

LATIN AMERICAN CONFERENCE

ON NATURAL AND APPLIED SCIENCES

NOVEMBER 5-6, 2021
VILLAHERMOSA, MEXICO

PROCEEDING BOOK

EDITORS

Dr. Germán Martínez Prats
Dra. Francisca Silva Hernández
Dr. Mijael Altamirano Santiago
Dra. Isi Verónica Lara Andrade



UNIVERSIDAD JUÁREZ
AUTÓNOMA DE TABASCO
"ESTUDIO EN LA DUDA. ACCIÓN EN LA FE"



MA|rket
S|ociety
REV|ew

ISBN: 978-625-7464-56-7



UNIVERSIDAD JUÁREZ
AUTÓNOMA DE TABASCO

“ESTUDIO EN LA DUDA. ACCIÓN EN LA FE”

PROCEEDING BOOK

November 5-6, 2021
Villahermosa, Mexico

EDITORS

Dr. Germán Martínez Prats
Dra. Francisca Silva Hernández
Dr. Mijael Altamirano Santiago
Dra. Isi Verónica Lara Andrade

ISBN: 978-625-7464-56-7

LATIN AMERICAN INTERNATIONAL CONFERENCE ON NATURAL AND APPLIED SCIENCES

November 5-6, 2021

Villahermosa, Mexico

PROCEEDING BOOK

EDITORS

Dr. Germán Martínez Prats
Dra. Francisca Silva Hernández
Dr. Mijael Altamirano Santiago
Dra. Isi Verónica Lara Andrade

All rights reserved. No part of this publication may be reproduced, distributed, or transmitted in any form or by any means, including photocopying, recording, or other electronic or mechanical methods, without the prior written permission of the publisher, except in the case of brief quotations embodied in critical reviews and certain other noncommercial uses permitted by copyright law.

Institution of Economic Development and Social
Research

Publications® (The Licence Number of Publicator:

2014/31220) TURKEY TR: +90 342 606 06 75

USA: +1 631 685 0 853

E mail: iksadyayinevi@gmail.com

www.iksadyayinevi.com

It is responsibility of the author to abide by the
publishing ethics rules IKSAD Publications – 2021©

Issued: 06.12.2021

ISBN: 978-625-7464-56-7

ABOUT CONFERENCE

LATIN AMERICAN INTERNATIONAL CONFERENCE ON NATURAL AND APPLIED SCIENCES

DATE - PLACE

Universidad Juárez Autónoma de Tabasco, México

İKSAD- www.iksad.org.tr

PARTICIPANT ORGANIZATIONS

Universidad Juárez Autónoma de Tabasco, México

*Universidad Abierta y a Distancia UNAD, Colombia
Institute Of Economic Development And Social Research*

Violence and Abuse Studies Platform

LANGUAGES

English, Spanish, Turkish, Russian

EVALUATION PROCESS

All applications have undergone a double-blind peer review process

PRESENTATION

Oral presentations

INTERNATIONAL PARTICIPANT COUNTRIES

*USA, Morocco, India, Iraq, Iran, China, Ukraine, Moldova, Ethiopia, Macedonia,
Algeria, France, Poland, Slovakia, UK, Spain, Latvia, Argentina, Mexico, Romania,
Indonesia, Pakistan, Bulgaria, Vietnam, Nigeria, Azerbaijan, Canada, Kosova,
Saudi Arabia, Kyrgyzstan*

(67)

Turkey (56)

ORGANIZING AND SCIENTIFIC COMMITTEES

Dra. Felipa Sánchez Pérez

Universidad Juárez Autónoma de Tabasco, México Chairman of the conference

Dra. Francisca Silva Hernández

Universidad Juárez Autónoma de Tabasco, México

Dr. Germán Martínez Prats

Universidad Juárez Autónoma de Tabasco, México

Dr. Jose Alberto Del Rivero Del Rivero

Universidad Juárez Autónoma de Tabasco, México

Dr. Rafael Ricardo Renteria Ramos

Universidad Abierta y a Distancia UNAD, Colombia

Dr. Ragif Huseynov

Managing Director of Khazar Educational Center, Azerbaijan

Dr. Raiba Jafarova

Associate Professor of Azerbaijan State Agricultural University, Azerbaijan

Assoc. Prof. Dr. Resmiyye Abdullayeva

Institute of Economics, Azerbaijan

Assist. Prof. Dr. Maral Jamalova

Azerbaijan State University of Economics, Azerbaijan

Bunyamin Seyidov

PhD student of Institute of Philosophy and Sociology, Azerbaijan

PHOTO GALLERY



PHOTO GALLERY

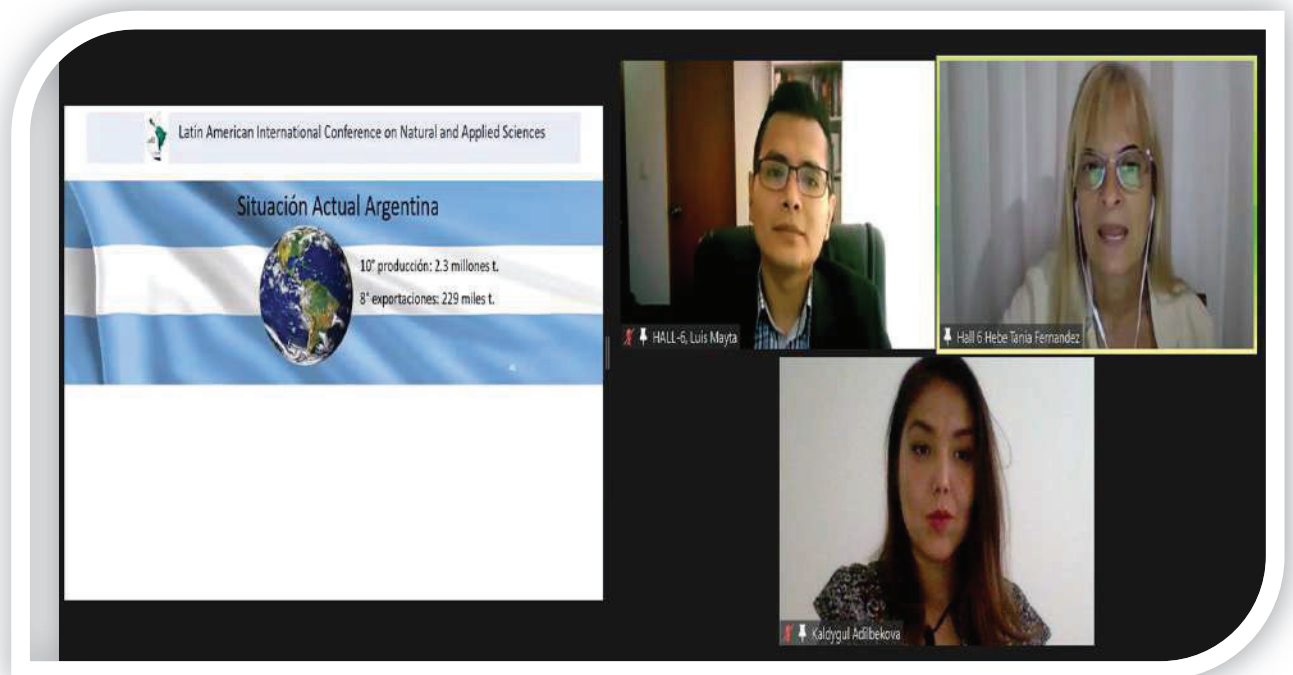


PHOTO GALLERY

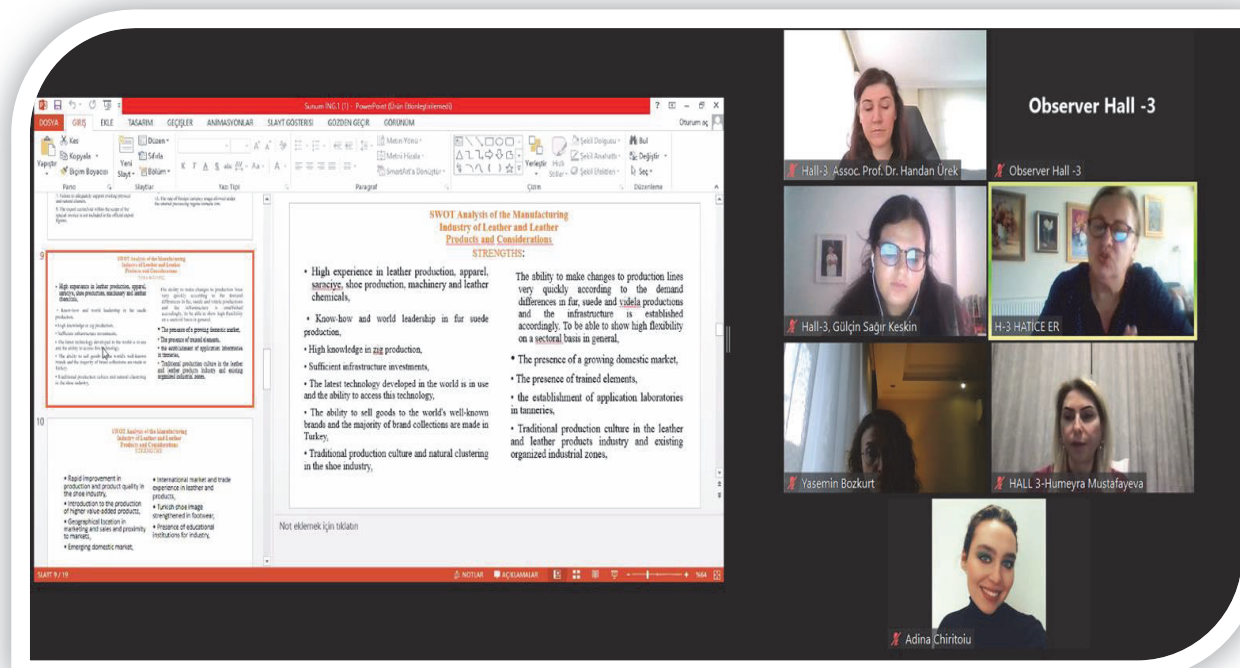
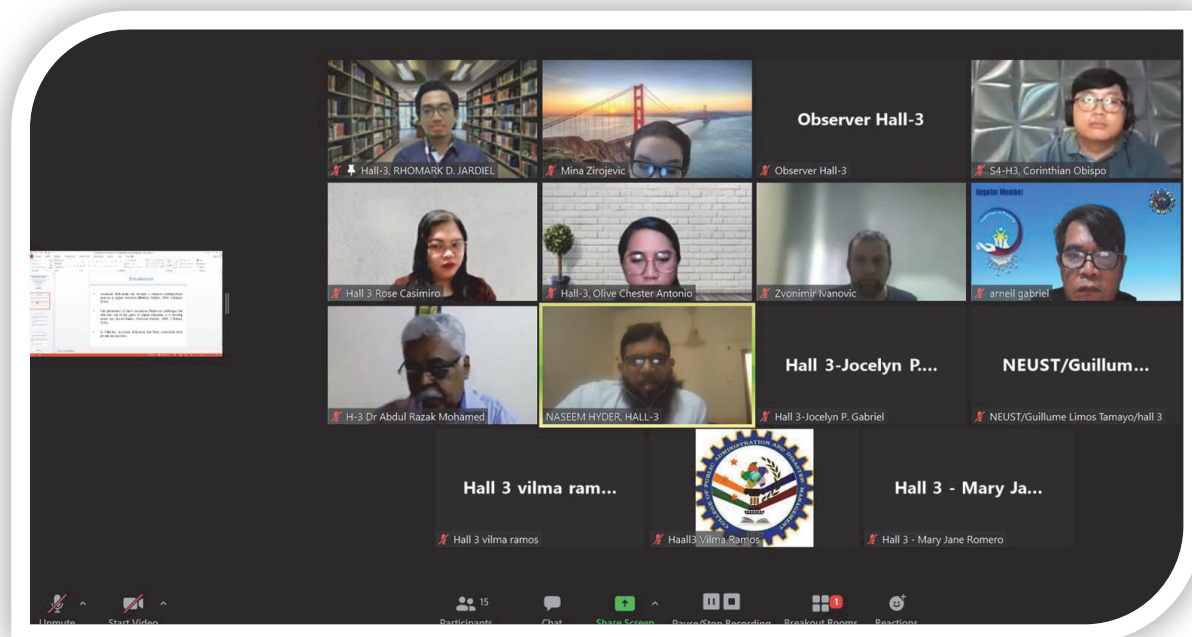



PHOTO GALLERY

Recording... You are viewing Hall-5, Md. Mahbubor Rahman's screen View Options

Properties of Carbon Fiber

- ✓ High Thermal Resistance
- ✓ Fire Resistance (Not Flammable)
- ✓ High Tensile Strength to Weight ratio
- ✓ High Rigidity
- ✓ Corrosion Resistance
- ✓ Electrical Conductivity
- ✓ Fatigue Resistance
- ✓ Low Thermal Expansion
- ✓ Non-poisonous
- ✓ Biologically Compatible
- ✓ X-ray Permeable



Observer Hall-5

Observer Hall-5

Hall-5, Dr.Rekha Suman

HS, Ezgi GURGENC

Hall-5, Md. Mahbubor Rahman

Recording...

Observer Hall-5

HS-Yener CESUR

Observer Hall-5

HS, Ezgi GURGENC

Hall-5, Dr.Rekha Suman

h-S Belfarhi

mai duc nghia

Hall-5, Sibel AKBULUT

Hall-5, Zakaria LAFDAILI

HATİCE ER

ONDOKUZ MAYIS UNİVERSİTESİ

Gizem Furuncu

ERHAN YAVAŞCI

HATİCE ER

Yüksel Ardali

Gizem Furuncu

ERHAN YAVAŞCI

PHOTO GALLERY

Design requirements of SEM

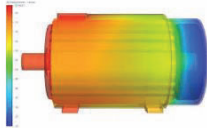
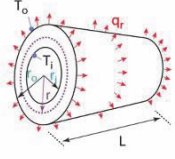
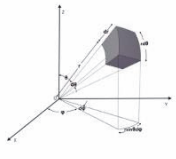
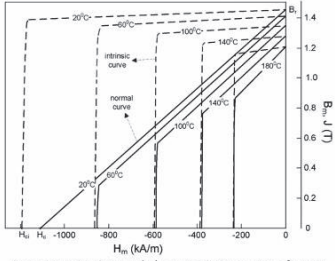
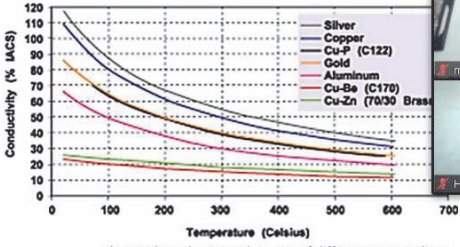




Fig.) Heat conduction equation in cylindrical coordinates

$$\frac{\partial^2 T}{\partial r^2} + \frac{1}{r} \frac{\partial T}{\partial r} + \frac{1}{r^2} \frac{\partial^2 T}{\partial \phi^2} + \frac{\partial^2 T}{\partial z^2} + \frac{\dot{q}}{k} = \frac{1}{\alpha} \frac{\partial T}{\partial t}$$


Demagnetisation and characteristic curves of a PM (TDI Neorec53B iron-based rare-earth magnet)



Electrical conductivity changing of different type winding materials by temperature

6.11.2021

I. INTRODUCTION


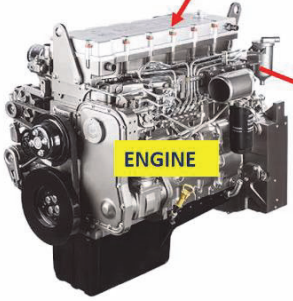






PHOTO GALLERY

II. MATERIALS AND METHODS

Table 2. Engine and simulation parameters

Type	6CHE, unified combustion
Number of cylinders	6
Cylinder diameter x piston stroke (mm)	105x125
Power (Hp/rpm)	130/2600
Compression ratio	16.4
Engine speed of simulation	1600 rpm
Number of nozzle holes x diameter x spray direction	4 x 0.32 x 140°
Injection timing °BTDC	18° BTDC
Injection pressure (bar)	210
Rod length	215 mm
IVC, EVO	
IVO	16° BTDC
IVC	52° BTDC
EVO	52° BTDC
EVC	16° BTDC



Observer Hall-5

Observer Hall-5

H5-Yener CESUR

Hall-5 - Dr.Rekha Suman

mai duc nghia


EXPANSION THEOREM

TEOREM : If $f(x)$ has a continuous second derivative in each $\Omega_i (i = 1, 2, \dots, n + 1)$ and satisfies the boundary-transmission conditions (2)-(5), then $f(x)$ can be expanded into an absolutely and uniformly convergent series of eigenfunctions of the boundary-value-transmission problem (1)-(5) on Ω , i.e.,

$$f(x) = \sum_{m=0}^{\infty} r_m \psi_m(x) \quad (16)$$

where $r_m = r_m(f)$ are the Fourier coefficients of f given by

$$r_m = \sum_{k=0}^n \frac{1}{a_{k+1}^2} \prod_{i=0}^k \theta_{i34} \prod_{i=k+1}^{n+1} \theta_{i12} \int_{\xi_{k+0}}^{\xi_{k+1}-0} f(x) \psi_m(x) dx. \quad (17)$$



Observer Hall-5

Observer Hall-5

H-5 hayati olgar

H5-Kadriye Aydemir

Hall-5, Mehsin...

Hall-5, Mehsin Attaya

ve elektronik olarak imzalayın

PHOTO GALLERY

Observer Hall-5

Observer Hall-5

H5-Fatih Hatipoğlu

H5-Ertan GRUC

H5-M. Burak ATEŞ

HCC is more common → **10 ages later**

However, it can also be observed at earlier ages (for example, at 25 months).

No gender predisposition.

No breed predisposition.

Liver
Large intestine
Small intestine

Slide 3 / 27 Türkiye (Türkiye) Erişilebilirlik: Özetlere göz atın

H6-MO-Lenforma-TR-ENG.ppt [Uyumluluk Modu] - Microsoft PowerPoint

LATIN AMERICAN INTERNATIONAL CONFERENCE ON NATURAL AND APPLIED SCIENCES

Method

Doku parçaları 4-5 mm kalınlığında olacak şekilde küçültüldü ve daha sonra tekrar %10'luk formaldehit solüsyonunda 24 saat süreyle tespit edildi. Rutin doku takip işlemlerinden sonra hazırlanan preparatlar Hematoksile-Eozin (HE) ile boyandı. Preparatlar ışık mikroskopunda incelendi

Tissue pieces were thinned to a thickness of 4-5 mm and then fixed in 10% formaldehyde solution for 24 hours again. After routine tissue processing procedures, the preparations were stained with Hematoxylin-Eosin (HE) The slides were examined under a light microscope.

H5-özgür özdemir

H5-Mustafa Ortatati

H5-Zeynep ÇELİK

Hall 5 Badiye V.H

Hall 5 Badiye V.H

Slide 6 / 23 "Varsayılan Tasarım" Türkiye

PHOTO GALLERY

Recording...

Latin American International Conference on Natural and Applied Sciences

DATES : NOVEMBER 5-6, 2021
VILLAHERMOSA, MEXICO

In general, EMPs often have a benign clinical course in dogs and cats and may be cured with complete surgical excision. Noncutaneous, non-oral EMP may have a more aggressive behavior; however, dogs treated with surgery alone or a combination of surgery and adjuvant systemic chemotherapy can have extended survival times.
(Sternberg R et all. 2009)



Genel olarak EMP'ler genellikle kedilerde iyi seyir gösterir. Deri dışı, oral EMP daha agresif olabilir; birlikte, tek veya cerrahi sistemik kemoterapi ile tedavi edilen köpeklerde sağkalım süreleri uzayabilir.
(Sternberg R et all. 2009)

Observer Hall-5

Observer Hall-5

H5-Fatih Hatipoğlu

H5-M. Burak ATEŞ

H5-Mustafa Ortatalı

PowerPoint Slide Show - [Dr Vaishali H. Badiye] - PowerPoint

You are viewing Hall 5 Badiye V.H.'s screen

View Options

INTRODUCTION

The agriculture industry is the prime source of revenue generation industry for the world population. Diseases caused by insect pests have made vulnerable effects on human health and crop health as well as it will directly impact the revenue generation sources.

Insects are the most dominant species on the earth and a very important and integral part of the ecosystem belongs to the phylum Arthropoda. They are beneficial for human society but some of them are very harmful to growing crops, stored products. They attack crops either by directly eating them or infecting them by the transmission of bacteria or viruses

IPM is an environment-friendly well-organized that works on the long-term prevention of pest's disease or harm caused by insects through a combination of techniques like the use of biological agents viz parasitoids, crop field tactics, modification of crop methods, and use of genetically treated varieties of crops.

Slide 3 of 21

Hall 5 Badiye V.H.

H5-Ertan CRUC

H5-Fatih Hatipoğlu

H5-Zeynep ÇELİK

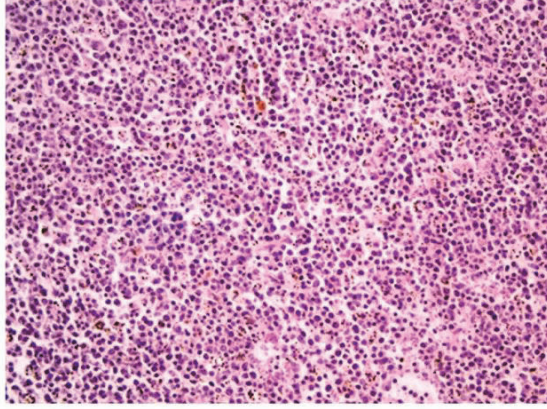
PHOTO GALLERY

Recording...

Latin American
International Conference on
Natural and Applied Sciences
DATES : NOVEMBER 5-6, 2021
VILLAHERMOSA, MEXICO

Microscopic findings

In the histopathological examination, it was determined that there was no capsule around the tumoral mass, and it was observed that the tumor cells were especially collected in the sinusoids.



Mikroskopik bulgular

Histopatolojik incelemede, tümör kütlesinin etrafında bulunmadığı belirlenmiştir. Tumor hücreleri özellikle sinüzoidlerde toplandığı görüldü.

Observer Hall-5

H5-Fatih Hatipoğlu

H5-M. Burak ATEŞ

H5-Mustafa Ortatatlı

Recording...

H-6 observer

José Leonardo Mattos

H-6 observer

Hall 6 Hebe Tania Fernandez

Luis Chávez

Pablo Mtz

HALL-6, Luis Mayta

Hall 6, Gerardo Sánchez

Luis Gonzalez

Hall 6- DAVID BONFIL

HALL-6 Edwin Bustamante

Miguel Manzano

Miguel Manzano

Aramak için buraya yazın

14°C

TUR

18:28



LATIN AMERICAN INTERNATIONAL CONFERENCE ON NATURAL AND APPLIED SCIENCES

**November 5-6, 2021
Villahermosa, Mexico**

CONFERENCE PROGRAM

Online (with ZOOM Conference)

Zoom Meeting ID: 858 8536 2635

Zoom Password: 543120

IMPORTANT, PLEASE READ CAREFULLY

- To be able to make a meeting online, login via <https://zoom.us/join> site, enter ID instead of "Meeting ID
- or Personal Link Name" and solidify the session.
- The presentation will have **15 minutes** (including questions and answers).
- The Zoom application is free and no need to create an account.
- The Zoom application can be used without registration.
- The application works on tablets, phones and PCs.
- Speakers must be connected to the session **10 minutes before** the presentation time.
- All congress participants can connect live and listen to all sessions.
- During the session, your camera should be turned on at least %70 of session period
- Moderator is responsible for the presentation and scientific discussion (question-answer) section of the session.

TECHNICAL INFORMATION

- Make sure your computer has a microphone and is working.
- You should be able to use screen sharing feature in Zoom.
- Attendance certificates will be sent to you as pdf at the end of the congress.
- Moderator is responsible for the presentation and scientific discussion (question-answer) section of the session.

**Before you login to Zoom please indicate your name surname and hall number,
exp. Hall-1, Shahla Tahirgizi**

ÖNEMLİ, DİKKATLE OKUYUNUZ LÜTFEN

- Kongremizde Yazım Kurallarına uygun gönderilmiş ve bilim kurulundan geçen bildiriler için online (video konferans sistemi üzerinden) sunum imkanı sağlanmıştır.
- Sunumlar için **15 dakika** (soru ve cevaplar dahil) süre ayrılmıştır.
- Online sunum yapabilmek için <https://zoom.us/join> sitesi üzerinden giriş yaparak "Meeting ID or Personal Link Name" yerine ID numarasını girerek oturuma katılabilirsiniz.
- Zoom uygulaması ücretsizdir ve hesap oluşturmaya gerek yoktur.
- Zoom uygulaması kaydolmadan kullanılabilir.
- Uygulama tablet, telefon ve PC'lerde çalışıyor.
- Her oturumdaki sunucular, sunum saatinden **10 dk öncesinde** oturuma bağlanmış olmaları gerekmektedir.
- Tüm kongre katılımcıları canlı bağlanarak tüm oturumları dinleyebilir.
- Moderatör – oturumdaki sunum ve bilimsel tartışma (soru-cevap) kısmından sorumludur.

TEKNİK BİLGİLER

- Bilgisayarınızda mikrofon olduğuna ve çalıştığına emin olun.
- Zoom'da ekran paylaşma özelliğine kullanabilmelisiniz.
- Katılım belgeleri kongre sonunda tarafınıza pdf olarak gönderilecektir
- Kongre programında yer ve saat değişikliği gibi talepler dikkate alınmayacaktır

Zoom'a giriş yaparken önce lütfen adınızı, soyadınızı ve SALON numaranızı yazınız
Örnek: Salon-1, Shahla Tahirgizi

-Opening Ceremony-

05.11.2021

Mexico Local Time: 08:³⁰–09:⁰⁰

Ankara Local Time: 16:³⁰–17:⁰⁰

Dr. Mustafa Latif EMEK

President of IKSAD Institute

Dra. Felipa Sánchez Pérez

Universidad Juárez Autónoma de Tabasco, México

CHAIRMAN OF THE CONFERENCE

Dr. Germán Martínez Prats

Universidad Juárez Autónoma de Tabasco, México

Dra. Francisca Silva Hernandez

Universidad Juárez Autónoma de Tabasco, México

LATIN AMERICAN INTERNATIONAL CONFERENCE ON NATURAL AND APPLIED SCIENCES
November 05-06, 2021 Villahermosa, Mexico

05.11.2021

Session-1, Hall-4

Mexico Time: 05⁰⁰-07³⁰

Ankara Time: 13⁰⁰-15³⁰

HEAD OF SESSION: Dr. Gümrah UYSAL

TOPIC TITLE	AUTHORS	AFFILIATION
BIG DATA MODELING	Emine BAŞ	Selçuk University, Konya, Turkey
ON MODIFIED BIVARIATE PICARD INTEGRAL OPERATORS WHICH FIX SOME EXPONENTIAL FUNCTIONS	Gümrah UYSAL	Karabük University
AI-ASSISTED COMPARISON OF LIVE NETWORK MEASUREMENTS AND PERFORMANCE METRICS IN DWDM SYSTEMS	Mustafa Serdar Osmanca Murat YÜCEL	Gazi University
BIO-INSPIRED HYBRIDIZATION OF ARTIFICIAL NEURAL NETWORKS: AN APPLICATION FOR CLASSIFICATION TASKS	Ouail MJAHER, Salah EL HADAJ El Mahdi ELGUARMAH, Soukaina MJAHER	Cadi Ayyad University, Marrakech, Morocco
FISH SCHOOL SEARCH ALGORITHM FOR SOLVING MULTI-OBJECTIVE U-SHAPED DISASSEMBLY LINE BALANCING PROBLEM	Pengfei Yao Surendra M. Gupta	Northeastern University Boston, USA
DEVELOPMENT OF CPR B2 ca s1a d1 CLASS SIGNAL CABLES	Erdoğan YÜKSEL Can ALTINGÖZ Furkan ŞEN Ahmet FEYZİOĞLU	Türk Prysmian Kablo ve Sistemleri A.Ş. R&D Center, Bursa, Turkey. Marmara University
CURING EFFECT IN RTM PROCESS	Ahmed Ouezgan Said Adima Aziz Maziri El Hassan Mallil Jamal Echaabi	Hassan II University of Casablanca, Morocco.
EFFECT OF TIN SUBSTITUTION ON STRUCTURAL, ELECTRICAL AND HUMIDITY-SENSING CHARACTERISTICS OF TUNGSTEN OXIDE NANOPARTICLES	Karunesh Tiwari Anam Zaidi Shalini	Babu Banarasi Das University Lucknow, Uttar Pradesh, India
MATERIALS CLASSIFICATION OF PROFITABLE AND NEW SOFT CONTACT LENSES USING MATLAB	Amenah Emad Mohammed Redha	Dijlah University College, Iraq

LATIN AMERICAN INTERNATIONAL CONFERENCE ON NATURAL AND APPLIED SCIENCES
November 05-06, 2021 Villahermosa, Mexico

05.11.2021

Session-1, Hall-5

Mexico Time: 05⁰⁰-07³⁰

Ankara Time: 13⁰⁰-15³⁰

HEAD OF SESSION: Assoc. Prof. Dr. Onur Akyıldırım

TOPIC TITLE	AUTHORS	AFFILIATION
SYNTHESIS AND IN VITRO ANTIOXIDANT PROPERTIES OF SOME NEW 1-BENZYL-3-ALKYL(ARYL)-4-(3-METHOXY-4-PHENYLMETHOXY-BENZYLIDENAMINO)-4,5-DIHYDRO-1H-1,2,4-TRIAZOL-5-ONES	Onur Akyıldırım Özlem Gürsoy-Kol Haydar Yüksek	Kafkas University, Kars, Turkey
A STUDY ON THEORETICAL/EXPERIMENTAL SPECTROSCOPIC AND ELECTRONIC PROPERTIES OF 1-ACETYL-3-METHYL-4-(4-METHYLBENZOXY)- BENZYLIDENEAMINO]-4,5-DIHYDRO-1H-1,2,4-TRIAZOL-5-ONE	Hilal Medetalibeyoğlu Haydar Yüksek	Kafkas University, Kars, Turkey
SYNTHESIS AND IN VITRO ANTIOXIDANT PROPERTIES OF SOME NOVEL 1,3,4-TRISUBSTITUE-4,5-DIHYDRO-1H-1,2,4-TRIAZOL-5-ONES	Onur Akyıldırım Özlem Gürsoy-Kol Haydar Yüksek	Kafkas University, Kars, Turkey
INVESTIGATION OF THE USAGE OF CORAL WASTE FISH SCALS AS A CATALYST IN PRODUCTION OF BIODIESEL	Gediz UĞUZ	Ondokuz Mayıs University, Turkey
INTERACTIONS of [Cu(5-nphen)(tyr)(H ₂ O)]NO ₃ · 2H ₂ O COMPLEX with BOVINE SERUM ALBUMINE (BSA)	Duygu İNCİ Rahmiye AYDIN	Kocaeli University, Turkey Bursa Uludag University, Turkey
SYNTHESIS AND CHARACTERIZATION OF NEW MANNICH BASES CONTAINING 1,2,4-TRIAZOLE RING	Bahar BANKOĞLU YOLA Haydar YÜKSEK	Iskenderun Technical University, Turkey Kafkas University, Kars, Turkey
SYNTHESIS OF NOVEL 3-[[1-(MORPHOLIN-4-YL-METHYL)-3-ALKYL/ARYL-4,5-DIHYDRO-1H-1,2,4-TRIAZOL-5-ONE-4-YL]-AZOMETHINE}-PHENYL 2,5-DICHLOROBENZENESULFONATES	Fevzi Aytemiz Haydar Yüksek	Kafkas University, Kars, Turkey
STRUCTURAL AND SPECTROSCOPIC ANALYSIS WITH DFT OF 3-METHYL-4-[2-(2-THIENYLCARBONYLOXY)-3-METHOXYBENZYLIDENAMINO]-4,5-DIHYDRO-1H-1,2,4-TRIAZOL-5-ONE	Gül KOTAN Haydar YÜKSEK	Kafkas University, Kars, Turkey

LATIN AMERICAN INTERNATIONAL CONFERENCE ON NATURAL AND APPLIED SCIENCES
November 05-06, 2021 Villahermosa, Mexico

05.11.2021

Session-1, Hall-6

Mexico Time: 05⁰⁰-07³⁰

Ankara Time: 13⁰⁰-15³⁰

HEAD OF SESSION: Priyanka Singh

TOPIC TITLE	AUTHORS	AFFILIATION
RECENT DIAGNOSTIC AIDS IN ORAL CANCER DETECTION	Shikha Saxena Priyanka Singh	RUHS College of Dental Sciences, Jaipur, Rajasthan King George's Medical University, Lucknow (UP), India
AURICULAR ACUPRESSURE FOR SMOKING CESSATION: A SYSTEMATIC REVIEW OF RANDOMIZED CONTROLLED TRIALS	Ying-Ying Zhang Ze-Yu Yu JianPing Liu	Beijing University, China
FEATURES OF THE LIPID SPECTRUM AND THE PROBLEM OF ACHIEVING THE TARGET LEVEL OF LOW-DENSITY LIPOPROTEINS DURING A CORONARY EVENT	Madina Nurzhanova Gulnara Kapanova	Al-Farabi Kazakh National University, Kazakhstan
ORAL CANCER SCREENING. CURRENT APPROACHES AND FUTURE PROSPECTS	Ivashchuk Oleksandr Hovornyan Serhiy	Bukovinian State Medical University
INTRA-ABDOMINAL HYPERTENSION AS ONE OF THE FACTORS OF OCCURRENCE OF POSTOPERATIVE EVENTRAT	Ivashchuk Alexander Ivanovich Morar Igor Kalinovich	Буковинский государственный медицинский университет, Украина
PRIMARY MYELOFIBROSIS IN PATIENTS UNDER 40 YEARS OLD	Sgibneva-Bobeiko Nina Vasily Musteatsa Maria Robu	State University of Medicine and Pharmacy "N. Testemitanu ", Moldova
VELSCOPE INSTRUMENT FOR DETECTION OF ORAL SOFT TISSUE CONDITION IN PROSTHODONTIC PATIENTS	Aneta Mijoska Sasho Jovanovski Daniela Srbinoska Vesna Trpeska Blagoja Dashtevski Marjan Petkov	University St. Cyril and Methodius, Skopje, N. Macedonia
EVALUATION OF ORAL SOFT TISSUES AT GERIATRIC PATIENTS WITH DENTAL PROSTHESIS	Aneta Mijoska Sasho Jovanovski Daniela Srbinoska Vesna Trpeska Emilija Bajraktarova Valjakova	University St. Cyril and Methodius, Skopje, N. Macedonia

LATIN AMERICAN INTERNATIONAL CONFERENCE ON NATURAL AND APPLIED SCIENCES
November 05-06, 2021 Villahermosa, Mexico

05.11.2021

Session-2, Hall-5

Mexico Time: 09⁰⁰-11³⁰

Ankara Time: 17⁰⁰-19³⁰

HEAD OF SESSION: Dr. Gül KOTAN and Dr. Mustafa Latif EMEK

TOPIC TITLE	AUTHORS	AFFILIATION
SOME QUANTUM CHEMICAL CALCULATIONS OF 3-n-PROPYL-4-(3-ACETOXY-4-METHOXYBENZYLIDENAMINO)-4,5-DIHYDRO-1H-1,2,4-TRIAZOL-5-ONE	Önder ALBAYRAK Gül KOTAN Haydar YÜKSEK	Kafkas University, Kars, Turkey
ELECTRONIC, THERMODYNAMIC, GEOMETRIC AND NONLINEAR OPTIC ANALYSIS OF 1-(2,6-DIMETILMORFOLIN-4-IL-METIL)-3-ETHYL-4-(4-HYDROXYBENZYLIDENAMINO)-4,5-DIHYDRO-1H-1,2,4-TRIAZOL-5-ONE	Songül BOY Gül KOTAN Haydar YÜKSEK	Kafkas University, Kars, Turkey
INHIBITION OF THERMAL AND SHEAR INDUCED AGGREGATION OF ALBUMIN (BOVINE SERUM ALBUMIN) BY CENTELLA ASIATICA EXTRACT	Laipubam Gayatri Sharma, Lalit Mohan Pandey	Indian Institute of Technology, Guwahati, India
SYNTHESIS OF ZEOLITIC MATERIALS INCORPORATED IN THE PRESENCE OF DIFFERENT STRUCTURING ORGANIC MOLECULES	TABTI Affaf LAUNAY Franck BABA AHMED Abd Rezzak Serier Mohamed	University of Relizane Ahmed Zabana, Algeria. University of Oran ,Ahmed Ben Bella, Algeria. Ivry-sur-SeineSorbonne Universities, France.
INVESTIGATION OF THEORETICAL AND EXPERIMENTAL SPECTROSCOPIC PROPERTIES OF 3-p-METHYLBENZYL-4-[3-ETHOXY-4-(4-METHOXYBENZOXY)-BENZYLIDENEAMINO]-4,5-DIHYDRO-1H-1,2,4-TRIAZOL-5-ONE	Hilal Medetalibeyoğlu Haydar Yüksek	Kafkas University, Kars, Turkey
SYNTHESIS AND CHARACTERIZATION OF NEW 1-(4-AMINOCARBONYLPIPERIDIN-4-YL-METHYL)-3-ALKYL(ARYL)-4-(3-METHOXY-4-ISOBUTYRYLOXY-BENZYLIDENEAMINO)-4,5-DIHYDRO-1H-1,2,4-TRIAZOLE-5-ONES	Sevda MANAP Haydar YÜKSEK	Kafkas University, Kars, Turkey
EVALUATION OF THEORETICAL AND EXPERIMENTAL PROPERTIES OF 3-METHYL-4-(3-ACETOXY-4-METHOXY-BENZYLIDENAMINO)-4,5-DIHYDRO-1H-1,2,4-TRIAZOL-5-ONE	Önder Albayrak Murat Beytur Haydar Yüksek	Kafkas University, Kars, Turkey
TEMPERATURE-RESPONSIVE NANOGELS CONTAINING SPIONS AND MIRNAS FOR TARGETED DELIVERY IN WOUND HEALING AND SKIN REGENERATION APPLICATIONS. THE EURONANOMED PROJECT TENTACLES	Alessandro Paolini Stefania Paola Bruno Arkadijs Sobolevs Aiva Plotniece Marcin K. Chmielewski Natalia Krówczyńska Ludovic Le Hégarat Kevin Hogeveen Monika Sramkova Alena Gabelova Andrea Caporali Nicolás Cassinelli Beatriz Sanz Andrea Masotti	Riga, Latvia. Poland. France Slovakia United Kingdom Spain

LATIN AMERICAN INTERNATIONAL CONFERENCE ON NATURAL AND APPLIED SCIENCES
November 05-06, 2021 Villahermosa, Mexico

05.11.2021

Session-2, Hall-6

Mexico Time: 09⁰⁰-11³⁰

Ankara Time: 17⁰⁰-19³⁰

HEAD OF SESSION: José Leonardo de Oliveira Mattos

TOPIC TITLE	AUTHORS	AFFILIATION
ESTUDIO DE ESPECTROSCOPIA FTIR DE EXTRACTOS DE HOJAS DE PISTACIA LENTÍSCUS	Hayat Jaadan , Mustafa Akodad , Saadia Belmalha	Université Mohamed Premier, - Géologie, Ecole Nationale d'Agriculture de Meknès, Meknès-Maroc
EFFECTO DEL ADICIONADO DE ADITIVOS Y HARINA DE CHIA EN LA INDUSTRIA AVICOLA ARGENTINA	Hebe FERNÁNDEZ Angelo MAZZOCCHI Dardo CÓCCARO Carmen Salerno	Universidad Nacional del Sur, Buenos Aires, Argentina.
PROPAGACIÓN ASEJUAL POR ACODOS AÉREOS DE QUÉNUA (POLYLEPIS RUGULOSA BITTER) UTILIZANDO CUATRO ENRAÍZADORES CON DOS SUSTRATOS NATURALES EN CONDICIONES DE VÍVERO	Luis Mayta, Edwin Bustamante, Eduardo Molinari, Elio Ponce	Sociedad Minera Cerro Verde, Chess Consulting & Project,
SPECIES DIVERSITY WITHIN THE UPPER/MIDDLE PARAÍBA DO SUL RIVER BASIN AND ADJACENT DRAINAGES CLADE, OF THE AUSTRALOHETEROS AUTRANI GROUP (TELEOSTEI, CICHLIDAE)	José Leonardo de Oliveira Mattos Marcos Aurélio da Silva Adrian Indermaur Axel Makay Katz Walter Salzburger Felipe Polivanov Ottoni	Universidade Federal do Rio de Janeiro University of Basel Federal University of Maranhão
THERMAL CHARACTERIZATION OF SURFACTANT SOLUTIONS AND PHASE TRANSITION IDENTIFICATION USING THE LEWIS-NIELSEN MODEL	Luis M. Montes-de-Oca R. Medina-Esquivel Zambrano-Arjona , P. Martínez- Torres	Universidad Michoacana de San Nicolás de Hidalgo, Morelia, Michoacán, México Universidad Autónoma de Yucatán, Yucatán, Mexico
ESTUDIO ELECTROQUÍMICO DE UN ACERO INOXIDABLE Y ACERO AL CARBONO EN SOLUCIÓN DE EXTRACTO DE CEMENTO CON IONES CLORURO	David Bonfil Ceferino Lucien Veleza Ángel Bacellis	Centro de investigación y de estudios avanzados (CINVESTAV)
EFFECTO DEL CA EN LA ALEACIÓN DE MG-CA0.3 SOBRE LA ACTIVIDAD ELECTROQUÍMICA EN SOLUCIÓN DE HANK Y PROPIEDADES DE DEPÓSITOS DE AG-NANO PARTÍCULAS	José Luis González-Murguía Lucien Veleza	Centro de Investigación y de Estudios Avanzados del IPN (CINVESTAV)
ACTIVIDAD ELECTROQUÍMICA DE MG DE ALTA PUREZA EN SOLUCIÓN FISIOLÓGICA DE HANK	Miguel Manzano Canul Lucien Veleza José Luis González-Murguía	Centro de Investigación y de Estudios Avanzados del IPN (CINVESTAV)
COMPORTAMIENTO DE LA CORROSIÓN DEL NANOCOMPUESTO AM60-ALN Y LA ALEACIÓN AM60 EXPUESTAS A UN AMBIENTE SIMULADO DE LLUVIA ÁCIDA	Luis Chávez Lucien Veleza	Centro de Investigación y de Estudios Avanzados del IPN (CINVESTAV)
ACTIVIDAD ELECTROQUÍMICA DE LA MATRIZ METÁLICA EXTRUIDA AM60 EN UN ENTORNO DE SOLUCIÓN MARINA SIMULADA	Gerardo Sánchez Lucien Veleza Luis Chávez	Centro de Investigación y de Estudios Avanzados del IPN (CINVESTAV)

05.11.2021

Session-3, Hall-3

Mexico Time: 12⁰⁰-14³⁰

Ankara Time: 20⁰⁰-22³⁰

HEAD OF SESSION: Binyam Zigta

TOPIC TITLE	AUTHORS	AFFILIATION
LIVER FAILURE WITH MECHANICAL JAUNDICE	Elena Mostiuk	Taras Shevchenko National University of Kyiv
THE GENOMIC AND TRANSCRIPTOMIC APPROACHES IN OPIUM POPPY	Tuğba Gürkök Tan Gülşen Güçlü	Çankırı Karatekin University, Turkey Sivas Cumhuriyet University Turkey.
EFFECT OF THERMAL RADIATION AND CHEMICAL REACTION ON MHD FLOW OF BLOOD IN STRETCHING PERMEABLE VESSEL	Binyam Zigta	Wachemo University, Ethiopia
BURNOUT SYNDROME AT MEDICAL STAFF FROM ROMANIA	Boboc Daniela	School Center for Inclusive Education from Constanta - Romania
C-MAC® VS. MCGRATH® VIDEO LARYNGOSCOPE IN PATIENTS UNDERGOING GENERAL ANESTHESIA WITH OROTRACHEAL INTUBATION: A PROSPECTIVE, RANDOMIZED CLINICAL TRIAL	Christopher Ryalino Tjokorda Gde Agung Senapathi Jhoni Pardomuan Pasaribu	Udayana University, Indonesia
POSSIBLE EFFECTS AFTER A COVID VACCINATION AT THE MOLECULAR AND CHEMICAL LEVEL FOR PATIENTS WITH CELIAC DISEASE	Felicia Andrei Anca Dragomirescu	Timiș County Emergency Clinical Hospital, Romania University of Medicine and Pharmacy "Victor Babes", Romania
STRUCTURE OF TANISIT CELLS AND THEIR FUNCTIONAL ROLE IN THE NERVOUS SYSTEM	Fatih TAŞ Ender ERDOĞAN	Siirt University, Turkey

LATIN AMERICAN INTERNATIONAL CONFERENCE ON NATURAL AND APPLIED SCIENCES
November 05-06, 2021 Villahermosa, Mexico

05.11.2021

Session-3, Hall-4

Mexico Time: 12⁰⁰-14³⁰

Ankara Time: 20⁰⁰-22³⁰

HEAD OF SESSION: Nida Khan

TOPIC TITLE	AUTHORS	AFFILIATION
EFFECT OF MAXIMAL DOSES OF DEXTRAN-POLYACRYLAMIDE POLYMERS AND THEIR AS CARRIERS OF SILVER AND GOLD NANOPARTICLES ON LIVER	Valentyna Kurovska Oksana Kaleinikova Iryna Byelinska Natalia Kutsevol Taras Blashkiv	Taras Shevchenko National University of Kyiv, Kyiv, Ukraine Bogomoletz Institute of Physiology, Kyiv, Ukraine
COMPARISON OF IRON, ZINC AND FERRITIN AMONG SMALL FOR GESTATIONAL AGE AND APPROPRIATE FOR GESTATIONAL AGE MOTHERS	Nida Khan Sadia Fatima Rubina Nazli Tasleem Akhtar Jamila Haider	Institute of Basic Medical Sciences, Khyber Medical University, Peshawar Pakistan Health Research Council, Khyber Medical College, Peshawar Shaheed Benazir Bhutto Women University, Peshawar.
DNA NANOTECHNOLOGY AND THERAPEUTICS	Baig, Mirza Muhammad Faran Ashraf	The University of Hong Kong
ENDOSCOPIC APPROACHES IN OTORHINOLARYNGOLOGY	Proletina Bozdukova, Tsvetelina Grigorova	ENT resident at UMHAT Burgas
ENT MANIFESTATIONS IN COVID-19	Daniel Petkov Tsvetelina Grigorova	UMHAT Burgas
PROTECTIVE EFFECT OF MURRAYA KOENIGII AGAINST TESTICULAR DAMAGES INCURRED IN SKIN TUMOR BEARING MICE	Aniqa Aniqa Sarvnrinder Kaur	Panjab University, Chandigarh
E-HEALTH APPLICATIONS IN TURKEY	Fatih Altan Mehmet Doğan	Erciyes University
COVID-19 VACCINATIONS AND COVID-19 VACCINATION RATES IN TURKEY	Fatih Altan Mehmet Doğan	Erciyes University

LATIN AMERICAN INTERNATIONAL CONFERENCE ON NATURAL AND APPLIED SCIENCES
November 05-06, 2021 Villahermosa, Mexico

05.11.2021

Session-3, Hall-5

Mexico Time: 12⁰⁰-14³⁰

Ankara Time: 20⁰⁰-22³⁰

HEAD OF SESSION: Assoc. Prof. Dr. Grozi Delchev

TOPIC TITLE	AUTHORS	AFFILIATION
GRAIN YIELDS OF DURUM WHEAT (TRITICUM DURUM DESF.) AND YIELD STABILITY AFFECTED OF CERTAIN PREPARATIONS AND VARIOUS TERMS OF SOWING	Petar Nikolov Grozi Delchev	Obrazcov Chiflik, Ruse, Bulgaria Trakia University, Bulgaria
EFFECTIVE ROLE OF CHITOSAN-SILVER NANOCOMPOSITE ON FOOD PRESERVATION	K.R.Padma K.R.Don	Sri Padmavati Mahila Visvavidyalayam University, Tirupati Bharath University, Chennai, Tamil Nadu, India
GENETIC VARIABILITY, ASSOCIATION AND DIVERSITY STUDY AMONG THE SUNFLOWER GENOTYPES AT SEEDLING STAGE BASED ON DIFFERENT MORPHO-PHYSIOLOGICAL PARAMETERS UNDER POLYETHYLENE GLYCOL INDUCED STRESS	Ms. Uzma Ayaz	The University of Poonch Rawalakot, Pakistan
WOODEN BREAST SYNDROME AND FACTORS AFFECTING ITS DEVELOPMENT	Tuğçe UZUN Aylin AĞMA OKUR	Tekirdağ Namık Kemal University Tekirdag/TÜRKİYE
IN VITRO WOUND HEALING POTENCY OF METHANOLIC LEAF EXTRACT OF ARISTOLOCHIA SACCATA IS POSSIBLY MEDIATED BY ITS STIMULATORY EFFECT ON COLLAGEN-1 EXPRESSION	K.R.Padma K.R.Don	Sri Padmavati Mahila Visvavidyalayam (Women's) University, Tirupati, AP Bharath University, Chennai, Tamil Nadu
FREQUENCY-BASED AGRI-IOT TECHNIQUES IN AGRICULTURE	DEEPA SONAL SHAILESH KUMAR SHRIVASTAVA BINAY KUMAR MISHRA	V.K.S. University, India
DIFFERENT HUMIC ACID DOSES EFFECT ON GEMLİK OLIVE SAPLINGS IN MANISA KÖPRÜBAŞI DISTRICT	Ayça AKÇA UÇKUN Ünal KAYA , Suna BAŞER , Alptug ÇANTAL , Merve TÜRKYILMAZ	Olive Research Institute Argem Agricultural Engineering LTD.ŞTİ.
EFFECT OF SMALL-SCALE FISH CAGE CULTURE ON SEDIMENT QUALITY OF THE SOUTHERN CASPIAN SEA: CASE STUDY IN IRANIAN COAST-NOWSHAHR	Nasrollahzadeh Saravi H. Vahedi, F. Makhlough A. Baluei, M.	Caspian Sea Ecology Research Center (CSERC), Iranian Fisheries Science Research Institute (IFSRI), Agricultural Research, Education and Extension Organization (AREEO), Sari, Iran.

LATIN AMERICAN INTERNATIONAL CONFERENCE ON NATURAL AND APPLIED SCIENCES
November 05-06, 2021 Villahermosa, Mexico

05.11.2021

Session-3, Hall-6

Mexico Time: 12⁰⁰-14³⁰

Ankara Time: 20⁰⁰-22³⁰

HEAD OF SESSION: Assist. Prof. Dr. Fevzi Altuner

TOPIC TITLE	AUTHORS	AFFILIATION
PURPLE POTATO VARIETIES AS RICH ANTHOCYANINS SOURCE FOR FOOD, PHARMACEUTICALS AND COSMETICS	Alexandra Mihaela NAGY (FRĂȚILĂ) Corina CĂȚANĂ Paula BOBOC (OROS) Camelia SAVA SAND	Lucian Blaga University Sibiu, Romania. University of Agricultural Sciences and Veterinary Medicine, Cluj-Napoca, Romania.
RESPONSE OF SPHAGNUM MOSS TO DIFFERENT SOWING METHODS FOR THE PURPOSE OF THEIR USE IN CONTEMPORARY STREET ART	Paula BOBOC (OROS) Rita-Daniela FARTADI Corina CĂȚANĂ	Lucian Blaga University Sibiu, Romania. University of Agricultural Sciences and Veterinary Medicine, Cluj-Napoca, Romania.
PROCESSING SPECIMENS FOR VIRTUAL HERBARIUM	Rita-Daniela FARTADI Paula BOBOC (OROS) Corina CĂȚANĂ	Lucian Blaga University Sibiu, Romania. University of Agricultural Sciences and Veterinary Medicine, Cluj-Napoca, Romania.
EVALUATION OF SOMATIC CELL COUNT OF RAW MILK DEPENDING ON SEASONAL VARIATION	Melike CINIVIZ Gokce KESER Irmak ARAL BASKAYA Lutfiye YILMAZ ERSAN Tulay OZCAN Omer Utku COPUR	Bursa Uludag University, Turkey
EFFECT OF SALT CONCENTRATION ON THE STRUCTURE AND PREFERENCE OF MIHALIC CHEESE	Gokce KESER Melike CINIVIZ Irmak ARAL BASKAYA Tulay OZCAN Lutfiye YILMAZ ERSAN Omer Utku COPUR Ozlem KANER	Bursa Uludag University, Turkey
THE EFFECT OF SOWING FREQUENCY ON YIELD AND YIELD COMPONENTS OF OAT CULTIVARS IN VAN ECOLOGICAL CONDITIONS	Fevzi ALTUNER Mehmet ULKER	Van Yuzuncu Yil University, Van-TURKEY
THE EFFECT OF NITROGEN FERTILIZER DOSES ON YIELD AND YIELD PROPERTIES ON OAT CULTIVARS	Fevzi ALTUNER Mehmet ULKER	Van Yuzuncu Yil University, Van-TURKEY
STUDY ON SPATIAL SURFACE SEDIMENT QUALITY AT TWO MAIN TRIBUTARIES OF GAVEH AND GHESHLAGH RIVERS OF THE ZHAVEH DAM-WEST OF IRAN	Nasrollahzadeh Saravi H. Vahedi, F. Naderi Jolodar, M. Makhlough A. Behrozi, Sh. Baluei, M. Kardarrostami, M.	Caspian Sea Ecology Research Center (CSERC), Iranian Fisheries Science Research Institute (IFSRI), Agricultural Research, Education and Extension Organization (AREEO), Sari, Iran.

06.11.2021

Session-4, Hall-4

Mexico Time: 05⁰⁰-07³⁰

Ankara Time: 13⁰⁰-15³⁰

HEAD OF SESSION: Dr. Ayça AKÇA UÇKUN

TOPIC TITLE	AUTHORS	AFFILIATION
MANAGEMENT OF THE FOODS SUPPLY CHAIN WITH INTO ACCOUNT HUMAN HEALTH	Fethi Boudahri , Abderazzak Baba Ahmed, Rabab Boukli Hacene,	Manufacturing Enginneering Loboratory of Tlemcen Tlemcen, Algeria University of Relizane, Relizane, Algeria
SOCIO-DEMOGRAPHIC AND PRODUCTION STRUCTURES OF POMEGRANATE PRODUCING ENTERPRISES IN HATAY	Zeynep DEMETGÜL Nuran TAPKI	Hatay Mustafa Kemal University, TÜRKİYE
EVALUAION OF CHROMIUM CONTAMINATION ON AGRICULTURAL SOIL AND ON DURUM WHEAT	Baba Ahmed Abderrazzak Boudahri Fethi Tabti Affaf	Ahmed Zabana university, University of Tlemcen, Algeria Ahmed Zabana university, Relizane, Algeria
EVALUATION OF THE PRODUCTION OF SOME FIELD PLANTS GROWED IN CENTRAL ANATOLIAN CONDITIONS IN SALT CONDITIONS	M. Sevba ÇOLAK Ahmet ÖZTÜRK	Ankara University, Turkey
ARTIFICIAL RAIN ON THE VERGE OF DROUGHT	M. Sevba ÇOLAK Ahmet ÖZTÜRK	Ankara University, Turkey
INVESTIGATION OF THE EFFECTS OF SEFERİHISAR REGION CLIMATIC AND TOPOGRAPHIC CONDITIONS ON OLIVE PHENOLOGY AND POMOLOGY	Ayça AKÇA UÇKUN Murat TUĞAÇ Suna BAŞER Sedef ÖZDEN Aişe DELİBORAN Tülin PEKCAN,	Olive Research Institute Soil, Fertilizer And Water Resources Central Research Institute
100% NATURAL, DIFFERENT WITH REPAIRING AND HEALING PROPERTIES DEVELOPMENT OF CREAM WITH POMATO CONTAINING HERBAL EXTRACTS	Merve KADAL Aşlı BAHADIR	Rebul Kozmetik Sanayi ve Ticaret A.Ş. Ar-Ge Merkezi, İstanbul, Turkey.
METHODS OF GENETIC ENGINEERING IN PLANTS BREEDING	Dzhamirze R.R., Ph.D Esaulova L.V., Ph.D. Slabchenko A. S.,	Federal State Budgetary Scientific Institution «Federal Scientific Rice centrwe»

LATIN AMERICAN INTERNATIONAL CONFERENCE ON NATURAL AND APPLIED SCIENCES
November 05-06, 2021 Villahermosa, Mexico

06.11.2021

Session-4, Hall-5

Mexico Time: 05⁰⁰-07³⁰

Ankara Time: 13⁰⁰-15³⁰

HEAD OF SESSION: Dr. Rekha Suman

TOPIC TITLE	AUTHORS	AFFILIATION
TESTING AND EVALUATION OF ELECTRODIALYSIS METHOD ON DESALINATION	Sinem KAYA Yüksel ARDALI	Ministry of Environmet and Urbanisation, Samsun, Turkey Ondokuz Mayıs University
INVESTIGATION OF STRUCTURAL PROPERTIES OF AL/P-SI/CDO:NIO/AL PHOTODIODE FABRICATED BY SOL-GEL SPIN COATING METHOD	Ezgi GURGENC Aydın DİKİCİ Fehmi ASLAN	Firat University
THE EFFECT OF HEAT TREATMENT STRATEGIES ON THERMAL STABILIZATION OF POLYACRYLONITRILE FIBERS IN CARBON FIBER PRODUCTION	Kemal Şahin TUNÇEL Md. Mahbubor RAHMAN Tuba DEMİREL İsmail KARACAN	Siirt University, Siirt, Turkey Bangladesh University, Bangladesh Erciyes University, Kayseri, Turkey
NUMERICAL STUDY OF THE EFFECT OF EXTERNAL MAGNETIC FIELDS ON THE TURBULENT NATURAL CONVECTION OF NANOFLUIDS IN A TWO-DIMENSIONAL CAVITY	Zakaria LAFDAILI Sakina El-Hamdani Mohamed El Hattab Lahoucine Belarche	University Ibn Zohr, Agadir, Morocco
STUDY OF METHODS OF EXTRACTİNG A WİLD PLANT FROM THE ALGERİAN SAHARA	Belfarhi Leila Tahraoui Abdelkrime Bairi Abdelmedjid Ibtissem Chouba Naziha Amri Nadia Boukris	University of Badji Moukhtar, Annaba, Algeria
ENVIRONMENT AND SUSTAINABLE DEVELOPMENT GOALS IN INDIA	Dr. Rekha Suman	Himachal Pradesh University
INVESTIGATION OF TRIBOLOGICAL CHARACTERISTICS OF COPPER-TITANIUM ALLOYS PROCESSED BY MULTI-AXIAL CRYO-FORGING	Ramesh S , Gajanan M Naik , Gajanan Anne	RV Institute of Technology and Management, Banglore,
DESIGN AND CONTROL OF INDUSTRIAL TYPE LIQUID LEVEL CONTROL SYSTEM WITH PID	Ahmet TOP Yener CESUR Muammer GÖKBULUT	Firat University, Elazığ, Turkey
EXPERIMENTAL AND NUMERICAL PERFORMANCE ANALYSIS OF SMOKE EXTRACTION MOTORS USED IN SPECIAL FAN APPLICATIONS AT HIGH TEMPERATURE	Cansu AKSOY Sibel AKBULUT	Volt Electric Motors Company Izmir, Turkey
A SIMULATION STUDY ON THE PROCESS OF FUEL INJECTION OF DIESEL- VEGETABLE OIL MIXTURE OF DIESEL 6CHE YANMAR ENGINE BY KIVA-3V SOFTWARE	Mai Duc Nghia	Air Force Officer's college, VietNam

LATIN AMERICAN INTERNATIONAL CONFERENCE ON NATURAL AND APPLIED SCIENCES
November 05-06, 2021 Villahermosa, Mexico

06.11.2021

Session-5, Hall-4

Mexico Time: 08⁰⁰-10³⁰

Ankara Time: 16⁰⁰-18³⁰

HEAD OF SESSION: Dr. Günay BEYHAN

TOPIC TITLE	AUTHORS	AFFILIATION
EXPERT SYSTEM RULE-BASED OPTIMIZATION IN ASSIGNING COURSES OF STUDY	Ismail Olaniyi MURAINA Segbenu Joseph ZOSU Moses Adeolu AGOI	Adeniran Ogunsanya College of Education, Lagos Nigeria Lagos State University, Lagos Nigeria Adeniran Ogunsanya College of Education, Lagos Nigeria
PLANNING OF URBAN TRANSFORMATION AFTER THE EARTHQUAKE IN A LOCAL AREA WITH ZONING WITH HEDONIC AND PRIME METHODS	SELİM TAŞKAYA	Artvin, Turkey
DETERMINATION OF SOME PERFORMANCE CHARACTERISTICS OF CONSTRUCTION TIMERS FROM LAMINATED WOOD MODIFIED WITH CARBON FIBER	Turan Maharrambay AHMADLI, Erkan AVCI Kamala YUSİFOVA	Muğla Sıtkı Kocman University, Azerbaijan Architectura and Construction University, Baku
BURIED WITH RESISTIVITY METHOD IN THE ANCIENT CITY OF ALABANDA DETECTION OF ARCHEOLOGICAL RESIDENTS	Suat DEMİR Günay BEYHAN	Sakarya University
APPLICATION OF REMOTE SENSING METHODS TO GROUND RESEARCH	Ahmet FAZLI ZENGİN Günay BEYHAN Suat DEMİR	Sakarya University
ABOUT THE NATURE OF THE ENVIRONMENTAL REQUIREMENTS	Michail Michailov	PhD – SWU “Neofit Rilski” - Bulgaria
FLIGHT SAFETY RISK ANALYSIS AT AIRPORTS: THE CASE OF SAMSUN ÇARŞAMBA AIRPORT	Ömer Faruk UZUN Faik Ahmet SESLİ	Sinop University, Turkey Ondokuz Mayıs University, Turkey

LATIN AMERICAN INTERNATIONAL CONFERENCE ON NATURAL AND APPLIED SCIENCES
November 05-06, 2021 Villahermosa, Mexico

06.11.2021

Session-5, Hall-5

Mexico Time: 08⁰⁰-10³⁰

Ankara Time: 16⁰⁰-18³⁰

HEAD OF SESSION: Dr. Hayati OLĞAR

TOPIC TITLE	AUTHORS	AFFILIATION
DERIVATIONS PERIOD 2 OF PRIME RINGS	Mehsin Jabel Atteya	Al-Mustansiriyah University, Iraq
SPECTRAL PROPERTIES FOR BOUNDARY VALUE PROBLEMS OF STURM-LIOUVILLE TYPE	Oktay Sh. MUKHTAROV Kadriye AYDEMİR Hayati Olğar	Gaziosmanpaşa University, Tokat, Turkey. Amasya University, Turkey Gaziosmanpaşa University, Turkey.
INVESTIGATION OF SOME PROPERTIES OF PERIODIC STURM-LIOUVILLE PROBLEM WITH TRANSMISSION CONDITIONS	Oktay Sh. MUKHTAROV Kadriye AYDEMİR Hayati Olğar	Gaziosmanpaşa University, Tokat, Turkey. Amasya University, Turkey Gaziosmanpaşa University, Turkey.
PARTICLE-LADEN FLOW into A POROUS CHANNEL: ENTRY and BOUNDARY CONDITIONS	M.H. Hamdan	University of New Brunswick, New Brunswick, Canada
SOME QUALITATIVE PROPERTIES OF WEAK EIGENFUNCTIONS OF MULTI-INTERVAL STURM-LIOUVILLE PROBLEMS	Oktay Sh. MUKHTAROV Hayati OLĞAR Kadriye AYDEMİR	Gaziosmanpaşa University, Tokat, Turkey. Amasya University, Turkey Gaziosmanpaşa University, Turkey
OPERATOR-POLYNOMIAL TREATMENT OF A DISCONTINUOUS STURM-LIOUVILLE PROBLEM	Hayati OLĞAR	Gaziosmanpasa University, Turkey.
DISCRETENESS OF THE SPECTRUM AND RIESZ BASISITY OF THE WEAK EIGENFUNCTIONS FOR MANY-INTERVAL STURM-LIOUVILLE PROBLEMS	Oktay Sh. MUKHTAROV Hayati OLĞAR Kadriye AYDEMİR	Gaziosmanpasa University, Tokat, Turkey. Azerbaijan National Academy of Sciences, Baku, Azerbaijan Amasya University, Turkey.
3-D MHD FLOW OF NON-NEWTONIAN HYBRID NANOLIQUID ABOVE A STRETCHING SURFACE	Dr. G.P. Ashwinkumar P. Nanda	Vijayanagara Sri Krishnadevaraya University, Bellary, India.
SIGNIFICANCE OF THERMAL RADIATION ON MHD FLOW OF HYBRID NANOFLUID OVER A STRETCHING SURFACE	Dr. G.P. Ashwinkumar B. Ranjana	Vijayanagara Sri Krishnadevaraya University, Bellary, India.

LATIN AMERICAN INTERNATIONAL CONFERENCE ON NATURAL AND APPLIED SCIENCES
November 05-06, 2021 Villahermosa, Mexico

06.11.2021

Session-6, Hall-3

Mexico Time: 11⁰⁰-13³⁰

Ankara Time: 19⁰⁰-21³⁰

HEAD OF SESSION: Houda EL KHEYYAT

TOPIC TITLE	AUTHORS	AFFILIATION
A REACTION DIFFUSION MODEL TO DESCRIBE THE TOXIN EFFECT ON THE FISH-PLANKTON POPULATION	Ouedraogo Hamidou	Université JOSEPH KI ZERBO/ IBAM
USE OF SORGHUM GRAIN IN POULTRY NUTRITION	Aylin AGMA OKUR Kadir ERTEN Hasan Ersin SAMLI	Tekirdag Namik Kemal University , Tekirdag/TURKEY
BIOMETRIC CHARACTERIZATION OF LOCAL GOATS FROM THE ARGAN GROVE OF AGADIR IN MOROCCO	Houda EL KHEYYAT Saïd EL MADIDI	University Ibn Zohr, Agadir, Morocco
ETHNOBOTANICAL STUDY AIMED AT INVESTIGATING THE USE OF MEDICINAL PLANTS OF APIACÉE FAMILY IN THE NORTH RÉGION (MOROCCO)	NOUIOURA Ghizlane TOURABI Maryem DERWICH El houssine	Université sidi Mohammed ben Abdellah, Fès, Maroc.
FISHERY, MORPHOMETRY AND MERISTIC COUNTS OF DECAPTERUS MACROSOMA (BLEEKER, 1851) OFF COCHIN COAST	A. U. Arun Revathy R	St. Peters College, Kolenchery, Kerala, India Nirmala College, Kerala, India
OPPORTUNITIES OF USING GREEN FEED FOR ANIMAL FEEDING IN HYDROPONIC AGRICULTURE SYSTEM	Ezgi KARPUZ Kadir ERTEN Fisun KOC	Tekirdag Namik Kemal University, TURKEY
THE HONEY OF RHODENDRON	Münire TURHAN	Bingöl University
EFFECT OF VARIETY AND SUCROSE CONCENTRATION ON BANANA (MUSA SPP) VARIETIES ON IN VITRO PROPAGATION	Nazar AL GHASHEEM, M.S. SHARADA, M.S. SUDARSHANA	Medicinal Plant Tissue Culture Laboratory, University of Thi Qar , Iraq

06.11.2021

Session-6, Hall-4

Mexico Time: 11⁰⁰-13³⁰

Ankara Time: 19⁰⁰-21³⁰

HEAD OF SESSION: Skender Demaku

TOPIC TITLE	AUTHORS	AFFILIATION
ASSESSMENT WATER QUALITY OF THE LUMBARDHI RIVER, IN THE PRIZREN AREA, BY THE PHYSICO-CHEMICAL ANALYSIS AND HEAVY METALS	Skender Demaku Gani KASTRATI	University of Pristina, Prishtina, Kosovo UBT College, - Republic of Kosovo
EFFECT OF THE MAGNETIC FIELD ON MIXED CONVECTION IN A CAVITY HEATED FROM THE TOP FILLED WITH A NANOFLUID	EL HATTAB Mohamed LAFDAILI Zakaria	Ibn Zohr University, ENSA, Agadir, Morocco
PRODUCTION OF INDUSTRIAL BIOMOLECULES BY ACTINOMYCETES ISOLATED FROM SOIL IN SAUDI ARABIA	Maha Fahad Algourabi, Nashwa Ibrahim Hagagy, Lobna Abdelkefi-Mesrati	University of Jeddah, Jeddah, Saudi Arabia.
THE SURVEY OF WATER QUALITY BASED ON THE PHYTOPLANKTON AND SAPROBIC INDEX IN ZHAWEH DAM TRIBUTARIES (KORDESTAN PROVINCE, IRAN)	Asieh Makhloogh Nasrollahzadeh Saravi H. Naderi, M. Eslami, F.	Caspian Sea Ecology Research Center (CSERC) Ecology Dept. Iran Iranian Fisheries Science Research Institute (IFSR), Tehran, Iran
REMOVAL OF SULFATE FROM LEATHER INDUSTRY WASTEWATER WITH DIFFERENT ACTIVATED CARBON ADSORPTIONS	Ali Rıza DİNÇER İbrahim Feda ARAL Elçin GENÇ	Tekirdağ Namık Kemal University, Tekirdağ, Turkey Çevre Gıda ve Endüstriyel Analiz Laboratuvarı, Merkez Mah. Tatlıpınar Sok. Mert Plaza

LATIN AMERICAN INTERNATIONAL CONFERENCE ON NATURAL AND APPLIED SCIENCES
November 05-06, 2021 Villahermosa, Mexico

06.11.2021

Session-6, Hall-5

Mexico Time: 11⁰⁰-13³⁰

Ankara Time: 19⁰⁰-21³⁰

HEAD OF SESSION: Mehmet Burak ATES

TOPIC TITLE	AUTHORS	AFFILIATION
HISTOPATHOLOGICAL CHARACTERIZATION OF HEPATOCELLULAR CARCINOMA IN A DOG	Mehmet Burak ATES Mehmet TUZCU Mustafa ORTATATLI	Selcuk University, Konya, Turkey.
INFILTRATIVE RENAL LYMPHOMA IN A 1-YEAR-OLD MALE STRAY CAT	Mustafa ORTATATLI Ertan ORUC Ozgür OZDEMIR	Selcuk University, Konya, Turkey.
SUBCUTANEOUS MULTIPLE MASTOCYTOMA IN AN 8-YEAR-OLD MALE ENGLISH SETTER	Ozgur OZDEMIR Mehmet Burak ATES Mehmet TUZCU	Selcuk University, Konya, Turkey.
HEMANGIOPERICYTOMA IN A 17-YEAR-OLD FEMALE GOLDEN DOG	Ertan ORUC Ozgur OZDEMIR Mehmet Burak ATES	Selcuk University, Konya, Turkey.
THE CASE OF MULTIPLE EPIDERMAL INCLUSION CYSTS IN A 2-YEARS-OLD HOUND DOG	Zeynep CELIK Osman DAGAR Aysegul BULUT Rabia SALIK Gokhan AKCAKAVAK Aysenur TURAL Beatriz PADRON PEREZ Fatih HATİPOGLU	Selcuk University, Konya, Turkey. Kyrgyz-Turkish Manas University, Bishkek, Kyrgyzstan.
A CASE OF PERICARDITIS FIBRINOSA CAUSED BY HISTOPHILUS SOMNI IN A 2-MONTH-OLD SIMMENTAL BREED CALF	Mehmet TUZCU Nevin TUZCU Zeynep CELIK Gokhan AKCAKAVAK	Selcuk University, Konya, Turkey. Bozok University, Yozgat, Turkey,
EXTRAMEDULLARY PLASMACYTOMA IN SPLEEN OF 12-YEAR-OLD FEMALE GOLDEN RETRIEVER DOG	Mustafa ORTATATLI Ertan ORUC Zeynep CELIK Fatih HATİPOGLU	Selcuk University, Turkey. Kyrgyz-Turkish Manas University, Bishkek, Kyrgyzstan.
A SURVEY STUDY OF INSECT PEST ORDERS AND THEIR MANAGEMENT STRATEGIES IN DIFFERENT AREAS OF VIDARBHA REGION	Badiye V.H., Gajbe P.U Saha R.S.	SMM College of Science, Nagpur (Maharashtra, India)
EDIBLE ORNAMENTAL FLOWERS SEED COLLECTION - PRESENT STATUS AND FUTURE PERSPECTIVES AT CENTER FOR BIODIVERSITY AND CONSERVATION, UASVM CLUJ-NAPOCA, ROMANIA	Corina CĂȚANĂ Alina MITROI Paula BOBOC (OROS)	University of Agricultural Sciences and Veterinary Medicine, Cluj-Napoca, Romania.

KONGRE KÜNYESİ	I
BİLİM KURULU	II
KONGRE PROGRAMI	III
İÇİNDEKİLER	IV

İÇİNDEKİLER		
Author	Title	No
Onur Akyıldırım Özlem Gürsoy-Kol Haydar Yüksek	SYNTHESIS AND IN VITRO ANTIOXIDANT PROPERTIES OF SOME NEW 1- BENZYL-3-ALKYL(ARYL)-4-(3-METHOXY-4PHENYLMETHOXYBENZYLIDENAMINO)-4,5-DIHYDRO-1H-1,2,4-TRIAZOL-5-ONES	1
Emine BAŞ	BIG DATA MODELING	9
Erdinç YÜKSEL Can ALTINGÖZ Furkan ŞEN Ahmet FEYZİOĞLU	DEVELOPMENT OF CPR B2ca s1a d1 CLASS SIGNAL CABLES	14
Gümrah Uysal	ON MODIFIED BIVARIATE PICARD INTEGRAL OPERATORS WHICH FIX SOME EXPONENTIAL FUNCTIONS	16
Ahmed Ouezgan Said Adima Aziz Maziri El Hassan Mallil Jamal Echaabi	CURING EFFECT IN RTM PROCESS	24
Mustafa Serdar Osmanca Murat YÜCEL	AI-ASSISTED COMPARISON OF LIVE NETWORK MEASUREMENTS AND PERFORMANCE METRICS IN DWDM SYSTEMS	25
Karunesh Tiwari Anam Zaidi Shalini	EFFECT OF TIN SUBSTITUTION ON STRUCTURAL, ELECTRICAL AND HUMIDITY-SENSING CHARACTERISTICS OF TUNGSTEN OXIDE NANOPARTICLES	31
Ouail MJAHE Salah EL HADAJ El Mahdi ELGUARMAH Soukaina MJAHE	BIO-INSPIRED HYBRIDIZATION OF ARTIFICIAL NEURAL NETWORKS: AN APPLICATION FOR CLASSIFICATION TASKS	32
Pengfei Yao Surendra M. Gupta	FISH SCHOOL SEARCH ALGORITHM FOR SOLVING MULTI-OBJECTIVE USHAPED DISASSEMBLY LINE BALANCING PROBLEM	44
Amenah Emad mohammed redha	MATERIALS CLASSIFICATION OF PROFITABLE AND NEW SOFT CONTACT LENSES USING MATLAB	53
Onur Akyıldırım Özlem Gürsoy-Kol Haydar Yüksek	SYNTHESIS AND IN VITRO ANTIOXIDANT PROPERTIES OF SOME NOVEL 1, 3, 4-TRISUBSTITUE-4,5-DIHYDRO-1H-1, 2, 4-TRIAZOL-5-ONES	61
Hilal Medetalibeyoğlu Haydar Yüksek	INVESTIGATION OF THEORETICAL AND EXPERIMENTAL SPECTROSCOPIC PROPERTIES OF 3-p-METHYLBENZYL-4-□3-ETHOXY-4- (4-METHOXYBENZOXY)-BENZYLIDENAMINO]-4,5-DIHYDRO-1H-1,2,4-TRIAZOL-5-ONE	68
Hilal Medetalibeyoğlu	STUDY ON THEORETICAL/EXPERIMENTAL	77

Haydar Yüksek	SPECTROSCOPIC AND ELECTRONIC PROPERTIES OF 1-ACETYL-3-METHYL-4-(4-METHYLBENZOXY)-BENZYLIDENAMINO]-4,5-DIHYDRO-1H-1,2,4- TRIAZOL-5-ONE	
Duygu İNCİ Rahmiye AYDIN	INTERACTIONS of [Cu(5 nphen)(tyr)(H ₂ O)]NO ₃ ·2H ₂ O COMPLEX with BOVINE SERUM ALBUMINE (BSA)	88
Bahar BANKOĞLU YOLA Haydar YÜKSEK	SYNTHESIS AND CHARACTERIZATION OF NEW MANNICH BASES CONTAINING 1, 2, 4- TRIAZOLE RING	95
Fevzi Aytemiz Haydar Yüksek	SYNTHESIS OF NOVEL 3- {[1-(MORPHOLIN-4-YL-METHYL)-3-ALKYL/ARYL- 4,5-DIHYDRO-1H-1,2,4- TRIAZOL-5-ONE-4- YL]-AZOMETHINE}-PHENYL 2,5- DICHLOROBENZENESULFONATES	100
Gül KOTAN Haydar YÜKSEK	STRUCTURAL AND SPECTROSCOPIK ANALYSIS WITH DFT OF 3-METHYL-4- [2-(2- THIENYLCARBONYLOXY) METHOXYBENZYLIDENAMINO)-4,5- DIHYDRO-1H- 1,2,4-TRIAZOL-5-ONE	105
Shikha Saxena Priyanka Singh	RECENT DIAGNOSTIC AIDS IN ORAL CANCER DETECTION	117
Ying-Ying Zhang Ze-Yu Yu Jian-Ping Liu	AURICULAR ACUPRESSURE FOR SMOKING CESSATION: A SYSTEMATIC REVIEW OF RANDOMIZED CONTROLLED TRIALS	118
Madina Nurzhanova Gulnara Kapanova	FEATURES OF THE LIPID SPECTRUM AND THE PROBLEM OF ACHIEVING THE TARGET LEVEL OF LOW-DENSITY LIPOPROTEINS DURING A CORONARY EVENT	120
Ivashchuk Oleksandr Hovornyan Serhiy	ORAL CANCER SCREENING. CURRENT APPROACHES AND FUTURE PROSPECTS.	126
Aneta Mijoska Sasho Jovanovski Daniela Srbinoska Vesna Trpevska Emilija Bajraktarova Valjakova	EVALUATION OF ORAL SOFT TISSUES AT GERIATRIC PATIENTS WITH DENTAL PROSTHESIS	127
Aneta Mijoska Sasho Jovanovski Daniela Srbinoska Vesna Trpeska Blagoja Dashtevski Marjan Petkov	VELSCOPE INSTRUMENT FOR DETECTION OF ORAL SOFT TISSUE CONDITION IN PROSTHODONTIC PATIENTS	129
Önder ALBAYRAK Gül KOTAN Haydar YÜKSEK	SOME QUANTUM CHEMICAL CALCULATIONS OF 3-n-PROPYL-4-(3-ACETOXY-4-METHOXYBENZYLIDENAMINO)-4,5-DIHYDRO-1H- 1, 2, 4- TRIAZOL-5-ONE	131
Songül BOY Gül KOTAN Haydar YÜKSEK	ELECTRONIC, THERMODYNAMIC, GEOMETRIC ANALYSIS OF 1-(2,6- DIMETILMORFOLIN-4-IL- METIL)-3-ETHYL-4-(4 HYDROXYBENZYLIDENAMINO)-4,5-DIHYDRO-1H- 1, 2, 4-TRIAZOL-5-ONE	143
Laipubam Gayatri Sharma Lalit Mohan Pandey	INHIBITION OF THERMAL AND SHEAR INDUCED AGGREGATION OF ALBUMIN (BOVINE SERUM ALBUMIN) BY CENTELLA ASIATICA EXTRACT	153
Affaf TABTI	SYNTHESIS OF ZEOLITIC MATERIALS	154

Franck LAUNAY Abd Rezzak BABA AHMED Mohamed Serier	INCORPORATED IN THE PRESENCE OF DIFFERENT STRUCTURING ORGANIC MOLECULES	
Sevda MANAP Haydar YÜKSEK	SYNTHESIS AND CHARACTERIZATION OF NEW 1-(4-AMINOCARBONYLPYPERIDIN -4-YL-METHYL)-3-ALKYL(ARYL)-4-(3-METHOXY-4-ISOBUTYRYLOXY-BENZYLIDENEAMINO)-4,5-DIHYDRO-1H-1,2,4-TRIAZOLE-5-ONES	162
Hayat Jaadan Mustafa Akodad Saadia Belmalha	ESTUDIO DE ESPECTROSCOPIA FTIR DE EXTRACTOS DE HOJAS DE PISTACIA LENTISCUS	167
Hebe FERNÁNDEZ Angelo MAZZOCCHI Dardo CÔCCARO Carmen Salerno	EFFECTO DEL ADICIONADO DE ADITIVOS Y HARINA DE CHIA EN LA INDUSTRIA AVICOLA ARGENTINA	168
Luis Mayta Edwin Bustamante Eduardo Molinari Elio Ponce	PROPAGACIÓN ASEJUAL POR ACODOS AÉREOS DE QUEÑUA (POLYLEPIS RUGULOSA BITTER) UTILIZANDO CUATRO ENRAIZADORES CON DOS SUSTRATOS NATURALES EN CONDICIONES DE VIVERO	169
José Leonardo de Oliveira Mattos Marcos Aurélio da Silva Adrian Indermaur Axel Makay Katz Walter Salzburger Felipe Polivanov Ottoni	SPECIES DIVERSITY WITHIN THE UPPER/MIDDLE PARAÍBA DO SUL RIVER BASIN AND ADJACENT DRAINAGES CLADE, OF THE AUSTRALOHEROS AUTRANI GROUP (TELEOSTEI, CICHLIDAE)	177
Luis M. Montes-de-Oca R. Medina-Esquivel M. A. Zambrano-Arjona P. Martínez-Torres	THERMAL CHARACTERIZATION OF SURFACTANT SOLUTIONS AND PHASE TRANSITION IDENTIFICATION USING THE LEWIS-NIELSEN MODEL	178
David Bonfil Ceferino Lucien Veleva Ángel Bacellis	ESTUDIO ELECTROQUÍMICO DE UN ACERO INOXIDABLE Y ACERO AL CARBONO EN SOLUCIÓN DE EXTRACTO DE CEMENTO CON IONES CLORURO.	179
José Luis González-Murguá Lucien Veleva	EFFECT OF CA ON THE ELECTROCHEMICAL ACTIVITY OF THE MG-CA0.3 ALLOY EXPOSED TO HANK'S PHYSIOLOGICAL SOLUTION AND PROPERTIES OF AG NANO-PARTICLE DEPOSITS	180
Miguel Manzano Canul José Luis González-Murguía Lucien Veleva	ACTIVIDAD ELECTROQUÍMICA DE MG EXTRUIDO EN SOLUCIÓN FISIOLÓGICA DE HANK	196
Elena Mostiuk	LIVER FAILURE WITH MECHANICAL JAUNDICE	197
Binyam Zigta	EFFECT OF THERMAL RADIATION AND CHEMICAL REACTION ON MHD FLOW OF BLOOD IN STRETCHING PERMEABLE VESSEL	199
Boboc Daniela	BURNOUT SYNDROME AT MEDICAL STAFF FROM ROMANIA	200
Christopher Ryalino Tjokorda Gde Agung Senapathi Jhoni Pardomuan Pasaribu	C-MAC® VS. MCGRATH® VIDEO LARYNGOSCOPE IN PATIENTS UNDERGOING GENERAL ANESTHESIA WITH OROTRACHEAL INTUBATION: A PROSPECTIVE, RANDOMIZED CLINICAL TRIAL	201
Fatih TAŞ	STRUCTURE OF TANISIT CELLS AND THEIR	202

Ender ERDOĞAN	FUNCTIONAL ROLE IN THE NERVOUS SYSTEM	
Valentyna Kurovska Oksana Kaleinikova Iryna Byelinska Natalia Kutsevol Taras Blashkiv	EFFECT OF MAXIMAL DOSES OF DEXTRAN- POLYACRYLAMIDE POLYMERS AND THEIR AS CARRIERS OF SILVER AND GOL NANOPARTICLES ON LIVER	204
Nida Khan Sadia Fatima Rubina Nazli Tasleem Akhtar Jamila Haider	COMPARISON OF IRON, ZINC AND FERRITIN AMONG SMALL FOR GESTATIONAL AGE AND APPROPRIATE FOR GESTATIONAL AGE MOTHERS	206
Proletina Bozdukova	ENDOSCOPIC APPROACHES IN OTORHINOLARYNGOLOGY	208
Daniel Petkov Tsvetelina Grigorova	ENT MANIFESTATIONS IN COVID-19	209
Aniqa Aniqa Sarvnarinder Kaur	PROTECTIVE EFFECT OF MURRAYA KOENIGII AGAINST TESTICULAR DAMAGES INCURRED IN SKIN TUMOR BEARING MICE	210
Mehmet Doğan Fatih Altan	COVID-19 VACCINES AND THE RATES OF COVID- 19 VACCINATION IN TURKEY	211
Mehmet Doğan Fatih Altan	E-HEALTH APPLICATIONS IN TURKEY	215
Petar Nikolov Grozi Delchev	GRAIN YIELDS OF DURUM WHEAT (TRITICUM DURUM DESF.) AND YIELD STABILITY AFFECTED OF CERTAIN PREPARATIONS AND VARIOUS TERMS OF SOWING	222
K.R.Padma K.R.Don	IN VITRO WOUND HEALING POTENCY OF METHANOLIC LEAF EXTRACT OF ARISTOLOCHIA SACCATA IS POSSIBLY MEDIATED BY ITS STIMULATORY EFFECT ON COLLAGEN-1 EXPRESSION	230
K.R.Padma K.R.Don	EFFECTIVE ROLE OF CHITOSAN-SILVER NANOCOMPOSITE ON FOOD PRESERVATION	231
Uzma Ayaz	GENETIC VARIABILITY, ASSOCIATION AND DIVERSITY STUDY AMONG THE SUNFLOWER GENOTYPES AT SEEDLING STAGE BASED ON DIFFERENT MORPHOPHYSIOLOGICAL PARAMETERS UNDER POLYETHYLENE GLYCOL INDUCEDSTRESS	232
Tuğçe UZUN Aylin AĞMA OKUR	WOODEN BREAST SYNDROME AND FACTORS AFFECTING ITS DEVELOPMENT	233
Aylin AĞMA OKUR Kadir ERTEN Hasan Ersin SAMLI	USE OF SORGHUM GRAIN IN POULTRY NUTRITION	242
DEEPA SONAL SHAILESH KUMAR SHRIVASTAVA BINAY KUMAR MISHRA	FREQUENCY-BASED AGRI-IOT TECHNIQUES IN AGRICULTURE	251
Ayça AKÇA UÇKUN Suna BAŞER Ünal KAYA Alptug ÇANTAL Merve TÜRKYILMAZ	EFFECT OF DIFFERENT HUMIC ACID DOSES ON GEMLIK OLIVE SAPLINGS IN MANISA KÖPRÜBAŞI DISTRICT	252

Ayça AKÇA UÇKUN Murat TUĞAÇ Suna BAŞER Sedef ÖZDEN Aişe DELİBORAN Tülin PEKCAN	INVESTIGATION OF THE EFFECTS OF SEFERİHISAR REGION CLIMATIC AND TOPOGRAPHIC CONDITIONS ON OLIVE PHENOLOGY AND POMOLOGY	259
Alexandra-Mihaela Nagy (Frătilă) Camelia Sava Sand Paula Boboc (Oros) Corina Cătană	PURPLE POTATO VARIETIES AS RICH ANTHOCYANINS SOURCE FOR FOOD, PHARMACEUTICALS AND COSMETICS	274
Paula Boboc (Oros) Rita-Daniela Farțadi Corina Cătană	RESPONSE OF SPHAGNUM MOSS TO DIFFERENT SOWING METHODS FOR THE PURPOSE OF THEIR USE IN CONTEMPORARY STREET ART	279
Rita Daniela Farțadi Paula Boboc (Oros) Corina Cătană	PROCESSING SPECIMENS FOR VIRTUAL HERBARIUM	287
Melike Ciniviz Gokce Keser Irmak Aral Baskaya Lutfiye Yilmaz Ersan Tulay Ozcan Omer Utku Copur	EVALUATION OF SOMATIC CELL COUNT OF RAW MILK DEPENDING ON SEASONAL VARIATION	291
Gokce Keser Melike Ciniviz Irmak Aral Baskaya Tulay Ozcan Lutfiye Yilmaz Ersan Omer Utku Copur Ozlem Kaner	EFFECT OF SALT CONCENTRATION ON THE STRUCTURE AND PREFERENCE OF MIHALIC CHEESE	298
Fevzi ALTUNER Mehmet ULKER	THE EFFECT OF SOWING FREQUENCY ON YIELD AND YIELD COMPONENTS OF OAT CULTIVARS IN VAN ECOLOGICAL CONDITIONS	304
Fevzi ALTUNER Mehmet ULKER	THE EFFECT OF NITROGEN FERTILIZER DOSES ON YIELD AND YIELD PROPERTIES ON OAT CULTIVARS	311
Makhlough A. Nasrollahzadeh Saravi H. Naderi, M. Eslami, F.	THE SURVEY OF WATER QUALITY BASED ON THE PHYTOPLANKTON AND SAPROBIC INDEX IN THE ZHAVEH DAM TRIBUTARIES (KURDISTAN PROVINCE, IRAN)	320
Fethi Boudahri Abderazzak Baba Ahmed Rabab Boukli Hacene	MANAGEMENT OF THE FOODS SUPPLY CHAIN WITH INTO ACCOUNT HUMAN HEALTH	321
Zeynep DEMETGÜL Nuran TAPKI	SOCIO-DEMOGRAPHIC AND PRODUCTION STRUCTURES OF POMEGRANATE PRODUCING ENTERPRISES IN HATAY	328
Baba Ahmed Abderrazzak Boudahri Fethi Tabti Affaf	EVALUATION OF CHROMIUM CONTAMINATION ON AGRICULTURAL SOIL AND ON DURUM WHEAT	330
Ahmet ÖZTÜRK M. Sevba ÇOLAK	ARTIFICIAL RAIN ON THE VERGE OF DROUGHT	331
M. Sevba ÇOLAK	YIELD EVALUATIONS OF SOME FIELD CROPS	340

Ahmet ÖZTÜRK	GROWN IN CENTRAL ANATOLIAN IN SALTY CONDITIONS	
Merve KADAL Ash BAHADIR	DEVELOPMENT OF 100% NATURAL POMAD CREAM CONTAINING DIFFERENT HERBAL EXTRACTS WITH REPAIRING AND HEALING PROPERTIES	350
Dzhamirze R.R. Esaulova L.V. Slabchenko A. S.	METHODS OF GENETIC ENGINEERING IN PLANTS BREEDING	352
Sinem KAYA Yüksel ARDALI	TESTING AND EVALUATION OF ELECTRODIALYSIS METHOD ON DESALINATION	360
Nasrollahzadeh Saravi H. Vahedi, F. Makhloogh A. Baluei, M.	EFFECT OF SMALL-SCALE FISH CAGE CULTURE ON SEDIMENT QUALITY OF THE SOUTHERN CASPIAN SEA: CASE STUDY IN IRANIAN COAST-NOWSHAHR	367
Ezgi GURGENC Aydın DİKİCİ Fehmi ASLAN	INVESTIGATION OF STRUCTURAL PROPERTIES OF AL/P-Si/CDO:NIO/AL PHOTODIODE FABRICATED BY SOL-GEL SPIN COATING METHOD	368
Zakaria LAFDAILI Sakina El-Hamdani Mohamed El Hattab Lahoucine Belarche	NUMERICAL STUDY OF THE EFFECT OF EXTERNAL MAGNETIC FIELDS ON THE TURBULENT NATURAL CONVECTION OF NANOFLUIDS IN A TWODIMENSIONAL CAVITY	372
Belfarhi Leila Leila Belfarhi Tahraoui Abdelkrime Bairi Abdelmedjid Ibtissem Chouba Naziha Amri Nadia Boukris	STUDY OF METHODS OF EXTRACTING A WILD PLANT FROM THE ALGERIAN SAHARA	373
Rekha Suman	ENVIRONMENT AND SUSTAINABLE DEVELOPMENT GOALS IN INDIA	375
Ramesh S Gajanan M Naik Gajanan Anne	INVESTIGATION OF TRIBOLOGICAL CHARACTERISTICS OF COPPERTITANIUM ALLOYS PROCESSED BY MULTI-AXIAL CRYO-FORGING	376
Ahmet TOP Yener CESUR Muammer GÖKBULUT	DESIGN AND CONTROL OF INDUSTRIAL TYPE LIQUID LEVEL CONTROL SYSTEM	377
Cansu AKSOY Sibel AKBULUT	EXPERIMENTAL AND NUMERICAL PERFORMANCE ANALYSIS OF SMOKE EXTRACTION MOTORS USED IN SPECIAL FAN APPLICATIONS AT HIGH TEMPERATURE	387
Mai Duc Nghia	A SIMULATION STUDY ON THE PROCESS OF FUEL INJECTION OF DIESEL - VEGETABLE OIL MIXTURE OF THE YANMAR 6CHE DIESEL ENGINE BY KIVA-3V SOFTWARE	396
Ismail Olaniyi MURAINA Segbenu Joseph ZOSU Moses Adeolu AGOI	EXPERT SYSTEM RULE-BASED OPTIMIZATION IN ASSIGNING COURSES OF STUDY	403
Selim Taşkaya	PLANNING OF URBAN TRANSFORMATION AFTER THE EARTHQUAKE IN A LOCAL AREA WITH ZONING WITH HEDONIC AND PRIME METHODS	408

Turan Maharrambay AHMADLI Erkan AVCI Kamala YUSİFOVA	DETERMINATION OF SOME PERFORMANCE CHARACTERISTICS OF CONSTRUCTION TIMERS FROM LAMINATED WOOD MODIFIED WITH CARBON FIBER	410
SUAT DEMİR GÜNAY BEYHAN	DETECTION OF BURIED ARCHAEOLOGICAL BY RESISTIVITY METHOD IN THE ANCIENT CITY OF ALABANDA	411
Fazlı Ahmet Zengin Günay Beyhan Suat Demir	APPLICATION OF REMOTE SENSING METHODS TO GROUND RESEARCH	422
M. As. Michailov	ABOUT THE NATURE OF THE ENVIRONMENTAL REQUIREMENTS	429
Ömer Faruk UZUN Faik Ahmet SESLİ	FLIGHT SAFETY RISK ANALYSIS AT AIRPORTS: THE CASE OF SAMSUN ÇARŞAMBA AIRPORT	430
Kadriye AYDEMİR Oktay Sh. MUKHTAROV Hayati Olğar	INVESTIGATION OF SOME PROPERTIES OF PERIODIC STURM-LIOUVILLE PROBLEM WITH TRANSMISSION CONDITIONS	440
Oktay Sh. MUKHTAROV Kadriye AYDEMİR Hayati Olğar	SPECTRAL PROPERTIES FOR BOUNDARY VALUE PROBLEMS OF STURMLIOUVILLE TYPE	445
Oktay Sh. MUKHTAROV Hayati OLĞAR Kadriye AYDEMİR	SOME QUALITATIVE PROPERTIES OF WEAK EIGENFUNCTIONS OF MULTIINTERVAL STURM-LIOUVILLE PROBLEMS	449
Hayati OLĞAR	OPERATOR-POLYNOMIAL TREATMENT OF A DISCONTINUOUS STURMLIOUVILLE PROBLEM	455
Hayati OLĞAR Oktay Sh. MUKHTAROV Kadriye AYDEMİR	DISCRETENESS OF THE SPECTRUM AND RIESZ BASISITY OF THE WEAK EIGENFUNCTIONS FOR MANY-INTERVAL STURM-LIOUVILLE PROBLEMS	461
G.P. Ashwinkumar P. Nanda	3-D MHD FLOW OF NON-NEWTONIAN HYBRID NANOLIQUID ABOVE A STRETCHING SURFACE	472
G.P. Ashwinkumar B. Ranjana	SIGNIFICANCE OF THERMAL RADIATION ON MHD FLOW OF HYBRID NANOFLUID OVER A STRETCHING SURFACE	473
Luis Chávez Lucien Veleza	COMPORTAMIENTO DE LA CORROSIÓN DEL NANOCOMPUESTO AM60- ALN Y LA ALEACIÓN AM60 EXPUESTAS A UN AMBIENTE SIMULADO DE LLUVIA ÁCIDA	474
Gerardo Sánchez Luis Chávez Lucien Veleza	ACTIVIDAD ELECTROQUÍMICA DE LA MATRIZ METÁLICA EXTRUIDA AM60 EN UNA SOLUCIÓN QUE SIMULA EL AMBIENTE MARINO	475
FELICIA ANDREI ANCA DRAGOMIRESCU	POSSIBLE EFFECTS AFTER A COVID VACCINATION AT THE MOLECULAR AND CHEMICAL LEVEL FOR PATIENTS WITH CELIAC DISEASE	476
Ouedraogo Hamidou	A REACTION DIFFUSION MODEL TO DESCRIBE THE TOXIN EFFECT ON THE FISH-PLANKTON POPULATION	477
Houda EL KHEYYAT Saïd EL MADIDI	BIOMETRIC CHARACTERIZATION OF LOCAL GOATS FROM THE ARGAN GROVE OF AGADIR IN MOROCCO	478
NOUIOURA Ghizlane	ETHNOBOTANICAL STUDY AIMED AT	4789

TOURABI Maryem DERWICH El houssine	INVESTIGATING THE USE OF MEDICINAL PLANTS OF APIACEE FAMILY IN THE NORTH REGION (MOROCCO)	
U. Arun Revathy R	FISHERY, MORPHOMETRY AND MERISTIC COUNTS OF DECAPTERUS MACROSOMA (BLEEKER, 1851) OFF COCHIN COAST	480
Ezgi KARPUZ Kadir ERTEN Fisun KOC	USAGE POSSIBILITIES OF GREEN FODDER GERMINATED IN HYDROPONIC SYSTEM IN ANIMAL NUTRITION	481
Nazar AL GHASHEEM M.S. SHARADA M.S. SUDARSHANA	EFFECT OF VARIETY AND SUCROSE CONCENTRATION ON BANANA (MUSA SPP) VARIETIES ON IN VITRO PROPAGATION	491
Skender DEMAKU Gani KASTRATI	ASSESSMENT WATER QUALITY OF THE LUMBARDHI RIVER, IN THE PRIZREN AREA, BY THE PHYSICO-CHEMICAL ANALYSIS AND HEAVY METALS	498
EL HATTAB Mohamed LAFDAILI Zakaria	EFFECT OF THE MAGNETIC FIELD ON MIXED CONVECTION IN A CAVITY HEATED FROM THE TOP FILLED WITH A NANOFLUID	510
Maha Fahad Algouraibi Nashwa Ibrahim Hagagy Lobna Abdelkefi-Mesrati	PRODUCTION OF INDUSTRIAL BIOMOLECULES BY ACTINOMYCETES ISOLATED FROM SOIL IN SAUDI ARABIA	511
Ali Rıza DİNÇER Elçin GENÇ İbrahim Feda ARAL	REMOVAL OF SULFATE FROM LEATHER INDUSTRY WASTEWATER WITH DIFFERENT ACTIVATED CARBON ADSORPTIONS	512
Mehmet TUZCU Nevin TUZCU Zeynep CELIK Gokhan AKCAKAVAK	A CASE OF PERICARDITIS FIBRINOSA CAUSED BY HISTOPHILUS SOMNI IN A TWO-MONTH-OLD SIMMENTAL BREED CALF	522
Ozgur OZDEMIR Mehmet Burak ATES Mehmet TUZCU	SUBCUTANEOUS MULTIPLE MASTOCYTOMA IN AN 8-YEAR-OLD MALE ENGLISH SETTER	529
Ertan Oruc Ozgur Ozdemir Mehmet Burak Ates	HEMANGIOPERICYTOMA IN A 17-YEAR-OLD FEMALE GOLDEN RETRIEVER DOG	534
Mustafa ORTATATLI Ertan ORUC Ozgur OZDEMIR	INFILTRATIVE RENAL LYMPHOMA IN A 1-YEAR- OLD MALE STRAY CAT	539
Mustafa ORTATATLI Ertan ORUC Zeynep CELIK Fatih HATİPOĞLU	EXTRAMEDULLARY PLASMACYTOMA IN SPLEEN OF 12-YEAR-OLD FEMALE GOLDEN RETRIEVER DOG	543
Mehmet Burak ATES Mehmet TUZCU Mustafa ORTATATLI	HISTOPATHOLOGICAL CHARACTERIZATION OF HEPATOCELLULAR CARCINOMA IN A DOG	549
Zeynep CELIK Osman DAGAR Aysegul BULUT Rabia SALIK Gokhan AKCAKAVAK Aysenur TURAL	THE CASE OF EPIDERMAL INCLUSION CYST IN A 2-YEARS-OLD HOUND DOG	557

Beatriz PADRON PEREZ		
Fatih HATİPOĞLU		
Badiye V.H. Gajbe P.U Saha R.S.	“A SURVEY STUDY OF INSECT PEST ORDERS AND THEIR MANAGEMENT STRATEGIES IN DIFFERENT AREAS OF VIDARBHA REGION”.	563
Corina CĂTANĂ Alina MITROI Paula BOBOC (OROS)	EDIBLE ORNAMENTAL FLOWERS SEED COLLECTION – PRESENT STATUS AND FUTURE PERSPECTIVES AT CENTER FOR BIODIVERSITY AND CONSERVATION, UASVM CLUJ-NAPOCA, ROMANIA	564
Tuğba Gürkök Tan Gülşen Güçlü	THE GENOMIC AND TRANSCRIPTOMIC APPROACHES IN OPIUM POPPY	565
Mehsin Jabel Atteya	DERIVATIONS PERIOD 2 OF PRIME RINGS	578
Kemal Şahin TUNÇEL Mahbubor RAHMAN Tuba DEMİREL İsmail KARACAN	THE EFFECT OF HEAT TREATMENT STRATEGIES ON THERMAL STABILIZATION OF POLYACRYLONITRILE FIBERS IN CARBON FIBER PRODUCTION	583
Önder Albayrak Murat Beytur Haydar Yüksek	EVALUATION OF THEORETICAL AND EXPERIMENTAL PROPERTIES OF 3-METHYL-4- (3-ACETOXY-4-METHOXY-BENZYLIDENAMINO)- 4,5-DIHYDRO-1H-1,2,4-TRIAZOL-5-ONE	595
M.H. Hamdan	PARTICLE-LADEN FLOW INTO A POROUS CHANNEL: ENTRY AND BOUNDARY CONDITIONS	603
Münire TURHAN	THE HONEY OF RHODENDRON	614
Gediz UĞUZ	INVESTIGATION OF THE USAGE OF CORAL WASTE FISH SCALS AS A CATALYST IN PRODUCTION OF BIODIESEL	626

SYNTHESIS AND IN VITRO ANTIOXIDANT PROPERTIES OF SOME NEW 1-BENZYL-3-ALKYL(ARYL)-4-(3-METHOXY-4-PHENYLMETHOXY-BENZYLIDENAMINO)-4,5-DIHYDRO-1H-1,2,4-TRIAZOL-5-ONES

Assoc. Prof. Dr. Onur Akyıldırım

Kafkas University, Faculty of Engineering and Architecture, Department of Chemical Engineering, 36100, Kars, Turkey
ORCID ID: 0000-0003-1090-695X

Prof. Dr. Özlem Gürsoy-Kol

Kafkas University, Faculty of Science and Letters, Department of Chemistry, 36100, Kars, Turkey
ORCID ID: 0000-0003-2637-9023

Prof. Dr. Haydar Yüksek

Kafkas University, Faculty of Science and Letters, Department of Chemistry, 36100, Kars, Turkey
ORCID ID: 0000-0003-1289-1800

Abstract

4,5-Dihydro-1H-1,2,4-triazol-5-one derivatives have a wide range of biological properties such as antioxidant, antitumor, anti-inflammatory, antifungal, antimicrobial, hypoglycemic, analgesic, hypocholesteremic, antiviral, antihypertensive, antiparasitic and anti-HIV properties known to have activity. Compounds with a 1,2,4-triazole ring generally have potential biologically active properties. For this reason, extensive research has been carried out on many derivatives of 1,2,4-triazole compounds in medicine, pharmaceuticals and industry, both on synthesis and on many properties. It is known that new derivatives of compounds containing 1,2,4-triazole ring are synthesized and these are used in many areas of chemistry. In this study, five new 1-benzyl-3-alkyl(aryl)-4-(3-methoxy-4-phenylmethoxy-benzylidenamino)-4,5-dihydro-1H-1,2,4-triazol-5-ones (**4**) having 4,5-dihydro-1H-1,2,4-triazol-5-ones ring were synthesized and characterized by elemental analysis, IR, ¹H NMR, ¹³C NMR and UV spectral data. In addition, the antioxidant activities of these compounds were investigated using different antioxidant methodologies: 1,1-diphenyl-2-picryl-hydrazil (DPPH) free radical scavenging, reducing power and metal chelating activities.

Keywords: 1,2,4-triazol-5-one, antioxidant activity, Schiff base, synthesis.

1. Introduction

Some studies have been done on some 4,5-dihydro-1H-1,2,4-triazol-5-one derivatives (Alkan vd., 2007; Ikizler & Yuksek, 1993; Yuksek vd., 1997, 2004). In vivo analgesic and anti-inflammatory activities have been studied for some 1,2,4-triazole-derived compounds (Abdelazeem vd., 2021). In a recent study, the antibacterial properties of 1,2,4-triazole-derived Schiff bases were investigated (Li vd., 2021). N-acetyl derivatives of compounds with 1,2,4-triazole ring have been synthesized; in vitro antioxidant and antibacterial activities of these compounds were studied (Manap, 2021).

Today, it is accepted by scientists that antioxidants are an important research area. The damage caused by oxidative stress has been widely discussed in terms of antioxidants' capacity to protect organisms and cells. Natural sources are either synthesized or obtained that can provide active ingredients to prevent or reduce the effect of oxidative stress on the cell (Hussain *et al.*, 2003). In a recent study, it was determined that heterocyclic 1,2,4-triazole compounds were evaluated in terms of *in vitro* antimicrobial, anticancer, antioxidant and anti-urease activities (Kumari *et al.*, 2021).

In this study, five new 1-benzyl-3-alkyl(aryl)-4-(3-methoxy-4-phenylmethoxy-benzylidenamino)-4,5-dihydro-1H-1,2,4-triazole-5-ones (**4**) were synthesized. In addition, antioxidant activities of newly synthesized compounds were investigated using different antioxidant methodologies: 1,1-diphenyl-2-picryl-hydrazil (DPPH) free radical scavenging, reducing power and metal chelating activities.

2. Materials and Methods

Chemical reagents and all solvents used in this study were purchased from Merck AG, Aldrich and Fluka. The starting compounds 3-alkyl(aryl)-4-amino-4,5-dihydro-1H-1,2,4-triazol-5-ones **2** were prepared from the reactions of the corresponding ester ethoxycarbonylhydrazones **1** with an aqueous solution of hydrazine hydrate as described in the literature (Ikizler & Yuksek, 1993). Compound **3** was obtained from the reaction of compounds **2** with 3-methoxy-4-hydroxy-benzaldehyde through recently reported method (Manap, S, 2009). Melting points were determined in open glass capillaries using an Electrothermal digital melting point apparatus and are uncorrected. The IR spectra were obtained on a Perkin-Elmer Instruments Spectrum One FT-IR spectrometer. ^1H and ^{13}C NMR spectra were recorded in deuterated dimethyl sulfoxide with TMS as internal standard using a Varian Mercury spectrometer at 200 MHz and 50 MHz, respectively. UV absorption spectra were measured in 10 mm quartz cells between 200 and 400 nm using a PG Instruments Ltd T80 UV / Vis spectrometer. Extinction coefficients (ϵ) are expressed in $\text{L mol}^{-1} \text{cm}^{-1}$. Elemental analyses were carried out on a Leco 932 Elemental Combustion System (CHNS-O) for C, H and N.

2.1. General procedure for the synthesis of compound 4. 3-Alkyl(Aryl)-4-(3-methoxy-4-hydroxy-benzylidenamino)-4,5-dihydro-1H-1,2,4-triazol-5-one (**3**) (0.01 mol) was treated with Na (0.02 mol) dissolved in absolute ethanol (100 mL), and this solution was refluxed for 2 h. After cooling until room temperature to this solution was added benzyl bromide (0.02 mol) and this mixture was refluxed for 5 h and filtered. The filtrate was evaporated *in vacuo* and the crude product was recrystallized from ethanol to afford compound.

2.1.1. 1-Benzyl-3-methyl-4-(3-methoxy-4-phenylmethoxy-benzylidenamino)-4,5-dihydro-1H-1,2,4-triazol-5-one (4a). Yield 2.69 g (63%); mp 120 °C; IR (KBr): ν C=O 1698, C=N 1605, monosubstituted benzenoid ring 746 and 697 cm^{-1} ; ^1H NMR (200MHz, DMSO- d_6): δ 2.28 (s, 3H, CH_3), 3.83 (s, 3H, OCH_3), 4.89 (s, 2H, NCH_2), 5.16 (s, 2H, OCH_2), 7.13-7.45 (m, 13H, Ar-H), 9.58 (s, 1H, $\text{N}=\text{CH}$); ^{13}C NMR (50MHz, DMSO- d_6): δ 10.96 (CH_3), 47.98 (NCH_2), 55.40 (OCH_3), 69.76 (OCH_2), 109.12, 112.84, 122.61, 125.99, 127.54, 127.60 (arom-C), 127.90 (2C), 127.98 (2C), 128.42 (2C), 128.52 (2C), 136.49, 136.66, 143.27, 149.43 (arom-C), 149.20 (triazole C_3), 150.75 ($\text{N}=\text{CH}$), 154.73 (triazole C_5); UV λ_{max} (ϵ): 330 (21865), 320 (28435), 236 (19507), 220 (29293), 210 (27331) nm; Anal. Calcd. for $\text{C}_{25}\text{H}_{24}\text{N}_4\text{O}_3$ (428.49): C, 70.08; H, 5.65; N, 13.08. Found: C, 67.77; H, 5.54; N, 12.93.

2.1.2. 1-Benzyl-3-ethyl-4-(3-methoxy-4-phenylmethoxy-benzylidenamino)-4,5-dihydro-1H-1,2,4-triazol-5-one (4b). Yield 3.11 g (69%); mp 153 °C; IR (KBr): ν C=O 1697, C=N 1601, 1587, monosubstituted benzenoid ring 746 and 698 cm^{-1} ; ^1H NMR (200MHz, DMSO- d_6): δ 1.19 (t, 3H, CH_2CH_3 , $J=6.25$ Hz), 2.69 (q, 2H, CH_2CH_3 , $J=7.03$ Hz), 3.83 (s, 3H, OCH_3), 4.91 (s, 2H, NCH_2), 5.16 (s, 2H, OCH_2), 7.13-7.44 (m, 13H, Ar-H), 9.58 (s, 1H, $\text{N}=\text{CH}$); UV λ_{max} (ϵ): 330 (23642), 320 (26771), 236 (18612), 216 (26600), 210 (24024) nm; Anal. Calcd. for $\text{C}_{26}\text{H}_{26}\text{N}_4\text{O}_3$ (442.52): C, 70.57; H, 5.92; N, 12.66. Found: C, 67.63; H, 5.74; N, 12.32.

2.1.3. 1-Benzyl-3-n-propyl-4-(3-methoxy-4-phenylmethoxy-benzylidenamino)-4,5-dihydro-1H-1,2,4-triazol-5-one (4c). Yield 2.13 g (47%); mp 140 °C; IR (KBr): ν C=O 1697, C=N 1599, 1585, monosubstituted benzenoid ring 759 and 698 cm^{-1} ; ^1H NMR (200MHz, DMSO- d_6): δ 0.93 (t, 3H, $\text{CH}_2\text{CH}_2\text{CH}_3$, $J=7.03$ Hz), 1.67 (sext, 2H, $\text{CH}_2\text{CH}_2\text{CH}_3$), 2.65 (t, 2H, $\text{CH}_2\text{CH}_2\text{CH}_3$), 3.82 (s, 3H, OCH_3), 4.91 (s, 2H, NCH_2), 5.16 (s, 2H, OCH_2), 7.13-7.44 (m, 13H, Ar-H), 9.56 (s, 1H, $\text{N}=\text{CH}$); ^{13}C NMR (50MHz, DMSO- d_6): δ 13.41 ($\text{CH}_2\text{CH}_2\text{CH}_3$), 18.85 ($\text{CH}_2\text{CH}_2\text{CH}_3$), 26.57 ($\text{CH}_2\text{CH}_2\text{CH}_3$), 48.03 (NCH_2), 55.41 (OCH_3), 69.78 (OCH_2), 109.31, 112.96, 121.20, 122.40, 126.05 (arom-C), 127.47 (2C), 127.89 (2C), 128.43 (2C), 128.52 (2C), 136.50, 136.69, 143.30, 145.87, 149.35 (arom-C), 149.21 (triazole C_3), 150.75 ($\text{N}=\text{CH}$), 154.80 (triazole C_5); UV λ_{max} (ϵ): 332 (19791), 318 (24177), 236 (17383), 218 (24491), 210 (20000) nm.

2.1.4. 1-Benzyl-3-(p-methylbenzyl)-4-(3-methoxy-4-phenylmethoxy-benzylidenamino)-4,5-dihydro-1H-1,2,4-triazol-5-one (4d). Yield 2.49 g (48%); mp 152 °C; IR (KBr): ν C=O 1701, C=N 1589, 1,4-disubstituted benzenoid ring 820, monosubstituted benzenoid ring 763 and 697 cm^{-1} ; ^1H NMR (200MHz, DMSO- d_6): δ 2.23 (s, 3H, CH_3), 3.84 (s, 3H, OCH_3), 4.01 (s, 2H, CH_2), 4.93 (s, 2H, NCH_2), 5.15 (s, 2H, OCH_2), 7.13-7.44 (m, 17H, Ar-H), 9.53 (s, 1H, $\text{N}=\text{CH}$); UV λ_{max} (ϵ): 330 (16966), 320 (22660), 236 (16000), 218 (25850), 210 (19500) nm.

2.1.5. 1-Benzyl-3-(p-chlorobenzyl)-4-(3-methoxy-4-phenylmethoxy-benzylidenamino)-4,5-dihydro-1H-1,2,4-triazol-5-one (4e). Yield 4.16 g (75%); mp 150 °C; IR (KBr): ν C=O 1702, C=N 1588, 1,4-disubstituted benzenoid ring 820, monosubstituted benzenoid ring 748 and 683 cm^{-1} ; ^1H NMR (200MHz, DMSO- d_6): δ 3.82 (s, 3H, OCH_3), 4.08 (s, 2H, CH_2), 4.93 (s, 2H, NCH_2), 5.14 (s, 2H, OCH_2), 7.13-7.44 (m, 17H, Ar-H), 9.55 (s, 1H, $\text{N}=\text{CH}$); ^{13}C NMR (50MHz, DMSO- d_6): δ 10.96 (CH_3), 30.50 (CH_2Ph), 48.00 (NCH_2), 55.50 (OCH_3), 69.80 (OCH_2), 108.52, 112.75, 122.97, 125.96 (arom-C), 127.49 (2C), 127.88 (2C), 128.36 (2C), 128.41 (2C), 128.54 (2C), 130.56 (2C), 131.41 (arom-C), 134.61 (2C), 136.46, 136.55 (arom-C), 144.80 (2C), 149.48 (arom-C), 149.21 (triazole C_3), 150.78 ($\text{N}=\text{CH}$), 154.06 (triazole C_5); UV λ_{max} (ϵ): 332 (17561), 320 (23284), 216 (31054) nm; Anal. Calcd. for $\text{C}_{31}\text{H}_{27}\text{N}_4\text{O}_3\text{Cl}$ (539.03): C, 69.08; H, 5.05; N, 10.39. Found: C, 66.81; H, 4.98; N, 10.24.

2.2. Antioxidant activity. Butylated hydroxytoluene (BHT) was purchased from E. Merck (Merck KGaA, Darmstadt, Germany). Ferrous chloride, α -tocopherol, 1,1-diphenyl-2-picrylhydrazyl (DPPH), 3-(2-pyridyl)-5,6-bis(phenylsulfonic acid)-1,2,4-triazine (ferrozine), butylated hydroxyanisole (BHA) and trichloroacetic acid (TCA) were bought from Sigma (Sigma-Aldrich GmbH, Steinheim, Germany).

2.2.1. Reducing power. The reducing power of the newly synthesized compounds was assigned according to the method of Oyaizu (Oyaizu, 1986). Different concentrations of the samples (50-250 $\mu\text{g/mL}$) in DMSO (1 mL) were mixed with phosphate buffer (2.5 mL, 0.2 M,

pH = 6.6) and potassium ferricyanide (2.5 mL, 1%). The mixture was incubated at 50°C for 20 min. after which a portion (2.5 mL) of trichloroacetic acid (10%) was added to the mixture, which was then centrifuged for 10 min at 1000 x g. The upper layer of solution (2.5 mL) was mixed with distilled water (2.5 mL) and FeCl₃ (0.5 mL, 0.1%), and then the absorbance at 700 nm was measured in a spectrophotometer. Higher absorbance of the reaction mixture showed greater reducing power.

2.2.2. Free radical scavenging activity. Free radical scavenging activity of compounds was measured by DPPH[•], using the method of Blois (Blois, 1958). Concisely, 0.1 mM solution of DPPH[•] in ethanol was prepared, and this solution (1 mL) was added to sample solutions in DMSO (3 mL) at different concentrations (50-250 µg/mL). The mixture was shaken vigorously and allowed to stand at room temperature for 30 min. Then the absorbance was measured at 517 nm in a spectrophotometer. Lower absorbance of the reaction mixture showed higher free radical scavenging activity. The DPPH[•] concentration (mM) in the reaction medium was calculated from the following calibration curve and assigned by linear regression (R: 0.997):

$$\text{Absorbance} = 0.0003 \times \text{DPPH}^{\bullet} - 0.0174$$

The capability to scavenge the DPPH radical was calculated using the following equation:

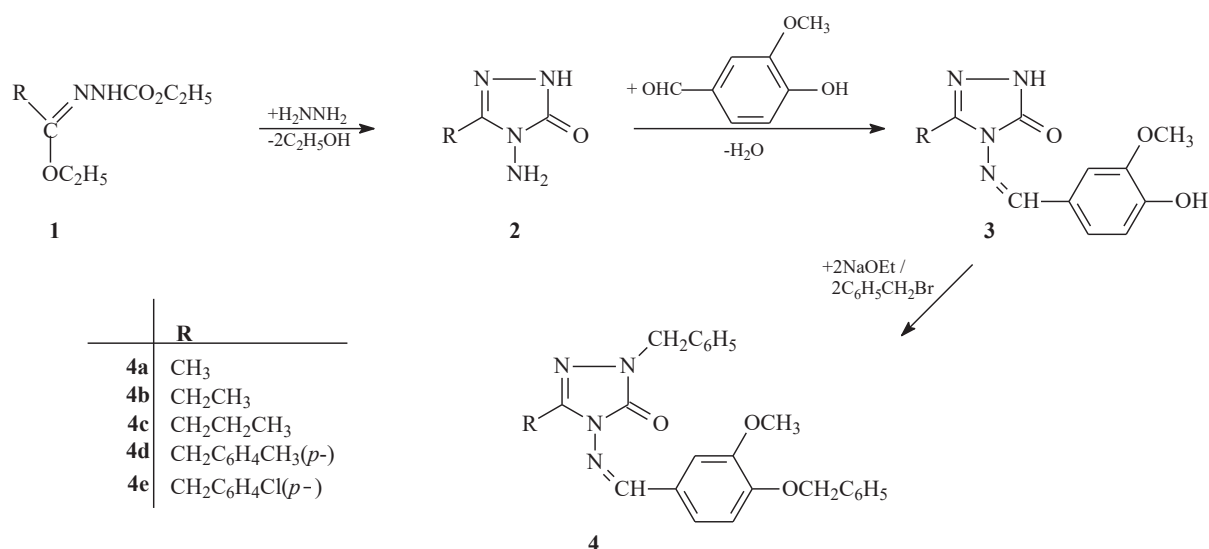
$$\text{DPPH}^{\bullet} \text{ scavenging effect (\%)} = (A_0 - A_1/A_0) \times 100$$

where A₀ is the absorbance of the control reaction and A₁ is the absorbance in the presence of the samples or standards.

2.2.3. Metal chelating activity. The method of Dinis et al were used to estimate the chelation of ferrous ions by the synthesized compounds and standards (Dinis vd., 1994). Briefly, the synthesized compounds (50-250 µg mL⁻¹) were added to a 2 mM solution of FeCl₂ (0.05 mL). The reaction was initiated by the addition of 5 mM ferrozine (0.2 mL) and the mixture was shaken vigorously and left standing at room temperature for 10 min. After the mixture had reached equilibrium, the absorbance of the solution was then measured at 562 nm in a spectrophotometer. All test and analyses were run in triplicate and averaged. The percentage of inhibition of ferrozine-Fe²⁺ complex formation was given by the formula: % Inhibition = (A₀ - A₁/A₀) x 100, where A₀ is the absorbance of the control, and A₁ is the absorbance in the presence of the samples or standards. The control did not contain compound or standard.

3. Results and Discussion

The 1-benzyl-3-alkyl(aryl)-4-(3-methoxy-4-phenylmethoxy-benzylidenamino)-4,5-dihydro-1H-1,2,4-triazol-5-ones **4a-e** were prepared. Compound **4** was synthesized by the reaction of **3** type compound with benzyl bromide in sodium ethoxide (Scheme 1).



Scheme 1. Synthesis route of compounds 2-4.

The structures of five new **4** type 1-benzyl-3-alkyl(aryl)-4-(3-methoxy-4-phenylmethoxybenzylidenamino)-4,5-dihydro-1H-1,2,4-triazol-5-ones were identified using IR, ¹H NMR, ¹³C NMR, UV and elemental analyses data.

3.1. Antioxidant activity. The antioxidant activities of 5 new compounds **4a-e** were determined. Several methods are used to determine antioxidant activities. The methods used in the study are given below:

3.1.1. Total reductive capability using the potassium ferricyanide reduction method.

The reductive capabilities of compounds are evaluated by the extent of conversion of the Fe³⁺ / ferricyanide complex to the Fe²⁺ / ferrous form. The reducing powers of the compounds were detected at different concentrations, and results were compared with BHA, BHT and α -tocopherol. The reducing capacity of a compound could assist as a significant indicator of its potential antioxidant activity (Meir vd., 1995). The antioxidant activity of assumed antioxidant has been attributed to various mechanisms, among which are prevention chain initiation, binding of transition metal ion catalyst, decomposition of peroxides, prevention of continued hydrogen abstraction, reductive capacity and radical scavenging (Yildirim vd., 2001). In the present study, all the amount of the compounds showed lower absorbance than standard antioxidants. Therefore, no activities were seen to reduce metal ions complexes to their lower oxidation state or to join in any electron transfer reaction. In other saying, compounds did not show the reductive activities.

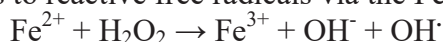
3.1.2. DPPH[•] radical scavenging activity. The model of scavenging the stable DPPH radical pattern is an extensively used method to assess antioxidant activities in a relatively short time compared with other methods. The impact of antioxidants on DPPH radical scavenging was assumed to be because of their hydrogen donating ability (Baumann, 1979). DPPH is a stable free radical and accepts an electron or hydrogen radical to become a stable diamagnetic molecule (Soares vd., 1997). The reduction capability of DPPH radicals was detected by decrease in its absorbance at 517 nm induced by antioxidants. The absorption maximum of a stable DPPH radical in ethanol was at 517 nm. The decline in absorbance of DPPH radical brought forth by antioxidants, owing to reaction between antioxidant molecules and radical, progresses, which result in the scavenging of the radical by hydrogen donation. It

is visually obvious as a discoloration from purple to yellow. Hence, DPPH \cdot is usually used as a substrate to evaluate antioxidative activity of antioxidants (Duh, 1999). In the study, antiradical activities of compounds and standard antioxidants such as BHA, BHT and α -tocopherol were established by using DPPH \cdot method. Scavenging effect values of compound **4a**, BHA and α -tocopherol at different concentrations are given. Compound **4a** showed low activity as a radical scavenger. The other compounds showed no activity.

3.1.3. Ferrous ion chelating activity. The chelating effect towards ferrous ions by the compounds and standards was determined. Ferrozine can quantitatively make up complexes with Fe $^{2+}$. In the presence of chelating agents, the complex formation is interrupted with the conclusion that the red colour of the complex is decreased. Measurement of colour reduction thus allows estimation of the chelating activity of the coexisting chelator (Yamaguchi vd., 2000). Transition metals have crucial role in the generation oxygen free radicals in living organism. The ferric iron (Fe $^{3+}$) is the relatively biologically inactive form of iron. Nevertheless, it can be reduced to the active Fe $^{2+}$, depending on condition, particularly pH (Strlic vd., 2002) and oxidized back through. Fenton type reactions with the production of hydroxyl radical or Haber-Weiss reactions with superoxide anions. The production of these radicals may cause lipid peroxidation, protein modification and DNA damage. Chelating agents may not activate metal ions and potentially inhibit the metal-dependent processes (Finefrock vd., 2003). Furthermore, the production of highly active ROS such as O $_2^{\cdot-}$, H $_2$ O $_2$ and OH \cdot is also catalyzed by free iron through Haber-Weiss reactions:



Iron is known as the most important lipid oxidation pro-oxidant because of its high reactivity among the transition metals. The ferrous state of iron accelerates lipid oxidation by corrupting the hydrogen and lipid peroxides to reactive free radicals via the Fenton reactions:



Fe $^{3+}$ ion also produces radicals from peroxides, though the rate is tenfold less than that of Fe $^{2+}$ ion, which is the most powerful pro-oxidant among the various types of metal ions (Calis vd., 1993). Ferrous ion chelating activities of the compounds **4a-e**, BHT, BHA and α -tocopherol are given. In this study, metal chelating capacity was significant since it reduced the concentrations of the catalyzing transition metal. It was stated that chelating agents that form σ -bonds with a metal are effective as secondary antioxidants since they reduce the redox potential thereby stabilizing the oxidized form of metal ion (Gordon, M. H, 1990). The obtained data reveal that all compounds uncovers that all the compounds, except **4b**, show a marked capacity for iron binding, suggesting that their action as peroxidation protectors may be regarding their iron binding capacity. Instead, free iron is known to have low solubility and a chelated iron complex has greater solubility in solution, which can be contributed merely by the ligand. Additionally, the compound-iron complex may also be active, since it can participate in iron-catalyzed reactions.

4. Conclusions

The synthesis and in vitro antioxidant evaluation of new 4,5-dihydro-1H-1,2,4-triazol-5-one derivatives are defined. All of the compounds, apart from **4b**, reveal a marked capacity for iron binding. The data here reported could be of the possible interest because of the observed metal chelating activities of the studied compounds could prevent redox cycling. Design and synthesis of novel small molecules which can definitely protective role in biological systems are in view in modern medicinal chemistry. These results may also provide some guidance for the development of novel triazole-based therapeutic target.

Acknowledgements. This work was supported by the Turkish Scientific and Technological Council (Project Number: TBAG 108T984).

5. References

- Abdelazeem, A. H., El-Din, A. G. S., Arab, H. H., El-Saadi, M. T., El-Moghazy, S. M., & Amin, N. H. (2021). Design, synthesis and anti-inflammatory/analgesic evaluation of novel di-substituted urea derivatives bearing diaryl-1,2,4-triazole with dual COX-2/sEH inhibitory activities. *Journal of Molecular Structure*, 1240, 130565. <https://doi.org/10.1016/j.molstruc.2021.130565>
- Alkan, M., Yuksek, H., Islamoglu, F., Bahceci, S., Calapoglu, M., Elmastas, M., Aksit, H., & Ozdemir, M. (2007). A study on 4-acylamino-4,5-dihydro-1H-1,2,4-triazol-5-ones. *Molecules*, 12(8), 1805-1816. <https://doi.org/10.3390/12081805>
- Baumann, J. W., G. ;. Bruchhausen, FV. (1979). Prostaglandin synthetase inhibiting O₂-radical scavenging properties of some flavonoids and related phenolic compounds. *Naunyn-Schmiedebergs Arch Pharmacol*, 308, 27–32.
- Blois, M. S. (1958). Antioxidant determinations by the use of a stable free radical. *Nature*, 181(4617), 1199–1200.
- Calis, I., Hosny, M., Khalifa, T., & Nishibe, S. (1993). Secoiridoids from *Fraxinus-Angustifolia*. *Phytochemistry*, 33(6), 1453-1456. [https://doi.org/10.1016/0031-9422\(93\)85109-5](https://doi.org/10.1016/0031-9422(93)85109-5)
- Dinis, T., Madeira, V., & Almeida, L. (1994). Action of Phenolic Derivatives (acetaminophen, Salicylate, and 5-Aminosalicylate) as Inhibitors of Membrane Lipid-Peroxidation and as Peroxyl Radical Scavengers. *Archives of Biochemistry and Biophysics*, 315(1), 161-169. <https://doi.org/10.1006/abbi.1994.1485>
- Duh, P. D. (1999). Antioxidant activity of water extract of four Harng Jyur (*Chrysanthemum morifolium* Ramat) varieties in soybean oil emulsion. *Food Chemistry*, 66(4), 471-476. [https://doi.org/10.1016/S0308-8146\(99\)00081-3](https://doi.org/10.1016/S0308-8146(99)00081-3)
- Finefrock, A. E., Bush, A. I., & Doraiswamy, P. M. (2003). Current status of metals as therapeutic targets in Alzheimer's disease. *Journal of the American Geriatrics Society*, 51(8), 1143-1148. <https://doi.org/10.1046/j.1532-5415.2003.51368.x>
- Gordon, M. H. (1990). *Food Antioxidants*. Elsevier.
- Hussain, H. H., Babic, G., Durst, T., Wright, J. S., Flueraru, M., Chichirau, A., & Chepelev, L. L. (2003). Development of novel antioxidants: Design, synthesis, and reactivity. *Journal of Organic Chemistry*, 68(18), 7023-7032. <https://doi.org/10.1021/jo0301090>
- Ikizler, A., & Yuksek, H. (1993). Acetylation of 4-Amino-4,5-Dihydro-1H-1,2,4-Triazol-5-Ones. *Organic Preparations and Procedures International*, 25(1), 99-105. <https://doi.org/10.1080/00304949309457935>
- Kumari, M., Tahlan, S., Narasimhan, B., Ramasamy, K., Lim, S. M., Shah, S. A. A., Mani, V., & Kakkar, S. (2021). Synthesis and biological evaluation of heterocyclic 1,2,4-triazole scaffolds as promising pharmacological agents. *Bmc Chemistry*, 15(1), 5. <https://doi.org/10.1186/s13065-020-00717-y>
- Li, B., Zhang, Z., Zhang, J.-F., Liu, J., Zuo, X.-Y., Chen, F., Zhang, G.-Y., Fang, H.-Q., Jin, Z., & Tang, Y.-Z. (2021). Design, synthesis and biological evaluation of pleuromutilin-Schiff base hybrids as potent anti-MRSA agents in vitro and in vivo. *European Journal of Medicinal Chemistry*, 223, 113624. <https://doi.org/10.1016/j.ejmech.2021.113624>
- Manap, S. (2009). Bazı yeni 3-alkil(aril)-4-(3,4-disubstituebenzilidenamino)-4,5-dihidro-1H-1,2,4-triazol-5-on türevlerinin sentezi, yapılarının aydınlatılması, antioksidan ve asitlik özelliklerinin incelenmesi [Master Thesis]. Kafkas University.

- Manap, S. (2021). Synthesis and in vitro antioxidant and antimicrobial activities of novel 3-alkyl(aryl)-4-[3-methoxy-4-(2-furylcarbonyloxy)-benzylidenamino]-4,5-dihydro-1H-1,2,4-triazol-5-ones, and their N-acetyl, N-Mannich base derivatives. *Journal of the Iranian Chemical Society*. <https://doi.org/10.1007/s13738-021-02386-7>
- Meir, S., Kanner, J., Akiri, B., & Philosophhadas, S. (1995). Determination and Involvement of Aqueous Reducing Compounds in Oxidative Defense Systems of Various Senescing Leaves. *Journal of Agricultural and Food Chemistry*, 43(7), 1813-1819. <https://doi.org/10.1021/jf00055a012>
- Oyaizu, M. (1986). Studies on products of browning reaction antioxidative activities of products of browning reaction prepared from glucosamine. *The Japanese journal of nutrition and dietetics*, 44(6), 307–315.
- Soares, J. R., Dinis, T. C. P., Cunha, A. P., & Almeida, L. M. (1997). Antioxidant activities of some extracts of *Thymus zygis*. *Free Radical Research*, 26(5), 469-478. <https://doi.org/10.3109/10715769709084484>
- Strlic, M., Radovic, T., Kolar, J., & Pihlar, B. (2002). Anti- and prooxidative properties of gallic acid in Fenton-type systems. *Journal of Agricultural and Food Chemistry*, 50(22), 6313-6317. <https://doi.org/10.1021/jf025636j>
- Yamaguchi, F., Ariga, T., Yoshimura, Y., & Nakazawa, H. (2000). Antioxidative and anti-glycation activity of garcinol from *Garcinia indica* fruit rind. *Journal of Agricultural and Food Chemistry*, 48(2), 180-185. <https://doi.org/10.1021/jf990845y>
- Yildirim, A., Mavi, A., & Kara, A. A. (2001). Determination of antioxidant and antimicrobial activities of *Rumex crispus* L. extracts. *Journal of Agricultural and Food Chemistry*, 49(8), 4083-4089. <https://doi.org/10.1021/jf0103572>
- Yukse, H., Demirbas, A., Ikizler, A., Johansson, C. B., Celik, C., & Ikizler, A. A. (1997). Synthesis and antibacterial activities of some 4,5-dihydro-1H-1,2,4-triazol-5-ones. *Arzneimittel-Forschung/Drug Research*, 47(4), 405-409.
- Yukse, H., Ocak, Z., Alkan, M., Bahceci, S., & Ozdemir, M. (2004). Synthesis and determination of pK(a) values of some new 3,4-disubstituted-4,5-dihydro-1H-1,2,4-triazol-5-one derivatives in non-aqueous solvents. *Molecules*, 9(4), 232-240. <https://doi.org/10.3390/90400232>

BIG DATA MODELING

Lecturer Dr. Emine BAŞ
(ORC-ID: 0000-0003-4322-6010)

Kulu Vocational School, Selçuk University, 42075, Konya, Turkey

Abstract- Big data is a fast growing data set. Controlling this fast growing data is one of the biggest problems that must be overcome. Using this big data, advanced forecasts can be easily made. Deciding which data to use in a big dataset is a different problem step. How to make meaningful data from large data is a separate problem step. The purpose of this special issue on Modeling and Management of Big Data is to discuss research and experience in modelling and to develop as well as deploy systems and techniques to deal with Big Data. This study has been discussed on the place of use of big data sets, the advantages of big data sets and the problems of big data sets.

Keywords: *Big data, Optimization, Social Network*

I. INTRODUCTION

Big Data has various definitions in the literature. Some of those are specified below:

Big Data is the amount of data beyond the ability of technology to store, manage and process efficiently (Manyika et.al, 2011). Big Data is a term which defines the hi-tech, high speed, high-volume, complex and multivariate data to capture, store, distribute, manage and analyze the information (TechAmerica Foundation, 2014). Big data is high volume, high velocity, and/or high variety information assets that require new forms of processing to enable enhanced decision making, insight discovery and process optimization (Gartner, 2014; Gürsakal, 2014). Big Data Technologies are new generation technologies and architectures which were designed to extract value from multivariate high volume data sets efficiently by providing high speed capturing, discovering and analyzing (Gantz and Reinsel, 2011).

Twenty first century has seen the explosion of data collection in many areas. The ease of acquisition of data as a result of technological revolution has made this feasible (Fan, 2013). Massive data and high dimensionality characterizes many contemporary problem domains such as biomedical sciences, engineering, finance and social sciences. This means machine learning problems handling such spatio-temporal problems may have to deal with tens of thousands of features extracted from documents, images and other objects. Typical key features of big data include very large samples as well as very high dimensionality (Bhattacharya and his friends, 2016).

II. BIG DATA MODEL

Big Data Definition:

Various studies in the literature show that big data has 3, 4 or 5 characteristics; 3 of whom are common at all: Volume, Velocity and Variety. Others are Veracity and Value (Hashem et.al, 2015; Elragal, 2014; Fadiya et.al., 2014; Yang et.al., 2014; López et.al., 2015, Özköse et al., 2015). The first definition of Big Data was developed by Meta Group (now part of Gartner) by describing their three characteristics called “3V”: Volume, Velocity and Variety. Based on data quality, IBM has added a fourth V called: Veracity.

However, Oracle has added a fourth V called: Value, highlighting the added value of Big Data (Baaziz & Quoniam, 2013a). 5 characteristics of big data is shown in Figure 2.1.

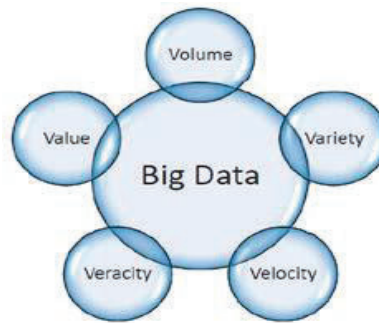


Figure 2. 1 Characteristics of Big Data (Elragal, 2014)

These 5 characteristics are explained as follows (Hashem et.al, 2015; Elragal, 2014; Fadiya et.al., 2014; Yanget.al., 2014; López et.al., 2015):

Volume: It is the most important characteristic of big data. It represents the size of the big data set.

Variety: Various data come to the companies from numerous resources (internal or external). These data entries from separate resources cause variance in data set. External data are hardly ever structural.

Velocity: The production rate of big data is notably high. The heavy increase in data means that the data should be analyzed more swiftly. The faster the data increases, the faster the need for the data increases; therefore the process shows increase as well.

Veracity: It is the accuracy of the data. The data should be acquired from correct resources and its security should be provided. Only authorized people should have the access permission.

Value: A result should be generated after all of the procedures and the result should enrich the process.

Classification of Big Data:

The characteristic of big data can be understood better by dividing it into classes. These classes are Data Sources, Content Format, Data Stores, Data Staging and Data Processing (Hashem et.al, 2015).

Data Sources : Web & Social, Machine, Sensing, Transactions and IoT

Content Format : Structured, Semi-Structured and Unstructured

Data Stores : Document-oriented, Column-oriented, Graph based and Key-value

Data Staging : Cleaning, Normalization and Transform

Data Processing : Batch and Real time

Big Data Process:

Big data process is shown below(Özköse et al., 2015):

- Data Management
 - ✓ Acquisition and Recording
 - ✓ Extraction, Cleaning and Annotation
 - ✓ Integration, Aggregation and Representation
- Analytics
 - ✓ Modeling and Analysis
 - ✓ Interpretation

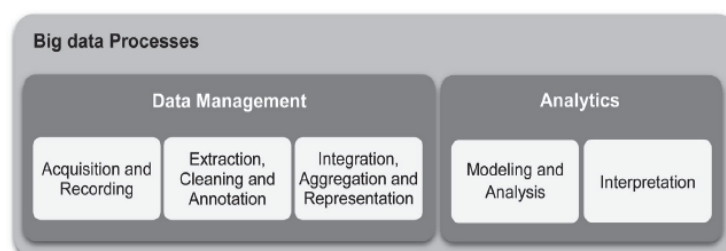


Figure 2.2. Big Data Process (Gandomi and Haider, 2015)

Usage Areas of Big Data:

Big data is used efficiently in numerous fields. Some of them are listed below(Özköse et al., 2015):

- Automotive industry,
- High technology and industry,
- Oil and gas,
- Telecommunication sector,
- Medical field,
- Retail industry,
- Packaged consumer products,
- Media and show business,
- Travel and transport sector,
- Financial services,
- Social media and online services,
- Public services,
- Education and research,
- Health services,
- Law enforcement and defense industry.

Methods Used in Big Data:

Text Analytics: Text analytics is used for information retrieval from data. E-mails, blogs, online forums, news and call center records are all examples of text data. Text analytics involve machine learning, statistical analysis and computational linguistics. Text analytics enable to extract meaningful summaries from large scale data (Gandomi and Haider, 2015).

Audio Analytics: Audio analytics is used to extract information from unstructured audio data. Call centers and health services are commonly used utilization areas of audio analytics. Audio analytics can be used in numerous fields such as increasing the customer experience, the performance of customer representative and the sales rate; comprehending several tasks such as customer behaviors and the troubles of products (Gandomi and Haider, 2015).

Video Analytics: Video analytics is the usage of various techniques to extract meaningful information, track and analyze video streams. Marketing and operations management is the main application area of video analytics (Gandomi and Haider, 2015).

Social Media Analytics: Social media analytics is the analysis of the structured and unstructured data on the social media channels. Social media can be categorized as follows (Gandomi and Haider, 2015):

- Social networks (Facebook, LinkedIn),
- Blogs (BlogSpot, WordPress),
- Microblogs (Twitter, Tumblr),
- Social news (Digg, Reddit),
- Social bookmarks (Delicious, StumbleUpon),
- Media sharing (Instagram, YouTube),
- Wiki (Wikipedia, Wikihow),
- Question-and-answer sites (Yahoo! Answers, Ask.com),
- Review sites (Yelp, TripAdvisor).

Predictive Analytics: Predictive analytics is based upon estimating future considering current or stale data. Predictive analysis is used to capture the relationships of data and discover the patterns. Predictive analytics which is primarily based on statistical methods, is highly applicable on many disciplines (Gandomi and Haider, 2015).

III. CHALLENGES OF BIG DATA

The objective of this special issue was to conduct a survey of the recognised techniques to deal with big data. The results indicate that the current strategies, methodologies and architectural models are not adequate for solving problems arising from this data complexity. In conclusion, while much work in this area has been accomplished, there is still much to be done in order to manage big data efficiently and exploit the opportunities hidden in the data. Big Data bring many attractive opportunities, as has been stated, along with some challenges, involving several issues such as complexity in data capture, storage, analysis and visualization. Future research should focus on the critical aspects which are the challenges to be addressed in the successful and efficient modeling and management of big data (Gil and Song, 2016). These challenges (Labrinidis & Jagadish 2012; Kaisler, 2013; Chen & Zhang, 2014) could be divided into several steps as shown in Fig. 3.1.

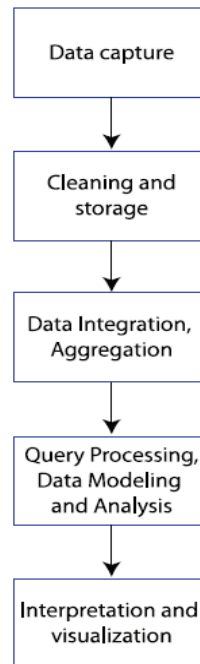


Figure 3.1. Challenges to better address the opportunities of big data.

- (i) *Data capture*: Many data are recorded from diverse data generating sources.
- (ii) *Cleaning and storage*: The objective in this case is to store the data in a structured form suitable for analysis.
- (iii) *Data Integration, Aggregation*: Besides the former challenge, the reality is that very often the variety of the sources makes it hard to deal with the information .
- (iv) *Query Processing, Data Modeling and Analysis*. In order to query, model and analyse data, data mining is a set of techniques to extract precious information from data. There are several techniques which include clustering analysis, classification, regression and association rule learning. However, Big Data mining is more challenging compared with traditional data mining algorithms. In the current status of data mining is analysed since new mining techniques are necessary due to the volume, variability, and velocity, of those data.
- (v) *Interpretation and visualization*. Choosing proper data representation tools is crucial when we try to visualize Big Data due to the complexity of the data (Petcu et al. ,2013; Gil and Song, 2016)

Some mechanisms in order to solve this situation are:

- The People's Ontology [Open Information Extraction]. Mine a database of entities and classes from the Web.
- Recovering Table Semantics.
- Recovering Binary Relationships.
- Attribute Correlations.

- Synonym Discovery.

IV. CONCLUSION

Big Data is the amount of data beyond the ability of technology to store, manage and process efficiently. Many problems are solved using large data. Many forward-looking estimates are available. The large data we have described in the past as waste data has become useful in many areas today. But the big data has many challenges. The results indicate that the current strategies, methodologies and architectural models are not adequate for solving problems arising from this data complexity. In conclusion, while much work in this area has been accomplished, there is still much to be done in order to manage big data efficiently and exploit the opportunities hidden in the data (Gil and Song, 2016).

REFERENCES

- [1] Baaziz A., “How to use Big Data technologies to optimize operations in Upstream Petroleum Industry”, 21st World Petroleum Congress.
- [2] Fan Jianqing. Features of big data and sparsest solution in high confidence set. Past, present, and future of statistical science 2013:505.
- [3] Bhattacharya M., Islam R., Abawajy J., “Evolutionary optimization: A big data perspective”, Journal of Network and Computer Applications 59(2016)416–426.
- [4] Gantz, J., & Reinsel, D. (2011). Extracting value from chaos. *IDC iView*, (1142), 9-10.
- [5] Gürsakal, N., *Büyük Veri*, Dora Kitabevi, Bursa, 2014.
- [6] Manyika, J., Chui, M., Brown, B., Bughin, J., Dobbs, R., Roxburgh, C., ... & McKinsey Global Institute. (2011). Big data: The next frontier for innovation, competition, and productivity.
- [7] Fadiya, S. O., Saydam, S., & Zira, V. V. (2014). Advancing big data for humanitarian needs. *Procedia Engineering*, 78, 88-95.
- [8] Özköse H., Arı E. S., Gencer C., “Yesterday, Today and Tomorrow of Big Data”, *Procedia - Social and Behavioral Sciences* 195 (2015) 1042 – 1050.
- [9] Elragal, A. (2014). ERP and Big Data: The Inept Couple. *Procedia Technology*, 16, 242-249.
- [10] Hashem, I. A. T., Yaqoob, I., Anuar, N. B., Mokhtar, S., Gani, A., & Khan, S. U. (2015). The rise of “big data” on cloud computing: Review and open research issues. *Information Systems*, 47, 98-115.
- [11] López, V., del Río, S., Benítez, J. M., & Herrera, F. (2015). Cost-sensitive linguistic fuzzy rule based classification systems under the MapReduce framework for imbalanced big data. *Fuzzy Sets and Systems*, 258, 5-38.
- [12] Yang, C., Zhang, X., Zhong, C., Liu, C., Pei, J., Ramamohanarao, K., & Chen, J. (2014). A spatiotemporal compression based approach for efficient big data processing on Cloud. *Journal of Computer and System Sciences*, 80(8), 1563-1583.
- [13] Baaziz A., Quoniam L., 2013b, The information for the operational risk management in uncertain environments: Case of Early Kick Detection while drilling of the oil or gas wells, *International Journal of Innovation and Applied Studies (IJIAS)*, Vol. 4 No. 1, Sep. 2013.
- [14] Gandomi, A., & Haider, M. (2015). Beyond the hype: Big data concepts, methods, and analytics. *International Journal of Information Management*, 35(2), 137-144.
- [15] Gil D., Song Il-Y., “Modeling and Management of Big Data: Challenges and opportunities”, *Future Generation Computer Systems* 63 (2016) 96–99.
- [16] A. Labrinidis, H. Jagadish, Challenges and opportunities with big data, *Proc. VLDB Endow.* 5 (12) (2012) 2032–2033.
- [17] S. Kaisler, F. Armour, J.A. Espinosa, W. Money, Big data: Issues and challenges moving forward, in: *System Sciences (HICSS)*, 2013 46th Hawaii International Conference, IEEE, 2013, pp. 995–1004.
- [18] C.P. Chen, C.-Y. Zhang, Data-intensive applications, challenges, techniques and technologies: A survey on big data, *Inform. Sci.* 275 (2014) 314–347.
- [19] D. Petcu, G. Macariu, S. Panica, C. Craciun, Portable cloud applications from theory to practice, *Future Gener. Comput. Syst.* 29 (6) (2013) 1417–1430.

CPR B2_{ca} s1a d1 SINIFI SİNYAL KABLOLARININ GELİŞTİRİLMESİ**DEVELOPMENT OF CPR B2_{ca} s1a d1 CLASS SIGNAL CABLES****Erdinç YÜKSEL**

Türk Prysmian Kablo ve Sistemleri A.Ş. Ar-Ge Merkezi, Bursa, Türkiye.

ORCID NO: <https://orcid.org/0000-0002-3141-763X>**Can ALTINGÖZ**

Türk Prysmian Kablo ve Sistemleri A.Ş. Ar-Ge Merkezi, Bursa, Türkiye.

ORCID NO: <https://orcid.org/0000-0002-6363-8920>**Furkan ŞEN**

Türk Prysmian Kablo ve Sistemleri A.Ş. Ar-Ge Merkezi, Bursa, Türkiye.

ORCID NO: <https://orcid.org/0000-0003-4661-7957>**Ahmet FEYZİOĞLU**

Marmara Üniversitesi, Teknoloji Fakültesi, Makine Mühendisliği, İstanbul, Türkiye.

ORCID ID: <https://orcid.org/0000-0003-0296-106X>**ÖZET**

Günümüz dünyasında, mülkiyetin ve insan sağlığının yangından korunması, bina güvenliğinin ayrılmaz bir parçasıdır. Güvenlik, hizmet ve ekonomik yatırım getirisi açısından önemli olan kablo sistemlerinin güvenilirliği ve uzun vadeli istikrarı büyük önem taşımaktadır. Bu amaçla binaların kablo tesisatında alev geciktirici ve yangına dayanıklı kablolar kullanılmaktadır. Genellikle yangınlar sağlığa zarar verir ya da büyük maddi hasara neden olur. Hatta bazı durumlarda ölümle sonuçlanabilir. Bu nedenle bilim, araştırma ve teknik uygulama çabalarının yangınları önlemeye ve sonuçlarını en aza indirmeye yönelik olduğu anlaşılabılır bir durumdur. Teknik standardizasyon, yangın güvenliğini artırmak için önemli bir araçtır. Bu kapsamda tüm sertifikasyon ve etiketleme süreci EN 50575 standardında tanımlanmıştır. Bu standart, inşaat işlerinde kalıcı olarak kurulan kablolar için yangın gerekliliklerini detaylandırarak, CE işaretinin uygulanabilmesi için bir Performans Beyanı (DoP-Declaration of Performance) yapılmasını sağlar. Tüm yapı ürünlerinin (kablolar dahil) yangın performansına tepkisinin sınıflandırılması CPR (Construction Product Regulation-Yapı Ürünleri Yönetmeliği) altında 2016 yılında 2016/364/EU kapsamında yayınlanmış olup, kablolar için CE işaretinin oluşturulması 1 Temmuz 2017 tarihinde zorunlu hale gelmiştir. CPR, “yangına tepki” ve “yangında devre bütünlüğü (yangına dayanıklılık)” olmak üzere yangın güvenliğinin bu iki parametreyle değerlendirilmesidir. Günümüzde CPR yönetmeliğine uygun kabloların kullanımı sadece bina içinde değil aynı zamanda tünel, geçit vb. kapalı alanlarda da yaygınlaşmaktadır. Demiryolu uygulamalarının kapalı geçişlerde kullanılan kablolarında şartnamelerde belirtilen CPR sınıfına uygunluk aranmaktadır. Su sızdırmazlık özelliği olan ve yanma performansı yüksek demiryolu kabloları tamamen yepyeni bir konsept olup AR-GE faaliyetlerinin yürütülmesi ihtiyacını doğurmuştur. Bu gerekliliklerden yola çıkılarak bu çalışmada ilgili şartnamelerde talep edilen kuru su sızdırmaz sinyal kablolarının, en yüksek performans seviyesindeki CPR B2_{ca} s1a d1 sınıfı olarak geliştirilmesi amaçlanmıştır. Su sızdırmazlık kablonun uzun dönem ömrünü korumasını sağlayan önemli bir parametredir. Projede; kuru su sızdırmaz demiryolu kabloların aynı zamanda CPR B2_{ca} S1a d1 performansını sağlayan versiyonlarının geliştirilmesi için çalışmalar yapılmıştır. A-2YTF(L)2YB2Y ve A-2YTF(L)HBH tipi kablolar proje kapsamında ele alınmıştır. 1 dörtden 10 dörtdüye kadar farklı kesitlerde kablolar üzerinde çalışmalar

yapılmıştır. Uygun malzeme seçimi yapıldıktan sonra prototip kabloların tasarımı için Prysmian Group bünyesinde geliştirilmiş olan Common Analisi (CA) kablo tasarım programı kullanılmıştır. Kabloların belirlenen kesitleri için numune üretimleri gerçekleştirilmiştir. Üretim aşamaları arasında izolasyon, eğirme, dolgulama, zırhlama ve kılıflama gibi safhalar bulunmaktadır. Eğirme safhası ve dış kılıf safhaları projenin en kritik prosesleri olarak ön plana çıkmaktadır. Hem su sızdırmazlığın sağlanması hem de elektriksel parametrelerin şartname değerlerini sağlaması için kablo özünün formasyonu incelenmiştir. Prototip üretimi sonrası kablolar üzerinde elektriksel, malzeme, su sızdırmazlık ve yanma testleri uygulanmıştır. Proje kapsamında kazanılan üretim yeteneği ve bilgi birikimi ile yenilikçi bir ürün grubunun ortaya çıkması sağlanmıştır.

Anahtar Kelimeler: CPR, Kablo Teknolojisi, Kablo Testleri, Sinyal Kablosu

ABSTRACT

In today's world, protecting property and human health from fire is an integral part of building safety. The reliability and long-term stability of cable systems, which are important for safety, service and economic return on investment, are of great importance. For this purpose, flame retardant and fire-resistant cables are used in the wiring of buildings. Generally, fires are harmful to health or cause major property damage. In some cases, it can even result in death. Therefore, it is understandable that the efforts of science, research and technical practice are aimed at preventing fires and minimizing their consequences. Technical standardization is an important tool to improve fire safety. In this context, the entire certification and labeling process is defined in the EN 50575 standard. This standard details fire requirements for cables permanently installed in construction works and provides for a Declaration of Performance (DoP) to be applied for CE marking. The classification of the reaction to fire performance of all building products (including cables) was published in 2016/364/EU under the CPR (Construction Product Regulation) in 2016, and the application of the CE marking for cables became mandatory on 1 July 2017. CPR is the evaluation of fire safety with these two parameters, "reaction to fire" and "circuit integrity in fire (fire resistance)". Today, the use of cables in accordance with the CPR regulation is becoming widespread not only inside the building but also in indoor areas such as tunnels and passages. Cables used in indoor parts of railway applications are required to comply with the CPR class specified in the specifications. Railway cables which have water-tight and high combustion performance, are a completely new concept and have led to the need for R&D activities.

Based on these requirements, in this study, it is aimed to develop the dry water-tight signal cables demanded in the relevant specifications as CPR B2_{ca} S1a d1 class with the highest performance level. Water-tight ability is an important parameter that ensures the long-term life of the cable. In the project, studies have been carried out to develop versions of dry water-tight railway cables that also provide CPR B2_{ca} S1a d1 performance. A-2YTF(L)2YB2Y and A-2YTF(L)HBH type cables are discussed in the project. It has been studied on cables with different cross-sections from 1 quad to 10 quad. After choosing the suitable material, the Common Analisi (CA) cable design program developed by the Prysmian Group was used for the design of the prototype cables. Sample production was carried out for the determined cross sections of the cables. The production stages include such stages as insulation, spinning, filling, armoring and sheathing. The spinning phase and the outer sheathing phases stand out as the most critical processes of the project. The formation of the core of the cable was examined in order to ensure both water tightness and the specification values of the electrical parameters. After the prototype production, electrical, material, water tightness and combustion tests were applied on the cables. As a result of the production capability and know-how gained within the scope of the project, an innovative product group was created.

Keywords: CPR, Cable Technology, Cable Tests, Signal Cable

ON MODIFIED BIVARIATE PICARD INTEGRAL OPERATORS WHICH FIX SOME EXPONENTIAL FUNCTIONS

Gümrah Uysal

Karabük University, ORCID: 0000-0001-7747-1706

Abstract

In this study, we handle bivariate counterparts of the Picard operators introduced by Agratini, Aral and Deniz [Positivity 21(3), 1189–1199 (2017)] and prove some theorems analogous to that of proved by Aral, Yılmaz and Deniz [Positivity 24(2), 427–439 (2020)].

Keywords: Modified bivariate Picard integral operators, weighted pointwise convergence, weighted Korovkin-type theorem

1. Introduction

In order to keep pace with recent emerging trends in approximation theory, by the aid of definitions of classical operators, the researchers prefer to derive new linear positive operators that fix some exponential functions to compare the convergence rates of various operators with their older versions. In particular, with the help of such developments, it is predicted that better results will be obtained by taking advantage of the breakthroughs of the approximation theory in applications, such as image restoration, three-dimensional modeling and so forth. Integral operators have left their mark on an important part of the entire literature of approximation theory. For further reading, we refer the readers to [10, 19]. Indeed, there is a wide spectrum on integral operators ranging from the Korovkin-type approximation (see [2]) to current engineering investigations.

The current study is addressed to the problem of exponential approximation in the sense of modifying operators in order to reproduce exponential functions by using bivariate Picard-type operators.

Let \mathbf{N} denote the set of all positive integers, \mathbf{R} denote the set of all real numbers and $\mathbf{R}^2 = \mathbf{R} \times \mathbf{R}$. Here, using ideas similar to that of [3, 12, 15], we consider a bivariate counterpart of modified Picard operators which are introduced in [1]:

$$P_n^*(g; x) = \frac{\sqrt{n}}{2} \int_{-\infty}^{\infty} g(\alpha_n(x) + s) e^{-\sqrt{n}|s|} ds, \quad x \in \mathbf{R}, n \in \mathbf{N}, \quad (1)$$

where $\alpha_n(x) = x - \alpha_n$ with $\alpha_n = \frac{1}{2a} \ln \left(\frac{n}{n-4a^2} \right)$, $a > 0$, $n \geq n_a := [4a^2] + 1$ and $[.]$ denotes floor function and $g, g: \mathbf{R} \rightarrow \mathbf{R}$, is a function such that the operators defined in equation (1) are well-defined. The operators defined in equation (1) are well-defined for the classes of functions for which the integrals finitely exist. Besides, they reproduce constant functions and e^{2ax} with $a > 0$ which are defined on \mathbf{R} . Also, as $a \rightarrow 0^+$ the classical versions of the operators defined in equation (1) are obtained. A bivariate counterpart of sequence of operators defined in equation (1) is as follows:

$$P_{n,m}^*(f; x, y) = \frac{\sqrt{nm}}{4} \int_{-\infty}^{\infty} \int_{-\infty}^{\infty} f(\alpha_n(x) + s, \beta_m(y) + t) e^{-\sqrt{n}|s|} e^{-\sqrt{m}|t|} ds dt, \quad (2)$$

where $(x, y) \in \mathbf{R}^2$, $n, m \in \mathbf{N}$, $\alpha_n(x) := x - \alpha_n$ with $\alpha_n := \frac{1}{2a} \ln \left(\frac{n}{n-4a^2} \right)$, where $a > 0$, $n \geq n_a := [4a^2] + 1$, $\beta_m(y) := y - \beta_m$ with $\beta_m := \frac{1}{2b} \ln \left(\frac{m}{m-4b^2} \right)$, where $b > 0$, $m \geq m_b := [4b^2] + 1$.

$[4b^2] + 1$ and $\lfloor \cdot \rfloor$ denotes floor function. These operators can be seen as a version of modified bivariate Picard operators fixing constant functions, e^{2ax} , e^{2by} and $e^{2(ax+by)}$ defined on \mathbf{R}^2 with $a, b > 0$. Also, as $a, b \rightarrow 0^+$ the classical versions of the operators defined in equation (2) are obtained. We should note that definition of multivariate Picard operators can be found in [3]. In [9], the authors considered the modification of bivariate Bernstein operators reproducing some exponential functions. For some approximation properties of univariate and multivariate Picard-type operators, we refer the interested readers to [3-6, 16, 17, 22, 23] and the references therein. Especially, some modifications of Picard-, Gauss-Weierstrass- and spline-type operators preserving some exponential functions can be found in [1, 5, 7, 24]. Also, some theorems about unified type univariate or multivariate integral operators are available in [7, 18-21].

In this study, we prove bivariate versions of some theorems given in [6]. Now, using exponential weighted Lebesgue space notion (see [8]; see also [6, 11, 16]) and following [8, 12, 16], mutatis mutandis, we consider the space $L_{p,a,b}(\mathbf{R}^2)$ with $a, b > 0$ and $1 \leq p < \infty$ which is consisting of all functions $f: \mathbf{R}^2 \rightarrow \mathbf{R}$ for which p -th power of $e^{-a|x|}e^{-b|y|}f(x, y)$ is integrable in the sense of Lebesgue, namely, $\int_{-\infty}^{\infty} \int_{-\infty}^{\infty} |e^{-a|x|}e^{-b|y|}f(x, y)|^p dx dy < \infty$. Here, $e^{-a|x|}e^{-b|y|}$ with $a, b > 0$ and $(x, y) \in \mathbf{R}^2$ is an exponential-type bivariate weight function.

The norm used in this space is given by

$$\|f\|_{L_{p,a,b}(\mathbf{R}^2)} := \left(\int_{-\infty}^{\infty} \int_{-\infty}^{\infty} |e^{-a|x|}e^{-b|y|}f(x, y)|^p dx dy \right)^{1/p}.$$

Throughout this manuscript, we assume, without specifically mentioning, that the sequence of operators $\{P_{n,m}^*\}_{\substack{n \geq n_a \\ m \geq m_b}}$ is as defined in equation (2) and is considered on appropriate domains

where integrals reach finite value.

2. Aims and Scope

Our aim is to state and prove bivariate analogues of Theorem 5.2, Theorem 6.2 and Theorem 6.3 in [6] for modified bivariate Picard operators.

3. Material and Method

Main materials of this study are the results of [1, 6, 13] and the classical proof schemes. Some closely related works can be given as [10, 19, 20].

4. Main Results

We start this part with an existence lemma concerning the operators defined in equation (2).

Lemma 4.1. If $f \in L_{p,a,b}(\mathbf{R}^2)$ ($1 \leq p < \infty$ and $a, b > 0$), then for sufficiently large numbers n and m , $P_{n,m}^*f \in L_{p,a,b}(\mathbf{R}^2)$ and the following inequality holds:

$$\|P_{n,m}^*f\|_{L_{p,a,b}(\mathbf{R}^2)} \leq e^{a|\alpha_n|}e^{b|\beta_m|} \frac{\sqrt{nm}}{(\sqrt{n}-a)(\sqrt{m}-b)} \|f\|_{L_{p,a,b}(\mathbf{R}^2)}.$$

Proof. Let $p > 1$. In view of notion of norm in $L_{p,a,b}(\mathbf{R}^2)$ and multidimensional version of generalized Minkowski inequality (see, for example, [19]), we directly have

$$\begin{aligned} \|P_{n,m}^*f\|_{L_{p,a,b}(\mathbf{R}^2)} &= \left(\int_{-\infty}^{\infty} \int_{-\infty}^{\infty} |e^{-a|x|}e^{-b|y|}P_{n,m}^*(f; x, y)|^p dx dy \right)^{1/p} \\ &\leq e^{a|\alpha_n|}e^{b|\beta_m|} \frac{\sqrt{nm}}{(\sqrt{n}-a)(\sqrt{m}-b)} \|f\|_{L_{p,a,b}(\mathbf{R}^2)}. \end{aligned}$$

The case $p = 1$ is similar. The proof is completed.

Definition 4.1 is based on the definition of μ -Lebesgue point given in [18] and Definition 6.1 given in [6]. This kind of Lebesgue point definition is more preferable from the practical point of view because it shortens the proof steps.

Definition 4.1. A point $(x, y) \in \mathbf{R}^2$ at which the limit relation expressed as

$$\lim_{h,k \rightarrow 0^+} \frac{1}{hk} \int_0^h \int_0^k \left| \frac{[f(\alpha_n(x) + s, \beta_m(y) + t) + f(\alpha_n(x) + s, \beta_m(y) - t) + f(\alpha_n(x) - s, \beta_m(y) + t) + f(\alpha_n(x) - s, \beta_m(y) - t) - 4f(x, y)]}{e^{as}e^{bt}} \right|^p dsdt = 0$$

holds is named as weighted p –Lebesgue point of $f \in L_{p,a,b}(\mathbf{R}^2)$ with $a, b > 0$ and $p \geq 1$.

Bivariate version of Theorem 6.2 in [6] for modified bivariate Picard operators is stated in the following theorem.

Theorem 4.1. If $f \in L_{p,a,b}(\mathbf{R}^2)$ ($1 \leq p < \infty$ and $a, b > 0$), then

$$\lim_{n,m \rightarrow \infty} P_{n,m}^*(f; x, y) = f(x, y)$$

holds at each $(x, y) \in L_{p,a,b}(\mathbf{R}^2)$ which stands for weighted p –Lebesgue point of $L_{p,a,b}(\mathbf{R}^2)$ whose definition is given in Definition 4.1.

Proof. Let $p = 1$. On the basis of the following well-known calculation

$$\frac{\sqrt{nm}}{4} \int_{-\infty}^{\infty} \int_{-\infty}^{\infty} e^{-\sqrt{n}|s|} e^{-\sqrt{m}|t|} dsdt = 1,$$

we have

$$P_{n,m}^*(f; x, y) = \frac{\sqrt{nm}}{4} \int_0^{\infty} \int_0^{\infty} \left[\begin{aligned} &[f(\alpha_n(x) + s, \beta_m(y) + t) + f(\alpha_n(x) + s, \beta_m(y) - t) \\ &+ f(\alpha_n(x) - s, \beta_m(y) + t) + f(\alpha_n(x) - s, \beta_m(y) - t)] \\ &\times e^{-\sqrt{n}s} e^{-\sqrt{m}t} \end{aligned} \right] dsdt.$$

Furthermore, the following equality holds:

$$\begin{aligned} &P_{n,m}^*(f; x, y) - f(x, y) \\ &= \frac{\sqrt{nm}}{4} \int_0^{\infty} \int_0^{\infty} \left[\begin{aligned} &[f(\alpha_n(x) + s, \beta_m(y) + t) + f(\alpha_n(x) + s, \beta_m(y) - t) \\ &+ f(\alpha_n(x) - s, \beta_m(y) + t) + f(\alpha_n(x) - s, \beta_m(y) - t) \\ &- 4f(x, y)] \end{aligned} \right] \\ &\times e^{-\sqrt{n}s} e^{-\sqrt{m}t} dsdt. \end{aligned}$$

Taking absolute value of both sides of the above equality and using monotonicity of Lebesgue integral, we obtain

$$\begin{aligned} &|P_{n,m}^*(f; x, y) - f(x, y)| \\ &\leq \frac{\sqrt{nm}}{4} \int_0^{\infty} \int_0^{\infty} \left| \begin{aligned} &[f(\alpha_n(x) + s, \beta_m(y) + t) + f(\alpha_n(x) + s, \beta_m(y) - t) \\ &+ f(\alpha_n(x) - s, \beta_m(y) + t) + f(\alpha_n(x) - s, \beta_m(y) - t) \\ &- 4f(x, y)] \end{aligned} \right| e^{-as} e^{-bt} \\ &\times e^{-(\sqrt{n}-a)s} e^{-(\sqrt{m}-b)t} dsdt. \end{aligned}$$

In view of Definition 4.1, for all $\varepsilon > 0$, there exists $\delta > 0$ such that

$$\int_0^h \int_0^k \left| \frac{[f(\alpha_n(x) + s, \beta_m(y) + t) + f(\alpha_n(x) + s, \beta_m(y) - t) + f(\alpha_n(x) - s, \beta_m(y) + t) + f(\alpha_n(x) - s, \beta_m(y) - t) - 4f(x, y)]}{e^{as}e^{bt}} \right| dsdt < \varepsilon hk, \quad (3)$$

where $0 < h, k \leq \delta$. For this $\delta > 0$, we can write

$$|P_{n,m}^*(f; x, y) - f(x, y)|$$

$$\begin{aligned}
 &\leq \frac{\sqrt{nm}}{4} \int_0^\delta \int_0^\delta \left| \frac{[f(\alpha_n(x) + s, \beta_m(y) + t) + f(\alpha_n(x) + s, \beta_m(y) - t) + f(\alpha_n(x) - s, \beta_m(y) + t) + f(\alpha_n(x) - s, \beta_m(y) - t) - 4f(x, y)]}{-4f(x, y)} \right| e^{-as} e^{-bt} \\
 &\quad \times e^{-(\sqrt{n}-a)s} e^{-(\sqrt{m}-b)t} ds dt \\
 &+ \frac{\sqrt{nm}}{4} \iint_D \left| \frac{[f(\alpha_n(x) + s, \beta_m(y) + t) + f(\alpha_n(x) + s, \beta_m(y) - t) + f(\alpha_n(x) - s, \beta_m(y) + t) + f(\alpha_n(x) - s, \beta_m(y) - t) - 4f(x, y)]}{-4f(x, y)} \right| e^{-as} e^{-bt} \\
 &\quad \times e^{-(\sqrt{n}-a)s} e^{-(\sqrt{m}-b)t} ds dt \\
 &=: A_{1,\delta}(n, m) + A_{2,\delta}(n, m),
 \end{aligned}$$

where $D = [0, \infty) \times [0, \infty) \setminus (0, \delta] \times (0, \delta]$.

Using inequality (3) and method of integration by parts for double integrals (see, for example, [14, 21]), we get

$$|A_{1,\delta}(n, m)| \leq \varepsilon \left(\frac{\sqrt{n}}{\sqrt{n}-a} \right) \left(\frac{\sqrt{m}}{\sqrt{m}-b} \right).$$

Since $\varepsilon > 0$ is arbitrarily small, for sufficiently large numbers n and m , we observe that $|A_{1,\delta}(n, m)| \rightarrow 0$ as $n, m \rightarrow \infty$ independent of δ . Also, we clearly have $|A_{2,\delta}(n, m)| \rightarrow 0$ as $n, m \rightarrow \infty$ for each fixed $\delta > 0$ and sufficiently large numbers n and m . The proof is completed for this case. For the case $p > 1$, the proof is analogous. The proof is completed.

A bivariate version of Theorem 5.2 in [6] for modified bivariate Picard integral operators is stated in the following theorem.

Theorem 4.2. If $f \in L_{p,a,b}(\mathbf{R}^2)$ ($1 \leq p < \infty$ and $a, b > 0$), then there holds

$$\lim_{n,m \rightarrow \infty} \|P_{n,m}^* f - f\|_{L_{p,a,b}(\mathbf{R}^2)} = 0.$$

Proof. In order to prove this theorem, we will use the criteria given in Theorem 2 in paper [13] by Gadjiev and Aral. First of all, our weight function clearly satisfies the conditions of indicated theorem. Keeping in mind that $P_{n,m}^*$ is a uniformly bounded sequence of linear positive operators acting on $L_{p,a,b}(\mathbf{R}^2)$ by Lemma 4.1, we will verify the following conditions in [13]:

- (i) $\lim_{n,m \rightarrow \infty} \|P_{n,m}^* e_0 - e_0\|_{L_{p,a,b}(\mathbf{R}^2)} = 0$
- (ii) $\lim_{n,m \rightarrow \infty} \|P_{n,m}^* e_1 - e_1\|_{L_{p,a,b}(\mathbf{R}^2)} = 0$
- (iii) $\lim_{n,m \rightarrow \infty} \|P_{n,m}^* e_2 - e_2\|_{L_{p,a,b}(\mathbf{R}^2)} = 0$
- (iv) $\lim_{n,m \rightarrow \infty} \|P_{n,m}^* e_3 - e_3\|_{L_{p,a,b}(\mathbf{R}^2)} = 0,$

where, $e_0(s, t) = 1$, $e_1(s, t) = s$, $e_2(s, t) = t$ and $e_3(s, t) = s^2 + t^2$ are bivariate test functions defined on \mathbf{R}^2 . To verify conditions (i)-(iv), in the sequel of this proof, we will use Lemma 1 in [1] in which the required moments for our proof exist for univariate case.

By Lemma 1 in [1], there hold:

$$P_{n,m}^*(e_0; x, y) = 1, \quad P_{n,m}^*(e_1; x, y) = \alpha_n(x), \quad P_{n,m}^*(e_2; x, y) = \beta_m(y) \quad \text{and} \quad P_{n,m}^*(e_3; x, y) = \alpha_n^2(x) + \beta_m^2(y) + \frac{2}{n} + \frac{2}{m}.$$

Using direct computation as in [6, 22], we get:

$$\begin{aligned}
 &\lim_{n,m \rightarrow \infty} \|P_{n,m}^* e_0 - e_0\|_{L_{p,a,b}(\mathbf{R}^2)} = 0, \\
 &\lim_{n,m \rightarrow \infty} \|P_{n,m}^* e_1 - e_1\|_{L_{p,a,b}(\mathbf{R}^2)} \\
 &= \lim_{n,m \rightarrow \infty} \left(\int_{-\infty}^{\infty} \int_{-\infty}^{\infty} |e^{-a|x|} e^{-b|y|} [\alpha_n(x) - x]|^p dx dy \right)^{1/p}
 \end{aligned}$$

$$= \lim_{n,m \rightarrow \infty} \frac{1}{2a} \ln \left(\frac{n}{n-4a^2} \right) \left(\frac{2}{ap} \right)^{\frac{1}{p}} \left(\frac{2}{bp} \right)^{\frac{1}{p}} = 0$$

and

$$\begin{aligned} & \lim_{n,m \rightarrow \infty} \|P_{n,m}^* e_2 - e_2\|_{L_{p,a,b}(\mathbf{R}^2)} \\ &= \lim_{n,m \rightarrow \infty} \left(\int_{-\infty}^{\infty} \int_{-\infty}^{\infty} |e^{-a|x|} e^{-b|y|} [\beta_m(y) - y]|^p dx dy \right)^{1/p} \\ &= \lim_{n,m \rightarrow \infty} \frac{1}{2b} \ln \left(\frac{m}{m-4b^2} \right) \left(\frac{2}{bp} \right)^{\frac{1}{p}} \left(\frac{2}{ap} \right)^{\frac{1}{p}} = 0. \end{aligned}$$

For the last case, we proceed in the following way:

$$\begin{aligned} & \|P_{n,m}^* e_3 - e_3\|_{L_{p,a,b}(\mathbf{R}^2)}^p \\ &= \int_{-\infty}^{\infty} \int_{-\infty}^{\infty} \left| e^{-a|x|} e^{-b|y|} [\alpha_n^2(x) + \beta_m^2(y) + \frac{2}{n} + \frac{2}{m} - x^2 - y^2] \right|^p dx dy \\ &\leq 2^p \int_{-\infty}^{\infty} \int_{-\infty}^{\infty} e^{-pa|x|} e^{-pb|y|} |\alpha_n^2(x) - x^2 + \beta_m^2(y) - y^2|^p dx dy \\ &\quad + 2^p \int_{-\infty}^{\infty} \int_{-\infty}^{\infty} e^{-pa|x|} e^{-pb|y|} \left| \frac{2}{n} + \frac{2}{m} \right|^p dx dy \\ &\leq 2^{2p} \int_{-\infty}^{\infty} \int_{-\infty}^{\infty} e^{-pa|x|} e^{-pb|y|} |\alpha_n^2(x) - x^2|^p dx dy \\ &\quad + 2^{2p} \int_{-\infty}^{\infty} \int_{-\infty}^{\infty} e^{-pa|x|} e^{-pb|y|} |\beta_m^2(y) - y^2|^p dx dy \\ &\quad + 2^p \int_{-\infty}^{\infty} \int_{-\infty}^{\infty} e^{-pa|x|} e^{-pb|y|} \left| \frac{2}{n} + \frac{2}{m} \right|^p dx dy \\ &=: 2^{2p} I_1(n, m) + 2^{2p} I_2(n, m) + 2^p I_3(n, m). \end{aligned}$$

Simple calculations lead to

$$\lim_{n,m \rightarrow \infty} I_1(n, m) = 0,$$

since

$$\begin{aligned} I_1(n, m) &\leq 2^p \frac{1}{2^{2p} a^{2p}} \frac{2}{bp} \ln^{2p} \left(\frac{n}{n-4a^2} \right) \frac{2}{ap} \\ &\quad + 2^{2p} \frac{1}{2^p a^p} \frac{2}{bp} \ln^p \left(\frac{n}{n-4a^2} \right) \frac{2}{a} (ap)^{-p} \Gamma[p]; \end{aligned}$$

$$\lim_{n,m \rightarrow \infty} I_2(n, m) = 0,$$

since

$$\begin{aligned} I_2(n, m) &\leq 2^p \frac{1}{2^{2p} b^{2p}} \frac{2}{ap} \ln^{2p} \left(\frac{m}{m-4b^2} \right) \frac{2}{bp} \\ &\quad + 2^{2p} \frac{1}{2^p b^p} \frac{2}{ap} \ln^p \left(\frac{m}{m-4b^2} \right) \frac{2}{b} (bp)^{-p} \Gamma[p], \end{aligned}$$

and directly there holds that

$$\lim_{n,m \rightarrow \infty} I_3(n, m) = 0.$$

Thus, the proof is completed.

Now, we prove a bivariate version of Theorem 6.3 in [6].

Theorem 4.3. Assume that $f \in L_{p,a,b}(\mathbf{R}^2)$ ($1 \leq p < \infty$ and $a, b > 0$) and the following limit relation:

$$\lim_{h,k \rightarrow 0^+} \frac{1}{hk} \int_0^h \int_0^k \left\| \begin{aligned} &[f(\alpha_n(\cdot) + s, \beta_m(\cdot) + t) + f(\alpha_n(\cdot) + s, \beta_m(\cdot) - t) \\ &+ f(\alpha_n(\cdot) - s, \beta_m(\cdot) + t) + f(\alpha_n(\cdot) - s, \beta_m(\cdot) - t) \\ &- 4f(\cdot, \cdot)] \end{aligned} \right\|_{L_{p,a,b}(\mathbf{R}^2)} ds dt$$

= 0

holds.

Then

$$\lim_{n,m \rightarrow \infty} \|P_{n,m}^* f - f\|_{L_{p,a,b}(\mathbf{R}^2)} = 0.$$

Proof. Let $p > 1$. In view of generalized Minkowski inequality (see, for e.g., [19]), we see that

$$\begin{aligned} &\|P_{n,m}^* f - f\|_{L_{p,a,b}(\mathbf{R}^2)} \\ &\leq \frac{\sqrt{nm}}{4} \int_0^\infty \int_0^\infty \left\| \begin{aligned} &[f(\alpha_n(\cdot) + s, \beta_m(\cdot) + t) + f(\alpha_n(\cdot) + s, \beta_m(\cdot) - t) \\ &+ f(\alpha_n(\cdot) - s, \beta_m(\cdot) + t) + f(\alpha_n(\cdot) - s, \beta_m(\cdot) - t) \\ &- 4f(\cdot, \cdot)] \end{aligned} \right\|_{L_{p,a,b}(\mathbf{R}^2)} \end{aligned}$$

$$\times e^{-\sqrt{ns}} e^{-\sqrt{mt}} ds dt$$

holds. We prove similar to the classical pointwise convergence theorem's way.

Now, in view of suppositions of our theorem, for all $\varepsilon > 0$, there exists $\delta > 0$ such that

$$\begin{aligned} &\int_0^h \int_0^k \left\| \begin{aligned} &[f(\alpha_n(\cdot) + s, \beta_m(\cdot) + t) + f(\alpha_n(\cdot) + s, \beta_m(\cdot) - t) \\ &+ f(\alpha_n(\cdot) - s, \beta_m(\cdot) + t) + f(\alpha_n(\cdot) - s, \beta_m(\cdot) - t) \\ &- 4f(\cdot, \cdot)] \end{aligned} \right\|_{L_{p,a,b}(\mathbf{R}^2)} ds dt \\ &< \varepsilon hk, \end{aligned} \tag{4}$$

where $0 < h, k \leq \delta$.

For this $\delta > 0$, we may split the integral in such a way that the following inequality holds:

$$\begin{aligned} &\|P_{n,m}^* f - f\|_{L_{p,a,b}(\mathbf{R}^2)} \\ &\leq \frac{\sqrt{nm}}{4} \int_0^\delta \int_0^\delta \left\| \begin{aligned} &[f(\alpha_n(\cdot) + s, \beta_m(\cdot) + t) + f(\alpha_n(\cdot) + s, \beta_m(\cdot) - t) \\ &+ f(\alpha_n(\cdot) - s, \beta_m(\cdot) + t) + f(\alpha_n(\cdot) - s, \beta_m(\cdot) - t) \\ &- 4f(\cdot, \cdot)] \end{aligned} \right\|_{L_{p,a,b}(\mathbf{R}^2)} \\ &\times e^{-\sqrt{ns}} e^{-\sqrt{mt}} ds dt \\ &+ \frac{\sqrt{nm}}{4} \iint_D \left\| \begin{aligned} &[f(\alpha_n(\cdot) + s, \beta_m(\cdot) + t) + f(\alpha_n(\cdot) + s, \beta_m(\cdot) - t) \\ &+ f(\alpha_n(\cdot) - s, \beta_m(\cdot) + t) + f(\alpha_n(\cdot) - s, \beta_m(\cdot) - t) \\ &- 4f(\cdot, \cdot)] \end{aligned} \right\|_{L_{p,a,b}(\mathbf{R}^2)} \end{aligned}$$

$$\times e^{-\sqrt{ns}} e^{-\sqrt{mt}} ds dt$$

$$=: G_{1,\delta}(n, m) + G_{2,\delta}(n, m),$$

where $D = [0, \infty) \times [0, \infty) \setminus (0, \delta] \times (0, \delta]$.

Using inequality (4) and method of integration by parts for double integrals (see, for example, [14, 21]), we have $|A_{1,\delta}(n, m)| \leq \varepsilon$. Since $\varepsilon > 0$ is arbitrarily small, we observe that $|G_{1,\delta}(n, m)| \rightarrow 0$ as $n, m \rightarrow \infty$ independent of δ . Since our kernel function is an approximate identity (see [10]), we clearly have $|G_{2,\delta}(n, m)| \rightarrow 0$ as $n, m \rightarrow \infty$ for each fixed $\delta > 0$ and sufficiently large numbers n and m . The proof is completed for this case. For the case $p = 1$, the proof is analogous. The proof is completed.

5. Conclusion

In this study, some theorems analogous to that of given in [6] for the operators defined in equation (2). We can say that bivariate case is consistent with univariate case for proved theorems. In future works, weighted uniform convergence in appropriate function spaces, and rate of convergence using a modulus of continuity are thought to be examined for indicated operators.

References

1. O. Agratini, A. Aral and E. Deniz, “On two classes of approximation processes of integral type”, *Positivity*, vol. 21, pp. 1189–1199, 2017.
2. F. Altomare and M. Campiti, *Korovkin-type Approximation Theory and its Applications*, Appendix A by Michael Pannenberg and Appendix B by Ferdinand Beckhoff, *De Gruyter Studies in Mathematics* 17, Walter de Gruyter & Co., Berlin, 1994.
3. G. A. Anastassiou and S. G. Gal, *Approximation Theory: Moduli of Continuity and Global Smoothness Preservation*, Birkhäuser Boston Inc., Boston, MA, 2000.
4. G. A. Anastassiou and A. Aral, “Generalized Picard singular integrals”, *Comput. Math. Appl.*, vol. 57, pp. 821–830, 2009.
5. A. Aral, “On generalized Picard integral operators”, in: *Advances in Summability and Approximation Theory*, Springer, Singapore, pp. 157–168, 2018.
6. A. Aral, B. Yılmaz and E. Deniz, “Weighted approximation by modified Picard operators”, *Positivity*, vol. 24, pp. 427–439, 2020.
7. C. Bardaro, I. Mantellini, G. Uysal and B. Yılmaz, “A class of integral operators that fix exponential functions”, *Mediterr. J. Math.*, vol. 18, Paper No. 179, pp. 1–21, 2021.
8. M. Becker, D. Kucharski and R. J. Nessel, “Global approximation theorems for the Szász-Mirakjan operators in exponential weight spaces”, in: *Linear Spaces and Approximation (Proc. Conf., Math. Res. Inst., Oberwolfach, 1977)*, *Internat. Ser. Numer. Math.*, vol. 40, Birkhäuser, Basel, pp. 319–333, 1978.
9. K. Bozkurt, F. Özaraç and A. Aral, “Bivariate Bernstein polynomials that reproduce exponential functions”, *Commun. Fac. Sci. Univ. Ank. Ser. A1 Math. Stat.*, vol. 70, pp. 541–554, 2021.
10. P. L. Butzer and R. J. Nessel, *Fourier Analysis and Approximation, Volume 1: One-dimensional Theory*, *Pure and Applied Mathematics*, vol. 40. Academic Press, New York-London, 1971.
11. Z. Ditzian and V. Totik, *Moduli of Smoothness*, Springer, New York, 1987.
12. B. Firlej, M. Lesniewicz and L. Rempulska, “Approximation of functions two variables by some operators in weighted spaces”, *Rendiconti del Seminario Matematico della Università di Padova*, vol. 101, pp. 63–82, 1999.
13. A. D. Gadjeiev and A. Aral, “Weighted L_p -approximation with positive linear operators on unbounded sets”, *Appl. Math. Lett.*, vol. 20, pp. 1046–1051, 2007.
14. E. W. Hobson, *The Theory of Functions of a Real Variable and the Theory of Fourier's Series*, Cambridge University Press (Kessinger Publishing, LLC reprint 2008), vol. 1, England, 1921.
15. A. İzgi, “Order of approximation of functions of two variables by new type gamma operators”, *Gen. Math.*, vol. 17, pp. 23–32, 2009.
16. A. Lesniewicz, L. Rempulska and J. Wasiak, “Approximation properties of the Picard singular integral in exponential weighted spaces”, *Publ. Math.*, vol. 40, pp. 233–242, 1996.

17. L. Rempulska and K. Tomczak, “On some properties of the Picard operators”, Arch. Math. (Brno), vol. 45, pp. 125–135, 2009.
18. B. Rydzewska, “Approximation des fonctions de deux variables par des integrales singulieres doubles”, Fasc. Math., vol. 8, pp. 35–45, 1974.
19. E. M. Stein, Singular Integrals and Differentiability Properties of Functions, Princeton University Press, New Jersey, 1970.
20. S. Siudut, “Some remarks on double singular integrals”, Comment. Math. (Prace Mat.), vol. 34, pp. 173–181, 1994.
21. R. Taberski, “On double integrals and Fourier series”, Ann. Polon. Math., vol. 15, pp. 97–115, 1964.
22. G. Uysal, “Approximation by m-singular modified Picard operators”, in: Proceeding Book of International Symposium on Recent Developments, in Science, Technology and Social Sciences, 20-22 December, Ankara, pp. 255-261, 2019.
23. G. Uysal, “Normwise convergence of m-singular modified Picard operators”, in: Proceeding Book of International May 19 Innovative Scientific Approaches Congress II, 27-29 December, Samsun, pp. 582-588, 2019.
24. B. Yılmaz, G. Uysal, A. Aral, “Reconstruction of two approximation processes in order to reproduce e^{ax} and e^{2ax} , $a > 0$ ”, J. Math. Inequal., vol. 15, pp. 1101-1118, 2021.

CURING EFFECT IN RTM PROCESS

Ahmed Ouezgan

Applied Research Team on Composites, Management, and Innovation, High National School of Electricity and Mechanics (ENSEM), Hassan II University of Casablanca, Morocco.

Said Adima

Applied Research Team on Composites, Management, and Innovation, High National School of Electricity and Mechanics (ENSEM), Hassan II University of Casablanca, Morocco.

Aziz Maziri

Applied Research Team on Composites, Management, and Innovation, High National School of Electricity and Mechanics (ENSEM), Hassan II University of Casablanca, Morocco.

El Hassan Mallil

Applied Research Team on Composites, Management, and Innovation, High National School of Electricity and Mechanics (ENSEM), Hassan II University of Casablanca, Morocco.

Jamal Echaabi

Applied Research Team on Composites, Management, and Innovation, High National School of Electricity and Mechanics (ENSEM), Hassan II University of Casablanca, Morocco.

Abstract.

The resin transfer molding (RTM) process is a composite manufacturing processing, belongs to the liquid composite molding (LCM) family. In this process, a fibrous reinforcement materials are first cut and placed into a stationary bed of a rigid mold, then a thermosetting resin is injected, through an injection machine, to fill the fabric preform. Then, the saturated preform is polymerized, when this stage is finished, the part is ready to be ejected from the mold. The isothermal RTM technique is widely used by many industrial sectors, such as automotive and aeronautic for manufacturing small to mid-size high performance composite components. However, this technique has major limitation in manufacturing large composite parts with high fiber volume fraction due to the pressure equipment, cost investment and process time that dramatically increases proportional to the part dimension of the manufactured part. One of the promising strategies to overcome this limitations is to control the evolution of resin viscosity through the time by changing temperature, but this leads to accelerate the degree of cure which in turns increases the viscosity of resin and excites the polymerization of resin before the part is completely filled. In this paper, the curing effect during the RTM filling stage is investigated to study its effects on the filling time, resin pressure distribution and resin flow front profile.

Keywords: Isothermal RTM; Non-isothermal RTM; curing effect; filling stage.

AI-ASSISTED COMPARISON OF LIVE NETWORK MEASUREMENTS AND PERFORMANCE METRICS IN DWDM SYSTEMS

Mustafa Serdar Osmanca

Gazi Üniversitesi, Fen Bilimleri Enstitüsü

ORCID NO: 0000-0002-6939-2765

Prof. Dr. Murat YÜCEL

Gazi Üniversitesi, Teknoloji Fakültesi, Elektrik-Elektronik Müh.

ORCID NO: 0000-0002-0349-4013

ABSTRACT

Fast and complete transmission of data is very important in communication technology. Systems with increased capacity should be used in proportion to the increasing need for data transmission and the increasing number of users. Fiber optic communication systems are widely used in communication to meet these expectations. Fiber optic networks have become the most preferred systems with their high bandwidth, high speed and transmission capacity up to very long distances.

Performance monitoring in fiber optic communication systems is very important for the system to work efficiently. One of the most important indicators in performance data is the FEC (Forward Error Correction) parameter. In order to determine the FEC parameter in the most accurate way, artificial intelligence-assisted determination of the input parameters in the live network and evaluation of which parameter is the most effective are presented. As input, optical channel capacity, fiber distance traveled by optical channel, total regeneration number of optical channel, average span lengths, average cable attenuation between two dwdm systems, expected cable attenuation based on fiber optic cable distance and total number of channels in dwdm link are used. In the light of these data, it has been observed that the decision tree artificial intelligence algorithm estimates the most accurate FEC parameter. The most important data affecting the FEC parameter as input were also examined, and it was determined that these were the number of channels, fiber attenuation and fiber distance. These data were also compared with the network parameters and it was observed that they exactly matched the live network parameters.

Key Words: WDM, Decision tree, FEC, fiber optic communication, span loss

1. INTRODUCTION

With the development of technology, there has been an extraordinary increase in voice, data and image transmission. In this situation, the need for higher speed has increased the need for fiber optic communication systems that provide transmission at the speed of light. There is almost no signal loss in fiber optic cables. Data transmission over longer distances can be achieved with fiber optic systems. Fiber optic cable is highly resistant to environmental effects and provides information security. Although the initial cost is higher, fiber optic systems provide the most efficient, economical and shortest time to access information.

The increasing need for faster data transmission in the world causes new researches on fiber optic communication systems. In this study, WDM, a fiber optic transmission technique that provides data transmission over the same medium by using multiple different light wavelengths in optical communication, and FEC (Forwarding Error Correction), which is followed as a quality parameter in this transmission technique, were examined. The effect of 7 inputs, which are effective on the FEC parameter, is observed over the live network using the Decision tree algorithm, artificial intelligence and machine learning technique. The estimation of the specified input and FEC output with artificial intelligence algorithm, comparison and interpretation of this estimation with the real network outputs were made.

2. FIBER OPTIC COMMUNICATION SYSTEMS

Optical communication system consists of three main parts; receiver, transmission medium and transmitter. Optical communication systems use high carrier frequencies (~ 100 THz) in the visible or near infrared region of the electromagnetic spectrum. To distinguish them from microwave systems whose carrier frequency is typically by five orders of magnitude (~ 1 GHz) smaller, they are sometimes referred to as light wave systems. Fiber optic communication systems are light wave systems that use optical fibers to transmit information [1].

WDM is a technology that provides a significant increase in total data rate by multiplexing optical signals of different wavelengths, each in a separate transmitter, allowing them to be carried over a single optical fiber. The use of WDM effectively increases the total bandwidth per optical fiber by summing the bitrate of each channel. Thus, a WDM system can transmit information at a terabit capacity per second (Tb/s) [2].

Optical modulators are elements that perform different functions such as phase, amplitude, frequency and polarization modulation in optical fiber systems, and most of them act as solid state elements. The source light is modulated by the electrical control signal by changing the optical properties of the modulator material. The control signal is associated with the properties of matter through electro-optical, acoustic-optic and magneto-optical mechanisms [3].

Optical modulators are also divided into analog or digital modulators according to the type of information signal used. In analog modulation, the light change emitted from the optical source is continuous, while in digital modulation there are discrete changes in light intensity. Digital modulated systems have a lower signal-to-noise ratio than analog modulated systems. The analog quantities used in modulation are density, optical phase, polarization, and color. In digital modulation, frequency modulation, on-off density modulation, Doppler shift, pulse width or delay time modulation and hybrid systems techniques are used [3].

The basic performance indicators for high-speed transmissions in the Optical Transmission layer are as follows, and the most important performance indicator calculated with these performance inputs is the FEC (Forwarding Error Correction) parameter. Input values that may have an effect on the FEC values taken as output in the data set in this study are summarized below:

- A) Optical Channel Capacity (10Gb/s, 40Gb/s, 100Gb/s, etc) (OCH Capacity)
- B) Total fiber distance traveled by Optical Channel (km) (Total link Distance)
- C) Total optic regeneration number of the Optic Canal (Span Number),
- D) Average span lengths (Total distance traveled by Optical Channel / Total optical regeneration number of Optical Channel) (Average Link Span Length)
- E) A to B Average cable attenuation between two DWDM systems, (dB) (average total attenuation from A to B)
- F) B to A Average cable attenuation between two DWDM systems, (dB) (average of total attenuation from B to A)
- G) Fiber optic cable expected attenuation value (Total fiber optic cable expected attenuation value)
- H) Average Fiber Kilometric Loss (dB/km),
- I) Number of channels in DWDM links,

The explanation of the FEC parameter is;

Since the data ,which is wanted to be transmitted through a transmission line, face with error during transmission, error control and correction concepts are being studied. Coding has an important part in error controlling and it is performed by adding extra bits to the each message and every code word has limited error correction capability. FEC fixes transmission line errors within some limits, without retransmission is needed [4]

3.SIMULATION SETUP

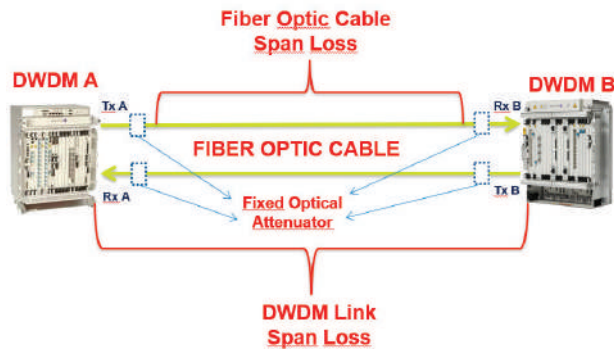


Figure 1: Diagram of 2 DWDM systems Used in Live Network

The network, which the examinations are made, is a fiber optic mesh connected to each other at different distances and carries active traffic flows. The fact that the obtained data are real measurement values has ensured that the outputs are more realistic and reliable. The most important feature of this network is that there are multiple connections between large and different DWDM systems. Similarly, there are different channel numbers and different channel rates carried from each channel. In Figure 1, a sample connection diagram between the two systems of the examined network is given. The whole network is connected to each other in this design.



Figure 2: Turkey-wide DWDM Map

In Figure 2, as an example, the dwdm map of Turkey and its links can be seen.

As the Data Set, the FEC (Forward Error Correction) values, which is one of the most important quality parameters of the optical channels carried on the DWDM network, investigated with artificial intelligence algorithms. It are used to determine which of the metrics examined can cause the distortions in case of high the FEC value, which indicates that there are distortions during the transportation of the service.

In DWDM systems, there are channel cards with optical channel source and carrier. Errors in the service are corrected due to the FEC algorithm, eliminating the problems that occur during the transfer of data and ensuring that the migrated services are not affected. However, the high FEC errors also show that there are some problems in DWDM optical channels, and in this study, studies have been carried out on what metrics may cause the FEC value to be high in DWDM Optical Channels.

The decision tree, which is the artificial intelligence algorithm used in the examinations, can be briefly mentioned as follows;

In this study classification method that creates a model in the form of a tree structure consisting of decision nodes and leaf nodes according to feature and target is used. The decision tree algorithm is developed by dividing the data set into smaller pieces. The first node is called the root node. A decision tree can consist of both categorical and numerical data and a decision node may contain one or more branches.(5)

The summary table taken from the live network as a data set is as follows;

FEC	OCH Adı	OCH KAPASİTESİ (10G, 40G, 100G)	TOPLAM LİNK MESAFESİ (KM)	SPAN SAYISI	LİNK FİBER UZUNLUĞU	A TO B FİBER KABLO 1550 NM TOPLAM ZATIFLAMASI	B TO A FİBER KABLO 1550 NM TOPLAM ZATIFLAMASI	FİBER KABLO 1550 NM BEKLENEN ZATIFLAMA	FİBER KİLOMETRİK KAYBI (dB/km)	LİNK KANAL SAYISI
188784226426	Ulus_10634-Gantep(Sahinbey)_12783-OCH-265314	100000	1100	18	61	20	18	275	0,33	77
188784226426	Hatay_13106-Kilis_17901-OCH-83478	10000	915	16	57	279	278	229	4,88	58
188654204621	Bozayaz_13301-Mersin_B.Evler_13307-OCH-83967	10000	913	12	76	281	264	228	3,70	56
17253253595	Mersin_13305-Adana_10111-OCH-45940	100000	89	2	45	4	7	22	0,09	64
171536459762	Kars_13601-Erzurum_Saraylı_1250-OCH-81627	10000	761	12	63	218	221	190	3,43	58
14441868283	Hatay_13106-Kilis_17901-OCH-83478	10000	915	16	57	279	277	229	4,88	58
127528229242	Bozayaz_13301-Mersin_B.Evler_13307-OCH-83967	10000	913	12	76	281	264	228	3,69	56
9759563677	Kars_13601-Erzurum_Saraylı_1250-OCH-81627	10000	761	12	63	217	221	190	3,42	58
50612931046	Ulus_10630_100G-Kapitan_Sari_18608-OCH-04108	10000	11072	208	53	2510	2514	2768	47,15	17
39275210198	NE_12221-Kapitan_Mavi_18604-OCH-272087_FAZ3-C	10000	426	20	21	168	162	106	7,89	78
36524381446	Kayseri_13805-Incesu_10615-OCH-85953	10000	1186	15	79	263	276	297	3,33	32
36524381446	Kayseri_13805-Incesu_10615-OCH-85953	10000	1186	15	79	263	276	297	3,33	32
34963551392	ULUS_KUCUKSANAYI_ASON_CH1_TRANSIT_061651	10000	6637	110	60	1936	1847	1659	32,09	0

Table:1 Example of Dataset Set

About 800 channel data sets and the FEC parameter values for each channel from the live network are used as database. With the Decision tree algorithm, each input value was handled individually and analyzed according to the FEC value, and estimation was made with continuous values.

20% of the data set was used as validation data. According to the results of the analysis:

Max tree depth	6
Train RMSE	17469779731.6389
Validation RMSE	1390551895.6316
Training time (sec)	0.0094

Table:2 Decision Tree Algorithm outputs

For the purpose of this study, the closest estimation sample to the FEC value from the Live Network was obtained with the Decision Tree algorithm.

In order to find out which parameter is the most important affecting the FEC value, the outputs were observed by making changes in the data set.

The most important input affecting the FEC value in these parameters are Channel Number (I), Fiber Attenuation (D) and Fiber Distance (E) and these values match exactly when compared to the live network.

4. RESULTS AND DISCUSSION

The most important indicators taken from the Live Network in terms of effect on the FEC parameter were analyzed with the decision tree mechanism, which is one of the artificial intelligence algorithms.

In this analysis; The FEC parameter is used as the output value. It has been observed that the decision tree algorithm predicts the closest output to the Live network value as accuracy in the data set.

As a result the effect of the inputs in the data set on the FEC parameter is observed separately and it has been observed that the parameters that affect the FEC parameter are Channel Number (I), Fiber Attenuation (D) and Fiber Distance (E) which overlaps with the live network measurements.

5. REFERENCES

- [1] Agrawal, G. P., Fiber-Optic Communication Systems, Wiley-Interscience, New York, 2010.
- [2] Hiçdurmaz, Ö., Yüksek Hızlı DWDM Sistemlerinde Optik Fiberdeki FWM Ve ASE Etkisi Altında İletim Performansının Analizi ve Optimizasyonu, Doktora Tezi, Uludağ Üniversitesi, Fen Bilimleri Enstitüsü, Bursa, 2013.
- [3] Tarı, E., Optik Modülatörlerde Performans Analizi, Yüksek Lisans Tezi, Yıldız Teknik Üniversitesi, Fen Bilimleri Enstitüsü, İstanbul, 2010.
- (4) Das, A., Digital Communication: Principles and System Modelling. Germany: Springer. 191-211, 2010.
- (5) Allett, E.J., 1986. Environmental impact assessment and decision analysis. Journal of Operational Research Society, 37(9)

EFFECT OF TIN SUBSTITUTION ON STRUCTURAL, ELECTRICAL AND HUMIDITY-SENSING CHARACTERISTICS OF TUNGSTEN OXIDE NANOPARTICLES

Karunesh Tiwari

Department of Physics, Babu Banarasi Das University Lucknow, Uttar Pradesh, India-226028

Anam Zaidi

Department of Physics, Babu Banarasi Das University Lucknow, Uttar Pradesh, India-226028

Shalini

Department of Physics, Babu Banarasi Das University Lucknow, Uttar Pradesh, India-226028

Abstract: In this paper we report humidity sensing studies of $\text{SnO}_2\text{-WO}_3$ nanocomposite. Pellets of $\text{SnO}_2\text{-WO}_3$ nanocomposites have been made by mechanical mixing of SnO_2 and WO_3 powder in weight % ratio of 5% : 95% and annealing them from 300°C - 600°C for 3 hours. Sensitivities of pellets annealed at 300°C, 400°C, 500°C and 600°C are 4.67, 3.27, 6.53 and 23.81 $\text{M}\Omega/\%\text{RH}$ respectively. The SEM micrograph and XRD pattern confirm that grains are of nanosize. The hysteresis (between humidification and desiccation, measured in the RH range of 15 – 90 %RH) is less than 6 %RH. . Activation energy is 0.069 eV in the temperature range 50°C to 300°C. The response time and recovery time of the sample annealed at 600°C is 138 seconds and 874 seconds respectively.

Keywords: SnO_2 , WO_3 , nanocomposite, Humidity sensor, Activation energy

BIO-INSPIRED HYBRIDIZATION OF ARTIFICIAL NEURAL NETWORKS: AN APPLICATION FOR CLASSIFICATION TASKS

Ouail MJAHER

Faculty of Sciences and Technology, Department of Applied Mathematics and Computer Sciences, Cadi Ayyad University, Marrakech, Morocco

Salah EL HADAJ

Faculty of Sciences and Technology, Department of Applied Mathematics and Computer Sciences, Cadi Ayyad University, Marrakech, Morocco

El Mahdi ELGUARMAH

Faculty of Sciences and Technology, Department of Applied Mathematics and Computer Sciences, Cadi Ayyad University, Marrakech, Morocco
Royal School of Aeronautics, Department of Applied Mathematics and Computer Sciences, Marrakech, Morocco

Soukaina MJAHER

Faculty of Sciences and Technology, Department of Applied Mathematics and Computer Sciences, Cadi Ayyad University, Marrakech, Morocco

Abstract

In this work, series of hybridized artificial neural network (ANN) models with bio-inspired metaheuristic algorithms such as particle swarm optimization (PSO-ANN), differential evolution (DE-ANN), genetic algorithm (GA-ANN) and ant lion optimizer (ALO-ANN) algorithms, were designed for classifying four kinds of data.

Initially, a complete analysis is carried out using the back-propagation (BP) algorithm to optimize the various neural networks. We explored architectures with one, two and three layers. Secondly, the connection weights and bias of neurons in each of the previous architectures are optimized using the GA, PSO, ALO and DE metaheuristics. A preliminary investigation allowed to refine the choices concerning the parameters of each algorithm or metaheuristic. The four data types selected belong to different domains and present a variety of choices between the number of classes, variables and examples. Data are characterized by the most discriminating variables. As parameters of performance, efficiencies, purities and errors of classifications are computed from the confusion matrices. Due to the stochastic nature of metaheuristics, each of these optimization algorithms was executed for 500 epochs and 20 runs for stability.

The overall performances are promising; the obtained results are in agreement with the complexity of the classification tasks. In all simulation runs, it can be observed that metaheuristic algorithms have been able to find optimal parameters. GA-ANN and ALO-ANN approaches are comparative, when PSO-ANN and DE-ANN show better performance. PSO allows to minimize the classification error

and to improve efficiencies and purities of classifications. It can be clearly shown that all the results using the PSO based ANN has higher values of efficiency and therefore higher discrimination ability. The analysis takes into account the dependence of the results with respect to the parameters of each method. A compromise between good performance and acceptable computing time is also sought.

Keywords: Classification, Metaheuristic, Neural Network, Optimization

1. INTRODUCTION

The general goal of artificial intelligence is to imitate the ability of human brain to observe, analyze, learn, and make a decision, especially for complex problem [1]. A considerable amount of research in the field of Machine Learning (ML) is concerned with developing methods that automate classification tasks [2] in several real-world applications, in such fields as civil engineering [3,4], medicine [5], land use [6], high energy physics [7-8], investment [9], and marketing [10].

The use of metaheuristic to optimize ML method helps to achieve faster convergence with minimum iterations, which in turn increases the efficiency of an algorithm. In recent years, many bio-inspired meta-heuristic optimization algorithms were developed and successfully used for optimization of machine learning algorithms like Artificial Neural Network (ANN) [11-20].

This paper focuses on four meta-heuristic optimization algorithms, such as Genetic Algorithm (GA), Particle Swarm Optimization (PSO), Ant Lion Optimization (ALO) and Differential Evolution (DE), to find the optimal solution for ANN learning and their application to classification problems. These hybrid ANNs classifiers are applied to four datasets relevant to classification and prediction taken from public Machine Learning Repository such as Mammographic Mass Data Set [21], Seed Data Set [22], Somerville Happiness Survey [23] and Rotor Fault Diagnosis Data Set [24].

The rest of the paper is organized as follows: Section 2 exposes the ANN principle and the four chosen meta-heuristic optimization algorithms and presents the four considered datasets. In Section 3 the comparative results between Backpropagation Neural Network (BPNN) and the four hybrid ANN (PSO-ANN, ALO-ANN, GA-ANN and DE-ANN) are given. Section 4 is dedicated to conclusions and perspectives of our work.

2. METHODOLOGY AND DATA

As we had introduced, our work consists in optimizing a neural network by the use of metaheuristic methods. In this section, we will give an overview of the methods adopted as well as the data having been the subject of our various applications.

2.1. Back-propagation Neural Network (BPNN)

The architecture of a multilayered neural network is organized into levels of nodes (neurons): one input layer, one output layer and one or several hidden layers [25, 26]. Each neuron in a level l is thus directly connected to all the neurons of the following layer $(l+1)$ (Figure 1). All the neurons i of a layer l in this network, produce a response $S_i^{(l)}$ by computing a weighted sum of the outputs $S_j^{(l-1)}$ of the j neurons in the layer $(l-1)$ to which they are connected. This sum is then transformed through a nonlinear sigmoid function f :

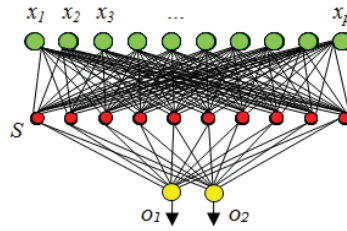


Figure 1. Architecture of a multilayer neural network

$$S_i^{(l)} = f\left(\sum_{j=1}^{N_{l-1}} W_{ij}^{(l)} S_j^{(l-1)} - \theta_i^{(l)}\right) \quad (1)$$

where $\theta_i^{(1)}$ is the threshold of the neuron i in layer l , $W_{ij}^{(1)}$ the connection weight between the neurons i of layer l and j (of layer $l-1$), N_{l-1} : Number of units in the layer $l-1$

$$f(x) = \frac{1-e^{-x}}{1+e^{-x}} \quad (2)$$

Notice that, for $l = 1$, $S_i^{(1)} = x_i$ ($i=1, \dots, n$), and for a q layer network the outputs are: $o_i = S_i^{(q)}$, ($i=1, \dots, m$). The training of this network is supervised and uses the "gradient descent method" with an error back-propagation algorithm which is composed by the following steps [27]:

a) Propagation of an event p across the network. Then all the neurons responses are computed.

b) Error back-propagation: for every introduced data, the network seeks to minimize, on the output layer, a quadratic error $E^{(p)}$ existing between the output (feature) value $o_i^{(p)}$ and the desired output or target value $d_i^{(p)}$ of the m neurons.

$$E^{(p)} = \sum_{i=1}^m (o_i^{(p)} - d_i^{(p)})^2 \quad (3)$$

Thus the gradient of $E^{(p)}$ is back-propagated to modify the weights' value. For an arbitrary weight (or threshold) W_{ij} :

$$W_{ij}(t) = W_{ij}(t-1) + \Delta W_{ij}(t) \quad \text{and} \quad \Delta W_{ij}(t) = -\eta \frac{\partial E}{\partial W_{ij}} + \alpha \Delta W_{ij}(t-1) \quad (4)$$

where η and α are two learning parameters of the network. The numbers t and $t-1$ denote the calculation steps. These two steps are several times repeated, presenting to the network the set of the learning examples in order to converge the total error E towards a minimum ($E = \sum_p E^{(p)}$).

2.2. Genetic Algorithm (GA)

The genetic algorithm (GA), developed by John Holland, is a heuristic search based on Charles Darwin theory of natural evolution and selection "the one that is best endowed, survives" [28-29]. It is useful for solving several kinds of problems with high complexity, and is presented as a graph of three main operators: selection, crossover and mutation. Population size, the number of generations, the probability of mutations and crossovers, and the selection method that represents crucial parameters that highly affect GA efficiently.

The GA process begins iterations with a generated random set of individuals, called Population, and considered as solutions to the problem to solve. That set of individuals are then tested against the objective function. The objective function is a set of criteria used to determine how fit each individual are. Each individual or solution is a chromosome identified by a set of joined parameters called Genes and is evaluated then assigned to a fitness value, calculated using the objective function. The selection procedure retains then the best performing chromosomes, called parents, according to their fitness values.

GA operates on a population (a number of potential solutions n_{pop}). The population at time t is represented by the time-dependent variable $S(t)$, with $S(0)$ a random initial population. Algorithm 1 shows the GA structure [30].

Algorithm 1: GA Algorithm

- 1: Randomly Generate initial random population of n_{pop} elements.
 - 2: $t=1$
 - 2: Repeat
 - 3: Calculate the fitness $S(t)$ of the chromosome and remember the highest fitness value.
 - 4: Select parents according to the roulette wheel mechanism.
 - 5: Crossover the parent's chromosomes.
 - 6: Mutate the chromosomes.
 - 7: $i=i+1$
 - 7: until the end criterion is satisfied.
-

2.3. Differential Evolution Algorithm (DE)

The differential evolution algorithm (DE), is a population-based metaheuristic search algorithm proposed in 1997 by Storn and Price [31]. The DE process begins iterations with a generated random set of individuals, or Population, and considered as solutions to the problem to solve. That set of individuals are then tested against the objective function. Then primarily, the next steps consists of two operations: mutation and recombination depending upon minor variation. In differential evolution, solutions are known as genome or chromosome. Each chromosome start with mutation followed by recombination. New child is created using target vector used to generate a donor vector that is then used during the recombination to obtain the trial vector [31]. DE operates on a population (a number of potential solutions n_{pop}). The population at time t is represented by the time-dependent variable $S(t)$, with the initial population of random estimates being $S(0)$. Algorithm 2 shows the DE structure.

Algorithm 2: DE Algorithm

- 1: Randomly Generate initial random population of n_{pop} elements.
 - 2: $t=1$
 - 2: Repeat
 - 3: Calculate the fitness $S(t)$ of the chromosome and remember the highest fitness value.
 - 4: Mutate the chromosomes.
 - 5: Crossover the parent's chromosomes.
 - 6: Select Childs for next generation.
 - 7: $i=i+1$
 - 8: until the end criterion is satisfied.
-

2.4. Particle Swarm Optimization (PSO)

Particle swarm optimization (PSO) is a population based stochastic optimization process [32]. A PSO process is initialized with a random population of solutions. The prospective solutions, called particles, move via the problem space by following the current optimal solutions [33]. Every particle has a fitness value to evaluate by the objective function, and a velocity which directs its flying. In every iteration, the particle swarm optimizer updates its velocity and position using the two best attributes: the best solution it has reached named p_{best} and the global best value named g_{best} . We find in Algorithm 3, the main steps of PSO.

Algorithm 3: PSO Algorithm

-
- 1: Initialize population.
 - 2: Repeat
 - 3: Evaluate individual fitness.
 - 4: Update personal best p_{best} .
 - 5: Update global best g_{best} .
 - 6: Generate a new population.
 - 7: Update velocity.
 - 8: Update position.
 - 9: until the end criterion is satisfied.
-

2.5. Ant Lion Optimization (ALO)

Ant lion optimization (ALO) algorithm [34,35] is based on ant lions hunting mechanism. It consists on random walk exploration and random agent selection based on five main hunting steps: random walk of agents, construction traps, entrapment of ants in the trap, catching prey and reconstruction traps. The ALO optimizer roulette wheel and random ants walks can disregard local optima.

The detailed ALO algorithm is described in Algorithm 4.

Algorithm 4: ALO Algorithm

-
- 1: Initialize randomly the first population of Ants and Antlions.
 - 2: Calculate the fitness value of Ants and Antlions.
 - 3: Find the best Antlion which has the optimal fitness and save it as the elite.
 - 4: Repeat
 - 5: For each Ant
 - 6: Select an Antlion using Roulette wheel.
 - 7: Update parameters.
 - 8: Create and normalize a random walk.
 - 9: Update the position of ant.
 - 10: End for
 - 11: Calculate the fitness of all Ants.
 - 12: Replace an Antlion with its corresponding elite if becomes fitter.
 - 13: Update the elite if an Antlion has fitter value than it.
 - 14: until the end criterion is satisfied.
-
-

2.6. Data

As introduced, we have explored our approach on four types of data: Mammographic Mass Data [21], Seed Data [22], Sommerville Happiness survey [23] and Fault data [24]. We find in Table 1, the characteristics of these data.

Table 1. Data Characteristics.

Dataset	Number of Classes and instances	Data Attributes
Mammographic Mass Data [21]	2 classes 516 benign 445 malignant	5 including 3 BIRADS Attributes [21]
Seed Data [22]	3 classes 70 Kama, 70 Rosa, 70 Canadian	7 Seed shape attributes.
Sommerville Happiness survey [23]	2 classes 75 Happy, 75 Unhappy	6 characteristic attributes of a city lifestyle
Fault data [24]	4 classes (1 Healthy and 3 Faulty) 200 Healthy , 200 Faulty 1, 200 Faulty 2, 200 Faulty 3	6 attributes corresponding to the frequencies and amplitudes of the first 3 peaks of the Welch spectrum

3. RESULTS AND DISCUSSION

We present in this section the results of the implementation of our approach. We start by classifying the data considered using BPNN, followed by classifications by hybridized neural networks. It should also be noticed that the learning of neural networks is carried out on 80% of the data considered and the remaining 20% of data were used for the validation of the NNs. For all the neural networks considered, whether they are optimized using BP algorithm, or hybridized with a metaheuristic, the input layer contains N_{var} neurons, and the hidden layer only 1 neuron. The desired response of this output neuron is coded according to the number of classes that the data contains.

A very interesting point, concerning the number of weights and thresholds to optimize for each ANN, should be recalled here. For the case of an architecture ($N_{var} : n_1 : n_2 : n_3 : 1$), of a neural network with 3 hidden layers (composed respectively of n_1 , n_2 and n_3 neurons), knowing that the input layer contains N_{var} neurons and the output layer of a single neuron, the number of weights N_W and thresholds N_T are as follows.

$$N_W = N_{var} n_1 + n_1 n_2 + n_2 n_3 + n_3 \quad \text{and} \quad N_T = n_1 + n_2 + n_3 + 1 \quad (5)$$

This means that for the architecture (5: 10: 25: 20: 1), for example, we have to optimize the values of 820 weights and 56 biases.

In fact, the optimization of an RN consists in modifying the weights and thresholds until the error is minimized or the iterations are finished.

In the case of the BPNN classification, the weights and thresholds are improved thanks to the calculations given in section 2, for all architectures with 1, 2 and 3 hidden layers (and between 5 and 35 neurons by layer). In the case of ANN hybridized by PSO, ALO, GA and

DE, the parameters (weight and thresholds) are the ingredients (particles, antlion or genes) to be handled until the end of the iterations.

We tested all structures with 1, 2 and 3 hidden layers, containing between 5 and 35 neurons each, with a number of iterations ranging from 100 to 1000. In addition, we explored these ANN (for PSO-ANN, ALO-ANN, GA-ANN and DE-ANN) with populations ranging from 20 to 100 individuals. Table 2 shows the parameters of each method used.

Notice that, after a training phase, efficiencies β_i , and purities η_i and errors ε_i corresponding to the classifications are computed from the validation confusion matrix A (A_{ij}), (A_{ij} being the value of examples of genuine class C_i classified as class C_j). For each class C_i we have:

$$\beta_i = \frac{A_{ii}}{\sum_l A_{il}}, \quad \eta_i = \frac{A_{ii}}{\sum_l A_{li}}, \quad \varepsilon_i = 1 - \beta_i \quad (6)$$

Table 2. Algorithms parameters tuning

Algorithm	PARAMETERS TUNING	Algorithm	PARAMETERS TUNING
Genetic Algorithm	Number of runs = 50 Number of features = 5-7 Maximum number of iterations = 1000 Number of population elements = 100 Crossover probability (pc) = 0.8 Mutation rate = 0.02 Mutation probability (pm) = 0.3 Selection pressure = 8	Particle Swarm Optimization	Number of runs = 50 Number of features = 5-7 Maximum number of iterations = 1000 Number of population elements = 100 Inertia weight = 0.72 Inertia weight damping ratio = 0.99 Personal learning coefficient = 1.49 Global learning coefficient = 1.49
Differential Evolution	Number of runs = 50 Number of features = 5-7 Maximum number of iterations = 1000 Number of population elements = 100 Crossover probability (pc) = 0.8 Mutation rate = 0.02 Mutation probability (pm) = 0.3 Selection pressure = 8	Ant Lion Optimization	Number of runs = 50 Number of features = 5-7 Maximum number of iterations = 1000 Number of search agents = 1000

The first point worth noting is the dependence of the classification efficiency on the neurons number (whatever their distribution in the network). This observation is valid regardless of

the approach used in optimizing this said network. We illustrate this property in Figure 2, where the efficiency of classifications is plotted with respect to the number of neurons in the network. The best results are summarized in Table 3. For a better comparison, between the different approaches, we present in Table 4, the best results of each approach taking into account all the data.

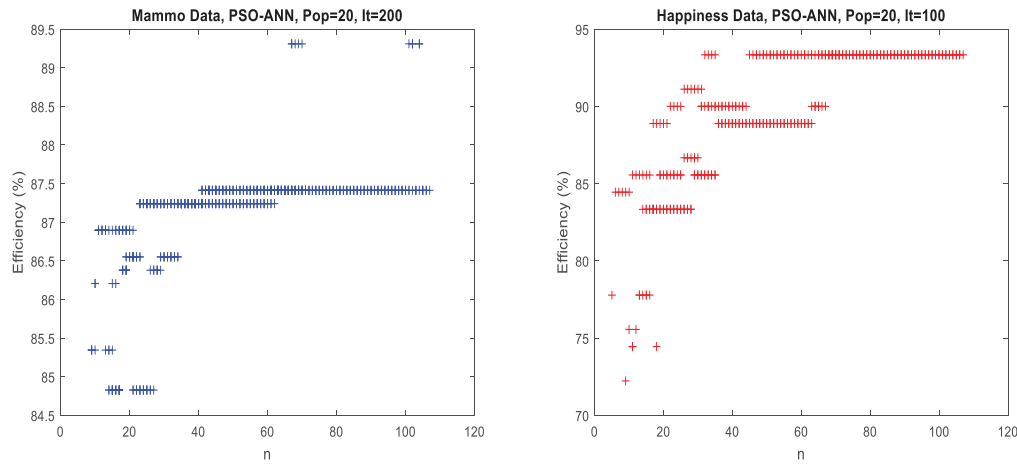


Figure 2. Efficiency vs Neurons for PSO-ANN, a) Mammo Data, b) Happiness Data

Table 3. Best Results for Mammo and Happiness Data

Method	Data	Architecture	Efficiency (%)	DATA	Architecture	Efficiency (%)
BPNN	Mammo	(5: 15: 1)	85.00	Happiness	(6: 19: 1)	74.44
		(5: 12: 31: 1)	85.34		(6: 19: 24: 1)	86.67
		(5: 12: 12: 18: 1)	86.55		(6: 17: 24: 7: 1)	88.89
PSO-ANN	Mammo	(5: 13: 1)	85.17	Happiness	(6: 32: 1)	93.33
		(5: 34: 33: 1)	88.27		(6: 23: 22: 1)	93.33
		(5: 34: 33: 34: 1)	89.31		(6: 22: 23: 21: 1)	93.33
GA-ANN	Mammo	(5: 26: 1)	85.04	Happiness	(6: 14: 1)	80.27
		(5: 18: 17: 1)	85.69		(6: 14: 12: 1)	89.41
		(5: 18: 19: 17: 1)	89.02		(6: 14: 17: 13: 1)	90.72
DE-ANN	Mammo	(5: 17: 1)	85.92	Happiness	(6: 5: 1)	78.33
		(5: 13: 12: 1)	88.12		(6: 21: 19: 1)	89.33
		(5: 31: 23: 14: 1)	89.17		(6: 21: 17: 16: 1)	90.13
ALO-	Mam	(5: 23: 1)	85.19	Happi	(6: 5: 1)	75.27

ANN	mo	ness
	(5: 19: 18: 1)	(6: 26: 26: 1)
	(5: 26: 24: 27: 1)	(6: 33: 33: 32: 1)
	85.70	87.56
	87.31	90.15

Table 4. Best Results for all Datasets

EFFICIENCY (%)				
Method	Mammo Data	Happiness Data	Seed Data	Fault Data
BPNN	86.55	88.89	96.02	92.16
PSO-ANN	89.31	93.33	99.23	95.00
ALO-ANN	87.31	90.15	97.18	93.10
GA-ANN	89.02	90.72	98.12	94.25
DE-ANN	89.17	90.13	98.26	94.31

4. CONCLUSION

The quality of learning depends on the parameters adopted for metaheuristics, which prompted us to run the code several times (50 runs). Moreover, the number of iterations is here of great importance, without forgetting the precision-computation time dilemma. The results are also initialization dependent; consequently several runs are necessary to achieve the expected performance.

All of the bio-inspired methods have given promising results. Combinations with bio-inspired metaheuristic methods (ALO, PSO, GA and DE) gave better results than those of BPNN. PSO-ANN appears to be more efficient than ALO-ANN, GA-ANN, and DE-ANN (and BPNN) for the data chosen and the runs performed.

On the same performances comparing to the classical BPNN, the Hybrid Neural Networks PSO-ANN, GA-ANN and DE-ANN gave each good results going up to 5% more efficiency.

As perspectives, the metaheuristic algorithms can be tuned more effectively. In addition, other metaheuristics can be explored in the same way as other types of ANN.

REFERENCES

- [1]. M. M. Najafabadi, F. Villanustre, T. M. Khoshgoftaar, N. Seliya, R. Wald, and E. Muharemagic, "Deep learning applications and challenges in big data analytics", *Journal of Big Data*, vol. 2, no. 1, pp. 1–21, 2015.
- [2]. Sesmero, M.P.; Alonso-Weber, J.M.; Gutierrez, G.; Ledezma, A.; Sanchis, A. "An ensemble approach of dual base learners for multi-class classification problems". *Inf. Fusion* 2015, 24, 122–136.
- [3]. Khaledian, Y.; Miller, B.A. "Selecting appropriate machine learning methods for digital soil mapping". *Appl. Math. Model.* 2020, 81, 401–418

-
- [4]. Wang, Q.; Li, Q.; Wu, D.; Yu, Y.; Tin-Loi, F.; Ma, J.; Gao, W. "Machine learning aided static structural reliability analysis for functionally graded frame structures". *Appl. Math. Model.* 2020, 78, 792–815.
 - [5]. Bhardwaj, A.; Tiwari, A. "Breast cancer diagnosis using Genetically Optimized Neural Network model". *Expert Syst. Appl.* 2015, 42, 4611–4620.
 - [6]. Iounousse, J.; Er-Raki, S.; El Motassadeq, A.; Chehouani, H. "Using an unsupervised approach of Probabilistic Neural Network (PNN) for land use classification from multitemporal satellite images". *Appl. Soft Comput.* 2015, 30, 1–13.
 - [7]. Mjahed, M. (2005). "Higgs Search at LHC by Neural Networks". *Nuclear Physics B (Proc. Suppl.)* 140: 799-801.
 - [8]. Mjahed, M. (2003). "Search for the standard model Higgs boson using neural networks and discriminant analysis", *Nuclear Physics B Vol 119C*: 1027-1029.
 - [9]. Del Vecchio, C.; Fenu, G.; Pellegrino, F.A.; Di Foggia, M.; Quatrone, M.; Benincasa, L.; Iannuzzi, S.; Acernese, A.; Corraa, P.; Glielmo, L. "Support Vector Representation Machine for superalloy investment casting optimization." *Appl. Math. Model.* 2019, 72, 324–336.
 - [10]. Kaefer, F.; Heilman, C.M.; Ramenofsky, S.D. "A neural network application to consumer classification to improve the timing of direct marketing activities". *Comput. Oper. Res.* 2005, 32, 2595–2615.
 - [11]. Sarker, I.H. "Machine Learning: Algorithms, Real-World Applications and Research Directions". *SN Comput. Sci.* 2, 160 (2021). <https://doi.org/10.1007/s42979-021-00592-x>
 - [12]. Dash, Nilamadhab & Priyadarshini, Rojalina & Mishra, Brojo & Misra, Rachita. (2017). Bio-Inspired Computing through Artificial Neural Network. 10.4018/978-1-5225-1008-6.ch011.
 - [13]. Braik, Malik & Al-Zoubi, Hussein & Al-Hiary, Heba. (2021). "Artificial neural networks training via bio-inspired optimisation algorithms: modelling industrial winding process, case study". *Soft Computing*. 25. 1-25. 10.1007/s00500-020-05464-9.
 - [14]. Rahman, Md. Mijanur. (2015). "An Implementation for Combining Neural Networks and Genetic Algorithms." *International Journal of Computer Science and Technology*. 6. 218-222.
 - [15]. Ahmadizar, Fardin & Soltanian, Khabat & AkhlaghianTab, Fardin & Tsoulos, Ioannis. (2015). "Artificial neural network development by means of a novel combination of grammatical evolution and genetic algorithm." *Engineering Applications of Artificial Intelligence*. 39. 1-13. 10.1016/j.engappai.2014.11.003.
 - [16]. Sheikholarefin, Saeid & Esfandiari, Mj & Bondarabadi, H.A. (2016). "A combination of particle swarm optimization and multi-criterion decision-making for optimum design of reinforced concrete frames." *International journal of optimization in civil engineering*. 245-268.
 - [17]. Mjahed, M. (2006). "Search for the Higgs boson at LHC by using Genetic Algorithms, " *Nuclear Instruments and Methods A* 559(1): 172-179.
 - [18]. Juan A. Lazzús, "Neural network-particle swarm modeling to predict thermal properties," *Mathematical and Computer Modelling*, Volume 57, Issues 9–10, 2013, Pages 2408-2418, ISSN 0895-7177, <https://doi.org/10.1016/j.mcm.2012.01.003>
 - [19]. Tam T. Truong, Seunghye Lee, Jaehong Lee, "An artificial neural network-differential evolution approach for optimization of bidirectional functionally graded beams, "
-

-
- Composite Structures, Volume 233, 2020, 111517, ISSN 0263-8223, <https://doi.org/10.1016/j.compstruct.2019.111517>.
- [20]. Hongping Hu, Yangyang Li, Yanping Bai, Juping Zhang, Maoxing Liu, "The Improved Antlion Optimizer and Artificial Neural Network for Chinese Influenza Prediction", Complexity, vol. 2019, Article ID 1480392, 12 pages, 2019. <https://doi.org/10.1155/2019/1480392>
- [21]. M. Elter, R. Schulz-Wendtland and T. Wittenberg. UCI Machine Learning Repository. Mammographic mass Data Set. Available: <http://archive.ics.uci.edu/ml/datasets/mammographic+mass>
- [22]. M. Charytanowicz, J. Niewczas, P. Kulczycki, P. A. Kowalski, S. Lukasik, S. Zak. UCI Machine Learning Repository. seeds Data Set. [<https://archive.ics.uci.edu/ml/datasets/seeds>]. The Institute of Agrophysics of the Polish Academy of Sciences in Lublin.
- [23]. W.W. Koczkodaj, T. Kakiashvili, A. Szymanska, J. Montero-Marin, R. Araya, J. Garcia-Campayo, K. Rutkowski, D. Strzalka. UCI Machine Learning Repository. Somerville Happiness Survey Data Set. Available: <https://archive.ics.uci.edu/ml/datasets/Somerville+Happiness+Survey>.
- [24]. Mjahed Soukaina, Salah El Hadaj, Khadija Bouzaachane, Said Raghay. (2020) "Helicopter Main Rotor Fault Diagnosis by Using GA- and PSO-based Classifiers." Studies in Informatics and Control, 29(1) 5-15, March 2020. <https://doi.org/10.24846/v29i1y202001>
- [25]. Michie, D., Spiegelhalter, D. J., Taylor, C. C. (1995). Machine Learning, Neural and Statistical Classification. Ellis Horwood, USA.
- [26]. C.M. Bishop. (1995). Neural Networks for Pattern Recognition, Oxford: Oxford University Press.
- [27]. S. Singh, "Backpropagation learning algorithm based on Levenberg Marquardt algorithm," in Proceedings of the Fourth International Workshop on Computer Networks & Communications, vol. 2, Chennai, India, October 2012.
- [28]. J. H. Holland. (1975). Adaptation in Natural and Artificial Systems, University of Michigan Press.
- [29]. Z. Michalewicz. (1996). Genetic Algorithms + Data Structures = Evolution Programs, 3 ed. Berlin, Heidelberg: Springer Berlin Heidelberg.
- [30]. Mjahed, M. (2010). Optimization of Classification Tasks by using Genetic Algorithms. In Proceedings of Informatics and Systems (INFOS), (IEEE conference), Cairo, Egypt, March 2010, pp.1-4.
- [31]. Kenneth V. Price Rainer M. Storn Jouni A. Lampinen, (2005), Differential Evolution: A Practical Approach To Global Optimization, Springer. ISBN 978-3-540-20950-8.
- [32]. Kennedy, J., Eberhart, R. C., Shi, Y. (2001). Swarm Intelligence. Morgan Kaufmann Publishers Inc., San Francisco, CA.
- [33]. P. Rini, M. Shamsuddin, S. Yuhaniz. (2011). "Particle Swarm Optimization: technique, system and challenges," International Journal of Computer Applications 14: 0019–0027.
- [34]. S. Mirjalili. (2015). "The ant lion optimizer", Advances in Engineering Software, 83: 0-98.
- [35]. S. Kumar and A. Kumar, "A brief review on antlion optimization algorithm," 2018
-

International Conference on Advances in Computing, Communication Control and Networking (ICACCCN), 2018, pp. 236-240, doi: 10.1109/ICACCCN.2018.8748862.

BIOGRAPHY

Ouail MJAHER was born in Morocco, 1997, He received his Engineering degrees in Computer Sciences from the National School of Applied Sciences (ENSA) of Marrakech, Morocco, in 2020. He is currently pursuing the Ph.D. at Cadi Ayyad University of Marrakech, Morocco. His main research interests include Artificial Intelligence based Classification, Supervised and Non-supervised Machine Learning, Big data reduction and Intelligent Cyber Security Intrusion Detection.

FISH SCHOOL SEARCH ALGORITHM FOR SOLVING MULTI-OBJECTIVE U-SHAPED DISASSEMBLY LINE BALANCING PROBLEM

Pengfei Yao

Department of Mechanical and Industrial Engineering
Northeastern University Boston, MA, 02115, USA.

Surendra M. Gupta

Department of Mechanical and Industrial Engineering
Northeastern University Boston, MA, 02115, USA.

Abstract

The rapid advancement of society and economy has led to the acceleration of product diversification and improvement. One obvious consequence of product improvement is the creation of many end-of-life (EOL) products. Landfilling is not a suitable option for EOL products since it is not ecofriendly. Product recovery is an ecofriendly strategy to deal with EOL products. Remanufacturing is one of the most widely used options for product recovery. Disassembly is the first and one of the most crucial steps of remanufacturing. Disassembly aims to physically separate EOL products into its different parts and/or subassemblies. Workstations are linked together on a disassembly line to perform disassembly tasks. Balancing the disassembly line is essential for creating profits and achieving other objectives. A U-shaped disassembly line has many advantages compared to a straight-line layout since operators and/or robotic machines can work on both sides of the line. Single profit or a cost-based objective is not enough or practical for the real-world disassembly cases. Reducing the number of workstations, increasing smoothness, early removal of hazardous part(s) and early removal of highly demanded part(s) are the four objectives considered in this paper. Fish school search (FSS) is a novel meta-heuristic optimization algorithm which is based on the simulation of social behaviors of biologic fish. Since disassembly line balancing problem (DLBP) belongs to the NP-hard class, heuristics and meta-heuristics are best suited techniques for solving the DLBP in a reasonable computational time. In this paper, the FSS algorithm is used and implemented on a U-shaped and a straight-line disassembly line and tested. Results demonstrate that the U-shaped layout offers superior performance compared to the straight-line layout. Results also show that the FSS algorithm has the ability to find near-optimal solutions and is superior to other meta-heuristic algorithms in many aspects.

Keywords: Remanufacturing, Disassembly line balancing problem (DLBP), U-shaped disassembly line, Fish school search (FSS) algorithm.

INTRODUCTION

Rapid development of economic and technology has accelerated product diversification. Product diversification together with customers' demand accelerate product upgrades. One obvious consequence of product upgrades is increasing number of end-of-life (EOL) products since life cycle of products is shortened. Rapidly updated electrical and electronic products result in a lot of wastage (Li and Janardhanan, 2021) and waste problem directly threatens the health of both environment and individuals (Wang et al., 2021). Landfilling is the traditional way of solving EOL products and waste, but it is not suitable in today's situation because of increasing pressure of environmental problems (Chen et al., 2021). Increasing environmental awareness in society and stricter environmental regulations have forced firms to take more suitable product recovery actions (Akpınar, Ilgin, and Aktas, 2021). Product recovery aims to maximize the recovery value as well as minimize the amount of disposal of EOL products (Gao et al., 2021) and has received greater attention in recent years (Edis, Edis, and Ilgin, 2021). The concept of environmentally conscious manufacturing and product recovery was first highlighted by Gungor and Gupta (1999) which aspires to add green manufacturing to the whole life cycle of a product. Remanufacturing and recycling are two popular options of product recovery, which are widely used in real world cases. Disassembly is a key and necessary step to complete the separation of reusable parts and harmful substances from EOL products (Yin et al., 2021) and it is also the first and one of the most crucial steps for remanufacturing and recycling. Disassembly tasks are operated on a paced line linked with different workstations and operators and/or robots which are assigned to each workstation. Partial and complete disassembly are two groups of disassembly research (Yao and Gupta, 2021). There are four popular types of a disassembly lines, namely, straight-line, parallel, U-shaped and two-sided. A U-shaped disassembly line is much more productive and efficient compared to a straight-line configuration since operators or robots can work on both sides of the line. Based on the importance of a disassembly line, balancing the disassembly line is critical. Disassembly line balancing problem (DLBP) was, for the first time, proposed by Gungor and Gupta (1999), which can be simply described as the optimum assignment of disassembly tasks to workstations within the domain of predetermined constraints.

The rest of paper is structured as follows: literature review is included in the next section. The section that follows introduces the detailed disassembly line balancing problem, and introduces the mathematical model and related constraints. This is followed by a section that covers detailed results and comparison of the performance of several algorithms. The last section provides the conclusion and directions for future research.

LITERATURE REVIEW

There are four types of a disassembly lines as mentioned in the previous section, viz., straight-line, parallel, U-shaped and two-sided. Each line has its special characteristics and using

different line on a same disassembly problem may lead to different results. DLBP literature has focused more on straight-line configuration (Ozceylan et al., 2019) than other configurations and only a handful of papers addressed U-shaped disassembly lines. Agrawal and Tiwari (2008) first studied U-shaped DLBP, and they proposed a collaborative ant colony algorithm to solve it. Later Avikal and Mishra (2012) and Avikal, Jain, and Mishra (2013) introduced different heuristic methods to balance a U-shaped disassembly line. A pareto hybrid ant colony and genetic algorithm was proposed by Zhang et al. (2018) with the consideration of multiple objectives. Li, Kucukkoc, and Zhang (2019), for the first time, studied sequence dependent U-shaped DLBP. Wang, Gao, and Li (2020) considered partial disassembly on a U-shaped disassembly line. Most recently, Li and Janardhanan (2021) considered profit-oriented U-shaped partial DLBP using a mixed-integer linear programming model. Yao and Gupta (2021a) and Yao and Gupta (2021b) have, for the first-time, applied cat swarm algorithm (CSO) and small world optimization algorithm (SWOA) on a U-shaped disassembly line respectively. Wang et al. (2021) combined a meta-heuristic algorithm with multi-criterion decision making (MCDM) and variable neighborhood search (VNS) theory to balance a U-shaped layout. Yao and Gupta (2021d) and Yao and Gupta (2021c) first introduced invasive weed optimization algorithm (IWO) and ant colony optimization algorithm (ACO) on a U-shaped line respectively and compared their performances with several other meta-heuristics. Yao and Gupta (2021e) first proposed a teaching-learning-based optimization algorithm (TLBO) on U-shaped disassembly line.

DLBP aims to adjust task sequence to better achieve determined objectives, therefore DLBP belongs to optimization problem field. For small size cases, mathematical approaches and exact methods can find the optimal solution(s) in short time. But for large size cases, these methods do not have the ability to find near-optimal solution(s) in a reasonable computational time. Therefore, heuristics and meta-heuristics are introduced in DLBP field. McGovern and Gupta (2007) proved that DLBP belongs to NP-hard problem. After that, novel heuristics and meta-heuristics are proposed to help balance the disassembly line. Fish school search (FSS) algorithm was originally proposed in Bastos-Filho et al. (2008) based on the simulation of social behavior of biologic fish. In this paper, FSS algorithm is applied on a straight-line layout and a U-shaped disassembly line. The performance of FSS is compared with several other meta-heuristics and presented in section 4.

In this paper, four different objectives are considered, viz., minimization of number of workstations, minimization of idle times, removal of hazardous part(s) early and removal of high demand part(s) early. This paper uses Pareto optimal theory to classify near-optimal solutions.

To the best of the authors' knowledge, in this paper, FSS has been applied on a U-shaped disassembly line for the time. The performance of FSS is compared with several other meta-heuristic algorithms and results show that FSS has the ability of finding near-optimal solution(s)

and in some cases, shows superior performance. In addition, the same case was performed on both a U-shaped disassembly line and a straight-line configuration and compared. The results show that the U-shaped layout indeed has some advantages compared to the straight-line layout, especially when considering the minimization of idle times.

PROBLEM DEFINITION

Disassembly line balancing problem (DLBP) consists of several objectives and basic constraints. Basic constraints include cycle time constraint and precedence relationships constraints. The assumptions of the problem are as follows:

1. There is only one type of EOL products.
2. Complete disassembly is considered in this paper.
3. Task processing/removal time is deterministic.
4. Cycle time is known.

Notation

N Number of tasks

i, j Task index, $i, j = 1, 2, \dots, N$

M Number of workstations

m Workstation index, $m = 1, 2, \dots, M$

ws_m binary variable, 1, if workstation m is opened; 0, otherwise

t_i Processing/removal time of task i

h_i binary variable, 1, if task i is hazardous; 0, otherwise

d_j demand value of task j

CT Cycle time

T_m Total task processing times of workstation m

F_a Objective function, $a = 1, 2, 3, 4$

Decision variables:

x_{im} 1, if task i is assigned at the front side of workstation m ; 0, otherwise

y_{jm} 1, if task j is assigned at the back side of workstation m ; 0, otherwise

s_i Position number of task i in sequence

Objectives:

$$\text{Min } F_1 = \sum_{m=1}^M ws_m \quad (1)$$

$$\text{Min } F_2 = \sum_{m=1}^M (CT - T_m)^2 \quad (2)$$

$$\text{Min } F_3 = \sum_{i=1}^N (s_i * h_i) \quad (3)$$

$$\text{Min } F_4 = \sum_{i=1}^N (s_i * d_i) \quad (4)$$

Formulation (1) describes finding minimum number of workstations. Total of idle times is shown in equation (2) which is nonlinear equation. Equation (3) describes removal of hazardous part(s) early and equation (4) facilitates removal high demand part(s) early.

Constraints:

$$\sum_{m=1}^M (x_{im} + y_{im}) = 1 \quad (5)$$

$$\sum_{i=1}^N (x_{im} + y_{im}) \geq 1 \quad (6)$$

$$CT \geq T_m \quad (7)$$

$$x_{im}, y_{im} = \{0,1\} \forall i, m \quad (8)$$

Constraint (5) ensures that one task can only be assigned to one side of one workstation. Constraint (6) says that one workstation can operate one or more tasks. Constraint (7) is the cycle time constraint which means that the cycle time should be larger than or equal to the total of task processing times of each workstation.

RESULTS

FSS algorithm was coded in MATLAB and applied on a straight-line and a U-shaped line separately. The case is acquired from McGovern and Gupta (2006) and is used to test the ability of FSS algorithm for solving DLBP. FSS algorithm was run 20 times on the straight-line disassembly line and 20 times on the U-shaped disassembly line separately. Case information, viz., task number, task processing/removal time, hazardous index, and demand values are shown in Table 1. Table 2 lists 4 randomly picked solutions for straight-line and another 4 randomly picked solutions for U-shaped line. The task sequences are listed in the last column of Table 2. Since multiple objectives are considered in this paper, pareto front strategy was used to classify these near-optimal solutions. From Table 2, all the 8 solutions found the best value for the minimum number of workstations. On the straight-line layout, the best value found for the second objective is 211, but on U-shaped line, the minimum total of idle times is 207. Also, average values calculated for the three objectives show that U-shaped disassembly line performs better in many aspects and this type of layout indeed improves line efficiency and productivity. The performance of FSS algorithm is compared with nine other meta-heuristic algorithms, viz.,

genetic algorithm (GA), ant colony optimization (ACO), improved ant colony optimization (IACO), hybrid group neighborhood search algorithm (HGNS), improved artificial bee colony optimization (IABC), small world optimization algorithm (SWOA), cat swarm optimization (CSO), invasive weed optimization (IWO), and teaching-learning-based optimization (TLBO). Detailed performance data of various algorithms are taken from McGovern and Gupta (2006), Zhang et al. (2018), Zhu et al. (2014), Zhu, Zhang, and Guan (2020), Yao and Gupta (2021a), Yao and Gupta (2021b), Yao and Gupta (2021c), Yao and Gupta (2021d), and Yao and Gupta (2021e).

Table 1. Case information

Task number	Task processing time	Hazardous index	Demand value
1	14	0	0
2	10	0	500
3	12	0	0
4	17	0	0
5	23	0	0
6	14	0	750
7	19	1	295
8	36	0	0
9	14	0	360
10	10	0	0

Table 2. Performance of straight-line and U-shaped disassembly line

Line type	F_1	F_2	F_3	F_4	Task sequence
Straight-line	5	211	5	8885	6,4,5,10,7,9,8,1,2,3
	5	259	4	10060	5,6,1,7,4,10,8,9,2,3
	5	211	5	9605	6,4,10,5,7,1,8,9,2,3
	5	219	4	9340	5,6,1,7,4,9,8,10,2,3
U-shaped	5	207	5	9695	5,9,10,6,7,1,4,8,2,3
	5	211	4	9480	5,6,10,7,9,1,4,8,2,3
	5	249	3	8685	5,6,7,4,9,1,10,8,2,3
	5	211	4	8950	6,10,5,7,1,8,9,4,2,3

Table 3 presents detailed comparison of 10 different meta-heuristic algorithms on straight-line disassembly layout. Table 4 lists performances of 6 meta-heuristic algorithms on U-shaped disassembly line. Results in Table 4 are based on the average values of near-optimal solutions found with setting the first two objectives as primary objectives. From Table 3 and Table 4, FSS shows great ability on finding near-optimal solutions for the DLBP. Particularly on minimizing the number of workstations and minimizing total of idle times, FSS performs better than most of other meta-heuristic algorithms.

Table 3. Performance of 10 meta-heuristics on straight-line layout

Objective	GA	ACO	IACO	HGNS	IABC	SWOA	CSO	IWO	TLBO	FSS
F_1	5	5	5	5	5	5	5	5	5	5
F_2	211	211	211	219	211	211	211	211	211	211
F_3	4	4	4	4	4	4	5	4	6	5
F_4	9730	10090	9730	7510	9730	9480	8880	9480	8100	8885

Table 4. Performance of 6 meta-heuristics on U-shaped disassembly line

Objective	SWOA	CSO	IWO	ACO	TLBO	FSS
F_1	5	5	5	5	5	5
F_2	207	207	207	207	207	207
F_3	4	5	5	5	5	5
F_3	8980	9696	8915	8915	8915	9695

CONCLUSION

FSS algorithm has, for the first time, been proposed and implemented on a U-shaped DLBP. Comparison results show that FSS performs well and is suitable for DLBP research. Special disassembly types like partial and sequence-dependent disassembly need more research attention. Also, novel meta-heuristic algorithms can also be proposed and implemented on U-shaped DLBP.

REFERENCES

- Agrawal, S. and Tiwari, M.K., 2008. A collaborative ant colony algorithm to stochastic mixed-model U-shaped disassembly line balancing and sequencing problem. *International Journal of Production Research*, 46(6), pp.1405-1429.
- Akpınar, M.E., Ilgin, M.A. and Aktaş, H., 2021. Disassembly Line Balancing by Using Simulation Optimization. *Alphanumeric Journal*, 9(1), pp.63-84.
- Avikal, S., Jain, R. and Mishra, P., 2013. A heuristic for U-shaped disassembly line balancing problems. *MIT International Journal of Mechanical Engineering*, 3(1), pp.51-56.
- Avikal, S. and Mishra, P.K., 2012. A new U-shaped heuristic for disassembly line balancing problems. *PRATIBHA: International Journal of Science, Spirituality, Business and Technology*, 1(1), pp.21-27.
- Bastos Filho, C.J., de Lima Neto, F.B., Lins, A.J., Nascimento, A.I. and Lima, M.P., 2008, October. A novel search algorithm based on fish school behavior. In *2008 IEEE international conference on systems, man and cybernetics* (pp. 2646-2651). IEEE.

- Chen, J.C., Chen, Y.Y., Chen, T.L. and Yang, Y.C., 2021. An adaptive genetic algorithm-based and AND/OR graph approach for the disassembly line balancing problem. *Engineering Optimization*, pp.1-17.
- Edis, E.B., Edis, R.S. and Ilgin, M.A., 2022. Mixed integer programming approaches to partial disassembly line balancing and sequencing problem. *Computers & Operations Research*, 138, p.105559.
- Gao, Y., Lou, S., Zheng, H. and Tan, J., 2021. A data-driven method of selective disassembly planning at end-of-life under uncertainty. *Journal of Intelligent Manufacturing*, pp.1-21.
- Gungor, A., & Gupta, S. M., 1999. Disassembly line balancing. *Proceedings of the 1999 Annual Meeting of the Northeast Decision Sciences Institute*, Newport, Rhode Island, March 24-26, pp.193-195.
- Gungor, A. and Gupta, S.M., 1999. Issues in environmentally conscious manufacturing and product recovery: a survey. *Computers & Industrial Engineering*, 36(4), pp.811-853.
- Li, Z. and Janardhanan, M.N., 2021. Modelling and solving profit-oriented U-shaped partial disassembly line balancing problem. *Expert Systems with Applications*, p.115431.
- Li, Z., Kucukkoc, I. and Zhang, Z., 2019. Iterated local search method and mathematical model for sequence-dependent U-shaped disassembly line balancing problem. *Computers & Industrial Engineering*, 137, p.106056.
- McGovern, S.M. and Gupta, S.M., 2006. Ant colony optimization for disassembly sequencing with multiple objectives. *The International Journal of Advanced Manufacturing Technology*, 30(5-6), pp.481-496.
- Özceylan, E., Kalayci, C.B., Güngör, A. and Gupta, S.M., 2019. Disassembly line balancing problem: a review of the state of the art and future directions. *International Journal of Production Research*, 57(15-16), pp.4805-4827.
- Wang, K., Gao, L. and Li, X., 2020. A multi-objective algorithm for U-shaped disassembly line balancing with partial destructive mode. *Neural Computing and Applications*, pp.1-22.
- Wang, K., Li, X., Gao, L., Li, P. and Gupta, S.M., 2021. A genetic simulated annealing algorithm for parallel partial disassembly line balancing problem. *Applied Soft Computing*, 107, p.107404.
- Wang, Y., Xie, Y., Ren, Y. and Zhang, C., 2021, February. A MCDM-Based Meta-Heuristic Approach for U-shaped Disassembly Line Balancing Problem. In *Journal of Physics: Conference Series* (Vol. 1828, No. 1, p. 012159). IOP Publishing.

- Yao, P. and Gupta, S. M., 2021a. Cat Swarm Optimization Algorithm for Solving Multi-Objective U-Shaped Disassembly Line Balancing Problem. *Proceedings of the International Conference on Remanufacturing*, March 24-25, pp. 222-230.
- Yao, P. and Gupta, S. M., 2021b. Small World Optimization Algorithm for Solving Multi-Objective U-Shaped Disassembly Line Balancing Problem, *Proceedings of the 2021 Annual Meeting of the Northeast Decision Sciences Institute*, Virtual, March 26-27, 659-668.
- Yao, P. and Gupta, S. M., 2021c. Ant Colony Optimization Algorithm for Solving U-Shaped Disassembly Line Balancing Problem with Multiple Objectives, *Proceedings of the 4th International Conference on Innovative Studies of Contemporary Sciences*, Tokyo, Japan, July 29-31, pp. 21-26.
- Yao, P. and Gupta, S. M., 2021d. Invasive Weed Optimization Algorithm for Solving Multi-Objective U-Shaped Disassembly Line Balancing Problem", *Proceedings of the 12th International Congress on Mathematics, Engineering and Natural Sciences*, Paris, France, July 9-11, pp. 286-292.
- Yao, P. and Gupta, S. M., 2021e. Teaching-Learning-Based Optimization Algorithm for Solving Multi-Objective U-Shaped Disassembly Line Balancing Problem, *Proceedings of the 5th International New York Conference on Evolving Trends in Interdisciplinary Research and Practices*, Manhattan, New York City, October 3-5, pp. 21-28.
- Yin, T., Zhang, Z., Zhang, Y., Wu, T. and Liang, W., 2022. Mixed-integer programming model and hybrid driving algorithm for multi-product partial disassembly line balancing problem with multi-robot workstations. *Robotics and Computer-Integrated Manufacturing*, 73, p.102251.
- Zhang, Z., Wang, K., Zhu, L. and Cheng, W., 2018. Pareto Hybrid Ant Colony and Genetic Algorithm for Multi-Objective U-Shaped Disassembly Line Balancing Problem. *Journal of Southwest Jiaotong University*, 53(3), pp.628-637.
- Zhu, X., Zhang, Z., Zhu, X. and Hu, J., 2014. An ant colony optimization algorithm for multi-objective disassembly line balancing problem. *China Mechanical Engineering*, 25(8), p.1075.
- Zhu, L., Zhang, Z. and Guan, C., 2020. Multi-objective partial parallel disassembly line balancing problem using hybrid group neighbourhood search algorithm. *Journal of Manufacturing Systems*, 56, pp.252-269.

MATERIALS CLASSIFICATION OF PROFITABLE AND NEW SOFT CONTACT LENSES USING MATLAB

Amenah Emad mohammed redha

Iraqi Ministry of Higher Education and Scientific Research/Dijlah University College

Abstract

This paper presents the materials classification of profitable and new soft contact lenses using MATLAB. The industry and marketplace of contact lens have demonstrated a high level of vitality and evolved into rapid development area in which science daily perform continually cooperate. The relative study of the basic profitable and nano-phonic materials characteristics to produced by integration of fullerene nano-particles are derivative in essential materials for soft contact lenses. Basically, the contact lens material is sensitizing of monomer 2-hydroxyethyl methacrylate and fullerene which is derivative to use because it have efficient transmission properties in ultraviolet visible and close to the spectrum of infrared. To classify the materials of soft contact lenses, the optomagnetic scope should be used under the different between spreader reflected light and reflect polarized illumination. In this work, biomedical applications industry and applied science has been applied to provide enough material classifications in soft contact lenses depend on WAT techniques. The result shows an identical wavelengths peak value of incorporate fullerene, C60 and C60 (OH) 24.

Keywords: Materials Classification, Soft Contact Lenses, MATLAB

1. INTRODUCTION

Contact lenses manufacturing and its marketplace stability development in many reorganization and numerous creation sections is continually happening by inventive materials and the design of optical [1, 2]. The possibility of this products is not simply via expansion of materials and collection, except via original analytical and beneficial explanation. The poly 2-hydroxyethyl is the most material used in soft contact lens which the major component of soft lenses [3, 4]. Many researchers introduce numerous studies to improve and develop the characteristics of soft contact lens material due to its important in this time such as [5-15]. These studies is refers to achieve best vision correction, better wearing comfort, less medical difficulties and providing adequate amount of oxygen for the cornea during wearing the lenses. This work investigate the optomagnetic spectroscopy usage to examine the features of the essential and nano-phonic materials that provided by integrating the fullerene with its derivatives in the essential fabric for soft lenses. By adding the optical material to the essential fabric in proportion is considerably advanced the optical property to obtain the nanophotonic material. The incorporated C60 with nanophotonics materials generate different optical specifications due to icosahedra group as more symmetry rudiments which determine the energy of nanophotonic materials. In addition, the fullerene have numerous function in the material to prepare the nano-phonic lenses. The fullerene could be considered as accountable for enhanced electromagnetic specifications in light transmitting which is suitable to optic courage and eyes [16-20]. The contact lens transmission properties could be believed including fullerene to modify the Electroencephalogram signals in the patient who wearing this lenses [21-25]. The possibility to use these lenses could be manifold in daily wear, reduce light intensity when the eyes has high sensitivity, better retina protection from ultraviolet radiation and possibility of depression treatments [25-29].

2. MATERIALS AND METHOD

The electromagnetic radiation is a visible light to the eye of human and dependable for vision. The specification of this radiation is including a wavelength from (380-780) nm and frequency from $(3.1-7.9) \times 10^{14}$ Hz. The physical meaning of optomagnetic spectroscopy is depending on basic principles of geometric optics under refraction and reflection phenomena and wave optic polarization. Under Brewster angle, the technique to obtain linearity polarization light (i.e. $E=E_s$) is reflected. In case of polarized light reaches the dielectric surface which might be achievable to examine its performance via two perpendicular mechanism or parallel with polarization surface. The reflection of light density is depending on the incidence angle. Hence, at specific angle value of incidence, at what time the reflected light happen to polarized and contain merely s-function, the p-function become equivalent with zero. The reflected waves as seen from microscopic point of view are generated by oscillation of electric dipoles sample that wave reflection. This oscillation is transverse to wave propagation direction. In case of polarized waves in incidence plan is arrive at the plane, the dipoles will oscillate in same surface due to the reflected light which will not spreader in the incidence surface except vertical to this plane. In addition, the wave should be polarized vertical to the incidence plan in order to reflect which mean so as to merely constituent that is not incidence plan could be reflected and further parts will be very weak. The spread white light so as to arrive at the surface beneath Brewster angle form is reflect signal as retain main polarized in the plane vertical to the incidence surface under s-polarized. These categories of polarized could happen beneath single incidence only to meet the Brewster equation condition. The most important is to use the reality that the summation of reflected and refracted waves should be in 90° to compute the Brewster angle as shown in Figure 1.

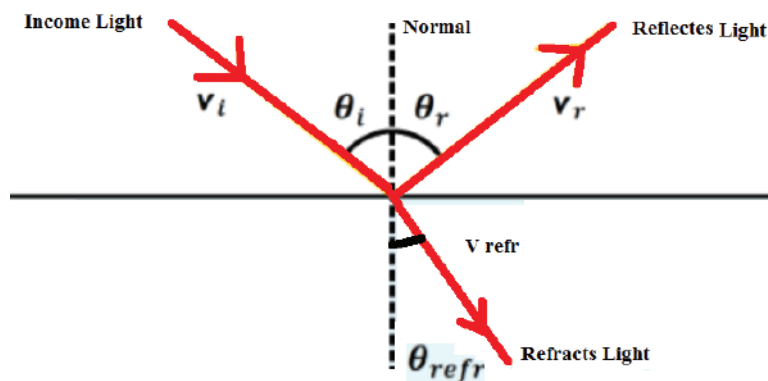


Figure 1: Reflection and Refraction of the light

The response difference to white light under uniform magnetic and electric component is reflected polarized light under muted component of subdued electric guide to famous magnetic oscillation. The oscillation is origin from modification of incident emission based on optical characteristic in the example under test. base on the optical and magnetic property of material, the optomagnetic spectroscopy are nearby to the conformation conditions in hankie which is reasoned by the reduction of incident light by the fabric. The optomagnetic spectroscopy techniques are depend on the disparity among spreader reflection light and polarization reflected lighting. By using the digital camera, the prototype is photograph under spread white light and reflection polarization lighting. Subsequently, the obtained digital images have been processed. Many important advantages could be provided by digital photography such as operation speed, data achievement and low cost. The digitalized data allows the image analysis

through decomposition of data into color components from red, blue and green components. For Brewster spectroscopy, this device could be used to implement the techniques including with typical digitalized camera and sufficient organization for amplification and light basis tailored. In order to transform the picture to histogram of diffusion, the digital processing of images could be applied to show the intensity of pixel on the scale from 1 to 256. The shade of minimum density is corresponding to 1 and the shade of maximum intensity is corresponding to 256. Hence, by following the histograms role, the images are exhibit as band at which the allocation of all intensities is illustrated on the scale from 1 to 256. Every component originates from the equivalent wavelengths variety of visible spectrum. The possibility of this techniques is because of each components inside the camera sensor is based on 256 height. Meaning that, the organized spectrum evidence of visible light is at 768 points (256×3). The digital footage consists of implied data regarding the wavelength with strength of spread light and reflection polarization light. The incident white light with different data layers based on light incident angle is illustrated in Figure 2.

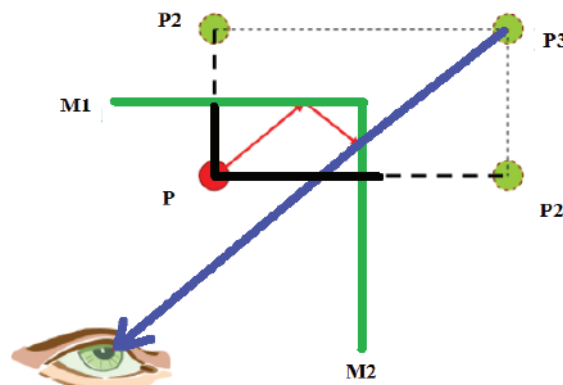


Figure 2: light white incident depend on light angle

This work introduce the digital image in the form of RGB arrangement, consequently essential pixel information in the channels of blue and red for light spread and replicate polarized light is selected. The information examination algorithms are depending on chromatic illustration named Maxwell triangle and spectral convolution process depend on red-blue and white light polarized ratio. Hence, R-B and W-P abbreviation denote by extract the blue from red wavelength of lighting and reflection polarization light are use in shadow convolution algorithms in order to compute the information of opt magnetic spectroscopy. This procedure contain an sample illuminating with spread light, first digital image acquisition and the illumination samples with polarized light and other acquisition of digital images. After recorded of 10 photography repetitions that takes 10 second for every example in digital record, the methods is track by processing of spectral images so as to take position in the following steps:

- a. The first step of photographing represented by cropped the region of interest and extract this region decomposes into its channel components red, blue and green will provided by 3 mono chromatic image which represent the intensity allocation of sub-visibly spectrum exhibit as histogram.
- b. In the second step, the convolution spectrum implementation is the red and blue channels after shaped the dissimilarity among the obtained reply by polarized light and white light.

c. In the 3rd step, the performing of sample spectral analysis that classify depend on wavelength and intensity.

3. EXPERIMENT SETUP

New kind of contact lenses with 2 dissimilar kinds of included nano-particles represented by fullerol and fullerene be use in this work. Firstly, the nano-materials is supplementary throughout the process of polymerization with poly hydroxyethyl methacrylate as basic materials. In all samples, the polymerization was homogeneous and new nano-photonics material for soft contact lenses was produced. A reference sample is polymerization is carried out without nano-materials. In this experiment, the used equipments is a device type NL-B50 with digital camera from canon model and Nano lab. The power solution and lighting were achieved by LED diode with lighting circuit based on Brewster angle at 53^0 in the vertical and 120^0 in the horizontal plane. A circular shape surface has been used in the working space with diameter of 26 mm. The soft lenses be store inside desiccators as its hygroscopic type. During the experiment, the calcium chloride was inserted inside the device in order to attract the dampness from the surroundings. Soft contact lenses were photographed for three types of materials. By using these techniques, the 120 images are obtained distributed as 60 by means of concave side in the lens and 10 pictures and light and 10 pictures with polarization lighting in every example. In addition, the other 60 imagery is the convex face of the lens. All images processing were done in Photoshop due to low shadows that generate too much noise in the spectrum under test. The chosen part of each photo is processed which suppose to obtained without shadow. Cropped size of 1600 x 1200 pixels were used in the image processing. By using MATLAB programs code, novel crop imagery could be treat to obtain the results. The results obtained represented in diagram anywhere the feature standards of wavelength and intensity is significant.

4. WORK RESULTS

In order to examine the features of essential material and nano-photonics materials, the optomagnetic spectroscopy technique is used. The results obtained are by incorporating the fullerene nano-particles and derivative in essential materials for soft contact lenses. By mean of separate canals, blue, red and green, colors mechanism, the digital images has been analyzed and then progression by spectral convolution algorithms to provide the concluding results in diagrams. Figure 3 show the peak value of para-magnetic properties over zero height and diamagnetic under zero height property in contrast to wavelength differences.

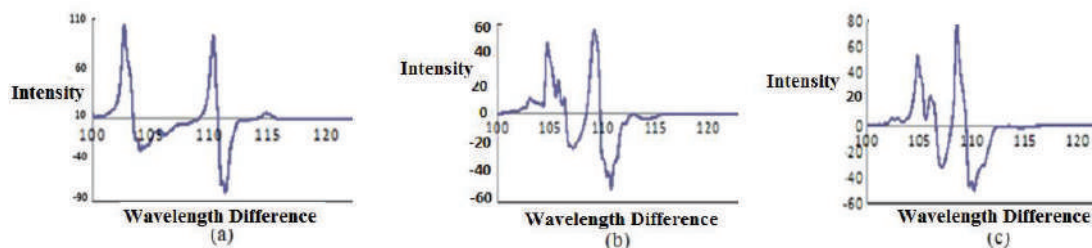


Figure 3: spectrums of average peaks in soft contact lenses: (a): essential material (b): incorporate fullerene (c): incorporate fullerol

The materials investigation for soft contact lenses photo-graphed by means of convex side of the lenses in shape 3 illustrate the recorded samples performs differently. Obviously, the basic material in Figure 3a, there are four picks, two negative and two positive and the average wavelengths and amplitude of first and second peaks are 102, 103, 110, and 87 respectively. The negative peaks is (104, -29) and (111, -79) and the material with incorporate fullerene and C60 in Figure 3b. The wavelength and amplitude in positive peaks are (104, 43) and (109, 53). For negative peaks the amplitude is (106, -21) and (110, -50). In the case of material with incorporate fullerol C60 (OH)24 in shape 3c, present a positive peaks at (104, 53) and (108, 74) and the negative at (107, -30) with (110, -50). For every 10 graphs of lens convex side, the maximum peak value of positive and negative was selected as average climax value. All this average values and standard deviation value is illustrated by Table 1.

Table 1: standards deviation and typical value of amplitude and wavelength in convex side

Soft Contact Lens Type	Wavelength Value	Wavelength Standard Deviation	Amplitude Value	Amplitude Standard Deviation
Essential Material +	104	3	108	10
Essential Material -	111	0.32	-89	16
Essential Material & Fullerene +	107	2	71	9
Essential Material & Fullerene -	110	0.37	-56	6
Essential Material & Fullerol +	108	1	87	10
Essential Material & Fullerol -	109	0.2	-53	4

Figure 4 shows the obtained results of photo-graphing the concave side of contact lens in this research. Figure 4a shows the basic material with many peaks whose average wavelength and amplitude are 101, 62, 102, 39, 104, -20, 105, -19, 109, 24, 110, 18 and 110, -37 respectively.

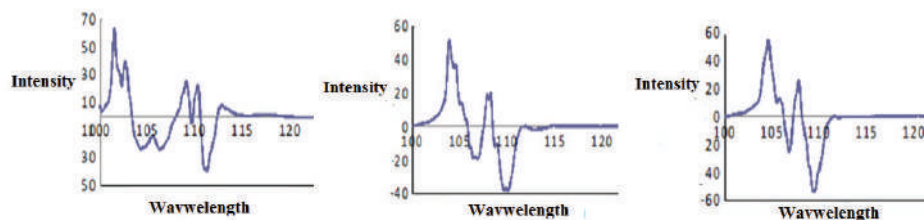


Figure 5: Average spectrums of materials (a): basic material (b): with incorporate fullerene (c): with incorporate fullerol

The amplitude and wavelength of optimistic peak for material by means of incorporate fullerene C60 showing in Figure 4b are 103, 51, 107, 18 while the negative peaks are 106, -18,

109, -37. In case of the material with incorporate fullerol C60(OH)24 as illustrated in Figure 4c, the positive climax happen at 104, 55 and 107, 25, and the negative peaks occur at 106, -23, 109, -49. In every 10graphics of lens concave side, the maximum amplitude peak positive and negative was selected with average values. Table 2 illustrates the average values and standard deviation values.

Table 2: standard deviation and average value of amplitude and wavelength

Soft Contact Lens Type	Wavelength Value	Wavelength Standard Deviation	Amplitude Value	Amplitude Standard Deviation
Essential Material +	101	0,2	68	10
Essential Material -	111	0.39	-47	3
Essential Material & Fullerene +	103	0.19	56	5
Essential Material & Fullerene -	110	0.3	-44	4
Essential Material& Fullerol +	104	1	59	8
Essential Material& Fullerol -	109	0.2	-59	7

the wavelength of material with integrated fullerene and the material with incorporate fullerol are totally identical while shifted by 2nm contrast with basic material. the peak amplitude is varies up to 20 units which is observe so as to in all cases the peaks happen at wavelength is 102 nm to 114nm whilst the amplitude contain somewhat better difference and variations. from these results one could conclude that the differences in the intensity and wavelength peak are happen obviously for basic materials of soft contact lens and incorporate fullerol and fullerene. this is because of different surface treated and influence in two types of nanomaterials in soft contact lens. the convex side is crushed whilst the concave side is casted by many process reason.

5. CONCLUSION

This work introduced a materials classification of profitable and new soft contact lenses using wavelength transformation algorithms. To investigate the basic and nono-photonic material characteristics, the optogenetic spectroscopy techniques are used. Hence, by incorporating the nano-particles of fullerene with associated derivatives in the essential material for soft contact lenses is inspected and examined. Hence, when the material with C60, folderol, C60(OH)24 and fullerene is incorporated, the peaks are nearly close in each type and identical wavelength while different intensities. The amplitude peak varies up to 20 units which observe that the 3 materials occur the climaxes at wavelength in the variety from 102 to 114nm. In same time, the intensities have somewhat higher variations which could be illustrate same influence in both nano-materials because of different facade treatment contact lenses. In the imaging of soft contact lens in convex side, the paramagnetic amplitude properties are better than the imaging in the concave side which is probable to notice the variation in influences of a nano-photonic compare with the basic material with optogenetic spectroscopy technique. In addition, reliable

acquired results were obtained and the optogenetic spectroscopy procedure is qualitative to use for classification the facade structure of materials. Depend on obtain drawing and waveforms; the similarities and differences of dissimilar contact lenses influences.

ACKNOWLEDGMENT

WE WOULD LIKE TO THANK DEAN OF DIJLAH UNIVERSITY COLLEGE FOR HIS SUPPORT TO DONE THIS WORK

REFERENCES

- [1]. Christopher Stephen Andrew Musgrave 1 and Fengzhou Fang, " Contact Lens Materials: A Materials Science Perspective", Materials 2019, 12
- [2]. Hevnen M. et al., " Activity of Deposited Lysozyme on Contemporary Soft Contact Lenses Exposed to Differing Lens Care Systems", Dove Medical Press Ltd, Clinical Ophthalmology 2021;15 1727–1733, 2021
- [3]. Morgan PB, Woods C, Tranoudis I, et al. International contact lens prescribing in 2019. Contact Lens Spectrum. 2020;35:26–32. 2019
- [4]. Nichols JJ, Chalmers RL, Dumbleton K, et al. The case for using hydrogen peroxide contact lens care solutions: a review. Eye Contact Lens. 2019;45:69–82. 2019
- [5]. Nichols, J. Contact Lenses 2017. In Contact Lens Spectrum; PentaVision LLC: Ambler, PA, USA, 2018; pp 20–25.
- [6]. Kirchhof, S.; Goepferich, A.M.; Brandl, F.P. Hydrogels in ophthalmic applications. Eur. J. Pharm. Biopharm. 2015, 95, 227–238.
- [7]. Xu, J.; Xue, Y.; Hu, G.; Lin, T.; Gou, J.; Yin, T.; He, H.; Zhang, Y.; Tang, X. A comprehensive review on contact lens for ophthalmic drug delivery. J. Control. Release 2018, 281, 97–118.
- [8]. Vidal-Rohr, M.; Wolffsohn, J.S.; Davies, L.N.; Cerviño, A. Effect of contact lens surface properties on comfort, tear stability and ocular physiology. Contact Lens Anterior Eye 2018, 41, 117–121.
- [9]. Lee, D.; Cho, S.; Park, H.S.; Kwon, I. Ocular drug delivery through pHEMA-Hydrogel contact lenses Co-loaded with lipophilic vitamins. Sci. Rep. 2016, 6, 1–8.
- [10]. Zhao, J.; Mayumi, K.; Creton, C.; Narita, T. Rheological properties of tough hydrogels based on an associating polymer with permanent and transient crosslinks: Effects of crosslinking density. J. Rheol. (N.Y.) 2017, 61, 1371–1383
- [11]. Musgrave, C.S.A.; Nazarov, W.; Bazin, N. The effect of para-divinyl benzene on styrenic emulsion-templated porous polymers: A chemical Trojan horse. J. Mater. Sci. 2017, 52, 3179–3187
- [12]. Abdollahi, E.; Khalafi-Nezhad, A.; Mohammadi, A.; Abdouss, M.; Salami-Kalajahi, M. Synthesis of new molecularly imprinted polymer via reversible addition fragmentation transfer polymerization as a drug delivery system. Polymer (U. K.) 2018, 143, 245–257.
- [13]. Zhang, C.; Liu, Z.; Wang, H.; Feng, X.; He, C. Novel Anti-Biofouling Soft Contact Lens: L –Cysteine Conjugated Amphiphilic Conetworks via RAFT and Thiol—Ene Click Chemistry. Macromol. Biosci. 2017, 17, 1600444.
- [14]. Ko, J.; Cho, K.; Han, S.W.; Sung, H.K.; Baek, S.W.; Koh, W.-G.; Yoon, J.S. Hydrophilic surface modification of poly(methyl methacrylate)-based ocular prostheses using poly(ethylene glycol) grafting. Colloids Surf. B Biointerfaces 2017, 158, 287–294.
- [15]. Shokrollahzadeh, F.; Hashemi, H.; Jafarzadehpur, E.; Mirzajani, A.; Khabazkhoob, M.; Yekta, A.; Asgari, S. Corneal aberration changes after rigid gas permeable contact lens wear in keratonic patients. J. Curr. Ophthalmol. 2016, 28, 194–198.

-
- [16]. Yuksel Elgin, C.; Iskeleli, G.; Aydin, O. Effects of the rigid gas permeable contact lense use on tear and ocular surface among keratoconus patients. *Contact Lens Anterior Eye* 2018, 41, 273–276.
- [17]. Yuksel Elgin, C.; Iskeleli, G.; Aydin, O. Effects of the rigid gas permeable contact lense use on tear and ocular surface among keratoconus patients. *Contact Lens Anterior Eye* 2018, 41, 273–276
- [18]. Ruan, J.L.; Chen, C.; Shen, J.H.; Zhao, X.L.; Qian, S.H.; Zhu, Z.G. A gelated colloidal crystal attached lens for noninvasive continuous monitoring of tear glucose. *Polymers* 2017, 9, 125.
- [19]. Tseng, R.C.; Chen, C.C.; Hsu, S.M.; Chuang, H.S. Contact-lens biosensors. *Sensors* 2018, 18, 2651.
- [20]. Kim, J.; Kim, M.; Lee, M.S.; Kim, K.; Ji, S.; Kim, Y.T.; Park, J.; Na, K.; Bae, K.H.; Kim, H.K.; et al. Wearable smart sensor systems integrated on soft contact lenses for wireless ocular diagnostics. *Nat. Commun.* 2017, 8, 14997.
- [21]. Seo, E.; Kumar, S.; Lee, J.; Jang, J.; Park, J.H.; Chang, M.C.; Kwon, I.; Lee, J.S.; Huh, Y. il Modified hydrogels based on poly(2-hydroxyethyl methacrylate) (pHEMA) with higher surface wettability and mechanical properties. *Macromol. Res.* 2017, 25, 704–711.
- [22]. Sulley, A.; Young, G.; Hunt, C. Factors in the success of new contact lens wearers. *Contact Lens Anterior Eye* 2017, 40, 15–24.
- [23]. Maulvi, F.A.; Desai, A.R.; Choksi, H.H.; Patil, R.J.; Ranch, K.M.; Vyas, B.A.; Shah, D.O. Effect of surfactant chain length on drug release kinetics from microemulsion-laden contact lenses. *Int. J. Pharm.* 2017, 524, 193–204.
- [24]. Ubholz, B.; Chröder, S.V.E.N.S.; Ihranyan, A.L.M. Light scattering in poly (vinyl alcohol) hydrogels reinforced with nanocellulose for ophthalmic use. *Opt. Mater. Express* 2017, 7, 2824–2837.
- [25]. Dutta, D.; Kamphuis, B.; Ozcelik, B.; Thissen, H.; Pinarbasi, R.; Kumar, N.; Willcox, M.D.P. Development of silicone hydrogel antimicrobial contact lenses with Mel4 peptide coating. *Optom. Vis. Sci.* 2018, 95, 937–
- [26]. Ubholz, B.; Chröder, S.V.E.N.S.; Ihranyan, A.L.M. Light scattering in poly (vinyl alcohol) hydrogels reinforced with nanocellulose for ophthalmic use. *Opt. Mater. Express* 2017, 7, 2824–2837.
- [27]. Stach, S.; Țălu, Ș.; Trabattoni, S.; Tavazzi, S.; Głuchaczka, A.; Siek, P.; Zajac, J.; Giovanzana, S. Morphological Properties of Siloxane-Hydrogel Contact Lens Surfaces. *Curr. Eye Res.* 2017, 42, 498–505.
- [28]. Salzillo, R.; Schiraldi, C.; Corsuto, L.; D’Agostino, A.; Filosa, R.; De Rosa, M.; La Gatta, A. Optimization of hyaluronan-based eye drop formulations. *Carbohydr. Polym.* 2016, 153, 275–283.
- [29]. Moustafa, M.A.; Elnaggar, Y.S.R.; El-Refaie, W.M.; Abdallah, O.Y. Hyalugel-integrated liposomes as a novel ocular nanosized delivery system of fluconazole with promising prolonged effect. *Int. J. Pharm.* 2017, 534, 14–24
-

SYNTHESIS AND *IN VITRO* ANTIOXIDANT PROPERTIES OF SOME NOVEL 1,3,4-TRISUBSTITUE-4,5-DIHYDRO-1*H*-1,2,4-TRIAZOL-5-ONES

Assoc. Prof. Dr. Onur Akyıldırım

Kafkas University, Faculty of Engineering and Architecture, Department of Chemical
Engineering, 36100, Kars, Turkey
ORCID ID: 0000-0003-1090-695X

Prof. Dr. Özlem Gürsoy-Kol

Kafkas University, Faculty of Science and Letters, Department of Chemistry, 36100,
Kars, Turkey
ORCID ID: 0000-0003-2637-9023

Prof. Dr. Haydar Yüksek

Kafkas University, Faculty of Science and Letters, Department of Chemistry, 36100,
Kars, Turkey
ORCID ID: 0000-0003-1289-1800

Abstract

*It is known that 1,2,4-Triazole-derived compounds have a wide range of biological activities. Due to the wide biological activities of 1,2,4-triazole compounds, many different derivatives of these compounds have been synthesized. Therefore, the properties of compounds containing 1,2,4-triazole ring are reported both in vitro and in vivo studies. Compounds with high activity are commonly used as active pharmaceutical ingredients. In this study, three new 1-phenacyl-3-methyl-4-(3-methoxy-4-benzoylmethoxy-benzylidenamino)-4,5-dihydro-1*H*-1,2,4-triazol-5-one (4a), 1-phenacyl-3-(*p*-methylbenzyl)-4-(3-methoxy-4-benzoylmethoxy-benzylidenamino)-4,5-dihydro-1*H*-1,2,4-triazol-5-one (4b) and 1-phenacyl-3-(*p*-chlorobenzyl)-4-(3-methoxy-4-hydroxy-benzylidenamino)-4,5-dihydro-1*H*-1,2,4-triazol-5-one (4c) compounds were synthesized by the reaction of 3-alkyl(aryl)-4-(3-methoxy-4-hydroxy-benzylidenamino)-4,5-dihydro-1*H*-1,2,4-triazol-5-one (3) compound with phenacyl bromide in sodium ethoxide. These new compounds were characterized by elemental analysis, IR, ¹H NMR, ¹³C NMR and UV spectral data. They were then analyzed for their potential antioxidant activities in vitro by three different methods: reducing power, free radical scavenging and metal chelating activity. These antioxidant activities were compared with standard antioxidants, such as BHA, BHT and α-tocopherol.*

Keywords: Schiff base, 1, 2, 4-triazole, synthesis, antioxidant activity.

1. Introduction

Various studies have been conducted on 1,2,4-triazoles and their anticancer (Maddali vd., 2021), antiviral, antitumor (Jilloju vd., 2021), antimicrobial (Amin vd., 2021), antiproliferative and antioxidant properties (Sicak, 2021) have been reported.

In a recent study, *N*-acetyl derivatives of 1,2,4-triazole-derived compounds were synthesized and their *in vitro* antioxidant and *in vitro* antibacterial properties were investigated (Manap, 2021). A series of compounds derived from 4,5-dihydro-1*H*-1,2,4-triazol-5-one were synthesized and their *in vitro* antioxidant activities were analyzed. In addition, antimicrobial

activities against bacteria and yeast were investigated (Yukse vd., 2013). The synthesis, spectroscopic examinations and antioxidant activity of the 1-acetyl-3-methyl-derived compound bearing 1,2,4-triazole ring were investigated (Gokce vd., 2014).

In current study, three new 1-phenacyl-3-methyl-4-(3-methoxy-4-benzoylmethoxybenzylidenamino)-4,5-dihydro-1*H*-1,2,4-triazol-5-one (**4a**), 1-phenacyl-3-(*p*-methylbenzyl)-4-(3-methoxy-4-benzoylmethoxybenzylidenamino)-4,5-dihydro-1*H*-1,2,4-triazol-5-one (**4b**) and 1-phenacyl-3-(*p*-chlorobenzyl)-4-(3-methoxy-4-hydroxybenzylidenamino)-4,5-dihydro-1*H*-1,2,4-triazol-5-one (**4c**) compounds were synthesized. The antioxidant activities of the newly synthesized compounds were investigated using antioxidant methodologies such as 1,1-diphenyl-2-picrylhydrazil (DPPH) free radical scavenging, reducing power and metal chelating activities.

2. Materials and Methods

Reagents and solvents used in this study were purchased from Merck AG, Aldrich and Fluka. The starting compounds 3-alkyl(aryl)-4-amino-4,5-dihydro-1*H*-1,2,4-triazol-5-ones **2** were prepared from the reactions of the corresponding ester ethoxycarbonylhydrazones **1** with an aqueous solution of hydrazine hydrate as described previously (Ikizler & Yuksek, 1993). Compound **3** was obtained from the reaction of compounds **2** with 3-methoxy-4-hydroxybenzaldehyde through a recently reported method (Manap, S, 2009). Melting points were determined in open glass capillaries using an Electrothermal digital melting point apparatus and are uncorrected. The IR spectra were obtained on a Perkin-Elmer Instruments Spectrum One FT-IR spectrometer. ¹H and ¹³C NMR spectra were recorded in deuterated dimethyl sulfoxide with TMS as internal standard using a Varian Mercury spectrometer at 200 MHz and 50 MHz, respectively. UV absorption spectra were measured in 10 mm quartz cells between 200 and 400 nm using a PG Instruments Ltd T80 UV / Vis spectrometer. Extinction coefficients (ϵ) are expressed in L mol⁻¹ cm⁻¹. Elemental analyses were carried out on a Leco 932 Elemental Combustion System (CHNS-O) for C, H and N.

2.1. General procedure for the synthesis of compound 4. Na (0.02 mol) was dissolved in 100 mL absolute ethanol and this solution was mixed with 3-alkyl(aryl)-4-(3-methoxy-4-hydroxybenzylidenamino)-4,5-dihydro-1*H*-1,2,4-triazol-5-one (**3**) (0.01 mol), followed by reflux for 2 h. After cooling of this solution to room temperature, phenacyl bromide (0.02 mol) was added into this and this mixture was refluxed for 5 h and then filtered. The filtrate was evaporated through vacuo and the crude product was recrystallized from corresponding solvent to afford compound.

2.1.1. 1-Phenacyl-3-methyl-4-(3-methoxy-4-benzoylmethoxybenzylidenamino)-4,5-dihydro-1*H*-1,2,4-triazol-5-one (4a**).** Yield 2.80 g (58%); mp 400 °C; IR (KBr): ν C=O 1725, 1695, C=N 1598, 1580, monosubstituted benzenoid ring 759 and 690 cm⁻¹; ¹H NMR (200MHz, DMSO-*d*₆): δ 2.40 (s, 3H, CH₃), 3.95 (s, 3H, OCH₃), 5.21 (s, 2H, NCH₂), 5.43 (s, 2H, OCH₂), 6.78-6.83 (m, 1H, Ar-H), 7.22-7.64 (m, 8H, Ar-H), 7.97-8.01 (m, 4H, Ar-H), 9.71 (s, 1H, N=CH); ¹³C NMR (50MHz, DMSO-*d*₆): δ 11.76 (CH₃), 51.61 (NCH₂), 56.27 (OCH₃), 71.80 (OCH₂), 110.00, 113.88, 114.82, 122.99, 123.84 (arom-C), 128.28 (2C), 128.37 (2C), 128.43, 128.62 (arom-C), 129.12 (2C), 134.17 (2C), 134.80, 138.87, 144.93 (arom-C), 150.63 (triazole C₃), 151.23 (N=CH), 154.38 (triazole C₅), 154.91, 154.38 (2C=O); UV λ_{\max} (ϵ): 316 (16300), 204 (21454) nm; *Anal.* Calcd. for C₂₇H₂₄N₄O₅ (484.51): C, 66.93; H, 4.99; N, 11.56. Found: C, 64.52; H, 5.31; N, 12.55.

2.1.2. 1-Phenacyl-3-(*p*-methylbenzyl)-4-(3-methoxy-4-benzoylmethoxybenzylidenamino)-4,5-dihydro-1*H*-1,2,4-triazol-5-one (4b). Yield 3.61 g (63%); mp 105 °C; IR (KBr): ν C=O 1710, 1695, C=N 1596, monosubstituted benzenoid ring 760 and 689 cm^{-1} ; ^1H NMR (200MHz, DMSO- d_6): δ 2.23 (s, 3H, CH₃), 3.83 (s, 3H, OCH₃), 4.03 (s, 2H, CH₂), 5.25 (s, 2H, NCH₂), 5.42 (s, 2H, OCH₂), 7.08-7.35 (m, 15H, Ar-H), 7.58 (d, 2H, Ar-H), 9.45 (s, 1H, N=CH); UV λ_{max} (ϵ): 320 (19784), 296 (13497), 238 (22383), 214 (26000) nm.

2.1.3. 1-Phenacyl-3-(*p*-chlorobenzyl)-4-(3-methoxy-4-hydroxybenzylidenamino)-4,5-dihydro-1*H*-1,2,4-triazol-5-one (4c). Yield 4.03 g (68%); mp 172 °C; IR (KBr): ν OH 3235, C=O 1705, 1690, C=N 1597, monosubstituted benzenoid ring 753 and 688 cm^{-1} ; ^1H NMR (200MHz, DMSO- d_6): δ 3.84 (s, 3H, OCH₃), 4.13 (s, 2H, CH₂), 5.45 (s, 2H, NCH₂), 6.89 (d, 1H, Ar-H), 7.20-7.72 (m, 9H, Ar-H), 8.05 (d, 2H, Ar-H), 9.48 (s, 1H, N=CH), 9.92 (s, 1H, OH); UV λ_{max} (ϵ): 320 (19645), 294 (13734), 240 (25980), 220 (26094) nm; *Anal.* Calcd. for C₂₅H₂₁N₄O₄Cl (476.92): C, 62.96; H, 4.44; N, 11.75. Found: C, 63.18; H, 4.68; N, 9.10.

2.2. Antioxidant activity. Butylated hydroxytoluene (BHT) was purchased from E. Merck (Merck KGaA, Darmstadt, Germany). Ferrous chloride, α -tocopherol, 1,1-diphenyl-2-picrylhydrazyl (DPPH \cdot), 3-(2-pyridyl)-5,6-bis(phenylsulfonic acid)-1,2,4-triazine (ferrozine), butylated hydroxyanisole (BHA) and trichloroacetic acid (TCA) were bought from Sigma (Sigma-Aldrich GmbH, Steinheim, Germany).

2.2.1. Reducing power. The reducing power of the newly synthesized compounds was investigated according to Oyaizu's method (Oyaizu, 1986). Different concentrations of the samples (50-250 $\mu\text{g/mL}$) in DMSO (1 mL) were mixed with phosphate buffer (2.5 mL, 0.2 M, pH = 6.6) and potassium ferricyanide (2.5 mL, 1%). The mixture was incubated at 50 °C for 20 min after which a portion (2.5 mL) of trichloroacetic acid (10%) was added to the mixture, which was then centrifuged for 10 min at 1000 x g. The upper layer of solution (2.5 mL) was mixed with distilled water (2.5 mL) and FeCl₃ (0.5 mL, 0.1%), and then the absorbance was measured using a spectrophotometer at 700 nm. Higher absorbance of the reaction mixture showed a greater reducing power.

2.2.2. Free radical scavenging activity. Free radical scavenging activity of compounds was measured by DPPH \cdot , using the method of Blois (Blois, 1958). Concisely, 0.1 mM solution of DPPH \cdot in ethanol was prepared, and this solution (1 mL) was added to sample solutions in DMSO (3 mL) at different concentrations (50-250 $\mu\text{g/mL}$). The mixture was shaken vigorously and incubated at room temperature for 30 min. Then the absorbance was measured at 517 nm in a spectrophotometer. Lower absorbance of the reaction mixture showed higher free radical scavenging activity. The DPPH \cdot concentration (mM) in the reaction medium was calculated from the following calibration curve and assigned by linear regression (R: 0.997):

$$\text{Absorbance} = 0.0003 \times \text{DPPH}\cdot - 0.0174$$

The capability to scavenge the DPPH radical was calculated using the following equation:

$$\text{DPPH}\cdot \text{ scavenging effect (\%)} = (A_0 - A_1/A_0) \times 100$$

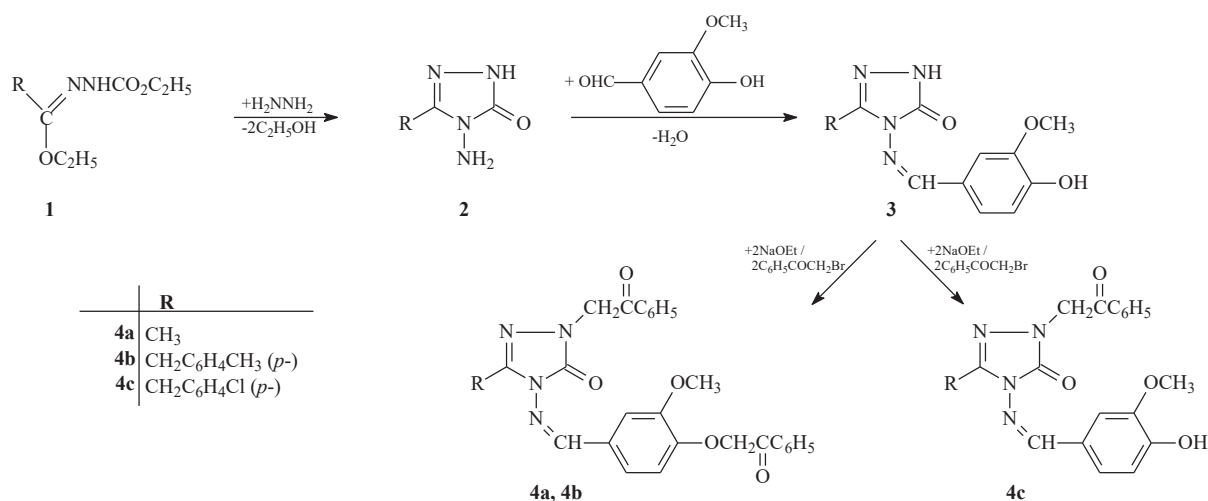
where A_0 is the absorbance of the control reaction and A_1 is the absorbance in the presence of the samples or standards.

2.2.3. Metal chelating activity. The method of Dinis *et al* were used to estimate the chelation of ferrous ions by the synthesized compounds and standards (Dinis *et al.*, 1994). Briefly, the synthesized compounds (50-250 $\mu\text{g mL}^{-1}$) were added to a 2 mM solution of FeCl₂ (0.05 mL). The reaction was initiated by the addition of 5 mM ferrozine (0.2 mL) and

the mixture was shaken vigorously and incubated at room temperature for 10 min. After the mixture had reached equilibrium, the absorbance of the solution was then measured at 562 nm in a spectrophotometer. All test and analyses were run in triplicate and averaged. The percentage of inhibition of ferrozine-Fe²⁺ complex formation was given by the formula: % Inhibition = $(A_0 - A_1/A_0) \times 100$, where A_0 is the absorbance of the control, and A_1 is the absorbance in the presence of the samples or standards. The control did not contain any compound or standard.

3. Results and Discussion

The 1-phenacyl-3-methyl-4-(3-methoxy-4-benzoylmethoxy-benzylidenamino)-4,5-dihydro-1*H*-1,2,4-triazol-5-one (**4a**), 1-phenacyl-3-(*p*-methylbenzyl)-4-(3-methoxy-4-benzoylmethoxy-benzylidenamino)-4,5-dihydro-1*H*-1,2,4-triazol-5-one (**4b**) and 1-phenacyl-3-(*p*-chlorobenzyl)-4-(3-methoxy-4-hydroxy-benzylidenamino)-4,5-dihydro-1*H*-1,2,4-triazol-5-one (**4c**) compounds were prepared. Compound **4** was synthesized by the reaction of **3** type compound with phenacyl bromide in sodium ethoxide (Scheme 1).



Scheme 1. Synthesis route of compounds **2-4**.

The structures of three new 1-phenacyl-3-methyl-4-(3-methoxy-4-benzoylmethoxy-benzylidenamino)-4,5-dihydro-1*H*-1,2,4-triazol-5-one (**4a**), 1-phenacyl-3-(*p*-methylbenzyl)-4-(3-methoxy-4-benzoylmethoxy-benzylidenamino)-4,5-dihydro-1*H*-1,2,4-triazol-5-one (**4b**) and 1-phenacyl-3-(*p*-chlorobenzyl)-4-(3-methoxy-4-hydroxy-benzylidenamino)-4,5-dihydro-1*H*-1,2,4-triazol-5-one (**4c**) compounds identified using IR, ¹H NMR, ¹³C NMR, UV and elemental analyses data.

3.1. Antioxidant activity. The antioxidant activities of three new compounds **4a-c** were determined. Several methods were used to determine antioxidant activities. The methods used in the study are given below:

3.1.1. Total reductive capability using the potassium ferricyanide reduction method.

The reductive capabilities of compounds were evaluated by the extent of conversion of the Fe³⁺ / ferricyanide complex to the Fe²⁺ / ferrous form. The reducing powers of the compounds were detected at different concentrations, and results were compared with BHA, BHT and α -tocopherol. The reducing capacity of a compound could assist as a significant indicator of its

potential antioxidant activity (Meir vd., 1995). The antioxidant activity of a compound depends on several mechanisms, such as prevention of chain initiation, binding of transition metal ion catalyst, decomposition of peroxides, prevention of continued hydrogen abstraction, reductive capacity and radical scavenging (Yildirim vd., 2001). In the present study, all the amount of the compounds showed lower absorbance than standard antioxidants. Therefore, no activities were seen to reduce metal ions complexes to their lower oxidation state or to join in any electron transfer reaction. In other words, compounds did not show any reductive activities.

3.1.2. DPPH[•] radical scavenging activity. The model of scavenging the stable DPPH radical pattern is an extensively used method to assess antioxidant activities in a relatively short time compared with other methods. The impact of antioxidants on DPPH radical scavenging was assumed to be because of their hydrogen donating ability (Baumann, 1979). DPPH is a stable free radical and accepts an electron or hydrogen radical to become a stable diamagnetic molecule (Soares vd., 1997). The reduction capability of DPPH radicals was detected by decrease in its absorbance at 517 nm induced by antioxidants. The absorption maximum of a stable DPPH radical in ethanol was at 517 nm. The decline in absorbance of DPPH radical brought forth by antioxidants, owing to reaction between antioxidant molecules and radical, progresses, which result in the scavenging of the radical by hydrogen donation. It is visually obvious as a discoloration from purple to yellow. Hence, DPPH[•] is usually used as a substrate to evaluate antioxidative activity of antioxidants (Duh, 1999). In the study, antiradical activities of compounds and standard antioxidants such as BHA, BHT and α -tocopherol were established by using DPPH[•] method. Scavenging effect values of compounds **4a**, **4b**, **4c**, BHA and α -tocopherol at different concentrations are given. Compounds **4a**, **4b**, **4c** showed low activity as radical scavengers.

3.1.3. Ferrous ion chelating activity. The chelating effect towards ferrous ions by the compounds and standards was determined. Ferrozine can quantitatively make up complexes with Fe^{2+} . In the presence of chelating agents, the complex formation is interrupted, which was understood by the decrease in the tone of red color of the complex. Measurement of colour reduction thus allows estimation of the chelating activity of the coexisting chelator (Yamaguchi vd., 2000). Transition metals have crucial role in the generation oxygen free radicals in living organism. The ferric iron (Fe^{3+}) is the relatively biologically inactive form of iron. Nevertheless, it can be reduced to the active Fe^{2+} , depending on condition, particularly pH (Strlic vd., 2002) and oxidized back through. Fenton type reactions with the production of hydroxyl radical or Haber-Weiss reactions with superoxide anions. The production of these radicals may cause lipid peroxidation, protein modification and DNA damage. Chelating agents may not activate metal ions and potentially inhibit the metal-dependent processes (Finefrock vd., 2003). Furthermore, the production of highly active ROS such as $\text{O}_2^{\cdot-}$, H_2O_2 and OH^{\cdot} is also catalyzed by free iron through Haber-Weiss reactions:



Iron is known as the most important lipid oxidation pro-oxidant because of its high reactivity among the transition metals. The ferrous state of iron accelerates lipid oxidation by corrupting the hydrogen and lipid peroxides to reactive free radicals via the Fenton reactions:



Fe^{3+} ion also produces radicals from peroxides, though the rate is tenfold less than that of Fe^{2+} ion, which is the most powerful pro-oxidant among the various types of metal ions (Calis vd., 1993). Ferrous ion chelating activities of the compounds **4a-c**, BHT, BHA and α -tocopherol are given. In this study, metal chelating capacity was significant since it reduced the concentrations of the catalyzing transition metal. It was stated that chelating agents that form

σ -bonds with a metal are effective as secondary antioxidants since they reduce the redox potential thereby stabilizing the oxidized form of metal ion (Gordon, M. H, 1990). The obtained data reveal that **4b** compound, except **4a** and **4c**, show a marked capacity for iron binding, suggesting that their action as peroxidation protectors may be associated with their iron binding capacity. Instead, free iron is known to have low solubility and a chelated iron complex has greater solubility in solution, which can be contributed merely by the ligand. Additionally, the compound-iron complex may also be active, since it can participate in iron-catalyzed reactions.

4. Conclusions

The synthesis and *in vitro* antioxidant evaluation of new 4,5-dihydro-1H-1,2,4-triazol-5-one derivatives are defined. **4b** compound, apart from **4a** and **4c**, reveal a marked capacity for iron binding. The data here reported could be of the possible interest because of the observed metal chelating activities of the studied compound could prevent redox cycling. Design and synthesis of novel small molecules which can definitely protective role in biological systems are in view in modern medicinal chemistry. These results may lead to development of other novel therapeutic targets based on triazole.

Acknowledgements. This work was supported by the Turkish Scientific and Technological Council (Project Number: TBAG 108T984).

5. References

- Amin, N. H., El-Saadi, M. T., Ibrahim, A. A., & Abdel-Rahman, H. M. (2021). Design, synthesis and mechanistic study of new 1,2,4-triazole derivatives as antimicrobial agents. *Bioorganic Chemistry*, 111, 104841. <https://doi.org/10.1016/j.bioorg.2021.104841>
- Baumann, J. W., G. J. Bruchhausen, FV. (1979). Prostaglandin synthetase inhibiting O₂-radical scavenging properties of some flavonoids and related phenolic compounds. *Naunyn-Schmiedeberg's Arch Pharmacol*, 308, 27–32.
- Blois, M. S. (1958). Antioxidant determinations by the use of a stable free radical. *Nature*, 181(4617), 1199–1200.
- Calis, I., Hosny, M., Khalifa, T., & Nishibe, S. (1993). Secoiridoids from Fraxinus-Angustifolia. *Phytochemistry*, 33(6), 1453-1456. [https://doi.org/10.1016/0031-9422\(93\)85109-5](https://doi.org/10.1016/0031-9422(93)85109-5)
- Dinis, T., Madeira, V., & Almeida, L. (1994). Action of Phenolic Derivatives (acetaminophen, Salicylate, and 5-Aminosalicylate) as Inhibitors of Membrane Lipid-Peroxidation and as Peroxyl Radical Scavengers. *Archives of Biochemistry and Biophysics*, 315(1), 161-169. <https://doi.org/10.1006/abbi.1994.1485>
- Duh, P. D. (1999). Antioxidant activity of water extract of four Harng Jyur (Chrysanthemum morifolium Ramat) varieties in soybean oil emulsion. *Food Chemistry*, 66(4), 471-476. [https://doi.org/10.1016/S0308-8146\(99\)00081-3](https://doi.org/10.1016/S0308-8146(99)00081-3)
- Finefrock, A. E., Bush, A. I., & Doraiswamy, P. M. (2003). Current status of metals as therapeutic targets in Alzheimer's disease. *Journal of the American Geriatrics Society*, 51(8), 1143-1148. <https://doi.org/10.1046/j.1532-5415.2003.51368.x>
- Gokce, H., Akyildirim, O., Bahceli, S., Yuksek, H., & Kol, O. G. (2014). The 1-acetyl-3-methyl-4-[3-methoxy-4-(4-methylbenzoxy)benzylidenamino]-4,5-dihydro-1H-1,2,4-triazol-5-one molecule investigated by a joint spectroscopic and quantum chemical calculations.

- Journal of Molecular Structure*, 1056, 273-284.
<https://doi.org/10.1016/j.molstruc.2013.10.044>
- Gordon, M. H. (1990). *Food Antioxidants*. Elsevier.
- Ikizler, A., & Yuksek, H. (1993). Acetylation of 4-Amino-4,5-Dihydro-1H-1,2,4-Triazol-5-Ones. *Organic Preparations and Procedures International*, 25(1), 99-105.
<https://doi.org/10.1080/00304949309457935>
- Jilloju, P. C., Persoons, L., Kurapati, S. K., Schols, D., De Jonghe, S., Daelemans, D., & Vedula, R. R. (2021). Discovery of (+/-)-3-(1H-pyrazol-1-yl)-6,7-dihydro-5H-[1,2,4]triazolo[3,4-b][1,3,4] thiadiazine derivatives with promising in vitro anticoronavirus and antitumoral activity. *Molecular Diversity*. <https://doi.org/10.1007/s11030-021-10258-8>
- Maddali, N. K., Ivaturi, V. K. V., Murthy Yellajosula, L. N., Malkhed, V., Brahman, P. K., Pindiprolu, S. K. S. S., Kondaparthi, V., & Nethinti, S. R. (2021). New 1,2,4-Triazole Scaffolds as Anticancer Agents: Synthesis, Biological Evaluation and Docking Studies. *Chemistryselect*, 6(26), 6788-6796. <https://doi.org/10.1002/slct.202101387>
- Manap, S. (2009). *Bazı yeni 3-alkil(aryl)-4-(3,4-disubstituebenzilidenamino)-4,5-dihidro-1H-1,2,4-triazol-5-on türevlerinin sentezi, yapılarının aydınlatılması, antioksidan ve asitlik özelliklerinin incelenmesi* [Master Thesis]. Kafkas University.
- Manap, S. (2021). Synthesis and in vitro antioxidant and antimicrobial activities of novel 3-alkyl(aryl)-4-[3-methoxy-4-(2-furylcarbonyloxy)-benzylidenamino]-4,5-dihydro-1H-1,2,4-triazol-5-ones, and their N-acetyl, N-Mannich base derivatives. *Journal of the Iranian Chemical Society*. <https://doi.org/10.1007/s13738-021-02386-7>
- Meir, S., Kanner, J., Akiri, B., & Philosophhadass, S. (1995). Determination and Involvement of Aqueous Reducing Compounds in Oxidative Defense Systems of Various Senescing Leaves. *Journal of Agricultural and Food Chemistry*, 43(7), 1813-1819.
<https://doi.org/10.1021/jf00055a012>
- Oyaizu, M. (1986). Studies on products of browning reaction antioxidative activities of products of browning reaction prepared from glucosamine. *The Japanese journal of nutrition and dietetics*, 44(6), 307-315.
- Sicak, Y. (2021). Design and antiproliferative and antioxidant activities of furan-based thiosemicarbazides and 1,2,4-triazoles: Their structure-activity relationship and SwissADME predictions. *Medicinal Chemistry Research*, 30(8), 1557-1568.
<https://doi.org/10.1007/s00044-021-02756-z>
- Soares, J. R., Dinis, T. C. P., Cunha, A. P., & Almeida, L. M. (1997). Antioxidant activities of some extracts of *Thymus zygis*. *Free Radical Research*, 26(5), 469-478.
<https://doi.org/10.3109/10715769709084484>
- Strlic, M., Radovic, T., Kolar, J., & Pihlar, B. (2002). Anti- and prooxidative properties of gallic acid in Fenton-type systems. *Journal of Agricultural and Food Chemistry*, 50(22), 6313-6317. <https://doi.org/10.1021/jf025636j>
- Yamaguchi, F., Ariga, T., Yoshimura, Y., & Nakazawa, H. (2000). Antioxidative and anti-glycation activity of garcinol from *Garcinia indica* fruit rind. *Journal of Agricultural and Food Chemistry*, 48(2), 180-185. <https://doi.org/10.1021/jf990845y>
- Yildirim, A., Mavi, A., & Kara, A. A. (2001). Determination of antioxidant and antimicrobial activities of *Rumex crispus* L. extracts. *Journal of Agricultural and Food Chemistry*, 49(8), 4083-4089. <https://doi.org/10.1021/jf0103572>
- Yukse, H., Akyildirim, O., Yola, M. L., Gursoy-Kol, O., Celebier, M., & Kart, D. (2013). Synthesis, In Vitro Antimicrobial and Antioxidant Activities of Some New 4,5-Dihydro-1H-1,2,4-triazol-5-one Derivatives. *Archiv Der Pharmazie*, 346(6), 470-480.
<https://doi.org/10.1002/ardp.201300048>

INVESTIGATION OF THEORETICAL AND EXPERIMENTAL SPECTROSCOPIC PROPERTIES OF 3-p-METHYLBENZYL-4-[3-ETHOXY-4-(4-METHOXYBENZOXY)-BENZYLIDENAMINO]-4,5-DIHYDRO-1H-1,2,4-TRIAZOL-5-ONE

Asst. Prof. Dr. Hilal Medetalibeyoğlu

Kafkas University, Faculty of Science and Letters, Department of Chemistry,
36100, Kars, Turkey
ORCID ID: 0000-0002-1310-6811

Prof. Dr. Haydar Yüksek

Kafkas University, Faculty of Science and Letters, Department of Chemistry,
36100, Kars, Turkey
ORCID ID: 0000-0003-1289-1800

Abstract

In the present study, 3-p-methylbenzyl-4-[3-ethoxy-4-(4-methoxybenzoxy)-benzylidenamino]-4,5-dihydro-1H-1,2,4-triazol-5-one was optimized by using B3LYP/6-31G(d,p) basis set. All quantum chemical calculations were carried out using the Gaussian09W program package and the GaussView molecular visualization program. The ^1H -NMR and ^{13}C -NMR spectral values of the titled compound were calculated utilizing the B3LYP/6-31G(d,p) basis set. To determine the ^1H -NMR and ^{13}C -NMR isotropic shift values, the gauge independent atomic orbital (GIAO) methodology was used. The IR vibrational frequency values of the titled compound were calculated using B3LYP/6-31G(d,p) basis set. The IR vibrational frequency values were defined using the veda4f software. The UV-vis spectral calculations in the solvents of the titled compound were performed via the same basis set. TD-DFT computations in the solvents (ethanol, DMSO, and methanol) were used to identify the UV-Vis spectral analyses. All spectral results were compared with experimental ones suggested by Alkan and coworkers. The theoretically studied frontier molecular orbital analyses were used to determine the compound's electronic properties (ionization potential, electron affinity, molecular softness, molecular hardness, and electronegativity). Moreover, the highest occupied molecular orbital-lowest unoccupied molecular orbital (HOMO-LUMO), bond lengths, bond angles, dihedral angles, molecular electrostatic potential maps (MEP), and Mulliken atomic charges of the titled compound were investigated. The results of the correlational analysis between experimental and theoretical data were evaluated.

Keywords: 1,2,4-Triazol-5-one, Schiff base, HOMO-LUMO, MEP, UV-vis.

1. Introduction

1,2,4-Triazole heterocycle represents the key pharmacophore in various biologically-active compounds including antibacterial, antiviral against HIV, antifungal, anti-inflammatory, analgesic, and anticancer activities (Gao vd., 2019; Grytsai vd., 2020; Jiang vd., 2020; Tratat, 2020; Zampieri vd., 2019). In the present

study, we present a comprehensive investigation on the molecular structure, vibrational spectra, optic, thermal, and electronic properties of the title compound. According to our literature searches, results based on quantum chemical calculations and FT-IR, UV-vis, NMR spectral studies and HOMO–LUMO analysis on the title compound have not been reported elsewhere. Herewith, experimental and theoretical studies have been performed to give a detailed description of the molecular structure, electronic, optic, thermal NMR, UV-vis, and vibrational harmonic spectra of 3-p-methylbenzyl-4-[3-ethoxy-4-(4-methoxybenzoyloxy)-benzylidenamino]-4,5-dihydro-1H-1,2,4-triazol-5-one (Alkan vd., 2014). Furthermore, the title compound was analyzed computationally for nonlinear optical properties.

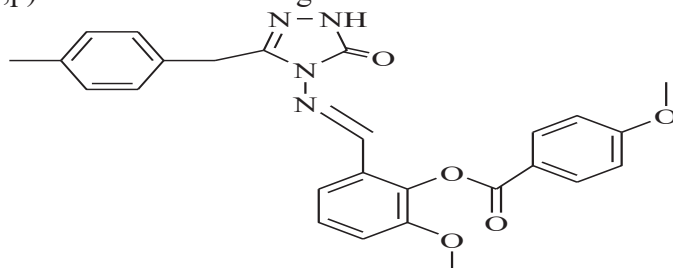
2. Materials and Methods

Gaussian09W program package was used for the DFT calculations (Frisch vd, 2009). The visualization for the verification of the optimized molecular structure was performed using the Gaussview program (Dennington vd, 2016). The geometry optimization of the titled compound was performed by using B3LYP method with 6-311G(d) basis set. The GIAO (Gauge-Including Atomic Orbital) ^1H and ^{13}C NMR chemical shift values in DMSO were calculated by the same basis set (Pulay & Hinton, 2007). The standard error rate was calculated according to $\delta_{\text{calc}} = a \delta_{\text{exp}} + b$ formula. The spectral data of the title compound were carried out with the same level of theory. The veda4f program was used for identification of computed IR data (Jamróz, 2013). The UV–Vis spectrum was obtained through time-dependent density functional theory (TD-DFT). The important electronic properties such as electronegativity, chemical hardness, chemical softness and chemical potential are calculated by the utilization of numerical values of the ionization energy and electron affinity (Foresman & Frisch, 2015). The nonlinear optical behaviour of the title compound was investigated by defining dipole moment (μ), polarizability (α), anisotropic polarizability ($\Delta\alpha$) and first static hyperpolarizability (β) on the same level of theory (Luo vd., 2011).

3. Results and Discussion

3.1. Molecular Structure

The structure with minimum global energy the title compound obtained by using B3LYP/6-31G(d,p) level is shown in Figure 1.



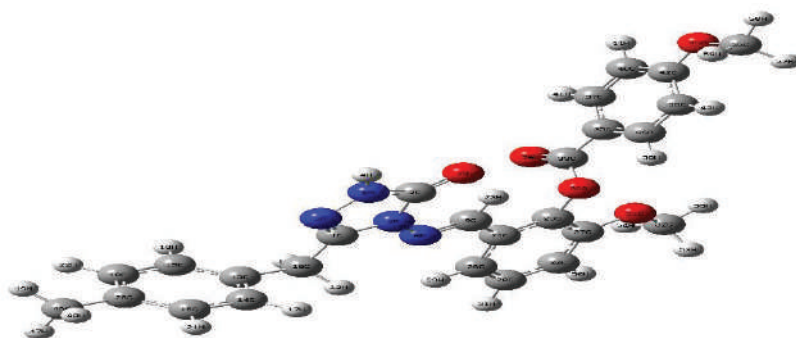


Figure 1. Optimized molecular structure of 3-p-methylbenzyl-4-[3-ethoxy-4-(4-methoxybenzoxy)-benzylidenamino]-4,5-dihydro-1H-1,2,4-triazol-5-one with B3LYP/6-31G(d,p) level of theory.

3.2. Vibrational frequencies

The titled compound has 59 atoms and the number of the normal vibrations are 171. The observed and calculated vibrational frequencies, the calculated IR intensities and assignments of vibrational frequencies for titled compound are summarized in Table 1.

Table 1. The calculated and experimental frequency values of the titled compound

	$\nu(\text{NH})$	$\nu(\text{C=O})$	$\nu(\text{C=O})$	$\nu(\text{C=N})$	$\nu(\text{C=N})$	$\nu(\text{C=O})$	ν substituted benzenoid ring
*Experimental	3163	1738	1700	1606	1578	1254	844
B3LYP (Scaled)	3699	1823	1821	1653	1629	1282	872
B3LYP (Unscaled)	3573	1761	1759	1597	1574	1239	842

* The experimental values were taken from ref (Alkan vd.,2014).

$$\diamond \quad \nu_{\text{calc}} = 1,0726 \nu_{\text{exp}} - 157,11 \quad R^2 = 0,9991$$

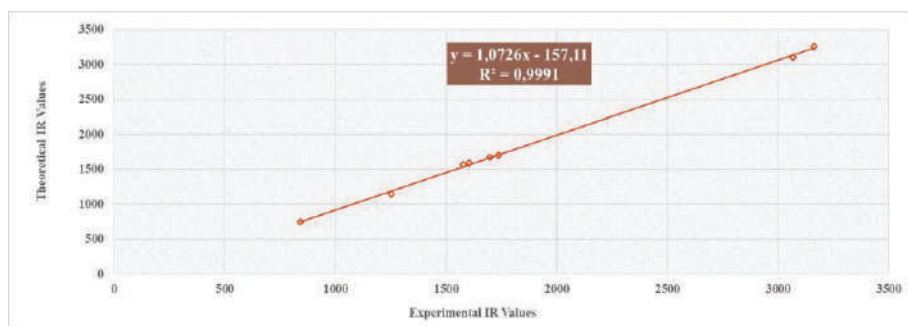


Figure 2. The correlation graphics for IR of the title compound.

3.3.NMR spectral analysis

In this study, the optimized molecular geometry of the titled compound was obtained by using B3LYP method with 6-31G(d,p) basis level in DMSO solvent. By considering the optimized molecular geometry of the titled compound the ^1H and ^{13}C NMR chemical shift values were calculated at the same level by using Gauge-Independent Atomic Orbital (GIAO) method (Wolinski vd., 1990).

$$\diamond \delta_{\text{exp}} = 1,039\delta_{\text{cal}} + 9,273 \text{ (R}^2 = 0,9968 \text{)} (^{13}\text{C-NMR in DMSO})$$

$$\diamond \delta_{\text{exp}} = 1,0145\delta_{\text{cal}} + 0,174 \text{ (R}^2 = 0,8703 \text{)} (^1\text{H-NMR in DMSO})$$

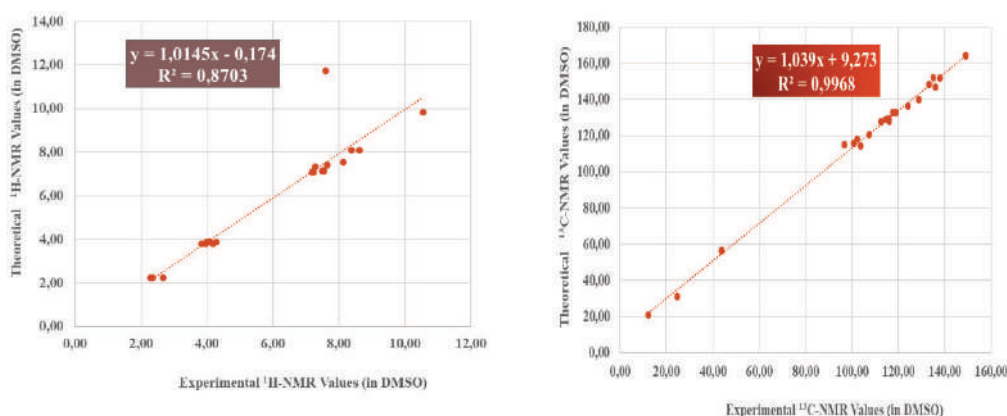


Figure 3. The NMR correlation graphics of the title compound.

Table 2. The calculated and experimental ^{13}C and ^1H NMR isotropic chemical shift values of the title compound

o	N	B3LYP/D MSO	*Exp.	No	B3LYP/ DMSO	*Exp.
	4		163,93	23-		9,85
2-C		149,09	H		10,56	
	3		164,44	39-		8,09
3-C		148,97	H		8,62	
	2		151,62	41-		8,09
7-C		137,88	H		8,39	
	1		146,77	29-		7,54
-C		136,08	H		8,14	
	2		152,09	31-		7,40
-C		135,01	H		7,64	
	9		148,33			11,72
-C		133,09		4-H	7,60	
	2		139,87	17-		7,13
5-C		128,87	H		7,54	
	2		136,23	21-		7,15
0-C		124,03	H		7,52	
	3		132,67	22-		7,15
7-C		119,02	H		7,52	

	3		132,67	19-		7,13
6-C		118,90	H		7,49	
	1		132,99	50-		7,32
3-C		117,45	H		7,27	
	2		127,76	44-		7,10
4-C		116,04	H		7,23	
	1		129,44	43-		7,10
4-C		115,95	H		7,20	
	1		129,44	12-		3,89
5-C		115,80	H		4,08	
	1		129,11	11-		3,89
8-C		114,61	H		4,06	
	1		129,11	58-		3,87
6-C		114,58	H		4,29	
	2		127,49	59-		3,87
8-C		112,61	H		3,98	
	3		120,59	57-		3,87
5-C		107,34	H		3,98	
	4		114,88	53-		3,79
0-C		103,68	H		3,96	
	2		118,08	54-		3,79
6-C		102,25	H		3,83	
	3		115,76	55-		3,79
0-C		100,82	H		4,18	
	3		114,88	47-		2,25
8-C		96,64	H		2,68	
	5		56,13	49-		2,25
6-C		43,78	H		2,35	
	5		56,65	48-		2,25
2-C		43,72	H		2,28	
	1		30,95			
0-C		24,56				
	4		21,07			
6-C		12,38				

* The experimental values were taken from ref (Alkan vd.,2014).

3.4. Electronic Properties

Theoretical, the molecular structure, the highest occupied molecular orbital-lowest unoccupied molecular orbital (HOMO-LUMO), electronic transition, electronegativity(χ), hardness(η), molecular electrostatic potential maps (MEP) and Mulliken atomic charges of the titled compound has been investigated.

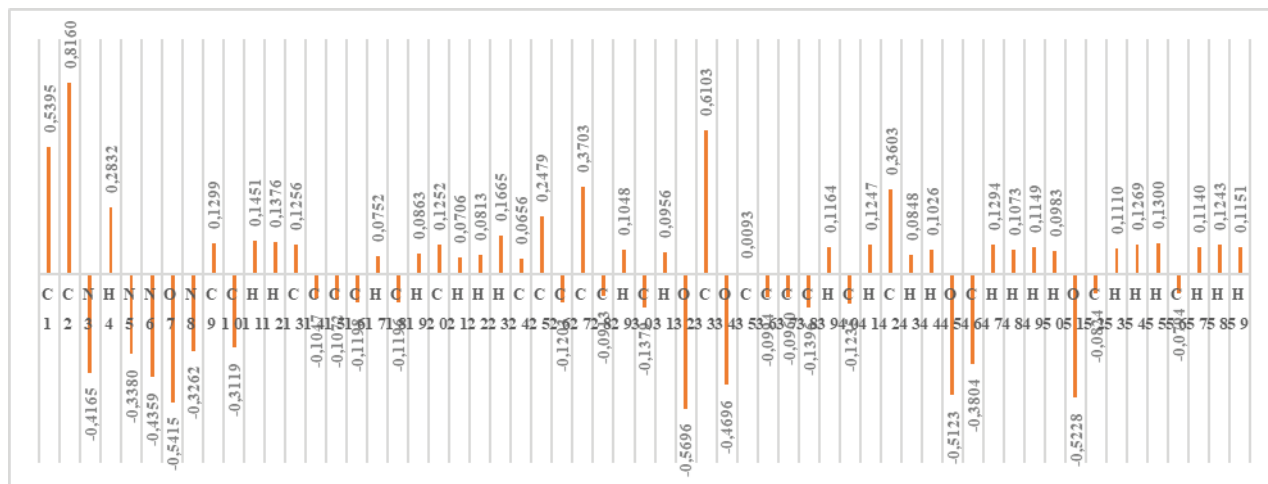


Figure 4. The Mulliken atomic charges of the title compound

Table 3. The theoretical UV-vis, oscillator power values with TD-DFT/B3LYP of the title compound

*Experimental λ (nm)	λ (nm)	Excitation Energy (eV)	Oscillator Power (f)
296.00 (28.25)	319.0 4	3.8862	0.2042
256.00 (29.00)	313.7 7	3.9534	0.2194
214.00 (19.65)	293.5 1	4.2242	0.0100

* The experimental values were taken from ref (Alkan vd.,2014).

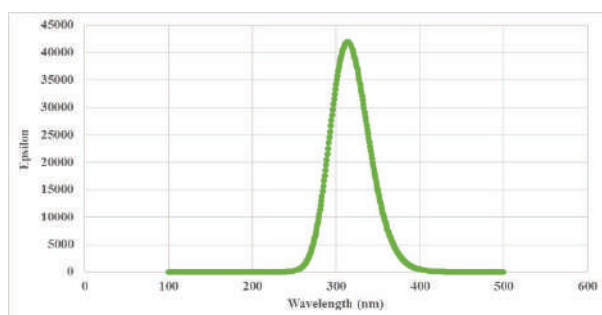


Figure 5. The obtained (DFT/B3LYP) UV-vis spectra graphics of the title compound

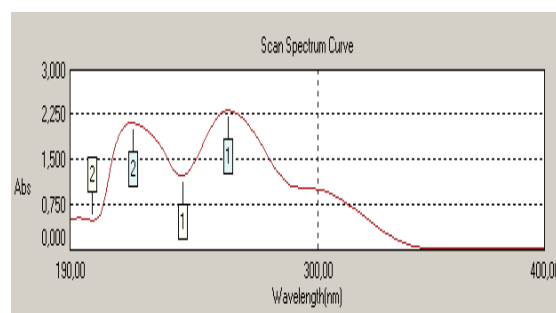


Figure 6. The experimental UV-vis spectra of the title compound

$$\diamond \lambda_{\text{calc.}} = 0.3128\lambda_{\text{exp.}} - 228.91 \quad R^2 = 0.9053 \quad (\text{UV-vis in Ethanol})$$

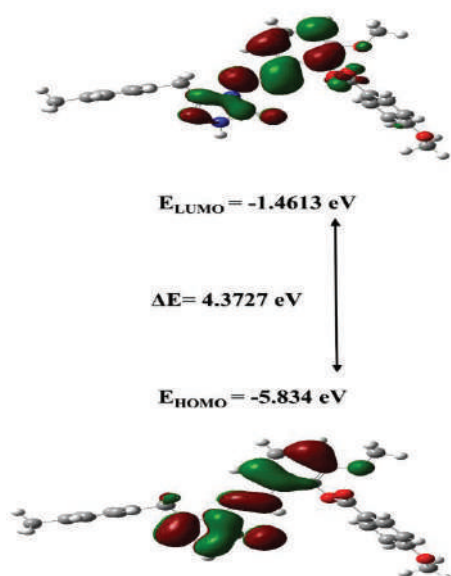


Figure 7. The calculated HOMO-LUMO energies of the title compound with the B3LYP/6-31G(d,p) level of theory

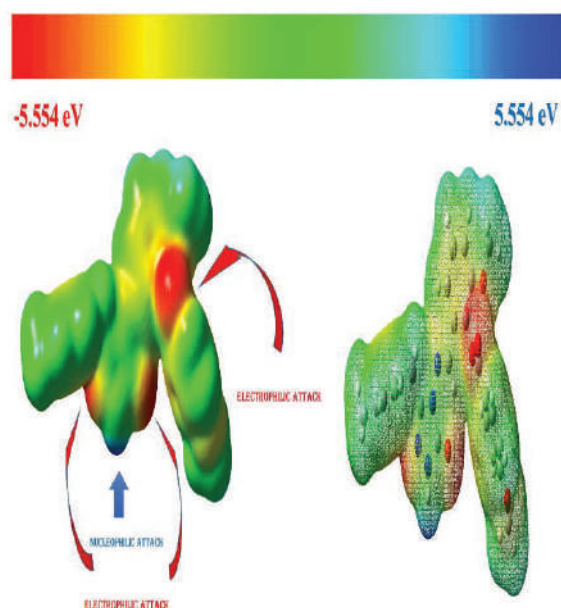


Figure 8. The calculated MEPS map of the title compound with the B3LYP/6-31G(d,p) level of theory

Table 4. The electronic properties of the title compound

Electronic Properties	eV	B3LYP (eV)
E_{HOMO}	-5,83	
E_{LUMO}	-1,46	
I; Ionization Potential	$I = -E_{\text{HOMO}}$	5,83
A; Electron Affinity	$A = -E_{\text{LUMO}}$	1,46
ΔE; Energy Gap	$\Delta E = (E_{\text{LUMO}} - E_{\text{HOMO}})$	4,37
χ; Electronegativity	$\chi = (I + A) / 2$	3,65
η; Molecular Hardness	$\eta = (I - A) / 2$	2,19
S; Molecular Softness	$S = 1/\eta$	0,46
μ; Chemical Potential	$\mu = -\chi$	-3,65
ω; Electrophilic Index	$\omega = \mu^2 / 2\eta$	3,04
ε; Nucleophilic Index	$\varepsilon = \mu \cdot \eta$	-7,98

3.5.Non-linear Optical Properties

The linear polarizability (α), first hyperpolarizability (β), and total static dipole moment (μ) of the title compound were computed at the B3LYP/6-31G(d,p) level of theory. The computed β value was determined to be around 44 times that of urea ($0.1947 \times 10^{-30} \text{ cm}^5/\text{esu}$). These findings suggested that the title compound would make an excellent candidate for a non-linear optical material.

Table 5. The total energy, the electric dipole moment μ , the average polarizability and first hyperpolarizability β_{total} of the title compound

	Urea	B3LYP
E		-1293.1760 (Hartree)
μ	1.3197	7.4117 D
Δ_{α} (esu)		43.5510 (10^{-24} cm ⁵ /esu)
β	0.1974	8.5818 (10^{-30} cm ⁵ /esu)

4. Conclusion

The molecular structures, vibrational frequencies, ¹H and ¹³C NMR chemicals shifts, UV–vis spectroscopies, HOMO-LUMO analyses, atomic charges and NLO properties of 3-p-methylbenzyl-4-[3-ethoxy-4-(4-methoxybenzoxy)-benzylidenamino]-4,5-dihydro-1H-1,2,4-triazol-5-one have been calculated by using B3LYP/6-31G(d,p) level. By considering the experimental parameters, it can be easily stated that the vibrational frequencies, ¹H and ¹³C NMR chemical shifts the parameters calculated theoretically agree quite well with the experimental findings (Alkan vd., 2014). These results may also provide some guidance for the development of novel triazole-based materials.

5. References

- Alkan, M., Gürbüz, A., Yüksek, H., Gürsoy Kol, Ö. & Ocak, Z. (2014). Synthesis and non-aqueous medium titrations of some new 3- alkyl(aryl)-4-[2-(4-methoxybenzoxy)-3-methoxy]-benzylidenamino-4,5-dihydro-1H-1,2,4-triazol-5-ones. *Caucasian Journal of Science*, 1(1), 138-148.
- Foresman, J., & Frisch, A. (2015). *Exploring Chemistry with Electronic Structure Methods*, 3rd edition.
- Gao, F., Wang, T., Xiao, J., & Huang, G. (2019). Antibacterial activity study of 1,2,4-triazole derivatives. *European Journal of Medicinal Chemistry*, 173, 274-281. <https://doi.org/10.1016/j.ejmech.2019.04.043>
- GaussView, Version 6, Dennington, Roy; Keith, Todd A.; Millam, John M. Semichem Inc., Shawnee Mission, KS, 2016. (t.y.).
- Grytsai, O., Valiashko, O., Penco-Campillo, M., Dufies, M., Hagege, A., Demange, L., Martial, S., Pagès, G., Ronco, C., & Benhida, R. (2020). Synthesis and biological evaluation of 3-amino-1,2,4-triazole derivatives as potential anticancer compounds. *Bioorganic Chemistry*, 104, 104271. <https://doi.org/10.1016/j.bioorg.2020.104271>
- Jamróz, M. H. (2013). Vibrational Energy Distribution Analysis (VEDA): Scopes and limitations. *Spectrochimica Acta Part A: Molecular and Biomolecular Spectroscopy*, 114, 220-230. <https://doi.org/10.1016/j.saa.2013.05.096>
- Jiang, G.-W., Chang, Q., Liang, D.-Y., Zhang, Y.-T., Meng, Y.-J., & Yi, Q.-Q. (2020). Preparation and antitumor effects of 4-amino-1,2,4-triazole Schiff base derivative. *The Journal of International Medical Research*, 48(2), 300060520903874. <https://doi.org/10.1177/0300060520903874>
- Luo, S. J., Yang, J. T., Du, W. F., & Laref, A. (2011). Mechanism of Linear and Nonlinear Optical Properties of the Urea Crystal Family. *The Journal of Physical Chemistry A*, 115(20), 5192-5200. <https://doi.org/10.1021/jp200164s>
- Frisch, M. J., Trucks, G. W., Schlegel, H. B., Scuseria, G. E., Robb, M. A., Cheeseman, J. R., Scalmani, G., Barone, V., Mennucci, B., Petersson, G. A., Nakatsuji, H., Caricato, M., Li X., Hratchian, H. P., Izmaylov, F.A., Bloino, J., Zheng, G., Sonnenberg, J. L., Hada, M., Ehara, M., Toyota, K., Fukuda, R., Hasegawa, J., Ishida, M., Nakajima, T.,

- Honda, Y., Kitao, O., Nakai, H., Vreven, T., Montgomery, J. A., Peralta, Jr., J. E., Ogliaro, F., Bearpark, M., Heyd, J. J., Brothers, E., Kudin, K. N., Staroverov, V. N., Kobayashi, R., Normand, J., Raghavachari, K., Rendell, A., Burant, J. C., Iyengar, S.S., Tomasi, J., Cossi, M., Rega, N., Millam, J. M., Klene, M., Knox, J. E., Cross, J. B., Bakken, V., Adamo, C., Jaramillo, J., Gomperts, R., Stratmann, R. E., Yazyev, O., Austin, A. J., Cammi, R., Pomelli, C., Ochterski, J. W., Martin, R. L., Morokuma, K., Zakrzewski, V. G., Voth, G. A., Salvador, P., Dannenberg, J. J., Dapprich, S., Daniels, A. D., Farkas, Ö., Foresman, J. B., Ortiz, J. V., Cioslowski, J., and Fox, D. J., Gaussian 09 (Gaussian, Inc., Wallingford CT, 2009).
- Pulay, P., & Hinton, J. F. (2007). Shielding Theory: GIAO Method. İçinde EMagRes. American Cancer Society. <https://doi.org/10.1002/9780470034590.emrstm0501>
- Tratrat, C. (2020). 1,2,4-Triazole: A Privileged Scaffold for the Development of Potent Antifungal Agents - A Brief Review. *Current Topics in Medicinal Chemistry*, 20(24), 2235-2258. <https://doi.org/10.2174/1568026620666200704140107>
- Wolinski, K., Hinton, J. F., & Pulay, P. (1990). Efficient implementation of the gauge-independent atomic orbital method for NMR chemical shift calculations. *Journal of the American Chemical Society*, 112(23), 8251-8260. <https://doi.org/10.1021/ja00179a005>
- Zampieri, D., Cateni, F., Moneghini, M., Zacchigna, M., Laurini, E., Marson, D., De Logu, A., Sanna, A., & Mamolo, M. G. (2019). Imidazole and 1,2,4-Triazole-based Derivatives Gifted with Antitubercular Activity: Cytotoxicity and Computational Assessment. *Current Topics in Medicinal Chemistry*, 19(8), 620-632. <https://doi.org/10.2174/1568026619666190227183826>

A STUDY ON THEORETICAL/EXPERIMENTAL SPECTROSCOPIC AND ELECTRONIC PROPERTIES OF 1-ACETYL-3-METHYL-4-(4-METHYLBENZOXY)-BENZYLIDENAMINO]-4,5-DIHYDRO-1H-1,2,4-TRIAZOL-5-ONE

Asst. Prof. Dr. Hilal Medetalibeyoğlu

Kafkas University, Faculty of Science and Letters, Department of Chemistry, 36100,
Kars, Turkey
ORCID ID: 0000-0002-1310-6811

Prof. Dr. Haydar Yüksek

Kafkas University, Faculty of Science and Letters, Department of Chemistry, 36100,
Kars, Turkey
ORCID ID: 0000-0003-1289-1800

Abstract

In the current study, 1-acetyl-3-methyl-4-(4-methylbenzoxy)-benzylidenamino]-4,5-dihydro-1H-1,2,4-triazol-5-one was optimized by using the B3LYP/6-311G(d) basis set. The Infrared spectral data of the titled compound were computed by using the same basis set. The veda4f program was used to define the IR values. The theoretical IR absorption frequencies were compared with those obtained from experimental data. The gauge independent atomic orbital (GIAO) methodology is used to obtain the ^1H -NMR and ^{13}C -NMR isotropic shift values. According to the equivalence of $\delta_{\text{exp}} = a + b \cdot \delta_{\text{calc}}$, experimental and theoretical values were added and drawn the correlation graphs. The standard error values were determined utilizing the Sigma Plot program with the a and b constants as regression coefficients. The correlational analysis results (R^2) were determined to study the consistency and accuracy of the theoretical and experimental parameters suggested by Yüksek and coworkers. The HOMO–LUMO energies and the corresponding electronic properties (ionization potential, electron affinity, molecular softness, molecular hardness, and electronegativity) were examined. To predict the UV-Vis spectral analysis, TD-DFT computations in the solvents were done. The molecular electrostatic potential (MEP), Mulliken atomic charges, electronic absorption maximum wavelengths, and nonlinear optical (NLO) properties (i.e., the first hyperpolarizability and polarizability) of the titled compound were studied. All correlational analysis results between the experimental and theoretical findings were determined.

Keywords: 1,2,4-triazol-5-one, DFT, 6-311G(d), MEP, HOMO-LUMO

1. Introduction

1,2,4-triazoles are biologically important compounds and possess antifungal and antiviral activities (Dincel vd., 2021; El-Sebaey, 2020). Some derivatives of 1,2,4-triazole are reported for their antitumor, anticancer anticonvulsants and antidepressants activities (Pasupuleti vd., 2020; Slaihim vd., 2019; Wang vd., 2020). The efficient electron-transport and hole-blocking characteristics of highly electron-deficient triazole derivatives are used to develop organic lightemitting diodes (Manship vd., 2020; Savateev vd., 2017; Thottempudi & Shreeve, 2011). The triazole being nitrogen rich is

used as linkers for metal organic frameworks, these compounds are useful to produce nitrogen rich porous carbon which work as efficient electrochemical catalyst for oxygen reduction reaction in fuel cell as compared to conventional carbon support (Nguyen vd., 2020). The presence of delocalized π -electrons and intermolecular interactions in the organic compounds results for the enhancement of NLO properties in these materials (Altürk vd., 2017; Maza vd., 2020). The quest to explore such materials is a major concern due to their various practical applications (Laachir vd., 2020; Ye vd., 2018). The organic nonlinear materials have high optical sensitivities with greater optical thresholds for enhancing laser force as compared to inorganic materials (Zacharias vd., 2018). A number of theoretical studies are also devoted to explore structure and properties of 1,2,4-triazoles. In this study, 1-acetyl-3-methyl-4-(4-methylbenzoxymethylideneamino)-4,5-dihydro-1H-1,2,4-triazol-5-one and its analysis was carried out through using the B3LYP/6-311G(d) basis set. The combined computational and experimental tools (Yüksek vd., 2016) have been used to find its structural, spectroscopic and electronic aspects. Also, the title compound was analyzed computationally for nonlinear optical properties.

2. Materials and Methods

Gaussian09W program package was used for the DFT calculations (Frisch vd., 2009). The visualization for the verification of the optimized molecular structure was performed using the Gaussview program (Dennington vd., 2016). The geometry optimization of the titled compound was performed by using B3LYP method with 6-311G(d) basis set. The GIAO (Gauge-Including Atomic Orbital) ^1H and ^{13}C NMR chemical shift values in DMSO were calculated by the same basis set (Pulay & Hinton, 2007). The standard error rate was calculated according to $\delta_{\text{calc}} = a \delta_{\text{exp}} + b$ formula. The spectral data of the title compound were carried out with the same level of theory. The veda4f program was used for identification of computed IR data (Jamróz, 2013). The UV-Vis spectrum was obtained through time-dependent density functional theory (TD-DFT). The important electronic properties such as electronegativity, chemical hardness, chemical softness and chemical potential are calculated by the utilization of numerical values of the ionization energy and electron affinity (Foresman & Frisch, 2015). The nonlinear optical behaviour of the title compound was investigated by defining dipole moment (μ), polarizability (α), anisotropic polarizability ($\Delta\alpha$) and first static hyperpolarizability (β) on the same level of theory (Luo vd., 2011).

3. Results and Discussion

3.1. Molecular Structure

The structure with minimum global energy the title compound obtained by using B3LYP/6-311G(d) level is shown in Figure 1.

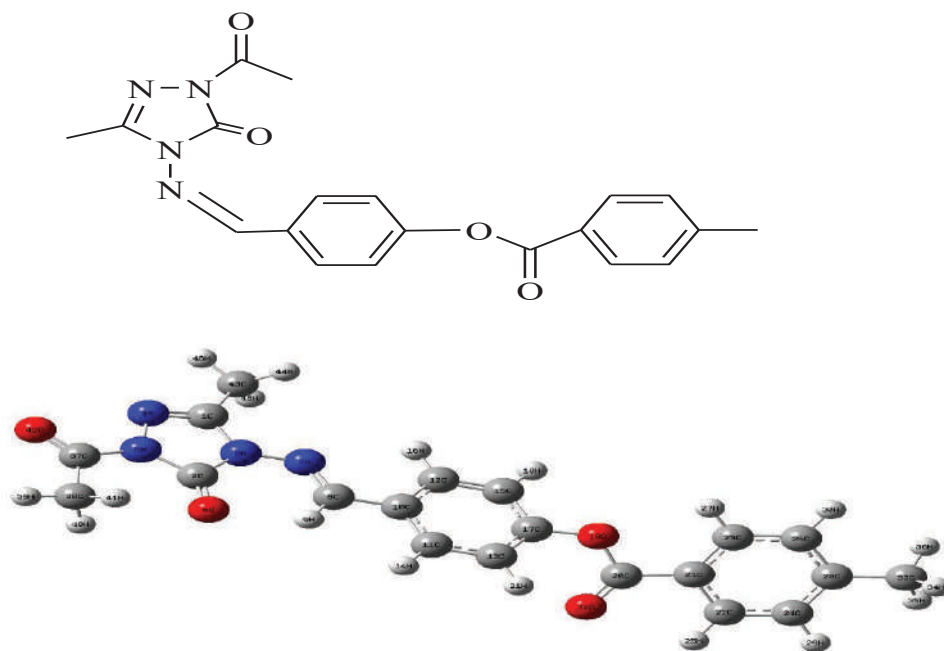


Figure 1. Optimized molecular structure of 1-acetyl-3-methyl-4-(4-methylbenzoxy)-benzylidenamino]-4,5-dihydro-1H-1,2,4-triazol-5-one with B3LYP/6-311G(d) level of theory.

3.2. vibrational frequencies

V

The titled compound has 46 atoms and the number of the normal vibrations are 132. The observed and calculated vibrational frequencies, the calculated IR intensities and assignments of vibrational frequencies for titled compound are summarized in Table 1.

Table 1. The calculated and experimental frequency values of the titled compound

Exp.	Unscal ed	Scale d	Vibrational Frequencies	% PED
406,49	419,97	405,69	τ CCCO (13)	3,42
454,03	468,82	452,88	δ NNC (16), δ CCN (11)	5,69
477,03	489,29	472,65	γ CCCC (44)	6,98
536,93	574,64	555,11	δ COC (11)	6,34
566,47	587,56	567,58	τ HCCN (36), γ ONNC (49)	3,68
603,82	620,49	599,39	ν CC (12), δ CCC (12)	12,66
634,74	660,44	637,99	τ NNCC (51), γ CNNC (12)	0,53
676,63	701,85	677,99	τ CCCC (30), γ OCOC (29), γ CCCC (16),	12,28
735,12	761,49	735,60	τ HCCC (34), γ OCOC (37)	36,90
771,52	803,29	775,98	ν CC (15), δ CCC (17)	5,12
836,58	875,25	845,49	ν CC (11), δ CCO (18)	26,86
880,78			ν CC (12), NN (11), δ OCN (10), δ NCC (10), δ	
	925,85	894,37	NNC (12)	16,39
966,23	1014,11	979,63	ν CC (10), δ HCH (20), τ HCCC (49)	10,98

1015,2		1031,6	δ HCH (44), τ HCCC (47), τ HCCN (48), γ ONNC	
7	1068,00	8	(14)	41,96
1057,8		1052,2		
4	1089,30	6	δ NNC (11), τ HCCN (11)	71,41
1106,3		1106,6		
7	1145,58	3	δ HCC (60)	5,68
1170,1		1186,8		
6	1228,59	2	ν OC (21), δ HCC (22)	327,00
1205,3		1244,1		
0	1287,93	4	ν CC (13), NN (14), δ NCN (16)	15,46
1259,2		1271,1		
9	1315,87	3	ν NC (34), δ CNN (10), ν OC (21)	636,68
1318,5		1338,6		
8	1385,79	7	ν NC (11), δ HCN (27), δ HCH (14)	114,89
1364,6		1383,9		
2	1432,60	0	δ HCN (13), δ HCH (70)	31,76
1413,5		1411,5		
5	1461,26	8	δ HCN (24)	94,57
1455,0		1456,5		
2	1507,83	7	δ HCH (61), τ HCCC (20)	10,16
1507,1		1497,6		
7	1550,38	7	δ HCC (36)	23,88
1600,4		1620,8		
4	1677,87	2	ν NC (62)	118,53
1696,1		1725,9		
0	1786,74	9	ν OC (77)	283,98
1732,6		1737,8		
5	1799,01	4	ν OC (87)	266,20
1765,9		1765,5		
4	1827,72	8	ν OC (87)	337,29
2851,9		2926,4		
1	3029,49	9	ν CH (100)	28,15
2919,4		2978,4		
2	3083,26	3	ν CH (99)	22,72
3014,2		3106,1		
7	3215,50	7	ν CH (96)	3,97
3063,1		3130,6		
5	3240,86	7	ν CH (100)	2,64



, stretching; δ , bending; γ , out-of-plane bending; τ , torsion

*The experimental values were taken from ref (Yüksek vd., 2016).

v

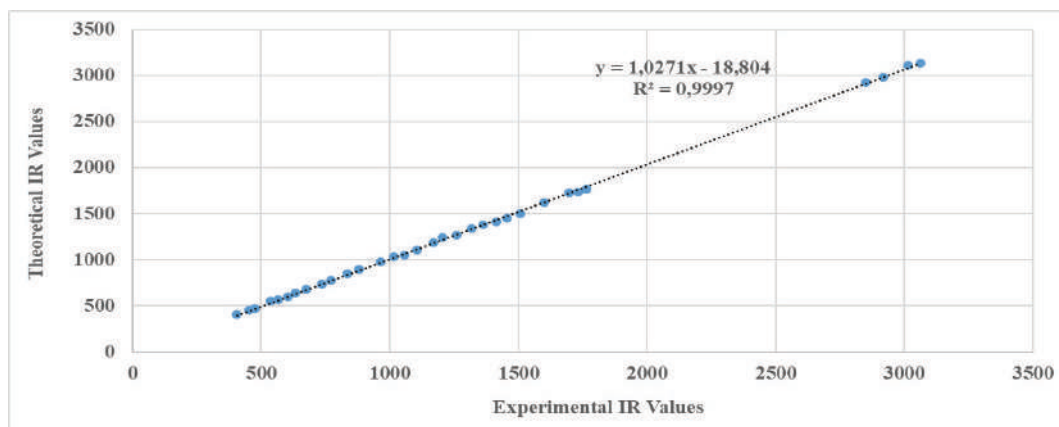


Figure 2. The correlation graphics for IR of the title compound.

3.3. MR spectral analysis

N

In this study, the optimized molecular geometry of the titled compound was obtained by using B3LYP method with 6-311G(d) basis level in DMSO solvent. By considering the optimized molecular geometry of the titled compound the ^1H and ^{13}C NMR chemical shift values were calculated at the same level by using Gauge-Independent Atomic Orbital (GIAO) method (Wolinski vd., 1990).

❖

$$\delta_{\text{exp}} = 0,9785\delta_{\text{cal}} + 0,3604 \quad (R^2 = 0,9935) \quad (^1\text{H-NMR in DMSO})$$

δ

Table 2. The calculated and experimental ^{13}C and ^1H NMR isotropic chemical shift values of the title compound

No	B3LYP/DMSO	*Experimental	Diff.
9-H	9,58	9,65	0,11
16-H	8,06	8,06	0,21
27-H	7,92	8,00	0,13
25-H	7,86	8,00	0,07
31-H	7,51	7,46	0,27
14-H	7,27	8,06	-0,58
29-H	7,20	7,44	-0,02
30-H	7,17	7,44	-0,05
18-H	7,07	7,46	-0,18
34-H	2,32	2,37	0,25
40-H	2,30	2,44	0,15
41-H	2,28	2,44	0,13
44-H	2,16	2,33	0,13
45-H	2,15	2,33	0,12
35-H	2,10	2,37	0,03

36-H	2,00	2,37	-0,07
46-H	1,81	2,33	-0,22
39-H	1,64	2,44	-0,50
RMSD			0,245

*The experimental values were taken from ref (Yüksek vd., 2016).

3.4. Electronic Properties

Theoretical, the molecular structure, the highest occupied molecular orbital-lowest unoccupied molecular orbital (HOMO-LUMO), electronic transition, electronegativity(χ), hardness(η), molecular electrostatic potential maps (MEP) and Mulliken atomic charges of the titled compound has been investigated.

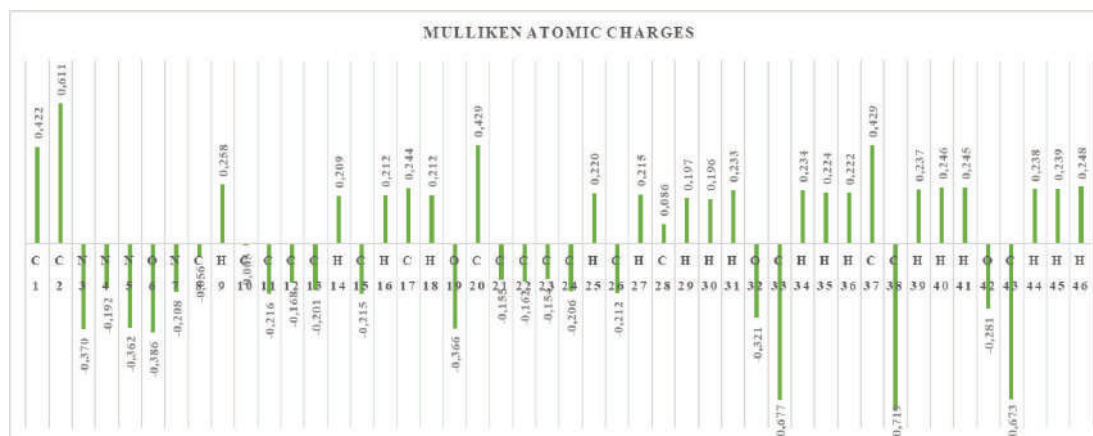


Figure 3. The Mulliken atomic charges of the title compound

Table 3. The theoretical UV-vis, oscillator power values with TD-DFT/B3LYP of the title compound

*Experimental λ (nm)	λ (nm)	Excitation Energy (eV)	Oscillator Power (f)
290.00	313.97	3.9489	1.0323
	278.73	4.4482	0.0145
252.00	271.19	4.5718	0.0012

*The experimental values were taken from ref (Yüksek vd., 2016).

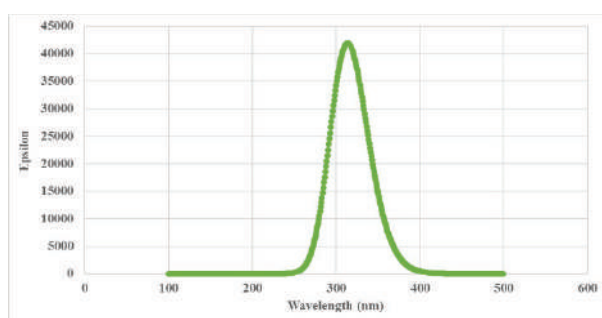


Figure 4. The obtained (DFT/B3LYP) UV-vis spectra graphics of the title compound

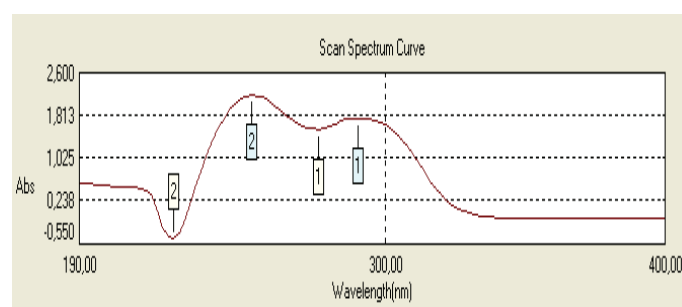


Figure 5. The experimental UV-vis spectra of the title compound

$$\diamond \quad \lambda_{\text{calc.}} = 1,1258 \lambda_{\text{exp.}} - 12,509 \quad R^2 = 1.000 \quad (\text{Uv-vis in Ethanol})$$

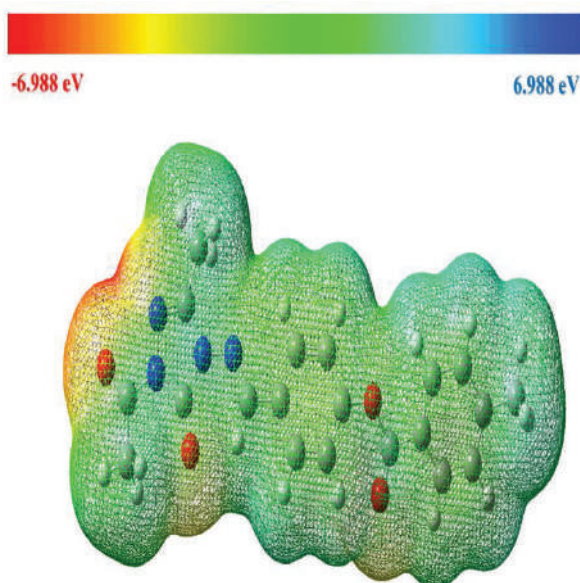
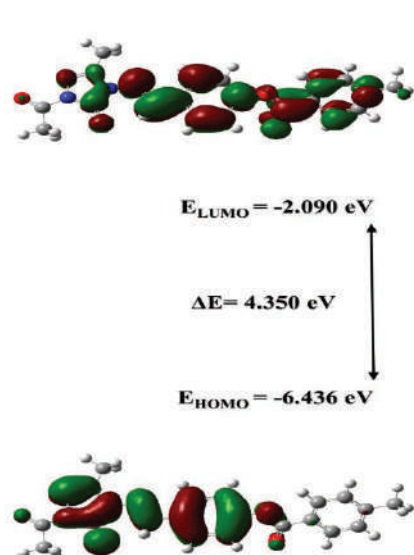


Figure 6. The calculated HOMO-LUMO energies of the title compound with the B3LYP/6-311G(d) level of theory

Figure 7. The calculated MEPS map of the title compound with the B3LYP/6-311G(d) level of theory

Table 4. The electronic properties of the title compound

Electronic Properties	eV	B3LYP (eV)
E_{HOMO}	-6,44	
E_{LUMO}	-2,09	
I; Ionization Potential	$I = -E_{\text{HOMO}}$	6,44
A; Electron Affinity	$A = -E_{\text{LUMO}}$	2,09
ΔE; Energy Gap	$\Delta E = (E_{\text{LUMO}} - E_{\text{HOMO}})$	4,35
χ; Electronegativity	$\chi = (I + A) / 2$	4,26
η; Molecular Hardness	$\eta = (I - A) / 2$	2,17
S; Molecular Softness	$S = 1/\eta$	0,46
μ; Chemical Potential	$\mu = -\chi$	-4,26
ω; Electrophilic Index	$\omega = \mu^2 / 2\eta$	4,18
ε; Nucleophilic Index	$\varepsilon = \mu \cdot \eta$	-9,26

3.5. Non-linear Optical Properties

The linear polarizability (α), first hyperpolarizability (β), and total static dipole moment (μ) of the title compound were computed at the B3LYP/6-311G(d) level of theory. The computed β value was determined to be around 44 times that of urea ($0.1947 \times 10^{-30} \text{ cm}^5/\text{esu}$). These findings suggested that the title compound would make an excellent candidate for a non-linear optical material.

Table 5. The total energy, the electric dipole moment μ , the average polarizability and first hyperpolarizability β_{total} of the title compound

	Urea	B3LYP
E		-1293.1760 (Hartree)
μ	1.3197	7.4117 D
Δ_{α} (esu)		43.5510 (10^{-24} cm ⁵ /esu)
β	0.1974	8.5818 (10^{-30} cm ⁵ /esu)

4. Conclusion

The molecular structures, vibrational frequencies, ¹H and ¹³C NMR chemicals shifts, UV–vis spectroscopies, HOMO-LUMO analyses, atomic charges and NLO properties of 1-acetyl-3-methyl-4-(4-methylbenzoxy)-benzylidenamino]-4,5-dihydro-1H-1,2,4-triazol-5-on have been calculated by using B3LYP/6-311G(d) level. By considering the experimental parameters, it can be easily stated that the vibrational frequencies, ¹H and ¹³C NMR chemical shifts the parameters calculated theoretically agree quite well with the experimental findings (Yüksek vd., 2016). These results may also provide some guidance for the development of novel triazole-based materials.

5. References

- Altürk, S., Avcı, D., Tamer, Ö., & Atalay, Y. (2017). Comparison of different hybrid DFT methods on structural, spectroscopic, electronic and NLO parameters for a potential NLO material. *Computational and Theoretical Chemistry*, 1100, 34-45. <https://doi.org/10.1016/j.comptc.2016.12.007>
- Dincel, E. D., Ulusoy-Güzeldemirci, N., Şatana, D., & Küçükbaşmacı, Ö. (2021). Design, synthesis, characterization and antimicrobial evaluation of some novel hydrazinecarbothioamide, 4-thiazolidinone and 1,2,4-triazole-3-thione derivatives. *Journal of Heterocyclic Chemistry*, 58(1), 195-205. <https://doi.org/10.1002/jhet.4159>
- El-Sebaey, S. A. (2020). Recent Advances in 1,2,4-Triazole Scaffolds as Antiviral Agents. *ChemistrySelect*, 5(37), 11654-11680. <https://doi.org/10.1002/slct.202002830>
- Foresman, J., & Frisch, A. (2015). *Exploring Chemistry With Electronic Structure Methods*, 3rd edition. GaussView, Version 6, Dennington, Roy; Keith, Todd A.; Millam, John M. Semichem Inc., Shawnee Mission, KS, 2016. (t.y.).
- Jamróz, M. H. (2013). Vibrational Energy Distribution Analysis (VEDA): Scopes and limitations. *Spectrochimica Acta Part A: Molecular and Biomolecular Spectroscopy*, 114, 220-230. <https://doi.org/10.1016/j.saa.2013.05.096>
- Laachir, A., Guesmi, S., Ketatni, E. M., Saadi, M., El Ammari, L., Mentré, O., Esserti, S., Faize, M., & Bentiss, F. (2020). A new homobimetallic cobalt(II) complex based on the tetradentate 3,5-bis(2-pyridyl)-1H-1,2,4-triazole ligand: Synthesis, crystal structure, Hirshfeld analysis, spectroscopic characterization, magnetic properties and antimicrobial activities. *Polyhedron*, 189, 114722. <https://doi.org/10.1016/j.poly.2020.114722>
- Luo, S. J., Yang, J. T., Du, W. F., & Laref, A. (2011). Mechanism of Linear and Nonlinear Optical Properties of the Urea Crystal Family. *The Journal of Physical Chemistry A*, 115(20), 5192-5200. <https://doi.org/10.1021/jp200164s>
- Frisch, M. J., Trucks, G. W., Schlegel, H. B., Scuseria, G. E., Robb, M. A., Cheeseman, J. R., Scalmani, G., Barone, V., Mennucci, B., Petersson, G. A., Nakatsuji, H., Caricato, M., Li X., Hratchian, H. P., Izmaylov, F.A., Bloino, J., Zheng, G., Sonnenberg, J. L., Hada, M., Ehara,

- M., Toyota, K., Fukuda, R., Hasegawa, J., Ishida, M., Nakajima, T., Honda, Y., Kitao, O., Nakai, H., Vreven, T., Montgomery, J. A., Peralta, Jr., J. E., Ogliaro, F., Bearpark, M., Heyd, J. J., Brothers, E., Kudin, K. N., Staroverov, V. N., Kobayashi, R., Normand, J., Raghavachari, K., Rendell, A., Burant, J. C., Iyengar, S.S., Tomasi, J., Cossi, M., Rega, N., Millam, J. M., Klene, M., Knox, J. E., Cross, J. B., Bakken, V., Adamo, C., Jaramillo, J., Gomperts, R., Stratmann, R. E., Yazyev, O., Austin, A. J., Cammi, R., Pomelli, C., Ochterski, J. W., Martin, R. L., Morokuma, K., Zakrzewski, V. G., Voth, G. A., Salvador, P., Dannenberg, J. J., Dapprich, S., Daniels, A. D., Farkas, Ö., Foresman, J. B., Ortiz, J. V., Cioslowski, J., and Fox, D. J., Gaussian 09 (Gaussian, Inc., Wallingford CT, 2009).
- Manship, T. D., Smith, D. M., & Piercey, D. G. (2020). An Improved Synthesis of the Insensitive Energetic Material 3-Amino-5-Nitro-1,2,4-triazole (ANTA). *Propellants, Explosives, Pyrotechnics*, 45(10), 1621-1626. <https://doi.org/10.1002/prep.202000097>
- Maza, S., Kijatkin, C., Bouhidel, Z., Pillet, S., Schaniel, D., Imlau, M., Guillot, B., Cherouana, A., & Bendeif, E.-E. (2020). Synthesis, structural investigation and NLO properties of three 1,2,4-triazole Schiff bases. *Journal of Molecular Structure*, 1219, 128492. <https://doi.org/10.1016/j.molstruc.2020.128492>
- Nguyen, V. H., Nguyen, H. H., & Do, H. H. (2020). 1,2,4-triazole-derived N-heterocyclic carbene complexes of platinum(II) as catalysts for hydroamination reactions and active anticancer agents. *Inorganic Chemistry Communications*, 121, 108173. <https://doi.org/10.1016/j.inoche.2020.108173>
- Pasupuleti, B. G., Khongsti, K., Das, B., & Bez, G. (2020). 1,2,3-Triazole tethered 1,2,4-trioxanes: Studies on their synthesis and effect on osteopontin expression in MDA-MB-435 breast cancer cells. *European Journal of Medicinal Chemistry*, 186, 111908. <https://doi.org/10.1016/j.ejmech.2019.111908>
- Pulay, P., & Hinton, J. F. (2007). Shielding Theory: GIAO Method. *Çinde EMagRes*. American Cancer Society. <https://doi.org/10.1002/9780470034590.emrstm0501>
- Savateev, A., Pronkin, S., Epping, J. D., Willinger, M. G., Antonietti, M., & Dontsova, D. (2017). Synthesis of an electronically modified carbon nitride from a processable semiconductor, 3-amino-1,2,4-triazole oligomer, via a topotactic-like phase transition. *Journal of Materials Chemistry A*, 5(18), 8394-8401. <https://doi.org/10.1039/C7TA01714F>
- Slaïhim, M. M., Al-Suede, F. S. R., Khairuddean, M., Khadeer Ahamed, M. B., & Shah Abdul Majid, A. M. (2019). Synthesis, characterisation of new derivatives with mono ring system of 1,2,4-triazole scaffold and their anticancer activities. *Journal of Molecular Structure*, 1196, 78-87. <https://doi.org/10.1016/j.molstruc.2019.06.066>
- Thottempudi, V., & Shreeve, J. M. (2011). Synthesis and Promising Properties of a New Family of High-Density Energetic Salts of 5-Nitro-3-trinitromethyl-1H-1,2,4-triazole and 5,5'-Bis(trinitromethyl)-3,3'-azo-1H-1,2,4-triazole. *Journal of the American Chemical Society*, 133(49), 19982-19992. <https://doi.org/10.1021/ja208990z>
- Wang, C., Li, Y., Liu, T., Wang, Z., Zhang, Y., Bao, K., Wu, Y., Guan, Q., Zuo, D., & Zhang, W. (2020). Design, synthesis and evaluation of antiproliferative and antitubulin activities of 5-methyl-4-aryl-3-(4-arylpiperazine-1-carbonyl)-4H-1,2,4-triazoles. *Bioorganic Chemistry*, 104, 103909. <https://doi.org/10.1016/j.bioorg.2020.103909>
- Wolinski, K., Hinton, J. F., & Pulay, P. (1990). Efficient implementation of the gauge-independent atomic orbital method for NMR chemical shift calculations. *Journal of the American Chemical Society*, 112(23), 8251-8260. <https://doi.org/10.1021/ja00179a005>
- Ye, Z., Ding, M., Wu, Y., Li, Y., Hua, W., & Zhang, F. (2018). Electrochemical synthesis of 1,2,4-triazole-fused heterocycles. *Green Chemistry*, 20(8), 1732-1737. <https://doi.org/10.1039/C7GC03739B>
- Yüksek, H., Koca, E., Beytur, M., Gürsoy-Kol, Ö., Aytemiz, F., Alkan, M. (2016). Synthesis, Antioxidant and Antimicrobial Activities of Some 1-Acetyl-3-alkyl(aryl)-4-[4-(4-

methylbenzoxy)-benzylidenamino]-4,5-dihydro-1H-1,2,4-triazol-5-ones. *Journal of Chemical and Pharmaceutical Research*, 8 (7): 905-911.

Zacharias, A. O., Varghese, A., Akshaya, K. B., Savitha, M. S., & George, L. (2018). DFT, spectroscopic studies, NBO, NLO and Fukui functional analysis of 1-(1-(2,4-difluorophenyl)-2-(1H-1,2,4-triazol-1-yl)ethylidene) thiosemicarbazide. *Journal of Molecular Structure*, 1158, 1-13. <https://doi.org/10.1016/j.molstruc.2018.01.002>

INTERACTIONS of [Cu(5-nphen)(tyr)(H₂O)]NO₃·2H₂O COMPLEX with BOVINE SERUM ALBUMINE (BSA)

Assoc. Prof. Dr. Duygu İNCİ

Kocaeli University, Faculty of Arts and Sciences, Department of Chemistry, Kocaeli, Turkey
ORCID NO: 0000-0002-0483-9642

Prof. Dr. Rahmiye AYDIN

Bursa Uludag University, Faculty of Arts and Sciences, Department of Chemistry, Bursa, Turkey
ORCID NO: 0000-0003-4944-0181

ABSTRACT

In the recent years, bioinorganic chemistry has provided numerous examples of structures with affinity towards biomolecules, including nucleic acids and proteins, and showing potential to be developed into therapeutic agents. Coordination compounds show unique properties offering interesting opportunities in designing new biologically active molecules, such as redox activity, variety of geometries and coordination numbers offered by metal ions, resulting in high structural diversity. Among various serum albumins, bovine serum albumin (BSA) is the most extensively studied owing to its structural homology with human serum albumin (HSA). Consequently, the studies on interaction of metal complexes with protein are useful in the design of biologically active molecules.

For the first time in this study, the interactions of the [Cu(5-nphen)(tyr)(H₂O)]NO₃·2H₂O complex, which was previously synthesized and published by our group, with bovine serum albumin (BSA) were investigated using electronic absorption and fluorescence (synchronized fluorescence, fluorescence resonance energy transfer (FRET), two-dimensional (2D) and three-dimensional (3-D) fluorescence) spectroscopy techniques and BSA quenching mechanism was found. Again, for the first time in this study, DPPH and H₂O₂ radical scavenging activities of the synthesized complex were investigated in comparison with standard ascorbic acid, trolox and BHT.

Keywords: Cu(II) complex, mixed ligand complex, BSA interaction, radical scavenging activity

ÖZET

Son yıllarda, biyoinorganik kimya, nükleik asitler ve proteinler dahil olmak üzere biyomoleküllere afinitesi olan ve terapötik ajanlara dönüşme potansiyeli gösteren çok sayıda yapı örneği sağlamıştır. Koordinasyon bileşikleri, yapısal çeşitlilikle sonuçlanan redoks aktivitesi, çeşitli geometriler ve metal iyonları tarafından sunulan koordinasyon numaraları gibi yeni biyolojik olarak aktif moleküllerin tasarlanmasında ilginç özellikler sunan benzersiz özellikler gösterir. Çeşitli serum albüminleri arasında, insan serum albümini (HSA) ile yapısal homolojisi nedeniyle sığır serum albümini (BSA) en kapsamlı çalışılanıdır. Sonuç olarak, metal komplekslerinin protein ile etkileşimi üzerine yapılan çalışmalar, biyolojik olarak aktif moleküllerin tasarımında yararlıdır.

İlk kez bu çalışmada, grubumuz tarafından daha önce sentezlenmiş ve yayınlanmış olan [Cu(5-nphen)(tyr)(H₂O)]NO₃·2H₂O kompleksinin, sığır serum albümini (BSA) ile etkileşimleri elektronik absorpsiyon ve floresans (senkronize floresans, floresans rezonans enerji transferi (FRET), iki boyutlu (2D) ve üç boyutlu (3-D) floresans) spektroskopisi teknikleri kullanılarak araştırıldı ve BSA sönmeme mekanizması bulundu. Yine ilk kez bu çalışmada, kompleksin DPPH ve H₂O₂ radikali

yakalama aktiviteleri standart olarak kullanılan askorbik asit, trolox ve BHT ile karşılaştırmalı olarak araştırıldı.

Anahtar Kelimeler: Cu(II) kompleksi, , karışık ligand kompleksi, BSA etkileşimi, radikal giderme aktivitesi

1. INTRODUCTION

Serum albumins play an important role in the transport of metal ions and their complexes to cells and tissues. Human serum albumin (HSA) and bovine serum albumin (BSA) belong to the group of the most studied proteins [1]. Bovine serum albumin possesses amino acid sequence that has 76% similarity to the human serum albumin [2]. Investigations of the interactions of serum albumin proteins and metal complexes used as drugs, is of great importance, because it can lead to a decrease or increase in the biological activity of the drug. Because of the extraordinary binding capacity of different ligands and metal complexes, they are also used as model systems for studying interactions with bioactive molecules [3,4]. Free radicals are implicated as a major factor in the development of oxidative damage diseases which can be promoted by drugs [5]. As a consequence, there is an important need for antioxidants as a defence against free radical attack.

[Cu(5-nphen)(tyr)(H₂O)]NO₃·2H₂O was synthesized and investigated crystal structures as described in our previously studies [6]. Furthermore, for the first time in this study, binding studies of the complex to BSA (by using electronic absorption and fluorescence spectroscopy (type of quenching, binding constant, number of binding locations, thermodynamic parameters, FRET analysis, and 2D and 3D fluorescence analyses) and radical scavenging activities were performed.

2. EXPERIMENTAL

2.1. Materials and measurements

All chemicals were of reagent grade, purchased from different sources, and were used without further purification. NaCl, tris-(hydroxymethyl)aminomethane-HCl, BSA, hydrogen peroxide, 6-hydroxy-2,5,7,8-tetramethylchromane-2-carboxylic acid (Trolox), 1,1-diphenyl-picrylhydrazyl (DPPH), butylated hydroxytoluene (BHT) and ascorbic acid were provided from Sigma-Aldrich. The spectrophotometric studies were performed using a GBC Cintra 303 UV-Visible spectrophotometer connected with a Peltier thermocell. Emission intensity measurements were carried out using a Jasco FP-750 spectrofluorometer.

2.2. BSA interaction studies

BSA trials were made in Tris-HCl buffer (5 mM Tris-HCl / 50 mM NaCl buffer at pH 7.2). The electronic absorption spectra of solutions containing the BSA, BSA+the complex at 20 µM concentrations were measured. In fluorescence experiments were researched at a constant concentration of BSA (1 µM) while varying the complex concentration (0-20 µM). To investigate BSA binding activity of the complex, fluorescence experiments were performed at different temperatures (298.2, 310.2 and 318.2 K) and calculated the following equation.

$$\frac{I_0}{I} = 1 + K_q \tau_0 \cdot [\text{Complex}] = 1 + K_{SV} \cdot [\text{Complex}] \quad (1)$$

I_0 and I are the fluorescence emission intensity in the absence and presence of the complex, respectively. $[Complex]$, K_q and τ_0 are the total concentration of the complex, the quenching rate constant and the average lifetime of biopolymer in the absence of the quencher ($\tau_0=10^{-8}$ s) [7], respectively. In a static quenching, the binding constant (K_A) and the number of binding sites (n) could be calculated with the following equation. K_A is the binding constant to a site and n is the number of binding sites per albumin.

$$\log(I_0 - I) = \log K_A + n \log [Complex] \quad (2)$$

In BSA binding studies, the thermodynamic parameters of the BSA+the complex systems could be calculated on the basis of the van't Hoff equation:

$$\ln K = -\frac{\Delta H}{RT} + \frac{\Delta S}{R} \quad (3)$$

$$\Delta G = \Delta H - T\Delta S = -RT \ln K_A \quad (4)$$

ΔG is the free energy change, K_A binding constant, T is temperature, and R is the gas constant. ΔG , ΔH and ΔS could be determined from the plotted graph of $\ln K$ versus $1/T$. FRET theory was used to thoroughly research the interaction with BSA+the complex systems. The energy transfer efficiency (E) of the complex obtained using the following equation.

$$E = 1 - \frac{I}{I_0} = \frac{R_0^6}{(R_0^6 + r^6)} \quad (5)$$

I and I_0 are the fluorescence emission intensities of BSA in the presence and absence of the complex (1 μM). r is the distance between BSA and the complex, R_0 is the critical distance when the transfer efficiency is 50%. These parameters might be calculated by following equations.

$$R_0^6 = 8.8 \times 10^{-25} K^2 \phi J N^{-4} \quad (6)$$

$$J = \frac{\sum F(\lambda) \varepsilon(\lambda) \lambda^4 \Delta \lambda}{\sum F(\lambda) \Delta \lambda} \quad (7)$$

$F(\lambda)$ is the fluorescence emission intensity of the BSA at the certain wavelength (λ), $\varepsilon(\lambda)$ is the molar absorption coefficient of the complex at the certain wavelength (λ) and its unit is $\text{cm}^{-1} \text{M}^{-1}$ [8]. The range of synchronous scanning was also used to comprehensive research the interaction with BSA+the complex systems. The three dimensional (3D) and countour plot (2D) excitation and emission spectra of BSA, BSA+ complex systems were recorded in the range of 220-350 nm.

2.3. Radical scavenging studies

The radical scavenging activities of the complex were evaluated using DPPH and H_2O_2 assay according to the method described in previous literature [9-10]. Trolox, Asc and BHT were used as reference compounds. The percentage of radical scavenging by reference compounds and the complex were calculated using the following equation:

$$\% \text{ Radical activity} = [(A_0 - A_c) / A_0] * 100 \quad (8)$$

A_0 and A_c are the absorbance in the absence and presence of the complex, respectively. The 50 % radical scavenging activity (IC_{50}) was computed using the percentage of activity.

3. RESULTS AND DISCUSSION

3.1. BSA binding activities

The electronic absorption spectra show BSA in the absence and presence of the complex. The absorption intensity of BSA was enhanced as the complex were added (Figure 1a). Therefore, possible quenching mechanism of BSA by the complex was a static quenching process. To determine the BSA binding behaviors of the complex, fluorescence quenching experiments were performed. The $\log K_{sv}$ and $\log K_q$ is given in Table 1. For the complex, the Stern-Volmer plots were linear and the values of K_{sv} decreased with increasing temperature, this shows static quenching (Figure 1b). With regard to the K_q values, the quenching process seems to be static quenching. The $\log K_A$ and n for the complex are listed in Table 1. The values of n for BSA were approximately equal to 1 for the complex, suggesting that there was one binding site in BSA. For the complex, the negative values of ΔH and ΔS indicated that hydrogen bonds and van der Waals interactions play major roles in the binding process and stabilizes the BSA+complex formation (Table 2). The values of r and E % of the complex were presented in Table 2. Found r values are 0.56 nm for the complex, respectively. The energy transferred to the complex from BSA is 48.01 % (Figure 1c). According to 2D and 3D results, the analysis of the peaks “a” and “b” showed that the binding of the complex with BSA affected conformational and microenvironment of amino acid residues in BSA (Figure 2).

Table 1 The quenching constant (K_{sv} and K_q), modified Stern-Volmer constant (K_a), binding constant (K_A) and number of binding sites (n) of BSA + Complex

Compounds	T	$\log K_{sv}$	$\log K_q$	$\log K_A$	n
Complex	298.2	4.80 ± 0.05	12.80 ± 0.05	4.79 ± 0.04	0.97
	310.2	4.57 ± 0.05	12.57 ± 0.05	4.27 ± 0.03	0.95
	318.2	4.31 ± 0.07	12.31 ± 0.07	3.99 ± 0.02	0.91

Table 2 The thermodynamic parameters (ΔG° , ΔH° , ΔS°) and the distance parameters (r and % E transfer) of BSA + Complex

Compounds	T	ΔG° (kJmol ⁻¹)	ΔH° (kJmol ⁻¹)	ΔS° (Jmol ⁻¹ K ⁻¹)	r (nm)	E (%)
Complex	298.2	-27.40				
	310.2	-25.56	-73.01	-152.99	0.56	48.01
	318.2	-24.38				

3.2. Radical scavenging activity

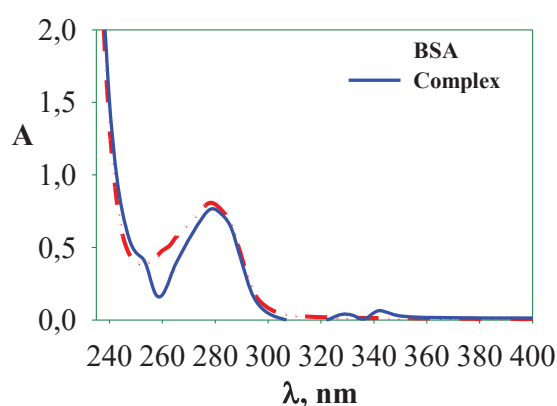
In this work, radical scavenging activity of the complex was investigated by DPPH and H₂O₂ methods. The IC₅₀ values of the complex, BHT, Trolox and Ascorbic acid are given Table 3. The radical scavenging effect of the complex and standards on H₂O₂ radical decreased in the order of ascorbic acid > BHT > trolox > the complex and DPPH radical decreased in the order of trolox > the complex > BHT > ascorbic acid > the complex. Comparing both methods with each other, it was observed that the complex had better H₂O₂ scavenging activity. As a result, the complex could be potential candidate as an antioxidant agent.

Table 3 The antioxidant and radical scavenging activities of the complex

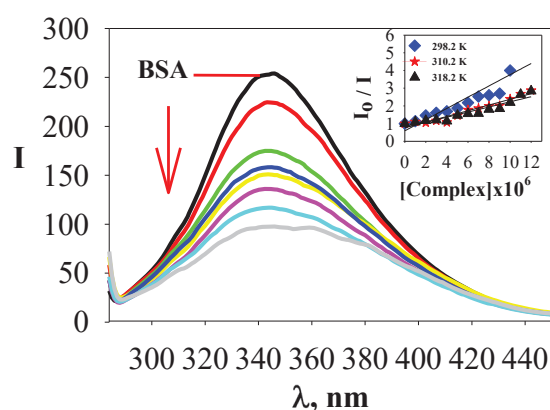
Compounds	IC ₅₀ (μM)		Ref
	DPPH	H ₂ O ₂	
Complex	18.56 ± 0.05	2.37 ± 0.04	*
Ascorbic acid	25.6	0.02	[11]
Trolox	7.73	0.12	[11]
BHT	15.04	0.03	[11]

*This work.

a)



b)



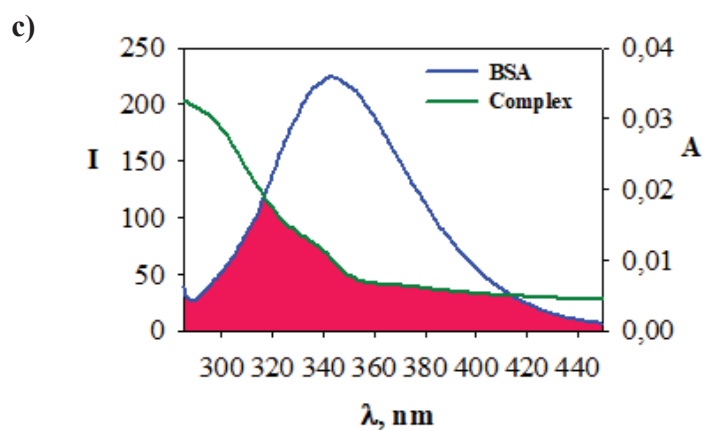


Figure 1. a) Electronic absorption spectra of the complex upon addition of BSA; b) Effects of the complex on the fluorescence spectra of BSA c) The emission spectrum of BSA and electronic absorption spectrum of the complex. A shaded region represents the overlapping area of both spectra.

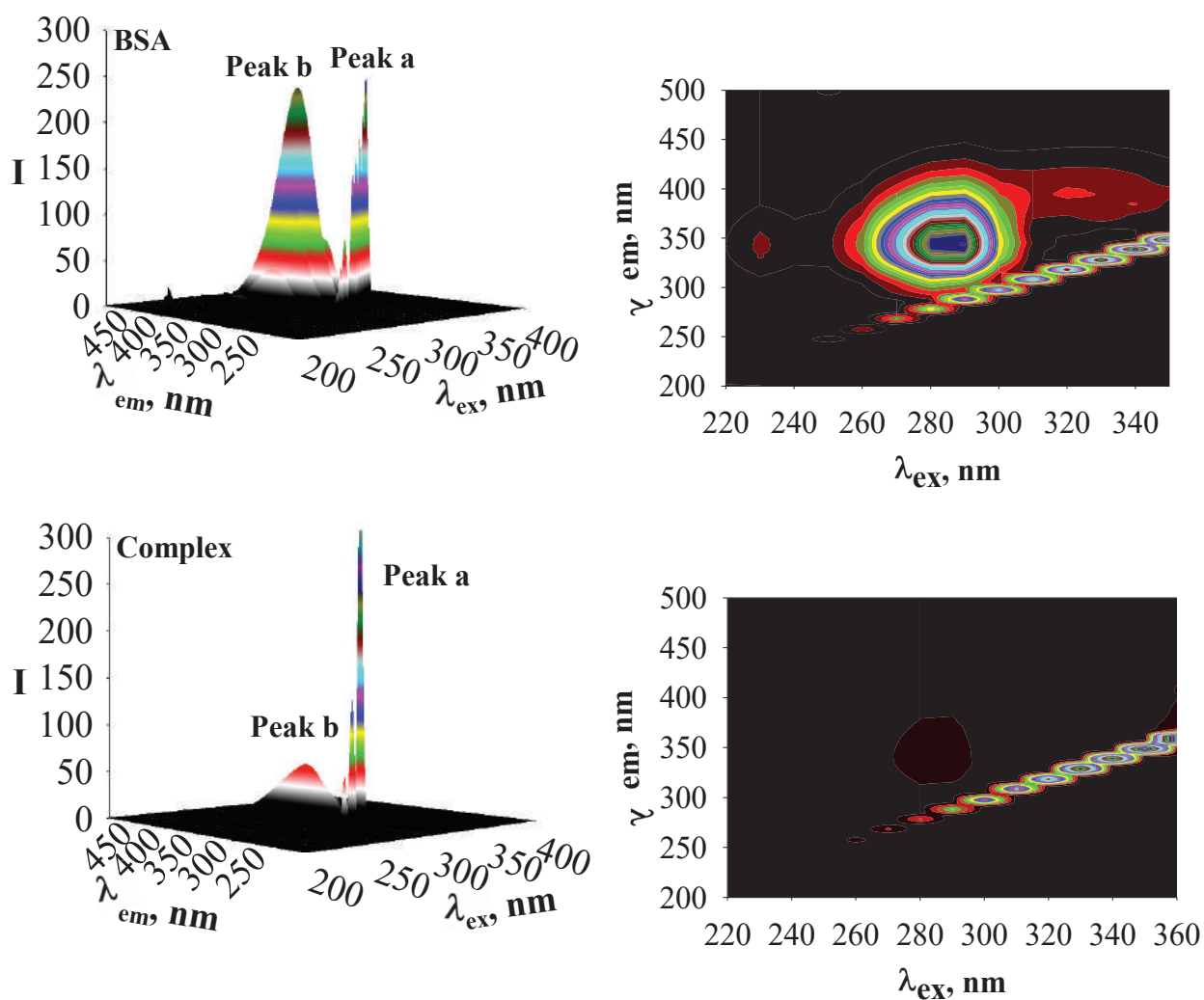


Figure 2. 2D and 3D fluorescence spectra of BSA, BSA+complex

4. CONCLUSIONS

The interaction of the complex with BSA by spectroscopic methods including electronic and fluorescence spectroscopy were investigated. The quenching in BSA could occur via a static mode, indicating that the complex binds to BSA via hydrogen bonding and van der Waals forces. The binding distances between BSA and the complex were evaluated based on FRET and the results indicated that the quenching of BSA by the complex involved static quenching. The results from 2D and 3D fluorescence results indicated that the microenvironment of tyrosine and tryptophan residues on proteins was altered with the addition of the complex. Furthermore, the complex showed radical scavenging activity when compared to standard antioxidants such as ascorbic acid, trolox and BHT.

5. REFERENCES

- [1] Carter D, Ho JX. *Adv. Protein Chem.* 1994;45:153-203.
- [2] Curry S, Mandelkow H, Brick P, Franks N. *Nat. Struct. Biol.* 1998;5:827-835.
- [3] Reynolds JA, Herbert S, Polet H, Steinhardt J. *Biochemistry* 1967;6:937-947.
- [4] Sklar LA, Hudson BS, Simoni RD. *Biochemistry* 1977;16:5100-5108
- [5] Barnham KJ, Masters CL, Bush AI. *Nat. Rev. Drug Discov.* 2004;3:205-214.
- [6] İnci D, Aydın R, Vatan Ö, Yılmaz D, Gençkal HM, Zorlu Y, Cavaş T. *Spectrochim Acta A Mol Biomol Spectrosc.* 2015; 145: 313-324.
- [7] Lakowicz JR. *Principles of Fluorescence Spectroscopy*, 1999, p. 237.
- [8] Wang F, Huang W, Dai ZX. *J Mol Struct.* 2008; 875: 509.
- [9] Gulcin İ. *Toxicology* 2006; 217(2–3): 213-220.
- [10] Ruch RJ, Cheng SJ, Klaunig JE. *Carcinogenesis* 1989; 10(6): 1003-1008.
- [11] İnci D, Aydın R, Vatan Ö, Şahin O, Çinkılıç N. *New J Chem.* 2019; 43(12): 4681-4697.

SYNTHESIS AND CHARACTERIZATION OF NEW MANNICH BASES CONTAINING 1,2,4-TRIAZOLE RING

Dr. Bahar BANKOĞLU YOLA

Science and Technology Application and Research Laboratory, Iskenderun Technical
University, 31200, Hatay, Turkey
ORCID NO: 0000-0002-2931-077X

Prof. Dr. Haydar YÜKSEK

Department of Chemistry, Kafkas University, 36100, Kars, Turkey
ORCID NO: 0000-0003-1289-1800

Abstract: In the present study, seven novel bis-[3-alkyl(aryl)-4-(3-ethoxy-4-hydroxy)-benzylideneamino-4,5-dihydro-1*H*-1,2,4-triazol-5-on-1-yl-methyl]-piperazines (**6**) were obtained from the reactions of 3-alkyl(aryl)-4-(3-ethoxy-4-hydroxy)-benzylidenamino-4,5-dihydro-1*H*-1,2,4-triazole-5-ones (**5**) with morpholine in the presence of formaldehyde according to the Mannich reaction. The structures of novel compounds were characterized by using IR, ¹H-NMR and ¹³C-NMR spectra.

Keywords: 4,5-Dihydro-1*H*-1,2,4-triazol-5-one, Synthesis, Schiff base, Mannich base

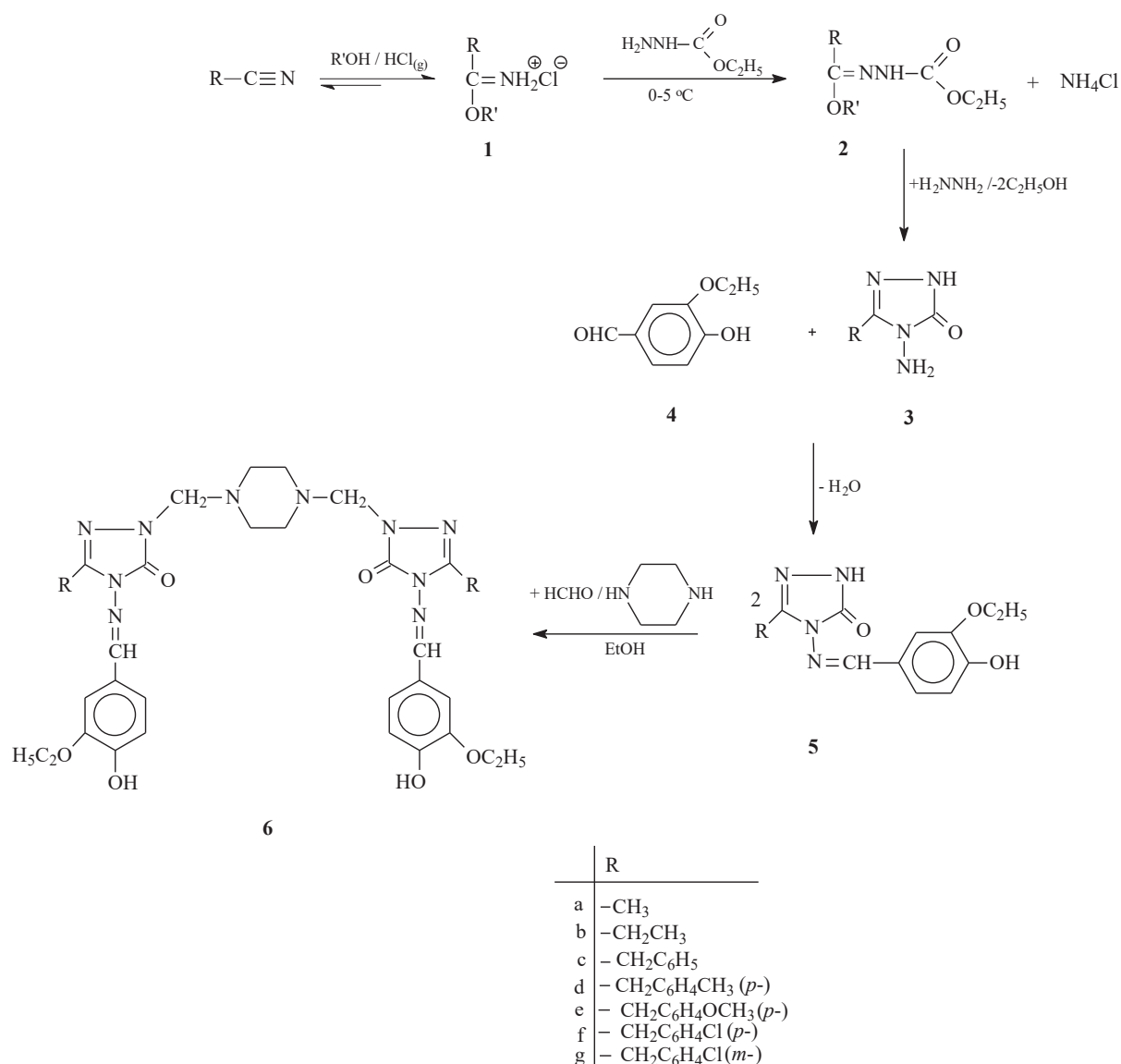
1. Introduction

The classical Mannich reaction is a three-component condensation reaction. This reaction is known as the condensation reaction between structurally diverse substrates (X-H) containing at least one active hydrogen atom and an aldehyde or ketone (generally R¹-CHO) and a primary or secondary amine. The Mannich reaction was first performed in Germany in 1992 by two scientists named Mannich and Krosche. It is known that this method, which is still preferred today, is used in the synthesis of many compounds (Hellmann, 1960), (Roman, 2015).

Mannich bases are industrially important compounds and their importance has been increasing in the light of industrial developments in recent years. So much so that it has found many practical applications in the processing of natural macromolecular materials such as leather, paper and textiles, in the production of synthetic polymers, as additives used in the petroleum industry, products used in water treatment, analytical reagents, cosmetics, dyes, etc. In spite of it, the most important application of the Mannich reaction lies in the field of medicinal chemistry (Atul Kumar, 2010), (Jakub Iwanejko, 2014), (Maurilio Tramontini, 1988). This allegation is supported by the a remarkable number of papers published each year. The majority of these studies consist of examining some activities of new Mannich bases such as anticancer, antibacterial, antifungal and antioxidant (Roman, 2015) (Fatimah S. Al-Khattaf a, 2021), (Samra Farooq, 2021).

In this study, bis-[3-alkyl(aryl)-4-(3-ethoxy-4-hydroxy)-benzylideneamino-4,5-dihydro-1*H*-1,2,4-triazol-5-on-1-yl-methyl]-piperazines (**6**) were obtained from the reactions of 3-alkyl(aryl)-4-(3-ethoxy-4-hydroxy)-benzylidenamino-4,5-dihydro-1*H*-1,2,4-triazole-5-ones (**5**) with piperazine in the presence of formaldehyde according to the Mannich reaction. Synthesis of type **3** compounds was carried out by starting from nitriles with the pinner

method of amino compounds containing 1,2,4-triazole ring registered in the literature (Yüksek 2005).



2. Materials and Methods

Chemical reagents and all solvents used in this study were purchased from Merck AG, Aldrich and Fluka. The IR spectra were obtained on an Alpha-P Bruker FT-IR spectrometer. ¹H and ¹³C NMR spectra were recorded in deuterated dimethyl sulfoxide with TMS as internal standard using a Bruker Ultrashield Plus Biospin spectrometer at 400 MHz and 100 MHz, respectively.

The corresponding compound 1 (0.01 mol) was refluxed with acetic anhydride (15 mL) for 0.5 h. After addition of absolute ethanol (50 mL), the mixture was refluxed for an hour more. Evaporation of the resulting solution at 40-45 °C in vacuo and several recrystallizations of the residue from EtOH gave pure compounds **6** as colorless crystals.

3. Results

N,N'-Bis-[3-metil-4-(3-etoksi-4-hidroksi)-benzilidenamino-4,5-dihidro-1*H*-1,2,4-triazol-5-on-1-il-metil]-piperazin (6a): IR (ATR) (cm⁻¹): 3134 (OH), 1698 (C=O), 1596 (C=N), 893 ve 798 (1,2,4-trisubstitue benzen halkası). ¹H-NMR (DMSO-*d*₆) (Ek Şekil 95): δ 1.36 (t, 6H, 2OCH₂CH₃; *J* = 6.80 Hz), 2.30 (s, 6H, 2CH₃), 2.58 (s, 8H, 4CH₂), 4.08 (q, 4H, 2OCH₂CH₃; *J* = 6.80 Hz), 4.50 (s, 4H, 2NCH₂N), 6.89 (d, 2H, ArH; *J* = 8.00 Hz), 7.25 (dd, 2H, ArH, *J* = 8.00, 1.60 Hz), 7.38 (d, 2H, ArH, *J* = 1.60 Hz), 9.47 (s, 2H, 2N=CH), 9.75 (s, 2H, 2OH). ¹³C-NMR (DMSO-*d*₆): δ 10.95 (2CH₃), 14.64 (2OCH₂CH₃), 49.39 (4CH₂), 63.96 (2OCH₂CH₃), 65.70 (2NCH₂N), [111.64 (2CH), 115.75 (2CH), 122.70 (2CH), 124.57 (2C), 142.85 (2C), 150.60 (2C)] (ArC), 147.18 (2Triazol C₃), 150.31 (2Triazol C₅), 155.42 (2N=CH).

N,N'-Bis-[3-etil-4-(3-etoksi-4-hidroksi)-benzilidenamino-4,5-dihidro-1*H*-1,2,4-triazol-5-on-1-il-metil]-piperazin (6b): IR (ATR) (cm⁻¹): 3300 (OH), 1692 (C=O), 1593 (C=N), 866 ve 797 (1,2,4-trisubstitue benzen halkası). ¹H-NMR (DMSO-*d*₆) (Ek Şekil 98): δ 1.21 (t, 6H, 2CH₂CH₃; *J* = 7.60 Hz), 1.36 (t, 6H, 2OCH₂CH₃; *J* = 6.80 Hz), 2.58 (s, 8H, 4CH₂), 2.69 (q, 4H, 2CH₂CH₃; *J* = 7.60 Hz), 4.08 (q, 4H, 2OCH₂CH₃; *J* = 6.80 Hz), 4.51 (s, 4H, 2NCH₂N), 6.90 (d, 2H, ArH; *J* = 8.40 Hz), 7.25 (dd, 2H, ArH, *J* = 8.40, 2.00 Hz), 7.38 (d, 2H, ArH, *J* = 1.60 Hz), 9.47 (s, 2H, 2N=CH), 9.71 (s, 2H, 2OH). ¹³C-NMR (DMSO-*d*₆): δ 10.00 (2CH₂CH₃), 14.63 (2OCH₂CH₃), 18.42 (2CH₂CH₃), 49.42 (4CH₂), 63.94 (2OCH₂CH₃), 65.74 (2NCH₂N), [111.66 (2CH), 115.77 (2CH), 122.60 (2CH), 124.60 (2C), 146.63 (2C), 150.60 (2C)] (ArC), 147.16 (2Triazol C₃), 150.43 (2Triazol C₅), 155.39 (2N=CH).

N,N'-Bis-[3-benzil-4-(3-etoksi-4-hidroksi)-benzilidenamino-4,5-dihidro-1*H*-1,2,4-triazol-5-on-1-il-metil]-piperazin (6c): IR (ATR) (cm⁻¹) 3128 (OH), 1702 (C=O), 1585 (C=N), 905 ve 798 (1,2,4-trisubstitue benzen halkası), 770 ve 703 (monosubstitue benzen halkası). ¹H-NMR (DMSO-*d*₆) (Ek Şekil 101): δ 1.38 (t, 6H, 2OCH₂CH₃; *J* = 6.80 Hz), 2.61 (s, 8H, 4CH₂), 4.03-4.09 (m, 8H, CH₂Ph + 2OCH₂CH₃), 4.56 (s, 4H, 2NCH₂N), 6.87 (d, 2H, ArH; *J* = 8.00 Hz), 7.17 (dd, 2H, ArH, *J* = 8.00, 2.00 Hz), 7.21-7.24 (m, 2H, ArH), 7.28-7.32 (m, 10H, ArH), 9.44 (s, 2H, 2N=CH), 9.71 (s, 2H, 2OH). ¹³C-NMR (DMSO-*d*₆): δ 14.62 (2OCH₂CH₃), 31.10 (2CH₂Ph), 49.45 (4CH₂), 63.83 (2OCH₂CH₃), 65.86 (2NCH₂N), [110.77 (2CH), 115.61 (2CH), 123.09 (2CH), 124.58 (2C), 144.73 (2C), 150.57 (2C)] (ArC), [126. 71 (2CH), 128.45 (4CH), 128.63 (4CH), 135.82 (2C)] (C₃-ArC), 147.17 (2Triazol C₃), 150.35 (2Triazol C₅), 154.60 (2N=CH).

N,N'-Bis-[3-(*p*-metilbenzil)-4-(3-etoksi-4-hidroksi)-benzilidenamino-4,5-dihidro-1*H*-1,2,4-triazol-5-on-1-il-metil]-piperazin (6d): IR (ATR) (cm⁻¹) 3130 (OH), 1701 (C=O), 1588 (C=N), 897 ve 799 (1,2,4-trisubstitue benzen halkası), 799 (1,4-disubstitue benzen halkası). ¹H-NMR (DMSO-*d*₆): δ 1.38 (t, 6H, 2OCH₂CH₃; *J* = 6.80 Hz), 2.24 (s, 6H, 2PhCH₃), 2.60 (s, 8H, 4CH₂), 4.00 (s, 4H, 2CH₂Ph), 4.06 (q, 4H, 2OCH₂CH₃; *J* = 6.80 Hz), 4.55 (s, 4H, 2NCH₂N), 6.87 (d, 2H, ArH; *J* = 8.00 Hz), 7.10 (d, 4H, ArH; *J* = 8.00 Hz), 7.15-7.19 (m, 2H, ArH), 7.20 (d, 4H, ArH; *J* = 8.00 Hz), 7.30 (d, 2H, ArH; *J* = 1.60 Hz), 9.44 (s, 2H, 2N=CH), 9.70 (s, 2H, 2OH). ¹³C-NMR (DMSO-*d*₆): δ 14.62 (2OCH₂CH₃), 20.56 (2PhCH₃), 30.72 (2CH₂Ph), 49.45 (4CH₂), 63.82 (2OCH₂CH₃), 65.85 (2NCH₂N), [110.78 (2CH), 115.61 (2CH), 123.09 (2CH), 124.61 (2C), 144.87 (2C), 150.56 (2C)] (ArC), [128. 51 (4CH), 129.01 (4CH), 132.68 (2C), 135.78 (2C)] (C₃-ArC), 147.18 (2Triazol C₃), 150.35 (2Triazol C₅), 154.53 (2N=CH).

N,N'-Bis-[3-(*p*-metoksibenzil)-4-(3-etoksi-4-hidroksi)-benzilidenamino-4,5-dihidro-1*H*-1,2,4-triazol-5-on-1-ilmetil]-piperazin (6e): IR (ATR) (cm⁻¹) 3063 (OH), 1705 (C=O), 1591 (C=N), 879 ve 804 (1,2,4-trisubstitue benzen halkası), 804 (1,4-disubstitue benzen halkası). ¹H-NMR (DMSO-*d*₆): δ 1.39 (t, 6H, 2OCH₂CH₃; *J* = 6.80 Hz), 2.61 (s, 8H, 4CH₂), 3.70 (s,

6H, 2OCH₃), 3.99 (s, 4H, 2CH₂Ph), 4.08 (q, 4H, 2OCH₂CH₃; $J = 6.80$ Hz), 4.55 (s, 4H, 2NCH₂N), 6.87 (d, 4H, ArH; $J = 8.40$ Hz), 6.89 (d, 2H, ArH; $J = 8.00$ Hz), 7.19 (dd, 2H, ArH; $J = 8.40, 1.60$ Hz), 7.24 (d, 4H, ArH; $J = 8.80$ Hz), 7.32 (d, 2H, ArH; $J = 1.20$ Hz), 9.45 (s, 2H, 2N=CH), 9.73 (s, 2H, 2OH). ¹³C-NMR (DMSO-*d*₆) (Ek Şekil 108): δ 14.62 (2OCH₂CH₃), 30.25 (2CH₂Ph), 49.44 (4CH₂), 54.99 (2OCH₃), 63.82 (2OCH₂CH₃), 65.84 (2NCH₂N), [110.84 (2CH), 115.62 (2CH), 123.04 (2CH), 124.62 (2C), 145.02 (2C), 150.54 (2C)] (ArC), [113.88 (4CH), 127.54 (2CH), 129.70 (4CH), 158.08 (2C)] (C₃-ArC), 147.18 (2Triazol C₃), 150.35 (2Triazol C₅), 154.59 (2N=CH).

N,N'-Bis-[3-(*p*-klorobenzil)-4-(3-etoksi-4-hidroksi)-benzilidenamino-4,5-dihidro-1*H*-1,2,4-triazol-5-on-1-ilmetil]-piperazin (6f): IR (ATR) (cm⁻¹): 3187 (OH), 1705 (C=O), 1587 (C=N), 852 ve 798 (1,2,4-trisubstitue benzen halkası), 798 (1,4-disubstitue benzen halkası). ¹H-NMR (DMSO-*d*₆) (Ek Şekil 110): δ 1.38 (s, 6H, 2OCH₂CH₃; $J = 6.80$ Hz), 2.60 (s, 8H, 4CH₂), 4.04 (s, 4H, 2OCH₂CH₃; $J = 6.80$ Hz), 4.08 (s, 4H, 2CH₂Ph), 4.55 (s, 4H, 2NCH₂N), 6.87 (d, 2H, ArH; $J = 8.00$ Hz), 7.17 (dd, 2H, ArH; $J = 8.00, 2.00$ Hz), 7.26 (d, 2H, ArH; $J = 2.00$ Hz), 7.33-7.39 (m, 8H, ArH), 9.44 (s, 2H, 2N=CH), 9.72 (s, 2H, 2OH). ¹³C-NMR (DMSO-*d*₆): δ 14.62 (2OCH₂CH₃), 30.45 (2CH₂Ph), 49.42 (4CH₂), 63.83 (2OCH₂CH₃), 65.89 (2NCH₂N), [110.80 (2CH), 115.62 (2CH), 123.11 (2CH), 124.51 (2C), 144.38 (2C), 150.61 (2C)] (ArC), [128.40 (4CH), 130.53 (4CH), 131.40 (2C), 134.82 (2C)] (C₃-ArC), 147.18 (2Triazol C₃), 150.34 (2Triazol C₅), 154.75 (2N=CH).

N,N'-Bis-[3-(*m*-klorobenzil)-4-(3-etoksi-4-hidroksi)-benzilidenamino-4,5-dihidro-1*H*-1,2,4-triazol-5-on-1-ilmetil]-piperazin (6g): IR (ATR) (cm⁻¹): 3200 (OH), 1673 (C=O), 1581 (C=N), 900 ve 825 (1,2,4-trisubstitue benzen halkası), 867, 790 ve 703 (1,3-disubstitue benzen halkası). ¹H-NMR (DMSO-*d*₆) (Ek Şekil 113): δ 1.38 (t, 6H, 2OCH₂CH₃; $J = 6.80$ Hz), 2.61 (s, 8H, 4CH₂), 4.07 (q, 4H, 2OCH₂CH₃; $J = 6.80$ Hz), 4.10 (s, 4H, 2CH₂Ph), 4.56 (s, 4H, 2NCH₂N), 6.87 (d, 2H, ArH; $J = 8.00$ Hz), 7.17 (dd, 2H, ArH; $J = 8.00, 1.60$ Hz), 7.26-7.34 (m, 8H, ArH), 7.44 (s, 2H, ArH), 9.44 (s, 2H, 2N=CH), 9.75 (s, 2H, 2OH). ¹³C-NMR (DMSO-*d*₆): δ 14.62 (2OCH₂CH₃), 30.64 (2CH₂Ph), 49.45 (4CH₂), 63.86 (2OCH₂CH₃), 65.90 (2NCH₂N), [110.64 (2CH), 115.60 (2CH), 123.23 (2CH), 124.51 (2C), 144.20 (2C), 150.63 (2C)] (ArC), [126.76 (2CH), 127.33 (2CH), 128.72 (2CH), 130.28 (2CH), 132.99 (2C), 138.27 (2C)] (C₃-ArC), 147.23 (2Triazol C₃), 150.32 (2Triazol C₅), 154.72 (2N=CH).

4. Discussion

In this study, because of their potential biological activity, the bis-[3-alkyl(aryl)-4-(3-ethoxy-4-hydroxy)-benzylideneamino-4,5-dihydro-1*H*-1,2,4-triazol-5-on-1-yl-methyl]-piperazines were obtained. The structures of six new compounds were identified with IR, ¹H-NMR and ¹³C-NMR spectral data.

References

- Atul Kumar, M. K. (2010). Non-ionic surfactant catalyzed synthesis of Betti base in water. *Tetrahedron Letters*, 1582-1584.
- Fatimah S. Al-Khattaf a, A. M. (2021). Antimicrobial and cytotoxic activities of isoniazid connected. *Journal of Infection and Public Health*, 533-542.
- Hellmann, H. O. (1960). α -Aminoalkylierung. *Verlag Chemie*, 289.
- Jakub Iwanejko, E. W. (2014). Stereoselective preparation of chiral compounds in Mannich-type reactions of a bicyclic imine and phenols or indole. *Tetrahedron Letters*, 6619-6622.
- Maurilio Tramontini, L. A. (1988). Mannich bases in polymer chemistry. *Polymer*, 771-788.
- Roman, G. (2015). Mannich bases in medicinal chemistry and drug design. *European Journal of Medicinal Chemistry*, 743-816.
- Samra Farooq, I.-U. H. (2021). Synthesis, characterization and biological evaluation of N-Mannich base derivatives of 2-phenyl-2-imidazoline as potential antioxidants, enzyme inhibitors, antimicrobials, cytotoxic and anti-inflammatory agents. *Arabian Journal of Chemistry*, 103050-103072.
- Yüksek, H. Ü. (2005). Non-Aqueous Medium Titrations of Some New 4-Benzylidenamino-4,5-dihydro-1H-1,2,4-triazol-5-one Derivatives. *Molecules*, 961-970.

SYNTHESIS OF NOVEL 3-{[1-(MORPHOLIN-4-YL-METHYL)-3-ALKYL/ARYL-4,5-DIHYDRO-1H-1,2,4-TRIAZOL-5-ONE-4-YL]-AZOMETHINE}-PHENYL 2,5-DICHLOROBENZENESULFONATES

Dr. Fevzi Aytemiz

Kafkas University, Faculty of Science and Letters, Department of Chemistry, 36100,
Kars, Turkey ORCID ID: 0000-0002-5982-9038

Prof. Dr. Haydar Yüksek

Kafkas University, Faculty of Science and Letters, Department of Chemistry, 36100,
Kars, Turkey ORCID ID: 0000-0003-1289-1800

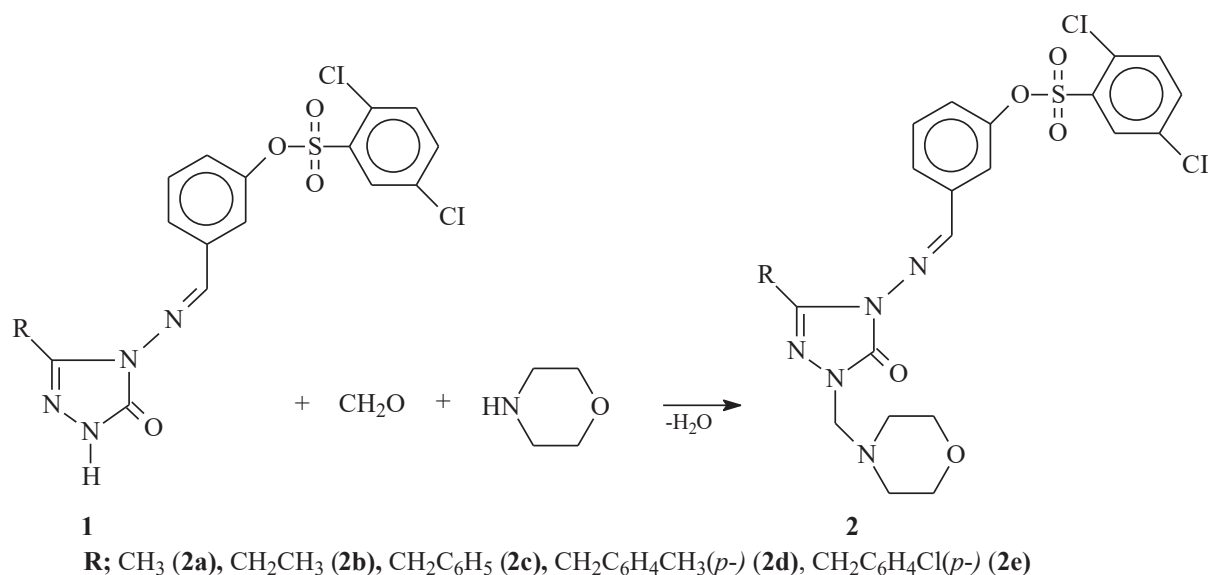
ABSTRACT

In this study, 3-[(3-alkyl/aryl-4,5-dihydro-1H-1,2,4-triazol-5-one-4-yl)-azomethine]-phenyl 2,5-dichlorobenzenesulfonates (**1**) were treated with morpholine in the presence of formaldehyde to obtain 5 new 3-{[1-(morpholin-4-yl-methyl)-3-alkyl/aryl-4,5-dihydro-1H-1,2,4-triazole-5-one-4-yl]-azomethine}-phenyl 2,5-dichlorobenzenesulfonates (**2**). These novel compounds characterized by IR, ¹H NMR and ¹³C NMR spectral data.

Keywords: 4,5-Dihydro-1H-1,2,4-triazol-5-one, Synthesis, Mannich base, Characterization

INTRODUCTION

1,2,4-Triazole derivatives are recorded to own a wide variety of pharmacological activities like antioxidant (Gürsoy-Kol & Ayazoglu, 2017), antibacterial (Yüksek vd., 1997), antiparasitic (Saadeh vd., 2010), anti-inflammatory (Uzgören-Baran vd., 2012), analgesic (Chidananda vd., 2012), antitumor (Demirbaş vd., 2002), anti-HIV (Li vd., 2013), antiviral (Henen vd., 2012) properties. The Mannich reaction is a three-component condensation reaction containing compounds of active hydrogen, formaldehyde, and a secondary amine (Karthikeyan vd., 2006). Aminomethylation of aromatic substrates by the Mannich reaction is important for the synthesis and modification of biologically active compounds (Tramontini & Angiolini, 1994). Mannich bases have found many practical applications such as leather, paper and textile, production of synthetic polymers, petroleum industry, analytical reagents, cosmetics, paints (Tramontini & Angiolini, 1990). However, the importance of Mannich bases has increased recently due to their applications in pharmaceutical chemistry. They have also been found to have antibacterial, antifungal, anticancer, antituberculosis, analgesic, and anti-inflammatory properties (Amir & Shikha, 2004; Ashok vd., 2007; Pathak vd., t.y.; Shivarama Holla vd., 2002; Walczak vd., 2004).



Scheme 1. Synthesis route of compounds **2**

EXPERIMENTAL

Chemical reagents used in the study were supplied from Sigma (Sigma-Aldrich GmbH, Germany), Fluka (Switzerland) and Merck AG, (Germany). Melting points were identified using a Stuart SMP30 melting point apparatus with open glass capillaries (United Kingdom). ^1H and ^{13}C NMR spectra were recorded in deuterated dimethyl sulfoxide (DMSO- d_6) using a Bruker spectrometer (Germany) at 400 MHz and 100 MHz, respectively.

General procedure for the synthesis of 3-[[1-(morpholin-4-yl-methyl)-3-alkyl/aryl-4,5-dihydro-1H-1,2,4-triazol-5-one-4-yl]-azomethine}-phenyl 2,5-dichlorobenzenesulfonates (**2**)

The corresponding compound **1** (5 mmol) was dissolved absolute ethanol and to this solution were added formaldehyde (% 37, 20 mmol) and morpholine (10 mmol). The reaction mixture was refluxed for 4 hours and filtered. The solution was left at room temperature for 1 overnight and after cooling of the mixture in the -18°C refrigerator. The solid formed was obtained by filtration, washed with cold ethanol. Several recrystallizations of the crude product from ethanol gave pure compounds **2**.

3-[[1-(morpholin-4-yl-methyl)-3-methyl-4,5-dihydro-1H-1,2,4-triazol-5-one-4-yl]-azomethine}-phenyl 2,5-dichlorobenzenesulfonates (**2a**)

White solid; yield: 78.68%; m.p. 257°C ; IR (cm^{-1}) ν_{max} : 1703 (C=O), 1606, 1571 (C=N), 1362 and 1184 (SO_2), 891 and 798 (1,3-disubstituted benzenoid ring). ^1H -NMR (400 MHz, DMSO- d_6) (ppm) δ H: 2.24 (s, CH_3), 2.72 (t, CH_2NCH_2 ; $J = 4.40$ Hz), 3.56 (t, CH_2OCH_2 ; $J = 4.40$ Hz), 4.53 (s, NCH_2N), [7.30(dd, 1H, $J=8.40$, 2.00 Hz); 7.57-7.59 (m, 2H); 7.81 (d, 1H, $J=8.00$ Hz); 7.94-7.95 (m, 3H)] (Ar-C), 9.71 (s, $\text{N}=\text{CH}$); ^{13}C -NMR (100 MHz, DMSO- d_6) (ppm) δ C: 10.98 (CH_3), 49.93 (CH_2NCH_2), 65.93 (NCH_2N), 66.02 (CH_2OCH_2), [119.42 (CH), 122.37 (CH), 127.78 (CH), 130.77 (C), 131.16 (CH), 131.28 (CH), 132.71 (C), 133.67 (C), 134.33 (CH), 135.96 (C), 136.44 (CH), 151.05 (C)] (Ar-C), 144.20 (triazole C_3), 149.05 (2triazole C_5), 151.48 ($\text{N}=\text{CH}$).

3-[[1-(morpholin-4-yl-methyl)-3-ethyl-4,5-dihydro-1H-1,2,4-triazol-5-one-4-yl]-azomethine}-phenyl 2,5-dichlorobenzenesulfonates (**2b**)

White solid; yield: 81.96%; m.p. 109°C; IR (cm⁻¹) ν_{\max} : 1712 (C=O), 1572 (C=N), 1361 and 1181 (SO₂), 895 and 793 (1,3-disubstituted benzenoid ring). ¹H-NMR (400 MHz, DMSO-d₆) (ppm) δ H: 2.23 (s, CH₃, J =7.20 Hz), 2.58 (t, CH₂NCH₂; J = 4.40 Hz), 2.67 (s, CH₂, J =7.20 Hz), 3.56 (t, CH₂OCH₂; J = 4.40 Hz), 4.54 (s, NCH₂N), [7.34 (dq, 1H, J =8.40, 1.20 Hz); 7.57-7.58 (m, 2H); 7.60 (d, 1H, J =8.40 Hz); 7.80 (d, 1H, J =7.60 Hz); 7.93-7.95 (m, 3H)] (Ar-C), 9.69 (s, N=CH); ¹³C-NMR (100 MHz, DMSO-d₆) (ppm) δ C: 10.01(CH₂CH₃), 18.46(CH₂CH₃), 49.94 (CH₂NCH₂), 65.97 (NCH₂N), 66.02 (CH₂OCH₂), [119.29 (CH), 124.60 (CH), 127.95 (CH), 130.75 (C), 131.21 (CH), 131.28 (CH), 132.71 (C), 133.66 (C), 134.31 (CH), 135.78 (C), 136.41 (CH), 150.19 (C)] (Ar-C), 146.72 (triazole C₃), 149.07 (triazole C₅), 152.00 (N=CH).

3-*{[1-(morpholin-4-yl-methyl)-3-benzyl-4,5-dihydro-1H-1,2,4-triazol-5-one-4-yl]-azomethine}*-phenyl 2,5-dichlorobenzenesulfonates (2c)

White solid; yield: 81.15%; m.p. 118°C; IR (cm⁻¹) ν_{\max} : 1710 (C=O), 1601, 1572 (C=N), 1379 and 1190 (SO₂), 890 and 690 (1,3-disubstituted benzenoid ring), 738 and 690 (monosubstituted benzenoid ring). ¹H-NMR (400 MHz, DMSO-d₆) (ppm) δ H: 2.59 (t, CH₂NCH₂; J = 4.40 Hz), 3.56 (t, CH₂OCH₂; J = 4.80 Hz), 4.07 (s, CH₂Ph), 4.58 (s, NCH₂N), [7.23-7.34 (m, 6H); 7.55 (t, 1H, J =8.00 Hz); 7.64 (m, 1H); 7.76 (d, 1H, J =8.00 Hz); 7.90-7.94 (m, 3H)] (Ar-C), 9.67 (s, N=CH); ¹³C-NMR (100 MHz, DMSO-d₆) (ppm) δ C: 30.91 (CH₂Ph), 49.96 (CH₂NCH₂), 66.02 (NCH₂N), 66.07 (CH₂OCH₂), [119.69 (CH), 124.41 (CH), 127.92 (CH), 130.74 (C), 131.15 (CH), 131.25 (CH), 132.70 (C), 133.66 (C), 134.29 (CH), 135.72 (C), 136.40 (CH), 150.07 (C)] (Ar-C), [126.85 (CH), 128.54 (2CH), 128.68 (2CH), 135.49 (C)] (Ar-C linked to triazole C₃), 144.86 (triazole C₃), 149.00 (triazole C₅), 152.01 (N=CH).

3-*{[1-(morpholin-4-yl-methyl)-3-p-methylbenzyl-4,5-dihydro-1H-1,2,4-triazol-5-one-4-yl]-azomethine}*-phenyl 2,5-dichlorobenzenesulfonates (2d)

White solid; yield: 79.6%; m.p. 124°C; IR (cm⁻¹) ν_{\max} : 1699 (C=O), 1580 (C=N), 1357 and 1192 (SO₂), 890 and 795 (1,3-disubstituted benzenoid ring), 839 (1,4-disubstituted benzenoid ring). ¹H-NMR (400 MHz, DMSO-d₆) (ppm) δ H: 2.25 (t, CH₃), 2.58 (t, CH₂NCH₂; J = 4.40 Hz), 3.56 (t, CH₂OCH₂; J = 4.40 Hz), 4.00 (s, CH₂Ph), 4.57 (s, NCH₂N), [7.13 (d, 2H, J =8.00Hz); 7.20 (d, 2H, J =8.00 Hz); 7.28 (dq, 1H, J =8.40, 1.20 Hz); 7.56 (t, 1H, J =8.00 Hz); 7.64 (t, 1H, J =2.00Hz); 7.90-7.91 (m, 2H); 7.9 5(t, 1H J =1.60 Hz)] (Ar-C), 9.66 (s, N=CH); ¹³C-NMR (100 MHz, DMSO-d₆) (ppm) δ C: 20.59 (PhCH₃), 30.53(CH₂Ph), 49.99 (CH₂NCH₂), 66.02 (NCH₂N), 66.02 (CH₂OCH₂), [119.63 (CH), 124.40 (CH), 127.98 (CH), 130.74 (C), 131.17 (C), 131.25 (CH), 132.70 (C), 133.66 (C), 134.30 (CH), 135.96 (C), 136.61 (CH), 150.07 (C)] (Ar-C), [128.35 (2CH), 129.04 (2CH), 132.35 (C), 135.74 (C)] (Ar-C linked to triazole C₃), 145.02 (triazole C₃), 149.01 (triazole C₅), 150.07 (N=CH).

3-*{[1-(morpholin-4-yl-methyl)-3-p-chlorobenzyl-4,5-dihydro-1H-1,2,4-triazol-5-one-4-yl]-azomethine}*-phenyl 2,5-dichlorobenzenesulfonates (2e)

White solid; yield: 77.66%; m.p. 135°C; IR (cm⁻¹) ν_{\max} : 1700 (C=O), 1594 (C=N), 1355 and 1192 (SO₂), 890 and 798 (1,3-disubstituted benzenoid ring), 798 (1,4-disubstituted benzenoid ring). ¹H-NMR (400 MHz, DMSO-d₆) (ppm) δ H: 2.58 (t, CH₂NCH₂; J = 4.40 Hz), 3.56 (t, CH₂OCH₂; J = 4.40 Hz), 4.08 (s, CH₂Ph), 4.57 (s, NCH₂N), [7.27-7.30 (m, 1H); 7.34-7.41 (m, 4H); 7.56 (t, 1H, J =8.00 Hz); 7.64 (t, 1H, J = 2.00 Hz); 7.78 (d, 1H, J =7.60 Hz); 7.91 (m, 2H); 7.95 (t, 1H, J =1.60 Hz)] (Ar-C), 9.67 (s, N=CH); ¹³C-NMR (100 MHz, DMSO-d₆) (ppm) δ C: 30.23 (CH₂Ph), 49.94 (CH₂NCH₂), 66.02 (NCH₂N), 66.10 (CH₂OCH₂), [119.81 (CH), 124.43 (CH), 127.88 (CH), 130.81 (C), 131.17 (CH), 131.25 (CH), 132.70 (C), 133.65 (CH), 134.29 (CH), 135.68 (C), 136.41 (CH), 150.06 (C)] (Ar-C), [128.40 (2CH), 130.75

(2CH), 131.57 (C), 134.62 (C)] (Ar-C linked to triazole C₃), 144.55 (triazole C₃), 148.99 (triazole C₅), 152.13 (N=CH).

RESULTS AND DISCUSSION

In the present study, new Mannich base (**2a-2e**) were designed and synthesized. The new synthesized compounds were identified using spectral data (IR, ¹H NMR and ¹³C NMR).

REFERENCES

- Amir, M., & Shikha, K. (2004). Synthesis and anti-inflammatory, analgesic, ulcerogenic and lipid peroxidation activities of some new 2-[(2,6-dichloroanilino) phenyl]acetic acid derivatives. *European Journal of Medicinal Chemistry*, 39(6), 535-545. <https://doi.org/10.1016/j.ejmech.2004.02.008>
- Ashok, M., Holla, B. S., & Poojary, B. (2007). Convenient one pot synthesis and antimicrobial evaluation of some new Mannich bases carrying 4-methylthiobenzyl moiety. *European Journal of Medicinal Chemistry*, 42(8), 1095-1101. <https://doi.org/10.1016/j.ejmech.2007.01.015>
- Chidananda, N., Poojary, B., Sumangala, V., Kumari, N. S., Shetty, P., & Arulmoli, T. (2012). Facile synthesis, characterization and pharmacological activities of 3,6-disubstituted 1,2,4-triazolo[3,4-b][1,3,4]thiadiazoles and 5,6-dihydro-3,6-disubstituted-1,2,4-triazolo[3,4-b][1,3,4]thiadiazoles. *European Journal of Medicinal Chemistry*, 51, 124-136. <https://doi.org/10.1016/j.ejmech.2012.02.030>
- Demirbaş, N., Ugurluoğlu, R., & Demirbaş, A. (2002). Synthesis of 3-alkyl(Aryl)-4-alkylidenamino-4,5-dihydro-1H-1,2,4-triazol-5-ones and 3-alkyl-4-alkylamino-4,5-dihydro-1H-1,2,4-triazol-5-ones as antitumor agents. *Bioorganic & Medicinal Chemistry*, 10(12), 3717-3723. [https://doi.org/10.1016/S0968-0896\(02\)00420-0](https://doi.org/10.1016/S0968-0896(02)00420-0)
- Gürsoy-Kol, Ö., & Ayazoğlu, E. (2017). Antioxidant activities and acidic properties of some novel 4-[3,4-di-(4-nitrobenzoxy)-benzylidenamino]-4,5-dihydro-1H-1,2,4-triazol-5-one derivatives. *Arabian Journal of Chemistry*, 10, S2881-S2889. <https://doi.org/10.1016/j.arabjc.2013.11.015>
- Henen, M. A., El Bialy, S. A. A., Goda, F. E., Nasr, M. N. A., & Eisa, H. M. (2012). [1,2,4]Triazolo[4,3-a]quinoxaline: Synthesis, antiviral, and antimicrobial activities. *Medicinal Chemistry Research*, 21(9), 2368-2378. <https://doi.org/10.1007/s00044-011-9753-7>
- Karthikeyan, M. S., Prasad, D. J., Poojary, B., Subrahmanya Bhat, K., Holla, B. S., & Kumari, N. S. (2006). Synthesis and biological activity of Schiff and Mannich bases bearing 2,4-dichloro-5-fluorophenyl moiety. *Bioorganic & Medicinal Chemistry*, 14(22), 7482-7489. <https://doi.org/10.1016/j.bmc.2006.07.015>
- Li, Z., Cao, Y., Zhan, P., Pannecouque, C., Balzarini, J., De Clercq, E., & Liu, X. (2013). Synthesis and Anti-HIV Evaluation of Novel 1,2,4-triazole Derivatives as Potential Non-nucleoside HIV-1 Reverse Transcriptase Inhibitors. *Letters in Drug Design & Discovery*, 10(1), 27-34. <https://doi.org/10.2174/157018013804142429>

- Pathak, P., Novak, J., Shukla, P. K., Grishina, M., Potemkin, V., & Verma, A. (t.y.). Design, synthesis, antibacterial evaluation, and computational studies of hybrid oxothiazolidin-1,2,4-triazole scaffolds. *Archiv Der Pharmazie*, n/a(n/a), e2000473. <https://doi.org/10.1002/ardp.202000473>
- Saadeh, H. A., Mosleh, I. M., Al-Bakri, A. G., & Mubarak, M. S. (2010). Synthesis and antimicrobial activity of new 1,2,4-triazole-3-thiol metronidazole derivatives. *Monatshefte Für Chemie - Chemical Monthly*, 141(4), 471-478. <https://doi.org/10.1007/s00706-010-0281-9>
- Shivarama Holla, B., Narayana Poojary, K., Sooryanarayana Rao, B., & Shivananda, M. K. (2002). New bis-aminomercaptotriazoles and bis-triazolothiadiazoles as possible anticancer agents. *European Journal of Medicinal Chemistry*, 37(6), 511-517. [https://doi.org/10.1016/S0223-5234\(02\)01358-2](https://doi.org/10.1016/S0223-5234(02)01358-2)
- Tramontini, M., & Angiolini, L. (1990). Further advances in the chemistry of mannich bases. *Tetrahedron*, 46(6), 1791-1837. [https://doi.org/10.1016/S0040-4020\(01\)89752-0](https://doi.org/10.1016/S0040-4020(01)89752-0)
- Tramontini, M., & Angiolini, L. (1994). *Mannich Bases-Chemistry and Uses*. CRC Press.
- Uzgören-Baran, A., Tel, B. C., Sarıgöl, D., Öztürk, E. İ., Kazkayası, İ., Okay, G., Ertan, M., & Tozkoparan, B. (2012). Thiazolo[3,2-b]-1,2,4-triazole-5(6H)-one substituted with ibuprofen: Novel non-steroidal anti-inflammatory agents with favorable gastrointestinal tolerance. *European Journal of Medicinal Chemistry*, 57, 398-406. <https://doi.org/10.1016/j.ejmech.2012.07.009>
- Walczak, K., Gondela, A., & Suwiński, J. (2004). Synthesis and anti-tuberculosis activity of N-aryl-C-nitroazoles. *European Journal of Medicinal Chemistry*, 39(10), 849-853. <https://doi.org/10.1016/j.ejmech.2004.06.014>
- Yüksek, H., Demirbaş, A., İkizler, A., Johansson, C. B., Celik, C., & İkizler, A. A. (1997). Synthesis and antibacterial activities of some 4,5-dihydro-1H-1,2,4-triazol-5-ones. *Arzneimittel-Forschung*, 47(4), 405-409.

STRUCTURAL AND SPECTROSCOPIC ANALYSIS WITH DFT OF 3-METHYL-4-[2-(2-THIENYLCARBONYLOXY)-3-METHOXYBENZYLIDENAMINO)-4,5-DIHYDRO-1H-1,2,4-TRIAZOL-5-ONE

Assist. Prof. Dr. Gül KOTAN

Kafkas University, Kars Vocational School, Kars, Turkey
ORCID: 0000-0002-4507-9029

Prof. Dr. Haydar YÜKSEK

Kafkas University, Department of Chemistry, Kars, Turkey
ORCID: 0000-0003-1289-1800

ABSTRACT

In this study, 3-Methyl-4-[2-(2-thienylcarbonyloxy)-3-methoxybenzylidenamino)-4,5-dihydro-1H-1,2,4-triazol-5-one were calculated using Gaussian 09W program on the computer. For this purpose, firstly, positions of the molecule atoms were determined by drawing three-dimensional atomic structure in the GaussView5.0 program. Then, the optimization of the molecule was performed by choosing the 6-311++G(d,p) basis set and the DFT/ B3LYP method. The infrared (IR) harmonic vibration frequencies were calculated using the Veda 4 program and scaled values were obtained by scaled with a certain scala factor. The obtained computational spectral values were compared with experimental values and IR spectrums were created. All quantum chemical calculations were carried out using optimized molecular structure. Proton Nuclear Magnetic Resonance ($^1\text{H}/\text{NMR}$) spectral values was calculated and in the DMSO solvent and in the gas phase according to GIAO method. Also, non-linear optic analysis (NLO), geometric (bond angles, bond length) and electronic properties (electron affinity (A), electronegativity (χ), softness (σ), global hardness (η) and ionization potential (I), thermodynamic parameters, dipole moment, the highest occupied molecular orbital-lowest unoccupied molecular orbital energy (HOMO-LUMO) analysis, mulliken charges, $E_{\text{LUMO}}-E_{\text{HOMO}}$ energy gap (ΔE_g), total energy of title molecule were calculated. Finally, electron spin potential (ESP), molecular electrostatic potential (MEP) and contour surface map were defined.

Keywords: B3LYP, GIAO, Veda4, HOMO-LUMO.

INTRODUCTION

Schiff bases are formed by the condensation mechanism of aldehydes or ketones with secondary amines (Lindoy, 1971; Holm, 1966) Schiff base derivatives of triazoles have an important place in modern heterocyclic compounds. This is because the compounds are shown significant biological activity such as inflammatory, antitubercular, antifungal, antimicrobial, antibacterial, antitumoral, anticonvulsant, herbicidal activities (Jin, 2018; Soni, 2010; Shanty, 2017; Alkan, 2008; Pontiki, 2008; Bensaber, 2014; Gowda, 2011; Kaur, 2012; Wang, 2010). Recently, quantum chemical calculations of heterocyclic molecules have widely been used to theoretically predict the structural, spectroscopic, thermodynamic and electronic properties of molecular systems (Kotan, 2021; Kotan, 2020; Beytur, 2021; Kotan,

2019; Yüksek, 2017; Gökçe, 2013). The Gaussian 09W (Frisch, 2009) package program, which has many basic set and theory options including molecular ab-initio methods, is used. All of the theoretical studies were done with the Density Functional Theory (B3LYP) method. The structure of molecules and their spectroscopy, geometric, electronic, nonlinear optical properties were investigated. The compound was analyzed with IR, ^1H -NMR, and theoretical infrared spectrum were drawn. 3-Methyl-4-[2-(2-thienylcarbonyloxy)-3-methoxybenzylidenamino)-4,5-dihydro-1*H*-1,2,4-triazol-5-one has been optimized using B3LYP/6-311G++(d,p) basis set (Frisch, 2009; Wolinski, 1990) ^1H -NMR and ^{13}C -NMR isotropic shift values were calculated by the method of GIAO (Wolinski, 1990) using the program package Gaussian G09W. Experimental and theoretical values were inserted into the graphic according to equation of $\delta_{\text{exp}} = a + b \cdot \delta_{\text{calc}}$. IR absorption frequencies of analysed molecule were calculated by method. The veda4f program (Jamróz, et al., 2004) was used in defining IR data, which were scaled with determined scala factor (Merrick, 2007). Experimental data obtained from the literature (Gürbüz, 2020). Furthermore, theoretical bond lengths and bond angles, dipole moments, mulliken charges, thermodynamics properties, electronic parameters, countour maps, HOMO-LUMO energies and total energy of the molecule were calculated.

MATERIALS AND METHODS

Theoretical

The calculations were carried out with density functional theory (DFT) method using 6-311G++(d,p) basis sets at the Gaussian 09W program package on a computing system (Frisch, 2009). Firstly, the compound was optimized by using the DFT(B3LYP) method and 6-311++G(d,p) basis set (Frisch, 2009; Wolinski, 1990). Then, ^1H -NMR isotropic shift values were calculated with method of GIAO (Wolinski, 1990). The veda4f program was used in defining IR data (Jamróz, 2004). Theoretically calculated IR data are scaled with appropriate scala factors (Merrick, 2007). The theoretical infrared spectrum are visualized with the using scaled theoretical spectroscopik value. Besides, the HOMO-LUMO energy, bond lengths energy gap (ΔE_g), thermodynamic parameters, bond angles, electronic properties, total energy, mulliken charges and dipole moment were calculated on the computer.

RESULT AND DISCUSSION

Calculations

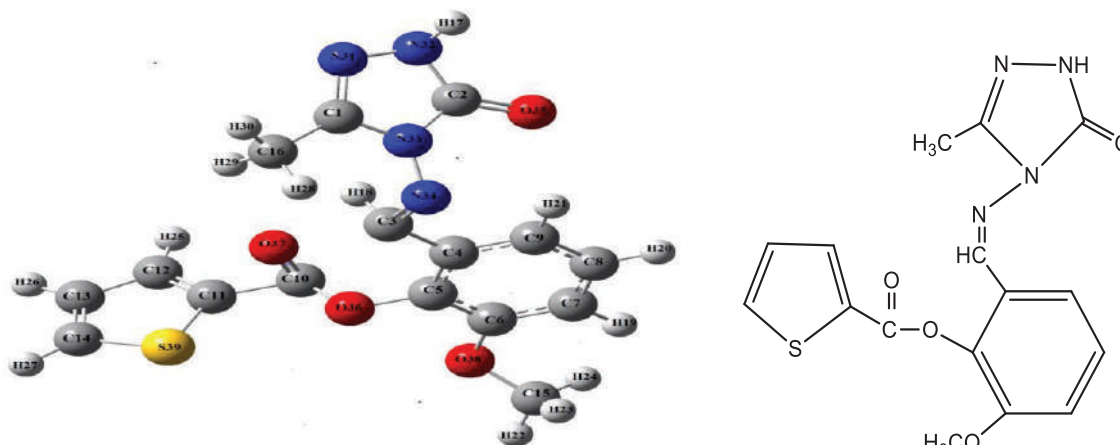


Figure 1. The optimized structure and molecule formula.**Molecular Geometry (Bond Lengths and Bond Angles)****Table 1.** The theoretical bond lengths of molecule

Bond lengths	B3LYP	bond lengths	B3LYP	bond lengths	B3LYP
C(1)-N(31)	1.29	C(3)-C(4)	1.46	S(39)-C(11)	1.74
C(1)-N(33)	1.38	C(4)-C(5)	1.40	C(5)-C(6)	1.40
C(1)-C(16)	1.48	C(4)-C(9)	1.39	C(6)-O(38)	1.35
N(31)-N(32)	1.38	C(5)-O(36)	1.38	O(38)-C(15)	1.42
N(32)-H(17)	1.00	O(36)-C(10)	1.37	C(15)-H(22)	1.08
N(32)-C(2)	1.36	C(10)-O(37)	1.20	C(15)-H(23)	1.09
C(2)-N(33)	1.41	C(10)-C(11)	1.46	C(15)-H(24)	1.09
C(2)-O(35)	1.21	C(11)-C(12)	1.37	C(6)-C(7)	1.39
N(33)-N(34)	1.36	C(12)-H(25)	1.08	C(7)-H(19)	1.08
C(16)-H(28)	1.08	C(12)-C(13)	1.41	C(7)-C(8)	1.39
C(16)-H(29)	1.09	C(13)-H(26)	1.08	C(8)-H(20)	1.08
C(16)-H(30)	1.09	C(13)-C(14)	1.37	C(8)-C(9)	1.38
N(34)-C(3)	1.28	C(14)-H(27)	1.07	C(9)-H(21)	1.08
C(3)-H(18)	1.08	C(14)-S(39)	1.72		

Table 2. The significant bond lengths of molecule

Bond length (Å)	Theoretical B3LYP6-311++G(d,p) (Å)	Literature(Å)
N34=C3	1.28/ 1.28	1.28
N-C	1.41-1.29	1.32
C=O	1.21	1.21
N-N	1.38-1.36	1.35
Phenyl C-C	1.38-1.40	1.38
C-O	1.36-1.42	

The highest bond angle is N(32)-C(2)-O(35) 129.98 while, the lowest bond angle C(11)-S(39)-C(14) 91.05.

Table 3. The bond angles of molecule

Bond angles	B3LYP	Bond angles	B3LYP
N(31)-C(1)-N(33)	111.26	C(11)-S(39)-C(14)	91.05
N(31)-N(32)-H(17)	120.40	S(39)-C(14)-H(27)	119.70
H(17)-N(32)-C(2)	125.22	H(27)-C(14)-C(13)	127.92
N(32)-C(2)-O(35)	129.98	C(14)-C(13)-H(26)	123.44
O(35)-C(2)-N(33)	128.77	H(26)-C(13)-C(12)	124.16
N(33)-C(1)-C(16)	123.51	C(13)-C(12)-H(25)	125.06
C(1)-C(16)-H(28)	108.58	H(25)-C(12)-C(11)	122.07
C(1)-C(16)-H(29)	110.90	C(4)-C(5)-C(6)	121.55
C(1)-C(16)-H(30)	110.91	C(5)-C(6)-O(38)	115.72
C(1)-N(33)-C(2)	108.29	C(6)-O(38)-C(15)	118.57
N(33)-N(34)-C(3)	119.05	O(38)-C(15)-H(22)	111.13
N(34)-C(3)-H(18)	122.26	O(38)-C(15)-H(23)	111.34

H(18)-C(3)-C(4)	118.39	O(38)-C(15)-H(24)	105.68
C(3)-C(4)-C(5)	119.19	C(5)-C(6)-C(7)	118.89
C(3)-C(4)-C(9)	122.27	C(6)-C(7)-H(19)	120.46
C(4)-C(5)-O(36)	119.76	H(19)-C(7)-C(8)	119.69
O(36)-C(10)-O(37)	118.58	C(7)-C(8)-H(20)	119.05
O(37)-C(10)-C(11)	110.82	H(20)-C(8)-C(9)	119.93
C(10)-C(11)-S(39)	123.44	C(8)-C(9)-H(21)	121.12
C(10)-C(11)-C(12)	125.22	H(21)-C(9)-C(4)	118.72

Mulliken Charges

The electronegative atoms in the compound are S, N and O atoms which have negative charge values. The mulliken charge values of H atoms were found to be positive. C1, C2, C4, C5, C6, C11, C12, C14 atoms surrounded by electronegative atoms in the compound have positive charges. C12 atom was found to have the highest atomic charge of 1.117, and are shown in the Table 4.

Table 4. The theoretical mulliken charges datas

DFT/B3LYP		DFT/B3LYP		DFT/B3LYP	
C1	0.081	C14	0.261	N31	-0.059
C2	0.443	C15	-0.289	N32	-0.230
C3	-0.335	C16	-0.489	N33	-0.064
C4	0.678	H17	0.391	N34	-0.067
C5	0.134	H18	0.253	O35	-0.373
C6	0.001	H19	0.219	O36	0.057
C7	-0.046	H30	0.178	O37	-0.123
C8	-0.596	H20	0.155	O38	-0.134
C9	-0.424	H21	0.263	H27	0.263
C10	-1.258	H22	0.161	H28	0.177
C11	0.063	H23	0.145	H29	0.181
C12	1.117	H24	0.176	S39	-0.179
C13	-0.969	H25	0.219		

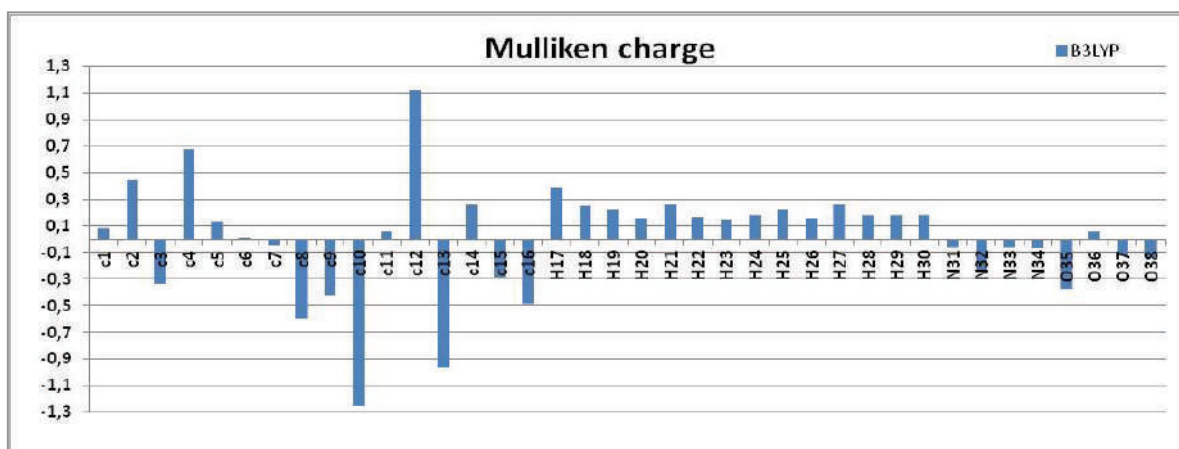


Figure 2. The mulliken atomic charge data of the molecule

The vibration frequency of the compound

Theoretically IR values were calculation veda 4f programme. The calculated harmonic vibrational frequency values were scaled with 0.9844 for DFT(B3LYP)6-311++G(d,p) level. The possitive frequency in the data was found. IR spectrums were drawn with obtained values according to B3LYP method. Theoretically IR values were compare with experimentally IR values and found corresponding with each other of values.

Table 5. Significant vibrational frequencies (cm⁻¹)

Vibrational Frequencies	Experimenta l	Scaled 6- 311++G(d,p)
$\delta OCC(14), \delta CCC(12)$	532	529
$\nu NN(14), \delta NCN(15)$	574	573
$\tau OCCC(22), \tau CCCC(21)$	607	599
$\nu NC(14), \nu CC(10), \delta NNC(14), \delta CNN(19)$	741	743
$\tau HCCC(46)$	779	778
$\tau HCCC(28)$	795	792
$\nu SC(50)$	863	856
$\nu CC(16), \nu OC(22), \delta CCC(15)$	936	937
$\nu OC(33), \delta HCC(18), \delta CCC(14)$	1009	1016
$\nu CC(28), \delta HCC(36)$	1048	1047
$\nu OC(25), \tau HCOC(13)$	1172	1174
$\nu CC(20), \delta HCC(10), \delta CCC(21)$	1217	1209
$\nu CC(22), \delta HCC(46), \delta HCS(11)$	1249	1248
$\delta HCC(21)$	1266	1261
$\nu CC(13), \delta HCN(13)$	1313	1327
$\delta HCN(42), \nu NC(20)$	1358	1355
$\delta HNN(59), \delta HCH(15)$	1383	1375
$\delta HCH(30), \delta HCN(59)$	1413	1398
$\nu CC(20), \delta HCC(22)$	1439	1430
$\delta HCH(46), \tau HCCN(17)$	1460	1463
$\delta HCH(58), \tau HCOC(11)$	1481	1481
$\nu CC(10), \delta HCC(26)$	1521	1540
$\nu CC(10), \delta HCC(10), \delta CCC(18)$	1574	1587
$\nu NC(67)$	1607	1634
$\nu OC(75)$	1698	1759
$\nu OC(73)$	1733	1761
$\nu OC(89)$	2946	2963
$\nu CH(56)$	2972	2998
$\nu CH(56)$	3022	3172
$\nu CH(53)$	3104	3189
$\nu NH(100)$	3207	3621

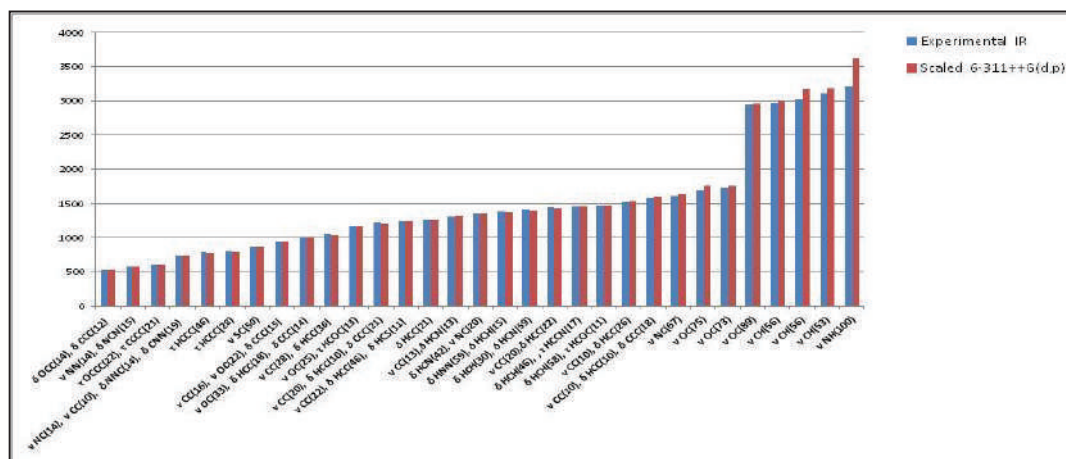


Figure 3. The experimental and scaled vibrational frequencies (cm^{-1})

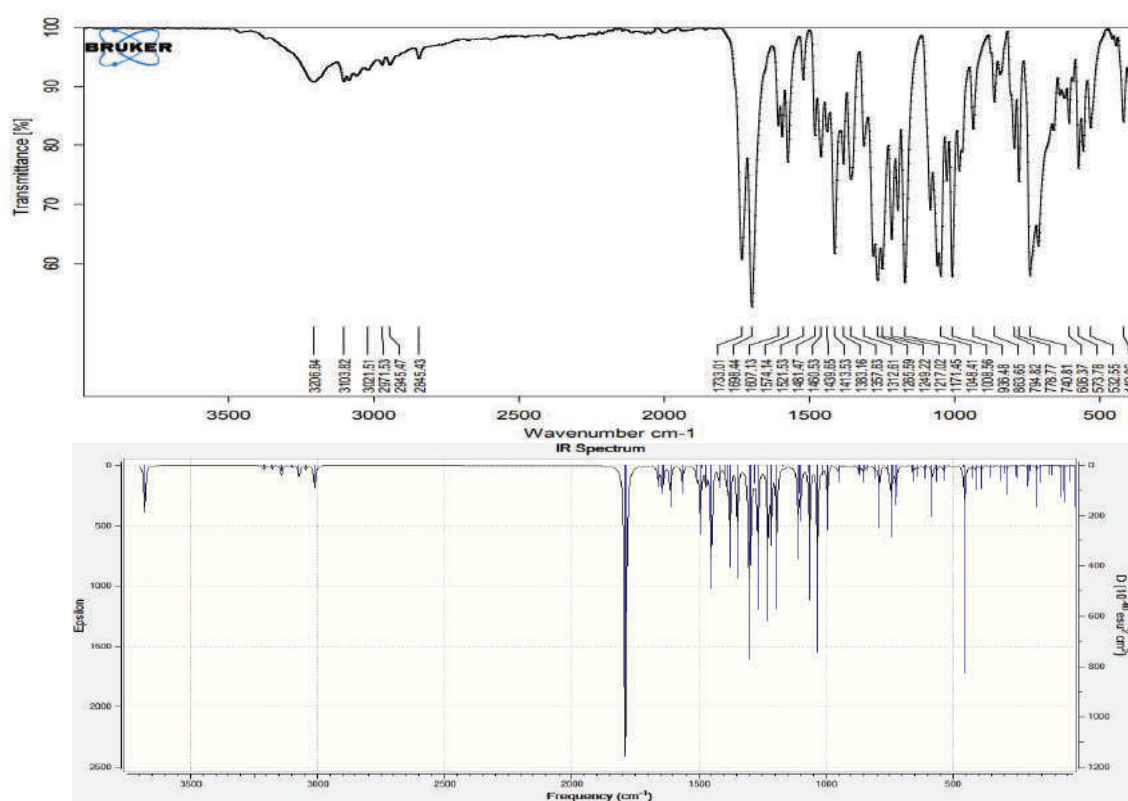


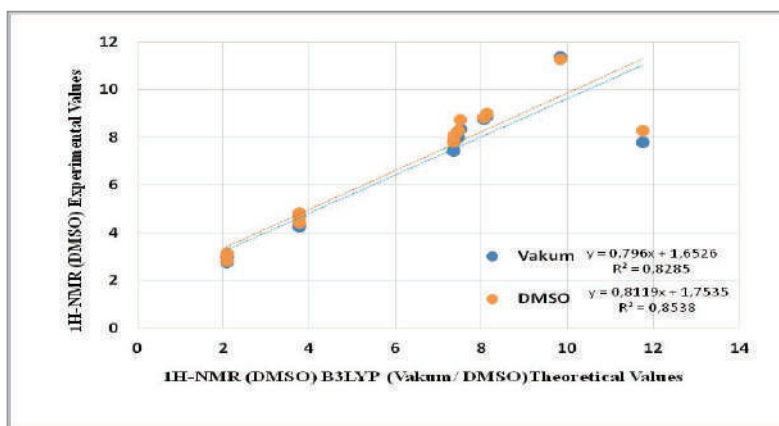
Figure 4. Theoretical IR spectra simulated with B3LYP/6-311G++(d,p)

The NMR Analysis

R values for the molecule were evaluated in gases medium and DMSO solvent according to DFT(B3LYP) 6-311++G(d,p) methods. Theoretical and experimental ^1H chemical shift and R values were calculated and, a linear correlation was observed between the results.

Table 6. $^1\text{H-NMR}$ (vakum-DMSO) isotropic chemical shifts (δ/ppm)

No	Experimental	B3LYP	Different	B3LYP	Different
H17	11,74	7,81	3,93	8,28	3,46
H18	9,81	11,37	-1,56	11,28	-1,47
H19	8,04	8,77	-0,73	8,85	-0,81
H20	7,45	8,02	-0,57	8,30	-0,85
H21	7,32	7,44	-0,12	7,85	-0,53
H22	8,10	8,91	-0,81	9,02	-0,92
H23	7,36	7,84	-0,48	8,10	-0,74
H24	7,50	8,36	-0,86	8,75	-1,25
H25	3,75	4,32	-0,57	4,83	-1,08
H26	3,75	4,25	-0,50	4,41	-0,66
H27	3,75	4,72	-0,97	4,56	-0,81
H28	2,05	3,00	-0,95	3,12	-1,07
H29	2,05	3,01	-0,96	3,15	-1,10
H30	2,05	2,75	-0,70	2,83	-0,78

**Figure 5.** Compared values of calculated and experimental $^1\text{H-NMR}$ chemical shifts values of titled compound with DFT(B3LYP) 6-311++G(d,p) (gas phase/ DMSO).

Frontier molecular orbital analysis

HOMO-LUMO energy values of compound was obtained by 4.328 eV value for B3LYP 6-311G++G(d,p) basis set (figure 6). Using HOMO-LUMO energy gap electron affinity (A), global hardness (η), electronegativity (χ), chemical potential (μ), softness (S), ionization potential (I), chemical potential (Pi), electrophilic index(ω), Nucleophilic index (IP) for the compound was calculated and are showed in Table 8.

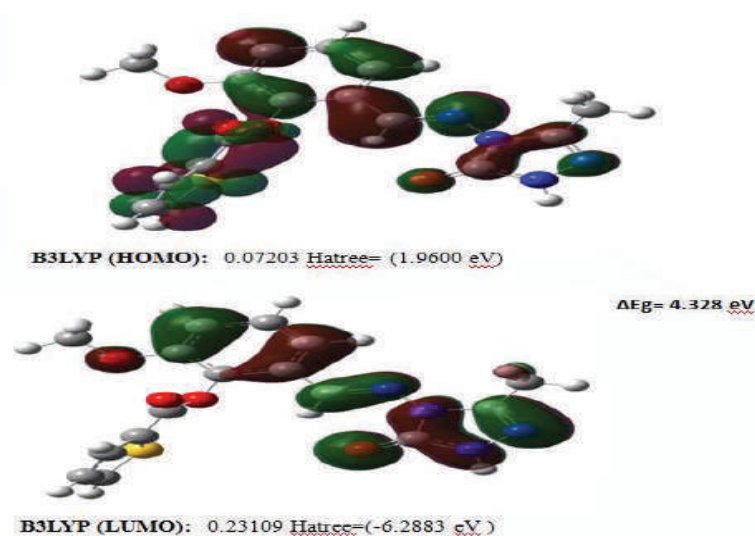


Figure 6. HOMO-LUMO energy of the molecule

Table 7. The calculated electronic structure parameters of the molecule

		Hatree	eV	kcal/mol	KJ/mol
	LUMO	-0,07203	-1,95999	-45,199	-189,115
	HOMO	-0,23109	-6,28812	-145,01	-606,727
E	Electron affinity	0,07203	1,95999	45,199	189,115
I	Ionization potential	0,23109	6,28812	145,01	606,727
ΔE	Energy gap	0,15906	4,32813	99,8106	417,612
χ	Electronegativity	0,15156	4,12405	95,1044	397,921
Pi	Chemical potential	-0,15156	-4,12405	-95,1044	-397,921
ω	Electrophilic index	0,000913419	0,02485	0,57317	2,39818
IP	Nucleophilic index	-0,01205357	-0,32799	-7,56365	-31,6466
S	Molecular softness	12,5739	342,144	7890,14	33012,7
η	Molecular hardness	0,07953	2,16407	49,9053	208,806

Thermodynamics properties

Thermodynamics parameters were calculated with (B3LYP) functionals in DFT method at the 6-311++G(d,p) basis set at 298.150 K and under 1 atm pressure.

Table 8. The thermodynamics parameters of the molecule

		B3LYP			B3LYP
Rotational temperatures (Kelvin)			Entropy S(cal/mol-K)		
A		0.01209	Translational		43.520
B		0.00681	Rotational		35.790
C		0.00462	Vibrational		88.626
Rotational constants (GHZ)			Total		167.936
A		0.25184	Zero-point correction (Hartree/Particle)		0.286373
B		0.14184	Thermal correction to Energy		0.309333
C		0.09622	Thermal correction to Enthalpy		0.310277
Thermal Energies E(kcal/mol)			Thermal correction to Gibbs Free Energy		0.230485
Translational		0.889	Sum of electronic and zero-point Energies	-	1536.230418
Rotational		0.889	Sum of electronic and thermal Energies	-	1536.207459
brational		192.332	Sum of electronic and thermal Enthalpies	-	1536.206515
Total		194.109	Sum of electronic and thermal Free Energies	-	1536.286307
Thermal Capacity CV(cal/mol-K)			Zero-point vibrational energy (Kcal/mol)		179.70193
Translational		2.981			
Rotational		2.981			
Vibrational		78.978			
Total		84.940			

The Surface Maps

The total density, molecular electron potential (MEP) and contour maps of the molecule were determined. From these surface maps were possible to determine the charge distribution and charge density, electronegative and positive regions of the molecule. The electronegative atoms in the structure were surrounded by red, the N-H proton is blue, while the other is yellow or green.

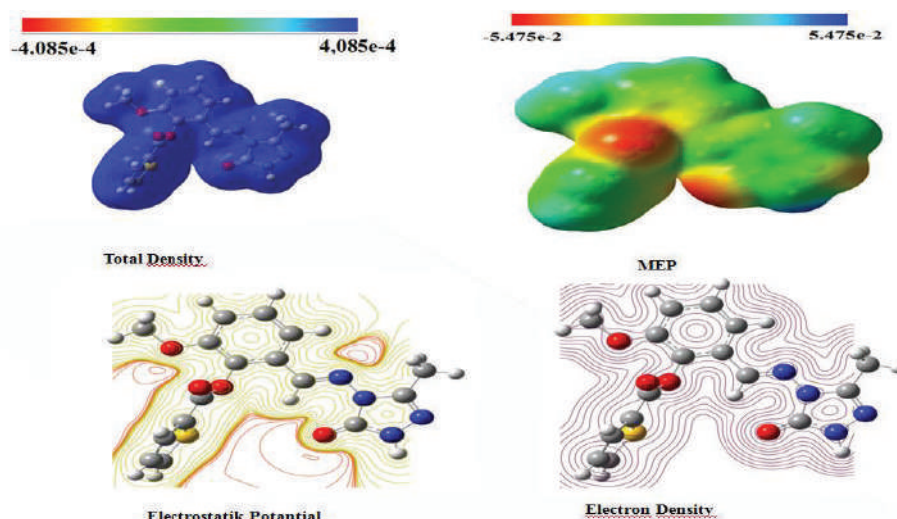


Figure 7. The MEP, Total density and Countour Maps of molecule

CONCLUSION

In this theoretical work, calculations of determining target molecule were carried out by DFT (B3LYP) methods with the 6-311++G(d, p) basis sets at the program package Gaussian G09W. The ^1H chemical shifts and FT-IR data in the calculations are seen to be compatible with the empirical data. A linear correlation was observed in the R^2 values, but there is a slight deviation in the H-NMR correlation graph. The reason for this deviation is the N-H acidic proton (H17) in the molecule. Also, the infrared data was not found negative frequency and the only reason for this is the stability of the molecule. In addition, the LUMO-HOMO energy, geometric properties, ΔE energy gap, total energy, electronic some properties, dipole moments, thermodynamics data were calculated. The reliability of different methods in theoretical computation was discussed. The surface maps of molecule were visualized, and the most electrophilic and nucleophilic regions were detected.

REFERENCES

- Lindoy, L. F. (1971). Metal-ion control in the synthesis of Schiff base complexes. *Quarterly Reviews, Chemical Society*, 25(3), 379-391.
- Holm, R. H., Everett Jr, G. W., & Chakravorty, A. (1966). Metal complexes of Schiff bases and β -ketoamines. *Progress in Inorganic Chemistry*, 83-214.
- Jin, R. Y., Zeng, C. Y., Liang, X. H., Sun, X. H., Liu, Y. F., Wang, Y. Y., & Zhou, S. (2018). Design, synthesis, biological activities and DFT calculation of novel 1, 2, 4-triazole Schiff base derivatives. *Bioorganic chemistry*, 80, 253-260.
- Soni, B., Ranawat, M. S., Sharma, R., Bhandari, A., & Sharma, S. (2010). Synthesis and evaluation of some new benzothiazole derivatives as potential antimicrobial agents. *European journal of medicinal chemistry*, 45(7), 2938-2942.
- Shanty, A. A., Philip, J. E., Sneha, E. J., Kurup, M. R. P., Balachandran, S., & Mohanan, P. V. (2017). Synthesis, characterization and biological studies of Schiff bases derived from heterocyclic moiety. *Bioorganic chemistry*, 70, 67-73.

- Alkan, M., Yüksek, H., Gürsoy-Kol, Ö., & Calapoğlu, M. (2008). Synthesis, acidity and antioxidant properties of some novel 3, 4-disubstituted-4, 5-dihydro-1H-1, 2, 4-triazol-5-one derivatives. *Molecules*, 13(1), 107-121.
- Pontiki, E., Hadjipavlou-Litina, D., & Chaviara, A. T. (2008). Evaluation of anti-inflammatory and antioxidant activities of copper (II) Schiff mono-base and copper (II) Schiff base coordination compounds of dien with heterocyclic aldehydes and 2-amino-5-methyl-thiazole. *Journal of enzyme inhibition and medicinal chemistry*, 23(6), 1011-1017.
- Bensaber, S. M., Allafe, H. A., Ermeli, N. B., Mohamed, S. B., Zetrini, A. A., Alsabri, S. G., ... & Gbaj, A. M. (2014). Chemical synthesis, molecular modelling, and evaluation of anticancer activity of some pyrazol-3-one Schiff base derivatives. *Medicinal Chemistry Research*, 23(12), 5120-5134.
- Gowda, J., Khader, A. M. A., Kalluraya, B., Shree, P., & Shabaraya, A. R. (2011). Synthesis, characterization and pharmacological activity of 4-{[1-substituted aminomethyl-4-arylideneamino-5-sulfanyl-4, 5-dihydro-1H-1, 2, 4-triazol-3-yl] methyl}-2H-1, 4-benzothiazin-3 (4H)-ones. *European journal of medicinal chemistry*, 46(9), 4100-4106.
- Kaur, H., Kumar, S., Chaudhary, A., & Kumar, A. (2012). Synthesis and biological evaluation of some new substituted benzoxazepine and benzothiazepine as antipsychotic as well as anticonvulsant agents. *Arabian Journal of Chemistry*, 5(3), 271-283.
- Wang, B. L., Shi, Y. X., Ma, Y., Liu, X. H., Li, Y. H., Song, H. B., ... & Li, Z. M. (2010). Synthesis and biological activity of some novel trifluoromethyl-substituted 1, 2, 4-triazole and bis (1, 2, 4-Triazole) Mannich bases containing piperazine rings. *Journal of agricultural and food chemistry*, 58(9), 5515-5522.
- Kotan, G., (2021). Novel Mannich Base Derivatives: Synthesis, Characterization, Antimicrobial and Antioxidant Activities. *Letters in Organic Chemistry*, 18(10), 830-841.
- Kotan, G., Gökçe, H., Akyıldırım, O., Yüksek, H., Beytur, M., Manap, S., & Medetalibeyoğlu, H. (2020). Synthesis, Spectroscopic and Computational Analysis of 2-[(2-Sulfanyl-1 H-benzo [d] imidazol-5-yl) iminomethyl] phenyl Naphthalene-2-sulfonate. *Russian Journal of Organic Chemistry*, 56(11), 1982-1994.
- Beytur, M., & Avinca, I. (2021). Molecular, Electronic, Nonlinear Optical and Spectroscopic Analysis of Heterocyclic 3-Substituted-4-(3-methyl-2-thienylmethyleneamino)-4, 5-dihydro-1H-1, 2, 4-triazol-5-ones: Experiment and DFT Calculations. *Heterocyclic Communications*, 27(1), 1-16.
- Kotan, G., Medetalibeyoğlu, H., Beytur M., Akyıldırım O., Yüksek H. (2019). Synthesis and Theoretical Analyses of Novel 5-mercapto-2-(5-methyl-furan-2-yl-methylidenamino)-1,3,4-thiadiazole Molecule. *Iğdır Üniversitesi Fen Bilimleri Enstitüsü Dergisi*, 9(2): 1023-1034, ISSN: 2146-0574, eISSN: 2536-4618, DOI: 10.21597/jist.542004.
- Yüksek, H., Kotan, G., Medetalibeyoğlu, H., Gürbüz, A., Alkan M. (2017). B3LYP ve HF Temel Setleri Kullanılarak Bazı 3-Alkil-4-(2-asetoksi-3-metoksibenzilidenamino)-4,5-dihidro-1H-1.2.4-triazol-5-on Bileşiklerinin Deneysel ve Teorik Özelliklerinin İncelenmesi. *CBÜ Fen Bil. Dergi*, Cilt 13, Sayı 1, 193-204.
- Gökçe, H., Bahçeli, S., Akyıldırım, O., Yüksek, H. and Gürsoy-Kol, Ö. (2013). The Syntheses, Molecular Structures, Spectroscopic Properties (IR, Micro-Raman, NMR and UV-vis) and DFT Calculations of Antioxidant 3-alkyl-4-[3-methoxy-4-(4-methylbenzoxy)benzylidenamino]-4,5-dihydro-1H-1,2,4-triazol-5-one Molecules *Letters in Organic Chemistry*, 10(6): 395-441.
- Frisch, M.J., Trucks, G.W., Schlegel, H.B., Scuseria, G.E., Robb, M.A., Cheeseman, J.R., Scalmani, G., Barone, V., Mennucci, B., Petersson, G.A., Nakatsuji, H., Caricato, M., Li, X., Hratchian, H.P., Izmaylov, A.F., Bloino, J., Zheng, G., Sonnenberg, J.L., Hada, M., Ehara, M., Toyota, K., Fukuda, R., Hasegawa, J., Ishida, M., Nakajima, T., Honda, Y., Kitao, O., Nakai, H., Vreven, T., Montgomery, J.A., Jr.Vreven, T., Peralta, J.E., Ogliaro,

- F., Bearpark, M., Heyd, J.J., Brothers, E., Kudin, N., Staroverov, V.N., Kobayashi, R., Normand, J., Raghavachari, K., Rendell, A., Burant, J.C., Iyengar, S.S., Tomasi J., Cossi, M., Rega, N., Millam, J.M., Klene, M., Knox, J.E., Cross J.B., Bakken, V., Adamo, C., Jaramillo, J., Gomperts, R., Stratmann, R.E., Yazyev, O., Austin, A.J., Cammi, R., Pomelli, C., Ochterski, J.W., Martin, L.R., Morokuma, K., Zakrzewski, V.G., Voth, G.A., Salvador, P., Dannenberg, J.J., Dapprich, S., Daniels A.D., Farkas, O., Foresman, J.B., Ortiz, J.V., Cioslowski, J., & Fox, D.J. (2009). Gaussian Inc., Wallingford, CT.
- Wolinski, K., Hilton, J.F. and Pulay, P.J. (1990). *Am. Chem. Soc.*, 112, 512.
- Jamróz, M.H. (2004). Vibrational Energy Distribution Analysis: VEDA 4 program, Warsaw.
- Merrick J.P., Moran D., Radom L. (2007). An Evaluation of Harmonic Vibrational Frequency Scale Factors. *Journal of Physical Chemistry*, 111(45), 11683-11700.
- Gürbüz, A., Alkan, M., Manap, S., Ozdemir, G., Yüksek, H., Gürsoy-Kol, Ö. (2020). Investigation of antioxidant of novel 4-[2-(2-thienyl-carbonyloxy)-3-methoxybenzylideneamino]-4,5-dihydro- 1H-1,2,4-triazol-5-one derivatives, *International Journal of Pharmaceutical, Chemical and Biological Sciences (IJPCBS)*, 10(1), 1-8.

RECENT DIAGNOSTIC AIDS IN ORAL CANCER DETECTION**Dr. Shikha Saxena, Associate Professor,**Department of Oral Pathology and Microbiology, RUHS College of Dental Sciences, Jaipur,
Rajasthan, India.Orcid no.- <https://orcid.org/0000-0002-3655-1096>**Dr. Priyanka Singh**Associate Professor, Department of Oral Pathology and Microbiology,
Faculty of Dental Sciences, King George's Medical University, Lucknow (UP), IndiaOrcid no.- <https://orcid.org/0000-0002-1616-1867>**Abstract:**

Oral cancers are one of the most common cancers worldwide today. The diagnosis of oral cancer at an early stage has a good prognosis as the survival rate is high (around 80%). However, the majority of oral cancer cases are diagnosed at a later stage with a considerably poor 5-year survival rate of 50% according to World Health Organization statistics. Thus, an effective management strategy for oral cancer will depend on its early identification and intervention which would pave the way for superior prognosis. Many diagnostic tools / aids have been explored with the aim of early detection of oral precancer and cancer. The basic chair-side procedures or relatively advanced aids come with a set of limitations along with subjectivity as one of the setbacks. The advent and exploitation of molecular techniques in the field of health diagnostics, is demanding the molecular typing of the oral potentially malignant diseases and also of oral cancer. The recent diagnostic techniques in oral cancer and precancer detection includes lab-on-chip, microfluidics, nano diagnostics, liquid biopsy, omics technology and synthetic biology in early detection of oral precancer and cancer. Oral cancer being multifactorial in origin with the chief participation of altered genetics and epigenetics would demand high-end diagnostics for designing personalized therapy. Hence, the present paper highlights the role of various advanced diagnostic aids in detection of oral precancer and cancer.

Keywords: Oral Cancer, Toluidine Blue Staining, Oral Brush Biopsy, Chemiluminescence.

AURICULAR ACUPRESSURE FOR SMOKING CESSATION: A SYSTEMATIC REVIEW OF RANDOMIZED CONTROLLED TRIALS

Ying-Ying Zhang
Ze-Yu Yu
Jian-Ping Liu

Institutions:

1 Centre for Evidence-Based Chinese Medicine, Beijing University of Chinese
Medicine, Beijing, China;

*Jian-ping Liu is corresponding author.

E-mail: yuchen8240@126.com (Y.-Y. Zhang); zeyu.yu@bucm.edu.cn (Z.-Y. Yu);
liujp@bucm.edu.cn (J.-P. Liu)

Objective: Acupressure has been widely used for smoking cessation due to convenience and good compliance. Our aim was to evaluate its therapeutic effects and safety for smoking cessation.

Methods: Randomized controlled trials (RCTs) comparing acupressure with sham acupressure or conventional therapy for smoking cessation were included. Ten databases were searched from their inception to February 2021. Two review authors independently screened studies, extracted data, and assessed the risk of bias. Meta-analysis was conducted with Rev Man 5.4 software. Grading of Recommendations Assessment, Development and Evaluation (GRADE) was applied to assess the quality of evidence. The primary outcome was abstinence rate at short-term (1-3months), mid-term (3-6months), and long-term (≥ 6 months). The secondary outcomes were nicotine withdrawal symptoms, daily cigarettes

consumption, nicotine dependence, exhaled carbon monoxide (CO), relapse rate, craving for cigarettes and adverse events.

Results: Eleven RCTs involving 883 smokers were identified. The overall risk of bias was not serious. Acupressure was found more effective than sham acupressure or conventional therapy in improving short-term (RR 1.41, 95% CI [1.04 to 1.91]; low certainty; 8 trials, n=637) and mid-term abstinence rate (RR 1.63, 95% CI [1.27 to 2.09]; low certainty; 8 trials, n=749). However, the long-term abstinence effect was not significant between two groups (RR 1.85, 95% CI [0.59 to 5.82]; moderate certainty; 2 trials, n=74). Additionally, acupressure was also superior to sham acupressure in relieving short term withdrawn symptoms (MD -2.68, 95% CI [-5.34 to -0.03]; 4 trials, n=180) and reducing the level of exhaled CO (MD -3.84, 95% CI [-5.03 to -2.66]; 2 trials, n=103).

Conclusions: Low certainty evidence suggests that acupressure maybe effective in achieving short-term and middle-term smoking cessation, as well as relieving short-term withdrawn symptoms. No serious adverse events were reported in the included trials. Further large, long-term follow-up RCTs are warranted to verify its benefits and safety.

Keywords: acupuncture; acupressure; smoking cessation; randomized controlled trials; systematic review.

FEATURES OF THE LIPID SPECTRUM AND THE PROBLEM OF ACHIEVING THE TARGET LEVEL OF LOW-DENSITY LIPOPROTEINS DURING A CORONARY EVENT

Madina Nurzhanova

al-Farabi Kazakh National University, The Republic of Kazakhstan, Almaty city,
al Farabi str.71

Gulnara Kapanova

al-Farabi Kazakh National University, The Republic of Kazakhstan, Almaty city,
al Farabi str.71

Abstract

This article presents the features of the lipid spectrum in patients with acute coronary syndrome, in comparison with the groups with myocardial infarction (MI) and Unstable angina pectoris (NS), as well as the results of adherence to lipid-lowering therapy with the peculiarities of achieving target levels of the lipid spectrum. The results obtained represent that the groups are identical in terms of the lipid spectrum and that the levels of individual values of the lipid spectrum differ from the norm, and patients are also with low adherence to lipid-lowering therapy and do not reach the target levels for low-density lipoprotein cholesterol (LDL-C) recommended by the European Society of Cardiology (ESC) from 2019.

Key words: acute coronary syndrome, lipid spectrum, dyslipidemia, low density lipoproteins, myocardial infarction, unstable angina

Introduction

Coronary heart disease (CHD), and above all, acute coronary syndrome (ACS) - myocardial infarction (MI) and unstable angina (UA), are the leading cause of death and disability in the population of developed countries [1]. According to the forecasts of the World Health Organization (WHO), by 2030 about 23.6 million people will die from CHD, mainly from heart disease and stroke, which will remain the only leading causes of death [2]. The term “acute myocardial infarction” (MI) should be used when there is evidence of myocardial injury (as determined by an increase in cardiac troponin levels by at least one value above the 99th percentile of the normal reference value) and myocardial necrosis in clinical situations allowing suggest myocardial ischemia [3]. Unstable angina (NS) is a form of ACS, with dynamic observation of which the release of enzymes and biomarkers of myocardial necrosis was not detected [4].

The most dangerous of the acute manifestations of coronary heart disease is associated with the presence of an unstable atherosclerotic plaque in the coronary arteries [5, 6]. It is well

known that the development of atherosclerosis of vessels of various localization, including coronary arteries, is based on lipid metabolism disorders, or dyslipidemia [7, 8]. Dyslipidemia includes a wide range of lipid metabolism disorders, and this is when the concentrations of lipids and lipoproteins in the blood go beyond the normal range, can be caused by both acquired (secondary) and hereditary (primary) causes [9].

According to the new recommendations and revised ESC concepts for the treatment of dyslipidemias, it has been established that for secondary prevention, patients at very high risk are recommended to reduce low-density lipoprotein cholesterol (LDL-C) by at least $\geq 50\%$ of the baseline, and the recommended target values for cholesterol LDL cholesterol is < 1.4 mmol / L (< 55 mg / dL). For patients with cardiovascular disease (CVD) of atherosclerotic genesis who have had a second vascular event within 2 years (not necessarily of the same nature as the first event) while taking the maximum tolerated dose of statin, the target level of LDL-C can be indicator < 1.0 mmol / L (< 40 mg / dL). For primary prevention in very high-risk patients who do not have familial hypercholesterolemia, an LDL-C reduction of at least $\geq 50\%$ from baseline is recommended, and the recommended LDL-C target is < 1.4 mmol / L (< 55 mg / dL). Individuals of very high risk (without CVD of atherosclerotic genesis in the presence of other RF) are recommended the same target values of LDL-C in primary prevention. For high-risk patients, a decrease in LDL-C of at least $\geq 50\%$ from baseline is recommended, and the recommended targets for LDL-C are < 1.8 mmol / L (< 70 mg / dL). For moderate-risk patients, LDL-C targets are < 2.6 mmol / L (< 100 mg / dL). For low-risk individuals, LDL-C targets are < 3.0 mmol / L (< 116 mg / dL) (ESC Dyslipidemia Guidelines: Lipid Modification to Reduce Cardiovascular Risk 2019).

Purpose of the study: to describe the features of the lipid spectrum and the achievement of target levels of the lipid spectrum in patients with acute coronary syndrome (ACS) in a comparative analysis

Materials and methods:

The study was carried out retrospectively based on the materials of the case histories of the cardiology department of the City Clinical Hospital No. 7 of Almaty city for the period 01.01.2018-01.09.2021 according to the inclusion and exclusion criteria in the study, a total of 142 patients (case histories) with acute coronary syndrome (ACS) were included in the study. The age of the patients varied from 41 to 83 years (men accounted for 99 (69.7%), women accounted for 43 (30.3%)). Two groups were allocated in accordance with the clinical diagnosis: Myocardial infarction (MI) - 78 patients, and Unstable angina pectoris (UA) - 64 patients. All patients were assessed cardiovascular risk (CVR) according to the SCORE scale, according to which 87 (61.3%) patients had very high CVR, 55 (38.7%) patients had high CVR, in our study, patients with intermediate and there was no low CVR.

The study included the main characteristics of the patients, including laboratory and instrumental data carried out in the hospital, data of the medical history of cardiovascular diseases (CVD). Further, a comparison was made between the two groups, where the features of the lipid spectrum, adherence to treatment with an emphasis on lipid-lowering treatment, taking into account the main risk factors for coronary heart disease (CHD), comorbidities, lipid-lowering treatment, achievement of target levels of LDL-C and other features were assessed and described.

Statistical analysis: data, the distribution of which obeys the normal law, are presented as the mean \pm standard deviation ($M \pm SD$), in other cases - the median, lower and upper quartiles, discrete variables are presented as frequencies with percentages. Statistical processing of the research data was carried out using the SPSS 22.0 software. The distribution normality was checked using the Kolmogorov - Smirnov test. During the analysis, the following methods were used: to compare quantitative values with a normal distribution - Student's t-test, in cases other than a normal distribution - Mann-Whitney U test. The association was assessed using the Pearson Chi-square test, Odds Ratio and Confidence Interval. Differences were considered statistically significant at $p < 0.05$. Including the odds ratio (OR) was considered statistically significant if the 95% confidence interval (CI) for the odds ratio in its interval does not include one.

Results and Discussions:

According to the results of the study, the average age for all patients was 63.7 ± 7.7 years (66.8 ± 8.1 for the MI group and 63.4 ± 8.2 years for the UA group). There were significantly more men in both groups than women ($p < 0.05$), but the groups were comparable in age ($p > 0.05$).

Table 1 - Comparative characteristics of basic data

indicators	MI, n=78	UA, n=64	p
Age, years	66.8 ± 8.3	63.4 ± 8.2	0.19
Weight, kg	78.9 ± 8.7	77.7 ± 10.7	0.34
BMI, kg / m ²	28.2 ± 3.2	27.7 ± 3.2	0.38
WC, cm	98.9 ± 15.4	96.8 ± 17.7	0.32
SBP, mm Hg	122.2 ± 12.6	138.1 ± 11.6	0.02
DBP, mm Hg	76.9 ± 17.5	88.1 ± 11.3	0.01
HR, beats / min.	79.9 ± 8.4	75.4 ± 10.5	0.33

(BMI - body mass index, HR - waist circumference, SBP - systolic blood pressure, DBP - diastolic blood pressure, HR - heart rate)

Also, according to Table 1, groups by anthropometric characteristics are comparable to each other ($p > 0.05$), but it must be emphasized that the average subject mass index (BMI) in both groups coincides with the excess BMI category. When analyzing the waist size by gender, then in more in half of the patients, the waist was above normal (the norm for women up to 80 cm, for men up to 94 cm according to the data of the European Society of Cardiology from 2019), which is a criterion for abdominal obesity. According to objective data of hemodynamic characteristics, the level of blood pressure on admission was lower in the group

with MI compared to the group with UA, since patients with MI receive more often

indicators	MI, n=78	UA, n=64	p
Total cholesterol, mmol / l	4.85±1.1	4.7±1.2	0.09
LDL-C, mmol / L	3.9±1.2	3.5±1.1	0.07
HDL-C, mmol / L	1.15±0.25	1.18±0.3	0.11
TG, mmol / L	1.95±0.7	2.0±0.9	0.28
Atherogenic coefficient	3.9±1.2	3.2±1.1	0.02
LDL-C ≤1.4 mmol / L	0	0	-
LDL-C ≤1.8 mmol / L	0	0	-
LDL-C ≤2.6 mmol / L	0	0	-

cardiogenic shock, and the groups did not differ statistically in terms of heart rate.

The lipid spectrum, according to Table 2, it can be concluded that the lipid spectrum indices differ from the norm for patients with coronary artery disease in both groups, and the statistical does not differ between the groups ($p > 0.05$). But according to the data of the atherogenic coefficient it was higher in the group with MI (3.9 ± 1.2 and 3.2 ± 1.1 mmol / L, $p = 0.02$).

Table 2 - The state of the lipid spectrum in both groups

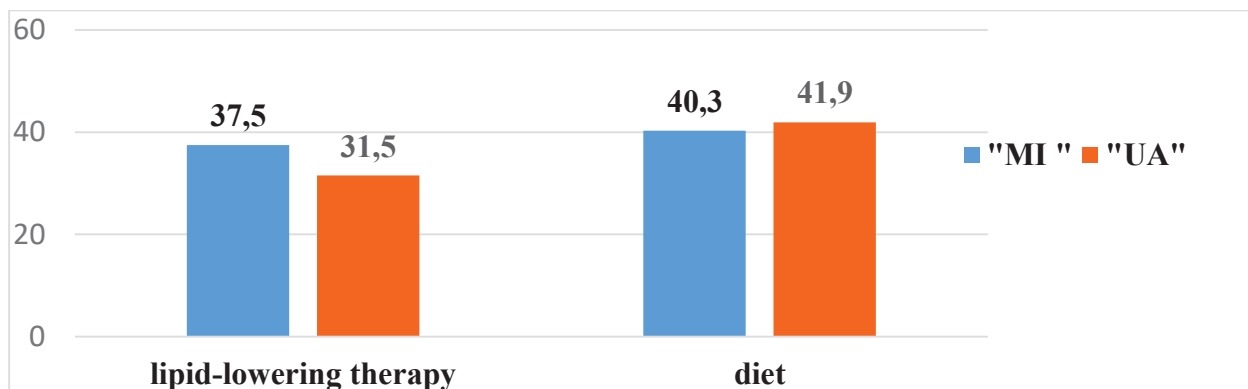
(Cholesterol-cholesterol, LDL-low-density lipoprotein, HDL-high-density lipoprotein, TG-triglycerides)

With very high and high cardiovascular risk (CVR), all patients (100%) in both groups do not reach the target LDL-C level in terms of LDL-C levels (all patients have an LDL-C level higher than 1.8 mmol / L). LDL cholesterol indices for all patients ranged from 1.83 to 7.46 mmol / L (for a holistic presentation, the data are also presented as Me [Q25; Q75] - 3.81 [2.68; 4.11]).

Also, for some known risk factors for coronary artery disease and concomitant diseases, such as: smoking and alcohol consumption, history of arterial hypertension, the statistical groups do not differ ($p > 0.05$), but in the group with a history of MI, diabetes mellitus and Chronic kidney disease are more common than in the group with UA (<0.05).

According to Diagram 1, adherence to treatment for lipid-lowering therapy is low in both groups (MI - 19 (37.5%) and UA - 17 (31.5%)), and the statistical difference does not differ (OR 0.83, CI 0.37- 1.8, χ^2 0.69, $p > 0.05$).

Diagram 1 - Adherence to lipid-lowering therapy and diet



Of the analyzed case histories, 19 (13.4%) patients do not remember the names of the medications they were taking, these patients were not included in the statistical processing. Comparative analysis of LDL cholesterol in patients initially taking and not taking lipid-lowering therapy did not statistically differ ($p > 0.05$). Of the lipid-lowering drugs, more than 90% of cases are statins, and in the rest of the cases, patients received combined lipid-lowering therapy (statins in combination with ezetimibe). With regard to adherence to the diet (diet No. 9 or No. 10), there is also low adherence, and the groups do not differ statistically ($p > 0.05$). All of the above data are potent modified risk factors for coronary artery disease (CVD), which means it is of particular importance in the management of CVD risk factors.

Conclusion: The results obtained represent that the groups on the lipid spectrum are identical to each other and the average values differ from the norm, as well as patients with low adherence to lipid-lowering therapy and do not reach the target levels for low-density lipoprotein cholesterol (LDL-C) recommended by the European Society of Cardiology (ESC) from 2019

Bibliography

1. European guidelines on cardiovascular disease prevention in clinical practice: full text. Fourth Joint Task Force of the European Society of Cardiology and other societies on cardiovascular disease prevention in clinical practice. Eur. J. Cardiovasc. Prev. Rehabil. 2007 Sep; 14 Suppl 2: S1-113.
2. ESC Guidelines for the management of acute coronary syndromes in patients presenting without persistent ST-segment elevation: The Task Force for the management of acute coronary syndromes in patients presenting without persistent ST-segment elevation of the European Society of Cardiology / C.W. Hamm, J.-P. Bassand, S. Agewall [et al.] // Eur Heart J. - 2011. - No. 32. - P. 2999-3054.
3. 2017 ESC GUIDELINES FOR THE MANAGEMENT OF ACUTE MYOCARDIAL INFARCTION IN PATIENTS PRESENTING WITH ST-SEGMENT ELEVATION The Task Force for the management of acute myocardial infarction in patients presenting with ST-segment elevation of the European Society of Cardiology (ESC)
4. AHA / ACC Guideline for the management of patients with non-ST-elevation acute coronary syndromes: a report of the American College of Cardiology / American Heart Association task force on practice guidelines. / E. A. Amsterdam, N.K. Wenger, R. G. Brindis et al. / J. Am. Coll. Cardiol.-2014.-No. 64.P. 139-228

5. Libby, P. Mechanisms of acute coronary syndromes and their implications for therapy [Text] / P. Libby. // N. Engl. J. Med. - 2013. - Vol. 368. - P. 2004-2013.
6. Update on acute coronary syndromes: the pathologists' view [Text] / E. Falk, M. Nakano, J.F. Bentzon [et al.]. // Eur. Heart J. - 2013. - Vol. 34 (10). - P. 719-728.
7. Arutyunov, A.G. Correction of cardiovascular risk with statins. Problems and unsolved issues at the present stage / A.G. Arutyunov, G.P. Arutyunov // Heart. - 2015. - T. 14, No. 4. - S. 193-212.
8. Bubnova, M.G. High-intensity lipid-lowering therapy and low level of low-density lipoprotein cholesterol: is this approach justified in clinical practice? A look at the problem / M.G. Bubnova // Russian Journal of Cardiology. - 2018. - T. 23, No. 6. - S. 191-200.
9. Ezhov MV, Sergienko IV, Aronov DM, et al. Diagnostics and correction of lipid metabolism disorders in order to prevent and treat atherosclerosis. Atherosclerosis and dyslipidemia. 2017.Vol. 3.S.5-22.

ORAL CANCER SCREENING. CURRENT APPROACHES AND FUTURE PROSPECTS.**Prof. Dr. Ivashchuk Oleksandr**

Bukovinian State Medical University Department of Oncology and radiology

Dr. Hovornyan Serhiy

Bukovinian State Medical University Department of Oncology and radiology

Keywords: oral cancer, screening methods, deep learning.

Background. It is well-known, that oncological diseases are the second most common reason for death in the world, taking approximately 10 million human lives every year. At the same time, every third of these cases could be prevented by early diagnosis and timely specific treatment. Oral cancer is included in the list of 10 leading types of cancer death in Ukrainian men, and in 38,8% of these cases, patients did not survive 1 year after they detected cancer. Mostly, it is because this type of oncological disease is usually detected lately, after the appearance of metastasis in lymph nodes and other tissues. At this stage of cancer, the specific treatment is poor-effective and even impossible. The situation could have been fixed by an effective method of early diagnosis and timely oral cancer suspicion. Therefore, it is important to find out the methods of oral cancer screening, since our knowledge in this area is not sufficient.

The aim of the research. Analyze screening approaches, their specificity, and sensitivity, as well as the applicability and applicability of existing screening techniques to global screening program requirements, and determine the prospects of oral cancer screening research.

Methods. This study used a literature review to find information on the above-mentioned topic from various scientific and methodological sources.

Results. The findings of this study reveal that no successful attempts to provide organized or opportunistic screening programs have been made, and none of them have been adopted by any level of the healthcare system. The primary method of screening was a physical inspection of the mouth cavity with various adjuvant approaches, although none of these were sufficiently specific or sensitive for an organized screening program. Physical examination of the mouth cavity with various light adjuvant systems, on the other hand, has yielded promising results for opportunistic screening. Spectroscopy and polarimetry of tissues and oral cavity fluids may be an efficient tool for early diagnosis, according to research trends. The interpretation of acquired values is the method's main drawback. Convolutional neural networks and other Artificial Intelligence technologies, in our opinion, can overcome this challenge.

Conclusions. None of the currently available screening technologies are sufficiently compliant, practical, effective, sensitive, and cost-effective. As a result, our study highlights the necessity of developing an improved oral cancer screening tool with artificial intellect elements based on deep learning technologies.

EVALUATION OF ORAL SOFT TISSUES AT GERIATRIC PATIENTS WITH DENTAL PROSTHESIS

Ass. Prof. Dr. Aneta Mijoska

University St. Cyril and Methodius, Faculty for Dentistry, Department of Prosthodontics, Skopje,
N. Macedonia
ORCID ID 0000-0002-3093-0327

Ass. Prof. Dr. Sasho Jovanovski

University St. Cyril and Methodius, Faculty for Dentistry, Department of Prosthodontics,
Skopje, N. Macedonia
ORCID ID 0000-0003-1612-5062

Dr. Daniela Srbinoska

University Dental Clinical Centre St. Pantelejmon, Department of Orthodontics,
Skopje, N. Macedonia

Dr. Vesna Trpevska

University Dental Clinical Centre St. Pantelejmon, Department of Orthodontics, Skopje, N.
Macedonia
ORCID ID 0000-0002-4000-882X

Ass. Prof. Dr. Emilija Bajraktarova Valjakova

University St. Cyril and Methodius, Faculty for Dentistry, Skopje, N. Macedonia

ABSTRACT

Degenerative oral changes occur during ageing in geriatric patients, and they should be carefully treated for achieving better prosthodontics treatment. The aim was to evaluate data on the prevalence of oral mucosal lesions in elderly patients in relation to age, gender, educational level and wearing dental prosthesis. Prevalence of lesions was assessed by clinical examination of a sample of 300 elderly patients aged 60 years and older. Detailed oral examinations of the oral cavity and GOHAI questionnaire were performed at the university clinic and geriatric facilities. Lesions were categorized into six main groups: tongue lesions, white lesions, ulcerative lesions, pigmentation lesions, denture-related lesions and miscellaneous. At least one oral mucosal lesion was diagnosed in 200 participants (66%). The prevalence rate was significantly higher in men than in women (78, 2% men 65, 7% women $P < 0.05$) correlated to smoking. The most prevalent lesions were fissured tongue (34.2%), benign tumors (17.1%), hairy tongue (16.5%), and white lesions (12.6%). The prevalence was significantly higher in the

60 to 69 year old group (80, 8%) than in the 70 years and older group (67.4%). Denture stomatitis was observed in 7, 5 % of the participants in the 70 years and older group compared with 3.2% in the 65 to 69 year old group. There was a high prevalence of oral mucosal lesions among elders, and the presence was related to age, gender, low education level, smoking and poor oral habits.

Keywords: geriatric, oral soft tissue, prosthodontics

A validation of the study was carried out and it was approved by the ethics committee of the Faculty for dentistry Ss Cyril and Methodius University Skopje on 18.12.2018. No. 02-38363.

VELSCOPE INSTRUMENT FOR DETECTION OF ORAL SOFT TISSUE CONDITION IN PROSTHODONTIC PATIENTS

Ass. Prof. Dr. Aneta Mijoska

University St. Cyril and Methodius, Faculty for Dentistry, Department of prosthodontics,
Skopje, N. Macedonia
ORCID ID 0000-0002-3093-0327

Ass. Prof. Dr. Sasho Jovanovski

University St. Cyril and Methodius, Faculty for Dentistry, Department of prosthodontics,
Skopje, N. Macedonia
ORCID ID 0000-0003-1612-5062

Dr. Daniela Srbinoska

University Dental Clinical Centre St. Pantelejmon, Department of orthodontics,
Skopje, N. Macedonia

Dr. Vesna Trpeska

University Dental Clinical Centre St. Pantelejmon, Department of orthodontics,
Skopje, N. Macedonia
ORCID ID 0000-0002-4000-882X

Ass. Prof. Dr. Blagoja Dashtevski

University St. Cyril and Methodius, Faculty for Dentistry, Department of prosthodontics, Skopje,
N. Macedonia
ORCID ID 0000-0001-9346-1751

Assoc.Prof.Dr. Marjan Petkov

University St. Cyril and Methodius, Faculty for Dentistry, Department of prosthodontics,
Skopje, N. Macedonia

ABSTRACT

Early detection of oral mucosa diseases and potentially malignant disorders requires careful examination because of high malignant transformation frequency. Almost 90% of oral cancers occur in patients older than 50 years. The aim of study was to determine the value of VELscope as adjunct tool for oral examination in geriatric prosthodontics patients. Clinical protocol for 300 patients over 60 years old was questionnaire with risk factors, clinical observation and VELscope mucosal tissue examination with scoring of the changes and dysplasia level. Tissue changes were classified as inflammatory, traumatic, dysplastic and other. Abnormal tissue was associated with

auto fluorescence loss and dark appearance in contrast to the surrounding tissue. In 21% of patients abnormal premalignant lesions were detected. Leukoplakia was the most common premalignant disorder 42 (12, 6%), 16 (4, 8%) had lichen planus, 6 (1, 8%) cheilitis actinica and 5 patients (1, 5%) were diagnosed with squamous cell carcinoma. We found 118 inflammatory lesions (35, 4%) where 58 (17, 4%) were denture stomatitis, 18 (5, 4%) angular cheilitis, traumatic lesions were found in 38 patients (11, 4%) and 4 (1, 2%) were diagnosed with epulis fissuratum. In 54 patients (16, 2%) we diagnosed infectious changes from which aphtous ulcerations and candidiasis were most common. VELscope can be used as a part of diagnostic process to detect abnormal tissue and oral lesions that might have been overlooked. However surgical excision biopsy as the golden standard for the detection of the lesion's histology is obligated for final diagnose.

Keywords: oral mucosa, VELscope, dysplasia, florescence visualization

SOME QUANTUM CHEMICAL CALCULATIONS OF 3-*n*-PROPYL-4-(3-ACETOXY-4-METHOXYBENZYLIDENAMINO)-4,5-DIHYDRO-1*H*-1,2,4-TRIAZOL-5-ONE

Önder ALBAYRAK

Kafkas University, Ataturk Vocational School of Health Services, Kars, Turkey.

ORCID: 0000-0002-6573-6137,

Assist. Prof. Dr. Gül KOTAN

Kafkas University, Kars Vocational School, Kars, Turkey

ORCID: 0000-0002-4507-9029

Prof. Dr. Haydar YÜKSEK

Kafkas University, Department of Chemistry, Kars, Turkey

ORCID: 0000-0003-1289-1800

ABSTRACT

The theoretical calculations of 3-*n*-propyl-4-(3-acetoxy-4-methoxybenzylidenamino)-4,5-dihydro-1*H*-1,2,4-triazol-5-one molecule were studied the DFT/B3LYP 6-311++G(d,p) basis set. The molecule, firstly, were optimized to find the geometries where the energy is minimum. The target molecule's Proton Nuclear Magnetic Resonance and Carbon-13 Nuclear magnetic Resonance (^1H and ^{13}C -NMR) isotropic shift values were calculated by the method of the gauge independent atomic orbital (GIAO) using the program package Gaussian G09. According to the $\delta_{\text{exp}} = a + b \cdot \delta_{\text{calc}}$ equation, regression analysis was performed using experimental and calculated values and correlation graphs were drawn. Experimental spectroscopic values were obtained from the literature. The Veda 4 program was used to determined IR vibration frequency and the calculated these values are multiplied with scala factor. The calculated theoretical IR data compared with experimental data, and theoretical infrared graphs were created. Also, the surface map such as molecular electrostatic potential (MEP) was visualized. The dipole moments, the HOMO-LUMO energy, the thermodynamic analysis, ΔE energy gap, the total energy, the non-linear optic analysis (NLO) (i.e., the first hyperpolarizability and polarizability), the electronic parameters such as electron affinity, molecular softness, molecular hardness, ionization potential and electronegativity, the geometric properties (bond length and bond angles), the mulliken charge for molecule were calculated.

Keywords: DFT, 1,2,4-triazol-5-one, GIAO, HOMO-LUMO

INTRODUCTION

It is formed by the reaction of aldehydes or ketones with secondary amines, which have a C=N imine group in their structure. Schiff bases are commonly synthesized structures among heterocyclic compounds. Because Schiff bases with 1,2,4-triazole have biological activity

(Zhang, et al., 2017; Cai, et al., 2020; Peyton, et al., 2015; Kotan, et al., 2021; Bahçeci, 2016; Manap, et al., 2020). The quantum chemical calculation methods have widely been used to theoretically predict the spectroscopic, structural, electronic and thermodynamic properties of molecular systems. The Density Functional Theory (DFT) ensure support for experimental structural and spectroscopic studies (Kotan, et al., 2021; Gökçe, et al., 2013; Kotan et al., 2017; Beytur, 2021). In this study, having a large number of theory and basic set options, including molecular mechanics, semi-empirical and ab-initio methods, Gaussian 09W (Frisch, et al., 2009; Wolinski, 1990) package is used. DFT(B3LYP) functional are used at the determination of the structure of molecules. Firstly, The molecule was optimized using Gauss view 5.0 package program (Dennington, 2007). The experimental data of the compound were taken from the literature (Bahçeci, et.al., 2017). The structure of the compound was analyzed with compared IR, ^1H -NMR experimental and theoretical spectral data were drawn. ^1H -NMR isotropic shift values were calculated by the method of GIAO using the program package Gaussian G09W (Frisch et al., 2009). Using experimental (Bahçeci, et.al., 2017) and theoretical values were done regresyon analysis and R^2 values were calculated. The FIT-IR vibration absorption frequencies of analysed molecule were determined with the veda4f program (Jamróz, 2004). There was no negative value in the IR results. Furthermore, molecule's experimental and theoretical, theoretical bond lengths, dipole moments, mulliken charges, HOMO-LUMO energies, thermodynamic ve electronic parameters and total energy of the molecule were calculated.

THEORETICAL CALCULATIONS

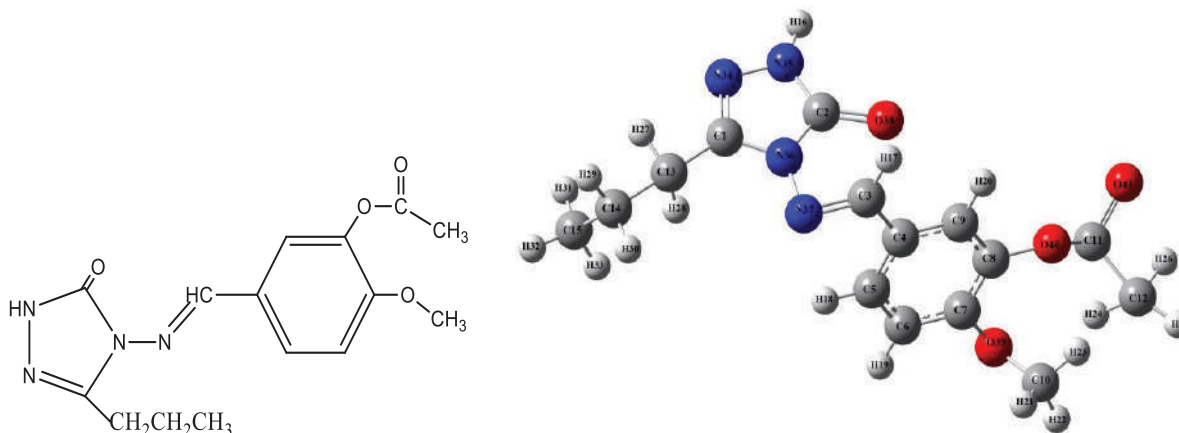


Figure 1. Gausview structure and molecule formula

NMR Analysis

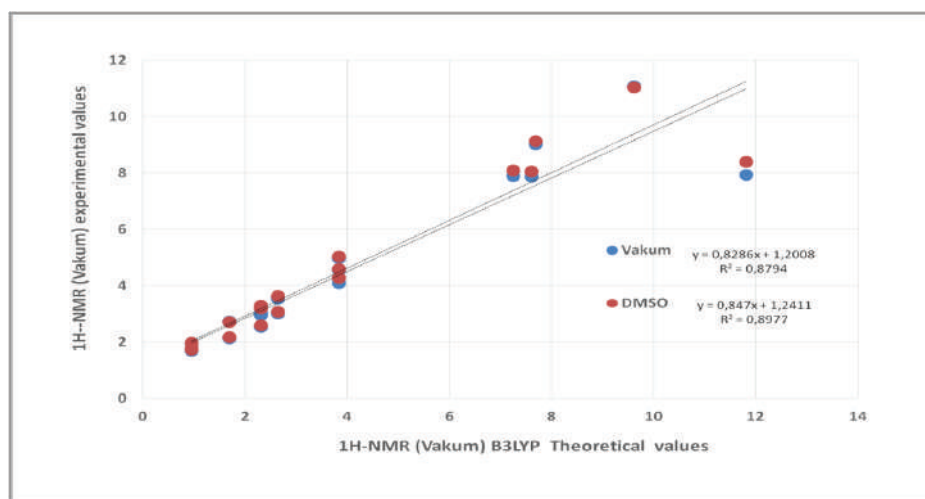
Molecule was optimized by using the B3LYP/6-311++G(d,p) basis set (Frisch et al., 2009; Wolinski, 1990). Starting from this optimized structure with ^1H -NMR spectral data (Table 1) and IR spectral values according to GIAO (Wolinski, 1990) method was calculated using the method of Gaussian G09W program package in gas phase. The correlation graphs for chemical shifts drawn with ^1H -NMR, ^{13}C -NMR and ^1H -NMR(DMSO), ^1H -NMR(vakum/DMSO) spectral data of the molecule (Fig. 2) Theoretically calculated IR data are multiplied with appropriate adjustment factors and the data obtained according to DFT(B3LYP) method are formed using theoretical infrared spectrum (Fig. 3).

Table 1. The calculated and experimental $^1\text{H-NMR}(\text{vakum})/\text{NMR}(\text{DMSO})\text{B3LYP 6-311++G(d,p)}$ isotropic chemical shifts of the molecule (δ/ppm)

Experimental	B3LYP (vakum)	Difference	B3LYP (DMSO)	Difference
11.8	7.94	3.86	8.40	3.40
9.6	11.07	-1.47	11.03	-1.43
7.68	9.01	-1.33	9.14	-1.46
7.24	7.89	-0.65	8.09	-0.85
7.59	7.87	-0.28	8.06	-0.47
3.83	4.10	-0.27	4.27	-0.44
3.83	4.56	-0.73	4.59	-0.76
3.83	4.97	-1.14	5.04	-1.21
2.3	2.96	-0.66	3.20	-0.90
2.3	2.53	-0.23	2.59	-0.29
2.3	3.04	-0.74	3.30	-1.00
2.63	3.02	-0.39	3.08	-0.45
2.63	3.53	-0.90	3.63	-1.00
1.68	2.14	-0.46	2.17	-0.49
1.68	2.73	-1.05	2.72	-1.04
0.95	1.69	-0.74	1.73	-0.78
0.95	1.96	-1.01	1.98	-1.03
0.95	1.73	-0.78	1.8	-0.85

The relation between R^2 values of the compound

B3LYP(vakum)6-311++G(d,p): ^1H : 0.8794; B3LYP(DMSO)6-311++G(d,p): ^1H : 0.8977.
There is such a relationship between R^2 -values of the compound.

**Figure 2.** The $^1\text{H-NMR}$ Vakum/ DMSO correlation graphs for chemical shifts of the molecule.

The vibration frequency of the compound

Theoretically IR values were calculation veda 4f programme (Jamróz, 2004) and scala values were obtain. The negative frequency in the data was not found. This result, structure of compound were shown stable. IR spectrums were drawn with obtained values according to

DFT(B3LYP) method. Theoretically IR values were compare with experimentally IR values. The result of this compare were found corresponding with each other of values. The experimental carbonyl peak (C=O) in 1705, 1765 cm^{-1} and theoretical (C=O) peak in 1755, 1804 cm^{-1} were observed. The NH peak was assigned 3178 cm^{-1} (experimental), 3620 cm^{-1} (theoretical). The experimentally C=N peak was observed at the 1604, 1590 cm^{-1} and same peak theoretically 1611, 1636 cm^{-1} .

Table 3. The calculated IR vibration frequencies values of the molecule

Vibrations	Experimental	B3LYP	Scaled B3LYP
τ CCNC(40)		13,58	13
τ CCCN(15), τ CNNC(15)		21,64	21
δ CCC(17), δ CCN(62)		33,71	33
τ CCNC(24), τ CCCN(19), τ CNNC(26)		41,96	41
τ CCCC(13), τ CNNC(29)		47,76	47
δ CCC(33), δ CCN(34)		64,79	64
τ CCCC(18), τ CNCC(13)		74,50	73
ν CC(33), δ CNN(10)		76,16	75
τ CCCC(19), τ CNNC(29)		86,11	85
δ CCN(30)		88,28	87
ν CC(10), δ CNC(33), δ CCC(16)		93,84	92
τ HCCC(16), τ CCCC(29)		106,14	104
τ HNNC(11), τ HCCC(11), τ CNNC(17)		149,34	147
ν CC(17), δ CCC(11), δ CNC(16)		165,06	162
τ HCCC(16), τ NCNN(19), τ CCCC(10)		187,08	184
τ HCCN(24), τ CCNC(12)		189,57	187
ν NC(13), δ HCC(17), δ HCN(27)		207,86	205
ν CC(22), δ HCC(22)		236,21	233
ν NC(17), ν CC(15), δ HNN(10)		243,47	240
ν NC(21), ν CC(24), δ CCC(10)		257,59	254
ν CC(23), δ CCC(10)		295,04	290
ν CC(14), δ CCC(14)		304,91	300
ν CC(46), δ HCC(17)		323,89	319
δ OCC(15), τ NNCC(13)		327,89	323
δ CCN(10), τ HNNC(10), τ NNCC(13)		368,18	362
δ NNC(12), δ OCC(17), δ CNN(10)		407,91	402
δ COC(11)		436,32	430
τ HNNC(18)		471,95	465
τ HNNC(45)		474,3	467
δ OCC(14), τ OCCC (20)		511	503
δ OCC(16), τ OCOC (10)		565,18	556
δ OCC(13)		575,64	567
δ OCN(15), τ OCOC (34)		593,58	584
τ OCOC(10), τ CCCC(13)		608,92	599
τ CCCC(14)		617,73	608
ν CC(13), τ NNCC(10)		652,28	642
ν CC(16), δ CCC(11)		683,62	673
τ HCCN(10)		713,33	702
τ ONNC(46)		735,46	724
τ HCCC(12), τ CCCC(16)		742,97	731
δ HCC(11), τ HCCN(31)		748,02	736

$\nu NN(11), \delta CCC(12)$	769,1	757
$\nu CC(10), \tau HCCC(17)$	793,76	781
$\nu NC(14), \nu CC(10), \delta NNC(14), \delta CNN(19)$	817,4	805
$\nu OC(10), \delta NNC(14)$	845,99	833
$\tau HCCC(28)$	859,12	846
$\nu OC(10), \tau HCCC(16)$	878,16	864
$\tau HCCC(10)$	880,3	867
$\nu CC(50), \tau HCCC(17)$	899,52	885
$\tau HCCC(23), \tau CCCC(12)$	918,86	905
$\nu OC(11), \delta HCC(11), \delta CCC(14)$	971,25	956
$\delta HCC(75)$	983,2	968
$\tau HCNN(86)$	1010,94	995
$\delta HCH(10), \delta CCO(10), \tau HCCO(39)$	1021,21	1005
$\nu OC(75), \delta CCC(11)$	1025,22	1009
$\nu CC(44), \delta NNC(11)$	1030,83	1015
$\nu NC(87), \delta NCC(18)$	1048,32	1032
$\tau HCCO(30), \tau OCOC(21)$	1063,12	1047
$\nu NC(14), \nu NN(28)$	1078,77	1062
$\nu CC(19), \delta CCC(13), \tau HCCC(17)$	1109,88	1093
$\nu OC(21), \delta HCC(27)$	1121,17	1104
$\tau HCCN(25), \tau CCCN(12), \tau HCCC(10)$	1136,29	1119
$\delta HCH(15), \tau HCOC(45)$	1167,93	1150
$\nu OC(11), \delta CCC(39)$	1169,79	1152
$\delta HCC(10), \tau HCOC(11)$	1196,17	1178
$\nu CC(10), \delta CCC(10), \tau HCOC(17), \tau HCCO(10)$	1205,48	1187
$\nu NC(21), \nu NN(15)$	1213,74	1195
$\delta HCC(19), \delta CCC(10)$	1241,78	1222
$\delta HCC(43)$	1259,35	1240
$\nu NN(11), \delta HCC(24), \delta NCN(11)$	1281,98	1262
$\nu OC(18), \delta HCC(19)$	1276 1282,57	1263
$\nu CC(15), \delta HCC(16), \tau HCCN(12)$	1305,14	1285
$\tau HCCN(24)$	1318,25	1298
$\delta HCC(45), \tau HCCN(11)$	1328,15	1307
$\delta HCN(18), \tau HCCN(34)$	1380,63	1359
$\delta HNN(26), \delta HCN(42), \tau HCCN(19)$	1387,87	1366
$\delta HCH(61)$	1399,33	1378
$\delta HNN(42), \delta HCN(13)$	1401,78	1380
$\delta HCH(30)$	1413,05	1391
$\nu CC(32)$	1433,03	1411
$\nu NC(13), \delta HCN(22)$	1462,03	1439
$\delta HCH(50)$	1471,74	1449
$HCCO(20)$	1472,71	1450
$\delta HCH(25)$	1476,47	1453
$\delta HCH(49)$	1490,14	1467
$\delta HCH(32)$	1495,56	1472
$\tau HCOC(13)$	1498,84	1475
$\delta HCH(48)$	1506,44	1483
$\delta HCH(26)$	1507,98	1484
$\nu CC(10), \delta HCC(10), \delta HCC(18)$	1538,32	1514
$\nu CC(18), \delta HCC(13)$	1600,08	1575

ν NC(52)	1590	1636,45	1611
ν NC(18), ν CC(38), δ HCC(10)		1641,81	1616
ν NC(45), ν CC(14)	1604	1661,46	1636
ν OC(73)	1705	1782,76	1755
ν OC(89)	1765	1832,27	1804
ν CH(56)		3016,03	2969
ν CH(53)		3019,63	2973
ν CH(43)		3029,62	2982
ν CH(80)		3046,66	2999
ν CH(43)		3050,97	3003
ν CH(51)		3059,17	3011
ν CH(62)		3081,47	3033
ν CH(17)		3085,25	3037
ν CH(32)		3089,51	3041
ν NH(100)		3098,27	3050
ν CH(56)		3113,25	3065
ν CH(53)		3133,73	3085
ν CH(43)		3150,21	3101
ν CH(80)		3157,94	3109
ν CH(43)		3183,91	3134
ν CH(51)		3186,39	3137
ν CH(62)		3205,08	3155
ν NH(100)	3178	3676,95	3620

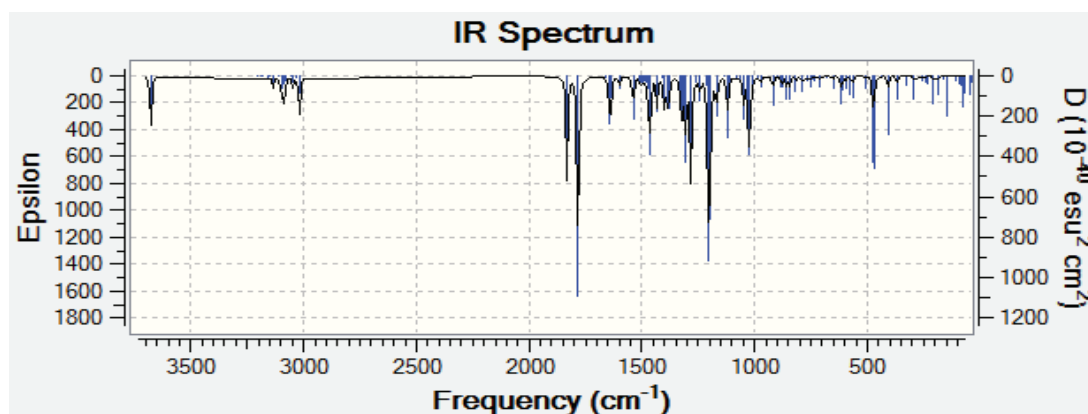


Figure 3. Theoretical IR spectrums and simulated with DFT/B3LYP/6-311++G(d,p) level of the molecule.

Geometric properties (bond angle, length)

The bond length/ angle of the molecule were found based on the stable optimized structure in terms of the arrangement of atoms. Computationally provided data and some length and angle values available in the literature were compared. The calculated and obtained data with 6-311++G(d,p) set for DFT(B3LYP), respectively; C1-N34; C1-N36; C2-N35; C2-N36; C3-N37 bond lengths 1.29, 1.39; 1.36, 1.41; 1.28 were found and is shown in Table 1. The bond lengths registered in the literature are C=N; 1.27 Å and C-N; It is 1.47 Å (Sudha et al., 2018). The C-C and C-H lengths in the benzene ring present in the structure were also compared with the lengths in the literature. Accordingly, the mean values of C-C bond lengths of the benzene ring for B3LYP, respectively, according to the data obtained with the are 1.39, 1.38; The mean C-H bond length was calculated as 1.08, 1.07 Å. The values of C-C bond lengths in the benzene ring in the literature are 1.39 Å and C-H; It was measured as 1.08 Å (Sudha et al.,

2018). As a result of the comparison of the computational data obtained from the bond lengths with the DFT(B3LYP) method and the 6-311++G(d,p) set, and the data obtained from the literature, it has been concluded that the values are the same or very close to each other.

Table 5. The calculated bond length and angle B3LYP/6-311++G(d,p) of the molecule.

Bond Angles	B3LYP	Bond Angles	B3LYP	Bond lengths	B3LYP	Bond lengths	B3LYP
N(34)-C(1)-N(36)	111.08	C(4)-C(5)-C(6)	120.430	C(1)-N(34)	1.29	C(4)-C(5)	1.40
N(34)-N(35)-H(16)	120.454	C(4)-C(9)-C(8)	120.447	C(1)-N(36)	1.39	C(4)-C(9)	1.40
H(16)-N(35)-C(2)	125.203	C(5)-C(6)-H(19)	121.131	C(1)-C(13)	1.49	C(5)-H(18)	1.08
N(35)-C(2)-O(38)	129.920	C(5)-C(6)-C(7)	120.754	N(34)-N(35)	1.37	C(5)-C(6)	1.38
O(38)-C(2)-N(36)	128.770	H(19)-C(6)-C(7)	118.113	N(35)-H(16)	1.00	C(6)-H(19)	1.08
N(36)-C(1)-C(13)	124.918	C(6)-C(7)-O(39)	119.961	N(35)-C(2)	1.36	C(6)-C(7)	1.39
C(1)-C(13)-H(27)	106.769	O(39)-C(10)-H(21)	110.427	C(2)-N(36)	1.41	C(7)-O(39)	1.36
C(1)-C(13)-H(28)	109.015	O(39)-C(10)-H(22)	106.057	C(2)-O(38)	1.21	O(39)-C(10)	1.43
C(1)-C(13)-C(14)	113.595	O(39)-C(10)-H(23)	111.205	N(36)-N(37)	1.37	C(10)-H(21)	1.09
H(29)-C(14)-H(30)	106.894	H(21)-C(10)-H(23)	109.742	C(13)-H(27)	1.09	C(10)-H(22)	1.08
H(29)-C(14)-C(15)	109.908	H(21)-C(10)-H(22)	109.505	C(13)-H(28)	1.09	C(10)-H(23)	1.09
H(30)-C(14)-C(15)	109.893	H(22)-C(10)-H(23)	109.835	C(13)-C(14)	1.54	C(7)-C(8)	1.39
C(14)-C(15)-H(31)	111.309	O(39)-C(7)-C(8)	121.494	C(14)-H(29)	1.09	C(8)-O(40)	1.39

C(14)- C(15)- H(32)	111.075	C(7)-C(8)- O(40)	119.035	C(14)- H(30)	1.09	O(40)- C(11)	1.38
C(14)- C(15)- H(33)	111.249	C(7)-C(8)- C(9)	120.822	C(14)- C(15)	1.53	C(11)- O(41)	1.19
H(31)- C(15)- H(32)	107.683	C(8)-C(9)- H(20)	118.998	C(15)- H(31)	1.09	C(11)- C(12)	1.50
H(31)- C(15)- H(33)	107.657	C(8)- O(40)- C(11)	117.796	C(15)- H(32)	1.09	C(12)- H(24)	1.09
H(32)- C(15)- H(33)	107.690	O(40)- C(11)- O(41)	123.317	C(15)- H(33)	1.09	C(12)- H(25)	1.09
C(1)- N(36)-C(2)	108.322	O(41)- C(11)- C(12)	126.717	N(37)- C(3)	1.28	C(12)- H(6)	1.08
N(36)- N(37)-C(3)	119.106	C(11)- C(12)- H(24)	109.277	C(3)- H(17)	1.08	C(8)-C(9)	1.38
N(37)- C(3)-H(17)	121.959	C(11)- C(12)- H(25)	110.574	C(3)-C(4)	1.46	C(9)- H(20)	1.08
H(17)- C(3)-C(4)	117.717	C(11)- C(12)- H(26)	109.379				
C(3)-C(4)- C(5)	122.964	H(24)- C(12)- H(25)	107.642				
C(3)-C(4)- C(9)	118.239	H(24)- C(12)- H(26)	109.442				
C(4)-C(5)- H(18)	119.200	H(25)- C(12)- H(26)	110.495				

Table 7. The calculated mulliken charges datas of the molecule.

	B3LYP		B3LYP		B3LYP
C1	-0.294	C14	-0.007	H27	0.202
C2	0.438	C15	-0.603	H28	0.178
C3	-0.319	H16	0.389	H29	0.160
C4	0.962	H17	0.257	H30	0.157
C5	-0.163	H18	0.130	H31	0.135
C6	0.028	H19	0.214	H32	0.147
C7	0.166	H20	0.190	N34	-0.011
C8	-1.052	H21	0.129	N35	-0.217
C9	-0.593	H22	0.164	N36	-0.043
C10	-0.272	H23	0.190	N37	-0.004
C11	0.149	H24	0.176	O38	-0.364
C12	-0.551	H25	0.182	O39	-0.127
C13	-0.238	H26	0.174	O40	-0.017
				O41	-0.176

FMO Analysis

Frontier Molecular orbitals (FMO), such as HOMO-LUMO, help us determine the electron transitions in the molecule and the chemical reactivity of the molecule (Fukui, 1982). LUMO stands for low energy vacant molecular orbital and HOMO stands for high energy filled molecular orbital. Also known as "LUMO" electron donating orbital, "HOMO" electron donating orbital. The energy gap " ΔE_g " between these orbitals is significant and the lower it is, the more stable the molecule. The B3LYP, 6-311G(d,p) HOMO-LUMO energies of the molecule were found theoretically $\Delta E_g = 4.34$ eV for B3LYP/6-311G(d,p) are shown in Figure 2. In addition to these, the following electronic parameters were calculated using the Elumo, Ehomo and ΔE_g value (Table 8).

Table 8. The calculated electronic structure parameters of the molecule

		Hatree	ev	kcal/mol	KJ/mol
	LUMO	-0,07228	-1,96679	-45,3559	-189,771
	HOMO	-0,2318	-6,30744	-145,455	-608,591
A	Electron Affinity	0,07228	1,96679	45,3559	189,771
I	Ionization Potential	0,2318	6,30744	145,455	608,591
ΔE	Electronegativity	0,15952	4,34065	100,099	418,82
χ	Chemical Potential	0,15204	4,13711	95,4056	399,181
Pi	Electrophilic Index	-0,15204	-4,13711	-95,4056	-399,181
ω	Nucleophilic Index	0,000921873	0,02508	0,57848	2,42038
IP	Molecular Softness	-0,01212671	-0,32998	-7,60955	-31,8387
S	Molecular Hardness	12,5376	341,157	7867,39	32917,5
η	Electron Affinity	0,07976	2,17033	50,0496	209,41

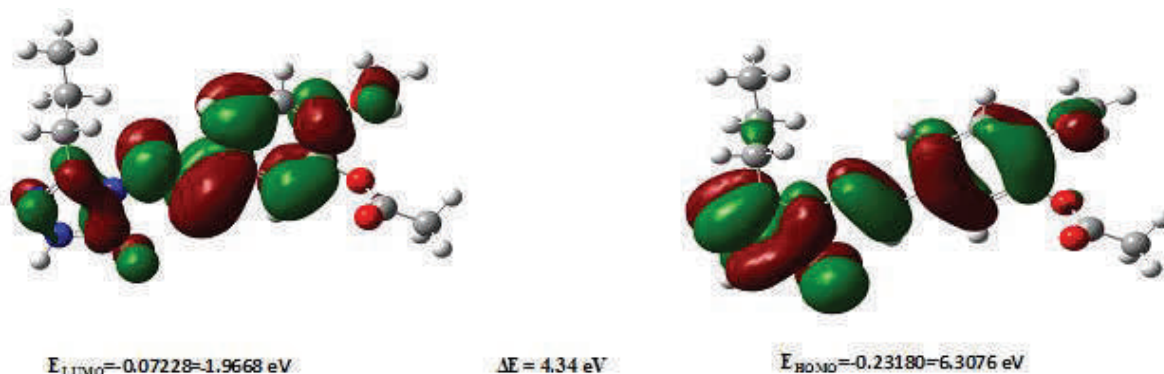


Figure 5. HOMO-LUMO energy calculated with DFT/B3LYP/6-311++G(d,p) of the molecule.

Thermodynamics properties

Thermodynamics parameters were calculated with (B3LYP) functionals in DFT method at the 6-311G++(d,p) basis set at 298.150 K and under 1 atm pressure.

Rotational temperatures (Kelvin)	DFT		DFT
A	0.02197	Zero-point correction (Hartree/Particle)	0.323066
B	0.00527	Thermal correction to Energy	0.346394
C	0.00440	Thermal correction to Enthalpy	0.347339
Rotational constants (GHZ)		Thermal correction to Gibbs Free Energy	0.266255
A	0.45769	Sum of electronic and zero-point Energies	- 1102.2938 63
B	0.10981	Sum of electronic and thermal Energies	- 1102.2705 35
C	0.09175	Sum of electronic and thermal Free Energies	- 1102.3506 74
Thermal Energies E(kcal/mol)		Sum of electronic and thermal Enthalpies	- 1102.2695 91
Translational	0.889	Zero-point vibrational energy (Kcal/mol)	202.7268
Rotational	0.889	Entropy S(cal/mol-K)	
Vibrational	215.588	Translational	43.168
Total	217.366	Rotational	35.498
Thermal Capacity CV(cal/mol-K)		Vibrational	91.988
Translational	2.981	Total	170.654
Rotational	2.981		
Vibrational	77.820		
Total	83.781		

CONCLUSIONS

Quantum chemical methods such as DFT are used to obtain geometrical parameters and calculate the IR, ^1H -NMR and ^{13}C -NMR spectra of the compound. The calculated chemical shifts are compared with the experimental observations. The chemical shifts calculated by B3LYP/6-311++G(d,p) method are in a very good agreement with the experimental data. The normal mode vibrational frequencies calculated at the B3LYP method of theory are in accordance with the recorded IR spectrum. In addition, vibrational bands assignments and analysis of the fundamental modes of the compound are performed.

REFERENCES

- Zhang, S., Xu, Z., Gao, C., Ren, Q. C., Chang, L., Lv, Z. S., & Feng, L. S. (2017). Triazole derivatives and their anti-tubercular activity. *European journal of medicinal chemistry*, 138, 501-513.
- Cai, T., Liao, Y., Chen, Z., Zhu, Y., & Qiu, X. (2020). The Influence of Different Triazole Antifungal Agents on the Pharmacokinetics of Cyclophosphamide. *Annals of Pharmacotherapy*, 54(7), 676-683.
- Peyton, L. R., Gallagher, S., & Hashemzadeh, M. (2015). Triazole antifungals: a review. *Drugs Today*, 51(12), 705-718.
- Kanabar, D., Farrales, P., Kabir, A., Juang, D., Gnanmony, M., Almasri, J., ... & Muth, A. (2020). Optimizing the aryl-triazole of cjoc42 for enhanced gankyrin binding and anti-cancer activity. *Bioorganic & Medicinal Chemistry Letters*, 30(17), 127372.
- Yüksek, H., Özdemir, G., Manap, S., Yılmaz, Y., Kotan, G., Gürsoy-Kol, Ö., & Alkan, M. (2020). Synthesis and Investigations of Antimicrobial, Antioxidant Activities of Novel Di-[2-(3-alkyl/aryl-4, 5-dihydro-1H-1, 2, 4-triazol-5-one-4-yl)-azomethinephenyl] Isophtalates and Mannich Base Derivatives. *ACTA Pharmaceutica Scientia*, 58(1).
- Bahçeci, Ş., Yıldırım, N., Gürsoy-Kol, Ö., Manap, S., Beytur, M., & Yüksek, H. (2016). Synthesis, characterization and antioxidant properties of new 3-alkyl (aryl)-4-(3-hydroxy-4-methoxybenzylidenamino)-4, 5-dihydro-1H-1, 2, 4-triazol-5-ones. *Rasayan J Chem*, 9(3), 494-501.
- Manap, S., Gürsoy-Kol, Ö., Alkan, M., & Yüksek, H. (2020). Synthesis, in vitro antioxidant and antimicrobial activities of some novel 3-substituted-4-(3-methoxy-4-isobutyryloxybenzylideneamino)-4, 5-dihydro-1H-1, 2, 4-triazol-5-one derivatives.
- Kotan, G., Gökce, H., Akyıldırım, O., Yüksek, H., Beytur, M., Manap, S., & Medetalibeyoğlu, H. (2020). Synthesis, Spectroscopic and Computational Analysis of 2-[(2-Sulfanyl-1 H-benzo [d] imidazol-5-yl) iminomethyl] phenyl Naphthalene-2-sulfonate. *Russian Journal of Organic Chemistry*, 56(11), 1982-1994.
- Gokce, H., Bahceli, S., Akyildirim, O., Yuksek, H., & Kol, O. G. (2013). The Syntheses, Molecular Structures, Spectroscopic Properties (IR, Micro-Raman, NMR and UV-vis) and DFT Calculations of Antioxidant 3-alkyl-4-[3-methoxy-4-(4-methylbenzoxy) benzylidenamino]-4, 5-dihydro-1H-1, 2, 4-triazol-5-one Molecules. *Letters in Organic Chemistry*, 10(6), 395-441.
- Kotan, G., & Yüksek, H. (2016). Theoretical And Spectroscopic Studies of 1-(Morpholine-4-yl-Methyl)-3-Benzyl-4-(4-Isopropyl-Benzylidenamino)-4,5-Dihydro-1H-1,2,4-Triazol-5-One Molecule. *Journal of The Turkish Chemical Society Section A: Chemistry*, 3(3), 381-392.
- Beytur, M., & Avinca, I. (2021). Molecular, Electronic, Nonlinear Optical and Spectroscopic Analysis of Heterocyclic 3-Substituted-4-(3-methyl-2-thienylmethyleneamino)-4, 5-

- dihydro-1H-1, 2, 4-triazol-5-ones: Experiment and DFT Calculations. *Heterocyclic Communications*, 27(1), 1-16.
- Frisch, M.J., Trucks, G.W., Schlegel, H.B., Scuseria, G.E., Robb, M.A., Cheeseman, J.R., Scalmani, G., Barone, V., Mennucci, B., Petersson, G.A., Nakatsuji, H., Caricato, M., Li, X., Hratchian, H.P., Izmaylov, A.F., Bloino, J., Zheng, G., Sonnenberg, J.L., Hada, M., Ehara, M., Toyota, K., Fukuda, R., Hasegawa, J., Ishida, M., Nakajima, T., Honda, Y., Kitao, O., Nakai, H., Vreven, T., Montgomery, J.A., Jr. Vreven, T., Peralta, J.E., Ogliaro, F., Bearpark, M., Heyd, J.J., Brothers, E., Kudin, N., Staroverov, V.N., Kobayashi, R., Normand, J., Raghavachari, K., Rendell, A., Burant, J.C., Iyengar, S.S., Tomasi, J., Cossi, M., Rega, N., Millam, J.M., Klene, M., Knox, J.E., Cross, J.B., Bakken, V., Adamo, C., Jaramillo, J., Gomperts, R., Stratmann, R.E., Yazyev, O., Austin, A.J., Cammi, R., Pomelli, C., Ochterski, J.W., Martin, L.R., Morokuma, K., Zakrzewski, V.G., Voth, G.A., Salvador, P., Dannenberg, J.J., Dapprich, S., Daniels, A.D., Farkas, O., Foresman, J.B., Ortiz, J.V., Cioslowski, J., & Fox, D.J. (2009). Gaussian Inc., Wallingford, CT.
- Wolinski K., Hilton J.F. and Pulay P. J. (1990). Am. Chem. Soc. 112 512.
- Dennington, R.; Keith, T.; Millam, J. (2007). GaussView, Version 4.1. 2. *Semichem Inc., Shawnee Mission, KS*.
- Bahçeci, Ş., Yıldırım, N., Alkan, M., Gürsoy-Kol, Ö., Manap, S., Beytur, M., Yüksek, H., (2017). Investigation of Antioxidant, Biological and Acidic Properties of New 3-Alkyl(Aryl)-4-(3-acetoxy-4-methoxybenzylidenamino)-4,5-dihydro-1H-1,2,4-triazol-5-ones. *The Pharmaceutical and Chemical Journal*, 4(4), 91-101
- Jamróz, M.H. (2004). Vibrational Energy Distribution Analysis: VEDA 4 program, Warsaw.
- Sudha, N., Abinaya, B., Arun Kumar, R., & Mathammal, R. (2018). Synthesis, Structural, Spectral, Optical and Mechanical Study of Benzimidazolium Phthalate crystals for NLO Applications. *Journal of Lasers Optics & Photonics*, 5(2), 1-6.
- Fukui, K., (1982). Role of Frontier Orbitals in Chemical Reactions. *Science*, 747-754.

ELECTRONIC, THERMODYNAMIC, GEOMETRIC ANALYSIS OF 1-(2,6-DIMETILMORFOLIN-4-IL-METIL)-3-ETHYL-4-(4-HYDROXYBENZYLIDENAMINO)-4,5-DIHYDRO-1*H*-1,2,4-TRIAZOL-5-ONE

Assist. Prof. Dr. Songül BOY

Kafkas University, Ataturk Vocational School of Health Services, Kars Turkey
ORCID: 0000-0002-6508-8600

Assist. Prof. Dr. Gül KOTAN

Kafkas University, Kars Vocational School, Kars, Turkey
ORCID: 0000-0002-4507-9029

Prof. Dr. Haydar YÜKSEK

Kafkas University, Department of Chemistry, Kars, Turkey
ORCID: 0000-0003-1289-1800

ABSTRACT

The quantum chemical computations of 1-(2,6-Dimethylmorpholine-4-il-methyl)-3-ethyl-4-(4-hydroxybenzylidenamino)-4,5-dihydro-1*H*-1,2,4-triazol-5-one were performed using DFT/B3PW91 method in the 6-311G(d, p)(d,p) basis set. The molecule was optimized for the most stable positions of the atoms. This Gauss-view optimized structure was used for all calculations. Firstly, the nuclear magnetic rezonans (^{13}C -NMR and ^1H -NMR) data were calculated with the GIAO method in the Gaussian O9W package program and the results were compared with the experimental values obtained from the literature. The R value were calculated by performing regression analysis using all experimental and calculation spectral data. The Veda 4 program was used to calculate theoretical infrared (IR) vibration frequencies which were scaled with certain scala factor. Furthermore, the thermodynamic parameters such as (heat capacity CV^0 , entropy S^0 and enthalpy H^0), geometric properties (bond angle and length), electronic parameters (global hardness (η), electron affinity (A), electronegativity (χ), softness (σ) and ionization potential (I), $E_{\text{LUMO}}-E_{\text{HOMO}}$ energy gap, HOMO-LUMO energy), dipole moment, mulliken atomic charges, non-linear optic (NLO) (i.e., the first hyperpolarizability and polarizability) analysis were studied. The molecular electrostatic potential (MEP) surface map was designed, and thus the electronegative and electropositive regions of the molecule were determined. Additionally, electrostatic spin potential map (ESP) and electron contour map of molecule were obtained.

Keywords: 6-311++ G(d, p), GIAO, HOMO-LUMO. NLO

INTRODUCTION

1,2,4- Triazole derivatives have been associated with diverse biological activities, such as antibacterial, antifungal, anti-inflammatory, antihypertensive and antiviral (Raval, et.al., 2009; Al-Soud, et.al., 2004). In addition, metal complexes of triazoles give very good results in the treatment of bladder, testis, ovary, brain tumors. Also because of 1,2,4-triazoles having pharmacological activity, they are found in the structure of many drugs used in chemotherapy. Synthesized compound in this study is a Mannich base. Mannich bases have applications in the field of medicinal chemistry, the product of synthetic polymers, the petroleum industry, as products used in water treatment, cosmetics, the dyes industry. In addition, Mannich bases have biological activity such as anticancer, antibacterial, antimycobacterial, anti-inflammatory, analgesic, antifungal, antitumor (Kumar, et.al., 2010). Today, many properties of molecules have been started to be calculated without the need for experimentations using theoretical methods. Quantum chemical calculations are commonly used for interpretation, understanding and prevision of experimental results such as ^1H and ^{13}C NMR spectral data, IR frequency values, bond angles, bond length, dihedral angles, Mulliken atomic charges, HOMO-LUMO energies, dipole moment, thermodynamic properties. Furthermore, these calculations are used to determine the optical and electronic properties of organic compounds and to elucidate their structure-activity relationship (SAR). In this study, the molecule was optimized by using 6-311G(d,p) basis set of the B3LYP method (Frisch, et.al., 2009). The optimized molecular structure, vibrational frequencies, atomic charges and frontier molecular orbitals (HOMO and LUMO) of the titled compound have been calculated by using B3LYP method with 6-311G(d,p) basis set. All quantum chemical calculations were carried out by using Gaussian09W program package and the GaussView molecular visualization program (Frisch et.al., 2009). The molecular structure and vibrational calculations of the molecule were computed by using B3LYP (Becke, 1993) density functional method with 6-311G(d, p) basis set in ground state. IR absorption frequencies of the titled compound were calculated by the same basis set. Then, they were compared with experimental data which are shown to be accurate. Infrared spectrum was composed by using the data obtained from the method (Boy et.al., 2021). The assignments of fundamental vibrational modes of the titled compound were performed on the basis of total energy distribution (TED) analysis by using veda4f program (Jamroz, 2004). Thermodynamic properties of analyzed molecule were calculated by the same basis set. Also, the molecular structure, the highest occupied molecular orbital-lowest unoccupied molecular orbital (HOMO-LUMO), electronic transition, electronegativity, hardness, molecular electrostatic potential maps (MEP), Mulliken atomic charges of the titled compound have been investigated by the same basis set.

MATERIALS AND METHODS

The compound was optimized by using the B3LYP/6-311G(d,p) basis set (Frisch et.al., 2009; Wolinski, et. al.). ^1H -NMR and ^{13}C -NMR isotropic shift values were calculated by the method of GIAO using the program package Gaussian G09W (Wolinski, et. al.). Experimental and theoretical values were inserted into the graphic according to equation of $\delta_{\text{exp}} = a + b \cdot \delta_{\text{calc}}$. The standard error values were found via Sigma Plot program with regression coefficient of a and b constants. IR absorption frequencies of analyzed molecule were calculated by B3LYP/6-311G(d,p) methods. The veda4f program was used in defining IR data, which were calculated theoretically (Jamroz, et al., 2004). The experimental (Boy, et.al., 2021) and the obtained

theoretical values were compared and found by regression analyses that are accurate, Besides, the calculations such as bond angles, bond lengths, the HOMO-LUMO energy and mulliken charges of compound was calculated.

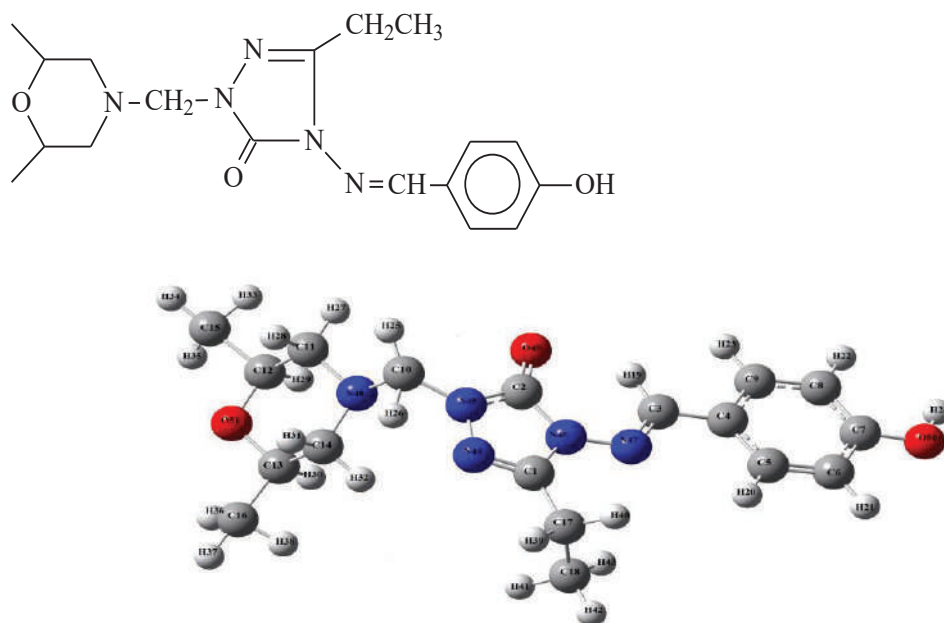


Figure 1. Optimized molecular structure of molecule with B3LYP/ 6-311G(d,p) level.

RESULT AND DISCUSSIONS

Molecular Structure

The optimized molecular geometric parameters (bond angles, bond lengths) of the molecule by using B3LYP/6-311G(d,p) level are listed in Table 1. N4-C3 bond length was observed as 1.28 Å (experimental) and 1.28 Å (B3LYP), respectively. The lowest bond length of O(50)-H(24) as 0.96 Å (B3LYP) was measured. All bond angles were close to each other, but the highest angle was between N(45)-C(2)-O(49).

Table 1. The calculated bond angles and bond lengths of the titled compound

Bond Angles (°)	B3LY P	Bond Angles (°)	B3LY P	Bond lengths	B3LY P	Bond lengths	B3LY P
N(44)-C(1)- N(46)	111.0 5	H(25)-C(10)- N(48)	112.8 7	C(1)- N(44)	1.29	C(9)- H(23)	1.08
N(44)-N(45)- C(10)	122.0 6	H(26)-C(10)- N(48)	108.4 9	C(1)- N(46)	1.38	C(4)-C(9)	1.40
C(10)-N(45)- C(2)	124.8 0	C(10)-N(48)- C(11)	112.6 7	C(1)- C(17)	1.49	C(10)- H(25)	1.09
N(45)-C(2)- O(49)	129.2 6	C(10)-N(48)- C(14)	113.3 3	N(44)- N(45)	1.38	C(10)- H(26)	1.10

O(49)-C(2)- N(46)	128.5 7	N(48)-C(11)- H(27)	112.0 5	N(45)- C(10)	1.44	C(10)- N(48)	1.45
N(45)-C(2)- N(46)	102.1 4	N(48)-C(11)- H(28)	108.6 8	N(45)- C(2)	1.37	N(48)- C(11)	1.46
N(44)-C(1)- C(17)	124.9 1	H(27)-C(11)- H(28)	108.1 8	C(2)- N(46)	1.41	C(11)- H(27)	1.09
C(1)-C(17)- C(18)	113.5 1	H(27)-C(11)- C(12)	108.5 2	C(2)- O(49)	1.22	C(11)- H(28)	1.10
C(1)-C(17)- H(39)	106.5 7	H(28)-C(11)- C(12)	109.3 5	N(46)- N(47)	1.37	C(11)- C(12)	1.52
C(1)-C(17)- H(40)	108.7 9	N(48)-C(11)- C(12)	109.9 9	C(17)- H(39)	1.09	C(12)- H(29)	1.10
C(17)-C(18)- H(41)	110.8 6	C(11)-C(12)- H(29)	107.8 7	C(17)- H(40)	1.09	C(12)- C(15)	1.51
C(17)-C(18)- H(42)	110.0 9	H(29)-C(12)- C(15)	110.0 3	C(17)- C(18)	1.53	C(15)- H(33)	1.09
C(17)-C(18)- H(43)	111.1 0	C(11)-C(12)- C(15)	112.7 8	C(18)- H(41)	1.09	C(15)- H(34)	1.09
H(41)-C(18)- H(42)	108.0 6	O(51)-C(12)- C(15)	107.4 1	C(18)- H(42)	1.09	C(12)- O(51)	1.43
H(42)-C(18)- H(43)	108.1 6	C(12)-C(15)- H(33)	110.1 3	C(18)- H(43)	1.09	O(51)- C(13)	1.43
H(41)-C(18)- H(43)	108.4 5	C(12)-C(15)- H(34)	110.5 9	N(47)- C(3)	1.28	C(13)- C(16)	1.51
C(1)-N(46)- C(2)	108.1 4	C(12)-C(15)- H(35)	110.6 6	C(3)- H(19)	1.08	C(13)- H(30)	1.10
N(46)-N(47)- C(3)	118.9 8	H(33)-C(15)- H(34)	108.2 4	C(3)-C(4)	1.46	C(16)- H(36)	1.09
N(47)-C(3)- H(19)	121.7 6	H(33)-C(15)- H(35)	108.4 6	C(4)-C(5)	1.40	C(16)- H(37)	1.09
H(19)-C(3)- C(4)	117.6 4	H(34)-C(15)- H(35)	108.7 0	C(5)- H(20)	1.08	C(16)- H(38)	1.09
C(3)-C(4)- C(5)	122.9 6	H(29)-C(12)- O(51)	108.5 2	C(5)-C(6)	1.38	C(13)- C(14)	1.52
C(3)-C(4)- C(9)	118.7 2	C(12)-O(51)- C(13)	112.8 6	C(6)- H(21)	1.08	C(14)- H(31)	1.10
C(4)-C(5)- H(20)	119.0 1	O(51)-C(13)- H(30)	108.4 1	C(6)-C(7)	1.40	C(14)- H(32)	1.09
C(4)-C(5)- C(6)	120.9 9	O(51)-C(13)- C(14)	110.1 6	C(8)- H(22)	1.08		
C(5)-C(6)- H(21)	121.3 0	H(30)-C(13)- C(14)	108.0 9	C(7)-C(8)	1.39		
C(5)-C(6)- C(7)	119.8 8	C(13)-C(14)- H(31)	108.9 0	C(7)- O(50)	1.36		
C(6)-C(7)- C(8)	120.0 3	C(13)-C(14)- H(32)	109.8 5	O(50)- H(24)	0.96		
C(6)-C(7)-	117.1	C(13)-C(14)-	110.2	C(8)-C(9)	1.39		

O(50)	7	N(48)	1
C(7)-O(50)-	109.9	H(31)-C(14)-	111.1
H(24)	9	N(48)	3
O(50)-C(7)-	122.7	H(32)-C(14)-	108.9
C(8)	9	N(48)	6
C(7)-C(8)-	119.6	H(31)-C(14)-	107.7
C(9)	2	H(32)	2
C(7)-C(8)-	120.1	O(51)-C(13)-	107.3
H(22)	8	C(16)	5
H(22)-C(8)-	120.1	H(30)-C(13)-	109.9
C(9)	8	C(16)	5
C(8)-C(9)-	119.3	C(13)-C(16)-	110.5
H(23)	6	H(36)	9
H(23)-C(9)-	119.4	C(13)-C(16)-	110.1
C(4)	9	H(37)	7
C(2)-N(45)-	124.8	C(13)-C(16)-	110.6
C(10)	0	H(38)	1
N(45)-C(10)-	106.6	H(36)-C(16)-	108.2
H(25)	7	H(37)	4
N(45)-C(10)-	106.2	H(36)-C(16)-	108.6
H(26)	5	H(38)	4
H(25)-C(10)-	108.9	H(37)-C(16)-	108.4
H(26)	8	H(38)	9

Vibrational frequencies

Theoretically IR values were calculation veda 4f programme and scala values were obtain. The negative frequency in the data was not found. This result, structure of compound were shown stable. IR spectrums were drawn with obtained values according to DFT method. Theoretically IR values were compare with experimentally IR values. The result of this compare were found corresponding with each other of values. Experimentally carbonyl peak (C=O) in 1688 cm^{-1} and theoretically (C=O) peak in 1762 cm^{-1} were observed. The OH peak was signed in 3180 cm^{-1} (experimental), 3525 cm^{-1} (calculated). Experimentally C=N peak $1607, 1586\text{ cm}^{-1}$ while theoretically 1618 cm^{-1} (B3LYP) was observed and these values were listed in the Table 2.

Table 2. The calculated and observed frequencies values of the titled compound

vibrational frequencies	Experimental IR	Scaled 6-311G(d, p)
ν (OH)	3180	3525
ν (C=O)	1688	1762
ν (C=N)	1607, 1586	1618

NMR Spectral Analysis

In nuclear magnetic resonance (NMR) spectroscopy, the isotropic chemical shift analysis allows us to identify relative ionic species and to calculate reliable magnetic properties which provide the accurate predictions of molecular geometries (Rani et.al.,2010; Subramanian et.al.,2010). In this framework, the optimized molecular geometry of the titled compound was obtained by using B3LYP method with 6-311G(d, p) basis level in DMSO solvent. By considering the optimized molecular geometry of the titled compound the ^1H and ^{13}C NMR chemical shift values were calculated at the same level by using Gauge-Independent Atomic Orbital (GIAO) method. Theoretically and experimentally values were plotted according to $\delta_{\text{exp}} = a \cdot \delta_{\text{calc.}} + b$, R^2 were found using the SigmaPlot program (Table 3 and Figure 5)

Table 3. The calculated and experimental ^{13}C / ^1H NMR isotropic chemical shifts of the titled compound

No	Experimenta l	B3LYP(vakum)	Difference	B3LYP(DMSO)	Difference
C1	146,76	152,95	-6,19	154,95	-8,19
C2	150,52	154,46	-3,94	155,38	-4,86
C3	155,08	154,65	0,43	155,83	-0,75
C4	124,66	133,79	-9,13	132,62	-7,96
C5	129,72	131,15	-1,43	130,61	-0,89
C6	115,89	120,57	-4,68	120,32	-4,43
C7	161,21	165,55	-4,34	166,41	-5,2
C8	115,89	115,68	0,21	117,57	-1,68
C9	129,72	138,85	-9,13	140,07	-10,35
C10	65,98	67,55	-1,57	67,31	-1,33
C11	55,03	59,20	-4,17	58,85	-3,82
C12	71,49	76,43	-4,94	58,7	12,79
C13	71,49	75,70	-4,21	76,82	-5,33
C14	55,64	59,25	-3,61	55,92	-0,28
C15	17,88	18,41	-0,53	18,28	-0,4
C16	18,84	19,91	-1,07	19,73	-0,89
C17	18,46	23,62	-5,16	23,73	-5,27
C18	10,12	13,52	-3,4	13,29	-3,17
H19	9,52	11,16	-1,64	11,11	-1,59
H20	7,66	9,08	-1,42	9,13	-1,47
H21	6,86	7,82	-0,96	7,91	-1,05
H22	6,86	7,21	-0,35	7,63	-0,77
H23	7,66	8,05	-0,39	8,26	-0,6
H24	10,2	4,67	5,53	5,57	4,63
H25	4,55	5,12	-0,57	5,17	-0,62
H26	4,55	4,37	0,18	4,53	0,02

H27	2,61	3,25	-0,64	3,37	-0,76
H28	2,3	2,64	-0,34	2,77	-0,47
H29	3,91	4,33	-0,42	4,35	-0,44
H30	3,91	4,18	-0,27	4,23	-0,32
H31	2,02	2,49	-0,47	2,61	-0,59
H32	3,54	3,86	-0,32	3,85	-0,31
H33	1,04	1,55	-0,51	1,76	-0,72
H34	1,04	1,65	-0,61	1,63	-0,59
H35	1,13	1,99	-0,86	1,92	-0,79
H36	1,04	1,72	-0,68	1,69	-0,65
H37	1,13	2,02	-0,89	1,96	-0,83
H38	1,04	1,51	-0,47	1,71	-0,67
H39	2,72	3,08	-0,36	3,14	-0,42
H40	2,72	3,65	-0,93	3,74	-1,02
H41	1,23	2,39	-1,16	1,72	-0,49
H42	1,23	1,89	-0,66	2,04	-0,81
H43	1,23	1,68	-0,45	2,33	-1,1

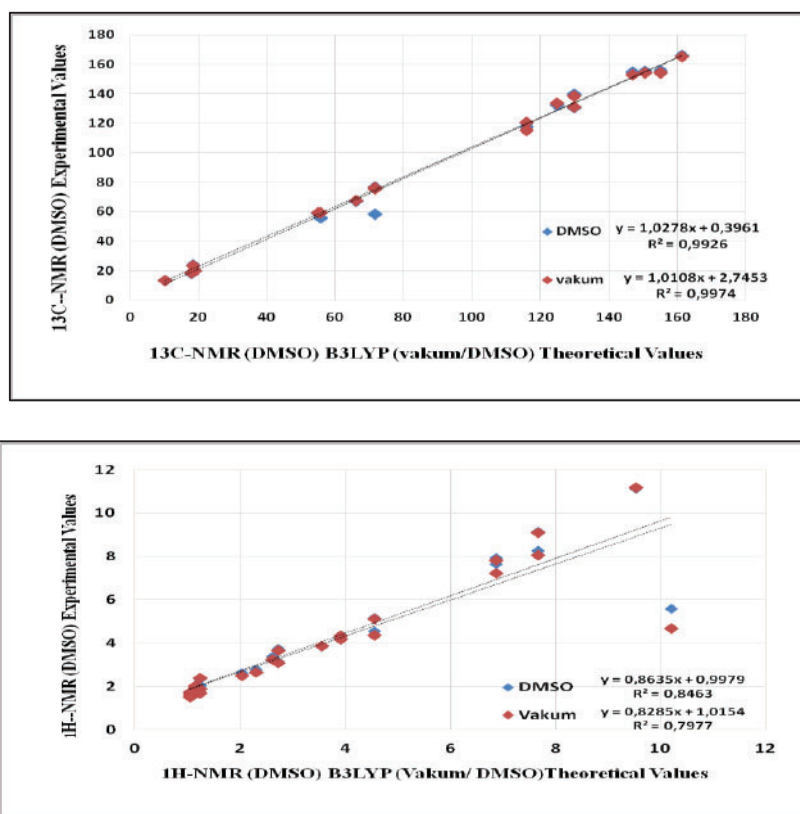


Figure 2. The correlation graphics for $^{13}\text{C}/^1\text{H}$ -NMR(vakum/DMSO)

Electronic and Thermodynamic Properties

The some N and O atoms which have negative charge values. The mulliken charge values of H atoms were found to be positive. C2, C4, C5, C10 atoms surrounded by electronegative atoms in

the compound have positive charges. C5 atom was found to have the highest atomic charge of 0.716.

Table 4. Mulliken atomic charges of the titled compound

Atoms	B3LYP	Atoms	B3LYP	Atoms	B3LYP
C1	-0.098	H19	0.283	H37	0.161
C2	0.164	H20	0.156	H38	0.139
C3	-0.294	H21	0.205	H39	0.186
C4	0.654	H22	0.138	H40	0.173
C5	0.716	H23	0.157	H41	0.137
C6	-0.637	H24	0.267	H42	0.155
C7	-0.273	H25	0.229	H43	0.165
C8	-0.093	H26	0.150	N44	-0.057
C9	-1.177	H27	0.134	N45	-0.181
C10	0.341	H28	0.138	N46	-0.046
C11	-0.221	H29	0.164	N47	-0.116
C12	-0.007	H30	0.157	N48	0.336
C13	-0.027	H31	0.155	O49	-0.329
C14	-0.532	H32	0.154	O50	-0.222
C15	-0.574	H33	0.137	O51	-0.035
C16	-0.610	H34	0.163		
C17	-0.249	H35	0.163		
C18	-0.444	H36	0.160		

The HOMO-LUMO energy gap was assigned as 4.31eV at 6-311G(d,p) level and in the gas phase and shown at the Figure 6. All electronic parameters of the molecule were calculated by using the HOMO-LUMO energy difference.

Table 5. The electronic properties of the titled compound

	Electronic Parameters	Hatree	eV	kcal/mol	KJ/mol
	Electron Affinity	-0,06447	-1,75427	-40,4551	-169,266
	Ionization Potential	-0,22309	-6,07044	-139,99	-585,723
A	Energy gap	0,06447	1,75427	40,4551	169,266
I	Electronegativity	0,22309	6,07044	139,99	585,723
ΔE	Chemical potential	0,15862	4,31616	99,5345	416,457
χ	Electrophilic index	0,14378	3,91235	90,2224	377,494
Pi	Nucleophilic index	-0,14378	-3,91235	-90,2224	-377,494
ω	Molecular softness	0,000819775	0,02231	0,51441	2,15232
IP	Molecular hardness	-0,01140319	-0,31029	-7,15554	-29,9391
S	Electron Affinity	12,6088	343,093	7912,03	33104,3
η	Ionization Potential	0,07931	2,15808	49,7673	208,228

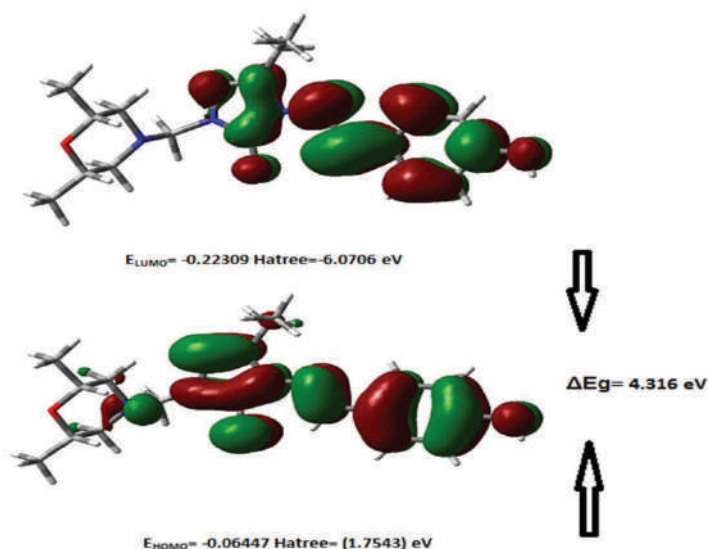


Figure 3. The calculated HOMO-LUMO energies of the titled compound with the B3LYP/6-311G(d,p) level

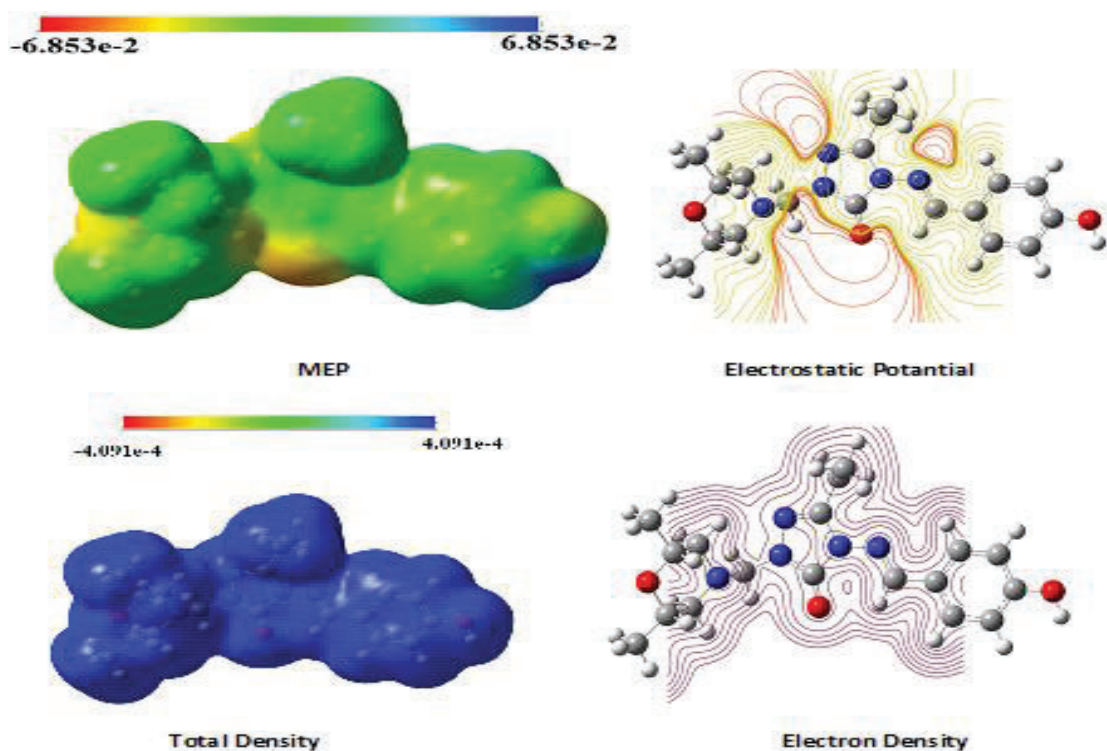


Figure 4. TD, ESP, MEP and countour mapped surfaces of molecule

CONCLUSIONS

The molecular structure, vibrational frequencies, ^1H and ^{13}C NMR chemicals shifts, MEP, HOMO-LUMO analyses and atomic charges for Mannich base 1-(2,6-dimethylmorpholin-4-yl-

methyl)-3-ethyl-4-(4 hydroksibenzylideneamino)-4,5-dihydro-1*H*-1,2,4-triazol-5-one have been calculated by using B3LYP/6-311G(d,p) level. By considering the experimental results, it can be easily stated that the vibrational frequencies, ^1H and ^{13}C NMR chemical shifts parameters obtained theoretically are in a very good agreement with the experimental ones .

REFERENCES

- Raval, J. P., Patel, H. V., Patel, P. S., & Desai, K. R. (2010). A convenient, rapid microwave assisted synthesis of some novel 3-[(4-chloro-3-methylphenoxy) methyl]-6-aryl-5, 6-dihydro-[1, 2, 4] triazolo [3, 4-b][1, 3, 4] thiadiazoles using acidic alumina. *Journal of Saudi Chemical Society*, 14(4), 417-421.
- Al-Soud, Y. A., Al-Dweri, M. N., Al-Masaudi, N. A., (2004). Synthesis, antitumor and antiviral properties of some 1,2,4-triazole derivatives, *Farmaco* (59), 775-78.
- Kumar, A., Gupta, M. K., & Kumar, M. (2010). Non-ionic surfactant catalyzed synthesis of Betti base in water. *Tetrahedron letters*, 51(12), 1582-1584.
- Boy, S., Türkan, F., Beytur, M., Aras, A., Akyıldırım, O., Karaman, H. S., & Yüksek, H. (2021). Synthesis, design, and assessment of novel morpholine-derived Mannich bases as multifunctional agents for the potential enzyme inhibitory properties including docking study. *Bioorganic Chemistry*, 107, 104524.
- Frisch, M. J. E. A., Trucks, G. W., Schlegel, H. B., Scuseria, G. E., Robb, M. A., Cheeseman, J. R., ... & Fox, D. J. (2009). gaussian 09, Revision d. 01, Gaussian, Inc., Wallingford CT, 201.
- Frisch, A., Nielson, A.B., & Holder, A.J. (2003). Gaussview User Manual, Gaussian, Inc., Wallingford, CT, [3]
- Wolinski, K., Hilton, J.F., Pulay, P. (1990). *J. Am. Chem. Soc.*, 112, 512.
- Beck, A. D. (1993). Density-functional thermochemistry. III. The role of exact exchange. *J. Chem. Phys*, 98(7), 5648-6.
- Jamróz, M.H. (2004). Vibrational Energy Distribution Analysis: VEDA 4 program, Warsaw.
- Rani, A. U., Sundaraganesan, N., Kurt, M., Cinar, M., & Karabacak, M. (2010). FT-IR, FT-Raman, NMR spectra and DFT calculations on 4-chloro-N-methylaniline. *Spectrochimica Acta Part A: Molecular and Biomolecular Spectroscopy*, 75(5), 1523-1529.
- Subramanian, N., Sundaraganesan, N., & Jayabharathi, J. (2010). Molecular structure, spectroscopic (FT-IR, FT-Raman, NMR, UV) studies and first-order molecular hyperpolarizabilities of 1, 2-bis (3-methoxy-4-hydroxybenzylidene) hydrazine by density functional method. *Spectrochimica Acta Part A: Molecular and Biomolecular Spectroscopy*, 76(2), 259-269.
- Wade, Jr. L.G. (2006) Organic Chemistry, 6nd ed.; Pearson Prentice Hall: New Jersey.
- Wolinski K., Hilton J.F. and Pulay P. J. (1990). *Am. Chem. Soc.* 112 512.

INHIBITION OF THERMAL AND SHEAR INDUCED AGGREGATION OF ALBUMIN (BOVINE SERUM ALBUMIN) BY CENTELLA ASIATICA EXTRACT

Laipubam Gayatri Sharma

Indian Institute of Technology, Guwahati, India, 781039

Lalit Mohan Pandey

Indian Institute of Technology, Guwahati, India, 781039

Abstract

Protein aggregation phenomena owing to its numerous disadvantages in the pharmaceutical industry as well as being the seed cause of neurodegenerative diseases [1], remains one of the important topic in scientific research. Various natural sources are now being focussed for solving the protein aggregation issue as no side effects are accompanied. *Centella asiatica* (CA) is one such plant which is a perennial medicinal herb known for its neuroprotection property and memory enhancement. Its antioxidative action, free radical scavenging and modulation of cholinergic activities are some of the properties which attributes to the neuroprotection ability[2]. Apart from this, it is very likely that components of the CA could bind to the bigger macromolecule protein and peptides. This small molecule binding then aids to the native structure stabilization when exposed to various external stimuli. Therefore, in light of the above possibility, we checked the inhibition action of CA extract against thermal and shear induced aggregation of a model protein, BSA at 60°C and shear force of 300s⁻¹. Three types of extract were tested namely CA ethyl acetate extract (CEE), CA methanolic extract (CME) and CA water extract (CWE), which were extracted sequentially with increasing polarity of the solvent. The aggregation kinetics was monitored through Thioflavin T (Th-T) assay and dynamic light scattering (DLS) and the aggregate morphology were analysed via AFM. The interaction of the extract and the protein was thermodynamically investigated through isothermal titration calorimetry (ITC). The characterization of the extract was performed through the high resolution liquid chromatography mass spectrometry (HRLCMS) and the antioxidative action via DPPH free radical scavenging assay. 300 µg/ml CWE, CME and CEE conferred scavenging activity on DPPH radical with the inhibitory percent of 42.48, 53.35 and 16.87 % respectively. The dissociation constant K_d determined from ITC for CEE, CWE and CME with BSA was found to be 0.13 mM⁻¹, 2.3 mM⁻¹ and 139 M⁻¹ respectively. From this study it was found that CA extract could significantly inhibit the aggregation of BSA and CEE extract was found to performed the best.

Keywords: protein aggregation, centella asiatica, shear, thermal

References

1. Ross, C.A. and M.A. Poirier, Protein aggregation and neurodegenerative disease. *Nature medicine*, 2004. **10**(7): p. S10-S17.
2. Arora, R., et al., Comparison of three different extracts of *Centella asiatica* for anti-amnesic, antioxidant and anticholinergic activities: in vitro and in vivo study. *Biomedicine & Pharmacotherapy*, 2018. **105**: p. 1344-1352.

SYNTHESIS OF ZEOLITIC MATERIALS INCORPORATED IN THE PRESENCE OF DIFFERENT STRUCTURING ORGANIC MOLECULES

Affaf TABTI

Institute of Science and Technology, University of Relizane Ahmed Zabana, Algeria.
LCM Materials Chemistry Laboratory, University of Oran 1, Ahmed Ben Bella, Algeria.

Franck LAUNAY

Surface Reactivity Laboratory, site Le Raphael, 3 rue Galilée, 94200 Ivry-sur-Seine Sorbonne Universities, UPMC-Paris 06, UMR 7197, France.

Abd Rezzak BABA AHMED

Mohamed Serier

Institute of Science and Technology, University of Relizane Ahmed Zabana, Algeria.

Abstract

The main objective of this study is to synthesize microporous materials of MFI type purely silicic (silicalite-1) incorporated into the transition metal. The synthesis of these materials is carried out in fluorinated and alkaline media, in the presence of the various structuring organic molecules, diethylamine (DEA), tetrapropylammonium hydroxide (TPAOH), tetrapropylammonium bromide (TPABr), o-phenylene diamine ($C_6H_8N_2$ (o)) and under very precise conditions of crystallization temperature and crystallization time (175°C, 24 hours). The silicalite incorporated synthesized was characterized by X-ray fluorescence, X-ray diffraction, IR spectroscopy and UV-Vis. spectroscopy.

Keywords: TS-1, XRF, XRD, IR, UV-Vis., synthesis, agents structuring., template effect

1. INTRODUCTION

Syntheses of microporous materials require the presence of an inorganic structuring agent (alkaline or alkaline-earth cations) or organic (amines, quaternary amines, alcohols, etc.). These species intervene as true molecular agents around which crystallizes the mineral matter. After synthesis, they are occluded in the porosity and the porous material is obtained after extraction or removal by calcination.

The synthesis of TS-1 was first made in 1983 using TPAOH as an organic template. [1] The TPAOH used as an organic structuring agent that can act as a reagent directing the structure and provide the alkalinity necessary for the crystallization of the zeolite. [2] Many researchers have proposed other structuring agents cheaper than TPAOH, which takes the same cation TPA^+ . [3],[4]-[5]

To reduce the cost of synthesizing TS-1, many efforts have been made to use inexpensive small organic amines as a template instead of expensive TPAOH. Although the use of small inexpensive organic amines devices to replace the expensive TPAOH, such as TPABr, ammonia, diethylamine, hexanediamine, ethylenediamine, n-butylamine, is a promising strategy for the synthesis of low-cost TS-1. [6]-[7]

TS-1 can prepared also with tetrapropylammonium bromide (TPA-Br) as template. Mueller and al [8] and Gang and al [9] synthesized TS-1 in the presence of TPABr as organic structuring agent using ammonia as source of alkali, the size of the zeolite obtained was often greater than 10 μ m, much larger than that typical of TS-1 synthesized using TPAOH as a structuring agent, so micronuclei were obtained [11]-[12] what is undesirable. Zuo and al. demonstrated synthesis of the TS-1 with crystal size of 200 nm using the TPA-Br. [10]

The formation of microporous materials in the presence of diethylamine (DEA) as an organic template is favored by static conditions, high concentrations of DEA and a low temperature (393 K). The role of diethylamine is extended to the stabilization of nuclei.[13]

The hydrophilic / hydrophobic balance is illustrated by the work of Brukett and Davis on the synthesis of the MFI type zeolite in the presence of tetrapropylammonium cation (TPA⁺) as an organic structuring agent. According to the authors, the organic species must not be too hydrophilic to be able to present structuring properties, they also introduce the concept of "hydration ,hydrophobic ». [14]-[15]

The structuring agents can play different roles such as: compensation action of the negative charge of the mineral framework (case of silico aluminophosphates for example), action of filling the microporosity, structuring action ("template" effect) by a preorganization of the mineral species around the organic entity and / or orientation of the crystallization by adaptation to the shape and symmetry of the organic entity, chemical action by modifying the properties of the gel and / or the solution (hydrophilic or hydrophobic nature of the organic entity). Organic species) and thermodynamic action, in particular by the stabilization of construction units.

In this study, we are interested in the preparation of titatium silicalite-1 from aqueous solutions of tetrapropylammonium hydroxide or bromide (TPAOH, TPABr), diethylamine (DEA), ortho phenylenediamine (C₆H₈N₂(o)) as structuring agents, the synthesis protocol of titanium silicalite-1 is carried out under conditions of crystallization temperature greater than 100°C and crystallization time at 24 hours.

2. EXPERIMENTAL

2.1 TS-1 synthesis conditions

We report the conditions (a temperature of 175°C and a crystallization time of 24 hours) of synthesis of TS-1 in Table 1.

Table 1: TS-1 synthesis conditions.

Silicalite-1 incorporated in titanium	Molar compositions	Crystallization time	Crystallization temperature
MS1	.1Na ₂ O-DEA-SiO ₂ -0.01TiO ₂ - 15H ₂ O	24 hours	175°C
MS2	KF-0.08TPAOH-SiO ₂ -	24 hours	175°C

0.01TiO ₂ -20H ₂ O			
MS3	DEA-0.04TPABr-SiO ₂ -	24 hours	175°C
0.01TiO ₂ -13H ₂ O			
MS4	0.1	24 hours	175°C
a ₂ O-0.1C ₆ H ₈ N ₂ (o)-SiO ₂ -			
0.01TiO ₂ -7H ₂ O			

2.2 TS-1 synthesis procedure

For the synthesis of TS-1, we introduce in a beaker successively, 7.5g of Ludox, 4.41g of water, we add 3.65g of DEA, 0.55 g KOH and 0.057 g of TiO₂ with strong stirring up to obtaining a gel for 2 hours and at room temperature (25 ° C.). This gel of molar composition: 0.1 K₂O-DEA-SiO₂-0.01TiO₂-10H₂O is transferred into an autoclave which will subsequently be placed in an oven heated to 175 ° C. After a period of crystallization of 24 hours the autoclave is cooled, the recovered product is filtered, washed several times with distilled water and dried at 80 ° C, this is applied to the synthesis of all the materials (MS1, MS2, MS3 and that of MS4). To release the pores of the synthesized material, the final product is calcined at a temperature of 550 ° C for 6 hours. We adopt the same process of synthesis for all samples.

3. CHARACTERIZATION OF TS-1

Silicalite incorporated into titanium synthesized using diethylamine (DEA), tetrapropylammonium hydroxide or bromide (TPAOH, TPABr) and ortho phenylenediamine (C₆H₈N₂) as a structuring agents was characterized by X-ray fluorescence, X-ray diffraction, IR spectroscopy and visible UV spectroscopy.

3.1 X-ray fluorescence of TS-1

The X-ray fluorescence of TS-1 synthesized from the DEA as a structuring agent showed that 43.60% of titanium species were incorporated, 52% of titanium species for that synthesized with TPAOH and 49.26% of titanium species incorporated. with the TPABr. Table 2 collates the values of the molar ratios of the TS-1 given by FX.

Table 2: Molar ratios of the TS-1 given by FX.

TS-1	Molar ratio			Molar ratio of TS-1 given by FX
	Ti/Si	SA	SA/Si	

				Ti	Si	Ti/Si
MS1	0.01	DEA	1	0.28	41.30	0.0043
MS2	0.01	TPAOH	0.08	0.33	45.48	0.0052
MS3	0.01	TPABr	0.4	0.30	45.10	0.0049

SA: structuring agent

3.2 X-ray diffraction of TS-1

On the diffractograms of the samples (MS1, MS2 and MS3) (Figure 1), we observe the peaks at $2\theta = 23.09, 23.29, 23.68, 23.92$ and 24.3° . These values are consistent with those published by IZA (International Zeolite Association). [16]

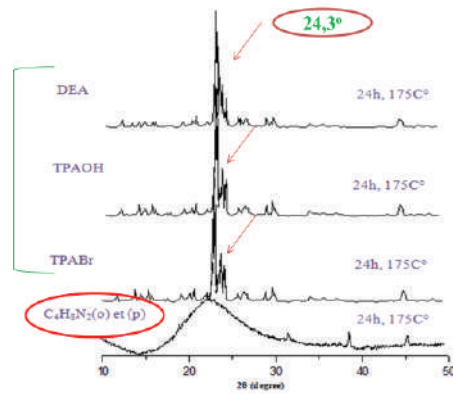


Figure 1: Diffractograms of TS-1 (MS1,MS2,MS3 and MS4).

TS-1 crystallizes in the orthorhombic system [17], let us note that the diffraction peak at $2\theta = 24.3^\circ$ in the XRD diagram indicates the change of the monoclinic symmetry of Silicalite-1 (S-1) towards symmetry. orthorhombic of TS-1. [18] No significant diffraction peak was observed at 2θ of 25.4° for all of the samples, which indicated the absence of crystalline of TiO_2 . [19]

The relative crystallinity of the samples (MS1, MS2, MS3 and MS4) is based on the three characteristic peaks of the MFI type zeolite at Bragg angles $2\theta = 23, 24$ and 24.5° . [20] The sample for which the sum of the diffraction intensities ($I_{23^\circ} + I_{24^\circ} + I_{24.5^\circ}$) sample is the highest is considered as a reference product, that is to say having a 100%

$$\text{Relative crystallinity (\%)} = \frac{(I_{23^\circ} + I_{24^\circ} + I_{24.5^\circ}) \text{ sample}}{(I_{23^\circ} + I_{24^\circ} + I_{24.5^\circ}) \text{ reference}}$$

The results of the relative crystallinity, calculated from the previous formula are presented in Figure 2.

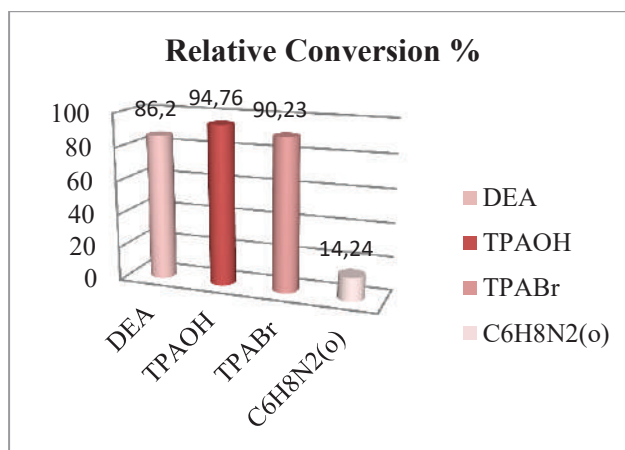


Figure 2: The relative crystallinity of the samples using DEA, TPAOH, TPABr and C₆H₈N₂(o) as organic structurants.

3.3 Infra Red Spectroscopy (FT-IR)

The FT-IR spectra of the samples, MS3, MS6, ME3 and MF3 (are shown in Figure 3) synthesized with the various structuring agents (diethylamine, tetrapropylammonium hydroxide and tetrapropylammonium bromide) have vibration bands at 1230, 1100, 800, 550 and 450 cm⁻¹.

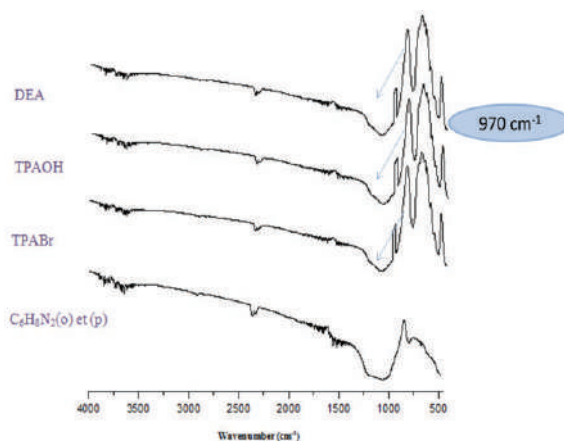


Figure 3: IR spectra of TS-1.

The asymmetric elongation of Si-O-Si is attributed to adsorption band 1100 and 1230 cm⁻¹. The absorption band around 552 and 457 cm⁻¹ is attributed to the rocking vibration of Si-O-Si. [21] The absorption bands at 1230 and 547 cm⁻¹ are assigned to the characteristic vibration of the tetrahedral structure of the MFI type zeolite. [22]

The absorption band that appears at 970 cm⁻¹ indicates the presence of titanium atoms in the structure of TS-1 [23], this band corresponds to the vibration mode of the Si-O group of [SiO₄] bonded to atoms

Ti (IV) with tetrahedral coordination [16] and is assigned to the asymmetric elongation of the vibration mode of the Si-O-Ti bridge according to Boccuti and Thangaraj et al. [24]-[25]

As shown in Figure 3, the bands at 553 cm^{-1} and 965 cm^{-1} demonstrate the successful incorporation of Ti into the MFI framework of the TS-1. [19]

3.4 UV visible spectroscopy

The UV-vis spectra of TS-1 shown in Figure 4 show a similar form published in the literature for this type of zeolite. [26]-[27] The intense band at 212 nm corresponds to a charge transfer transition involving tetra-coordinate sequences isolated from Ti^{4+} ions and oxygen atoms of the Ti-O-Si species of the zeolite. [24],[28]-[29] The absence of peaks at 260-270 nm indicates a large ordered arrangement of Ti-O-Si bonding. [30]

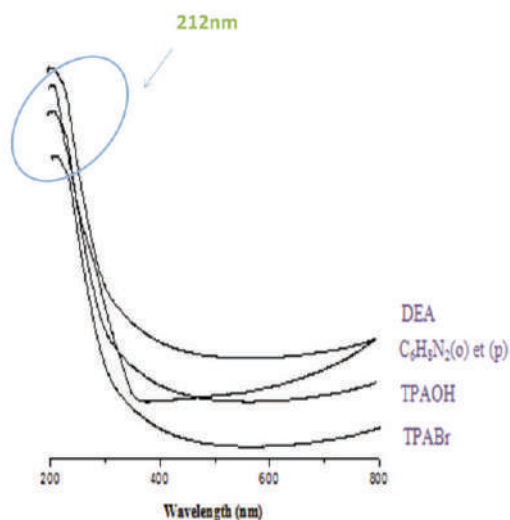


Figure 4: Visible UV spectra of TS-1

Conclusion

According to the results obtained, in this part of the synthesis of materials incorporated on the transition metal (titanium, Ti), in the presence of the different structuring agents, we can say that the materials synthesized using diethylamine (DEA), tetrapropylammonium hydroxide (TPAOH) and tetrapropylammonium bromide (TPABr) as organic structuring agents, allowed us to have well crystalline silicic zeolites of MFI type structure. This is confirmed by :

- The diffractograms of these materials which indicate the presence of characteristic peaks appearing at $2\theta = 23.09, 23.29, 23.68, 23.92$ and 24.3° . These materials have a high relative crystallinity (86.20%, 94.76% and 90.23%).
- The presence of absorption bands at 1230 and 547 cm^{-1} are assigned to the characteristic vibration of the tetrahedral structure of the MFI type. This was given by infrared spectroscopy.
- Appearance of the intense band at 212 nm in UV-Vis. spectrum which corresponds to silicalite incorporated in titanium.

On the other hand, the synthesis of titanium silicalite-1 in the presence of organic molecule, ortho phenylenediamine ($C_6H_8N_2$) as structuring agent, gave us poorly crystallized material with an amorphous structure. This material has a low relative crystallinity (14.24%).

References

- [1] M. Taramasso, G. Perego and B. Notari, US Pat., US4410501, 1983.
- [2] M. Taramasso, G. Perego, and B. Notari, US 4 410 501, 1983.
- [3] Y. Zuo, M. Liu, T. Zhang, C. Meng, X. Guo and C. Song, ChemCatChem, 2015, pp 2660–2668, 7. DOI: 10.1002/cctc.201500440
- [4] U. Müller and W. Steck, Studies in Surface Science and Catalysis, 1994, pp 203–210, 84. DOI: 10.1016/S0167-2991(08)64115-4
- [5] P. Chen, X. Chen, X. Chen and H. Kita, Journal of Membrane Science., 2009, pp 369–378, 330. DOI.org/10.1016
- [6] Li, G.; Guo, X.; Wang, X.; Zhao, Q.; Bao, X.; Han, X.; Lin, L. Applied Catalysis A: General 1999, pp 11–18, 185. DOI : org/10.1016/S0926-860X(99)00115-5
- [7] Iwasaki, T.; Isaka, M.; Nakamura, H.; Yasuda, M.; Watano, S. Microporous Mesoporous Mater. 2012, pp 1–6, 150. DOI :org/10.1016/j.micromeso.2011.09.023
- [8] Müller, U.; Steck, W. Ammonium-Based Alkaline-Free Synthesis of MFI-Type Boron and Titanium Zeolites. In Stud. Surf. Sci. Catal.; Weitkamp, J., Karge, H. G., Pfeifer, H., Hölderich, W., Eds.; Elsevier: Amsterdam, 1994; pp 203–210, 84,. DOI : org/10.1016/S0167-2991(08)64115-4 Studies in Surface Science and Catalysis
- [9] Gang, L.; Xinwen, G.; Xiangsheng, W.; Qi, Z.; Xinhe, B.; Xiuwen, H.; Liwu, L. Synthesis of Titanium Silicalites in Different Template Systems and Their Catalytic Performance. Applied Catalysis A: General. 1999, pp 11–18, 185 (1),. DOI: 10.1016/S0926-860X(99)00115-5.
- [10] Zuo, Y.; Liu, M.; Zhang, T.; Meng, C.; Guo, X.; Song, C. Enhanced Catalytic Performance of Titanium Silicalite-1 in Tuning the Crystal Size in the Range 1200–200 Nm in a Tetrapropylammonium Bromide System. ChemCatChem. 2015, pp 2660–2668, 7 . DOI: 10.1002/cctc.201500440.
- [11] Wang X S, Guo X W. Catalysis Today, 1999, pp 177-186 , 51, DOI : org/10.1016/S0920-5861(99)00020-6
- [12] Tuel A. Zeolites, 1996, pp 108-117, 16,. DOI : org/10.1016/0144-2449(95)00109-3
- [13]. N.R .Forbes, L.V.C. Rees. Zeolites. 1995, pp 452–459, 15. DOI: org/10.1016/0144-2449(95)00016-Y
- [14] S.L. Burkett, M.E. Davis, Chemistry of Materials. 1995, pp 1453-1463, 7. DOI : 10.1021/cm00056a009
- [15]. S.L. Burkett, M.E. Davis, Chemistry of Materials. 1995, pp 920-928, 7. DOI : 10.1021/cm00053a017
- [16] M.M.J. Treacy, J.B. Higgins, Collection of Simulated XRD Powder Patterns for Zeolites, 4th edition, Structure Commission of the International Zeolite Association, Elsevier, Amsterdam, 2001, p.367.
- [17] Y. G. Li, Y. M. Lee and J. F. Porter, Journal of Materials Science, 2002, pp 1959-1965, 37.
- [18] VAN-HUY NGUYEN, HSIANG-YU CHAN and JEFFREY C S WU Journal of Chemical Sciences 2013, pp 859–867, 125. DOI: 10.1007/s12039-013-0449-z
- [19] Catalysts 0800049 v2 2018 Yuecheng Luo, Jiahui Xiong, Conglin Pang, Guiying Li * and Changwei Hu * Catalysts 2018, 8, 1-14, 49. DOI:10.3390/catal8020049

-
- [20] C.P. Nicolaidis, *Applied Catalysis A: General* 1999, pp 211-217, 185. doi.org/10.1016/S0926-860X(99)00112-X
- [21] M.C. Capel-Sanchez, V.A. dela Pena-O'Shea, L. Barrio, J.M. Compos-Martin, J.L.G. Fierro, *Top. Catal.* 2006, pp 27-34, 41 . DOI: 10.1007/s11244-006-0091-9 *Topics in Catalysis*
- [22] R.S. Drago, S.C. Dias, J.M. McGilvray, A.L.M.L. Mateus, *J. Phys. Chem. A* 1998, pp 1508–1514, 102. **DOI:** 10.1021/jp973249k *Physical Chemistry B*
- [23] J F .Bengoa, N G .Gallegos, S G .Marchetti, A M .Alvarez, M V .Cagnoli, A A.Yeramian, *Micropor, Mesopor, Mater*, 1998, pp 163-172, 24 . Bengoa, J.F., Gallegos, N.G, Marchetti, S.G, Alvarez, A.M., Cagnoli, M.V., Yeramian, A.A., “Influence of TS-1 structural properties and operation conditions on venzene catalytic oxidation with H₂O₂.”, *Microporous and Mesoporous Materials*. 1998, pp 163-172, 24, DOI:10.1016/S1387-1811(98)00157-7
- [24] M.R. Boccuti, K.M. Rao, A. Zecchina, G. Leofanti, G. Petrini, *Studies in Surface Science and Catalysis*. 1989, pp 133-144 ,48 , doi.org/10.1016/S0167-2991(08)60677-1
- [25] A. Thangaraj, R. Kumar, S.P. Mirajkar, P. Ratnasamy, *Chin. J. Catal.* 1991, 130, 1-8. doi.org/10.1016/0021-9517(91)90086-J
- [26]. G N .Vayssilov, *Catal. Rev.-Sci. Eng.* 1997,pp209-251,39. *Catalysis Reviews. Science and Engineering*. DOI:10.1080/01614949709353777
- [27]. J H C .Van Hooff, J W.Roelofsen, H .Van Bakkum, E M .Flanigen, J C Jansen,.Elsevier, Amsterdam, *Stud. Surf.Sci. Catal*, 1991 ,58.
- [28]. W .Zhang, M .Froba, J .Wang, P T .Tanev, J .Wong, T J .Pinnavaia, *J. Am ChemSoc*, 1996, pp 9164-9171, 118,. **DOI:** 10.1021/ja960594z *Journal. American Chemical Society*,
- [29]. S .Baweked, Q .He, N F .Dummer, A F .Carly, DW .Knight, D .Bethell, C J .Kiely, G J .Hutchings, *Catal. Sci. Technol*, 2011, pp 747-759,1. **DOI:** 10.1039/C1CY00122A *Catalysis Science & Technology*
- [30]. J A .Martens, D.De Vos, C E A .Kirschhock, P P.Pescarmona, B .Sels,.Vankelecom I F J. *Topics in Catalysis.*, 2009, pp 1119–1130, 52. DOI: 10.1007/s11244-009-9279-0)
-

SYNTHESIS AND CHARACTERIZATION OF NEW 1-(4-AMINOCARBONYLPYPERIDIN-4-YL-METHYL)-3-ALKYL(ARYL)-4-(3-METHOXY-4-ISOBUTYRYLOXY-BENZYLIDENEAMINO)-4,5-DIHYDRO-1H-1,2,4-TRIAZOLE-5-ONES

Dr. Öğr. Üyesi Sevda MANAP

Kafkas University, Department of Chemistry, Kars/Turkey

ORCID NO: 0000-0002-5025-9622

Prof. Dr. Haydar YÜKSEK

Kafkas University, Department of Chemistry, Kars/Turkey

ORCID NO: 0000-0003-1289-1800

ABSTRACT

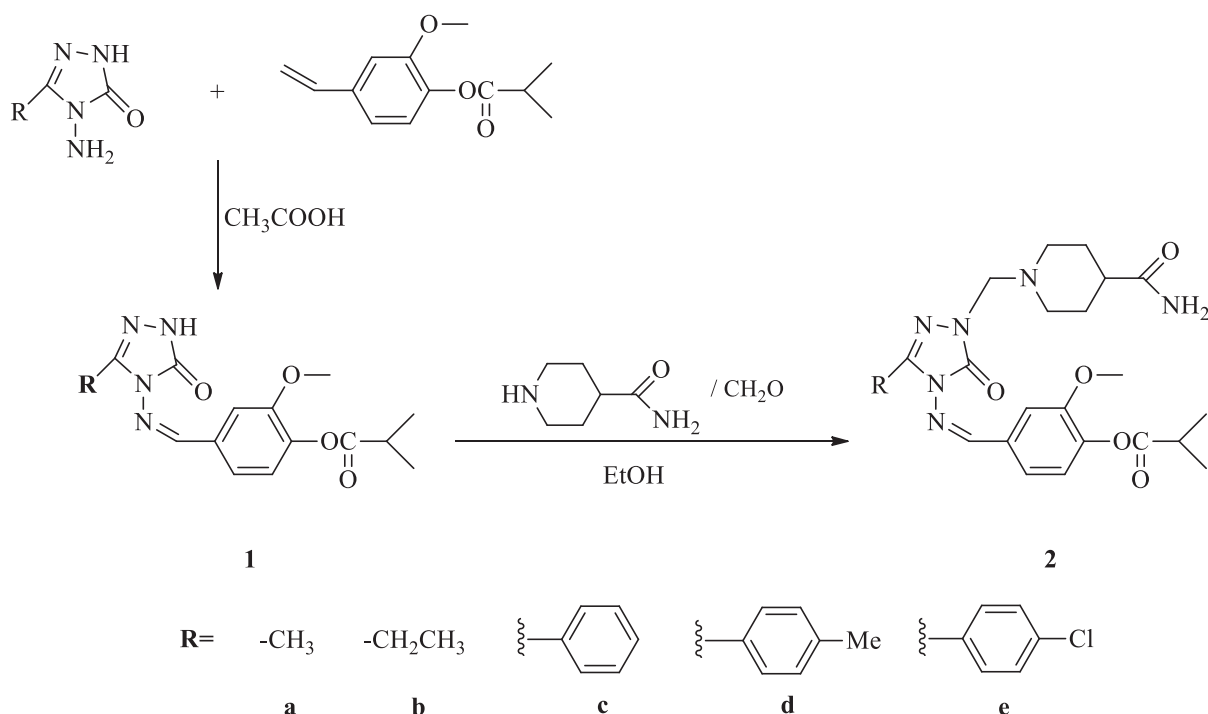
In the present study, 3-alkyl(aryl)-4-(3-methoxy-4-isobutyryloxy benzylidene amino)-4,5-dihydro-1H-1,2,4-triazol-5-ones (**1**) reacted with 4-piperidinecarboxamide in the presence of formaldehyde to obtain five novel 1-(4-aminocarbonylpiperidin-4-yl-methyl)-3-alkyl(aryl)-4-(3-methoxy-4-isobutyryloxy-benzylideneamino)-4,5-dihydro-1H-1,2,4-triazole-5-ones (**2**). The structures of compounds **2** were established from IR, ¹H NMR and ¹³C NMR spectral data.

Keywords: 1,2,4-Triazol-5-one, Schiff base, Mannich base, Synthesis, Characterization

INTRODUCTION

Triazoles are heterocyclic compounds that contain three nitrogen atoms. Some modern medicines contain triazole moieties. 1,2,4-Triazole derivatives have been found to have a broad spectrum of biological activities. The classical Mannich reaction, a three-component condensation between structurally diverse substrates containing at least one active hydrogen atom, an aldehyde component and an amine reagent leads to a class of compounds known as Mannich bases (Roman, 2015). Mannich bases have practices in the pharmaceutical field and another industries, like petroleum, the cosmetics, the dyes and the food industries, etc. The primary advantage of the Mannich reaction is that it permits two different molecules to be bonded together in one step (Tramontini and Angiolini, 1994). Mannich bases obtained from 1,2,4-triazole derivatives have been reported to possess biological activities including antilipase, antioxidant, antibacterial, and antifungal features (Manap et al., 2020; Ceylan, 2016; Wang et al., 2017).

Making use of the Mannich reaction we got a series of new derivatives containing a 4-piperidinecarboxamide substituent coupled with a 1,2,4-triazole ring. In this paper, the synthesis of 5 novel 1-(4-aminocarbonylpiperidin-4-yl-methyl)-3-alkyl(aryl)-4-(3-methoxy-4-isobutyryloxy-benzylideneamino)-4,5-dihydro-1H-1,2,4-triazole-5-ones (**2a-e**) were synthesized by the reactions of 3-alkyl(aryl)-4-(3-methoxy-4-isobutyryloxy benzylidene amino)-4,5-dihydro-1H-1,2,4-triazol-5-ones (**1a-e**) with formaldehyde and 4-piperidinecarboxamide (Scheme 1).



Scheme 1. Synthesis pathway of compounds **2**

EXPERIMENTAL

Chemical reagents and all solvents used in this study were purchased from Merck AG, Aldrich and Fluka. Melting points which were uncorrect were determined in open glass capillaries using an Stuart SMP30 digital melting point apparatus. The IR spectra were obtained on a ALPHA-P BRUKER FT-IR spectrometer. ^1H and ^{13}C NMR spectra were recorded in deuterated dimethyl sulfoxide with TMS as internal standard using a BRUKER ULTRASHIELD PLUS BIOSPIN spectrometer at 400 MHz and 10 MHz, respectively.

General procedure for the synthesis of 1-(4-aminocarbonylpiperidin-4-yl-methyl)-3-alkyl(aryl)-4-(3-methoxy-4-isobutyryloxy-benzylideneamino)-4,5-dihydro-1H-1,2,4-triazole-5-ones (**2**)

The corresponding compound **1** (5 mmol) (Manap, 2017) has been dissolved in 100 mL of ethanol followed by addition of piperidine-4-carboxamide (0.05 mol) and formaldehyde (37%, 10 mmol). The reaction mixture has been refluxed for 3 hours. After standing at RT overnight, the solid has been filtered and crystallized from ethanol. The solid has been recrystallized from the same solvent and purified by drying *in vacuo* to obtain pure compounds **2** as white crystals.

1-(4-aminocarbonylpiperidin-4-yl-methyl)-3-methyl-4-(3-methoxy-4-isobutyryloxy-benzylideneamino)-4,5-dihydro-1H-1,2,4-triazole-5-ones (2a)

White solid. Yield: 72 %; mp; 181°C. **IR (cm⁻¹):** 3412 and 3288 (NH₂), 1755, 1700, 1644 (C=O), 1619, 1580 (C=N), 1240 (COO). **¹H-NMR (400 MHz, DMSO-*d*₆) δ:** 1.24 (d, 6H, 2CH₃; *J* = 6.80 Hz), [1.49-1.55 (m, 2H), 1.67 (d, 2H; *J* = 10.80 Hz), 1.96 (m, 1H), 2.25-2.29 (m, 2H), 2.91 (d, 2H; *J* = 11.60 Hz)] (Piperidine H), 2.31 (s, 3H, CH₃), 2.84 (hept, 1H, CH; *J* = 7.20 Hz), 3.84 (s, 3H, OCH₃), 4.53 (s, 2H, NCH₂N), [6.71 (s, 1H, NH), 7.15 (s, 1H, NH)] (NH₂), 7.22 (d, 1H, ArH; *J* = 8.40 Hz), 7.46 (dd, 1H, ArH; *J* = 8.00, 1.60 Hz), 7.59 (d, 1H, ArH; *J* = 1.60 Hz), 9.70 (s, 1H, N=CH); **¹³C-NMR (100 MHz, DMSO-*d*₆) δ:** 10.94 (CH₃), 18.72 (2CH₃), [28.41 (2CH₂), 41.08 (CH), 49.72 (2CH₂)] (Piperidine C), 33.15 (CH), 56.05 (OCH₃), 66.33 (NCH₂N), [111.82(CH), 120.63(CH), 123.38(CH), 132.16(C), 142.06 (C), 150.21 (C)] (ArC), 142.90 (Triazole C₃), 151.32 (N=CH), 153.65 (Triazole C₅), 174.19 (COO), 176.37 (CONH₂).

1-(4-aminocarbonylpiperidin-4-yl-methyl)-3-ethyl-4-(3-methoxy-4-isobutyryloxy-benzylideneamino)-4,5-dihydro-1H-1,2,4-triazole-5-ones (2b)

White solid. Yield: 73 %; mp; 183°C. **IR (cm⁻¹):** 3404 and 3191 (NH₂), 1757, 1696, 1648 (C=O), 1593, 1574 (C=N), 1267 (COO). **¹H-NMR (400 MHz, DMSO-*d*₆) δ:** 1.21-1.23 (m, 3H, CH₂CH₃), 1.24 (d, 6H, 2CH₃; *J* = 6.80 Hz), [1.49-1.53 (m, 2H), 1.67 (d, 2H; *J* = 10.80 Hz), 1.97 (m, 1H), 2.25-2.30 (m, 2H), 2.92 (d, 2H; *J* = 11.60 Hz)] (Piperidine H), 2.74 (q, 2H, CH₂CH₃; *J* = 7.20 Hz), 2.84 (hept, 1H, CH; *J* = 6.80 Hz), 3.83 (s, 3H, OCH₃), 4.55 (s, 2H, NCH₂N), [6.71 (s, 1H, NH), 7.15 (s, 1H, NH)] (NH₂), 7.22 (d, 3H, ArH; *J* = 8.00 Hz), 7.46 (dd, 1H, ArH; *J* = 8.40, 1.60 Hz), 7.58 (d, 1H, ArH; *J* = 2.00 Hz), 9.69 (s, 1H, N=CH); **¹³C-NMR (100 MHz, DMSO-*d*₆) δ:** 10.01 (CH₂CH₃), 18.38 (CH₂CH₃), 18.73 (2CH₂), [28.41 (2CH₂), 41.09 (CH), 49.74 (2CH₂)] (Piperidine C), 33.18 (CH), 56.04 (OCH₃), 66.37 (NCH₂N), [111.58 (CH), 120.53 (CH), 123.41 (CH), 132.20 (C), 142.06 (C), 150.35 (C)] (ArC), 146.64 (Triazole C₃), 151.32 (N=CH), 153.66 (Triazole C₅), 174.20 (COO), 176.37 (CONH₂).

1-(4-aminocarbonylpiperidin-4-yl-methyl)-3-benzyl-4-(3-methoxy-4-isobutyryloxy-benzylideneamino)-4,5-dihydro-1H-1,2,4-triazole-5-ones (2c)

White solid. Yield: 76 %; mp; 172°C. **IR (cm⁻¹):** 3370 and 3190 (NH₂), 1762, 1711, 1648 (C=O), 1603, 1582 (C=N), 1244 (COO), 757 and 704 (monosubstituted benzenoid ring). **¹H-NMR (400 MHz, DMSO-*d*₆) δ:** 1.24 (d, 6H, 2CH₃; *J* = 6.80 Hz), [1.53-1.54 (m, 2H), 1.67 (m, 2H), 1.98 (m, 1H), 2.29-2.30 (m, 2H), 2.93 (d, 2H; *J* = 11.60 Hz)] (Piperidine H), 2.83 (hept, 1H, CH₃; *J* = 6.80 Hz), 3.83 (s, 3H, OCH₃), 4.11 (s, 2H, CH₂Ph), 4.58 (s, 2H, NCH₂N), [6.72 (s, 1H, NH), 7.17 (s, 1H, NH)] (NH₂), 7.19-7.25 (m, 2H, ArH), 7.30-7.35 (m, 4H, ArH), 7.38 (dd, 1H, ArH; *J* = 8.00, 1.60 Hz), 7.49 (d, 1H, ArH; *J* = 2.00 Hz), 9.64 (s, 1H, N=CH); **¹³C-NMR (100 MHz, DMSO-*d*₆) δ:** 18.72 (2CH₃), [28.42 (2CH₂), 41.09 (CH), 49.75 (2CH₂)] (Piperidine C), 31.05 (CH₂Ph), 33.17 (CH), 56.01 (OCH₃), 66.46 (NCH₂N), [110.73 (CH), 121.19 (CH), 123.35 (CH), 132.14 (C), 142.08 (C), 150.24 (C)] (Ar-C), [126.76 (CH), 128.52 (2CH), 128.82 (2CH), 135.76 (C)] (C3 linked to ArC), 144.72 (Triazole C₃), 151.29 (N=CH), 152.97 (Triazole C₅), 174.20 (COO), 176.35 (CONH₂).

*1-(4-aminocarbonylpiperidin-4-yl-methyl)-3-(*p*-methylbenzyl)-4-(3-methoxy-4-isobutyryloxy-benzylideneamino)-4,5-dihydro-1H-1,2,4-triazole-5-ones (2d)*

White solid. Yield: 71 %; mp; 166°C. **IR (cm⁻¹):** 3364 and 3192 (NH₂), 1756, 1709, 1649 (C=O), 1604, 1583 (C=N), 1239 (COO), 812 (1,4-disubstituted benzenoid ring). **¹H-NMR (400 MHz, DMSO-*d*₆) δ:** 1.24 (d, 6H, 2CH₃; *J* = 6.80 Hz), [1.50-1.53 (m, 2H), 1.68 (d, 2H; *J* = 10.40 Hz), 1.97 (m, 1H), 2.28-2.31 (m, 2H), 2.93 (d, 2H; *J* = 11.20 Hz)] (Piperidine H), 2.25 (s, 3H, PhCH₃), 2.84 (hept, 1H, CH; *J* = 6.80 Hz), 3.83 (s, 3H, OCH₃), 4.05 (s, 2H, CH₂Ph), 4.58 (s, 2H, NCH₂N), [6.72 (s, 1H, NH), 7.17 (s, 1H, NH)] (NH₂), 7.12 (d, 2H, ArH; *J* = 8.00 Hz), 7.20 (d, 2H, ArH; *J* = 8.00 Hz), 7.22 (d, 1H, ArH; *J* = 7.20 Hz), 7.38 (dd, 1H, ArH; *J* = 8.40, 2.00 Hz), 7.50 (d, 1H, ArH; *J* = 1.60 Hz), 9.64 (s, 1H, N=CH); **¹³C-NMR (100 MHz, DMSO-*d*₆) δ:** 18.72 (2CH₃), 20.57 (PhCH₃), [28.42 (2CH₂), 41.09 (CH), 49.75 (2CH₂)] (Piperidine C), 30.66 (CH₂Ph), 33.18 (CH), 55.99 (OCH₃), 66.44 (NCH₂N), [110.72 (CH), 121.20 (CH), 123.36 (CH), 132.16 (C), 142.08 (C), 150.23 (C)] (ArC), [128.49 (2CH), 129.08 (2CH), 132.62 (C), 135.86 (C)] (C3 linked to ArC), 144.86 (Triazole C₃), 151.29 (N=CH), 152.91 (Triazole C₅), 174.20 (COO), 176.35 (CONH₂).

1-(4-aminocarbonylpiperidin-4-yl-methyl)-3-(p-chlorobenzyl)-4-(3-methoxy-4-isobutyryloxy-benzylideneamino)-4,5-dihydro-1H-1,2,4-triazole-5-ones (2e)

White solid. Yield: 77 %; mp; 186°C. **IR (cm⁻¹):** 3359 and 3185 (NH₂), 1756, 1716, 1646 (C=O), 1598, 1577 (C=N), 1234 (COO), 802 (1,4-disubstituted benzenoid ring). **¹H-NMR (400 MHz, DMSO-*d*₆) δ:** 1.24 (d, 6H, 2CH₃; *J* = 7.20 Hz), [1.50-1.54 (m, 2H), 1.68 (d, 2H; *J* = 10.40 Hz), 1.98 (m, 1H), 2.26-2.29 (m, 2H), 2.92 (d, 2H; *J* = 11.20 Hz)] (Piperidine H), 2.84 (hept, 1H, CH; *J* = 7.20 Hz), 3.83 (s, 3H, OCH₃), 4.12 (s, 2H, CH₂Ph), 4.58 (s, 2H, NCH₂N), [6.73 (s, 1H, NH), 7.17 (s, 1H, NH)] (NH₂), 7.21 (d, 1H, ArH; *J* = 8.40 Hz), 7.35-7.41 (m, 5H, ArH), 7.48 (d, 1H, ArH; *J* = 2.00 Hz), 9.65 (s, 1H, N=CH); **¹³C-NMR (100 MHz, DMSO-*d*₆) δ:** 18.72 (2CH₃), [28.41 (2CH₂), 41.05 (CH), 49.72 (2CH₂)] (Piperidine C), 30.53 (CH₂Ph), 33.18 (CH), 56.02 (OCH₃), 66.49 (NCH₂N), [110.80 (CH), 121.17 (CH), 123.36 (CH), 132.27 (C), 142.12 (C), 150.22 (C)] (ArC), [128.38 (2CH), 130.74 (2CH), 131.49 (C), 134.86 (C)] (C3 linked to ArC), 144.38 (Triazole C₃), 151.30 (N=CH), 153.12 (Triazole C₅), 174.19 (COO), 176.36 (CONH₂).

RESULTS AND DISCUSSION

In the present study, new 1,2,4-triazole derivatives (**2a-2e**) were designed and synthesized. The new synthesized compounds were identified using spectral data (IR, ¹H NMR and ¹³C NMR).

REFERENCES

- Ceylan, S. (2016). Synthesis and biological evaluation of new Mannich and Schiff bases containing 1,2,4-triazole and 1,3,4-oxadiazole nucleus. *Medical Chemistry Research*. 25, 1958–1970.
- Manap, S. (2017). Bazı vanilin türevlerinin 3-Alkil(Aril)-4-amino-4,5-dihidro-1*H*-1,2,4-triazol-5-on'lar ile reaksiyonlarının incelenmesi. Doktora Tezi, Kafkas Üniversitesi Fen Bilimleri Enstitüsü, Kars.
- Manap, S., Gursoy-Kol, Ö., Alkan, M. and Yüksek, H. (2020). Synthesis, *in vitro* antioxidant and antimicrobial activities of some novel 3-substitued-4-(3-methoxy-4-isobutyryloxybenzylideneamino)-4,5-dihydro-1*H*-1,2,4-triazol-5-one derivatives. *Indian Journal of Chemistry*. 59B, 271-282.
- Roman, G. (2015). Mannich bases in medicinal chemistry and drug design. *European Journal of Medicinal Chemistry*, 89(2015), 743-816.
- Tramontini, M. and Angiolini, L. (1994). *Mannich Bases: Chemistry and Uses*, CRC Press, Boca Raton, Florida, USA, p. 2.
- Wang, B.L., Zhang, L.Y., Liu, X.H., Ma, Y., Zhang, Y., Li, Z.M. and Zhang, X. (2017). *Bioorganic and Medicinal Chemistry Letters*. 27, 5457-5462.

ESTUDIO DE ESPECTROSCOPIA FTIR DE EXTRACTOS DE HOJAS DE PISTACIA LENTISCUS

Hayat Jaadan

Université Mohamed Premier, Faculté Pluridisciplinaire de Nador, Département Biologie-
Géologie, Laboratoire OLMAN-RL, BP300, Selouane, 62702 Nador

Ecole Nationale d'Agriculture de Meknès, Département de Protection des Plantes et de
l'Environnement, BP S/40 50 000 Meknès-Maroc

Mustafa Akodad

Université Mohamed Premier, Faculté Pluridisciplinaire de Nador, Département Biologie-
Géologie, Laboratoire OLMAN-RL, BP300, Selouane, 62702 Nador

Saadia Belmalha

Ecole Nationale d'Agriculture de Meknès, Département de Protection des Plantes et de
l'Environnement, BP S/40 50 000 Meknès-Maroc

Pistacia lentiscus L. es una importante planta medicinal, perteneciente a la familia de las Anacardiáceas (Pistaciaceae), conocida como "drou" en árabe local, y "Fadhiss" en amazigh y utilizada en el tratamiento de diferentes enfermedades y problemas.

Para estudiar la composición química de los extractos de las hojas de *Pistacia Lentiscus* L, cosechadas en el Cabo de las Tres Horcas en el Noreste de Marruecos, se escanearon los diferentes extractos en el rango de longitud de onda de 8.300 - 350 cm⁻¹ con una resolución de 0,5 cm⁻¹ utilizando el espectrómetro FTIR Spectrum Two Perkinelmer y se detectaron los picos característicos y sus grupos funcionales. Se registraron los valores de los picos FTIR. Cada análisis se repitió tres veces para la confirmación del espectro.

Los resultados del espectro FTIR obtenidos en este estudio demostraron señales de absorción para rangos de números de onda múltiples, que se identificaron en la composición de grupos funcionales del extracto de hidrolato, metanol, acetato de etilo de alcohol y fenoles (O-H), ácidos carboxílicos (estiramiento de C-O), grupo metilo y aldehído (estiramiento de enlaces C-H), estiramiento de C=O (grupo aldehído), alquenos (estiramiento de C=C), aminas y amidas (flexión de N-H), nitro (N=O) y aromáticos (estiramiento de C-C).

EFFECTO DEL ADICIONADO DE ADITIVOS Y HARINA DE CHIA EN LA INDUSTRIA AVICOLA ARGENTINA

Hebe FERNÁNDEZ

Universidad Nacional del Sur, Departamento de Agronomía, Bahía Blanca,
Buenos Aires, Argentina.

Angelo MAZZOCCHI

Universidad Nacional del Sur, Departamento de Agronomía, Bahía Blanca,
Buenos Aires, Argentina.

Dardo CÓCCARO

Universidad Nacional del Sur, Departamento de Agronomía, Bahía Blanca,
Buenos Aires, Argentina.

Carmen Salerno

Universidad Nacional del Sur, Departamento de Agronomía, Bahía Blanca,
Buenos Aires, Argentina.

RESUMEN

La harina de chía (HC) es una fuente importante de ácidos grasos poliinsaturados omega n-3 (AGPI) con beneficios sobre el crecimiento aviar. Sin embargo, estos AGPI aumentan la susceptibilidad a la peroxidación lipídica. El hidroxitirosol es un novedoso subproducto antioxidante del olivo que actúa contra los procesos oxidativos. En desventaja, la HC presenta fibra soluble (FS). Las enzimas carbohidrasas adicionadas a la dieta hidrolizan la FS aumentando la eficiencia y utilización de los nutrientes. El objetivo del presente experimento fue evaluar el uso combinado de harina de chía a través de la combinación chía/antioxidante y, por otro lado, a través de la combinación chía/antioxidante y enzimas sobre el peso de la carcasa y rendimiento de diferentes cortes comerciales. Noventa pollos parrilleros machos Cobb fueron divididos al azar en 30 grupos, alojados en 30 corrales y asignados a cinco repeticiones por cada tratamiento. Las dietas fueron: 1) C: control; 2) W₃: dieta con 10% HC; 3) W₃+Ez: dieta con 10% HC + 0,05% complejo enzimático comercial Biomix (Ez); 4) W₃+Ez+H: dieta con 10% HC + 0,05% Ez + HT (7 mg/kg PV/d); 5) W₃+H: dieta con 10% HC + HT (7 mg/kg PV/d); 6) H: dieta con HT (7 mg/kg PV/d). El experimento se extendió desde los 22 hasta los 42 días de vida, momento en el que se realizó la faena y se obtuvieron muestras de cinco animales por tratamiento. El mayor peso de carcasa y pechuga (P<0,05) correspondió a la dieta H. El HT podría mejorar la síntesis de aminoácidos y el metabolismo hormonal promoviendo el desarrollo muscular. Si bien, el agregado del complejo enzimático y/o HT a la HC no quedó reflejado en los parámetros evaluados, se plantean nuevos estudios que involucren el uso de diferentes dosis y tiempos de suministro del complejo enzimático y del antioxidante.

Palabras claves: aves, fenoles, ácido linolénico, hidrolasas.

PROPAGACIÓN ASEJUAL POR ACODOS AÉREOS DE QUEÑUA (POLYLEPIS RUGULOSA BITTER) UTILIZANDO CUATRO ENRAIZADORES CON DOS SUSTRATOS NATURALES EN CONDICIONES DE VIVERO

Luis Mayta

Laboratorio de Biotecnología Vegetal; Sociedad Minera Cerro Verde, Perú

Edwin Bustamante

Laboratorio de Biotecnología Vegetal; Sociedad Minera Cerro Verde, Perú

Eduardo Molinari

Chess Consulting & Project y Universidad Nacional Agraria La Molina, Perú

Elio Ponce

Laboratorio de Biotecnología Vegetal; Sociedad Minera Cerro Verde, Perú

Resumen

La rehabilitación de zonas afectadas por labores antropicas con especies nativas es un problema serio en la zona andina, ya que no se cuenta con suficientes métodos de propagación de especies autóctonas con respaldo científico, por ello investigó sobre la propagación de la “queñua” *Polylepis rugulosa* en el vivero de Uchumayo pertenecientes a Sociedad Minera Cerro Verde S.A.A., con el objetivo de comparar la eficiencia de los enraizadores y sustratos utilizados en la propagación vegetativa. La recolección del material vegetativo se realizó en los bosques de Tuctumpaya del distrito de Pochi, ya que presenta condiciones ideales (libres de plagas y enfermedades) de árboles idóneos (buena genética), se compró fibra de coco y musgo *Sphagnum* para los sustratos. Estos fueron empleados en la investigación para llenar 300 acodos aéreos de 80 gramos cada uno, que fueron desinfectados con Vitavax, el riego se aplicó en horas de la tarde y el deshierbe se realizó siempre que fuera necesario. Se aplicó un diseño de bloques completamente al azar, con arreglo factorial 5×2, para un total de diez tratamientos con diez repeticiones cada uno, estableciendo 30 unidades experimentales con 3 acodos aéreos por unidad experimental. Se aplicó la prueba de especificidad de LSD Fisher al 95% de probabilidad estadística con el fin de identificar los mejores tratamientos. Se evidenció una sobrevivencia a los 60 días, indistintamente en todos los tratamientos, el porcentaje de sobrevivencia del mejor tratamiento fue del 75%. En cuanto a la variable «porcentaje de prendimiento», que mide la capacidad del acodo para formar raíces viables, se evidenció que el tratamiento T8 (ácido húmico + fibra de coco) destacó por proveer el mejor resultado (30%).

Palabras clave: acodos aéreos, enraizadores, *Polylepis rugulosa*, propagación vegetativa, queñua, sustratos

1. INTRODUCCIÓN

Los bosques de queñua (*Polylepis Ruiz & Pavón*) son de gran interés ecológico, sistemático y biogeográfico al presentar un sistema biológico único y uno de los más vulnerables de los altos andes [1]. Los queñuales están distribuidos en pequeños parches aislados, relictos de

un hábitat ampliamente distribuido durante el pleistoceno, por la fuerte presión antrópica de la tala, la quema y el sobrepastoreo, que han llevado a la pérdida de grandes extensiones de bosque y a cambios en los patrones de regeneración natural de los bosques [2]. Las especies más basales se encuentran en el norte del Perú, por lo que se le considera el centro de origen de *Polylepis*, en tanto la mayoría de las especies se ubica en el sur de Perú y se le considera centro de diversificación [3].

Perú reporta 19 especies, de las cuales 4 son endémicas [4,5]. En la provincia de Arequipa, *Polylepis rugulosa* es la única especie arbórea dominante de los bosques relictos altoandinos ubicados en las laderas los volcanes Chachani, Pichupichu y Misti [6]. El bosque del Pichupichu es el que posee la mayor extensión, con 29 832 ha, y el más cercano a la ciudad de Arequipa. Es considerado como ecosistema importante por ser un reservorio de agua [7]. Adicionalmente los bosques de queñua son importantes económicamente para las comunidades campesinas aledañas al ser utilizadas como combustible, material de construcción, elaboración de utensilios de cocina y mangos de herramientas, entre otros usos [8,9].

La propagación vegetativa en especies nativas representa una alternativa para su manejo, al disminuir el tiempo de producción de plántulas en condiciones controladas, pero conservando características genotípicas y fenotípicas de las plantas madre [10]. De esta forma, la propagación vegetativa en queñua es importante por la baja viabilidad que presentan las semillas y el bajo porcentaje de germinación de esta [11]. El empleo de acodos es un método de multiplicación vegetativa que estimula la formación de raíces adventicias en tallos adheridos a la planta madre, en el caso de acodos aéreos, estos se realizan en la parte superior de la planta. Es necesario recalcar que el acodo en general suele presentar mejores resultados que la multiplicación vegetativa por estacas, al acelerarse la obtención de plantas, ya que el acodo no se separa de la planta y recibe nutrientes a través del xilema [12]. Para que la propagación vegetativa tenga mayor éxito de prendimiento, el uso de enraizadores naturales o químicos ayudan a la proliferación y formación de raíces [13], de igual manera, el sustrato cumple una función importante para el normal crecimiento y desarrollo de las plantas y este debe contener una buena proporción de nutrientes y una adecuada textura [14].

El objetivo de la presente investigación es lograr el enraizamiento de queñua (*Polylepis rugulosa* Bitter) por medio de acodos aéreos bajo el efecto de tres enraizadores y la utilización de dos sustratos naturales en condiciones de vivero.

2. MATERIALES Y MÉTODOS

2.1. Área del experimento

El presente trabajo se desarrolló en el Laboratorio de Biotecnología de Sociedad Minera Cerro Verde, distrito de Uchumayo, departamento de Arequipa, Perú. Para esta investigación se utilizaron 100 plantas madre de queñua, obtenidas de la comunidad campesina de Tuctumpaya, las cuales fueron aclimatadas en las instalaciones del vivero de Uchumayo.

2.2. Obtención de acodos aéreos

2.2.1. Selección de plantas madre

Se procedió a la selección de las plantas de queñua considerando las características deseadas entre ellas la turgencia de la planta, el tamaño, tomando en cuenta que sea una planta completamente sana para la realización del estudio y se considerará la edad propicia de la planta, siendo una planta genéticamente idéntica se le denomina donadora o planta madre.

2.2.2. Selección de ramas

Se obtuvo de la planta madre o donadora, para ello se considerará una longitud menor a 30cm dado que más larga estropeará el trabajo del acodado, un grosor de 0.5 a 1cm, que sea una rama joven ya que contiene tejido en formación.

2.2.3. Preparación del plástico y envoltorio para el acodo

Para la realización del envoltorio del acodo se utilizó fundas plásticas resistentes de 8 cm de ancho por 15 cm de largo siendo las mismas de color oscuro dado que las raíces son fotosensibles, además de la utilización de goma elástica para sujetar el acodo a las ramas.

2.2.4. Incisión de la rama

Esta denominación se le da a la formación del anillo que se hace al realizar un corte de 0.5 cm a la corteza sin afectar drásticamente a la planta, removiendo el cambium de la rama seleccionada para facilitar el enraizamiento de la planta, no se debe hacer este procedimiento muy profundo, podría causar el desprendimiento de la rama.

2.3. Elaboración del acodo

Se utilizó todos los procedimientos mencionados anteriormente, comenzando con la selección de la rama indicada, el retiro de hojas que intervengan en el procedimiento, se realizó la incisión a la rama y se sujetó la funda plástica con 20 g del sustrato (sustrato de turba, sustrato de fibra de coco y musgo Sphagnum) por los extremos con goma elástica para que quede firme, finalmente se humedeció el sustrato con 10 mL de enraizador (agua, Root Hor®, Kelpa®, ácidos húmicos y fúlvicos y ANA) y se les desinfectó con Vitavax®.

2.4. Mantención de humedad en el acodo

Se aplicó en los acodos por inyección, mediante la utilización de una jeringa de 10 mL, las soluciones a los distintos sustratos para mantener la humedad, de 1 a 2 veces por semana, además se realizó un riego cada semana en el área de investigación.

2.5. Diseño experimental.

Para el trabajo de investigación se utilizó un diseño experimental completamente al azar (DCA), con arreglo factorial de 2 actores ($A \times B$), con cinco niveles para el factor A y dos niveles para el factor B; con 10 repeticiones y 10 tratamientos con una prueba de especificidad de LSD Fisher a un nivel de significancia del 5%.

Enraizador		Sustrato	
E0	Agua	S1	Musgo
E1	Root Hor	S2	Fibra de Coco
E2	Kelpa		
E3	AH		
E4	ANA puro		

Tabla 1. Factores de estudio evaluados en la propagación de queñua.

Sustrato (S)	S1	S2
--------------	----	----

Enraizador (E)		
E0	E0S1	E0S2
E1	E1S1	E1S2
E2	E2S1	E2S2
E3	E3S1	E3S2
E4	E4S1	E4S2

Tabla 2. Combinación factorial del experimento.

2.5.1. Parámetros evaluados

Los parámetros evaluados fueron: longitud del brote o rama, descomposición de tejidos, porcentaje de prendimiento, porcentaje de acodos enraizados, número de raíces, longitud de raíces y diámetro de raíces.

2.5.2. Análisis estadístico

Para el análisis de datos las variables en estudio se emplearon el análisis de varianza (ANOVA), usando la prueba F a un nivel de significancia de 0,05 y para la comparación múltiple de medias entre las medias se utilizó la prueba de significancia de LSD Fisher a una probabilidad $\alpha = 0,05$.

2.5.3. Población y muestra

La población fueron 100 plantas madre con tratamiento, la unidad experimental es una planta madre con tres acodos aéreos y 10 por tratamiento.

Tratamiento		Descripción
T1	E0S1	Agua + musgo
T2	E0S2	Agua + Fibra de coco
T3	E1S1	Root hor ® + Musgo
T4	E1S2	Root hor ® + Fibra de coco
T5	E2S1	Kelpa ® + Musgo
T6	E2S2	Kelpa ® + Fibra de coco
T7	E3S1	Ácido húmico + Musgo
T8	E3S2	Ácido húmico + Fibra de coco
T9	E4S1	ANA + Musgo
T10	E4S2	ANA + Fibra de coco

Tabla 3. Tratamientos del experimento.

3. RESULTADOS Y DISCUSIÓN

3.1. Resultados

3.1.1. Longitud de los brotes

Después de ser sometidos a los acodos aéreos, los tratamientos 8 y 9 fueron los que presentaron los resultados más sobresalientes (25.78 y 25.88 cm de longitud, respectivamente), tal y como se observa en la figura 1.



Figura 1. Longitud de brote con respecto al tratamiento.

3.1.2. Descomposición de tejidos

Los tratamientos 4, 5 y 10 fueron los que presentaron un mayor porcentaje de tejidos descompuestos por masa al término de la evaluación (16.67, 20 y 16.67 % respectivamente), lo que es un claro indicativo de la poca sobrevivencia en estos tratamientos, tal y como se observa en la figura 2.

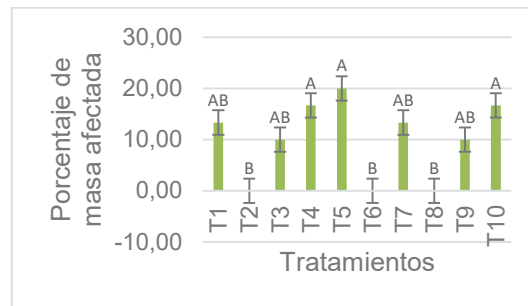


Figura 2. Porcentajes de descomposición de tejidos.

3.1.3. Prendimiento de acodos aéreos

El mejor prendimiento fue mostrado en el tratamiento 8 (30.33%), seguido cercanamente por los tratamientos 6, 9, 2 y 10, los que se diferencian claramente de los demás tratamientos, tal y como se observa en la figura 3.



Figura 3. Porcentajes de prendimiento.

3.1.4. Crecimiento de raíces

El tratamiento 10 es el que presenta el mayor número de raíces (7.73), seguido de los tratamientos 6 y 8 (3.87 y 4.10, respectivamente), tal y como se observa en la figura 4.



Figura 4. Número de raíces.

Con respecto a la longitud de raíces las que presentaron los mejores resultados fueron el tratamiento 6 y el tratamiento 8 (2.02 y 2.04 cm, respectivamente), como se observa en la figura 5.

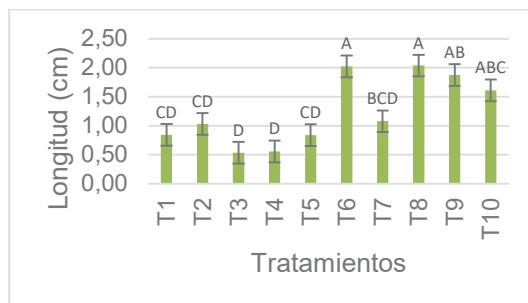


Figura 5. Longitud de raíces.

Los tratamientos 8, 9 y 10 (0.1, 0.1 y 0.12 mm respectivamente) otorgaron los mejores diámetros, tal y como se observa en la figura 6. En general, el desempeño de los tratamientos para la promoción y el crecimiento de raíces parecen ser mejores con el tratamiento 8.

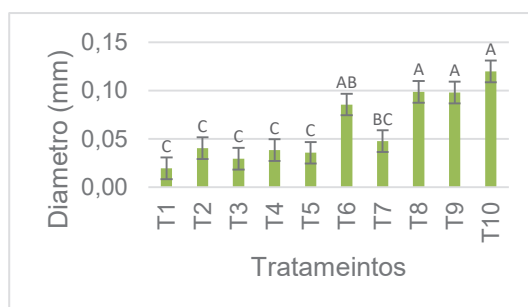


Figura 6. Diámetro de raíces.

3.2. Discusión

La aplicación de enraizadores y sustratos bajo condiciones de vivero incrementó significativamente en la propagación de acodos aéreos de queñua. El tratamiento 8 (ácido húmico y fibra de coco) fue el más efectivo para promover la longitud de brote, el prendimiento y la poca descomposición de tejido.

Se le atribuye este éxito a la fibra de coco porque, por ser un sustrato más poroso con mayor retención de agua y mayor disponibilidad del elemento fósforo (P) resultante de las fertilizaciones hidrosolubles, hace que la planta acelere la formación de pelos absorbentes y raíces secundarias [15].

El musgo, por otro lado, dio resultados contrarios, debido a que la compactación redujo la aireación y el espacio poroso en la zona de las raíces, lo que reduce así la asimilación del fósforo [15].

Los resultados obtenidos, son semejantes a los de Soto [16], quien evaluó el efecto de tres dosis de Root Hor en la propagación vegetativa de queñual (*Polylepis* sp.), señalando que el material, mientras menos lignificado sea, permitirá mayor actividad de las células vegetativas, propiciando la rápida formación de raíces por los enraizadores, lo que permitió la sobrevivencia de los esquejes. También indicó que un limitante para las yemas enraizadas es edad, ya que las más viejas suelen morir con más frecuencia al ser trasplantadas.

También verificamos que los bioestimulantes son productos que, solos o mezclados, realmente contribuyen a mejorar el crecimiento de las plantas al gatillar procesos fisiológicos específicos. Son caracterizados por sus diferentes modos de acción y varias

formas de uso, son capaces de mejorar la nutrición y desarrollo de los vegetales [17] como el caso del ácido húmico utilizado en el tratamiento 8, el cual es el tratamiento que recomendamos.

4. CONCLUSIONES

Se concluye que el tratamiento que presenta la mejor respuesta para el tratamiento de los acodos aéreos es el tiramiento 8 el cual contiene ácidos húmicos y fibra de coco, que le proporciona a la planta los elementos esenciales para la generación de raíces de buena calidad al tiempo que provee un ambiente físico que le permite llevar a cabo las funciones fisiológicas necesarias con normalidad.

Los autores consideran que los presentes resultados, novedosos por provenir del uso de una técnica poco usada en plantas nativas como el acodamiento aéreo, contribuirán al conocimiento para la conservación in y ex situ de plantas arbóreas en otras zonas de alta biodiversidad que se encuentren amenazadas por la actividad humana.

AGRADECIMIENTOS

Se agradece el financiamiento de esta investigación a Sociedad Minera Cerro Verde que permitió se haga posible el desarrollo del trabajo de investigación bajo el contrato N°37031903237 – CLS-236-2019.7

REFERENCIAS

- [1]. M. Kessler y A. N. Schmidt-Lebuhn. "Taxonomical and distributional notes on *Polylepis* (Rosaceae)," *Organisms Diversity and Evolution*, vol. 6, pp. 67–70, Feb. 2006
- [2]. R. C. Torres, D. Renison, I. Hensen, R. Suárez y L. Enrico. "Polylepis australis' regeneration niche in relation to seed dispersal, site characteristics and livestock density," *Forest Ecology and Management*, vol. 254, pp. 255–260, Ene. 2008
- [3]. W. Mendoza y A. Cano. "Diversidad del género *Polylepis* (Rosaceae, Sanguisorbeae) en los Andes peruanos," *Revista peruana de biología*, vol. 18, pp. 197–200, Sep. 2011.
- [4]. B. B. Simpson. "A revision of the genus *Polylepis* (Rosaceae: Sanguisorbeae)," *Smithsonian contributions to botany*, vol. 43, pp. 1–62, Ene. 1979.
- [5]. Missouri Botanical Gardens. (2021) Tropicos, [Online]. Available: <https://tropicos.org/home>
- [6]. W. Mendoza, A. Cano y R. Vento. "Bosques de *Polylepis* de la Reserva Nacional de Salinas y Aguada Blanca, Arequipa y Moquegua, Perú," *Biodiversidad de la Reserva Nacional de Salinas y Aguada Blanca*, pp. 167–173, 1ra ed., H. Zeballos, J. A. Ochoa y E. López, Eds. Arequipa, Perú: Desco, Profonampe y Sernanp, 2010.
- [7]. S. M. Soto Huaira, V. Gamarra-Toledo, C. Medina y E. López. "Composición de la Dieta de las Aves de los Bosques de Queñua (*Polylepis rugulosa*) en Arequipa, Suroeste Del Perú," *Ornitología Neotropical*, vol. 30, pp. 217–223, Nov. 2019.
- [8]. J. Recharte, R. Arévalo y M. Glave. "Bosques de montaña: Ecosistemas relictos," *Islas en el cielo: conservación de ecosistemas, afirmación de la cultura y prosperidad en las montañas del Perú*, pp. 11–19, 1ra ed., J. Recharte, R. Arévalo y M. Glave, Eds. Lima, Perú: Instituto de Montaña, 2003.
- [9]. M. Kessler, *Bosques de Polylepis*, 1ra ed., La Paz, Bolivia: Universidad Mayor de San Andrés, 2006.

-
- [10]. G. P. Servat, W. Mendoza, N. Hurtado y R. Castañeda. “Crecimiento, Regeneración y Fenología de árboles de *Polylepis pauta* Hieron. (Rosaceae) en el Ecotono del Bosque Montano del Valle del Río Apurímac,” *Monitoring Biodiversity: Lessons from a Trans-Andean Megaproject*, pp. 245–253, 1ra ed., A. Alonso, F. Dallmeier y G. P. Servat, Eds. Washington D. C., United States of America: Smithsonian Institution Scholarly Press, 2013.
- [11]. T. Huarhua Chipani, “Propagación vegetativa de esquejes de queñua (*Polylepis incana*) con la aplicación de dos enraizadores naturales y tres tipos de sustratos en condiciones de vivero Cuajone, Torata-Moquegua,” tesis, Universidad José Carlos Mariátegui, Moquegua, Perú, Ago. 2017.
- [12]. R. J. Pérez Concha, “Propagación por acodo aéreo de *Terminalia amazonia* (J. F. Gmel.) Exell, usando tres concentraciones de auxinas,” tesis, Universidad Nacional de Cajamarca, Cajamarca, Perú, Abr. 2017.
- [13]. R. Hoyos, “Determinación de sustratos y efecto de cuatro niveles de ácido naftalenacético (ANA) sobre el enraizamiento de esquejes de queñua (*Polylepis tarapacana*),” tesis, Universidad Técnica de Oruro, Oruro, Bolivia, Abr. 2004.
- [14]. D. P. León Araujo, “Propagación de dos Especies de Yagual (*Polylepis incana* y *Polylepis racemosa*) utilizando dos Enraizadores Orgánicos y dos Enraizadores Químicos en el Vivero Forestal del CREA en el Cantón y Provincia del Cañar,” tesis, Escuela Superior Politécnica de Chimborazo, Riobamba, Ecuador, Ago. 2008.
- [15]. A. M. Bustamante Estrada, “Enraizamiento de *Euphorbia pulcherrima* en cuatro sustratos y dos concentraciones del ácido indol-3-butírico,” tesis, Escuela Agrícola Panamericana Zamorano, Francisco Morazán, Honduras, Nov. 2014.
- [16]. L. I. Soto Choccelahua, “Programación vegetativa de esquejes de queñual (*Polylepis* sp.) bajo diferentes dosis del en raizador Root-hor en el distrito de Carampoma – Huarochirí - Lima,” tesis, Universidad Nacional de Huancavelica, Huancavelica, Perú, Oct. 2013.
- [17]. F. A. Álvarez Gavilanes, “Enraizamiento con ácidos húmicos y extracto de gas en estacas de mora (*Rubus glaucus* Benth.),” tesis, Universidad Técnica Estatal de Quevedo, Quevedo, Ecuador, Ago. 2008.

BIOGRAFÍA

Luis Fernando Mayta Anco (Arequipa, 1993) es un botánico peruano, bachiller y biólogo por la Universidad Nacional San Agustín de Arequipa, con experiencia en nomenclatura y sistemática de astéridas. Actualmente se desempeña como Coordinador del Componente de Investigación en el Laboratorio de Biotecnología Vegetal de la Sociedad Minera Cerro Verde, donde lleva a cabo estudios fisiológicos en plantas nativas de los Andes del sur del Perú.

SPECIES DIVERSITY WITHIN THE UPPER/MIDDLE PARAÍBA DO SUL RIVER
BASIN AND ADJACENT DRAINAGES CLADE, OF THE AUSTRALOHEROS
AUTRANI GROUP (TELEOSTEI, CICHLIDAE)

Dr. José Leonardo de Oliveira Mattos – Universidade Federal do Rio de Janeiro

Ms. Marcos Aurélio da Silva - University of Basel

Dr. Adrian Indermaur - University of Basel

Dr. Axel Makay Katz - Universidade Federal do Rio de Janeiro

Dr. Walter Salzburger - University of Basel

Dr. Felipe Polivanov Ottoni - Federal University of Maranhão

Abstract

The *Australoheros autrani* species group is divided into three clades: the Upper/middle Paraíba do Sul river basin and adjacent drainages clade, the Northern Mata Atlântica clade, and the Southern Mata Atlântica clade. In this present analysis we included six additional haplotypes from a stream of the upper Paranaíba River drainage, of the upper Paraná river basin, being the first record for *Australoheros autrani* species group in this river drainage. Two distinct species delimitation methods approaches based on molecular data were here performed: a tree-based method as proposed by Wiens and Penkrot (WP) and a character-based DNA barcoding (CBB). In our analysis the monophyly of both *A. autrani* species group and the Upper/middle Paraíba do Sul river basin and adjacent drainages clade were corroborated. In addition, a unique color pattern that consists in the presence of metallic blue or green blotches in the anal-fin base of life or fresh specimens was here considered as diagnostic for the *A. autrani* species group. Both distinct species delimitation methods here implemented had identical results. The combined analyses (WP and CBB) delimited three lineages (species) within the Upper/ Middle Paraíba do Sul river basin and adjacent drainages clade: *Australoheros barbosae*, *A. macacuensis*, and *A. robustus*, that are considered here considered as valid species. The six new haplotypes were included clustered with haplotypes of the species *A. barbosae*. The species *Australoheros paraibae* and *A. tavaresi* were considered here as junior synonyms of *A. barbosae*, while *Australoheros mattosi* was considered as a junior synonym of *A. robustus*. *Australoheros montanus* was tentatively included within this clade due to the presence of that unique aforementioned diagnostic color pattern. Despite it was not included in the molecular analyses, it is considered as valid. The result of this work highlighted the importance of using molecular data and approaches in taxonomy and species delimitation, providing more accurate estimates of biodiversity, and help to solve taxonomic issues and problems, as well as challenging the ‘taxonomic impediment’. In addition, the result of this work challenge the hypothesis of a single species of the genus for all the river basins of eastern Brazil, as suggested by Říčan et al. (2011).

Keywords: Cichlinae, molecular systematics, Neotropical region

THERMAL CHARACTERIZATION OF SURFACTANT SOLUTIONS AND PHASE TRANSITION IDENTIFICATION USING THE LEWIS-NIELSEN MODEL

Luis M. Montes-de-Oca

Instituto de Física y Matemáticas, Universidad Michoacana de San Nicolás de Hidalgo,
Morelia, Michoacán, México

R. Medina-Esquivel

Facultad de Ingeniería, Universidad Autónoma de Yucatán, A.P. 150, Cordemex, Mérida,
Yucatán, Mexico

M. A. Zambrano-Arjona

Facultad de Ingeniería, Universidad Autónoma de Yucatán, A.P. 150, Cordemex, Mérida,
Yucatán, Mexico

P. Martínez-Torres

Instituto de Física y Matemáticas, Universidad Michoacana de San Nicolás de Hidalgo,
Morelia, Michoacán, México

Keywords. Thermal characterization, self-assembly, critical micellar concentration, nanofluids.

Systems formed by surfactants have a wide range of applications in the fabrication of optical devices, foams, heat transfer, among others. Surfactant molecules in polar media tend to self-assemble into different structures like spherical micelles, tubular micelles, hexagonal phases, or lamellar structures; while in non-polar media as oils, tend to form inverted micelles. Self-assembly strongly depends on the molecular geometry of surfactants; in particular, the length and width of their hydrophilic and hydrophobic regions. The knowledge of self-assembly of these systems is of great interest for the fabrication of Pickering emulsions and particle-stabilized foams. Several methods had been used in the characterization of these nanofluids to find important parameters like the critical micellar concentration (CMC) in surfactants and the critical aggregation concentration (CAC) in nanoparticle suspensions. These methods include the measurement of surface parameters as surface tension or pressure and in-bulk measurements of electrical conductivity, fluorescence, osmotic pressure, and thermal conductivity. Despite the mentioned methods, very little has been done about the thermal characterization of these complexes. Previous work reports the use of the hot wire method to find the thermal conductivity and the study of the heat transfer through the liquid. In this work, we propose the study of anionic and cationic surfactants in water using the thermal wave resonator cavity technique, which is a non-invasive method to obtain the thermal diffusivity of the samples. Also, we use the mathematical effective thermal model of Lewis-Nielsen to explain the behavior of our experiments. It was possible to identify the critical micellar concentration and the transition from spherical micelles to rod-like micelles.

ESTUDIO ELECTROQUÍMICO DE UN ACERO INOXIDABLE Y ACERO AL CARBONO EN SOLUCIÓN DE EXTRACTO DE CEMENTO CON IONES CLORURO.

David Bonfil Ceferino

Centro de investigación y de estudios avanzados (CINVESTAV)

Lucien Veleza

Centro de investigación y de estudios avanzados (CINVESTAV)

Ángel Bacellis

Centro de investigación y de estudios avanzados (CINVESTAV)

Esta investigación trata sobre la actividad electroquímica de corrosión del acero al carbono B450C y acero inoxidable ferrítico SS 430, expuestos por 30 días a la solución alcalina (pH=13.38 inicial) de extracto de cemento Portland en la presencia de cloruros ($5 \text{ g L}^{-1} \text{ NaCl}$), simulando el ambiente del poro de concreto. Se registró el cambio del Ph de la solución y el registro de pérdida de masa, además se hicieron los análisis de caracterización superficial: Microscopía electrónica de barrido SEM-EDS, espectroscopía fotoelectrónica de rayos X (XPS) y difracción de rayos X (XDR). Asimismo, como las pruebas electroquímicas de registro del potencial a circuito abierto (OCP) y las curvas de polarización potenciodinámicas (PDP). La alcalinidad de la solución disminuyó hasta pH ≈ 9.5 , lo que provocó la pérdida del estado pasivo de B450C y su valor final de potencial de corrosión (OCP) fue de -464 mV . Mientras tanto, el acero inoxidable mantuvo su capa pasiva y su valor del OCP fue de $+175 \text{ mV}$ al final de este ensayo. Los análisis de SEM-EDS y XPS sugirieron la presencia de fases de Cr (C, N), V (C, N), así como de SiC y un bajo contenido de Mn en la superficie de SS 430, mientras en la superficie del acero al carbono fueron las fases de SiC, MnS y Mn_3C . Después de la exposición al extracto de cemento, los productos de corrosión son óxidos/hidróxidos, y la presencia de cristales de CaCO_3 . La capa de corrosión de B450C no es uniforme en su morfología y algunos productos de corrosión se extienden en forma de filamentos (corrosión filiforme). Los ataques de corrosión para el acero inoxidable SS430 son locales y muestran el inicio de picaduras. La curva anódica potenciodinámica del acero SS 430 reveló un rango amplio de potenciales de estado pasivo con baja velocidad de densidad de corriente, mientras el acero al carbono B450C tuvo amplia actividad de corrosión. Por otro lado, el proceso catódico del SS 430 tuvo inicialmente a polarización pequeña de 30 a 40 mV dificultad para la reducción del O_2 a través de su capa pasiva.

Palabras Clave: Corrosión, concreto, acero inoxidable y acero al carbono

EFFECT OF CA ON THE ELECTROCHEMICAL ACTIVITY OF THE MG-CA0.3 ALLOY EXPOSED TO HANK'S PHYSIOLOGICAL SOLUTION AND PROPERTIES OF AG NANO-PARTICLE DEPOSITS

José Luis González-Murguá

Department of Applied Physics, Center for Research and Advanced Studies (CINVESTAV-IPN),
Mérida, Yucatán, México

Lucien Veleza

Department of Applied Physics, Center for Research and Advanced Studies (CINVESTAV-IPN),
Mérida, Yucatán, México

Abstract

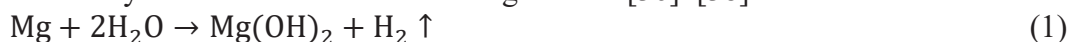
This research compares the degradation of Mg and the Mg-Ca0.3 alloy, as possible materials for temporary implants, when exposed for up to 14 days in Hank's solution. The combination of immersion and electrochemical tests (polarization curves, PDP), as well as techniques for surface characterization (SEM-EDS and XPS) allowed to reveal the effect of Ca on the degradation of Mg. The change in pH over time, the lower loss of mass ($\sim 20\%$), lower concentration of Mg^{2+} ions released ($\sim 360\%$), and the lower level of surface degradation, allowed to suggest the positive effect of Ca as part of the Mg-Ca0.3 alloy, suggesting a lower electrochemical activity compared to that of Mg. To provide antibacterial properties of the Mg-Ca0.3 surface, electroless deposits of Ag nanoparticles (Ag-NPs) were made, which were characterized by SEM-EDS, XRD, UV-Vis and contact angle. The antibacterial capacity of the Ag-NPs deposits was tested against the growth of *Staphylococcus aureus* and *Escherichia coli* bacteria, using the agar diffusion test. A greater antibacterial effect was observed with respect to *S. aureus*, attributed to the more negative zeta potential of this bacterium, which is why it attracts more Ag^+ ions released, which cause damage to the bacterial cell membrane.

Keywords: Ag Nano-particles, Antibacterial Properties, Bacterial Zeta Potential, Corrosion, Hank's Solution, Magnesium.

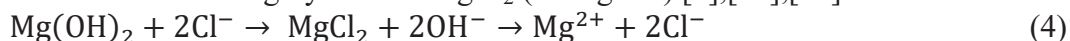
1. INTRODUCTION

Mg is the lightest metal with a density of 1.738 g cm^{-3} which is close to the cortical bone ($1.75\text{--}2.1 \text{ g cm}^{-3}$), with an elastic modulus of 45 GPa ($\approx 20 \text{ GPa}$ of cortical bone), its rapidly cooled alloys can reach a strength/weight ratio of 490 kN m kg^{-1} [1]–[4], hence it is considered as a more suitable material than the biomedical titanium alloy $\text{Ti}_6\text{Al}_4\text{V}$ (4.47 g cm^{-3}) [5]. Mg alloys have attracted much research interest as biodegradable, resorbable and biocompatible materials, when used as temporary implants in physiological environments [6]–[12]. The Mg^{2+} ion released is non-toxic and is essential for protein synthesis, activation of a variety of enzymes, regulation of the activities of the central nervous and neuromuscular system, regulation of blood glucose level, promoting normal blood pressure, in addition to playing an important role in the prevention and treatment of hypertension disorders, cardiovascular diseases and diabetes [13]–[15]. The average Mg^{2+} ion requirement is $\sim 375 \text{ mg day}^{-1}$ for a human body [16]. Magnesium has been commercially applied as a biomaterial for wound closure, orthopedic, microsurgical, and cardiovascular [9],[17]–[20]. Moreover, they have stimulating effects on the growth of new bone tissue because magnesium ions (Mg^{2+}) exhibit a strong affinity to bind with phosphate ions present in the human body, influencing the mineralization of bone tissue through the formation of hydroxyapatite $[\text{Ca}_{10}(\text{PO}_4)_6(\text{OH})_2]$, or possible similar compounds, which can inhibit the corrosion process [21]–[25]. In aqueous media, because of the very negative redox potential of Mg ($-2.38 \text{ V}_{\text{SHE}}$), its anodic dissolution (Equation 1) is accompanied by the main cathodic reaction of hydrogen evolution over a wide pH range [21]–

[35]. The hydrogen volume measurement is not a reliable method for the corrosion process monitoring, because the oxygen reduction Eq. 2 and the water reduction Eq. 3 may also occur as secondary cathodic reactions on the Mg surface [36]–[38].



In physiological solutions composed of a high content of NaCl (up to 3.5%), the Cl^- ions penetrate the pores of the poorly soluble (0.009 g L^{-1}) corrosion product of $\text{Mg}(\text{OH})_2$, causing its partial transformation to highly soluble MgCl_2 (54.3 g L^{-1}) [8],[18],[39]:



The mainly disadvantages that Mg may present in physiological media are: anticipated loss of mechanical integrity (implant failure); H_2 gas generated as a byproduct of corrosion (affecting the healing process); alkalinization at the surface interface Eq. 4, which accelerates the process of $\text{Mg}(\text{OH})_2$ corrosion product formation and disorder in the physiological reactions that depend on the pH [40]–[42]. To reduce the rapid degradation of Mg, calcium was used as an alloying element. The metal Ca (1.55 g cm^{-3}) was chosen as it is the major component in the human bones, as a hydroxyapatite complex $[\text{Ca}_{10}(\text{PO}_4)_6(\text{OH})_2]$, which provides the rigidity and stability of the bone, as well as, the ions of Ca are essential for the chemical signals of cells [42],[43]. In a solid solution its percentage can reach up to 1.34 % wt. according to the binary phase diagrams of Mg-Ca [22],[44]. The microstructure of Mg-Ca alloys systems includes α -Mg (hexagonal crystalline structure) and Mg_2Ca phase, in which crystalline cell presents double parameter values ($a = 0.623$, $c = 0.1012$) compared to those of Mg [45]–[48]. In the literature, there are controversial results for the electrochemical behavior of the Mg_2Ca intermetallic particles present in the matrix of Mg-Ca alloys and there is not a clear justification for their biodegradation mechanism [14],[29],[49]–[52]. It has been noted that the electrochemical activity of Mg_2Ca particles needs to be investigated with precision to determine their effect on the biodegradation process of Mg-Ca implants [53]–[55]. The increasing fight against bacterial infections during the surgery requires the development of medical devices and materials with antimicrobial properties [56]. The bacterial proliferation and its surface adhesion on solids are crucial, caused mainly by the interaction between the solid surface potential (electric charge) and the zeta potential charge of the bacteria cellular surface [57], in an addition to other factors, such as pH of the solution and its chemical composition, the hydrophobicity of the solid surface and ionic strength. Several studies have revealed the antimicrobial efficiency of Ag-nanoparticles (NPs), although the mechanism of their effect is not yet fully understood [58]–[61]. It was suggested that Ag-NPs initially bind to the bacteria cell, altering its permeability and respiration, followed by penetration into and the intracellular release of Ag-ions [62]. The silver exhibits a significant antibacterial action in the dark, where there is no light (within the human body), making this metal an attractive material for biomedical applications [63]. The deposition of Ag-NPs on Mg-alloys surface could be one approach to provide antimicrobial protection for the implantable medical device surface, to combat associated infections.

The aim of this work is to provide more detailed information on the effect of Ca on the electrochemical degradation process of Mg-Ca0.3 alloy, when exposed to Hank's physiological solution (at 37°C) for up to 14 days, compared with that of pure Mg. The change of surface morphology and composition was characterized by SEM-EDS and XPS techniques. The pH of the Hank's solution and concentration of the released Mg-ions were monitored. Mass losses, potentiodynamic polarization (PDP) curves, EIS diagrams, fluctuations of corrosion current and potential (EN), revealed an additional information. Ag-NPs of different size, electroless deposited on Mg-Ca0.3 surface, were characterized by means of the UV-Vis spectroscopy, SEM-EDS, XRD

and the contact angle test. The bacteria *S. aureus* (*Staphylococcus aureus*) and *E. coli* (*Escherichia coli*) were selected as models of Gram-positive and Gram-negative bacteria for testing the antibacterial properties of the Ag-NPs. The ability to prevent bacteria growth was proved by the agar disk diffusion method (Kirby–Bauer test).

2. MATERIALS AND METHODS

2.1. Samples and Solution Preparation

Hank's physiological solution was prepared with the following analytical grade reagents (7.2 initial pH): NaCl 8.0 g L⁻¹, glucose 1.0 g L⁻¹, NaHCO₃ 0.35 g L⁻¹, and KCl 0.30 g L⁻¹; in a low content: KH₂PO₄, MgSO₄·7H₂O, MgCl₂·6H₂O, CaCl₂, and ultrapure deionized water (18.2 MΩ·cm) [64]–[66]. Mg (99.9 wt.%) and Mg-Ca alloy (Ca 0.3 wt.% and the balance Mg) were manufactured by an extrusion process and supplied by Helmholtz-Zentrum Hereon, Institute of Materials and Process Design (Geesthacht, Germany) as cylindrical bars (diameter = 1 cm). According to the manufacturer the nominal composition (wt.%) is Al (0.016), Cu (0.0019), Fe (0.0019), Ni (0.0014), Zn (0.0060), Ca (0.23) and Mg (Bal.). The tested materials were cut into a 3-mm thick discs; some of them were used for the immersion test, while others were prepared as electrodes for electrochemical experiments. All samples were abraded with SiC paper to 4000 grits, using ethanol as a lubricant, and then sonicated in ethanol for 5 min and dried in air at room temperature.

2.2. Immersion Test and Surface Characterization

According to the ISO 16428 [64] and ASTM G31-12a [67] standards, Mg and the Mg-Ca0.3 alloy samples were submerged in 20 mL of Hank's physiological solution at 37°C, with a daily renewal of electrolyte for 14 days in triplicate. The residual solutions were stored to measure their pH by a pH meter and the concentration of the released Mg²⁺ ions by photometry (HI83200, Hanna Instruments, Woonsocket, RI, USA). To evaluate the mass loss and the corrosion damage on the surface after each exposure period, the formed layer of products was chemically removed, according to the standards ASTM G1-03 [68], using the solution of 200 g L⁻¹ CrO₃, 10 g L⁻¹ AgNO₃, and 20 g L⁻¹ Ba(NO₃)₂. The values of initial mass w_0 and final mass w_1 were measured by an analytical balance (VE-204, Velab, CDMX, México) and then the mass loss was calculated ($\Delta m = w_1 - w_0$). The morphology and composition of the layers formed on the Mg and Mg-Ca0.3 surfaces, before and after exposure to Hank's physiological solution, were characterized by: SEM-EDS (SEM-EDS, XL-30 ESEM-JEOL JSM-7600F, JEOL Ltd., Tokyo, Japan) and XPS (K-Alpha Surface, Thermo Scientific, Waltham, MA, USA), after sputtering the specimens' surface with a scanning argon-ion during 15 s.

2.3. Electrochemical Characterization

The corrosion process of Mg and Mg-Ca0.3 in Hank's solution (at 21°C) was studied with the potentiodynamic polarization curves (vs. OCP) were recorded at a scanning rate of 10 mV s⁻¹, in a potential range from -1 V to +1 V. Mg and Mg-Ca0.3 samples were elaborated as working electrodes in a typical three-electrode cell configuration, inside a Faraday cage. A saturated calomel electrode (SCE) as a reference electrode (SCE, Gamry Instruments, Philadelphia, PA, USA). The electrodes were connected to a potentiostat /galvanostat/ZRA Interface-1000E (Gamry Instruments, Philadelphia, PA, USA).

2.4. Characterization of Antibacterial Properties of Ag-NPs Deposits on Mg-Ca0.3 Surface

2.4.1. Agar Disk Diffusion Antibacterial Test

Agar and nutrient broth Mueller-Hinton were used as the non-selective medium that promotes the growth of bacteria: Gram-positive *S. aureus* ATCC 6538 and Gram-negative *E. coli* ATCC 25922. The antibacterial agar disk-diffusion method (Kirby–Bauer method) [69]–[71] was carried out, which consists of initial inoculation of a bacteria spread layer (100 μm) on the agar disk. The suspensions with bacteria were adjusted by optical density (spectro-photometry) at 625 nm, to match the turbidity equivalent to the 0.5 McFarland standard (1.5×10^8 CFU mL⁻¹) and adjusted to

1.5×10^6 CFU mL⁻¹ by serial dilutions. All samples were sterilized with ethyl alcohol and placed in a box with ultraviolet light for 1 h, as well as all glassware were sterilized in an autoclave at 121°C and 15 psi (for 20 min). The samples of the Mg-Ca0.3 alloy without and with deposit of Ag-NPs in triplicate, were placed on the agar disk and incubated at 37°C for 24 h (in the dark). The diameter of the inhibition halo around the alloys, where the bacteria did not grow, was then measured, and compared.

2.4.2. Zeta Potential Measurement of Bacteria

The zeta potential (NANO ZEN 3600, Malvern Instruments Ltd., Worcestershire, UK) of *E. coli* and *S. aureus* bacteria in Muller-Hinton culture medium (at 21.5°C) was measured at different pH values by auto-titration (MPT-2, Malvern Instruments Ltd., Worcestershire, UK), to better understand their interactions with sample surfaces. The titrants were solutions of 0.1 and 0.5 mol L⁻¹ of NaOH or 0.5 mol L⁻¹ of HCl. Zeta potential values are the average of triplicate measurements for each pH value.

3. RESULTS AND DISCUSSION

3.1. Surface Characterization of Mg and Mg-Ca0.3

The SEM images (Figure 1) of the freshly polished surfaces of the samples were compared, as well as the EDS analysis of sites (labeled as 1, 2, 3, and 4) is presented in Figure 1C, as also the suggested compounds of MgO (site 3) and Mg₂Ca particles (site 4), reported by metallurgical studies [72],[73]–[75].

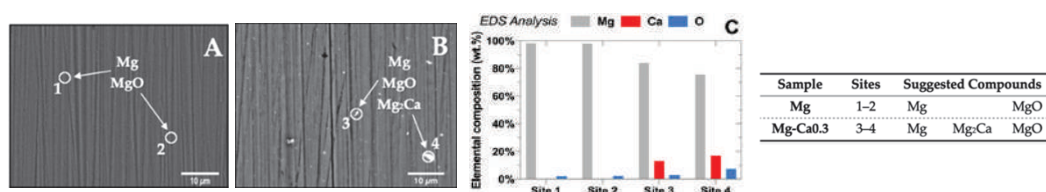


Figure 1. SEM images (2000×) of the Mg (A) and Mg-Ca0.3 (B) reference surfaces. (C) EDS analysis of sites marked on the SEM images and the suggested compounds.

3.2. Test Solution Monitoring and Mass Loss Measurement

The pH of Hank's solution (Figure 2A) showed increasing and decreasing tendencies, which were influenced by the formation of OH⁻ ions (Equations 2 and 3) and the evolution of H₂ (Equation 1) during the corrosion process. Consequently, when the pH solution was shifted to more alkaline values, the precipitation of Mg(OH)₂ corrosion product was favored. On the other hand, the glucose [CH₂OH(CHOH)₄CHO], which is a part of Hank's solution (1.00 g L⁻¹), can be rapidly transformed into gluconic acid [CH₂OH(CHOH)₄COOH], which acidifies the electrolyte and causes partial destruction of the Mg(OH)₂ film [76]. It has been reported that the gluconic acid promotes the growth of the hydroxyapatite layer, due to the chelation reaction with Ca²⁺ ions [75]. The pH of Hank's solution (at 14 days) reached alkaline value of ~8.3 for Mg samples, while that of Mg-Ca0.3 the value decreased to pH ~6.3. The values of mass loss (Δm) and concentration of the released Mg²⁺ ions (Figure 2B) were a consequence of the change in pH over time. Therefore, after 14 days of immersion in Hank's solution, the mass loss of Mg-Ca0.3 (3.76 mg cm⁻²) was ~20% lower than that of the Mg samples (4.66 mg cm⁻²). The concentration of released Mg²⁺ ions was 365% lower for the Mg-Ca0.3 alloy than that for Mg. It can be suggested that a fraction of the mass loss and concentration of released Mg²⁺ ions are the result of attacks by Cl⁻ ions and formation of soluble MgCl₂ (Equations 4 and 5).

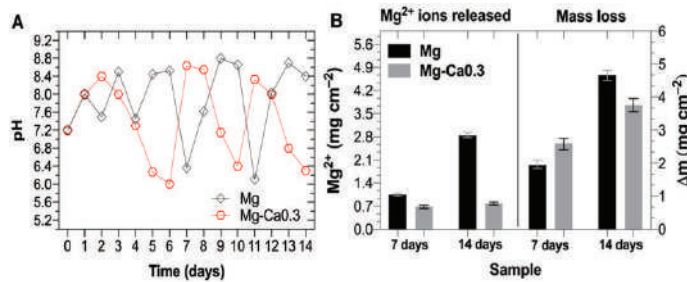


Figure 2. Changes in times of: (A) Hank's solution pH up to 14 days during the exposure of Mg and Mg-Ca0.3 samples up to 14 days; (B) concentration of the released Mg²⁺ ions and measured mass loss (Δm) at 7 and 14 days. (Electrolyte renewal every 24 h).

3.3. SEM-EDS Analysis After Exposure to Hank's Solution

The Mg (Figure 3A) and Mg-Ca0.3 (Figure 3B) surfaces showed cracked layers (at 14 days). These cracks can connect the α -Mg with Hank's solution, improving the release of Mg²⁺ ions and the evolution of the H₂ bubble (the pressure of H₂ bubbles may cause cracks or fractures in the layers). The EDS analysis, the main elements on Mg-Ca0.3 alloy surfaces are Mg, O, and Ca, and Cu, Al, Fe, Ni, and Zn appear in small amounts (below 1% wt.), which may present cathodic activity, being effective sites for hydrogen evolution [77]. The presence of P element could be considered as a part of the formed Mg₃(PO₄)₂ and as well as participating in the compound hydroxyapatite [Ca₁₀(PO₄)₆(OH)₂] [78],[79]. After the removal of the formed layers, the cross-sectional images (Figure 3C,D) revealed that the corrosion attacks have been less aggressive in depth, ~5.5 times in Mg-Ca0.3 surface (Figure 3D) than those in Mg (Figure 3C). It is also evident that the localized attacks have been more pronounced on the Mg surface (Figure 3E) than those on the Mg-Ca0.3 surface (Figure 3F). The intermetallic Mg₂Ca particles appeared on the surface of Mg-Ca0.3 (Figure 3F, sites 9 and 10) even after the removal of the formed layers, suggesting their role as local cathodic sites.

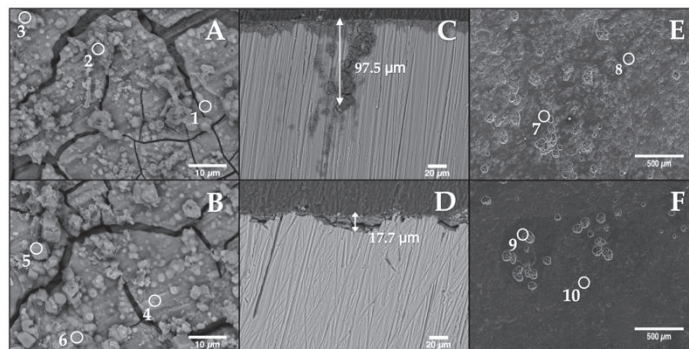


Figure 3. SEM images of the morphological surfaces changes after immersion in Hank's solution for 14 days: (A) Mg and (B) Mg-Ca0.3 (2000×); cross-sections (500×): (C) Mg and (D) Mg-Ca0.3; surfaces after the removal of layers (50×): (E) Mg and (F) Mg-Ca0.3.

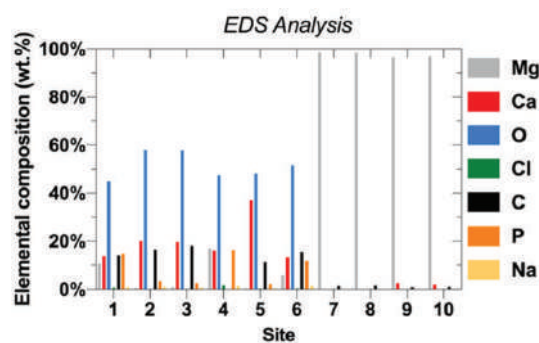


Figure 4. EDS analysis of corresponding sites marked in the SEM images (Figure 3A,B,E,F).

3.4. XPS Analysis After Exposure to Hank's Solution

The XPS analysis was performed as a complementary, to correlate with the EDS elemental composition of the sample surfaces after exposure for 14 days to Hank's solution. The high-resolution spectra (Figure 5) revealed the presence of Mg, Ca, O, C, P, Cl, and Na elements. The main peaks of Mg 2p (at 50.28 eV) and O 1s (at 531.48 eV) were associated with $\text{Mg}(\text{OH})_2$ compound [80]–[82]. The secondary peak of Mg 2p (at 44.98 eV), together with the peaks of P 2p (at 133.43 eV) and Ca 2p (at 347.51 and 351.18 eV) were attributed to $\text{Mg}_3(\text{PO}_4)_2$ and calcium phosphate $[\text{Ca}_{10}(\text{PO}_4)_6(\text{OH})_2]$ compounds. The peaks C 1s and O 1s were considered as a part of CaCO_3 [83]–[85].

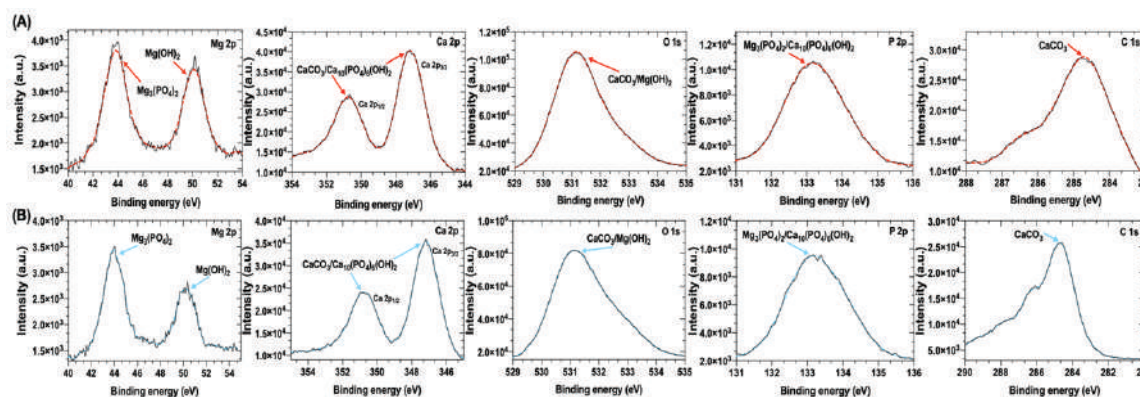


Figure 4. XPS high-resolution spectra of (A) Mg and (B) Mg-Ca0.3 surfaces after exposure to Hank's solution for 14 days (at 37 °C).

3.5. Potentiodynamic Polarization Curves (PDP) After Exposure to Hank's Solution

The cathodic branches have a kinetics controlled by the activation process, while the anodic branches tended to reach a limiting current value related to a barrier effect of the formed corrosion layers on the Mg and Mg-Ca0.3 surfaces. The followed strong increase in the anodic current was attributed to the chloride ions, which transformed the insoluble compound of $\text{Mg}(\text{OH})_2$ to soluble MgCl_2 . The tendency to the next limiting current (at a higher anodic polarization) could be related to the formation of phosphate and carbonate salts on the surfaces, which may act as protective layers, reducing the speed of the anodic process [86]–[88].

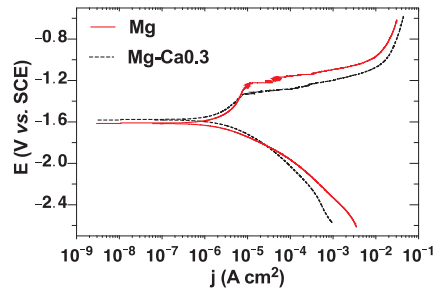


Figure 5. Potentiodynamic polarization (PDP) curves of Mg and Mg-Ca0.3 after 24 h of immersion in Hank's solution.

The limiting anodic current values of Mg-Ca0.3, presenting two surface states, seem to be lower than those of Mg, as well also the cathodic current values. The corrosion potential and current density (j_{corr}) were not calculated by Tafel extrapolation because the presence of precise linear Tafel regions in the PDP curves was not considered. According to the procedure of ASTM G102-89 [89], the value of the polarization resistance (R_p) was estimated from the anodic branch at a polarization of ± 5 mV, as well as the respective value of corrosion current density j_{corr} ($\Delta E/\Delta I$). The “apparent” Tafel constant (B') was calculated through the Stern–Geary relation with the Eq. 5, and the calculated mass loss rate (MR) with the Eq. 6 [89]:

Sample	R_p ($\text{k}\Omega \text{ cm}^2$)	B' (mV)	j_{corr} ($\mu\text{A cm}^{-2}$)	MR ($\text{g m}^{-2} \text{ d}^{-1}$)
Mg	31.57	38.52	1.22	0.12
Mg-Ca0.3	32.81	33.79	1.03	0.10

$$j_{\text{corr}} = \frac{B'}{R_p} \quad (5)$$

$$\text{MR} = K \cdot j_{\text{corr}} \cdot \text{EW} \quad (6)$$

where K is a constant (8.954×10^{-3}), and EW is the approximate equivalent weight of the samples (~ 11.17 for Mg).

The higher value of Mg-Ca0.3 polarization resistance (R_p) to the corrosion process, compared to that of Mg (Table 1) has led to lower values of j_{corr} and MR. These facts suggest the positive effect of Ca as a part of the Mg-alloy, although of a very low content (0.3 wt.%).

Table 1. Values of R_p , j_{corr} , B' , and MR for Mg and Mg-Ca0.3 in Hank's solution (at 27°C).

3.6. SEM and UV-Vis of Ag-Nanoparticles (NPs) on the Surface of Mg-Ca0.3

The UV-Vis absorption band with a maximum at around 290 nm that decreases up to 320 nm (Figure 6A) is attributed to electronic interband transition between electrons in s-orbitals and p-empty orbitals of metallic silver [90],[91]. The minimum observed at 320 nm in all samples is related to the well-known decrease of the imaginary part (k) of the refraction index characteristic of

metallic silver [92]. This wavelength outlines the limits between interband transition, from 320 nm toward lower wavelengths. A maximum of the adsorbance near to 400 nm is a result of the electron density resonance phenomena (surface plasmon resonant band). The bandwidth, asymmetry, and position depend on the Ag-NPs particle size and size distribution. The interaction of the particles with the substrate also affects the optical response due to the localization of the plasmon fluctuations (localized surface plasmon resonance, LSPR). The change in color is influenced by the LSPR band, when the Ag-NPs show difference in morphology, size, and shape. The SEM images (Figure 6C) reveal that the Ag-NPs are well-isolated and in a very low size (Figure 6D) by using the electrolyte of low concentration of Ag^+ (10^{-3} M, 1 min), because of the slow growth rate. However, at one order higher concentration of Ag^+ (10^{-2} M, 1 min), the better connection between Ag-particles leads to the formation of agglomerates, as the diffusion of the Ag-ions is more facilitated to the substrate. It is considered that this effect of short-range interaction induces the LSPR band in the long wavelength region [90],[91],[93], that is why the photograph of the surface becomes darker at higher concentration of Ag-NPs agglomerates. The Ag-NPs and agglomerate size distribution on the Mg-Ca03 surface is presented in Figure 6D.

Figure 6. ELD of Ag-nanoparticles on Mg-Ca0.3 surface from 10^{-3} M and 10^{-2} M AgNO_3 solutions at different times: (A) UV-Vis absorption spectra (evolution over time), (B) representative circular images, (C) SEM micrographs of selected areas (5000 \times), and (D) Ag-NPs and agglomerate size distribution on the Mg-Ca0.3 surface.

3.7. XRD of Ag-Nanoparticles (NPs) on the Surface of Mg-Ca0.3

XRD spectra (Figure 7) indicated the pattern of the hexagonal Mg-metal matrix and the presence of nanostructured Ag crystals of FCC cell structure. The calculated average size of Ag (T) nanocrystallites was 10 nm, according to the Debye-Scherrer's equation [94]–[96]:

$$T = \frac{K \cdot \lambda}{B \cdot \cos(\theta_B)} \quad (7)$$

where K is a dimensionless factor (0.9); λ is the wavelength of the X-rays (1.5406 Å); B is the mean width of the peak at a half of the height (fwhm), considered for the calculation; and θ_B is the angle corresponding to the maximum of the reflection.

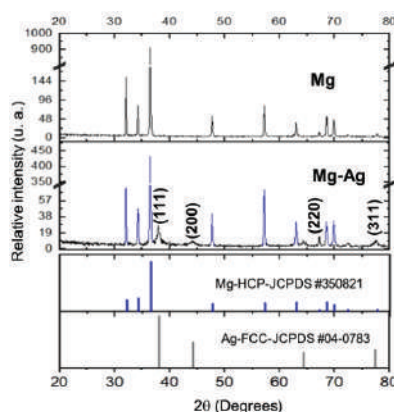


Figure 7. XRD spectra of Ag-NPs deposited on Mg-Ca0.3 surface (from 10^{-3} M, $t = 6$ min). The column bar graphs correspond to HCP Mg-JCPDS #350821 and FCC Ag-JCPDS #04-0783.

3.8. Contact Angle and Surface Free Energy (SFE) of Ag-NPs on the Surface of Mg-Ca0.3

The results following the ASTM D5725-99 [97] methodology, revealed that the contact angle (Figure 8A) depends on the molar concentration of the solution for Ag-NPs electroless deposition, as well as, on the time for deposition (quantity of Ag-NPs on the Mg-Ca0.3 alloy, Figure 6C). The angle value was greater than 120° on the B surfaces (substrate Mg-Ca0.3), as well as on all Ag-NPs deposits formed by 10^{-3} M and 10^{-2} M AgNO_3 , at different times. Therefore, these surfaces are considered as superhydrophobic [98]–[101]. For this analysis the nomenclature was M1 (10^{-3} M; 1,3,6 min) to M4 (10^{-2} M; 1 min), from lowest to highest concentration of deposit of Ag-NPs. The calculated SFE (Figure 8B) showed a decrease in the positive values of B, M1, and M2 surfaces, while the M3 y M4 surfaces presented very negative values. The last fact suggests that these surfaces will exhibit a poor cell bacterial adhesion, as well as wettability properties [98]–[106].

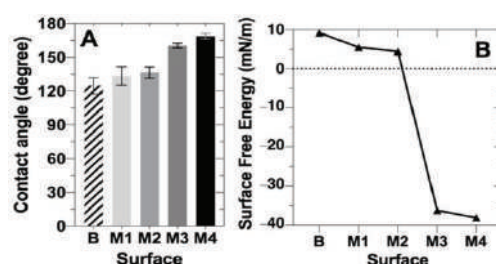


Figure 8. (A) Contact angle values and (B) calculated surface free energy (SFE) of the surfaces.

3.9. Zeta Potential Measurement of *E. coli* and *S. aureus*

The data in Figure 9 showed that zeta potential of *E. coli* and *S. aureus* (bacteria concentration of 10^8 CFU mL^{-1}) tended to be more negative values with respect to the pH of the Mueller–Hinton culture broth ($\text{pH} \approx 7.0$ and up to 11), to understand the electrostatic interactions between bacteria and Ag-NPs deposits on the Mg-Ca0.3 surface. The pH of the culture broth was chosen to be like that of the pH range of change of Hank's solution during the exposure of Mg-Ca0 (Figure 2A). At the initial pH of 7.0 the zeta potential was more negative for *S. aureus* (-5.67 mV) than that of *E. coli* (-3.16 mV), followed by a sudden shift at $\text{pH} \approx 7.25$ to more negative values close to each other and ending at ≈ -11 mV at $\text{pH} = 11$.

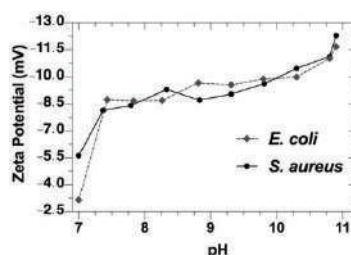


Figure 9. Zeta potential of *E. coli* and *S. aureus* bacteria vs. pH of Mueller–Hinton culture broth.

3.10. Agar Disk-Diffusion Test of Ag-NPs on the Surface of Mg-Ca0.3

The graph of the agar disk diffusion test (Figure 10A) shows the halos (diameters) of the zone of inhibition vs. the growth of the bacteria studied. No zone of inhibition was observed on the bare Mg-Ca0.3 substrate. It was logical to observe a greater antibacterial capacity on the M4 substrate, whose surface is covered by agglomerates of Ag-NP in an extended area (Figure 6C,D). For all the

samples, *S. aureus* presented a larger zone of inhibition than *E. coli*, which indicated that *S. aureus* is more sensitive to the Ag-NPs than *E. coli*. After measuring the diameters of the inhibition halos, the percent inhibition growth diameter (PIDG) (Figure 10B) was determined according to the following equation [107]:

$$\text{PIDG (\%)} = \left(\frac{\text{Diameter of sample} - \text{Diameter of control}}{\text{Diameter of control}} \right) \cdot (100) \quad (8)$$

where diameter of control is the diameter of the Mg-Ca0.3 samples (1 cm), and the diameter of sample is the average diameter of the zone of inhibition after agar disk-diffusion test of three replicates.

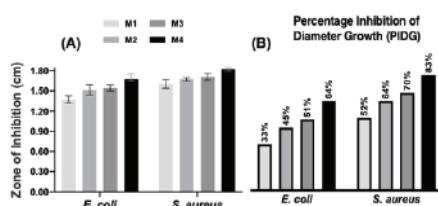


Figure 10. The graph of the (A) zone of inhibition and (B) PIDG, for the sample surfaces exposed to *E. coli* and *S. aureus* on agar for 24 h at 37°C in an incubator (dark conditions).

The exact antimicrobial mechanism of Ag-NPs is still not completely known; however, it is suggested that it depends on chemisorbed Ag^+ ions, released from the silver partial oxidation because of its sensitivity to oxygen [108]. Studies report that the Ag-NPs can generate long-lasting antibacterial activity due to the consequent release of Ag^+ ions which kill the bacteria [109]–[112]. On the other hand, considering that the surface charge of Ag-NPs is not actually measured [113], their interaction with bacteria cell is still open to discussion.

4. CONCLUSIONS

The mass loss and concentration values of the released Mg^{2+} ions were a consequence of the change in pH over time at the end of the experiment. The mass loss of Mg-Ca0.3 was ~ 20% less than that of the Mg samples. The concentration of Mg^{2+} ions released was ~ 3.6 times lower for the Mg-Ca0.3 alloy than for the Mg. A fraction of the mass loss and the concentration of Mg^{2+} ions released are the result of the formation of soluble MgCl_2 , as well as the chelating effect of gluconic acid.

The intermetallic Mg_2Ca particles appeared on the surface of Mg-Ca0.3 even after the removal of the formed layers, suggesting their role as local cathodic sites

The total polarization resistance (R_p), estimated from the PDP data indicated that R_p for Mg-Ca0.3 was higher than that of Mg, suggesting the Ca positive effect.

The electroless deposited Ag-nanoparticles (Ag-NPs) on Mg-Ca0.3 were characterized by the time evolution of the UV-Vis absorption spectra and change in color of the Mg-Ca0.3 substrate. The XRD spectra indicated the presence of nanostructured Ag crystals of FCC cell, in which the calculated average size was 10 nm.

The measured contact angle of the Ag-NPs ($>120^\circ$) indicated that their surfaces may be considered as superhydrophobic, and thus, they may exhibit an antibacterial behavior. The calculated surface free energy (SFE) showed a tendency to very negative values, which suggest that the Ag-NPs exhibit a poor cell bacteria adhesion, as well as poor wettability properties.

The ability to prevent growth of *S. aureus* (Staphylococcus aureus) and *E. coli* (Escherichia coli) bacteria, in the presence of Ag-NPs, was proved by the agar disk diffusion method (Kirby–Bauer test). The greater antibacterial effect of *S. aureus* was attributed to its more negative zeta-potential, attracting more the released Ag^+ ions from the Ag-NPs.

ACKNOWLEDGMENT

J. Luis González-Murguía acknowledges the Mexican National Council for Science and Technology (CONACYT) for the scholarship granted to him for his Ph.D. study. The authors gratefully thank the National Laboratory of Nano- and Biomaterials (LANNBIO-CINVESTAV) for allowing the use of DRX, SEM-EDS and XPS facilities, and to Daniel Aguilar, Victor Rejón Moo and Willian Cauich for their support in data acquisition. The projects: FOMIX-Yucatán 2008-108160, CONACYT LAB-2009-01-123913, 292692, 294643, 188345 y 204822.

REFERENCES

- [1]. Kim, S.G.; Inoue, A.; Masumoto, T. "Increase of Mechanical Strength of a Mg₈₅Zn₁₂Ce₃ Amorphous Alloy by Dispersion of Ultrafine hcp-Mg Particles". *Mater. Trans. JIM* 1991, 32, 875–878,
- [2]. The American Foundry Society Technical Department. *Magnesium Alloys*; Schaumburg, IL, USA, 2006.
- [3]. Staiger, M.P.; Pietak, A.M.; Huadmai, J.; Dias, G. "Magnesium and its alloys as orthopedic biomaterials: A review". *Biomaterials* 2006, 27, 1728–1734.
- [4]. Richards, A.M.; Coleman, N.W.; Knight, T.A.; Belkoff, S.M.; Mears, S.C. "Bone density and cortical thickness in normal, osteopenic, and osteoporotic sacra". *J. Osteoporos.* 2010, 504078.
- [5]. Li, L.C.; Gao, J.C.; Wang, Y. "Evaluation of cyto-toxicity and corrosion behavior of alkali-heat-treated magnesium in simulated body fluid". *Surf. Coat. Technol.* 2004, 185, 92–98.
- [6]. Kirkland, N.T. "Magnesium biomaterials: Past, present and future". *Corros. Eng. Sci. Technol.* 2012, 47, 322–328,
- [7]. Li, N.; Zheng, Y. Novel. "Magnesium Alloys Developed for Biomedical Application: A Review". *J. Mater. Sci. Technol.* 2013, 29, 489–502.
- [8]. Zheng, Y.; Gu, X.; Witte, F. "Biodegradable metals." *Mater. Sci. Eng. R Rep.* 2014, 77, 1–34.
- [9]. Luthringer, B.J.; Feyerabend, F.; Willumeit-Römer, R. "Magnesium-based implants: A mini-review". *Magnes. Res.* 2014, 27, 142–154.
- [10]. Tkacz, J.; Slouková, K.; Minda, J.; Drábiková, J.; Fintová, S.; Doležal, P.; Wasserbauer, J. "Influence of the Composition of the Hank's Balanced Salt Solution on the Corrosion Behavior of AZ31 and AZ61 Magnesium Alloys". *Metals* 2017, 7, 465.
- [11]. Riaz, U.; Shabib, I.; Haider, W. "The current trends of Mg alloys in biomedical applications—A review". *J. Biomed. Mater. Res. Part B Appl. Biomater.* 2018, 107, 1970–1996.
- [12]. Chen, Y.-T.; Hung, F.-Y.; Syu, J.-C. "Biodegradable Implantation Material: Mechanical Properties and Surface Corrosion Mechanism of Mg-1Ca-0.5Zr Alloy". *Metals* 2019, 9, 857.
- [13]. Pleshchitsker, A. "Biological Role of Magnesium". *Clin. Chem.* 1958, 4, 429–451.
- [14]. Hartwig, A. "Role of magnesium in genomic stability". *Mutat. Res.* 2001, 475, 113–121.
- [15]. Chen, Q.; Thouas, G.A. "Metallic implant biomaterials". *Mater. Sci. Eng. R Reports* 2015, 87, 1–57,
- [16]. Song, G.; Song, S. "A Possible Biodegradable Magnesium Implant Material". *Adv. Eng. Mater.* 2007, 9, 298–302.
- [17]. Chen, Y.; Xu, Z.; Smith, C.; Sankar, J. "Recent advances on the development of magnesium alloys for biodegradable implants". *Acta Biomater.* 2014, 10, 4561–4573.
- [18]. Zhao, D.; Witte, F.; Lu, F.; Wang, J.; Li, J.; Qin, L. "Current status on clinical applications of magnesium-based orthopaedic implants: A review from clinical translational perspective". *Biomaterials* 2017, 112, 287–302.
- [19]. Seitz, J.-M.; Wulf, E.; Freytag, P.; Bormann, D.; Bach, F.-W. "The Manufacture of Resorbable Suture Material from Magnesium". *Adv. Eng. Mater.* 2010, 12, 1099–1105.
- [20]. Chng, C.B.; Lau, D.P.; Choo, J.Q.; Chui, C.K. "A bioabsorbable microclip for laryngeal microsurgery: Design and evaluation". *Acta Biomater.* 2012, 8, 2835–2844.

-
- [21]. Zreiqat, H.; Howlett, C.R.; Zannettino, A.; Evans, P.; Schulze-Tanzil, G.; Knabe, C.; Shakibaei, K.M. "Mechanisms of magnesium-stimulated adhesion of osteoblastic cells to commonly used orthopaedic implants". *J. Biomed. Mater. Res.* 2002, 62, 175–184.
- [22]. Yamasaki, Y.; Yoshida, Y.; Okazaki, M.; Shimazu, A.; Kubo, T.; Akagawa, Y.; Uchida, T. "Action of FGMgCO₃Ap-collagen composite in promoting bone formation". *Biomaterials* 2003, 24, 4913–4920.
- [23]. Revell, P.A.; Damien, E.; Zhang, X.S.; Evans, P.; Howlett, C.R. "The Effect of Magnesium Ions on Bone Bonding to Hydroxyapatite Coating on Titanium Alloy Implants". *Key Eng. Mater.* 2003, 254, 447–450.
- [24]. Park, J.B.; Bronzino, J.D. "Biomaterials: Principles and Applications"; CRC Press: Boca Raton, FL, USA, 2003; pp. 1–20, ISBN 0-8493-1491-7.
- [25]. Prakasam, M.; Locs, J.; Salma-Ancane, K.; Loca, D.; Largeteau, A.; Berzina-Cimdina, L. "Biodegradable Materials and Metallic Implants-A Review". *J. Funct. Biomater.* 2017, 8, 44.
- [26]. Yamasaki, Y.; Yoshida, Y.; Okazaki, M.; Shimazu, A.; Uchida, T.; Kubo, T.; Akagawa, Y.; Hamada, Y.; Takahashi, J.; Matsuura, N. "Synthesis of functionally graded MgCO₃ apatite accelerating osteoblast adhesion". *J. Biomed. Mater. Res.* 2002, 62, 99–105.
- [27]. Wolf, F.I.; Cittadini, A. "Chemistry and biochemistry of magnesium". *Mol. Asp. Med.* 2003, 24, 3–9.
- [28]. Song, G.L. "Corrosion electrochemistry of magnesium (Mg) and its alloys". In *Corrosion of Magnesium Alloys*, 1st ed.; Song, G.L., Ed.; Woodhead Publishing: Cambridge, UK, 2011; pp. 3–65.
- [29]. Bahmani, A.; Arthanari, S.; Shin, K.S. "Formulation of corrosion rate of magnesium alloys using microstructural parameters". *J. Magnes. Alloys* 2020, 8, 134–149.
- [30]. Pourbaix, M. "Atlas of Electrochemical Equilibria in Aqueous Solution"; Pergamon Press: Oxford, UK, 1966.
- [31]. Jenkins, H.D.B. *Handbook of Chemistry and Physics*, 73rd ed.; CRC Press: Boca Raton, FL, USA, 1992; p. 5585.
- [32]. Atkins, P.; De Paula, J. *Atkins' Physical Chemistry*, 10th ed.; Oxford University Press: Oxford, UK, 2014; pp. 255–257.
- [33]. Cui, L.; Liu, H.; Xue, K.; Zeng, W.; Li, R.; Guan, S. "In Vitro Corrosion and Antibacterial Performance of Micro-Arc Oxidation Coating on AZ31 Magnesium Alloy: Effects of Tannic Acid". *J. Electrochem. Soc.* 2018, 165, C821–C829.
- [34]. Curioni, M.; Salamone, L.; Scenini, F.; Santamaria, M.; Di Natale, M. "A mathematical description accounting for the superfluous hydrogen evolution and the inductive behaviour observed during electrochemical measurements on magnesium". *Electrochim. Acta* 2018, 274, 343–352.
- [35]. Makar, G.L.; Kruger, J. "Corrosion of magnesium". *Inter. Mater. Rev.* 1993, 38, 138–153.
- [36]. Silva, E.L.; Lamaka, S.V.; Mei, D.; Zheludkevich, M.L. "The reduction of dissolved oxygen during magnesium corrosion". *Chemistry Open* 2018, 7, 664–668.
- [37]. Strebl, M.; Bruns, M.; Virtanen, S. Editors' choice—Respirometric in situ methods for real-time monitoring of corrosion rates: Part I. Atmospheric corrosion. *J. Electrochem. Soc.* 2020, 167, 021510.
- [38]. Wang, C.; Mei, D.; Wiese, G.; Wang, L.; Deng, M.; Lamaka, S.V.; Zheludkevich, M.L. "High rate oxygen reduction reaction during corrosion of ultra-high-purity magnesium." *NPJ Mater. Degrad.* 2020, 4, 42.
- [39]. Li, S.; Yang, X.; Hou, J.; Du, W. "A review on thermal conductivity of magnesium and its alloys". *J. Magnes. Alloys* 2020, 8, 78–90.
-

-
- [40]. Zhang, E.; Yin, D.; Xu, L.; Yang, L.; Yang, K. "Microstructure, mechanical and corrosion properties and biocompatibility of Mg–Zn–Mn alloys for biomedical application". *Mater. Sci. Eng. C* 2009, 29, 987–993.
- [41]. Sankar, M.; Vishnu, J.; Gupta, M.; Manivasagam, G. "Magnesium-Based Alloys and Nanocomposites for Biomedical Application, Applications of Nanocomposite Materials in Orthopedics"; Woodhead Publishing: Cambridge, UK, 2018; pp. 83–109.
- [42]. Nie, J.F.; Muddle, B.C. "Precipitation hardening of Mg–Ca(–Zn) alloys". *Scr. Mater.* 1997, 37, 1475–1481.
- [43]. Ilich, J.Z.; Kerstetter, J.E. "Nutrition in bone health revisited: A story beyond calcium." *J. Am. Coll. Nutr.* 2000, 19, 715–737.
- [44]. ASM International. Alloy Phase Diagram. In *Handbook ASM; The Materials Information Company*: 1992; Volume 3, p. 79.
- [45]. Villars, P.; Calvert, L.D.; Pearson, W.B. *Pearson's Handbook of Crystallographic Data for Intermetallic Phases*; ASM International, Materials Park: Russell, OH, USA, 1985.
- [46]. Li, Z.J.; Gu, X.N.; Lou, S.Q.; Zheng, Y.F. "The development of binary Mg–Ca alloys for use as biodegradable materials within bone". *Biomaterials* 2008, 29, 1329–1344.
- [47]. Kirkland, N.T.; Birbilis, N.; Walker, J.; Woodfield, T.; Dias, G.J.; Staiger, M.P. "In-vitro dissolution of magnesium–calcium binary alloys: Clarifying the unique role of calcium additions in bioresorbable magnesium implant alloys". *J. Biomed. Mater. Res.* 2010, 95, 91–100.
- [48]. Zheng, H.; Yu, L.; Lyu, S.; You, C.; Chen, M. "Insight into the Role and Mechanism of Nano MgO on the Hot Compressive Deformation Behavior of Mg–Zn–Ca Alloys". *Metals* 2020, 10, 1357.
- [49]. Wen, C.E.; Mabuchi, M.; Yamada, Y.; Shimojima, K.; Chino, Y.; Asahina, T. "Processing of biocompatible porous Ti and Mg". *Scr. Mater.* 2001, 45, 1147–1153.
- [50]. Saris, N.E.; Mervaala, E.; Karppanen, H.; Khawaja, J.A.; Lewenstam, A. "Magnesium: An update on physiological, clinical and analytical aspects." *Clin. Chim. Acta* 2000, 294, 1–26.
- [51]. Okuma, T. "Magnesium and bone strength". *Nutrition* 2001, 17, 679–680.
- [52]. Wan, Y.; Xiong, G.; Luo, H.; He, F.; Huang, Y.; Zhou, X. "Preparation and characterization of a new biomedical magnesium–calcium alloy". *Mater. Des.* 2008, 29, 2034–2037.
- [53]. Witte, F.; Hort, N.; Vogt, C.; Cohen, S.; Kainer, K.U.; Willumeit, R. "Degradable biomaterials based on magnesium corrosion". *Curr. Opin. Solid State Mater. Sci.* 2008, 12, 63–72.
- [54]. Harandi, S.E.; Mirshahi, M.; Koleini, S.; Idris, M.H.; Jafari, H.; Kadir, M.R.A. "Effect of calcium content on the microstructure, hardness and in-vitro corrosion behavior of biodegradable Mg–Ca binary alloy". *Mater. Res.* 2013, 16, 11–18.
- [55]. Coelho, P.G.; Jimbo, R. "Osseointegration of metallic devices: Current trends based on implant hardware design." *Arch. Biochem. Biophys.* 2014, 561, 99–108.
- [56]. Necula, B.S.; Fratila-Apachitei, L.E.; Berkani, A.; Apachitei, I.; Duszczyk, J. "Enrichment of anodic MgO layers with Ag nanoparticles for biomedical applications". *J. Mater. Sci. Mater. Med.* 2009, 20, 339–345.
- [57]. Hori, K.; Matsumoto, S. "Bacterial adhesion: From mechanism to control". *Biochem. Eng. J.* 2010, 48, 424–434.
- [58]. Sondi, I.; Salopek-Sondi, B. "Silver nanoparticles as antimicrobial agent: A case study on *E. coli* as a model for Gram-negative bacteria", *J. Colloid Interface Sci.* 2004, 275, 177–182.
- [59]. Alt, V.; Bechert, T.; Steinrücke, P.; Wagener, M.; Seidel, P.; Dingeldein, E.; Domann, E.; Schnettler, R. "An in vitro assessment of the antibacterial properties and cytotoxicity of nanoparticulate silver bone cement". *Biomaterials* 2004, 25, 4383–4391.
-

-
- [60]. Kim, J.S.; Kuk, E.; Yu, K.; Kim, J.; Park, S.; Lee, H.; Kim, S.; Park, Y.; Park, Y.; Hwang, C.; et al. "Antimicrobial effects of silver nanoparticles". *Nanomedicine* 2007, 3, 95–101.
- [61]. Shahverdi, A.R.; Fakhimi, A.; Shahverdi, H.R.; Minaian, S. "Synthesis and effect of silver nanoparticles on the antibacterial activity of different antibiotics against *Staphylococcus aureus* and *Escherichia coli*". *Nanomedicine* 2007, 3, 168–171.
- [62]. Burduşel, A.-C.; Gherasim, O.; Grumezescu, A.; Mogoantă, L.; Ficai, A.; Andronescu, E. "Biomedical Applications of Silver Nanoparticles: An Up-to-Date Overview". *Nanomaterials* 2018, 8, 681.
- [63]. Liu, Y.; Li, C.; Luo, S. et al. "Inter-transformation between silver nanoparticles and Ag^+ induced by humic acid under light or dark conditions". *Ecotoxicology* 2020, 30, 1376–1385.
- [64]. ISO 16428. Implants for Surgery—Test Solutions and Environmental Conditions for Static and Dynamic Corrosion Tests on Implantable Materials and Medical Devices; Switzerland, 2005.
- [65]. Kuwahara, H.; Al-Abdullat, Y.; Mazaki, N.; Tsutsumi, S.; Aizawa, T. "Precipitation of Magnesium Apatite on Pure Magnesium Surface during Immersing in Hank's Solution". *Mater. Trans.* 2001, 42, 1317–1321.
- [66]. Abidin, N.I.Z.; Martin, D.; Atrens, A. "Corrosion of high purity Mg, AZ91, ZE41 and $\text{Mg}_{20}\text{Zn}_{10}\text{Mn}$ in Hank's solution at room temperature". *Corros. Sci.* 2011, 53.
- [67]. ASTM G31-12a. Standard Guide for Laboratory Immersion Corrosion Testing of Metals; ASTM International: West Conshohocken, PA, USA, 2021.
- [68]. ASTM G1-03. Standard Practice for Preparing, Cleaning and Evaluating Corrosion Test Specimens; ASTM International: West Conshohocken, PA, USA, 2017.
- [69]. Heatley, N.G. "A method for the assay of penicillin", *Biochem. J.* 1944, 38, 61–65.
- [70]. Clinical and Laboratory Standards Institute. M02-A11, Performance Standards for Antimicrobial Disk Susceptibility Tests: Approved Standard; Clinical and Laboratory Standards Institute: Wayne, PA, USA, 2012.
- [71]. Balouiri, M.; Sadiki, M.; Ibnsouda, S.K. "Methods for in vitro evaluating antimicrobial activity: A review". *J. Pharm. Anal.* 2016, 6, 71–79.
- [72]. Bakhsheshi Rad, H.R.; Hasbullah Idris, M.; Abdul Kadir, M.R.; Farahany, S. "Microstructure analysis and corrosion behavior of biodegradable Mg–Ca implant alloys". *Mater. Des.* 2012, 33, 88–97.
- [73]. Liu, Y.; Liu, X.; Zhang, Z.; Farrell, N.; Chen, D.; Zheng, Y. "Comparative, real-time in situ monitoring of galvanic corrosion in Mg– Mg_2Ca and Mg– MgZn_2 couples in Hank's solution". *Corros. Sci.* 2019, 161, 108185.
- [74]. Ding, Z.Y.; Cui, L.Y.; Chen, X.B.; Zeng, R.C.; Guan, S.K.; Li, S.Q.; Zhang, F.; Zou, Y.H.; Liu, Q.Y. "In vitro corrosion of micro-arc oxidation coating on Mg–1Li–1Ca alloy—The influence of intermetallic compound Mg_2Ca ". *J. Alloys Compd.* 2018, 764, 250–260.
- [75]. Khorasani, F.; Emamy, M.; Malekan, M.; Mirzadeh, H.; Pourbahari, B.; Krajnák, T.; Minárik, P. "Enhancement of the microstructure and elevated temperature mechanical properties of as-cast Mg– Al_2Ca – Mg_2Ca in-situ composite by hot extrusion". *Mater. Charact.* 2019, 147, 155–164.
- [76]. Zeng, R.C.; Li, X.T.; Li, S.Q.; Zhang, F.; Han, E.H. "In vitro degradation of pure Mg in response to glucose". *Sci. Rep.* 2015, 5, 13026.
- [77]. Song, G.L.; Atrens, A. "Corrosion Mechanisms of Magnesium Alloys". *Adv. Eng. Mater.* 2000, 1, 11–33.
- [78]. Thakur, V.K.; Thakur, M.K.; Kessler, M.R. *Handbook of Composites from Renewable Materials*; John Wiley & Sons: Hoboken, NJ, USA, 2017.
-

-
- [79]. Zhang, Y.F.; Hinton, B.; Wallace, G.; Liu, X.; Forsyth, M. "On corrosion behaviour of magnesium alloy AZ31 in simulated body fluids and influence of ionic liquid pretreatments". *Corros. Eng. Sci. Technol.* 2012, 47, 374–382.
- [80]. Santamaria, M.; Di Quarto, F.; Zanna, S.; Marcus, P. "Initial surface film on magnesium metal: A characterization by X-ray photoelectron spectroscopy (XPS) and photocurrent spectroscopy (PCS)". *Electrochim. Acta* 2007, 53, 1314–1324.
- [81]. Fournier, V.; Marcus, P.; Olefjord, I. "Oxidation of magnesium". *Surf. Inter. Anal.* 2002, 34, 494–497.
- [82]. Moulder, J.F.; Stickle, W.F.; Sobol, P.E.; Bomben, K.D. *Handbook of X-Ray Photoelectron Spectroscopy*; Physical Electronics Inc.: Chanhassen, MN, USA, 1992.
- [83]. Felker, D.L.; Sherwood, P.M.A. "Magnesium Phosphate ($\text{Mg}_3(\text{PO}_4)_2$) by XPS". *Surf. Sci. Spectra* 2001, 8, 38–44.
- [84]. Nelson, A.E. Mature Dental Enamel "[Calcium Hydroxyapatite, $\text{Ca}_{10}(\text{PO}_4)_6(\text{OH})_2$] by XPS". *Surf. Sci. Spectra* 2002, 9, 250–259.
- [85]. Baer, D.R.; Moulder, J.F. "High Resolution XPS Spectrum of Calcite (CaCO_3)". *Surf. Sci. Spectra* 1993, 2, 1.
- [86]. Yamamoto, A.; Hiromoto, S. "Effect of inorganic salts, amino acids and proteins on the degradation of pure magnesium in vitro". *Mater. Sci. Eng. C* 2009, 29, 1559–1568.
- [87]. Xin, Y.; Hu, T.; Chu, P.K. "Degradation behaviour of pure magnesium in simulated body fluids with different concentrations of HCO_3^- ". *Corros. Sci.* 2011, 53, 1522–1528.
- [88]. Atrens, A.; Song, G.L.; Cao, F.; Shi, Z.; Bowen, P.K. "Advances in Mg corrosion and research suggestions". *J. Magnes. Alloys* 2013, 1, 177–200.
- [89]. ASTM G102–89. *Standard Practice for Calculation of Corrosion Rates and Related Information from Electrochemical Measurements*; ASTM International: West Conshohocken, PA, USA, 1989.
- [90]. Pinchuk, A.; Hilger, A.; Von Plessen, G.; Kreibig, U. "Substrate effect on the optical response of silver nanoparticles". *Nanotechnology* 2004, 15, 1890–1896.
- [91]. Jain, P.K.; El-Sayed, M.A. "Noble Metal Nanoparticle Pairs: Effect of Medium for Enhanced Nanosensing". *Nano Lett.* 2008, 8, 4347–4352.
- [92]. Johnson, P.B.; Christy, R.W. "Optical constants of the noble metals". *Phys. Rev. B* 1972, 6, 4370–4379.
- [93]. Kumura, S.; Sugita, T.; Nakamura, K.; Kobayashi, N. "An improvement in the coloration properties of Ag deposition-based plasmonic EC devices by precise control of shape and density of deposited Ag nanoparticles". *Nanoscale* 2020, 12, 23975–23983.
- [94]. Holzwarth, U.; Gibson, N. "The Scherrer equation versus the 'Debye-Scherrer equation'". *Nat. Nanotechnol.* 2011, 6, 534.
- [95]. Loua, C.-W.; Chenb, A.-P.; Lic, T.-T.; Linbde, C.-H. "Antimicrobial activity of UV-induced chitosan capped silver nanoparticles". *Mater. Lett.* 2014, 128, 248–252.
- [96]. Singaravelan, R.; Bangaru Sudarsan Alwar, S. "Electrochemical synthesis, characterisation and phytogetic properties of silver nanoparticles". *Appl. Nanosci.* 2015, 5, 983–991.
- [97]. ASTM D5725-99. *Standard Test Method for Surface Wettability and Absorbency of Sheeted Materials Using an Automated Contact Angle Tester*, Annual Book of ASTM Standards; ASTM Committee on Standards, ASTM: West Conshohocken, PA, USA, 2008.
- [98]. Carré, A.; Mittal, K.L. *Superhydrophobic Surface*; CRC Press: Boca Raton, FL, USA, 2009; pp. 3–17.
- [99]. Yeganeh, M.; Mohammadi, N. "Superhydrophobic surface of Mg alloys: A review". *J. Magnes. Alloys* 2018, 6, 59–70.
-

-
- [100]. Mahmood, M.H.; Maleque, M.A.; Rahman, M. "Hard-Hydrophobic Nano-CuO Coating via Electrochemical Oxidation for Heat Transfer Performance Enhancement". *Arab. J. Sci. Eng.* 2021, 1–11.
- [101]. Sanchez-Perez, A.; Cano-Millá, N.; Moya Villaescusa, M.J.; Montoya Carralero, J.M.; Navarro Cuellar, C. "Effect of Photofunctionalization with 6 W or 85 W UVC on the Degree of Wettability of RBM Titanium in Relation to the Irradiation Time". *Appl. Sci.* 2021, 11, 5427.
- [102]. Li, X.-M.; Reinhoudt, D.; Crego-Calama, M. "What do we need for a superhydrophobic surface?. A review on the recent progress in the preparation of superhydrophobic surfaces". *Chem. Soc. Rev.* 2007, 36, 1350–1368.
- [103]. Zhang, X.; Shi, F.; Niu, J.; Jiang, Y.; Wang, Z. "Superhydrophobic surfaces: From structural control to functional application". *J. Mater. Chem.* 2008, 18, 621–633.
- [104]. Guo, Z.; Liu, W.; Su, B.-L. "Superhydrophobic surfaces: From natural to biomimetic to functional". *J. Colloid Interface Sci.* 2011, 353, 335–355.
- [105]. Zhang, Y.-L.; Xia, H.; Kim, E.; Sun, H.-B. "Recent developments in superhydrophobic surfaces with unique structural and functional properties". *Soft Matter* 2012, 8, 11217–11231..
- [106]. Latthe, S.S.; Gurav, A.B.; Maruti, C.S.; Vhatkar, R.S. "Recent Progress in Preparation of Superhydrophobic Surfaces: A Review", *J. Surf. Eng. Mater. Adv. Technol.* 2012, 2, 76–94.
- [107]. Himratul-Aznita, W.H.; Mohd-Al-Faisal, N.; Fathilah, A.R. "Determination of the percentage inhibition of diameter growth (PIDG) of Piper betle crude aqueous extract against oral *Candida* species". *J. Med. Plants Res.* 2011, 5, 878–884.
- [108]. Lok, C.N.; Ho, C.M.; Chen, R.; He, Q.Y.; Yu, W.Y.; Sun, H.; Tam, P.K.H.; Chiu, J.F.; Che, C.M. "Silver nanoparticles: Partial oxidation and antibacterial activities". *J. Biol. Inorg. Chem.* 2007, 12, 527–534.
- [109]. Spadaro, J.A.; Berger, T.J.; Barranco, S.D.; Chapin, S.E.; Becker, R.O. "Antibacterial Effects of Silver Electrodes with Weak Direct Current". *Antimicrob. Agents Chemother.* 1974, 6, 637–642.
- [110]. Gupta, A.; Matsui, K.; Lo, J.F.; Silver, S. "Molecular basis for resistance to silver cations in *Salmonella*". *Nat. Med.* 1999, 5, 183–188.
- [111]. Choi, O.; Deng, K.K.; Kim, N.J.; Ross, L.; Surampalli, R.Y.; Hu, Z. "The inhibitory effects of silver nanoparticles, silver ions, and silver chloride colloids on microbial growth". *Water Res.* 2008, 42, 3066–3074.
- [112]. Shao, Y.; Zeng, R.C.; Li, S.Q.; Cui, L.Y.; Zou, Y.H.; Guan, S.K.; Zheng, Y.F. "Advance in Antibacterial Magnesium Alloys and Surface Coatings on Magnesium Alloys: A Review". *Acta Metall. Sin.* 2020, 33, 615–629,
Choi, O.; Hu, Z. "Size Dependent and Reactive Oxygen Species Related Nanosilver Toxicity to Nitrifying Bacteria", *Environ. Sci. Technol.* 2008, 42, 4583–4588.
-

ACTIVIDAD ELECTROQUÍMICA DE MG EXTRUIDO EN SOLUCIÓN FISIOLÓGICA DE HANK

Miguel Manzano Canul

José Luis González-Murguía

Lucien Veleza

Departamento de Física Aplicada, Centro de Investigación y de Estudios Avanzados (CINVESTAV-IPN), Unidad Mérida, Yucatán, México

Este estudio presenta el proceso de degradación del Mg expuesto durante 7 y 14 días al medio fisiológico (solución de Hank), como un material posible de implantes temporales en el cuerpo humano. Los resultados de las pruebas de inmersión, pruebas electroquímicas (potencial de corrosión, OCP y curvas de polarización, PDP) y la caracterización superficial han sido colaborados. El análisis elemental (EDS) y los espectros de XPS revelan una película formada por $\text{Mg}(\text{OH})_2$, producto de corrosión de Mg, depósitos cristalinos de NaCl y CaCO_3 , así mismo de los fosfatos $\text{Mg}_3(\text{PO}_4)$ y el hidroxiapatita $\text{Ca}_{10}(\text{PO}_4)_6(\text{OH})_2$. Después de eliminar las películas formadas en la superficie, las imágenes SEM muestran corrosión localizada, como aparentes picaduras, que podría atribuirse a la evolución de gas hidrógeno, un proceso simultaneo durante la degradación del Mg. El potencial de corrosión a circuito abierto (OCP) se ha desplazado desde un valor inicial de -1.70 V (SCE) hacia valores menos negativos, alcanzando el valor de -1.59 V, debido a la formación de la capa de productos, que actúa como barrera física con el medio. Las mediciones de pH, iones Mg^{2+} liberados y pérdida de masa permiten corroborar una tendencia de aumento ligero en la velocidad de corrosión.

Palabras Clave: Magnesio, Degradación, Solución de Hank, PDP, XPS, SEM-EDS.

LIVER FAILURE WITH MECHANICAL JAUNDICE

Elena Mostiuk

Department of Fundamental Medicine Taras Shevchenko National University of Kyiv
Educational and Scientific Centre «Institute of Biology and Medicine», assistant of the chair,
Ph.D. in Medicine.

Abstract

The article describes pattern between the degree of activity of hepatic fat cells and the degree of development of fibrosis in the liver tissue in the patients with obstructive jaundice of benign origin. This pattern is not included in the traditional diagnosis of morphological and functional violations in liver tissue with severe inflammation with prolonged obstruction of the biliary tract, that is a significant disadvantage in the treatment of profile patients.

Keywords: liver tissue, fat cells (Ito cells), fibrosis, mechanical jaundice, liver failure, staged surgical tactics.

Introduction

Mechanical jaundice is accompanied by high intoxication, which leads to the development of liver failure. Mechanical jaundice is the cause of pathological changes in the liver and other organs of the patient with the development of multiple organ failure, leading to high mortality. At the same time, traditional surgical correction of mechanical jaundice is not always effective, and postoperative mortality remains high (15-45%).

Despite the fact that minimally invasive surgical methods and advanced detoxification methods are actively used, many patients develop liver failure after surgery, which was not diagnosed in the preoperative period.

There is evidence of the possible participation of fat cells (Ito cells) in the development of liver failure, which, together with fibroblasts, are responsible for the development of liver fibrosis due to their increased secretion of extracellular matrix, such as collagen and fibronectin.

A number of experimental studies indicate relations between oxidative stress and the development of fibrosis in various organs, including the liver. Oxidative stress acts as an activator of liver fat cells.

It was noted that activated Ito cells are able to synthesize cytokines that enhance their action, such as tumor necrosis factor (TNF- α), fibroblast growth factor (FGF), IL-2 and IL-8 in response to an intrahepatic increase in concentration proinflammatory cytokines and growth factors, which causes the progression of hepatofibrosis.

Thus, an important point in choosing the tactics of surgical treatment is the detection of hepatic lipocytes in biopsies of liver tissue.

The aim of the study was to determine the features of the morphological structure of the connective tissue of the liver and the presence of activated Ito cells in patients with mechanical jaundice.

Materials and methods

We have examined 128 patients of different age and sex with extrahepatic cholestasis of benign genesis.

The main reasons for the development of obstructive jaundice in the examined patients were the following: calculous cholecystitis, stenosing papillitis, stricture of the common bile duct, pseudocyst of the pancreas.

During the operation, fragments of liver tissue were taken, which were examined morphologically using histochemical reactions, light and electron microscopy. To detect fat cells in liver cells, staining of frozen sections with Sudan III and Sudan IV was used.

To determine collagen types I and III in tissue samples, staining with picrofuchsin was used. Collagen study was carried out in polarized light on a "Polmy-A" microscope. To determine the activity of Ito cells, the material was fixed in a 10% solution of neutral formalin, dehydrated in alcohols of increasing concentration, and embedded in celloidin. Sections 5–7 μm thick were stained with hematoxylin and eosin, as well as picrofuchsin. To fix material for electron microscopy the liver tissue fragments we used a 4% glutaraldehyde solution, then decalcified in a Trilon B solution, fixed in a solution of osmic acid, dehydrated in alcohols of increasing concentration, then in acetone and embedded in epoxy resin. It was carried out in accordance with the methodological instructions of Weekly.

Semi-thin and ultra-thin sections were prepared using a UMTP-ZM microtome. Semi-thin sections were stained with toluidine blue and basic fuchsin. Ultra-thin slices were contrasted according to Reynolds.

The ultrastructural organization of liver cells was studied using an EMV-100BR electron microscope.

Results and its discussion

In patients with extrahepatic cholestasis of benign genesis, significant violations of the morphological state of the liver tissue were revealed. Microscopic analysis of liver samples shows fibrosis in the area of the bile ducts, dilated portal tracts with lymphohistiocytic infiltration. In the foci of fibrosis, an increased number of fat cells and fibroblasts are found, which led to an increased production of collagen I and III type.

Liver lipocytes are characterized by a large number of fat droplets in the cytoplasm, which occupy almost the entire volume of the cytoplasm, and a small hyperchromic nucleus with areas of chromatin condensation located centrally or asymmetrically.

It also revealed Ito-cells with a moderate content of lipid droplets in the cytoplasm and myofibroblast-like cells, the cytoplasm of which is filled with filamentous structures.

Analysis of the material obtained shows that all patients with mechanical jaundice were found to have hepatic lipocytes, collagen types I and III, myofibroblast-like cells, which confirms the development of stromal liver fibrosis.

Morphological changes in liver tissue sclerosis were confirmed by a high level of fibroblast growth factor (FGF) in the blood of patients.

The severity of the inflammatory reaction in the hepatopancreatoduodenal zone in patients with mechanical jaundice was characterized by a high content of inflammatory cytokines IL-2, IL-8, TNF- α in blood, which led to the activation of Ito cells and the main diagnostic criteria for prognosis the development of sclerosis and liver failure.

The properties of connective tissue largely depend on the functional activity of Ito cells and the severity of infiltrative processes.

The degree of impairment of the functional state of the connective tissue is one of the factors that determine the further development and outcome of the disease. Therefore, the morphological study of liver biopsies in patients with mechanical jaundice provides useful information for determining the possible volume and stages of surgical treatment, and also makes it possible to determine the postoperative management of patients.

Conclusions

1. Determination of the functional state of the components of connective tissue is of great prognostic value in patients with mechanical jaundice.

2. Assessment of the state of connective tissue provides important information for the choice of surgical treatment tactics, as well as for the development of methods for the prevention of preoperative and postoperative complications using modern detoxification methods and staged surgical tactics.

EFFECT OF THERMAL RADIATION AND CHEMICAL REACTION ON MHD FLOW OF BLOOD IN STRETCHING PERMEABLE VESSEL

Dr. Binyam Zigta

Wachemo University College of Natural and Computational Science
ETHIOPIA

Abstract: In this paper theoretical analysis of blood flow in the presence of thermal radiation and chemical reaction under the influence of time dependent magnetic field intensity has been studied. The unsteady non linear partial differential equations of blood flow considers time dependent stretching velocity, the energy equation also accounts time dependent temperature of vessel wall and concentration equation includes time dependent blood concentration. The governing non linear partial differential equations of motion, energy and concentration are converted into ordinary differential equations using similarity transformations solved numerically by applying ode45. MATLAB code is used to analyze theoretical facts. The effect of physical parameters viz., permeability parameter, unsteadiness parameter, Prandtl number, Hartmann number, thermal radiation parameter, chemical reaction parameter and Schmidt number on flow variables viz., velocity of blood flow in vessel, temperature and concentration of blood has been analyzed and discussed graphically. From the simulation study the following important results are obtained: velocity of blood flow increases with both increment of permeability and unsteadiness parameter. Temperature of the blood increases in vessel wall as Prandtl number and Hartmann number increases. Concentration of the blood decreases as time dependent chemical reaction parameter and Schmidt number increases.

Keywords: Stretching velocity, similarity transformations, time dependent magnetic field intensity, thermal radiation, chemical reaction.

BURNOUT SYNDROME AT MEDICAL STAFF FROM ROMANIA

Boboc Daniela

Teacher at the School Center for Inclusive Education from Constanta - Romania;

ABSTRACT

Burnout syndrome is common in the life of medical staff, but in the case of intensive care doctors it is increasing lately. Exhaustion causes a decrease in both functionality and physical and mental condition. The yield is lower and for this reason performing medical duties can become difficult for medical staff suffering from burnout syndrome. The coronavirus pandemic has affected everyone but I believe that the most affected category of people are the medical staff working in intensive care. The first line, as it is usually called this category of medical staff, coped this pandemic, but the sacrifices were great. The guard shifts were numerous, the patients were many and in a very serious condition, some being killed by this virus. Some doctors began to show signs of chronic fatigue, depression and what was worse, they began to become more indifferent to those around them. Those characteristics are the main signs of burnout. However, the Romanian medical system was overworked but faced with success the large number of patients. The mobile hospitals were also full at one time. At the same time, this mobilization led to the appearance of burnout syndrome. I chose to do a paper on burnout syndrome among intensive care professionals because they have been the most affected in the last year and will certainly have difficulties for a while after the pandemic will diminish. Now that the number of people diagnosed with coronavirus - Delta has started to increase again, the situation is serious. In this paper we will present a case study of a young woman resident in intensive care at the Infectious Diseases Hospital in Constanta – Romania.

I think it is a serious problem and should not be treated with indifference.

Keywords: burnout syndrome, medical staff, intensive care, chronic fatigue

C-MAC® VS. MCGRATH® VIDEO LARYNGOSCOPE IN PATIENTS UNDERGOING GENERAL ANESTHESIA WITH OROTRACHEAL INTUBATION: A PROSPECTIVE, RANDOMIZED CLINICAL TRIAL

Christopher Ryalino

Department of Anesthesiology and Intensive Care Faculty of Medicine,
Udayana University Indonesia

Tjokorda Gde Agung Senapathi

Department of Anesthesiology and Intensive Care Faculty of Medicine,
Udayana University Indonesia

Jhoni Pardomuan Pasaribu

Department of Anesthesiology and Intensive Care Faculty of Medicine,
Udayana University Indonesia

Abstract

Background: Intubation is an essential procedure to secure the airway in critically ill patients and also a common procedure in general anaesthesia. In this modern era, there are various video laryngoscopes (VL) available in the market which help anaesthesiologist to improve the success rate of intubation, moreover in patient with difficult airway. The goal of this study was to compare the effectiveness of C-MAC® and McGrath® VL in orotracheal intubation.

Patients and Methods: The study was conducted at a tertiary public hospital in Bali, Indonesia. The study was registered in Clinical Trials Registry (NCT04936516). We included 68 patients underwent general anaesthesia for elective, non-maxillofacial surgeries. All subjects provided written informed consent. The inclusion criteria were American Society of Anaesthesiologists (ASA) physical status 1 to 3, aged 18-65 years old, with a body mass index of $<35 \text{ kg/m}^2$. Those with cervical instability and who showed predictors and/or history of difficult intubation were excluded. The subjects were randomly divided into two groups: Group C (C-MAC®) and Group M (McGrath®). All intubations were carried out by third-year anaesthesia registrars to minimize skill bias. We measured the effectiveness of the devices in terms of time-to-intubation, ease of intubation, total attempts, failure to intubate, larynx and glottis visualization, degree, hemodynamic stability, and complications.

Results: Time-to-intubation is significantly shorter in Group C compared to Group M (12(5) vs. 23(14) seconds, $p < 0.001$). Glottic visualization, measured by POGO (percentage of glottic opening) score, is also significantly better in Group C than Group P ($p = 0.011$). Attempts for successful intubation, ease of intubation, larynx visualization, and hemodynamic stability showed no statistically significant difference between the two groups. There are no documented complications in both groups.

Conclusion: C-MAC® is more effective than McGrath® in terms of intubation time and glottic visualization.

Keywords: video laryngoscope, intubation, general anaesthesia, POGO score

TANISİT HÜCRELERİNİN YAPISI VE SİNİR SİSTEMİNDEKİ FONKSİYONEL ROLÜ

STRUCTURE OF TANISIT CELLS AND THEIR FUNCTIONAL ROLE IN THE NERVOUS SYSTEM

Fatih TAŞ

Siirt Üniversitesi Tıp Fakültesi, Histoloji ve Embriyoloji Anabilim Dalı, Siirt, Türkiye
ORCID ID: 0000-0001-9817-4241

Ender ERDOĞAN

Selçuk Üniversitesi Tıp Fakültesi, Histoloji ve Embriyoloji Anabilim Dalı, Konya, Türkiye
ORCID ID: 0000-0002-6220-9243

ÖZET

Tanisit hücreleri, 1954 yılında Horstmann tarafından tanımlanmıştır. Tanisitler, beyin ventriküllerini döşeyen ve hipotalamusun derinliklerine uzanan, bölgede işlevleri olan özelleşmiş endim hücreleridir. Tanisitler, yetişkin memelilerde ventriküler sistemde ve bu sistemi çevreleyen sirkumventriküler organlarda bulunmaktadır. En çok beyin 3. ventriküler bölgesinde ve spinal kordun kanalis sentralisinde yer almaktadır. Tanisitlerin her birinin kendi ayrı karakteristik özellikleri olan, dört farklı alt tipi bulunmaktadır. Bu alt-tipler: $\alpha 1$, $\alpha 2$, $\beta 1$ ve $\beta 2$ 'dir. α tanisitleri, üçüncü ventrikül lümeniyle, medial basal hipotalamusun damarları ve nöronları arasında köprü oluştururken; β tanisitleri, ventriküler beyin omurilik sıvısı (BOS) ve portal kan arasındaki anatomik bağlantıyı sağlamaktadır. Bu dört grup tanisitlerin her biri farklı ve önemli fonksiyonel molekülleri ortaya çıkarmaktadır. Bunlara örnek olarak; glukoz ve glutamat taşıyıcılar, periferik hormonlar, nöropeptidler için reseptör serileri, büyüme faktörünü dönüştürücü moleküller ve özel bir protein olan P85 verilebilir.

Tanisitler, nöroglia grubu hücrelerden olup, BOS ile portal kapillerler arası köprü kuran ve nöroendokrin fonksiyonlara sahip bipolar hücrelerdir. Bipolar hücreler olan tanisitlerin, bazal tarafı nöronlar ve kapiller damarlar ile ilişkiliyken, apikal tarafı da ventriküllerdeki serebral sıvı ile ilişkilidir. Tanisitlerle, endim hücreleri arasında bazı farklılıklar bulunmaktadır. Endim hücreleri kabaca kuboiddir, birçok siliyaya sahiptir ve sadece çok kısa bir uzantıya sahiptir. Buna karşılık tanisitler ise, sillerden, mikrovilluslardan ya da diğer özelleşmiş apikal hücre uzantılarından yoksundur. Fakat tanisitler de beyin parankimasına uzanan, uzun çıkıntılara sahiptir. Bu uzantılar tanisitlerin, çekirdeklerde yer alan nöronlarla sıkı bir kontak kurulmasını sağlamaktadır. Tanisit hücrelerinin fonksiyonel özellikleri arasında; BOS'un taşınımı, Gonadotropin salgılatıcı hormon (Gn-RH) salgılamadaki rolü, GLUT-1 ve GLUT-2 gibi glikoz taşıyıcısı molekülleri bünyesinde bulundurması, tiroid hormonunu aktive eden deiyodinaz tip II'yi içermesi, lezyonlu aksonun rejenerasyonunu desteklemesi ve nöral kök hücre olarak hareket etmesi sayılabilir. Sonuç olarak tanisit hücrelerinin geniş fonksiyonel rolü, bu hücrelerin nörodejeneratif hastalıklar başta olmak üzere, medikal hastalıkların tanı ve tedavisinde kullanılabileceğini düşündürmektedir.

Anahtar Kelimeler: Tanisitler, Endim hücreleri, BOS, Nörodejeneratif hastalıklar

ABSTRACT

Tanycyte cells were described by Horstmann in 1954. Tanycytes are specialized ependymal cells that line the brain ventricles and extend deep into the hypothalamus. Tanycytes are found in the ventricular system of adult mammals and in the circumventricular organs surrounding this system. It is mostly located in the third ventricular region of the brain and canalis centralis of the spinal cord. There are four different subtypes of tanycytes, each with their own distinct characteristics. These subtypes are: $\alpha 1$, $\alpha 2$, $\beta 1$ and $\beta 2$. While α tanycytes form a bridge between the lumen of the third ventricle and the vessels and neurons of the medial basal hypothalamus; β tanycytes provide the anatomical link between ventricular cerebrospinal fluid (CSF) and portal blood. Each of these four groups of tanycytes reveals different and important functional molecules. As an example of these; glucose and glutamate transporters, peripheral hormones, receptor series for neuropeptides, growth factor converting molecules and a special protein P85 can be given.

Tanycytes are bipolar cells that form a bridge between CSF and portal capillaries and have neuroendocrine functions. The basal side of tanycytes, which are bipolar cells, is associated with neurons and capillaries, while the apical side is associated with cerebral fluid in the ventricles. There are some differences between tanycytes and ependymal cells. Ependymal cells are roughly cuboid, have many cilia, and have only a very short extension. In contrast, tanycytes lack cilia, microvilli, or other specialized apical cell extensions. But tanycytes also have long projections that extend to the brain parenchyma. These extensions allow the tanycytes to establish a tight contact with the neurons in the nuclei. Among the functional properties of tanycyte cells; Transport of CSF, release of Gonadotropin-releasing hormone (Gn-RH), containing glucose transporter molecules such as GLUT-1 and GLUT-2, containing deiodinase type II that activates thyroid hormone, supporting regeneration of lesioned axon and acting as neural stem cell countable. In conclusion, the wide functional role of tanycyte cells suggests that these cells can be used in the diagnosis and treatment of medical diseases, especially neurodegenerative diseases.

Keywords: Tanycytes, Ependymal cells, CSF, Neurodegenerative diseases

EFFECT OF MAXIMAL DOSES OF DEXTRAN-POLYACRYLAMIDE POLYMERS AND THEIR AS CARRIERS OF SILVER AND GOLD NANOPARTICLES ON LIVER

Valentyna Kurovska

Taras Shevchenko National University of Kyiv, Kyiv, Ukraine

Oksana Kaleinikova

Bogomoletz Institute of Physiology, Kyiv, Ukraine

Iryna Byelinska

Taras Shevchenko National University of Kyiv, Kyiv, Ukraine

Natalia Kutsevol

Taras Shevchenko National University of Kyiv, Kyiv, Ukraine

Taras Blashkiv

Bogomoletz Institute of Physiology, Kyiv, Ukraine

Key words: dextran-polyacrylamide polymers, silver and gold nanoparticles, liver, toxicity

Problem. One of the tasks of modern medicine is to search new agents which give an opportunity to treat diseases at the cellular level. In this regard polymer nanocomposites are promising agents which could be used as nanocarriers for the delivery and release of water-soluble medicines. **Objectives.** To study the effect of maximal doses of the dextran-polyacrylamide polymers and their effect as carriers of silver and gold nanoparticles on liver. **Research methods.** Nanocarriers on the base of branched dextran-polyacrylamide polymers had been synthesized in our laboratory. They are supposed to be used as a potential mean for transport of silver and gold nanoparticles. "Uncharged" star-like polymer matrices (D-PAA) consist of a dextran core and grafted polyacrylamide chains. "Charged" matrices (D-PAA (PE) - dextran-polyacrylamide polyelectrolyte) also consist of a dextran core and grafted partially hydrolyzed polyacrylamide chains. An alkaline hydrolysis changes part of the amide groups to hydroxyl groups, which determines the negative charge of the macromolecule. The hydrodynamic dimensions of both types of macromolecules are 70-80 nm. Spherical shaped gold nanoparticles with size of 2-5 nm were loaded into D-PAA. Silver nanoparticles synthesized in D-PAA also characterized by spherical shape and had a size 8-15 nm.

Experiments were carried out using 25 males of white laboratory Albino mice. Age of animals was 10 weeks, weight 25-30 g. The animals were divided into five groups: I – control, II – D-PAA, III – D-PAA (PE), IV – Au-D-PAA, V – Ag-D-PAA. Substances were diluted with 0,3 ml saline and injected intravenously into the tail vein once a day per five days. On the third day after the last (fifth) treatment, the animals were withdrawn from the experiment under ether

anesthesia in compliance with the rules of euthanasia. The right lobe of the liver was removed immediately, forthwith fixed in Bouin's solution for 7 days, embedded in paraffin. Slides were stained with hematoxylin-eosin according to the standard technique.

Results. A pronounced blood stasis in central veins, collagen deposits and neutrophilic infiltration around them, necrosis of the parenchyma of the centrilobular zone, and an increase of eosinophilia of the hepatocytes' cytoplasm have been observed in the livers of animals of the II group. These signs indicate inflammatory process, portal hypertension, and the death of hepatocytes in the centrilobular zones. The changes in the III group were similar to those in the previous one and demonstrated toxic damage to the liver. The signs of apoptosis have been indicated here as well in form of hyperchromic small nuclei and acidophilic apoptotic bodies. The changes what indicated toxic damage to the liver as well as the cell death mainly by apoptosis have been observed in the IV group in addition to the aforementioned pathological processes. The alteration of cells in the form of excessive accumulation of glycogen and small-droplet fatty inclusions, karyomegaly, pyknotic nuclei and eosinophilic alteration of hepatocytes cytoplasm, a presence of inclusions in Kupffer's cells were typical for this group. The similar picture we have obtained in group V. Along with this in groups IV and V some of the changes could be considered as signs of the liver's compensatory responses to the damage (hypertrophic regeneration). E.g., eosinophilic alteration of hepatocytes, focal infiltration with neutrophils and necrosis, blood stasis in the central veins, alteration in the form of excessive accumulation of glycogen and small-drop fatty degeneration, hepatocellular hypertrophy, accompanied by compression of the sinusoids belong to these features.

It makes picture we obtained quite mosaic. If apoptosis and necrosis indicate the damaging effect of nanoparticles, the signs of regeneration raise questions about the time of their appearance. Regeneration develops at the first stages of lesion and indicates an attempt of cells to fight the ongoing processes. It may point out the presence of mechanisms that operate in this cell and allowed it to avoid death.

Conclusions. Hence, our results demonstrate that maximal doses of studied substances cause harmful effect on the liver. The optimal dosages, which could be used with therapeutic aim as well as frequency of their administration are needed to be studied.

COMPARISON OF IRON, ZINC AND FERRITIN AMONG SMALL FOR GESTATIONAL AGE AND APPROPRIATE FOR GESTATIONAL AGE MOTHERS

Nida Khan

M.Phil Scholar, Biochemistry Department, Institute of Basic Medical Sciences, Khyber Medical University, Peshawar.

ORCID: <https://orcid.org/0000-0002-6214-8719>

Dr. Sadia Fatima

Biochemistry Department, Institute of Basic Medical Sciences, Khyber Medical University, Peshawar.

Prof. Dr. Rubina Nazli

Biochemistry Department, Institute of Basic Medical Sciences, Khyber Medical University, Peshawar.

Dr. Tasleem Akhtar

Pakistan Health Research Council, Khyber Medical College, Peshawar.

Dr. Jamila Haider

Microbiology Department, Shaheed Benazir Bhutto Women University, Peshawar.

ABSTRACT

Small for Gestational Age (SGA) newborns are one of the vulnerable groups that have a high risk of growth failure and many childhood and adulthood disorders. Every year more than 30 million mothers give birth to SGA babies. Regardless of its high prevalence, very few studies exist on risk factors and consequences of SGA born in Pakistan. So this study was achieved to assess the nutritional status of SGA and AGA (Appropriate for Gestational Age) mothers by estimating their iron, zinc and ferritin levels. This case-control study was conducted at different Basic Health Units from October 2020 to June 2021. In this study mothers of SGA newborns (cases n=40) were compared with mothers of AGA newborns (control n=40). Information regarding socio-demographic, socio-economic and reproductive history of mothers was recorded on predesigned questionnaires. Dietary data of mothers was taken through multiple pass 24-hours dietary recall questionnaire. Blood samples were collected for finding the Hemoglobin, Iron, Ferritin and Zinc levels of selected SGA and AGA mothers. Data analysis was done using SPSS version 20. In this research study, differences in the hemoglobin (Hb), serum levels of iron, ferritin and zinc were observed in eighty post-natal mothers having age range between 16 – 35 years (Mean \pm SD; 24.75 \pm 5.06 years). Overall 40% of mothers had Body Mass Index (BMI) in normal range. In SGA group, the frequency of mothers having normal BMI was less than AGA mothers (SGA=30%, AGA= 50%). Comparison of birth interval, previous SGA history, antenatal visits and smoking exposure in both groups were found significant. Total anemic

mothers (Hb<12g/dL) were 48.8% in which 43.6% were SGA. Iron deficiency was more common in SGA group (55%). The prevalence of iron deficiency anemia was 26.3% in which 49.2% were SGA mothers. Zinc deficiency in SGA mothers was observed to be 53.4%. The energy intake of SGA mothers on daily basis was significantly lower than AGA mothers. It is concluded that mothers of both the groups were malnourished, anemic and iron deficient. Zinc deficiency was most prevalent in SGA group. No significant difference was found between biochemical parameters of SGA and AGA group.

Keywords: Small for gestational age, Appropriate for gestational age, Iron, Zinc, Ferritin, Basic Health Units, Peshawar

ENDOSCOPIC APPROACHES IN OTORHINOLARYNGOLOGY

Proletina Bozdukova

ENT resident at UMHAT Burgas

Abstract

Introduction: Endoscopic approaches in otorhinolaryngology successfully entered in our specialty and is well spreading in more and more fields of it. [1]

Aim: The aim of this study is to present the wide range of mini invasive surgical techniques in the area of ear, nose and throat.

Methods: We made a research among different data bases for the endoscopic methods used in different countries. We also made a comparison with these used in Bulgaria and mainly in our clinic.

Results: Functional endoscopic sinus surgery is the best established mini invasive surgical approach in Bulgaria and in Europe. [2] Sleep endoscopy is a method of choice for diagnostic of the socially significant obstructive sleep apnea. Endoscopic laser microsurgery is widely used for benign and malignant laryngeal diseases. Because of tendency to minimize invasiveness of surgery the endoscopy expands into other fields of otorhinolaryngology: otosurgery, neck soft tissue surgery (thyroid and parathyroid surgery), salivary gland surgery, skull base surgery. [3]

Conclusion: A lot of conditions and disease are good for endoscopic treatment and because of that these methods should be established more and more in Bulgaria and abroad.

References

[1] S I Rosenberg 1, H Silverstein, T O Willcox, M A Gordon, Endoscopy in otology and neurotology, <https://pubmed.ncbi.nlm.nih.gov/8172296/>

[2] Jiannis K Hajjioannou, DavaChaido, Panagiotis Kousoulis, Diagnostic and operative endoscopy in otorhinolaryngology: Traditional and emerging techniques, https://www.researchgate.net/publication/292935706_Diagnostic_and_operative_endoscopy_in_otorhinolaryngology_Traditional_and_emerging_techniques

[3] Jan Betka , Karl Hörmann, Manuel Bernal-Sprekelsen ,Jan Plzák, Endoscopic/External Approaches in Otorhinolaryngology and Head and Neck Surgery, <https://www.hindawi.com/journals/bmri/2015/958453/>

ENT MANIFESTATIONS IN COVID-19

Daniel Petkov
UMHAT Burgas

Tsvetelina Grigorova
UMHAT Burgas

Abstract

Introduction: We detect, analyze and discuss the different ear nose throat (ENT) manifestations those were reported in COVID19 hospitalised patients in the university hospital of Burgas. [1]

Aim: The aim of the study is to find common ENT symptoms for developing the disease in COVID19 positive patients. [2]

Materials and methods: We made a questionnaire among the hospitalized patients and a research in the PubMed databases, Web of Science and others.

Results: Within the included 98 COVID-19 laboratory - confirmed positive patients, the most common ENT manifestations of COVID-19 were sore throat (15%). Other common otorhinolaryngological manifestations of the disease were - pharyngeal erythema, runny nose, nasal congestion, enlargement of the tonsils, infection of the upper respiratory tract.

Conclusions: As a conclusion we can say that ENT manifestations for COVID-19 are not common as fever and cough. Nevertheless the disease is still spreading and with all the mutations we should continue the evaluation of the clinical manifestation. [3]

Key words: COVID19, ENT, symptoms, manifestations, ear, nose, throat

References

- [1] Mohammad Waheed El-Anwar, Saad Elzayat, Yasser Ahmed Fouad, ENT manifestation in COVID-19 patients, <https://pubmed.ncbi.nlm.nih.gov/32586739/>
- [2] Geng Ju Tuang, Adi Farhan Abdul Wahab, Salina Husain, Otolaryngology manifestations of COVID-19: a contemporary viewpoint, <https://pmj.bmj.com/content/early/2021/04/19/postgradmedj-2021-140169>
- [3] Priyanka Chaurasia, Vaibhav Kuchhal, ENT manifestations in Covid-19 positive patients, <https://www.ijhcr.com/index.php/ijhcr/article/view/391>

PROTECTIVE EFFECT OF MURRAYA KOENIGII AGAINST TESTICULAR DAMAGES INCURRED IN SKIN TUMOR BEARING MICE

Aniqa Aniqa

Department of Biophysics, Panjab University, Chandigarh

Sarvnrinder Kaur

Department of Biophysics, Panjab University, Chandigarh

Keywords: Skin cancer, Testicular damage, *Murraya koenigii*

Problem: Exposure to polycyclic aromatic hydrocarbons (PAHs) is a significant factor responsible for skin carcinogenesis. 7,12-Dimethylbenz(a)anthracene (DMBA), a PAHs, is a known carcinogen, teratogen and toxicant. During carcinogenesis, DMBA and its metabolites produce a lot of free radicals and create oxidative stress. This oxidative stress further targets the different cell organelles. Consequences of the damages initiated by DMBA also affect several vital organs such as the brain, liver, testis, etc., by complex biological reactions, like increase in mutation rate, alteration in the cellular membrane, structural proteins, metabolic enzymes, and signalling proteins.

Objectives: The present study was aimed to evaluate the possible role of Hydroethanolic *Murraya koenigii* leaves extract (HEMKLE) against damages incurred during DMBA/TPA induced skin tumorigenesis in mice.

Research methods: For the study, 40 male LACA mice were segregated into four groups, namely: Control, DMBA/TPA, HEMKLE, and HEMKLE+DMBA/TPA. Skin tumors were induced by topical application of 7,12-Dimethylbenz(a)anthracene (DMBA) [500 nmol/100 ul of acetone] and 12-O-tetradecanoyl phorbol-13-acetate (TPA) [1.7 nmol/100 ul of acetone] and HEMKLE (200 mg/kg b. w.) was administered orally.

Results: The protective response of HEMKLE to testicular damages during skin tumorigenesis was evident by the increase in sperm motility and sperm count, restoration of endogenous antioxidant enzymes, and histo-architecture of testis in the HEMKLE + DMBA/TPA group when compared to DMBA/TPA group. HEMKLE also decreased (p0.05) the mRNA and protein expression of pro-apoptotic genes (caspase-9 and caspase-3) and increased the anti-apoptotic gene, i.e. Bcl-2 in HEMKLE + DMBA/TPA group when compared to DMBA/TPA group, suggesting its anti-apoptotic effects.

Conclusions: The decrease in oxidative stress and apoptosis, restoration of antioxidant enzymes, and histo-architecture of testes suggest that HEMKLE markedly protected the damage initiated during skin carcinogenesis.

COVID-19 VACCINES AND THE RATES OF COVID-19 VACCINATION IN TURKEY

Mehmet Doğan

Prof. Dr. University of Erciyes, Halil Bayraktar Vocational School of Health Services,
Kayseri, TURKEY

Fatih Altan

University of Erciyes, Halil Bayraktar Vocational School of Health Services, Kayseri, TURKEY

ABSTRACT

The most important global health problem of the 21st century is undoubtedly the COVID-19 pandemic. The COVID-19 vaccines, which are available in a very short time as a result of intensive studies, are the most effective method of combating the pandemic. The aim of this study is to evaluate the COVID-19 vaccines and vaccination rates used in Turkey. The aim of this study is to evaluate the COVID-19 vaccines and vaccination rates applied in Turkey.

COVID 19 vaccination rates were evaluated by the Ministry of Health of the Republic of Turkey between 11 January and 15 October 2021. In addition, COVID-19 vaccine types, access routes to the vaccine and post-vaccine side effects were evaluated.

The first COVID-9 vaccine in Turkey was started on January 11, 2021, by applying it to the Minister of Health. The "inactivated vaccine", which stimulates immunity without harming the body by disintegrating and neutralizing the virus, was the first type of vaccine administered in Turkey. In addition to inactivated vaccines, messenger RNA (mRNA) vaccines have been introduced. mRNA, a vaccine containing mRNA that carries the genetic code of the virus. The Ministry of Health made the COVID-19 vaccine applications by grouping method. First stage; health workers, the elderly, the disabled, those working and staying in protection homes, and individuals over the age of 65 have started to be vaccinated. At the last stage, all individuals over the age of 18 can get vaccinated. All individuals coming from the vaccine group can choose the vaccine they want. For vaccination appointments, they can get their vaccinations by making an appointment on the day they want from the Central Physician Appointment System (MHRS) and e-Pulse application. As of October 15, 2021, a total of 113 million 709 thousand 533 (1st, 2nd and 3rd doses) vaccines were administered. 47 million 119 thousand 99 people have had 2 doses of vaccine and the rate is 75.91% among the population aged 18 and over who have received at least two doses. This rate is 55.9% in the whole population. Although there are rare allergic reactions, mild side effects such as fatigue, headache, fever, chills, muscle/joint pain, vomiting, diarrhea, pain, redness and swelling at the injection site are common.

As in all infectious diseases, the risk of person-to-person transmission of the disease will decrease with the vaccination of a sufficient part of the population in the COVID-19 pandemic. Thus, since the risk of spreading the disease in the community will decrease, unvaccinated individuals will also be protected. It is important to increase vaccination studies in order to reach the necessary rates for herd immunity.

Keywords: Turkey, COVID-19, Vaccine

INTRODUCTION

COVID-19 (Coronavirus); It emerged in China on December 31, 2019 and spread rapidly, causing a pandemic. It has been effective in many fields such as education, trade and tourism, especially health. It has experienced periods when people could not go out even in order to meet their basic consumption needs. In the fight against the pandemic, which is a public health problem that concerns the whole world, scientists have developed vaccines after intense studies and vaccines developed in many countries have begun to be implemented. While Turkey takes part in the scientific process with domestic vaccine studies, it also fights the coronavirus pandemic by supplying the vaccines developed (Doğan & Bayraktar, 2020).

Immunity is the situation created by the resistance factors developed by the microorganisms in which the infectious agent is located against the infectious agents. Substances that, when given to the organism in an appropriate way, create an immune response and protect the person from infectious diseases are called vaccines (Aşı Portalı, 2021). The Expanded Immunization Program (EPI) was developed by the World Health Organization (WHO) in 1974 to prevent deaths from vaccine-preventable diseases. Turkey was included in the EPI in 1981. It started with IPE, DBT (Diphtheria, Pertussis Tetanus), Polio (polio), Measles, BCG (TB) vaccine. IPE; Hepatitis B vaccine was added in 1998, Measles Rubella Mumps (MMR) and Hemophilus influenza Type b (Hib) vaccines in 2006, Conjugated Pneumococcus (KPA) in 2008, Hepatitis A in 2012 and Varicella vaccine in 2013 (Etiler, 2018; Şimşek, 2020; Ertem & Çan, 2014).

The “antigen” is the basic element that provides immunization among the components of the vaccine. “Suspension Liquid” containing vaccine elements such as another vaccine component, complex liquids containing protein and antigen, sterile water, physiological saline. It consists of "chemical substances" such as "condoms, stabilizers, antibiotics" used to keep vaccines intact and prevent bacterial growth in them. In addition, it consists of "Adjuvants", which are aluminum salts used to increase and prolong the immune response formed by the main antigen. Vaccines; It is classified according to the source and properties of the antigen, the method of administration of the vaccine and the application technique. According to the source of the antigen; virus, bacteria and toxoid vaccines, according to the characteristics of the antigen; They are classified as live (attenuated), Inactive, toxoid and biotechnological vaccines. There are also oral and parenteral vaccines according to the application technique of the vaccine. According to the method of application of the vaccine, it consists of routine, to be applied when necessary and optional vaccines. Routine vaccination; The vaccination calendar applied to childhood in Turkey can be given as an example. Influenza vaccine can be given as an example of optional vaccines. COVID-19 vaccines can also be given as examples of vaccines to be applied when necessary (Günay, 2009; Doğan, 2020).

Inactivated (Sinovac / Turcovac) and mRNA (Biontech / Pfizer) vaccines have been applied in Turkey since January 11, 2021. Inactivated vaccines, the virus is fragmented and inactivated, and immunity is stimulated without harming the body. mRNA vaccines are involved in protein synthesis, which is naturally produced in the human body. The purpose of these vaccines is to act as an individual's mRNA and to create a warning against the virus. While inactivated vaccines can be stored at 2-8°C, the most important disadvantage of mRNA vaccines is that they are stored at -70°C. Although rare, there are allergic reactions, but mild side effects such as fatigue, headache, fever, chills, muscle/joint pain, vomiting, diarrhea, pain, redness and swelling in the

injection area are common. The Ministry of Health made the COVID-19 vaccine applications by grouping method. First stage; health workers, the elderly, the disabled, those working and staying in protection homes, and individuals over the age of 65 have started to be vaccinated. At the last stage, all individuals over the age of 18 can get vaccinated. All individuals in the vaccine group can choose the vaccine they want. For vaccination appointments, they can get their vaccinations by making an appointment on the day they want from the Central Physician Appointment System (CPAS) and e-Pulse application. As of October 15, 2021, a total of 113 million 709 thousand 533 (1st, 2nd and 3rd doses) vaccines have been administered in Turkey. 47 million 119 thousand 99 people have had 2 doses (fully vaccinated) vaccine, and the rate of people who have been vaccinated at least two doses is 55.9% in the whole population (COVID-19 AŞIŞI, 2021).

Individual measures are as important as public measures in the fight against the pandemic. It is important for the countries to obtain and make available the vaccines developed by the public, and for the individuals who are vaccinated to be vaccinated individually. The aim of this study is to evaluate the COVID-19 vaccines and vaccination rates applied in Turkey.

METHODS

COVID 19 vaccination rates were evaluated by the Ministry of Health of the Republic of Turkey between 11 January and 15 October 2021. In addition, COVID-19 vaccine types, access routes to the vaccine and post-vaccine side effects were evaluated.

RESULT

While the vaccination rate increased gradually until 15 May 2021, after a variable course from this date until 15 July, a gradual decrease was observed until October. Between July 15 and August 2021, approximately 12.8 million people were vaccinated the most. The share of the vaccinated people in this period in the population is 15.2%. As of October 15, 2021, 2 doses of vaccination of approximately 47 million people in total have been completed, while the share of those vaccinated in the population is 55.9%. Data on COVID-19 vaccination in Turkey are shown in Table 1.

Table 1. Data on COVID-19 Vaccination in Turkey

Date	2 Doses Vaccinated (Fully Vaccinated)	Number of Persons Completed 2 Doses of Vaccine	Proportion to Whole Population (%)	Increase Rate (%)
11 January-15 February 2021	573.879	573.879	0.7	0.7
15 February -March 2021	3.349.666	2.775.787	4.0	3.3
15 March-April 2021	7.737.134	4.387.468	9.2	5.2
15 April-May 2021	10.792.375	3.055.241	12.8	5.6
15 May-June 2021	13.973.218	3.180.843	16.6	3.8
15 June-July 2021	20.013.130	6.039.912	23.7	7.1
15 July-August 2021	32.807.818	12.794.688	38.9	15.2
15 August-September 2021	41.182.546	8.374.728	48.8	9.9

15 September -October 2021	47.119.099	5.936.553	55.9	7.1
-------------------------------	------------	-----------	------	-----

CONCLUSION

The protection of susceptible individuals through individuals who are immune in the community is called community immunity. In order to prevent infectious disease outbreaks, it is necessary to exceed a certain immunity level in the society. Despite the increase in the number of individuals vaccinated in Turkey, the desired figures have not been reached yet. In order to gain community immunity, COVID-19 vaccination rates will be achieved by vaccinating a sufficient part of the population.

REFERENCES

- Aşı Portalı. (2021, Ekim 15). <https://asi.saglik.gov.tr/>
- COVID-19 Aşısı. (2021, Ekim 15). <https://covid19asi.saglik.gov.tr/>
- Ertem M, Çan G. (2014). Turkey's Health Report 2014. In: Communicable Diseases, (Vaccine Preventable Diseases), Turkish Society of Public Health Specialists, Trakya University Publishing. 1st, Edirne, Turkey, pp. 77– 85.
- Etiler N. (2018). Vaccine Guide for Primary Health Care Workers. Turkish Medical Association Publishing. 1st, Ankara, pp.1-87.
- Doğan, M. (2020). Vaccines in Turkey's Immunization Schedule. Karadeniz Uygulamalı Bilimler Kongresi (s. 9-14). Artvin: UBAK.
- Doğan, M., & Bayraktar, M. (2020). COVID-19 with a Public Health Perspective: Measures Taken in Turkey and Public Compliance with the Measures. Iran J Public Health, 67-75.
- Günay, O. (2009). Bağışıklama Hizmetleri. Y. Öztürk, & O. Günay içinde, Halk Sağlığı (s. 793-800). Kayseri: Erciyes Üniversitesi.
- Şimşek Orhon F. (2020). An Overview of the Extended Immunization Program. Osmangazi Journal of Medicine, Social Pediatrics Special Issue March pp.6-14.

E-HEALTH APPLICATIONS IN TURKEY

Mehmet Doğan

Prof. Dr. University of Erciyes, Halil Bayraktar Vocational School of Health Services,
Kayseri, TURKEY

Fatih Altan

University of Erciyes, Halil Bayraktar Vocational School of Health Services, Kayseri, TURKEY

The aim of this study is to introduce e-health applications in Turkey. Although it was first used to describe electronic medical records, e-health does not only mean the transfer and the storage of personal and social data about health with the information and technology now dominating every field of medicine in accordance with the changing nature of healthcare delivery; It is expressed as the use of information and communication technologies in the prevention of diseases, the realization of diagnosis and treatment, the monitoring of the treatment process and the management of health.

With the "National Health Information System", which is among the basic components of the Health Transformation Program, which was implemented in Turkey in 2003, it is aimed to ensure both standardization at the national level and to establish fast, accurate and effective communication in the field of health. For this purpose, various e-health applications such as National Health Data Dictionary, Family Medicine Information System, Central Physician Appointment System, Core Resource Management System, MEDULA, e-Nabız have been implemented. With these applications, it is aimed to increase the efficiency and quality indicators of the health services offered. In addition, e-health applications are used in solving existing problems in the health sector, preventing potential problems, determining priorities, planning resources and investments in the health sector, and evaluating service quality.

As a result, e-health applications have contributed to better quality of health service delivery, effective, easy and fast communication between patient-physician, in-house and outside the institution, and to reduce costs.

Keywords: E-health, information system, e-Nabız, MEDULA, information technology

INTRODUCTION

e-Health is expressed as the internet-based use of information technologies for effective health service delivery, rapid access to information and sustainable data transfer with stakeholders (Akdağ, 2010). According to another definition, it is defined as making information and communication technologies available to citizens with all their functions. This technology is used to improve the health status of individuals, to provide easy and fast access to health services, and to provide effective, efficient and quality service to all stakeholders in the health sector (Ömürbek & Altın, 2009).

E-health is at the intersection of public health and medical information systems regarding health services and health education through internet-based technologies. To put it more broadly, it creates not only technical development, but also the attitude, behavior and mentality that contributes to the development of local, regional and global health services together with information and communication technologies. This definition shows that e-health does not only consist of the internet and medicine, it includes more than that. Therefore, the letter “e” in the concept of e-health also denotes a series of “e” in addition to its electronic meaning. These are (Eysenbach, 2001);

- **Efficiency:** Expectations from e-health application are to increase efficiency in health services and thus reduce costs. One possible way to reduce costs would be through avoidance of unnecessary diagnostic or treatment interventions, improved communication opportunities between healthcare organizations, and patient participation.
- **Enhancing Quality of Care:** Increasing productivity not only reduces costs, but also increases quality. E-health can improve the quality of health services by, for example, making comparisons between different service providers, directing consumers' patient flows to the best quality providers within the scope of quality assurance.
- **Evidence Based:** The service delivery of e-health applications should not only be evaluated in terms of effectiveness and effectiveness, but also scientifically proven.
- **Empowerment:** E-health, empowering consumers and patients, opens new avenues for patient-centered healthcare and enables evidence-based intervention by making medical and personal electronic records accessible to consumers over the internet.
- **Encouragement:** e-Health promotes a new relationship between the patient and healthcare professionals towards a true partnership where participation in decisions is ensured.
- **Education:** e-Health refers to the continuity of medical education of physicians with online resources, as well as education about preventive health services such as continuing medical education and health education of consumers.
- **Enabling Information Exchange and Communication:** e-Health enables the exchange of standardized information and communication between health institutions.
- **Extending:** e-Health extends the scope of health care beyond its traditional borders. This happens both geographically and conceptually. E-health enables consumers to easily obtain health services online from global service providers.

These services cover many applications, from simple advice to more complex interventions or a drug product.

- **Ethics:** e-Health includes new forms of patient-physician interaction. Online professional practices pose new challenges and threats to ethical issues such as informed consent, privacy and equity issues.
- **Equity:** While making healthcare more equitable is one of the promises of e-health, there are also serious threats that e-health can deepen the gap between the “haves” and the “have-nots”. People without money, skills, and access to computers and networks cannot use computers effectively. As a result, these patient populations (indeed, those who will benefit most from health information) are the least likely to benefit from advances in information technology unless political measures ensure equal access for all.

1. e-Health Applications

e-Health applications consist of National Health Data Dictionary, Family Medicine Information System, Core Resource Management System and e-Prescription applications. In order for these systems to work more efficiently, some auxiliary source modules integrated with these systems are needed. These systems consist of MEDULA, e-Nabız applications.

e-Health is expressed as a fast, secure and expanding information system that enables the collection and integration of data produced electronically in health institutions in certain standards. With this application, data and information that will meet the needs of all stakeholders are produced. In other words, Health-Net can be expressed as a health data bank model that allows the collection of health information of all citizens in a single center. At the same time, e-Health provides secure communication and has high bandwidth. With this application, it is aimed to increase the efficiency and quality indicators of the health services offered. It is used in solving existing problems in the health sector, preventing potential problems, determining priorities, planning resources and investment in the health sector, and evaluating service quality.

When the infrastructure features of the e-Health application are examined, it is possible to mention some features. These are (Akdağ & Erkoç, 2011);

- Transferring data and information produced from different software in health institutions into standard data,
- Decision support system, where necessary and sufficient information can be accessed for the analysis of health expenditures, disease burden and demographic factors,
- Monitoring and reporting indicators shared with international organizations (WHO, EUROSTAT, OECD),
- International data exchange determined within the framework of the legislation,
- The ability to access and manage the health records of the citizens of the country,

- There are features such as quick access to information thanks to early warning systems.

1.1. National Health Data Dictionary

The increasing importance of information in almost every field in the developing world has increased the need for obtaining information correctly and important studies have been started to meet this need. It is seen that many international standards have been developed especially in the field of health informatics. These standards are; It brings rules on how to follow a method in the stages of defining, transferring, storing, protecting and analyzing data. The National Health Data Dictionary is a dictionary study that is used in health institutions in our country and will be used as a reference by hospital information systems. The glossary consists of hierarchical inter-term relationships with datasets in different categories. (<https://e-saglik.gov.tr>).

The most important function of the USVS is that it is based on "interoperability". For this reason, the following points should be taken into consideration while adding new data elements to the system (Akdağ & Erkoç, 2011):

- Whether it will be used for policy development, monitoring, evaluation, auditing, statistics, analysis and reporting, Whether it is useful in obtaining any information,
- Whether there is any data in the patient's file,
- Whether there is data that the physician needs to reach quickly in the electronic environment, although it should be in the patient's file,
- Whether the data to be included in the dictionary is data that requires the physician to enter and save in the information system.

1.2. Family Medicine Information System Application

The Family Medicine practice, which was put into practice as a requirement of the Health Transformation Program, brought along important innovations in the collection of data from the primary health care services of the Ministry of Health, as well as the delivery of health services. At the forefront of these innovations is Family Medicine Information System. It is not correct to consider Family Medicine Information System as just a computer program. This system is also described as newly developed standards for data collection from primary health care services in provinces where family medicine is practiced. With Family Medicine Information System, family physicians record the health service provided electronically and transmit the recorded data directly to the Ministry of Health in electronic environment with the data sets (Minimum Health Data Sets) determined by the Ministry of Health (Akdağ, 2010).

1.3. Central Physician Appointment System

The Ministry of Health has put into effect the Health Transformation Program in order to reach health services more effectively and efficiently in Turkey and has carried out the studies within the scope of this program to a large extent. One of the most important works of this program is the Central Physician Appointment System. This system is

(<https://www.mhrs.gov.tr/>); It is a system where citizens can make an appointment with the hospitals and dentists they want from the live operators, the web or the Central Physician Appointment System mobile application by calling the hospitals, oral and dental health centers and family physicians affiliated to the Ministry of Health.

- It is one of the 20 basic public services accepted by the European Union.
- It is centralized the appointment systems, which are distributed in public hospitals and affiliated health institutions. It also claims to be the first and only system in the world that manages the appointment systems of public hospitals from a single center.
- It is “Alo 182” can provide services to citizens at an accessibility level of 99.6% from our hospitals and family physicians via the call center, the internet, and mobile applications.
- It contributes to the development of new health policies with the data collected from the appointment system.

1.4. Core Resource Management System

This system produces accurate and up-to-date information in the follow-up and direction of human, material and financial resources in the Ministry of Health and its affiliates (Akdağ, 2010). Core Resource Management System; It is the system where the Ministry of Health, all personnel of the ministry, institution and building information, material information and private health institutions are monitored. The Human Resources Management System, where personnel movements are tracked, Material Resources Management System, where movables in all material warehouses within the Ministry of Health are actively followed, Investment Tracking System, where real estate is tracked, belongs to all private health institutions operating in Turkey. It has sub-modules such as the Private Health Institutions Management System, where all the process steps are followed, and the Basic Health Statistics Module, which is used to collect health statistics across the country” (Digital Hospital, 2019). Core Resource Management System consists of four modules. These are (<https://dijitalhastane.saglik.gov.tr/>);

1.5. MEDULA

MEDULA has been implemented since 01 August 2006. It is a system that ensures that the invoice information of the health services provided by the health institutions for the insured and beneficiaries is transferred to the General Health Insurance System and the invoice costs are transferred to the health institution. The system ensures that these periods are realized without interfering with the internal processes of health institutions. Pharmacies, health centers, diagnosis and treatment centers, public and private hospitals are integrated with the MEDULA system through web services. With this system, it is aimed that the citizens benefit from the health services offered in the best way. Some purposes of MEDULA (Birinci, 2013);

- Making the payments to the institution quickly and accurately,
- To make estimations and risk analyzes of future health expenditures,
- Ability to track changes in expenditure items
- It can be listed as obtaining comprehensive and high quality statistical information.

1.6. Electronic Prescription (e-Prescription)

It is an application that allows prescribing information to be written, stored and transferred between institutions in electronic environment. With the implementation of this system, paper-based prescription will decrease and after a while, paper-based prescription practice will come to an end. Thanks to the system, physicians prescribe the drugs to be given to the patients electronically, and patients can receive their drugs from pharmacies with a tracking number (Birinci, 2013). e-Prescription has been put into practice in Turkey since 01.07.2012.

e-Prescription application occupies an important place as a standard application in health information systems recently. It is the most comprehensive support system of health information systems, and it has been determined that more than one third (230 thousand prescriptions) of office-based prescriptions written in the USA in 2011 were made with the e-prescription system. With the e-prescription application, which is one of the important innovations in health recently, physicians can monitor drugs, drug contents and which diseases are used for the treatment of drugs through web-based systems (Gider, Ocak, & Top, 2015).

1.7. e-Nabız System

e-Nabız is an application that citizens and health professionals can access health data collected from health institutions via the internet and mobile devices. It is a personal health record system where the patient can manage all health information and access his/her medical history from a single place, regardless of where the examination, examination and treatment is performed. It is the world's largest and most comprehensive health informatics system, which can be accessed securely over the internet, enabling the health records to be evaluated by physicians within the framework of the authority granted by the individuals themselves, for which the duration and limit have been determined, thus increasing the quality and speed of the diagnosis and treatment process, and establishing a strong communication network between the patient and the physician. is the infrastructure. The health information in e-Nabız, the diagnoses made about the diseases of the individuals, the analyzes made, the medical images taken, the prescribed drugs, the allergies detected and similar information, since the system was put into use, are sent to the e-Nabız system in electronic environment by the health care providers. consists of The information can only be seen by the physicians authorized by the persons or by the persons who are in the system and who are allowed permanent or temporary permission (<https://enabiz.gov.tr/>).

RESULT

e-Health has become an area that adds innovation, speed, efficiency and flexibility to the healthcare industry. With e-Health, national and international health systems can be connected to each other and contribute to the development of the global health level. In addition, electronic communication of all health institutions and the ability to monitor health records in electronic environment provide important benefits not only for health institutions, but also for patients and their relatives and other stakeholders.

Since citizens can access their health records electronically, they can monitor their health information checks, data on service costs and many other data they need through e-health applications. It also provides benefits in many ways, such as making it easier for physicians to make decisions, better managing the processes of hospitals, improving their relations with suppliers, and establishing policies at the Ministry level. As a result, e-health applications have contributed to better quality of health service delivery, effective, easy and fast communication between patient-physician, in-house and outside the institution, and to reduce costs.

REFERENCES

- Akdağ, R. (2010). Türkiye Sağlıkta Dönüşüm Programı: ilerleme Raporu. Ankara: T.C. Sağlık Bakanlığı.
- Akdağ, R., & Erkoç, Y. (2011). Türkiye Sağlıkta Dönüşüm Değerlendirme Raporu: 2003-2010. Ankara: Sağlık Bakanlığı.
- Birinci, Ş. (2013). Hastane Bilgi Yönetim Sistemleri. H. Sur, & T. Palteki içinde, Hastane Yönetimi (s. 285-304). İstanbul: Nobel Tıp Kitabevi.
- Central Physician Appointment System. (2021, 06 11). T.C Sağlık Bakanlığı Merkezi Hekim Randevu Sistemi: <https://www.mhrs.gov.tr/Vatandas/hakkimizda.xhtml> adresinden alındı
- Core Resource Management System. (2021, 06 11). T.C. Sağlık Bakanlığı Dijital Hastane. <https://dijitalhastane.saglik.gov.tr/aglik.gov.tr/> adresinden alındı
- e-Sağlık. (2021,06 11). T. C. Sağlık Bakanlığı e-Sağlık, <https://e-saglik.gov.tr/> adresinden alındı
- Eysenbach, G. (2001). What is e-health? Journal of Medical Internet Research, 3(2), e20.
- Gider, Ö., Ocak, S., & Top, M. (2015). Sağlık Hizmetlerinde Elektronik Reçete (E-Reçete) Uygulamasının Değerlendirilmesi. Bilgi Ekonomisi ve Yönetimi Dergisi, 48, 15-25.
- Ömürbek, N., & Altın, F. G. (2009). Sağlık Bilişim Sistemlerinin Uygulanmasına İlişkin Bir Araştırma: İzmir Örneği. SDÜ Fen Edebiyat Fakültesi Sosyal Bilimler Dergisi(19), 211-232.

GRAIN YIELDS OF DURUM WHEAT (TRITICUM DURUM DESF.) AND YIELD STABILITY AFFECTED OF CERTAIN PREPARATIONS AND VARIOUS TERMS OF SOWING

Petar Nikolov

Institute of Agriculture and Seed Science "Obrazcov Chiflik", Ruse, Bulgaria,

Grozi Delchev

Trakia University, Faculty of Agriculture, Stara Zagora, Bulgaria,
ORCID: ID/0000-0003-2443-5474

Abstract

During 2019-2021, two field experiments with durum wheat cultivar Predel (*Triticum durum* Desf.) were performed in the experimental field of the Field Crops Institute, Chirpan and in the experimental field of the Trakia University, Stara Zagora. Three sowing dates were tested: Early sowing (05 - 10 October), Normal sowing (20 - 25 October - standard) and Late sowing (05 - 10 November). In early sowing, 2 retardants were studied: Cearon 480 SL - 1 l/ha and Medax top - 1 l/ha and 2 insecticides: Proteus 110 OD - 625 ml/ha and Mageos - 100 g/ha, as well as the mixtures between them. During late sowing, 2 stimulators were studied: Naturamin plus - 1.5 l/ha and Raiza mix - 750 ml/ha and 2 foliar liquid fertilizers: Mix for cereal SC - 1.5 l/ha and Trimax SC - 1.5 l/ha, as well as the mixtures between them. These preparations and fertilizers are imported after stage 3 - 4 leaves of durum wheat, in the so-called "Closure of crops". In the case of early sowing variants, this stage occurs in autumn, and in the case of late sowing variants, the stage occurs in spring. Early sowing of durum wheat leads to a decrease in grain yield in both regions - Chirpan and Stara Zagora. In the case of late sowing of durum wheat, the yield reduction is smaller. The combined use of Cearon and Medax top retardants with the insecticides Proteus and Mageos leads to higher grain yields compared to their use alone. The combined use of the stimulators Naturamin plus and Raiza mix with the foliar fertilizers Mix for cereals and Trimax also leads to higher grain yields compared to their use alone. The most unstable are the tank mixture Naturamin plus + Trimax in Chirpan region, followed by the independent and joint use of the retardants Cearon and Medax top and the insecticides Proteus and Mageos in Stara Zagora region. All variants from Chirpan region are the most technologically valuable. They combine high grain yields with high or good stability over different years.

Keywords: durum wheat, sowing dates, growth regulators, foliar fertilizers, grain yield, yield stability

1. INTRODUCTION

Durum wheat is a species with a winter-spring character. With earlier sowing until the onset of the cold months, it may enter stem elongation stage and freeze completely. The most optimal terms for sowing in Bulgaria are from 15.10 to 10.11. Any further delay can lead to damage and frost of the crop due to its weaker development. According to many authors, very early or very late sowing leads to problems with diseases and enemies (Sharma et al. 2003; Singh, 2004; Bassu et al., 2010; Gorczyca, 2018).

The aim of the present study is to study the productivity of durum wheat and the stability of yields under different weather conditions under the influence of certain pesticides, growth regulators and complex foliar fertilizers and different sowing dates.

2. MATERIAL AND METHODS

During 2019-2021, two field experiments with durum wheat cultivar Predel (*Triticum durum* Desf.) were performed in the experimental field of the Field Crops Institute, Chirpan and in the experimental field of the Trakia University, Stara Zagora, by the block method, in 4 replications, with the size of the harvest plot 15 m², after predecessor sunflower. The soil type is a chromic cambisols, poorly stocked with N₂, P₂O₅ and K₂O. Three sowing dates were tested: Early sowing (05 - 10 October), Normal sowing (20 - 25 October - standard) and Late sowing (05 - 10 November). In early sowing, 2 retardants were studied: Cearon 480 SL – 1 l/ha and Medax top - 1 l/ha and 2 insecticides: Proteus 110 OD - 625 ml/ha and Mageos - 100 g/ha, as well as the mixtures between them. During late sowing, 2 stimulators were studied: Naturamin plus - 1.5 l/ha and Raisa mix - 750 ml/ha and 2 foliar fertilizers: Mix for cereal SC - 1.5 l/ha and Trimax SC - 1.5 l/ha, as well as the mixtures between them.

These preparations and fertilizers are treated after stage 3 - 4 leaves of durum wheat, in the so-called "Closure of crops". In the case of early sowing variants, this stage occurs in autumn, and in the case of late sowing variants, the stage occurs in spring.

The productivity of durum wheat was determined by the obtained grain yields. The data were processed by analysis of variance (Shanin 1977; Barov, 1982; Lidanski, 1988). The stability of the tested variants with respect to the years was assessed by the stability variants σ^2 and S_i^2 according to Shukla (1972), ecovalence W_i according to Wricke (1962) and the stability criterion YS_i according to Kang (1993).

3. RESULTS AND DISCUSSION

When sowing durum wheat in optimal terms yields of 5518 kg/ha for the Chirpan region and 4102 kg/ha for the Stara Zagora region is obtained (Table 1). The reason for the lower yields in Stara Zagora is the poor nutrient and water regimes of the chromic cambisols soil in this area. In the Chirpan region, the leached vertisol soil is characterized by much higher soil fertility.

Early sowing of durum wheat leads to a reduction in grain yields in both areas. On average for the study period the decrease for the Stara Zagora region is by 16.6% compared to the normal sowing. For the Chirpan region the reduction of the yield is smaller - by 12.7% compared to the normal sowing. The decrease in yields in the early sowing of durum wheat is due to two reasons. The first reason is the development of virus diseases such as Wheat stroke mosaic caused by the Wheat streak mosaic virus transmitted by the mites *Aceria tulipae* and *Aceria tossicella* and Yellow barley blight caused by the Barley yellow dwarf virus transmitted by the aphids *Rhopalosiphon padi* and *Sitobion avenae* (Juroszek and von Tiedemann, 2011, 2012; Nilsen and Kirby, 2016). The second reason is damage to some wheat plants in winter, as a result of reduced cold tolerance due to their premature entry into stem elongation stage and the associated hardening of the plants. Unlike common wheat (*Triticum aestivum* L.), which is of the winter type and has a longer vernalization period, durum wheat (*Triticum durum* Desf.) is of the winter-spring type, with a short vernalization period and in warm autumn is predisposed to early stem elongation (Singh and Jain, 2000; Modhej, 2012).

Late sowing of durum wheat also leads to a reduction in grain yields in both areas. The reduction is less than that of early sowing. On average for the period the decrease for Stara Zagora region is by 9.3% compared to the normal sowing. For Chirpan region the reduction of the yield is almost the same - by 10.5% compared to the normal sowing. The decrease in yields in the late sowing of durum wheat is due to the short vegetation in November, leading to less hardening of the plants and

difficult to reach the optimal phase of the 4th leaf for wintering of durum wheat. As a result, some plants are damaged during the winter months.

The use of the insecticides Proteus and Mageos in early sowing leads to an increase in grain yield in both regions - Chirpan and Stara Zagora. On average for the period the increase varies from 11.3% to 12.7%. This increase is due to the limitation of viral diseases, as the insecticides Proteus and Mageos destroy the vectors of viruses.

The uses of retardants Cearon and Medax top in early sowing, also lead to increased yields in both areas. The increase in yield with the use of retardants alone is less than with the use of insecticides alone. On average for the period the increase varies from 6.1% to 7.2%. This shows that in early sowing the reduction in yield is due more to the attack of viruses than to the premature entry of durum wheat into the stem elongation stage.

The combined uses of retardants Cearon and Medax top with the insecticides Proteus and Mageos, lead to higher grain yields compared to their use alone. On average for the period the increase compared to the untreated variant with early sowing is from 18.0% to 20.3%. For Chirpan region the average increase in yield compared to the normal sowing period is from 3.6% to 4.5%. For Stara Zagora region, the combined use of insecticides and retardants almost compensates for the shortcomings of early sowing - the yields are 98.4% - 99.7% compared to normal sowing. Despite all the less developed plants in the Stara Zagora region overwinter more difficult.

The use of the stimulators Naturamin plus and Raiza mix during late sowing leads to an increase in grain yield in both regions - Chirpan and Stara Zagora. On average for the period, the increase compared to the untreated variant with late sowing varies from 9.2% to 11.7%.

Table 1. Grain yields affected of certain preparations and various terms of sowing, kg/ha (2019-2021)

Variants			2019	2020	2021	Mean	% compared to control	% compared to normal sowing
Chirpan								
Early sowing	-	-	4993	5024	4441	4819	100	87.3
		Proteus	5736	5481	4963	5393	111.9	97.7
		Mageos	5724	5436	4922	5361	111.3	97.2
	Cearon	-	5361	5429	4712	5166	107.2	93.6
		Proteus	6017	5884	5281	5727	118.8	103.8
		Mageos	5970	6034	5414	5799	120.3	104.5
	Medax top	-	5385	5348	4738	5157	107.0	93.5
		Proteus	5947	5979	5368	5765	120.0	104.4
		Mageos	6029	5940	5332	5715	118.6	103.6
	Normal sowing – St,		5853	5604	5122	5518	-	100
Late sowing	-	-	5197	5055	4569	4940	100	89.5
		Mix for cereals	5689	5481	4968	5379	108.9	97.0
		Trimax	5666	5436	4979	5360	108.5	97.1
	Naturamin plus	-	5736	5520	4999	5512	111.6	99.9
		Mix for cereals	6222	6205	5829	6085	123.2	110.3
		Trimax	6029	6389	5742	6053	122.5	109.7
	Raiza mix	-	5724	5498	4973	5393	109.2	97.7
		Mix for cereals	6058	6181	5552	5930	120.0	107.5

			Trimax	6192	6243	5609	6015	121.8	109.0
Stara Zagora									
Early sowing	-	-	3850	3333	3081	3421	100	83.4	
		Proteus	4332	3786	3427	3848	112.5	93.8	
		Mageos	4314	3773	3484	3857	112.7	94.0	
	Cearon	-	4056	3553	3282	3630	106.1	88.5	
		Proteus	4546	3973	3663	4061	118.7	99.0	
		Mageos	4515	3946	3644	4035	118.0	98.4	
	Medax top	-	4069	3563	3290	3641	106.4	88.8	
		Proteus	4555	3946	3648	4059	118.6	98.9	
		Mageos	4582	4000	3690	4091	119.6	99.7	
Normal sowing – St,			4457	4167	3808	4102	-	100	
Late sowing	-	-	3920	3834	3538	3722	100	90.7	
		Mix for cereals	4283	4225	3888	4132	111.0	100.7	
		Trimax	4265	4206	3877	4116	110.6	100.3	
	Naturamin plus	-	4323	4191	3865	4125	110.8	100.6	
		Mix for cereals	4675	4608	4246	4500	120.9	109.7	
		Trimax	4555	4490	4139	4395	118.1	107.1	
	Raiza mix	-	4310	4252	3918	4156	111.7	101.3	
		Mix for cereals	4564	4497	4143	4401	118.2	107.3	
		Trimax	4662	4570	4212	4481	120.4	109.4	
LSD, kg/ha:									
F.A	p≤5%=47	p≤1%=61	p≤0.1%=79						
F.B	p≤5%=38	p≤1%=50	p≤0.1%=64						
F.C	p≤5%=117	p≤1%=154	p≤0.1%=198						
AxB	p≤5%=66	p≤1%=87	p≤0.1%=111						
AxC	p≤5%=203	p≤1%=267	p≤0.1%=342						
BxC	p≤5%=166	p≤1%=218	p≤0.1%=279						
AxBxC	p≤5%=287	p≤1%=378	p≤0.1%=484						

The use of foliar fertilizers Mix for cereals and Trimax in late sowing also leads to an increase in grain yield in both areas. For Stara Zagora region the increase in grain yield on average for the period is higher and varies from 10.6% to 11.0%. For Chirpan region the increase is smaller - from 8.5% to 8.9%. The reason for the higher effect of foliar fertilizers in Stara Zagora is the lower supply of nutrients to the chromic cambisols soil compared to the leached vertisol soil in Chirpan.

The combined use of the stimulators Naturamin plus and Raiza mix with the foliar fertilizers Mix for cereals and Trimax leads to higher grain yields compared to their use alone. On average for the period in both regions the increase compared to the untreated variant with late sowing is from 18.1% to 23.2%. The average increase in grain yield compared to the normal sowing period is from 7.1% to 10.3%.

Through the analysis of the variant in terms of grain yield (Table 2) it is established that the areas of derivation of the experiments have the greatest influence on this indicator - 71.4% of the total variation. The reason for this is the differences in soil conditions in the two regions related to their different reserves of moisture and nutrients. The strength of the influence of the preparations and the terms of sowing is 12.7%, and of the years - 8.9%. The influence of regions, preparations, sowing dates and years is very well proven at $p \leq 0.01$. There is a proven interaction of the regions with the conditions of the years (AxB) - 0.4%, of the preparations and the terms of sowing with the

conditions of the years (AxC) - 0.7% and of the regions with the preparations and terms of sowing (BxC) - 0.9%. The interactions of the regions with the conditions of the years (AxB) and of the regions with the preparations and the sowing terms (BxC) are very well proved at $p \leq 0.01$. The interaction between the preparations and the sowing dates with the conditions of the years (AxC) was proved at $p \leq 0.5$. The interaction between the three experimental factors (AxBxC) - 0.5% has not been proven.

Table 2. Analysis of variance for grain yield

Source of variation	Degrees of freedom	Sum of squares	Influence of factor, %	Mean squares	Fisher's criterion	Level of significance
Total	455	3539672	100	-	-	-
Tract of land	3	13904	0.4	4634.7	10.9	***
Variants	113	3381624	95.5	29925.9	70.4	***
Factor A – Years	2	314104	8.9	157052.0	369.4	***
Factor B – Places	1	2531216	71.4	2531216.0	5953.0	***
Factor C – Preparations and terms of sowing	18	449896	12.7	24994.2	58.8	***
AxB	2	15560	0.4	7780.0	18.3	***
AxC	36	24232	0.7	673.1	1.6	*
BxC	18	30192	0.9	1677.3	3.9	***
AxBxC	36	16424	0.5	456.2	1.1	ns
Pooled error	339	144144	4.1	452.2	-	-
* $p \leq 5\%$ ** $p \leq 1\%$ *** $p \leq 0.1\%$						

Based on the proven interactions regions x year, preparations and sowing dates x year and areas x preparations and sowing dates, the stability of the manifestations of each variant in terms of durum wheat grain yield was assessed (Table 3). The Shukla stability variants σ_i^2 and S_i^2 , the Wricke ecovalence W_i and the Kang YSi stability criterion were calculated.

The Shukla stability variants (σ_i^2 and S_i^2), which take into account the linear and nonlinear interactions, respectively, unilaterally evaluate the stability of the variants. These variants, which show lower values, are considered more stable because they interact less with environmental conditions. The negative values of the indicators σ_i^2 and S_i^2 are considered to be 0. At significantly high values of either of the two parameters - σ_i^2 or S_i^2 , the variants are considered unstable. In Wricke's W_i ecovalence, the higher the value of the indicator, the more unstable the corresponding variant.

Using these three parameters of stability, it was found that the most unstable are the tank mixture Naturamin plus + Trimax in the Chirpan region, followed by the independent and joint use of retardants Cearon and Medax top and insecticides Proteus and Mageos in the Stara Zagora region. In them, the values of the variance variants σ_i^2 and S_i^2 according to Shukla and the ecovalence W_i according to Wricke are the highest and mathematically proven. The instability is mainly due to the significant differences in grain yields in these variants during the different years of experience, as soil and meteorological conditions affect them the most. In these variants there is instability of linear and nonlinear type - proven values of σ_i^2 and S_i^2 . In case of late sowing in the Stara Zagora

region, without additional treatments, there is instability of linear type - proven values of σ_i^2 . S_i^2 values are unproven. With the independent use of the retardant Cearon, the stimulator Naturamin plus, the leaf fertilizer Mix for cereals in the Chirpan region and early sowing in the region Stara Zagora, without additional treatments, there is instability of nonlinear type - proven values of S_i^2 . The values of σ_i^2 are unproven. The other variants show high stability in terms of grain yield, despite the changes in meteorological conditions during the growing season of durum wheat.

In order to make an overall assessment of the effectiveness of each variant, both its influence on the yield of durum wheat grain and its stability - the reaction of the crop to this variant in different years - must be taken into account. Very valuable information about the technological value of the variants is given by Kang's YS_i indicator for simultaneous assessment of yield and stability, based on the reliability of the differences in grain yield and the variant of the interaction with the environment. The value of this criterion is that using non-parametric methods and statistical proof of differences, we obtain a summary assessment, sorting the options in descending order according to their economic value.

Table 3. Stability parameters of certain preparations and various terms of sowing for grain yield with relation to years

Variants			\bar{x}	σ_i^2	S_i^2	W_i	YS_i
Chirpan							
Early sowing	-	-	4819	504.6	1009.5	996.1	21+
		Proteus	5393	206.0	-14.7	430.2	30+
		Mageos	5361	305.8	30.2	619.5	28+
	Cearon	-	5166	895.4	1719.4*	1736.6	26+
		Proteus	5727	276.3	180.5	563.4	35+
		Mageos	5799	578.6	116405	1136.3	37+
	Medax top	-	5157	351.2	635.7	705.5	25+
		Proteus	5765	547.2	1107.8	1076.7	36+
		Mageos	5715	39.3	7.0	112.6	34+
Normal sowing – St,			5518	47.4	-24.1	129.8	33+
Late sowing	-	-	4940	10.2	30.5	59.4	23+
		Mix for cereals	5379	83.9	-26.1	198.9	29+
		Trimax	5360	19.3	-13.6	76.5	27+
	Naturamin plus	-	5512	1192.9	1719.3*	2300.3	32+
		Mix for cereals	6085	596.4	245.5	1170.4	41+
		Trimax	6053	3213.9**	5297.2**	6129.6	32+
	Raiza mix	-	5393	119.9	-25.3	297.3	30+
		Mix for cereals	5930	100.2	1996.3*	1973.0	38+
		Trimax	6015	665.8	1541.4	1301.5	39+
Stara Zagora							
Early sowing	-	-	3421	1125.0	2153.8*	2171.6	-2
		Proteus	3848	1468.2*	1975.7*	2821.9	-2
		Mageos	3857	1294.2*	2225.4*	2492.2	-1
	Cearon	-	3630	1024.6	1923.4*	1981.4	-1
		Proteus	4061	1597.8*	2498.0*	3067.5	2
		Mageos	4035	1548.5*	2461.6	2974.7	0
	Medax top	-	3641	1043.8	1945.0*	2017.8	0
		Proteus	4059	1712.3*	2527.4*	3284.4	1

		Mageos	4091	1680.2*	2602.5*	3223.5	3
Normal sowing – St,			4102	636.7	1263.1	1246.3	8
		-	3722	1445.9*	333.3	2779.5	-3
	-	Mix for cereals	4132	547.7	70.5	1077.8	11
		Trimax	4116	580.9	60.7	1140.6	9
Late sowing	Naturamin plus	-	4125	299.2	-26.6	606.8	10
		Mix for cereals	4500	391.1	2.7	781.0	16
		Trimax	4395	451.4	68.3	895.2	13
	Raiza mix	-	4156	587.9	79.2	1154.0	12
		Mix for cereals	4401	429.7	66.7	854.1	14
		Trimax	4481	308.7	23.9	625.0	15
Mean			4786				18.4
LSD (p=0.05)			138				

Kang's generalized stability criterion YS_i , taking into account both stability and yield value, gives a negative assessment of late and early sowing in Stara Zagora region, without additional treatments and the independent use of insecticides Proteus and Mageos and retardant Cearon, characterizing them as unstable and low yielding.

According to this criterion, all variants from Chirpan region are the most technologically valuable. These options combine high values of grain yield and high or good stability of this indicator in different years.

From the point of view of the technology for growing durum wheat, the variants with joint and independent use of the stimulants Naturamin plus and Raiza mix and the leaf fertilizers Mix for cereals and Trimax in Stara Zagora region, as well as the variant with normal sowing in this region are highly appreciated. They combine good grain yields with good stability during the individual years of the study.

The variants with joint use of the insecticides Proteus and Mageos and of the retardants Cearon and Medax top in Stara Zagora region receive low marks and should be avoided.

4. CONCLUSIONS

Early sowing of durum wheat leads to a decrease in grain yield in both regions - Chirpan and Stara Zagora.

In the case of late sowing of durum wheat, the yield reduction is smaller.

The combined use of Cearon and Medax top retardants with the insecticides Proteus and Mageos leads to higher grain yields compared to their use alone.

The combined use of the stimulators Naturamin plus and Raiza mix with the foliar fertilizers Mix for cereals and Trimax also leads to higher grain yields compared to their use alone.

The most unstable are the tank mixture Naturamin plus + Trimax in Chirpan region, followed by the independent and joint use of the retardants Cearon and Medax top and the insecticides Proteus and Mageos in Stara Zagora region.

All variants from Chirpan region are the most technologically valuable. They combine high grain yields with high or good stability over different years.

REFERENCES

- [1].A. Gorczyca. "Fusarium head blight incidence and mycotoxin accumulation in three durum wheat cultivars in relation to sowing date and density." The Science of Nature, vol. 105 (1), pp. 1-11, 2018.
- [2].A. K. Singh and G. L. Jain. "Effect of sowing time, irrigation and nitrogen on grain yield and quality of durum wheat (Triticum durum)." Indian Journal of Agricultural Sciences, vol. 70 (8), pp. 532-533, 2000.

-
- [3].A. Modhej, "Effects of post-anthesis heat stress and nitrogen levels on grain yield in wheat (T. durum and T. aestivum) genotypes." *International Journal of Plant Production*, vol. 2 (3), pp. 257-268, 2012.
- [4].E. C. Oerke, "Crop losses to pests". *Journal of Agricultural Science*, vol. 144, pp. 31-43, 2006.
- [5].G. Shukla, "Some statistical aspects of partitioning genotype - environmental components of variability." *Heredity*, vol. 29, pp. 237-245, 1972.
- [6].G. Wricke, "Über eine Methode zur Erfassung der Ökologischen Streikbreiten Feldersuchen." *Pflanzen zu Recht*, vol. 47, pp. 92-96, 1962.
- [7].M. Kang, "Simultaneous selection for yield and stability: Consequences for growers." *Agronomy Journal*, vol. 85, pp. 754-757, 1993.
- [8].N. Nielsen and T. Kirby. "Sowing Density and Cultivar Effects on Pith Expression in Solid - Stemmed Durum Wheat." *Agronomy Journal*, vol. 108 (1), pp. 219-228, 2016.
- [9].P. Juroszek and A. von Tiedemann. "Plant diseases, insect pests and weeds in a changing global climate: a review of approaches, challenges, research gaps, key studies and concepts." *Journal of Agricultural Science*, doi: 10.1017 / S0021859612000500, 2012.
- [10]. P. Juroszek and A. von Tiedemann. "Potential strategies and future requirements for plant disease management under a changing climate. *Plant Pathology*, vol. 60, pp. 100–112, 2011.
- [11]. S. Bassu, F. Giunta and M. Motzo. "Effects of sowing date and cultivar on spike weight and kernel number in durum wheat." *Crop and Pasture Science*, vol. 61 (4), pp. 287-295, 2010.
- [12]. S. N. Sharma, R. S. Sain, and R. K. Sharma. "The genetic control of flag leaf length in normal and late sown durum wheat. *Journal of Agricultural Science*, vol. 141 (3-4), pp. 323-331, 2003.
- [13]. S. Singh, "Occurrence and impact of a new leaf rust race on durum wheat in northwestern Mexico from 2001 to 2003." *Plant disease*, vol. 88 (7), pp. 703-708, 2004.
- [14]. T. Lidanski, *Statistical methods in biology and agriculture*, Sofia, pp. 376, 1988.
- [15]. V. Barov, *Analysis and schemes of the field experience*. NAPO, Sofia, pp. 668, 1982.
- [16]. Yo. Shanin, *Methodology of the field experience*. BAS, pp. 384, 1977.
-

IN VITRO WOUND HEALING POTENCY OF METHANOLIC LEAF EXTRACT OF ARISTOLOCHIA SACCATA IS POSSIBLY MEDIATED BY ITS STIMULATORY EFFECT ON COLLAGEN-1 EXPRESSION

K.R.Padma

Assistant Professor, Department of Biotechnology, Sri Padmavati Mahila Visvavidyalayam (Women's) University, Tirupati, AP Orcid No:0000-0002-6783-3248.

K.R.Don

Reader, Department of Oral Pathology and Microbiology, Sree Balaji Dental College and Hospital, Bharath Institute of Higher Education and Research (BIHER) Bharath University, Chennai, Tamil Nadu, India
Orcid No: 0000-0003-3110-8076.

Abstract

Background: Identification and assessment of therapeutic potential of natural products derived from medicinal plants have led to the discovery of innovative and economical drugs to treat several diseases, including chronic wounds. In vitro cell based scratch assay is an appropriate and inexpensive method for initial understanding of wound healing potential of medicinal plant extracts. The current study was aimed at investigating the wound healing capacity of Aristolochia saccata leaf extract by using scratch assay as a primary model, where proliferative and migratory capabilities of test compounds could be monitored through microscopy studies. A. saccata is an evergreen climbing shrub belongs to the family Aristolochiaceae.

Methods: Methanolic extraction of the plant material was done using Soxhlet apparatus and the cytotoxicity of the extract on L929 cells was studied by 3-(4,5-dimethylthiazol-2-yl)-2,5-diphenyltetrazolium bromide (MTT) assay. L929 is a human fibroblast cell line. In vitro scratch assay was performed to evaluate the wound healing properties of A. saccata leaf extract and possible mechanism of action was analyzed by flow cytometric expression studies of an extracellular matrix (ECM) factor, collagen type-1.

Results: MTT assay revealed that A. saccata leaf extract had no cytotoxic effect on the cells and at higher concentrations, the extract showed mild toxicity resulting in the death of just 2.88% cells. Scratch assay showed 34.05%, 70.00%, 93.52% wound closure at 12hrs, 24hrs and 48hrs of incubation respectively. These results were similar compared to positive control which showed 37.60, 56.41 and 99.05% of wound closure. Further, flow cytometry-based studies revealed that the A. saccata leaf extract induced the expression of ECM remodelling factor collagen-1.

Conclusion: Our study revealed the wound healing capabilities of A. saccata In vitro. Hence, A. saccata could be recommended as a potential source of wound healing agents.

Keywords: Plant biology, Cell biology, Pharmaceutical science, Molecular biology, Biotechnology, Biochemistry

EFFECTIVE ROLE OF CHITOSAN-SILVER NANOCOMPOSITE ON FOOD PRESERVATION

K.R.Padma

Assistant Professor, Department of Biotechnology, Sri Padmavati Mahila Visvavidyalayam
(Women's) University, Tirupati, AP. Orcid No:0000-0002-6783-3248.

K.R.Don

Reader, Department of Oral Pathology and Microbiology, Sree Balaji Dental College and
Hospital, Bharath Institute of Higher Education and Research (BIHER) Bharath University,
Chennai, Tamil Nadu, India
Orcid No: 0000-0003-3110-8076.

ABSTRACT

Canning is the general term applied to the process of packaging a food in a container and subjecting it to a thermal process for the purpose of extending its useful life. An optimal thermal process will destroy pathogenic (disease-causing) bacteria, kill or control spoilage organisms present, and have minimal impact on the nutritional and physical qualities of the food. Although we think of canning in terms of steel or possibly aluminium cans, the principles apply equally well to a variety of food containers such as glass jars, plastic and foil-laminated pouches, semi rigid plastic trays or bowls, as well as metal cans of any one of several shapes, including cylindrical, oval, oblong, or rectangular. Therefore in our present study we have provided the optimum preparation parameters of chitosan-silver nanoparticles composite (CSNC) with promising antibacterial activity. Nevertheless, Chitosan utilized to alleviate silver nitrate and stabilise silver nanoparticles in the medium. Therefore, our current article revealed the significance of canning with coated chitosan silver nanoparticle as a best method for preservation of several food items.

Keywords: Chitosan silver nanoparticles composite, Chitosan, Preservation method, container, canning.

GENETIC VARIABILITY, ASSOCIATION AND DIVERSITY STUDY AMONG THE SUNFLOWER GENOTYPES AT SEEDLING STAGE BASED ON DIFFERENT MORPHO-PHYSIOLOGICAL PARAMETERS UNDER POLYETHYLENE GLYCOL INDUCED STRESS

Ms. Uzma Ayaz

The University of Poonch Rawalakot, Pakistan

Abstract

Drought stress directly affects growth along with productivity of plants by altering plant water status. Sunflower (*Helianthus annuus* L.) an oilseed crop, is adversely affected by biotic stresses. The present study was carried out to study the genetic variability and diversity among the sunflower genotypes at seedling stage based on different morph-physiological parameters under Polyethylene Glycol (PEG) induced stress. A total of twenty seven genotypes including two hybrids, eight advanced lines and seventeen accessions of sunflower (*Helianthus annuus* L.) were tested at germination and seedling stages in Polyethylene Glycol. Correlation and principle component analysis confirmed that germination percentage, root length, proline content, shoot length, chlorophyll content, Stomatal frequency and survival percentage are positively correlated with each other hence; these traits were responsible for most of variation among genotypes. The cluster analysis results showed that genotypes Ausun, line-2, line-8, 17559, 17578, Hysun-33, 17555, and 17587 as more diverse among all the genotypes. These most divergent genotypes could be utilized in the development of inbreed which could be subsequently used in the heterosis breeding.

Key words: Sunflower, drought, stress, polyethylene glycol

WOODEN BREAST SYNDROME AND FACTORS AFFECTING ITS DEVELOPMENT

Tuğçe UZUN

Tekirdag Namik Kemal University Faculty of Agriculture, Dept. of Animal Science
Tekirdag/TURKEY
ORCID: 0000-0003-3424-8576

Aylin AĞMA OKUR

Tekirdag Namik Kemal University Faculty of Agriculture, Dept. of Animal Science
Tekirdag/TURKEY
ORCID: 0000-0001-6678-765X

Abstract

It is aimed to summarize the information about the “Wooden Breast” syndrome, which was first detected in 2014 and has gained increasing importance from that date in the poultry farming sector day by day, and the factors affecting its formation. The share and importance of poultry meat and egg production in the livestock sector have been increasing in recent years. Especially broiler meat production and consumption is rising in the world. Animal protein sources are accepted as the most valuable protein source due to their high digestibility in human nutrition. According to 2019 data, the total meat consumption per person in the world is 43.5 kg, of which approximately 39% (16.9 kg) is poultry meat (BESD-BIR, 2021a). Advantages of poultry rearing and poultry products (meat, egg) for consumers’ perspectives are relatively low preparing and cooking time, low feed conversion ratio (FCR), nutritional properties of meat and eggs, affordability in terms of prices, and being consumable in all religions and cultures (Kuttappan et al., 2016; Baltic et al., 2019; Baldi et al., 2020).

The most notable and increasing myopathies in the last 10 years are Deep Pectoral Muscle (DPM), Pale-Soft-Water (PSE), White Striping (WS), Spaghetti Breast (SB), and Wooden Breast (WB) syndromes. It is thought that these myopathies might have been present before 2010, however, their detection and reporting could be new in meat processing facilities (Aviagen, 2019; Sihvo, 2019; Bailey et al., 2020; Zampiga et al., 2020).

WB syndrome is a myopathy that was first reported in Finland in 2014 and can be detected after slaughter. No effective biomarker for detection in live animals has yet been found (Sihvo et al., 2014; Kuttappan et al., 2016; Baltic et al., 2019; Cauble et al., 2020). The pectoralis major muscle is the most valuable part of the broiler carcass and forms approximately one-fifth of the birds' body weight (Baltic et al., 2019). The most important characteristic that distinguishes WB syndrome from other myopathies, is that it is seen only in the pectoralis major muscle. When the WB breast meat is examined microscopically, it has been reported that the muscle fibers appear less oval or round in shape (Zotte et al., 2017). Studies demonstrated that it has a larger cross-sectional area than normal muscle, high intramuscular collagen, and high pH after slaughtering (Huang and Ahn, 2018; Velleman, 2020). In addition, it has been stated that disease lesions such as regional oxygen deficiency, oxidative stress, fibrosis, increased intracellular calcium, and muscle fiber type changes can be seen. It has also been determined that the superficial area of the pectoralis muscle tends to be more affected

than the deep parts of the muscle (Mutryn et al., 2015; Baltic et al., 2019; Baldi et al., 2020).

Factors causing WB syndrome have been reported, such as breed, sex, rapid growth rate, high breast meat yield, age, energy and amino acid levels of the feed, pectoral muscle hypertrophy, oxidative stress, potassium, and phosphorus addition to the feed, feed restriction, selenium, vitamin E, phytase enzyme supplementation, decrease in motility might play an active role, and also have negative effects on breast meat quality (Tekeli et al., 2016; Bowker et al., 2019; Zhang et al., 2021). When comparing healthy breast meat and breast meat affected by WB syndrome, consumers can easily distinguish physical and sensory differences even with their sensory organs. As a result, consumer preferences are negatively affected, due to the firmness of meat and meat products with WB syndrome.

When the breast meat with WB syndrome was examined histologically, it was determined that polyphasic muscle degeneration with varying degrees of fibrosis, inflammatory cell accumulation, cellular unwanted fluid accumulation, necrosis, and lymphocytic (LYM-white blood cell type) clusters were observed in the pectoralis major muscle (Kuttappan et al., 2016; Abasht et al., 2019). At the same time, increased creatine kinase levels were detected in plasma. In addition, abnormalities in cell structure and shape, muscle fiber fragmentation, deterioration of healthy tissue-mass formation, irregular fat formation (lipidosis), calcium accumulation, oxygen deficiency (hypoxia), oxidative stress, etc. other typical symptoms of existing tissue damage have been demonstrated (Mutryn et al., 2015; Griffin et al., 2017; Zotte et al., 2017). Furthermore, studies have shown that it does not pose a pathological threat in terms of microbiological, chemical, and biological use as human food. This myopathy also negatively affects meat processing and causes economic losses in the poultry industry. To sum up, studies on WB syndrome are increasing and gaining great importance considering all the reasons mentioned above.

Keywords: Wooden breast, myopathy, muscle fibre, pH, broiler

Odunsu Göğüs Eti Sendromu ve Oluşumunu Etkileyen Faktörler

1. GİRİŞ

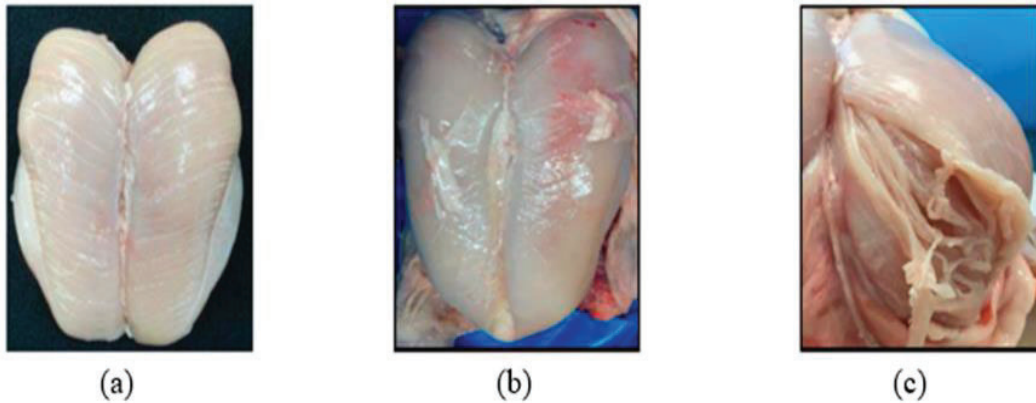
Beyaz et ve yumurta üretiminin hayvancılık sektöründeki payı ve önemi son yıllarda giderek artmaktadır. Özellikle tavuk eti üretimi ve tüketimi dünya çapında yaygınlaşmaktadır. Hayvansal protein kaynakları, insan beslenmesinde yarıyışlılığının yüksekliği nedeniyle, en değerli protein kaynağı olarak kabul edilmektedir. Dünyadaki hayvansal protein kaynaklarının tüketim değerleri incelendiğinde, %45'i büyükbaş hayvanların et ve sütünden, %31'i kümes hayvanlarının et ve yumurtasından, %20'si domuzların etinden ve %4'ü ise küçükbaş hayvanların etinden ve sütünden olacak şekilde karşılanmaktadır. Kanatlı hayvanların; üretim süresinin göreceli olarak düşük olması, yem dönüşüm oranının (YDO) düşük olması, etinin ve yumurtasının besleyici özellikleri, fiyatları bakımından satın alınabilirliği, tüketime hazırlama kolaylıkları, tüm dinlerde ve kültürlerde tüketilebilir olması gibi avantajları bulunmaktadır (Kuttappan ve ark., 2016; Baltic ve ark., 2019; Baldi ve ark., 2020).

Çizelge 1. Dünyadaki ve Türkiye’deki kişi başı et tüketim değerleri (kg)
Table 1. Meat consumption values per capita in the world and in Turkey (kg)

Et türleri	Dünya		Türkiye	
	2018	2019	2018	2019
Büyükbaş Hayvan Eti	9.3	9.4	12.9	13.6
Kanatlı Eti	16.3	16.9	21.6	21.0
Küçükbaş Eti	2.0	2.0	1.4	1.5
Domuz eti	15.8	14.3	-	-
TOPLAM	44.4	43.5	35.9	36.1

BESD-BİR (2021a, 2021b) verilerinden derlenmiştir.

Çizelge 1’de Türkiye’de ve Dünya’da toplam et tüketim değerleri yer almaktadır (BESD-BİR, 2021a, 2021b). Bilim insanları ve üreticiler; beyaz et talebini karşılayabilmek amacıyla, kısa sürede işleme ağırlığına ulaşabilecek tavuk ırkları elde etmek için ıslah çalışmaları üzerine yoğunlaşmıştır. Tavukçuluk sektöründe yıllar içinde gelişen ıslah metotları, bakım ve besleme konularındaki iyileşmeler ile kısa sürede yüksek canlı ağırlığa ulaşan hibrit ırklar üretilmeye başlanmıştır. Etlik piliçlerdeki bu hızlı büyüme oranı, yem dönüşüm oranı (FCR), yüksek göğüs verimi, canlı ağırlık artışı, işleme ağırlığına ulaşma süresinin kısalması, genetik vb. faktörler, kasta birtakım miyopatilere sebep olmuştur. Son 10 yılda en çok dikkat çeken ve artış gösterenler miyopatiler; Derin Pektoral Kası (DPM), Solgun-Yumuşak-Sulu (PSE), Beyaz Çizgi (BÇ), Spagetti Göğüs Eti (SGE) ve Odunsu Göğüs Eti (OGE) sendromlarıdır. Bu miyopatilerin 2010 yılından önce de mevcut olabileceği, ancak işleme tesislerinde saptanıp rapor edilmeye başlamasının yeni olabileceği düşünülmektedir (Aviagen, 2019; Sihvo, 2019; Bailey ve ark., 2020; Zampiga ve ark, 2020). Şekil 1’de Beyaz çizgi, Odunsu göğüs eti ve Spagetti göğüs eti miyopatilerine ait görüntüler verilmiştir.



Şekil 1. Etlik piliçlerde görülen (a) Beyaz çizgi, (b) Odunsu göğüs eti, (c) Spagetti göğüs eti miyopatilerine ait görüntüler (Soglia ve ark., 2019)

Figure 1. Appearances of (a) White striping, (b) Wooden breast, (c) Spaghetti meat myopathies in broilers (Soglia et al. 2019)

Odunsu Göğüs Eti (OGE), ilk defa Finlandiya’da 2014 yılında fark edilmiş bir miyopati olup, kesim sonrasında saptanabilmektedir. Henüz canlı hayvanlarda saptanmasında etkili bir biyo-belirteç bulunamamıştır (Sihvo ve ark, 2014; Kuttappan ve ark., 2016; Baltic ve ark., 2019; Cauble ve ark, 2020). OGE sendromu, etlik piliçlerin pektolaris major kasında görülmekte ve kaslara verdiği sertlikten dolayı halk arasında “Odunsu Göğüs (Wooden Breast)” adını almıştır (De Brot ve ark., 2016; Kuttappan ve ark., 2016;

Cauble ve ark., 2020). Oluşum sebepleri tam olarak bilinmemekle birlikte, ticari koşullarda yetiştirilen etlik piliçlerin hızlı büyüme oranı başta olmak üzere, genetik yapıları, cinsiyetleri, yedikleri yemin besin madde içeriği, kısıtlı yemleme uygulanması ve oksidatif stres gibi faktörlerden etkilendiği düşünülmektedir. Bununla birlikte, OGE sendromunun etiolojisi birçok yönü ile halen belirsizliğini korumaktadır (Tekeli ve ark., 2016; Bowker ve ark., 2019; Zhang ve ark., 2021).

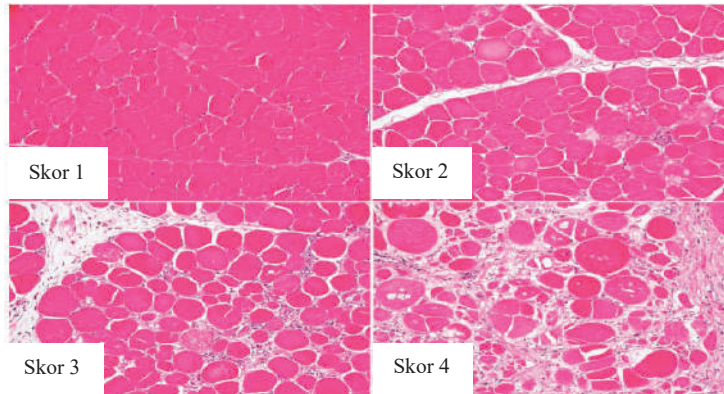
Bu derleme çalışması ile en son saptanan miyopati olan “Odunsu Göğüs Eti” sendromu, oluşumunu etkileyen faktörler, etlik piliçler ve et kalitesi üzerindeki etkileri konularında bilgiler vermek amaçlanmıştır.

2. ODUNSU GÖĞÜS ETİ SENDROMU

OGE sendromunun makroskopik olarak incelenmesi ile pektoral kaslarda sertlik, şişkinlik, küçük kanama lekeleri, viskoz yapıda yangı sıvısı, yüksek pH ve solgun bir görüntü ile karşılaşılmış, söz konusu bölgenin elle muayenesi ile de OGE sendromunun saptanabileceği bildirilmiştir (Mutryn ve ark., 2015; Hosotani ve ark., 2020). OGE miyopatisinin bir diğer karakteristik özelliği ise; sadece pektolaris major kasında gözlemlenmesidir. Etlik piliç karkasında en önemli kasın pektolaris major kası olduğu ve vücut ağırlığının %20’ sini oluşturduğu bilinmektedir (Baltic ve ark., 2019).

Beyaz Çizgi (BÇ) miyopatisinde ise göğüs eti ve butta, lif dejenerasyonu sebebiyle kas liflerine paralel olarak beyaz çizgi gözlemlenmiştir. Bu görünümün altında kas nekrozu ve kas lifleri üzerindeki yağ mineralizasyonunun etkilerinin olduğu tahmin edilmektedir (Mutryn ve ark., 2015; Huang ve Ahn, 2018; Bowker ve ark., 2019; Zampiga ve ark., 2020). Beyaz çizgi ve odunsu göğüs eti miyopatileri, göğüs etlerinde tek başına veya birlikte gözlemlenebildiği saptanmıştır (De Brot ve ark., 2016; Tekeli ve ark., 2016; Griffin ve ark., 2017; Soglia ve ark., 2019).

OGE sendromuna sahip göğüs filetosunun mikroskopik incelenmesi sonucu, kaslardaki liflerin yuvarlak veya buna benzer şekillerde olduğu görülmüştür (Zotte ve ark., 2017; Şekil 2). Kesim sonrası sağlıklı bir kasa göre daha yüksek pH’a ait olduğu yapılan çalışmalarla ortaya konmuştur (Huang ve Ahn, 2018; Velleman, 2020).



Şekil 2. Göğüs eti filetosunda hafif (1 ve 2), orta (3) ve şiddetli (4) safhalarda gözlemlenen Odunsu göğüs eti sendromunun mikroskopik görüntüleri (Chen ve ark., 2019)

Figure 2. Microscopic images of Wooden breast meat syndrome observed in breast fillets in mild (Score 1 and 2), moderate (Score 3) and severe (Score 4) stages (Chen et al., 2019)

OGE sendromuna sahip göğüs filetosunun histolojik incelenmesi sonucunda pektolaris major kasında fibroz, kas dejenerasyonu, yangı görüldüğü tespit edilmiştir (Kuttappan ve ark., 2016; Abasht ve ark., 2019). Aynı zamanda plazma kreatin kinaz seviyelerinde

artış saptanmıştır. Ayrıca hücre yapısı ve şeklindeki anormalliklerin (çekirdeklerin içselleştirilmesi, bölünmüş hücre görünümü, poligonal hücre kaybı vb.) var olan hasarın diğer tipik belirtileri olduğu ortaya konmuştur (Mutryn ve ark., 2015; Griffin ve ark., 2017; Zotte ve ark., 2017). Şekil 3'te ileri safhadaki OGE sendromuna sahip göğüs eti ile sağlıklı göğüs etinin üzerine 200 g ağırlık konulduğunda aralarındaki sertlik farklılıkları gösterilmiştir (Kuttapan ve ark., 2016).



Şekil 3. (a) İleri safhadaki Odunsu göğüs eti sendromu görülen göğüs etine, (b) Sağlıklı göğüs etine ağırlık ile baskı uygulandığındaki görünüşleri (Kuttapan ve ark., 2016).

Figure 3. (a) The appearance of the breast meat with severe wooden breast meat syndrome, (b) The appearance of healthy breast meat when pressure is applied with weight (Kuttapan et al., 2016).

3. ODUNSU GÖĞÜS ETİ SENDROMU VE OLASI SEBEPLERİ

Son yıllarda kanatlı hayvan etine yönelik tüketici talebindeki artıştan dolayı tavukçuluk sektörü, etlik piliçlerin daha genç yaşlarda hızlı bir şekilde daha fazla vücut ağırlığına ulaşabilmesini istemektedir. Böylelikle uygun rasyon seçimiyle ilk 2 hafta günlük 20-40 g canlı ağırlık artışı, ardından kesim yaşına kadar (yaklaşık 42 gün) günde 100 g canlı ağırlık artışı sağlanıp 3-4 kg modern etlik piliç üretimi yapmak amaçlanmaktadır (Abasht ve ark., 2019; Baltic ve ark., 2019).

Yapılan araştırmalar neticesinde ticari olarak üretilen göğüs filetolarının yaklaşık %5-10'unun OGE sendromunu sergilediği gözlemlenmiştir. OGE sendromunun en erken 14 günlük olduktan sonra görülmeye başladığı ve 3-4 haftalık olduktan sonra filetoda dejenerasyon (bozulma) belirtileri görüldüğü tespit edilmiştir (Hosotani ve ark., 2020; Zhang ve ark., 2021). Ancak kas dejenerasyonunun en çok 5-6 haftalıkken (kesim dönemi) belirgin olduğu bildirilmiştir (Baltic ve ark., 2019; Sihvo, 2019).

3.1. Odunsu Göğüs Eti Sendromuna Etki Eden Faktörler

1) Pektoral kas hipertrofisi: Hacimce artan kas lifleri, kılcal damarların azalmasına neden olur. Bu sebepten kan akışı yavaşlar, vücuttaki oksijen miktarı azalır ve bu durum damar iltihabına sebep olabilir. Pektoral kasında görülen bu değişikliklerle, odunsu göğüs eti sendromu miyopatilerinin oluşabileceği ifade edilmiştir (Soglia ve ark., 2019).

2) Hızlı Büyüme Oranı ve Yüksek Göğüs Verimi: Etlik piliçlerde görülen hızlı büyüme; göğüs kasının normalden fazla gerilmesine ve kılcal damarlardan oluşan ağların sayısında düşüslere sebep olmaktadır. Normalden daha hızlı gelişen etlik piliçlerde dolaşım azlığından ötürü kas lifleri dejenerasyona uğrar. Bu sebepten fibrozis ve vücuttaki oksijen seviyesindeki azalmadan ötürü hipoksi ortaya çıkar. Bu değişikliklerle, odunsu göğüs eti sendromu gibi miyopatilerin oluşabileceği ifade edilmiştir (Kuttappan ve ark., 2017; Zotte ve ark., 2017; Huang ve Ahn, 2018).

3) Yemin Enerji Düzeyi: Yüksek enerjili yemle beslemek daha yüksek vücut ağırlığına sahip etlik piliç üretimi sağlar ve büyüme oranını artırır. Yemlerde yüksek lipid seviyesi ve daha düşük protein miktarı etlik piliçlerde OGE ve BÇ oluşumunu

artırdığı ifade edilmiştir (Trocino ve ark., 2015; Griffin ve ark., 2017; Huang ve Ahn, 2018).

4) Aminoasit Düzeyi: Daha düşük sindirilebilir amino asit ile beslemek yani rasyonda aminoasit sınırlamasına gitmenin etlik piliçlerde odunsu göğüs etinin görülme oranı azalttığı bildirilmiştir. Aynı zamanda yapılan araştırmalar, etlik piliç rasyonuna esansiyel aminoasitlerden olan sindirilebilir lizin ve arginin ilavesinin olumlu etki yapacağı yönündedir (Cruz ve ark., 2017; Bodle ve ark., 2018).

5) Fitaz Enzimi İlavesi: Rasyona katkı maddesi olarak fitaz enziminin eklenmesi oksijen homeostasisinin (dengesinin) iyileştirilmesi yoluyla etlik piliçlerdeki Odunsu göğüs eti şiddetini %5 azalttığı bildirilmiştir (Cauble ve ark., 2020).

6) Potasyum (K) ve Fosfor (P) İlavesi: Potasyum ve fosfor iyonları, etlik piliçlerde hızlı büyüme sırasında üretilen hidrojen iyonlarının ortadan kaldırılmasında önemli rol oynamaktadır. Rasyondaki K ve P düzeylerinin azalmasına bağlı olarak; hızlı büyüyen, yüksek göğüs verimli etlik piliçlerin kaslarında asit-baz dengesinin bozulduğu tespit edilmiştir. Yapılan bazı araştırmalar, rasyona potasyum ve fosfor ilavesinin etlik piliçlerde OGE miyopatisinin oluşumunu azaltabileceğini varsaymaktadır (Livingston ve ark., 2019).

7) Hareket Kabiliyeti: Hareket kabiliyeti genellikle daha ağır ve hızlı büyüyen etlik piliçlerde daha zayıftır. Yürüyüş skorunun, etlik piliç hareketliliği ölçen iyi bir belirleyici olduğu ifade edilmiştir. Yapılan bazı çalışmalar, tavuklardaki kanat hareketliliğindeki azalmanın da OGE lezyonlarıyla ilişkili olduğunu varsaymaktadır (Papah ve ark., 2017; Baltic ve ark., 2019).

OGE sendromuna ayrıca oksidatif stres, cinsiyet, yaş, yem kısıtlaması, selenyum ve E vitamini ilavesi vb. gibi faktörlerin de etki ettiği yapılan araştırmalar sonucu tespit edilmiştir (Radaelli ve ark., 2017; Sihvo ve ark., 2017; Soglia ve ark., 2017; Huang ve Ahn, 2018; Baltic ve ark., 2019).

3.2. Odunsu Göğüs Eti Sendromunun Et Kalitesi Üzerine Etkisi

Etlik piliç endüstrisi, et üretimi için kas büyümesini en üst düzeye çıkarmaya odaklanmıştır. Pektolaris major kasları ticari bakımdan önemli bir ekonomik değere sahiptir. Bu nedenle hızlı büyüme oranı, yüksek göğüs verimi, yem dönüşüm oranı (FCR) gibi konulardaki gelişmeler kanatlı endüstrisinin birincil ilgi odağı haline gelmiştir (Griffin ve ark., 2017; Zampiga ve ark., 2020). OGE sendromuna sahip etlerde protein seviyesi azalmakta, pH derecesinde artış meydana gelmek ve ette yağ birikmesi görülmektedir. Etteki bu değişimler; etin işleme verimini (su tutma kapasitesi kaybı, pişirme kaybı, kesme kuvveti artışı vb.) ve et kalitesini azaltmaktadır (Clark ve Velleman, 2017; Huang ve Ahn, 2018).

4. SONUÇ

Yapılan tüm çalışmaların sonucunda, OGE sendromunun başlangıcını engelleme veya et kalitesini olumlu yönde etkileme konularında etkili birer çözüm henüz konu edilmemiştir. Yapılan incelemelerde OGE sendromuna sahip etlerin tüketiminde sağlık açısından zararlı herhangi bir patolojik, kimyasal veya biyolojik bir bulguya ulaşılmadığından “tüketilebilir gıda” görüşüne varılmıştır. Fiziksel ve duyuşal farklılıklar tüketicilerin satın alma isteğini ve etin görsel-duyuşal albenisini olumsuz yönde etkilediğinden bu tür etler halk tarafından tercih edilmemektedir. Dolayısıyla da endüstrideki birçok sektör büyük ekonomik zararlara uğramaktadır. OGE sendromunun sebep olduğu göğüs filetolarındaki bu duyuşal-teknolojik olumsuzlukların üstesinden

gelebilmek için araştırmaları, bilime uygun çözümleri ve beslenme konusundaki yenilikleri ele almak gerekmektedir. Bu bağlamda et kalitesini belirleyen; renk, pH, kesme kuvveti, su tutma/bağlama yeteneği, protein içeriği, yağ oranı, selenyum, E vitamini gibi tüm parametreler dikkate alınmalıdır.

KAYNAKLAR

- [1]. A. D. Zotte, G. Tasoniero, E. Puolanne, H. Remignon, M. Cecchinato, E. Catelli, and M. Cullere, "Effect of "Wooden Breast" appearance on poultry meat quality, histological traits, and lesions characterization," *Czech J. Anim. Sci.*, 62(2): 51-57, 2017.
- [2]. A. Tekeli, A. Özcan, and H. R. Kutlu, "Etlik piliçlerde odunsu göğüs eti "Wooden Breast" sorunu," *Turkish Journal of Agriculture – Food Science and Technology*, 4(11): 962-967, 2016.
- [3]. A. Trocino, A. Piccirillo, M. Birolo, G. Radaelli, D. Bertotto, E. Filiou, M. Petracci, and G. Xiccato, "Effect of genotype, gender and feed restriction on growth, meat quality and the occurrence of white striping and wooden breast in broiler chickens," *Poultry Science*, 94: 2996-3004, 2015.
- [4]. Aviagen, "Breast Muscle Myopathies (BMM)," 0219-AVN-066, p.48. (http://en.aviagen.com/assets/Tech_Center/Broiler_Breeder_Tech_Articles/English/Breast-Muscle-Myopathies-2019-EN.pdf; Erişim tarihi: 28.04.2021), 2019.
- [5]. B. Abasht, N. Zhou, W. R. Lee, Z. Zhuo, and E. Peripolli, "The metabolic characteristics of susceptibility to wooden breast disease in chickens with high feed efficiency," *Poultry Science*, 98: 3246-3256, 2019.
- [6]. B. Bowker, H. Zhuang, S. C. Yoon, G. Tasoniero, and K. Lawrence, "Relationships between attributes of woody breast and White striping myopathies in commercially processed broiler breast meat," *Poultry Science*, 28: 490-496, 2019.
- [7]. B. C. Bodle, C. Alvarado, R. B. Shirley, Y. Mercier, and J. T. Lee, "Evaluation of different dietary alterations in their ability to mitigate the incidence and severity of woody breast and white striping in commercial male broilers," *Poultry Science*, 97: 3298-3310, 2018.
- [8]. BESD-BİR, "Dünya'da kişi başına düşen et tüketimleri," (<https://besd-bir.org/assets/uploaded/dunya-kisi-basina-et-tuketimi.pdf>; Erişim tarihi: 21.10.2021), 2021a.
- [9]. BESD-BİR, "Türkiye'de kişi başına düşen et tüketimleri," (<https://besd-bir.org/assets/uploaded/Tr-kisi-basina-turlere-gore-et-tuketimi.pdf>; Erişim tarihi: 21.10.2021), 2021b.
- [10]. D. L. Clark, and S. G. Velleman, "Spatial influence on breast muscle morphological structure, myofiber size, and gene expression associated with the wooden breast myopathy in broilers," *Poultry Science*, 95: 2930-2945, 2017.
- [11]. F. Soglia, J. Gao, M. Mazzoni, E. Puolanne, C. Cavani, M. Petracci, and P. Erthjerg, "Superficial and deep changes of histology, texture and particle size

- distribution in broiler wooden breast muscle during refrigerated storage,” *Poultry Science*, 96: 3465-3472, 2017.
- [12]. F. Soglia, M. Mazzoni, and M. Petracci, “Spotlight on avian pathology: current growth – related breast meat abnormalities in broilers,” *Avian Pathology*, 48(1): 1-3, 2019.
- [13]. G. Baldi, F. Soglia, and M. Petracci, “Current status of poultry meat abnormalities,” *Meat and Muscle Biology*, 4(2):4, 1-7, 2020.
- [14]. G. Radaelli, A. Piccirillo, M. Birolo, D. Bertotto, F. Gratta, C. Ballarin, M. Vascellari, G. Xiccato, and A. Trocino, “Effect of age on the occurrence of muscle fiber degeneration associated with myopathies in broiler chickens submitted to feed restriction,” *Poultry Science*, 96: 309-319, 2017.
- [15]. H. K. Sihvo, “Pathology of wooden breast myopathy in broiler chickens,” University of Helsinki Faculty of Veterinary Medicine, Finland, 2019.
- [16]. H. K. Sihvo, J. Linden, N. Airas, K. Immonen, J. Valaja, and E. Puolanne, “Wooden breast myodegeneration of pectoralis major muscle over the growth period in broilers,” *Veterinary Pathology*, 54(1): 119-128, 2017.
- [17]. H. K. Sihvo, K. Immonen, and E. Puolanne, “Myodegeneration with fibrosis and regeneration in the pectoralis major muscle of broilers,” *Veterinary Pathology*, 51(3): 619-623, 2014.
- [18]. J. R. Griffin, L. Moraes, M. Wick, and M. S. Lilburn, “Onset of White striping and progression into wooden breast as defined by myopathic changes underlying pectoralis major growth. Estimation of growth parameters as predictors for stage of myopathy progression,” *Avian Pathology*, 47(1): 2-13, 2017.
- [19]. L. R. Chen, M. M. Suyemoto, A. H. Sarsour, H. A. Cordova, E. O. Oviedo-Rondon, M. Wineland, H. J. Barnes and L. B. Borst, “Temporal characterization of wooden breast myopathy “Woody Breast” severity and correlation with growth rate and lymphocytic phlebitis in three commercial broiler strains and a random-bred broiler strain,” *Avian Pathology*, 48(4): 319-328, 2019.
- [20]. M. B. Papah, E. M. Brannick, C. J. Schmidt, and B. Abasht, “Evidence and role of phlebitis and lipid infiltration in the onset and pathogenesis of wooden breast disease in modern broiler chickens,” *Avian Pathology*, 46(6): 623-643, 2017.
- [21]. M. Baltic, A. Rajcic, M. Laudanovic, S. Nesic, T. Baltic, J. Ciric, and I. B. Lazic, “Wooden breast – a novel myopathy recognized in broiler chickens,” *IOP Conf. Series*, 333: 012037, 2019.
- [22]. M. F. Mutryn, E. M. Brannick, W. Fu, W. R. Lee, and B. Abasht, “Characterization of a novel chicken muscle disorder through differential gene expression and pathway analysis using RNA – sequencing,” *BioMed Central (BMC) Genomics*, 16: 399, 2015.
- [23]. M. Hosotani, T. Kawasaki, Y. Hasegawa, Y. Wakasa, M. Hoshino, N. Takahashi, H. Ueda, T. Takaya, T. Iwasaki, and T. Watanabe, “Physiological and pathological mitochondrial clearance is related to pectoralis major muscle pathogenesis in broilers with wooden breast syndrome,” *Frontiers in Physiology*, 11: 579, 2020.
- [24]. M. L. Livingston, C. D. Landon, H. J. Barnes, J. Brake, and K. A. Livingston, “Dietary potassium and available phosphorous on broiler growth performance, carcass characteristics, and wooden breast,” *Poultry Science*, 98: 2813-2822, 2019.
- [25]. M. Zampiga, F. Soglia, G. Baldi, M. Petracci, G. M. Strasburg, and F. Sirri, “Muscle abnormalities and meat quality consequences in modern turkey hybrids,” *Frontiers in Physiology*, 11: 554, 2020.

-
- [26]. R. A. Bailey, E. Souza, and S. Avendano, "Characterising the influence of genetics on breast muscle myopathies in broiler chickens," *Frontiers in Physiology*, 11: 1041, 2020.
- [27]. R. F. A. Cruz, S. L. Vieira, L. Kindlein, M. Kipper, H. S. Cemin, and S. M. Rauber, "Occurrence of White striping and wooden breast in broilers fed grower and finisher diets with increasing lysine levels," *Poultry Science*, 96: 501-510, 2017.
- [28]. R. N. Cauble, E. S. Greene, S. Orlowski, C. Walk, M. Bedford, J. Apple, M. T. Kidd, and S. Dridi, "Dietary phytase reduces broiler woody breast severity via potential modulation of breast muscle fatty acid profiles," *Poultry Science*, 99: 4009-4015, 2020.
- [29]. S. De Brot, S. Perez, H. L. Shivaprasad, K. Baiker, L. Polledo, M. Clark, and L. Grau-Roma, "Wooden breast lesions in broiler chickens in the United Kingdom," *Veterinary Record*, 178(6): 141. (<https://doi.org/10.1136/vr.103561>), 2016.
- [30]. S. G. Velleman, "Pectoralis major "Breast" muscle extracellular matrix fibrillar collagen modifications associated with the wooden breast fibrotic myopathy in broilers," *Frontiers in Physiology*, 11: 461, 2020.
- [31]. V. A. Kuttappan, B. M. Hargis, and C. M. Owens, "White striping and woody breast myopathies in the modern poultry industry," *Poultry Science*, 95: 2724-2733, 2016.
- [32]. V. A. Kuttappan, C. M. Owens, C. Coon, B. M. Hargis, and M. Vazquez-Anon, "Incidence of broiler breast myopathies at 2 different ages and its impact on selected raw meat quality parameters," *Poultry Science*, 96: 3005-3009, 2017.
- [33]. X. Huang, and D. U. Ahn, "The incidence of muscle abnormalities in broiler breast meat," *Korean Journal for Food Science of Animal Resources*, 38(5): 835-850, 2018.
- [34]. X. Zhang, K. V. To, T. R. Jarvis, Y. L. Campbell, J. D. Hendrix, S. P. Suman, S. Li, D. S. Antonelo, W. Zhai, J. Chen, H. Zhu, and M. W. Schilling, "Broiler genetics influences proteome profiles of normal and woody breast muscle," *Poultry Science*, 100: 100994, 2021.

USE OF SORGHUM GRAIN IN POULTRY NUTRITION**Aylin AGMA OKUR**

Tekirdag Namik Kemal University Faculty of Agriculture, Dept. of Animal Science
Tekirdag/TURKEY
ORCID: 0000-0001-6678-765X

Kadir ERTEN

Tekirdag Namik Kemal University Faculty of Agriculture, Dept. of Animal Science
Tekirdag/TURKEY
ORCID: 0000-0002-6307-1573

Hasan Ersin SAMLI

Tekirdag Namik Kemal University Faculty of Agriculture, Dept. of Animal Science
Tekirdag/TURKEY
ORCID: 0000-0002-5462-8384

Abstract

In recent years, one of the important reasons for the price increase in the feed of monogastric animals can be said to be the increase in the value of commonly used raw materials due to excessive competition. To prevent this condition, the use of alternative feed raw materials in the diets becomes very important. Sorghum is a product that is emerging and gaining importance to meet this need. World sorghum production is estimated to be 61.62 million metric tons in 2020/2021. The top 5 sorghum-producing countries in the world are the USA, Nigeria, Ethiopia, Sudan, and Mexico, respectively (Worldagriculturalproduction, 2021). Sorghum is a plant grown in the low rainfall regions of the world, especially in subtropical, tropical, and temperate climate zones (Smith and Frederiksen, 2000).

Sorghum has many varieties and is important for the food industry as well as the feed industry. It has been reported that the nutrient content of sorghum grain is 9.3% crude protein, 1.9% crude ash, 2.4% crude cellulose, 2.9% crude oil, and 3250 kcal/kg metabolizable energy (Mohamed et al., 2015; Anonymous, 2021). However, some anti-nutritional factors limit the use of sorghum grain. These metabolites are called tannins, and the amount of tannin they contain varies according to the variety. Tannins are compounds with phenolic structure and are natural defense mechanisms produced by plants to protect themselves (Rooney et al., 2021). They are divided into two as condensed and hydrolyzable tannins (Ünver et al., 2014).

Tannins in sorghum are in the group of condensed tannins. Unlike hydrolyzable tannins, it has been reported that condensed tannins do not have toxic effects (Kamalak, 2007). Adverse effects of condensed tannin content that poultry fed are reported as, decrease in growth rate, and feed consumption, formation of tannin-protein complexes that are difficult to digest, inhibition of digestive enzymes, increase in endogenous protein production, negative effects on digestive tract functions, and negative effects caused by absorption of tannins and tannin metabolites (Selle et al., 2010). In the perspective of animal nutrition, the effects of tannins may vary depending on the type, age,

physiological state of the animal, the content of the feed consumed, the tannin content, and structure of the plant (Ünver et al., 2014).

Sorghum tannins have also been reported to have beneficial effects. These are the fact that tannins are a good source of antioxidants (Naveena et al., 2008), and that they gain antibacterial properties by forming compounds with metal ions (Kaya and Yalçın, 1999; Hatano et al., 2005; Aydın and Üstün, 2007). It has been stated that it may result in a decrease in the number of people (Min and Hart, 2003).

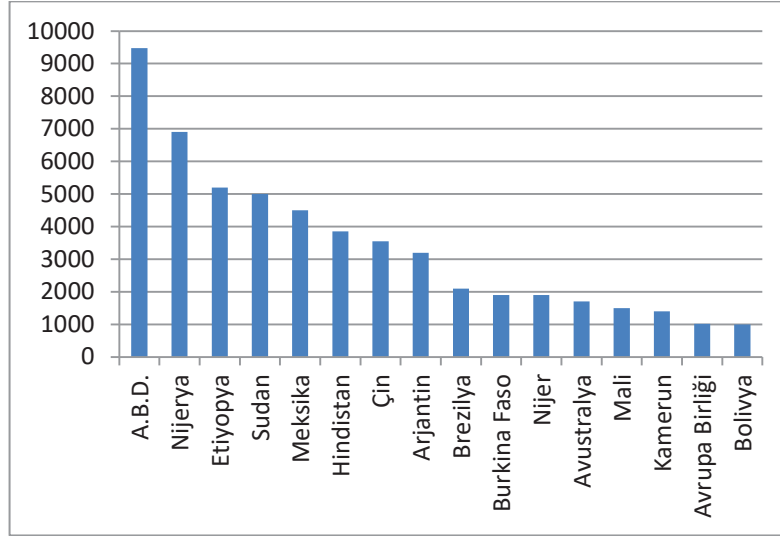
There are various methods to reduce the negative effects of tannins. These methods are mainly physical and chemical applications. While the physical methods are autoclaving, cooking, dehulling and soaking, the chemical methods are the use of wood ash, the addition of tallow, the addition of enzymes, the use of some tannin binding agents, germination, the use of alkali, and the application of urea. In the selection of the method to be used, the efficiency and cost of reducing tannin play a decisive role. Among the mentioned methods, it is also stated that enzyme addition, although not the most economical, gives better results than processing methods such as soaking and dehulling, and it is the most effective method. In various studies, it has been reported that the treatment of sorghum with both polyphenol oxidase and phytase enzymes caused a significant reduction in tannins. It has been revealed that the effectiveness of soaking, which is a cheap and old method, increases only if it is applied for a long time and at high temperatures. It is stated in the sources that the dehulling process is also an effective method. In addition to these methods, it is reported that extrusion and germination also have a reducing effect on tannins (Medugu ve ark., 2012; Iqbal ve ark., 2017; Hassan ve ark., 2020). With the effective use of these methods and the selection of suitable varieties, it will be possible to use sorghum grain in poultry feeds.

Keywords: Sorghum, tannin, poultry nutrition

Dane Sorgumun Kanatlı Beslemede Kullanımı

1. GİRİŞ

Sorghum (*Sorghum bicolor* L. Moench.), insan ve hayvan beslenmesi bakımından çeltik, arpa, buğday ve mısırın ardından gelen önemli bir tahıldır (Taylor, 2004). Tropikal ve subtropikal bölgelerde yaygın olarak yetiştirilen sorgum bitkisi, Kuzey Afrika kökenlidir (Smith ve Frederiksen, 2000). Suyun kısıtlı olduğu bölgelerde, mısıra alternatif olabilecek sorgumun hastalık ve zararlılara karşı dayanıklılığının yüksek olduğu bildirilmiştir (Klocke ve ark., 2014). Dünyada Amerika, Hindistan ve Afrika ülkelerinde fazla miktarda üretilmekte; insan gıdası, hayvan yemi ve endüstride de biyoyakıt olarak değerlendirilmesiyle önemli bir bitkidir (Meral ve Saydan Kanberoğlu, 2012). Dünya üretimi incelendiğinde Amerika Birleşik Devletleri Tarım Bakanlığı verilerine göre (USDA), Dünya sorgum üretiminin 2020/2021 döneminde 61,62 milyon metrik ton olacağı tahmin edilmektedir. Grafik 1’ de bir milyon metrik tonun üzerinde olan ülkeler görülmektedir (Worldagriculturalproduction, 2021).



Grafik 1. Ükelere Göre Sorgum Üretimi (Bir milyon metrik tonun üzerinde olan ülkeler worldagriculturalproduction.com (2021) 'a göre hazırlanmıştır (X1000)

2. Sorgumun Besin Madde İçeriği

Sorgumun içerdiği metabolize olabilir enerji (ME) içeriğinin 3250 kcal/kg; Ham protein (HP) içeriğinin ise %9,3; Ham kül %1,9; Ham Selüloz %2,4; Ham yağ içeriğinin %2,9 olduğu belirtilmiştir (Mohamed ve ark., 2015; Anonim, 2021; Şekil 1). Etlik piliçlerin günlük metabolize olabilir enerji ihtiyacını karşılamak için buğdaya dayalı ve sorguma dayalı olarak hazırlanan rasyonların benzer özelliklere sahip olduğu belirtilmiştir (Black ve ark., 2005). Rasyonlarda kullanıldığında, esansiyel aminoasitlerden lizin bakımından desteklenmesi gerektiği bildirilmiştir (Selle ve ark., 2010). Sorgumun içerdiği protein oranı arttıkça, lösin, izölösün, valin, aspartik asit ve glutamik asit içeriklerinin de arttığı saptanmıştır (Douglas ve ark., 1990).

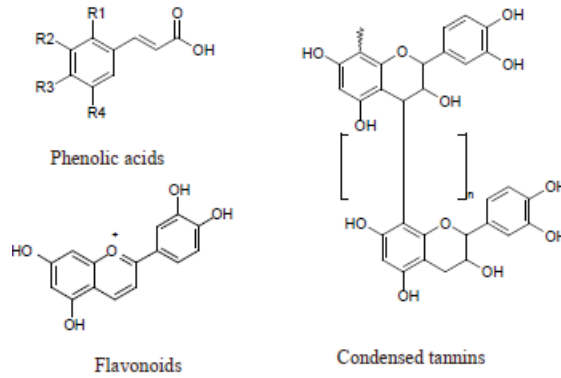


Şekil 1. Hasat dönemindeki sorgumun görünümü

2.1. Sorgumda bulunan anti-besleme faktörleri

Sorgumun içerdiği temel anti-besleme faktörü olarak tanenler saptanmıştır (Mohamed ve ark., 2015). Tanenler, bitkide doğal olarak bulunan savunma mekanizmalarıdır ve fenolik yapıdadırlar. Total fenol analizleri ile fenolik asitler, flavanoidler (antosiyeninler, flavonlar, flavonoller gb.) kondanse tanenler ve tirozin saptanmaktadır (Rooney ve ark., 2021; Şekil 2). Hayvan besleme açısından ise tanenlerin etkileri; bitkinin tanen içeriğine ve yapısına, hayvanın türüne, yaşına,

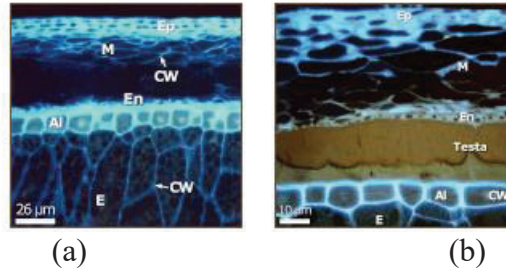
fizyolojik durumuna tükettiği yemin içeriğine bağlı olarak değişebilmektedir. Tanenler; kondanse (proantosiyanidinler) ve hidrolize olabilen tanenler olarak ikiye ayrılmaktadır (Ünver ve ark., 2014). Hidrolize olabilen tanenler çekirdek merkezi olarak poliol (genellikle D-glukoz) içeren moleküllerdir. Bu poliollerin hidroksi grupları kısmen veya tümüyle gallik asit veya elajik asit gibi fenolik gruplarla esterleşmiştir (Kanberoğlu, 2006). Kondanse tanenlerin hidrolize olabilen tanenlerden en önemli farkı, şeker içeren bir kısma sahip olmamalarıdır (Albertse, 2002). Karaciğerin hidrolize olabilen tanenlerin oluşturduğu metabolitleri ve fenolleri detoksifiye etmede yetersiz kalması sonucunda, toksik etki görülmektedir (Aydın ve Üstün, 2007; Üstün ve Aydın, 2007).



Şekil 2. Fenolik bileşiklerin yapıları (Rooney ve ark., 2021)

Tanenlerin, ruminantlarla karşılaştırıldığında tek midelilerde daha fazla olumsuz etkilerle karşılaşılmasına sebep olduğu bildirilmektedir (Yalçın, 2013). Etlik piliç rasyonlarında yüksek tanen içerikli sorgum kullanılması canlı ağırlık, yem tüketimi ve büyümede gerilemeye neden olmaktadır. Bu nedenle kanatlı hayvanlarının beslenmesinde tanen içeriği düşük sorgum çeşitleri kullanılması önerilmiştir (Şenköylü, 1985). Tanen içeriği %0,75 ve %1,5 arasında yem ile beslenen genç piliçlerin canlı ağırlığında %16 ve %41 oranında azalma meydana geldiği bildirilmiştir (Kubena ve ark., 2001). Yumurta tavuklarının yemlerinin %1 den fazla tanen içermesinin yumurta verimini olumsuz etkilediğini (Ünver ve ark., 2014), %5 ve üzerindeki tanen içeriğinin ise ölümlere neden olduğu bildirilmiştir (Kaya ve Yavuz, 1993; Yavuz ve ark., 1997).

Sorgum danesinin testa ve perikarp katmanlarında tanenler bulunmaktadır, ve testa kısmında B₁ B₂ genlerinin varlığı ile tanenlerin varlığı arasında önemli bir ilişki bulunduğu bildirilmiştir (Şekil 3; Selle ve ark, 2010; Rooney ve ark., 2021). Hidrolize olabilen tanenlerden farklı olarak, kondanse tanenlerin toksik etki göstermedikleri bildirilmiştir (Kamalak, 2007). Bazı sorgum çeşitlerinin danelerinde %2 veya daha fazla kondanse tanen olduğu (Butler ve ark., 1983), kırmızı sorgum çeşitlerinde %6 ile %8 arasında değiştiği bildirilmiştir. (Kumar ve ark., 2007). Kondanse tanen içeriği sebebiyle büyümede gerileme, yem tüketiminde düşme, sindirimi güç olan tanen-protein komplekslerinin oluşumu, sindirim enzimlerinin inhibisyonu, endojen protein üretiminin artması, sindirim kanalı fonksiyonları üzerine olumsuz etkileri, tanenlerin ve tanen metabolitlerinin emilmesinin sebep olduğu toksik etkiler sebebiyle tüketen kanatlı hayvanlarda olumsuz etkiler görüldüğü belirtilmiştir (Selle ve ark., 2010).



Şekil 3. Sorgum tanesinin florasan fotomikrograf ile alınan görüntüleri (Ep- epikarp; M- meskarp; CW- Hücre duvarı; En- endokarp; Al- Alevron; E- endosperm hücresi); a) Tanen içermeyen, b) Tanen içeren (renklenmiş testa) (Rooney ve ark., 2021)

Sorgum tanenlerinin çok iyi bir antioksidan kaynağı olduğu bildirilmiştir (Rooney ve ark., 2021; Çizelge 1). Yüksek tanen içeren yemlerle beslemenin sentetik antioksidan butilen hidroksi toluen'e (BHT) göre piliç etinde oksidatif bozulmaya karşı daha uzun süreli koruma sağladığı belirtilmiştir (Naveena ve ark., 2008).

Çizelge 1. Antioksidan aktivite düzeyleri (Rooney ve ark., 2021).

Farklı bitkisel kaynaklar	Antioksidan aktivitesi (KM'de)
Sorgum kepeği taneni	2400-3100
Yaban mersini	87-870
Çilek	356-400
Kırmızı Erik	452-600
Üzüm	100
Portakal	80-150
Karpuz	15

Tanenler metal iyonları ile bileşik oluşturarak antibakteriyel özellik kazanmaktadır (Kaya ve Yalçın, 1999). Demir ile kompleks oluşturan tannik asit, birçok mikroorganizmanın gelişimini engellemektedir (Hatano ve ark., 2005; Aydın ve Üstün, 2007). Kondanse tanen içeren yemlerin tüketimiyle bağırsaklardaki patojenlerin sayısının azalabileceği belirtilmiştir (Min ve Hart, 2003).

2.2. Tanenlerin olumsuz etkilerinin azaltılmasına yönelik uygulamalar

Tanenlerin olumsuz etkilerini azaltmak için çeşitli yöntemler bulunmaktadır. Bu yöntemler esas olarak fiziksel ve kimyasal uygulamalardır. Fiziksel yöntemler; otoklavlama, pişirme, kabukların ayrılması ve ıslatma iken, kimyasal yöntemler ise odun külü kullanımı, donyağı ilavesi, enzimlerin ilavesi, tanen bağlayıcı bazı ajanların kullanımı, çimlendirme, alkali kullanımı ve üre uygulamasıdır. Kullanılacak yöntemin seçiminde ise, tanen azaltmadaki etkinlikleri ve maliyetleri belirleyici rol oynamaktadır.

Lentinus edodes mantarının yumurtacı tavuklara sorgum daneleriyle fermente edilerek verilmesiyle yüksek yumurta verimi sağlanmış (Willis ve ark., 2009), etlik piliçlerde Lentinus edodes ile ilgili yürütülen farklı bir çalışmada ise Salmonella spp. sayısında azalma görülmüştür (Willis ve ark., 2010). Proantosiyanidinli (PA) sorgum diyetleriyle beslenen etlik piliçlere sindirim enzimi eklenmesinin tavukların düşük performansını yükseltmek için katkıda bulunduğu gözlenmiştir (Nyamambi ve ark., 2000). Proantosiyanidinlerin, antimikrobiyal, antiinflamatuvar (iltihap önleyici), antialerjik, antioksidan, antikansorejen, kalp hastalıkları, eklem iltihabı ve cilt yaşlanmalarını önleyici etkileri olduğu bildirilmiştir (Ağma Okur, 2010; Gönültaş ve Balaban Uçar, 2012).

Sorgum (*Sorghum vulgare* L.) taneleri 2, 4 ve 6. günlerde oda sıcaklığında çimlendirildiğinde, protein içeriğinin arttığı, tanen miktarının 6. günde belirgin şekilde azaldığı ve lizin içeriğinde %30'dan fazla artış olduğu gözlenmiştir. Sorgumun çimlendirilmesiyle kanatlı rasyonunda sentetik lizin ilavesinin azaltılabildiği bildirilmiştir (Okoh ve ark., 1989). Sorgumla beslenen etlik piliçlerde NaHCO_3 ilavesinin taneni azalttığı ve tavukların büyümesine katkı sağladığı saptanmıştır (Banda-Nyirenda ve Vohra, 1990). Daha ince partikül büyüklüğüne oranla, iri öğütülmüş sorgum ile beslenen piliçlerde ağırlık artışının daha yüksek olduğu belirtilmiştir (Nir ve ark. 1990). Sorgumda tanen azaltmak için kullanılan diğer yöntemler ise, alkali ile muamele (Iqbal ve ark., 2017), ıslatma (Kyarisiima ve ark., 2004) ve ekstrüzyondur (Singh ve ark., 2017).

Bahsedilen yöntemler arasında enzim ilavesinin, en ekonomik olmamakla birlikte, ıslatma, kabuktan ayırma gibi işleme yöntemlerine göre daha iyi sonuçlar verdiği ve en etkili yöntem olduğu da ifade edilmektedir. Çeşitli araştırmalarda, sorgumun hem polifenoloksidaz hem de fitaz enzimleri ile muamele edilmesinin tanenlerde önemli derecede bir azalmaya sebep olduğu belirtilmiştir. Ucuz ve eski bir yöntem olan ıslatmanın etkinliğinin ise, ancak uzun süreli ve yüksek sıcaklıkta uygulanması halinde arttığı ortaya konmuştur. Kabuk ayırma işleminin de etkili bir yöntem olduğu kaynaklarda ifade edilmiştir. Bu yöntemlere ilave olarak ekstrüzyonun ve çimlendirmenin de tanenleri azaltıcı etkisi olduğu bildirilmektedir (Medugu ve ark., 2012; Hassan ve ark., 2020).

3. Rasyona Sorgum İçeriğinin, Etlik Piliçler Üzerindeki Etkileri

3.1. Performans üzerine etkisi

Etlik piliçler ile ilgili çalışmalarda, mısır yerine başlangıç rasyonlarında %45, bitirme yemlerinde %60 oranında sorgum kullanımının canlı ağırlık, yemden yararlanma, ölüm oranı ve karkas ağırlığında önemli bir değişikliğe neden olmadığı (Hulan ve Proudfoot, 1982) Başka bir çalışmada sorgumun %45'e kadar mısırla değiştirilmesinin biyolojik olarak daha iyi olduğu ve piliç performansı üzerinde olumsuz bir etkisi olmadığı bildirilmiştir (Abdo ve ark., 2015). Enerji kaynağı olarak mısır yerine sorgumun katılmasının, hindilerin ve kesim-karkas özelliklerinde ve besi performansında önemli bir değişikliğe neden olmadığı için, mısırdan daha uygun fiyat döneminde bir kısmı ya da tamamı yerine sorgumun katılabileceği belirtilmiştir (Dosay ve Ak, 1996). Yumurtacı tavukların rasyonunda kullanılan mısırın (kontrol) yerine katılan farklı oranlardaki (%30, %40 ve %50) sorgumla (*Sorghum vulgare*, %0,67 tanen) yürütülen çalışmada, rasyona %30 katılan sorgum gurubunda toplam serum protein değeri, serum albumin seviyesi, kolesterol seviyesi ve kalsiyum seviyesi yüksek bulunurken, lipoprotein (LDL) seviyesi en düşük bulunmuştur. Sonuç olarak, sorgumun yumurtacı tavuk rasyonlarında antioksidan etkisiyle lipid peroksidasyonu düşürdüğü ve serum parametrelerini olumlu etkilediği belirlenmiştir (İmlik ve ark., 2009).

3.2. Ürün kalitesi üzerine etkisi

Ochieng ve ark. (2020), düşük tanen (yaklaşık %5) içeriğine sahip sorgumun rasyonlara ilave edilme düzeylerine göre et kalitesi üzerine olan etkilerini araştırmışlar, çalışmalarında kontrol rasyonu %55 mısır içermektedir. Muamelelerde ise rasyondaki mısırın %20, %40, %60 ve %100'ü yerine sorgum kullanılmıştır. Göğüs etinin kolesterol içeriği, sorgum düzeyinin rasyonda artmasıyla önemli düzeyde düşmüştür. But etinde ise rasyonun sorgum içeriğinin %22, 33 ve 44 olduğu gruplarda düşmüş, %0, 11 ve 55 sorgum içeren gruplarda ise istatistiki olarak yüksek bulunmuştur.

Aynı çalışmada Vitamin A ve E içerikleri saptanmış ve göğüs etinde her iki vitamin için de muameleler arası bir farklılık gözlenmemiştir. But etinde ise A vitamininde bir farklılık görülmezken, E vitamin değerleri % 33, 44 ve 55 sorgum içeren rasyonu tüketen hayvanlarda en düşük olarak saptanmıştır (Ochieng ve ark., 2020).

4. Sonuç ve Öneriler

Sorgumun hayvanların enerji ihtiyacını karşılamak için mısırın yerine kullanılabileceğini bildiren çalışmalar olduğu görülmüştür. Örneğin; Mohamed ve ark. (2015), etlik piliç rasyonlarına %0, 6, 12, 18 sorgum ilave edip, performans parametrelerine olan etkilerini incelemiş ve sorgumun %18 e kadar performansı olumsuz etkilemeden kullanılabileceğini belirtmişlerdir. Ochieng ve ark. (2020) ise çalışmalarında, düşük tanen içeren sorgumun etlik piliç rasyonlarında %33 ten daha yüksek oranda yer almaması gerektiğini bildirmişlerdir. Tanin düzeyini azaltmak için uygulanan yöntemlerin etkin kullanımı ve uygun çeşit seçimiyle, sorgum tanesinin kanatlı yemlerinde kullanımı mümkün olabilecektir.

KAYNAKLAR

- [1]. A. Ağma Okur, "Etlik Piliçlerde Yemlere Aromatik Yağlar ve Vitamin E İlavesinin Bağırsak Mikrobiyolojisi ve Oksidatif Stabilité Üzerine Etkileri," Namık Kemal Üniversitesi Fen Bilimleri Enstitüsü, Doktora Tezi, s. 99, Tekirdağ, 2010.
- [2]. A. Kamalak, "Kondanse tanenin olumsuz etkilerini azaltmak için kullanılan katkı maddeleri ve yemlere uygulanan işlemler," Kahramanmaraş Sütçü İmam Üniv. Fen ve Mühendislik Dergisi, 10: 144-150, 2007.
- [3]. A. Mohamed, M. Urge, and K. Gebeyew, "Effects of replacing maize with sorghum on growth and feed efficiency of commercial broiler chicken," Journal of Veterinary Science and Technology, 6 (3): 224, 2015.
- [4]. Anonim, "Sorghum," <https://www.feedtables.com/content/sorghum> (Access date: 27.10.2021), 2021.
- [5]. A. Singh, S. Gupta, R. Kaur, and H. R. Gupta, "Process optimization for anti-nutrient minimization of millets," Asian Journal of Dairy and Food Research, 36: 322-326, 2017.
- [6]. B. A. Ochieng, W. O. Owino, J. N. Kinyuru, J. N. Mburu, and M. G. Gicheha, "Effect of Low Tannin Sorghum Based feeds on broiler meat nutritional quality," Journal of Agriculture and Food Research, 2, 2020.
- [7]. B. Kanberoğlu, "Zeytin Karasuyunun Biyolojik Yolla İyileştirilmesinde Tannaz Enziminin Etkisi," Yüksek Lisans Tezi, Ege Üniversitesi, Fen Bilimler Enstitüsü, Biyomühendislik Anabilim Dalı, s. 277, İzmir, 2006.
- [8]. B. M. Naveena, A. R. Şen, S. Vaithyanathan, Y. Babji, and N. Kondaiah, "Comparative efficacy of pomegranate juice, pomegranate rind powder and BHT in cooked chicken patties," Meat Science, 80 (4):1304-308, 2008.
- [9]. B. Nyamambi, L. R. Ndlovu, J. S. Read, and J. D. Reed, "The effects of sorghum proanthocyanidins on digestive enzyme activity in vitro and in the digestive tract of chicken," Journal of the Science of Food and Agriculture, 80 (15): 2223-2231, 2000
- [10]. B. R. Min, T. N. Barry, G. T. Attwood, and W. C. McNabb, "The effect of condensed tannins on the nutrition and health of ruminants fed fresh temperate forages: A review," Animal Feed Science and Technology, 106 (3): 3-19, 2013.
- [11]. C. C. Kyarisiima, M. W. Okot, and B. Svihus, "Use of wood ash in the treatment of high tannin sorghum for poultry feeding," S. Afr. J. Anim. Sci. 34: 110-115, 2004.
- [12]. C. I. Medugu, B. Saleh, J. U. Igwebuike, and R. L. Ndirmbita, "Strategies to improve the utilization of tannin-rich feed materials by poultry," International Journal of Poultry Science, 11 (6): 417-423, 2012.
- [13]. C. W. Smith, and R.A. Frederiksen, "Sorghum: Origin, History, Technology and Production," New York, NY: John Wiley and Sons, p.824, 2000.

- [14]. D. B. Banda-Nyirenda, and P. Vohra, "Nutritional improvement of tannin-containing sorghums (*Sorghum bicolor*) by sodium bicarbonate," *Cereal Chemistry*, 67 (6): 533-537, 1990.
- [15]. E. H. Albertse, "Cloning, Expression and Characterization of Tannase from *Aspergillus* Species," PhD Thesis. University of the Free State, p.122, South Africa, 2002.
- [16]. E. Ünver, A. A. Okur, E. Tahtabiçen, B. Kara, and H. E. Şamlı, "Tannins and their impacts on animal nutrition," *Turkish Journal of Agriculture-Food Science and Technology*, 2 (6): 263-267, 2014.
- [17]. F. Üstün, and S. A. Aydın, "Tanenler 2, Toksisiteleri, beslenme üzerine etkileri, detannifikasyon," *İstanbul Üniv. Vet. Fak. Derg.* 33: 33-41, 2007.
- [18]. H. İmİK, A. K. Yıldırım, H. Polat, and R. Gümüş, "Yumurta tavuklarında rasyona farklı oranlarda katılan sorgumun (*Sorghum vulgare*) serum glikoz, lipid protein, glutatyon peroksidaz ve malondialdehit üzerine etkisi," *Kafkas Üniversitesi Veteriner Fakültesi Dergisi*, 15 (3): 417-422, 2009.
- [19]. H. W. Hulan, F. G. Proudfoot, "Nutritive value of sorghum grain for broiler chickens," *Can. J. Anim. Sci.*, 62: 869-875, 1982.
- [20]. H. Yavuz, F. Akar, M. Kerman, Y. Şanlı, E. Yarsan, A. Filazi, "Türkiye'de üretilen veya ithal edilen yem ve yem ham maddelerinin hayvan sağlığı ve verimliliği yönünden önem taşıyan nitrat-nitrit, tannik asit ve siyanür içerikleri üzerine araştırmalar," *Etlik Veterinerlik Mikrobiyoloji Dergisi*, 9 (1): 57-88, 1997.
- [21]. İ. Kaya, and S. Yalçın, "Baklagil tane yemleri ve ruminant rasyonlarında kullanımı," *Lalahan Hayvancılık Araştırma Enstitüsü Dergisi*, 39(1): 101-114, 1999.
- [22]. I. Nir, J. P. Melcion, and M. Picard, "Effect of particle size of sorghum grains on feed intake and performance of young broilers," *Poultry Science*, 69 (12): 2177-2184, 1990.
- [23]. J. H. Douglas, T. W. Sullivan, P. L. Bond, and F. J. Struwe, "Nutrient composition and metabolizable energy values of selected grain sorghum varieties and yellow corn," *Poultry Science*, 69 (7): 1147-1155, 1990.
- [24]. J. L. Black, R. J. Hughes, S. G. Nielsen, A. M. Tredrea, R. MacAlpine, and R. J. Van Barneveld, "The energy value of cereal grains, particularly wheat and sorghum, for poultry," *Proceedings of the Australian Poultry Science Symposium*, 17: 21-29, 2005.
- [25]. J. R. N. Taylor, "Africa, Overview: Importance of Sorghum in Africa," Department of Food Science, University of Pretoria, Pretoria 0002, South Africa, Tegemeo Institute of Agricultural Policy and Development, 2004.
- [26]. L. F. Kubena, J. A. Byrd, C. R. Young, and D. E. Corrier, "Effects of tannic acid on cecal volatile fatty acids and susceptibility to *Salmonella typhimurium* colonization in broiler chicks," *Poultry Science*, 80 (9): 1293-1298, 2001.
- [27]. L. G. Butler, D. J. Riedl, D. G. Lebryk, and H. J. Blytt, "Interaction of proteins with sorghum tannin: mechanism, specificity and significance," *Journal of the American Oil Chemists' Society*, 61 (5): 916-920, 1984.
- [28]. L. Rooney, C. McDonough, and L. Dykes, "Myths about sorghum tannins," <http://crsps.net/wp-content/downloads/INTSORMIL/Inventoried%209.6/3-0000-8-680.pdf> (Access date: 20.10.2021)
- [29]. M. Abdo, U. Mengistu, and G. Kefyalew, "Effects of replacing maize with sorghum on growth and feed efficiency of commercial broiler chicken. *Journal of Veterinary Science and Technology*, 6(3), 2015.
- [30]. M. Dosay, and İ. Ak, "Hindi besi rasyonlarında mısır yerine sorgumun enerji kaynağı olarak kullanılması olanakları," *Uludağ Üniversitesi Ziraat Fakültesi Dergisi*, sa.12, ss.1-9, 1998.

- [31]. M.A. Iqbal, S. Naveed, T.N. Pasha, R. Naseer, A. Mahmud, A. Rahman, and Y.A. Ditta, "Effect of different treatments on tannin contents of sorghum grain cultivars," *Pakistan Journal of Science*, 69(1), 17, 2017.
- [32]. N. L. Klocke, R. S. Currie, I. Kisekka, and L. R. Stone, "Corn and Grain Sorghum Response to Limited Irrigation, Drought, and Hail," *Applied Engineering in Agriculture*, 30(6): 915-924, 2014.
- [33]. N. Şenköylü, "Tanninler ve Sorgumun Kanatlı Hayvanların Beslenmesindeki Yeri," *Yem Sanayii Dergisi*, Sayı: 46, s. 13-17, Ankara, 1985.
- [34]. O. Gönültaş, and M. Balaban Uçar, "Fıstıkçamı (*Pinus pinea*) kabuğunun tanen bileşimi," *Kahramanmaraş Sütçü İmam Üniv. Doğa Bil. Der. Özel Sayı*, s. 80-84, 2012
- [35]. P. H. Selle, D. J. Cadogan, X. Li, and W. L. Byrden, "Implications of sorghum in broiler chicken nutrition," *Animal Feed Science and Technology*, 156 (3-4): 57-74, 2010.
- [36]. P. N. Okoh, R. P. Kubiczek, P. C. Njoku, and G. T. Iyeghe, "Some compositional changes in malted sorghum (*Sorghum vulgare*) grain and its value in broiler chicken diet," *Journal of the Science of Food and Agriculture*, 49 (3): 271-279, 1989.
- [37]. R. Meral., and G. Saydan Kanberoğlu, "Tahıllardan Etanol Üretimi," *Iğdır Üni. Fen Bilimleri Enst. Der.*, 2 (3): 61-68, 2012.
- [38]. S. A. Aydın, and F. Üstün, "Tanenler I kimyasal yapıları, farmakolojik etkileri, analiz yöntemleri," *İstanbul Üniversitesi Veteriner Fakültesi Dergisi*, 33 (1): 21- 31, 2007.
- [39]. S. Kaya, and H. Yavuz, "Yem ve yem hammaddelerinde bulunan olumsuzluk faktörleri ve hayvanlara yönelik etkileri. 1: Organik nitelikli olumsuzluk faktörleri," *Ankara Veteriner Fakültesi Dergisi*, 40 (4): 586-614, 1993.
- [40]. S. Yalçın, "Yemlerde Antinutrisyonel Faktörler, Yemler ve Yem Hijyeni ve Teknolojisi," *Genişletilmiş 5. Baskı*, s.261- 286, Ankara Üniv., Veteriner Fakültesi, Ankara, 2013.
- [41]. T. Hatano, M. Kusudo, K. Inada, T. Ogawa, S. Shiota, T. Tsuchiya, and T. Yoshida, "Effects of tannins and related polyphenols on methicillin-resistant *Staphylococcus aureus*," *Phytochemistry*, 66 (17): 2047-2055, 2005.
- [42]. V. Kumar, A. V. Elangovan, A. B. Mandal, P. K. Tyagi, S. K. Bhanja, and B. B. Dash, "Effects of feeding raw or reconstituted high tannin red sorghum on nutrient utilisation and certain welfare parameters of broiler chickens," *British Poultry Science*, 48 (2): 198-20, 2007.
- [43]. W. L. Willis, O. S. Isikhuemhen, J. W. Allen, A. Byers, K. King, and C. Thomas, "Utilizing fungus myceliated grain for molt induction and performance in commercial laying hens," *Poultry Science*, 88 (10): 2026-2032, 2009.
- [44]. W. L. Willis, O. S. Isikhuemhen, S. İbrahim, K. King, R. Minor, and E. I. Ohimain, "Effect of dietary fungus myceliated grain on broiler performance and enteric colonization with *Bifidobacteria* and *Salmonella*," *International Journal of Poultry Science*, 9 (1): 48-52, 2010.
- [45]. Worldagriculturalproduction, "Sorghum productions," <http://www.worldagriculturalproduction.com/crops/sorghum.aspx> (Access date: 21.10.2021).
- [46]. Z. M. Hassan, T. G. Manyelo, L. Selaledi, and M. Mabelebele, "The effects of tannins in monogastric animals with special reference to alternative feed ingredients," *Molecules*, 25, 4680, 2020.

FREQUENCY-BASED AGRI-IOT TECHNIQUES IN AGRICULTURE

DEEPA SONAL

Department of Computer Science, V.K.S. University, Arrah-802301, India,

SHAILESH KUMAR SHRIVASTAVA

Scientist-F & Head, DGRC, NIC, STPI Campus, Patna-800013, India

BINAY KUMAR MISHRA

Director, Department of Computer Science, V.K.S. University, Arrah-802301, India,

Abstract

With the ongoing growth of the Internet of Things (IoT), multiple large-scale IoT platforms can now analyze a high proportion of sensor data streams. These IoT frameworks are used to gather, process, and analyze data streams in real-time, making it easier to deliver smart solutions for decision-making. Current IoT-based solutions are primarily domain-specific, delivering stream processing and analytics for a narrow range of applications (smart cities, healthcare etc.). In this paper, we are proposing an Agri-IoT based model for continuous guarding of the agriculture field in order to protect the crops from being destructed by animal-raiding. These animal- attacks mostly happen in some specific months of the year. So a proper guarding system of the agricultural areas can be done using frequency based IoT techniques. In this research paper, a crop protection system of the field has been proposed using Agri-IoT Techniques.

Keywords: Agri-IoT, Crop protection, Agriculture, IoT, Field Guarding, Animal attacks

EFFECT OF DIFFERENT HUMIC ACID DOSES ON GEMLIK OLIVE SAPLINGS IN MANISA KÖPRÜBAŞI DISTRICT

Ayça AKÇA UÇKUN
0000-0002-5592-496X

Suna BAŞER
Olive Research Institute

Ünal KAYA
Olive Research Institute

Alptug ÇANTAL
Argem Agricultural Engineering LTD.ŞTİ.

Merve TÜRKYILMAZ
Argem Agricultural Engineering LTD.ŞTİ.

Abstract

In this study, the effects of different Humic acid doses on Gemlik olive saplings and shoot length and internode values were investigated. The research was carried out on 3-year-old olive saplings planted in a terrace in the Köprübaşı district of Manisa. The study consisted of the application of 4 different doses of humic acid (0, 250, 500, 750 mg kg⁻¹) to three-year-old olive saplings. Humic acid applications were applied for 2 years in 2020 and 2021, 1 week before the full flowering date. As a result of the research, shoot length and internode values of 250 ppm doses were found to be statistically significant ($p < 0.005$). As a result, positive effects of Humic acid applications on olive saplings were observed.

Keywords: Humic Acid, olive sapling, shoot length, internode

1. INTRODUCTION

Olea europaea L is known as one of the most important plants and common products of the Mediterranean basin, which is long-lived and easily adaptable to climatic conditions. Olive fruits are also commercially evaluated for their oil content or edible flesh. When the studies are examined, it is revealed that the yield of olive trees is generally at a low level due to poor soil fertility and low water holding capacity. As a result of these studies, it has been suggested that olive trees need organic fertilizer and that the organic matter content of the soil should increase (Fayed 2010).

According to Tatini et al. (1991) showed that humic acid substances increase the dry matter of leaves and roots, promote N uptake and nutrient accumulation, and increase the photosynthesis of trees. Due to the positive effect of humic substances on the visible growth of plants, these chemicals are used by growers as pesticides, etc. It is widely used instead of other substances such as inclusion of organic residues in the soil improves soil structure. Agricultural products obtained from organic agriculture are very important for human health. Humic acids are complex heterogeneous mixtures. For this reason, when the studies were examined, it was seen that organic residues did not cause significant increases in olive mineral and leaf concentrations in the first year, but turned into beneficial over time.

In a study, it was reported that the N and K content in the leaf in the vegetative development and flowering of "Picual" olive trees increased significantly with the application of organic fertilization (poultry manure), but no significant difference was observed in the leaf P content in both seasons. In another study, it was revealed that the application of leonardite extracts (extracted humic substances) to the leaves under field conditions stimulated shoot growth and promoted the accumulation of K, B, Mg, Ca and Fe in the leaves. Humic acids are called the main fractions of humic substances and the most active components of soil and compost organic matter. Humic acids have been shown to stimulate plant growth and have positive effects such as cellular respiration, photosynthesis, protein synthesis, water and nutrient uptake (Vaughan and Malcolm, 1985). In another study, it was determined that humic acids have a dose-dependent effect and are especially effective in the low concentration range (Chen and Aviad, 1990).

As a result of studies, optimal concentrations that can affect and stimulate plant growth were generally found in the range of 50-300 mg/L-1, but positive effects were also obtained at lower concentrations (Chen et al., 2004). Humic acids have indirect and direct effects on plant growth. Considering the indirect effects of humic acid, enrichment of soil nutrients, increase of microbial population, higher action exchange capacity, improvement of soil structure; When the direct effects are examined, they are described as various biochemical events in the cell wall, membrane or cytoplasm (Varanini and Pinton, 2001).

Humic substances are the main components of soil organic matter (65-70%) that help increase cell membrane permeability, respiration, photosynthesis, oxygen and phosphorus uptake, and stem cell growth (Cacco and Dell Agnolla, 1984). Humic acids can also be characterized as complex substances derived from the decomposition of organic substances. Agricultural humic acids are known to increase nutrient uptake, drought tolerance, seed germination and overall plant performance (Chen and Aviad, 1990). Benefits associated with the use of humic acid in alkaline soils with low organic matter include increased nutrient uptake, tolerance to drought and temperature extremes, and activity of beneficial soil microorganisms (Russo and Berlyn, 1990).

Studies on the effects of humic acids on plant growth have generally been conducted in controlled environments, for example on hydroponically grown herbaceous species or certain

substrates (Malik and Azam, 1985). In a study by Ferrara and Brunetti, 2010., it was revealed that humic acid applications (foliar applications) significantly increased the yield (kg/tree), fruit quality and chemical properties of "Aggizi" olive trees. It was observed that humic acid applied to olive trees, especially during the full flowering period, significantly increased the width, length and weight of the fruits compared to the control application. In another study, it was determined that humic acid is especially beneficial in releasing nutrients from the soil, thus facilitating the uptake of nutrients (Kauser et al. 1985).

According to Tatini et al. (1991) reported that humic acid substances increase the dry matter of leaves and roots, support N uptake and nutrient accumulation, and increase photosynthesis. In another study, "Aggizi" was added to olive trees under drippers during full bloom and humic acid was sprayed on the tree as a foliar application. In the study, fruit yield (kg/tree), average fruit volume, weight, meat/seed ratio were measured and an increase was observed (Tatini, 1991).

2. MATERIAL AND METHOD

2.1. Working area

This study was carried out in the orchards of 3-4 years old Gemlik olive cultivars in the Köprübaşı district of Manisa province in two seasons, 2020 and 2021.

2.2. Study Material

Gemlik olive, which is the study material, is the most important black table olive variety of the Marmara Region. It is also known in the region with the synonyms of Trilye, Kaplık, Kıvırcık and Kara. The center of origin is the Gemlik district of Bursa province. The tree is medium vigorous and round-spreading. Due to the easy rooting of the cuttings, early yielding and low periodicity tendency, it has spread rapidly in all our olive growing regions in recent years. In recent years, most of the new facilities have been established with this variety. Gemlik olive has medium size fruit (270-280 pcs/kg, meat/seed ratio is 6:1 and oil ratio: 24%. Gemlik olive variety constitutes 50% of the total trade volume of the country and 80% of the Marmara Region yield. (Anonymous, 2007).

The study material was planted with terracing at the foot of the mountain at 5x2.5 meters intervals in the Köprübaşı district of Manisa. Olive trees were irrigated with drip irrigation method once a month in summer at regular intervals. As fertilization, only different doses of humic acid were tried.

Application time of different humic acid doses

Different humic acid applications were applied 1 week before full bloom (end of April-early May) in 2020 and 2021. The full flowering period was determined as the date when 80% of the flowers of the trees opened.

Table 1: Different humic acid doses

Trial	Humic Acid Doses
Control	none
Humic Acid	750 ml
Humic Acid	500 ml
Humic Acid	250 ml

Soil analysis was carried out at 0-30 cm and 0-60 cm levels in the experimental area in November 2020. According to the results of the soil analysis, the data of the olive orchard are given below.



Figure 1. Olive saplings in the study area

Table 2: Soil analysis results of the trial area

Parameters	Depth	
	0-30 cm	0-60 cm
İşba %	35	34
E. C.	0.06	0.04
Milimhos/cm		
pH	5.99	5.42
Lime	1.67	1.90
Organic Matter	1.53	1.32
N %	0.05	0.03
P ppm	8.30	6.45
K ppm	54.41	55.14
Ca ppm	409.66	402.79
Mg ppm	53.77	55.13
Fe ppm	33.14	28.05
Mn ppm	1.35	1.30
Zn ppm	0.21	0.18
Cu ppm	0.11	0.10
B ppm	1.19	1.19

Leaf samples were taken from the opposite pairs of leaves in the olive resting period in February in the experimental area.

Table 3. Leaf analysis results of the experimental area

Parameters	Results	Reference Values (Ülgen ve Ateşalp, 1972)
N %	1.78	1,4- 2
P %	0.19	0.08-0.2
K %	0.95	0.7-1.4
Ca %	1.18	1.4-2.5
Mg %	0.15	0.2-0.45
Fe ppm	124.25	7-200
Mn ppm	53.97	25-70
Zn ppm	14.61	15-30
Cu ppm	4.19	6-18
B ppm	15.99	11-23

When the leaf analysis results of the experimental area are examined, Magnesium (%), Zinc (ppm), values are low, Nitrogen %, Phosphorus %, Potassium %, Calcium %, Magnesium %, Iron ppm, Manganese ppm, Zinc ppm, Copper ppm, Bor ppm found to be sufficient (Table 3).

When the soil analysis results of the experimental area were examined, it was determined that the soil pH was moderately acidic, calcareous and soils with good organic matter content. According to the results of the analysis, nitrogen, phosphorus, potassium, magnesium, manganese and zinc contents were found to be low. When looking at the other values, calcium and iron contents are high, copper content is sufficient and boron content is medium (Table 2).

2.3. Measurements

Shoot Length: A total of 12 shoot lengths (by measuring shoot lengths in meters and cm) were taken in 1 tree in each replication and in three shoots from 4 directions of the selected tree, 1 measurement at the beginning and end of vegetation in the 1st and 2nd years.

Between Nodes: The distance between two nodes will be measured on the shoots to be selected for shoot length measurement and recorded in cm.

3. CONCLUSION AND DISCUSSION

The effect of different humic acid doses on shoot length and internodes in Manisa Köprübaşı district between 2020-2021 was investigated. As a result of the study, 250 ppm dose was found to be statistically significant at different humic acid doses applied before full bloom in 2020 compared to control applications ($p < 0.005$). Other important doses are 500 ppm and 750 ppm, respectively.

When the effect of different humic acid doses applied before full bloom in 2021 on olive saplings was examined, the effect of 250 ppm dose was found to be statistically significant ($p < 0.005$) (Table 4).

Table 4: Effect of different humic acid doses on shoot length (%)

Years	Humic Acid Doses			
	Control	250 ppm	500 ppm	750 ppm
2020	29.47 d	33.72 a	31.12 b	30.56 c
2021	34.47 c	36.12 a	35.47 b	34.50 cd

Each row is statistically significant ($p < 0.005$)

When the effects of different humic acid doses on Gemlik olive saplings were examined, the internode effects of 250 ppm humic acid doses were statistically significant ($p < 0.005$) compared to the control in both years (2020 and 2021) (Table 5).

Table 5: Effect of Different Humic Acid Doses on the internodes (%)

Years	Humic Acid Doses			
	Control	250 ppm	500 ppm	750 ppm
2020	2.04 d	2.10 a	2.08 b	2.06 c
2021	1.77 d	2.98 a	2.80 b	2.75 c

Each row is statistically significant ($p < 0.005$)

Çılgin (2019). In the study, 5 humic acids (0, 100, 200, 300, 400 mg kg⁻¹) and 2 N doses (0 and 100 mg kg⁻¹) were applied to three different olive cultivars. As a result of the study, it was observed that the olive varieties used gave different responses to the applications.

In this context, it was determined that doses of 100 mg kg⁻¹ in Ayvalık and Gemlik cultivars and 200 mg kg⁻¹ in Manzanilla cultivars were effective.

Eman et al. (2011) applied humic acid in different combinations with 0.5% and 1% humic acid as a single application or a mixture of 0.25% and 0.5% some microelements (Zn, Fe and Mn) in “Coratina” olive saplings by spraying the olive saplings. . In the results obtained, it was reported that spraying of humic acid increased leaf macro and micro element contents and vegetative growth of olive saplings, especially when combined with micro elements, compared to untreated plants (control).

Yousef et al. (2011) evaluated humic and amino acids, macro and trace elements in two consecutive seasons in 2008 and 2009 after spraying the “Chemlali” olive saplings individually and separately.

Shoot and root characteristics, leaf macro and trace elements were examined. The researchers determined that the application of (Humic acid + amino acids + macro elements + micro elements) was the most effective application compared to the other application, Due to these applications gave the best results in plant height, number of branches, number of leaves, and also with control of plant diameter and leaf area. On the other hand, they reported that this application increased root length and root weight compared to the control plant.

The findings of our study revealed parallel results with other studies. In the final result, the positive effect of humic acid applications on olive saplings was determined. It has been determined that humic acid is especially useful in releasing nutrients from the soil, thus facilitating the uptake of nutrients (Kausar et al. 1985).

REFERENCES

- [1].Anonymous, 2007, Adaptation of some important domestic and foreign varieties to our regions, National Olive and Olive Oil Symposium, 15-17 p.
- [2].Cacco, G. and G. Dell Agnolla, 1984. Plant growth regulator activity of soluble humic substances. *Can. J. Soil Sci.*, 64: 25-28.
- [3].Chen, Y, and T. Aviad, 1990. Effects of humic substances on plant growth. In: McCarthy P, Calpp CE, Malcolm RL. Bloom, Readings. ASA and SSSA, Madison, WI. pp: 161-186.
- [4].Chen, Y., M. De Nobile, T. Aviad, 2004. Stimulatory effects of humic substances on plant growth. In: Soil organic matter in sustainable agriculture (Magdoff F., Weil R.R., eds). CRC Press, NY, USA. pp: 103-129.
- [5].Çılgin, İ., 2019. Effects of Humic Acid Applications on Sapling Growth in Different Olive Varieties, Ege University, Master Thesis.
- [6].Fayed, T. A., 2010. Response of four olive cultivars to common organic manures in Libya *AmEuras.J.Agric.Envirion. Sci.*, 8(3): 275-291.
- [7].Ferrara, G. and G. Brunetti, 2010. Effects of the times of application of a soil humic acid on berry quality of table grape (*Vitis vinifera* L.) cv Italia Span *J. Agric. Res.*, 8(3): 1-6.
- [8].Eman A. Abd El-Gawad; Mohamed M.M. Kandiel; Amany A. Abbass and Adel A. Shaheen (2011): Effect of some endocrine disrupting chemicals on fish reproduction. Ph.D thesis (Fish Diseases and Management). Faculty of Veterinary Medicine, Benha University.
- [9].Kausar, A., F. Malik, Azam, 1985. Effect of humic acid on corn seedling growth. *Environmental and Experimental Botany*, 25: 245-252.

- [10]. Tattini, M., Bertoni, P., Landi, A. and Traversi, M.L., 1991, Effect of humic acids on growth and biomass portioning of container-grown olive plants, In II Symposium on Horticultural Substrates and Their Analysis, XXIII IHC 294:75-80 pp.
- [11]. Malik, K.A., F. Azam, 1985. Effect of humic acid on wheat (*Triticum aestivum* L.). *Environ Exp Bot* 25, 245- 252. Muscolo A., Cutrupi S., Nardi S., 1998. Iaa Detection In humic substances. *Soil Biol Biochem*, 30: 1199-1201.
- [12]. Russo, R.O. and G.P. Berlyn, 1990. The use of organic biostimulants to help low input sustainable agriculture. *J. Sustainable Agric.*, 1(2): 19-42.
- [13]. Vaughan, D. and Linehan, D.J., 1976, The growth of wheat plants in humic acid solutions under axenic conditions. *Plant and Soil*, 44:448-449 pp.
- [14]. Varanini, Z., R. Pinton, 2001. Direct versus indirect effects of soil humic substances on plant growth and nutrition. In: *The rhizosphere: biochemistry and organic substances at the soil plant interface* (Pinton R., Varanini Z., Nannipieri P., eds). Marcel Dekker Inc, NY, USA. pp: 141-157.
- [15]. Yousef A.A., Al-Saleh S., Al-Kaabi A., Al-Jawfi M. (2011) Laboratory investigation of the impact of injection-water salinity and ionic content on oil recovery from carbonate reservoirs, paper SPE 137634, SPE Reserv. Evalu. Eng. 14, 5, 578–593.

INVESTIGATION OF THE EFFECTS OF SEFERIHISAR REGION CLIMATIC AND TOPOGRAPHIC CONDITIONS ON OLIVE PHENOLOGY AND POMOLOGY

Dr. Ayça AKÇA UÇKUN

Olive Research Institute
0000-0002-5592-496X

Murat TUĞAÇ

Soil, Fertilizer And Water Resources Central Research Institute

Dr. Suna BAŞER

Olive Research Institute

Sedef ÖZDEN

Olive Research Institute

Aişe DELİBORAN

Olive Research Institute

Tülin PEKCAN

Olive Research Institute

Abstract

The ecological factors limiting cultivation of olive, which is an important and strategic product of our country, are climate and topographic conditions. In this study, it is aimed to reveal the effects of the climatic and topographical conditions of the Erkence olive cultivar, which grows in Selçuk region, one of the important regions of the Aegean region, on the phenology of the Erkence olive, using GIS (Geographical Information System). For this purpose, maps containing the climatic and topographic characteristics of 6 local regions selected from Seferihisar region were created by using GIS method. Phenological observations, pomological measurements, soil and leaf analysis results were compared in order to determine the climatic and topographic effect.

When all the results were compared, it was found that each local region has its own characteristics and its effects on olive on a local region basis were statistically significant ($p < 0.05$). The factors limiting and supporting olive cultivation are integrated with geographical conditions. The climatic and topographic conditions of a region vary on the basis of region, local region and village. Even within the same region, different climatic and topographic processes may occur. This affects the yield and quality of olive. This study once again emphasized the importance of assessing the geographic factors present on a small local basis when evaluating olive and olive oil processes.

Keywords: Olive; phenology; pomology; CBS; climate.

1. INTRODUCTION

Due to its geographical and special location characteristics, our country is located in a geography dominated by the Mediterranean climate. The olive tree is also a product of the Mediterranean climate, which has an important economic and strategic importance (Sağlıker, 2005). In this study, the effects of climatic and topographic parameters on the phenological and pomological characteristics of the Memecik olive cultivar in the Seferihisar region were emphasized. The phenological studies included in our study are defined as the researches on the life cycles of plants and animals that are repeated every year. Pomological measurements, on the other hand, are the measurements made with the aim of investigating the physical properties of fruit trees at the stage of growing fruits (Atalay, 2004).

Climatic and topographic conditions in olive cultivation affect the yield and quality of olives. Considering the effects of rain water, which is among the climatic conditions; Winter and spring rains provide olive blooming and increase fruit set. The water to be given to the olive trees in the summer, on the other hand, meets the water need while forming the seed of the fruit. Subsequent irrigation reduces the June shedding of fruits. However, irrigation increases the table value of table olives with the coarsening of olives and provides oil formation in oil production (Özilbey, 1986). In the Aegean and Mediterranean Regions, the relative humidity of olives grown on the coast is very important. Olive fruit set is positively affected in the humid spring period in some regions (Buldan and Çukur, 2003). Considering the wind effects, the winds blowing from the north-west in the winter season bring plenty of precipitation. However, light winds blowing in April and early May contribute to the fertilization of olive flowers. However, light breezes passing through the olive trees prevent the spread of some diseases such as ring spot disease. Another situation is that the humid winds blowing in summer partially prevent the olive trees from remaining dry. Winds blowing in winter (intersection) reduce the moisture holding capacity of the soil. In some regions, the drying winds (samyeli) blowing from the southern region at the end of May reduce the pollination of the flowers (Ayaz and Varol, 2015).

Low and high temperatures negatively affect the growth, quality and yield of olives in olive cultivation. While low temperatures cause defoliation and shoot deaths on olives, high temperatures cause burns in flowers, reduction of fruit sizes, and branch and shoot burns. Studies have shown that temperatures have a decisive effect on the growing, phenological and pomological properties of olives (Efe, 2009).

It is of particular importance to map the climatic and topographic conditions of the olive growing areas and to examine the climatic effects of the varieties that dominate the region. Geographic Information System (GIS) is used in determining the maps of the most suitable areas where agricultural products can be grown and in making climatic and topographic analyzes of agricultural products. The reason for this is that accurate, reliable and up-to-date information about agricultural areas can be accessed with GIS (Gündüzoğlu, 2004).

In this study, it is aimed to reveal the effects of climatic and topographic conditions revealed by GIS on the phenological and pomological conditions of olives in different local areas dominated by the Erkence olive variety in the Seferihisar region. This study was carried out with the aim of eliminating the deficiencies in the literature on the climatic and topographic processes of olives.

2. MATERIAL AND METHOD

Our study was designed with the Erkence olive variety. Nearly 90% of the olive tree existence in the Karaburun peninsula consists of the Erkence olive variety. The oil rate of the Erkence olive variety is 25.4% and it is a variety with high periodicity. It reaches harvest maturity in October-November (Tutar, 2010).

In our study, 6 different local regions in the Karaburun peninsula were selected (Table 1). These local regions are Gödence, Beyler, Gölcük, Orhanlı, Kavakdere, Ulaş. In order to determine the differences in our local regions where the experiment was conducted, it was harvested in the 2020/2021 crop season and all locations were harvested on 7.10.2020 on the same day (Table 1).

Table 1: Seferihisar region selected local regions and date of harvested fruits

Locations		Harvest	Leaf/Soil Samples
SEFERİHİSAR	Gödence	7.10.2020	13.10.2020
	Gölcük	7.10.2020	13.10.2020
	Beyler	7.10.2020	13.10.2020
	Orhanlı	7.10.2020	13.10.2020
	Ulaş	7.10.2020	11.10.2020
	Kavakdere	7.10.2020	13.10.2020

2.1. Features Examined in the Study

Obtaining Meteorological Data: Climate data was obtained from the General Directorate of Meteorology. The monthly averages of the temperature (°C) and relative humidity (%) changes recorded in the orchards of the Erkence variety, where the applications were made, were calculated.

Remote Sensing Methods (GIS): The Remote Sensing application has been carried out in a way that includes data generation and data processing methods from aerial photographs and satellite images, as well as remote sensing operations such as band arithmetic, image enhancement, classification, vegetation index, accuracy analysis on images.

Creating Slope Maps: While creating slope maps, slope values calculated over digital terrain model are displayed in desired thematic intervals.

Creating Altitude Maps: While creating altitude maps, the altitude data is read from the digital terrain model and the desired height range values are displayed thematically.

Agricultural Ecological Zoning Maps: In Agricultural Ecological Zoning; It is the creation of similar homogeneous areas by bringing together the climate, topographic, soil and land cover parameters that make up the land features through GIS. The classification system will be based on the UNESCO (1979) system.

Olive Phenology: In the determination of olive phenology, the BBCH (2001) literature was taken as a reference. While examining the phenology of the experimental regions, priority was given to 3 periods. The first of these is the period of shoot, leaf and bud formation, the other is the period of flower and fruit setting, and the last period is the ripening and color period.

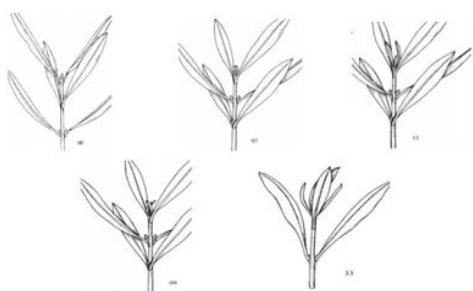


Figure 1. Olive shoot, leaf and bud formation phenology (BBCH, 2001)

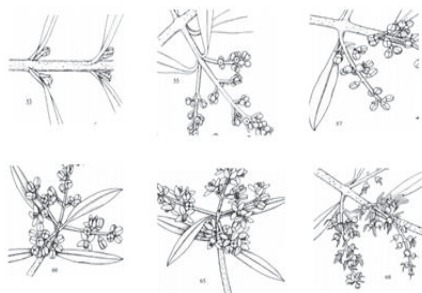


Figure 2. Olive flower and fruit formation phenology (BBCH, 2001)

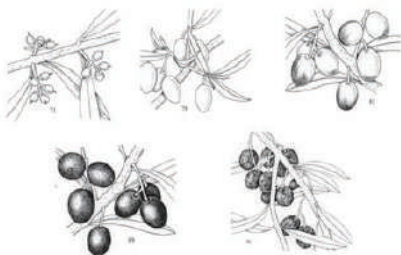


Figure 3. Olive ripening and color change phenology (BBCH, 2019)

Yield and Fruit Characteristics: By following the maturity index values of the fruits, at the optimum maturity stage; (each tree 1 replication) x (3 tree replications) x (24 orchards) = 72 fruit samples were taken and yield and quality analyzes were made.

Hundred fruit weight: 100 fruit weight of olive samples was carried out as stated in AOCS (1971).

Fruit volume: 100 fruits were taken and placed in a measuring tape containing a certain amount of water, and the amount of overflowing water was determined and calculated as mm³.

Meat/pit ratio: The meat/kernel ratios of olive samples were carried out as specified in AOCS (1971).

The number of fruit in kg (calibration): It is called the size criterion in olives. It has been evaluated according to the number of grains in 1 kg.

Color determination: Fruit color was determined by measuring CIE L*, a*, b* from the surface of 25 olive fruits taken from each replication using a colorimeter (Minolta CR-300, Japan) from both sides of the equator region.

Maturity index: It was calculated according to Boskou (1996) in 100 olives selected randomly from each replication.

Olives are cut in half;

0= Fruit skin is dark green,

1= Fruit skin is yellow or yellowish green,

2= Fruit skin is yellowish green, but fruit flesh is reddish dotted,
 3= Fruit skin is reddish or slightly violet,
 4= Fruit skin is black and fruit flesh is completely green,
 5= The skin of the fruit is black and the flesh is violet towards the half of the core,
 6= The skin of the fruit is black and the flesh is violet right up to the core,
 7= Fruit skin is black and fruit flesh is completely black, classified according to 8 categories.
 maturity index; The number of fruits included in each class was calculated by multiplying by the value of that class and dividing by the total number of fruits evaluated.

Soil Analysis: Soil samples were taken from a depth of 0-30 cm, representing the whole parcel, during the period (post-harvest) when leaf samples were taken (Kacar and Katkat, 2010). The dried soil samples and the physical and chemical analyzes by passing through a 2 mm sieve and the methods to be used in these analyzes are given below.

pH: 1:2.5 soil: determined by pH meter in water solution (Mclean, 1982)

Electrical Conductivity: 1:2.5 in soil: water solution to be determined by EC meter (Mclean, 1982)

Organic Matter: Determined by the Walkley-Black method (Jackson, 1962).

Total Nitrogen: The N content of the samples is determined by the Dumas Method (McGeehan and Naylor, 1988).

Available P: Olsen et al. (1954), the soil samples are extracted with 0.5 M NaHCO₃ (pH: 8.5) and determined by the Ascorbic Acid Method in the obtained filtrate (Kacar, 1985).

Retrievable K, Ca and Mg: Soil samples are determined by ICP-OES Device in the filtrate obtained after extraction with 1 N Ammonium Acetate (pH: 7) (Carson, 1980).

Retrievable Fe, Cu, Mn and Zn: Soil samples are determined by ICP-OES Device in the filtrate obtained after extraction with DTPA (pH: 7.3) (Lindsay and Norvell, 1978).

Obtainable B: Soil samples are extracted with 0.01 M Mannitol + 0.01 M Calcium Chloride solution and determined by ICP-OES Device (Kacar and Fox, 1966).

Leaf Analysis: Leaf samples were duly taken from all over the trees after harvest, with opposite leaf pairs in the middle of the annual end shoots (Güner, 1969). During the harvest period, fruit samples were taken from each orchard and analyzed as stated below. After the leaf and fruit samples taken are brought to the laboratory, they are washed first with tap water, then with 0.1 N HCl and 2 times with deionized water, after which the excess water is removed with blotting paper, dried at 70 °C for 48 hours (until they reach a constant weight) and covered with tungsten. It was ground in the mill and made ready for analysis (Kacar, 1972).

Total N: The N content of the samples was determined by the Dumas Method (McGeehan and Naylor, 1988).

Total P, K, Ca, Mg, Fe, Cu, Mn, Zn and B: Leaf samples are burned with concentrated H₂O₂ + HNO₃ acid in a microwave digestion device and determined by ICP-OES Device in the obtained filtrate (Zarcinas et al., 1987).

3. FINDINGS AND DISCUSSION

3.1. Evaluation of Meteorological Data

The meteorological data of the Seferihisar region are given below (Table 2).

The annual precipitation requirement in olive cultivation is 700-800 mm. Feeding the olive with rain water and adequate irrigation in the dry period encourages flowering and fruit set. However, it increases the pit formation and oil formation of the olive grain (Buldan and Çukur, 2003). In our country, the relative humidity of the Aegean and Mediterranean regions, especially the coastline, has positive effects on olive flowering, fruit set and fruit ripening processes. At the same time, the presence of relative humidity prevents burns and drying caused by high temperatures encountered in the flowering and fruit set period of olives (Yıldırım et al., 2008).

Table 2: Seferihisar region meteorological climate data

Meteorological Elements	Months												Yearly
	1	2	3	4	5	6	7	8	9	10	11	12	
Average Temperature °C	7.9	8.0	10.3	14.2	19.0	23.8	26.3	25.7	22.0	17.5	12.6	9.4	16.40
Highest Temperature °C	11.9	12.3	15.2	19.4	24.4	29.3	32.0	31.6	28.0	23.1	17.3	13.3	21.49
Lowest Temperature °C	4.4	4.4	6.0	9.4	13.4	17.6	20.4	20.1	16.5	12.7	8.6	6.1	11.63
Average Precipitation (mm)	109.5	85.9	71.5	46.5	25.1	4.2	0.7	0.9	11.6	35.2	95.6	133.8	620.38
Average Wind Speed	1.9	2.1	1.9	1.7	1.7	1.9	2.1	2.0	1.7	1.6	1.7	1.9	1.86
Sunbathing Time	136.6	140.5	197.3	236.1	290.4	353.0	375.0	353.1	294.3	231.2	152.4	111.6	2871.31
Humidity %	70.7	68.5	68.0	67.0	63.3	56.1	54.2	57.2	60.6	66.0	70.0	72.5	64.51

When the meteorological climate data (average of many years) taken for the Seferihisar region are examined, the average precipitation is determined as 620 mm (Table 2). Olive cultivation was found to be low in terms of ideal water demand. Therefore, irrigation is recommended during the dry season in summer. However, the relative humidity was found to be 64 %. It has been observed that relative humidity has a positive effect on olives in the Seferihisar region (Table 2).

Buldan and Çukur (2003) in a study examining the effects of winds on olives, revealed that the winds blowing from the north-west (northernwest wind) in winter increase the precipitation and the light winds blowing in the spring will contribute to the fertilization of the olive and the humid winds blowing in the summer reduce the dehydration of the trees. The location of the Seferihisar region shows that it is advantageous for olive cultivation.

When the meteorological climate data (average for many years) taken for the Seferihisar region are examined, the average wind speed is 1.86 m/s (Table 2). Olive cultivation was found to be low in terms of ideal water demand. Therefore, irrigation is recommended during the dry season in summer. However, the relative humidity was found to be 64% and the evaporation to be 97%. Although it is seen that relative humidity has a positive effect on olives in the Karaburun peninsula, the importance of irrigation in summer is emphasized once again due to the high evaporation rate (Table 2).

The temperature demand of olive cultivation is optimum 15 °C. When the Seferihisar region was examined, it was seen that the average temperature was sufficient for olive cultivation.

Examination of climatic and topographic conditions mapped with GIS. Geographic Information Systems is an information system that performs the functions of collecting, storing, processing and

presenting graphical and non-graphical information to be obtained by using location in integrity (Yomralıoğlu, 2015).

The Geographic Information System and altitude and ecological region maps of the Seferihisar region are given below (Figure 3 and Figure 4).

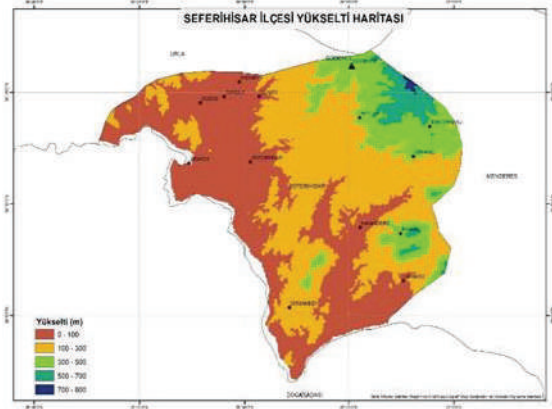


Figure 3. Elevation map of Seferihisar region created with GIS

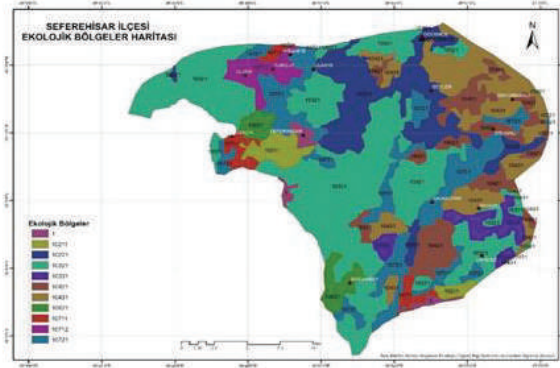


Figure 4. Seferihisar region ecological region map created with GIS

The information on the maps given above on the basis of regions and the determined olive phenology are given below (Table 3).

Location Seferihisar Region	Fenoloji			Altitude Map	Ecoregion	Drought Index	Hottest average	Coldest Average	Slope	Table 3. Ecological map information and phenology of Seferihisar region There are Gödençe, Beyler, Gölcük and Orhanlı districts at an altitude of 300- 500 m above sea level. Gödençe village was determined as the place where the phenology was seen at the latest and the altitude was the highest. As the altitude increases, the temperature decreases and accordingly the
	1 April	14 May	6 Oct							
Gödençe	07	55	81	300-500 m	10221	0.5-0.75 (semi)	>20 °C	0-10 °C	%2-12	
Beyler	07	57	81	300-500 m	10221	0.5-0.75 (semi)	>20 °C	0-10 °C	%2-12	
Gölcük	07	57	81	300-500 m	10321	0.5-0.75 (semi)	>20 °C	0-10 °C	%2-12	
Orhanlı	09	57	81	300-500 m	10421	0.5-0.75 (semi)	>20 °C	0-10 °C	%2-12	
Kavakdere	50	60	85	0-100 m	10721	0.75-1 (humid)	20-30 °C	0-10 °C	%2-12	
Ulaş	51	61	89	0-100 m	10721	0.75-1 (humid)	20-30 °C	0-10 °C	%2-12	

upper limit of olive growth is determined. The slope, on the other hand, plays a role in the cultivation of olives by affecting the soil and groundwater (Uslu, 1971).

At an altitude of 0-100 m above sea level, there are Kavakdere and Ulaş village. Since Kavakdere and Ulaş Villages are located in a humid region according to the agricultural ecological map and are close to sea levels, phenology was seen earlier in these villages. Humid air from the sea and large water surfaces is beneficial for olives. In humid weather, sweating in the leaves of the tree decreases and thirst is not experienced. Olive tree leaves benefit from the humidity in the air when they cannot get enough moisture from the soil in summer. The relative humidity of the air is one of the criteria that increases the product quality in table cultivation. In areas where relative humidity is sufficient, the water consumption of olives also decreases (Ayaz and Varol 2015).

An increase in temperature above the normal in May-June causes shrinkage of the leaves due to excessive transpiration. Since the extreme heat in the spring prevents fertilization, there is no fruit set (Aykas, 2004). The Erkence olive variety, which is dominant in Seferihisar district, has a strong periodicity tendency. The year 2020 is a period of extinction especially for Erkence olives. The high temperatures seen between 18-27 May 2020 also caused the low olive flowers to burn, especially in areas close to sea level, and led to flower shedding, and fruit set and yield losses were observed especially in the dehydrated areas.

The pomological characteristics of Erkence olive varieties grown in local regions in the Seferihisar region are given in Tables 4 and 5.

Seferihisar	10 Fruit Volume (ml) mean	100 Fruit Weight (g) mean	100 g of fruit weight	Table 4. Some pomological characteristics of olives in Seferihisar region
Ulamış	13 ± 0.03^c	330.7 ± 0.03^c	31 ± 0.08^c	Pomological measurements made in some local areas in the Seferihisar region were found to be statistically significant (Table 4). Statistically significant differences in
Beyler	14 ± 0.02^b	340.4 ± 0.02^b	29 ± 0.06^d	
Kavakdere	16 ± 0.04^a	400.8 ± 0.05^a	24 ± 0.04^e	
Gölcük	12 ± 0.03^d	250.4 ± 0.04^f	45 ± 0.04^a	
Orhanlı	12 ± 0.12^d	270.2 ± 0.01^e	36 ± 0.03^b	
Gödençe	13 ± 0.08^c	310.5 ± 0.02^d	36 ± 0.06^b	

z Differences between the means in each column were determined by Duncan's test according to $P < 0.05$. * Significant relative to $P \leq 0.05$ or ** $P \leq 0.01$

measurements of 100 fruit weights of harvested fruits. On the basis of local regions, Kavakdere (400 g) has the highest fruit weight, while Gölcük (250 g) has the lowest fruit weight (Table 4). The elevation has very positive effects on olive cultivation. In other regions, the 100 fruit weights are respectively Beyler (340 g), Ulamış (330 g), Gödençe (310 g), Orhanlı (270 g) local regions (Table 4).

Considering the number of grains per 100 g of the harvested fruits, the highest amount of grains (45 pieces) and the least amount of grains (24 pieces) were seen in Kavakdere location. It was observed that fruit weight and grain amount were inversely proportional. Akca Uckun (2020) examined the effects of different heights and different harvest times of Ayvalık (Edremit) olive cultivar on fruit and olive oil quality in a study he conducted. At the end of the study, it has been revealed that the yield and quality of olive fruits grown in high regions are higher and the positive effects of height on olives. It has been seen that this study is compatible with the study of Akca Uckun (2020).

Table 5. Some pomological characteristics of olives in Seferihisar region

In the study, the maturity index was found to be statistically significant on the basis of local regions, and the maturity index values were found to vary

Seferihisar	Maturity Index	Meat/Pit Ratio	L	a	b
Ulaşı	2.4	3.69 ± 0.05 ^b	56.032 ± 0.05 ^a	0.778 ± 0.05 ^a	26.60 ± 0.05 ^e
Beyler	1.5	3.30 ± 0.03 ^c	48.918 ± 0.03 ^d	-2.699 ± 0.03 ^c	30.117 ± 0.04 ^c
Kavakdere	1.3	4.33 ± 0.04 ^a	56.14 ± 0.02 ^a	-3.529 ± 0.04 ^e	35.188 ± 0.05 ^a
Gölcük	1.0	2.90 ± 0.03 ^d	47.06 ± 0.04 ^e	-2.811 ± 0.03 ^d	28.089 ± 0.03 ^d
Orhanlı	1.3	2.77 ± 0.02 ^e	53.407 ± 0.03 ^b	-3.775 ± 0.04 ^f	34.318 ± 0.04 ^b
Gödençe	1.9	2.68 ± 0.05 ^{ef}	47.26 ± 0.03 ^e	-1.055 ± 0.05 ^b	23.633 ± 0.03 ^f

z Differences between the means in each column were determined by Duncan's test according to $P < 0.05$. * Significant relative to $P \leq 0.05$ or ** $P \leq 0.01$

The skin

color of the fruits varies from green to yellowish green, light violet and violet. In the local region of Ulaşı, the color of the fruit skin was violet compared to other regions. The reason for this is that the phenological process is early compared to other regions due to its location close to sea level (Table 5). Considering the meat/seed ratios, the Ulaşı local region again had the highest value (3.69).

In the study, color measurements were found to be statistically significant. A L^* value of 56,032 in the Ulaşı local region indicates that violet color is evident, a^* value of 26.6 indicates that the green color decreases considerably, and a b^* value of 0.778 indicates that the color of the fruit's flesh becomes darker (Table 5). The fruit color has taken a color from green to black with phenology. Nergiz and Engez (2000) found that the weight of olive fruits increased with maturity. When compared with these results, it is seen that the fruit color change is compatible with the maturity index values.

Irrigation is generally not done on calcareous and barren soils, especially in marginal areas where olive cultivation is carried out. The geography of the olive groves and the topographic conditions have a direct effect on the general structure of the olive trees. (Aydogdu, 2011). According to the results of the soil analysis performed at 6 different locations in the Seferihisar region, it was determined that the Orhanlı location was moderately calcareous (5.43%), while the other locations (Beyler, Ulaşı, Gödençe, Gölcük, Kavakdere) were found in calcareous areas (1-4%) (Table 5). It has also been observed that the Erkence olive trees in the Seferihisar region are generally not irrigated. In the Seferihisar region, the pH value is slightly acid in the Ulaşı location (6.70); Gölcük (5.96), Gödençe (5.70), Kavakdere (6.09) medium acid; Orhanlı (7.81), Beyler (7.97) were slightly alkaline. However, the phosphorus values are; Ulaşı high (26.49 ppm), Gölcük, Orhanlı, Beyler, Kavakdere moderate values, Gödençe low (6.56 ppm) values (Table 5). When potassium values are examined, Gödençe, Beyler, Ulaşı (50-100 ppm) are low; Gölcük, Orhanlı, Kavakdere mean values were determined. Boron and Iron values were found to be high in all locations.

Ca values, on the other hand, are high in Orhanlı, Beyler, medium in Gölcük, Ulaş, Gödençe and Kavakdere. The nitrogen (%) value was found to be low in the Orhanlı location, while the other regions were found to be moderate (0.09-0.17%) (Table 5).

Looking at other studies; In the olive groves of Aydın region, where Manzanilla variety is found, the soil was found to be poor in N content, low in available P content, low in K content, moderate in Ca content, and poor in Mg content (Akıllıoğlu, 2009). In Bursa region, the soils are generally clay loam, sandy loam and clay textured, neutral or slightly alkaline, mostly lime-rich and unsalted, the total available N, available P and Zn contents of the soils are moderate, and the K and Fe contents are found to be sufficient (Aksoy, Tümsavaş, 2000). In Bursa (Yalova) location, it was revealed that the soils where the Gemlik olive variety is grown have a clay loam texture, very low lime content, and neutral and acidic soil reactions (Uysal et al., 2016). In a study conducted in the GAP Region, it was determined that Fe and Zn deficiency were observed in sloping agricultural areas (Eryüce et al., 1993). In the Hatay region, it has been observed that the N contents are between the optimum limits, the P contents are incomplete, and the K contents are between the optimum limits (Toplu, 2000). It has been revealed that the soils in the Şanlıurfa region are generally very calcareous, slightly alkaline, unsalted, and the amount of organic matter is insufficient (Siyonmez et al., 2017). In the orchards of the Halhalı olive variety in Derik district of Mardin province, the levels of P, K, Ca, Mg, Fe and Mn of the leaves were found to be sufficient, while the levels of N, Zn, Cu and B were insufficient (Doran et al., 2008).

Seferihisar bölgesinde yaprak analiz sonuçlarına göre, Azot değeri Ulaş (1.34 %), According to the leaf analysis results in Seferihisar region, Nitrogen value was found to be low in Ulaş (1.34%), Gölcük (1.23%), Orhanlı (1.17%), Gödençe (1.60%), Kavakdere (1.78%), Beyler (1.50%) were found to be sufficient. Phosphorus, Iron and Boron are at sufficient levels (Table 6). Zinc and Manganese values were found to be low in Beyler location (11.43, 17.21 ppm) and sufficient in other regions. It has been determined that zinc deficiency occurs in the form of chlorosis in young leaves, the leaves become smaller, the plant becomes stunted, and the old leaves become stunted, wilted and twisted (Marschner, 1995). Potassium value is low in Gödençe (0.48) and sufficient in other regions. Copper and Calcium values are low in Gödençe and Beyler locations, but sufficient in other locations (Table 6).

It was observed that the content of N, P, K, Zn and B elements in young leaves, Ca, Mg, Mn, Cu and Fe elements in the old leaves were higher in olive (Fernandez-Escobar et al., 1999). Since the Erkence olives in the Seferihisar region are old trees, it has emerged in accordance with the soil analysis results. Although the iron element in the soil is not found in the structure of chlorophyll, chlorophyll production decreases in iron deficiency. Iron element is effective on the protein mechanism in the plant (Kacar and Katkat, 2010). Iron deficiency is seen because the soils of dry areas contain large amounts of lime and have high pH. It also occurs with high levels of heavy metals such as manganese, copper, zinc, chromium and nickel (Aktaş and Ateş, 1998). It has emerged that copper is a plant nutrient required by the plant for chlorophyll production, respiration and protein synthesis. It affects protein and carbohydrate metabolism. It has been found to play a role in symbiotic nitrogen fixation. The element Mn in the soil plays a role in the breakdown of water in photosynthesis and the absorption of iron, calcium and magnesium. It acts together with iron in the formation of chlorophyll and increases plant seed germination and fruit ripening (Kacar and Katkat, 2010). When the Zn element is examined, it has been revealed that as the pH in the soil increases, the Zn solubility decreases (Kantarci, 2000).

Table 6. Seferihisar Region Soil Analysis Results

4. CONCLUSION															
The factors limiting and supporting olive cultivation are integrated with geographical conditions. The climatic and topographic conditions of a region vary on the basis of region, local region and village. Different climatic and topographical processes can be experienced within the same region. This affects the yield and quality of olives. When evaluating olive and olive oil processes, it is necessary to look at the geographical factors present on a small local basis. This study showed that the climatic and topographic conditions affecting olives have differences even on the basis of local regions.															
Seferihisar Region	% İşıba	E.C. Milihmho s/cm	P h	% Li me	% Or ga ni c M att er	% N	P (p m)	K (pp m)	Ca (pp m)	Mg (pp m)	Fe (p m)	M n (p m)	Z n (p m)	C u (p m)	B (p m)
Ula mış	4 3	0.23	6. 7 0	1. 50	3. 57	0 . 1 6	26 . 4 9	71. 18	21 59. 82	376 . 42	25 . 0 1	28 . 1 7	2 . 2 . 1 2	2. 9 7	3. 6 1
Gölc ük	4 8	0.29	5. 9 6	1. 82	2. 35	0 . 1 1	13 . 5 7	118 . 62	13 48. 64	196 . 67	58 . 2 6	29 . 4 9	1. 3 1	1. 2 7	4. 1 4
Orha nlı	3 9	0.41	7. 8 1	5. 43	2. 22	0 . 0 7	15 . 1 7	134 . 43	47 50. 65	163 . 81	8. 90	18 . 8 5	0. 9 3	7. 8 0	4. 3 2
Göd ence	3 9	0.10	5. 7 0	1. 83	3. 03	0 . 0 9	6. 56	50. 40	77 0.0 9	177 . 50	42 . 7 6	14 . 3 5	0. 4 2	0. 7 3	4. 3 0
Kav akde re	3 7	0.42	6. 0 9	1. 55	1. 91	0 . 1 1	12 . 2 0	117 . 57	11 47. 96	190 . 16	25 . 1 2	27 . 6 6	0. 8 4	1. 2 8	4. 3 0
Beyl er	4 7	0.32	7. 9 7	3. 72	2. 16	0 . 1 1	3. 79	68. 78	45 44. 10	249 . 98	16 . 8 4	21 . 7 8	0. 5 3	1. 0 6	4. 1 3

s by Climatic and Topographic Conditions and Determination of Geographical Indication Standardization".

-Thank you to TAGEM for its contribution.

‘There is no conflict of interest between the authors’

REFERENCES

- [1].Akça Uçkun, A., Aksoy U., (2020). Effect of Yield And Quality on Olive And Olive Oil In Olive Orchards Located At Different Altitudes, *Acta Scientific Agriculture* (ISSN: 2581-365X), Volume 4 Issue 7 July 2020.
 - [2].Akıllıoğlu A., (1995) “Aydın Yöresi Zeytinliklerinin Beslenme Durumu” II. Ulusal Bahçe Bitkileri Kongresi Tebliğleri. Cilt I., Adana, s:711-715.
 - [3].Aktaş M ve Ateş A., (1998). Bitkilerde Beslenme Bozuklukları Nedenleri Tanınmaları. Nurol Matbaacılık A.Ş. Ostim-Ankara..
 - [4].Anonim, 2018. www.naturalresources.sa.gov.au/.../140916-standard-tests-a...Erişim tarihi: 15.05.2018.
 - [5].Aydoğdu, E., (2011). Domat ve Uslu Zeytin Çeşitlerinde Yaprakların Besin Element İçerikleri ve Bunların Mevsimsel Değişimlerinin İncelenmesi, Çukurova Üniversitesi, Fen Bilimleri Enstitüsü, Yüksek Lisans Tezi.
 - [6].Atalay Y. (2004) Doğa Bilimleri Sözlüğü (I. Baskı), Meta Basım Matbaacılık Hizmetleri, İzmir.
 - [7].Ayaz, M, Varol, N . (2015). İklim Parametrelerindeki Değişimlerin (Sıcaklık, Yağış, Kar, Nispi Nem, Sis, Dolu ve Rüzgar) Zeytin Yetiştiriciliği Üzerine Etkileri. *Zeytin Bilimi* 5 (1) , 33-40.
 - [8].AOCS. (1971). Official and tentative methods of analysis of the American Oil Chemists Society, Champaign, IL, USA.
 - [9].Boskou, D., (1996). Olive Oil Chemistry and Technology. History and Characteristics of the Olive Tree. AOCS Press, Champaign, Illinois : 1 - 6.
 - [10]. Buldan Y ve Çukur H. (2003). Edremit Körfezinde Zeytincilik. Doğal Ortam – İnsan, Tarih Yayınları, İzmir.
 - [11]. Carson, P. L., 1980. Recommended Potassium Test. In: Recommended Chemical Soil Test Procedures for the North Central Region. Rev. Ed. North Central Regional Publication No: 221, North Dakota Agric. Exp. Stn. North Dakota State University, Fargo, USA, 20-21p
 - [12]. Doran, İ., Koca, Y.K., Pekkolay, B., Mungan, M., (2008). Derik Yöresi Zeytinliklerinin Beslenme Durumunun Tespiti. *Akdeniz Üniversitesi Ziraat Fakültesi Dergisi*. 21(1): 131-138.
 - [13]. Efe, R. (2009). “Sıcaklık şartlarının Türkiye’de Zeytinin (*Olea europaea* L. subsp. *europaea*) Yetiğmesine, Fenolojik ve Pomolojik Özelliklerine Etkisi”, *Ekoloji* 18, 70: 17-26, İstanbul.
 - [14]. Eryüce, N., (1979). Ayvalık Bölgesi Yağlık Zeytin Çeşidi Yapraklarında Bazı Besin Elementlerinin Bir Vegetasyon Periyodu İçindeki Değişimleri. *Ege Üniversitesi Fen Bilimleri Enstitüsü, Doktora Tezi*, Bornova, İzmir, 114s.
 - [15]. FAO. (1990). Micronutrient, Assessment at the Country Level: An International Study. FAO Soil Bulletin by Sillanpaa. Rome.
 - [16]. Gündüzoğlu, G. (2004). Batı Anadolu’da CBC yöntemiyle (zeytin örneğinde) doğal ortam analizi. 3. Coğrafi Bilgi Sistemleri Bilişim Günleri, Fatih Üniv., İstanbul. 8 s.
 - [17]. Follet RH, (1969). Zn, Fe, Mn and Cu in Colorado Soils. Ph. D. Dissertation. Colorado State University.
 - [18]. Güner, H., (1969). Toprak Verimliliği Yönünden Toprakların Kimyasal Analizleri.Türkiye Toprak İlmi Derneği ve 3. Bilimsel Toplantı Tebliğleri. Yayın No:1 sayfa 313-322.
 - [19]. Jackson, M. L., (1962). Soil Chemical Analysis. Prentice Hall Inc. Eng. Cliffs, Newyork, U.S.A., 183-187p.
-

-
- [20]. Özilbey N. (1986). Zeytinde sulama, Zeytin Yetiştiriciliği Kursu, Yayın no: 61, , Bornova-İzmir, s: 107-121.
- [21]. Kacar, B., Fox, R. L., (1966). Boron Status of Some Turkish Soils. University of Ankara, Yearbook of The Faculty of Agriculture, Ankara, 9-11p.
- [22]. Kacar, B., (1972). Bitki ve Toprağın Kimyasal Analizleri. II. Bitki Analizleri, A. Ü. Ziraat Fakültesi Yayınları 453, Uygulama Klavuzu, 155, A. Ü. Basımevi, Ankara, s: 646.
- [23]. Kacar, B. (1995). Bitki ve Toprağın Kimyasal Analizleri. III. Toprak Analizleri. Ankara Üniv. Zir. Fak. Eğt. Araş. ve Gel. Vakfı Yay. No: 3, Ankara. 705 s.
- [24]. Kacar, B., Katkat, A.V., (2010). Bitki Besleme. Nobel Yayınları, No:849,. Ankara, s.659.
- [25]. Kaya, U., Kurucu, Y., (2011). Zeytin Ağaç Sayımında Yüksek Çözünürlüklü Uydu Görüntüsünün Kullanımı, Zeytincilik Araştırma Enstitüsü Dergisi, 2(1):1-12.
- [26]. Lindsay, W. L., Norwell, W. A., 1978. Development of A DTPA Soil Test For Zinc, Iron, Manganese and Copper. Soil Science Society Of America Journal, 42:421-428.
- [27]. Mcgeehan, S.L., Naylor, D.V., (1988). Automated Instrumental Analysis of Carbon and Nitrogen in Plant and Soil Samples. Journal of Comm. Soil Sci. Plant Anal., 19(4): 493-505.
- [28]. Mclean, E. O., (1982). Soil PH and Lime Requirement in Methods of Soil Analysis (A. L. Page et al. editör). Part II, 2nd, American Society of Agronomy Inc. Publisher, Madison, Wisconsin, U.S.A., 199-224p.
- [29]. Nergiz, C. and Engez, Y., (2000). Compositional Variation of Olive Fruit During Ripening. Food Chemistry, 69: 55-59.
- [30]. Marschner, H. (1995). Mineral Nutrition of Higher Plants 2nd Ed.p.1-889. Acad. Press. New York, USA <http://aob.oxfordjournals.org/content/78/4/527.full.pdf+html>.
- [31]. Tutar M. (2010). Erken zeytin çeşidinde farklı tiplerin belirlenmesi. Doktora Tezi, Ege Üniversitesi Fen Bilimleri Enstitüsü, İzmir, 73.
- [32]. Sağlıker H. (2005). Doğu Akdeniz Bölgesinde iki farklı ana materyalde yetişen *Olea europaea* L., *Pinus brutia* ten. ve *Pistacia terebinthus* L. topraklarında karbon mineralizasyonu. Ekoloji 14, 54, 20-24.
- [33]. Sanz-CORTÉS, F., J.Martínez-Calvo, M.L.Badenesh.Bleiholder, H. Hack, G. Llacer, U.Meier. (2002). Zeytin Ağaçlarının Fenolojik Büyüme Aşamaları (*Olea Europaea* L.). Ann' E.Uygula. Biol. 140,151-157.
- [34]. Söylemez S, Öktem AG, Kara H, Almaca ND, Ak BE, Sakar E., 2017. Şanlıurfa yöresi zeytinliklerinin beslenme durumunun belirlenmesi. Harran Tarım ve Gıda Bilimleri Dergisi 21(1): 1-15.
- [35]. Uslu, S. (1971). Ege Bölgesi Ve Bilhassa Edremit Güre Havzasında Toprak Koruması Bakımından Zeytin Ve Orman Münasebetleri, Journal Of The Faculty Of Forestry Istanbul University.
- [36]. Uysal, E., Albayrak, B., Kayalı, F., Karakoç, A., Bıyıklı, M., Daş, Ö.B., (2016). Armutlu Yöresinde Yetiştirilen Zeytinliklerde Verim ile Bazı Toprak Özellikleri Arasındaki İlişkinin Belirlenmesi. Nevşehir Bilim ve Teknoloji Dergisi TARGİD Özel Sayı s. 19-31.
- [37]. Ülgen, N. ve M. Ateşalp, (1972). Toprak ve Gübre Araştırma Enstitüsü Teknik Yayınlar Serisi Sayı:21 Metin Matbaası, Ankara.
- [38]. Ülgen, N. ve N. Yurtsever, (1974). Türkiye Gübre ve Gübreleme Rehberi. Toprak ve Gübre Araştırma Enstitüsü Teknik Yayın No:28.
- [39]. Ankara.Toplu, C. (2000). Hatay İli Değişik Üretim Merkezlerindeki Zeytinliklerin Verimlilik Durumları, Fenolojik, Morfolojik ve Pomolojik Özellikleri İle Beslenme Durumları
-

Üzerindeki Araştırmalar. Doktora Tezi, Çukurova Üniversitesi Bahçe Bitkileri Ana Bilim Dalı, Adana, s. 195.

[40]. Yıldırım, O. (2008). Sulama Sistemlerinin Tasarımı (Genişletilmiş 3. Baskı). Ankara Üniversitesi Ziraat Fakültesi Ders Kitabı No: 518, Yayın No: 1565, , Ankara, s. 354.

[41]. Yomralıoğlu, T., (2015). Coğrafi Bilgi Sistemleri Temel Kavramlar ve Uygulamalar (3. Baskı), Akademi Kitabevi, Trabzon.

[42]. Wolf, B. (1971). The Determination of Boron in Soil Extracts, Plant Materials, Composts, Manures, Water and Nutrient Solutions. Soil Science and Plant Analysis (2), 363-374.

[43]. Zarcinas, B.A., Cartwright, B., Spauncer, L.P., (1987). Nitric Acid Digestion and Multielement Analysis of Plant Material by Inductively Coupled Plasma Spectrometry. Commun. Soil Sci. Plant Anal., 18:131-147p.

[44].

PURPLE POTATO VARIETIES AS RICH ANTHOCYANINS SOURCE FOR FOOD, PHARMACEUTICALS AND COSMETICS

Alexandra-Mihaela Nagy (Frățilă)

Lucian Blaga University of Sibiu, Faculty of Agricultural Science, Food Industry and Environmental Protection, Sibiu, Romania, <https://orcid.org/0000-0002-1195-2109>,

Camelia Sava Sand

Lucian Blaga University of Sibiu, Faculty of Agricultural Science, Food Industry and Environmental Protection, Sibiu, Romania, <https://orcid.org/0000-0001-5245-1602>,

Paula Boboc (Oros)

University of Agricultural Sciences and Veterinary Medicine, Center for Biodiversity and Conservation, Department of Horticulture and Landscaping, Cluj-Napoca, Romania, <https://orcid.org/0000-0003-3760-5460>,

Corina Cătană

University of Agricultural Sciences and Veterinary Medicine, Center for Biodiversity and Conservation, Department of Horticulture and Landscaping, Cluj-Napoca, Romania, <https://orcid.org/0000-0002-6041-215X>

Abstract

In recent years, anthocyanins in food, pharmaceuticals and cosmetics are increasingly used for their beneficial antioxidant capacity and coloring effects. Anthocyanins are rarely found as free molecules (aglycon form), they being rather linked to sugars (forming glucosides) and linked to phenolic acids. Anthocyanin-derived pigments comprise a diverse group of intensely colored pigments within the orange, red, purple and blue range. Crop landraces have substance, symbolic and sign values. Loss of biodiversity exposes the corporate sector to a range of risks and opportunities that can affect profit, asset values and cash flow. There is an increased demand for new raw material sources. Priority activities to prevent biodiversity loss are surveying and inventorying various plant genetic resources and improvement of plant genetic resources. Potatoes are commonly white or light-yellow due to phenolics and flavonoids found as glucosides. The antioxidant capacity of anthocyanins from purple flesh potato varieties can be determined by available analytical methods. The present paper focuses on separation and identification of the main anthocyanin aglycons from different purple flesh potato varieties as a strong source for food, pharmaceuticals and cosmetics. The total anthocyanin content was determined from the UV-Vis spectra (200-650nm) registered from a methanol-HCl 1% extract of potato, quantifying the specific absorption at 535nm. To identify the aglycon, the retention times and the specific UV-Vis absorption of each peak, as registered by Photo Diode Array, was considered. Our data show that purple flesh potato studied varieties having violet colors distributed differently and with various intensities in the flesh pulp contain mainly malvidin, peonidin and pelargonidin. Concerning the combination of anthocyanidin aglycons with different flavonoids and phenolic acids we can assume, according to UV-Vis data that there are mainly combination with coumaric acid. No determination of sugar groups linked to anthocyanins were done.

Keywords: Anthocyanins, In vitro Plant Pigments, Purple Flesh Potato

1. INTRODUCTION

For both humans and animals, the potato (*Solanum tuberosum* L.) has been considered a major source of food since ancient times. The potato has gained significant global

importance due to its extraordinary yield per unit area, compared to other crops [1]. More recently, in Bangladesh, the waste from potato peeling is used in the production of bio-oil and non-condensable gases, which has a positive impact on fuel economy and ensures the proper management of household waste to ensure a clean environment [2].

This plant has major importance on the diet of the population in many European countries, even in Romania it is considered to be 'the second bread' [3]. According to statistical data, a person consumes a quantity between 80 and 150 kg of potatoes per year. In Romania the average is 90 kg for each person in one year.

Purple potatoes (*Solanum tuberosum* var. *Violette*) are native to Peru and grown mainly in South America [4], but these varieties have begun to spread worldwide since they are highly sought after was said that this type of potato is the healthiest vegetable in the world [5].

Potatoes contain 6 types of alkaloids, namely alpha-solanine, beta-solanine, gamma-solanine, alpha-chaconin, beta-chaconin and gamma-chaconin, alkaloids that can be identified in all plant organs [6]. Especially varieties with colored pulp (from pink to dark purple), contain substantial amounts of anthocyanins, compounds that can act as antioxidants and can have beneficial effects on human health [7]. Of course, in addition to anthocyanins and other phytonutrients (carotenoids, phenols, flavonoids), minerals (K, Mg, N, Fe, Cu, Zn) and vitamins (C, A, B₁, B₂, B₆) have benefits for the health of the human body [8]. They can be used easily for pharmaceutical or cosmetic purposes.

By replicated laboratory and field trials was developed a protocol for virus-free/resistant colorful potato. Potato clones with high anthocyanin pigment were evaluated for their antioxidant properties, total phenolics content, and total anthocyanin content. The correlation of these three parameters is studied.

The paper presents a taxonomy study by molecular approaches. Evaluation of the colorful potato germplasm with the regard of molecular marker assisted breeding program which will generate new virus-resistant and/or -free potato germplasm is discussed.

2. MATERIALS AND METHODS

2.1. Plant materials

Samples of old cultivated germplasm from local Transylvanian empirically created potato crop diversity centers, "P1", "P2" and "P3" taken from seed lots produced during the 2001 and 2002 growing seasons, from local growers source were used as starting plant material. The tubers were selected according to their morphological type. The nodes dormancy was break down by a GA3 treatment (3%).

2.2. Media and cultural conditions

For initiation was made the selection of nodes followed by their detachment from the tuber with a small part of suber. After that, the material was sterilization in 5% hypochlorite for 15-20 min, followed by 3-5 rinses in sterile water. The next step was the placement of nodes on a modified MS (1962) plus glycine (4 mg/l), kinetin (4mg/l), sucrose (20 g/l) and agar (8 g/l), pH value of 5.7.

After 6 weeks of culture the meristems were harvested from the axillary shoots (8-12/ plant). Apical shoot tips (0.2-0.5 mm) containing a meristematic dome with 1-2 leaf primordial were cultured on a MS (1962) medium supplemented with Biotin (2mg/l), Glycine (2mg/l), GA3 (1,00mg/l) Myo-inositol (200mg/l).

Multiplication of virus free material was done by cuttings, transferred on MS (1962) medium supplement with PGRs every 3 weeks. Plants were grown into a vegetation room, under full time fluorescent tubes illumination, at 25°C temperature.

Tuberization was induced in the presence of the ascorbic acid (1,5 mg/l), on liquid medium, on a rotative shaker (60 rpm).

2.3. Experimental data

Each tube was considered an experimental unit. Depending on the availability of plant materials, the length of plantlets (cm), root length (cm) and root number per plantlet varied with experiments. Collected data were subjected to analysis.

2.4. Quantification of anthocyanins

Quantification of dry weight, starch and total anthocyanins in potato samples were obtained from 3 parallel determinations for each of the three potato samples.

The total anthocyanin content was determined from the UV-Vis spectra (200-650nm) registered from a methanol-HCl 1% extract of potato, quantifying the specific absorbance at 535nm. To identify the aglicons, there were considered the retention times (according to standard separation) and the specific UV-Vis absorption of each peak, as registered by PhotoDiode Array.

3. RESULTS AND DISCUSSION

3.1. The effect of auxin and cytokinin on growth of the apical meristems of three old potato varieties

Growth and development of isolated meristem tips depend on the cultivar used and were strongly influenced by the presence of exogenous growth substances in a very vitamins rich culture substrate.

The test of different auxin-cytokinin interactions showed that the best combination was that of IBA (1.0 mg/l) and Kin (0.1 mg/l) completed with 1.0 mg/l GA₃.

In all three studied genotypes axillary shoots were formed within 3 weeks, whereas complete plantlets, including roots were obtained in 6-8 weeks.

Regarding the total length of plantlets was registered value between 14,4 and 7,75 cm and for genotypes P2 and P3 were registered negative significance of difference. For average mean of root length were registered negative significance of difference for P2 and P3 and for average mean of roots number per plantlet were registered positive significance of difference for P2 and P3 genotypes.

Table 1. The effect of auxin (IBA) and cytokinin (Kin) on growth of the apical meristems of three old potatoes varieties

Total length of plantlets (cm)					
Genotype	Mean	%	□d	Significance of difference	DL
P1	14,400	100.000	-	-	DL 5% = 0,137
P2	11,050	77	-3,35	ooo	DL 1% = 0,194
P3	7,750	54	-6,65	ooo	DL 0,1% = 0,277
Average mean of root length (cm)					
Genotype	Mean	%	□d	Significance of difference	DL
P1	3,745	100.000	-	-	DL 5% = 0,274

P2	2,400	64.085	- 1,345	ooo	DL 1% = 0,387
P3	1,750	46.729	- 1,995	ooo	DL 0,1% = 0,553
Average mean of roots number/plantlet					
Genotype	Mean	%	□d	Significance of difference	DL
P1	6,600	100.000	-		DL 5% = 0,052
P2	11,450	173.485	4,850	***	DL 1% = 0,073
P3	18,05	273.485	11,450	***	DL 0,1% = 0,105

The best tuberization rate was recorded on the P1 (46%) genotype, followed by P2 (23%) and after that P3 (11%).

3.2. HPLCs analysis results

The data show that the Romanian samples having violet colour, distributed differently and with various intensities into the pulp of the tuber contain mainly malvidin and derivatives of it, petunidin and delphinidin (peaks 7,5,4). These aglycons represent more than 75% of the anthocyanins. Then pelargonidin (peak6) and cyanidin (peak3).

Table 2. HPLCs of the hydrolysed extract

Sample	Peak no	HPLC peaks for HE (tR, min)	Specific absorbtion (nm)	Identification
P1	3	7.82	530	Cyanidin
	4	7.95	529	Delphinidin
	5	7.99	529	Petunidin
	6	9.10	530	Pelargonidin
	7	11.98	535	Malvidin
P2	1	7.40	530	NI
	2	-	-	-
	3	7.51	530	Cyanidin
	4	8.09	530	Delphinidin
	5	8.63	530	Petunidin
	6	10.38	534	Pelargonidin
	7	18.13	539	Malvidin
P3	1	7.42	530	NI
	2	7.96	530	NI
	3	8.50	530	Cyanidin
	4	8.96	529	Delphinidin
	5	9.54	533	Petunidin
	6	12.38	534	Pelargonidin
	7	19.34	535	Malvidin

No qualitative differemnces were observed between the samples P1,P2 and P3 just quantitative, the most rich in anthocyan being sample P3.

Concerning the combinations of anthocyanidic aglicons with different flavonoids and phenolic acids we can assume that in these potatoes there are mainly combinations with phenolics, mainly with coumaric acid.

No determinations of sugar groups linked to anthocyanins were done.

4. CONCLUSIONS

IBA is the best in obtaining rooted virus free plantlets. Tubers were obtained in 6-8 weeks by culturing cuttings on liquid MS (1962) medium supplemented with ascorbic acid.

The Romanian violet potatoes, distributed differently and with various intensities into the pulp of the tuber contain mainly aglycons like malvidin and petunidin and delphinidin representing more than 75% of the anthocyanins. Then pelargonidin and cyanidin, with no qualitative differences between samples.

ACKNOWLEDGMENT

This study was made using the infrastructure of the Center of Biodiversity and Conservation from University of Agricultural Sciences and Veterinary Medicine Cluj Napoca.

REFERENCES

- [1]. M.E. Camire, S. Kubow and D.J. Donnelly, "Potatoes and human health, Critical Reviews", Food Science and Nutrition, vol. 49, pp. 823-840, 2009.
- [2]. A. Razu, H. Ershad, M. Golam and I. Mohammad, "Potato (*Solanum tuberosum*) peel waste utilization for eco-friendly bio-oil production via pyrolysis", DUJASE, vol. 5(1&2), pp. 25-29, 2020.
- [3]. P. Iliev and I. Iliev, "Cultura extratimpurie a cartofului", Pomicultura, Viticultura și Vinificația, vol. 50(2), pp.7-9, 2014.
- [4]. L. Zhang, L. Zhao, X. Bian, K. Guo, L. Zhou and C. Wei, "Characterization and comparative study of starches from seven purple sweet potatoes", Food Hydrocolloids, pp. 1-37, 2018.
- [5]. A. Li, R. Xiao, S. He, X. An, Y. He, C. Wang, S. Yin, B. Wang, X. Shi and J. He, "Research Advances of Purple Sweet Potato Anthocyanins: Extraction, Identification, Stability, Bioactivity, Application, and Biotransformation", Molecules, vol. 24(21), pp. 3816, 2019.
- [6]. D. Schrenk, M. Bignami, L. Bodin, J.K. Chipman, J. del Mazo, C. Hogstrand, L. Hoogenboom, J.C. Leblanc, C.S. Nebbia, E., Nielsen, E. Ntzani, A. Petersen, S. Sand, T. Schwerdtle, C. Vleminckx, H. Wallace, L. Brimer, B. Cottrill, B. Dusemund, P. Mulder, G. Vollmer, M. Binaglia, L.R. Bordajandi, F. Riolo, R. Roldan-Torre and B. Grasl-Kraupp, "Risk assessment of glycoalkaloids in feed and food, in particular in potatoes and potato-derived products", EFSA Journal, vol. 18(8), pp. 6222, 2020.
- [7]. A.D. Navare, A. Goyer and R. Shakya, "Nutritional value of potatoes: vitamin, phytonutrient, and mineral content", USDA-ARS, Washington State University, 395-424, 2009.
- [8]. N.Z. Ngobese, T.S. Workneh, B.A. Alimi and S. Tesfay, S., "Nutrient composition and starch characteristics of eight European potato cultivars cultivated in South Africa", J Food Compos Anal, 55, 1-11, 2017.

RESPONSE OF SPHAGNUM MOSS TO DIFFERENT SOWING METHODS FOR THE PURPOSE OF THEIR USE IN CONTEMPORARY STREET ART

Paula Boboc (Oros)

University of Agricultural Sciences and Veterinary Medicine, Center for Biodiversity and Conservation, Department of Horticulture and Landscaping, Cluj-Napoca, Romania

Rita-Daniela Farțadi

University of Agricultural Sciences and Veterinary Medicine, Center for Biodiversity and Conservation, Department of Horticulture and Landscaping, Cluj-Napoca, Romania

Corina Cătană

University of Agricultural Sciences and Veterinary Medicine, Center for Biodiversity and Conservation, Department of Horticulture and Landscaping, Cluj-Napoca, Romania

Abstract

Moss-graffiti is a street art concept that has as premise the use of mosses instead paint-based sprays, which are toxic and difficult to remove from walls. The proposal to use natural coloring materials can be a concept that will take this art out of the problematic underground area, giving a new ecological direction to this type of street manifest. Moss-graffiti does not only mean the creation of beautiful images using mosses, but it also means the growth of live images, the introduction of nature in the urban environment. Usually containing a subliminal message, street art using mosses has become a new adventure of urban expression, a path in which nature literally puts its signature in the urban space. The main objective of this research is the study of moss sowing and finding a technical solution to create a moss-graffiti. The paper presents the comparative laboratory study of two recipes and the results obtained after their implementation. The paper gives a short presentation of the graffiti history, from the oldest times until nowadays, for a better understanding of its evolution and people's perception on moss-graffiti. For this purpose, a detailed research was done on different types of mosses biology and the requirements from the environment and the need for food. The study consisted in harvesting the mosses from nature, growing these in a laboratory (on artificial ground), tests regarding the preparation of mixtures based on mosses and other substances and observations on sowing techniques. The application of this study consists in finding a solution in order to assure the biotope factor in a polluted environment. The study shows the problems regarding the understanding of the biology of mosses growing on artificial ground and identifies the technical solution which assures the success of making a decorative panel designed for the urban space.

Keywords: Moss-Graffiti, Sphagnum Sowing, Artificial Medium, Technical Solution

1. INTRODUCTION

People are born creative and lifelong choices shape the way they choose to express themselves. The street is the visual environment that captivates people the easiest, that's why it has become a place where artists display their anti-system messages in a unique and convincing way with stencils, illustrations, paintings, mosaics, sculptures, posters.

Moss-graffiti is a street art concept whose basic idea is to use mosses to the detriment of paint-based sprays, which are toxic and difficult to remove from walls and buildings.

The main concern of landscapers is to beautify and bring color to the urban environment through plants. A landscaper's job is not just to beautify gardens and parks. It must go beyond the "gates of

the gates" and try to bring life to any space in the urban environment through plants. Moss-graffiti can inspire any space.

This paper tests the hypotheses that show that mosses are plants that need minimal environmental conditions to survive and that they can grow and develop on a wide range of supports and materials. The proposal to use natural "coloring" materials can be a concept that will take this art out of the problematic underground area, giving a new, ecological direction to this type of street manifestation, sometimes disturbing. Eco-graffiti lives with nature, without harming the environment, changing under the effect of its elements, creating an intense, unique contact with nature.

Moss-graffiti is a simple and effective way to bring street art to life, encouraging mosses growth and giving an excellent alternative to paint sprays.

Eco-graffiti fans use the most unexpected sources to express themselves and beautify city walls. Instead of sprays with paint use: earth, sponges to draw in the dust, vines already existing on the walls, furs and last but not least moss.

Edina Tokodi, is the first to bring mosses to the city walls. She is the founder of Mosstika, a collective of eco-minded street artists, a collective dedicated to green guerrilla tactics inspired by public art (classic graffiti) [16].

Moss-graffiti can even be used for indoor decoration, provided it provides optimal moisture for the survival of the mosses. The name of moss-graffiti starts from the main ingredient needed to make it: the mosses, which are harmless to the environment, are therefore "eco". Moss could help keep a consistent stage of humidity in an enclosed indoor room. In fact, moss not only soaks humidity but also emanates humidity [9].

The term of Graffiti originated from Greek *graphein* can be explained simply as a critical expression including social-cultural and political responses to opposing ideologies in urban public spaces [6].

The graffiti technique has its origins in antiquity, during the period of ancient Greece and the Roman Empire. "Historically, the term 'graffiti' originally referred to inscriptions, portraits, etc. found on the walls of ancient tombs or on ruins, as in the Catacombs of Rome or in Pompeii [15].

In Rome, their own walls in Roman houses and monuments were engraved with graffiti, examples of their work being found in Egypt. The eruption of Vesuvius has preserved graffiti scratched on the walls of Pompeii and offers a direct picture of street life in those times: vulgar Latin, insults, magic, political messages and declarations of love. However, not only the Greeks and Romans did graffiti: the Mayan site in Tikal, Guatemala, also contains ancient examples. Viking graffiti in Rome and Newgrange, Ireland [15].

The first famous graffiti of the 20th century was "Kilroy was here" followed by "Mr. Chad", a face only with eyes and a nose, leaning against the wall saying "What?" No rare commodity? " during rationalization. The art of graffiti is seen as an authentic work, with an emphasis on color and composition. The uses of graffiti go beyond the strict sphere of contemporary art, the techniques and styles being constantly innovated; Graffiti has penetrated society enough to become a part of popular culture. Brands such as Nike have included the aesthetic aspects of graffiti in their products, while other brands, such as IBM, have used graffiti as a marketing medium for the "Love, Peace & Linux" graffiti campaign on the streets of San Francisco, California is part of the company's outdoor strategy) [5], [15].

There are divided opinions about graffiti: Varnedoe and Gopnik (1990) see graffiti "as a whole compositional phenomenon, on the one hand as a childish joke, and on the other hand as an adult insult". Abel and Bucket (1977) see this in a completely different way: "a form of communication that is both personal and free from everyday social constraints that normally impedes the free

expression of thoughts. In 1970, research on graffiti was in full swing. At that time, researchers in many disciplines were interested in graffiti, resulting in a large amount of information about graffiti, information that is then analyzed [15].

Spray paints have harmful effects on the environment. They emit pollutants into the air. Paints contain toxic chemicals, and some may even contain chlorofluorocarbon or hydrocarbon gases to spray paint on a surface [17].

Concerned about caring for the environment, an anonymous artist uses natural pigments (coal, plant sap, earth) to create scenic landscapes [14]. As an alternative, moss graffiti is an ecological, environmentally friendly choice, which is beginning to become a much more accepted, practical and also aesthetic method of creating graffiti worldwide.

Moss-graffiti is becoming more and more accepted among street art lovers. Moss graffiti, because it can be used as paint, is a very versatile reason. This means that it can be used to design slogans or pictures. It can be both a literary and a physical metaphor. Despite being largely in the street art community, much of the use of moss-graffiti has an ecological theme or message [8].

Beyond the aesthetic effect that moss-graffiti creates, its use helps to increase the green surfaces in cities. If we chose to create moss-graffiti on different surfaces in cities, the level of pollution in the city would be considerably reduced. Studies conducted at Gheorghe Asachi "Technical University of Iasi, Romania, have shown that Sphagnum species are among the species with high absorption capacity of heavy metals (especially chromium), which recommends them as extremely useful in plating urban areas of on the edge of heavily circulated arteries [1].

Mosses play a notable environmental role in the global carbon cycle as the largest land depositary for carbon [4]. Sphagnum peatlands hold up large amounts of carbon dioxide from the air. When the rate of plant production in an ecosystem exceeds the rate of plant decomposition, carbon sequestration occurs [2].

The mosses belongs to the phylum Bryophyta. Bryophytes are autotrophic cryptogames comprising approximately 25,000 species. The history of bryophytes involves an alternation between sporophytic and gametophytic descents that differ in pattern and role. The actual plant is represented by the gametophytic descents, which is the most developed haploid generation in the whole plant kingdom. The spores germinate to form a branched or thallose protonema which resembles green algae. The germination as well as its growth is very sensitive to all kinds of natural and human influences which exceeds by far the sensitivity of the green gametophore [13]. The protonema produced from a spore forms one to several shoots, each of which grows to become an 'individual'. The individuals are thus at the very outset part of an assemblage. Several moss shoot has a genetically fixed method of ramification, depending on species, genus or family, a particular 'growth-form' in the narrower meaning of the term [10]. Bryophytes are generally small (less than 5 cm) but some can grow up to a length of 70 cm. Bryophytes thrive in humid climates, but can be found all over the world, even in arid. A wide range of species can grow in areas unable to be colonised by any other plant which is significant for many aspects in bioindication also. Bryophytes colonise nearly every kind of terrestrial substrate (e.g. bare stones, bark, skeletons, etc.) and grow in freshwater but are absent from saline waterbodies (salt lakes, oceans) [13]. Contrary from other plants, mosses does not need soil supplements to stimulate growth [11]. In most areas, mosses grow mainly in areas of shade, such as wooded zones and at extremities of streams. However, they can grow anywhere in cool, damp and cloudy climates, and some species are suitable to sunny, seasonally dry areas like alpine rocks or stabilized sand dunes [2], [12]. Wherever they occur, mosses require high levels of moisture to survive .

2. MATERIALS AND METHODS

The experiment took place at the Biodiversity Research Center of Univeristi of Agricultural Sciences an Veterinary Medicine Cluj-Napoca (UASVM Cluj-Napoca), Romania. The practical

study consisted in choosing the materials and substances for the preparation of the mixture and establishing a recipe for sowing *Sphagnum* moss in order to use it to create moss-graffiti. *Sphagnum* mosses was from different surfaces, such as stone or tree bark.

Preparing a moss-graffiti using the empirical method involves harvesting the mosses, crushing them and mixing them with different substances to promote the germination process.

In order to settle on a support, the mosses need a substrate that promotes germination, the so-called biofilm. Biofilm is an aggregate of microorganisms in which cells adhere to each other on a surface. These adherent cells are often embedded in a self-producing matrix of extracellular polymeric substances (EPS) [3].

EPS biofilm, also known as "sludge", is a polymeric conglomerate composed of extracellular DNA, proteins and polysaccharides. Biofilm can form on living or dead surfaces and can be spread in nature, in the polluted area (industry) or aseptic (hospitals) [7]. Frequent watering is necessary to promote the installation of mosses.

Following the model of the empirical method, two variants of obtaining the preparation and sowing techniques were tested.

Table 1. Required materials

Variant I	Variant II
100g moss (<i>Sphagnum</i> spp.)	100g moss (<i>Sphagnum</i> spp.)
150ml distilled water	50ml distilled water
10g sugar	50 ml beer
1,5g Gelrite	50g yogurt
	8g sugar
	1g Gelrite

In the case of Variant I (Figure 1), the sugar and Gelrite were weighed using the analytical balance, then the gel was placed in 50 ml of distilled water to mix. Because the gel needs heat to form, but also permanent mixing, the electric hob with magnetic stirring was used, at a temperature of 200°C and 8000 rpm, for 10 minutes. The moss was washed under a continuous stream of water for 10 minutes to remove existing impurities then grind with a scalpel.

After crushing the mosses, they are added over the rest of the water and sugar, after which, the pH value is measured and adjusted (optimal 5.5-5.7), to ensure that the solution is within the typical limits required by the development of plant cells (slightly acidic).

The solution was transferred to a spray container and sprayed on organic paper previously placed on a layer of cotton wool soaked in sterilized water.

To favor the sowing process, subsequent waterings were done with a solution consisting of water and macro-elements from the culture medium formula of Murashige and Skoog (1962) (Table 2).

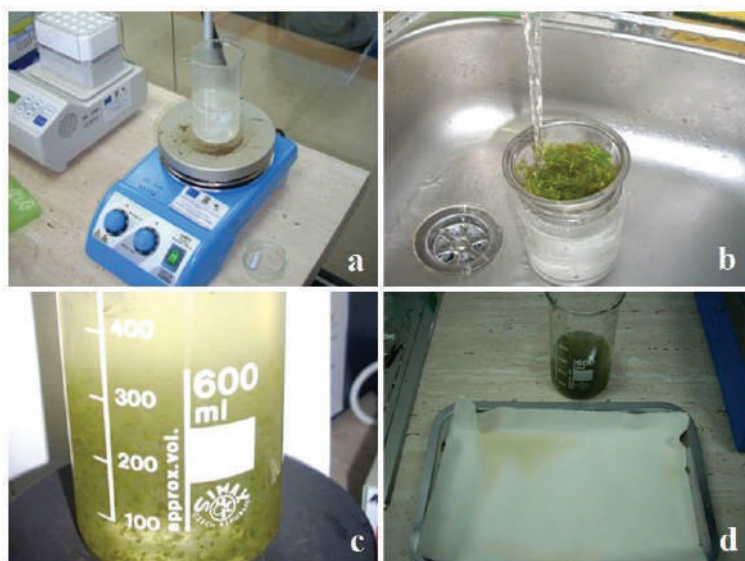


Figure 1. Aspects from the variant I Sphagnum seeding: a - preparation of the solution, b - preparation of the vegetal material, c - homogenization of the seeding solution, d - dispersion of the sample

Table 2. Macroelements in the composition of the basic Mourashige Skoog (1962) medium

Macroelements	mg/l
NH_4NO_3	1650
KNO_3	1900
$\text{CaCl}_2 \cdot 2\text{H}_2\text{O}$	440
$\text{MgSO}_4 \cdot 7\text{H}_2\text{O}$	370
KH_2PO_4	170

Like the previous experiment, for Variant II (Figure 2) the sugar and Gelrite were weighed with the analytical balance, then the gel was put in 50ml of water to mixed. Because the Gelrite needs heat to solidification, but also permanent mixing, was used the magnetic stirrer at 200°C and 8000 rpm for 10 minutes.

In a bowl was added the mosses, yogurt, beer and sugar, then grind with a blender at maximum speed for 7-10 minutes, until the mosses are crushed and a homogeneous composition was obtained, in which Gelrite will be added. Adjust the pH value (optimal 5.5-5.7).

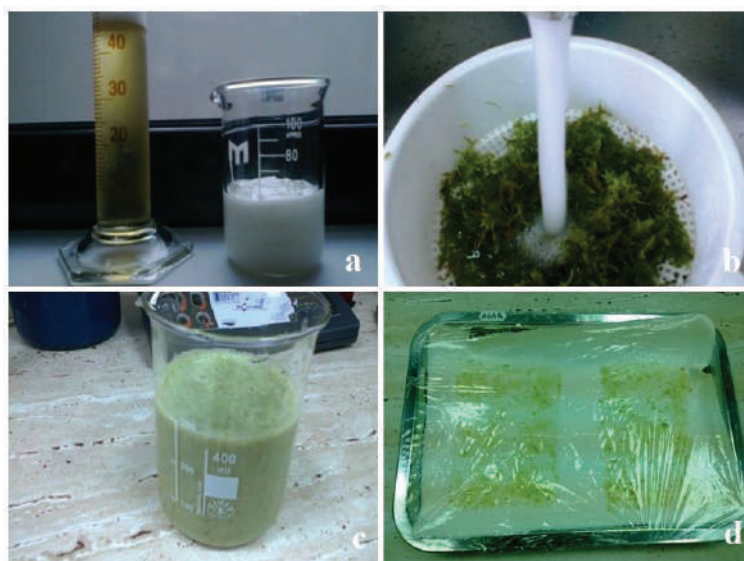


Figure 2. Aspects from the variant II *Sphagnum* seeding: a - preparation of the solution, b - preparation of the vegetal material, c - homogenization of the seeding solution, d - dispersion of the sample

After the whole composition was homogenized, using a brush, the composition was spread on a porous organic paper placed on a bed of cotton wool soaked in distilled water and kept in the vegetation chamber at a constant temperature of 20°C and a humidity of 65%. In order to maintain the humidity, a constant microclimate was ensured in the initiation phase by covering the experiment with food foil.

The original photos were taken with an ordinary camera and the structure images by taking the camera of the Olympus Microscope and the Motic Stereolup from the laboratory equipment.

3. RESULTS AND DISCUSSION

All these materials were used in different stages of the experiment to determine which of them best influences the process of germination and growth of mosses of the genus *Sphagnum*.

Variant I aims to observe how mosses can regenerate only from cells and whether new plants can be formed in the absence of plant tissue and in the absence of nutrients and bacteria in nature, necessary to form new colonies.

Variant II aims to observe how mosses can regenerate from shredded tissues, if they are placed in a suitable environment, having in composition, yogurt, two lactic bacteria *Lactobacillus delbrueckii* ssp. *Bulgaricus* and *Streptococcus thermophilus* and yeast *Sacharomyces* respectively, between which symbiotic relationships are created, which leads to the acceleration of the fermentation process and the formation of the fixing biofilm, necessary for the installation process of a *Sphagnum* moss colony.

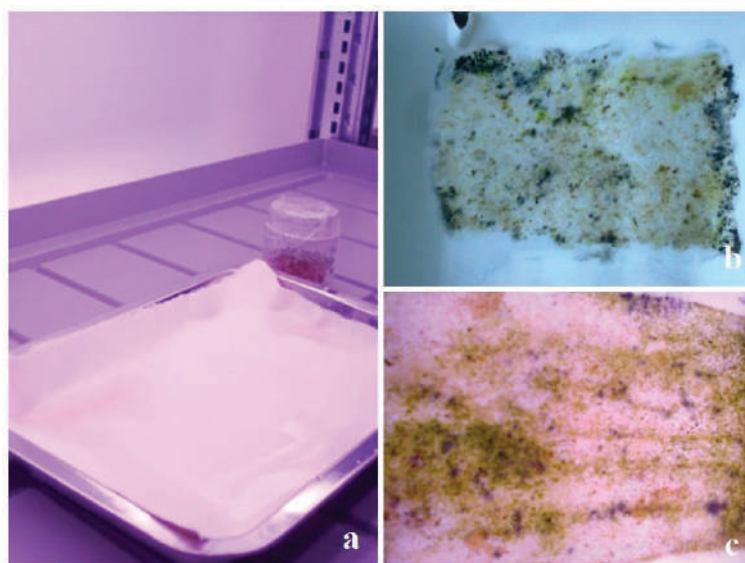


Figure 3. Aspects from moss growth: a - seeded sample in the vegetation room, b - variant I sample, c - variant II sample.



Figure 4. Visual observations: a - Sphagnum mosses after 6 months, b - Observations on the Motic Binocular Magnifier, c - Observations at the Motic Optical Microscope 10X objective

As in [12], an experiment in three steps was conducted. For Prototype A, the 600 g washed mosses were mixed in the blender with 100 ml water and 200 ml plain yogurt. The 100 ml water in Prototype A was replaced with 100 ml beer for Prototype B, to assess whether beer could speed up the initial growth of the moss. For Prototype C, the washed mosses were mixed with 100 ml water, 200 ml plain yogurt and 200 ml corn syrup. Different surfaces such as unfired brick, red brick, wood, tile and mortar wall were assessed. Prototype C succeeded in all three trials carried out. The difference between Prototype B and other prototypes was that it used beer as the primary liquid instead of water. Initially the foliage thickness for Prototype A was 5 mm when applied to the wall surfaces. Moss grew faster on a porous surface such as brick rather than on smooth surfaces.

4. CONCLUSIONS

Mosses are a valuable material for landscape art not only because of their appearance but also because of their role in the urban landscape. Along with lichens, mosses are valuable indicators of the degree of air pollution with SO_2 , CO_2 , heavy metal ions (Pb, Zn, Hg, Cd), and eco-graffiti arrangements can thus be a cheap and friendly tool for monitoring urban pollution.

The mosses can be placed on the slope or side walls of heavily circulated arteries in the urban area, thus ensuring an absorbent layer of traffic-specific toxins.

Mosses, due to their high ecological plasticity and the large number of existing species, are a cheap material for urban installations, easy to maintain due to their ability to survive and natural regeneration, without the need for fertilization or growth stimulation.

Different species of mosses should be tested in various indoor environment conditions to facilitate merchantability. The only disadvantage is finding solutions to ensure constant humidity throughout life.

REFERENCES

- [1].C. Balan, D. Bilba, M. Macoveanu, "Studies on chromium (III) removal from aqueous solutions by sorption on Sphagnum moss peat", *Journal of the Serbian Chemical Society*, Vol. 74(8-9), pp. 953-964, 2009.
- [2].M.T. Boquete, J. R. Aboal, A. Carballeira and J. A. Fernandez, "Do mosses exist outside of Europe? A biomonitoring reflection" *Science of the Total Environment*, vol. 593/594, pp. 567–570, Mar. 2017.
- [3].K. Czaczyk, K. Mysza, "Biosynthesis of Extracellular Polymeric Substances (EPS) and Its Role in Microbial Biofilm Formation", *Polish Journal of Environmental Studies*, vol. 16, pp. 799-806, 2007.
- [4].S. Deben, J. A. Fernandez, A. Carballeira and J. R. Aboal, "Using devitalized moss for active biomonitoring of water pollution", *Environmental Pollution*, vol. 210, pp. 315–322, Mar. 2016.
- [5].Duru, "5. The Affective Territory of Poetic Graffiti from Sidewalk to Networked Image". *Visualizing the Street: New Practices of Documenting, Navigating and Imagining the City*, edited by Pedram Dibazar and Judith Naef, Amsterdam: Amsterdam University Press, pp. 93-114, 2018.
- [6].G. Erdoğan, "Graffiti as a communication tool in public space: the case of Beyoğlu", *Journal of Human Sciences*, vol. 14, pp. 50-63, 2017.
- [7].S. Fulaz, S. Vitale, L. Quinn, E. Casey, "Nanoparticle–Biofilm Interactions: The Role of the EPS Matrix", *Trends in Microbiology*, Vol. 27, 2019.
- [8].E. Jackson, M. Kuha, "A Language Analysis of the Guerrilla Gardening Movement", 2015.
- [9].H. Kempter, M. Krachler, W. Shotyk, C. Zaccane, "Major and trace elements in sphagnum moss from four southern German bogs, and comparison with available moss monitoring data", *Ecological Indicators*, vol. 78, pp. 19–25, 2017.
- [10]. K. Mägdefrau, "Life-forms of Bryophytes" in Smith A.J.E. (eds) *Bryophyte Ecology*. Springer, Dordrecht 1982.
- [11]. C. P. B. Mesquita, J. E. Knelman, A. J. King, E. C. Farrer and K. N. Suding, "Plant colonization of moss-dominated soils in the alpine: microbial and biogeochemical implications", *Soil Biology Biochemistry*, vol. 111, pp. 135–142, Aug. 2017.
- [12]. C. Wang, H. Li, S. A. Neoh, "Moss-indoor vertical greenery system design protocol: Using moss as an indoor vertical greenery system in the tropics", *Indoor and Built Environment*, vol. 28(7), pp. 887-904, Aug. 2019.
- [13]. H. G. Zechmeister, K. Grodzińska, and G. Szarek-Łukaszewska "Bryophytes". *Bioindicators and biomonitors*, pp. 329–375, 2003.
- [14]. <https://www.cbc.ca/arts/this-alberta-artist-makes-paint-from-soil-and-rocks-and-here-s-how-she-does-it-1.5965730>
- [15]. <https://en.wikipedia.org/wiki/Graffiti>
- [16]. <http://www.mosstika.com/>
- [17]. <http://signaturefillingcompany.com/dangers-aerosol-products-stay-safe-using/>

PROCESSING SPECIMENS FOR VIRTUAL HERBARIUM**Rita Daniela Farțadi****Paula Boboc (Oros)****Corina Cătană**

University of Agricultural Sciences and Veterinary Medicine Cluj-Napoca, 0000-0002-1646-9327

Abstract

The germoplasm collections represent deposits of plant material, insured deposits in the short, medium and indefinite duration (preservation of callus and DNA samples, by cryopreservation). Each germoplasm collection has an additional herbarium. In Botany, the herbarium is a collection of small plants, leaves or flowers pressed between sheets of paper and kept in a special file in which there are also elements of taxonomic identification based on the morphology of plant specimens. The herbarium is the basic reference source of the taxonomist and has become a center of research as well as teaching and public information. Unfortunately, no matter how well the biological materials are processed, they degrade over time. Drying, pressing and preservation processes alter the morphology of the specimens. A virtual herbarium is a digitalized form, a collection of digital images of preserved plants or plant parts. It acts as an electronic gateway to collections of herbaria. It becomes a special type of museum and can also be considered a database with large amounts of raw data. The goals of the virtual herbariums are to make specimens data available electronically for use in biodiversity research projects, to reduce transport of actual specimens for projects where digital representations will be sufficient for study, and to provide a source of reference information. The herbarium concept has evolved so that today, the term is associated not only with specimens of preserved plants, but also with certain botanical activities. This paper proposes the creation of a virtual herbarium, a new technique for recording botanical objects, so that plants can be studied with unaltered colors and morphology. The information is stored in databases, complementary to the classical herbarium and all morphological descriptors that will allow the user to access large amounts of data, with the potential to expand analytical research.

Keywords: Herbarium, Virtual Herbarium, Technical Solution

1. INTRODUCTION

The digitization of natural history collections has evolved to the creation of databases for recording catalog data and specimen labels to include digital images of specimens. This was determined by several important factors, such as the need of increasing the overall accessibility of copies and to keep the original copies by limiting their manual handling. The largest herbarium collections in the world participate in international loan programs, in which a researcher can request a herbarium file that would be sent to study. This shipment contributes to the wear of the samples.

Virtual herbariums are the digitized form of physical herbaria with the role of increasing the longevity of specimens and international accessibility, via the World Wide Web.

2. MATERIAL AND METHODS**2.1. History of Herbarium**

The art of the herbarium was initiated by the Italian taxonomist Luca Ghini (1490-1556). The concept of preserving dried plant specimens is 450 years old. The oldest specimen of preserved plants is conserved in Rome, collected by the naturalist Gherardo Cibo, a student of Luca Ghini (1532) [1]. The first herbarium in the world was established in 1545 at the University of Padua, Italy. As the Renaissance developed, the Italians began to teach Botany and created the world's first botanical garden, also at the University of Padua, Italy. For the study of Botany, the students of those times were prepared the "Book" of mounted dried specimens (plants) "and called them" dry

gardens "or" Horti Sicci ". In the same year, the first botanical garden was established, the only garden that has uninterrupted activity from its establishment until today.

Depending on the location of the plant material and their functionality, herbariums are: international, national, regional, local, private, educational, for research [2].

According to Index Herbariorum, today there are 2.800 active herbariums in the world which are associated with them about 10.000 biodiversity specialists. Citing the same source, in 2003 there were 3240 active herbariums in the world [3].

2.2. Textile Fiber Herbarium

There is an interest in finding new forms of documentation, as close as possible to reality, given that, over time, morphological characters lose their structure or color. At the beginning of the 20th century, The Textile Herbarium Collection from Cluj-Napoca was created for both scientific and artistic purposes.



B.



C.



A.

Fig.1 – The Textile Fiber Herbarium USAMV
Taraxacum (A), Matricaria (B), Delphinium (C)
Source: original

2.3. Virtual Herbarium

Through this technique there were made electronic data samples available for use in biodiversity research projects; reducing the shipment of real specimens for projects in which digital representations will be sufficient for study; and to gather data elements (ex photographs and drawings, manuscripts, published papers, microscopic preparations, genetic sequences) derived from a specimen with the catalog entry data for that specimen.

The collections of images of the virtual herbarium are constantly updated, as the sheets of classic herbarium are available.

The concept of virtual herbarium comes as a result of the digital development of all theoretical and practical branches of biotechnology. Digitization of the herbarium involves both scanning the plant material and entering it in a specialized database.

2.4. Data bases

For this study there were analyzed three of the most important botanical databases in the world: Global Plants [4], Kew Herbarium Catalogue [5], Global Biodiversity Information Facility [6]. In order to properly compare the information found, the study was done searching the species *Myosotis alpestris*.

There is information about the location and the date of collecting, the collector, the altitude etc. Each database comes with its own presentation style and related information. The Kew Garden Catalogue is by far the most complex in terms of taxonomic documentation, but the Global Biodiversity Information Facility offers a new perspective through user-friendly and intuitive design by their interactive map and the facility of uploading real plant photos not only by scientist, but also by botany enthusiasts.

2.5. Equipment

The use of appropriate scanning equipment brings a useful end result in research. Professional scanners were used to scan the herbarium sheets at the University of Agricultural Sciences and Veterinary Medicine of Cluj-Napoca: BioScan 1600 and Microtek Scanner.

3. RESULTS AND DISCUSSION

The scan was produced using classic herbarium sheet of *Juglans regia*, existing in the Didactic Herbarium of the University of Agricultural Sciences and Veterinary Medicine from Cluj-Napoca, Romania. Using the scanning method, a digital herbarium file was obtained. It will be entered into the herbarium database so that it can be viewed and used by researchers and students.



A.

B.

Fig.1 – Herbarium USAMV (A), Herbarium digital scan on *Juglans Regia* (B)

Source: original

The benefits of such a project are:

- data accessibility: public data can be accessed by anyone with access to the internet, from any corner of the world
- easy transmission of information between authorized institutions or persons through databases
- the opportunity to update species information in real time
- elimination of the risk of degradation of plant material: although they are kept in optimal conditions of temperature, humidity and light intensity, the classic herbaceous leaves are endangered over time
- compacting collections to increase storage space
- the chance to popularize herbariums, botanical science and biotechnology

4. CONCLUSIONS

The database, accessible through a website, can play an important role in species conservation and habitat restoration. The website provides information about the species and their spaces: regional and state locations, habitat types and species that grow in these habitats, their conservation status and whether a (endemic) species is limited to a particular location. In addition, information about

plants grouped in niche collections, provides concentrated information, accessible anytime, to anyone and from anywhere.

Computerizing a germplasm collection or virtual herbarium has many advantages:

- allows the user to access large amounts of data, with the potential to expand analytical research
- once computerized, specimen data can be easily changed or corrected
- it becomes extremely easy to add additional fields to the database when an update or change is needed
- by maximizing the use of botanical information, the herbarium can be managed more efficiently
- data can be extracted quickly in different formats, obtaining statistical data.

ACKNOWLEDGMENT

This study was made using the infrastructure of the Biodiversity and Conservation Center from USAMV Cluj-Napoca, as well as having access to the didactic herbarium of the university.

REFERENCES

1. <https://herbariumworld.wordpress.com/2018/03/05/at-the-beginning-luca-ghini/> (last access – nov 2021)
2. <https://www.brown.edu/research/projects/herbarium/about/what-herbarium> (last access – nov 2021)
3. <http://sweetgum.nybg.org/science/ih/map/> (last access – nov 2021)
4. https://plants.jstor.org/stable/10.5555/al.ap.specimen.us01164037?searchUri=filter%3Dname%26so%3Dps_group_by_genus_species%2Basc%26Query%3Dmyosotis%2Balpestris (last access – nov 2021)
5. <https://apps.kew.org/herbcat/detailsQuery.do?imageId=677068&pageCode=1&presentPage=1&queryId=4&sessionId=47C59F25911C7AF52B8487EF749207FF&barcode=K001085874> (last access – nov 2021)
6. <https://www.gbif.org/species/5341187> (last access – nov 2021)

EVALUATION OF SOMATIC CELL COUNT OF RAW MILK DEPENDING ON SEASONAL VARIATION

Melike Ciniviz

Bursa Uludag University, Faculty of Agriculture, Department of Food Engineering, Turkey,
0000-0001-6089-1659

Gokce Keser

Bursa Uludag University, Faculty of Agriculture, Department of Food Engineering, Turkey,
0000-0003-1611-7847

Irmak Aral Baskaya

Bursa Uludag University, Faculty of Agriculture, Department of Food Engineering, Turkey,
000-0001-5475-210X

Lutfiye Yilmaz Ersan

Bursa Uludag University, Faculty of Agriculture, Department of Food Engineering, Turkey,
0000-0001-9588-6200

Tulay Ozcan

Bursa Uludag University, Faculty of Agriculture, Department of Food Engineering, Turkey,
0000-0002-0223-3807

Omer Utku Copur

Bursa Uludag University, Faculty of Agriculture, Department of Food Engineering, Turkey,
0000-0002-1951-7937

Abstract

Determination of somatic cell count is accepted as an important criterion in terms of food safety to evaluate udder health and milk quality. Changes in the number of somatic cells of milk occur as a result of mastitis, which stimulates the defence system or causes intramammary infection. There is a positive correlation between the increase in the number of somatic cells and viable microorganism counts in milk and the degree of mastitis. In this study, the number of somatic cells and SCC were determined in cow milk obtained from local raw milk collection centers in summer and winter periods. According to the results of this study, the lowest somatic cell count of milk in winter was 12×10^3 cells/mL and the highest was 726×10^3 cells/mL, while the lowest was 132×10^3 cells/mL and the highest was 555×10^3 cells/mL in summer. The SCC of milk was determined as $3,50 \times 10^4$ - $6,16 \times 10^6$ cfu/mL in winter and $1,20 \times 10^4$ - $1,11 \times 10^6$ cfu/mL in summer.

Keywords: Milk, Somatic Cell, Total Viable Microorganism, Season

1. INTRODUCTION

Milk, due to its complex biochemical composition and high water activity, serves as an excellent culture medium for the growth and activity of microorganisms. It is very difficult to prevent the contamination of milk with microorganisms due to the farm environment, the animal's health and milking conditions. The importance of maintaining the quality of raw milk is recognized by milk producers worldwide [1]. Therefore, the microbial content of milk is an important attribute in determining its quality [2], [3]. The presence of high total

viable microorganism and somatic cell count (SCC) in raw milk indicate milking or general hygiene problems [3]. Microbial contamination in raw milk can occur through different microorganisms [4]. In dairy industry, total microorganism number are a mandatory quality indicator of raw milk. The most important microorganisms used as hygiene indicators to determine quality of milk are psychotropic, aerobic mesophilic, and coliform bacteria. High number of mesophilic bacteria is accepted as an indicator of inadequate hygiene practices [5]-[7]. Milk is defined as a biological fluid with high nutritional value containing water, protein, lipid, carbohydrate, minerals, etc. In addition, milk includes milk-secreting epithelial cells called as SC. SC of milk composed of 25% epithelial cells (udder secretory tissue) and 75% leucocytes (white blood cells) including macrophages, polymorphonuclear neutrophil cells (PMNs), erythrocytes and lymphocyte [3], [8]. The amount of SCs in milk, often referred to as SCC is used as a mandatory indicator of udder health. SCs are recognized as one of the most important components of defence against disease and infections in the mammary gland [9], [10]. As a result of inflammation in cow mammary glands, high SCC and infection level of pathogens causing mastitis aim a decrease in milk yield [11], [12]. Milk SCC in a healthy cow is $<1 \times 10^5$ cells/mL under normal conditions. SCC greater than 2×10^5 cells/mL has been reported to be indicative of inflammation in the udder [13]. Most of these assessments are based on an increase in SCC above the limit value of 400,000 (4×10^5) cells/mL due to the fact that infection has occurred in the udder [14]-[16]. In the European Union, it is thought that if the SCC is more than 2×10^5 cells in 1 mL of raw milk, the udder may be infected, and if it is higher than 4×10^5 cells, the udder may be infected and it is not suitable for human consumption. In the dairy industry, the SCC limit for acceptance of milk differs depend on countries. For instance; SCC for bovine milk in Germany, Canada and the USA were determined as 1×10^5 , 5×10^5 and 7.5×10^5 cells/mL, respectively [17], [18]. High SCC negatively affects the quality of raw milk and reduces its shelf life [5]. In many countries, the maximum SCC international export standard has been reported as 400,000 cells/mL [19]-[21]. The maximum acceptable level of SCC in the European Union is based on geometric averages collected over 3-month periods [22]. The most important factors affecting SSC of raw milk and their effects are shown in Table 1 [10], [23].

Table 1. The most important factors affecting SSC of raw milk and their effects [8], [10], [24]

Factors		Effect on SCC in milk
Inflammatory Factors	Bacteria (Mastitis)	This inflammation of the mammary gland can be characterized by an increase in SCC. Treating infected and culling chronic mastitis animals cause a decrease in SCC.
	Virulence factors	
	Physical agents	
	Chemical agents	
Environmental factors	Milking techniques	Lower SCC in machine than in manual milking. Unhygienic and incomplete milking factors cause an increase in SCC.
	Milking machine	
	Hygiene	
	Housing	Changes in housing and feed cause an increase

	Dietary	in SCC. Feeding antioxidants cause a decrease in SCC.
	Seasons	Hot-humid climates causes an increase in SCC.
	Stress	Under stress of milk production, immunity of animals becomes low leading to more SCC.
	Farming system	Clean animal surroundings cause a decrease in SCC.
Host factors	Daily variations /Milking time	Higher SCC in evening compared to morning milking.
	Number and stage of lactation	SCC increases with increasing age, parity and stage of lactation.
	Age/Parity	
	Health of udder	Regular udder screening cause a decrease in SCC.
Other factors	Counting methods	Standardization of SCC counters is essential and equipment in order to guarantee accuracy and reproducibility of results.
	Conservation and storage samples	The conservation of the sample (temperature and time), the type of preservative and the temperature of the analysis affect the accuracy of the SCC results.

As SCC increases in milk (100×10^3 to 1000×10^3 cells/mL), lactose, fat and casein contents in milk, milk yield and gel firmness reduces while pH of milk, whey protein, non-protein nitrogen, blood components such as Na, K, Cl, immunoglobulins and serum albumins increase [25]. Determining the SCC of milk have been used automated devices. Coulter Milk Cell Counter and Fossomatic are the most commonly-used equipments. Fossomatic with a fluorescent dye counts the number of fluorescing particles while Coulter Milk Cell Counter counts particles as they flow through an electric field. Also, direct microscopic method has been used to determine SCC [26].

Considering all the above-mentioned facts, the aim of the present stud was to determine the total number of viable microorganisms and somatic cell of cow milk collected during winter and summer period.

2. MATERIALS AND METHODS

In the study, cow's milk was obtained from 23 different farms in 3-month periods. TVM and SCC were determined in cow's milk for the winter (January-February-March) and summer (May-June-July) periods.

2.1. The Total Count of Viable Microorganisms

Raw milk samples taken as sterile were diluted. 1 mL sample was taken from the dilution process with the help of a sterile pipette in petri dishes. Afterwards, 12-15 mL of medium was added to the petri dish, in which 1 mL of sample was added, and homogeneous mixing was ensured in the petri dish. It was kept in an incubator at 30°C for 72 hours. After 72 hours, the colonies were counted and the results were given as cfu/mL [27].

2.2. Somatic Cell Count

Delaval brand (Type: Cellcounter DCC) device was used for the determination of SCC. There is a special cassette compartment for placing milk samples inside the device. Raw milk samples were injected into the bowl of the device. The instrument automatically diluted the sample to 3 over 10 dilutions. Direct reading was then performed. Then direct reading was done. Results as multiplying with 1000 were calculated [28].

3. RESULTS AND DISCUSSION

Results of TVM were shown in Table 2. The TVM of milk collected during winter period varied from $3,50 \times 10^4$ - $6,16 \times 10^6$ while these numbers in summer period varied from $1,20 \times 10^4$ - $1,11 \times 10^6$. Several studies show a clear association between teat hygiene and raw milk quality, where disinfection lowers the amount of bacteria [29]-[31]. Many farms related factors contribute to the variation in milk TVM. The factors presented here show some of the major causes for variations found in this literature study. Mastitis is a major reason for rising bacterial counts, as reported in numerous studies [32], [33]. TVM can vary with lactation stage, being higher in late lactation [34]. In a study, higher TVM were found in milk from larger farms, characterized by barn conditions, robotic milking, and breed [31]. Milk collected in summer months when cows are grazing outdoors revealed modestly higher counts [34], [35]. Doyle et al. [36], observed higher TVM in milk after milking preparations, especially in milk from grazing cows. It was suggested that bacteria originating from outdoor environment may have difficulties adhering to teat skin, and instead shed down into the milk [37]. Milking system has also been observed to be associated with differences in bacterial counts.

Table 2. The total count of viable microorganisms

Season	Number of Samples	Range Min- Max.(cfu/mL)	Average
Winter	69	$3,50 \times 10^4$ - $6,16 \times 10^6$	$2,94 \times 10^5$
Summer	69	$1,20 \times 10^4$ - $1,11 \times 10^6$	$2,94 \times 10^5$

The SCC of cow's milk were presented in Table 3. According to the results of SCC, the mean result of 69 samples in winter was 345×10^3 cell/mL, while the average result of 69 samples in summer was 305×10^3 cell/mL. The SCC of the samples collected in winter was almost higher than in summer. The mean SCC was below the limit values specified in the European Union regulation in both periods and Turkish Food Codex Communiqué [38]. In the studies, the factors affecting the number of somatic cells have changed according to years, seasons and months. It has been reported that the reason for the increase in the number of somatic cells in the summer season is the heat stress in the cows, the differentiation of their diets, mastitis infection, multiple births and milking in the last lactation periods. It has been stated that the amount of SCC increase in the winter season and in the months of this season may be related to the deficiency of vitamin A, which has the feature of protecting the epithelial structure met from the pasture in summer [39]. As a

result, it has been determined that the cow's milk processed in the dairy enterprise during the 6-month period is in accordance with the limits determined in the relevant communiqués of the European Union Commission in terms of the number of somatic cells.

Table 3. Somatic cell counts

Season	Number of Samples	Range Min.-Max. (cell/mL)	Average (cell/mL)
Winter	69	12x10 ³ -726x10 ³	345x10 ³
Summer	69	132x10 ³ -555x10 ³	305x10 ³

4. CONCLUSION

The results of this study indicate that parity, stage of lactation, age of animals and calving season significantly affected TVM and SCC. Improving milking management, reducing stress, providing extra care during the first month of lactation, and milking at a uniform interval will help to decrease SCC in milk and the prevalence of mastitis. It is suggested that monthly control of SCC may be effective for improving milk production and milk quality in cows.

REFERENCES

- [1] S. Gschwendtner, T. Alatossava, S. Kublik, M. M. Fuka, M. Schlöter, and P. Munsch-Alatossava, "N₂ gas flushing alleviates the loss of bacterial diversity and inhibits psychrotrophic pseudomonas during the cold storage of bovine raw milk," *PLOS One*, 11:e0146015, 2016.
- [2] M. A. Reta, A. H. Addis, "Microbiological Quality Assessment of Raw and Pasteurized Milk," *International Journal of Food Science and Microbiology*, Vol. 2 (6), pp. 087-091, 2015.
- [3] B. E. Gillespie, M. J. Lewis, S. Boonyayatra, M. L. Maxwell, A. Saxton, S. P. Oliver, and R. A. Almeida, "Short communication: Evaluation of bulk tank milk microbiological quality of nine dairy farms in Tennessee," *J. Dairy Sci.*, 95:4275–4279, 2012.
- [4] A. M. Elmoslemany, G. P. Keefe, I. R. Dohoo, and B. M. Jayarao, "Risk factors for bacteriological quality of bulk tank milk in Prince Edward Island dairy herds, Part 2: bacteria count-specific risk factors," *J. Dairy Sci.* 92:2644–2652, 2009.
- [5] D. M. Barbano, Y. Ma, and M. V. Santos, "Influence of raw milk quality on fluid milk shelf life," *J. Dairy Sci.* 89:E15–E19, 2006.
- [6] R. A. Miller, D. J. Kent, K. J. Boor, N. H. Martin and M. Wiedmann, "Different management practices are associated with mesophilic and thermophilic spore levels in bulk tank raw milk," *J. Dairy Sci.* 98:4338–4351. 2015.
- [7] L. A. Nero, F. De Carvalho, "Raw Milk, Balance Between Hazards and Benefits," Academic Press., 2019,
- [8] M. Talukder, H. M M. Ahmed, "Effect of somatic cell count on dairy products: a review," *Asian J. Med. Biol. Res.* 3 (1), 1-9, 2017.
- [9] M.J. Paape, J. Mehrzad, X. Zhao, J. Detilleux and C. Burvenich, "Defense of the bovine mammary gland by polymorphonuclear neutrophil leukocytes," *J. Mam. Gland. Biol.*, 7:109-121, 2002.
- [10] N. Sharma, N.K. Singh and M.S. Bhadwal, "Relationship of somatic cell count and mastitis: an overview," *Asian Aus. J. Anim Sci.*, 24: 429-438, 2011.

-
- [11] H. Hogeveen, K. Huijps, and T. J., "Lam, Economic aspects of mastitis: New developments," *N. Z. Vet. J.* 59:16–23, 2011.
- [12] U. Geary, N. Lopez-Villalobos, N. Begley, F. McCoy, B. O'Brien, L. O'Grady, and L. Shalloo, "Estimating the effect of mastitis on the profitability of Irish dairy farms," *J. Dairy Sci.* 95:3662–3673, 2012.
- [13] National Mastitis Council, "Guidelines on normal and abnormal raw milk based on somatic cell counts and signs of clinical mastitis," NMC, 2015.
- [14] Y. H. Schukken, D. J. Wilson, F. Welcome, L. Garrison-Tikofsky, and R. N. Gonzalez, "Monitoring udder health and milk quality using somatic cell counts," *Vet. Res.* 34:579–596, 2003.
- [15] A. Bradley and M. Green, "Use and interpretation of somatic cell count data in dairy cows," *In Pract.* 27:310–315, 2005.
- [16] International Dairy Federation, "Guidelines for the use and interpretation of bovine milk somatic cell counts (SCC) in the dairy industry," *Bulletin of the International Dairy Federation, IDF*, Brussels, 466/2013.
- [17] J. Olechnowicz and J.M. Jaskowski, "Somatic cells count in cow's bulk tank milk" *J. Vet. Med. Sci.*, 74:681-686, 2012.
- [18] D. Schwarz, U.S. Diesterbeck, S. Konig, K. Brugemann, K. Schlez, M. Zschock, W. Wolter and C.P. Czerny, "Flow cytometric differential cell counts in milk for the evaluation of inflammatory reactions in clinically healthy and subclinically infected bovine mammary glands," *J. Dairy Sci.*, 94: 5033-5044, 2011.
- [19] H. D. Norman, J. E. Lombard, J. R. Wright, C. A. Kopral, J. M. Rodriguez, and R. H. Miller, "Consequences of alternative standards for bulk tank somatic cell count of dairy herds in the United States," *J. Dairy Sci.* 94:6243–6256, 2011.
- [20] FDA, "Grade A Pasteurized Milk Ordinance," US Department of Health and Human Services. Washington, DC. 2014.
- [21] USDA-AMS, "Notice to the industry," <http://www.ams.usda.gov>, 2014.
- [22] S. J. More, T. A. Clegg, P. J. Lynch, and L. O'Grady, "The effect of somatic cell count data adjustment and interpretation, as outlined in European Union legislation, on herd eligibility to supply raw milk for processing dairy products" *J. Dairy Sci.*, 96:3671–3681, 2013.
- [23] K. M. Hunt, J. E. Williams, B. Shafii, M. K. Hunt, R. Mehre, R. Ting, M. K. McGuire and M.A. McGuire, "Mastitis is associated with increased free fatty acids, somatic cell count and interleukin-8 concentrations in human milk," *Udderfeeding Med.*, 8:105-110, 2013.
- [24] N. B. Burke, K. A. Zacharski, M. Southern, P. Hogan., M. P. Ryan and C. C. Adley, "The Dairy Industry: Process, Monitoring, Standards, and Quality," *Intech open book series*, 2018.
- [25] A. Gulati, "Effect of Dairy Cow Diets on the Composition and Processing Characteristics of Milk, Department of Chemistry," Maynooth University, Doctoral thesis, 2019.
- [26] C. Gonzalo, J. C. Boixo, J. A. Carriedo, F. S. Primitivo, "Evaluation of Rapid Somatic Cell Counters Under Different Analytical Conditions in Ovine Milk," *J. Dairy Sci.*, 87:3623–3628, 2004.
- [27] L. A. Boczek, E. W. Rice, C. H. Johnson, "Total Viable Counts | Spread Plate Technique," *Encyclopedia of Food Microbiology (Second Edition)*, 636-637. 2014.
-

-
- [28] H. Kesenkaş, Ö. Kınık, A. O. Yerlikaya, E. Özer, “Keçi sütünde somatik hücre sayısı ve malondialdehit miktarı arasındaki ilişkinin belirlenmesi,” *Ege Üniv. Ziraat Fak. Derg.*, 55 (4):397-403, 2018.
- [29] L. Bava, S. Colombini, M. Zucali, M. Decimo, S. Morandi, T. Silvetti, M. Brasca, A. Tamburini, G. M. Crovetto, A. Sandrucci, “Efficient milking hygiene reduces bacterial spore contamination in milk,” *Journal of Dairy Research*, 84 (3):322–328, 2017.
- [30] A.J. Bradley, K.A. Leach, M.J. Green, J. Gibbons, I. C. Ohnstad, D.H. Black, B. Payne, V.E. Prout and J. E. Breen, “The impact of dairy cows’ bedding material and its microbial content on the quality and safety of milk – a cross sectional study of UK farms,” *International Journal of Food Microbiology*, 269:36–45, 2018.
- [31] G. Bernes, A. Höjer, Å. Lundh, M. Johansson, K. H. Saedén, M. Hetta, Dicksved, J. Sun and D. Nilsson, “Vad påverkar mikrofloran i mjölken på gård och mejeri?,” Umeå, 2019.
- [32] O. D. Múnera-Bedoya, L.D Cassoli, P.F. Machado and M.F. Cerón-Muñoz, “Influence of attitudes and behavior of milkers on the hygienic and sanitary quality of milk,” *PLoS ONE*, 12(9), e0184640, 2017.
- [33] S.B. Skeie, M. Håland, I.M. Thorsen, J. Narvhus, & D. Porcellato, “Bulk tank raw milk microbiota differs within and between farms: A moving goalpost challenging quality control,” *Journal of Dairy Science*, 102(3), 1959–1971, 2019.
- [34] M. E. Kable, Y. Srisengfa, Z. Xue, L.C. Coates and M.L. Marco, “Viable and Total Bacterial Populations Undergo Equipment- and Time-Dependent Shifts during Milk Processing,” *Applied and Environmental Microbiology*, 85;(13), 2019.
- [35] H. Priyashantha, Å. Lundh, A. Höjer, G. Bernes, D. Nilsson, M. Hetta, K. H. Saedén, A.H. Gustafsson, and M. Johansson, “Composition and properties of bovine milk: A case study from dairy farms in northern Sweden; Part I. Effect of dairy farming system,” *Journal of Dairy Science*, 2021.
- [36] C.J. Doyle, D. Gleeson, P.W. O’Toole and P.D. Cotter, “Impacts of Seasonal Housing and Teat Preparation on Raw Milk Microbiota: a High Through put Sequencing Study,” *Applied and Environmental Microbiology*, 83 (2), 2017b.
- [37] S. D. David, “Raw milk and the first amendment: Implications for public health policy and practice,” *Public Health Reports*, 129;5, 455-457. (2014),
- [38] Anonymous, “Çiğ Sütün Arzina Dair Tebliğ,” Sayı: 30050, Tebliğ No: 2017/20, 2017.
- [39] L. Goncalves, “Total bacterial count as an attribute for raw milk quality,” *Swedish University of Agricultural Sciences, SLU* 2021:31, 2018.
-

EFFECT OF SALT CONCENTRATION ON THE STRUCTURE AND PREFERENCE OF MIHALIC CHEESE

Gokce Keser

Bursa Uludag University, Faculty of Agriculture, Department of Food Engineering,
Bursa/TURKEY
0000-0003-1611-7847

Melike Ciniviz

Bursa Uludag University, Faculty of Agriculture, Department of Food Engineering,
Bursa/TURKEY
0000-0001-6089-1659

Irmak Aral Baskaya

Bursa Uludag University, Faculty of Agriculture, Department of Food Engineering,
Bursa/TURKEY
000-0001-5475-210X

Tulay Ozcan

Bursa Uludag University, Faculty of Agriculture, Department of Food Engineering,
Bursa/TURKEY
0000-0002-0223-3807

Lutfiye Yilmaz Ersan

Bursa Uludag University, Faculty of Agriculture, Department of Food Engineering,
Bursa/TURKEY
0000-0001-9588-6200

Omer Utku Copur

Bursa Uludag University, Faculty of Agriculture, Department of Food Engineering,
Bursa/TURKEY
0000-0002-1951-7937

Ozlem Kaner

Sutas Dairy, Bursa/TURKEY

Abstract

Mihalic cheese, one of the most important traditional cheeses of Turkey, has salty, hard and hole formed properties. It is traditionally produced using sheep's milk and both by boiling the curd and maturing in brine. In the production of Mihalic cheese, salting is carried out with two or three different brine applications. In this study, pH, total dry matter, salt, textural and sensory properties were determined in Mihalic cheeses from cow's milk collected from the different artisanal producers. As a result of this study, average pH, total dry matter, salt and salt in dry matter values were determined as 5.52, 63.50% and 4.98%, 7.78%. It was determined that the removal of moisture from the curd during ripening and hardening of the cheese was directly related to the salt content and texture.

Keywords: Mihalic Cheese, Salt, Sensory, Texture

1. INTRODUCTION

It has been reported that there are more than 200 types of cheese in Turkey. The most important cheeses produced in Turkey are White Cheese, Kashar, Tulum, Mihalic, Dil, Otlu, Orgu, Cerkez, Halloumi, Lor and Civil [1], [2]. Mihalic cheese that of traditional cheese is one of the oldest cheeses produced in Turkey. It is generally produced in Bursa and Balikesir in the Marmara region and known as Maglic, Mahlic, Kelle or Manyas cheese. It is a hard cheese with a cream or yellow colour, salty and slightly acidic. It is produced both by boiling the curd and ripening in brine [3], [4]. Propionic acid bacteria constitute the dominant flora of Mihalic cheese and the cheese has characteristic 2-4 mm roundish holes due to propionic acid fermentation. Mihalic cheese are produced both raw and pasteurized sheep's or cow's milk. However, Mihalic cheese as artisanal is typically made from raw milk with spontaneous fermentation and without a starter culture. Natural microorganisms in raw milk cause spontaneous fermentation in Mihalic cheese [3]. Raw or pasteurized sheep milk is coagulated in wooden barrels called 'Polim' at 32-35°C. After coagulation, the curd is cut into the size of a grain of rice. Then, the curds are scalding gradually by adding boiling water and rested. Afterwards, the curd is transferred to a cotton cloth for whey separation. Pressure is applied to separate serum from curd in industrial production. The drained curd is cut into 3-5 kg blocks and curd is brined respectively in 15% NaCl for 2 days, 18% NaCl for 2-3 days and 22% NaCl for 2-10 days. Then cheeses are ripening in the cold room (about 3 months) (Figure 1.) [5]. Cheese ripening is influenced by the microflora of the raw milk, starter cultures, native enzymes of milk, manufacturing and ripening conditions. Cheese ripening is a complex process involving many biochemical reactions such as glycolysis, proteolysis and lipolysis. These biochemical reactions that take place during the ripening of cheese enhance the textural and sensory properties of cheese [6]–[8].

Raw milk
Renneting
Coagulation
Cutting coagulum
Adding boiling water
Mixing/scalding
Whey separation
Drainage
Cutting curd into blocks
First brine 15% brine for 2 days
Second brine 18% brine for 2–3 days
Third brine 22% brine for 2–10 days
Ripening

Figure 1. Artisanal production of Mihalic cheese [5]

Cheese salting has significant influence on cheese quality such as i: inhibition pathogenic microorganisms, and hence the safety of cheese, ii: inhibition various enzymes, enhances the syneresis of cheese curd, resulting in whey separation, enhances protein hydration which influences protein solubility and protein conformation, and iii: improve cheese texture, functionality, and flavour [9]. In this study, to determine physicochemical (pH, salt and total dry matter), textural and sensorial properties of cheese samples collected from artisanal manufacturers were investigated.

1. MATERIALS AND METHODS

In this study, Mihalic cheese samples were collected from the different artisanal producers in the Bursa-Balikesir region. Cheese samples properties are given in the Table 1. Cheeses produced using cow's milk were preferred, considering the ripening times of the selected samples or the producer difference. pH, salt, total dry matter, textural and sensory properties of Mihalic cheese samples were determined. The total dry matter and salt content of samples were measured in a Foodscan (Tekafos, Type: 78810, Serial No: 91702627; 2010) device in double parallel. Hardness values of Mihalic cheese samples were determined with TA. XTplus Texture Analyzer (Stable Micro Systems Ltd., U.K.). Sensory properties of samples were evaluated by panellists trained at Bursa Uludag University.

Table 1. Properties of Mihalic cheeses

Sample Code	Ripening Properties	Sample Code	Ripening Properties
CF-1	1.5 months	CF-6	3 months
CF-2	1.5 months	CF-7	3 months
CF-3	1.5 months	CF-8	12 months
CF-4	1.5 months	CF-9	14 months
CF-5	3 months	CF-10	15 months

2. RESULTS AND DISCUSSION

Physicochemical analysis results of Mihalic cheese samples are given in Table 2. pH values of Mihalic cheese samples was detected in the range of 5.22 ± 0.000 - 5.76 ± 0.007 . Regarding the pH, there were significant differences among the cheeses ($p < 0.01$). In previous studies, Bulut [10] reported that the average pH value of Mihalic cheeses, produced by ripening for three months from raw and pasteurized milk is 4.78. Golge and Sahan [11] reported that the pH values of different Mihalic cheeses prepared from cow and sheep milk are between 5.28 and 6.11. 15 of the cheeses, and the average pH value was determined as 5.51 [4]. These differences in pH values were thought to be due to the starter cultures present or added to the milk, depending on the use of raw or pasteurized milk [12].

Table 2. Physicochemical properties of Mihalic cheeses

Sample Code	pH	TDM (%)	Salt (%)	Salt in DM (%)
CF-1	5.70 ± 0.000^b	60.90 ± 0.057^{fg}	3.96 ± 0.014^f	6.50 ± 0.017^f
CF-2	5.62 ± 0.000^c	63.93 ± 0.106^d	3.66 ± 0.007^g	5.72 ± 0.002^g
CF-3	5.55 ± 0.010^d	61.24 ± 0.071^f	4.05 ± 0.057^f	6.61 ± 0.085^f
CF-4	5.25 ± 0.000^g	60.02 ± 0.163^h	5.93 ± 0.071^d	9.89 ± 0.091^b
CM-5	5.22 ± 0.000^h	59.44 ± 0.078^i	4.08 ± 0.042^{ef}	6.86 ± 0.062^c
CM-6	5.70 ± 0.010^b	60.81 ± 0.163^g	4.22 ± 0.042^e	6.94 ± 0.051^e
CM-7	5.48 ± 0.010^e	64.95 ± 0.099^c	7.72 ± 0.057^a	11.89 ± 0.069^a
CO-8	5.55 ± 0.000^d	68.30 ± 0.042^b	6.21 ± 0.049^c	9.08 ± 0.067^d
CO-9	5.41 ± 0.000^f	73.75 ± 0.156^a	7.12 ± 0.071^b	9.65 ± 0.076^c

CO-10	5.76±0.007 ^a	61.67±0.163 ^c	2.87±0.057 ^h	4.65±0.080 ^h
Minimum	5.22	59.44	2.87	4.65
Maximum	5.76	73.75	7.72	11.89
Average	5.52	63.50	4.98	7.78

Total dry matter (TDM) content of samples was determined as 59.44±0.078 - 73.75±0.156% (Table 2). Donmez et al. [13] reported that the dry matter ratio of Mihalic cheese as 75.50% in their study to compare different cheese types. Ozer et al. [14] determined the dry matter ratio of Mihalic cheeses, which they prepared using goat milk and ripening for three months, as 53.70-64.59%. Bulut [10] reported that the average dry matter content of Mihalic cheeses, which produced from raw and pasteurized milk and ripening for three months, was 56.19%. Mihalic cheese is ripened in brine, during ripening dry matter components (water-soluble proteins, peptides and salt) transfer into the brine. Therefore, it causes changes in dry matter. In addition, the dry matter may change with the characteristics of the raw milk used, the production method and the effect of the starter culture or existing bacterial activity [1].

The amount of salt in Mihalic cheese was determined as a minimum of 2.87±0.057% and a maximum of 7.72±0.057%. The amount of salt in dry matter was determined as 4.65±0.080 - 11.89±0.069%. In cheese technology salt affects the product characteristics, taste, aroma, surface, rind, consistency, structure of the cheese, development of microflora and proteolysis. Regarding the salt and salt in dry matter, there were significant differences among the cheeses ($p<0.01$). The highest salt and salt in dry matter content were found in sample CM-7 (7.72±0.057/11.89±0.069%). The salt content of Mihalic cheese samples prepared by Ozer et al. [14] using goat's milk and ripening for three months was determined as 3.51 - 10.06%. Bulut [10] reported that the average salt content of Mihalic cheeses, which produced from raw and pasteurized milk and ripened for three months, was 7.39%. Golge and Sahan [11] determined the salt content of different Mihalic cheeses, which they prepared using cow and sheep milk, between 3.27 - 8.18%. In studies, the amount of salt in Mihalic cheeses was determined as 5.09 - 6.73% by Ozer and Kesenkas [8] and 3.83 - 8.07% by Ozcan and Kurdal [3]. Factors affecting salt content can be explained as milk types, differences process, fermentation, brine concentration and storage conditions [9].

Table 3. Sensory and textural properties of Mihalic cheeses

Sample Code	SENSORY PROPERTIES		TEXTURE
	Appearance	Acceptability	Hardness
CF-1	7.62±0.907 ^a	8.12±1.254 ^a	1714.09±37.823 ^d
CF-2	7.98±0.976 ^a	6.80±3.824 ^a	3546.835±14.036 ^{bc}
CF-3	7.58±1.653 ^a	6.78±3.820 ^a	2784.98±67.797 ^{cd}
CF-4	7.86±0.498 ^a	6.70±3.778 ^a	4806.975±1068.035 ^b
CM-5	6.80±0.447 ^a	6.36±3.626 ^a	2634.03±166.764 ^{cd}
CM-6	7.98±0.976 ^a	8.36±1.322 ^a	3577.42±335.027 ^{bc}
CM-7	7.66±0.910 ^a	6.54±3.736 ^a	3951.19±130.291 ^{bc}

CO-8	7.20±9.000 ^a	6.18±8.800 ^a	4140.86±416.07 ^{bc}
CO-9	7.90±0.894 ^a	6.56±3.707 ^a	11009.39±1167.999 ^a
CO-10	8.06±0.684 ^a	6.78±3.826 ^a	1746.13±70.442 ^d
Minimum	6.80	6.18	1714.09
Maximum	8.06	8.36	11009.39
Average	7.66	6.92	3991.19

Sensory and textural properties of Mihalic cheeses are given Table 3. Acceptability and appearance values of samples were not significant differences among Mihalic cheeses ($p>0.01$). However, significant differences were found in the textural hardness values among the samples ($p<0.01$).

Table 4. Pearson's correlation coefficients among data of analyzed Mihalic cheeses

	Dry Matter	Salt	Salt in DM	Hardness
Dry Matter	1			
Salt	0.640**	1		
Salt in Dry Matter	0.452**	0.924**	1	
Hardness	0.807**	0.665**	0.537**	1

** Correlation is significant at the 0.01 level

Pearson's correlation coefficients among data analyzed were presented in Table 4. Dry matter of samples was highly and positively correlated with salt ($r=+0.640$, $p<0.01$), salt in dry matter ($r=+0.452$, $p<0.01$) and hardness ($r=+0.807$, $p<0.01$). Salt content of cheese samples was positively correlated with salt in dry matter ($r=+0.974$, $p<0.01$) and hardness ($r=+0.665$, $p<0.01$). In addition, positive correlation was found between salt in dry matter and hardness ($r=+0.537$, $p<0.01$).

3. CONCLUSION

In conclusion, the differences between pH, total dry matter, salt and salt in dry matter values of Mihalic cheese samples were significant. It can be thought that the differences between the characteristics of the samples are related to the type and rate of milk used in cheese making, the ripening conditions time, the salt content of the brine and the production method. The brine used in cheese production affects the taste/aroma development, textural properties and microbial activities in cheese. The separation of water from the cheese during ripening and the hardness of the cheese are directly related to the salt content of the cheeses. The presence of different starter cultures in cheese production also affects the proteolytic and lipolytic activity and this causes differences in the hardness and structure of the cheeses. In addition, the differences in the present study are due to the fact that cheeses are produced with traditional or industrial methods, with/without using starter culture, from raw/pasteurized milk.

REFERENCES

- [1] B. Bulut Solak, and N. Akin, "Determination of some properties of traditional Mihalic cheese made from raw and pasteurized cow's milk during ripening period," Middle-East Journal of Scientific Research, vol. 13, 1180–1185, 2013.

-
- [2] M. Yalman, S. O. Tepeli, and N. N. D. Zorba, "Mold flora of traditional cheeses produced in Turkey," *Turkish Journal of Agriculture Food Science and Technology*, vol. 4, 926–933, 2016.
- [3] T. Ozcan, and E. Kurdal, "The effect of using a starter culture, lipase and protease enzymes on ripening of Mihalic cheese," *Journal Dairy Technology*, vol. 65, 585–593, 2012.
- [4] S. Aday, and Y. Karagul Yuceer, "Physicochemical and sensory properties of Mihalic cheese," *International Journal of Food Properties*, vol. 17, 2207–2227, 2014.
- [5] A. A. Hayaloglu, B. H. Ozer, and P. F. Fox, "Cheeses of Turkey: 2. Varieties ripened under brine," *Dairy Science and Technology*, vol. 88, 225–244, 2008.
- [6] E. A. Foegeding, J. Brown, M. Drake, and C. R. Daubert, "Sensory and mechanical aspects of cheese texture," *International Dairy Journal*, vol. 13, 585–591, 2003.
- [7] H. H. Xu, Y. Y. He, X. H. Zhao, and T. J. Li, "Variations of Hausdorff dimension and selected textural indices of Cheddar and Gouda cheeses during storage," *International Journal of Food Properties*, vol. 16, 81–90, 2013.
- [8] E. Ozer, and H. Kesenkas, "The effect of using different starter culture combinations on ripening parameters, microbiological and sensory properties of Mihalic cheese," *Journal of Food Science and Technology*, vol. 56, 1202–1211, 2019.
- [9] P. F. Fox, T. P. Guine, T. M. Cogan, and P. L. H. McSweeney, "Fundamentals of cheese science," 2nd. ed., Newyork: Springer, 2017.
- [10] Bulut, B. Changes in chemical composition and microbial flora of Mihalic cheeses that produced from raw and pasteurize milk during ripening periods. Selcuk University, Konya, Turkey, 2006.
- [11] O. Golge, and N. Sahan, "Geleneksel yöntemle üretilen kelle peynirlerinin bazı kalite özellikleri," *Türkiye 10. Gıda Kongresi*, ss. 677–680, Erzurum, 2008.
- [12] A. R. Shahab Lavasani, M. R. Ehsani, S. Mirdamadi, and M. A. Ebrahim Zadeh Mousavi, "Changes in physicochemical and organoleptic properties of traditional Iranian cheese Lighvan during ripening," *International Journal of Dairy Technology*, vol. 65, 64–70, 2012.
- [13] M. Donmez, A. K. Seckin, O. Sagdic, and B. Simsek, "Chemical characteristics, fatty acid compositions, conjugated linoleic acid contents and cholesterol levels of some traditional Turkish cheeses," *International Journal of Food Sciences and Nutrition*, vol. 56, 157–163, 2005.
- [14] Z. Ozer, H. Aloğlu, and A. Sanlıdere, "Keci sütü kullanılarak yapılan Mihalic peynirinin özelliklerinin belirlenmesi," *SEYES Süt Endüstrisinde Yeni Eğilimler Sempozyumu*, ss. 141, İzmir, 2003.
-

THE EFFECT OF SOWING FREQUENCY ON YIELD AND YIELD COMPONENTS OF OAT CULTIVARS IN VAN ECOLOGICAL CONDITIONS

Fevzi ALTUNER

Van Yuzuncu Yil University, Gevas Vocational School, Department of Plant and Animal Production, Van-TURKEY.

ORCID: 0000-0002-2386-2450.

Mehmet ULKER

Van Yuzuncu Yil University, Faculty of Agriculture, Department of Field Crops, Van-TURKEY

ABSTRACT

In this study, it was aimed to determine the effects of three different sowing densities (350, 450 and 550 seeds/m²) on yield and yield properties of three oat cultivars (Chekota, Faikbey and Seydisehir) in Van ecological conditions in the 2009-2010 growing season. The research was carried out according to the Randomized Blocks in Split Split Plots Trial Design with three replications.

In the study, the effects of cultivars on the number of clusters per panicle (NCP) and grain yields (GY), and the effects of plant density on the number of days per panicle (NDP), the NCP, GY and total yield (TY) were found insignificant. Also, the effects of cultivars and plant density interactions on all traits were found insignificant.

The effects of plant density on panicle length (PL) were found significant ($P<0.05$). The PL varied between 23.76-25.47 cm according to the sowing density. The effects of sowing density on plant height (PH) were found very significant ($P<0.01$). The PH varied between 111.88-118.19 cm according to sowing density.

The effects of cultivars on the NDP were found to be very significant ($P<0.01$) and the NDP varied between 81.97 and 86.83 days. The effects of the cultivars on the PL were found significant ($P<0.05$) and the PL varied between 22.97-26.06 cm. The effects of cultivars on the PH were found to be very significant ($P<0.01$) and PH varied between 109.35-118.89 cm. The effects of cultivars on TY were found to be significant ($P<0.05$) and TY varied between 939.68-1028.75 kg/da. The highest TY was obtained from Seydisehir and Faikbey cultivars in the same group. The GY was found to be around 244.27 kg/da according to the general average of the cultivars and sowing densities.

According to the TY values, it was concluded that higher TY could be obtained from Faikbey and Seydisehir varieties with the lowest sowing density (350 m²) in Van conditions.

Keywords: *Avena sativa* L. Sowing density, Yield, Yield components,

INTRODUCTION

Cultivated plants have reached their present forms in more than ten thousand years (Oral, 2015). Cool climate cereals have an important place among cultivated plants in the world. Oat, on the other hand, ranks third after wheat and barley among cool climate cereals (Topal et al., 2015). Today, oats are cultivated on 9.5 million hectares, 23.1 million tons of production and 2453.1 kg/ha yield are obtained (FAOSTAT, 2019). In Turkey, which has decreased rapidly in the last 20 years, oats are cultivated on 113.2 thousand hectares of land, with a production of 314.5 thousand tons and a yield of 2780 kg/ha (TUIK, 2020).

Oat, which is generally used in animal nutrition, is also preferred in poultry farming, with its hulled structure that facilitates digestion. It is extremely nutritious as it contains approximately 3500 calories in 1 kg of grain (Topal et al., 2015). Recently, it has started to be preferred in human nutrition due to its rich dietary fiber content, amino acid diversity and β -glucan content. High nutritional value and low production cost increase the interest in oats (Mut et al., 2016) and many researches are carried out for this purpose (Yaver and Ertac, 2013).

Among the cool climate cereals, the climate demands of oats are higher. It has low resistance to drought and cold (Colville and Frey, 1986) and the desire for vernalization is evident (Kun, 1996). There is no oat production in the province of Van, which has a continental climate. However, since it is a good alternation plant, it will be a good alternative if suitable varieties are used in the province. Embedded sowing method was used in the study. Thus, the plant, which is sensitive to cold, spends the winter under snow cover and germinates in early spring (Altuner and Ulker, 2019). In this study, it was aimed to determine the effects of some oat cultivars and sowing densities on the yield characteristics in the climatic conditions of Van Province.

MATERIAL AND METHODS

The research was established in the area located at the southeast border of Van Yuzuncu Yıl University Campus area 38° 33 north latitude 43° 18 east longitude in the growing season of 2009-2010. The climate data of the research area during the season are given in Table 1 and the soil characteristics are given in Table 2.

Table 1. Climate data of 2009-2010 season*

Months	Rainfall (mm)		Average Temp. (C ^o)		Relative Humidity (%)	
	2009-2010	LTA	2009-2010	LTA	2009-2010	LTA
October	15.9	50.8	10.5	12.1	46.8	59.9
November	91.1	49.2	4.4	5	61.1	65.1
December	34.8	41.6	1.8	-0.3	63.5	69.4
January	51.6	36	0.1	-2.1	63.4	70.4
February	71.1	38.7	1.3	-0.7	65.5	71.1
March	38.3	51.9	5.7	3.4	58.9	67.4
April	46.3	55.7	8.3	8.7	62.2	62
May	69.8	42.8	13.2	13.4	61.1	57.7
June	41	17	19.7	18.9	43.6	48.7
July	10.8	8.2	23.9	22.8	34.2	43.9
Total	470.7	391.9				
Average			8.89	8.1	56	61.6

* Data from the General Directorate of Meteorology. LTA: Long Term Average

According to Table 1, there was a total of 80 mm more precipitation than the LTA average in the season 20019-2010, and it is seen that this occurs especially in the form of snowfall in winter and rain in May and June. It is understood that there is no serious deviation in the average temperature and relative humidity values during the season compared to the LTA.

Table 2. Physical and chemical properties of the soils of the trial area*

Depth (cm)	Texture Class	pH	Lime (%)	Available Phosphorus (ppm)	Total N (%)	Organic Matter (%)	Total Salt (%)
0-20	Sandy loam	7.67	12.3	0.38	0.087	1.75	0.011
20-40	Sandy loam	7.67	14.3	0.17	0.081	1.63	0.012

* Van Yuzuncu Yıl University Faculty of Agriculture Plant Nutrition and Soil Science Department Laboratory results

According to the soil analysis results in Table 2, the soil of the trial area was found to be calcareous, unsalted, slightly alkaline reaction, low organic matter content, and insufficient in terms of nitrogen and phosphorus content.

Seydisehir and Faikbey oat varieties used in the research were obtained from Konya Bahri Dagdas Agricultural Research Institute, and Chekota was obtained from the Gecit Kusagi Agricultural Research Institute. In the study, three sowing densities were applied as 350, 450 and 550 seeds/m². It was sowed in December and 10 kg/da of DAP, N-P-K (18-46-0) fertilizer was applied with sowing. In the experiment, the plots were formed 5 m in length, 6 rows and 20 cm between rows. The research, which was established according to the Randomized Blocks in Split Split Plots Trial Design with three replications. Weed control was done mechanically when necessary.

Features such as the number of days per panicle, panicle length, number of clusters per panicle and plant height were measured on 20 randomly selected plants that provided the plot average. Grain yield and total yield were obtained by harvesting the remaining area (0.8 m x 5m = 4.0 m²) by throwing 50 cm from the heads of the plots and one row from each side.

Statistical analysis of the data was performed with the IBM-SPSS (version 22.0) software program, and the comparisons between the means were carried out with the help of Duncan Multiple Comparison Test.

RESULTS AND DISCUSSION

The average values for the characteristics examined in the study are given in Table 3. In the study, the effects of cultivars on the number of days per panicle, panicle length and plant height were very significant ($P < 0.01$), and the effects on total yield were significant ($P < 0.05$). The effects of sowing frequencies on plant height were also very important ($P < 0.01$), while the effects on cluster length were significant ($P < 0.05$).

The effects of variety and sowing density interactions on all parameters were insignificant.

Table 3. Effects of sowing density on the investigated properties of oat cultivars group table*

<i>Number of Days Per Panicle (days)</i>					<i>Panicle Length (cm)</i>				
Cultivars	Sowing Densities			Means	Cultivars	Sowing Densities			Means
	D1	D2	D3			D1	D2	D3	
Chekota	81.5	81.5	82.92	81.97 B	Chekota	22.07	23.46	23.4	22.97 AB
Faikbey	87.83	86.25	86.42	86.83 A	Faikbey	24.82	26.96	26.42	26.06 A
Seydisehir	83.92	87	88.25	86.39 A	Seydisehir	24.39	26	25.67	25.35 A
Means	84.42	84.92	85.86	85.07	Means	23.76 AB	25.47 A	25.16 A	24.8
C.V. = % 5.50					C.V. = % 8.54				

<i>Number of Clusters Per Panicle (clusters/panicle)</i>					<i>Plant Height (cm)</i>				
Cultivars	Sowing Densities			Means	Cultivars	Sowing Densities			Means
	D1	D2	D3			D1	D2	D3	
Chekota	50.05	48.13	47.44	48.54	Chekota	106.25	113.29	108.52	109.35 B
Faikbey	50.74	50.65	48.63	50.01	Faikbey	113.23	121.37	119.82	118.14 A
Seydisehir	48.41	50.18	48.19	48.92	Seydisehir	116.16	119.91	120.61	118.89 A
Means	49.73	49.65	48.09	49.16	Means	111.88 B	118.19 A	116.31 A	115.46
C.V. = % 7.98					C.V. = % 7.69				

<i>Grain Yield (kg/da)</i>					<i>Total Yield (kg/da)</i>				
Cultivars	Sowing Densities			Means	Cultivars	Sowing Densities			Means
	D1	D2	D3			D1	D2	D3	
Chekota	252.4	269.1	247.21	256.24	Chekota	977.09	978.71	863.26	939.68 B
Faikbey	206.89	254.65	251.48	237.68	Faikbey	957.13	947	965.54	956.55 AB
Seydisehir	246.24	220.87	249.53	238.88	Seydisehir	1096.52	982.1	1007.62	1028.75 A
Means	235.18	248.21	249.41	244.27	Means	1010.25	969.27	945.47	975.00
C.V. = % 24.15					C.V. = % 18.60				

* There is no statistically significant difference between the values shown with the same letters in the same row and column. Sowing densities: D1: 350 seeds/m², D2: 450 seeds/m², D3: 550 seeds/ m²

Number of Days Per Panicle (day)

In the study, the effects of cultivars on the number of days per panicle were found to be statistically very significant ($P < 0.01$). According to the cultivars, the number of days per panicle varied between 81.97-86.63 days. The highest number of days per panicle were obtained from the Faikbey and Seydisehir in the same group and the lowest from the Chekota variety.

In the study, sowing frequencies did not have a significant effect on the number of days per panicle. According to the general average of sowing frequencies, the number of days per panicle was 85.07 days.

In a study (Sari et al., 2011), the number of days per panicle on oat yield components in two locations was determined between 116.0-126.0 days in location 1 and between 115.0-127.0 days in location 2. In another study (Sonmez, 2020), the number of days per panicle was determined between 131.3-145.0 days. The common feature of these studies is that they are sowed in winter. In a study sowed as a summer season (Erbas, 2012), the number of days per panicle was determined between 54.0-76.0 days. The number of days per panicles obtained in our study are longer than this. This shows that the number of days per panicle vary according to ecology.

Panicle Length (cm)

In the study, the effects of cultivars on panicle lengths were found to be very significant ($P < 0.01$). According to the cultivars, the panicle length varied between 22.97-26.06 cm. The highest panicle lengths were obtained from Faikbey and Seydisehir in the same group, and the lowest from Chekota cultivar.

In the study according to the sowing densities, the differences between the panicle lengths were found to be significant ($P < 0.05$). The panicle length varied between 23.76-25.47 cm, according to the sowing frequency. Accordingly, panicle lengths were taken from the highest frequencies of D3 and D2 in the same group and the lowest from D1 frequency.

Erbas (2012) determined the panicle lengths between 14.7-25.8 cm, according to the cultivars. Our results are similar to this study. Panicle lengths were determined by Hisir (2009) between 28.4-30.3 cm and Maral et al. (2009) determined that it varies between 27.3-33.2 cm and the difference between them is significant. Our results are lower than these studies.

Number of Clusters Per Panicle (clusters/panicle)

In the study, the effects of cultivars and sowing frequencies on the number of clusters per panicle were insignificant. According to general averages of the varieties and the planting density, the number of clusters per panicle were 49.16 clusters/panicle

Number of clusters per panicle in one study (Erbas, 2012) varied between 9.4-49.8 clusters, and in another study (Sari, 2012) found between 38.3-46.4 clusters in location-1 and 41.3-44 clusters in location-2 according to the averages of two years. Contrary to our results, the differences between the number of clusters per panicle were found to be significant, in these two studies.

Plant Height (cm)

In the study, the effects of cultivars on plant height were found to be very significant ($P < 0.01$). Plant heights varied between 109.35-118.89 cm, according to the cultivars. The highest plant heights were obtained from the Seydisehir and Faikbey in the same group, and the lowest from the Chekota cultivar.

The effects of sowing frequencies on plant height were found to be very significant ($P < 0.01$). According to planting frequency, plant heights varied between 111.88-118.19 cm. The highest plant heights were obtained from D2 and D3 frequencies in the same group, and the lowest from D1.

The results of our research were similar to Dumlupınar et al. (2016) (103-151 cm). Our results are higher than the data determined by Erbas (2012) (66.0-109.2 cm).

Grain Yield (kg/da)

There was no significant effect of cultivars and planting frequency on grain yield. According to the general averages of the varieties and of sowing density, grain yield was 244.27 kg/da. Contrary to our results, in some studies (Dumlupınar et al., 2016; Mut et al., 2016) it was determined that according to varieties, the differences between grain yields are significant.

Total Yield (kg/da)

In the study, the effects of cultivars on total yield were found to be significant ($P < 0.05$). According to the varieties, the total yields were between 939.68-1028.75 kg/da. The highest total yields were obtained from Seydisehir and lowest Chekota cultivars.

Sowing frequency did not have a significant effect on total yield.

Our results lower than data of total yields determined by Maral et al. (2013), Hısır (2009) and Sabanduzen and Akcura (2017), (1531, 1512.85 and 1874.0 kg/da, according to the averages respectively).

CONCLUSION

The effects of the oat varieties used in the study and the sowing frequency applied on the investigated characteristics are listed below.

Oat varieties and sowing density interactions did not have any significant effect as statistically on the examined properties.

The effects of the cultivars on the number of days per panicle, panicle length and plant height were statistically very significant ($P < 0.01$), while the effects on the total yield were significant ($P < 0.05$). The effects on the grain yield and the number of clusters per panicle were insignificant. According to the cultivars, the number of days per panicle varied between 81.97-86.39 days and the highest was obtained from Faikbey and Seydisehir cultivars in the same group. According to the cultivars, the panicle lengths varied between 22.97-26.06 cm and the highest were taken from Faikbey and Seydisehir cultivars in the same group. The plant heights of the cultivars varied between 109.35-118.89 cm and the highest were obtained from Seydisehir and Faikbey cultivars in the same group. According to the cultivars, the total yields ranged between 939.36-1028.75 kg/da and the highest total yields were obtained from Seydisehir cultivars.

The effect of sowing frequency on plant height was statistically very significant ($P < 0.01$), while the effect on panicle length was significant ($P < 0.05$). Apart from these, the effects of sowing frequencies on other parameters were insignificant. According to the cultivars, the panicle lengths varied between 23.76-25.47 cm and the highest were taken from frequencies of 450 and 550 seeds/m², in the same group. According to the cultivars, plant heights varied between 111.88-118.19 cm and the highest were obtained from frequencies 450 and 550 seeds/m², in the same group.

According to the general average of the variety and planting density, grain yield was 244.27 kg/da. When evaluated together grain yield with the total yield, it has been seen that a satisfactory product can be obtained with the oat varieties used in the research and the embedding sowing method and with sowing frequency of 350 seeds/m² in Van ecological conditions.

ACKNOWLEDGEMENT

This research was created from the PhD. thesis of Fevzi ALTUNER, which was supported by the project "Van YYU BAP 2010-FBE-D125".

REFERENCES

- Altuner, F., Ulker, M. (2019). The Effect of Different Sowing Frequencies and Nitrogen Fertilizer Doses on Yield and Yield Components in Oat (*Avena sativa* L.). Academic Studies on Natural and Health Sciences, 1(23): 299-319.
- Colville, D. C., Frey, K. J. (1986). Development rate and growth duration of oats in response to delayed sowing. Agronomy journal, 78(3), 417-421.

- Dumlupinar, Z., Ercan, K., Tekin, A., Herek, S., Kurt, A., Kecec, E., Olgun, M., Dokuyucu, T., Akkaya, A. (2016). Performances of the local oat lines in Kahramanmaraş conditions. Kahramanmaraş Sutcu Imam University Journal of Natural Sciences, 19 (4): 438-444.
- Erbas, O. D. (2012). Determination of Agricultural and Some Quality Traits of Oat (*Avena sativa* L.) Genotypes (master's thesis, unpublished). Bozok University, Institute of Science and Technology, Yozgat.
- FAOSTAT (2019). World Oat Production Information for 2019. <http://www.fao.org/faostat/en/#data/QCL> (Accessed on 29.07.2021).
- Hisir, Y. (2009). Determination of Genetic Differences and Progression of Turkey Oat Genotypes in Terms of Physiological, Morphological and Agricultural Characteristics (PhD thesis, unpublished). Sutcu Imam University, Institute of Science and Technology, Kahramanmaraş.
- Kun, E. (1996). Cereals-1 (Cool Climate Cereals). A.U. Faculty of Agriculture Publications. No:1451, Ankara. 322.
- Maral, H. (2009). The Response of Oat Varieties to Nitrogen Fertilization in terms of Grain Yield, Nitrogen Use and Yield Characteristics (master's thesis, unpublished). Sutcu Imam University, Institute of Science and Technology, Kahramanmaraş.
- Maral, H., Dumlupinar, Z., Dokuyucu, T., Akkaya, A. (2013). Response of Six Oat (*Avena sativa* L.) Cultivars to Nitrogen Fertilization for Agronomical Traits. Turkish Journal of Field Crops, 18(2): 254-259.
- Mut, Z., Erbas Kose, O., Akay, H. (2016). Grain yield and some quality characteristics of hullless oat varieties. Anatolian Journal of Agricultural Sciences, 31 (1): 96-105.
- Oral, E. (2015). The Effect of Different Plant Densities and Nitrogen Doses on Yield and Some Yield Components in Triticale (*X Triticosecale wittmack*) in Van Ecological Conditions (PhD thesis unpublished). Van Yuzuncu Yil University, Institute of Science and Technology, Van.
- Sabanduzen, B., Akcura, M. (2017). Investigation of yield and yield components of some oat genotypes in Canakkale conditions. Turkish Journal of Agriculture and Natural Sciences, 4 (2): 101-108.
- Sari, N., Imamoglu, A. (2011). Determination of advanced oat lines suitable for Menemen ecological conditions. Anadolu Journal, 21 (1): 16-25.
- Sari, N. (2012). Relationships Between Yield and Yield Components in Oat (*Avena sativa* L.) (master's thesis, unpublished). AMU, Institute of Science and Technology, Aydın.
- Sonmez, A. C. (2020). Determination of Biological Yield and Some Physiological Properties of Winter Oat (*Avena sativa* L.) Breeding Material . Journal of the Institute of Science and Technology, 10 (4), 3042-3051. DOI: 10.21597/jist.687596.
- Topal, A., Sade, B., Soylu, S., Akar, T., Mut, Z., Ayrancı, R., Sayım I., Ozkan, I., Yilmakart, M. (2015). National grain council barley - rye- oat- triticale report. http://uhk.org.tr/dosyalar/uhkarpa_kasim2015.pdf. (Access date: 10.06.2017).
- TUIK (2020). Turkey Oat Production Information for 2020. TURKSTAT. <https://biruni.tuik.gov.tr/medas/?kn=92&locale=tr> (Access date: 29.07.2021).
- Yaver, E., Ertac, N. (2013). The composition of oats, its uses in the grain industry and its effects on human health. Journal of Food and Feed Science - Technology / Journal of Food and Feed Science - Technology, 13:41-50.

THE EFFECT OF NITROGEN FERTILIZER DOSES ON YIELD AND YIELD PROPERTIES ON OAT CULTIVARS

Fevzi ALTUNER

Van Yuzuncu Yil University, Gevas Vocational School, Department of Plant and Animal Production, Van-TURKEY. ORCID: 0000-0002-2386-2450.

Mehmet ULKER

Van Yuzuncu Yil University, Faculty of Agriculture, Department of Field Crops, Van-TURKEY.

ABSTRACT

In this study, it was aimed to determine the effects of four nitrogen fertilizer doses (0, 4, 8 and 12 kg N/da) on yield and yield properties of three oat cultivars (Chekota, Faikbey and Seydisehir) in Van ecological conditions in the 2009-2010 growing season. The research was carried out according to the Randomized Blocks in Split Split Plots Trial Design with three replications. Sowing was done in December by embedding method.

In the study, the effects of cultivars on the panicle maturation time, the number of grain per panicle, plant height and thousand grain weights were very important ($P < 0.01$). The effects of cultivars on the number of panicles per squaremeter and grain yield were statistically insignificant. The effects of nitrogen fertilizer doses on the number of panicles per squaremeter were very significant ($P < 0.01$). The effects of nitrogen fertilizer doses on other parameters other than the number of panicles per squaremeter were statistically insignificant. The effects of variety and nitrogen fertilizer dose interactions on all parameters examined were insignificant.

According to the cultivars, the panicle maturation time was between 35.19-37.39 days, the number of grain per panicle was between 78.22-91.82 grains/panicle, the plant heights were between 109.35-118.89 cm, and the thousand grain weights ranged between 32.87-34.78 g. According to the nitrogen fertilizer doses, the number of panicle per squaremeter varied between 547.41-621.18 panicles/m².

According to the general averages of variety and grain yields, grain yields were 244.26 kg/da. As a result, it has been seen that Chekota, Faikbey and Seydisehir oat varieties can be grown by embedding sowing method in Van ecological conditions with the lowest nitrogen dose.

Keywords: *Avena sativa* L. Sowing density, Yield, Yield components,

INTRODUCTION

Oats ranks third in the world after wheat and barley among cool climate cereals (Topal et al., 2015). Oat, which has a cultivation area of 9.5 million ha in the world, has a production of 23.1 million tons and a yield of 2453.1 kg/ha (FAO, 2019). In Turkey, oats are cultivated on area of 113.2 thousand hectares and 314.5 thousand tons of production is carried out from here with 2780 kg/ha yield (TUIK, 2020). The lack of sufficient amount of oat varieties that are tolerant to different ecologies in Turkey is one of the important obstacles limiting its cultivation (Sari and Imamoglu, 2011).

Oat, which is generally used in animal nutrition, has recently started to be preferred in human nutrition. In addition to its rich dietary fiber and protein content, the use of oats as food, which can be consumed by people with gluten intolerance, is becoming widespread (Dumlupinar, 2010).

Nitrogen fertilization is the most important application of increasing the yield among maintenance operations, and an increase of 60% can be achieved with adequate fertilization (Sezen, 1991). Nitrogen fertilization provides a yield increase of 0.36-1.48 tons/ha, more than the number of panicle per squaremeter, in some oat varieties (Jelic et al., 2013; Huza et al., 2017; Gao et al., 2019). In addition, additional nitrogen fertilization provides additional yield increase in oats as in other grains (Hausherr et al., 2018).

Oat cultivation is not carried out in the Van province, where the typical continental climate conditions of the Eastern Anatolia Region are dominant. However, the cultivation of high-yielding varieties that are compatible with the ecology of the region will ensure that an alternative plant to barley used in animal nutrition is added to the plant pattern. In addition, oats can be used as an alternation plant in regional agriculture. In the study, it was tried to determine the changes in yield and yield components of nitrogen fertilizer doses applied to three oat varieties. Thus, besides the adaptation and performance test of oat varieties used in the province, the effects of nitrogen fertilization were determined. Due to its high sensitivity to climatic limitations (Colville and Frey, 1986), sowings were made using the embedding method.

MATERIAL AND METHODS

The research was established on the southeast border of Van Yuzuncu Yil University Campus in 2009-2010. The climate data of the province of Van for the 2009-2010 season and for Long Term Average (LTA) are given in Table 1. According to Table 1, it is seen that a total of 470.7 mm precipitation was received during the research season. This amount of precipitation is 80 mm more than the total of the LTA. It is understood that especially during the season, precipitation in November, January, February, May and June causes this excess.

It is observed that the average temperature and relative humidity average values during the season are close to the LTA (Table 1).

Table 1. Climate data of 2009-2010 season*

Months	Rainfall (mm)		Average Temp. (C ^o)		Relative Humidity (%)	
	2009-2010	LTA	2009-2010	LTA	2009-2010	LTA
October	15.9	50.8	10.5	12.1	46.8	59.9
November	91.1	49.2	4.4	5	61.1	65.1
December	34.8	41.6	1.8	-0.3	63.5	69.4
January	51.6	36	0.1	-2.1	63.4	70.4
February	71.1	38.7	1.3	-0.7	65.5	71.1
March	38.3	51.9	5.7	3.4	58.9	67.4
April	46.3	55.7	8.3	8.7	62.2	62
May	69.8	42.8	13.2	13.4	61.1	57.7
June	41	17	19.7	18.9	43.6	48.7
July	10.8	8.2	23.9	22.8	34.2	43.9
Total	470.7	391.9				
Average			8.89	8.1	56	61.6

* Data from the General Directorate of Meteorology. LTA: Long Term Average

Some physical and chemical properties of the soils of the trial area are shown in Table 2. According to the laboratory results of Van Yuzuncu Yil University Faculty of Agriculture, Department of Plant Nutrition and Soil Science, the organic matter content of the trial soils is low, phosphorus and nitrogen content is low, with slightly alkaline reaction, salt-free and lime content is high.

Table 2. Physical and chemical properties of the soils of the trial area*

Depth (cm)	Texture Class	pH	Lime (%)	Available Phosphorus (ppm)	Total N (%)	Organic Matter (%)	Total Salt (%)
0-20	Sandy loam	7.67	12.3	0.38	0.087	1.75	0.011
20-40	Sandy loam	7.67	14.3	0.17	0.081	1.63	0.012

* Van Yuzuncu Yil University Faculty of Agriculture Plant Nutrition and Soil Science Department Laboratory results

Of the oat varieties used in the research, Chekota was taken from the Gecit Kusagi Agricultural Research Institute, while Faikbey and Seydisehir were obtained from the Bahri Dagdas Agricultural Research Institute. In the experiment, 4 fertilizer applications were made as 0 (control), 4, 8 and 12 kg N/da. Sowing was done in December by embedding sowing

method. With this method, it is aimed that the seeds spend the winter under snow cover and germinate in early spring. After the diammonium phosphate DAP (N-P-K: 18-46-0) fertilizer applied with sowing, the remaining fertilizer was given in the form of 33% Ammonium Nitrate (NH_4NO_3) in the spring, except for the control plots, before the stemming period. In the experiment, the plots were set as 6 m², with a length of 5 m, 20 cm between rows and with 6 rows. The Randomized Blocks in Split Split Plots Trial Design was applied with three replications. Grain yield and total yield values were harvested from the remaining 4 m² area after 50 cm from the plot heads and one row from the sides as an edge effect. Other observations were made on 20 randomly selected plants in each plot.

IBM-SPSS (version 22.0) computer analysis program was used in the statistical analysis of the data obtained in the study. The significance of the differences between the means was determined by the Duncan Multiple Data Test.

RESULTS AND DISCUSSION

The average values of the data obtained in the study are given in Table 3. According to this, the effects of cultivars on the panicle maturation time, the number of grains per panicle, plant height and thousand grain weight were statistically very significant ($P < 0.01$). Similarly, the effects of nitrogen fertilizer doses on the number of panicles per squaremeter were very significant ($P < 0.01$), while the effects on other parameters were statistically insignificant ($P > 0.05$). The effects of variety and nitrogen fertilizer interactions on all parameters were statistically insignificant ($P > 0.05$).

Table 3. Effects of sowing density on the investigated properties of oat cultivars group table*

Panicle Maturation Time (day)						Number of Panicles Per Squaremeter (panicles/m ²)					
Cultiva rs	Nitrogen Doses				Mean s	Cultiva rs	Nitrogen Doses				Means
	N0	N4	N8	N12			N0	N4	N8	N12	
Chekot	37.4	37	37.5	37.5	37.39	Chekot	572	614.2	576	588.4	587.66
a	4		6	6	A	a		2		4	5
Faikbe	35.5	35.1	35.8	35.3	35.47	Faikbe	516.4	606.2	568.89	649.7	585.33
y	6	1	9	3	B	y	4	2		8	25
Seydis	35.7	34.8	34.4	35.6	35.19	Seydis	553.7	643.1	594.22	574.6	591.44
ehir	8	9	4	7	B	ehir	8	1		7	5
	36.2	35.6	35.9	36.1			547.4	621.1	579.70	604.2	588.14
Means	6	7	6	9	36.02	Means	1 B	8 A	AB	9 A	75
C.V. = % 5.26						C.V. = % 20.20					
Number of Grain Per Panicle (grain/panicle)						Plant Height (cm)					
Cultiva rs	Nitrogen Doses				Mean s	Cultiva rs	Nitrogen Doses				Means
	N0	N4	N8	N12			N0	N4	N8	N12	
Chekot	90.4	79.5	81.0	87.5	84.63	Chekot	110.0			108.8	109.35
a	3	9	1	1	B	a	8	110.2	108.29	4	B
Faikbe	94.7	91.8	88.1	92.5	91.82	Faikbe	117.8	116.6	120.6	117.4	118.14
y	6	4	8	2	A	y	9	1		4	A
Seydis	84.5	72.4	82.0	73.8	78.22	Seydis	117.7	120.3	116.68	120.7	118.89
ehir	3	3	9	5	C	ehir	4	9		6	A

89.9 81.2 83.7 84.6
Means 1 9 6 3 84.90
C.V. = % 13.36

115.2 115.7 115.6
Means 4 3 115.19 8 115.46
C.V. = % 7.69

Grain Yield (kg/da)						Thousand Grain Weight (g)					
Cultivars	Nitrogen Doses				Mean	Cultivars	Nitrogen Doses				Means
	N0	N4	N8	N12			N0	N4	N8	N12	
Chekota	234.32	277.91	256.17	256.53	256.23	Chekota	33.2	32.8	32.69	32.77	32.87B
Faikbey	234.93	238.79	232.09	244.9	237.68	Faikbey	34.66	33.54	35.65	35.28	34.78A
Seydisehir	247.7	255.3	227.2	225.32	238.88	Seydisehir	34.11	34.74	32.3	34.3	33.86AB
Means	238.98	257.33	238.49	242.25	244.26	Means	33.99	33.69	33.55	34.12	33.84
C.V. = % 24.15						C.V. = % 7.87					

* There is no statistically significant difference between the values shown with the same letters in the same row and column. Nitrogen doses: N0 (control), N4 (4 kg N/da), N8 (8 kg N/da), N12 (12 kg N/da)

Panicle Maturation Time (day)

In the study, according to the cultivars the differences between the panicle maturation time were found to be statistically very significant ($P < 0.01$). The panicle maturation time of the cultivars varied between 35.19-37.39 days. According to the cultivars, the highest panicle maturation time was observed in Chekota and the lowest in Seydisehir and Faikbey cultivars in the same group.

According to the nitrogen fertilizer doses the differences between the panicle maturation time were insignificant ($P > 0.05$). At the same time, according to the interactions of varieties and nitrogen fertilizer doses the differences between the panicle maturation times were insignificant ($P > 0.05$).

Similar to our findings, in a study (Tosun et al., 2010) it was determined that the panicle maturation time ranged from 27 to 57 days. In another study (Hisir, 2009), the panicle maturation times were lower than the results of our study (26.6-28.6). Similar to our research, Sonmez (2020) determined that according to genotypes the difference between panicle maturation time is significant and the panicle maturation times vary between 30.8-34.5 days.

Number of Panicles Per Squaremeter (panicles/m²)

In the study, according to the varieties the differences between the number of panicles per squaremeter were insignificant. According to the nitrogen fertilizer doses the differences between the number of panicles per squaremeter were very significant ($P < 0.01$). According to the fertilizer doses, the number of panicles per squaremeter varied between 547.41-621.18 panicles/m². The highest number of panicles per squaremeter were obtained from the N4, N8 and N12 doses in the same group and the lowest from the N0 control dose.

According to the variety and nitrogen fertilizer interactions, the differences in the number of panicles per square meter were insignificant.

Similar to our research, it was determined by Hisir (2009) that according to the varieties the difference between the number of panicles per squaremeter were insignificant and varied between 523.0-647.5 panicles/m². In some studies, data were obtained contrary to our results. Narlioglu, (2016) determined that according to genotypes the difference between the number of panicles per squaremeter were significant and varied between 206.3-503.3 panicles/m². It was determined by Maral (2009) that according to the varieties and fertilizer doses the differences between the number of panicles per squaremeter were significant and the number of clusters per squaremeter varied between 323.0-487.0 panicleless/m² according to the fertilizer doses.

Number of Grain Per Panicle (grain/panicle)

In the study, according to the cultivars the differences between the number of grains per panicle were found to be very significant ($P < 0.01$). The number of grains per panicle of cultivars were between 78.22-91.82 grains/panicle. The lowest number of grains per panicle were seen in Seydisehir and the highest in Faikbey cultivars.

According to the nitrogen fertilizer doses the differences between the number of grains per panicle were found to be insignificant.

According to the variety and nitrogen fertilizer interactions, the differences between the number of grains per panicle were also insignificant.

In some studies (Erbaş, 2012; Dumlupınar et al., 2016; Gungor et al., 2017), results similar to our research were obtained and the differences in the number of grains per panicle were found to be significant. Contrary to our research, in a study (Maral, 2009), it was determined that the effects of nitrogen fertilizer doses on the number of grains per panicle were significant and ranged from 61.0 to 84.0 grains/panicle.

Plant Height (cm)

In the study, according to the cultivars the differences between plant heights were found to be statistically very significant ($P < 0.01$). The plant heights of the cultivars were between 109.35-118.89 cm. The highest plant heights were seen in Seydisehir and Faikbey cultivars in the same group, and the lowest in Chekota cultivar.

According to nitrogen fertilizer doses there were no statistically significant difference between plant heights. The differences between plant heights were insignificant in terms of variety and nitrogen fertilizer interactions.

In some studies (Erbaş, 2012; Sari, 2012), similar results were found with our research and it was determined that according to cultivars the differences between plant heights were significant. Contrary to our research, it was determined by Maral (2009) that according to the cultivars the differences between plant heights were insignificant, but were significant for nitrogen fertilizer doses and varied between 97.7-105.6 cm.

Grain Yield (kg/da)

According to the varieties, nitrogen fertilizer doses and interactions the differences between the grain yields were insignificant.

According to the general averages of the variety and nitrogen fertilizer grain yields were 244.26 kg/da.

Contrary to our findings, in some studies (Sabanduzen and Akcura, 2017; Mut et al., 2016; Ceyhan, 2005), according to the cultivars, in another study (Maral, 2009) according to varieties and nitrogen fertilizer doses, it was found that the differences between grain yields were significant, and grain yields were found between 120.4-210.3 kg/da. Similar to our

research, it was determined by Hamill (2002) that the effects of cultivar, sowing frequency and their interactions on the differences in grain yield were statistically insignificant. In this study, it was seen that the effect of fertilizer doses on grain yield was significant only in locations with low soil nitrogen.

Thousand Grain Weight (g)

In the study, the differences between the thousand-grain weights according to the cultivars were found to be very significant ($P < 0.01$). The thousand-grain weights of the cultivars were between 32.87-34.78 g. The thousand-grain weights were highest in Faikbey and lowest in Seydisehir and Chekota cultivars in the same group.

According to the nitrogen fertilizer doses the differences between the thousand grain weights were insignificant.

According to the variety and nitrogen fertilizer interactions the differences between thousand grain weights were found to be insignificant.

Contrary to our findings, in some studies (Dumlupinar et al., 2016; Mut et al., 2016; Sari et al., 2011), it was determined that the differences between thousand-grain weights were significant. Maral et al. (2013) determined that cultivars and fertilizer doses had a significant effect on the differences between thousand-grain weights.

CONCLUSION

In this study, the effects of 0, 4, 8 and 12 kg/da nitrogen fertilizer doses applied to Chekota, Faikbey and Seydisehir oat cultivars on some yield and yield characteristics were investigated. Obtained results are given below.

According to the cultivars, the differences between the panicle maturation time, the number of grains per panicle, the plant height and the thousand grain weight were found to be very significant ($P < 0.01$). The panicle maturation time of the cultivars varied between 35.19-37 days and the highest was found in the Chekota cultivar. The number of grains per panicle varied between 78.22-91.82 grains/panicle and the highest was found in Faikbey variety. Plant heights varied between 109.35-118.9 cm and the highest were obtained from Seydisehir and Faikbey cultivars in the same group. Thousand grain weights varied between 32.87-34.78 g and the highest were taken from Faikbey variety.

The effect of nitrogen fertilizer doses on the differences in the number of panicles per squaremeter were very significant ($P < 0.01$), while the effect on other parameters were statistically insignificant. According to the fertilizer doses, the number of panicles per squaremeter varied between 547.41-621.18 panicles/m² and the highest were taken from the applications other than control dose.

The effect of cultivar and nitrogen fertilizer interactions on all parameters examined were insignificant.

According to the general average of the variety and nitrogen fertilizer doses, the grain yield was 244.26 kg/da. Considering the grain yield, it was concluded that the three oat varieties with the embedding sowing method and with the lowest fertilizer dose can be grown in Van ecological conditions.

ACKNOWLEDGEMENT

This research was created from the PhD. thesis of Fevzi ALTUNER, which was supported by the project of "Van YYU BAP 2010-FBE-D125".

REFERENCES

- Ceyhan, M. (2005). Evaluation of Some Oat Varieties in Adana and Kahramanmaras Locations in Terms of Yield and Yield Components (master's thesis, unpublished). SIU, Institute of Science and Technology, Kahramanmaras.
- Colville, D. C., Frey, K. J., (1986). Development rate and growth duration of oats in response to delayed sowing. *Agronomy journal*, 78(3), 417-421.
- Dumlupinar, Z. (2010). Characterization of local oat genotypes originating in Turkey with avenin proteins in terms of morphological, phenological and agronomic characteristics (PhD thesis unpublished). KSU, Institute of Science and Technology, Kahramanmaras.
- Dumlupinar, Z., Ercan, K., Tekin, A., Herek, S., Kurt, A., Kecec, E., Olgun, M., Dokuyucu, T., Akkaya, A. (2016). Performances of the local oat lines in Kahramanmaras conditions. *Kahramanmaras Sutcu Imam University Journal of Natural Sciences*, 19 (4): 438-444.
- Erbas, O. D. (2012). Determination of Agricultural and Some Quality Traits of Oat (*Avena sativa* L.) Genotypes (master's thesis, unpublished). Bozok University, Institute of Science and Technology, Yozgat.
- FAO (2019). World Oat Production Information for 2019. <http://www.fao.org/faostat/en/#data/QCL> (Accessed on 29.07.2021).
- Gao, K., Yu, Y.F., Xia, Z.T., Yang, G., Xing, Z.L., Qi, L.T., Ling, L.Z. (2019). Response of height, dry matter accumulation and partitioning of oat (*Avena sativa* L.) to planting density and nitrogen in Horqin Sandy Land. *Sci. Rep.* 9, 7961.
- Gungor, H., Dokuyucu, Dumlupinar, Z., T., Akkaya, A. (2017). Determination of the relationship between yield and some agricultural characteristics in oat (*Avena spp.*) by correlation and path analysis. *Journal of Tekirdag Faculty of Agriculture*, 14 (1): 61-68.
- Hamill, M. L., 2002. The effect of cultivar, seeding date, seeding rate and nitrogen fertility on oat (*Avena sativa* L.) yield and milling quality.
- Hausherr Luder, R.M., Qin, R., Richner, W., Stamp, P., Noulas, C. (2018). Spatial variability of selected soil properties and its impact on the grain yield of oats (*Avena sativa* L.) in small fields. *J. Plant Nutr.* 41, 2446–2469.
- Hisir, Y. (2009). Determination of Genetic Differences and Progression of Turkey Oat Genotypes in Terms of Physiological, Morphological and Agricultural Characteristics (PhD thesis, unpublished). Sutcu Imam University, Institute of Science and Technology, Kahramanmaras.
- Huza, R., Duda, M., Kadar, R., Racz, I., Ceclan, A. (2017). The influence of technological factors on yield and quality of spring oats at ARDS Turda. *Res. J. Agric. Sci.* 49, 80–84.
- Jelic, M., Dugalic, G., Milivojevic, J., Djekic, V. (2013). Effect of liming and fertilization on yield and quality of oat (*Avena sativa* L.) On an acid luvisol soil. *Rom. Agric. Res.* 30, 249–258.
- Maral, H. (2009). The Response of Oat Varieties to Nitrogen Fertilization in terms of Grain Yield, Nitrogen Use and Yield Characteristics (master's thesis, unpublished). Sutcu Imam University, Institute of Science and Technology, Kahramanmaras.
- Maral, H., Dumlupinar, Z., Dokuyucu, T., Akkaya, A. (2013). Response of Six Oat (*Avena sativa* L.) Cultivars to Nitrogen Fertilization for Agronomical Traits. *Turkish Journal of Field Crops*, 18(2): 254-259.
- Mut, Z., Erbas Kose, O., Akay, H. (2016). Grain yield and some quality characteristics of hullless oat varieties. *Anatolian Journal of Agricultural Sciences*, 31 (1): 96-105.

- Narlioglu, A. (2016). Evaluation of Some Oat Genotypes in terms of Yield and Quality Criteria and Silage Characteristics (master's thesis, unpublished). SIU, Institute of Science and Technology, Kahramanmaraş.
- Sabanduzen, B., Akcura, M. (2017). Investigation of yield and yield components of some oat genotypes in Canakkale conditions. Turkish Journal of Agriculture and Natural Sciences, 4 (2): 101-108.
- Sari N., Imamoglu, A. (2011). Determination of advanced oat lines suitable for Menemen ecological conditions. Anadolu, J. of AARI 21(1): 16-25.
- Sari, N. (2012). Relationships Between Yield and Yield Components in Oat (*Avena sativa* L.) (master's thesis, unpublished). AMU, Institute of Science and Technology, Aydın.
- Sezen, Y. (1991). Fertilizers and Fertilization. Ataturk University Publications No: 679. Faculty of Agriculture Publications. No:3003, Textbooks Serial No: 55, Erzurum.
- Sonmez, A. C. (2020). Determination of Biological Yield and Some Physiological Properties of Winter Oat (*Avena sativa* L.) Breeding Material . Journal of the Institute of Science and Technology, 10 (4), 3042-3051. DOI: 10.21597/jist.687596.
- Topal, A., Sade, B., Soylu, S., Akar, T., Mut, Z., Ayrancı, R., Sayım I., Ozkan, I., Yilmakart, M. (2015). National grain council barley - rye- oat- tritcale report. http://uhk.org.tr/dosyalar/uhkarpa_kasim2015.pdf. (Access date: 10.06.2017).
- Tosun, F., Sencar, O., Kirtok, Y. (2010). Micro and macro yield trials of summer oat varieties under irrigated conditions. Journal of Ataturk University Faculty of Agriculture, 13: 3-4.
- TUIK (2020). Turkey Oat Production Information for 2020. TURKSTAT. <https://biruni.tuik.gov.tr/medas/?kn=92&locale=tr> (Access date: 29.07.2021).

THE SURVEY OF WATER QUALITY BASED ON THE PHYTOPLANKTON AND SAPROBIC INDEX IN THE ZHAVEH DAM TRIBUTARIES (KURDISTAN PROVINCE, IRAN)

Makhlough A.

Caspian Sea Ecology Research Center (CSERC), Iranian Fisheries Science Research Institute (IFSRI), Agricultural Research, Education and Extension Organization (AREEO), Sari, Iran

Nasrollahzadeh Saravi H.

Caspian Sea Ecology Research Center (CSERC), Iranian Fisheries Science Research Institute (IFSRI), Agricultural Research, Education and Extension Organization (AREEO), Sari, Iran

Naderi, M.

Caspian Sea Ecology Research Center (CSERC), Iranian Fisheries Science Research Institute (IFSRI), Agricultural Research, Education and Extension Organization (AREEO), Sari, Iran

Eslami, F.

Iranian Fisheries Science Research Institute (IFSRI), Agricultural Research, Education and Extension Organization (AREEO), Tehran, Iran
ORCID:0000-0002-6798-2673

Abstract

The structure of Zhavveh Dam has been built on Sirvan River, after the cross of the two main branches of Gave-Rood and Gheshlagh Rivers, with the aim of being used in agriculture and industries. There are agricultural lands along the Gaveh-Rood branch. The Gheshlagh branch enters the dam after crossing the outskirts of Sanandaj and industrial areas and receiving various types of sewage. Due to the importance of water quality as water supply for human society, in this study, the structural pattern of phytoplankton and saprobic index based on its species in 5 stations (from upstream to the tower of Dam) are investigated. According to the results, Bacillariophyta, Cyanophyta and Chlorophyta phyla with 88, 35 and 36 species, respectively, were dominant in abundance and number of species. Maximum and minimum phytoplankton abundance was reported at station 2 (Near the wastewater treatment site) in summer (3008 million/m³) and winter (212 million/m³), respectively. While in station 1 (upstream), maximum and minimum abundance were recorded in winter (59 million/m³) and spring (30 million/m³), respectively. The number and abundance of species resistant to pollutions were higher in warm season than cold season. In station (1) the lowest value of saprobic index (1.00-2.07) and the highest quality (very little to moderate pollution) was reported in all seasons. The highest values of saprobic index were obtained at different stations in spring (<4, very severe pollution). The average saprobic index in cold seasons (autumn and winter) was lower than warm seasons. Pollution near to the treatment plant also had a severe adverse effect on water quality at following stations. In general, regardless of the change in the severity of pollution, the common pollution with organic matter in the middle class indicates the inadequate water quality in this basin.

Keywords: Phytoplankton, Biological index, Pollution, Zhavveh, Iran

MANAGEMENT OF THE FOODS SUPPLY CHAIN WITH INTO ACCOUNT HUMAN HEALTH

Fethi Boudahri

Manufacturing EnginneeringLoboratory of Tlemcen
Tlemcen, Algeria
University of Relizane, Relizane, Algeria

Abderazzak Baba Ahmed

University of Relizane, Relizane, Algeria

Rabab Boukli Hacene

Manufacturing EnginneeringLoboratory of Tlemcen
Tlemcen, Algeria

Abstract

The supply chain of agricultural products has received a great deal of attention lately due to issues related to public health. Something that has become apparent is that in the near future the design and operation of agricultural supply hains will be subject to more stringent regulations and closer monitoring, in particular those for products destined for human consumption (agri-foods). The supply chain of agri-foods, as any other supply chain, is a network of organizations working together in different processes and activities in order to bring products and services to the market, with the purpose of satisfying customers' demands. This work is concerned with the planning of a real agri-food supply chain for poultry products. For this concrete case we chose two products namely chicken and turkey-cock meat. More precisely the problem is to redesign the existing supply chain and to optimize the distribution planning. Furthermore, environmental costs of road transportation in terms of CO₂ emissions are taken into account in the computations. The proposed integrated approach permits to minimize the total costs of the agri-food supply chain not only in terms of economy but also in terms of public health (ecology). As mentioned in our paper, the entire problem is decomposed into two problems, and each sub problem is solved in sequential manner, to get the final solution. LINGO optimization solver (Version 12.0) has been used to get the solution to the problem.

Keywords: Agri_foods Supply chain; distribution network; optimization; CO₂ emissions.

1. INTRODUCTION

The term agri-food supply chains (ASC) have been coined to describe the activities from production to distribution that bring agricultural or horticultural products from the farm to the table [1]. ASC are formed by the organizations responsible for production (farmers), distribution, processing, and marketing of agricultural products to the final consumers. The supply chain of agri-foods, as any other supply chain, is a network of organizations working together in different processes and activities in order to bring products and services to the market, with the purpose of satisfying customers' demands [2]. What differentiates ASC from other supply chains is the importance played by factors such as food quality and safety [3]. Other relevant characteristics of agri-foods include their limited shelf life, their demand and price variability, which makes the underlying supply chain more complex and harder to manage than other supply chains. Agri-food supply chains (ASC) identified for two types; the first one is the supply chain of fresh agri-foods, and the second one is the supply chain for non-perishable agri-foods. Fresh products include highly perishable crops such as fresh milk, meat, fruits and vegetables whose useful life can be measured in days; non-perishable products are those that can be stored for longer periods of time such as grains, potatoes, and nuts [4]. Food safety has become the subject of significant public and regulatory attention in various countries.

Food safety is often an experience or credence attribute that consumers cannot detect through search activities prior to purchase [5]. The handling and consumption of poultry meat is recognized as a major cause of foodborne illness in humans globally particularly when eaten raw, undercooked or recontaminated and stored following cooking [17]. This implies that the traditional supply chain practices may be subject to revision and change. One of the aspects that may be the subject of considerable scrutiny is the planning activities performed along the supply chains of agricultural products. This study is an extension of other work but this time I added a special cost due to fuel during delivery of poultry products for the security of health human. The term agri-food supply chains (ASC) has been coined to describe the activities from production to

2. PROBLEM DESCRIPTION

Production-distribution networks provide an effective tool to model manufacturing and logistics activities of a firm. The production-distribution system design problem involves the determination of the best configuration regarding location, size, technology content and product range to achieve the firm's long-term goals [15].

Our problem is to determine the centroid of the cluster customers (set of retailers), and location / allocation between the slaughterhouses and the cluster customers (set of retailers).

A cluster of customers includes customers in the closest distance with a condition that the amount of demands from different customers of this customer clusters (sets of retailers) is less than the capacity of the truck transport used. We used two types of transport trucks; one capacity of 400 chickens which sum customer orders of this customer clusters is less than 400 chickens and the other 800 chickens where customer orders of the customer clusters is greater than 400 chickens and less than 800 chickens. Once the customer clusters are defined with their positions and capabilities, it remains for us to locate the different slaughterhouses and allocate the customer clusters to slaughterhouse, in such a way that capacity of vehicles (truck transport) and slaughterhouses are respected.

Assumptions

The The assumptions made in this model are given as follows:

- (1) The demand delivered to customers each day as an average of the order.
- (2) The capacity of each customer cluster (sets of retailers) must not exceed vehicles capacity.
- (3) The Processing capacity in slaughterhouses is always less than the sum of orders for each customer clusters assigned to this slaughterhouse i.
- (4) The location/allocation plan covers a planning horizon within which no substantial changes are incurred in customer demands and in the transportation infrastructure.

Model Parameters

i : Index for customers; $i \in I$,

j : Index for customer clusters; $j \in J$

k : Index for slaughterhouse; $k \in K$

l : Index for products; $l \in L$

v : Index for vehicles classified according to their authorized gross weight; $v \in V$

$I = \{1, \dots, r\}$ for Set of customers;

$J = \{1, \dots, t\}$ for Set of customer clusters;

$K = \{1, \dots, s\}$ for Set of slaughterhouses;

$L = \{1, \dots, p\}$ for Set of products;

$V = \{1, \dots, q\}$ for Set vehicles;

x_i, y_i : Geometric position of the customer i ;

x'_j, y'_j : Geometric position of the customer cluster j ;

x_k, y_k : Geometric position of the slaughterhouse k ;

n_j : Number of customers assigned to customer cluster j ;

Q_j : Capacity of a vehicle that travels to the customer cluster j ;
 D_{cli} : Demand of customer i for product l ;
 D_{clj} : Demand for a product l by the customer cluster j ;
 V_{ljk} : volume of l product shipped from customer cluster j to slaughterhouse k ;
 FC_k : Fixed cost for establishing a slaughterhouse k ;
 D_{jk} : Euclidian distance from slaughterhouse k to the centroid of customer cluster j ;
 p_l : Unit volume of the products;
 $C_{jk}^v(v; km)$: Transportation costs per kilometer from site k to site j by vehicle v . These transportation costs involve costs for operating vehicle v , infrastructures costs, fuel consumption when v is empty and tolls;
 $C_{jk}^v(v; t/km)$: Transportation costs per ton/kilometer from site k to site j by vehicle v . These costs are for fuel consumption per ton and environmental costs;
 These latter are calculated in two steps. First the emission factor per vehicle per ton. kilometer is assessed with the quantification method developed by ADEME. Then carbon dioxide emissions due to transportation are priced with the European Trading Scheme of carbon allowances on the European Energy Exchange, see [16].
 Q_{li} : Slaughterhouse Capacity i for product l ;

Decision Variables

$Y_{ij} = 1$, if the customer i is assigned to customer cluster j , $= 0$, otherwise;
 $Z_{jk} = 1$, if the customer cluster j is allocated to slaughterhouse k , $= 0$, otherwise;
 $X_k = 1$, if the slaughterhouse k is open, $= 0$ otherwise;

Model formulation

The mathematical model formulated for the minimization of Total Cost (TC) transportation in the city of Tlemcen (Algeria) (see Fig. 1) in order to cover the entire order requested. Since the problem is highly complex, it cannot be solved in a single stage.

For this purpose, the entire problem is decomposed into two problems; each problem is solved in a sequential manner, while accounting for dependence between them.

The objective criterion is decomposed into the following problems:

- (1) Capacitated Centered Clustering Problem (CCCP) [problem 1].
- (2) Location- Allocation Problem [problem 2].

2.1. Capacitated Centered Clustering Problem (CCCP)

The capacitated centered clustering problem consists in partitioning a set of n points into p disjoint clusters with a known capacity. Each cluster is specified by centroid. The objective is to minimize the total dissimilarity within each cluster, such that a given capacity limit of the cluster is not exceeded [11]. The mathematical model of CCCP is given as follows:

$$\text{Min } Z1 = \sum_{k \in K} \sum_{j \in J} \|(x_i - x'_j) + (y_i - y'_j)\|^2 Y_{ij} \dots \dots \dots (1)$$

Subject to:

$$\sum_{j \in J} Y_{ij} = 1, \forall i \in I \dots \dots \dots (1.1)$$

$$\sum_{k \in K} Y_{ij} = n_j, \forall j \in J \dots \dots \dots (1.2)$$

$$\sum_{i \in I} x_i Y_{ij} \leq n_j x'_j, \forall j \in J \dots \dots \dots (1.3)$$

$$\sum_{i \in I} y_i Y_{ij} \leq n_j y'_j, \forall j \in J \dots \dots \dots (1.4)$$

$$\sum_{j \in J} (Dc_{li} * p_l) Y_{ij} \leq Q_j \dots \dots \dots (1.5)$$

$$(x_i, y_i), (x'_j, y'_j) \in R^2, n_j \in N, Y_{ij} \in \{0,1\}, \dots \dots \dots (1.6)$$

The problem (1) aims at defining the set of customer's clusters by minimizing the total distance between these customers and the centre of the clusters. Constraints (1.2) specify that each customer is allocated to exactly one cluster. Inequalities (1.2) set the number of customers at each cluster. Constraints (1.3) and (1.4) define the geometric position of each cluster's centre. Constraint (1.5) imposes that a customer cluster must be less than the capacity of truck transportation and Constraints (1.6) define the space boundaries for the set of parameters and variables of the problem. It should be stressed that after the customers have been grouped into clusters, begins a second step calculation during which they have to be allocated to the slaughterhouses to be opened.

2.2. Location- Allocation Problem

The objective of the problem (2) is to minimize the cost function composed of fixed and variable costs. The fixed costs are linked to the opening of slaughter- houses and include investment costs for the land, the land tax and the slaughter units. The variable costs include the economics well as the ecological transportation costs.

The mathematical model is given as follows:

$$\text{Min} Z_2 = \sum_{k \in K} FC_k X_k + \sum_{l \in L} \sum_{v \in V} \sum_{i \in I} \sum_{k \in K} (C_{jk}^{v;km} + C_{jk}^{v;km,t}) V_{ljk} D_{jk} Z_{jk} \dots (2)$$

Subject to:

$$\sum_{i \in I} Z_{jk} = 1, \quad \forall j \in J \dots \dots \dots (2.1)$$

$$\sum_{i \in I} V_{ljk} * Z_{jk} = Dc_{lj}, \forall l \in L, \forall j \in J \dots \dots \dots (2.2)$$

$$\sum_{j \in J} V_{ljk} \leq Q_{lk} X_k, \forall l \in L, \forall k \in K. \dots \dots \dots (2.3)$$

$$V_{ljk} \geq 0, \forall l \in L, \quad \forall j \in J, \forall k \in K \dots \dots \dots (2.4)$$

$$Z_{ij} \in \{0,1\} \dots \dots \dots (2.5)$$

$$X_i \in \{0,1\} \dots \dots \dots (2.6)$$

The objective function (2) minimizes total costs, which are the sum of fixed facility costs and total demand weighted distance multiplied by the cost per unit distance per unit demand.

Constraint (2.1) assumes that each customer cluster j (sets of retailers) is assigned to exactly one slaughterhouse i . Constraint (2.2) states that customer cluster j (sets of retailers) can only be assigned to open slaughterhouse. Constraint (2.3) ensures that the sum of demands covered by the slaughterhouse i does not exceed the maximum capacity of this slaughterhouse. Constraint (2.4) guarantee non negativity of the products flows.

Constraints (2.5) and (2.6) impose binary conditions.

The objective criterion of the model is considered as the minimization of total cost, which is nothing but the summation of objectives of the above two sub problems or the summation of all above costs which is given as follows:

$$\text{Min } Z = Z_1 + Z_2$$

3. METHODOLOGY AND RESULTS

As mentioned earlier, the entire problem is decomposed into two problems; each problem is solved in sequential manner, to get the final solution. Optimization Branch & Bound solver has been used to get the solution to the problem.

The inputs to the phase 1 or CCCP are the coordinates of locations of customer's i (x_i, y_i), The input data can be taken from the small sized benchmark problems. For this, we used AutoCAD software to position the different customer. After solving phase 1 with the objective of minimization of total cost (Z_1), we can get the centroid of each customer clusters with their coordinates (x'_j, y'_j), total number of customers assigned to each customer cluster (n_j). These results (output phase1) are configured in the table I.

The output of phase 1 along with the coordinates of locations of slaughterhouse (x_k, y_k), fixed cost for establishing a slaughterhouse k (F_{Ck}), capacity of a slaughterhouse i (Q_i) and the distance from slaughterhouse k to centroid of each customer clusters j (D_{ij}) will become the input to the Phase 2 and it has been assumed that the number of slaughterhouses is equal to the integer part of total number of customer clusters.

After solving phase 2 with the objective of minimization of total cost (Z_2), we can get location of slaughterhouses needed to cover the total demands of customer cluster j and allocated slaughterhouses k to customer cluster j , in such a way that capacity of vehicles and slaughterhouses are respected. These results (output phase2) are presented in the table II.

Table 1. Result Of Problem 1

Cluster N°	n_j	Cluster's centre position	Assigned customers number
1	1	(8819.19 ; 5632.02)	5
2	1	(8854.72 ; 5646.22)	7
3	1	(8856.22 ; 5617.00)	6
4	1	(8880.51 ; 5638.30)	8
5	8	(7758.02 ; 6679.99)	3/4/11/17/18/102/103/104
6	12	(9007.11 ; 6033.94)	10/12/13/14/15/16/20/88/89/90/91/105
7	8	(7540.73 ; 6046.07)	1/53/54/56/57/58/59/112
8	0	/	
9	7	5112.69 ; 5767.09)	46/64/66/67/68/69/70
10	8	(7568.44 ; 5825.43)	2/9/19/49/51/52/55/60
11	10	(10043.23 ; 9490.09)	79/80/81/82/83/84/92/93/94/95
12	8	(7478.42 ; 5177.42)	23/26/30/32/33/34/50/111
13	5	(7146.53 ; 5353.10)	21/22/27/47/65
14	10	(7532.64 ; 4847.30)	24/25/28/29/31/35/36/37/38/48
15	0	/	
16	12	(10685.80 ; 9767.27)	71/72/73/74/75/76/77/78/85/86/87/110
17	10	(7726.06 ; 9343.55)	96/97/98/99/100/101/109
18	10	(6974.03 ; 4724.97)	39/40/41/42/43/44/45/61/62/63
19	1	(747842 ; 5177.42)	113

Table 2. Result Of Problem 2

Slaughterhouse number	Location decision	Allocated cluster number	Corresponding capacity for Product1 product2	
1	opened	2	680	20
		3	680	20
		11	420	16
		13	375	19
		14	395	21
		16	395	15
		19	454	05
2	closed	none	0	0
3	opened	12	380	19
		18	340	28
4	closed	none	0	0
5	opened	1	680	20
		9	405	16
6	closed	none	0	0
7	opened	4	680	20
		5	370	24
		6	430	10
		7	400	19
		10	380	22
		17	295	14

4. CONCLUSION

In recent years, many companies (production or service) are trying to reactivate their logistics networks.

The objective of this work is to reform the distribution network of chicken meat in city of Tlemcen, because of different retailers claim on the market instability of the chicken's meat (prices, lags behind the delivery, food safety ...).

To this aim, a two step mathematical model has been built and solved in a sequential manner. Once the customers have been grouped into clusters, the slaughterhouses to set up, to close or to reopen have been located, and the clusters of retailers have been allocated to them. LINGO 12 has been used to solve the three programs and to obtain exact solutions by using Branch and Bound with default parameters of the solver.

The encouraging results obtained in this work, suggest devoting our further research activities to:

- Introduce the vehicle routing to optimize the transportation problem for each cluster.
- Apply other methodologies such as heuristics and meta-heuristics to solve real life problems where size is important

REFERENCES

- [1] Performance indicators in agri-food production chains. In: Quantifying the Agri-Food Supply Chain. Springer, Netherlands (Chapter 5), pp.49–66
- [2] Christopher. M., 2005. Logistics and Supply Chain Management. Prentice Hall, London.
- [3] Salin, V., 1998. Information technology in agri-food supply chains. International Food and Agribusiness Management Review 1 (3), 329–334.
- [4] Omar ahumada and al, application of planning models in the agri-food supply chain : A review, European journal of operational reseearch 195(2009) 1-20.
- [5] E. Tsola, E.H. Drosinos, P. Zoiopoulos , Impact of poultry slaughter house modernisation and updating of food safety management systems on the microbiological quality and safety of products, Food Control 19 (2008) 423–431.
- [6] Abdullah Dasci, Vedat Verter, A continuous model for production±distribution system design, European Journal of Operational Research 129 (2001) 287±298.
- [7] European Energy Exchange, <http://www.eex.com/en/>
- [8] P. Whytea,, K. McGilla, C. Monahanb, J.D. Collinsa; The effect of sampling time on the levels of micro-organisms recovered from broiler carcasses in a commercial slaughter plant; Food Microbiology 21 (2004) 59–65

SOCIO-DEMOGRAPHIC AND PRODUCTION STRUCTURES OF POMEGRANATE PRODUCING ENTERPRISES IN HATAY

Zeynep DEMETGÜL

Hatay Mustafa Kemal Üniversitesi Rektörlüğü Strateji Geliştirme Daire Başkanlığı.

Antakya, Hatay/TÜRKİYE

Orcid no: 0000-0001-7121-416X

Dr. Öğr.Üyesi Nuran TAPKI

Hatay Mustafa Kemal Üniversitesi Ziraat Fakültesi Tarım Ekonomisi Bölümü.

Antakya, Hatay/TÜRKİYE

Orcid no: 0000-0001-5044-795X

ABSTRACT: The aim of this study was to determine the socio-demographic structures of pomegranate fruit producers with problems that arise during production and suggesting solutions in Hatay, Turkey. The amount of pomegranate production in Hatay province was 23,766 tons and the planting area was 13,811 decares in 2019 (TUIK, 2020). Hatay province met 4.25% of Turkey's total pomegranate production in 2019. The districts of Kırıkhan, Hassa, Antakya, Yayladağı and Arsuz, where pomegranate production is most intense in Hatay province. Data were collected by face-to-face interviews with a total of 63 pomegranate producers. It has been observed that fruit planting area in Hatay has increased by 33% since 2005. Between 2005 and 2019 years, the yield increased by 48% and the production amount increased by 4.96 times. The examined enterprises were divided into three different groups according to the size of the pomegranate planting area. 22.20% of the farmers were women and 77.80% were men. 95.20% of the entrepreneurs were between 15-64 ages and 4.80% were between 65 and over ages. The average number of family members in enterprises was determined as 4.68 people. The average experience of farmers was 19.21 years. Eleven entrepreneurs (17.46%) were university graduates and three of them were college graduates. Business owners consisted of the highest secondary and high school graduates with a proportional share of 39.68%. Five percent of them were uneducated. While 23.80% of enterprises kept records for the production, 76.20% did not. Record keeping in the enterprises was in the form of bookkeeping and was not a professional qualification. While 24 of the operators did animal production besides plant production, 39 did not. The average pomegranate planting areas was calculated for first, second and third group enterprises as 2.5, 19.30 and 88.66 decares, respectively. While the total land size of the enterprises was 32.83 decares, the average pomegranate production area was 15.77 decares. The share of pomegranate planting area in the total planting area of the enterprises was 48.03% proportionally. The average number of parcels in the examined enterprises was 2.27. There was no sharecropping was found in the first and second group enterprises. Partnership was carried out in only one enterprise from the third group of enterprises. While corn ranks first in the plant productin of enterprises, pomegranate ranks fourth. 52.38% of the enterprises obtained the saplings from their own gardens, 23.81% from private nurseries, 6.35% from the Provincial and District directorates of the Ministry of Agriculture and Forestry, and 17.46% from other pomegranate producers. 77.78% of the producers used regularly chemical fertilizer. While 77.78% of the enterprises used chemical medicine regularly, 22.22% did not used. While drip irrigation or flood irrigation was used in enterprises, there were enterprises that did both. 25.40% of the enterprises were drip irrigation, 60.32% were flood irrigation and 14.28% were irrigation in both irrigation methods. The entrepreneurs stated that the cost of

garden maintenance was high. Finding workers for maintenance was one of the biggest problems. Therefore, enterprises generally employed Syrian refugees as workers. Two of the enterprises were members of an organization related to pomegranate cultivation. The 22.22% of the enterprises has benefited from diesel support and 19.05% of enterprises has benefited fertilizer, and fodder crops supports. Operators agree that pomegranate fruit was a profitable product recently. The entrepreneurs stated that growing first quality products was especially important for the exporting and they faced problems such as chemical medicine, harvesting, irrigation, fertilization, maintenance, and sapling supply. 49 of the farmers stated that they had problems with the supply of saplings. 57.14% of the farmers had problems for the supplying of high quality seedlings. 30.61% of the farmers had high seedling prices, 8.16% of them stated that they had problems with the name of the varieties and 4.08% of them had problems due to the supply of high-yield seedlings. 34.88% of the enterprises had high irrigation costs and 65.11% had water shortage problems. 64.15% of enterprises considered high labor costs as an important problem. There were some problems related to harvesting processes in the enterprises. Forty-nine enterprises had harvesting problems. 51.02% of enterprises indicated that the problem of loss in harvest, 20.41% of them not being able to harvest on time, and 28.57% of them had high harvest cost problem. The producers stated that the inputs used in pomegranate production were very high, prices of fruit were low. It has been observed that there was a lack of knowledge in product breeding. It has been observed that especially the criteria for first quality product cultivation were not known. For this reason, it was necessary to increase the knowledge level of producers about pomegranate production and to be trained. Supports to be made by the state in pomegranate production could be positive for the production and productivity increase. It has been observed that pomegranate fruits and its products were rising value worldwide. The results revealed that pomegranate production will become more widespread in the coming years in the Hatay province, if the cost was reduced, the sales price was increased to an appropriate level, the quality and affordable saplings were supplied and the lack of knowledge of the producers was eliminated. Because, Hatay province has suitable geographical location and is a gastronomy city in Turkey.

Keywords: Turkey, Hatay province, pomegranate, enterprises, production, socio-demographic

References

TÜİK (2020). Turkish Statistical Institute (TSI). <http://www.tuik.gov.tr/> (access date 15 January 2020).

ACKNOWLEDGE

This study was produced from a Master's thesis and was supported by Hatay Mustafa Kemal University Scientific Research Projects Coordinatorship (Project No: 20.YL.034).

EVALUATION OF CHROMIUM CONTAMINATION ON AGRICULTURAL SOIL AND ON DURUM WHEAT

Baba Ahmed Abderrazzak

Ahmed Zabana university, Relizane, Algeria
Laboratory of Inorganic Chemistry and Environment, Department of
Chemistry, Faculty of Sciences, University of Tlemcen, Algeria

Boudahri Fethi

Ahmed Zabana university, Relizane, Algeria

Tabti Affaf

Ahmed Zabana university, Relizane, Algeria

Abstract

The goal of this work is therefore to determine the impact of chromium from the agricultural soil to the roots, then the aerial parts of the durum wheat during different seasons. This soil is irrigated by water laden with heavy metals, sewage wastewater and thus atmospheric emissions from the roads of the city Hammam Bouhrara located 35km from the city of Tlemcen and this through a multidisciplinary approach such as:

- Physical parameters by particle size analysis of the durum wheat soil.
- The physico-chemical conditions of the soil.
- Determine the total chromium contents present in the soil by sequential extraction according to Tessier and in the different organs of the durum wheat by extraction with aqua regia.

The extraction carried out on the ground showed total contents higher than the limit standards, thus generating an accumulation by chromium.

As for cultivated durum wheat, the study indicates a significant accumulation, particularly in grains and to a lesser extent in stems and leaves.

Keywords: Durum wheat, soil contamination, sequential extraction, chromium.

ARTIFICIAL RAIN ON THE VERGE OF DROUGHT**Prof. Dr. Ahmet ÖZTÜRK**

Ankara University, Faculty of Agriculture, Department of Farm Structures and Irrigation,
Ankara, Turkey. Orcid ID: 0000-0003-0201-1726

Dr. M. Sevba ÇOLAK

Ankara University, Faculty of Agriculture, Department of Farm Structures and Irrigation,
Ankara, Turkey. Orcid ID: 0000-0003-4752-6491

ABSTRACT

The rate of usable fresh water resources in total water is below 1% in the world. The water need of humanity is met with this small ratio. However, this water is not homogeneously distributed on the earth and shows significant changes on the basis of regions and countries. Our planet is getting warmer day by day due to global warming. The warming atmosphere causes more evaporation of water on earth. As a result, water resources are decreasing in many arid and semi-arid climate regions and even some lakes are drying up.

Ensuring the continuity of water resources is an important problem for countries. Many countries in the world are struggling against drought seriously. Water supply is the main problem of some countries. Under these conditions, each country takes various steps and conducts research for the safety of its own water resources.

Precipitation is the most important parameter for the security of water resources of countries. However, in order for precipitation to occur, there must first be moisture in the air and then successively cooling, condensation, growth of droplets and feeding of clouds with new clouds. The reason for the low precipitation in many parts of the world is not only the lack of moisture, but also the absence of cooling and condensation even though there is humidity.

Drought is defined as a type of natural disaster that can recur, spread over one or more seasons, occur due to decreasing precipitation and increasing temperatures, and affect all natural resources depending on the presence of water. The absence of drought depends on regular and sufficient rainfall. In order to be protected from the negative effects of drought, the best way to benefit from the precipitation is taken all over the world. For this purpose, techniques such as the construction of storage structures for the storage of water during its existence, rainwater harvesting, artificial rain, and moisture extraction from the atmosphere are applied.

Artificial rain is a method in which other necessary conditions for precipitation are met and precipitation is triggered when there is moisture in the air. Artificial rain is a method used not only for water supply, but also to help extinguish fires, disperse fog in airports, obtain energy or prevent heavy rains that may occur.

The main purpose of creating artificial rain is to create an artificial cooling and distribute the condensation nuclei to the environment in a way that eliminates the situation where there is no cooling in the air, or there is no condensation nuclei, although there is no condensation.

The seeding process of clouds can be achieved by plane, balloon, rockets, sending from the ground or more recently, drones. Whatever method is applied, the main purpose is to spread the seed (silver iodide) to the most suitable place in the cloud.

In this study, issues such as drought, precipitation, the formation of precipitation are mentioned and information about artificial rain applied in areas where precipitation is not sufficient is given. What the artificial rain technique is, for which purposes it is applied and how it is applied are explained in detail. In addition, information is given about the possibility of artificial rain to be a solution for drought.

Precipitation produced by cloud seeding is actually taken from the potential of a possible precipitation. Artificial rain techniques do not convert moisture that will never fall into precipitation. The obtained precipitation is the moisture present in the cloud that will already become precipitation when natural conditions allow. In this respect, when evaluated globally, the water provided by artificial rain is actually a rain stolen from the future.

Since the cloud will disappear as a result of the conversion of the existing cloud to water with artificial rain, the water supply will never be continuous. If there was a technology such as transferring the clouds in humid regions to arid regions, in this case, water supply in arid regions could be provided continuously with artificial rain and drought could be prevented. With current technology, artificial rain will never be an effective method of drought prevention due to the lack of clouds.

KURAKLIĞIN EŞİĞİNDE YAPAY YAĞMUR

ÖZET

Dünyamızda bulunan kullanılabilir tatlı su kaynaklarının toplam su içindeki oranı % 1 den azdır. İnsanlığın tüm su ihtiyacı bu küçük oran ile sağlanmaktadır. Ancak bu su yeryüzüne homojen dağılmamış olup, bölgeler ve ülkeler bazında önemli değişim göstermektedir. Dünyamız küresel ısınma nedeniyle her geçen gün ısınmaktadır. Isınan atmosfer yeryüzündeki suların daha fazla buharlaşmasına neden olmaktadır. Bunun sonucu olarak birçok kurak ve yarı kurak iklim bölgesinde su kaynakları azalmakta hatta bazı göller kurumaktadır.

Su kaynaklarının devamlılığını sağlamak ülkeler açısından önemli bir sorundur. Dünya da birçok ülke kuraklığa karşı ciddi mücadele vermektedir. Su temini bazı ülkelerin en temel sorunu durumundadır. Bu şartlar altında her ülke kendi su kaynaklarının güvenliği için çeşitli adımlar atmakta ve araştırmalar yürütmektedir.

Yağış ülkelerin su kaynaklarının güvenliği için en önemli parametredir. Ancak yağışın oluşması için öncelikle havada nem bulunması ve bundan sonra ardı ardına soğuma, yoğunlaşma, damlacıkların büyümesi ve bulutların yeni bulutlarla beslenmesi gibi olayların oluşması gerekmektedir. Dünyanın birçok yerine az yağış düşmesinin sebebi sadece nem eksikliği olmayıp, nem olduğu halde soğuma ve yoğunlaşmanın olmamasıdır.

Kuraklık, tekrar edebilen, bir veya birden çok mevsime yayılan, azalan yağışlar ve artan sıcaklıklar nedeniyle oluşan ve su varlığına bağlı olarak tüm doğal kaynakları etkileyen bir doğal afet türü olarak tanımlanmaktadır. Kuraklığın ortaya çıkmaması düzenli ve yeterli miktardaki yağışlara bağlıdır. Kuraklığın olumsuz etkilerinden korunmak için, bütün dünyada yağışlardan en iyi ölçüde yararlanma yoluna gidilmektedir. Bu amaçla, suyun var olduğu dönemde depolanması için depo yapılarının inşaa edilmesi, yağmur suyu hasadı, yapay yağmur, atmosferden nem sağımı gibi teknikler uygulanmaktadır.

Yapay yağmur, havada nem bulunduğu durumda, yağış için gerekli diğer şartların sağlandığı ve yağışın tetiklendiği bir yöntemdir. Yapay yağmur sadece su temini için değil, yangınların söndürülmesine yardımcı olmak, hava alanlarında sisin dağıtılması, enerji elde etmek ya da oluşabilecek şiddetli yağışları engellemek amaçlarıyla başvurulmuş bir yöntemdir.

Yapay yağmur oluşturmada asıl amaç, havada bulunan ancak soğumanın olmaması veya soğuma olduğu halde yoğunlaşma çekirdekleri bulunmadığı için yoğunlaşmanın gerçekleşmemesi durumunu ortadan kaldıracak şekilde, suni bir soğuma yaratmak ve ortama yoğunlaşma çekirdekleri dağıtmaktır.

Bulutların tohumlama işlemi, uçakla, balonla, roketlerle, yeryüzünden göndererek ya da son zamanlarda dronlarla sağlanabilmektedir. Hangi yöntem uygulanırsa uygulansın temel amaç tohumlayıcının (gümüş iyodür) bulut içerisinde en uygun yere yayılımıdır.

Bu çalışmada kuraklık, yağış, yağış oluşumu gibi konulara değinilmiş ve yağışın yeterli olmadığı alanlarda başvurulmuş yapay yağmur hakkında bilgiler verilmiştir. Yapay yağmur tekniğinin ne olduğu, hangi amaçlar için başvurulduğu, nasıl uygulandığı ayrıntılı anlatılmıştır. Ayrıca yapay yağmurun kuraklık için çözüm olabilme imkanı hakkında bilgiler verilmiştir.

Bulut tohumlama yapılarak yağdırılan yağış aslında yağabilecek bir yağışın potansiyelinden alınmaktadır. Yapay yağmur teknikleri hiçbir zaman asla düşmeyecek bir nemi yağış haline çeviriyor değildir. Yani indirilen yağış, bulutta mevcut olan ve doğal şartlar elverdiğinde zaten yağış haline gelecek olan nemdir. Bu açıdan tüm dünya bir bütün kabul edildiğinde, yapay yağmur ile temin edilen su aslında gelecekte günümüze çalınan bir yağıştır.

Mevcut bulutun yapay yağmur ile suya dönüştürülmesi sonucunda bulut ortadan kaybolacağı için, yapay yağmur ile su temini asla sürekli olmayacaktır. Nemli bölgelerdeki bulutların, kurak bölgelere nakledilmesi gibi bir teknoloji olsaydı, bu durumda kurak bölgelerde sürekli olarak yapay yağmur ile su temini sağlanabilir ve kuraklığın önüne geçilebilirdi. Mevcut teknolojisiyle yapay yağmur, bulut yetersizliğinden dolayı, asla kuraklık önlemede etkili bir yöntem olmayacaktır.

1. GİRİŞ

Dünyamızda bulunan kullanılabilir tatlı su kaynaklarının toplam su içindeki oranı % 1 den azdır. İnsanlığın tüm su ihtiyacı bu küçük oran ile sağlanmaktadır. Ancak bu su yeryüzüne homojen dağılmamış olup, bölgeler ve ülkeler bazında ciddi bir değişim göstermektedir. Ülkelerin sahip olduğu su kaynakları ya kişi başına düşen miktar ya da toplam miktar olarak verilmektedir. Kişi başına düşen miktarlara göre en şanslı ülke düşük nüfusundan dolayı

İzlanda iken, toplam miktar açısından en şanslı ülke Kanada'dır. Kanada o kadar fazla miktarda tatlı suya sahiptir ki; bu miktar diğer bütün ülkelerin sahip olduğundan fazladır. Yani dünyadaki tatlı ve kullanılabilir suyun yarısından fazlasına Kanada sahiptir. Bu dağılım bozukluğu o kadar kötüdür ki; dünyada en fazla ve en az suya sahip ülkelerin su oranları 10 bin kata kadar varabilmektedir. Bu dağılıma etkili en önemli parametre ülkenin bulunduğu coğrafi bölgedir.

Dünyamızın sıcaklığı son yüz yılda 1.5 derece kadar artmıştır. Bu artışa neden olan en önemli etken atmosferde yer alan sera gazı dediğimiz gazların miktarının artmış olmasıdır. Güneşten gelen ışınlar daha yeryüzüne ulaşmadan bu gazlar tarafından tutularak ısı enerjisine çevrilmekte ve atmosferin ısınması sağlanmaktadır. Isınan atmosfer nedeniyle yeryüzünden buharlaşma artmakta, bu durum da ardından kuraklığı getirmektedir. Aslında dünyadaki su miktarında bir artma ve azalma söz konusu değildir. Ancak atmosferdeki ısı artışıyla yeryüzünde insanlığın kullanımında olan su, buharlaşarak atmosferin nem içeriğini yükseltmekte, bu durum da suyun çevrimindeki dengenin bozulmasına sebep olmaktadır.

Dünyada sera gazlarının emisyon hacimlerinin yüksek olması iklim değişiminin en temel nedeni olarak gösterilmektedir. Bu nedenle İklim değişiminin önlenmesine yönelik sera gazları emisyonlarını sınırlandıracak şekilde uluslararası anlaşmalar yürürlüğe konmuş olsa bile, hala bu anlaşmalara uymayan ülkeler bulunmaktadır.

Günümüzde ülkeler su varlıklarını koruyacak ciddi önlemler almaya yönelik çalışmalar yürütmektedir. Türkiye'nin bulunduğu bölge, iklim değişikliğinden dolayı en çok etkilenecek kuşakta yer almaktadır. Türkiye günden güne azalan su kaynakları, kuruyan gölleriyle artık tehlikenin eşiğine gelmiş durumdadır. Dünyanın birçok ülkesi gibi Türkiye'ye de düşen yağış miktarlarında ciddi azalma söz konusudur.

Bu çalışmada kuraklığın tanımlaması ve yağış ile ilişkilendirilmesi, yağış oluşumunun ayrıntıları, yapay yağmur ve yapay yağmurun oluşturulma teknikleri ile yapay yağmurun uygulama alanları hakkında bilgiler verilmiştir.

2. KURAKLIK NEDİR?

Kuraklık, tekrar edebilen, bir veya birden çok mevsime yayılan, azalan yağışlar ve artan sıcaklıklar nedeniyle oluşan ve su varlığına bağlı olarak tüm doğal kaynakları etkileyen bir doğal afet türü olarak tanımlanmaktadır (Partigöç ve Soğancı, 2019).

Kuraklık Birleşmiş Milletler Çölleşme ile Mücadele Sözleşmesinde (BMÇMS) “yağışların kaydedilen normal seviyelerinin önemli ölçüde altına düşmesi sonucu arazi ve su kaynaklarının olumsuz etkilenmesine ve hidrolojik dengenin bozulmasına sebep olan doğal olaydır” şeklinde tanımlanmaktadır (BMÇMS,1994). Burada asıl ifade her ne kadar yağışların normal seyrine göre azalması olsa da; etkinliği açısından farklı alanlarda olumsuzluklar görülmesi beklenmektedir. Bu nedenle kuraklık, meteorolojik, tarımsal, hidrolojik ve sosyo-ekonomik boyutlarıyla değerlendirilmektedir.

Kuraklığın önemli özellikleri olarak; başlangıç ve bitişinin belirsiz oluşu, kümülatif artması, aynı anda birden fazla kaynağa etkisi, ekonomik boyutunun yüksek olması sayılabilir. Kuraklığın niteliği olarak ise, frekans, şiddet, süre ve etki alanı sayılabilir (MGM, 2021)

Kuraklığın var olması için süre önemli bir etmendir. Bir bölgede birkaç yıl üst üste oluşan kurak periyot kuraklık olarak değerlendirilemez. Kuraklığa meteorolojik anlamda kuraklık diyebilmek için 30 yıllık bir süreyi kapsamaması gerekir. Kuraklığın seyri ve şiddeti de bu süre zarfında değişim gösterebilir. Uzun süren kuraklıklarda havanın kuruması, nem azlığı yaratarak orman ve su kaynaklarında azalmaya neden olduğundan, önemli boyutta yaşamsal, çevresel, ekonomik sorunları ortaya çıkarabilir. Nem azlığından dolayı su kaynaklarında azalma ve kirlenme, tarımsal ürünlerin üretiminde zorluk, halkın su ve gıda ürünlerine bağlı olarak sağlık sorunlarının ortaya çıkması gibi durumlar oluşabilir. Kuraklık ilk olarak su varlığına bağlı sektörler üzerinde özellikle de tarım alanlarında etkisini göstermektedir. Bu sebeple, tarım sektöründeki kuraklığın gözlenen etkilerinin diğer sektörlerden çok daha farklı olduğunu söylemek mümkündür. Tarımsal kuraklık adı verilen bu kavram, bitkilerin çıkış ve gelişme döneminde ihtiyaç duydukları suyun toprakta bulunamaması anlamına gelmekte olup, tarımsal verimliliği doğrudan etkilemektedir (Kapluhan, 2013).

Kuraklığın ortaya çıkmaması düzenli ve yeterli miktardaki yağışlara bağlıdır. Kuraklığın olumsuz etkilerinden korunmak için, bütün dünyada yağışlardan en iyi ölçüde yararlanma yoluna gidilmektedir. Bu amaçla, suyun var olduğu dönemde depolanması için depo yapılarının inşaa edilmesi, yağmur suyu hasadı, yapay yağmur, atmosferden nem sağımı gibi teknikler uygulanmaktadır.

3. YAĞIŞIN OLUŞUMU

Atmosferdeki nemin soğuyup yoğunlaşması sonucu ağırlaşarak sıvı veya katı partiküller halinde yeryüzüne düşmesi olayına yağış denir. Yağış, yaşamın sürdürülebilmesi için mutlak gerekli bir doğa olayıdır. Yağış sayesinde su döngüsü gerçekleşmekte ve yeryüzündeki suyun yenilenmesi sağlanmaktadır. Yağışın oluşabilmesi için olması gereken bazı şartlar mevcuttur. Bu şartlardan ilki atmosferde nem bulunmasıdır. Bu şart yerine alternatif getirilemeyecek olan mutlak bir şarttır. Yağışın oluşması için bu şarta ilave olarak dört olayın daha ardı ardına gerçekleşmesi gerekir. Bunlar;

1. Soğuma,
2. Yoğunlaşma,
3. Damlaların büyümesi,
4. Yağış alanındaki bulutların yeterli olması ve beslenmesidir.

3.1. Soğuma

Atmosferde buhar halinde nem olarak bulunan suyun yoğunlaşması için, çiğlenme noktası denilen sıcaklığın altında bir sıcaklığa ulaşması, yani soğuması gerekir. Çiğlenme noktası ortam sıcaklığı ve bağıl neme bağlı olarak değişim gösteren bir sıcaklık değeridir. Havanın soğuması ile çiğlenme, beklenen bir olaydır. Havanın soğuması dört farklı yolla olabilir.

- a. **Konveksiyonla soğuma:** Hareket eden sıcak bir hava kütesinin soğuk bir yeryüzüne (zemine) temas etmesi sonucu oluşan soğumadır.
- b. **Radyasyon kaybı ile soğuma:** Hava kütesinin genellikle açık havalarda ve genellikle geceleyin atmosferin derinliklerine yani uzaya doğru ısısını kaybetmesiyle oluşan soğumadır.

c. **Karışma ile soğuma:** Sıcak ve soğuk 2 hava kütesinin birbiriyle çarpışıp karışması sonrasında oluşan soğumadır.

d. **Adyabatik soğuma:** Çevresiyle ısı değişimi olmadan, havanın bulunduğu yerden yükselmesi ve daha soğuk üst tabakalarda ısınıp kaybetmesi şeklindeki soğumadır.

3.2. Yoğunlaşma

Yoğunlaşma, iki faktörün etkisiyle ortaya çıkar. Öncelikle hava sıcaklığının çığırma noktası dediğimiz değerin altına düşmesi gerekir. Çığırma noktası altına düşen bir soğuma çığırma için mutlak gereklidir. Bunun yanında yoğunlaşmanın olabilmesi için havada yoğunlaşma çekirdeklerinin yani üzerinde damlacıkların çığırma noktası yüzeylerin bulunması gerekir. Yoğunlaşma çekirdekleri, suyu üzerinde tutan 10 mikrondan küçük çaplı parçacıklardır. Havadaki toz ve buz kristalleri gibi yüzeyler yoğunlaşma çekirdeği görevi görürler.

3.3. Damlaların Büyümesi

Yoğunlaşma çekirdeklerinin etrafında ilk çığırma ile ince bir film gibi su tabakası oluşur. Bu su higroskopik su olarak adlandırılır. Soğuma ve yoğunlaşma devam ettikçe bu su kalınlaşır, kalınlaşır ve havada kalmaz hale gelir. Sonra da ağırlığından dolayı düşmeye başlar. Düşerken diğer su partikülleriyle birleşir ve bu şekilde yağış başlamış olur.

3.4. Yağış Alanındaki Bulutların Yeterli Olması ve Beslenmesi

Yağış başladıktan sonra eğer bulut yoğunluğu fazla değilse bu durumda yağış çok kısa süreli olacaktır. Ancak bulutlar yoğun veya yağış alanı, hareket eden bulutlarla sürekli besleniyorsa; bu durumda soğuma ve yoğunlaşmaya paralel olarak yağışın sürekliliği sağlanmış olur. Genellikle yoğun bulutluluk olduğunda daha uzun süreli ve düzgün şiddetli yağışlar oluşurken, yetersiz bulutlardan oluşan yağışlar kısa sürelidir.

4. YAPAY YAĞMUR

Yapay yağmur çalışmaları ilk olarak 1946 yılında Amerika Birleşik devletlerinde, dünyanın çeşitli bölgelerinde görülen kuraklığa çözüm arayışı olarak başlamıştır. Bu ilk çalışmalarda 2 bin ile 4 bin metre arasındaki bulutlara CO₂ buzu ile suni tohumlama yapılarak yağış oluşturulması hedeflenmiştir. (Anonim 2021a). Bu çalışmada CO₂ buzu toz halinde bulut içerisine serpiştirilmiş ve serpilmiş bu z kristalleri hem soğumaya yardımcı olmuş hem de yoğunlaşma çekirdekleri görevini yerine getirmiştir. 1947'de Bernard Vonnegut, gümüş iyodürü bulut tohumlama işleminde kullanmıştır. Gümüş iyodür, buz kristaline benzer bir kristal yapısına sahip olduğu için -4°C ve daha düşük sıcaklıklarda etkili bir buz çekirdeği olarak hizmet emektedir ve gümüş iyodürü kullanmak, kuru buz kullanmaktan daha kolaydır (Anonim 2021b).

4.1. Yapay Yağmur Nedir? Nasıl Uygulanır?

Yapay yağmur (bulut tohumlama), ön şart olan havada nem bulunması dışında, yağışın oluşması için gerekli olan diğer şartların (soğuma, yoğunlaşma, damlaların büyümesi) suni olarak yaratılması sonucunda yağış oluşturulması olayıdır. Yapay yağmur oluşturmada asıl amaç, havada bulunan ancak soğumanın olmaması veya soğuma olduğu halde yoğunlaşma

çekirdekleri bulunmadığı için yoğunlaşmanın gerçekleşmemesi durumunu ortadan kaldıracak şekilde, suni bir soğuma yaratmak ve ortama yoğunlaşma çekirdekleri dağıtmaktır.

Havada bulut olmadığı durumda yapay yağmur yağdırmak söz konusu değildir. Yapay yağmur tehlikeleri ve riskleri olan bir tekniktir. Aslında yağış mekanizması çok karmaşık olduğundan tohumlama konusunda belirsizlikler vardır. Tohumlama zamanı, rüzgâr profili, havanın yukarı yükselme hızı ve diğer hava şartları, süper soğumuş su damlacıkları, çekirdek konsantrasyonu, damlacıkların birleşip büyüme durumu ve yönü gibi pek çok faktöre bağlıdır. Genel olarak yağış tahmini yapılır ve diğer şartlar da uygunsa tohumlama yapılır. Tohumlamadan 15 dakika veya birkaç saat sonra yağış olabilir. Orta şiddetle sağanak üreten yaz kümülüs bulutları ile alçak kış bulutları yapay yağmur oluşturmak için uygun bulutlardır.

Yağmur yağdırmak için yapılan herhangi bir bulut tohumlama işleminde öncelikle tohumlamaya uygun bulutu bulmak gerekir. Bulut tohumlama işleminde ikinci aşama ise, yoğunlaşma çekirdeği olarak hizmet edecek olan higroskopik maddelerin, bulut içindeki en uygun yere, zamanında ve doğru miktarda ulaştırılmasıdır. Ayrıca, verimli bir yağış almak için tohumlama yapılacak bulut soğuk olmalıdır (Anonim 2021c). Bu nedenle bir dağ yamacından yükselmekte olan orografik bulutlar oldukça uygundur. Çünkü bunlar yükseldikçe zaten soğuyacaklardır. Ayrıca dikey gelişme göstermiş kümülüs grubu bulutlar da yoğun nem içerikleri nedeniyle tohumlamaya uygun bulutlardır.

Bulutların tohumlama işlemi, uçakla, balonla, roketlerle, yeryüzünden göndererek ya da son zamanlarda dronlarla sağlanabilmektedir. Hangi yöntem uygulanırsa uygulansın temel amaç tohumlayıcının (genellikle gümüş iyodür) bulut içerisinde en uygun yere yayılımıdır. Bulut içerisine yoğunlaşma çekirdeklerini yaymak için uçaklar başarılı bir şekilde kullanılmaktadır (şekil 1 a-b) (Anonim 2021c).



Şekil 1. a. Uçak kanadına takılmış bulut tohumlama fişekleri



Şekil 1. b. Uçaktan yapılan tohumlama işlemi

4.2. Yapay Yağmur Uygulama Alanları Nerelerdir?

Yapay yağmur dünya üzerinde farklı amaçlar için uygulanan bir teknik olmakla birlikte, en çok su temini için uygulanmaktadır. Bulutlardaki su yeryüzüne düşürülerek rezervuarlarda depolanması ve kurak dönemler için kullanılması hedeflenir. Depolanan sudan hidroelektrik olarak enerji temini de amaçlanabilir. İleri dönemlerde oluşacak yoğun yağışın önlenmesi yine bir amaç olabilir. Ayrıca özellikle havalimanı civarındaki sisin dağıtılması için de yine yapay yağmur teknikleri kullanılabilir. Hava trafiğinin engellenmemesi açısından bu kullanım mantıklı bir uygulamadır. Orman yangınlarında söndürme çalışmalarına yardımcı olarak da düşünülebilmektedir.

Bütün bu amaçlara ve uygulamalara rağmen, yapay yağmurun bir bölgenin toplam yağış miktarını değiştirmedikçe iddia eden bilim adamları da vardır. Çünkü birçok durumda yağdırılan yağış aslında daha sonra doğal yolla yağacak olan yağışın öne çekilmiş halidir.

5. YAPAY YAĞMURUN KURAKLIĞA ETKİSİ

Dünya ülkelerine bakıldığında yapay yağmur tekniklerinin çoğunlukla kurak ve yarı kurak iklim kuşağı ülkelerinde uygulandığı görülmektedir. Ancak bunun yanında su açısından hiç sorun yaşamayan hatta dünyada en fazla suya sahip ülkelerin de yapay yağmur uygulamalarına başvurduğu görülmektedir. Farklı iklim şartlarına sahip bu ülkelerdeki yapay yağmur uygulama amaçları da birbirinden farklıdır. Kurak bölgelerde temel amaç su kıtlığının biraz olsun giderilmesidir. Ancak Kanada, Rusya gibi nemli ve sulak bölgelerde ise asıl amaç yüklü bir yağış oluşumunun önüne geçmektir. Dolu ya da şiddetli bir sel olayı meydana gelmemesi için atmosferdeki suyun küçük parçalar halinde yağdırılması temel amaçtır.

Bazı dünya ülkeleri amacı ne olursa olsun yapay yağmur uygulamalarına karşıdır. Öyle ki; ilk çalışmaların yapıldığı Amerika'da bile şu an 48 eyalette yapay yağmur yasak olup sadece çöl iklimine sahip 2 eyalette izin verilmektedir (Anonim 2021d). Bulut tohumlama işleminin doğaya müdahale olduğunu ve bulutların yok olabileceğini, uygulanan bölgede önemli iklim olaylarının (sel, yıldırım vs.) meydana gelebileceğini, elde edilen suyun aslında toplam yağış içerisinde çok da büyük bir oran (%3-5) tutmadığını belirten bilim adamları vardır. Bununla birlikte, Dünya Meteoroloji Örgütü raporuna göre dünya çapında 80'den fazla bulut tohumlama projesi olduğu biliniyor (Anonim 2021e).

Bulut tohumlama yapılarak yağdırılan yağış aslında yağabilecek bir yağışın potansiyelinden alınmaktadır. Yapay yağmur teknikleri hiçbir zaman asla düşmeyecek bir nemi yağış haline

çeviriyor değildir. Yani indirilen yağış, zaten bulutta mevcut olan ve doğal şartlar elverdiğinde zaten yağış haline gelecek olan nemdir. Bu açıdan bakıldığında tüm dünya bir bütün kabul edildiğinde yapay yağmur ile temin edilen su aslında gelecekte günümüze çalınan bir yağıştır. Yapay yağmur ekstra bir su üretmeyip, potansiyel bir yağışın istenilen zamanda yağmasını temin etmektedir. Mevcut bulutun yapay yağmur ile suya dönüştürülmesi sonucunda bulut ortadan kaybolacağı için, yapay yağmur ile su temini asla sürekli olmayacaktır. Nemli bölgelerdeki bulutların, kurak bölgelere nakledilmesi gibi bir teknoloji olsaydı, bu durumda kurak bölgelerde sürekli olarak yapay yağmur ile su temini sağlanabilir ve kuraklığın önüne geçilebilirdi. Mevcut teknolojisiyle yapay yağmur, bulut yetersizliğinden dolayı, asla kuraklık önlemede etkili bir yöntem olmayacaktır.

Yapay yağmur kuraklık açısından bir çözüm yolu olmamasına rağmen, havadaki sisin dağıtılması, ya da aşırı yağışların önlenmesi açısından başvurulacak bir teknik olmaya devam edecektir.

6. KAYNAKLAR

Anonim (2021a). <https://tr.euronews.com/2021/08/01/video-yapay-yagmur-kuraklik-sorununu-cozecek-mi>. Erişim tarihi: 25.10.2021.

Anonim (2021b). <http://kktcmeteor.org/bilgi/suniyagis>. Erişim tarihi: 25.10.2021.

Anonim (2021c). <http://www1.mgm.gov.tr/genel/ss.aspx?s=suniyagis>. 25.10.2021.

Anonim (2021d). https://www.kibrispostasi.com/c35-KIBRIS_HABERLERI/n42007-meteoroloji-dairesinden-uyari-suni-yagmur-deneyi-felaketle-sonuc.

Anonim (2021e). <https://www.ceyrekmuhendis.com/kurakliga-farkli-bir-cozum-yapay-yagmur/>.

BMÇMS. (1994). [https://web.archive.org/web/20170425114748/http://www.cem.gov.tr/erozyon/Files/faaliyetler/dis_iliskiler/collesme_ile_mucadele_sozlesmesi/UNCCD_BM_Collesme_ile_Mucadele_Sozlesmesi_\(Turkce\).pdf](https://web.archive.org/web/20170425114748/http://www.cem.gov.tr/erozyon/Files/faaliyetler/dis_iliskiler/collesme_ile_mucadele_sozlesmesi/UNCCD_BM_Collesme_ile_Mucadele_Sozlesmesi_(Turkce).pdf)

MGM (2021). <https://www.mgm.gov.tr/veridegerlendirme/kuraklik-analizi.aspx?d=yontemsinif>

Partigöç, N. S. ve Soğancı, S., (2019). Küresel İklim Değişikliğinin Kaçınılmaz Sonucu: Kuraklık. *Dirençlilik Dergisi*, 3(2), 2019, (287-299), ISSN: 2602-4667.

Kapluhan, E. (2013). Türkiye’de Kuraklık ve Kuraklığın Tarıma Etkisi, *Marmara Coğrafya Dergisi*, 27.

YIELD EVALUATIONS OF SOME FIELD CROPS GROWN IN CENTRAL ANATOLIAN IN SALTY CONDITIONS

Dr. M. Sevba ÇOLAK

Ankara University, Faculty of Agriculture, Department of Farm Structures and Irrigation, Ankara, Turkey. Orcid ID: 0000-0003-4752-6491

Prof. Dr. Ahmet ÖZTÜRK

Ankara University, Faculty of Agriculture, Department of Farm Structures and Irrigation, Ankara, Turkey. Orcid ID: 0000-0003-0201-1726

Abstract

Salinity is one of the important problems of the world's soils. Millions of hectares of land are lost every year in the world due to the effect of salinity. Salinity, which can occur in all climatic zones, occurs more and quickly in arid conditions. For this reason, it is more common in regions where arid and semi-arid climatic conditions are dominant.

In arid and semi-arid regions, soluble salts can not be transported far due to insufficient precipitation, and salty ground waters can reach the soil surface by capillary rise, especially in hot and dry periods. Due to the high evaporation, the water evaporates from the soil surface, leaving the salts they carry with it on the soil surface or near the surface.

In this study, a theoretical analysis was made for the changes in the proportional yields and washing needs of sunflower, wheat, corn, sugar beet and alfalfa plants in Central Anatolia conditions, taking into account the water needs and salt tolerance of these plants.

It was taken into account that it was grown in different soil salinities (1.0, 3.0, 5.0, 10 and 15 dS/m) based on 5 different plants in Central Anatolian conditions. Irrigation water salinity levels were chosen to be one sample from each quality class and to represent each quality class (0.1, 0.6, 1.5, 2.5 and 5.0 dS/m).

In the study, first, irrigation water needs were determined. The irrigation water needs of sunflower, wheat, corn, sugar beet and alfalfa were found to be 642, 511, 648, 827 and 795 mm, respectively. The proportional yield values of these plants, which are assumed to be grown in different soil salinities, were examined; Proportional yield values decreased as soil salinity increased in all plants.

When the proportional yield values of sunflower were examined in the study, A decrease occurred in subjects with soil salinity of 5.0 dS/m and more. When the proportional yield values of wheat and sugar beet are examined, Decreases started to be seen at 10.0 dS/m soil salinity condition. On the other hand, in corn and alfalfa, there was a decrease in the proportional yield from the soil salinity condition of 3.0 dS/m. Corn was the plant with the highest soil salinity at 15 dS/m condition.

When the 5 different field crops grown in Central Anatolian conditions were grown in 5 different soil salinities, the decrease in their proportional yield was calculated and it was determined that corn, which is the most sensitive plant to salinity, could not get any yield at

15 dS/m condition. Sugar beet was the plant with the highest yield with 52.8% proportional yield value in the highest salinity condition.

As the soil salinity increased, the proportional yield values decreased. While sunflower yielded 283 kg/da in soil salinity condition of 1.0 dS/m, it yielded 138.67 kg/da in soil salinity of 15.0 dS/m. Wheat yielded 267 kg/da in soil salinity condition of 1.0 dS/m, where soil salinity is the lowest, while yielding 96.387 kg/da at 15.0 dS/m soil salinity. The corn plant is; While 876 kg/da of product was obtained under 1.0 dS/m soil salinity condition, 3.504 kg/da product was obtained under 10 dS/m soil salinity condition, and no product was obtained at 15.0 dS/m soil salinity. While the highest yield was obtained in sugar beet with 6926 kg/da, 3656.93 kg/da yield was obtained in the saltiest condition. While the alfalfa plant gave the highest yield with 3890 kg/da in the least salinity, the lowest yield occurred in the highest salinity with 198.39 kg/da.

Depending on the increase in soil salinity, significant decreases were observed in the proportional yields. If the order of sensitivity to salinity is made; The most sensitive plant was corn, and the most resistant plant was sugar beet.

Keywords: Soil salinity, proportional yield, irrigation water quality

ORTA ANADOLU KOŞULLARINDA YETİŞTİRİLEN BAZI TARLA BİTKİLERİNİN TUZLU ŞARTLARDA VERİMLERİNİN DEĞERLENDİRİLMESİ

Özet

Tuzluluk dünya topraklarının önemli sorunlarından biridir. Dünyada her yıl milyonlarca ha arazi tuzluluk etkisiyle elden çıkmaktadır. Bütün iklim kuşaklarında oluşabilen tuzluluk, kurak koşullarda daha fazla ve çabuk bir şekilde ortaya çıkar. Bu nedenle kurak ve yarı kurak iklim koşullarının egemen olduğu bölgelerde daha yaygın olarak karşılaşılmaktadır.

Kurak ve yarı kurak bölgelerde yetersiz yağıştan dolayı çözünebilir tuzlar uzaklara taşınamamakta, özellikle sıcak ve yağışsız olan dönemlerde, tuzlu taban suları kılcal yükselme ile toprak yüzeyine kadar ulaşabilmektedir. Evaporasyonun yüksek olması nedeniyle sular, toprak yüzeyinden buharlaşırken beraberinde taşıdıkları tuzları toprak yüzeyinde veya yüzeye yakın kısımlarda bırakmaktadır.

Bu çalışmada, Orta Anadolu koşullarında, farklı toprak tuzluluklarında ayçiçeği, buğday, mısır, şeker pancarı ve yonca bitkilerinin yetiştirildiği ve bu bitkilerin su ihtiyacı ve tuz toleransları dikkate alınarak, oransal verimlerinde meydana gelen değişiklikler ve yıkama ihtiyaçları için teorik bir çözümleme yapılmıştır.

Orta Anadolu koşullarında 5 farklı bitki baz alınarak farklı toprak tuzluluklarında (1.0, 3.0, 5.0, 10 ve 15 dS/m) yetiştirildiği dikkate alınmıştır. Sulama suyu tuzluluk düzeyleri ise her bir kalite sınıfından bir örnek olacak şekilde ve her bir kalite sınıfını temsil edilecek şekilde (0.1, 0.6, 1.5, 2.5 ve 5.0 dS/m) seçilmiştir.

Çalışmada öncelikle sulama suyu ihtiyaçları belirlenmiştir. Ayçiçeği, buğday, mısır, şeker pancarı ve yoncanın sulama suyu ihtiyaçları sırasıyla 642, 511, 648, 827 ve 795 mm olarak bulunmuştur. Farklı toprak tuzluluklarında yetiştirildiği varsayılan bu bitkilerin oransal verim

değerleri incelenmiş olup; bütün bitkilerde toprak tuzluluğu arttıkça oransal verim değerleri azalma göstermiştir.

Çalışmada ayçiçeği oransal verim değerleri incelendiğinde; toprak tuzluluğunun 5.0 dS/m ve daha fazlası olan konularda azalma meydana gelmiştir. Buğday ve şeker pancarı oransal verim değerleri incelendiğinde; 10.0 dS/m toprak tuzluluğu koşulunda azalmalar görülmeye başlanmıştır. Mısır ve yonca bitkisinde ise 3.0 dS/m toprak tuzluluğu koşulundan itibaren oransal verimde azalmalar meydana gelmiştir. En yüksek toprak tuzluluğuna sahip olan 15 dS/m koşulunda hiç verim alınamayan bitki mısır olmuştur.

Orta Anadolu koşullarında yetiştiriciliği en fazla yapılan 5 farklı tarla bitkisinin 5 farklı toprak tuzluluğunda yetiştirildiğinde oransal verimlerinde meydana gelen düşüşler hesaplanmış olup, tuzluluğa en hassas bitki olan mısırın 15 dS/m koşulunda hiç verim alınamadığı tespit edilmiştir. En yüksek tuzluluk koşulunda %52.8 oransal verim değeri ile en yüksek verimin elde edildiği bitki ise şeker pancarı olmuştur.

Toprak tuzluluğu arttıkça oransal verim değerleri de azalmıştır. Ayçiçeği 1.0 dS/m toprak tuzluluğu koşulunda 283 kg/da verim verirken, 15.0 dS/m toprak tuzluluğunda 138.67 kg/da ürün vermiştir. Buğday toprak tuzluluğunun en düşük olduğu 1.0 dS/m toprak tuzluluğu koşulunda 267 kg/da ürün verirken 15.0 dS/m toprak tuzluluğunda 96.387 kg/da ürün vermiştir. Mısır bitkisi ise; 1.0 dS/m toprak tuzluluğu koşulunda 876 kg/da ürün elde edilirken, 10 dS/m toprak tuzluluğu koşulunda 3.504 kg/da ürün elde edilmiş, 15.0 dS/m toprak tuzluluğunda ise hiç ürün elde edilmemiştir. Şeker pancarında ise 6926 kg/da ile en yüksek verim elde edilirken, en tuzlu koşulda 3656,93 kg/da ürün elde edilmiştir. Yonca bitkisi en yüksek verimi 3890 kg/da ile en az tuzluluk konusunda verirken, en düşük verim ise 198.39 kg/da ile en yüksek tuzluluk konusunda meydana gelmiştir.

Toprak tuzluluğu artışına bağlı olarak oransal verimlerde de önemli azalmalar görülmüştür. Tuzluluğa karşı duyarlılık sıralaması yapılırsa; en hassas bitki mısır olup, en dayanıklı bitkinin şeker pancarı olduğu görülmüştür.

Anahtar kelimeler: Toprak tuzluluğu, oransal verim, sulama suyu kalitesi

1. GİRİŞ

Küresel ısınmanın etkisiyle birlikte, kurak ve yarı kurak bölgelerde su kaynakları giderek azalmaktadır. Su kaynaklarının miktarında meydana gelen bu azalmayla birlikte kirlenmeler de oluşmuş ve suların kalitesi giderek bozulmuştur. Suyun kirlenmesi sadece tarımsal açıdan değil, aynı zaman da doğadaki yaşam için de çok büyük önem arz etmektedir (Çolak ve Öztürk 2021).

Dünya nüfusunun her kırk yılda bir aşağı yukarı iki misline yükselme eğilimi, su kaynaklarına olan ihtiyacı sürekli artırmakta ve suyu yeryüzünün en önemli servetlerinden birisi haline getirmektedir (Öztürk ve Çolak 2021).

Tuzluluk dünya topraklarının önemli sorunlarından biridir. Dünyada her yıl milyonlarca ha arazi tuzluluk etkisiyle elden çıkmaktadır. Bütün iklim kuşaklarında oluşabilen tuzluluk,

kurak koşullarda daha fazla ve çabuk bir şekilde ortaya çıkar. Bu nedenle kurak ve yarı kurak iklim koşullarının egemen olduğu bölgelerde daha yaygın olarak karşılaşılmaktadır.

Sulanan alanlarda tuzluluğa neden olan faktörlerin başında kullanılan sulama suyu gelmektedir. Sulamada kullanılan suyun içerdiği tuzluluk düzeyine bağlı olarak, tarımsal alanlarda tuzlulaşma sorunları ile karşılaşılmaktadır. Bunun dışında taban suyu yüksekliği, taban arazilerde yanıl sızmalar, kıyı alanlarda deniz etkileşimi gibi faktörler kök bölgesine tuzun taşınmasını sağlamaktadır. Bunun dışında iklim koşulları, uygulanan tarım şekli, sulama yöntemi, sulama suyu miktarı, drenaj durumu, sulama ve drenaj yönetimi, çiftçilerin bilgi birikimi, sosyolojik faktörler gibi birçok faktör de etkili olmaktadır (Yurtseven 2020).

Bitki verimi ve su kullanımı arasındaki ilişki, kurak ve yarı-kurak bölgelerde zirai araştırmanın ana konusunu oluşturmaktadır (Lyle ve Bordovsky, 1995, Zhang ve Oweis, 1999, Pandey vd. 2000). Sulama suyu uygulamasına karşın bitki verim duyarlılığının bilinmesi ekonomik sulama stratejilerinin belirlenmesinde kritik öneme sahiptir.

Bitkilerin tuza dayanımları oransal verim ve mutlak verim ile ifade edilmektedir. Tuzlu koşullarda bitkinin verdiği verimin, oransal olarak, normal tuzsuz koşullarda verdiği verim ile karşılaştırılması oransal verim olarak ifade edilmektedir. Agronomik bir kriter olup, bitkilerin tuza dayanımları konusunda iyi bir temel oluşturmaktadır. Aynı zaman da bitkilerin tuza dayanım listeleri oluşturulurken bu verim değerlerinden faydalanılmaktadır.

Tuzlu toprak koşulunda bitkinin verdiği verim ise mutlak verim değeridir. Tuza dayanım listeleri hazırlanırken oransal verim değerlerinden faydalanılsa da, sonuç olarak bitkinin bitki deseni içinde yer alması koşulu ekonomik değerlendirmelere bağlı olacağından, mutlak verim değerleri de yararlı olacaktır.

Bitkilerin tuza dayanımları ile ilgili pek çok veri bulunmaktadır. Tüm dünyada bu konu ile ilgili yapılmış ve halen yapılmakta olan pek çok çalışma vardır. Bu çalışmada, Orta Anadolu koşullarında, farklı toprak tuzluluklarında ayçiçeği, buğday, mısır, şeker pancarı ve yonca bitkilerinin yetiştirildiği ve bu bitkilerin su ihtiyacı ve tuz toleransları dikkate alınarak, oransal verimlerinde meydana gelen değişiklikler için teorik bir çözümleme yapılmıştır.

2. MATERYAL & YÖNTEM

Çalışmada Orta Anadolu bölgesinden Afyon, Aksaray, Ankara, Çankırı, Çorum, Eskişehir, Karaman, Kırıkkale, Kırşehir, Konya, Nevşehir, Niğde ve Yozgat illeri seçilmiş olup, bu bölgelerde yetiştiriciliği en fazla yapılan ayçiçeği, buğday, mısır, şeker pancarı ve yonca baz bitki olarak seçilmiştir. Bu bitkilerin beş farklı toprak tuzluluğunda (1.0, 3.0, 5.0, 10 ve 15 dS/m) yetiştirildiği koşulda oransal verimlerinde meydana gelen azalmalar hesaplanmıştır.

Araştırmada Orta Anadolu şartlarında yürütülen ve kısıntı uygulanmadan optimum verim alınan çalışmalardan elde edilen net su tüketimi değerleri kullanılarak hazırlanmış olan Tagem yayını “Türkiye’de Sulanan Bitkilerin Bitki Su Tüketimleri” adlı eserden araştırma bölgelerine ait değerlerin ortalaması kullanılmıştır.

Tuzlu koşullarda bitkinin verdiği verimin, oransal olarak, normal tuzsuz koşullarda verdiği verim ile karşılaştırılması oransal verimi ifade etmektedir. Bu agronomik kriter, bitkilerin tuza dayanımları konusunda iyi bir temel oluşturduğundan, normalde bitkilerin tuza dayanımları listelerinin oluşturulmasında kullanılır (Yurtseven 2020).

Bütün bitkiler tuzluluğa karşı aynı tepkiyi göstermezler. Bitkinin cinsine ve genetik-morfolojik özelliklerine bağlı olarak tuza karşı toleransları farklılık gösterir. Bazı bitkiler tuzlu koşullarda dahi ekonomik düzeyde ürün verebilirken, bazı bitkiler verimlerini azaltır. Tuzlu koşullarda ekonomik ürün verebilen bitkiler, bu koşulda topraktan suyu alabilmek için gerekli ozmotik düzenlemeyi yapabilen bitkilerdir, bunlar dayanıklı bitki olarak isimlendirilirler. Bitkilerin genel olarak tuza dayanımlarının bilinmesi çok önemlidir. Tuzlulaşmanın önlenemediği bir alanda, tuzluluğa dayanıklı bir bitkinin yetiştirilmesi ile belirli tuzluluk koşulunda ekonomik olarak tarım yapma olanağı çıkacaktır.

Tuzluluğun artması ile birlikte bir noktaya kadar verim potansiyelinde azalma oluşmazken, bu noktadan sonra, tuzluluğun artmaya devam etmesi ile verim potansiyeli de doğrusal olarak azalmaya başlar. Bu ilişkiyi aşağıdaki eşitlikle ifade edebiliriz;

$$Y = 100 - b (EC_e - a)$$

Y= Oransal verim değeri (%)

EC_e = Toprak saturasyon ekstraktı tuzluluk değeri (dS/m)

a = Tuzluluk eşik değeri

b = Birim tuzluluk artışına bağlı olarak verimdeki azalma miktarı.

3. BULGULAR

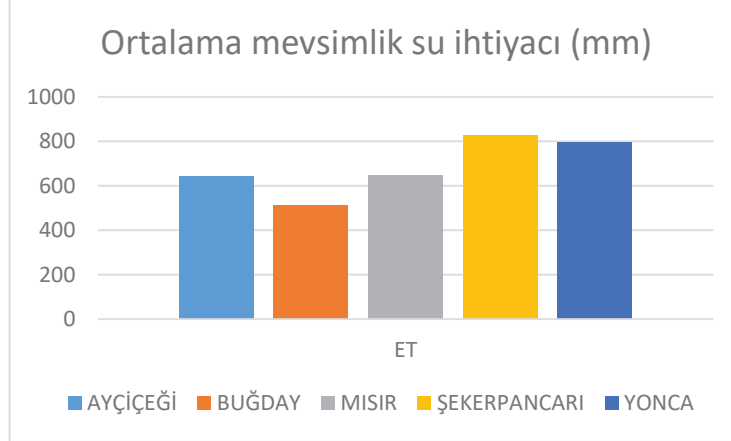
3.1. Sulama Suyu Miktarının Belirlenmesi

Çalışma alanlarında yetiştirilen 5 farklı baz bitkinin (ayçiçeği, buğday, mısır, şeker pancarı ve yonca), bu bölge koşullarındaki su tüketim değerleri hesaplanmıştır. Bitkilerin su tüketimini belirlemek için Tagem tarafından 2017 yılında hazırlanmış olan Türkiye’de Sulanan Bitkilerin Bitki Su Tüketimleri adlı eser esas alınmıştır. Her il için ve her bitki için su tüketim değerleri belirlenmiş, bu değerlerin ortalaması alınarak ortalama mevsimlik su ihtiyacı belirlenmiştir. Çizelge 3.1’de illere ait bitkilerin ortalama su tüketim değerleri verilmiştir.

Çizelge 3.1 Çalışma alanı ortalama mevsimlik su ihtiyacı

Proje İlleri	Ortalama mevsimlik su ihtiyacı (mm)				
	Ayçiçeği	Buğday	Mısır	Şeker pancarı	Yonca
Afyon	617	499	638	801	802
Aksaray	507	579	755	890	879
Ankara	661	506	620	845	802
Çankırı	591	457	564	761	743
Çorum	579	443	555	742	653
Eskişehir	662	520	674	821	725
Karaman	703	571	719	856	858
Kırıkkale	686	515	642	860	910
Kırşehir	730	517	688	919	885
Konya	678	518	692	823	832
Nevşehir	640	517	600	813	706
Niğde	706	570	724	879	882
Yozgat	580	428	552	745	663
Ort.	642	511	648	827	795

Şekil 3.1 incelendiğinde; 827 mm ile şeker pancarı en yüksek mevsimlik su ihtiyacına sahipken, 511 mm ile buğday en düşük su ihtiyacına sahiptir. Mevsimlik sulama suyu ihtiyaçları çalışma alanı içerisinde alınan 13 ilin ortalama değerlerine göre hesaplanmıştır.



Şekil 3.1 Çalışma alanı ortalama mevsimlik su ihtiyacı

3.2. Oransal Verim Değerlerinin Belirlenmesi

Çalışma alanı illerine ait 2020 yılı verim değerleri Tüik sayfasından elde edilmiş olup, bu değerler üzerinden hesaplamalar yapılmıştır. Ortalama ayçiçeği verimi 283 kg/da, buğday verimi 267 kg/da, mısır verimi 876 kg/da, şeker pancarı verimi 6926 kg/da, yonca verimi ise 3890 kg/da olarak hesaplanmıştır (Çizelge 3.2).

Çizelge 3.2 Çalışma alanı 2020 yılı verim değerleri (kg/da)

İller	2020 yılı verim değerleri (kg/da)				
	Buğday	Mısır	Ayçiçeği	Şeker Pancarı	Yonca
Afyonkarahisar	274	910	248	6998	3046
Aksaray	329	917	430	7465	6718
Ankara	270	1066	252	6425	2163
Eskişehir	272	980	366	6642	5008
Karaman	247	948	353	8656	6403
Konya	307	1035	417	7911	4930
Kırıkkale	214	929	328	6368	2053
Kırşehir	258	704	231	8039	1276
Nevşehir	238	1000	185	6834	4118
Niğde	328	885	-	7100	4873
Yozgat	221	449	179	7130	3350
Çankırı	253	-	149	4486	2759
Çorum	258	692	252	5984	3875
ORTALAMA	267	876	283	6926	3890

Çalışma alanı bitkilerine ait tuzluluk eşik değeri (a) ve birim tuzluluk artışına bağlı olarak verimdeki azalma miktarı (b) değerleri FAO kaynaklarından alınmıştır (Anonim 2021). Çizelge 3.3’de bitkilerin a ve b değerleri verilmiştir. Çizelge 3.3 incelendiğinde tuza dayanımı en fazla olan bitki şeker pancarı iken, en hassas olan bitkinin mısır olduğu görülmektedir.

Çizelge 3.3 Çalışma alanı bitkilerine ait a ve b değerleri

Ayçiçeği		Buğday		Mısır		Şeker Pancarı		Yonca	
a	b	a	b	a	b	a	b	a	b
4,8	5	6	7,1	1,7	12	7	5,9	2	7,3

Beş farklı toprak tuzluluğu koşulunda (1.0, 3.0, 5.0, 10.0 ve 15.0 dS/m) bitkilerde meydana gelen oransal verim azalmaları çizelge 3.4’de verilmiştir. 5.0 dS/m ve daha yüksek toprak tuzluluğu koşulunda oransal verimlerde düşüşler meydana gelmiştir. En fazla verim azalması mısır da meydana gelirken, en az azalma buğday ve şeker pancarında olmuştur.

Toprak tuzluluğunun en düşük olduğu 1.0 dS/m konusunda; bütün bitkilerde %100 verim elde edilmiştir. 3.0 dS/m toprak tuzluluğu koşulunda; ayçiçeği, buğday ve şeker pancarının verimlerinde bir azalma meydana gelmezken, mısır ve yonca da verim azalmaları görülmeye başlanmıştır. 5.0 dS/m toprak tuzluluğu koşulunda ise; buğday ve şeker pancarı %100 verim verirken, ayçiçeği, mısır ve yonca da azalmalar görülmüştür. 10.0 dS/m toprak tuzluluğu koşulunda ise; bütün bitkilerde verim azalmaları görülmüştür. En fazla toprak tuzluluğuna sahip olan 15.0 dS/m konusunda da mısır bitkisinde hiç verim alınamazken, diğer bitkilerde en düşük verimler elde edilmiştir.

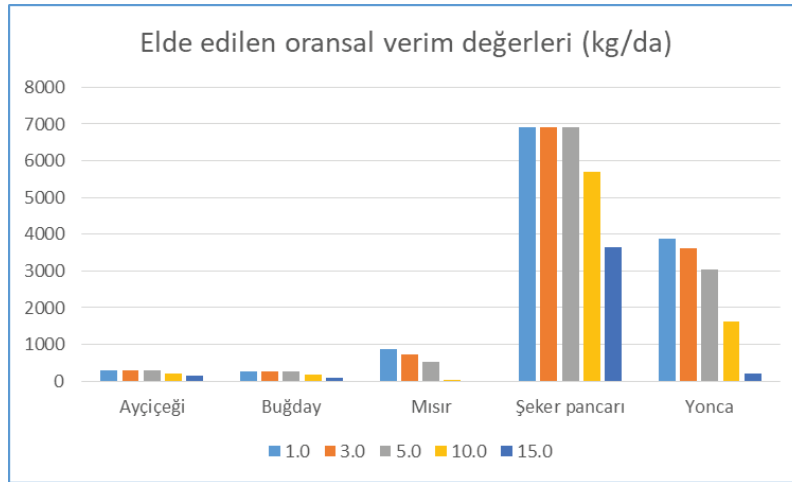
Çizelge 3.4 Elde edilen oransal verim değerleri (%)

Toprak Tuzlulukları (dS/m)	Ayçiçeği	Buğday	Mısır	Şeker pancarı	Yonca
1.0	100	100	100	100	100
3.0	100	100	84,4	100	92,7
5.0	99	100	60,4	100	78,1
10.0	74	71,6	0,4	82,3	41,6
15.0	49	36,1	0	52,8	5,1

Hesaplanan oransal verim değerleri, tam sulama koşulunda elde edilen verim değerleri ile düzeltilerek çizelge 3.5’deki değerler elde edilmiştir. Toprak tuzluluğu arttıkça oransal verim değerleri de azalmıştır. Ayçiçeği 1.0 dS/m toprak tuzluluğu koşulunda 283 kg/da verim verirken, 15.0 dS/m toprak tuzluluğunda 138.67 kg/da ürün vermiştir. Buğday toprak tuzluluğunun en düşük olduğu 1.0 dS/m toprak tuzluluğu koşulunda 267 kg/da ürün verirken 15.0 dS/m toprak tuzluluğunda 96.387 kg/da ürün vermiştir. Mısır bitkisi ise; 1.0 dS/m toprak tuzluluğu koşulunda 876 kg/da ürün elde edilirken, 10 dS/m toprak tuzluluğu koşulunda 3.504 kg/da ürün elde edilmiş, 15.0 dS/m toprak tuzluluğunda ise hiç ürün elde edilmemiştir. Şeker pancarında ise 6926 kg/da ile en yüksek verim elde edilirken, en tuzlu koşulda 3656,93 kg/da ürün elde edilmiştir. Yonca bitkisi en yüksek verimi 3890 kg/da ile en az tuzluluk konusunda verirken, en düşük verim ise 198.39 kg/da ile en yüksek tuzluluk konusunda meydana gelmiştir.

Çizelge 3.5 Elde edilen oransal verim değerleri (kg/da)

Toprak Tuzlulukları (dS/m)	Ayçiçeği	Buğday	Mısır	Şeker pancarı	Yonca
1.0	283	267	876	6926	3890
3.0	283	267	739,344	6926	3606,03
5.0	280,17	267	529,104	6926	3038,09
10.0	209,42	191,172	3,504	5700,1	1618,24
15.0	138,67	96,387	0	3656,93	198,39



Şekil 3.2 Elde edilen oransal verim değerleri (kg/da)

4. SONUÇ

Bu çalışmada, Orta Anadolu koşullarında 5 farklı bitkinin (ayçiçeği, buğday, mısır, şekerpancarı, yonca), beş farklı toprak tuzluluğunda (1.0, 3.0, 5.0, 10.0 ve 15.0 dS/m) yetiştirildiği varsayılarak, elde edilen oransal verim değerleri incelenmiştir. Çalışmada öncelikle bitkilerin sulama suyu ihtiyaçları belirlenmiş ve sırasıyla 642, 511, 648, 827 ve 795 mm olarak bulunmuştur.

Sulama suyu ihtiyacının tam olarak verildiği koşulda ayçiçeği verimi 283 kg/da, buğday verimi 267 kg/da, mısır verimi 876 kg/da, şekerpancarı verimi 6926 kg/da ve yonca verimi 3890 kg/da olarak belirlenmiştir.

Toprak tuzluluğu arttıkça oransal verim değerleri de azalmıştır. Ayçiçeği 1.0 dS/m toprak tuzluluğu koşulunda 283 kg/da verim verirken, 15.0 dS/m toprak tuzluluğunda 138.67 kg/da ürün vermiştir. Buğday toprak tuzluluğunun en düşük olduğu 1.0 dS/m toprak tuzluluğu koşulunda 267 kg/da ürün verirken 15.0 dS/m toprak tuzluluğunda 96.387 kg/da ürün vermiştir. Mısır bitkisi ise; 1.0 dS/m toprak tuzluluğu koşulunda 876 kg/da ürün elde edilirken, 10 dS/m toprak tuzluluğu koşulunda 3.504 kg/da ürün elde edilmiş, 15.0 dS/m toprak tuzluluğunda ise hiç ürün elde edilmemiştir. Şeker pancarında ise 6926 kg/da ile en yüksek verim elde edilirken, en tuzlu koşulda 3656,93 kg/da ürün elde edilmiştir. Yonca bitkisi en yüksek verimi 3890 kg/da ile en az tuzluluk konusunda verirken, en düşük verim ise 198.39 kg/da ile en yüksek tuzluluk konusunda meydana gelmiştir.

Toprak tuzluluğu artışına bağlı olarak oransal verimlerde de önemli azalmalar görülmüştür. Tuzluluğa karşı duyarlılık sıralaması yapılırsa; en hassas bitki mısır olup, en dayanıklı bitkinin şeker pancarı olduğu görülmüştür.

5. KAYNAKÇA

Anonim (2021). <http://www.fao.org/3/y4263e/y4263e0e.htm>. Erişim tarihi: 01.11.2021.

Çolak, M.S., Öztürk, A. (2021). The Effect Of Limited Irrigation On The Yields Of Some Field Crops Grown In Central Anatolian Conditions. 3. International Baku Scientific Research Congress October 15-16, 2021 / Baku Eurasia University, Baku, Azerbaijan. P.742-749. ISBN: 978-1-955094-17-7.

Lyle, W.M., Bordovsky, J.P., (1995). LEPA corn with limited water supplies. Trans. ASAE, 38, pp. 2455-2462.

Öztürk, A., Çolak, M.S. (2021). The Effects Of Different Irrigation Water Quality And Irrigation Methods On Salt Accumulation In The Soil. Middle East International Conference On Contemporary Scientific Studies – Vi. Saint Joseph University Of Beirut, Faculty Of Educational Sciences, On September 20-22, 2021. ISBN - 978-625-7464-25-3. Page: 412-421.

Pandey, R. K., Maranville, J. W., & Chetima, M.M. (2000). Deficit irrigation and nitrogen effects on maize in a Sahelian environment: II. Shoot growth, 91 nitrogen uptake and water extraction. Agricultural Water Management, 46(1), 15-27.

Yurtseven, E. (2020). Sulama Suyu Kalitesi ve Tuzluluk Ders Notları. Basılmamış. Ankara.

Zhang, H., Oweis, T., (1999). Water-yield relations and optimal irrigation scheduling of wheat in the Mediterranean region. Agric. Water Manag., 38, pp. 195-211.

%100 DOĞAL YAPIDA, ONARICI VE İYİLEŞTİRİCİ ÖZELLİK GÖSTEREN FARKLI BİTKİ ÖZLERİ İÇEREN POMAT YAPILI KREM GELİŞTİRİLMESİ

DEVELOPMENT OF 100% NATURAL POMAD CREAM CONTAINING DIFFERENT HERBAL EXTRACTS WITH REPAIRING AND HEALING PROPERTIES

Merve KADAL

Rebul Kozmetik Sanayi ve Ticaret A.ş. Ar-Ge Merkezi, İstanbul, Türkiye.

ORCID NO: <https://orcid.org/0000-0002-3343-2956>

Aslı BAHADIR

Rebul Kozmetik Sanayi ve Ticaret A.ş. Ar-Ge Merkezi, İstanbul, Türkiye.

ORCID NO: <https://orcid.org/0000-0001-6372-9622>

ÖZET

Son zamanlarda faydalarından çok yan etkilerin olması sebebiyle tüketicilerin sentetik ürünlere olan inancı azalmış dolayısıyla doğal yapıda bitkisel içerikli ürünlere yönelim artmıştır. Yüzyıllardan beri bitkilerin tamamı veya bir kısmı çeşitli cilt rahatsızlıklarında kullanıldığı bilinmektedir. Bununla birlikte bilimsel çalışmalar, klinik deneylere ve farmakolojik testlerin incelenmesine dayanarak bitkilerin çok büyük miktarlarda ve kompleks yapılarda cildi iyileştiren ve onaran fitokimyasallara sahip olduğunu göstermektedirler. Bu çalışmada 7 farklı bitki özünün birleşimi ile oluşturulan formülasyona sahip %100 doğal yapıda, onarıcı ve iyileştirici özellik gösteren pomat yapılı krem geliştirilmesi amaçlanmıştır. Geliştirilecek kremin, piyasada mevcut Hametan, Madecassol ve Bepanthol gibi ürünlerle benzer yapıda fakat işlev ve maliyet yönünden daha avantajlı olması hedeflenmiştir. Bu kapsamda ilk olarak ön formülasyon oluşturulması için çalışmalar yapılmıştır. Bu noktada formülasyon dahilinde kullanılacak bitki özleri ve diğer doğal kimyasal yapılar incelenerek raporlanmıştır. Elde edilen veriler dahilinde üretim ön planlaması çıkartılmıştır. Ön tasarımların sonucunda nihai üretimde kullanılacak test ve analizler belirlenerek ve formülasyon geliştirme çalışmaları başlatılmıştır. Formülasyon hazırlanırken ürün yapısında 7 farklı bitki özü, yatıştırıcı özelliği olan Madecassoside, cildin nem bariyerini koruma ve cilt kızarıklığını gidermek üzere Cantella Asiatica kullanılmıştır. Ciltte oluşan çizgiler ve yarıkları dolgunlaştırması üzerine Gotu Kola (Aslan Otu) kullanılmıştır. Devamında pomat krem içeriğine tahriş olmuşluğu azaltmasıyla bilinen ve iyileştirici etkisi bulunan Salycuminol, Aynısefa ve Kırmızı Pancar bitkileri eklenmiştir. Ayrıca içerikte cildin nem seviyesinin korunması, ürünün antioksidan özellik gösterebilmesi için Zerdeçal, Papatya gibi bitki özleri de kullanılmıştır.

Ürün formülasyonu tamamlandıktan sonra laboratuvar ortamında deneme üretimleri gerçekleştirilmiştir. Ürünlerin sürdürülebilir bir yapısı olması ve stabilite testinin uygulanması ardından, mikrobiyoloji testleri, paraben free testleri, dermatolojik testlerin uygulanması, fitalat testleri, renklendirici içermez, parafin ve mineral oil içermez testleri, silikon free testleri ve challenge testleri uygulanmıştır. Laboratuvar çalışma sonuçlarının ardından tekrarlanabilir sonuçlar elde edilmeye başlandığı andan itibaren pilot ölçekli deneme üretimi planlanıp laboratuvardaki şartlara bağlı kalınarak pilot ölçekli üretim gerçekleştirilmiştir. Hedef ürünle yüzde 98'in üzerinde bir benzerlik yakalanmıştır. Geliştirilen pomat yapılı kremin onarıcı, tahriş önleyici, nemlendirici, yaşlanmaya karşı olması, yara, iz ve yarıkların kapanmasına etkili olması ve hemen hemen her yaş grubunda kullanılabilir yapıda olması nihai ürününün sahip olduğu özelliklerdir.

Anahtar Kelimeler: Pomat Yapılı Krem, Formülasyon, Bitkisel Ürün

ABSTRACT

Recently, since there are more side effects than benefits, consumers' belief in synthetic products has decreased, so the tendency to products with natural herbal ingredients has increased. It is known that all or some of the plants have been used in various skin disorders for centuries. However, scientific studies, based on clinical trials and examination of pharmacological tests, show that plants have phytochemicals in very large quantities and complex structures that heal and repair the skin. In this study, it was aimed to develop a pomade cream with a restorative and healing properties in a 100% natural structure with a formulation created by combining 7 different plant extracts. Also, it is aimed that the cream to be developed will be similar in structure to products such as Hametan, Madecassol and Bepanthol available in the market, but more advantageous in terms of function and cost. In this context, firstly, studies were carried out to create a preformulation. At this point, plant extracts and other natural chemical structures to be used in the formulation were examined and reported. Production pre-planning was made within the scope of the obtained data. As a result of the preliminary designs, the tests and analyzes to be used in the final production were determined and formulation development studies were started. During the preparation of the formulation, 7 different plant extracts, Madecassoside with soothing properties, Cantella Asiatica were used to protect the skin's moisture barrier and eliminate skin redness in the product structure. Gotu Kola (Lion Grass) was used to fill the lines and clefts on the skin. Afterwards, Salycuminol, Calendula and Red Beet plants, which are known to reduce irritation and have a healing effect, were added to the pomade cream formula. In addition, plant extracts such as Turmeric, Chamomile were also used to maintain the moisture level of the skin in the formula and to provide the product with antioxidant properties.

After the product formulation was completed, trial productions were carried out in the laboratory environment. Microbiology tests, paraben free tests, dermatological tests, phthalate tests, colorant free, paraffin and mineral oil free tests, silicone free tests and challenge tests were performed after the products had a sustainable structure and stability test was applied. From the moment that reproducible results began to be obtained, pilot-scale trial production was planned, and pilot-scale production was carried out by adhering to the conditions in the laboratory. More than 98 percent similarity was achieved with the target product. The final product features of the developed pomade cream are reparative, anti-irritant, moisturizing, anti-aging, effective in closing wounds, scars and crevices also it can be used in almost every age group.

Keywords: Pomade Cream, Formulation, Herbal Product

METHODS OF GENETIC ENGINEERING IN PLANTS BREEDING**Dzhamirze R.R., Ph.D. in agriculture**

Federal State Budgetary Scientific Institution «Federal Scientific Rice centre»

Esaulova L.V., Ph.D. in agriculture

Federal State Budgetary Scientific Institution «Federal Scientific Rice centre»

Slabchenko A. S., student

Federal State Budgetary Educational Institution of Higher Education

“Kuban State Agrarian University named after I. T. Trubilin”,

Abstract. Breeding is the most effective and centralized means of increasing the size and quality of yield, ensuring environmental safety and sustainability of agroecosystems, reducing resource and energy costs for each additional unit of production. Modern plant breeding uses a whole range of methods based on the latest achievements of many biological sciences. Genetic engineering or transgenesis is becoming very important, and in the coming years, obviously, the main direction in the implementation of breeding programs for the integration of genes from different species, genera, families and even kingdoms, as a result of which one or more foreign genes can be incorporated into the genome, and the preference is given to traits with mono- or oligogenic control. Transgenesis can also improve the polygenic trait. The tasks of traditional breeding are much broader: they include both production and environment-improving directions, as well as the introduction of new species into crop. And finally, modern breeding methods make it possible to simultaneously manipulate dozens of traits, including polygenic ones, while the possibilities of transgenesis are limited to single genes. Obviously, along with the fundamentally new opportunities that are associated with the transfer of hereditary information between taxonomically distant organisms, the number of directions in which genetic engineering methods will be integrated into modern technology of plant breeding will constantly increase.

Key words: breeding, transgenesis, genetic engineering, bioengineering.

Genetic recombination is the exchange of genes between two chromosomes. According to the definition given by Pontecorvo in 1958, recombination is any process that can lead to the emergence of cells or organisms with two or more hereditary determinants, according to which their parents differed from each other and which are connected in a new way. Such recombination necessarily occurs in mammals during the formation of germ cells. During meiosis, homologous chromosomes exchange genes (so-called crossing over); it is these exchanges that make it possible to explain the redistribution

of hereditary traits in a number of generations. Genetic recombination occurs less frequently in viruses and bacteria than in animals. The exchange of genetic material, followed by recombination, occurs between organisms of the same or closely related species. Previously, European scientists put forward the assumption that all organisms possess restriction endonucleases that recognize foreign DNA that has entered the body, and cleave it, thus nullifying genetic recombination between evolutionarily distant genomes. But the latest achievements of Russian scientists in this area show that not all living organisms contain restriction enzymes. These enzymes are practically not found in higher animals, plants and humans. Most likely, the presence of restriction enzymes is an attribute of prokaryotic cells. The reason for the impossibility of natural genetic exchange between different species is not the presence of restriction enzymes, but the lack of homology in the nucleotide sequences of their DNA. Genetic engineering, in vitro recombination, do not require such homology [1].

Genetic engineering opens up new perspectives for plant breeding associated with the possibility of transferring genes from bacteria, fungi, exotic plants, and even humans and animals, which is unattainable for experimental mutagenesis and traditional breeding, including resistance genes [2].

A revolutionary achievement in the genetic transformation of plants was the identification of a natural vector - agrobacteria for gene transfer and the development of a method for micro-bombarding plant objects with metal microparticles with a preliminary deposited foreign DNA. Several outstanding advances in plant biochemistry and physiology have created the basis for integrating recombinant DNA technology into genetically engineered plant biotechnology. First, the discovery of phytohormones that regulate plant growth and development. Secondly, the development of methods for the cultivation of plants cells and tissues in vitro (these methods made it possible to grow cells, tissues and whole plants under sterile conditions and carry out their breeding on selective media, etc.) [3].

Modern plant breeding is a scientifically grounded technology for managing the heredity and variability of higher eukaryotes, which makes it possible to realize socio-economic, ecological, design-aesthetic and other goals. As a means of biological control over the adaptive and adapting responses of plants in order to continuously increase their production and environment-forming capabilities, the adaptive breeding system integrates the achievements of both applied and fundamental knowledge [4]. In other words, breeding acts as a synthetic discipline that makes extensive use of the achievements of physiology, biochemistry, soil science, microbiology, cytogenetics, ecology, and other sciences and functionally unites the stages of gene pool mobilization, breeding itself, variety testing and seed production, agroecological zoning and agroecosystem design.

In comparison with traditional breeding, the main tools of which are crossing and selection, the main advantages of genetic engineering are the ability to use fundamentally new genes that determine

agronomically important traits and new molecular genetic methods for monitoring transgenes (molecular gene markers), which greatly speed up the process of developing transgenic plants. In this situation, breeders are attracted by the possibility of targeted genetic "repair" of agricultural plants. [5].

Recombination breeding provides a continuous expansion of the range of available selection of genetic variability of economically valuable and adaptively significant traits, including a constant increase in the number of identified genetic donors of potential productivity and environmental resistance. For this, methods of endogenous and exogenous induction of genetic variability, overcoming sexual incompatibility between species of the same family, gametophytic selection, which allows, on the basis of large populations of pollen, to identify genotypes functionally equivalent to the desired sporophytes, etc., are widely used. Considering the possibilities of integrating breeding and genetic engineering, one should, first of all, determine fundamentally new and clearly expressed priorities of plant breeding itself, arising from the modern understanding of:

- the role of genome integration and the entire idiochrome in higher eukaryotes, manifested in the formation of blocks of coadapted genes and the preservation of their status quo during the transfer of hereditary information from one generation to another;
- the need to combine high potential productivity in varieties and hybrids, resistance to abiotic and biotic stressors, as well as production and environment-forming (soil-improving, phytomeliorative, phytosanitary, resource-restoring, design-aesthetic, etc.) functions;
- the importance of the transition from managing the variability of monogenic traits to combinatorics of quantitative (polygenic) traits, many of which are economically valuable;
- a clearly pronounced role of abiotic and biotic environmental factors that determine not only the direction and rates of natural selection (the "formative" influence of the biocenotic environment), but also act as inductors of genetic variability (mutational, recombination, reparation, transposition);
- the need to develop new or alternative areas of breeding, including phyto (bio) cenotic, ecotypic, bioenergetic, symbiotic, ecological, as well as apomictic, gamete, etc. [6].

Today, modern breeding as a science is characterized by a number of unresolved difficulties and problems, among them the most important are the following:

- the possibilities of traditional breeding itself are particularly limited when using germplasm of taxonomically unrelated and distant species. Since genetically determined prezygotic and postzygotic barriers are the main obstacle in this. As a result, when wild relatives of cultivated plants are used as donors of valuable traits, the duration and scale of the breeding process increase sharply.
- a further increase in yields for strategically important agricultural crops is constrained by the already achieved high yield index (0.5-0.8) corresponding to the modern level of scientific achievements.
- strengthening of the dependence of the variability of the yield quantity and quality on unregulated environmental factors, the share of which for the main grain crops exceeds 60%.

- the more traits the breeder seeks to combine in one variety or hybrid, the lower the rate of artificial selection is, as a result of which more time is required to develop a new variety. The presence of negative genetic and morphophysiological correlations between traits significantly reduces the rate of developing new varieties.
- with the introduction of large doses of mineral fertilizers and ameliorants, the use of a full set of pesticides and means of mechanization, there is an exponential increase in the cost of exhaustible resources for each additional yield unit, including food calorie, the dependence of the productivity of agroecosystems on technogenic factors increases, processes accelerate and the scale of environmental pollution and destruction increases.
- when combining breeding, agrotechnical and genetic engineering programs, in most cases, the genetic nature of economically valuable quantitative traits, as well as the effects of their interaction, are unknown.
- both in traditional breeding and when working with individual genes, the use of new genetic donors, as a rule, requires careful preliminary breeding work to optimize the selection process [6].

An analysis of breeding achievements in the 50-80s of the XX century also indicates that most of the improved agronomic traits that led to an increase in yield are polygenic, complex in nature. Varieties and hybrids with wide agroecological adaptation, slower aging of leaves, resistance to lodging, tolerance of flowers to abortion in conditions of high temperatures and drought, horizontal resistance to diseases, etc. have been developed. The main attention in modern breeding programs is paid to the combination of high potential productivity of varieties and the ability to resist the action of abiotic and biotic stressors. Among the main reasons for this orientation are the tendency to an increase in the gap between the potential and average yield of the most important agricultural crops, an increase in the dependence of yield quantity and quality on the use of man-made means, as well as weather fluctuations (the variability of yield over the years is 60-80% due to "whims" of weather). Consequently, further successful development of plant breeding requires the use of biological concepts, qualitatively new methods and technologies. [7, 8, 9].

It is known that the genetics of quantitative traits, ignoring the real genetic nature of their structural organization and functioning, for a long time was based on methods that reduce complex traits to simple ones ("main factors", etc.). Later, the dynamism of the formation of quantitative traits in morphogenesis was recognized, which determines the multivariate of the implementation of matrix structures (on the "gene-trait" path), the redistribution of the expression of genes and gene blocks during the formation of a complex trait, etc. Currently, quantitative traits are usually considered as a dynamic multivariate integrity, the genetic nature of all components of which is almost impossible to identify. As for genetic markers (marker-assisted-selection - MAS), realizing their effect on

quantitative traits, their identification remains very difficult, and their practical use in breeding is limited [3, 5].

Together with the use of the genetic potential of cultivated species, as well as taking into account numerous unsuccessful attempts to increase their cold tolerance and winter hardiness, salt and acid resistance, early maturity and photosynthetic productivity, in the coming period, special attention is paid to the introduction of new species into the culture (direction of "species change"), with great potential for adaptability to modern biotic, abiotic and anthropogenic factors. At the same time, the priority tasks are the "domestication" or "development" of new types of oilseeds, cereals, legumes, bulbs and root crops, many of which are not only resistant to environmental stressors, but are also characterized by a high content of biologically valuable substances and nutrients. At the same time, an increase in the yield of new crops will be provided due to the traits enhancing the potential productivity of plants and reducing the negative effect of abiotic and biotic factors limiting the magnitude and quality of the yield.

Especially great possibilities of genetic engineering open up in terms of the use of transgenic methods for the induction of meiotic recombination based on the transfer of endogenous crossing-over inductors into interspecific plant hybrids [3, 5, 6]. In recent years, it has been proven that the transfer of the rec A gene into tobacco plants allows increasing recombination variability.

In the process of integrating the methods of the adaptive system of breeding and transgenesis, primary attention is paid to increasing the resistance of varieties and hybrids to diseases, pests and weeds. The importance of this direction of breeding is evidenced by the fact that the total number of species potentially harmful to agroecosystems reaches 80-100 thousand, including over 30 thousand pathogens of fungal, bacterial and viral diseases, about 10 thousand arthropods, etc. an increase in the amount of pesticides used in agriculture (for example, in the USA a little more than 450 thousand tons per year), by the beginning of the XXI century, crop losses are on average about 35%, of which 14% are from pests, 12% from diseases and 9% from weeds [10]. The total cost of yield losses worldwide is estimated to be as high as \$ 50 trillion a year from diseases alone. In this regard, the combination of methods of traditional breeding and transgenesis in developing varieties with a pronounced resistance to unfavorable conditions, as well as multi-line and synthetic varieties, presents great prospects. This is due to the fact that genetic engineering methods make it possible to integrate several different resistance genes into a recipient plant at once, thus creating a "gene pyramid" that provides a complex resistance of the variety. However, there is no reason to assert that genetic engineering allegedly reduces the time for breeding varieties with the required characteristics [11], since for this they always use varieties already adapted to local environmental conditions (agroclicatic conditions and cultivation technologies), which take 5-10 years and more to develop.

In many objects, a correlation has been established between the characters manifested at the gametophytic and sporophytic levels [3, 12]. However, with the transition to selection at the haploid level, the relationship between the traits changes significantly [13], which in turn complicates the prognosis of their manifestation in diploids. To date, the possibility of introducing exogenous DNA into plants by means of germinating pollen has been proven [14].

Thus, gamete breeding and gametophytic selection can successfully solve some breeding and genetic problems:

- Improvement of the indicators of the reproductive structures themselves and, in particular, pollen (changes in aerodynamic properties and fertility; increase in the productivity of plant pollen, as well as the ability of pollen to germinate at low or, conversely, increased temperature, humidity, light and other stressful situations).
- Changes in sporophyte traits by assessing and selecting genetically different pollen grains, that is, using correlations between gametophyte and sporophyte traits.
- Evaluation of endogenous (including transgenesis) and exogenous induction of the frequency and spectrum of recombination variability, the manifestation of pollen traits in F1 hybrids, the nature of their inheritance, as well as the differential growth of pollen tubes "in vitro" and "in vivo".
- Improving the accuracy of hybridological analysis by taking into account the possibility of eliminating marked recombinant microgametes, as well as changing the ratios between phenotypic classes of plants in splitting generations.

Since gamete breeding based on direct (properties of the pollen itself) and indirect (correlation between the traits of gametophyte and sporophyte) pollen selection can significantly speed up the breeding process, it is obvious not only the possibility, but also the advisability of combining the methods of gamete breeding and transgenesis. This combination can be based on hybridization of transgenic forms with recipient varieties, as well as the use of pollen itself as a genetically modified object. The main advantages of combining gamete breeding and genetic engineering methods are, according to some scientists, both in the possibility of assessing a huge number of gametes for direct selection of the desired genotypes on specially developed and relatively easily regulated backgrounds, and in increasing the likelihood of identifying valuable sporophytes based on correlation analysis (indirect gametophytic selection).

In the integration of modern breeding and bioengineering methods, an extremely important role is played by the ability to use the latter to solve two fundamentally different, but equally priority tasks for plant breeding and seed production: 1) to distinguish between plant genotypes and to certify varieties; 2) identify genes controlling economically valuable and adaptively significant traits [15].

In **conclusion**, it should be noted that thanks to the advances in molecular biology and population genetics, the genetic heterogeneity of plants and pollen can now be assessed not only by

agronomic and biochemical traits, as it was in the time of N.I. Vavilov, but also at the molecular level (isozyme analysis, one-dimensional and two-dimensional electrophoresis, DNA restriction, etc.). When assessing genetic diversity, special attention should be paid to taking into account new alleles, as well as new combinations of genes (indicating the geographical origin and genealogy of samples, their geographic distance, degree of genealogical relationship, etc.). The biological diversity of research objects can also be judged by indicators of distance or divergence between traits. The choice of traits and their number in each specific case is determined taking into account the task at hand, and the traits themselves, including productivity and resistance, are evaluated in the offspring of selected material.

REFERENCES

1. Biotechnology: achievements and hopes: Translated from English / Ed., With a foreword. and add. of V. G. Debabov - M.: Mir 1987. – 411p.
2. Dzhamirze R.R. Integration of plant breeding and methods of genetic engineering. Ecological genetics of cultivated plants. – 2014, p. 49-59.
3. Zhuchenko A. A. Ecological genetics of cultivated plants (adaptation, recombinogenesis, agrobiocenosis). - Moldavian Research Institute of Irrigated Agriculture and Vegetable Growing. - Chisinau: Shtiintsa, 1980. – 587 p.
4. Zhuchenko A.A. Adaptive plant growing (ecological and genetic bases). Theory and practice. In three volumes. - M.: Publishing house "Agrorus", 2009. - 960 p.
5. Zhuchenko A.A., Balashova N.N. et al. Ecological and genetic foundations of tomato breeding, Institute of Ecological Genetics. - Chisinau: Shtiintsa, 1988. – 430 p.
6. Zhuchenko A.A. Adaptive system of plant breeding (ecological and genetic aspects). I and II volumes, Moscow, RUDN Publishing House, 2001. 1480 p.
7. Ostapenko N. V. Variability in productivity of rice varieties in competitive testing depending on weather and climatic conditions / N. V. Ostapenko, R. R. Dzhamirze, N. N. Chinchenko. Rice growing No. 3-4, 2015, p. 26-33.
8. Dzhamirze R. R., Ostapenko N. V., Lotochnikova T. N., Chinchenko N. N. Variability of traits and their correlation in different rice genotypes in dynamically changing climate conditions / Bulgarian Journal of Agricultural Science, 25 (No 4) 2019. – P. 625-632.
9. Dzhamirze R. R., Ostapenko N. V. and Chinchenko N. N. Correlation of technological indicators of grain and milled rice quality of new varieties depending on climate condition / International Scientific Conference «AGRITECH-2019: Agribusiness,

Environmental Engineering and Biotechnologies» 20–22 June 2019, Krasnoyarsk, Russian Federation. IOP Conference Series: Earth and Environmental Science. Volume 315, 2019. – P. 1-6.

10. Chemist's Handbook 21. www.chem21.info
11. Shelamova N.A. Prospects for the use of modern biotechnology abroad. Agroindustrial production: experience, problems and development trends, 2001, 1: 89-108.
12. Miryuta Yu. P., Miryuta O.K., Ilyina L.B., Golysheva M.I. Variability of varieties-populations and inbred lines of corn on the basis of fertilization selectivity // Genetics. 1967. No 7.P. 10–19.
13. Rotarenko V. A. The use of haploid plants in the scheme of recurrent selection in corn. Author's abstract. of Ph.D. thesis, Institute of Genetics, Academy of Sciences of Moldova, Chisinau, 2002.
14. Chesnokov Yu. V. Hereditary changes caused by the transfer of exogenous DNA into higher plants by means of germinating pollen. Dr. thesis. Chisinau, 2000.
15. Khavkin E.E. Environmental problems generated by transgenic plants / E.E. Khavkin // Ahova raslin: A two-month scientific and industrial journal. - 2001. - 5. - p. 5-6. - Material from the journal "Biotechnology and Transgenetics", No 1, 1999/2000.

TESTING AND EVALUATION OF ELECTRODIALYSIS METHOD ON DESALINATION**Sinem KAYA**

Ministry of Environment and Urbanisation, Central Directorate of Clean Air for Central Black Sea,
Samsun, Turkey.
0000-0002-5468-9662

Yüksel ARDALI

Ondokuz Mayıs University, Engineering Faculty, Environmental Engineering, Samsun, Turkey.
0000-0003-1648-951X

Abstract

The recent rapid population growth, drought and climate change become a threat to the sustainability of water resources entail necessary for societies to take administrative and economic precautions for the water supply. One of these precautions to acquire alternative water resources, use seawater with desalination. Electrodialysis (ED) method is widely used for this purpose. Polyvinylidene Fluoride (PVDF) membranes which placed in the ED cell, cation selectivity feature has been gained by compounds containing negative functional groups such as Camphor sulfonic acid (CSA). The morphologies and functional groups of the cation selective membranes obtained as a result of the modification were investigated by Scanning Electron Microscope (SEM) and Fourier Transform Infrared Spectroscopy (FT-IR) techniques. The presence of functional groups expected to be formed on the membrane surface as a result of the modification of PVDF membranes with CSA was proven by FT-IR spectra.

The surface morphologies of the modified membranes using the SEM technique were investigated. The increase in superficial pore sizes was clearly seen when the modified membranes were compared with the pores of the unmodified membranes. These studies concluded that the membrane modification process used in the Electrodialysis method was successful.

Keywords: Electrodialysis, cation exchange membrane, modification, desalination, FT-IR, SEM.

TUZSUZLAŞTIRMADA ELEKTRODİYALİZ YÖNTEMİNİN DENENMESİ VE DEĞERLENDİRİLMESİ

Özet

Son zamanlarda hızlı nüfus artışı, kuraklık ve iklim değişikliğinin, su kaynaklarının sürdürülebilirliği üzerinde tehdit oluşturması, toplumların su temininde idari ve ekonomik önlemler alma konusunda girişimde bulunmalarını zorunlu hale getirmiştir. Bu girişimlerden bir tanesi de alternatif su kaynağı elde etmek amacıyla deniz suyunun tuzsuzlaştırılarak kullanılması olmuştur. Elektrodializ (ED) bu amaçla yaygın olarak kullanılan bir yöntemdir. ED hücresi içerisine yerleştirilen Poliviniliden Florid (PVDF) membranlara katyon seçicilik özelliği; Kafur sülfonik asit (CSA) gibi pozitif fonksiyonel gruplar içeren bileşik ile modifikasyon işlemi sonucunda kazandırılmıştır. Modifikasyon sonucu elde edilen katyon seçici membranların morfolojileri ve fonksiyonel grupları Taramalı Elektron Mikroskop (SEM) ve Fourier Dönüşümlü Kızılıötesi Spektroskopisi (FT-IR) teknikleri ile incelenmiştir. PVDF membranın CSA ile modifikasyon işlemi sonucunda kazandırıldığı düşünülen fonksiyonel grupların varlığı FT-IR tekniği ile gözlenmiştir. Modifiye edilmiş membranların yüzey morfolojileri SEM tekniği ile incelenmiştir. Modifiye edilmiş ile modifiye edilmemiş membran karşılaştırıldığında modifiye edilmiş membranların gözenek boyutundaki artış açıkça görülmüştür. Bu çalışma ED yönteminde yapılan modifikasyon işleminin başarılı olduğunu göstermiştir.

Keywords: Elektrodializ, katyon seçici membrane, modifikasyon, tuzsuzlaştırma, FT-IR, SEM.

Giriş

Günümüzde su ihtiyacının sağlıklı, güvenli ve sürdürülebilir bir şekilde karşılanması birçok ülkenin gündemine aldığı önemli konulardan bir tanesidir. Hızlı nüfus artışı, kuraklık ve iklim değişikliği gibi etkenlerin su kaynaklarının güvenliği ve sürdürülebilirliği üzerinde tehdit oluşturduğu, sanayileşme ve turizm faaliyetlerinin artması ile birlikte su kaynaklarının hızlı bir şekilde tükenmeye başladığı görülmektedir. Artan su ihtiyacını karşılamak amacıyla yeraltı su kaynaklarına başvurulması mevcut su kaynaklarının ihtiyacı karşılamada yetersiz olduğunu göstermektedir.

Son yıllarda birçok ülke yeterli ve kaliteli su temini amacıyla idari ve ekonomik önlemler alma yolunda girişimlerde bulunmuştur. Bu girişimlerden bir tanesi de deniz suyunun tuzsuzlaştırılarak mevcut su kaynaklarına alternatif olarak yeni bir su kaynağı haline getirilmesi olmuştur. Özellikle su fakiri ve denize kıyısı olan birçok ülkenin su ihtiyacını karşılamada kaynak olarak deniz suyuna başvurduğu görülmektedir.

Deniz suyunun tuzsuzlaştırılmasında yaygın olarak termal yöntemler ve membran prosesleri kullanılmaktadır.

Son yıllarda deniz suyunun tuzsuzlaştırılmasında membran proseslerin gelişmesi ve maliyetlerinin azalması, bu teknolojilerinin kullanımını cazip hale getirmiştir. Termal yöntemlerin beraberinde kurulan ısıtma tesislerinin emisyonları göz önüne alındığında membran proseslerin çevreye olan etkileri daha az olup yüksek enerji verimliliğine sahiptir. Ekosisteme katkı sağlayan membran prosesleri deniz suyunun tuzsuzlaştırılmasında önemli bir yere sahiptir.

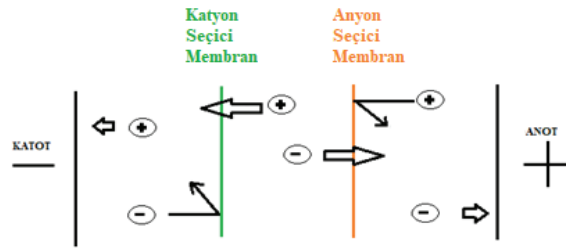
Membran arıtım yöntemlerinde önemli role sahip olan ED yönteminin ana bileşenleri iyon değiştirici membranlardır (Sadrazadeh, Razmi, et al., 2007). ED işlemi, adından da anlaşılacağı gibi elektroliz ve diyaliz İşlemlerinin bir araya gelmesi ile teşkil edilmektedir (Ergün E., 2008). Diyaliz işleminin verimliliğini arttırmak amacıyla sisteme elektrotlar yardımı ile akım uygulanması sonucu meydana çıkmıştır (Çetin B., 2006).

ED sistemi; ED hücre, pompa, güç kaynağı ve besleme suyundan meydana gelmektedir.

ED sisteminin ana bileşeni ED hücresidir. ED hücresini elektrotlar (anot ve katot), iyon seçici membranlar (anyon ve katyon seçici membranlar) meydana getirmektedir. ED hücresine verilen elektrik akımı ile birlikte iyonlar, iyon seçici membranlara doğru harekete geçer ve ayırım gerçekleştirilmiş olur. Katyonlar, katyon seçici membranlardan geçebilirken anyon seçici membranlardan geçemezler. Aynı şekilde anyonlarda, anyon seçici membranlardan geçebilirken katyon seçici membranlardan geçemezler (Çetin B., 2006).

ED işleminde difüzyon ve elektrik akımı en etkili mekanizmalardır (Tezakıl F., 2008). ED hücresinin tasarımı ve şekili giderilecek olan iyon konsantrasyonunda etkilidir (Valero., F., Barcelo, A., Arbos, R., 2020).

ED işleminin çalışma prensibi basitçe Şekil 1’de gösterilmektedir.



Şekil 1. ED işleminin basitçe çalışma prensibi

ED hücrede anyon ve katyon seçici membranlar birbirlerinden contalar vasıtası ile ayrılırmaktadır (Aytaç E., 2016).

Bir ED hücre içerisindeki iyon seçici membranların sayısı değişebilmek ile birlikte bir endüstriyel ölçekli ED hücresinde 100 ile 200 adet arasında bulunabilmektedir. Genellikle uygulamalarda levha ve dolambaçlı akışlı yığın tasarımlı hücreler kullanılmaktadır. Levha akışlı ED hücrelerinde membranlar dikey yerleştirilirken, dolambaçlı akışlı hücrelerde membranlar yatay yerleştirilmektedir (Strathmann, 2010).

ED hücre sistemleri en yaygın olarak deniz suyunun tuzsuzlaştırılmasında, birçok endüstride tuz ve asitin birbirinden ayırımında ve saf su üretimi işlemlerinde kullanılmaktadır (Aytaç E., 2016). 29

ED işleminde akım sürekli ve kesikli şekilde teşkil edilirken membranlarda tıkanma, kirlenme ve bozulma problemleri yaşanabilmektedir (Karabacakoglu B., 2001).

ED sisteminin verimi; hücre çifti sayısı, uygulanan voltaj, debi, çözelti konsantrasyonu ve sıcaklık gibi parametrelerden etkilenmektedir. Suyun sertliği ve organik açıdan kirliliği de membran tıkanmalarına sebep olacağından verimi etkileyen diğer önemli parametrelerdir (Káňavová et al., 2014).

ED işlemi; öncesinde basit bir ön arıtımın yeterli olması, düşük basınçta işletilebilmesi, yüksek basınçlı pompalara ihtiyaç duyulmaması, sessiz işletilebilmesi, membran koruyucuya ihtiyaç duyulmaması, işletme ve bakım maliyetinin düşük olması, iyon gideriminde yüksek verime sahip olması ve yüksek derişimli sularda etkili olması gibi avantajlara sahiptir. İyon dışındaki organik kökenli kirlleticiler üzerinde etkili olmaması ve enerji ihtiyacı ED işleminin dezavantajlarından (Scott, K., 1996).

ED işlemi tuzlu suyun tuzsuzlaştırılmasında 50 yılı aşkın süredir kullanılan bir yöntem olmak ile birlikte son yıllarda yaşanan gelişmeler ile gıda ve kimya olmak üzere çeşitli endüstrilerde de uygulanmaya başlanmıştır (Strathmann, 2010).

Materyal ve Yöntem

Materyaller

Çalışma boyunca membran modifikasyonunda kullanılan materyaller; PVDF membran, Klorosülfonik asit (HSO_3Cl), 1.2 Dikloroetan ($\text{C}_2\text{H}_4\text{Cl}_2$), Sülfirik asit (H_2SO_4), Anilin ($\text{C}_6\text{H}_5\text{NH}_2$), amonyum peoksodisülfat ($(\text{NH}_4)_2\text{S}_2\text{O}_8$), Amonyak (NH_3), Kafur Sülfonik asit (CSA), saf su ve vakumlu fırındır.

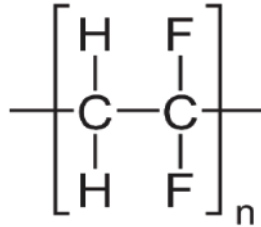
Membran Modifikasyonu Yöntemi

Membran modifikasyonu yöntemi şu şekilde gerçekleştirilmiştir. Membran modifikasyonu için hidrofilik özellikte PVDF membran kullanılmıştır. PVDF membranlara aşağıda belirtilen modifikasyon işlemleri yardımı ile anyon ve katyon seçicilik özelliği kazandırılmıştır.

Katyon seçici membranlar yapıları gereği negatif yüklü gruplara sahip olmalıdır. Ticari olarak temin edilen hidrofilik özelliğe sahip olan PVDF membranların üzerlerinde negatif yüklü gruplar oluşturmak üzere sülfonlama işlemi yapılmıştır.

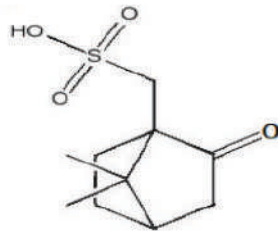
Sülfonlama işlemi sırasıyla şu şekilde gerçekleştirilmiştir. Membranlar hazırlanan Klorosülfonik asit çözeltisinde $80\text{ }^\circ\text{C}$ 'de 45 dk bekletilmiştir. Daha sonra membranlar sırası ile 1.2 Dikloroetan ve saf su ile yıkandıktan sonra $50\text{ }^\circ\text{C}$ 'de vakumlu fırında kurutulmuştur. Kurutulan membranlar 0,5 M Sülfirik asit ve anilin çözeltisinde 1 saat bekletilmiş ve sonrasında saf su ile yıkanmıştır. Sonrasında sırası ile 0,5 M amonyum peoksodisülfat çözeltisi içerisinde 4 saat 0,5 Molar amonyak çözeltisi içerisinde 12 saat bekletilmiş ve saf su ile yıkanmıştır. Son olarak membranlar 0,1 M CSA çözeltisinde 12 saat bekletilerek modifikasyon işlemi tamamlanmıştır (Farrokhzad et al., 2015). Elde edilen yeni membran S-PVDF-CSA adı ile tanımlanmıştır.

PVDF membranının kimyasal yapı formülü Şekil 2'de gösterilmiştir.



Şekil 2. PVDF'nin kimyasal yapı formülü (Anonim, 2021c)

PVDF membranların modifikasyonunda kullanılan CSA'nın kimyasal yapı formülü Şekil 3'te gösterilmiştir.



Şekil 3. Membran modifikasyonunda kullanılan CSA'nın kimyasal yapı formülü CSA

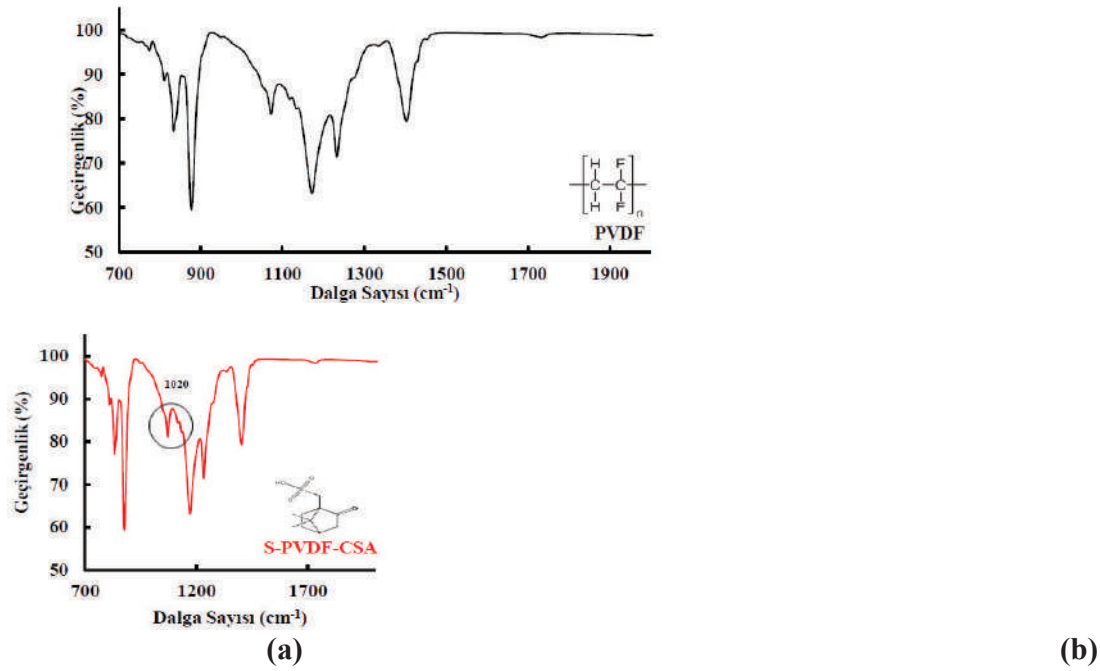
Membran Karakterizasyonu Yöntemleri

Modifikasyon sonucu elde edilen yeni membranların fonksiyonel grupları ve morfolojileri Perkin-Elmer Spectrum Two Model FT-IR ve Jeol JSM 7001 F Model Elektron Taramalı Mikroskobu (SEM) aracılığı ile incelenmiştir.

Sonuç ve Tartışma

Modifiye Edilmiş Membranların Fonksiyonel Gruplarının İncelenmesi

PVDF membranların CSA ile modifikasyonu sonucunda membran yüzeyinde oluşan fonksiyonel gruplar FT-IR spektrumları aracılığı ile belirlenmiştir. Modifikasyon işlemi sonucu elde edilen S-PVDF-CSA membranların ve işlem görmemiş PVDF membranının FT-IR spektrumları ayrı olarak Şekil 4'te gösterilmiştir.



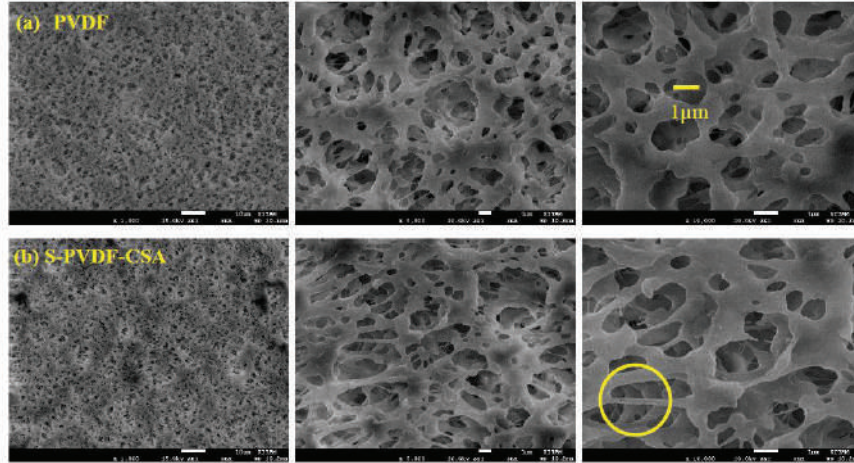
Şekil 4. Membranların ayrı IR spektrumları (a) PVDF (b) S-PVDF-CSA

IR spektrumları incelendiğinde; temel membran esas malzemesi olan ve PVDF için karakteristik C-H pik gerilmelerinin (en yüksek geçirimsizliğinin) 810 ve 870 cm⁻¹ dalga sayısı aralığında olduğu Şekil 4 (a)'da açıkça görülmektedir. 1100-1400 cm⁻¹ dalga sayısı aralığındaki keskin pik gerilmelerinin PVDF yapısındaki C-F bağlarını işaret ettiği Şekil 4 (a)'da görülmektedir. PVDF membran üzerindeki modifikasyon işleminin etkisi ile oluşan sülfon gruplarından kaynaklı S=O titreşimleri yaklaşık 980 ve 1020 cm⁻¹ dalga sayısı aralığında S-PVDF-CSA örneklerinde olduğu Şekil 4 (b)'de görülmektedir (Anonim, 2021d).

Şekil 4 (b)'de S-PVDF-CSA modifiye edilmiş PVDF membranın spektrumları modifiye edilmemiş PVDF membranın IR spektrumları ile karşılaştırıldığında geçirgenlik değerlerinin azalmış olduğu gösterilmektedir. Bu durum modifikasyon işleminin gerçekleştiğini göstermektedir.

Modifiye Edilmiş Membranların Morfolojilerinin İncelenmesi

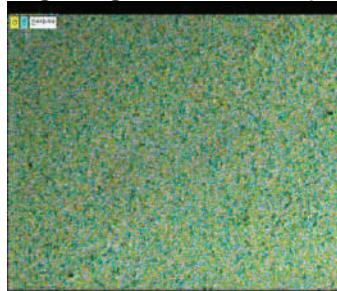
PVDF membranların modifikasyonu sonucunda elde edilen S-PVDF-CSA membranlarının ve modifikasyon işlemi görmemiş PVDF membranının morfolojileri Jeol JSM 7001 F Model Elektron Taramalı Mikroskobu (SEM) aracılığı ile görüntülenerek Şekil 5'te gösterilmiştir. Modifikasyon işlemi sonucunda membran yüzeyinde meydana gelen değişimleri fiziksel olarak göstermek için kıyaslama yapmak amacıyla, modifikasyon işlemi yapılmamış PVDF membranın SEM görüntülerinden faydalanılmıştır.



Şekil 5. Membranların x1000, x5000 ve x10000 büyütmede SEM görüntüleri (a) PVDF (b) S-PVDF-CSA

Şekil 5'te x1000, x5000 ve x10000 büyütmede alınan SEM görüntülerinden faydalanılarak modifikasyon işlemi sonucunda membranların yüzeyel gözenek boyutlarında değişiklik olup olmadığı, bu değişikliklerin homojenliği ve membranların mukavemeti, modifikasyonsuz PVDF membranların gözenekleri ile karşılaştırılmıştır. Şekil 5'te görüldüğü gibi modifikasyonsuz PVDF membranın x10000 büyütmede ortalama gözenek çapı yaklaşık 1 µm olarak gözlemlenmiştir. Modifikasyon işlemi sonucunda x10000 büyütmede elde edilen SEM görüntüsünde, modifikasyon işlemi sonucunda membranların modifikasyonsuz PVDF membranların gözenekleri ile karşılaştırıldığında yüzeyel gözenek boyutlarındaki artış açıkça görülmektedir. Ayrıca x10000 büyütmede S-PVDF-CSA modifikasyonlu membranlar incelendiğinde, gözenek boyutlarındaki aşırı artışı ile ipliksi yapıların oluşmasının membranların mukavemetinde azalma etkisi meydana getirmesi beklenmekte olduğu sonucuna varılmıştır.

PVDF membranların modifikasyonu sonucunda elde edilen S-PVDF-CSA membranların yüzeylerindeki modifikasyon bileşiklerindeki elementlerin varlığı Taramalı Mikroskobu Enerji Dağılımı Spektrometresi (SEM-EDS) aracılığı ile görüntülenerek Şekil 6'da gösterilmiştir.



Şekil 6. S-PVDF-CSA membranının SEM-EDS görüntüsü (S elementi dağılımı)

Şekil 6’da membran modifikasyonunda kullanılan CSA bileşiğinin yapısındaki sülfonik gruplardan kaynaklı kükürt (S) elementlerinin varlığı ve homojen dağılımı SEM-EDS görüntülerinde açıkça görülmektedir.

Referanslar

Sadrzadeh, M., Razmi, A., & Mohammadi, T. (2007). Separation of monovalent, divalent and trivalent ions from wastewater at various operating conditions using electrodialysis. *Desalination*, 205(1–3), 53–61. <https://doi.org/10.1016/j.desal.2006.04.039>.

Ergün E. (2008). *Elektordiyaliz Yöntemi ile Sulardan Florürün Giderilmesi*. . Selçuk Üniversitesi.

Çetin B. (2006). *Bakır ve Nikel İyonlarının Hibrit İyon Değişimi - Elektrodializ Süreci ile Giderilmesi*. Osmangazi Üniversitesi, Fen Bilimleri Enstitüsü.

Tezakıl F. (2008). *Sertlik Gideriminde Elektrodializ ve Elektrodeiyonizasyon Yöntemlerinin Kullanılması*. Osmangazi Üniversitesi.

Valero., F., Barcelo, A., Arbos, R. (2020). Electrodialysis Technology. Theory and Applications. In *Mean Field Simulation for Monte Carlo Integration*. <https://doi.org/10.1201/b14924-7>.

Strathmann, H. (2010). Electrodialysis, a mature technology with a multitude of new applications. *Desalination*, 264(3), 268–288. <https://doi.org/10.1016/j.desal.2010.04.069>.

Aytaç E. (2016). *Elektrodializ Yöntemi ile Atıksulardan Kurşun, Bakır ve Nikel Gideriminin Araştırılması*. Bülent Ecevit Üniversitesi.

Káňavová, N., Machuča, L., & Tvrzník, D. (2014). Determination of limiting current density for different electrodialysis modules. *Chemical Papers*, 68(3), 324–329. <https://doi.org/10.2478/s11696-013-0456-z>

Karabacakoğlu B. (2001). *Seyreltik Çözeltilerden Gümüş İyonlarının Uzaklaştırılmasında Elektrodializin Uygulanması*. Doktora Tezi. Osmangazi Üniversitesi.

Scott, K. (1996). Overview of the application of synthetic membrane processes. Industrial Membrane Separation Technology. *Modern at Large: Cultural Dimensions of Globalization*, 6276. <http://dx.doi.org/10.1016/j.cirp.2016.06.001%0A> <http://dx.doi.org/10.1016/j.powt> .

Anonim.(2021c). *PVDF’nin kimyasal yapı formülü*. http://tr.swewe.net/word_list.htm/?class_88_257&Kimyasal_adı

Anonim.(2021d). *Spectrum Table*. <https://www.sigmaaldrich.com/technical-documents/articles/biology/ir-spectrum-table.html>.

EFFECT OF SMALL-SCALE FISH CAGE CULTURE ON SEDIMENT QUALITY OF THE SOUTHERN CASPIAN SEA: CASE STUDY IN IRANIAN COAST-NOWSHAHR

Nasrollahzadeh Saravi H.

Caspian Sea Ecology Research Center (CSERC), Iranian Fisheries Science Research Institute (IFSRI),
Agricultural Research, Education and Extension Organization (AREEO), Sari, Iran.

Vahedi, F.

Caspian Sea Ecology Research Center (CSERC), Iranian Fisheries Science Research Institute (IFSRI),
Agricultural Research, Education and Extension Organization (AREEO), Sari, Iran.

Makhlough A.

Caspian Sea Ecology Research Center (CSERC), Iranian Fisheries Science Research Institute (IFSRI),
Agricultural Research, Education and Extension Organization (AREEO), Sari, Iran.

Baluei, M.

Caspian Sea Ecology Research Center (CSERC), Iranian Fisheries Science Research Institute (IFSRI),
Agricultural Research, Education and Extension Organization (AREEO), Sari, Iran.

Abstract

Due to the reduction of catching fish and use of saline and brackish waters, there are strong economic incentives to develop marine aquaculture. The aim of current study was to assess floating cage culture and the environmental quality statements based on different physico-chemical parameters and also compare its statements with the threshold values in the Iranian coastal waters of Caspian Sea (Nowshahr region). 142 water samples were collected along four distances (shadow, 100, 200 and 1000 meters) around the fish cage culture and four periods (before, start, middle and end of breeding) between autumn 2017 and autumn 2018. Sixteen physico-chemical parameters were analyzed based on standard methods. The principle component analysis (PCA) showed that first component alone accounts for 28.8% of the total variance. This component were contained SDD, DO%, Chl-a with loading factor (>0.6) and salinity, COD and NH_4 with loading factor (>0.4). The trophic level of Caspian Sea (TRIXcs) in the percentiles of 25-75% were observed 4.36-5.10. Stepwise regression test for the whole period showed that TRIXcs had a significant relationship with phosphorus, Chl-a and oxygen saturation ($p < 0.05$). Results also showed that values of whole 16 physico-chemical parameters (except BOD5) were less than threshold value and standards values criteria of some countries at marine ecosystems. The trophic status of this area changed from mesotrophic to meso-eutrophic and also high risk eutrophication process was predicted. Based on the universal and local criteria of Chl-a values, the water had high quality at most layers around the cages, and the quality was slightly reduced from the shadow of cage to a distance of 100 or 200 meters. In the southern part of the Caspian Sea, small-scale marine floating cages are now being installed, and the number of cages cannot have visible effects on the ecosystem.

Keywords: Physico-chemical parameters, Cage culture, Iranian coast, Caspian Sea, Iran

INVESTIGATION OF STRUCTURAL PROPERTIES OF AL/P-SI/CDO:NIO/AL PHOTODIODE FABRICATED BY SOL-GEL SPIN COATING METHOD

Ezgi GURGENC

Energy systems Engineering, Firat University, 0000-0002-0653-4041,

Aydın DİKİCİ

Energy systems Engineering, Firat University, 0000-0003-4892-2277

Fehmi ASLAN

Energy systems Engineering, Firat University, 0000-0002-5304-0503,

Abstract

Semiconductors such as titanium oxide (TiO₂), zinc oxide (ZnO), cadmium oxide (CdO) and nickel oxide (NiO) are often used in photodiode, photo sensor and optical applications. In addition to doping, one of the methods used to improve the properties of optoelectronic materials produced from metal oxide semiconductors is to obtain a new composite structure by mixing the semiconductors in different proportions [1-4]. In present study, pure cadmium oxide (CdO), nickel oxide (NiO) and different molar ratios of CdO:NiO thin films were deposited on p-Si layer by sol-gel spin coating technique. 2-methoxyethanol was used as the solvent and monoethanolamine was used as the stabilizer. Cadmium acetate was used as Cd source and Nickel acetate was used as Ni source for preparing sol-gel. p-Si sheet was cleaned with acetone, distilled water, ethanol and distilled water for 5 minutes each in ultrasonic bath. Then, this plate was immersed in 1:10 HF:H₂O solution for 30 seconds and ultrasonically washed in distilled water for 5 minutes. The bottom contact of the sheet, which was dried with nitrogen gas, was coated with Al and finally cut in 10*10 mm² dimensions. 0.5 M Cd and Ni in molar ratios of Cd:Ni (1:0, 0:1; 3:1; 1:3 and 1:1) were poured in to 10 ml solvent and mixed on a magnetic stirrer until all the powders were dissolved. 0.5 M stabilizer was dropwise to the mixture while stirring continue and was stirred at 80 °C for 2 h. Sol-gel solutions, which were left to rest for 24 hours at room temperature, were deposited on p-Si sheets at 3000 rpm for 30 seconds with dynamic spin coating technique and dried at 150 °C for 10 seconds. The dried samples were kept at room temperature for 10 minutes and the same procedures were repeated, and two-layer coating was carried out. The coated samples were calcined in the oven at 450 °C for 1 hour. FE-SEM, EDX and XRD analyzes were performed for structural characterizations. Thin films on the surface are composed of nano-sized structures and peaks of both elements were found in composite coatings in EDX analysis. In XRD analyzes it was observed that the peak intensities differed as the Cd/Ni ratio changed (Figure 1). The intense peaks observed in CdO thin film coating at 2θ angles of 33.01°, 38.29°, 55.28°, 65.91° and 69.25° corresponding to (111), (200), (220), (311) and (222) planes, respectively. The indexed peaks are fully consistent with the crystalline CdO (JCPDS 005-0640). The absence of secondary phases and impurities in the XRD diffraction peaks proves that CdO has been successfully formed. XRD analysis results of CdO thin film is in good agreement with literature studies [5], [6]. The intense peaks observed in NiO thin film coating at 2θ angles of 37.26°, 43.30°, 62.92°, 75.48° and 79.44° corresponding to (111), (200), (220), (311) and (222) planes, respectively. The indexed peaks are fully consistent with the cubic-structured crystalline NiO. No secondary or impurity peaks were observed. This indicates that NiO is crystalline and successfully formed. XRD analysis results of NiO thin film is in good agreement with literature studies [7], [8]. Characteristic peaks of both NiO and

CdO were observed in composite thin film coatings. This shows that the CdO:NiO composite thin film coatings were carried out successfully. The characteristic peaks of the element with higher ratio are higher in composite thin films. The characteristic peaks shifted to slightly higher 2 theta degrees compared to pure CdO and NiO. It has been concluded that pure and composite thin films have been successfully formed on p-Si and these films can find applications in optoelectronic and solar energy tracking systems.

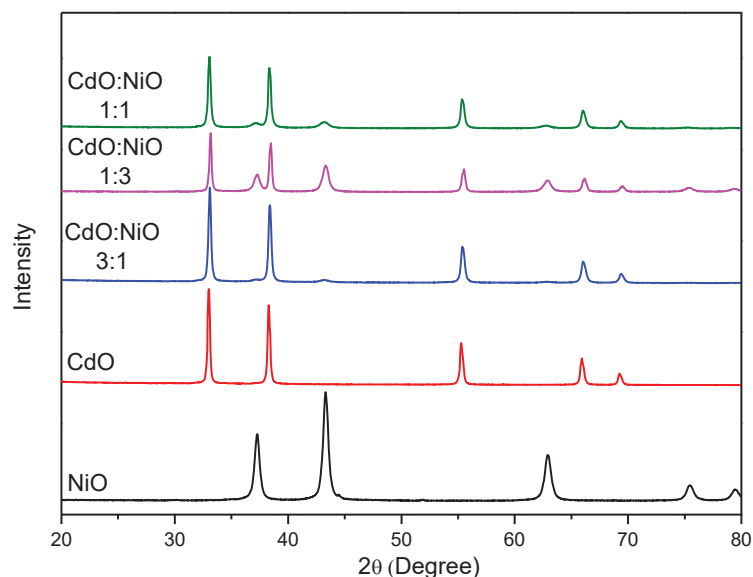


Figure 1. XRD results of thin films.

Keywords: Sol-gel spin coating technique, Thin Film, Composite, Solar energy, Photodiode.

Acknowledgement: The authors thank the Firat University Research Fund (FUBAP-TEKF.21.11) for their financial contribution to this research and the author Ezgi GURGENC would like to thank Council of Higher Education (CoHE) for its scholarship support with the 100/2000 Ph.D. scholarship.

References

- [1] F. Yakuphanoglu, Transparent metal oxide films based sensors for solar tracking applications, *Composites Part B: Engineering*, 92 (2016) 151-159.
- [2] B.A.H. Ameen, A. Yildiz, W. Farooq, F. Yakuphanoglu, Solar light photodetectors based on nanocrystalline zinc oxide cadmium doped/p-Si heterojunctions, *Silicon*, 11 (2019) 563-571.
- [3] N.M. Khusayfan, Electrical and photoresponse properties of Al/graphene oxide doped NiO nanocomposite/p-Si/Al photodiodes, *JAlIC*, 666 (2016) 501-506.
- [4] A. Sevik, B. Coskun, M. Soylu, The effect of molar ratio on the photo-generated charge activity of ZnO–CdO composites, *The European Physical Journal Plus*, 135 (2020) 65.
- [5] Ravichandran, A. T., Xavier, A. R., Pushpanathan, K., Nagabhushana, B. M., & Chandramohan, R. (2016). Structural and optical properties of Zn doped CdO nanoparticles synthesized by chemical precipitation method. *Journal of Materials Science: Materials in Electronics*, 27(3), 2693-2700.
- [6] Gupta, V. K., Fakhri, A., Tahami, S., & Agarwal, S. (2017). Zn doped CdO nanoparticles: structural, morphological, optical, photocatalytic and anti-bacterial properties. *Journal of colloid and interface science*, 504, 164-170.
- [7] Al-Ghamdi, A. A., Mahmoud, W. E., Yaghmour, S. J., & Al-Marzouki, F. M. (2009). Structure and optical properties of nanocrystalline NiO thin film synthesized by sol–gel spin-coating method. *Journal of Alloys and Compounds*, 486(1-2), 9-13.
- [8] Zhao, S., Shen, Y., Zhou, P., Zhang, J., Zhang, W., Chen, X., ... & Shen, Y. (2018). Highly selective NO₂ sensor based on p-type nanocrystalline NiO thin films prepared by sol–gel dip coating. *Ceramics International*, 44(1), 753-759.

NUMERICAL STUDY OF THE EFFECT OF EXTERNAL MAGNETIC FIELDS ON THE TURBULENT NATURAL CONVECTION OF NANOFLUIDS IN A TWO-DIMENSIONAL CAVITY

Zakaria LAFDAILI

Laboratory Mechanics, Processes, Energy and Environment (LMPEE),
National School of Applied Sciences, University Ibn Zohr, Agadir, Morocco

Sakina El-Hamdani

Laboratory Mechanics, Processes, Energy and Environment (LMPEE),
National School of Applied Sciences, University Ibn Zohr, Agadir, Morocco

Mohamed El Hattab

Laboratory Mechanics, Processes, Energy and Environment (LMPEE),
National School of Applied Sciences, University Ibn Zohr, Agadir, Morocco

Lahoucine Belarche

Equipe Matériaux, Mécanique et Génie Civil (E2MGC)
National School of Applied Sciences, University Ibn Zohr, Agadir, Morocco

Abstract

The present work consists in numerically studying the magnetohydrodynamics of the turbulent natural convection of nanofluids (Water + Ag / TiO₂ / Cu) in a differentially heated rectangular cavity. To predict the turbulent behavior of the flow, we used the standard $\kappa - \epsilon$ turbulence model. The governing equations of the physical problem are discretized by the finite volume method using the power law interpolation scheme to approximate the values of the functions of the various variables at the interfaces of the control volumes with respect to the nodes of the grid. The study focuses on the effect of physical parameters such as the Rayleigh number ($10^7 \leq Ra \leq 10^{10}$), the two-dimensional orientation of the magnetic field ($0 \leq \gamma < 2\pi$), the Hartmann number ($0 \leq Ha \leq 300$) and the volume fraction in nanoparticles ($0\% \leq \phi \leq 6\%$).

The results obtained show that the Rayleigh and Hartmann numbers have a considerable effect on the hydrodynamic and thermal fields. Indeed, the addition of the nanoparticles changes the thermal and electrical performance of the mixture, which significantly affects the convective heat exchange within the enclosure in the presence of a magnetic field. In addition, the orientation angle of this field strongly affects the hydrodynamic and thermal flow in nanofluids.

Keywords: Convection, natural, turbulence, nano-fluid, magnetic field.

STUDY OF METHODS OF EXTRACTING A WILD PLANT FROM THE ALGERIAN SAHARA

Belfarhi Leila

Permanent researcher at the CRAPC research center in Algiers
PhD student (Es science), Department of Animal Biology, University of Annaba

Leila Belfarhi

Laboratory of neuro-endocrinology, University of Badji Moukhtar, Annaba, Algeria; Center of Research in Physico-chemical analyses CRAPC, Tipaza, Algeria

Tahraoui Abdelkrime

Laboratory of neuro-endocrinology, University of Badji Moukhtar, Annaba, Algeria; Center of Research in Physico-chemical analyses CRAPC, Tipaza, Algeria

Bairi Abdelmedjid

Laboratory of neuro-endocrinology, University of Badji Moukhtar, Annaba, Algeria; Center of Research in Physico-chemical analyses CRAPC, Tipaza, Algeria

Ibtissem Chouba

University of Badji Moukhtar, Annaba, Algeria

Naziha Amri

Laboratory of neuro-endocrinology, University of Badji Moukhtar, Annaba, Algeria

Nadia Boukris

University of Badji Moukhtar, Annaba, Algeria; Service of Internal Medicine Hospital CHU IBEN SINA, Annaba, Algeria

Summary

The extraction of medicinal plants is a necessary step to isolate the bioactive molecules. However, this method is carried out using chemical solvents which can extract the molecules but also pollute the extract. Traditional methods of extraction are more efficient and can produce pure and unpolluted molecules. In this study two methods of extracting *Calotropis procera* were tested. The plant were obtained from the Sahara of Algeria. The first method was to extract the plant with chemical solvents. The plant powder was put in ethanol for 72 hours. After maceration, the ethanolic extract was filtered and the extract was decanted with solvents; chloroform, butanol and ethyl acetate. After filtration, the extracts appeared transparent green color. The extracts were kept in glass bottles and stored in the refrigerator. The second method is a cold extraction of the *Calotropis procera* plant without chemical solvents. The extract has not been filtered. A black to dark green extract was obtained. We put the extract in a UV-resistant bottle. The extracts obtained were immediately tested on rats and they were not stored in the refrigerator. The extracts of the *Calotropis procera* plant obtained by the two methods were tested for their protective effects vis-à-vis the toxicity of mercury. The results of the histopathology study of the kidney and liver of male Wistar rats treated with *Calotropis procera* extract obtained by cold extraction show that the renal glomeruli are of normal structure. The extract obtained by cold

extraction completely protected the liver of the rats. However, the extract obtained by chemical and hot extraction did not protect the kidneys and liver of rats from mercury toxicity. The results of this study demonstrate that cold extraction is a key to obtaining pure and effective molecules that can protect vital organs like the kidney and liver. The purpose of this communication is unveiled a new method of extracting plants used in the Sahara of Algeria to extract even the most complex plants such as *calotropis procera*.

Key word:

Cold extraction, chemical extraction, *calotropis procera*, antioxidants, kidney, liver.

Résumé

L'extraction des plantes médicinales est une étape nécessaire pour isoler les molécules bioactives. Cependant cette méthode est réalisée à l'aide des solvants chimiques qui peuvent extraire les molécules mais pollue aussi l'extrait. Les méthodes traditionnelles d'extraction sont plus efficaces et peuvent engendrer des molécules pure et non polluée. Lors de cette étude on a testé deux méthodes d'extraction d'une plante sauvage la *calotropis procera*. Les feuilles de la plante ont été récoltées à partir de la plante provenant de la willaya d'ILIZI du Sahara d'Algérie. La première méthode on a extrait la plante par des solvants chimiques. On a mis la poudre de la plante pendant 72 h dans l'éthanol. Après macérations on a filtré l'extrait éthanolique et on a procédé à la décantation de l'extrait par des solvants ; le chloroforme, le butanol et l'éthyle acétate. Après filtration on a obtenue des extraits de couleur vert transparent. Les extraits ont été maintenus dans des bouteilles en verre et stocké dans le réfrigérateur. La seconde méthode est une extraction à froids de la plante *calotropis procera* sans solvant chimique. L'extrait n'a pas été filtré. On a obtenu un extrait noir à vert foncé. On a mis l'extrait dans une bouteille anti-UV.

Les extraits de la plante *calotropis procréa* obtenue par les deux méthodes ont été testé pour leur effets protecteur vis-à-vis de la toxicité du mercure. Les résultats de l'étude histopathologie du rein et du foie des rats Wistar mâles traités avec l'extrait de la *Calotropis procera* obtenue par extraction à froids montre que les glomérules rénaux et sont de structure normale. L'extrait obtenu par extraction à froids a protégé totalement le foie des rats. Cependant l'extrait obtenu par extraction chimique n'a pas protégé les reins et le foie des rats contre la toxicité du mercure. Les résultats de cette étude démontrent que l'extraction des plantes est une clé pour obtenir des molécules pur et efficace qui peuvent protégée des organes vitaux comme le rein et le foie. Le but de cette communication est dévoilé une nouvelle méthode d'extraction des plantes algériennes à froids utilisée au Sahara d'Algérie pour extraire des plantes même les plus complexes comme la *calotropis procera*.

Mots clé :

Extraction à froids, extraction chimique, *calotropis procera*, antioxydants, reins, foie.

ENVIRONMENT AND SUSTAINABLE DEVELOPMENT GOALS IN INDIA

Dr. Rekha Suman

Assistant Professor, Sociology

University Institute of Legal Studies, AVA Loge, Himachal Pradesh University, Shimla-171004

Abstract

“There is enough for everyone’s need But not for everyone’s greed”

Mahatama Gandhi

Sustainable is a Latin born term which means to carry on, to endure, to live through, to maintain, to sanction, to prolong, to encourage, to support the life of living being. It may be described as a harmonious balance that manipulates development along with environmental imperatives. Human race is absolutely dependent upon nature for its existence, continuation and growth. Nature is a treasure trove which has an assortment of resources for human beings. Interdependence of humans with nature sometimes creates a problem which can affect our future generation. Humans, because of their greedy nature, are destroying the resources which is a matter of major concern, because our future on earth is at high risk. Human activities motivated by the attitude of unchecked consumerism and (false) invalid patterns of production and consumption have never been as mean and cruel towards the environment as in the modern era of scientific and technological innovations. The study will be based on secondary data and will be theoretical in nature. The objectives of the study shall be to highlight the initiatives of Stockholm conference related to environment, to highlight the initiatives of Government of India to achieve the Stockholm initiatives, to highlight the importance of environment and Sustainable Development Goals for future generation and to evaluate the law related to environment in India. It can be concluded that in new era the environment is degrading with the pace of development and human life is at high risk. It can be reduced only by adopting the sustainable development goals.

Keywords: Sustainable Development, Environment, Resources, Nature, Scientific

INVESTIGATION OF TRIBOLOGICAL CHARACTERISTICS OF COPPER-TITANIUM ALLOYS PROCESSED BY MULTI-AXIAL CRYO-FORGING

Ramesh S

Department of Mechanical Engineering, RV Institute of Technology and Management,
Bangalore, India-560076

Gajanan M Naik

Department of Mechanical Engineering, RV Institute of Technology and Management,
Bangalore, India-560076

Gajanan Anne

Department of Mechanical Engineering, National Institute of Technology Karnataka,
Surathkal, India-575025

Abstract

Cu-XTi alloys ($X = 1.5\%$ and 4.5%) were subjected to multi-axial forging (MAF) under cryogenic condition up to 3 passes successfully. Characteristics of the MAF processed alloys were analyzed using microstructural analysis, hardness and wear tests. Worn surface morphology and elemental analysis was done by scanning electron microscope (SEM). The hardness of samples increases with higher MAF passes due to strain hardening and grain refinement. Wear test was done for six different sliding distances (500 m, 1000 m, 1500 m, 2000 m, 2500 m and 3000 m), two different load (10 N and 20 N), and two different velocities (1 m/s, and 2 m/s) using the pin on disc wear test rig. Wear loss of as-received samples is higher than MAF processed samples due to an increase in hardness, but wear loss increases as the load increased. Coefficient of friction is reduced with the increase of MAF pass is due to strain hardening effect. The worn surface exhibits the plastic deformation regions, delamination, ploughing and formation of oxide layers which was revealed in X-Ray diffraction (XRD) analysis.

Keywords: Cu-Ti alloy, Multi-Axial Cryo Forging, Coefficient of Friction and Wear.

DESIGN AND CONTROL OF INDUSTRIAL TYPE LIQUID LEVEL CONTROL SYSTEM**Ahmet TOP**

Department of Electrical and Electronics Engineering, Faculty of Technology,
Firat University, Elazığ, Turkey
ORCID ID:0000-0001-6672-2119

Yener CESUR

Department of Electrical and Electronics Engineering, Faculty of Technology,
Firat University, Elazığ, Turkey

Muammer GÖKBULUT

Department of Electrical and Electronics Engineering, Faculty of Technology,
Firat University, Elazığ, Turkey
ORCID ID:0000-0003-1870-1772

Abstract

In this study, a liquid level control set equipped with a proportional control valve, solenoid valve, liquid level sensor, process controller and data acquisition card used in the industry is designed. These devices in the control system are mounted directly on the liquid tank and the control set is made in one piece. The level of the liquid is measured with the capacitive liquid level sensor, whose probe is adjusted according to the depth of the tank. This measured value is transmitted to the industrial controller as a feedback signal. With this controller, which operates the control algorithm depending on the entered reference value and the feedback signal, the on/off control of the liquid level is performed with a solenoid valve, while the PID control is performed with a proportional control valve. The feedback signal from the liquid level sensor and the control voltage of the valves are instantly transferred to the computer via the data acquisition card, and the graphics of the data are evaluated in the MATLAB/simulink program. The study is very suitable for examining system behaviors with different parameters and coefficients in on/off and continuous control forms. In addition, with this control set, it is ensured that the devices used in the industry are closely recognized and their usages learned.

Keywords: Liquid level control, On/off control, PID control

Introduction

Level measurement is used to determine the height, volumetric amount or mass amount of liquid or solid material in a tank [1]. In industrial systems related to fluid, the parameter that is the most frequent control requirement is level [2]. Liquids are generally used as fluids in control systems [3]. It is possible to see liquid level control in many different sectors such as nuclear power plants [4], food industry [5]. Proportional, integral, derivative (PID) control is the leading control method used in this process control [6-9]. In addition to the PID method, liquid level control applications with algorithms such as fuzzy logic [10-13], genetic algorithm [14], combination of PID and fuzzy logic control method [15-18] are also available in the literature.

Canbolat is introduced a new method for measuring the liquid level in the tank. Existing methods are generally based on the wide difference between the dielectric constants of liquids and air. The main advantage of the method is that it can be applied directly to non-conductive liquids without calibration with three capacitive sensors [19]. Terzic et al. They developed and used a single tube capacitive sensor, in which a neural network-based approach will be applied to accurately determine the fluid level in the automobile fuel tank while it is in motion. An acoustic sensor-based approach to measuring the liquid level in the fuel tank of moving vehicles is tried and validated with the Support Vector Machines classifier [20]. Altın and Bulut is developed a device that can detect the level in liquid tanks used in factories with an ultrasonic sensor and monitor the measurement data by transferring it to a remote

computer or smart phone with Bluetooth [21]. Varun Kumar et al., in their studies, monitors the liquid level in the container with an ultrasonic sensor, transfers this data to a remote display with the Arduino and Zigbee module, and informs with a message that the liquid level is reached a critical value with the GSM module [22]. Toghiani et al. modeled the cylinder capacitive sensor probe for measurement of the level of conductive liquids based on mathematical operations using MATLAB/Simulink [23].

In this study, a liquid level control set was designed and implemented by using elements such as industrial controller device, proportional valve, solenoid valve, industrial sensor, data acquisition device, which have a wide usage area in industry. Liquid level was measured with capacitive level sensor and closed loop control algorithm with this feedback signal was realized with industrial type controller. While the on/off control of the system with and without hysteresis was done with a solenoid valve, the PID control was made with a proportional valve that have 2-10 V DC control voltage. Level and valve voltage values were transferred to the computer with the data acquisition device and graphed in MATLAB/Simulink. As a result, an industry-compatible liquid level control set has been created where practical results can be observed and analyzed instantly.

2. Control System

Controlling can generally be defined as managing the desired output in a desired way [24]. The expected response from the output of the system may be to follow the reference value with the least error, to start and stop with on-off or to follow the reference without error. The control process is divided into two groups as two-position (on/off) or continuous output (PID) generating [25].

2.1 On-Off Control

In this control method, the system is either completely closed or completely open around the reference input value [26]. The input-output relation of the two-position controller, with the error signal $e(t)$ and the controller output $u(t)$, is as follows.

$$u(t) = \begin{cases} U_{\min}, & e(t) < 0 \\ U_{\max}, & e(t) \geq 0 \end{cases} \quad (1)$$

2.2. PID Control

Regardless of the control method in PID control, the output is constantly controlled against the entered reference value. This control method generally consists of different combinations of proportional, derivative and integral control forms [25]. Control signal $u(t)$;

$$u(t) = K_p e(t) + K_i \int_0^t e(t) dt + K_d \frac{de(t)}{dt} \quad (2)$$

It is calculated with the formula. With this controller, both the temporary and steady state of the system can be controlled [25].

3. System Architecture

The architecture of the liquid level control set, whose mechanical connection diagram is given in Figure 1 and electrical connection diagram in Figure 2, consists of the components shown in the diagrams.

(1) The ball valve, ensures the passage of liquid to the system.

(2) The solenoid valve is used for on-off control at the desired set value. It consists of a capsule molded from a glass-filled thermoplastic polyester (30%) material and a heat-resistant coil (resistant up to 200 °C). They can do more than 10 million on/off. It is suitable for use in high humidity environments [27].

(3) Manual valve creates a disruptive effect as well as evacuating the liquid from the tank.

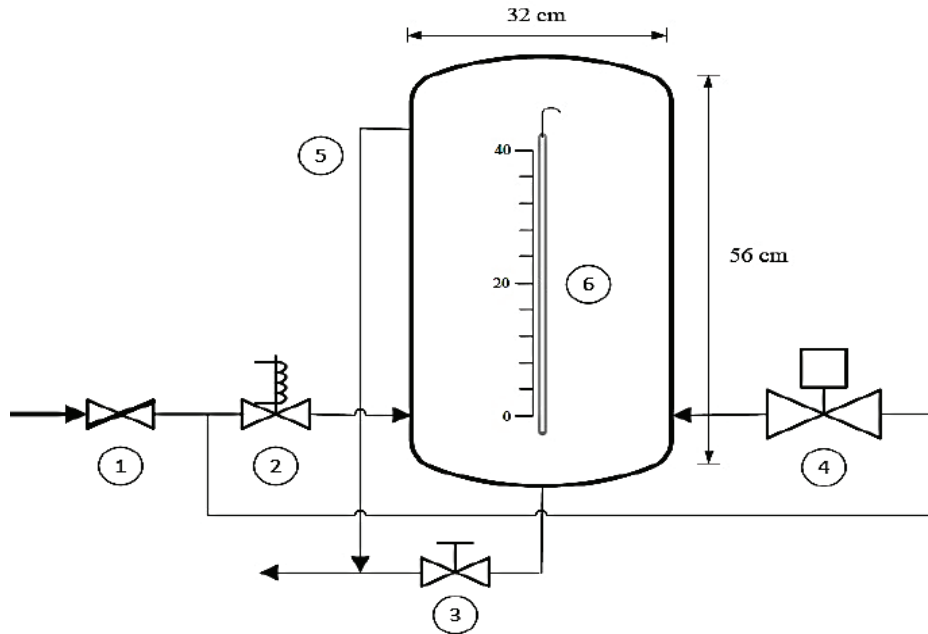


Figure 1. Mechanical diagram of liquid level control system

- (4) **The automatic control valve** realizes the fluid flow to realize the continuous control of the system with the voltage given within the limits. It is used for precise control of liquid flow in systems such as heating, ventilation and air conditioning. It adjusts the liquid flow proportionally according to the incoming control signal. It is compatible with controllers that have 2-10 V DC proportional outputs [28].
- (5) **The overflow pipe** provides safety liquid discharge from the maximum point of the tank level.
- (6) **The scaled transparent level indicator** is used to monitor the level of the process variable filled into the tank from outside the tank.

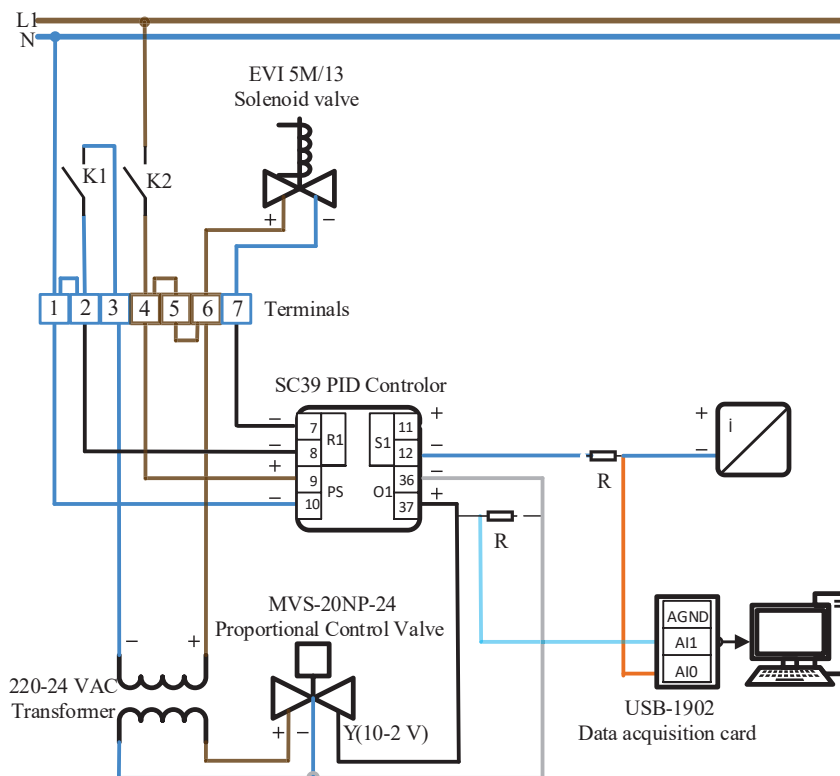


Figure 2. Electrical connection diagram of the liquid level control system

- (7) **The Standard Controller** is designed for the measurement and control of many process variables in industrial environments. They are safe and easy-to-use controllers that comply with international standards for multi-purpose process control use [29].

(8) **Capacitive Level Sensor** is used to measure the level in conductive liquids, low conductivity liquids, solid particulate and powdery materials, sticky and acid/basic liquids[30].

(9) **Data Acquisition Card** is used in fields such as signal testing, laboratory research and factory automation [31].

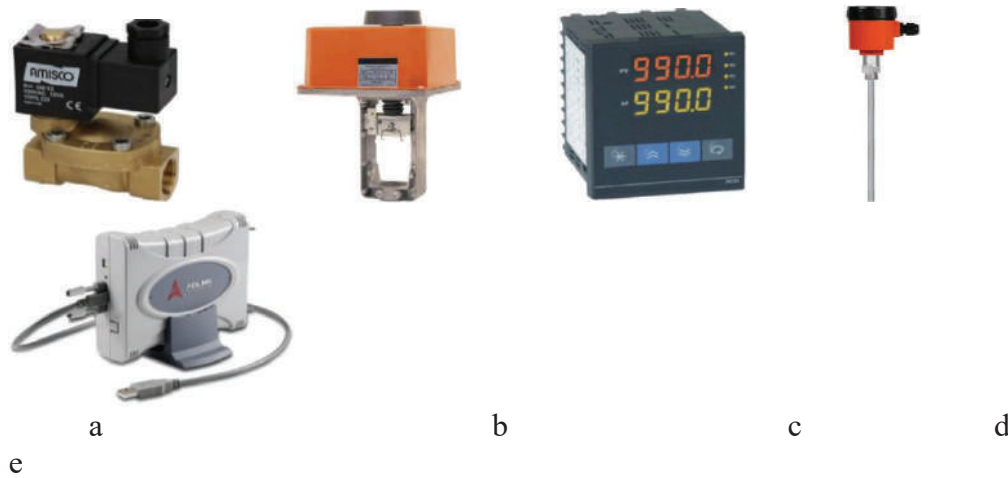


Figure 3. (a) Solenoid valve (Amisco), (b) Automatic control valve (Ontrol), (c) Controller (Tekon), (d) Capacitive level sensor (Ensim), (e) Data acquisition card (Adlink)

4.Experimental Results

The designed and realized liquid level set is shown in figure 4. Mechanical and electrical devices are mounted on the level tank and a portable, portable liquid level set is created in one piece.

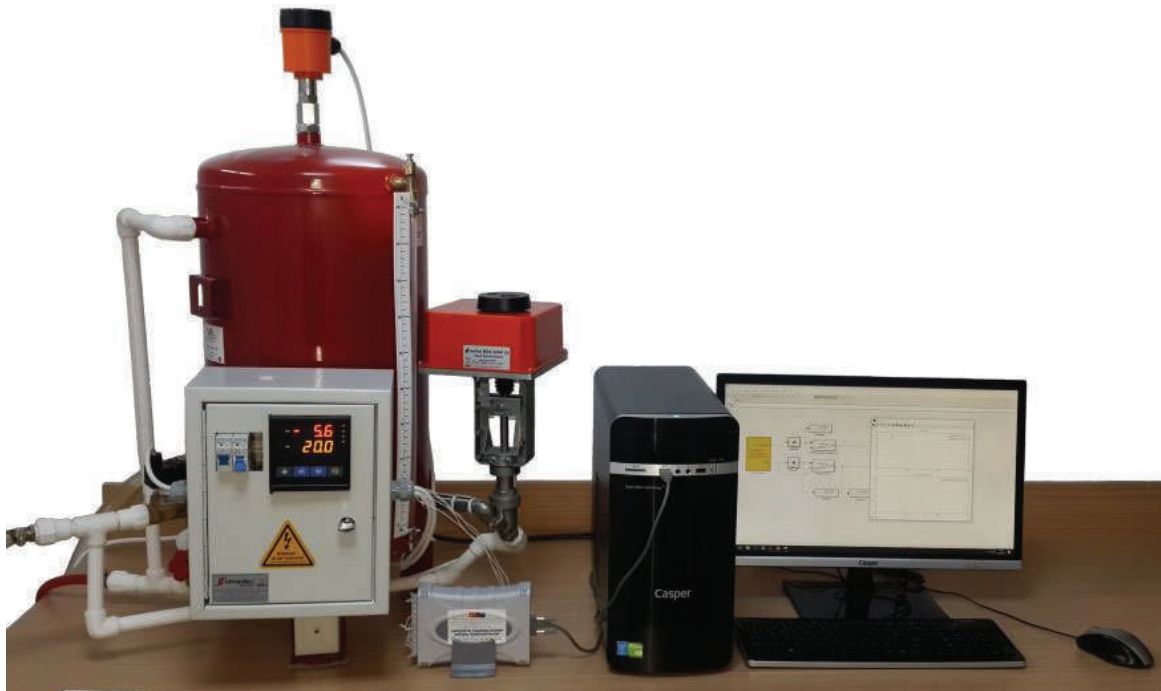


Figure 4. Liquid level control system

The system is used by connecting directly to the mains water and drain. The control panel electrically needs 220 V AC signal. After the control type and coefficients are determined with the controller on the panel, the control system can be operated in on/off and continuous control forms. The analog signal information measured from the sensor is 4 – 20 *mA* and the analog control signal 20 – 4 *mA* used in the control of the automatic control valve is converted to 2 – 10 V DC voltage with a resistor and transmitted to the data card.

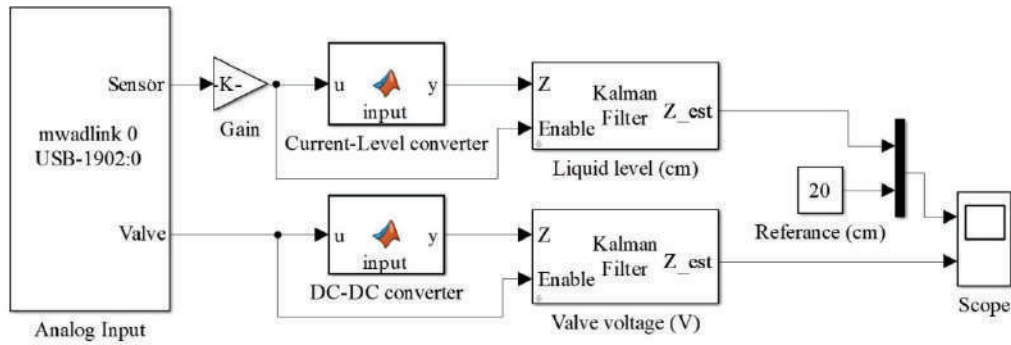


Figure 5. Data card MATLAB/Simulink interface

As seen in Figure 5, the graphs of these values taken with the USB port are drawn in the MATLAB/Simulink program. By extracting the operating curve of the sensor, the information received from the sensor was converted into level information by the curve fitting method in the simulink program. Then, the noise was reduced by passing through the kalman filter and the graph was drawn together with the set value. In experimental studies, on/off control of the system for different hysteresis values and P, PI and PID control for various coefficients were performed.

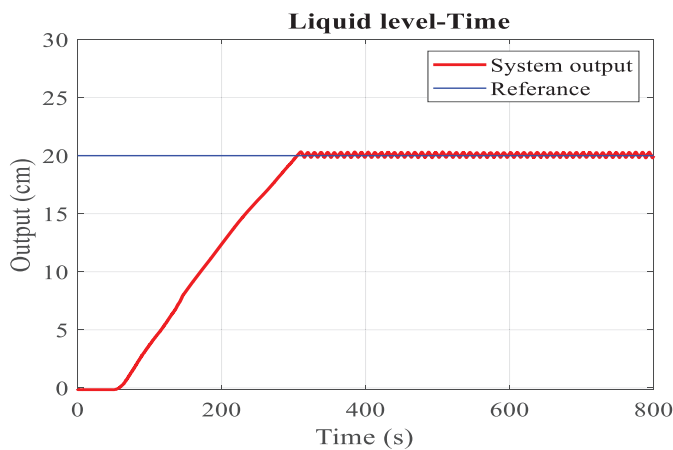


Figure 6. System on/off control, hysteresis=0
hysteresis=1

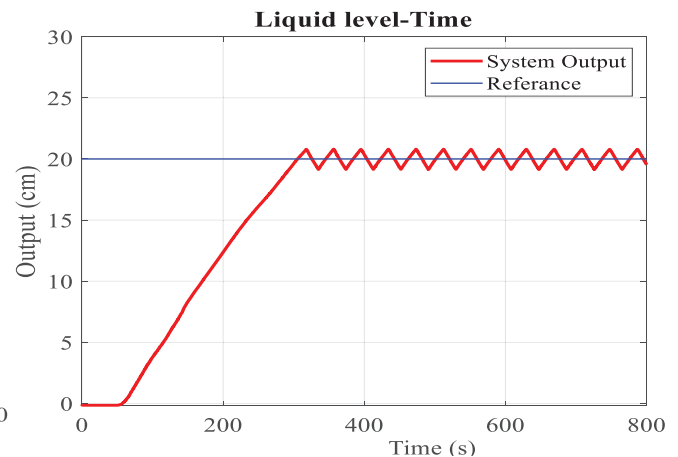


Figure 7. System on/off control, hysteresis=1

As can be seen in the graph in Figure 6, in the on/off control without hysteresis, after a delay of 50 seconds, the reference value was captured at 305 seconds and on/off occurred around the set.

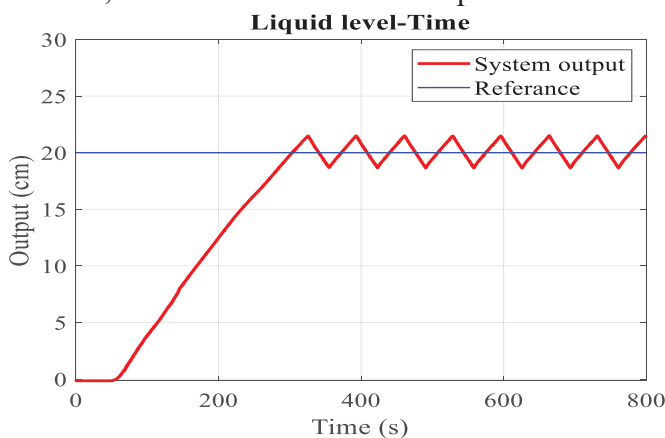


Figure 8. System on/off control, hysteresis=2
set values

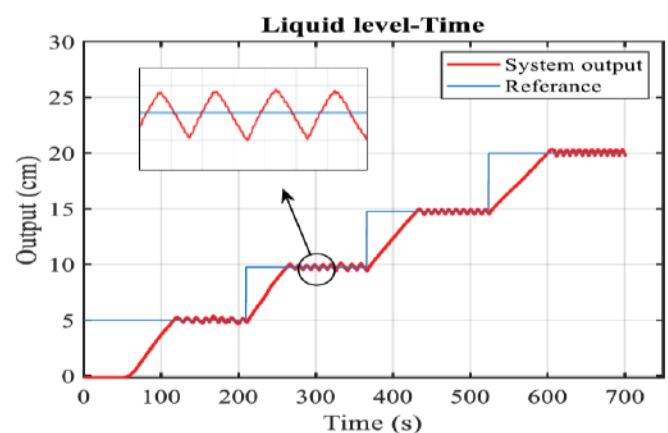


Figure 9. System on/off control for different set values
(hysteresis=0)

The graphics of on/off controls when hysteresis is 1 and hysteresis is 2 are given in figures 7 and 8, respectively. Here, as in the control when the hysteresis is 0, the system delay is 50 seconds and the time to reach the set point is 305 seconds. When hysteresis is 1, it oscillates around the set value at 19-21 cm

values, while when hysteresis is 2, it oscillates at 18-22 cm values. On/off control for 5-10-15 set values during system operation is as in figure 9.

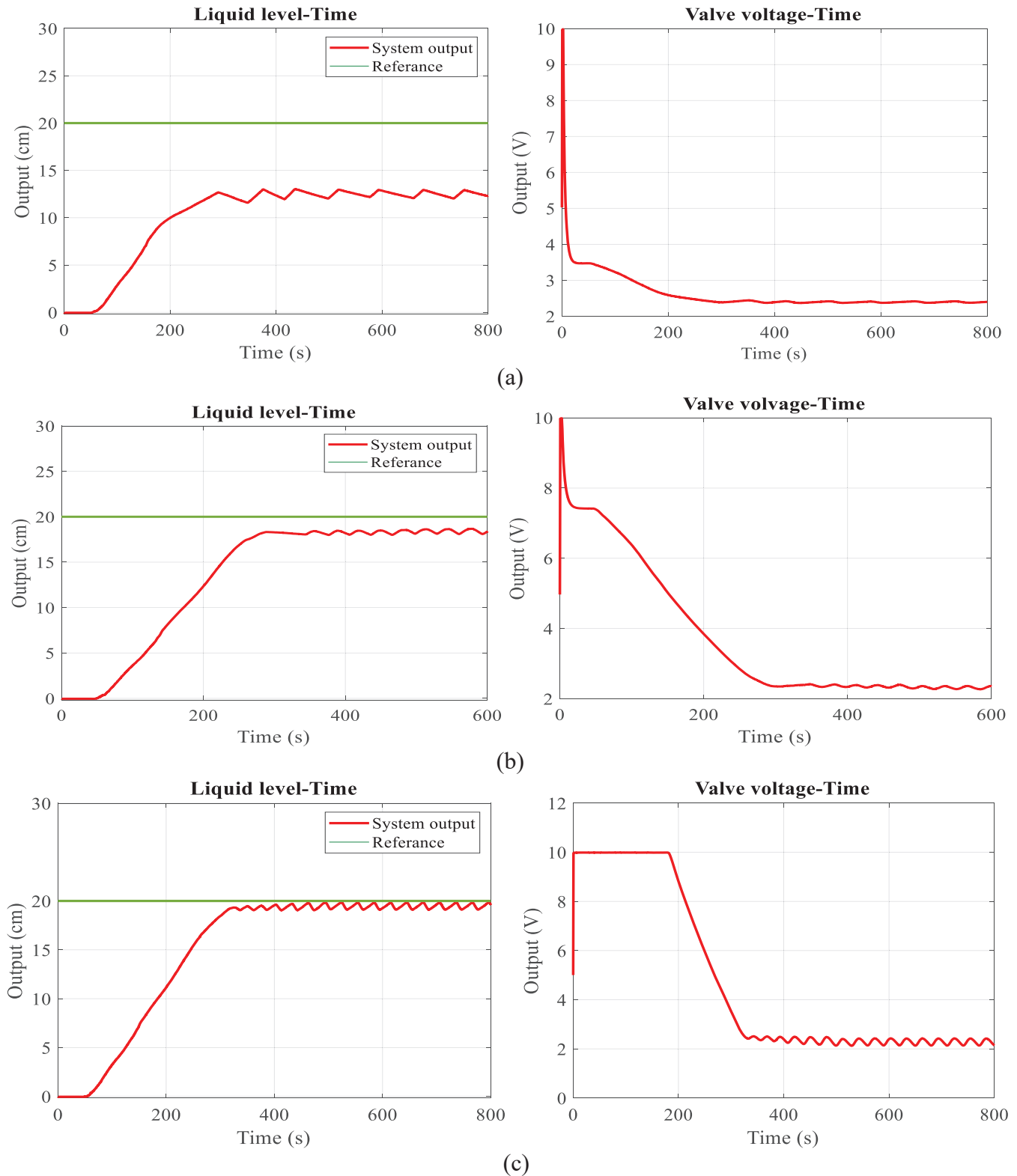
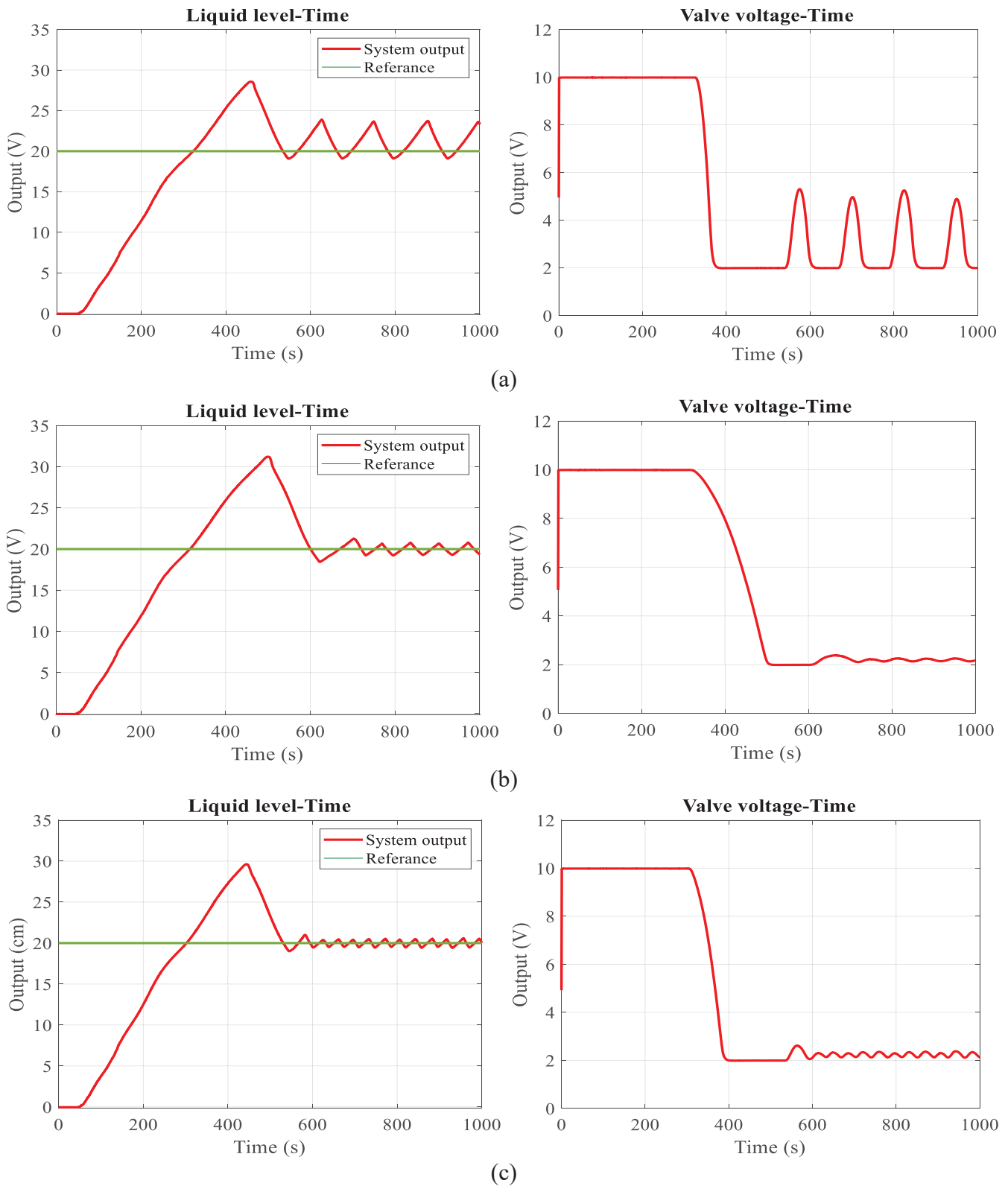


Figure 10. Proportional (P) control response of the liquid level control system for 20 cm reference value
a) PB=100%, b) PB=30%, c) PB=10%

When the proportional control charts in Figure 10 are examined, it is seen that the system delay is approximately the same and as the proportional band (PB) gets smaller, the system speed increases and the steady-state error decreases. The values of the graphics are given in Table 1.

Table 1. System P control according to different proportional band values

	PB = %100	PB = %30	PB = %10
System delay (s)	50.5	49.8	49.79
Time to reach steady state (s)	271	278	288
Steady state error (cm)	7,6	1,8	0,43

**Figure 11.** Proportional + integral (PI) control response for 20 cm set point of liquid level control system a) PB=20%,Ti=2, b) PB=80%, Ti=11, c) PB=20%, Ti=11

The responses of the system for different PI parameters are shown in figure 11.

Table 2. System PI control according to different proportional band and integral time constant values

	PB = %20, Ti = 2	PB = %80, Ti=11	PB = %20, Ti = 11
System delay (s)	51.3	50.4	50.56
Rise time (s)	348.1	315.1	302.4
Peak time (s)	458.8	500.4	443.4
Maximum overshoot (%)	32.71	56	48.1
Settlement time (s)	519.3	600.8	595.8
Steady state error (cm)	1.52	0	0

When the values in Table 2 are examined, it is seen that when the integral time constant (T_i) is increased for the same proportional band value, the settling time and the maximum overshoot increase, and the rise and peak times decrease. Also, the steady state error disappeared. When the integral time constant is kept the same and the proportional band value is increased, all values increased and the steady-state error value remained constant.

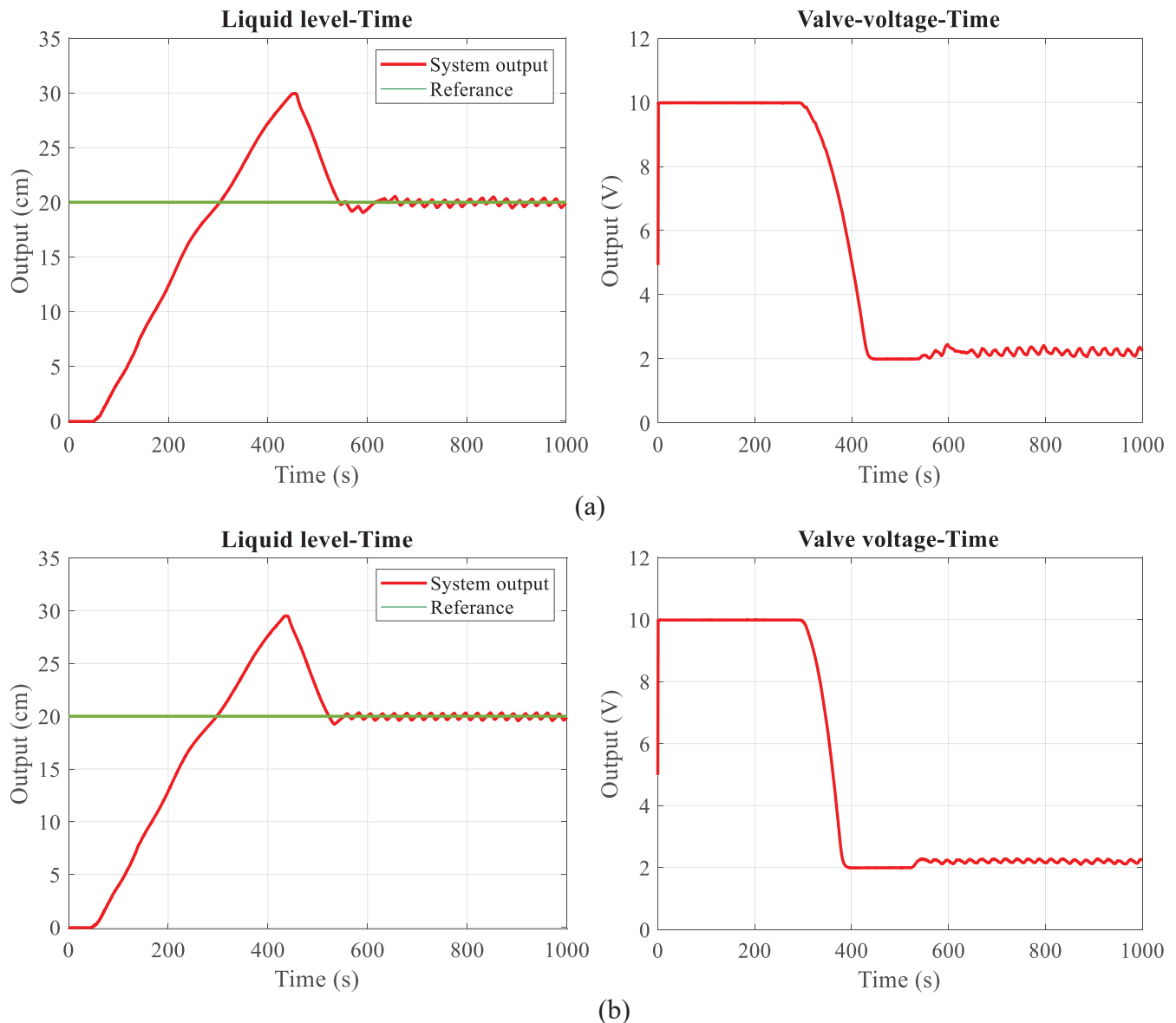


Figure 12. Proportional + integral + derivative (PID) control response for 20 cm set point of liquid level control system a) PB=30%, Ti=18, Td=12, b) PB=20%, Ti=11, Td=4

In Figure 12., the experimental control performance obtained by choosing different proportional band value, integral time constant and derivative time constant is given.

Table 3. System PID control according to different PB, Ti and Td values

	PB = %30, Ti = 18, Td = 12	PB = %20, Ti = 11, Td = 4
System delay (s)	50.02	49.56
Rise time (s)	305.4	298.5
Peak time (s)	452.7	436.4
Maximum overshoot (%)	49.75	45
Settlement time (s)	674	552.5
Steady state error (cm)	0	0

According to the PID performances in Table 3, when PB=20%, Ti=11, Td=4, all values decreased and better control was achieved. In addition, when compared to the PI control with PB=20%, Ti=11, it is seen that the rise, peak time and maximum overshoot are reduced, and the system follows the steady state in a shorter time without error.

Conclusion

In this study, a liquid level control set equipped with a control valve, sensor and process controller used in industrial areas was designed and implemented. After the mechanical and electrical drawings of the designed set were made, they were assembled in accordance with these drawings. Experimentally on/off and PID control were performed using the process controller on the set. Liquid level sensor output and valve control voltage were transferred to MATLAB program with the help of data acquisition card and monitored instantly. When the experimental results were examined, it was seen that the on/off controls with the solenoid valve showed the desired performance. When the results of the continuous control with the proportional control valve are compared, it is seen that the steady-state errors occur in the proportional control, this error is eliminated in the PI control, and in the PID control, both the steady-state error is eliminated and the transient overshoot and oscillations are reduced compared to other control forms. In addition, in the PID control, transient overshoot has occurred and continuous small oscillations have occurred in the steady state. When the system elements are examined separately, it is evaluated that this situation arises from the fact that the valve operates with more on-off effect due to the non-linear characteristic of the control valve, the on-off time being too long and the tank of the control set is quite small for the devices.

References

- [1] Şahbazlı, R. (2017). Su tanklarında sıvı seviye kontrol sisteminin geliştirilmesi (Master's thesis, Adnan Menderes Üniversitesi, Fen Bilimleri Enstitüsü).
- [2] Afşar, E. (2014). Proses kontrol eğitim seti tasarımı ve uygulaması (Master's thesis, Fen Bilimleri Enstitüsü).
- [3] ÜNSAL, A., DUYSAK, A., & ILICA, A. Eğitim Amaçlı Bir Kontrol Deney Seti Tasarımı ve Gerçekleştirilmesi The Design and Implementation of an Educational Control Testbed.
- [4] Yongsheng, Q., Yong, W., & Nan, S. (2013, August). Design of liquid level control system of nuclear power plant. In 2013 IEEE 11th International Conference on Electronic Measurement & Instruments (Vol. 2, pp. 583-586). IEEE.
- [5] Shujiao, B. I., & Feng, D. O. N. G. (2012, July). Modeling for liquid-level control system in beer fermentation process. In Proceedings of the 31st Chinese Control Conference (pp. 1739-1744). IEEE.
- [6] Isa, I. S., Meng, B. C. C., Saad, Z., & Fauzi, N. A. (2011, March). Comparative study of PID controlled modes on automatic water level measurement system. In 2011 IEEE 7th International Colloquium on Signal Processing and its Applications (pp. 237-242). IEEE.
- [7] Mehta, S. A., Katrodiya, J., & Mankad, B. (2011, December). Simulation, design and practical implementation of IMC tuned digital PID controller for liquid level control system. In 2011 Nirma University International Conference on Engineering (pp. 1-5). IEEE.
- [8] Yu, H. (2010, May). The Design and Realization of PID Liquid Level Control System Based on S7-200 and EM235. In 2010 International Conference on Intelligent Computation Technology and Automation (Vol. 3, pp. 762-765). IEEE.

- [9] ZHuo, W., Yanyan, J., & SHichao, W. (2012, June). The application of feedforward PID control in water level control system. In World Automation Congress 2012 (pp. 1-3). IEEE.
- [10] Li, Q., Fang, Y., Song, J., & Wang, J. (2010, March). The application of fuzzy control in liquid level system. In 2010 International Conference on Measuring Technology and Mechatronics Automation (Vol. 3, pp. 776-778). IEEE.
- [11] Abid, M. (2005, August). Fuzzy logic control of coupled liquid tank system. In 2005 International Conference on Information and Communication Technologies (pp. 144-147). IEEE.
- [12] Pan, Y., & Wang, Q. (2006, December). Research on a stable adaptive fuzzy control of nonlinear liquid level system. In 2006 Sixth International Conference on Hybrid Intelligent Systems (HIS'06) (pp. 65-65). IEEE.
- [13] Aydogmus, Z. (2009). Implementation of a fuzzy-based level control using SCADA. *Expert Systems with Applications*, 36(3), 6593-6597.
- [14] Zhou, K., Yan, B., Jiang, Y., & Huang, J. (2012, August). Double-tank liquid level control based on genetic algorithm. In 2012 4th International Conference on Intelligent Human-Machine Systems and Cybernetics (Vol. 2, pp. 354-357). IEEE.
- [15] Ahmad, A., Redhu, V., & Gupta, U. (2012). Liquid level control by using fuzzy logic controller. *International Journal of Advances in Engineering & Technology*, 4(1), 537.
- [16] Zhao, Y. (2010, April). Research on application of fuzzy PID controller in two-container water tank system control. In 2010 International Conference on Machine Vision and Human-machine Interface (pp. 679-682). IEEE.
- [17] Kayacan, E., & Kaynak, O. (2009). An adaptive grey PID-type fuzzy controller design for a non-linear liquid level system. *Transactions of the Institute of Measurement and Control*, 31(1), 33-49.
- [18] Xiao, Q., Zou, D., & Wei, P. (2010, August). Fuzzy adaptive PID control tank level. In 2010 International Conference on Multimedia Communications (pp. 149-152). IEEE.
- [19] Canbolat, H. (2009). A novel level measurement technique using three capacitive sensors for liquids. *IEEE transactions on Instrumentation and Measurement*, 58(10), 3762-3768.
- [20] Terzic, J., Nagarajah, C. R., & Alamgir, M. (2010). Fluid level measurement in dynamic environments using a single ultrasonic sensor and Support Vector Machine (SVM). *Sensors and Actuators A: Physical*, 161(1-2), 278-287.
- [21] Altın, S., & Bulut, F. (2016). Design of Ultrasonic Liquid Level Meter with Bluetooth Connection and Industrial Process Application. *Journal of Bartin University Engineering and Technological Sciences*, 4(1), 19-21.
- [22] Varun Kumar, S., Yokeshranj, P.V., Vignesh, V., Tamilselvan, S., 2018. Precision Level Measurement with Real Time Monitoring For Dynamically Changing Depths in a Container. *International Research Journal of Engineering and Technology (IRJET)*, 5(1) , 1512-1514.
- [23] Rizi, M. T., & Abadi, M. H. S. (2017). Analytical modeling of a coaxial cylindrical probe capacitive sensor based on MATLAB/Simulink for conductive liquids level measurements. *Turkish Journal of Electrical Engineering & Computer Sciences*, 25(4), 3024-3036.
- [24] Kıncay, O. Yapılarda otomasyon ve enerji yönetimi, otomatik kontrol ders notu. Yıldız Teknik Üniversitesi, İstanbul.
- [25] Gökbulut, M. Kontrol sistemlerinin analiz ve tasarımı, ders kitabı seçkin yayıncılık.
- [26] TOP A., Haydaroğlu C., Gökbulut M.,(2017) The Effects Of Pıd Parameters On Temperature Control Of Uninsulated Environment, *European Journal of Technique (EJT)*, 7(2), 146-157.
- [27] http://www.amisco.it/public/2019/EVI_5.pdf EVI 5M/13. 27 September 2021.
- [28] <https://www.ontrol.com.tr/sites/default/files/katalog/VM0018D.pdf> MVS – 20 NP – 24. 27 September 2021.
- [29] <http://www.tekon.com.tr/sc39.html> SC39 Kontrolör. 26 September 2021.
- [30] <https://www.ensim.com.tr/kapasitif-seviye-transmitterleri/> ECAP–101 26 September 2021.
- [31] https://www.adlinktech.com/Products/Data_Acquisition/USBDAQ/USB-1901_1902_1903?lang=en ADLINK USB 1902 27 September 2021..

EXPERIMENTAL AND NUMERICAL PERFORMANCE ANALYSIS OF SMOKE EXTRACTION MOTORS USED IN SPECIAL FAN APPLICATIONS AT HIGH TEMPERATURE

Cansu AKSOY

ORCID No: 0000-0001-5854-9061

Volt Electric Motors Company Izmir, Turkey

Sibel AKBULUT

ORCID No: 0000-0001-5211-00082

Volt Electric Motors Company Izmir, Turkey

Abstract

Today, asynchronous motors (AMs) are widely used in many industrial applications. As machine technology evolves, special motor demands are provided that require special design for specific purposes. Smoke extraction motors (SEMs); It is important that it exhibits a stable operating characteristic at high ambient temperature, especially in a special area where asynchronous motors are used. The high temperature stable operation feature of extraction motors used in area such as tunnel, airport, warehouse, underground passages, close parking requires many new design and production methods. Through special technology, it is ensured that the toxic gas and smoke formed in fire are discharged and a safe area is provided.

In this study, numerical analysis of three-phase totally enclosed air over (TEAO) smoke extraction motors which are designed, tested and proven to be used in special fan applications, in response to increasing ambient temperature, were compared with the experimental environment data and the motor performance under these conditions was investigated. In addition to the numerical and experimental results, general theoretical and design information about smoke extraction motors is shared in the study.

Moreover, it demonstrates the operating efficiency for motors that discharge air at high temperatures as a standard area of use. Furthermore, the data obtained in this study provide a reference for the design of high temperature AMs'.

Keywords: Asynchronous Motors (AMs), High-Temperature Fan Applications, Smoke Extraction Motors (SEMs)

1. INTRODUCTION

Asynchronous motors (AMS); due to their long maintenance periods, lack of brushes and compact structure, they are widely used in a wide range of industrial uses in parallel with the developments in motor driving technology.

Fan applications, which are one of the main application areas of AMs, do not provide compelling conditions for the motors when performed at low ambient temperatures. Despite this, Smoke Extraction Motors (SEMs) has extremely challenging requirements and high-level demands when considered as a special application area for AMs. Since it is aimed to extraction high temperature ambient air in SEMs applications, it is vital that the AMs subject to the design operate smoothly at the relevant temperature for the guaranteed period, depending on the design class and standard.

The motor classes used in SEMs applications are shown in Table 1. F300 class extraction motors are expected to operate for more than 120 minutes as standard and 120 minutes as optional. Difficult operating conditions require protection of the motor from high temperature air and smoke flowing outdoors for motor used in SEMs applications. For this purpose, motors with Totally Enclosed Air Over (TEAO) thermal design are commonly preferred for SEMs applications. The TEAO system complicates the transfer of heat generated by the rotor and stator windings to the external environment due to the fact that it completely closes the internal structure of the motor to the external environment. Although the use of TEAO type motors at ordinary ambient temperatures makes it possible to increase the motor inner temperature, in high temperature applications, insulating the motor from the outer environment delays the equalization of the motor inner temperature to the outdoor temperature for normal conditions and fan applications.

Table 1. Classification of SEMs

Class	Temperature C°	Minimum Functioning Period (Minute)
F200	200	120
F300	300	60
F400	400	120
F600	600	60
F842	842	30

High ambient temperature negatively affects the magnetic material forming the motor rotor and stator and the conductive material used in the motor stator, causing a decrease in the dielectric power of the motor [1], a decrease in the electrical conductivity of the conductors and a decrease in the saturation magnetization intensity of the magnetic material [2].

The temperature dependent relation of the conductivity and magnetic permeability properties of a conductive and magnetic material at high temperature are shown in Fig.1 is given in (a) and (b). As an indirect result of these characteristics, the increased motor internal temperature leads to a decrease in motor power [3].

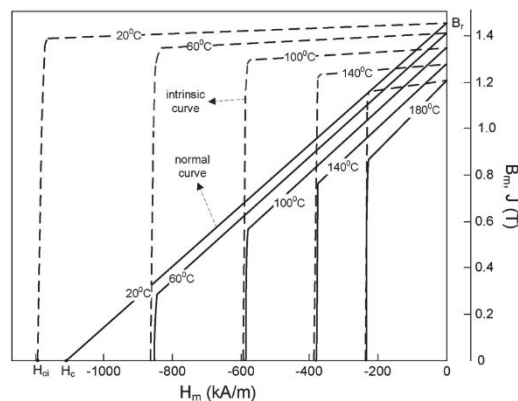


Figure 1. (a) Temperature dependent relation of magnetic permeability

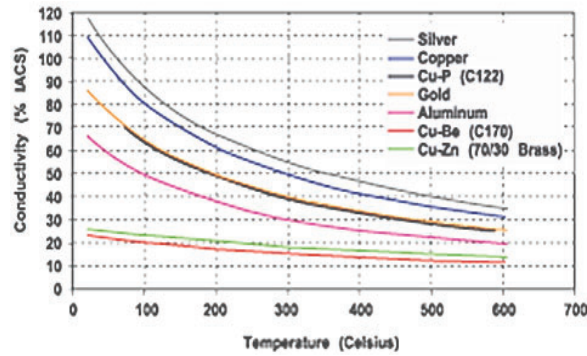


Figure 1. (b) Temperature dependent relation of conductivity

A fan is assembled to the TEAO motor design to circulate the inner air in order to prevent the motor inner temperature from rising locally in the winding inner parts and to allow the heat transferred from the outside environment and the heat produced in the motor to be uniformly distributed [4].

In this study, designs with variable power ranges for 2, 4, 6 pole design for TEAO type AMs, designed to work for 120 minutes in F300 standards, to be used in SEMs application were simulated on SPEED analysis software. Two different SEMs manufactured at 7.5 kW 2p and 55 kW 6p power were tested at 300 °C and compared with the simulation results obtained.

2. THERMAL CHALLENGES AND DESIGN REQUIREMENTS

In order to prevent the transfer of thermal energy of the high temperature air flowing over the AMs used for SEM application into the motor, minimizing the motor outer surface area comes to the fore as the main approach. Insulation of the outer surface of the motor, which is another preventive approach, is another application that is preferred due to compliance with the r_{cr} critical insulation diameter and can extend the active operation time of the motor. If the system is stable and the outer surface of the motor is modeled as a cylinder, then r_{cr} (m) is the heat transfer coefficient of the outer surface of the motor, k (W/m.C°) and h (W/m.C°) the convection coefficient of the outdoor fluid (air, smoke, etc.) critical insulation thickness can be calculated with the help of equation 1.

$$r_{cr} = k/h \quad (1)$$

The heat transferred to the motor due to high temperature air or smoke flowing through the motor can be calculated using equation 4 using equation 2 and 3, including the Re ; Reynolds number, Nu ; Nusselt number, Pr ; Prandtl number contained in equation 2[5].

$$Re = \frac{VD}{\nu}, \quad Nu = 0.91(Pr)^{\frac{1}{3}}(Re)^{\frac{1}{2}} \text{ for laminar flow, } Pr = \frac{c_p \mu}{\lambda} \quad (2)$$

$$Nu = 0.039x(Pr)^{0.6}(Re)^{0.6} \text{ for turbulent flow}$$

$$h = \frac{k}{D} Nu \quad (3)$$

$$\dot{Q} = hA_s(T_s - T_{\infty}) \quad (4)$$

In this assumption, motor lateral face areas are included in the calculation and motor covers are not included in the calculation.

3. NUMERICAL STUDY

In the study, 2, 4, 6-pole versions of SEMs designed at 3kW, 5.5kW, 18.5kW, 30kW and 45 kW were modeled with SPEED analysis software and the motor efficiencies depending on the obtained temperature are shown in figures 2(a), 2(b), 2(c).

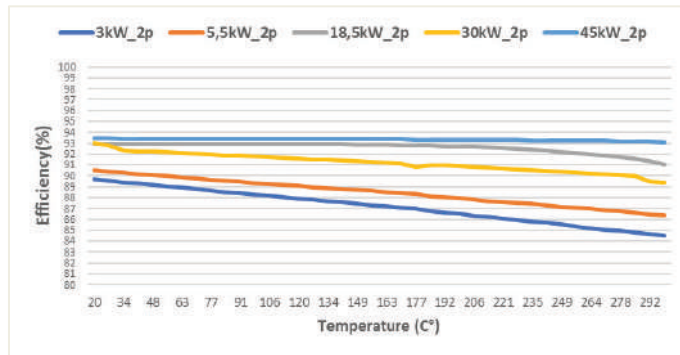


Figure 2. (a) 2-p temperature dependent efficiencies

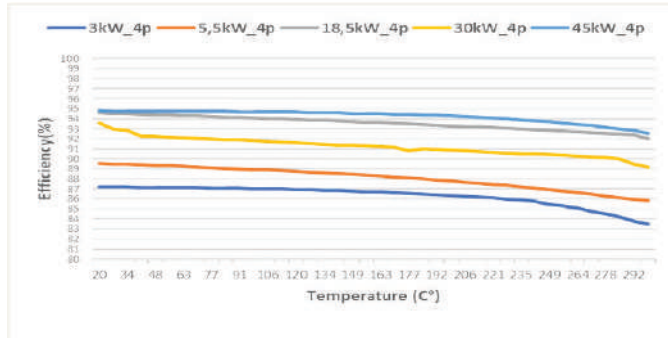


Figure 2. (b) 4-p temperature dependent efficiencies

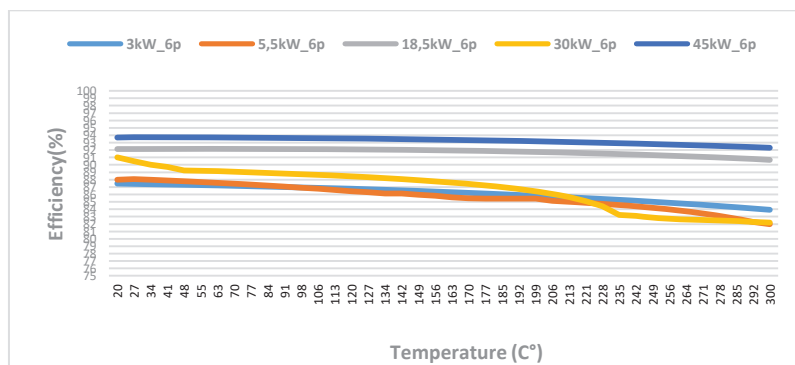


Figure 2. (c) 6-p temperature dependent efficiencies

The amounts of conductive and magnetic materials used depending on the motor design are listed in Table 2. Due to design optimization and target efficiency scale, it is not possible to establish a linear relationship between the amount of conductive and magnetic material used and the number of SEMs poles.

In additionally, the solver used in the analytical study provided the highest efficiency at the highest power, adhering to the motor design optimization.

Table 2. Optimum material quantities and minimum efficiency of designs

Power (kW)	Pole Number	Weight_Cu (kg)	Weight_Fe (kg)	Min Efficiency (%)
3	2	2,56	10,24	87,1
3	4	3,42	15,91	87,7
3	6	4,01	27,72	85,6
5,5	2	4,6	17,2	89,2
5,5	4	5,25	34,5	89,6
5,5	6	6,15	27,72	88
18,5	2	11,88	68,88	92,4
18,5	4	18,24	90,43	92,6
18,5	6	16,53	96,02	91,7
30	2	20,49	107,21	93,3
30	4	15,87	120,02	93,6
30	6	18,62	192,4	92,9
45	2	20,56	157,55	94
45	4	19,99	182,43	94,2
45	6	29,04	273,74	93,7

4. EXPERIMENTAL STUDY AND TEST SYSTEM

In the experimental part of the study, two different SEM prototypes 7,5 kW 2p and 55 kW 6p were produced. The same method was used the motor design as in the numerical study, the prototype design was completed with the results obtained, and the completed prototypes are given in Figure 3.

The high-temperature smoke-air environment is obtained by increasing the ambient air to high temperature in a closed environment, and the indoor environment requires the circulation of high-temperature gas by the manufactured fan-SEMs.

The process steps for the experimental study are shown in Table 3, and the time-dependent variation of the temperature measured from different points of the furnace is shown in Figure 4. The time-dependent variation of the static pressure measured from different points of the furnace is shown in Figure 5.

Table 3. Test procedure and process steps

-60	Fan switched on and SEM started warming up
0	Heating started
7	Target temperature was reached (300 C°)
22	Fan switched off
24	Fan switched on
60	No considerable changing on fan-SEM performance
90	No considerable changing on fan-SEM performance
120	No considerable changing on fan-SEM performance
129	Test completed and stopped

Since the SEMs design considered in the study was designed as class F300, the target ambient temperature of 300 ° C was reached in about 7 minutes. While the ambient temperature was stable between the 22nd and 24th minutes, the operation of the SEMs motor was stopped, the motor continued to operate in a controlled manner between the 24th and 120th minutes, and the test was terminated at the end of the 129th minute.



Figure 3. Prototype of SEM-fan couple

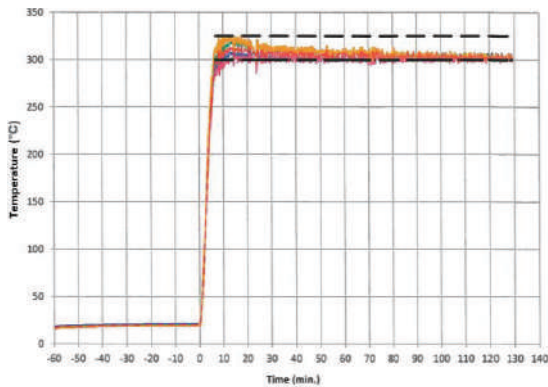


Figure 4. Furnace temperature measurement

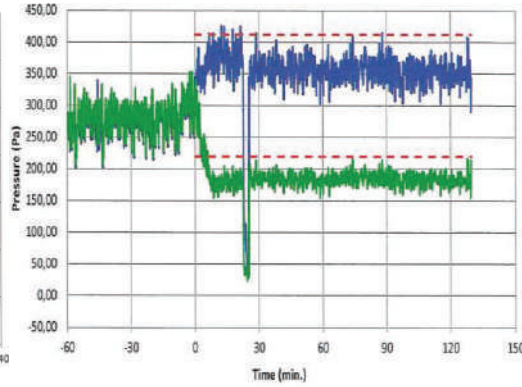


Figure 5. Furnace pressure measurement

4.1 Comparison of Numerical and Experimental Solution

The amounts of conductive and magnetic materials used depending on the motor design and target efficiency are listed in Table 4.

Table 4. Optimum material quantities and minimum efficiency of designs

Power (kW)	Pole Number	Weight Cu (kg)	Weight Fe (kg)	Min Efficiency (%)
7,5	2	5,8	19,6	88,1
7,5	4	5,03	30,87	88,7
7,5	6	9,8	51,96	87,2
55	2	67,34	172,8	94,3
55	4	23,6	193,16	94,6
55	6	33,87	323,51	94,1

The numerical solution results obtained for 7.5 kW 2p and 55 kW 6p motors are shown in Figure 5. Figure 5 shows that the efficiency has a greater decrease with increasing temperature, from 94,2% to 92,55% for 55kW 6p 89,2% to 85% for 7.5kW 2p between 20 and 300 degrees ambient temperature. The resistance of the material used in the stator winding increases with temperature. Therefore, the conductor losses in the stator increase. These losses increase the total loss of the motor and reduce the motor efficiency.

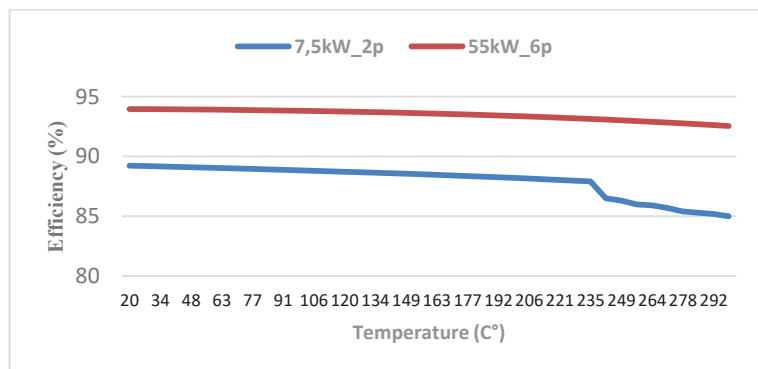


Figure 5. Temperature dependent efficiencies

Since the temperature of the motor is increased under constant power, the flux density decreases. Depending on the decrease in flux density, the motor speed decreases, while the torque increases at a certain rate according to the operating range of the motor. Temperature dependent torque graphs of 7.5 kW 2p and 55 kW 6p motors are given in Figure 6 (a) and (b).

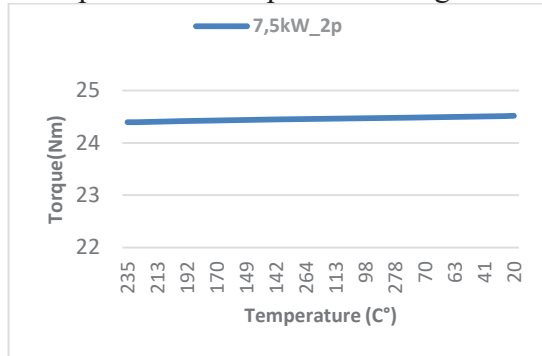


Figure 6. (a) 7.5 kW 2p temperature dependent torque

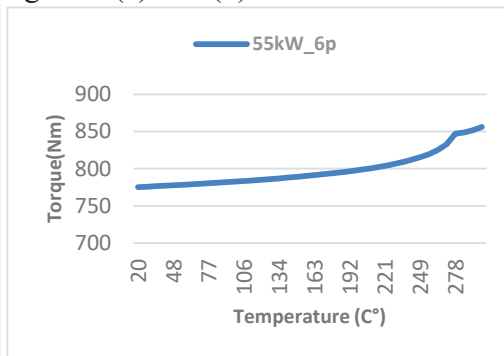


Figure 6. (b) 55 kW 6p temperature dependent torque

According to the test procedure given in Table 3, the current graphs of 7.5 kW 2p and 55 kW 6p motors over time are shown in Figure 7 (a) and (b) respectively. Testing the motor in a closed environment changes the air specification of the environment. Accordingly, the operating characteristics of the fan working connected to the motor changes and it causes the current and power of the motor to decrease during temperature rising. Power time graphs measured according to the test procedure for 7.5 kW 2p and 55 kW 6p motors are given in figure 8 (a) and (b) respectively.

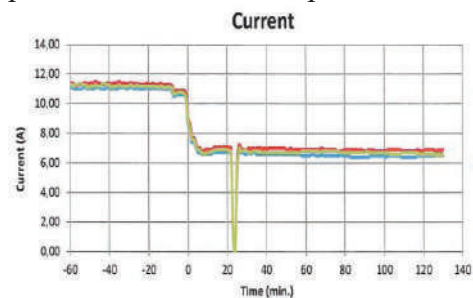


Figure 7. (a) 7.5 kW 2p time dependent current

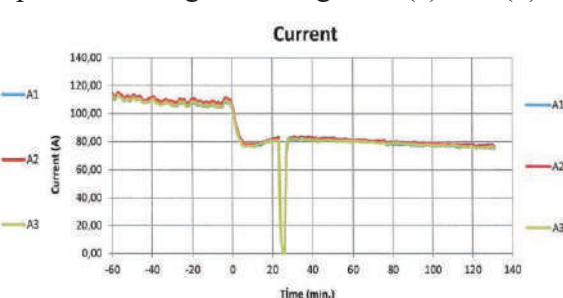


Figure 7. (b) 55 kW 6p time dependent current

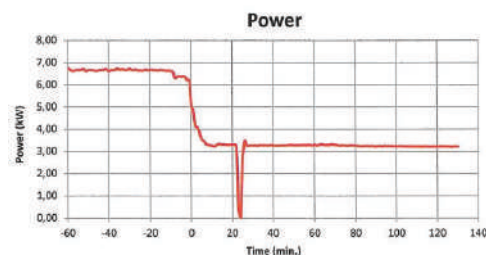


Figure 8. (a) 7.5 kW 2p time dependent power

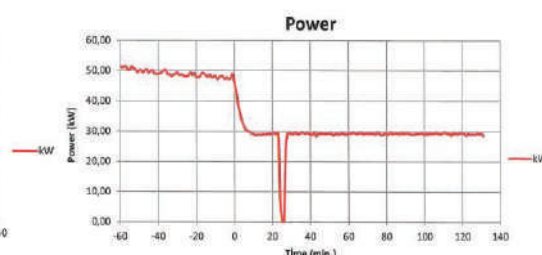


Figure 8. (b) 55 kW 6p time dependent power

5. CONCLUSION

Within the scope of the study, general information about smoke extraction motors was given and design requirements were shared.

Numerical analysis was performed under conditions close to the actual test environment, although the experimental study prototypes settled in the indoor environment and air to circulate heated air in a constant volume throughout the test that rise to the expansion of the pressure effect due to the inability to be included in the model, some differences between the results of the numerical analysis and experimental results have been observed.

Although classical electric motors try to transfer heat outside, at a high ambient temperature, SEM transfers heat from the external environment to the internal environment. Although the usual working environment for SEM is not high temperatures, it is possible that motors designed for SEM are preferred in environments that require constant high temperature operation, so it is extremely important that SEM maintains its efficiency with increasing temperature.

In addition to the insulation and size optimization studies mentioned in the previous sections, it is important to demonstrate new innovative approaches in order to ensure long-term operation at high temperatures application in SEMs.

REFERENCES

- [1] Yang Ying. Improvement of Electric Submersible Pump in High Temperature. China Science and Technology Fortune, 2010
- [2] [Shan Bai](#); [Shenglei Shi](#); [Peng Du](#) Analysis of the Performance of the Asynchronous Motor in the High Temperature, [10.1109/ISDEA.2012.82](#), 2013
- [3] Mao Man Hong. Test Research Extended High Temperature Motor Bearing Overhaul Cycle. Bearing. 2008
- [4] K Matsuoka, M Kondo, Y Shimizu, A Totally Enclosed Traction Motor Using a Permanent Magnet Synchronous Motor Electrical Engineering in Japan, Vol. 151, No. 3, 2005
- [5] [Yunus A. Çengel](#), [Afshin J. Ghajar](#), Isı ve Kütlev Transferi, 9786053552871, 2015

A SIMULATION STUDY ON THE PROCESS OF FUEL INJECTION OF DIESEL - VEGETABLE OIL MIXTURE OF THE YANMAR 6CHE DIESEL ENGINE BY KIVA-3V SOFTWARE

Mai Duc Nghia

Faculty of Mechanical Engineering, Air Force Officer's college, VietNam

Abstract

Currently, the problem of environmental pollution due to exhaust gases of internal combustion engines is very large. Although there are many technical improvements applied to new generation engines, the use of petroleum fuel still generates many harmful emissions, especially soot emissions from diesel engines. Therefore, the use of biofuel (vegetable oil) for the engine is necessary, to limit harmful emissions. However, because the characteristics of vegetable oil are different from that of diesel fuel, it is necessary to evaluate the fuel injection process and the formation of the combustion mixture in the engine, to adjust the injection parameters of the fuel system accordingly, improve thermal efficiency, reduce emissions for diesel engines. In this study, the article presents the process of fuel injection of diesel-vegetable oil mixture compared with diesel oil of the Yanmar 6CHE diesel engine using Kiva-3v software, the results show that the mixture fuel spray has penetration and smaller spray cone angle compared to diesel oil, this is the basis for adjusting injection pressure and injection timing of the engine fuel system when switching to using a diesel-vegetable oil mixture.

Keywords: diesel engine, soot emission, spray cone angle, spray penetration, kiva-3v software

1. INTRODUCTION

Diesel engines are popular used in road and waterway vehicles, including fishing boats of fishermen. Therefore, the demand for fuel and petroleum products is very high, leading to many problems that need to be solved such as: Fuel is increasingly depleted; environmental pollution caused by engine exhaust is increasing day by day, adversely affect human health and social development [1]. To overcome these limitations, many technological measures and solutions have been proposed and applied worldwide to ensure energy security and limit environmental pollution. Among the energy sources to replace petroleum currently in use such as: Solar energy, wind energy, etc., biofuels used for internal combustion engines are particular interest, because their unique characteristics suitable and feasible in finding raw materials for production [8]. Vegetable oil is a form of biofuel, but not synthesized into biodiesel, but mixed directly into diesel oil (mixture of diesel - coconut oil) used as fuel for diesel engines.

Vietnam is a country located in the tropical monsoon region, with great potential in developing raw materials for biofuel production. In which, coconut oil is considered as one of the abundant raw materials, because the natural and social conditions in Vietnam are suitable and favorable for the development of coconut trees. However, the characteristics of coconut oil are different from those of diesel oil such as viscosity, density, cetane number, so when used as a fuel, it will affect on the structure of spray (spray cone angle, spray penetration, etc.), the combustion mixture formation process and fuel combustion in the engine, because the above process is especially important for diesel engines [3], [6]. Therefore, evaluating the

structure of mixture fuel spray compared to diesel fuel, will help adjust the injection parameters of the engine fuel injection system appropriately, improve thermal efficiency, and reduce exhaust emissions poison, mainly soot [9], [11-12]. The following presents the research results on the injection process of diesel - coconut oil mixture fuel (15% coconut oil and 85% diesel-C15) of the Yanmar 6CHE diesel engine by simulation on Kiva-3v software.

2. MATERIALS AND METHODS

Diesel - Coconut oil mixture fuel:

Diesel-coconut oil mixture fuel (C15) is presented in Table 1, Yanmar 6CHE diesel engine (made in Japan), are used as engines for fishing vessel in Vietnam, engine specifications are given in Table 2.

Table 1. Properties of C15 fuel vs. DO

Fuel	Density (g/cm ³)	Cetane number (CN)	Viscosity at 40 ⁰ c (mm ² /s)	Calorific value (kcal/kg)	Flash point (⁰ c)
DO	0.8360	50	3.25	10.478	Min 60
C15	0.8420	52	3.65	10.650	75

Table 2. Engine and simulation parameters

Type	6CHE, unified combustion chamber
Number of cylinders	6
Cylinder diameter x piston stroke (mm)	105x125
Power (Hp/rpm)	130/2600
Compression ratio	16.4
Engine speed of simulation	1600 rpm
Number of nozzle holes x diameter x spray direction	4 x 0.32 x 140 ⁰
Injection timing ⁰ BTDC	18 ⁰ BTDC
Injection pressure (bar)	210
Rod length	215 mm
IVC, EVO	
IVO	16 ⁰ BTDC
IVC	52 ⁰ BTDC
EVO	52 ⁰ BTDC
EVC	16 ⁰ BTDC

Kiva-3v software:

Kiva – 3v software is developed by Los Alamos National Laboratory (Los Alamos National Laboratory – LANL) USA, is open source software, using Fortran language to simulate 2D and 3D turbulent fluid flows, has a chemical reaction like simulating the fuel injection and combustion process of an internal combustion engine [2]. The basis of the simulation process by Kiva -3v software is based on the conservation equations:

Conservation of mass: $\frac{\partial \rho_m}{\partial t} + \frac{\partial(\rho_m u_i)}{\partial x_i} = \frac{\partial}{\partial x_i} \left(\rho D \frac{\partial(\rho_m / \rho)}{\partial x_i} \right) + \dot{\rho}_m^s + \dot{\rho}_m^c$ (1)

Momentum equation: $\frac{\partial(\rho u_j)}{\partial t} + \frac{\partial}{\partial x_i} (\rho u_i u_j - \tau_{ij}) = -\frac{1}{\alpha^2} \frac{\partial p}{\partial x_j} + \rho F_j^s + \rho g_j - A_0 \frac{2}{3} \frac{\partial(\rho k)}{\partial x_i}$, $j = 1, 2, 3$ (2)

Conservation of energy: $\rho c_p \left(\frac{\partial T}{\partial t} + \frac{\partial T}{\partial x_i} \right) = k \frac{\partial^2 T}{\partial x_i^2} + \frac{\partial}{\partial x_i} \left(\rho D \sum_m h_m \frac{\partial(\rho_m / \rho)}{\partial x_i} \right) + A_0 \rho \varepsilon + \dot{Q}^s + \dot{Q}^c$ (3)

In the above equations: F^s is the rate of momentum gain per unit volume due to the spray ($\text{kg}\cdot\text{m/s}$); t : time (s); x_i : coordinates (m); p : pressure (N/m^2); $\rho = \sum_m \rho_m$: ρ_m is the mass-density of species m , ρ is the total mass-density (kg/m^3); $\dot{\rho}^s = \sum_m \dot{\rho}_m^s$: source terms of spray; $\dot{\rho}^c = \sum_m \dot{\rho}_m^c$: source terms of chemistry; u_i, u_j : the fluid velocity (m/s); T : is the fluid temperature (K); h_m the specific enthalpy of species m (J/kg); D : diffusion coefficient; Q^c, Q^s : The source terms due to chemical heat release and spray interactions; k, ε : the turbulent kinetic energy and its dissipation rate; A_0 and $1/\alpha^2$: parameter improves computational performance for flows with small Mach numbers (the quantity A_0 is zero in laminar calculations and unity when one of the turbulence models is used ($A_0 = 1$)).

The fuel injection process helps the spray to increase the surface area and mix with the air, increasing the rate of evaporation and combustion. Especially for direct injection engines, injection is the most effective measure to control combustion progress. In which, the spray kinetic energy is the main source of vortex generation, controlling the air-fuel mixing and the pre-mixed flame spread speed, greatly affecting the combustion, heat release and emissions formation process, thereby affecting the noise level, fuel consumption and emissions of the diesel engine [4-5], [7].

Description of the spray is characterized by physical parameters as shown in Figure 1 [10]. In which, the two basic parameters are spray tip penetration, spray cone angle, which creates the spray volume in the combustion chamber space and directly affect to the combustion mixture formation process of the diesel engines.

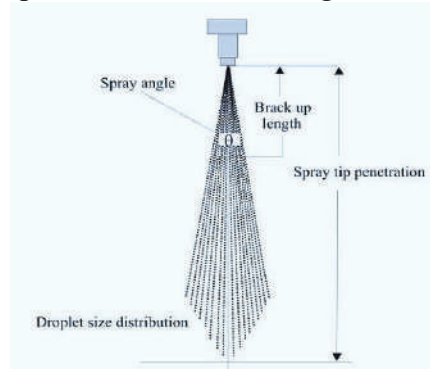


Figure 1. Structure of the fuel spray

The calculated parameters of spray structure [6], [9-10]:

+ Reynolds Number: $Re_i = v_i d_h \rho_i / \mu_i$; Weber Number: $We_i = v_i^2 d_h \rho_i / \sigma$ (4)

+ Ohnesorge Number: $Oh = \sqrt{We_i} / Re_i$; Taylor Viscosity Parameter: $T_a = Re_i / We_i = \sigma_i / \mu_i v_i$ (5)

+ Medium velocity of the injected Liquid fluid: $v_i = C_d \cdot 2(\Delta p / \rho_i)^{1/2}$ (6)

Where, C_d : Discharge coefficient of the nozzle; d_h : injection hole diameter (m); μ_i : fuel viscosity (mm^2/s); ρ_i : fuel density (kg/m^3); σ_i : surface tension of the fuel (N/m); p_{inj} : injection pressure (bar); p_c : end-stroke pressure of the engine (bar), $\Delta p = p_{inj} - p_c$.

The physical parameters that cause the fuel transition in the jet from one region to another are continuous and difficult to define, often based on the definition of the void fraction θ and expressed through equation 7:

$$\theta = 1 - \iiint \frac{4}{3} \pi r^3 d\bar{v} dr dT_d, \text{ according to Williams [9]} \quad (7)$$

Where, f : number of possible drops per unit spray volume; r : fuel drops radius; T_d : fuel drop temperature; \bar{v} is the fuel drop velocity in three dimensions.

According to Reitz [10], with the drops distribution in the spray as shown in Figure 1, when $\theta < 0.92$ is the liquid phase region and $\theta \gg 0.92$ is the gas phase region. $\theta < 0.5$, here begins the process of fuel drop break up, forming a spray structure.

Spray tip penetration S:

The injection front penetration (S) is defined as the total distance covered by the spray in a control volume, and it's determined by the equilibrium of two factors, first the momentum quantity with which the fluid is injected and second, the resistance that the idle fluid presents in the control volume, normally a gas. Due to friction effects, the liquids kinetic energy is transferred progressively to the working fluid. This energy will decrease continuously until the movement of the droplets depends solely on the movement of the working fluid inside the control volume.

$$\text{Time of break up spray: } t_b = 15.8(\rho_l \cdot d_h) / C_d \sqrt{2\rho_g \cdot \Delta p}, \text{ according to Hiroyasu and Arai [6]} \quad (8)$$

$$\text{Before break up: } 0 < t < t_b: S = 0.39 \cdot t(2\Delta p / \rho_l)^{1/2}, \text{ after break up: } t \geq t_b: S = 2.95(\Delta p / \rho_g)^{1/4} \cdot (d_h \cdot t)^{1/2} \quad (9)$$

Spray cone angle θ :

The cone angle (θ) is defined as the angle formed by two straight lines that stat from the exit orifice of the nozzle and tangent to the spray outline (sprays morphology) in a determined distance. The angle in a diesel spray is formed by two straight lines that are in contact with the spray's outline and at a distance equivalent to 60 times de exit diameter of the nozzles orifice. This angle usually is between 5 and 30 degrees. This determines greatly the fuels macroscopic distribution in the combustion chamber [6], [9]:

$$\theta = 0.05((d_h^2 \rho_g \cdot \Delta p) / \mu_g^2)^{1/4}, \text{ according to Hiroyasu [6]} \quad (10)$$

3. RESEARCH RESULTS AND DISCUSSIONS

Simulation results show that the C15 fuel spray has a shorter penetration and a smaller spray cone angle than DO fuel spray. This result is suitable with theoretical analyzes and studies related to the fuel properties that have been published previously. The grid model simulates the injection process of the diesel-coconut oil mixture fuel as shown in Figure 2.

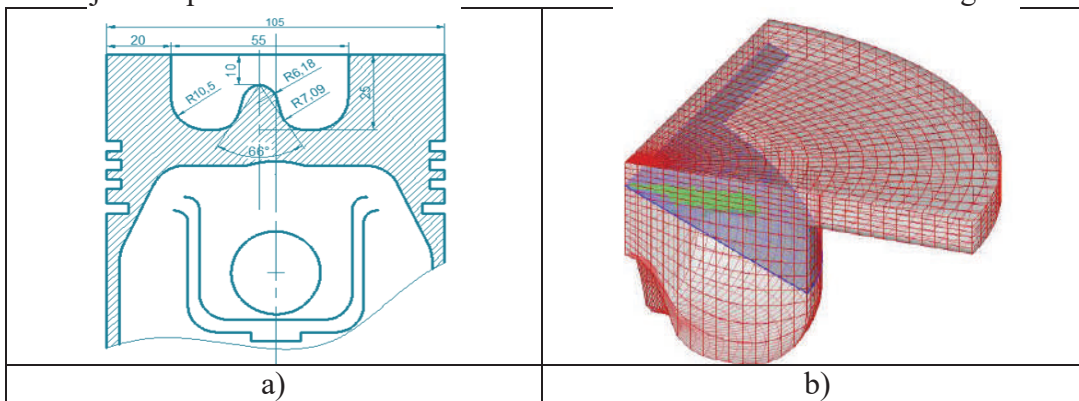


Figure 2. Dimensional drawing of the combustion chamber (a), grid model simulating the fuel injection process (b)

Universidad Juárez Autónoma de Tabasco, México

Universidad Juárez Autónoma de Tabasco, México



Universidad Juárez Autónoma de Tabasco, México

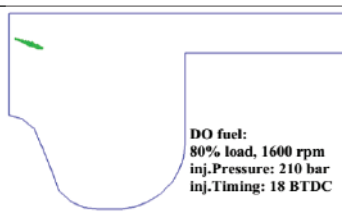
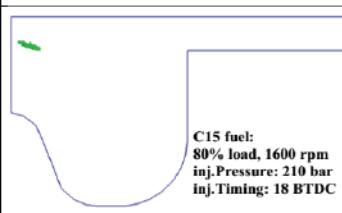
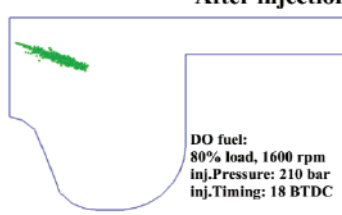
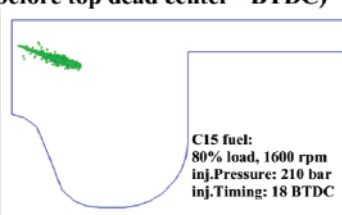
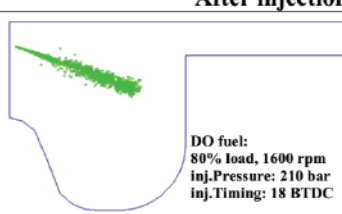
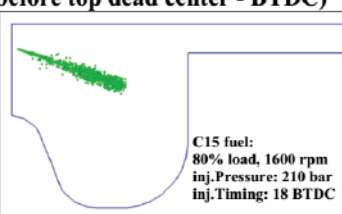
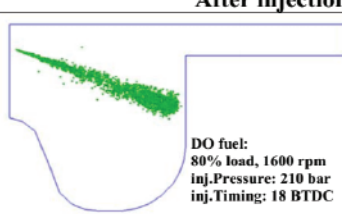
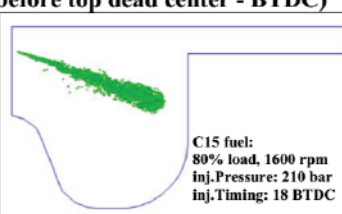
After injection timing (17 deg, before top dead center - BTDC)							
Penetration (DO fuel)	Parameters			Penetration (C15 fuel)	Parameters		
	X	Z	L		X	Z	L
 DO fuel: 80% load, 1600 rpm inj.Pressure: 210 bar inj.Timing: 18 BTDC	0.37	14.62	0.41	 C15 fuel: 80% load, 1600 rpm inj.Pressure: 210 bar inj.Timing: 18 BTDC	0.31	14.65	0.34
After injection timing (16 deg, before top dead center - BTDC)							
 DO fuel: 80% load, 1600 rpm inj.Pressure: 210 bar inj.Timing: 18 BTDC	0.86	14.36	0.97	 C15 fuel: 80% load, 1600 rpm inj.Pressure: 210 bar inj.Timing: 18 BTDC	0.77	14.42	0.86
After injection timing (15 deg, before top dead center - BTDC)							
 DO fuel: 80% load, 1600 rpm inj.Pressure: 210 bar inj.Timing: 18 BTDC	1.44	14.07	1.61	 C15 fuel: 80% load, 1600 rpm inj.Pressure: 210 bar inj.Timing: 18 BTDC	1.26	14.16	1.41
After injection timing (14 deg, before top dead center - BTDC)							
 DO fuel: 80% load, 1600 rpm inj.Pressure: 210 bar inj.Timing: 18 BTDC	1.87	13.83	2.11	 C15 fuel: 80% load, 1600 rpm inj.Pressure: 210 bar inj.Timing: 18 BTDC	1.69	13.91	1.91

Figure 4. Comparison of the C15 spray penetration and DO fuel

Where: $X = 0$, Z rotate -45° , text (55, 20), $Z_o = 14.8$, $L = \sqrt{X^2 + (Z_o - Z)^2}$ (11)

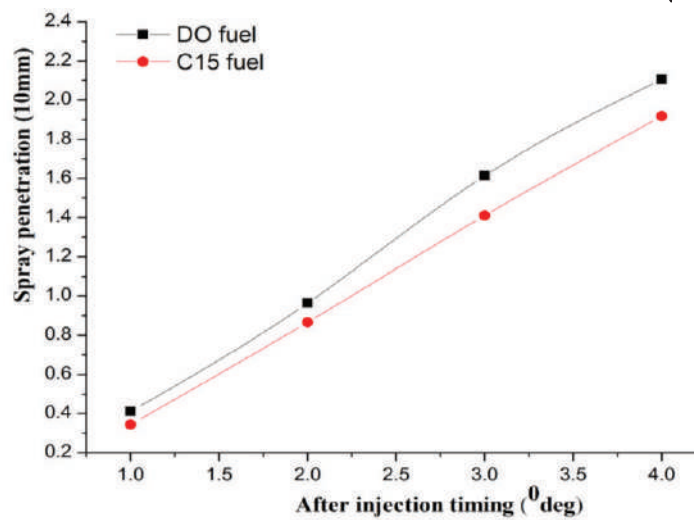


Figure 5. Spray tip penetration

4. CONCLUSIONS

On the basis of the results of theoretical analysis and simulation, it shows that the C15 fuel has a spray structure (spray tip penetration, spray cone angle) smaller than DO fuel spray. This reduces the combustion mixture formation process in the diesel engine, reduces the thermal efficiency and reduces the soot oxidation, which is an important basis for adjusting the injection pressure and injection timing of the diesel engine fuel system, when using diesel - vegetable oil mixture fuel.

REFERENCES

- [1]. Avinash Kumar Agarwal, Atul Dhar, 2013, Experimental Investigations of Performance, Emission and Combustion Characteristics of Karanja Oil Blends Fuelled DICI Engine, Elsevier Ltd. Renewable Energy 52, 283-291.
- [2]. Anthony A. Amsden, T-3, 1999, Kiva - 3v, Release 2, Improvements to Kiva-3v, Los Alamos National Laboratory
- [3]. Bernard Challen, Rodica Baranescu, 1999, Diesel Engine Reference Book, Oxford OX2 8DP.
- [4]. B.Desantes J. M, Payri R, Salvador F. J, 2003, Measurements of Spray Momentum for the Study of Cavitation in Diesel Injection Nozzles, SAE -01.
- [5]. Borman, G.L. and Johnson, J.H, 1962, Unsteady Vaporization Histories and Trajectories of Fuel Drops Injected into Swirling Air, in SAE Technical Paper 620271, Society of Automotive Engineers, Inc, USA.
- [6]. Carsten Baumgarten, 2006, Mixture Formation in Internal Combustion Engines, Springer - Verlag Berlin Heidelberg.
- [7]. Changlin Yang, Yoshiyuki Kidoguchi, Ryoji Kato, Kei Miwa, 2000, Effects of Fuel Properties on Combustion and Emissions of a Direct Injection Diesel Engine, Bulletin of the M.E.S.J, Vol. 28, No.2.
- [8]. C.Venkataramana Reddy, B.K.Venkanna, Swati B. Wadawadagi, 2010, Effect Of Injection Pressure on Performance, Emission and Combustion Characteristics of Direct Injection Diesel Engine Running on Blends of Pongamia Pinnata Linn Oil (Honge Oil) and Diesel Fue, Vol. 10 Issue 2, June.
- [9]. Daniela Siano, Fuel Injection, ISBN 978-953-307-116-9, Publisher: Sciyo, Chapters published August 17, 2010 under CC BY-NC-SA 3.0 license DOI: 10.5772/55402.
- [10]. Gunnar Stiesch, 2003, Modeling Engine Spray and Combustion Processes, Springer - Verlag Berlin Heidelberg.
- [11]. K. Mollenhauer, H. Tschöcke, 2010, Handbook of Diesel Engines, DOI 10.1007/978-3-540-89083-6, Springer - Verlag Berlin Heidelberg.
- [12]. Kannan. K, udayakumar. M, 2010, Experimental Study of the Effect of Fuel Injection Pressure on Diesel Engine Performance and Emission, journal of engineering and applied sciences, vol. 5 issue 5, p42.

EXPERT SYSTEM RULE-BASED OPTIMIZATION IN ASSIGNING COURSES OF STUDY

Ismail Olaniyi MURAINA

Department of Computer Science, Adeniran Ogunsanya College of Education, Lagos Nigeria
ORCID CODE: <https://www.orcid.org/0000-0002-9633-6080>

Segbenu Joseph ZOSU

Department of Mechanical Engineering, Lagos State University, Lagos Nigeria

Moses Adeolu AGOI

Department of Computer Science, Adeniran Ogunsanya College of Education, Lagos Nigeria

Abstract

The usual way of solving the general assignment problem by most institutions is to manually examine the full list of courses in some predefined order and for each course to a lecturer or lecturers of best-fitting. This procedure is a straight forward process that can be accomplished by a Head Of Department (HOD), using professional experience, HOD may use different criteria (Qualifications, Years of experience, area of specialization) to search for a lecturer with characteristics required by the course, to allocate courses to such lecturer. However, the procedure has the following significant drawbacks: It is tedious, repetitive, and time-consuming. Since the shortlist of matches is not prioritized within itself by using an expert system, it requires further manual work to rank-order the individuals in the shortlist and is thus likely to result in a sub-optimal choice, even for just a single course. The first course considered is likely to be assigned the best-found competent lecturer for the course (a greedy policy), even though that lecturer may be better suited to other courses that have not yet been assigned. In searching for best lecturer to a course fitting in most cases has led to a serious confusion of allocation. Given the above drawbacks, the potential for large amounts of data, and the need for a short response time, an automated procedure to optimize the set of assignments could offer a significant benefit; hence the reason for solving the assignment problem would be achieved successfully. This paper looks into effectiveness involving in the allocating the teachers to the relevant courses, the primary focus is rest on the teacher assignment problem using an expert system based approach with the use of visirule. The results of using the artificial intelligent (Expert system) proved to be easy of use, no undue repetitions and time saving compared to manual allocation method. Hence, the stress which head of departments are passing through over the years can be resolved by following the selection procedures generated by the system

Keywords: Expert system. Visirule, Assignment problem, Course allocation

Introduction

The assignment problem (AP) is a discrete and combinatorial problem where agents are assigned to perform tasks for efficiency maximization or cost (time) minimization. AP is a part of human resource project management (HRPM). The AP optimization model, with deterministic parameters describing agent-task performance, can be easily solved, but it is characteristic of

standard, well-known projects realized in a quiet environment Gaspars-Wieloch (2019). The assignment problem is a special case of the transportation problem where all sources and demand are equal to 1. The basic problem in operations research is to assign tasks to facilities on a one-to-one basis in an optimal way. The problem may be to find the best assignment of employees to jobs, the best player to a field position, equipment to a factory worker and many more examples. The main objective of assignment problem is to minimize the total time to complete a set of tasks, or to maximize skill ratings, or to minimize the cost of the assignments. Assignment problem has been used in a variety of application contexts such as personnel scheduling, manpower planning and resource allocation (Sonia, 2008).

Andrew and Collins (1971) developed a procedure for assigning teachers to courses based on a simple linear programming technique. According to Ravindran, (2008), the assignment problem (AP) is broadly known as a deterministic and combinatorial problem in operations research, discrete optimization, and project management. Ding (2020); Ding and Zeng (2018) carried out and analyzed the assignment problem with uncertain parameters. The first set of constraints implies that each lecturer is assigned to one and only one course and the second set of constraints implies that to each course is assigned one and only one lecturer. It should be noted that in addition to the minimization of assignment cost, an assignment problem may also consider other objective functions such as the minimization of completion time. When the assignment problem is considered with the minimization of assignment cost as the objective function, it is called the cost minimizing assignment problem, if it is time it is called time minimizing assignment problem. Assignment problem has been used in a variety of application contexts such as personnel scheduling, manpower planning and resource allocation (Sonia, 2008).

According to Simon, (2012) matching highly skilled people to available positions are a high-stakes task that requires careful consideration by experienced resource managers. A wrong decision may result in significant loss of value due to understaffing, under-qualification or over-qualification of assigned personnel, and high turnover of poorly matched workers. While the importance of quality matching is clear, dealing with pools of hundreds of jobs and resources in a dynamic market generates a significant amount of pressure to make decisions rapidly

Related Literatures

Odior, Charles-Owaba, and Oyawale, (2010) conducted a research on important research tool in operations research as it was applied to a particular structure of the multi-criteria assignment problem. The study addressed the problem of effectiveness of feasible solutions of a multi-criteria assignment problem which was done in two steps: the first one determined whether or not a given feasible solution of a multi-criteria assignment problem was a real efficient one while the second step was based on what will happened if the feasible solution was not real efficient, by providing a real efficient solution that dominated that not real efficient solution. Gunawan and Ng (2011) from Indonesia carried out a research which addressed time-tabling problem in a university. The study focused on the problem of assigning teachers to the courses and courses sections. In this study, a mathematical programming model was formulated, simulated annealing (SA) and tabu search (TS) algorithms were proposed to solve the problem. One phase involved allocating the teachers to the courses and determining the number of courses to be assigned to each teacher. The other phase involved assigning the teachers to the course sections in order to balance the teachers' load. At the end, the computational results showed that in general, tabu

search performed better than simulated annealing and other previous work. For the real data sets, the computational results showed that both proposed algorithms yielded better solutions when compared to manual allocation done by the university

Niknafs, Denzinger, and Ruhe, (2013) conducted a study on personnel assignment problem and proposed solution to solve the problem, the analysis results revealed potential solution approaches, the trends in application of existing solution methods, and some potential future research areas. It was observed that artificial intelligence and machine learning still have a good potential to contribute to this field of research in different applications. Gasparis-Wieloch (2019), suggested an algorithm combining binary programming with scenario planning and applying the optimism coefficient, which described the manager's nature (attitude towards risk). The procedure was designed for one-shot decisions (i.e., for situations where the selected alternative is performed only once) and pure strategies (the execution of a weighted combination of several decision variants is not possible) when considering new (innovation or innovative) projects or projects performed in very turbulent times

Goldsmith and Sloan (2021), carried a study on Conference Paper Assignment Problem (CPAP) which resolved the problem of assigning reviewers to conference paper submissions in a manner intended to minimize winging. It was assumed that papers were reviewed by members of a preset program committee (PC), each of whom has the opportunity to bid on papers prior to the assignment algorithm being run. In the study, they showed that CPAP was in P if the only information given was individual program committee members' preferences for individual papers. However, if both preferences and expertise (based on, say, keywords) were given, the problem was potentially more complex. Katta and Jay (2005) presented the problem of allocating a set of indivisible objects to agents in a fair and efficient manner.

The Visirule software is always used as a decision supporting tool, in which the rules are basically and precisely presented using Logic Programming Model. The RSA-Expert can be of great use to researchers in making a firm decision in utilizing suitable statistical data analysis in researches (Muraina, Rahman, Adeleke, & Aiyegbusi, 2013). Visirule allows experts / researchers to concentrate on explaining and establishing the structure of the logic correctly using their chosen tools - those embedded materials that can assist researcher to accomplish his mission (Spenser, 2007; Bilgi, kulkarni, & Spenser, 2010). The Visirule software, being free software, was used as a decision enabling tool, presented graphically based on a logic programming model (Muraina, Rahman and Adeleke, 2016). The Visirule software was used as a decision supporting tool, using Logic Programming Model to present RDS-Expert in a concisely and precisely way. The RDS Expert serves as a guide for researchers to use in making good decision regarding the type of research design fit their studies (Muraina and Adeleke, 2021).

Materials and Methods

The study used lecturers of Computer science, Adeniran Ogunsanya College of Education, Lagos, Nigeria as a case study. Qualifications, years of experience and area of specializations were considered in preparing the decision extracts used for the design of visirule.

Bachelor degrees as well as masters degrees programme done by the lecturers were used. The results were considered valid and reliable because they were all certified by accredited universities both locally and internationally. A lecturer was assigned series of courses based on criteria like qualifications, area of specializations or fields and years of experience

Results

The results show the graphical boxes that help the Head of Departments to just basically and conveniently assign courses to the best fitted lecturer in the department without wasting time and unnecessary repetition of efforts. The figure 1 shows the visirule paths to solve assignment problems

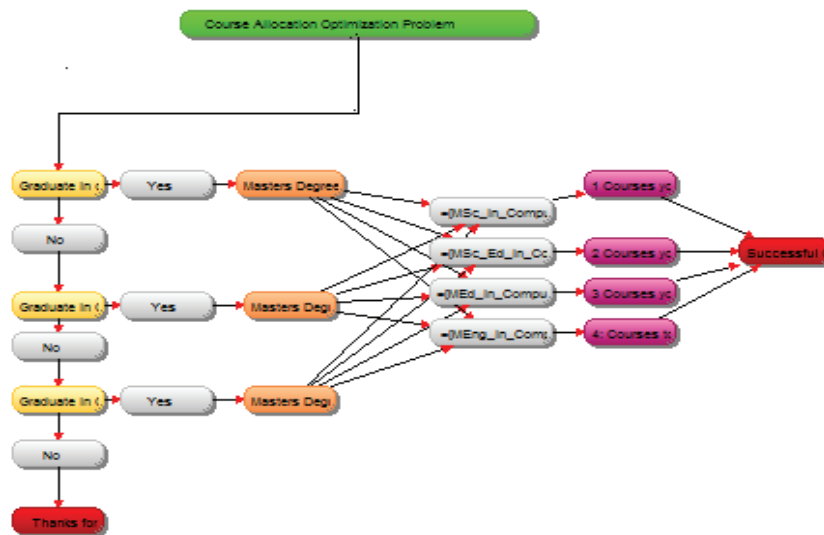


Fig. 1: Visirule Expert System Paths

Conclusion

A novel approach of using expert system is applied in this study which is far different from previous approaches. In this, no code is required in the use of visirule software and eventually the similar results are to be achieved with respect to past studies.

References

- Andrew, G. M. and Collins, R., (1971). Matching faculty to course, College University, Vol.46, No.2, pp.83-89
- Bilgi, N.B; Kulkami, R.R.V and Spenser, C (2010). An Expert System Using a Decision Logic Charting Approach for Indian Legal Domain with Specific Reference to Transfer of Property Act. *International Journal of Artificial Intelligence and Expert System (IJAE)*, 1(2), P 32-39
- Ding, Sib0 and Zeng. Xiao-Jun (2018). Uncertain random assignment problem. *Applied Mathematical Modelling* 56: 96–104. [[CrossRef](#)]
- Ding, Sib0. (2020). Uncertain random quadratic bottleneck assignment problem. *Journal of Ambient Intelligence and Humanized Computing* 11: 3259–64. [[CrossRef](#)]
- Gaspars-Wieloch, Helena (2019). The Assignment Problem in Human Resource Project Management under Uncertainty Department of Operations Research and Mathematical Economics, Poznań University of Economics and Business, 61-875 Poznań, Poland; Helena.gaspars@ue.poznan.pl

- Gunawan, Aldy and Ng, Kien Ming (2011). Solving the teacher assignment problem by two Metaheuristics. *International Journal of Information and Management Sciences*. 22, (1), 73-86. Research Collection School of Information Systems. Available at: https://ink.library.smu.edu.sg/sis_research/4003
- Muraina, I O and Adeleke I A (2021). Researchers' Artificial Intelligence Expert System Rule-Based Decision Making Using Visirule. *International Journal of Progressive Sciences and Technologies (IJPSAT)*, 28(1), pp.351-358
- Muraina, I O, Rahman, M A and Adeleke, I A (2016). Statistical Approaches and Decision Making Towards Bivariate and Multivariate Analyses with Visirule. *British Journal of Education, Society & Behavioural Science*, 14(2): 1-10
- Niknafs, Arash Denzinger, Jörg and Ruhe Günther (2013). A Systematic Literature Review of the Personnel Assignment Problem. *Proceedings of the International MultiConference of Engineers and Computer Scientists 2013 Vol II, IMECS 2013, March 13 - 15, 2013, Hong Kong*
- Odior, A O; Charles-Owaba, O E; Oyawale, F A (2010). Determining Feasible Solutions of a Multicriteria Assignment Problem. *J. Appl. Sci. Environ. Manage.* March, 2010 Vol. 14(1) 35 – 38
- Ravindran, A. (2008). *Operations Research and Management Science Handbook*. Boca Raton, London and New York: CRS Press.
- Sonia, P M C (2008). Two-Stage Time Minimizing Assignment Problem. *Omega articles on manufacturing magazines*. 36 (5): 730-740.

PLANNING OF URBAN TRANSFORMATION AFTER THE EARTHQUAKE IN A LOCAL AREA WITH ZONING WITH HEDONIC AND PRIME METHODS

İMARLI LOKAL BİR SAHADA DEPREM SONRASI KENTSEL DÖNÜŞÜMÜN HEDONİK ve EMSAL METODU İLE PLANLAMASI

Selim Taşkaya

Artvin Meslek Yüksekokulu Mimarlık ve Şehir Planlama Bölümü, Artvin, Türkiye.

Orcid No: <https://orcid.org/0000-0002-4290-3684>

ÖZET

İmarlı alanlar denilince aklımıza gelmesi gereken, insanların sağlık, ulaşım, barınma vb. gibi ihtiyaçlarını en iyi şekilde karşılanmasını sağlayan toprak düzeninin meydana getirilmesidir. Yol, konut, ticaret, yeşil, okul, hastane gibi alanların, belli imar sınırları geçirilerek bu sınır içerisinde oluşturulmasıdır. Bu alanlar oluştururken bazı kıstaslara dikkat edilmelidir. Jeolojik yapısı uygun olmayan yumuşak toprağa ya da fay hatlarının geçtiği arazi üzerine, su yataklarının kenarındaki gibi alanlara yerleşim yerlerinin inşa edilmemesi gerekir. Kentsel dönüşüm ise, bu tip tehlikeli alanlarda bulunan ya da yapı ömrünü tamamlamış inşaat stokunun dönüşümünü sağlayarak yeniden yapılandırmaktır. Türkiye’de 6306 sayılı yasal mevzuat çerçevesince bu işlemler yürütülür. Çalışmamız da, Ocak 2020 yılında Türkiye’nin Elazığ İlinde meydana gelen deprem sonrası zarar gören Mustafapaşa Mahallesi’ndeki lokal bir noktada inşaat stokunun bulunduğu alan kentsel dönüşüme sokularak yeniden inşası sağlanmıştır. Amaç, bir doğal afet sonrası hasar tespiti yapılarak, yeniden obölgenin planlamasını yapmaktır. Yöntem olarak ise, deprem öncesi kimi noktalarında bitşik yapı nizamı ya da ayırık nizam 5 kat olan alanların lokal bazlı bir imar planlaması ile yeniden imar adalarının oluşturulmasıdır. Eski inşaat toplam alanlarının projeleri ışığında bina ve daire bazlı m² ler tespit edilip, katların yüksekliği emsalleri, taks ve kaks oranları insanların eski düzenlerini çok değiştirmeyecek şekilde uygulanması emsal yöntemidir. Tabi bu emsaller uygulanırken, eski planda ilgili vatandaşın dairesinin konumu, ulaşım ve alışveriş noktalarına mesafesi vb. parametreler ışığında meydana gelebilecek deprem öncesi ve sonrası oluşturulacak planın ekonomik hesabının tespiti ise hedonik yöntemdir. Bu iki metod baz alınarak çalışma sahasındaki imar planı lokal kentsel dönüşüm faaliyetinin vatandaşla kamuya maaliyeti ve nasıl bir imar planının yapılması hakkında öneriler getirilmeye çalışıldı.

Anahtar Kelimeler: İmar planı, Kentsel Dönüşüm, Hedonik ve Emsal Metodu

ABSTRACT

When it comes to zoned areas, what should come to our minds is people's health, transportation, shelter, etc. It is the creation of the soil order that provides the best way to meet such needs. It is the creation of areas such as roads, housing, trade, green, school, hospital, within this border by passing certain zoning boundaries. When creating these areas, some criteria should be considered. Settlements should not be built on soft soil with an unsuitable geological structure or on land where fault lines pass, in areas such as on the edge of water beds. Urban transformation, on the other hand, is restructuring by transforming the construction stock that is located in such dangerous areas or has completed the life of the building. In Turkey, these procedures are carried out within the framework of the legal legislation numbered 6306. In our study, the area where the construction stock is located at a local point in Mustafapaşa Neighborhood, which was damaged after the earthquake that occurred in Turkey's Elazığ Province in January 2020, was transformed into urban transformation and reconstructed. The aim is to make a re-planning of the region by determining the damage after a natural disaster. As a method, it is the creation of zoning islands again with a local-based zoning planning of areas with a contiguous structure or 5 floors at some points before the earthquake. It is a precedent method to determine the m² based on buildings and flats in the light of the projects of the old construction total areas, and to apply the height of the floors, the equivalents of the floors, the tax and pay rates in a way that does not change the old order of the people much. Of course, while these precedents are being applied, the location of the relevant citizen's flat in the old plan, its distance to transportation and shopping points, etc. The determination of the economic calculation of the plan to be created before and after the earthquake that may occur in the light of the parameters is the hedonic method. Based on these two methods, suggestions were made about the cost of the local urban transformation activity in the study area to the public and how to make a zoning plan.

Keywords: Zoning plan, Urban Transformation, Hedonic and Precedent Method

DETERMINATION OF SOME PERFORMANCE CHARACTERISTICS OF CONSTRUCTION TIMERS FROM LAMINATED WOOD MODIFIED WITH CARBON FIBER

Turan Maharrambay AHMADLI

Muğla Sıtkı Kocman University, Mugla, Turkey

Erkan AVCI

Muğla Sıtkı Kocman University, Mugla, Turkey

Kamala YUSİFOVA

Azerbaijan Architectura and Construction University, Baku, Azerbaijan

Summary

The purpose of this study is to determine some of the performance properties of building lumber from laminated veneer lumber, modified with carbon fiber. In the study, 3 European spruce (*Picea abies*) trees of various thicknesses and unidirectional carbon fiber material were used as wood raw materials. The carbon fiber fabrics used are suitable for 4 different applications. Epoxy and polyurethane adhesives are used as glue. It complies with TS 5497 EN 408 standard for flexural strength and modulus of elasticity tests, TS EN 317 standards for water absorption and dimensional swelling rate, and EN 302-1 / 2004 standards for adhesion resistance tests. According to the test results, the maximum static bending resistance of the specimens was 73,324 N / mm² in laminated specimens using a single layer of CFRP building material and epoxy adhesive, while the average flexural modulus was a maximum of 11831.797 N / mm² in specimens. obtained by coating epoxy resin with carbon fiber. As a result of dimensional stability tests, the greatest increase in weight change (57.03%) for laminated specimens glued with epoxy resin, the maximum increase in thickness change (68.05%) for laminated specimens held together with two-layer polyurethane adhesive on the inner surface, maximum increase in width change The effect of adhesive and CFRP adhesive interaction on adhesion resistance was significant at a 95% confidence interval in tensile shear tests.

Tests have shown that CFRP reinforcement can be easily used in multilayer beams. Substantial improvements have been made in some mechanical properties and dimensional changes due to water. Using carbon fiber epoxy adhesive helps to protect the wood surface from external factors.

Key words: laminated wood material, carbon fiber (carbon fiber), adhesives, mechanical properties.

DETECTION OF BURIED ARCHAEOLOGICAL BY RESISTIVITY METHOD IN THE ANCIENT CITY OF ALABANDA

ALABANDA ANTİK KENTİNDE REZİSTİVİTE YÖNTEMİ İLE GÖMÜLÜ ARKEOLOJİK KALINTILARIN TESPİT EDİLMESİ

SUAT DEMİR

Yüksek Lisans Öğrencisi, Sakarya Üniversitesi, Mühendislik Fakültesi
Jeofizik Mühendisliği Bölümü

GÜNAY BEYHAN

Dr. Öğr. Üyesi, Sakarya Üniversitesi, Mühendislik Fakültesi
Jeofizik Mühendisliği Bölümü

Özet

Bu çalışma Aydın iline bağlı olan Çine ilçe merkezine yaklaşık 8 km uzaklıkta ki Alabanda Antik Kentinde yapılmıştır. Aydın Adnan Menderes Üniversitesi Arkeoloji Bölümü tarafından yürütülen ve yapılan kent planını çıkarma çalışması günümüzde de devam etmekte ve yapılar gün yüzüne çıkartılmaya çalışılmaktadır. Bu doğrultuda, söz konusu antik kentte kiliseye ait olduğu düşünülen gömülü yapıların varlığı ve kalıntılarının durumlarını belirlemek amacıyla jeofizik elektrik rezistivite tomografisi (ERT) yöntemi kullanılarak saha ölçümleri alınmıştır. Bu amaca yönelik olarak Kilise'ye ait olduğu düşünülen duvarlar içinde her biri 23 m olan kilise alt bölgesine ait 6 profil, kilise üst bölgesine ait 8 profil oluşturulmuş ve wenner dizilimi kullanılarak elektrik ölçümleri alınmıştır. Elektrotlar ve profiller arasındaki uzaklık 1'er m olarak karelelenmiş ve ölçümler alınmıştır. Profil boyu araziden dolayı 23 m seçilmiştir. Ölçüler ARES GF çok kanallı rezistivite cihazı ile alınmış ve kayıt altına alınmıştır. Elde edilen veriler RES2DINV / RES3DINV ters çözüm metodu kullanılarak 2B ve 3B kesit verileri oluşturulmuştur. Bu kesitlere dayanarak Kilise'ye ait kalıntıların veya varsayılan yapıların varlığı tespit edilmeye çalışılmıştır. Bu kalıntıların Kilise'nin hangi bölümlerine ait olduğu Jeofizik yöntemler ve aynı zamanda Arkeoloji disiplinleri dikkate alınarak yorumlamaya çalışılmıştır. Kilise bölgesinde devam eden ve planlanan kazı çalışmaları Jeofizik yorumların öngördüğü biçimde, Arkeolojik kurallarına uygun şekilde yapılmaktadır.

Anahtar kelimeler: Alabanda, Kilise, Elektrik Rezistivite Yöntemi, Arkeojeofizik, RES2DINV, RES3DINV

ABSTRACT

The study area is Church of the Alabanda Ancient City, located 8 km West of Çine town of Aydın province, in western Turkey. Field studies carried out by Archeology Department of Aydın Adnan Menderes University to map city plan of the Alabanda is still in progress. In order to determine presence and conditions of the buried structures, geophysical investigations by means of electrical resistivity tomography (ERT) were carried out in the Church. For this purpose, inside the walls of the Church, total 14 electrical profiles, which are 23 m in length were formed to measure electrical resistivity using the Wenner arrays. Both the profile separation and the distance between the electrodes were taken as 1 m. Measurements were ARES GF

multichannel resistivity instrument. 2D and 3D sections have been obtained from using RES2DINV and RES3DINV computer programs with robust inversion, respectively.

Keywords: Alabanda, Church, Electrical Resistivity Method, Archaeogeophysics, RES2DINV, RES3DINV

1. GİRİŞ

Jeofizik yöntemlerin günümüzde arkeolojik çalışmalarda da kullanılmaya başlanması, arkeolojik araştırma çalışmalarına yeni bir anlam, değer ve boyut kazandırmıştır. Jeofizik yöntemlerin uygulama hızı, kolaylığı, ucuzluğu ve kesinliği bu durumu daha da artırmıştır. Ayrıca bu yöntemin diğer bir büyük avantajı da; bütün jeofizik yöntemlerin arazi üzerinde uygulanabilirliği ve arkeolojik kalıntılara herhangi bir zarar vermeden ortaya çıkarmasıdır. Bu etkenleri göz önünde bulundurduğumuzda yakın zamanda jeofizik yöntemlerin arkeolojik çalışmalarda tercih edilip kullanılması sıklıkla önümüze örnek olarak çıkmakta ve büyük başarılar elde edilmektedir [Leucci vd., 2006; Negri vd., 2008; Tsokas vd., 2009; Drahor vd., 2011; Papadopoulos vd., 2012].

Önemli elektrik yöntemlerden biri olan rezistivite yönteminin başarısı gömülü yapı ve çevresindeki toprak arasında bulunan direnç farklılığı kuramına dayanmaktadır. Bu yöntem sayesinde duvarların, yapıların, yapı temellerinin, mağaraların, kalıntıların ve diğer arkeolojik yapıların tespit edilmesinde oldukça başarılı bir yöntem olduğu bilinmektedir.

Elektrik prospeksiyon yönteminde sıklıkla kullanılan ters çözüm teknikleri bloklu (robust) ve düzgünlük-kısıtlı (smoothness-constrained) en küçük kareler teknikleridir. Robust ters çözüm tekniği köşeli yapılarda, smoothness-constrained tekniğine göre daha kesin ve uygun sonuçlar sağlamaktadır [Loke vd., 2015; Loke vd., 2003]. Arkeolojik yapıları araştırma çalışmalarında aranan veya karşılaşılan kalıntılar da bu şekilde köşeli yapılar olduğundan dolayı bu tür çalışmalarda genellikle robust ters çözüm tekniği tercih edilmektedir [Drahor vd., 2018; De Domenico vd., 2006].

Tsokas ve diğerleri [Tsokas vd., 2007], Yunanistan'ın kuzeyinde Holy Dağları'nda bulunan Pratatton Kilisesi etrafında yeraltında gömülü yapıların varlığını araştırmak amacıyla elektrik yöntemi uygulamışlardır. Elde edilen tomografi haritalarından kilisenin etrafındaki temel duvar kalıntıları tespit edilmiş ve çalışma alanının jeolojisi hakkında bilgiler elde edilmiştir.

Bölgede son yıllarda arkeojeofizik alanında yapılan çalışmalarda meclis binası ve amfi tiyatro araştırma çalışmaları yer almaktadır [Papadopoulos vd., 2012; Perez-Gracia vd., 2008; Gaffney vd., 2007; Aubry vd., 2001]. Bu araştırmaları izleyen restorasyon, onarım, ayağa kaldırma ve kazı çalışmaları jeofizik çalışmaların önemini daha da artırmaktadır.

Bu alanda yapılan çalışmaların azlığından dolayı ulusal ve uluslararası bilgi ve deneyim ise oldukça kısıtlı olduğu bilinmektedir.

Bu çalışma Ege bölgesinin tarihsel ve kültürel açıdan önde illerinden olan Aydın'a bağlıdır. Çine ilçesinin batısında ve 8 km. uzağında bulunan, Doğanyurt köyünün (eski adı Araphisar) bulunduğu yerde konumlanmıştır. Alabanda antik kenti kazı alanımızda kilise olduğu tahmin edilen bir bölgede, 2B ve 3B elektrik öz direnç tekniğiyle gerçekleştirilen arazi uygulamasını ve sonuçlarını içermektedir.

Kısıtlı bilgi ve deneyim ışığı altında yapılan bu çalışmanın amacı, alanın jeofizik potansiyelini ortaya çıkarmak ve kilise olduğu tahmin edilen bölgenin alt ve üst kısımlarında barındırdığı yapıların geometrisini, kilise konumunu belirlemektir.

2. ARKEOJEOFİZİK TANIMI VE ÇALIŞMALARDA KULLANILAN YÖNTEMLER

2.1. Arkeojeofizik Çalışmaların Geçmişi

Geçmiş yıllardan şimdiki zamana süregelen ve varlığının en ufak, küçük bir nişanı olan ipuçlarından yola çıkan, arkeoloji biliminin doğası gereği birçok disiplinle ilişkilendirilebilir. Bu sayede yeniliğe açık bilimsel disiplinlerin doğuşuna, gelişmesine zemin oluşturmıştır. Bu gelişim zamanla değişik birçok bilim dalını içinde barındıran “arkeojeofizik” disiplininin oluşmasını da sağlamıştır.

Bu disiplinler içinde en önemlilerinden biri de geçmişe ışık tutan ve doğru tahminde bulunan arkeojeofiziktir. Jeofiziğin 1940’lı yıllarda arkeolojiye eşlik etmesiyle birlikte teknolojinin ve bilimsel gelişimin de yardımıyla, kazılardan önce ihtiyaç duyulan araştırmaları içinde ilk sırayı açık ara elinde bulundurmaktadır.

Tablo 1. Arkeojeofizik çalışmalar ve bu çalışmalara ait kullanılan yöntemler

Makale	Elektrik	Manyetik	GPR	Sismik	EM
Ekinci, Y.L., ve diğ., 2014	•	•			
Apostolopoulos V. G., 2014	•		•		•
Papadopoulos, N. ve diğ., 2012	•	•	•	•	
Tsourlos, P.I. ve Tsokas N. G., 2011	•				
Drahos, M.G. ve diğ., 2011	•	•	•		
Tsokas, N.G., ve diğ., 2009	•				
Tsokas, N.G., ve diğ., 2008	•				
Drahos, M.G. ve diğ., 2008	•	•			
Tsokas, N.G., ve diğ., 2007	•		•		
Leucci, G., ve diğ., 2007	•			•	
Drahos, M.G., 2006	•	•		•	•
De Domenico, D., ve diğ., 2006	•		•	•	
Tonkov, N., Loke, M. H., 2006	•				
Leucci G., Negri, S., 2006	•		•		

2.2. Arkeojeofizik Yöntemler

Arkeolojik çalışmalarda jeofiziğin ilk olarak tercih edilmesindeki en önemli kriter; kullanılan cihazların hiçbir durumda gömülü, yerin altında olduğunu varsaydığımız yapıya zarar vermemesidir. Jeofizik yöntemlerin sorunsuz, hızlı ve ayrıntılı sonuca bize ulaştırması ile pratik ve ucuz olması olarak sıralayabiliriz.

Arkeolojide jeofizik, yapının yer altında bulunduğu konumun, yani bulunduğu derinliğini ve büyüklüğünü küçücük olmasından, birkaç m büyüklüğe sahip olan yapıların tümüyle ilgilidir. Bu yapılarımız;

Duvarlar, fırınlar, çukurlar, temeller, ocaklar, kale duvarları, tiyatro, sokak, stadyum, tapınak, kilise, meclis binası, cadde, çarşı, büyük binalar, temeller ve evden arta kalan kalıntılar “arkeolojik” temelleri oluşturmaktadır.

Bu yöntemlerden bazıları;

- Manyetik Yöntem, Elektromanyetik Yöntem, Radar Yöntemi, Gravite Yöntemi, Elektrik Özdirenç Yöntemi



Şekil 1. Arkeojeofizik yöntemler



Şekil 5. Kilise alanının değişik cephelerden görüntüleri (kuzey ve güney)

3.1.1. Ters Çözüm Metodu

Jeofizik olarak karşımıza çıkan sorunlar ve sorunların çözümündeki prensip, anomaliye neden olan yapıyı veya kaynağı modellemeye çalışmaktır. Bu anomaliyi oluşturan kaynak, çalışılan bölgede yeraltında bulunan herhangi bir yapı veya yapılar kümesi olabilir. Bu durum problemin çok çözümlü olması sonucunu doğurur. Bu tür bir sorun görünür öz direnç verilerinin ters çözümüyle (inversion) aşılmaktadır.

Tüm ters çözüm yöntemlerinin amacı, yeraltındaki yapı için yanıtın bazı kısıtlamalara tabi tutulduğu ve ölçülen veriye uygun olan bir modeli belirlemeye çalışmaktır. Model parametreleri ve 2-B veya 3-B boyutlu rezistivite modelini tanımlayan matematiksel bağıntı kullanılarak bu modelin üreteceği yanıt yani kuramsal veri sonlu farklar [Dey vd., 1979a; Dey vd., 1979b] veya sonlu elemanlar [Silvester vd., 1990] yöntemleri sayesinde elde edilebilir.



Şekil 6. Ters çözüm işlemi genel akış şeması [Başokur vd., 2004]

Genel olarak ters çözüm işlemi, modelin oluşturacağı kuramsal anomaliyle gözlemsel anomali arasındaki uyum, verilen bir tolerans değerine ulaşınca kadar devam ettirilir. Bu uyum, RMS (root mean squares) ile gösterilen karesel hata değeriyle belirlenir ve

$$RMS = \sqrt{\frac{1}{N} \sum_{i=1}^N \left(\frac{g_i^{göz} - g_i^{hes}}{\sigma_i} \right)^2}$$

(1)

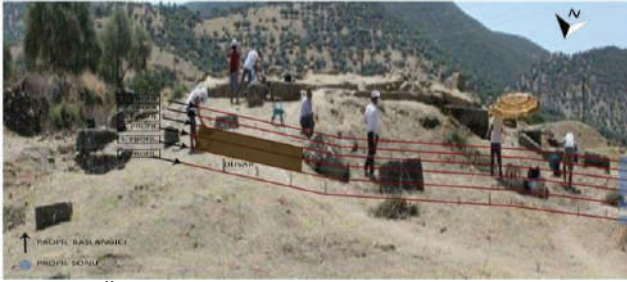
bağıntısıyla hesaplanır [Jackson vd., 1972]. Burada N veri sayısı, σ_i i'nci veriye ait standart sapma, $g_i^{göz}$ ve g_i^{hes} sırasıyla gözlenen ve hesaplanan anomali değerlerini göstermektedir.

Program hem sonlu farklar hem de sonlu elemanlar metoduyla görünür öz direnç değerlerinin hesaplanmasına olanak sağlar. Varsayılanlara göre eğer topoğrafya yoksa sonlu farklar metodu kullanılır. Topoğrafya içeriyorsa varsayılan seçim sonlu elemanlar metodudur. Program, bu bölümde anlatıldığı üzere ters çözüm işlemi için doğrusal olmayan bir en küçük kareler optimizasyon tekniğini kullanılır.

Ayrıca RESDIN2V programı sayesinde bir profil üzerinde alınan 2 boyutlu veriler birleştirilerek 3 boyutlu tomografi verileri oluşturulabilir ve bu 3 boyutlu veriler RESDIN3V programıyla ters çözüme tabi tutulup değerlendirilerek kat haritaları ve 3 boyutlu gösterimler elde edilebilir.

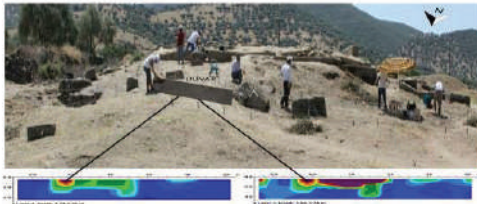
3.1.2. Kilise Alt Kısım

Elektrik öz direnç ölçümleri, doğu-batı uzanımlı ve her birisinin arası 1 m olacak şekilde yerleştirilmiştir. Kilisenin alt bölgesinde 6 adet paralel profil boyunca ARES GF çoklu elektrot sistemiyle 2012 temmuz ayında benimde içinde bulunduğum ekip tarafından tamamlanmıştır. Profil sayısının 6 ile kısıtlı kalmasına Şekil 7’de görüldüğü gibi arazinin mevcut durumu ve engebeli arama alanı durumuna neden olmuştur. Kiliseyi oluşturan yapıların yüzeydeki belirginliği ve küçük yüzey değişimleri göz önünde bulundurularak elektrotlar arası mesafe 1 m olarak seçilmiş ve uzunluk 23 m olacak şekilde karelajlanmıştır.



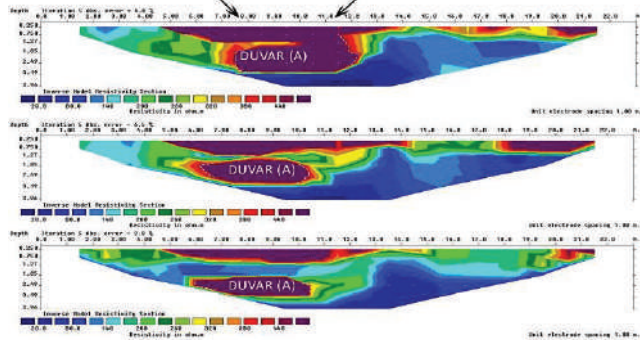
Şekil 7 Ölçü noktaları için gridlenmiş çalışma alanı kilise alt kısım

Mutlak hata (ABS error) değerlerinin yüzdesi % 2,4 – % 7,3’ü aşmamıştır. Ayrıca 2-B datalar Res2dinv programıyla birleştirilerek 3-B datalar elde edilmiş ve bu dataların da ters çözümü robust ters çözüm algoritması kullanılarak Res3dinv programıyla yapılmıştır.



Şekil 8 Kilise alt çalışma alanı derinlik kesiti

Kilise alt bölgesine ait olan, Şekil 8’de görülen çalışma alanında, kilise alt kısım çalışma alanındaki karartılı şekil mevcut duvarı temsil etmektedir.

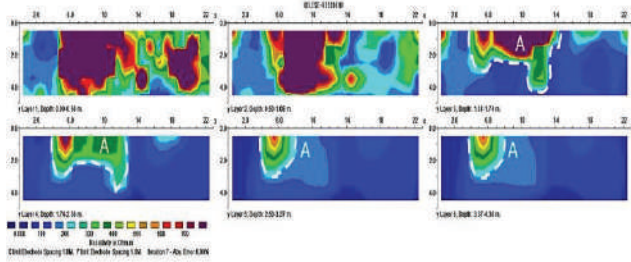


Şekil 9. Kilise alt kısım wenner elektrot dizilimi (yukarıdan aşağı 3. ,4. ve 5. profiller)

Kilise alt kısmındaki 3., 4. ve 5. profile ait olan wenner elektrot diziliminlerinde duvar yapısı Şekil 9’da toplu olarak belirtilmeye çalışılmıştır.

Kesitler, wenner elektrot dizilimi için 0,00 - 0,50 m, 0,50 - 1,08 m, 1,08 - 1,74 m, 1,74 - 2,50 m, 2,50 - 3,37 m ve 3,37 - 4,38'lik derinliklere aittir.

Bu kesitlere bakıldığında elektrik özdirenç değerleri Min: 36,41 ohm.m, Max: 1918,06 ohm.m arasında değişmektedir. Arkeolojik yapı kalıntılarını örten alüvyon zeminin özdirenci 36 – 345 ohm.m arasında değişmekte olduğu gözlemlenmektedir. Derinlik kesitlerinde şekil üzerinde gösterilmiş olan duvar yapısını, böylelikle özdirenç değerleri alüvyon zeminden daha yüksek dirence sahip olan kısımları temsil etmektedir. (Şekil 10.)



Şekil 10. Kilise alt 3-B derinlik kesiti (A duvar)

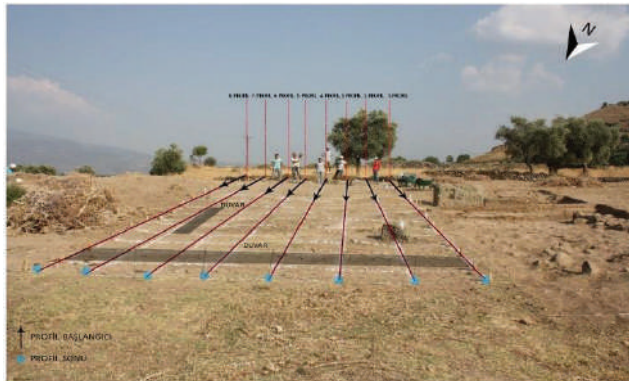
RES2DIN3V programı ile oluşturan wenner dizilime ait 1,08 – 1,74 m derinlik kesitinde A olarak isimlendirilen alan alüvyon ile örtülü olup Kilise'ye ait olduğu düşünülen kalıntı duvarı temsil etmektedir. Bu kalıntı duvar yapısı ve 1,74 – 2,50 – 3,37 ve 4,38 m derinlik kesitlerinde de görülmektedir. (Şekil 10)

3-B resistivite ters çözüm sonuçları kilise alt bölgede 6 iterasyonun ardından elde edilmiştir. Mutlak hata (ABS error) değerlerinin yüzdesi % 4,68'i aşmamıştır.

0,00 – 0,50 m ve 0,50 – 1,08 m derinliklerde ise yüzeye daha yakın olması sebebiyle antik kente ait olduğu düşünülen, taşınmış veya çevresel faktörlerden oraya ulaşmış, alüvyon zemininin, malzemelerin yüzeydeki görünüşü olarak değerlendirebiliriz.

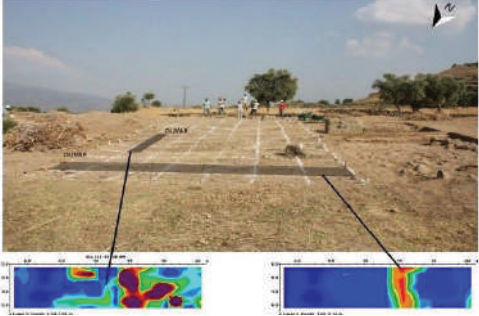
3.1.3. Kilise Üst Kısım

Elektrik özdirenç ölçümleri, kuzey uzanımlı ve her birisinin arası 1 m olacak şekilde yerleştirilmiştir. Kilisenin alt bölgesinde 8 adet paralel profil boyunca ARES GF çoklu elektrot sistemiyle 2012 temmuz ayında benim de içinde bulunduğum ekip tarafından tamamlanmıştır. Profil sayısının 8 ile kısıtlı kalmasına Şekil 11'de görüldüğü gibi arazinin mevcut durumu ve engebeli arama alanı durumuna neden olmuştur. Kiliseyi oluşturan yapıların yüzeydeki belirginliği ve küçük yüzey değişimleri göz önünde bulundurularak elektrotlar arası mesafe 1 m olarak seçilmiş ve uzunluk 23 m olacak şekilde karelemlenmiştir.

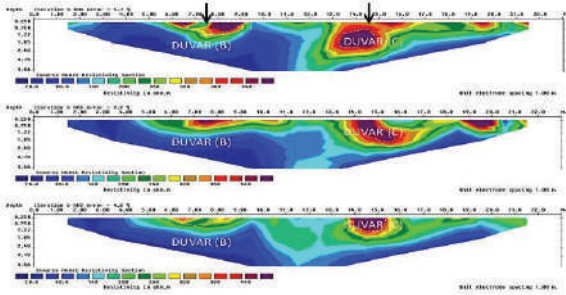


Şekil 11. Ölçü noktaları için gridlenmiş çalışma alanı kilise üst kısım

Mutlak hata (ABS error) değerlerinin yüzdesi % 2,3 – % 7,6'yı aşmamıştır. Ayrıca 2-B datalar Res2dinv programıyla birleştirilerek 3-B datalar elde edilmiş ve bu dataların da ters çözümü robust ters çözüm algoritması kullanılarak Res3dinv programıyla yapılmıştır.



Şekil 12. Kilise üst çalışma alanı 3-B derinlik kesiti



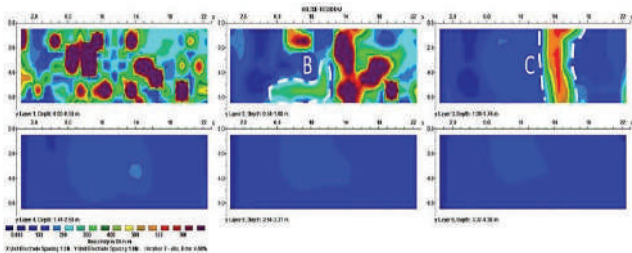
Şekil 13. Kilise üst kısım wenner elektrot dizilimi (yukarıdan aşağı 3., 4. ve 7. profiller)

Kilise üst kısmındaki 3., 4. ve 7. profile ait olan wenner elektrot diziliminlerinde duvar yapısı Şekil 13'de toplu olarak belirtilmeye çalışılmıştır.

Kesitler, wenner elektrot dizilimi için 0,00 - 0,50 m, 0,50 - 1,08 m, 1,08 - 1,74 m, 1,74 - 2,50 m, 2,50 - 3,37 m ve 3,37 - 4,38'lik derinliklere aittir.

RES3DINV programı ile oluşturan wenner dizilime ait, 0,50 - 1,08 m derinlik kesitinde B olarak isimlendirilen alan alüvyon ile örtülü olup Kilise'ye ait olduğu düşünülen duvar kalıntısını temsil etmektedir. (Şekil 14.)

1,08 - 1,74 m derinlik kesitinde C olarak isimlendirilen alan alüvyon ile örtülü olup Kilise'ye ait olduğu düşünülen duvar kalıntısını temsil etmektedir. (Şekil 14.)



Şekil 14. Kilise üst 3-B derinlik kesiti (B ve C duvar)

0,00 - 0,50 m de ise yüzeye daha yakın olması sebebiyle antik kente ait olduğu düşünülen, taşınmış veya çevresel faktörlerden oraya ulaşmış malzemelerin (yapıların) yüzeydeki görünüşü olarak değerlendirebiliriz.

Bu kesitlere bakıldığında elektrik öz direnç değerleri Min: 30,68 ohm.m, Max: 563,43 ohm.m arasında değişmektedir. Arkeolojik yapı kalıntılarını örten alüvyon zeminin öz direnci 30 - 178 ohm.m arasında değişmekte olduğu gözlemlenmektedir.

Derinlik kesitlerinde şekil üzerinde gösterilmiş olan duvar yapısını, böylelikle özdirenç değerleri alüvyon zeminden daha yüksek dirence sahip olan kısımları temsil etmektedir. (Şekil 14.)

4. SONUÇ VE ÖNERİLER

Bu çalışmada Wenner elektrot diziliminin düşey özdirenç değişimine (düşey yapılar) duyarlı olma ve yüksek çözüm gücü (resolution) özelliği sayesinde kilise alt ve kilise üst yapılarının sınırlarını daha net olarak belirlenmeye çalışılmıştır.

Kilise alt (Şekil 10.) ve üst (Şekil 14.) kısımlarına ait yapılar (duvar kalıntıları) her iki çalışma alanındaki elektrot diziliminde belirgin olarak görülmüştür.

Kiliseyi oluşturan duvar yapılarının bazı dağılmış kısımları wenner diziliminin yüksek sinyal gücü özelliği sayesinde, kiliseyi oluşturan yatay yapıların (duvar gibi) görülmesinde oldukça da fayda sağlamış ve yol göstermiştir.

Her iki çalışma yapılan bölgedeki kilise alt ve kilise üst elektrot diziliminden elde edilen veriler, kiliseyi oluşturan yapıların (duvar gibi) yeraltında gömülü olarak mevcut olduğunu açıkça göstermektedir. Jeofizik ölçümler ışığında belirlenen gömülü olan bu yapıların, yapılacak olan arkeolojik kazılarla yer yüzeyine zarar verilmeden çıkartılmalıdır.

Bir arada yaşayan kalabalık toplumların, kendi inançlarını daha iyi yaşamaları için büyük bir öneme sahip olan bu yapının, elde edilen verilere göre kilise olduğu düşünülmektedir. Bulunduğu konum ve yüzeyde çıplak gözle de görülen kabarıklık ve kalıntılardan yola çıkılarak yapının arkeolojik kazılarla ortaya çıkartılması ve verilecek karar doğrultusunda gerekirse, çıkan kalıntılara gerekli restorasyon çalışmalarının yapılması önemli ve gerekmektedir.

KAYNAKLAR

- [1]. Leucci, G., Geophysical investigation of the Temple of Apollo (Hierapolis,Turkey). Journal of Archaeological Science 33, 1505-1513, 2006.
- [2]. Negri, S., Leucci, G., Mazzone, F., High resolution 3D ERT to help GPR data interpretation for researching archaeological items in a geologically complex subsurface. Journal of Applied Geophysics 65, 111-120, 2008.
- [3]. Tsokas, G. N., Tsourlos, P. I., Stampolidis, A., Katsonopoulou, D., Soter, S., Tracing a Major Roman Road in the Area of Ancient Helike by Resistivity Tomography. Archaeological Prospection 16, 251-266, 2009.
- [4]. Drahor, M. G., Berge, M. A., Öztürk, C., Integrated geophysical surveys for the subsurface mapping of buried structure under and surrounding of the Agios Voukolos Church in Izmir, Turkey. Journal of Archaeological Science 38, 2231-2242, 2011.
- [5]. Papadopoulos, N. G., Sarris, A., Salvi, M. C., Dederix, S., Soupios, P., Dikmen, Ü., Rediscovering the small theatre and amphitheatre of ancient Ierapytna (SE Crete) by integrated geophysical methods. Journal of Archaeological Science 39, 1960-1973, 2012.
- [6]. Candansayar, M, E., Başokur, A, T., Detecting small-scale targets by the 2D inversion of two-sided three-electrode data: application to an archaeological survey. Geophysical Prospecting 49, 13-25, 2001
- [7]. Diamanti, N, G., Tsokas, G. N., Tsourlos, P, I., Vafidis, A., Integrated Interpretation of Geophysical Data in the Archaeological Site of Europolis. Archaeological Prospection 12, 79-91, 2005.
- [8]. Leucci, G., Greco, F., Giorgi, L. D., Mauceri, R., Three-dimensional image of seismic refraction tomography and electrical resistivity tomography survey in the castle of Occhiola' (Sicily, Italy). Journal of Archaeological Science 34, 233-242. 2007.
- [9]. Ekinici, Y. L., Balkaya, Ç., Aysel, Ş., Kaya, M, A., Lightfoot, C. S., Geomagnetic and geoelectrical prospection for buried archaeological remains on the Upper City of

Amorium, a Byzantine city in midwestern Turkey. *Journal of Geophysics and Engineering* 11, 015012, 2014.

[10]. Loke, M. H., Tutorial: 2-D and 3-D Electrical Imaging Surveys, 2015. www.geoelectrical.com, Erişim Tarihi : 14.04.2015.

[11]. Loke, M. H., Acworth, I., Dahlin, T., A comparison of smooth and blocky inversion methods in 2D electrical imaging surveys. *Exploration Geophysics* 34, 182-187, 2003.

[12]. Drahor, M. G., Berge, M. A., Kurtulmuş, T. Ö., Hartman, M., Spediel, M. A., Magnetic and Electrical Resistivity Tomography Investigations in a Roman Legionary Camp Site (Legio IV Scythica) in Zeugma, Southeastern Anatolia, Turkey. *Archaeological Prospection* 15, 159-186, 2008.

[13]. De Domenico, D., Giannino, F., Leucci, G., Bottari, C., Integrated geophysical surveys at the archaeological site of Tindari (Sicily, Italy). *Journal of Archaeological Science* 33, 961-970, 2006.

[14]. Batayneh, A., Khataibeh, J., Alrshdan, H., Tobasi, U., Aljahed, N., The Use of Microgravity, Magnetometry and Resistivity Surveys for the Characterization and Preservation of an Archaeological Site at Umm er- Rasas, Jordan, *Archaeological Prospection*, Vol. 14, p. 60-70, 2007.

[15]. Tsokas, G. N., Tsourlos, P. I., Vargemezis, G., Novack, M., Non- destructive Electrical Resistivity Tomography for Indoor Investigation: the Case of Kapnikarea Church in Athens, *Archaeological Prospection* Vol.15, p. 47-61, 2008.

[16]. Tsokas, G. N., Stampolidis, A., Mertzaniadis, I., Tsourlos, P. I., Hamza, R., Chrisafis, C., Ambonis, D., Tavlakis, I., Geophysical Exploration in the Church of Protaton at Karyes of Mount Athos (Holy Mountain) in Northern Greece, *Archaeological Prospection*, Vol.14, p. 75-86, 2007.

[17]. Perez-Gracia, V., Garcia, F., Pujades, L. G., Drigo, R. G., Capua, D., GPR Survey to Study the restoration of a Roman monument, *Journal of Cultural Heritage* 9, 89-96, 2008.

[18]. [Gaffney, C., Goodchild, H., Harrison, S., Geophysical and Topographical Survey of the Theatre at Ancient Sparta. *Birmingham Archaeology Report*, PN 1643, 2007.

[19]. Aubry, L., Benech, C., Marmet, E., Hesse, A., Recent achievements and trends of research for geophysical prospection of archaeological sites. *Journal of Radioanalytical and Nuclear Chemistry* 247, 621-628, 2001.

[20]. Bean, G. E., "Alabanda", *Princeton Encyclopedia of Classical Sites*, 1976.

[21]. Cohen, G. M., *The Hellenistic Settlements in Europe, the Islands, and Asia Minor*, University of California Press, 1996.

[22]. Berge, M. A., Elektrik Özdirenç Ters-Çözümüyle Çok Katmanlı Arkeolojik Yerleşmelerin Görüntülendirilmesi. Dokuz Eylül Üniversitesi, Fen Bilimleri Enstitüsü, Doktora Tezi, İzmir, 2011.

[23]. Berge, M. A., İki-Boyutlu Özdirenç Ters Çözüm Modellemesi. Dokuz Eylül Üniversitesi, Fen Bilimleri Enstitüsü, Yüksek Lisans Tezi, İzmir, 2005.

[24]. Dey, A., Morrison, H. F., Resistivity modeling for arbitrarily shaped two dimensional structures. *Geophysical Prospecting*, 27, 106-136, 1979a.

[25]. Dey, A., Morrison, H. F., Resistivity modeling for arbitrarily shaped three-dimensional structures. *Geophysics*, 44, 753-780, 1979b.

[26]. Silvester P.P., Ferrari R.L., *Finite elements for electrical engineers* (2nd. ed.). Cambridge University Press, 1990.

-
- [27]. Başokur, A. T., Düşey Elektrik Sondajı Verilerinin Yorumu, Ankara Üniversitesi, Mühendislik Fakültesi, Jeofizik Mühendisliği Ders Notları, Ankara, 2004.
- [28]. Jackson, D. D., Interpretation of inaccurate, insufficient and inconsistent data. Geophys. J. Roy. Astr. Soc., 28, 97-109, 1972.
- [29]. Karaaslan, H., Alabanda Antik Kenti Meclis binası içindeki gömülü yapıların elektrik yöntemle araştırılması / Investigation of structures in the Alabanda Bouleuterion by electrical resistivity method, Yüksek lisans Tezi, Sakarya 2015.
- [30]. Tavukçu, A. Y., Temür, A., Tavukçu, Z. A., Ceylan, M., Coşkun, S., Eker, K. 2018. ALABANDA 2017. Kazı Sonuçları Toplantısı., 40: 147-161.
- [31]. Candan, O., Dora, O. Ö., Oberhanslı, R., Koralay, E., Çetinkaplan, M., Akal, C., Satır, M., Chen, F., Kaya, O. 2011. Menderes Masifi'nin Pan-Afrikan Temelin Stratigrafisi ve Gondvana'nın Geç Neoproterozoyik/Kambriyen Evrimi ile İlişkisi. MTA Dergisi., 141: 25-68.
- [32]. Demirbaş, E. 2010. Kavşit (Çine-Aydın) Yöresinin Jeolojisi ve Feldispat Yataklarının İncelenmesi. Selçuk Üniversitesi, Fen Bilimleri Enstitüsü, Jeoloji Mühendisliği Bölümü, Yüksek Lisans Tezi.
-

APPLICATION OF REMOTE SENSING METHODS TO GROUND RESEARCH

UZAKTAN ALGILAMA YÖNTEMLERİNİN YER ARAŞTIRMALARINA
UYGULANMASI**Fazlı Ahmet Zengin**Sakarya Üniversitesi, Mühendislik Fakültesi, Jeofizik Mühendisliği Bölümü,
0000-0003-0068-1451**Günay Beyhan**Sakarya Üniversitesi, Mühendislik Fakültesi, Jeofizik Mühendisliği Bölümü,
0000-0003-1341-9049**Suat Demir**Sakarya Üniversitesi, Mühendislik Fakültesi, Jeofizik Mühendisliği Bölümü,
0000-0003-01031-5463

Özet

Uzaktan algılama, fiziksel bir temas olmaksızın gözlenen cisimden bilgi elde edilmesidir. Atmosferde veya uzayda hava araçları üzerinde bulunan algılayıcılar sayesinde yerdeki cisimler hakkında bilgi sahibi oluruz. Dünya genelinde maden arama çalışmalarında kullanılan uzaktan algılama teknikleri, madencilik yanında jeoloji, meteoroloji, tarım, coğrafi bilgi, oşinografi, çevre, haritacılık ve askeri amaçlı çalışmalar gibi farklı alanlarda yoğun olarak kullanılmaktadır. Uzaktan algılama yöntemiyle elde edilen görüntüler, maden arama çalışmalarında mineralizasyonun oluşma olasılığının fazla olduğu fay, çatlak ve kırıkların haritalanmasında minerallerin spektrum değerlerinden yararlanarak mineral zenginleşmesine sahip kayaların belirlenmesinde kullanılır.

İnceleme alanında hematit, kireçtaşı, grafit, grafit-şist, limonit ve killi- killi kumlu birimler gözlenmektedir. Sahada ekonomik değer taşıyan Hematit ve Grafit cevherleşmesi görülmektedir. Söz konusu cevherler yer yer çevre kayalarla ve faylarla sınırlandırılmaktadırlar. Cevherleşmenin bulunduğu faylar yüzeye yakın sığ faylardır. Yüzeydeki bütün kireçtaşlarının kataklastik parçalanmasının nedeni faylardır. Bu faylanmaların yeryüzüne ulaşmasına uygun zayıf ortamları oluştururlar. Çalışma sahasındaki ikincil ve üçüncül faylanmalar cevher içermektedir

Abstract

Remote sensing is the acquisition of information from the observed object without physical contact. Thanks to the sensors on the air vehicles in the atmosphere or in space, we have information about the objects on the ground. Remote sensing techniques, which are used in mineral exploration studies around the world, are used extensively in different fields such as geology, meteorology, agriculture, geographical information, oceanography, environment, cartography and military purposes as well as mining. The images obtained by remote sensing method are used to identify the rocks with mineral enrichment by making use of the spectral values of the minerals in the mapping of faults, cracks and fractures where mineralization is likely to occur in mineral exploration studies.

This study was carried out in Hendek district of Sakarya province. Hematite, limestone, graphite, graphite-schist, limonite and argillaceous sandy units are distinguished in the study area. Hematite and Graphite mineralization, which has economic value, is observed in the field. The ores in

question are limited in places by the surrounding rocks and faults. These secondary faults distributed in an elliptical manner caused tertiary faults in directions that make 60/120 degree angles to themselves. The first of these faults is compression regime (compressional character), the second and third of these faults are tension regime (dilatational character). At the same time, the tertiary faults are shallow. Tertiary faults are the cause of cataclastic disintegration of all limestones on the surface. These tertiary faults form weak environments suitable for reaching the earth's surface. Secondary and tertiary faults in our study area contain ore.

Keywords: Remote Sensing, Mining, Band Ratio, Mineralization, Spectral Analysis

1. GİRİŞ

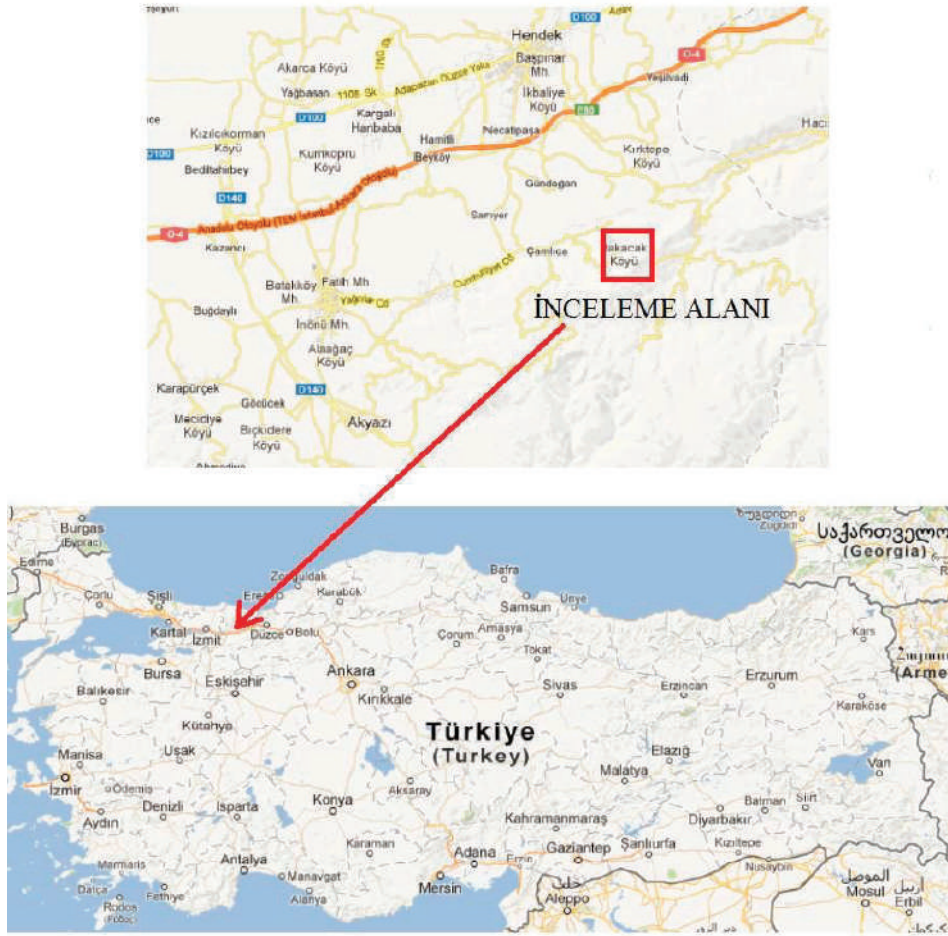
Gelişen toplumların hammadde tedariğini karşılamak için kullanılan fakat kısıtlı bir şekilde bulunan doğal kaynakların araştırılmasında, etkin yöntemler kullanarak teknolojinin doğru kullanılmasıyla birlikte bilgiye ve sonuca yüksek hızda ve kısa zamanda ulaşmak son derece önemli bir durum haline gelmiştir. Yer altında ve yer üstünde bulunan doğal kaynakların mevcut varlıklarının durumu ve potansiyellerinin belirlenmesi, geçen süre zarfında değişimlerinin izlenmesi, güncel durumlarının amacıyla yapılacak olan çalışmalarda, uzaktan algılama yöntemlerinden yararlanılması doğru, hızlı ve düşük maliyetli verilerin elde edilmesini sağlayacaktır. Uzaktan algılama yöntemleri cisimlerle direkt temas etmeden fiziksel özellikleri hakkında bilgi elde etme bilimi olarak tanımlanmaktadır. Uzaktan algılama yöntemi ile yeryüzünün farklı mekansal, spektral, radyometrik ve zamansal çözünürlüklerde görüntülenmesi ve izlenmesi mümkün olabilmektedir. Zamansal çözünürlük özellikle arazi örtüsü/kullanımında meydana gelen değişimlerin tespit edilmesi ve sürdürülebilir çevre çalışmaları açısından önem kazanmaktadır. Uydulardan alınan görüntüler farklı amaçlarla kullanılabilmekte ve aynı bölgede farklı çalışmaların birlikte yapılabilmesine olanak sağlamaktadır. Yeryüzünün düzenli olarak izlenmesi, kontrolü ve ulaşımı zor coğrafi bölgelerde çalışabilme imkânı, hızlı ve ekonomik olması uzaktan algılama teknolojisinin önemli avantajları olarak öne çıkmaktadır.

Madenlerin çoğu jeolojik birimler veya yapılar gibi yeryüzünde gözlenmezler. Bu sebepten madenlerin bulunmaları masraflı ve zor arazi şartlarındaki çalışmalar sonucunda mümkün olabilmektedir. Hedef madenlerin özelliklerine bağlı olarak uydu görüntüleri kullanılması sonucunda detay inceleme yapılarak araştırma sahanın daraltılması veya maden varlığının yüksek potansiyele sahip sahaların direk tespiti ile arama aşaması optimum zaman –maliyet ve yüksek başarı oranı ile tamamlanabilir.

Uzaktan algılama ile maden aramada;

- Yüzeyde mostra vermiş olan madenlerin tespiti
- Ana madenin tespitine yarayan alterasyon tiplerinin belirlenmesi
- Cevherleşmeye işaret eden bitkilerdeki anomalilerinin tespiti
- Yüzeylenen jeolojik yapıların tespiti
- Cevherleşmeye sahip litolojilerin belirlenmesi gibi yöntemler kullanılmaktadır.

Tespiti yapılmak istenen maden cevherleşmesine bağlı olarak bu yöntemlerin tamamının araştırılabileceği gibi genellikle en sık kullanılan yöntem maden cevherleşmesinin tespitine yarayan alterasyonların tespitidir.



Şekil 1. İnceleme alanı yer bulduru haritası
Figure 1. Location map of the review area

2. MATERYAL VE YÖNTEMLER

İnceleme alanında araştırılıp çıkarılan madenlerin konumları belirlenmiş, MTA tarafından hazırlanmış olan bölgenin jeoloji haritası sayısallaştırılarak sayısal yükseklik modeli elde edilmiş olup ile madenlerin jeoloji ve topoğrafya ile ilişkileri, stratigrafik seviyeleri gibi bilgiler elde edilmiştir. Uzaktan algılama çalışmalarında ArcMap, TntMips, Google Earth programları ile inceleme alanını kapsayan, Amerikan Jeolojik Araştırma Kurumu'ndan (USGS) alınan, 178-32 hat-sıra numaralı, 08.09.2021 tarihli, UTM projeksiyonlu, WGS 84 datumlu Landsat-8 uydu görüntüsü kullanılmıştır. Uydu görüntüleri atmosferdeki şartlar, güneş ışınların geliş açısı ve verilerin kaydı aşamasında gözlenebilen sistematik hatalar nedeniyle sistematik olan veya olmayan bir takım hatalar içerir. Landsat 8, görüntüler kaydedilirken geometrik ve radyometrik düzeltmeleri yapabilen teknik donanıma sahip bir uydudur. Uydu görüntülerinin kaydı esnasında sensörler araziden yayılan enerjiyi analog olarak algılar ve verilerin kaydı esnasında sahanın gerçek yansıma değerlerine göre bir takım sayısal değerlere dönüştürülerek kaydedilir. Bu nedenle çalışılacak sahadaki nesnelerin gerçek yansıma değerlerinin elde edilebilmesi amacıyla görüntü düzeltme (dönüştürme) işlemi gerçekleştirilir. Çalışma kapsamında Landsat 8 uydu görüntüsünün

yansıma değerleri elde edildikten sonra band oranlama, band aritmetiği, renkli kompozit görüntülerin oluşturulması gibi uzaktan algılama teknikleri kullanılmıştır.

3. SONUÇLAR VE TARTIŞMA

İşletme sahasında ölçülen doğrultuya dik yönde olmak üzere sahada 5m x 5m kareli olarak, yaklaşık 110m x 70m' lik bir alanda sistematik iki boyutlu Doğal Uçlaşma (Self Potential) ve Magnetik arama ölçümleri (prospeksiyon) uygulanmıştır. Daha sonra cevherleşme ve çevre kayaç ilişkisini, yapısal unsurları ve geometrisini ortaya koyabilmek için 12 profilde 2 Boyutlu Öz direnç ile 3 noktada 1 Boyutlu öz direnç (Schlumberger) ölçümleri de alınmıştır.(Şekil 2, Figure 2)

Uygulanan jeofizik yöntemler, arazi gözlemleri, açılan araştırma çukurları değerlendirildiğinde:

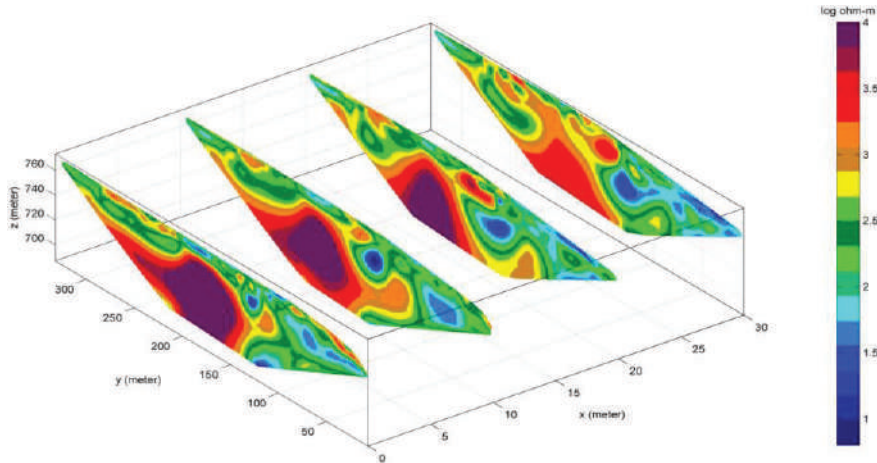
- İnceleme alanında hematit, kireçtaşı, grafit, grafit-şist, limonit ve killi- killi kumlu birimler gözlenmektedir.

- Sahada ekonomik değer taşıyan Hematit ve Grafit cevherleşmesi görülmektedir. Söz konusu

cevherler yer yer çevre kayaçlarla ve faylarla sınırlandırılmaktadırlar.

- Maden sahası açık işletme olarak üretim yapmaktadır. Şu ana kadar yaklaşık 15.000 ton blok (hematit + kireçtaşı) cevheri çıkarılmıştır.

- Eliptik bir şekilde dağılan bu ikincil faylar kendilerine 60/120 derecelik açılar yapan doğrultularda üçüncül faylanmalara neden olmuştur. Birincisi sıkıştırma rejimi (kompresyonel karakterli) olan bu fayların ikincisi ve üçüncüsü gerilim rejimi (dilatasyonel karakterli)' dir. Aynı zamanda üçüncül sıradaki faylar sıgıdır. Yüzeydeki bütün kireçtaşlarının kataklastik parçalanmasının nedeni üçüncül faylardır. İşte bu üçüncül faylanmaların yeryüzüne ulaşmasına uygun zayıf ortamları oluştururlar. Çalışma sahamızdaki ikincil ve üçüncül faylanmalar cevher içermektedir.
- Bölge genelinde cevherleşmenin büyük bir çoğunluğu tektonik yapılar boyunca yerleşmiştir.



Şekil 2. Rezistivite ölçü profillerinin blok diyagramı

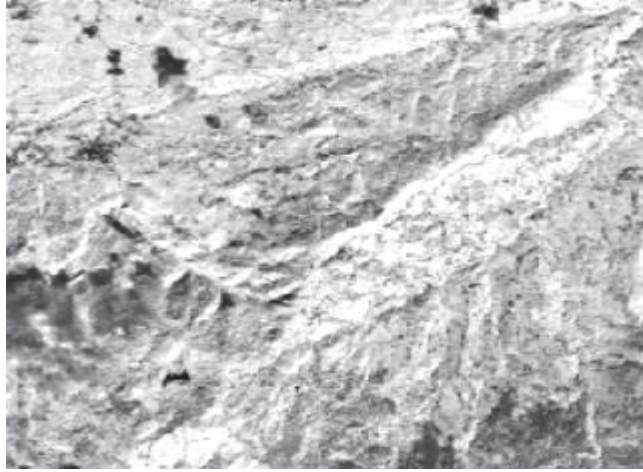
Figure 2. Resistivity Representation of measurement profiles in the form of a block diagram

Çalışma alanındaki cevherleşmelerin mineral birlikteliklerinin incelenmesi sonucunda hepsinin demirli mineraller (manyetit, limonit) içermesi ve hepsinde hidrotermal alterasyonun gözlenmesi sebebiyle literatürde alterasyon ve demirli minerallerin tespitinde yaygın olarak kullanılan;

- Kil mineralleri ve demir içeren minerallerin tespiti için 6/7 band oranı (Şekil 3/Figure 3, [1])

- Demirli minerallerin tespitine olanak tanıyan yöntemler;
 - 4/5 band oranı (Şekil 4/Figure 4, [1])
 - 5/4 band oranı (Şekil 5/Figure 5, [1])
 - R(4/2) G (5/4) B (5/7) renkli kompozit görüntü (Şekil 6/Figure 6, [2]) kompozit görüntü (Şekil 6, [2]) uzaktan algılama teknikleri kullanılmıştır.

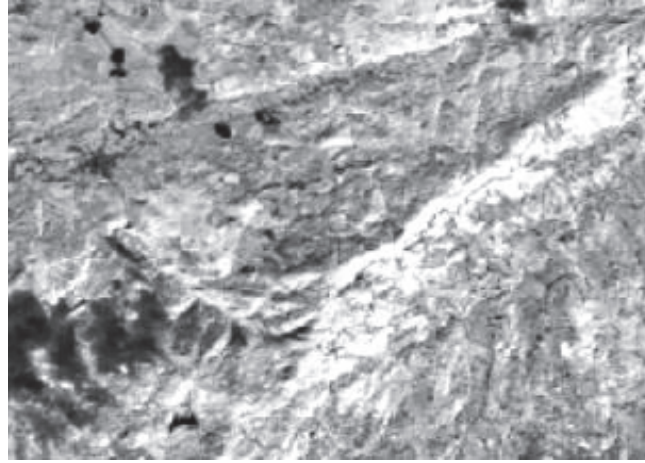
Uzaktan algılamada kullanılan band oranları iki farklı enerji aralığı kaydını içeren bandın matematiksel olarak oranlaması olduğundan elde edilen görüntü siyah-beyaz renklidir. Oranlanan bantların enerjileri ve belirlenmek istenilen mineralin bu enerjilere tepkisine bağlı olarak elde edilen görüntülerde sonuç kimi zaman açık kimi zaman koyu renklerle ifade edilir. 6/7 band oranı kil mineralleri ve demir oksitlerin tespiti için kullanılır ve koyu alanlar kil minerallerini işaret etmektedir (Şekil 3). 4/5 ve 5/4 band oranları demir tespiti için kullanılan bir oran olup, elde edilen görüntülerde 4/5'deki beyaz (Şekil 4), 5/4'deki siyah (Şekil 5) renkler demirli alanları işaret etmektedir (Bersi, 2016).



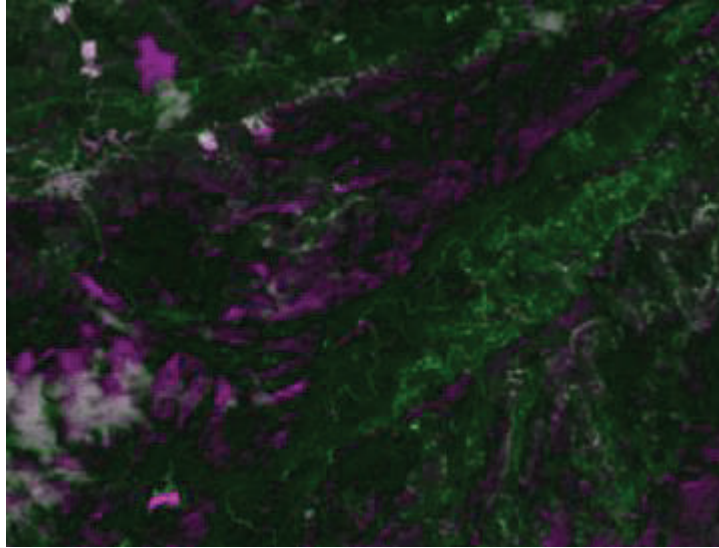
Şekil 3. Kil mineralleri ve demir içeren minerallerin tespiti için 6/7 band oranı
Figure 3. 6/7 band ratio for the content of clay minerals and iron-containing minerals



Şekil 4. Demirli minerallerin tespitini sağlayan bant oranları(4/5)
Figure 4. Band ratios enabling the detection of ferrous minerals(4/5)



Şekil 5. Demirli minerallerin tespitini sağlayan bant oranları(5/4)
Figure 5. Band ratios enabling the detection of ferrous minerals(4/5)



Şekil 6. Renkli Kompozit Görüntü
Figure 6. Color composite image

4. SONUÇLAR

İnceleme alanında yapılan önceki arazi çalışmalardan derlenen bilgilerin yorumlanması ve yapılan uzaktan algılama çalışmalarında elde edilen sonuç bölgenin maden potansiyeli bakımından bir diğer göstergesidir. Cevher ve/veya alterasyon oluşumunu işaret eden demirli mineraller ile kil minerallerinin tespiti amacıyla band oranları (6/7, 4/5, 5/4), (6/5)*(4/5) ile renkli kompozit görüntüler (4/2 5/4 5/7; 4/2 5/7 4/5; 4/2 5/7 5/4) oluşturulmuştur. Yapılan uzaktan algılama teknikleri ile elde edilen görüntülerin değerlerinin yorumlanması sonucunda mevcut yatakların konumları başarılı bir şekilde belirlenmiştir.

Jeolojik ve jeofizik olarak önceden çalışması yapılmış arazi çalışmasına ek olarak yapılan bu çalışma, arazi çalışmaları ve jeolojik gözlemler açısından zorlu coğrafik koşullara sahip sahaların uzaktan algılama yöntemlerinin kullanılarak maden sahalarının ve/veya potansiyel alanların belirlenmesi ile sonraki çalışmalara yön vermesi, yapılacak çalışmaların ilk başlarda belirlenen bölgelere göre planlanması sonucunda vakit ve maddi kazanç sağlaması açısından önemli olduğunu göstermiştir.

TEŞEKKÜRLER

Yapılan çalışmalar sırasında yardım sağlayan (makaleyi okuma, yazma, dil yardımı vb.)e Güney Beyhan Hocam'a Suat Demir 'e görüş ve katkıları için teşekkürlerimi sunarım.

REFERENCES

- [1].Bersi, M. Saibi, H. and Chabou, M. C. (2016). Aerogravity and remote sensing observations of an iron deposit in Gara Djebilet, southwestern Algeria. *Journal of African Earth Sciences*, 116, 134-150.
- [2].Salem, S. M. and El Gammal, E. A. (2015). Iron ore prospection East Aswan, Egypt, using remote sensing techniques. *Ore Geology Reviews*, 18, 195–206S. Zhang, C. Zhu, J. K. O. Sin, and P. K. T. Mok, “A novel ultrathin elevated channel low-temperature poly-Si TFT,” *IEEE Electron Device Lett.*, vol. 20, pp. 569–571, Nov. 1999.
- [3].Sabins, F. F. (1999). Remote sensing for mineral exploration. *Ore Geology Reviews*, 14, 157–183R. E. Sorace, V. S. Reinhardt, and S. A. Vaughn, “High-speed digital-to-RF converter,” U.S. Patent 5 668 842, Sep. 16, 1997.
- [4].Sultan, M. Arvidson, R. E. and Sturchio, N. C. (1986). Mapping of serpentinites in the Desert of Egypt using Landsat Thematic Mapper data. *Geology*, 14, 995–999. [https://doi.org/10.1130/0091-7613\(1986\)14%3C995:MOSITE%3E2.0.CO;2](https://doi.org/10.1130/0091-7613(1986)14%3C995:MOSITE%3E2.0.CO;2)FLEXChip Signal Processor (MC68175/D), Motorola, 1996.

ABOUT THE NATURE OF THE ENVIRONMENTAL REQUIREMENTS

Assoc. prof. M. As. Michailov

PhD – SWU “Neofit Rilski” - Bulgaria

Abstract

It is difficult to find a definition of "environmental requirements" in the literature. This phrase is used in practice, but it is not easy to explain. Definitions of the science "ecology" are usually used for this purpose, thus avoiding an answer to its essence. It can also be expressed through "requirements" for the "environmental friendliness" of something (or an object), but we still can't get a definition.

Due to the increasing and frequent use of this phrase, an attempt will be made here to create a definition through which to interpret and help in its use in practice.

It is proposed to express through "environmental requirements" the interaction of the two main factors (abiotic and biotic), the claims for their manifestation and their impact on life on Earth. The formation of a third group of environmental factors, etc. anthropogenic factors do not contribute to the interpretation and explanation of the Earth's processes. Through them an attempt is made to scientifically substantiate the actions of Man, but their essence is related to the satisfaction of his needs.

In view of the above, a more specific classification is proposed for the so-called "environmental requirements". First, it is necessary to distinguish between the different formulations for this type of concepts. Therefore, it is proposed to distinguish two groups of environmental requirements - one "naturally-conditioned" and the other "administrative-regulatory".

The difference between them is quite significant, because the first group combines requirements related to the implementation of various actions arising from the nature of different organisms to the environment in which they grow; while the second group systematizes the various (administratively created) normative documents through which to regulate the actions (and their consequences) of the Society related to impact on the Nature.

The presented research is the result of a very detailed study of the experience in different countries and world organizations on this topic. It should be noted that in most of the publications (including scientific ones) the emphasis is on the administrative-regulatory functions of this type of requirements. It seems that the essence of "environmental requirements" is in the regulation of administrative restrictions, which is wrong. An example is the number of normative documents for assessing the impact of various human activities on nature. Such assessments are allowed, but with a "significant impact" for which there is no definition.

From this position it is important to conduct research for a more correct study and use of terminology in the field of environment.

FLIGHT SAFETY RISK ANALYSIS AT AIRPORTS: THE CASE OF SAMSUN ÇARŞAMBA AIRPORT

Ömer Faruk UZUN

Sinop University, Department of Architecture and Urban Planning, Boyabat Vocational School, 57200, Sinop, Turkey
<https://orcid.org/0000-0002-0391-4495>

Faik Ahmet SESLİ

Ondokuz Mayıs University, Faculty of Engineering, Geomatic Engineering, 55270, Samsun, Turkey
<https://orcid.org/0000-0001-8352-734X>

ABSTRACT

Depending on the rapid population growth and advances in technology around the world, there is an increasing acceleration in transportation density with the developments in transportation vehicles. For this reason, it is quite natural for people to prefer vehicles that will transport them quickly, economically and safely. Air transportation is increasing its share in the transportation sector day by day with the advantages it has at this point, and the increase in the density of people moving in parallel with this share increase is inevitable. Although air transport is safer than other modes of transport, each flight also carries the potential for an accident. Also, if it happens, the death rate in accidents is very high. In this context, it is important to manage the airports and the surrounding areas where the most complex operations take place in the provision of flight operations. The criteria determined by the International Civil Aviation Organization (ICAO) will guide the management of the mentioned areas. In this study, an analysis method was created to measure the safety of airports by combining the criteria that ICAO has mentioned so far regarding the management of the areas around the airports. This analysis method, it was applied to Samsun Çarşamba Airport. The mentioned airport has been examined in 5 items in the flight safety risk analysis: 1- Facilities where people can be found collectively in the risk area around the airport, 2- Facilities where flammable and explosive products are sold in the risky area on the airport's landing-departure corridor, 3-High architectural structures within the risky area boundaries of airports, 4-Factors that may have a negative impact on pilots' vision, 5-Waste / Garbage facilities in the designated risky area around the airport. At the end of these 5 items examined, the airport received a risk score of 17,5. With the analysis method created, an airport in any part of the world will be objectively measurable in terms of flight safety and it will be easier to eliminate the risk factors.

Keywords: Flight safety, Risk analysis, Land management, Disaster management

1.INTRODUCTION

Due to the rapid population growth around the world, developments in transportation vehicles and advances in technology, there is an increasing acceleration in transportation density (Okumuş and Asil, 2007; Hatipoğlu and Işık, 2015; Erol and Kanbur, 2017). The increase in human mobility leads to a decrease in transportation costs, which in turn leads to changes in the preferences of the vehicles used in transportation (Rothkoph and Wald, 2008; Yaylalı and Dilek, 2009). For these reasons, it is quite normal for people to prefer vehicles that will

transport them quickly, economically and safely. Air transportation is increasing its share in the transportation sector day by day with the advantages it has at this point, and with this increase in share, the increase in human density is inevitable. It is clear that this intensity will increase the number of voyages. Although air transportation is safer than other modes of transportation, each flight also carries the potential for an accident. For this reason, it is of great importance to minimize the risks of these accidents, as in all kinds of transportation. In this context, it is important to manage the airports and the surrounding areas where the most complex operations take place in the provision of flight operations. The criteria determined by the International Civil Aviation Organization (ICAO) will guide the management of the mentioned areas. In this study, an analysis method was created to measure the safety of airports by combining the criteria that ICAO has mentioned so far regarding the management of the areas around the airports. Within the framework of the study, Samsun Çarşamba Airport in Turkey has been examined with this developed analysis method. The airport, which was built within the borders of Çarşamba district of Samsun in 1998 (DHMI, 2018), contributes to the economic, social and cultural development of the city with passenger and cargo transportation activities with an increasing momentum (Akgüngör and Demirel, 2004). Samsun province, which is located in the middle of the Black Sea Region, has become a regional center in terms of transportation and transportation when the advantage of population and workforce is added (Zeybek, 2006). This development at Çarşamba airport has had statistics that can be considered important on a world scale (Efendigil and Eminler, 2017; Doğan and Dikmen, 2018). According to the Turkish State Airports Authority (DHMI) data, 13930 passenger, commercial, freight and cargo flights were carried out at Samsun Çarşamba Airport in 2018, and the number of passengers carried exceeded 1 million. (Anonymous, 2018a). With the analysis method created, an airport in any part of the world will be objectively measurable in terms of flight safety and it will be easier to eliminate the risk factors.

2. Material and Method

2.1 Workspace

The field that constitutes the subject of the study; (41°18'13.0") north parallels (36°37'07.9") east meridians, (41°13'14.4") north parallels, (36°37'42.8") east meridians, (41°12'55.7") north parallels (36°30'55.8") east meridians and (41°17'51.6") north parallels are between geographic coordinate points located between (36°30'07.7") east meridians.

Samsun Çarşamba Airport, which is located on (41°15'56") North parallels and (36°32'55") East meridians and serves in civil status, is located in Çınarlık town of Çarşamba town in Samsun province, 25 km from the city center. . The facility, which started to be built on an area of 3.940.000 m² as of 1996, was equipped with technological systems that can land all kinds of aircraft even in rain and foggy weather, and opened to scheduled domestic and non-scheduled international air traffic for 24 hours on 15.12.1998. Currently, scheduled international flights are also available at the airport. The airport was accepted as an air border gate with the decision of the Council of Ministers dated 22.06.2000 and numbered 2000/918. Since the width of the taxiways at the airport is 24 m, the airport reference code is in category 4E (denotes aircraft that can land according to the wingspan), and when evaluated together with the shoulders, it is 39 m in total.

2.2 Technical Equipment Used in the Studies

Within the scope of the study, DJI Ryze branded drone, which is used to detect potential objects that may adversely affect the pilot's vision, Atlas ATML 60 branded laser meter, which is used for height measurements, Leica Viva GS10 GPS, which determines the coordinates of objects, and Nikon D5300 camera equipment, which is used to obtain images, were used. With reference to the "Turkish Civil Aviation General Directorate" (SHGM) "Havaalanı Hizmetleri El Kitabı" (Airport Services Handbook) (SHGM, 2007) created on the

basis of ICAO Annex-14, the height measurement processes of the elements that may violate the altitude criteria were carried out with a laser meter in the study area (Figure 1).



Figure 1. Height measurements in the study area

Objects that may adversely affect the vision of the pilots around the airports were determined. Firstly, the reflectivity properties of potential objects that may adversely affect the vision of the pilots in the study area in the Google Earth application of Google Labs were examined on the software. Afterwards, observation studies were carried out by climbing over the water reservoir of Sıtmasuyu Neighbourhood, which is a point that fully dominates the study area, and finally, a detailed scanning study was carried out with a drone by going to the study area (Figure 2).

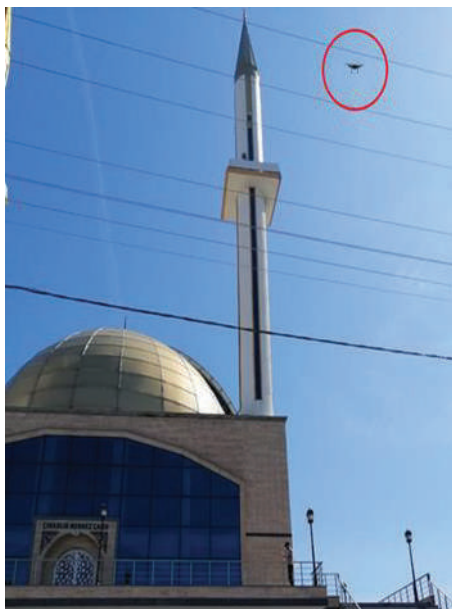


Figure 2. Reflective surface observation with drone in the study area

The distances of the areas where people are gathered together to the runway heads and the flammable and explosive facilities in the landing-departure corridor and its surroundings comply with the SHGM's "Construction Criteria around the Airport" by "Euclidean Distance" analysis under the distance analyzes tab in the Spatial Analyst Tools section of the ArcMap module of the ArcGIS software. The locations of these facilities were verified by going to the

study area. The suitability of the existence of Waste / Garbage Facilities that may cause mass bird movements around the airport according to the "Wild Animal Control and Reduction" manual of SHGM at the Airports was determined by the "Euclidean Distance" analysis under the distance analyzes tab in the Spatial Analyst Tools section of the ArcMap module of the ArcGIS software. The data obtained in the field were confirmed (Figure 3).

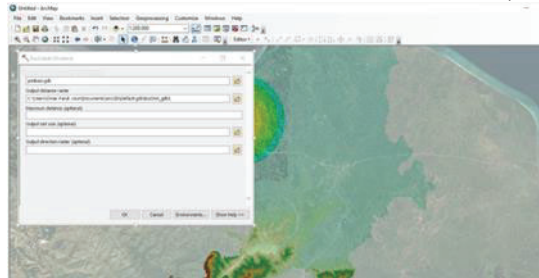


Figure 3. Calculations of the distances of the parameters to the reference points

The risk scores used in the "Flight Safety Risk Analysis" (UGRA) developed within the scope of the study express the probability of causing a flight accident, and high rates of loss of life and property in case of an accident. In the process of creating these risk scores, domestic and foreign; scientific studies, local government projects and news of media organs were used. As a result of the researches and investigations: Facilities where people can be found collectively in the risk area around the airport received 1 point, Facilities where flammable and explosive products are sold in the risky area on the airport's landing-departure corridor, as understood from the job descriptions received 1.5 points, High architectural structures within the risky area boundaries of airports received 2 points, Factors That May Have a Negative Impact on Pilots' Vision received 0.5 point, Waste / Garbage Facilities in the designated risky area around the airport received 3 points.

3. RESULTS AND DISCUSSION

The findings obtained in the studies carried out within the scope of the research and the relations of these findings with previous scientific studies and legal regulations are given below according to their subjects.

3.1. Investigation of Architectural and Other Structures in terms of Height

As Ulubay and Varol (2013) stated, high architectural structures within the risk limits of airports pose a potential accident hazard for both aircraft and people living in these structures, especially during take-off and landing of aircraft. By ICAO, the maximum height is limited to 45 meters in a radius of 3 km, taking the flight runway as its center (Anonymous, 2018b).

In the research carried out within the scope of the study, height measurements of energy transmission lines, structures, trees, etc. were made with laser meters in the area determined by the ArcGIS program (Figure 4), where the conical surface, which is the outermost line of the obstacle limitation surfaces, is located. In these measurements, the minaret of the Çınarlık Merkez Mosque, with a maximum height of 34 meters and a distance of 1003 meters from the center of the runway, was determined. According to these values, there is no threat that poses a risk to flight safety in terms of altitude. In terms of the sustainability of this situation, it is very important to keep the urban development process in the region under control.

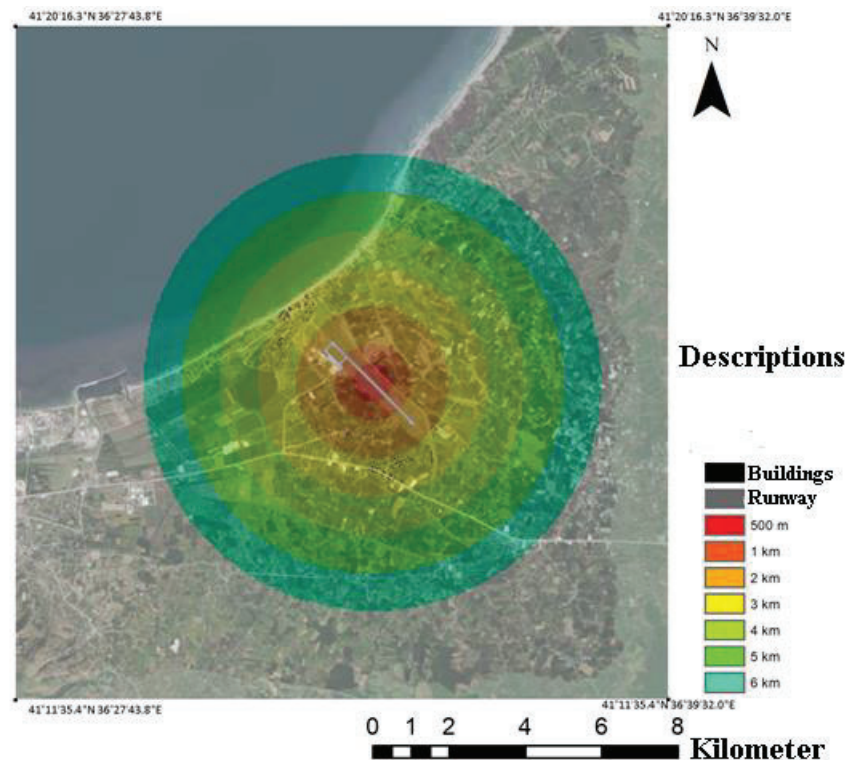


Figure 4. Area where height measurements are made

3.2. Identification of Factors That May Have a Negative Effect on Pilots's Vision

Today, the cause of accidents in aviation accidents is mostly human error (Kılıç, 2017; Uysal and Dokuman, 2017). It is stated that about one third of the factors that cause flight accidents are pilot error (SHY-13, 1992; Yüksel et al., 2006; Yavuz et al., 2015, Birgören, 2015) reported that 72 of 75 plane crashes between 1988 and 1990 were caused by pilot error, and one of the most important causes of pilot error was "distraction". For this reason, there should be no reflective and bright objects in the vicinity of the airports that will adversely affect the attention and vision of the pilots.

In the examinations made in the field, it has been determined that roof, facade cladding or similar materials that can reflect light at a high rate within the active field of view of the pilots are not used. The continuation of this situation is very important in preventing piloting errors, which are shown as the biggest cause of flight accidents.

3.3. The Distances of the Areas Where People Are Collected to the Runway Heads

In the study, 2 schools were identified that violated the rule stated in the Circular of SHGM (2012) on "Construction Criteria Around the Airport", that the settlements where people are gathered together should not be within 3000 meters of the runway head (Figure 5). It has been determined that Çınarlık Yalı Primary School and Çınarlık Primary School are at a distance of 978 m and 2080 m, respectively, from the start of the runway.

While Çınarlık Yalı Primary School has a total population of 56 including teachers and students, Çınarlık Primary School has a total population of 129 people (Anonymous, 2020a; Anonymous, 2020b). In the event that an air accident hits the areas where the schools are located, it is highly likely that the loss of life will be at very sad levels. For this reason, taking these schools out of the risk area is of vital importance in order to keep the losses to a minimum.

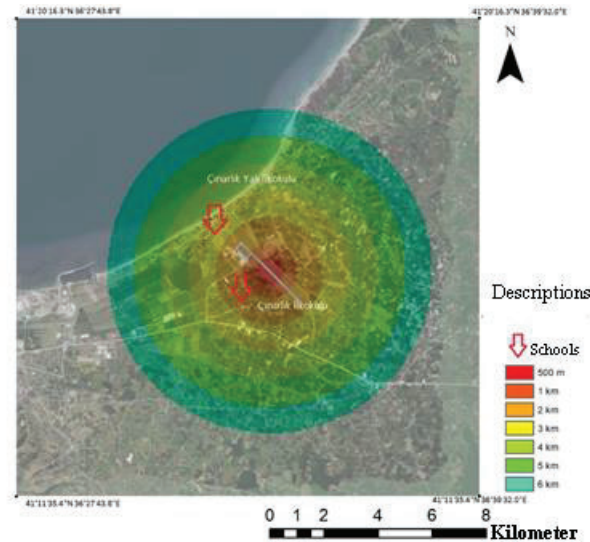


Figure 5. Schools around the airport

In the study, 8 mosques (Camii) violating the same circular were also detected (Figure 6). Çınarlık Köyü Mosque, Şehit Polis Tuncay Karataş Mosque, Eğerceli Merkez Mosque, Irmak Sırtı Köyü Köprü Başı Mosque, Sarı Kadı Mosque, Irmak Sırtı Köyü Merkez Mosque, Karakulak Mahallesi Mosque and Kurtuluş Mosques are respectively from the start of the runway. It was determined that they were at a distance of 1003 m, 2871 m, 1667, 1922 m, 2372 m, 2576 m, 2724 m, 1274 m. Like schools located in a risky area, places of worship are also buildings where people live together. It is clear that an air accident that may occur during worship will bring very serious consequences. For this reason, it is extremely important that places of worship are excluded from the risky area.

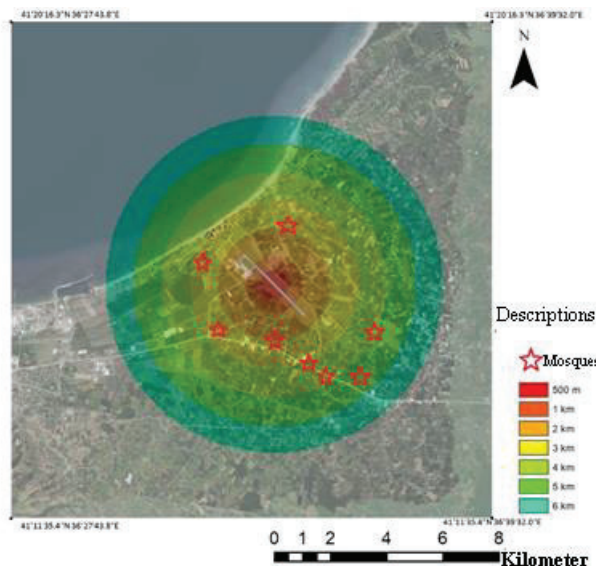


Figure 6. Mosques around the airport

3.4. Flammable and Explosive Facilities in and Around the Landing-Take Off Corridor

There is D-010 highway on the airport landing-departure corridor. According to the construction criteria envisaged around the airports, it is stated that there should not be any flammable, explosive facilities and warehouses within the 6000 meters area from the beginning of the runway (Anonymous, 2012).

In the study carried out, it may pose a risk for flight safety; the first ($41^{\circ}13'05.7''$) north parallels, ($36^{\circ}37'36.8''$) east meridians, the second ($41^{\circ}13'04.4''$) north parallels, ($36^{\circ}37'48.5''$) east meridians, the third ($41^{\circ}13'08.2''$) north parallels, ($36^{\circ}38'11.5''$) east meridians, fourth

(41°13'05.1") north parallels, (36°39'32.7") east meridians, and fifth (41°13'04.9")) north parallels, (36°39'42.9") east meridians coordinates, 5 fuel stations were identified (Figure 7). It has been determined that the furthest of these fuel oil facilities is 5961 meters per runway.

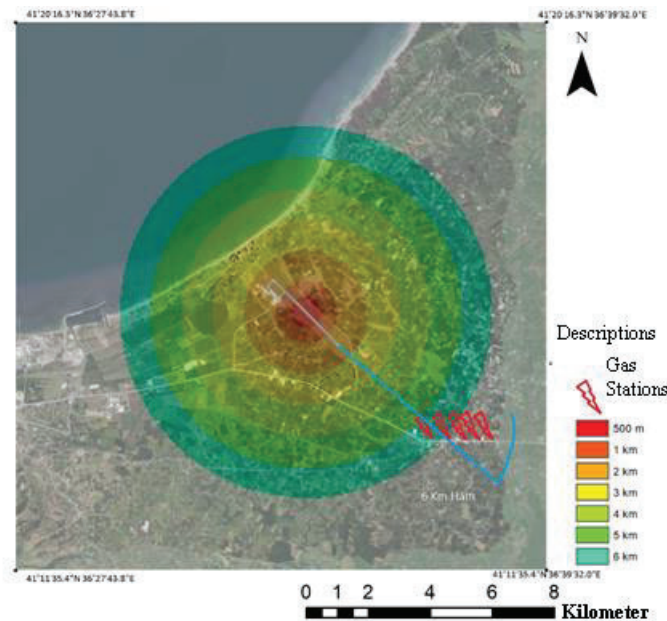


Figure7. Landing-take-off corridor and its surrounding fuel stations

3.5 Waste / Garbage Facilities in the Designated Risky Area Around the Airport

As SHGM (2016) can describe, garbage can be attractive to birds and cause birds to create a flight path. This situation jeopardizes his flight (Gülcan, 2019). In the 55-day accident that came with a small bird strike between 1912-2002; There will be 276 lives, and 108 passenger planes will become incapacitated (Abrate, 2016). 30% of cases do not develop while the planes are taking off and 60% of them are not developing on the airstrip. Few cases of bird strikes have been observed in rainy, snowy and swollen weather. In the study, it was determined that there was no garbage collection area in the conical surface. The closest garbage station to the airport belongs to Samsun Metropolitan Municipality, which is 18.75 km away and this distance is outside the risk limits of 13 km (SHGM, 2016).

3.6 UGRA Flight Safety Risk Analysis

Table 1. UGRA Flight Safety Risk Analysis

Risk Description	Risk score coefficient	Pieces	UGRA Risk Score
High architectural structures within the risky area boundaries of airports	2	0	0
Factors That May Have a Negative Impact on Pilots' Vision	0.5	0	0
Facilities where people can be found collectively in the risk area around the airport	1 point	10	10
Facilities where flammable and explosive products are sold in the risky area on the airport's landing-departure corridor	1.5 points	5	7.5
Waste / Garbage Facilities in the designated risky area around the airport	3	0	0
Total Score			17.5

4. CONCLUSION and RECOMMENDATIONS

There are a number of legal regulations in order to ensure flight safety. The most basic element of protection from airline accidents, which cause more loss of life and property when compared to other transportation sectors, is to avoid hazards. In this respect, it is of vital importance to fully comply with legal regulations. In this study, which examines the vicinity of Samsun Çarşamba Airport in terms of flight safety, it has been determined that some of the legal regulations created to ensure safety are not complied with. This shows that the deterrent of legal bases is not sufficient. It is a great shortcoming that the legislation on ensuring flight safety is violated at some points and there is no public pressure or any deterrent legal practice regarding this. In order to overcome this deficiency, it will be beneficial to carry out a number of studies by universities, non-governmental organizations and legal institutions, as in this study. As it is often emphasized in the study, it is clear that the issues that are not taken into account for flight safety may cause irreparable results in the future.

As a result of the knowledge and experience gained within the scope of the study, an analysis system called "Flight Safety Risk Analysis" (UGRA) was created and implemented at Samsun Çarşamba Airport. With this system, it is aimed to embody the issues that pose a danger to flight safety in numerical terms by scoring the elements that may cause more loss of life and property if they occur. With the application of UGRA to other airports, airports around the world will become objectively comparable in terms of flight safety. In this way, the

application will guide the authorities in many respects in the studies to be carried out to ensure safer flight operations.

References

- Abrate, S. (2016). Soft impacts on aerospace structures. *Progress in Aerospace Sciences*, 81, 1-17.
- Akgüngör, A. P. ve Demirel, A. (2011). Türkiye'deki ulaştırma sistemlerinin analizi ve ulaştırma politikaları. *Pamukkale Üniversitesi Mühendislik Bilimleri Dergisi*, 10 (3), 423-430.
- Anonymous, (2012). *Havaalanları çevresindeki yapılaşma kriterleri*. Ulaştırma Denizcilik ve Haberleşme Bakanlığı Sivil Havacılık Genel Müdürlüğü. <http://web.shgm.gov.tr/doc5/2549-7.pdf> (Date Accessed: 23.01.2020)
- Anonymous, (2018a). *Tüm uçak grafiği*. DHMİ. <https://www.dhmi.gov.tr/Lists/IstatistikList/Attachments/367/T%C3%9CM%20U%C3%87AK.pdf> (Date Accessed: 23.01.2020)
- Anonymous, (2018b). *Mâniaların kontrolü*. Devlet Hava Meydanları İşletmesi Yayınları El Kitabı, Havacılık Eğitim Dairesi Başkanlığı İşletme Eğitim Planlama ve Uygulama Müdürlüğü, Mayıs 2018.
- Anonymous, (2020a). Çınarlık Yalı İlkokulu. http://cinarlik_yali.meb.k12.tr/55/05/976681/okulumuz_hakkinda.html (Date Accessed: 19.05.2020)
- Anonymous, (2020b). T.C. Millî Eğitim Bakanlığı Samsun /Çarşamba-Çınarlık İlkokulu. <http://cinarlikio.meb.k12.tr> (Date Accessed: 19.05.2020)
- Birgören, N. (2015). *Uçuş emniyeti açısından ekip kaynak yönetimi uygulamalarının kabin ekibi üzerindeki etkisine ilişkin bir araştırma*. Basılmamış Yüksek Lisans Tezi. İstanbul Gelişim Üniversitesi Sosyal Bilimler Enstitüsü İşletme Anabilim Dalı, İstanbul.
- DHMİ, (2018). *İstatistikler*. <https://www.dhmi.gov.tr/sayfalar/istatistik.aspx> (Date Accessed: 15.09.2020).
- Doğan, Z. ve Dikmen, B. (2018). Türkiye'deki ulaştırma sektörü ve ulaştırma türlerinin karşılaştırılması. *Uluslararası Sosyal Araştırmalar Dergisi*, 11(56), 758-770. doi.org/10.17719/jisr.20185639046
- Efendigil, T. ve Eminler, Ö. (2017). Havacılık sektöründe talep tahminin önemi: yolcu talebi üzerine bir tahmin modeli. *Journal of Yaşar University*, 12, 14-30.
- Erol, A. ve Kanbur, E. (2017). Uçak bakım örgütlerinde iş sağlığı ve güvenliği yönetimi: çalışma sahalarından örnekler. *Al Farabi Uluslararası Sosyal Bilimler Dergisi*, 1(2), 181-192.
- Gülcan, O. (2019). Kuş çarpımları ve uçaklara etkileri üzerine bir gözden geçirme çalışması. *Engineer & The Machinery Magazine*, 60 (696), 192-220.
- Hatipoğlu, S. ve Işık, E. S. (2015). Havayolu ulaşımında hizmet kalitesinin ölçülmesi: İç hatlarda bir uygulama. *Kahramanmaraş Sütçü İmam Üniversitesi Sosyal Bilimler Dergisi*, 12(2), 293-312.
- Kılıç, (2017). Sivil ve askeri uçak kazalarında insan faktörü: örnek olay incelemesi: Helios Airways Flight Hcy522, Boeing 737. *Hava Kuvvetleri Komutanlığı, Havacılık Emniyeti Yönetim Sistemi (HEYS 2017) Sempozyumu*, Ankara, 12-13 April, 257-270.
- Okumuş, A. ve Asil, H. (2007). Hizmet kalitesi algılamasının havayolu yolcularının genel memnuniyet düzeylerine olan etkisinin incelenmesi. *İstanbul Üniversitesi İşletme Fakültesi Dergisi*, 36 (2), 7-29.

- Rothkoph, M. ve Wald, A., (2008). The role of innovation in the increasingly commoditized airline industry – insights from case studies. *Air Transport Research Society Kongresi*. Athens 8-11 July 2008.
- SHGM, (2007). Havaalanı hizmetleri el kitabı. http://web.shgm.gov.tr/documents/sivilhavacilik/files/pdf/kurumsal/yayinlar/HAD_T-01_manialarin_kontrolu.pdf (Date Accessed: 24.06.2020)
- SHGM, (2012). *Havaalanları çevresinde yapılaşma kriterleri*. <http://web.shgm.gov.tr/doc5/2549-7.pdf> (Date Accessed: 23.06.2020)
- SHGM, (2016). *Havaalanlarında yabancı hayvan kontrolü ve azaltımı*. [http://web.shgm.gov.tr/documents/sivilhavacilik/files/pdf/kurumsal/yayinlar/Havaalanlarinda Yabani Hayvan Kontrolu ve Azaltimi. pdf](http://web.shgm.gov.tr/documents/sivilhavacilik/files/pdf/kurumsal/yayinlar/Havaalanlarinda_Yabani_Hayvan_Kontrolu_ve_Azaltimi.pdf) (Date Accessed: 23.08.2020)
- SHY-13, (1992). Sivil Havacılık Genel Müdürlüğü, *Sivil Hava Araç Kazaları Soruşturma Yönetmeliği*, p 19.
- Uysal, M. Y. ve Dokuman, İ. (2017). Havacılık kaza ve olaylarında tasarım kaynaklı insan faktörleri. *Hava Kuvvetleri Komutanlığı, Havacılık Emniyeti Yönetim Sistemi (HEYS 2017) Sempozyumu*, Ankara, 12-13 April, 115-127
- Ulubay, A. ve Varol, M.B. (2013). Havaalanları etrafında emniyetli sahaların oluşturulması ve sunulması. *Havacılık ve Uzay Teknolojileri Dergisi*, 6 (1), 113-122.
- Yavuz, V., Temiz, C., Özdemir, E. T. ve Deniz, A. (2015). Avrupa bölgesi için kaza-kırım raporlarının incelenmesi. *Avrupa Bilim ve Teknoloji Dergisi*, 2(5), 155-160.
- Yaylalı, M. ve Dilek, Ö. (2009). Erzurum'da yolcuların havayolu ulaşım tercihlerini etkileyen faktörlerin tespiti. *Marmara Üniversitesi İktisadi ve İdari Bilimler Dergisi*, 26 (1), 1-21.
- Yüksel, M., Demirtaş, Ö., Kurt, M., Akay, D. (2006). Havacılık kazalarında insan faktörü. *Savunma Bilimleri Dergisi*, 5(1), 73-85.
- Zeybek, H. İ. (2006). Sosyo-ekonomik kriterlere göre Samsun ilinin, Karadeniz coğrafi bölgesi ve Türkiye'deki yeri. *Geçmişten Geleceğe Samsun Sempozyumu*, Samsun, 2006, p 4-6.

INVESTIGATION OF SOME PROPERTIES OF PERIODIC STURM-LIOUVILLE PROBLEM WITH TRANSMISSION CONDITIONS

Kadriye AYDEMİR

Amasya University, Faculty of Arts and Science, Department of Mathematics,
Amasya, Turkey.

ORCID ID: <https://orcid.org/0000-0002-8378-3949>

Oktay Sh. MUKHTAROV

Gaziosmanpaşa University, Faculty of Arts and Science, Department of Mathematics,
Tokat, Turkey.

Azerbaijan National Academy of Sciences, Institute of Mathematics and Mechanics,
Baku, Azerbaijan

ORCID ID: <https://orcid.org/0000-0001-7480-6857>

Hayati Olğar

Gaziosmanpaşa University, Faculty of Arts and Science, Department of Mathematics,
Tokat, Turkey.

ORCID ID: <https://orcid.org/0000-0003-4732-1605>

ÖZET

Bu çalışmada $L_2(-1,0) \oplus L_2(0,1)$ Hilbert uzayında

$$Ay := -y''(x) = \lambda y(x), \quad x \in [-1,0) \cup (0,1] \quad (1)$$

iki aralıklı Sturm-Liouville denkleminde

$$y(-1) = y(1) \quad (2)$$

$$y'(-1) = Ky'(1) \quad (3)$$

periyodik sınır şartlarından ve $x = 0$ geçiş noktasındaki

$$y(+0) = y(-0) \quad (4)$$

$$y'(+0) = \frac{1}{K}y'(-0) \quad (5)$$

geçiş şartlarından oluşan sınır-değer-geçiş probleminin bazı spektral özellikleri incelenmiştir. Burada $K > 0$ reel sayı, λ ise kompleks özdeğer parametresidir. Çalışmamızda problemin özdeğer ve özfonksiyonlarının bazı özellikleri araştırılmıştır. Ayrıca, araştırdığımız problemin karakteristik fonksiyonu tanımlanarak karakteristik fonksiyonun asimptotik ifadesi bulunmuştur.

Anahtar Kelimeler: Periodic Sturm-Liouville problemi, geçiş şartı, karakteristik fonksiyon.

ABSTRACT

The expansion in terms of the system of eigenfunctions for Sturm-Liouville type boundary value problems has a very important applications in many fields of natural sciences. Although periodic boundary conditions lead to spectral problems with unfamiliar solutions, the computation of expansions in terms of eigenfunction is a simple implementation of the procedure for solving many problems of mathematical physics. The spectral theory of differential operators, due to Sturm and Liouville, provides new expansions based on special type functions that reflect the physical properties of the particular system. The new expansions allow us to properly express solutions of many partial differential equations that would be otherwise be analytically difficult just as the trigonometric Fourier series enables us

to solve the heat flow problem. Therefore the spectral analysis of boundary value problems (BVP's) plays a crucial role in solving many important problems appearing in physics, engineering, physical chemistry, communication technology and etc. In solving of many BVP's by Fourier's method of separation of independent variables there arise Sturm-Liouville type eigenvalue problems. To justify the Fourier's method it is needed to prove the existence of infinitely many eigenvalues and to establish the expansion in a series of eigenfunctions. Now the Sturm-Liouville theory is one of the most actual and extensively developing field in spectral analysis of differential operators. In later years, the investigation of new concrete problems posed by physics led to the rapid development of Sturm-Liouville theory and the Sturm-Liouville problems remain one of the most current issues needed by spectral theory. Recently, Sturm-Liouville problems with transmission conditions have been an important research topic in mathematical physics. In this study, in the Hilbert space $L_2(-1,0) \oplus L_2(0,1)$ we shall examine some spectral properties of a new type boundary-value-transition problem consisting of a two-interval Sturm-Liouville equation

$$Ay := -y''(x) = \lambda y(x), \quad x \in [-1,0) \cup (0,1]$$

together with anti-periodic boundary conditions, given by

$$\begin{aligned} y(-1) &= y(1) \\ y'(-1) &= Ky'(1) \end{aligned}$$

and transition conditions at the interior point $x = 0$, given by

$$\begin{aligned} y(+0) &= y(-0) \\ y'(+0) &= \frac{1}{K} y'(-0) \end{aligned}$$

where $K > 0$ is the real number and λ is the complex eigenvalue parameter. In this study we shall investigate some properties of the eigenvalues and eigenfunctions of this problem. A Hilbert space suitable for the problem is constructed. We proved that the spectral semi-periodic problem under consideration has infinitely many real eigenvalues and the eigenfunctions belonging to distinct eigenvalues are orthogonal in this Hilbert space.

Keywords: Periodic Sturm-Liouville problems, transmission conditions, eigenfunctions.

GİRİŞ

Fizik ve başka doğa bilimlerinin birçok probleminin matematiksel modeli genelde kısmi diferansiyel denklemlerin bazı başlangıç ve sınır şartlarını sağlayan çözümlerin bulunmasına indirgenmektedir. Başlangıç ve sınır-değer problemlerinin çözümü için çok farklı yöntemler geliştirilmiştir. Örneğin; değişkenlerine ayırma yöntemi olarak da adlandırılan Fourier yönteminin uygulanabilmesi adi diferansiyel denklemler için sınır değer problemlerinin spektral özelliklerinin incelenmesini gerektirmektedir. Isı yayılımı probleminin çözümü üzerine çalışmalar yapıldığı süreçte ortaya çıkan, özdeğer parametresine bağlı adi diferansiyel denklemler için sınır değer problemleri ilk kez 19. yüzyılın ortalarında C. Sturm ve J. Liouville tarafından incelenmiştir. Sturm-Liouville problemi olarak adlandırılan özdeğer parametresini içeren özel tipten sınır değer problemleri matematiksel fiziğin önemli problemlerindendir. 1908 yılında George D. Birkhoff tarafından yayımlanmış [1] makalesinde

$$\frac{d^n y}{dx^n} + \lambda a_{n-1}(x, \lambda) \frac{d^{n-1} y}{dx^{n-1}} + \dots + \lambda^n a_0(x, \lambda) y = 0$$

formundaki özdeğer parametresine bağlı lineer diferansiyel denklemlerin çözümlerinin asimptotik davranışları incelenmiştir. Birkhoff bu çalışmasında kök fonksiyonları ve regüler sınır şartları kavramlarını tanımlamış(literatürde böyle şartlar Birkhoff anlamında regüler sınır şartları olarak adlandırılmaktadır), probleme uygun diferansiyel operatörün özfonksiyonlarından ve özfonksiyonlara bağlanmış fonksiyonlardan oluşan sisteminin tamlığı hakkında teorem ispatlamıştır. Daha sonra Tamarkin [2] çalışmasında parametreye bağlı lineer diferansiyel denklemler için temel çözümlerin asimptotiğini bulmuş, regüler sınır

şartları ile birlikte güçlü regüler sınır şartları kavramını tanımlamış ve bu sınır şartları altında özfonksiyonlar ve özfonksiyonlara bağlanmış fonksiyonların serisine açılım özelliklerini incelemiştir. Daha sonraki yıllarda fiziğin ortaya koyduğu yeni somut problemlerin araştırılması Sturm-Liouville teorisinin hızla gelişmesine yol açmıştır.

Günümüzde de Sturm-Liouville problemleri spektral teorisinin ihtiyaç duyduğu en güncel konulardan biri olmaya devam etmektedir. Lee [3] çalışmasında klasik Sturm-Liouville özdeğer problemi ile ilişkili spektral ve salınım teorisinin periyodik analoglarını sunmuştur. Berghe, Daele ve Meyer [4] çalışmasında regüler Sturm-Liouville problemlerinin özdeğerleri periyodik ve yarı-periyodik sınır koşulları altında araştırılmış ve yaklaşık özdeğerlerin hatasını azaltmak için basit bir lineer bağımlı çok adımlı yöntemin kullanılabileceği gösterilmiştir. [8], [9], [10], [11] çalışmalarında regular Sturm-Liouville problemi için geçiş şartlı problemler ele alınmıştır.

ESAS SONUÇLAR

$f: [a, b] \rightarrow R$ biçiminde karesi Lebesgue anlamında integrallenebilir fonksiyonların uzayını $L_2(-1,0)$ ile gösterelim.

$$Q = \{f(x) \mid f(x) \in L_2(-1,0) \oplus L_2(0,1)\}$$

biçiminde olan elemanların lineer uzayında $f(x)$, $g(x) \in Q$ fonksiyonlarının iç çarpımını

$$\langle f, g \rangle_{Q_k} = \int_{-1}^{-0} f(x) \overline{g(x)} dx + K \int_{+0}^1 f(x) \overline{g(x)} dx \quad (6)$$

eşitliği ile tanımlayalım.

Kolayca gösterilebilir ki, (6) eşitliği Q lineer uzayında bir iç çarpım fonksiyonu tanımlar. Bu iç çarpım uzayını Q_k ile gösterelim.

Lemma 1. $Q_k = (Q, \langle \cdot, \cdot \rangle_{Q_k})$ iç çarpım uzayı Hilbert uzayıdır.

Şimdi bu uzayda verilmiş (1) – (5) sınır-değer-geçiş problemi ile aynı özdeğerlere ve özfonksiyonlara sahip lineer operatör kurulacaktır.

(1) – (5) Sturm-Liouville sınır-değer geçiş probleminin ürettiği

$$G : Q \rightarrow Q$$

diferensiyel operatörü

$$D(G) = \left\{ f(x) = \begin{cases} f_1(x), & x \in [-1, 0) \\ f_2(x), & x \in (0, 1] \end{cases} \in Q \mid f_1(x), f_2(x), f_1'(x) \text{ ve } f_2'(x) \right.$$

fonksiyonları $[-1,0)$ ve $(0,1]$ aralıklarında mutlak süreklidirler sonlu $f(\pm 0)$ ve $f'(\pm 0)$ limit değerleri mevcuttur ve $f_1'' \in L_2(-1,0)$, $-f_2'' \in L_2(0,1)$, $f_1(-1) = f_2(1)$, $f_1'(-1) = f_2'(1)$, $f_1(0) = f_2(0)$, $f_1'(0) = K f_2'(0)$ }

tanım bölgesinde $Gf := -f''$ eşitliği ile tanımlansın.

Lemma 2. G operatörü yoğun tanımlı lineer operatördür, yani $\overline{D(G)} = Q$ eşitliği sağlanır.

Teorem 3. (1) – (5) eşitlikleri ile verilmiş sınır-değer-geçiş probleminin bütün özdeğerleri reeldir.

Not: Özdeğerler reel olduğu için genelliği bozmadan özfonksiyonların da reel değerli fonksiyonlar olduğunu kabul edebiliriz.

Teorem 4. (1) – (5) sınır-değer-geçiş probleminin iki farklı λ_m ve λ_n özdeğerlerine sırası ile uygun olan f_m ve f_n özfonksiyonları Q_k Hilbert uzayında ortogonaldirler. Yani;

$$\int_{-1}^{-0} f_m(x) f_n(x) dx + K \int_{+0}^1 f_m(x) f_n(x) dx = 0$$

eşitliği sağlanır.

Teorem 5. Q_k Hilbert uzayında yukarıdaki şekilde tanımlanan G operatörü simetriktir.

Bazı Yardımcı Başlangıç Değer Problemleri ve Çözümleri

Bu bölümde araştırdığımız (1) – (5) sınır-değer-geçiş problemi ile yakından ilgili olan ve sadece $[-1,0)$ ve $(0,1]$ alt aralıklarında verilmiş bazı yardımcı başlangıç-değer problemlerinin çözümleri tanımlanacaktır.

Her $\lambda \in \mathbb{C}$ için

$$\begin{aligned} -y''(x) &= \lambda y(x), & x \in [-1,0) \\ y(-1) &= 1 \\ y'(-1) &= 0 \end{aligned}$$

başlangıç-değer probleminin bir tek $R_1(x, \lambda)$ çözümü bulunur ve bu çözüm her bir $x \in [-1,0)$ değeri için λ değişkenine göre bütün kompleks düzlemde analitiktir. Yani $\forall x \in [-1,0)$ için λ parametresinin tam fonksiyonudur. (Titchmarsh, [13])

Her $\lambda \in \mathbb{C}$ için $R_2(x, \lambda)$ ile

$$\begin{aligned} -y''(x) &= \lambda y(x), & x \in (0,1] \\ y(1) &= 1 \\ y'(1) &= 0 \end{aligned}$$

eşitlikleri ile tanımlı başlangıç-değer probleminin çözümünü gösterelim. Bu çözüm de $\forall x \in (0,1]$ için λ parametresinin tam fonksiyonudur. (Titchmarsh, [13])

Benzer biçimde her $\lambda \in \mathbb{C}$ için $S_2(x, \lambda)$ ile

$$\begin{aligned} -y''(x) &= \lambda y(x), & x \in (0,1] \\ y(1) &= 0 \\ y'(1) &= 1 \end{aligned}$$

eşitlikleri ile tanımlı başlangıç-değer probleminin çözümünü $S_1(x, \lambda)$ ise

$$\begin{aligned} -y''(x) &= \lambda y(x), & x \in (0,1] \\ y(-1) &= 0 \\ y'(-1) &= 1 \end{aligned}$$

eşitlikleri ile tanımlı başlangıç-değer probleminin çözümünü gösterelim. Bu çözümler de her bir x değeri için λ değişkenine göre bütün kompleks düzlemde analitiktir, yani λ parametresinin tam fonksiyonudur. (Titchmarsh, [13])

Teorem 6. (1) – (5) sınır-değer-geçiş probleminin özdeğerleri

$$P(\lambda) = [S_2(+0, \lambda) + S_1(-0, \lambda) + KS_1'(-0, \lambda)][KR_2'(+0, \lambda) - R_1(-0, \lambda)] - [R_2(+0, \lambda) + R_1(-0, \lambda) + KR_1'(-0, \lambda)][KS_2'(+0, \lambda) - S_1(-0, \lambda)]$$

karakteristik fonksiyonunun sıfır yerleri ile çakışaktır.

Tanım 7. $P(\lambda)$ kompleks fonksiyonu (1) – (5) sınır-değer-geçiş probleminin karakteristik fonksiyonu olarak adlandırılır.

Teorem 8. (1) – (5) sınır-değer-geçiş probleminin $P(\lambda)$ karakteristik fonksiyonu tüm kompleks düzlemde analitiktir, yani tam fonksiyondur.

Teorem 9. $P(\lambda)$ karakteristik fonksiyonu $\lambda \rightarrow \infty$ için

$$P(\lambda) = -K \sin(2\sqrt{\lambda}) + O(e^{12Im\sqrt{\lambda}})$$

asimptotik eşitliğini sağlar.

Teorem 10. (1) – (5) sınır-değer-geçiş probleminin sayılabilir sonsuz sayıda özdeğeri mevcuttur ve bu özdeğerlerin sonlu yığılma noktası mevcut değildir.

Teşekkür: Bu çalışma, FMB-BAP 20-0440 (Bilimsel Araştırma Projeleri Koordinasyon Birimi) Proje numarası ile Amasya Üniversitesi tarafından desteklenmiştir.

KAYNAKLAR

- [1.] Birkhoff, G. D. (1908). On the Asymptotic Character of the Solution of the Certain Linear Differential Equations.
- [2.] Tamarkin, J. D., 1928. Some General Problems of The Theory of Ordinary Linear Differential Equations And Expansions of An Arbitrary Function in Series of Fundamental Functions. Math. Z., (27), 1-54.
- [3.] Lee, J.W. (1972). Spectral Properties and Oscillation Theorems for Periodic Boundary-Value Problems of Sturm Liouville Type. Journal of Differential Equations, 11, 592-606
- [4.] Berghe, G.V., Daele, M.V., Meyer, H.D. (1995). A modified difference scheme for periodic and semiperiodic Sturm-Liouville problems. Applied Numerical Mathematics, 18, 69-78.
- [5.] Aydemir, K., Mukhtarov, O. Sh. 2 (2014). Completeness Of One Two-Interval Boundary Value Problem With Transmission Conditions, Miskolc Mathematical Notes, 15:, 293303.
- [6.] Aydemir, K., Mukhtarov, O. Sh. (2017). Class of Sturm-Liouville problems with eigen-parameter dependent transmission conditions, Numerical Functional Analysis and Optimization , 38(10), 1260-1275.
- [7.] Kandemir, M., Mukhtarov, O. Sh. (2017). Nonlocal Sturm-Liouville problems with integral terms in the boundary conditions, Electronic Journal of Differential Equations, Vol. 2017, No. 11, pp. 112. 2017.
- [8.] Mukhtarov, O. Sh, Olğar, H.; Aydemir, K. (2015). Resolvent Operator and Spectrum of New Type Boundary Value Problems. Filomat 29, 1671–1680
- [9.] Mukhtarov, O. Sh, Olğar, H.; Aydemir, K. Jabbarov I. (2018). Operator-Pencil Realization Of One Sturm-Liouville Problem With Transmission Conditions. Applied And Computational Mathematics, 17(2), 284-294.
- [10.] Titchmars, E. C., 1962. Eigenfunctions Expansion Associated with Second Order Differential Equations I, second edn. Oxford Univ. press, London.

SPECTRAL PROPERTIES FOR BOUNDARY VALUE PROBLEMS OF STURM-LIOUVILLE TYPE

Oktay Sh. MUKHTAROV

Gaziosmanpaşa University, Faculty of Arts and Science, Department of Mathematics,
Tokat, Turkey.

Azerbaijan National Academy of Sciences, Institute of Mathematics and Mechanics,
Baku, Azerbaijan

ORCID ID: <https://orcid.org/0000-0001-7480-6857>

Kadriye AYDEMİR

³Amasya University, Faculty of Arts and Science, Department of Mathematics, Amasya,
Turkey.

ORCID ID: <https://orcid.org/0000-0002-8378-3949>

Hayati Olğar

Gaziosmanpaşa University, Faculty of Arts and Science, Department of Mathematics,
Tokat, Turkey.

ORCID ID: <https://orcid.org/0000-0003-4732-1605>

ÖZET

Bu çalışmada

$$Fu := -u''(x) = \mu u(x), \quad x \in [a_1, b_1) \cup (b_1, b_2) \cup (b_2, a_2] \quad (1)$$

Sturm-Liouville denkleminde

$$r_1 u := u(a_1) - u(a_2) = 0 \quad (2)$$

$$r_2 u := u'(a_1) - u'(a_2) = 0 \quad (3)$$

periyodik sınır şartlarından, b_1 noktasında

$$r_3 u := u(b_1^-) - u(b_1^+) = 0 \quad (4)$$

$$r_4 u := u'(b_1^-) - u'(b_1^+) = 0$$

(5)

biçiminde verilen geçiş şartlarından ve b_2 noktasındaki

$$r_5 u := u(b_2^-) - u(b_2^+) = 0 \quad (6)$$

$$r_6 u := u'(b_2^-) - u'(b_2^+) = 0$$

(7)

geçiş şartlarından oluşan sınır-değer-geçiş probleminin bazı spektral özellikleri incelenmiştir. μ ise kompleks özdeğer parametresidir. Çalışmamızda problemin özdeğer ve özfonksiyonlarının bazı özellikleri araştırılmıştır. Ayrıca, araştırdığımız problemin karakteristik fonksiyonu tanımlanarak karakteristik fonksiyonun asimptotik ifadesi bulunmuştur.

Anahtar Kelimeler: Periodic Sturm-Liouville problemi, geçiş şartı, karakteristik fonksiyon.

ABSTRACT

Motivated by problems of periodic motion in continuous media, such as the periodic flow in a rod, Sturm and Liouville were led in the first half of the 19th century to identify a class of boundary value problems for second order differential equations now referred to as Sturm-Liouville problems, that have inspired much of branches of modern analysis and spectral theory of linear operators and continue to do so. The direct problem of Sturm-Liouville theory is that of investigating the spectral data of various type Sturm-Liouville problems, i.e. the

investigation of some qualitative spectral aspects of eigenvalues and associated eigenfunctions. The existence of periodic and oscillatory solutions plays a key role in characterizing the behavior of boundary value problem. The spectral properties of boundary value problems for second order differential equations have been widely investigated due to their application in many fields of natural sciences, such as physics, mechanics, engineering, electromagnetics, quantum physics etc. In such applications, it is important to know the existence of periodic and oscillatory solutions of differential equations. Periodic boundary value problems for Sturm-Liouville type, in fact are one of the important areas of general spectral theory of differential operators since many problems of mathematical physics are modelled by this type of spectral problems. For example, consider the heated rod that has been bent into a circle. Then both ends this rod are physically the same. Thus, we would expect that the temperature and the temperature gradient at these endpoints to be the same. For this case we have periodic boundary conditions of the form

$$u(a) = u(b), u'(a) = u'(b).$$

It is well known that such type of boundary conditions lead to different types of eigenfunctions and eigenvalues. The purpose of this work is to study some spectral properties of periodic Sturm-Liouville problems of a new type which are defined on two disjoint intervals and contain additional transfer conditions.

In this paper, we shall consider discontinuous periodic eigenvalue problem which consisting of the differential equation

$$Fu := -u''(x) = \mu u(x), x \in [a_1, b_1) \cup (b_1, b_2) \cup (b_2, a_2] \quad (1)$$

with periodic boundary conditions

$$r_1 u := u(a_1) - u(a_2) = 0 \quad (2)$$

$$r_2 u := u'(a_1) - u'(a_2) = 0 \quad (3)$$

with impulsive conditions at the points of discontinuity b_1 and b_2

$$r_3 u := u(b_1^-) - u(b_1^+) = 0 \quad (4)$$

$$r_4 u := u'(b_1^-) - u'(b_1^+) = 0 \quad (5)$$

and

$$r_5 u := u(b_2^-) - u(b_2^+) = 0 \quad (6)$$

$$r_6 u := u'(b_2^-) - u'(b_2^+) = 0$$

(7)

where λ is a complex eigenvalue parameter.

Keywords: Sturm-Liouville problems, transmission conditions, eigenvalue.

GİRİŞ

Matematiksel fizik problemlerinin çözümü ihtiyacı klasik Sturm-Liouville teorisini geçmişte ve günümüzde özel bir ilgi odağı haline getirmiş ve bu teorinin geliştirilmesine vesile olmuştur. Örneğin, kristal örgüde iletken elektronun hareketi için basit bir model, periyodik potansiyele sahip Schrödinger denklemi biçiminde ifade edilir. Bu potansiyel, kristal örgüdeki iyonlar ve kristaldeki diğer elektronlardan kaynaklanan kuvvetlerin elektronun hareketi üzerindeki etkisini açıklar. Bu problemin tek boyutlu olduğu düşünülürse elektronun dalga fonksiyonu olan $V(x)$ potansiyeli periyodik bir fonksiyon olmak üzere bir boyutlu Schrödinger denklemi elde edilir. Periyodu a ile gösterilirse $V(x+a) = V(x)$ sağlanır. O halde

$$u(x) = \varphi\left(\frac{x}{a}\right), q(x) = \frac{2ma^2}{h} V\left(\frac{x}{a}\right), \lambda = \frac{2mE}{h^2}$$

değişken değişimleri yapıldıktan sonra u normal dalga fonksiyonu, λ enerji parametresi, $q(x+1) = q(x)$ olmak üzere Schrödinger denklemi

$$-u'' + q(x)u = \lambda u \quad (8)$$

biçimindeki Sturm-Liouville denkleminde indirgenir. (8) eşitliğinin spektrumu kesinlikle sürekli ve kapalı aralıkların birleşiminden veya boşluklarla ayrılmış bantlardan oluşur. Bu

bantların ve boşlukların varlığı, kristallerin iletkenlik özellikleri için önemli etkilere sahiptir. Enerjisi bantlardan birinde bulunan elektronlar kristal boyunca serbestçe hareket ederken enerjisi boşluklardan birinde bulunan elektronlar büyük mesafeler boyunca hareket edemez. Bir kristal, boş olmayan enerji bantları tamamen elektronlarla doluyorsa bir yalıtkan gibi davranır, bir metal gibi sadece kısmen doldurulmuş enerji bantlarına sahipse elektrik iletir. Yarı iletkenler genellikle tam bir valans bandına sahiptir, ancak küçük bir bant boşluğu enerjileri E_g ile termal enerji $k_B T$ aynı düzendedir. Sonuç olarak elektronlar valans bandından boş bir iletim bandına termal olarak uyarılabilir. Daha sonra uyarılmış elektronlar ve valans bandında bıraktıkları delikler elektriği iletirler. (8) eşitliğinin spektrumunu incelemek için periyodik katsayılı lineer adi diferansiyel denklemlere uygulanan Floquet teorisi kullanılır. Floquet teorisi ayrıca adi diferansiyel denklemlerin zaman-periyodik çözümlerinin kararlılığını incelemek için de kullanılır. $q(x)$ katsayısının periyodikliği çözümlerin periyodik olduğu anlamına gelmez.

Liu [1] çalışmasında

$$\begin{cases} x^n(t) = f(t, x(t), x(\alpha_1(t)), \dots, x(\alpha_m(t))), & t \in [0, T] \\ \Delta x^i(t_k) = I_{i,k}(x(t_k), \dots, x^{n-1}(t_k)), & k = 1, \dots, p \end{cases}$$

n . mertebeden fonksiyonel diferansiyel denkleminin impulse etkileri ve

$$x^i(0) = x^i(T), i = 0, \dots, n-1$$

periyodik sınır koşulları ile birlikte periyodik sınır değer probleminin çözümleri için varlık problemlerini araştırmıştır ve esas sonuçların önemini göstermek için örnekler sunmuştur. Wang[2] çalışmasında sabit nokta teoremi kullanılarak zaman ölçeklerinde doğrusal olmayan birinci dereceden impulsiv dinamik denklemlerinden ve periyodik sınır şartlarından oluşan sınır-değer problemleri için bazı spektral sonuçlar elde etmiştir. Bu makalede esas sonuçlara ait iki örnek verilmiştir. Malathi, Mohamed ve Bachok[3] makalesinde birinci dereceden adi diferansiyel denklemlerin sistemine indirgenme yapılmadan çekim tekniği kullanılarak doğrudan integrasyon (DI) yöntemiyle periyodik Sturm-Liouville (SL) problemlerinin özdeğerleri araştırılmıştır. Bu çalışmada Floquet teorisi, SL problemlerinin aşık olmayan bir çözümünü bulmak için uygulanır ve çekim teknikleri kullanılarak özdeğerlere yaklaşılr. DI yöntemiyle elde edilen sonuçlar ile birinci dereceden adi diferansiyel denklemlerin azaltılmasıyla karşılaştırılan hesaplama avantajları sunulmaktadır. [8], [9], [10], [11] çalışmalarında regular Sturm-Liouville problemi için geçiş şartlı problemler ele alınmıştır.

ESAS SONUÇLAR

Teorem 1. (1)– (7) periyodik sınır-değer geçiş problemi kendine eşleniktir.

Teorem 2. μ_n ve μ_m $[a_1, b_1) \cup (b_1, b_2) \cup (b_2, a_2]$ aralığında (1)– (7) probleminin farklı iki özdeğeri olsun. Bu özdeğerlere karşılık gelen u_n ve u_m özfonksiyonları için

$$\int_{a_1}^{b_1^-} u_n(x)u_m(x)dx + \int_{b_1^+}^{b_2^-} u_n(x)u_m(x)dx + \int_{b_2^+}^{a_2} u_n(x)u_m(x)dx = 0$$

eşitliği sağlanır. Bu eşitlik $L_2([a_1, b_1) \oplus (b_1, b_2) \oplus (b_2, a_2])$ Hilbert uzayında u_n ve u_m fonksiyonlarının ortogonal olduğunu gösterir.

Teorem 3. (1)– (7) periyodik sınır-değer geçiş probleminin tüm özdeğerleri reeldir.

(1) denkleminin iki çözümünü

$$S(x, \mu) = \begin{cases} S_1(x, \mu), & x \in [a_1, b_1) \\ S_2(x, \mu), & x \in (b_1, b_2) \\ S_3(x, \mu), & x \in (b_2, a_2] \end{cases} \quad \text{ve} \quad T(x, \mu) = \begin{cases} T_1(x, \mu), & x \in [a_1, b_1) \\ T_2(x, \mu), & x \in (b_1, b_2) \\ T_3(x, \mu), & x \in (b_2, a_2] \end{cases}$$

biçiminde tanımlansın.

$S_1(x, \mu)$, $[a_1, b_1)$ aralığında (1) denkleminin

$$S_1(a_1) = 1, S_1'(a_1) = 0$$

başlangıç şartlarını sağlayan bir çözümü olsun. Bu çözüm aracılığı ile (b_1, b_2) aralığında (1) denkleminin $S_2(x, \mu)$ çözümü

$$S_2(b_1^+) = S_1(b_1^-), \quad S_2'(b_1^+) = S_1'(b_1^-)$$

başlangıç şartları ile tanımlansın. $(b_2, a_2]$ aralığında (1) denkleminin $S_2(x, \mu)$ çözümü aracılığı ile tanımlayan ve

$$S_3(b_2^+) = S_2(b_2^-), \quad S_3'(b_2^+) = S_2'(b_2^-)$$

başlangıç şartlarını sağlayan çözümü $S_3(x, \lambda)$ olsun. Benzer şekilde $[a_1, b_1)$ aralığında (1) denkleminin $T_1(x, \lambda)$ çözümü

$$T_1(a_1) = 0, \quad T_1'(a_1) = 1$$

başlangıç şartları ile tanımlansın. (b_1, b_2) aralığında (1) denkleminin $T_2(x, \mu)$ çözümü

$$T_2(b_1^+) = T_1(b_1^-), \quad T_2'(b_1^+) = T_1'(b_1^-)$$

başlangıç şartları ile verilsin. $T_2(x, \mu)$ çözümü tarafından $[a_1, b_1)$ aralığında (1) denkleminin

$$T_3(b_2^+) = T_2(b_2^-), \quad T_3'(b_2^+) = T_2'(b_2^-)$$

başlangıç şartlarını sağlayan çözümü $T_3(x, \mu)$ olsun. Bu çözümlerin her biri μ kompleks spektral parametresinin tam fonksiyonudur.

Sonuç 4. $S(x, \mu)$ ve $T(x, \mu)$ fonksiyonları lineer bağımsızdır.

Teorem 6. (1)–(7) periyodik sınır-değer geçiş probleminin özdeğerleri

$$X(\mu) := W_\mu(S_2, T_2; b_2^+)W_\mu(S_2, T_2; b_2^-)[W_\lambda(S_3, T_3; a_1) + 1 - S_3(a_2) - T_3'(a_2)]$$

sınır fonksiyonunun sıfır yerleri ile çakışaktır.

Teşekkür: Bu çalışma, FMB-BAP 20-0440 (Bilimsel Araştırma Projeleri Koordinasyon Birimi) Proje numarası ile Amasya Üniversitesi tarafından desteklenmiştir.

KAYNAKLAR

- [1.] Liu, Y. (2007). Periodic Boundary Value Problems for Higher Order Impulsive Functional Differential Equations. SDÜ Fen Edebiyat Fakültesi Fen Dergisi (E-dergi), 2, 253-272.
- [2.] Wang, D.B. (2012). Periodic Boundary Value Problems for Nonlinear First-Order Impulsive Dynamic Equations on Time Scales. Advances in Difference Equations 2012, 12.
- [3.] Malathi, V., Mohamed, B. S., Bachok, B. T. (1996). Computing Eigenvalues Of Periodic Sturm-Liouville Problems Using Shooting Technique And Direct Integration Method. International Journal of Computer Mathematics, 68, 119-132.
- [4.] Aydemir, K., Mukhtarov, O. Sh. 2 (2014). Completeness Of One Two-Interval Boundary Value Problem With Transmission Conditions, Miskolc Mathematical Notes, 15:, 293303.
- [5.] Aydemir, K., Mukhtarov, O. Sh. (2017). Class of Sturm-Liouville problems with eigen-parameter dependent transmission conditions, Numerical Functional Analysis and Optimization, 38(10), 1260-1275.
- [6.] Kandemir, M., Mukhtarov, O. Sh. (2017). Nonlocal Sturm-Liouville problems with integral terms in the boundary conditions, Electronic Journal of Differential Equations, Vol. 2017, No. 11, pp. 112. 2017.
- [7.] Mukhtarov, O. Sh, Olğar, H.; Aydemir, K. (2015). Resolvent Operator and Spectrum of New Type Boundary Value Problems. Filomat 29, 1671–1680
- [8.] Mukhtarov, O. Sh, Olğar, H.; Aydemir, K. Jabbarov I. (2018). Operator-Pencil Realization Of One Sturm-Liouville Problem With Transmission Conditions. Applied And Computational Mathematics, 17(2), 284-294.
- [9.] Titchmarsh, E. C., 1962. Eigenfunctions Expansion Associated with Second Order Differential Equations I, second edn. Oxford Univ. press, London.

SOME QUALITATIVE PROPERTIES OF WEAK EIGENFUNCTIONS OF MULTI-INTERVAL STURM-LIOUVILLE PROBLEMS

Oktay Sh. MUKHTAROV

Gaziosmanpasa University, Faculty of Arts and Science, Department of Mathematics,
Tokat, Turkey.

Azerbaijan National Academy of Sciences, Institute of Mathematics and Mechanics,
Baku, Azerbaijan

ORCID ID: <https://orcid.org/0000-0001-7480-6857>

Hayati OLĞAR

Gaziosmanpasa University, Faculty of Arts and Science, Department of Mathematics, Tokat,
Turkey.

ORCID ID: <https://orcid.org/0000-0003-4732-1605>

Kadriye AYDEMİR

Amasya University, Faculty of Arts and Science, Department of Mathematics,
Amasya, Turkey.

ORCID ID: <https://orcid.org/0000-0002-8378-3949>

ÖZET

Bu çalışmada $a_1 < b_1 \leq a_2 < b_2$ şartını sağlayan iki ayırık (a_1, b_1) ve (a_2, b_2) aralıklarında tanımlı olan bir çok-aralıklı Sturm-Liouville denkleminde, a_1, b_2 noktalarında verilmiş iki tane sınır şartından ve de b_1, a_2 noktalarında verilmiş iki tane geçiş (iletişim) şartlarında oluşmuş bir sınır-değer-geçiş probleminin bazı spektral özellikleri incelenmiştir. İlk önce klasik Sobolev uzayları ile eşdeğer olan ve çok aralıklı sınır-değer-geçiş problemimize özgü olan yeni uzaylar ve bu uzaylara özgü iç çarpımlar tanımlanmıştır. Sınır-değer-geçiş problemimizin zayıf çözümü kavramı tanımlanmış ve Riesz temsil teoremi yardımıyla araştırdığımız çok aralıklı sınır-değer-geçiş problemi $A(\lambda) = A_0 + \lambda A_1$ olmak üzere $A(\lambda)\psi = 0$ biçiminde bir operatör denkleme indirgenmiştir. Daha sonra $A(\lambda)$ operatörü aracılığıyla çok aralıklı Sturm-Liouville probleminin simetrikliği, özdeğerlerinin reelliği ve özfonksiyonlarının ortogonallığı araştırılmıştır. Ayrıca, en az bir $\lambda_0 \in \mathbb{R}$ sayısı için $A(-\lambda_0) > 0$ olacak biçimde $A(\lambda)$ operatörünün pozitif tanımlı olduğu gösterilmiştir.

Anahtar Kelimeler: Multi-interval sınır-değer-geçiş problemi, sınır ve geçiş şartı, operatör.

ABSTRACT

The purpose of this study is to investigate various spectral properties of one non-classical Sturm-Liouville Problem (SLP, for short) the main feature of which is the nature of boundary conditions. Sturm-Liouville problems arise as the mathematical modelling of some systems and processes in the fields of physics, chemistry, aerodynamics, electrodynamics of electrical circuits, fluid dynamics, diffusion, magnetism, biology but more often as a result of using the method of separation of variables to solve the classical partial differential equations of physics, such as the Laplace's equation, the heat equation and the wave equation [1,7,8,11,13,17,19]. Also, many physical processes, such as the vibration of strings, the interaction of atomic particles, electrodynamics of complex medium, aerodynamics, polymer

rheology or the Earth's free oscillations yields Sturm-Liouville eigenvalue problems. The second-order self-adjoint linear differential equations

$$\left(p(x)u'(x)\right)' + (q(x) + \lambda \rho(x))u(x) = 0, \quad x \in I = [a, b]$$

together with boundary conditions of various types given at the ends $x=a, b$, first arose in the context of the separation of independent variables method for many initial and/or boundary value problems for linear partial differential equations appearing in many branches of applied mathematics. Two well-known works of Sturm on boundary value problems (BVP's) of this type, now called Sturm-Liouville problems (SLP's) published in 1836, are characterized by the general and qualitative nature of solutions. Although before Sturm the theory of differential equations was primarily concerned with the question of how to find exact solutions of a given differential equation of a special type, Sturm changed the question how to find some qualitative properties of a differential equation, such as the existence of a countable number of eigenvalues, the asymptotic behaviours of these eigenvalues and the corresponding eigenfunctions, comparison of solutions of similar differential equations with different coefficients, the location of the zeros of the solutions, etc., when its coefficients do not have a special form. The relevant spectral theory of differential operators has made significant progress since the time of these works by Sturm. There is an extensive literature on this topic [3,5,9,15,16,18]. Sarsenbi and Tengaeva [15] studied the basis properties of systems of eigenfunctions and associated functions for one kind of generalized spectral problems for a model second-order ordinary differential operator. Kerimov and Poladov [9] investigated the oscillation properties of eigenfunctions of the Sturm–Liouville problem with a spectral parameter in the boundary conditions. Moreover, they derived asymptotic formulas for eigenvalues and eigenfunctions and examined the basis properties in the Banach space $L_p, 1 < p < \infty$. Although this literature as such does not deal with similar, but multi-interval Sturm-Liouville operators, many of their results can be carried over to this case. Recently, the basis properties and eigenfunction expansions in various function spaces of the eigenfunction of the regular boundary value problems with spectral parameter in the boundary conditions have been investigated by many mathematicians. In [4,10,14,20] the authors studied the basis property in various function spaces of the eigenfunction of the Sturm-Liouville problems with nonclassical boundary conditions. An efficient approximation to the problems containing transmission conditions has been given by Mukhtarov and his colleagues [2,12,14]. This new approximation allows one to understand the geometrical meaning of the Hilbert space with the special inner product. The goal of this study is to establish some qualitative properties of the generalized solutions of one multi-interval Sturm-Liouville type boundary value problem, containing transmission conditions.

Namely in this study, some spectral properties of one multi-interval Sturm-Liouville type boundary value transmission problem which consist of a Sturm-Liouville equation with eigenparameter-dependent boundary conditions and transmission conditions will be investigated. Firstly, the weak solution will be defined for the problem under consideration. Second, this problem will be reduced to the operator-pencil equation. Finally, we prove that this operator-pencil is self-adjoint and positive definite for sufficiently large in absolute value negative values of the eigenparameter.

Keywords: Multi-interval Sturm-Liouville problems, boundary conditions and transmission conditions operator.

GİRİŞ

Doğa bilimlerinde, özellikle de fizikte ortaya çıkan bir çok somut problemlerin matematiksel modeli kurulurken genel olarak adi ve kısmi diferensiyel denklemler için sınır-değer problemleri ile karşılaşmaktadır. Bu tip problemlerin çözümü için en yaygın ve en etkin yöntemlerden biri spektral yöntemdir. Bu yöntem ilk defa ondokuzuncu yüzyılın ortalarında C. Sturm ve J. Liouville tarafından uygulanmıştır. Parabolik, eliptik yada hiperbolik denklem biçimindeki kısmi diferensiyel denklemlerin farklı başlangıç şartları altındaki çözümlerini, değişkenlerini ayırma yöntemi ile ararken ikinci mertebeden kısmi türevi bulunan değişkene göre Sturm-Liouville tipinde spektral problem ortaya çıkmaktadır. Değişkenlerine ayırma yönteminin esaslandırılması için, ortaya çıkan Sturm-Liouville tipinde spektral problemin özdeğerlerinin ve uygun özfonksiyonlarının farklı özelliklerinin araştırılması gerekmektedir. Uygulamalı matematik açısından bu kadar önemli olduğu için Sturm-Liouville problemleri ondokuzuncu yüzyılın ortalarından günümüze kadar yoğun bir biçimde araştırılmış ve araştırılmaya devam edilmektedir.

Yirminci yüzyılın ilk yarısında E.C. Titchmarsh, H. Weyl, A.C. Dixon, M.H. Stone ve başka bir çok matematikçinin çalışmaları Sturm-Liouville teorisine önemli katkılar sunmuştur. Yirminci yüzyılın ikinci yarısında ise J. Walter, A. Schneider, D.B. Hinton, P. Binding, P. Browne, K. Seddighi, M. Kasimov, B.M. Levitan, A. Zettl, A.A. Shkalikov ve başka matematikçiler hem Sturm-Liouville teorisinde hem de diferensiyel operatörler teorisinde önemli çalışmalar yapmışlardır. Son yıllarda fizikte ortaya çıkan çok-aralıklı somut problemlerin araştırılması ihtiyacı çözümü sadece sürekli değil hem de süreksizliğe sahip olan Sturm-Liouville problemlerine ilginin artmasına neden olmuştur. Süreksiz Sturm-Liouville problemleri sınır şartlarının yanısıra hem de sıçrama şartları (süreksizlik şartları) içermektedir. Son yıllarda O.Sh. Mukhtarov ve arkadaşları tarafından yapılmış çalışmalarda çok-çok geniş sınıftan sıçrama şartları içeren Sturm-Liouville problemlerinin bile kendine eşlenik diferensiyel operatörle temsil edilebilirliğini sağlayan yeni yöntemler geliştirilmiştir. Bu yöntemler sayesinde klasik biçiminde ifade edilemeyen birçok yeni tipten sınır değer problemlerinin spektral özelliklerini incelemek mümkün olmuştur.

Bu çalışmada iki aralıklı

$$\left(p_1(x)u_1'(x)\right)' + (q_1(x) + \lambda \rho_1(x))u_1(x) = 0, \quad x \in I_1 = (a_1, b_1) \quad (1)$$

$$\left(p_2(x)u_2'(x)\right)' + (q_2(x) + \lambda \rho_2(x))u_2(x) = 0, \quad x \in I_2 = (a_2, b_2) \quad (2)$$

diferensiyel denkleminde,

$$u_1'(a_1) = 0 \quad (3)$$

$$u_2'(b_2) = 0 \quad (4)$$

sınır şartlarından ve de verilmiş

$$u_2(a_2) = u_1(b_1) \quad (5)$$

$$\left(p_2u_2'\right)(a_2) = \left(p_1u_1'\right)(b_1) + \gamma_1 u_1(b_1) + \gamma_2 u_2(a_2) \quad (6)$$

geçiş şartlarından oluşmuş çok-aralıklı sınır-değer probleminin bazı spektral özellikleri incelenecektir. Problem incelenirken aşağıdaki şartların sağlandığını kabul edeceğiz:

- i. $p_i(x)$, $q_i(x)$ ve $\rho_i(x)$ ($i=1,2$) fonksiyonları sırasıyla $[a_i, b_i]$ aralığında ($i=1,2$) ölçülebilir, pozitif tanımlı ve Lebesgue anlamında integrallenebilir fonksiyonlardır,
- ii. λ kompleks özdeğer parametresidir,
- iii. γ_i ($i=1,2$) pozitif reel sayılardır,
- iv. $a_1 < b_1 \leq a_2 < b_2$.

Problemimize özgü Hilbert uzaylarının kurulması aşağıda tanımları verilen uzaylar yardımıyla yapılacaktır. Çeşitli tipten sınır değer problemlerinin (adi ve kısmi diferensiyel denklemler için) çalışılmasında standart $L_2(a, b)$ ve $W_2^m(a, b)$ Hilbert uzayları önemli bir rol oynamaktadır. Burada $L_2(a, b)$ ile $[a, b]$ aralığında karesi integrallenebilir kompleks değerli fonksiyonların klasik Lebesgue uzayını, $W_2^m(a, b)$ ile $[a, b]$ aralığında Lebesgue anlamında ölçülebilir ve $u'(x), u''(x), \dots, u^{(m)}(x)$ genelleştirilmiş türevleri bulunan ve her $k=1, 2, \dots, m$ için $u^{(k)}(x) \in L_2(a, b)$ olan fonksiyonların lineer uzayı gösterilmiştir.

Tanım 1. $L_2 := L_2(a_1, b_1) \oplus L_2(a_2, b_2)$ direkt toplam uzayının

$$H_2^1 = \{(u_1, u_2) \in L_2 : u_i \in W_2^1(a_i, b_i) (i=1, 2), u_2(a_2) = u_1(b_1)\}$$

lineer alt uzayı üzerinde $u = (u_1, u_2), v = (v_1, v_2)$ olmak üzere

$$\langle u, v \rangle_0 = \langle u_1, v_1 \rangle_{L_2(a_1, b_1)} + \langle u_2, v_2 \rangle_{L_2(a_2, b_2)}$$

iç-çarpımını tanımlayalım. Bu iç-çarpım uzayını H_0 ile gösterelim.

Teorem 2. H_0 iç-çarpım uzayı bir Hilbert uzayıdır.

Tanım 3. H_2^1 lineer uzayında başka bir iç-çarpımı $\langle u, v \rangle_1 := \langle u, v \rangle_0 + \langle u', v' \rangle_0$ biçiminde tanımlayarak elde edilen iç-çarpım uzayını H_1 ile gösterelim.

Teorem 4. H_1 iç-çarpım uzayı bir Hilbert uzayıdır.

Buraya kadar olan kısımda (1)–(6) çok-aralıklı Sturm – Liouville problemine özgü Hilbert uzaylarının kurulma aşaması tamamlanmıştır. Şimdi (1)–(6) problemi için zayıf özfonksiyon kavramı tanımlanacaktır.

Tanım 5. $u(x) \in H_1$ elemanı verilsin. Eğer $\forall v(x) \in H_1$ için

$$\begin{aligned} & \int_{a_1}^{b_1} (u_1'(x) \overline{v_1'(x)} + q_1(x) u_1(x) \overline{v_1(x)}) dx + \int_{a_2}^{b_2} (u_2'(x) \overline{v_2'(x)} + q_2(x) u_2(x) \overline{v_2(x)}) dx \\ & + \gamma_1 u_1(b_1) \overline{v_2(a_2)} + \gamma_2 u_2(a_2) \overline{v_2(a_2)} \\ & = \lambda \left[\int_{a_1}^{b_1} u_1(x) \overline{v_1(x)} dx + \int_{a_2}^{b_2} u_2(x) \overline{v_2(x)} dx \right] \end{aligned} \quad (7)$$

eşitliği sağlanırsa, o halde $u(x) \in H_1$ elemanına (1)–(6) Sturm-Liouville probleminin zayıf özfonksiyonu denir.

Buradan [14] çalışmasındaki yöntemden yararlanarak (1)–(6) iki-aralıklı Sturm-Liouville problemini (7) ile ifade edilen integral denklemine dönüştürmüş olduk. Aşağıdaki bilineer formları tanımladık.

$$P(u, v) =: \gamma_1 u_1(b_1) \overline{v_2(a_2)} + \gamma_2 u_2(a_2) \overline{v_2(a_2)}, \quad (8)$$

$$Q(u, v) =: \int_{a_1}^{b_1} u_1(x) \overline{v_1(x)} dx + \int_{a_2}^{b_2} u_2(x) \overline{v_2(x)} dx. \quad (9)$$

İlk önce aşağıdaki teoremi elde ettik.

Teorem 6. Her $u \in H_1$ için $P(u, \bullet)$ ve $Q(u, \bullet)$ fonksiyonelleri H_1 Hilbert uzayında süreklidir.

Daha sonra Riesz temsil teoreminden (bak [5] ve [10]) de yararlanarak aşağıdaki teoremi elde ettik.

Teorem 7. Her $u, v \in H_1$ için $\langle S_1 u, v \rangle_{H_1} := P(u, v)$ ve $\langle S_2 u, v \rangle_{H_1} := Q(u, v)$ eşitliklerini sağlayan $S_1 : H_1 \rightarrow H_1, S_2 : H_1 \rightarrow H_1$ lineer sınırlı operatörleri mevcuttur.

Aşağıdaki teoremi ise genel Fonksiyonel Analiz teorisinden ve [10] çalışmasında yer alan bazı yöntemlerden yararlanarak elde ettik.

Teorem 8. $S_1, S_2 : H_1 \rightarrow H_1$ operatörleri kompakt operatörlerdir.

Şimdi incelediğimiz (1)–(6) sınır değer geçiş problemine uygun S_1, S_2 operatörleri yardımı ile $S(u) := u + S_1 u$ olmak üzere $A(\lambda) u = S(u) - \lambda S_2 u$ ifadesini sağlayan operatör demetini tanımlayalım. Bu durumda $(\lambda, u(x))$ çifti özdeğer-özfonksiyon çifti ise o halde $A(-\lambda) u(x) = 0$ eşitliği sağlanır.

Tanım 9. [6] H Hilbert uzayı ve bu uzayda tanımlı bir A operatörü verilsin. Eğer A operatörü $\forall u \in H, u \neq 0$ için $\langle u, Au \rangle > 0$ eşitsizliğini sağlıyorsa, o halde A operatörüne H Hilbert uzayında pozitif tanımlı operatör denir.

Teorem 10. Öyle $\delta > 0$ reel sayısı vardır ki, her $\lambda > \delta$ reel sayısı için $A(-\lambda)$ operatörü H_1 Hilbert uzayında pozitif tanımlıdır.

KAYNAKLAR

- [1] Amara, Zh. Ben and A. A. Shkalikov, A.A. (1999). The Sturm-Liouville problem with physical and spectral parameters in the boundary condition, Math. Notes 66, 127–134.
- [2] Aydemir, K., Mukhtarov, O. Sh. (2017). Class of Sturm-Liouville problems with eigen-parameter dependent transmission conditions, Numerical Functional Analysis and Optimization, 38(10), 1260-1275.
- [3] Friedman, B. (1956). Principles and Techniques of Applied Mathematics, John Wiley and Sons New York.
- [4] Fulton, C. T. (1977). Two point boundary value problems with eigenvalue parameter contained in the boundary conditions. Proc. Roy. Soc. Edinburg, 77A, 293-308.
- [5] Gohberg, I.C. and Krein, M.G. (1969). Introduction to The Theory of Linear Non-Selfadjoint Operators, Translation of Mathematical Monographs, vol. 18, Amer. Math. Soc., Providence, Rhode Island.
- [6] Griffl, D.H. (2002). Applied Functional Analysis, Dover Publications, Inc., Mineola, New York.
- [7] Kaoullas, G. and Georgiou, G.C. (2015). Start-up and cessation Newtonian Poiseuille and Couette flows with dynamic wall slip, Meccanica, 50:1747–1760.
- [8] Kawano, A. and Morassi, A.. A Uniqueness Result On Detecting A Prey In A Spider Orb-Web, arXiv:1906.03610.
- [9] Kerimov, N.B., Poladov, R.G. (2012). Basis properties of the system of eigenfunctions in the Sturm–Liouville problem with a spectral parameter in the boundary conditions. ISSN 1064–5624. Doklady Math. 85(1), 8–13.
- [10] Ladyzhenskaia, O. A. (1985). The Boundary Value Problems Of Mathematical Physics, Springer-Verlag, New York.
- [11] Likov, A.V. and Mikhailov, Yu.A. (1963). The Theory Of Heat And Mass Transfer, Qosenergaizdat (Russian).

- [12] Mukhtarov, O.Sh., Olğar, H. and Aydemir, K. (2015). Resolvent Operator and Spectrum of New Type Boundary Value Problems, *Filomat*, 29:7, 1671-1680.
- [13] Nie, Y. and Linetsky, V. (2019). Sticky reflecting Ornstein-Uhlenbeck diffusions and the Vasicek interest rate model with the sticky zero lower bound. *Stochastic Models*, 1–19.
- [14] Olğar, H., Mukhtarov, O.Sh. and Aydemir, K. (2018). Some properties of eigenvalues and generalized eigenvectors of one boundary value problem, *Filomat*, 32:3, 911-920.
- [15] Sarsenbi, A.M., Tengaeva, A.A. (2012). On the basis properties of root functions of two generalized eigenvalue problems. ISSN 0012–2661. *Differ. Equ.* 48(2), 306–308.
- [16] Stakgold, I. (1971). *Boudary Value Problems of Mathematical Physics, II*, Macmillan Co., New York.
- [17] Tikhonov, A.N. and Samarskii, A.A. (1963). *Equations Of Mathematical Physics*, Oxford and New York, Pergamon.
- [18] Titchmars, E. C. (1962). *Eigenfunctions Expansion Associated with Second Order Differential Equations I*, second edn. Oxford Univ. press, London.
- [19] Voitovich, N.N., Katsenelbaum, B.Z. and Sivov, A.N. (1997). *Generalized Method Of Eigen-Vibration In The Theory Of Diffraction*, Nakua, Moskow. (Russian).
- [20] Yakubov, S. Y. (1994). *Completeness of root functions of regular differential operators*. Longman: Scientific and Technical.

OPERATOR-POLYNOMIAL TREATMENT OF A DISCONTINUOUS STURM-LIOUVILLE PROBLEM

Hayati OLĞAR

Gaziosmanpaşa University, Faculty of Arts and Science, Department of Mathematics,
Tokat, Turkey.

ORCID ID: <https://orcid.org/0000-0003-4732-1605>

ÖZET

Ayrık $[-1,0)$ ve $(0,1]$ aralıkları üzerinde

$$-f_1''(x, \lambda) + q_1(x)f_1(x, \lambda) = \lambda f_1(x, \lambda), \quad -1 < x < 0, \quad (1)$$

$$-f_2''(x, \lambda) + q_2(x)f_2(x, \lambda) = \lambda f_2(x, \lambda), \quad 0 < x < 1, \quad (2)$$

şeklinde tanımlı Sturm-Liouville denklemlerinden, $x=-1$ ve $x=1$ uç noktalarında verilmiş

$$\cos \alpha f_1(-1, \lambda) + \sin \alpha f_1'(-1, \lambda) = 0 \quad (3)$$

$$\cos \beta f_2(1, \lambda) + \sin \beta f_2'(1, \lambda) = 0 \quad (4)$$

sınır şartlarından ve $x=0$ süreksizlik noktasında verilmiş

$$f_1(-0, \lambda) - f_2(+0, \lambda) = 0 \quad (5)$$

$$f_1'(-0, \lambda) - f_2'(+0, \lambda) = a_1 f_1(-0, \lambda) + a_2 f_2(+0, \lambda) \quad (6)$$

geçiş şartlarından oluşan Sturm-Liouville tipindeki bir sınır değer geçiş problemini gözönüne alalım.

Burada λ kompleks spektral parametre, $q_1(x)$ ve $q_2(x)$ fonksiyonları sırasıyla $\Omega_1 := [-1, 0]$ ve $\Omega_2 := [0, 1]$ aralıkları üzerinde reel-değerli sürekli fonksiyonlar; a_1, a_2 reel değerli katsayılardır.

Bu çalışmanın temel amacı, (1)–(6) iki aralıklı sınır-değer-geçiş probleminin ürettiği ikinci mertebeden diferensiyel operatörlerin bazı spektral özelliklerinin incelenmesidir. Spektrumun asimptotik davranışlarının ve özfonksiyonlar sisteminin tamlık özelliklerinin araştırılması için bir operatör-teorik yöntem tanıtılacaktır. Bunun için (1)–(6) Sturm-Liouville problemine uygun Hilbert uzayı inşa edilmiştir. Daha sonra incelenecek olan (1)–(6) süreksiz sınır-değer-geçiş probleminin bir operatör-polinom denkleme indirgenebileceğini göz önünde bulundurarak uygun Sobolev uzaylarında bazı kendine eşlenik ve kompakt operatörler tanımlanacaktır. Son olarak bu operatör-demetinin kendine eşlenik ve λ özdeğer parametresinin mutlak değerce yeteri kadar büyük değerleri için pozitif olduğu ispat edilmiştir.

Anahtar Kelimeler: Çok-aralıklı Sturm-Liouville problemleri, zayıf özfonksiyonlar, geçiş şartları, operatör demeti.

ABSTRACT

The Sturm-Liouville theory is one of the most actual and extensively developing fields in theoretical and applied mathematics. Sturm-Liouville differential equation is a class of differential equation often encountered in solving partial differential equations of mathematical physics using the method of separation of variables. Its solutions define many of the well-known special functions, such as Bessel functions, Legendre polynomials, Chebyshev polynomials, or the various Hypergeometric functions arising in engineering and

science applications. The solutions of many problems in mathematical physics are involved in investigation of a spectral problem i.e., the investigation of the eigenvalues and corresponding eigenfunctions and the expansion of an arbitrary function in terms of eigenfunctions of a differential operator. The Sturm-Liouville problems with interior singularities have been studied in various formulations by many authors (see, for example [1,8] and references cited therein). In recent years there has been growing interest of discontinuous Sturm-Liouville problems with supplementary interaction conditions (so-called transmission conditions) (see, for example [1,4,11-13] and references cited therein). This kind of boundary-value problems appears in solving several classes of partial differential equations, particularly, in solving heat and mass transfer problems, in diffraction problems, in vibrating string problems when the string loaded additionally with point masses and in various type of physical transfer problems. Such properties as discreteness of the spectrum, coerciveness with respect to the spectral parameter, Abel basis property of a system of eigenfunctions and associated functions (so-called root functions), minimization principle of eigenvalues and etc. have been investigated in [8] and corresponding references cited therein.

The aim of this study is to investigate a many-interval Sturm-Liouville problem which consist of a many-interval Sturm-Liouville equation defined on two disjoint intervals with piecewise continuous potential under impulsive conditions (which are known by various names including interface conditions, jump conditions, transmission conditions, interface conditions etc.) and eigenparameter dependent boundary conditions. The problems with impulsive conditions have become an important area of research in recent years because of the needs of the modern technology, engineering, physics. Apart from being interesting in their own right, many-interval Sturm-Liouville problems have found numerous applications in various fields of science and technology. For example, they have recently been considered in the literature in connection with diverse areas, such as heat transfer [Belinskiy, Hiestand and Matthews, 2015], string theory [Gwak, Kim, Rey, 2016], fluid dynamics [Kaoullas and Georgiou, 2015], biology [Kawano and Morassi, 2019], mathematical finance [Nie and Linetsky, 2019] and quantum computing [Parra Rodriguez, Rico, Solano and Egusguiza, 2018]. Many of the mathematical problems encountered in the study of the boundary value transmission problems cannot be treated with the usual techniques within the standard framework of the boundary value problem. Naturally, solving of many-interval Sturm-Liouville problems including supplementary impulsive conditions are much more complicated to solve than classical Sturm-Liouville problems. For the background and applications the theory of boundary value transmission problems to different areas, we refer the reader to the monographs [10,16] and and some recent contribution [3,4,7,9,11,14].

Let us introduce to the consideration a new type Sturm-Liouville problem consisting of two-interval Sturm-Liouville equations

$$-f_1''(x, \lambda) + q_1(x)f_1(x, \lambda) = \lambda f_1(x, \lambda), \quad -1 < x < 0, \quad (1)$$

$$-f_2''(x, \lambda) + q_2(x)f_2(x, \lambda) = \lambda f_2(x, \lambda), \quad 0 < x < 1, \quad (2)$$

with boundary conditions

$$\cos \alpha f_1(-1, \lambda) + \sin \alpha f_1'(-1, \lambda) = 0 \quad (3)$$

$$\cos \beta f_2(1, \lambda) + \sin \beta f_2'(1, \lambda) = 0 \quad (4)$$

and with additional impulsive conditions

$$f_1(-0, \lambda) - f_2(+0, \lambda) = 0 \quad (5)$$

$$f_1'(-0, \lambda) - f_2'(+0, \lambda) = a_1 f_1(-0, \lambda) + a_2 f_2(+0, \lambda) \quad (6)$$

where λ is a complex spectral parameter, $q_1(x)$ and $q_2(x)$ are real-valued continuous functions in $\Omega_1 := [-1, 0]$ and $\Omega_2 := [0, 1]$ respectively; a_1, a_2 are real coefficients, $\alpha, \beta \in [0, 2\pi)$.

We define a new concept, the so-called generalized eigenfunction which is an generalization of a classical eigenfunction. Then we introduce to the consideration some compact operators such a way that the considered many-interval Sturm-Liouville problem can be reduced to the appropriate operator-polynomial equation in suitable functional space. By using these results we will establish some spectral properties of the considered many-interval Sturm-Liouville problem (1)–(6).

Keywords: Multi-interval Sturm-Liouville problems, weak eigenfunctions, transmission conditions, operator-pencil.

GİRİŞ

Ondokuzuncu yüzyılın ortalarında ilk olarak Sturm ve Liouville tarafından incelendiği için Sturm-Liouville problemi olarak adlandırılan, ikinci mertebeden adi diferansiyel denklemler için sınır-değer problemi günümüzde çok yoğun bir şekilde araştırılmış ve araştırılmaktadır. Başlangıçta, ısı iletimi problemlerine uygulanan Sturm-Liouville teorisinin daha sonra çok sayıda fiziksel problemlere uygulanabildiği görülmüştür. Diğer adıyla değişkenlerine ayırma yöntemi olarak da bilinen Fourier yönteminin uygulanması sonucunda birçok problem adi diferansiyel denklemler için sınır-değer problemine dönüştürülür. Ancak Fourier yönteminin esaslandırılması için elde edilen sınır-değer probleminin özfonksiyonlarının baz oluşturması ya da en azından, özfonksiyonların ve bu fonksiyonlara bağlanmış fonksiyonların tam olması gösterilmelidir. Matematik fiziğin birçok probleminin çözümünde kullanılan Fourier yöntemini uygulayabilmek için, verilmiş fonksiyonu adi diferansiyel denklemler için sınır-değer probleminin özfonksiyonları cinsinden açılımı şeklinde ifade etmek gerekir. Diğer bir ifadeyle adi diferansiyel denklem için sınır-değer probleminin özfonksiyonlarının hangi fonksiyon uzayında baz olduğunu incelemek gerekir. Bu soru beraberinde bir kaç problemin incelenmesini gerektirir. Bunlara özdeğerlerin asimptotik ifadelerinin bulunması, Green fonksiyonunun açılımının bulunması ve incelenmesi, rezolvent operatörünün bulunması, özfonksiyonlar sisteminin ve spektrumun asimptotik davranışlarının ve uygun özfonksiyonlar sisteminin tamlık özelliklerinin araştırılması için bir operatör-teorik yöntemin geliştirilmesi, genelleştirilmiş özfonksiyonlarının tanımlanması ve bu özfonksiyonların uygun Hilbert uzayında Riesz bazı oluşturması gibi özelliklerinin incelenmesi ve normunun değerlendirilmesi v.b. gösterilebilir.

[17] nolu çalışmada Walter, hem denkleminde hem de sınır şartlarının her ikisinde özdeğer parametresi bulunduran ikinci mertebeden adi diferansiyel denklem için sınır değer probleminin uygun Hilbert uzayında kendine eşlenik lineer operatörlerle bağlantısını kurmuş ve bu tip problemlerin operatör teorik yorumunu vermiştir. [5] nolu çalışmada Fulton, bu tipten problemlerin araştırılmasında Titchmarsh' ın [16] kitabındaki klasik yöntemlerin de uygulanabileceğini göstermiştir. Mukhtarov ve ark. [4,8,12,13] süreksizlik noktasına sahip ve sınır şartlarında özdeğer parametresi bulunduran süreksiz katsayılı sınır-değer-geçiş problemleri üzerine çalışmalar yapmışlardır. Ladyzhenskaia [10] daki çalışmasında bir Hilbert uzayında genelleştirilmiş çözümler kavramı yardımıyla, özdeğer probleminin bir operator denkleme indirgenmesine olanak sağlamıştır. Belinskiy ve ark. [3] deki çalışmalarında sınır şartlarının sadece bir tanesinde özdeğer parametresi bulunduran bir sınır-değer problemini

incelemişlerdir. Bu çalışmada ayrıca Hilbert uzayında bu sınıftan problemlerin özfonksiyonların Riesz bazı oluşturduğunu göstermişlerdir.

(1) – (6) PROBLEMİNE UYGUN HİLBERT UZAYLARININ KURULMASI VE GENELLEŞTİRİLMİŞ ÇÖZÜM KAVRAMININ TANIMLANMASI

Çeşitli tipten sınır değer problemlerinin spektral özelliklerinin araştırılmasında standart $L_2(\Omega), W_2^k(\Omega)$ Hilbert uzayları önemli bir rol oynamaktadır.

Ω , reel sayılar kümesinin herhangi bir sınırlı alt aralığı olsun. $L_2(\Omega)$ ile Ω aralığında karesi integrallenebilir kompleks değerli fonksiyonların klasik Lebesgue uzayını göstereceğiz. Bu uzayda tanımlı iç çarpımı ve karşılık gelen normu sırasıyla

$$\langle f, g \rangle_{L_2(\Omega)} = \int_{\Omega} f(x) \overline{g(x)} dx \quad \text{ve} \quad \|f\|_{L_2(\Omega)} = \sqrt{\langle f, f \rangle_{L_2(\Omega)}} \quad (7)$$

eşitlikleri ile tanımlayacağız.

$W_2^m(\Omega)$ ile Ω aralığında Lebesgue anlamında ölçülebilir olan ve $g'(x), g''(x), \dots, g^{(m)}(x)$ genelleştirilmiş türevleri bulunan ve her $k = 1, 2, \dots, m$ için $g^{(k)} \in L_2(\Omega)$ olan fonksiyonlarından oluşan Sobolev uzayını göstereceğiz. Bu uzay üzerinde tanımlı iç çarpımı

$$\langle f, g \rangle_{W_2^m(\Omega)} = \sum_{k=0}^m \langle f^{(k)}, g^{(k)} \rangle_{L_2(\Omega)} \quad (8)$$

eşitliği ile tanımlayacağız ($W_2^0(\Omega) := L_2(\Omega)$).

Bu çalışmada aşağıdaki gösterimlerden istifade edeceğiz. $\Omega_1 = [-1, 0), \Omega_2 = (0, 1]$ ve $\Omega = \Omega_1 \cup \Omega_2$,

$$f(x) = \begin{cases} f_1(x), & x \in \Omega_1 \\ f_2(x), & x \in \Omega_2 \end{cases}, \quad g(x) = \begin{cases} g_1(x), & x \in \Omega_1 \\ g_2(x), & x \in \Omega_2 \end{cases}, \quad q(x) = \begin{cases} q_1(x), & x \in \Omega_1 \\ q_2(x), & x \in \Omega_2 \end{cases}.$$

$L_2(\Omega), W_2^k(\Omega)$ uzayları ve yukarıdaki gösterimlerden yararlanarak (1) – (6) sınır-değer-geçiş problemine uygun $\oplus L_2(\Omega) = L_2(\Omega_1) \oplus L_2(\Omega_2)$, $W_2^1(\Omega) = W_2^1(\Omega_1) \oplus W_2^1(\Omega_2)$ ve $W_{2,q}^1(\Omega) = W_{2,q}^1(\Omega_1) \oplus W_{2,q}^1(\Omega_2)$ Hilbert uzaylarının direkt toplamalarında tanımlı olan iç çarpımları ve bu iç çarpımlara karşılık gelen normaları sırası ile aşağıdaki şekilde tanımlayacağız.

$$\langle f, g \rangle_{\oplus L_2(\Omega)} = \int_{\Omega_1} f_1(x) \overline{g_1(x)} dx + \int_{\Omega_2} f_2(x) \overline{g_2(x)} dx \quad (9)$$

$$\langle f, g \rangle_{\oplus W_2^1(\Omega)} = \int_{\Omega_1} \{f_1(x) \overline{g_1(x)} + f_1'(x) \overline{g_1'(x)}\} dx + \int_{\Omega_2} \{f_2(x) \overline{g_2(x)} + f_2'(x) \overline{g_2'(x)}\} dx \quad (10)$$

$$\langle f, g \rangle_{\oplus W_{2,q}^1(\Omega)} = \int_{\Omega_1} \{q_1(x) f_1(x) \overline{g_1(x)} + f_1'(x) \overline{g_1'(x)}\} dx + \int_{\Omega_2} \{q_2(x) f_2(x) \overline{g_2(x)} + f_2'(x) \overline{g_2'(x)}\} dx \quad (11)$$

$$\|f\|_{\oplus L_2(\Omega)} = \sqrt{\langle f, f \rangle_{\oplus L_2(\Omega)}}, \quad \|f\|_{\oplus W_2^1(\Omega)} = \sqrt{\langle f, f \rangle_{\oplus W_2^1(\Omega)}}, \quad \|f\|_{\oplus W_{2,q}^1(\Omega)} = \sqrt{\langle f, f \rangle_{\oplus W_{2,q}^1(\Omega)}} \quad (12)$$

Teorem 1. $\|f\|_{\oplus W_2^1(\Omega)}$ ve $\|f\|_{\oplus W_{2,q}^1(\Omega)}$ normları denktir.

Keyfi $\kappa \in \oplus W_2^1(\Omega)$ fonksiyonunu alalım ve $\bar{\kappa}$ fonksiyonu da κ fonksiyonunun kompleks eşleneği olsun. (1) – (2) diferensiyel denklemlerinin her iki tarafını $\bar{\kappa}$ eşlenik fonksiyonu ile çarparak $\Omega_i (i = 1, 2)$ aralıklarında integrallerini aldıktan sonra (3) – (6) sınır-geçiş şartlarını uygulayarak gerekli düzenlemeleri yaparsak

$$\begin{aligned} & \langle f, \kappa \rangle_{\oplus W_{2,q}^1(\Omega)} - \cot \alpha f_1(-1) \overline{\kappa_1(-1)} + \cot \beta f_2(1) \overline{\kappa_2(1)} + a_1 f_1(-0) \overline{\kappa_2(+0)} + a_2 f_2(+0) \overline{\kappa_2(+0)} \\ & = \lambda \langle f, \kappa \rangle_{\oplus L_2(\Omega)} \end{aligned} \quad (14)$$

eşitliğini elde ederiz.

Tanım 2. $f(x) \in \oplus W_2^1(\Omega)$ elemanı verilsin. Eğer (14) denklemi $\forall \kappa \in \oplus W_2^1(\Omega)$ için sağlanıyorsa $f(x) \in \oplus W_2^1(\Omega)$ fonksiyonu (1)–(6) sınır-değer-geçiş probleminin genelleştirilmiş çözümü olarak adlandırılır.

Teorem 3. (1)–(6) sınır-değer-geçiş probleminin her klasik $f \in \oplus W_2^2(\Omega)$ çözümü aynı zamanda bir genelleşmiş çözümdür.

Not : Bu teoremin tersi her zaman doğru değildir.

ESAS SONUÇLAR

Teorem 4.

$$-\cot \alpha f_1(-1) \overline{\kappa_1(-1)} + \cot \beta f_2(1) \overline{\kappa_2(1)} + a_1 f_1(-0) \overline{\kappa_2(+0)} + a_2 f_2(+0) \overline{\kappa_2(+0)} := \langle L_1 f, \kappa \rangle_{\oplus W_{2,q}^1(\Omega)} \quad (15)$$

eşitliği ile tanımlı L_1 operatörü $\oplus W_2^1(\Omega)$ Hilbert uzayında kendine eşlenik ve kompakt operatördür.

Teorem 5.

$$\langle f, \kappa \rangle_{\oplus L_2(\Omega)} := \langle L_2 f, \kappa \rangle_{\oplus W_{2,q}^1(\Omega)} \quad (16)$$

eşitliği ile tanımlı L_2 operatörü $\oplus W_2^1(\Omega)$ Hilbert uzayında kendine eşlenik, pozitif ve kompakt operatördür.

$\oplus W_2^1(\Omega)$ Hilbert uzayında sırasıyla

$$P(f) = f + L_1 f, \quad (17)$$

$$T(\lambda) f = P(f) - \lambda L_2 f \quad (18)$$

kuralları ile P operatörünü ve $T(\lambda)$ operatör-polinomunu tanımlayalım.

Teorem 6. $\lambda_0 \in \square$ nin yeterince büyük pozitif değerleri için $T(-\lambda_0)$ operatör-polinomu pozitif tanımlıdır.

Teorem 7. $\forall \lambda_0 \in \square$ için $T(-\lambda_0)$ operatörü kendine-eşleniktir.

Teorem 8. $\oplus W_2^1(\Omega)$ Hilbert uzayında

$$\chi(\lambda_0) = (T(-\lambda_0))^{-\frac{1}{2}} O_2 (T(-\lambda_0))^{-\frac{1}{2}} \quad (19)$$

biçiminde tanımlı $\chi(\lambda_0)$ operatörü pozitif, kendine-eşlenik ve kompakt operatördür.

Teorem 9. $f(x)$, (1)–(6) sınır-değer-geçiş probleminin herhangi bir özfonksiyonu olsun. Bu takdirde $g(x) = T(\lambda_0)f$ fonksiyonu $\chi(\lambda_0)$ operatörünün bir özelementidir.

KAYNAKLAR

- [1] Aydemir, K. and O. Sh. Mukhtarov, O.Sh. (2013). Green's Function Method for Self-Adjoint Realization of Boundary-Value Problems with Interior Singularities, Abstract and Applied Analysis, vol. 2013, Article ID 503267, 7 pages.
- [2] Belinskiy, B.P., Hiestand, J.W. and Matthews, J.V. (2015). Piecewise Uniform Optimal Design Of A Bar With An Attached Mass, Electronic Journal of Differential Equations, Vol. 2015, No. 206, pp. 1–17.
- [3] Belinskiy, B.P. and Dauer, J.P. (1997). On a regular Sturm - Liouville problem on a finite interval with the eigenvalue parameter appearing linearly in the boundary

conditions, Spectral theory and computational methods of Sturm-Liouville problem. Eds. D. Hinton and P. W. Schaefer, 1997.

[4] Binding, P.A, Browne, P.J., and Seddighi, K. (1993). Sturm-Liouville problems with eigenparameter dependent boundary conditions, *Proc. Edinburgh Math. Soc.*, 37(2), 57-72.

[5] Fulton, C.T. (1977). Two-point boundary value problems with eigenvalue parameter contained in the boundary conditions, *Proc. R. Soc. Edinburgh*, A77, 293-308.

[6] Gwak, S., Kim, J., Rey, S.J. (2016). Massless and massive higher spins from anti-de Sitter space waveguide, *Journal of High Energy Physics*, volume 2016, Article number: 24.

[7] Kaoullas, G. and Georgiou, G.C. (2015). Start-up and cessation Newtonian Poiseuille and Couette flows with dynamic wall slip, *Meccanica*, 50:1747–1760.

[8] Kandemir, M., Mukhtarov, O. Sh. (2017). Nonlocal Sturm-Liouville problems with integral terms in the boundary conditions, *Electronic Journal of Differential Equations*, Vol. 2017, No. 11, pp. 112. 2017.

[9] Kawano, A. and Morassi, A.. A Uniqueness Result On Detecting A Prey In A Spider Orb-Web, *arXiv:1906.03610*.

[10] Ladyzhenskaia, O. A. [1985]. *The Boundary Value Problems Of Mathematical Physics*, Springer-Verlag, New York.

[11] Mukhtarov, O. Sh, Olğar, H.; Aydemir, K. (2015). Resolvent Operator and Spectrum of New Type Boundary Value Problems. *Filomat* 29, 1671–1680

[12] Mukhtarov, O. Sh, Olğar, H., Aydemir, K., Jabbarov I. (2018). Operator-Pencil Realization Of One Sturm-Liouville Problem With Transmission Conditions. *Applied And Computational Mathematics*, 17(2), 284-294.

[13] Olğar, H., Mukhtarov, O.Sh. and Aydemir, K. (2018). Some properties of eigenvalues and generalized eigenvectors of one boundary value problem, *Filomat*, 32:3, 911-920.

[14] Nie, Y. and Linetsky, V. (2019). Sticky reflecting Ornstein-Uhlenbeck diffusions and the Vasicek interest rate model with the sticky zero lower bound. *Stochastic Models*, pages 1–19.

[15] Parra Rodriguez, A., Rico, E., Solano, E. and Egusguiza, I.L. (2018). Quantum Networks in Divergence-free Circuit QED, *Quantum Sci. Technol.* 3 (2018), no. 2, 024012, 46pp, *arXiv:1711.108817*.

[16] Titchmarsh, E. C., 1962. *Eigenfunctions Expansion Associated with Second Order Differential Equations I*, second edn. Oxford Univ. press, London.

[17] Walter, J. (1973). Regular eigenvalue problems with eigenvalue parameter in the boundary conditions. *Math. Z.* 133, 301-312.

DISCRETENESS OF THE SPECTRUM AND RIESZ BASISITY OF THE WEAK EIGENFUNCTIONS FOR MANY-INTERVAL STURM-LIOUVILLE PROBLEMS

Hayati OLĞAR

Gaziosmanpasa University, Faculty of Arts and Science, Department of Mathematics,
Tokat, Turkey.

ORCID ID: <https://orcid.org/0000-0003-4732-1605>

Oktay Sh. MUKHTAROV

Gaziosmanpasa University, Faculty of Arts and Science, Department of Mathematics,
Tokat, Turkey.

Azerbaijan National Academy of Sciences, Institute of Mathematics and Mechanics, Baku,
Azerbaijan

ORCID ID: <https://orcid.org/0000-0001-7480-6857>

Kadriye AYDEMİR

Amasya University, Faculty of Arts and Science, Department of Mathematics,
Amasya, Turkey.

ORCID ID: <https://orcid.org/0000-0002-8378-3949>

ÖZET

Bu çalışmanın temel amacı, ikinci mertebeden diferensiyel operatörler için çok-aralıklı süreksiz sınır-değer-geçiş problemlerinin araştırılmasıdır. İlk önce incelediğimiz çok-aralıklı Sturm-Liouville probleminin operatör-polinom formülasyonu sunulmuştur. Daha sonra bu çok-aralıklı Sturm-Liouville problemi operatör-demet denkleminde indirgenmiştir. Ayrıca uygun Sobolev uzaylarında bazı kendine eşlenik lineer operatörler tanımlanmıştır. Özdeğer ve özfonksiyonların bazı özellikleri incelenmiştir. Özellikle, uygun Hilbert uzayında spektrumun diskret (kesik) olduğu ve zayıf özfonksiyonlar sisteminin bir Riesz bazı oluşturduğu kanıtlanmıştır.

Anahtar Kelimeler: Çok-aralıklı Sturm-Liouville problemi, zayıf özfonksiyon, geçiş şartı, Riesz bazı.

ABSTRACT

The separation of independent variables allows to reduce many problems of quantum mechanics, physical chemistry, engineering, elasticity, electromagnetics and other areas of mathematical physics to a Sturm-Liouville type boundary value problems. To justify the separation of variables method it is needed to establish the discreteness of the spectrum and the completeness of the system of eigenfunctions. One of the main sources of inspiration for the differential operators and its important branch, the Sturm-Liouville theory are initial and/or boundary value problems for partial differential equations arise in various type of mathematical physics problems. The foundations of this theory were laid down by J. C. F. Sturm and J. Liouville in the mid-19th century while studying heat conduction problems. Initially applied to heat conduction problems, the Sturm-Liouville Theory was later found to be applicable to many concrete problems apparing physics, biology, engineering, finance etc. The Sturm-Liouville Theory, which is known by their names because it was first discussed by them, maintains its usefulness until today. Numerous articles and books have been written on this field. As it is known, boundary-value problems consisting of second-order ordinary linear differential equations and self-adjoint boundary conditions are generally known as Sturm-Liouville problems. In the boundary-value problem, which is also referred to as the classical Sturm-Liouville problem, the boundary conditions do not depend on the eigenvalue

parameter. For detailed information about classical Sturm-Liouville problems, [2,7,14] can be consulted. It is known that the most suitable space for these problems is the Hilbert space of square integrable functions, that is the space $L_2[a, b]$. However, when the spectral parameter occurs not only in the differential equations, but also in the boundary conditions, $L_2[a, b] \oplus \mathbb{R}^N$ -type direct sum spaces are more appropriate instead of $L_2[a, b]$ space. Because in this case, boundary value problems can be reduced to eigenvalue problems for linear differential operators defined in $L_2[a, b] \oplus \mathbb{R}^N$ -type spaces [4,12,13,15]. Kostyuchenko and Shkalikov in [6] discuss an operator-differential equation in connection with oscillations of an elastic semi-infinite cylinder. They reduced the problem to an operator polynomial equation of the form $L(\lambda)\psi=0$, where $L(\lambda)=\sum_{i=0}^n \lambda^i A_i$. Here A_0 is bounded linear operator

and self-adjoint, A_1 and A_2 are compact and self-adjoint linear operators. Belinskiy and Dauer [3] have considered the weak (generalized) solutions of a regular Sturm-Liouville problem on a finite interval with the eigenvalue parameter appearing linearly in the boundary conditions. In this study we shall investigate a many-interval Sturm-Liouville problem consisting of the following a multi-interval second order differential equations

$$\begin{aligned} -y_1''(x) + q_1(x)y_1(x) &= \mu y_1(x), \quad x \in [a, a + \varepsilon) \\ -y_2''(x) + q_2(x)y_2(x) &= \mu y_2(x), \quad x \in (a + \varepsilon, b - \varepsilon) \\ -y_3''(x) + q_3(x)y_3(x) &= \mu y_3(x), \quad x \in (b - \varepsilon, b] \end{aligned}$$

subject to the boundary conditions at the end points $x=a$ and $x=b$ given by

$$\begin{aligned} \alpha_1 y_1(a) + \alpha_2 y_1'(a) &= 0 \\ \beta_1 y_3(b) + \beta_2 y_3'(b) &= 0 \end{aligned}$$

and four transmission conditions at two points of interaction $x=a+\varepsilon$ and $x=b-\varepsilon$, given

$$\begin{aligned} y_2((a+\varepsilon)^+) - y_1((a+\varepsilon)^-) &= 0 \\ y_2'((a+\varepsilon)^+) &= y_1'((a+\varepsilon)^-) + \gamma_1 y_1((a+\varepsilon)^-) + \delta_1 y_2((a+\varepsilon)^+) \\ y_3((b-\varepsilon)^+) - y_2((b-\varepsilon)^-) &= 0 \\ y_3'((b-\varepsilon)^+) &= y_2'((b-\varepsilon)^-) + \gamma_2 y_2((b-\varepsilon)^-) + \delta_2 y_3((b-\varepsilon)^+) \end{aligned}$$

by

where $\mu \in \mathbb{R}$ is an eigenvalue parameter; $q_1(x), q_2(x), q_3(x)$ are real-valued functions which are continuous in each of the intervals $\Omega_1 := [a, a + \varepsilon)$, $\Omega_2 := (a + \varepsilon, b - \varepsilon)$ and $\Omega_3 := (b - \varepsilon, b]$; $|\alpha_1| + |\alpha_2| \neq 0, |\beta_1| + |\beta_2| \neq 0$ and $\gamma_i, \delta_i (i=1,2)$ are non-zero and positive real numbers.

The main goal of this work is the analysis of the eigenvalues and weak eigenfunctions of a new type Sturm-Liouville problems (SLP's), the so called many-interval SLP's, which differs from the standard SLP's in that the Sturm-Liouville equation are defined on finite number non-intersecting subintervals and the boundary conditions are set not only at the endpoints, but also at finite number internal points of interaction (such type of boundary conditions are known by various names including transmission conditions, jump conditions, interface conditions, etc.). Note that many-interval SLP's involving additional transmission conditions have found many applications in various areas of mathematical physics, such as in heat and mass transfer problems, in vibrating string problems, in fluid dynamics etc. Naturally, spectral

analysis of many-interval SLP's are much more complicated to analysis than classical one-interval SLP's. In this study we present an operator-polynomial formulation of the considered many-interval SLP's. Namely, we introduced some self-adjoint linear operators such a way that the considered many-interval SLP's can be interpreted as operator-pencil equation. We found some properties of eigenvalues and weak eigenfunction. In particular, we proved that the spectrum is discrete and the system of weak eigenfunctions forms a Riesz basis in appropriate Hilbert space.

Keywords: Multi-interval Sturm-Liouville problems, weak eigenfunctions, transmission conditions, operator-pencil.

GİRİŞ

Bağımsız değişkenlere ayırma yöntemi, kuantum mekaniği, fiziksel kimya, mühendislik, elastikiyet, elektromanyetik ve matematiksel fiziğin birçok problemini Sturm-Liouville tipi sınır değer problemlerine indirgemeye imkan vermektedir. Diferensiyel operatörler teorisinin ve de onun önemli bir dalı olan Sturm-Liouville teorisinin en esaslı ilham kaynaklarından biri matematik fizik problemlerinde ortaya çıkan kısmi türevli diferensiyel denklemler için başlangıç sınır değer problemleridir. Bu teorisinin esasları, J. C. F. Sturm ve J. Liouville tarafından 19. yüzyılın ortalarında ısı iletimi problemleri incelenirken konulmuştur. Başlangıçta ısı iletimi problemlerine uygulanan Sturm-Liouville Teorisinin daha sonra çok sayıda fizik, biyoloji, mühendislik ve finans problemlerine uygulanabildiği görülmüştür. İlk olarak kendileri tarafından ele alındığı için isimleriyle anılan Sturm-Liouville Teorisi günümüze kadar güncelliğini korumakta olup bu alanla ilgili sayısız makale ve kitap yazılmıştır. Bilindiği gibi ikinci mertebeden adi lineer diferensiyel denklem

$$y''(x) + q(x)y(x) = \lambda y(x), \quad x \in [a, b] \quad (1)$$

ve kendine eşlenik sınır şartlarından

$$\alpha_1 y(a) + \alpha_2 y'(a) = 0 \quad (2)$$

$$\beta_1 y(b) + \beta_2 y'(b) = 0 \quad (3)$$

oluşan sınır-değer problemleri genel olarak Sturm-Liouville problemleri olarak bilinmektedir. Klasik Sturm-Liouville problemi olarak da ifade edilen (1) – (3) sınır-değer probleminde sınır şartları özdeğer parametresine bağlı değildir. Klasik Sturm-Liouville problemleri ile ilgili ayrıntılı bilgiler için [2,7,14] kaynaklarına başvurulabilir. Bu problemler için en uygun uzayın karesi Lebesgue anlamında integrallenebilir fonksiyonlardan oluşan $L_2[a, b]$ Hilbert uzayı olduğu bilinmektedir. Ancak özdeğer parametresi lineer olarak sınır şartlarında da ortaya çıktığında $L_2[a, b]$ uzayı yerine $L_2[a, b] \oplus \mathbb{C}^N$ tipindeki uzaylar daha uygundur. Çünkü bu durumda sınır değer problemleri $L_2[a, b] \oplus \mathbb{C}^N$ tipindeki uzaylarda tanımlanmış operatörler için özdeğer problemlerine indirgenebilir [4,12,13,15]. 1983 yılında yayınlamış olan çalışmada Kostyuchenko ve Shkalikov [6],

$$n=2 \text{ için } L(\lambda)\psi=0, \quad L(\lambda)=\sum_{i=0}^n \lambda^i A_i \quad (4)$$

formundaki operatör demetlerini incelemişlerdir. Kostyuchenko ve Shkalikov bu çalışmalarında, en az bir $c \in \mathbb{C}$ reel sayısı için $L(c)$ – nin pozitif tanımlı olduğunu kabul etmişlerdir. 1985 yılında yayınlamış olduğu kitabında Ladyzhenskaia [8], bir Hilbert uzayında genelleştirilmiş çözümler kavramı yardımıyla, özdeğer probleminin bir operatör polinomal denkleme indirgenmesine olanak sağlamıştır. B. P. Belinsky and J.P. Dauer [3] çalışmasında, sınır şartlarında özdeğer parametresi lineer olarak bulunan regüler Sturm-Liouville probleminin özfonksiyonlarını incelemişlerdir. Ancak yukarıda bahsettiğimiz bütün çalışmalarda Sturm-Liouville problemleri, geçiş şartları içermeyen sınır değer problemleri

için incelenmiştir. O. Sh. Mukhtarov' un [1,5,9-11] çalışmalarında ise süreksiz katsayılı adi ve kısmi türevli diferensiyel denklemler için sınır değer geçiş problemleri araştırılmıştır.

Bu çalışmanın temel amacı, standart Sturm-Liouville problemlerinden farklı olan ve çok-aralıklı Sturm-Liouville problemleri olarak da adlandırılan yeni tip Sturm-Liouville problemlerinin (SLP'ler) özdeğerlerinin ve özfonksiyonlarının analizidir. Bu yeni tip Sturm-Liouville problemlerinin standart SLP'lerinden farkı Sturm-Liouville denkleminin sonlu sayıda kesişmeyen alt aralıklar üzerinde tanımlanması ve sıçrama şartları, geçiş şartları ya da arayüz şartları olarak da isimlendirilen sınır şartlarının sadece uç noktalarda değil, aynı zamanda sonlu sayıda iç etkileşim noktalarında da verilmesidir. İlave geçiş şartlarını içeren çok-aralıklı SLP'lerin, ısı ve madde transferi problemleri, telin titreşimi problemleri, akışkanlar dinamiği vb. gibi matematiksel fiziğin çeşitli alanlarında birçok uygulama zemini bulduğuna dikkat edilmesi gerekmektedir. Doğal olarak, çok-aralıklı SLP'lerin spektral analizi, klasik tek-aralıklı SLP'lerin analizinden çok daha karmaşıktır.

Bu çalışmada;

$$-y_1''(x) + q_1(x)y_1(x) = \mu y_1(x), x \in [a, a + \varepsilon] \quad (5)$$

$$-y_2''(x) + q_2(x)y_2(x) = \mu y_2(x), x \in (a + \varepsilon, b - \varepsilon) \quad (6)$$

$$-y_3''(x) + q_3(x)y_3(x) = \mu y_3(x), x \in (b - \varepsilon, b] \quad (7)$$

şeklinde tanımlı Sturm-Liouville denklemlerinden, $x = a$ ve $x = b$ uç noktalarında verilmiş

$$\alpha_1 y_1(a) + \alpha_2 y_1'(a) = 0 \quad (8)$$

$$\beta_1 y_3(b) + \beta_2 y_3'(b) = 0 \quad (9)$$

sınır şartlarından ve $x = a + c$ ve $x = b - c$ süreksizlik noktalarında verilmiş

$$y_2\left((a + \varepsilon)^+\right) - y_1\left((a + \varepsilon)^-\right) = 0 \quad (10)$$

$$y_2'\left((a + \varepsilon)^+\right) = y_1'\left((a + \varepsilon)^-\right) + \gamma_1 y_1\left((a + \varepsilon)^-\right) + \delta_1 y_2\left((a + \varepsilon)^+\right) \quad (11)$$

$$y_3\left((b - \varepsilon)^+\right) - y_2\left((b - \varepsilon)^-\right) = 0 \quad (12)$$

$$y_3'\left((b - \varepsilon)^+\right) = y_2'\left((b - \varepsilon)^-\right) + \gamma_2 y_2\left((b - \varepsilon)^-\right) + \delta_2 y_3\left((b - \varepsilon)^+\right) \quad (13)$$

geçiş şartlarından oluşan Sturm-Liouville tipindeki bir sınır değer geçiş probleminin bazı spektral özellikleri incelendi. Burada λ kompleks spektral parametre, $q_1(x), q_2(x)$ ve $q_3(x)$ fonksiyonları sırasıyla $\Omega_1 := [a, a + \varepsilon), \Omega_2 := (a + \varepsilon, b - \varepsilon), \Omega_3 := (b - \varepsilon, b]$ aralıkları üzerinde reel-değerli sürekli fonksiyonlar; $|\alpha_1| + |\alpha_2| \neq 0, |\beta_1| + |\beta_2| \neq 0$ ve $\gamma_i, \delta_i (i = 1, 2)$ sıfırdan farklı ve pozitif reel katsayılardır.

Şimdi dikkate alınan (5)–(13) sınır-değer-geçiş problemini araştırmak için ihtiyaç duyulan bazı yeni Hilbert uzayları tanımlayacağız ve bu uzaylarda geçerli olan bazı eşitsizlikleri ifade edeceğiz. $\Omega := \Omega_1 \oplus \Omega_2 \oplus \Omega_3$ ve $\Xi_0 := \bigoplus_{i=1}^3 L_2(\Omega_i)$ verilsin.

$\Xi_1 := \{y \in \Xi_0 : y_i \in W_2^1(\Omega_i) (i = 1, 2, 3), y_2(a + \varepsilon) = y_1(a + \varepsilon), y_3(b - \varepsilon) = y_2(b - \varepsilon)\}$ lineer uzayında

$$\langle y, z \rangle_{\Xi_1} = \int_{\Omega_1} \{y_1' \overline{z_1'} + y_1 \overline{z_1}\} dx + \int_{\Omega_2} \{y_2' \overline{z_2'} + y_2 \overline{z_2}\} dx + \int_{\Omega_3} \{y_3' \overline{z_3'} + y_3 \overline{z_3}\} dx \quad (14)$$

eşitliği ile iç çarpımı ve bu iç çarpıma karşılık gelen normu $\|y\|_{\Xi_1}^2 = \langle y, y \rangle_{\Xi_1}$ eşitliği ile

tanımlayalım; burada $y(x) = \begin{cases} y_1(x), & x \in \Omega_1 \\ y_2(x), & x \in \Omega_2 \\ y_3(x), & x \in \Omega_3 \end{cases}$ göstermişiz. Ξ_1 iç çarpım uzayının Hilbert uzayı

olduğu kolayca gösterilebilir. Şimdi Ξ_1 Hilbert uzayında yeni bir iç çarpımı $\langle y, z \rangle_{\Xi_{1,q}} = \langle y', z' \rangle_{\Xi_0} + \langle y, qz \rangle_{\Xi_0}$ eşitliği ile ve bu iç çarpıma karşılık gelen normu ise

$\|y\|_{\Xi_{1,q}}^2 = \langle y, y \rangle_{\Xi_{1,q}}$ şeklinde tanımlayalım. $q(x)$ fonksiyonu sınırlı, pozitif tanımlı ve ölçülebilir olduğundan dolayı $0 < m < M$ olacak biçimde öyle m ve M sayıları mevcuttur ki, $\forall y \in \Xi_1$ için

$$m \|y\|_{\Xi_1} < \|y\|_{\Xi_{1,q}} < M \|y\|_{\Xi_1} \quad (15)$$

eşitsizliği sağlanır.

Keyfi $\eta \in \Xi_1$ kompleks fonksiyonu alalım ve $\bar{\eta}$ fonksiyonu da η fonksiyonunun kompleks eşleniği olsun. (5)–(7) diferensiyel denklemlerinin her iki tarafını $\bar{\eta}$ eşlenik fonksiyonu ile çarpıp sonra Ω_i ($i = 1, 2, 3$) aralıklarında integrallerini alalım.

$$\sum_{i=1}^3 \int_{\Omega_i} \left\{ -y_i''(x) + q_i(x) y_i(x) \right\} \bar{\eta}_i(x) dx = \sum_{i=1}^3 \int_{\Omega_i} \mu y_i(x) \bar{\eta}_i(x) dx \quad (16)$$

Elde ettiğimiz (16) denkleminin sağındaki ilk terime kısmi integrasyon uygularsak

$$\begin{aligned} & \sum_{i=1}^3 \int_{\Omega_i} \left\{ y_i'(x) \bar{\eta}_i'(x) + q_i(x) y_i(x) \bar{\eta}_i(x) \right\} dx - y_3'(b) \bar{\eta}_3(b) + y_1'(a) \bar{\eta}_1(a) + y_2'(a+\varepsilon) \bar{\eta}_2(a+\varepsilon) \\ & - y_1'(a+\varepsilon) \bar{\eta}_1(a+\varepsilon) + y_3'(b-\varepsilon) \bar{\eta}_3(b-\varepsilon) - y_2'(b-\varepsilon) \bar{\eta}_2(b-\varepsilon) \\ & = \mu \sum_{i=1}^3 \int_{\Omega_i} y_i(x) \bar{\eta}_i(x) dx \end{aligned} \quad (17)$$

elde edilir. (8)–(13) sınır-geçiş şartlarını (17) ya uyguladıktan sonra düzenlersek

$$\begin{aligned} & \langle y, \eta \rangle_{\Xi_{1,q}} + \frac{\beta_1}{\beta_2} y_3(b) \bar{\eta}_3(b) - \frac{\alpha_1}{\alpha_2} y_1(a) \bar{\eta}_1(a) + [\gamma_1 y_1(a+\varepsilon) + \delta_1 y_2(a+\varepsilon)] \bar{\eta}_2(a+\varepsilon) \\ & + [\gamma_2 y_3(b-\varepsilon) + \delta_2 y_2(b-\varepsilon)] \bar{\eta}_3(b-\varepsilon) = \mu \langle y, \eta \rangle_{\Xi_0} \end{aligned} \quad (18)$$

eşitliği elde edilir. Böylece (17) eşitliği bütün terimleri Ξ_1 uzayının elemanları olan (18) ile temsil edilen bağıntıya dönüşür. Şimdi Ξ_1 Hilbert uzayında (5)–(13) sınır-değer-geçiş problemimize uygun zayıf çözümü tanımlayabiliriz.

Tanım 1. $y(x) \in \Xi_1$ elemanı verilsin. Eğer (18) denklemi $\forall \eta(x) \in \Xi_1$ için sağlanıyorsa $y(x) \in \Xi_1$ elemanı (5)–(13) sınır-değer-geçiş probleminin zayıf çözümü olarak adlandırılır.

SINIR-DEĞER-GEÇİŞ PROBLEMİNİN OPERATÖR-DEMETİ DENKLEMİNE İNDİRGENMESİ VE ESAS SONUÇLAR

Çalışmanın bundan sonraki kısmında aşağıdaki fonksiyonlardan yararlanılacaktır.

$$\begin{aligned} \tau_1(y, \eta) := & \frac{\beta_1}{\beta_2} y_3(b) \overline{\eta_3(b)} - \frac{\alpha_1}{\alpha_2} y_1(a) \overline{\eta_1(a)} + [\gamma_1 y_1(a + \varepsilon) + \delta_1 y_2(a + \varepsilon)] \overline{\eta_2(a + \varepsilon)} \\ & + [\gamma_2 y_3(b - \varepsilon) + \delta_2 y_2(b - \varepsilon)] \overline{\eta_3(b - \varepsilon)} \end{aligned} \quad (19)$$

$$\tau_2(y, \eta) := \sum_{i=1}^3 \int_{\Omega_i} y_i(x) \overline{\eta_i(x)} dx \quad (20)$$

Teorem 2. Verilen her bir $y(x) \in \Xi_1$ için $\tau_i(y, \eta) (i = 1, 2)$ fonksiyonları $\eta(x) \in \Xi_1$ değişkenine göre lineerdir.

Riesz temsil teoreminden yararlanarak $\tau_i(y, \eta) := \langle T_i y, \eta \rangle_{\Xi_{1,q}} (i = 1, 2)$ eşitliğini sağlayacak

$T_i : \Xi_1 \rightarrow \Xi_1 (i = 1, 2)$ operatörlerini tanımlayabiliriz.

Teorem 3. $T_1 : \Xi_1 \rightarrow \Xi_1$ ve $T_2 : \Xi_1 \rightarrow \Xi_1$ kendine eşlenik ve kompakt operatörlerdir.

Teorem 4. $T_2 : \Xi_1 \rightarrow \Xi_1$ operatörü pozitif operatördür.

Teorem 3. ve Teorem 4. gereği (18) ile verilen integral özdeşliği

$$\langle y, \eta \rangle_{\Xi_{1,q}} + \langle T_1 y, \eta \rangle_{\Xi_{1,q}} = \mu \langle T_2 y, \eta \rangle_{\Xi_{1,q}} \quad (21)$$

şeklinde yazılır. Eğer $y(x) \in \Xi_1$, (5)–(13) sınır-değer-geçiş probleminin zayıf bir çözümü ise bu takdirde (21) ifadesi $\forall \eta(x) \in \Xi_1$ için sağlanır. Yani Ξ_1 Hilbert uzayından alınan keyfi η değişkeni için (21) ifadesinin $y + T_1 y = \mu T_2 y$ lineer denklemi şeklinde yazılabileceğini söylemektedir.

Teorem 5. (5)–(13) sınır-değer-geçiş probleminin zayıf özfonksiyonları, Ξ_1 Hilbert uzayında

$$T(\mu) y(x) = 0, \quad T(\mu) = I + T_1 - \mu T_2 \quad (22)$$

operatör-polinom denklemini sağlar.

Teorem 6. $\forall \mu_0 \in \mathbb{C}$ için $T(-\mu_0)$ operatörü kendine-eşleniktir.

Teorem 7. (5)–(13) sınır-değer-geçiş probleminin zayıf özfonksiyonlar sistemi, Ξ_1 Hilbert uzayında Riesz bazı oluşturur.

KAYNAKLAR

- [1] Aydemir, K., Mukhtarov, O. Sh. (2017). Class of Sturm-Liouville problems with eigen-parameter dependent transmission conditions, Numerical Functional Analysis and Optimization, 38(10), 1260-1275.
- [2] Atkinson, F. V. (1964). Discrete and Continuous Boundary Problems, Academic Press, New York.
- [3] Belinsky, B. P. and Dauer, J. P. (1997). On a Regular Sturm-Liouville Problem on a Finite Interval with the Eigenvalue Parameter Appearing Linearly in the Boundary Conditions, Lecture Notes in Pure and Applied Mathematics, 191, Spectral Theory and Computational Methods of Sturm-Liouville Problems, 183–196.
- [4] Hinton, D. B. (1979). An Expansion Theorem for an Eigenvalue Problem with Eigenvalue Parameter in the Boundary Conditions, Quart J. Math. Oxford (2), 33-42.
- [5] Kandemir, M., Mukhtarov, O. Sh. (2017). Nonlocal Sturm-Liouville problems with integral terms in the boundary conditions, Electronic Journal of Differential Equations, Vol. 2017, No. 11, pp. 112. 2017.

- [6] Kostyuchenko, A. G. and Shkalikov, A. A. (1983). Self-adjoint Quadratic Operator Pencils and Elliptic Problems, *Functional Anal. Appl.* 17, 109.
- [7] Levitan, B. M. and Sargsyan, I. S. (1988) .*Sturm-Liouville and Dirac Operators* [in Russian], Nauka, Moscow.
- [8] Ladyzhenskaia, O. A. (1985). *The Boundary Value Problems of Mathematical Physics*, Springer – Verlag, New York.
- [9] Muhtarov, O. Ş. (1994) .Discontinuous Boundary Value Problem with Spectral Parameter in Boundary Condition, *Tr.J. of Mathematics*, 18, 183-192.
- [10] Mukhtarov, O. Sh, Olğar, H.; Aydemir, K. (2015). Resolvent Operator and Spectrum of New Type Boundary Value Problems. *Filomat* 29, 1671–1680.
- [11] Mukhtarov, O. Sh, Olğar, H.; Aydemir, K. Jabbarov I. (2018). Operator-Pencil Realization Of One Sturm-Liouville Problem With Transmission Conditions. *Applied And Computational Mathematics*, 17(2), 284-294.
- [12] Russakovskii, E. M. (1993). Sturm-Liouville problem with parameter in the boundary conditions, *Trudy Seminara imeni I. G. Petrovskogo*, 18.
- [13] Schneider, A. (1974). A Note on Eigenvalue Problems with Eigenvalue Parameter in the Boundary Conditions, *Math. Z.* 136, 163-167.
- [14] Titchmars, E. C. (1962). *Eigenfunctions Expansion Associated with Second Order Differential Equations I*, Second Edn. Oxford Univ. press, London.
- [15] Walter, J. (1973). Regular Eigenvalue Problems with Eigenvalue Parameter in the Boundary Conditions, *Math. Z.*, 133, 301-312.

3-D MHD FLOW OF NON-NEWTONIAN HYBRID NANOLIQUID ABOVE A STRETCHING SURFACE

Dr. G.P. Ashwinkumar

Department of Mathematics, Vijayanagara Sri Krishnadevaraya University, Bellary, India.

P. Nanda

Department of Mathematics, Vijayanagara Sri Krishnadevaraya University, Bellary, India.

Abstract

Three-dimensional unsteady magnetohydrodynamic stagnancy flow of hybrid nanoliquid, with nonlinear radiation and uneven heat rise/sag, is studied hypothetically. We considered Fe_3O_4 /graphene nanoparticles embedded in water. The physical problem is modelled mathematically and resolved using Runge–Kutta Fourth order with a shooting procedure. Influences of pertinent parameters on the flow and energy transport are noted numerically and graphically. Moreover, the wall friction and the local Nusselt number are computed and a comparative analysis of nano/hybrid nanofluids is performed with the help of streamlines and isotherms. It is found that the drive and energy transport of nano/hybrid nanofluid is highly influenced by the variation in the particle volume fraction as well as unsteadiness factor. Also, the average temperature of nanofluid in the saddle stagnation region is higher than that of hybrid nanofluid.

Keywords: Stagnation point; magnetohydrodynamic; hybrid nanofluid; uneven heat source/sink; nonlinear radiation.

SIGNIFICANCE OF THERMAL RADIATION ON MHD FLOW OF HYBRID NANOFLUID OVER A STRETCHING SURFACE

Dr. G.P. Ashwinkumar

Department of Mathematics, Vijayanagara Sri Krishnadevaraya University, Bellary, India.

B. Ranjana

Department of Mathematics, Vijayanagara Sri Krishnadevaraya University, Bellary, India.

Abstract

The pivotal aim of this research is to address the boundary layer analysis of two-dimensional unsteady hybrid nanofluid flow over a fat/slendering stretching surface. Thermal radiation and magnetohydrodynamic analysis are featured in this work. The transformed nonlinear ordinary differential equations are resolved using Runge–Kutta–Fehlberg technique. Then, a complete discussion of the influences of the flow regime on several thermofluidic parameters is presented. The significant outcome of the current investigation is that the increment in magnetic field and nanoparticle volume fraction parameters declines the skin friction. Furthermore, it is shown that when the radiation and the nanoparticle volume fraction are improved, the heat transfer rate triggers considerable evolution. The obtained results of this model closely match with those available in the literature as a limiting situation.

Keywords: Slendering stretching sheet, hybrid nanoliquid, MHD, Slip effects.

COMPORTAMIENTO DE LA CORROSIÓN DEL NANOCOMPUESTO AM60-ALN Y LA ALEACIÓN AM60 EXPUESTAS A UN AMBIENTE SIMULADO DE LLUVIA ÁCIDA

Luis Chávez

Centro de Investigación y de Estudios Avanzados del IPN (CINVESTAV)

Lucien Veleza

Centro de Investigación y de Estudios Avanzados del IPN (CINVESTAV)

Este trabajo de investigación compara la degradación del nanocompuesto AM60-AlN reforzado con 1% de nanopartículas de nitruro de aluminio (AlN) y de la aleación de magnesio AM60 al ser expuestas hasta 30 días en solución simulada de lluvia ácida (SAR). Distintas técnicas fueron empleadas para apoyar esta investigación entre ellas pruebas de inmersión, técnicas electroquímicas (OCP y EN) y métodos de caracterización superficial (SEM-EDS y XPS). La concentración de iones de Mg^{2+} liberados de la superficie del nanocompuesto fue menor que la aleación AM60. Debido al aumento en el tiempo del pH de la solución SAR, puede producirse una desaleación del Al, así como la formación de $Al(OH)_3$, según lo confirma XPS. Además, debido a la presencia de iones Cl^- en la solución SAR, se observó corrosión localizada, lo que sugiere un ruido Gaussiano fraccional con un proceso persistente y estacionario en el tiempo, de acuerdo con las pendientes de los gráficos de la densidad de potencia espectral (PSD) de las fluctuaciones de corriente.

Palabras Clave: Magnesio, Nitruro de aluminio, Corrosión, Nanocomposito, Lluvia acida, SEM-EDS, XPS

ACTIVIDAD ELECTROQUÍMICA DE LA MATRIZ METÁLICA EXTRUIDA AM60 EN UNA SOLUCIÓN QUE SIMULA EL AMBIENTE MARINO

Gerardo Sánchez

Departamento de Física Aplicada, Centro de Investigación y de Estudios Avanzados (CINVESTAV-IPN), Unidad Mérida, Yucatán, México

Luis Chávez

Departamento de Física Aplicada, Centro de Investigación y de Estudios Avanzados (CINVESTAV-IPN), Unidad Mérida, Yucatán, México

Lucien Veleza

Departamento de Física Aplicada, Centro de Investigación y de Estudios Avanzados (CINVESTAV-IPN), Unidad Mérida, Yucatán, México

Este estudio presenta el proceso de degradación de AM60, una aleación de Mg-Al propuesta para el uso en la construcción de automóviles, expuesta durante 14 días a una solución simulada de un ambiente marino. Los resultados de las pruebas de inmersión, cambio en el tiempo del potencial de corrosión (OCP) y de la superficie (SEM-EDS y XPS) han sido colaborados. El análisis de los datos obtenidos por EDS y XPS revela que sobre la superficie ha sido formada una película del $\text{Mg}(\text{OH})_2$, producto de corrosión principal y una menor cantidad de $\text{Al}(\text{OH})_3$. Después de la eliminación de las películas formadas, las imágenes SEM muestran ataques localizados, alrededor de las partículas intermetálicas de Al-Mn, con actividad catódica. El potencial de corrosión a circuito abierto se ha desplazado hacia valores más positivos, debido a la formación de la capa de productos, que actúa como una barrera física con el medio. Sin embargo, el cambio del pH de la solución y de la concentración de iones Mg^{2+} permiten corroborar una tendencia de aumento ligero de la velocidad de corrosión de AM60 en este ambiente marino, debido principalmente a la presencia de iones cloruros.

Palabras Clave: Aleaciones de Magnesio, Corrosión, Ambiente marino, Potencial de corrosión, iones de Mg^{+2} , pH.

POSSIBLE EFFECTS AFTER A COVID VACCINATION AT THE MOLECULAR AND CHEMICAL LEVEL FOR PATIENTS WITH CELIAC DISEASE

FELICIA ANDREI

University of Medicine and Pharmacy "Victor Babes", Faculty of Pharmacy, Department I, Piata
E. Murgu 2, 300041 Timisoara
Timiș County Emergency Clinical Hospital, 156 Liviu Rebreanu Boulevard, Timișoara 300723,
Romania

ANCA DRAGOMIRESCU

Timiș County Emergency Clinical Hospital, 156 Liviu Rebreanu Boulevard, Timișoara 300723,
Romania

ABSTRACT

A vaccination against the virus named COVID 19 is now available. Within a few months and intensive international research activities, a vaccine was developed which was first approved in the USA, Canada and then in England. In the EU, too, approval was given on December 21, 2020. There are currently three different active substances that differ from the vaccine type and producer.

Now, since weeks, many members of our celiac disease exchange groups are asking themselves or they are requesting the consultations of various medical specialists belonging to Metabolic Diseases and Diabetology, Gastroenterology, Allergology and Clinical Immunology, Internal and Family Medicine or even Clinical Pharmacists, whether the vaccine can be used for an autoimmune disease such as celiac disease (CD), or whether there is something against it. We have compiled currently available information, using also the existing patient database, adding the organic molecular study as a basis for further recommendations. The absolute novelty is the structural similarity of a part of the studied Gluten molecule (exorphin C and A5) with those of the Spike protein of the COVID 19 virus described in numerous dedicated articles. In addition, it appears that the cell attachment and penetration molecule is common in both cases.[1]

The conclusion of this study reveals that there are no globally known medical reasons to speak against the vaccine for an existing CD, on the contrary we can present the hypothesis of a bilateral benefit both in immunization against the pandemic agent of SAARS - COV 2 and in treating the difficult and often underdiagnosed celiac autoimmune disease.

KEY WORDS: Gluten, Exorphin, Celiac disease, Spike protein, COVID Vaccination

A REACTION DIFFUSION MODEL TO DESCRIBE THE TOXIN EFFECT ON THE FISH-PLANKTON POPULATION

Ouedraogo Hamidou

Department of mathematics,
Université JOSEPH KI ZERBO/ IBAM, OUAGADOUGOU

Abstract

This paper is aimed at the mathematical formulation, the analysis, and the numerical simulation of a prey-competitor-predator model by taking into account the toxin produced by the phytoplankton species. The mathematical study of the model leads us to have an idea on the existence of solution, the existence of equilibria, and the stability of the stationary equilibria. These results are obtained through the principle of comparison. Finally, the numerical simulations allowed us to establish a threshold of release of the toxin, above which we talk about the phytoplankton blooms.

keywords {Toxin effect, stability, bifurcation analysis, Pattern formation}

BIOMETRIC CHARACTERIZATION OF LOCAL GOATS FROM THE ARGAN GROVE OF AGADIR IN MOROCCO

Houda EL KHEYYAT

Biometrics and BioResources. Laboratory Biotechnologies and Valorization of Natural

Saïd EL MADIDI

Resources (BVRN). Faculty of Sciences, University Ibn Zohr, Agadir, Morocco

Abstract

A biometric study was carried out on 344 adult animals (318 females and 26 males), of three local goat breeds (Atlas, Barcha and Ghazalia) from the argan grove of Agadir province. 9 quantitative variables were used: height at the withers (HW), body length (BL), thorax depth (HD), chest circumference (CC), pelvic width (PW), ear length (EL), length horns (LH), height at the sacrum (HS), live weight (LW). 9 biometric indices were calculated: sub sternal gracefulness index (SSGI), atrial thorax index (ATI), body index (BI), height index (HI), relative thorax depth index (RHDI), proportionality index (PI), ear index (EI), body ratio (BR) and thoracic development (TD), in order to differentiate between races of the local population. The results showed a very significant difference and a high degree of heterogeneity between the races. Chest circumference, pelvic width, ear length and live weight were the most discriminating characteristics. Gender significantly influences all linear body measurements in this study. Biometric evidence suggesting the classification of the goats in the study area as an overall small, longiped, endomorphic body with a marked orientation for meat production. Statistical analysis of biometric traits will help define a goat breed morphological standard and guide genetic improvement programs.

Keywords: Biometrics - Local breed - Goat - Argan grove - Agadir.

ETHNOBOTANICAL STUDY AIMED AT INVESTIGATING THE USE OF MEDICINAL PLANTS OF APIACEE FAMILY IN THE NORTH REGION (MOROCCO)

NOUIOURA Ghizlane

Laboratoire des Substances Naturelles, Pharmacologie, Environnement, Modélisation, Santé & Qualité de Vie (SNAMEPEQ). Faculté des Sciences Dhar Mahraz, Université sidi Mohammed ben Abdellah, Fès, Maroc.

TOURABI Maryem

Laboratoire des Substances Naturelles, Pharmacologie, Environnement, Modélisation, Santé & Qualité de Vie (SNAMEPEQ). Faculté des Sciences Dhar Mahraz, Université sidi Mohammed ben Abdellah, Fès, Maroc.

DERWICH El houssine

Laboratoire des Substances Naturelles, Pharmacologie, Environnement, Modélisation, Santé & Qualité de Vie (SNAMEPEQ). Faculté des Sciences Dhar Mahraz, Université sidi Mohammed ben Abdellah, Fès, Maroc.

Abstract :

The ethnobotanical approach is based on the previous work by our research group, which consider the recommended standards for ethnopharmacological field studies. First, in order to locate informants, we made several visits to areas containing main population centers within the study area and administered closed questionnaires. These questionnaires contained questions regarding both the informant (including gender, age, education level, and family situation), and use of medicinal plants (vernacular name, therapeutic use, etc.). After analysis, using obtained data as a basis, we later developed both open and semi-structured interviews with informants. Other conventional methods of determining informant location, such as the snowball method and participant observation, were also followed.

The ethnobotany of Morocco has been comprised of a certain number of studies and publications with no particular relevance. This is especially true for those concerning the northern region of Morocco. Approaches to study ethnobotany, in the broadest sense of the term, have not been well developed. Further, data analysis has suffered from a lack of rigour due, in particular, to a lack of approved scientific methodologies for examining findings.

The aim of this study was to assess the knowledge and use of medicinal plants of apiacée family in the northern region of Morocco.

Keyword : apiacée family, therapeutic use, Ethnobotanical Study.

FISHERY, MORPHOMETRY AND MERISTIC COUNTS OF DECAPTERUS MACROSOMA (BLEEKER, 1851) OFF COCHIN COAST

U. Arun

Associate Professor, St. Peters College, Kolenchery, Kerala, India

Revathy R

Research Scholar, Department of Zoology, Nirmala College, Kerala, India

Abstract

Decapterus macrosoma (Short fin scad) constitutes an important element of the family Carangidae and one of the commercially exploited fish species off Cochin coast. Of the several species reported from the Indian waters, scad fisheries have much significance because it is used as food as well as bait. They are exploited mainly by diverse types of gears such as trawls and purse seines. The present study aimed to investigate fishery, morphometry and meristic counts of *D. macrosoma* along Cochin coast. The fishery study was conducted from April to December 2016 and the average catch-effort data by trawls was estimated at 3577.77 Kg and by purse seine, it was 1722.22 Kg. Period of peak abundance of fishery was estimated in the month of October-December (trawls: 4500- 5000Kg and purse seine: 2800Kg). The morphometric measurements of various body parts and meristic counts were studied by examination of 145 specimens ranging in size from 10.6 cm to 25 cm in total length and 10.99 gm to 102.7 gm in weight collected during October to November from Kalamukku fish landing centre. The linear relationship of the formula $y = bX + a$ were used for frame the growth pattern analysis. Twenty one morphometric and six meristic characters were analysed. Relation between the total length and other body measurements for the pooled data were subjected to multiple regression analysis using the software SPSS version 16.0. The observed results exhibited that various parameters show positive correlation with total length. From the present investigation, fin formula can be written as D: I, 13; V: 6-20; C: 26-40; A: 10-17. Meristic characters are remained constant and there is no change in meristic counts with the increase in body length.

Keywords: *Decapterus macrosoma*, Morphometry, Meristic, Multiple regression analysis.

USAGE POSSIBILITIES OF GREEN FODDER GERMINATED IN HYDROPONIC SYSTEM IN ANIMAL NUTRITION

Ezgi KARPUZ

Tekirdag Namik Kemal University Faculty of Agriculture, Dept. of Animal Science
Tekirdag/TURKEY

ORCID: 0000-0002-2470-3769

Kadir ERTEN

Tekirdag Namik Kemal University Faculty of Agriculture, Dept. of Animal Science
Tekirdag/TURKEY

ORCID: 0000-0002-6307-1573

Fisun KOC

Tekirdag Namik Kemal University Faculty of Agriculture, Dept. of Animal Science
Tekirdag/TURKEY

ORCID: 0000-0002-5978-9232

The increased livestock production has resulted in an increased demand for feeds and forage supply, where about 50-70% cost involvement with its feed supply attributing the forage and concentrates quality. Along with, the poor quality roughage e.g. straws comprises 90% of the cattle feed (Alçiçek et al., 2010) and grains comprises 50% of the total concentrate supply that bears high cost in the ruminant production. Therefore, quality improvement of existing feed resources and feeding green forage is necessary for the increased productivity of animals (Kılıç, 2016). Though the major constraints in production of green fodder by dairy farmers include unavailability of land for fodder cultivation due to small land holding size, more labor requirement and increasing labor cost for cultivation, more growth time, requirement of manure and fertilizer, uncertain rainfall, drought of water or saline water, natural calamities etc. (Naik et al., 2014). Hydroponic plant production is a cultivation system that provides the most suitable environment for seed germination and early plant growth, which is included in soilless agriculture technology. In this system, the grain germinated in a short time has high nutritional value and low cost. It provides alternative fresh green fodder to the farmers in all seasons of the year when the green grass needs for cattle and small cattle cannot be met from the pastures. Today, due to rapid industrialization and urbanization in Turkey and the world, there is a rapid decline in the availability of land for forage crops cultivation. This situation affects the productivity negatively because the green forage, which plays a major role in animal production, cannot be produced sufficiently. Therefore, the hydroponic method is an alternative green feed production method. In this method, hydroponic plants are grown using mineral nutrient solutions in a water solvent. It has been stated that feed production methods, which save more on soil and water, can show promising results to farmers, especially in arid regions (Indira et al., 2020). In literature studies, different forage plant species with hydroponic system; It has been reported that barley, oats, wheat, sorghum, alfalfa, cowpea and corn can be produced (Reddy et al., 1991; Snow et al., 2008; Al-Karaki and Al-Hashimi, 2012 Naik et al., 2012; Naik and Singh, 2013).

In the hydroponic farming system, it has been developed and arranged in a way to continuously supply fresh animal feed on a daily basis in closed growing rooms. The environmental conditions in the breeding rooms are controlled. Seeds with high germination are laid in specially prepared units and irrigated with timed automatic irrigation systems. According to the amount of fresh roughage that is targeted to be produced daily, production can be made in units of different sizes. In this system, the

systems that can produce 1 ton of fresh roughage per day are 4.6 x 11.6 x 2.3m in size, and 1377 liters of water and 18-40 kW of energy are needed per day (URL, 3). In this system, fresh feeds that reach 15-20 cm on the 7th day are taken from the units. The units are cleaned with water and the seeds are laid again and put into place. In the first application, the product is not taken in 7 days, but at the end of the 7th day, the product can be taken alternately every day. After the grains germinate, the roots take the appearance of carpet and the green part reaches 20-25 cm in 6-8 days. According to this, 6-10 times green feed can be obtained from the grains used (Kılıç, 2016).

Though, under tropical agroclimatic conditions maize, wheat and oat was suggested to be the best for hydroponic fodder production due to grain availability, fast growing nature and good biomass yield. However, limited research has been conducted on the feeding value of hydroponics fodder and the results are not consistent. Many researchers showed improved results in animal production (Tudor et al., 2003) while some researchers noticed no additional advantage in including hydroponic fodder in animal diets (Fazaeli et al., 2012). In this regard, first of all, studies should be carried out in which seeds with high germination ability are used and the cost is taken into account.

Keywords: Animal nutrition, hydroponic system, germination

Hidroponik Çimlendirilmiş Tohumların Hayvan Beslemede Kullanım Olanakları

1. GİRİŞ

Hidroponik bitki üretimi, topraksız tarım teknolojisi içerisinde yer alan tohumun çimlenmesi ve erken bitki gelişimine en uygun ortamın sağlandığı yetiştirme sistemidir. Bu sistemde kısa süre içerisinde çimlendirilen tahılın besin değeri yüksek, maliyeti düşüktür. Büyükbaş ve küçükbaş hayvanlar için yeşil ot ihtiyacının meralardan karşılanamadığı dönemlerde çiftçilere yılın her mevsiminde alternatif taze yeşil yem sağlar. Günümüzde, Türkiye’de ve Dünya’da hızlı sanayileşme ve kentleşme nedeniyle, yem bitkileri ekimi için arazi mevcudiyetinde hızlı düşüş yaşanmaktadır. Bu durum hayvansal üretimde büyük rol oynayan yeşil yemlerin yeterince üretilmemesi verimliliği olumsuz yönde etkilemektedir. Bu yüzden, hidroponik yöntem alternatif bir yeşil yem üretim metodudur. Bu metotta, bir su çözücü içinde mineral besin çözeltileri kullanarak topraksız bitki yetiştirmesi yapılmaktadır. Toprakta ve sudan daha fazla tasarruf sağlayan yem üretim yöntemleri, özellikle kurak bölgelerde çiftçilere umut verici sonuçlar gösterebileceği belirtilmiştir (İndira ve ark., 2020). Literatür çalışmalarında, hidroponik sistem ile farklı yem bitki türlerinin; arpa, yulaf, buğday, sorgum, yonca, börülce ve mısır üretiminin yapılabileceği bildirilmiştir (Reddy ve ark., 1991; Snow ve ark., 2008; Al-Karaki ve Al-Hashimi, 2012; Naik ve ark., 2012; Naik ve Singh, 2013).

2. HİDROPONİK ÜRETİMİN TARİHSEL GELİŞİMİ

Günümüzden 4000 yıl önceki Mısır kayıtlarında suda bitki yetiştirilmesinden bahsedilmektedir. Babil’in asma bahçeleri (Resim 1), Azteklerin ve Çinlilerin yüzen bahçeleri tarihte topraksız yetiştiriciliğe örnek olarak gösterilmektedir (Raviv ve ark., 2008).



Resim 1. Hidroponik üretim yapan Babil asma bahçeleri için kullanılan yapı (Anonim, 2020)

Bu sistemler ilk olarak 1699 yılında ilkel olarak İngiltere’de kullanılmıştır. Bitkilerin gelişimleri için gerekli mineralleri içeren bir çözelti ile durgun bir ortamda yetiştirilebileceği 1800’lerin ikinci yarısında ispatlanmıştır. 1860’lı yıllarda iki Alman araştırmacı besin çözeltisi içerisinde bitki yetiştiriciliğini gerçekleştirmiştir (Gül, 2008). Amerika’da, 1925-1935 yılları arasında topraksız yetiştiriciliğin uygulamaya aktarılması konusunda önemli gelişmeler kaydedilmiştir. İlk saha çalışması, Gericke tarafından 1937’de Kaliforniya Üniversitesinde besin çözeltisi içinde domates yetiştirilerek gerçekleştirilmiş ve bu tekniğe Yunanca su (hydro) ve çalışma (ponos) anlamına gelen iki kelimeden oluşan “hidroponik” (hydroponics) adı verilmiştir. Hidroponiğin ilk uygulanması ise, II. Dünya Savaşında, Pasifik Okyanusu’ndaki adalardaki askerlere taze sebze üretmek amacıyla su ve çakılın kullanılarak Amerikan ordusu tarafından gerçekleştirilmiştir (Gül, 2008).

3. HİDROPONİK ÜRETİMİN VERİMİ VE KALİTEYİ ETKİLEYEN FAKTÖRLER

Hidroponik sistemle üretilen filiz miktarı (verim) ve kalitesi aşağıdaki faktörlerden etkilenir;

Tahıl: Tahıl kalitesi, tahıl çeşidi ve tahıla uygulanan işlemler

Yetiştirme ortamı: Sıcaklık, nem ve küf oluşumu

Sistemin yönetimi: Su kalitesi ve pH, ısıtma süresi, besin kaynağı, tahıl katmanının derinliği, yoğunluğu ve büyüme süresi olarak sıralanabilir (Sneath ve McIntosh, 2003).

4. HİDROPONİK SİSTEMİN AVANTAJLARI

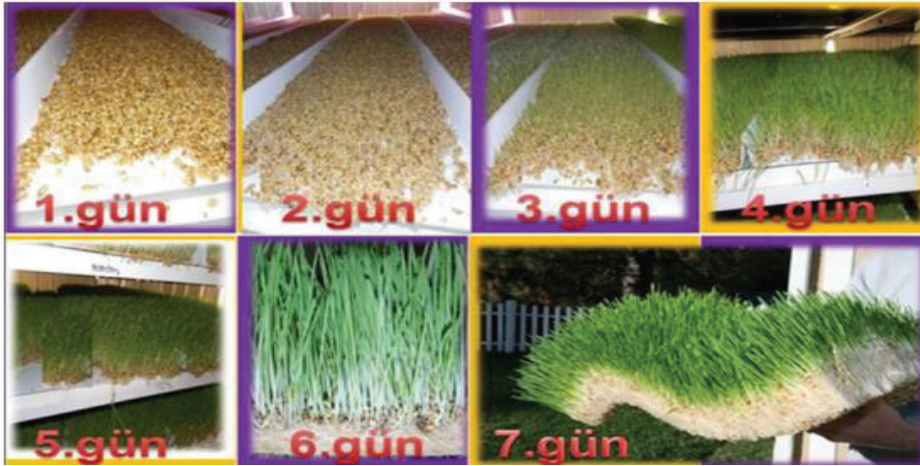
- Topraksızdır.
- İklim kontrolü sağlar.
- Su tasarrufu sağlar.
- Hızlı büyüme ve mahsul artışı sağlar.
- Besin maddelerinin etkin kullanımı sağlar.
- Daha iyi alan tahsisi olanağı sunar.
- pH'nın kontrolünü sağlar.
- Yabani ot zararlı veya toprakla ilgili hastalıklara rastlanmaz.
- Daha az tarımsal ilaç kullanımı sağlar.
- Emek ve zaman tasarrufu sağlar.
- Bitki atıklarının yakılmasını azaltır (Gaikwad, 2016).

5. HİDROPONİK SİSTEMİN DEZAVANTAJLARI

- Sistemi kurmak maliyetlidir.
- Üretim saha koşullarına göre sınırlıdır.
- Teknik bilgi gerektirir.
- Hastalık ve zararlılar hızla yayılabilir.
- Su bazlı mikro-organizma tehdidi.
- Sistem bütün bitkilerin üretimi için uygun değildir (Kılıç, 2016).

6. HİDROPONİK TARIM SİSTEMİNDE YEŞİL YEM ÜRETİM AŞAMALARI

Hidroponik tarım sisteminde kapalı yetiştirme odalarında günlük olarak sürekli taze hayvan yemi temin edecek şekilde geliştirilmiş ve düzenlenmiştir. Yetiştirme odalarında ortam şartları kontrollüdür. Çimlenmesi yüksek kaliteli tohumlar, özel hazırlanmış tavalara serilerek zaman ayarlı otomatik sulama sistemleri ile sulanır. Günlük üretilmesi hedeflenen taze kaba yem miktarına göre farklı ebatlarda tavalarda üretim olabilmektedir. Buna sistemde günde 1 ton taze kaba yem üretimi yapabilecek sistemler 4.6 x 11.6 x 2.3m ebatlarında olup, günde 1377 litre su ve 18-40 kw arasında enerjiye ihtiyaç duyulmaktadır (URL, 3). Bu sistemde 7. günde 15-20 santimetreye ulaşan yetişmiş taze yemler tavalardan alınır (Şekil 1). Tavalar suyla temizlenip tekrar tohum serilerek yerlerine sürülür. İlk uygulamada 7 günlük bir zamanda ürün alınmazken 7. günün sonunda münavebeli olarak her gün ürün alınabilmektedir. Taneler çimlendikten sonra kökler halı görünümünü alarak, 6-8 gün içerisinde yeşil aksam 20-25 cm boya ulaşmaktadır. Buna göre kullanılan tanelerin 6- 10 katı yeşil yem elde edilebilmektedir (Kılıç, 2016).



Şekil 1. Hidroponik tarım sisteminde kaba yem üretim aşamaları (URL, 3)

7. ÇİMLENDİRİLEN TAHILLARIN HAYVAN BESLEMEDE KULLANILMASI

Çimlendirilen tahılların filizleri ve kökleri; ruminant hayvanlar, atlar, tavuklar ve domuzda dahil olmak üzere birçok hayvanın beslenmesinde rahatlıkla kullanılabilir. (Kılıç, 2016).

7.1. Çimlendirilen Tahılların Ruminant Hayvanların Beslenmesinde Kullanımı

Hidroponik tarım sistemi ile yetiştirilmiş taze yemlerinin hayvanların refahına olumlu katkıları bulunduğu, yemin sindirilebilirliğini artırdığı, süt verimi (%8.7-10) ve sütteki yağ oranını (%14) artırdığı bilinmektedir (Sharif ve ark., 2013). Hastalıklara karşı direnci artırdığı, döl tutma oranını artırdığı bilinmektedir (Atıcı, 2012).

Tudor ve ark. 2003, sığırların beslenmesinde 15.4 kg ya da buna eşdeğer 1.8 kg kuru maddeyi (KM) karşılayacak kadar çimlendirilmiş taze yem verilmesinin hayvanların performansını iyileştirdiği bildirilmektedir. Aynı zamanda, çimlendirilmiş taze yemlerin sığırların beslenmesinde KM ihtiyacını karşılayabilecek oranda verilirse hayvanların performansını artırdığını bildirilmektedir Fazaeli ve ark. (2011)'nın, arpa çiminin buzağuların performansını etkisini değerlendirmek amacıyla yürüttükleri çalışmada sonunda çimlendirilmiş tahılda ağırlık, ham protein, gerçek protein, protein olmayan azot,

NDF, ADF, suda çözünür karbonhidratta artış, KM, organik madde ve lifsiz karbonhidrat oranında azalma olduğunu, yem dönüşüm oranında kontrol grubu ile beslenen buzağılarda çimlendirilmiş arpa içeren karma yeme göre daha yüksek olduğunu ve arpa çimi ile beslemenin yem maliyetini %24 artırdığı bildirilmiştir.

Ata (2016), tarafından yapılan çalışmada süttan kesilmiş İvesi kuzularında topraksız tarım ile elde edilen arpanın besi performansı üzerine etkisi incelenmiştir. Bu çalışmada iki gruba ayrılan kuzularda ilk grup toplam karışık rasyon diyetiyle (kontrol) beslenirken, ikinci gruptaki kuzular 90 günlük beslenme denemesinde tamamen hidroponik arpa ile serbest şekilde beslenmişlerdir. Sonuç olarak araştırmacı, hidroponik arpanın yem tüketimini, vücut ağırlığını, toplam ve ortalama günlük canlı ağırlık kazancını arttırdığını belirtmişlerdir.

Ramteke ve ark. (2019) yaptıkları bir derlemede süt ineklerini mısır danelerinden elde edilen 5-10 kg hidroponik taze yemin süt üretiminde %8-13 oranında artış sağladığını bildirmişlerdir. Ayrıca, araştırmacılar mısırdan elde edilen hidroponik yemin lezzetli, sindirilebilirliği yüksek ve besin maddelerince zengin olduğunu ortaya koyan araştırmalara yer vermişlerdir.

Sulser (2015) koçlarda ve koyunlarda çimlendirilmiş arpa kaba yemini, kontrol grubu (yonca kuru otu ve karışık arpa-mısır tanesinden oluşan rasyona ilave ettiklerinde hayvanların canlı ağırlık artışlarındaki farklılığın önemsiz olduğunu bildirmiştir. İvesi kuzuların rasyonuna toplam kuru maddede % 30 filizlenmiş arpa ile ikame edilmesinin, kuzularda besin madde sindirilebilirliğine ve yemden yararlanmaya olumlu yönde etkisi saptanmıştır.

Saidi (2014)'in yaptığı çalışmada 1 kg arpaya karşılık 8 günlük çimlenme periyodunda 6.6-7.5 kg yeşil yem elde edilmiş ve hidroponik arpa ile beslemenin yem maliyetini İvesi koyunlarında %42 düşürdüğünü tespit etmişlerdir.

Eshtayeh (2004), plastik tablalarda su kültürü yöntemiyle ürettiği saf arpa hasılı ve zeytin küspesinden oluşturduğu rasyonların koyunlarda canlı ağırlık ve süt kompozisyonu üzerine etkisini incelemiştir. Arpa hasılı oranının artması ile koyunların günlük süt miktarında artış olduğunu; sütte yağ, kuru madde değişimleri ve protein miktarında istatistiki açıdan önemli artışlar gözlemiştir. Saf arpa hasılı ve az orandaki zeytin küspesi uygulaması ile hayvanlarda canlı ağırlık artışı meydana getirdiğini bildirmiştir.

Del Castillo ve ark. (2013) yaptıkları çalışmada hidroponik sistemle üretilen arpa ve buğday hasılı ile besledikleri koyunlarının canlı ağırlık artışı üzerinde etkilerini incelemişlerdir. Hasıl ile beslenen koyunların günlük canlı ağırlık artışı 159 g, konsantre yem destekli serbest olatma sisteminde 136g, yalnız konsantre yemle beslenenlerde ise günlük ağırlık artışı 116 g olarak tespit edilmiştir. Sonuç olarak; hidroponik sistemle elde edilen hasılın teknik ve ekonomik yönden koyunların canlı ağırlık artışı bakımından ekonomik bir yöntem olduğunu bildirmişlerdir.

Kide ve ark. (2015), keçi rasyonlarına %80 oranında hidroponik olarak üretilen mısır ve arpanın besin madde sindirilebilirliği, canlı ağırlık artışı ve yemden yararlanmayı olumlu yönde etkilediklerini saptamışlardır. Araştırmacılar hidroponik üretimde 8 günlük çimlendirme sonucu 1 kg kuru daneden 8 kg mısır, 9 kg arpa elde etmişlerdir. Bunları %80 oranında yeme katmışlardır.

7.2. Diğer Hayvanların Beslenmesinde Kullanımı

Çimlendirilmiş yemler tavuklar, hindiler, kazlar, tavşanlar domuzlar vb. hayvanların beslenmesinde de kullanılabilir. Otlığa erişimin mümkün olmadığı bazı durumlarda, kimi tavuk yetiştiricileri vitamin temini için çimlenen tohumları kullanmaktadır. Çimlenme, tohumda bulunan beta karoten (vitamin A) miktarını arttırabilmekte ve sertifikalı organik kanatlı yetiştiriciliğinde yıl boyu var olan bir kaynak olarak, yemde kullanılması gereken sentetik vitamin miktarını azaltmak için avantaj sağlayabilmektedir. Ayrıca çimlendirilmiş yemleri yemeleri halinde kesilen tavukların derilerinin daha sarı renkte olduğu ve bunların yumurta sarılarının daha koyu renkte oldukları görülebilmektedir (URL, 4). Etlik piliçlerde çimlendirilmiş arpa kullanımı besin maddeleri sindirilebilirliğini yükseltmiş ve canlı ağırlık artışını %8 arttırmıştır. Yumurtacı tavukların rasyonlarına katıldığında ise yumurta üretimini

düşürdüğü bildirilmektedir (Sharif ve ark., 2013). Rasteh ve ark. (2014) rasyondaki arpayı %100 oranında çimlendirilmiş arpa ile değiştirerek beslemenin, yumurta tavuklarında yumurta verimi (%95.97 ve 87.61) ve yumurta kitlesini (61.08 ve 57.67 g) önemli miktarda arttırdığını saptamışlardır. Jemimah ve ark. (2018), yapmış olduğu çalışmada, hidroponik mısır yeminin Yeni Zelanda beyaz tavşanlarının büyüme performansı üzerine etkisini araştırmıştır. Çalışmada 1. grubu tamamen konsantre yem ile 2. grubu % 75 konsantre % 25 hidroponik mısır ile, 3. grubu ise % 50 konsantre %50 hidroponik mısır ile 30 gün boyunca beslemiştir. Deneme sonunda canlı ağırlık artışları sırasıyla; 262 g, 275 g ve 410 g olup, yemden yararlanma oranları ise 5.32, 5.22 ve 3.61 olarak bulmuşlar ve konsantre yeme % 50 oranında hidroponik mısır yemi karışımının yem maliyetini düşürdüğünü ve tavşanlarda önemli derecede vücut ağırlığı artışı sağladığından, tavşan beslemede bu oranın kullanılabileceğini bildirilmişlerdir. Brown ve ark. (2018), hidroponik yöntem ile üretilen mısır yemini kurudaki domuzların beslenmesinde kullanmış ve bu yemin domuzların beslenmesi ve yemde sindirilebilirlik üzerine etkilerini araştırmak için bir çalışma yapmışlardır. Çalışma sonucunda hidroponik mısır yeminin domuz beslemesine dahil edilmesi sonucunda kurudaki domuzların besin performansını ve yemin sindirilebilirliğini arttırdığı sonucuna varmışlardır.

4. SONUÇ VE ÖNERİLER

Ülkelerin coğrafik ve iklim şartları göz önüne alındığında kaliteli yeşil yemlerin bulunmadığı, özellikle kış ayında hidroponik sistemde üretilen hasıllar kaba yem açığını kapatmak için alternatif bir yöntem olabilir. Ancak, hidroponik yemin besleme değeri konusunda araştırma sayısı, aynı zamanda sonuçları da tutarlı değildir. Birçok araştırmacı, hidroponik sistemde üretilen hasılların hayvansal üretimde olumlu sonuçlar verdiğini gösterirken, bazı araştırmacılar, rasyonlara hidroponik yemin dahil edilmesinin ek bir avantaj yaratmadığını vurgulamıştır. Bu konuda öncelikle çimlenme kabiliyeti yüksek tohumların kullanıldığı ve maliyetinin dikkate alındığı çalışmalar yapılmalıdır. Ayrıca hidroponik üretimde kullanılan besin madde solüsyonun içeriği, iletkenliği, sıcaklık kontrolü, asitliği düzenleyiciler, su kalitesi ve ek besin madde takviyesi gibi ilave teknolojik uygulamaların dikkate alındığı yeni çalışmalar yapılmalıdır.

KAYNAKLAR

- [1]. A. Alçiçek A. Kılıç, V. Ayhan and M. Özdoğan, Türkiye’de kaba yem üretimi ve sorunları. Ziraat Mühendisleri Odası Dergisi, 10 s, 2010.
- [2]. A. Gül, Topraksız Tarım, Hasad Yayıncılık, 144 s, 2008.
- [3]. A. Sulser 2015. Hydroponic barley fodder feed tests on replacement rams and ewes. Journal of the Nacaa. 8(2). Erişim: Erişim: 15.10.2021.
- [4]. A.M. Snow, A.E. Ghaly and A. Snow. A comparative assessment of hydroponically grown cereal crops for the purification of aquaculture wastewater and the production of fish feed, American Journal of Agricultural and Biological Sciences, 3(1), 364-378, 2008.
- [5]. A.M.A. Saidi, The biological and economical feasibility of feeding barley green fodder to lactating awassi ewes, Open Journal of Animal Sciences, 5(2), 99-105, 2014.
- [6]. Anonim, Hidroponik üretim yapan Babil Asma Bahçeleri için kullanılan yapı, <https://bilgihanem.com/babilin-asma-bahceleri-hakkinda-bilgiler>, [Erişim Tarihi: 28.10.2021].
- [7]. D. Brown, J. W. Ng'ambi, Osinowo, O. A., A. T. Adeola, and O. A. Adebisi, Effects of feeding hydroponics maize fodder on performance and nutrient digestibility of weaned pigs, Applied Ecology and Environmental Research 16(3):2415-2422, 2018.
- [8]. D. Indira, P. Aruna, S.K. Swetha, and K. Kumar, Hydroponics as an alternative fodder for sustainable livestock production, World Journal of Advanced Research and Reviews, 5(2), 87-92, 2020.
- [9]. E. A. Raviv van Os, T. H. Gieling and J. H. Lieth, Technical equipment in soilless production systems. In M. Raviv, and J. H. Lieth (Eds.), Soilless culture, Theory and practice (pp. 157-207, 2008.
- [10]. F.S. Del Castillo, Del Carmen Moreno E. Pérez, E.C. Magaña and J.M. Gómez, Hydroponic wheat and barley fodder yields and their effect on weight gain in sheep, Revista Chapingo, Serie Horticultura, 19(4), 35-43, 2013.
- [11]. G. Al-Karaki, M. Al-Hashimi, Green Fodder Production and Water Use Efficiency of Some Forage Crops Under Hydroponic Conditions. ISRN Agronomy, 10: 1-5, 2012.
- [12]. G. Tudor, T. Darcy, P. Smith, F. Shallcross, The intake and live weight change of drought master steers fed hydroponically grown, young sprouted barley fodder (Auto Grass). Department of Agriculture Western Australia, 2003.
- [13]. H. Fazaeli, H.A. Golmohammadi, A.A. Shoayee, N. Montajebi, and S.H. Mosharraf, Performance of feedlot calves fed hydroponics fodder barley, Journal of Agricultural Science and Technology, 13(3), 367-375, 2011.
- [14]. H. Fazaeli, H.A. Golmohammadi, S.N. Tabatabayee and M. Asghari-Tabrizi, Productivity and nutritive value of barley green fodder yield in hydroponic system. World Appl. Sci. J. 16(4): 531-539, 2012.
- [15]. I.F.A. Eshtayeh, A new source of fresh green feed (hydroponic barley) for awass sheep. Master Dissertation, An-Najah National University, Nablus Palastine, 2004.
- [16]. K.D. Atıcı, Hasılatik yem derdini ortadan kaldırıyor, Tarım Gündem Dergisi, 9, 96-97, 2012.
- [17]. M. R. Rasteh, B. Dastar, M. S. Shargh, S. Zerehdaran and O. Ashayerizadeh, Effect of different levels of germinated barley on performance of laying hens and egg quality in different storage conditions, Animal Production Research, 3(1),43-51, 2014.
- [18]. M. Sharif, A. Hussain, M. Subhani, Use of sprouted grains in the diets of poultry and ruminants Indian Journal of Research. 2(10):4-7, 2013.
- [19]. M.R. Reddy, D.N. Reddyand, G.V.K. Reddy, Supplementation of barley fodder to paddy straw based rations of lactating crossbred cows, Indian Journal of Animal Nutrition, 8(4), 274-277, 1991.

- [20]. P. K. Naik, and N. P. Singh, Hydroponics fodder production: an alternative technology for sustainable livestock production against impending climate change, Model Training Course on Management Strategies for Sustainable Livestock Production against Impending Climate Change, 70-75, 2013.
- [21]. P. K. Naik, R. B. Dhuri, B. K. Swain and N.P. Singh, Nutrient Changes with the Growth of Hydroponics Fodder Maize, Indian Journal of Animal Nutrition, 29 (2), 161163, 2012.
- [22]. P.K. Naik, R. B. Dhuri, M. Karunakaran, B. K. Swain and N. P. Singh, Effect of feeding hydroponics maizefodder on digestibility of nutrients and milkproduction in lactating cows. Indian J. Anim. Sci. 84 (8): 880-883, 2014.
- [23]. R. Ramteke, R. Doneria and M. K. Gendley, Hydroponic techniques for fodder production, Acta Scientific Nutritional Health, 3(5), 127-132, 2019.
- [24]. S.P. Gaikwad, Cost effective green fodder production by hydroponic technique, [https://rkvy.nic.in/Uploads/SucessStory/MAHARASHTRA/2016/2016122954HYDROPO, 2016. NIC_Green%20Fodder%20\(%20Karad%20Satara%20\).pdf](https://rkvy.nic.in/Uploads/SucessStory/MAHARASHTRA/2016/2016122954HYDROPO, 2016. NIC_Green%20Fodder%20(%20Karad%20Satara%20).pdf), [Ziyaret Tarihi: 28.10.2021].
- [25]. T. Y. Chung, E. N. Nwokolo and J. S. Sim, Compositional and digestibility changes in sprouted barley and canola grains. Plant Foods for Human Nutrition. 39(3): 267-78, 1989.
- [26]. URL.3. İklim koşullarına bağlı kalmaksızın yılın 365 günü taze yeşil yem. Erişim adresi: <http://gfsturkiye.com/tr/wp-content/uploads/Sunul.pdf> Erişim: 14.08.2016.
- [27]. Ü. Kılıç, Kaba yem üretiminde hidroponik tarım sistemleri, Türk Tarım – Gıda Bilim ve Teknoloji Dergisi, 4(9),793-799, 2016.
- [28]. W. Kide, B. Desai, and J. Dhekale, Feeding effects of maize and barley hydroponic fodder on dry matter intake, nutrient digestibility and body weight gain of Konkan Kanyal goats. Life Sciences International Research Journal, ISSN 2347-869, 2015.

EFFECT OF VARIETY AND SUCROSE CONCENTRATION ON BANANA (MUSA SPP) VARIETIES ON IN VITRO PROPAGATION

Nazar AL GHASHEEM

Medicinal Plant Tissue Culture Laboratory, Department of studies in Botany, Manasagangotri,
Mysore - 570 006, Karnataka, India.
College of Agricultural and Marshlands, University of Thi Qar, Iraq.

M.S. SHARADA

Medicinal Plant Tissue Culture Laboratory, Department of studies in Botany, Manasagangotri,
Mysore - 570 006, Karnataka, India.

M.S. SUDARSHANA

Medicinal Plant Tissue Culture Laboratory, Department of studies in Botany, Manasagangotri,
Mysore - 570 006, Karnataka, India.

Basim Kassar HASAN

College of Agricultural and Marshlands, University of Thi Qar, Iraq.

Ihasn Jali AZEB

College of Agricultural and Marshlands, University of Thi Qar, Iraq.

Kawther ALGHASHEEM

College of Agricultural and Marshlands, University of Thi Qar, Iraq.

Abstract

This study was conducted in the laboratories of Botany Department and Labland Biotech - University of Mysore/India. The paper presents the effect of variety and sucrose concentration on Banana (*Musa spp*) varieties on in vitro propagation. Two variety(Robusta and Grandnine) were tested. The explants (shoots tip)were cultured on MS(Murashige and Skoog,1962)basal medium supplemented with 5mg/l Benzyl aminopurine(BAP) was used as cytokinine, on four variants(30,45,60 and 75)g/l,respectively, sucrose as carbon source and 7g agar. The results showed a significant correlation between varieties and sucrose concentrations, (60 g/l for Rubasta and 45 g/l for Grandnine variety) was superior to the rest of the sucrose concentrations used in the experiment in terms of the shoots number (40.33 and 29.11 multiplication rate), shoots height(2.71 and 3.06 cm), leaves number(5.22 and 5.11 leaf/plant), roots number(4.60 and 5.10 root/plant), roots length(2.90 and 3.54 cm), total weight (4.74 and 6.09 g/plant), fresh weight(4.54 and 5.81 g/plant) and dry weight (0.22 and 0.28 g/plant) respectively.

Keywords: shoots, Benzyl aminopurine, MS.

1. INTRODUCTION

Bananas belonging to Musaceae family under order Zingiberales and Genus *Musa* like *Musa sapientum* for used as dessert bananas and *Musa paradisiaca* for used as cooking bananas (plantains) which includes up 1000 species. [1],[2],[3] South East Asian region was Banana originated. [3],[4],[5] In 2019, India is recording the top country with 26.23% of the world's bananas production[6]. Micropropagation or plant tissue culture techniques are the clonal propagation of plants in closed tubes under aseptic conditions. Inside the tubes, the plants are

grown on culture media that supplemented with nutrients and growth hormones [7]. Plant tissue culture techniques provide a appropriate alternative for those plant species that confront obstruction to classical propagation [7]. Banana micropropagation in vitro is depending to embryo culture and shoots tip culture, because the seeds germination is low. [8] In vitro techniques of banana has been confirmed via many studies using different explants sources and methods such as [9],[10],[11],[12],[13],[14],[15]. Carbohydrates play an important role in plants tissue culture technique as an energy and carbon source, via adding it as a supplement to the culture media as well as an osmotic agent. [16] The aim of our study is to find out the effect of variety and appropriate concentration of sucrose on banana micropropagation.

2. Materials and Methods

2.1. Implements and accessories

All the implements required for plant tissue culture such as stainless steel forceps, blade holders, polypropylene sheets, aluminum stands were wrapped in two layers of clean newspaper and sealed with rubber bands. The implements were autoclaved at a temperature of 121 °C and at a pressure of 15 psi for 45 min. Once removed from autoclave, all items were dried in hot air oven overnight. The 250 ml size tissue culture bottles were filled with distilled water up to 2/3rd its volume and capped tightly with polypropylene caps and autoclaved for 45 min at a temperature of 121 °C and a pressure of 15 psi the previous day. The water was cooled to room temperature, prior to use. All the dissections of the tissues and sub culturing of explants/cultures were carried out with commercially available sterilized Surgeon blades of size 10 in a laminar air flow chamber.

2.2. Media preparation and sterilization

MS basal medium [17] was used for different growth stages during the micropropagation of *Musa* spp. And basal media with different concentrations of cytokinin and auxin used for different stages of micropropagation of Robusta and Grandnaine. The preparation of the media is as per standard tissue culture technique, which involves dissolving all the major salts, minor salts, iron stocks, vitamins, minerals and plant growth regulators in 75 % (V/V) of distilled water. In addition, 3 % (W/V) sucrose was added to the salt mixture and filtered through a nylon filter. The pH was adjusted to 5.7 with either 1N NaOH or 1N HCl. After the pH was adjusted, 0.8 % (W/V) of agar was dissolved in little less than the remaining 25 % (V/V) boiling water until complete homogenization. The final volume was made up to one liter or 100 %. 50 ml of this medium was dispensed into each of the tissue culture bottles and capped tightly. The bottles were sealed with polypropylene Kiln wrap and autoclaved for 15 min at 15 psi. The bottles were incubated at room temperature for a week to check the sterility of media and then used for inoculation purpose.

2.3. Explant selection and pretreatment

Two banana cultivars Robusta and Grandnaine (*Musa* spp.) were used as plant materials. Sword suckers of the 2 cultivars were separated from the mother plant and were chopped to appropriate size. The selected plants were washed thoroughly in running tap water. The suckers were wiped with 70 % ethyl alcohol. The explants were incubated in Dettol water (3 to 4 drops of liquid Dettol in 200 ml of water) for about 5 min and then washed thoroughly. The explants thus prepared were incubated in the pretreatment solution for 48 hrs, the solution was decanted and explants were rinsed several times with sterile distilled water.

2.4. Surface sterilization of explants

The surface sterilization was carried out in the inoculation room in a laminar airflow chamber. The pretreated explants were dissected to remove all the old, brown, overlapping scales and wiped with cotton dipped in 70 % ethyl alcohol solution. Explants were washed in sterile distilled water containing Tween 20 for 5 min with vigorous shaking. Then the explants were thoroughly rinsed with sterile distilled water for 2 to 3 times to remove all the traces of Tween 20. The explants were washed in 70 % ethyl alcohol for one min. The explants were finally surface sterilized in 0.4 % mercuric chloride for 30 min. The explants were washed with sterile distilled water several times to remove all the traces of mercuric chloride.

2.5. Initiation Stage

The surface sterilized explants were trimmed at the base, dry scales if any, were carefully removed and cut bits either with shoot tip, or the single node. One explant in each tissue culture bottle was inoculated in the initiation medium Ms supplemented with 5mg/l Benzyl aminopurine (BAP) was used as cytokinin. The initiation medium consisted of plain MS basal salts with 30 mg/l sucrose. The explants were incubated in growth room at a temperature of 25 ± 2 °C and were provided with 12 h photo period with a light intensity of 2500 lux from cool, white fluorescent tubes. After one week the cultures were screened for contamination. If contaminated, the jars were discarded, only clean cultures were retained for further use.

2.6. Multiplication Stage

After four weeks in the initiation medium, the buds were trimmed at the base and given a central longitudinal cut to injure the meristem tissue. The explants were cultured on MS basal medium supplemented with 5mg/l Benzyl aminopurine (BAP) was used as cytokinin, on four variants (30,45,60 and 75)g/l, respectively, sucrose as carbon source and 7g agar.

2.7. Data collection

In the experiment 5 replicates (3 explants in one tube culture) were used for each treatment and the experiment was repeated 3 times. Results were taken after 6 weeks from culture. The experiments were conducted as factorial experiments based on Completely Randomized Design (CRD). Data were recorded on (shoots number formed, shoots height, leaves number, roots number, roots length, total weight, fresh weight and dry) respectively were analyzed. Significance of differences between the results was estimated by Analysis of Variance (ANOVA) on SPSS version 20 program with the means compared with LSD test at < 0.05 .

3. Results and Discussion:

The results showed a significant correlation between varieties and sucrose concentrations, (60 g/l for Robusta and 45 g/l for Grandnine variety) was superior to the rest of the sucrose concentrations used in the experiment in terms of the shoots number (40.33 and 29.11 multiplication rate), shoots height (2.71 and 3.06 cm), leaves number (5.22 and 5.11 leaf/plant), roots number (4.60 and 5.10 root/plant), roots length (2.90 and 3.54 cm), total weight (4.74 and 6.09 g/plant), fresh weight (4.54 and 5.81 g/plant) and dry weight (0.22 and 0.28 g/plant) respectively.

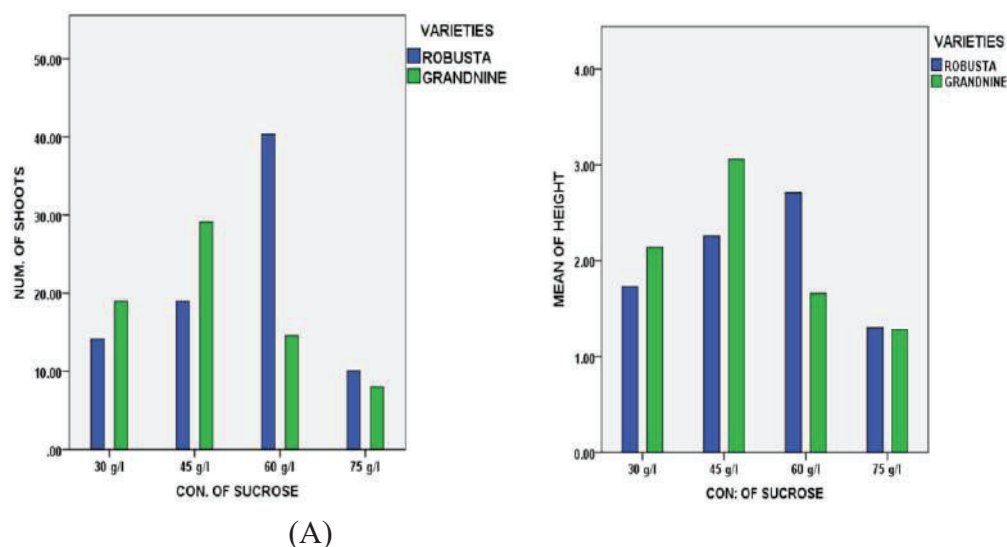


Figure 1. Effect of sucrose concentration on (A) shoots number formed (B) means shoots height. The results showed a significant correlation between varieties and sucrose concentrations, (75 g/l for Robusta and 75 g/l for Grandnine variety) was recede from the rest of the sucrose concentrations used in the experiment in terms of the shoots number (10.30 and 8.00 multiplication rate), shoots height (1.48 and 1.40 cm), leaves number (3.15 and 3.80 leaf/plant), roots number (1.10 and 1.22 root/plant), roots length (1.71 and 1.91 cm), total weight (2.28 and 1.98 g/plant), fresh weight (2.16 and 1.87 g/plant) and dry weight (0.12 and 0.11 g/plant) respectively.

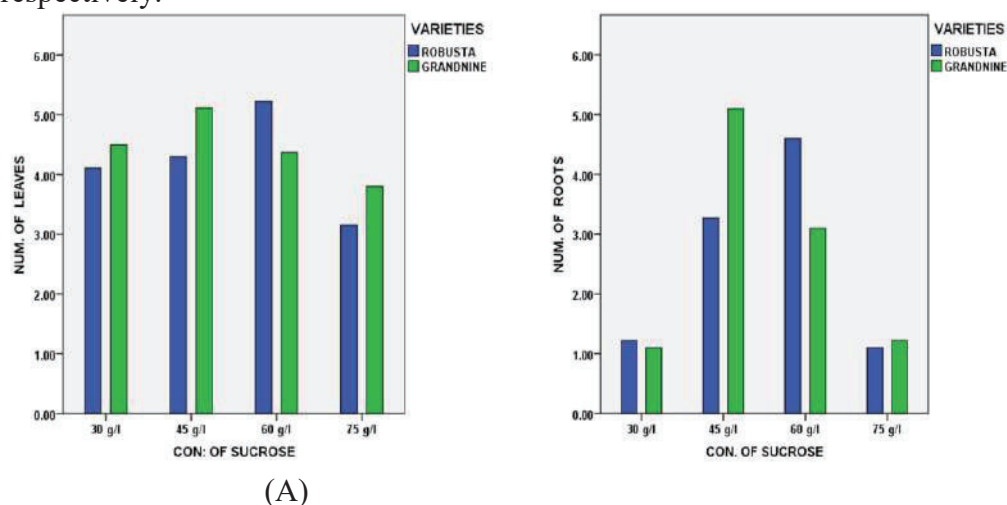


Figure 2. Effect of sucrose concentration on (A) leaves number formed (B) roots number formed. The results showed a significant correlation between varieties. Grandnine was superior on Robusta variety, the result of differences in the genetic materials of the species, leading to different responses in breeding.

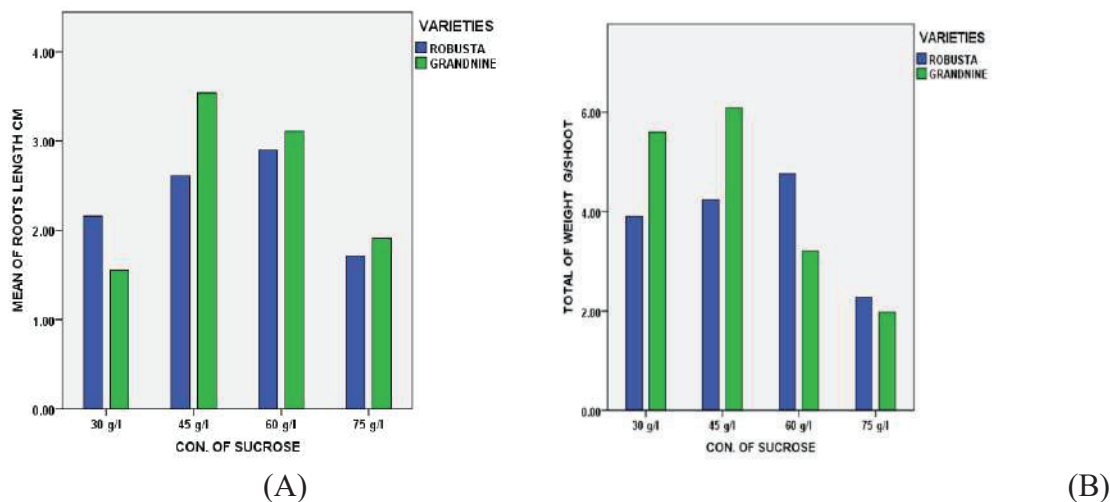


Figure 3. Effect of sucrose concentration on (A) mean of roots length (B) total weight.

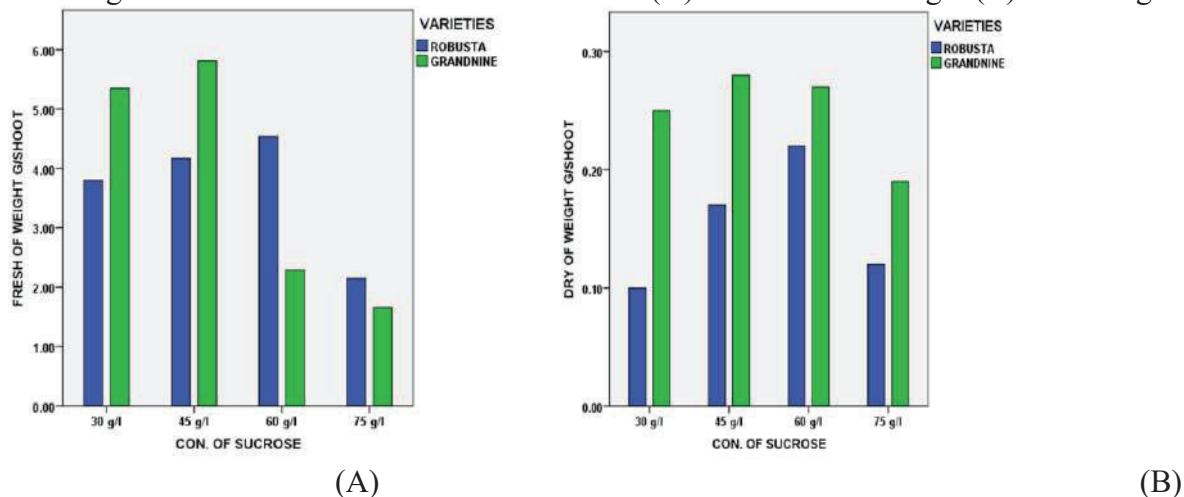


Figure 4. Effect of sucrose concentration on (A) fresh weight (B) dry weight.

According to Ref. [18] that while somatic transcriptional variance is influenced by external factors, there is also a genetic influence, with some genotypes increasing more instability than others in same culture conditions. Also, the study confirmed that increasing the concentration of sucrose in culture medium to a certain extent increased shoots number formed, shoots height, leaves number, roots number, roots length, total weight, fresh weight and dry weight. Ref. [19] showed that sucrose has a role in controlling the expression of several important enzymes and other proteins, may be due to the influence of sucrose in the metabolism of food to the cells and this means that increasing concentration of sucrose increased the amount of food inventory, which in turn helps plantlets on growth [20] or resulted in an increase of energy of carbon [21]. Also, increasing the concentration of sucrose to more than 70 g/L led to an increase in osmotic pressure, which leads to the plasma phenomenon in the cells and this phenomenon stopped the vital activities of the cells and stop of growth [22],[23]. Rustles similar studies Ref.[24] reported that MS medium supplemented with 60 g/l sucrose led to increased turmeric plant size, leaf and root, sucrose at 60 g/l produced the highest amount of dry weight.



Figure 5. Multiple shoot formation in Robusta variety after 6 weeks from culture.



Figure 6. Multiple shoot formation in Grandnaine variety after 6 weeks from culture.

4. Conclusions

The results showed a significant correlation between varieties and sucrose concentrations, (60 g/l) for Robusta was superior on shoots number and leaves number while (45g/l) for Grandnaine variety was superior on shoots height, roots number, roots length, total weight, fresh weight and dry weight, respectively..

ACKNOWLEDGMENT

The authors thankful the management of Labland Biotech Private Limited, Mysore, India for their assistance in completing this research.

REFERENCES

- [1].Espino R.R.C., Jamaludin S.H., Silayoi B., Nasution R.E. (1992). Musa L. (edible cultivars). In: Verheij EWM, Coronel RE (eds.) Plant Resources of South-East Asia No.2: Edible fruits and nuts. Prosea Foundation, Bogor.
- [2].Gebeyehu A. (2013). Effect of different combinations of 6-Benzylamino purine and Naphthalene acetic acid on multiple shoot proliferation of plantain (Musa spp) cv. Matoke from meristem derived explants. African Journal of Biotechnology; 12(7):709-719.
- [3].De Langhe E., Vrydaghs L., de Maret P., Perrier X., Denham T. (2009). Why bananas matter: An introduction to the history of banana domestication. Ethnobot Res Appl 7: 165-177.
- [4].Li L.F., Wang H.Y., Zhang C., Wang X.F., Shi F.X., Chen W.N. and Ge X.J. (2013). Origins and domestication of cultivated banana inferred from chloroplast and nuclear genes. PLoS ONE 8 (11): e80502. DOI:10.1371/journal.pone.0080502.
- [5].Wong C., Kiew R., Argent G., Set O., Lee S.K. and Gan Y.Y. (2002). Assessment of the validity of the sections in Musa (Muaceae) using AFLP. Annals of Botany 90, 231-238.
- [6].FAOSTAT. (2019). <https://www.fao.org/faostat/en>.
- [7].Hartmann H.T., Kester D.E., Davies F.T. Jr and Geneve R.L. (2002). Hartmann and Kester's Plant Propagation. Principles and practices 7th Ed Prentice-Hall International, UK Ltd London, UK.
- [8].Vuylsteke D.R. and SWENNEN R. (1993). Genetic improvement of plantains. In: (INIBAP) Proceedings of the workshop on Biotechnology Applications for Banana and Plantain Improvement, San José, Costa Rica, 27-31 January, 1992 169-176.
- [9].Jalil M., Khalid N. and Othman R.Y. (2003). Plant regeneration from embryogenic suspension cultures of Musa acuminata cv. Mas (AA). Plant Cell Tissue Organ Cult.75: 209-

214.

- [10]. Madhulatha P., Anbalagan M., Jayachandran S. and Sakthivel N. (2004). Influence of liquid pulse treatment with growth regulators on in vitro propagation of banana (*Musa spp.* AAA). *Plant Cell Tissue Organ Cult.* 76:189-192.
- [11]. Strosse H., Schoofs H., Panis B., Andre E., Reyniers K. and Swennen R. (2006). Development of embryogenic cell suspensions from shoot meristematic tissue in bananas and plantains (*Musa spp.*). *Plant Sci.* 170: 104-112.
- [12]. Wong W.C., Jalil M., Ong-Abdullah M., Othman R.Y. and Khalid N. (2006). Enhancement of banana plant regeneration by incorporating a liquidbased embryo development medium for embryogenic cell suspension. *J. Hortic. Sci. Biotechnol.* 81: 385-390.
- [13]. Venkatachalam L., Sreedhar R.V. and Bhagyalakshmi N. (2007). Micropropagation in banana using high levels of cytokinins does not involve any genetic changes as revealed by RAPD and ISSR markers. *Plant Growth Regul.* 51: 192-205.
- [14]. Resmi L. and Nair A.S. (2007). Plantlet production from the male inflorescence tips of *Musa acuminata* cultivars from South India. *Plant Cell Tissue Organ Cult.* 88: 333-338.
- [15]. Shirani S., Mahdavi F. and Maziah M. (2009). Morphological abnormality among regenerated shootsof banana and plantain (*Musa spp.*) after in vitro multiplication with TDZ and BAP from excised shoot tips. *Afr. J. Biotechnol.* 8(21): 5755-5761.
- [16]. Kumar S. and Singh M.P. (2009). *Plant Tissue Culture*. APH Publishing Corporation, New Delhi.
- [17]. Murashige, T. and Skoog, F. (1962). A Revised Medium for Rapid Growth and Bio Assays with Tobacco Tissue Cultures. *Plant Physiology*, 15, 473-497.
- [18]. KARP A. (1992). On the current understanding of somaclonal variation. In: Mifflin, B. J. (ed), *Oxford Surveys of Plant Molecular and Cell Biology*, vol. 7, Oxford University Press, Oxford, pp. 1—58.
- [19]. Dey P.M. and Harborne J.B. (1997). *Plant biochemistry*. Academic Press. New York, pp.409-421.
- [20]. Hazarika B.N. (2003). Acclimatization of tissue-cultured plants. *Current Science*, Vol.85, No.12. 1704-1712.
- [21]. Taha H.S., Bekheet S.A. and Saker M.M. (2001). Factors affecting in vitro multiplication of date palm. *Biologia Plantarum* 44(3):431-433.
- [22]. Zouine J. and El-Hadrami I. (2004). Somatic embryogenesis in *Phoenix dactylifera* L.: Effect of exogenous supply of sucrose on proteins, sugar, phenolics and peroxidases activities during the embryogenic cell suspension culture. *J. Biotechnology* 3(2):114-118.
- [23]. Al-Maarri K.W. and Al-Ghamdi A.S. (1997). Micropropagation of Five Date Palm Cultivars Through in vitro Axillary Buds Proliferation. *D.U.J. Agri.Sci.* Vol 13, 1997.
- [24]. Adeberg J. and M. Cousins. (2006). Thin films of liquid media for heterotrophic growth and storage. organ development: turmeric (*Curcuma longa*) as a model plant. *Hortscience*. 41:539-542.
-

ASSESSMENT WATER QUALITY OF THE LUMBARDHI RIVER, IN THE PRIZREN AREA, BY THE PHYSICO-CHEMICAL ANALYSIS AND HEAVY METALS

Skender DEMAKU

University of Pristina, Faculty of Natural Science and Mathematics, Department of Chemistry,
Prishtina, Kosovo

Gani KASTRATI

UBT College, Department of Food Science and Technologies - Republic of Kosovo;

Abstract

This scientific project, will enable us to have a more realistic overview of the water quality of the Lumëbardhë River, in the study area. Has been analyze physico-chemical parameters, such as; temperature, pH, EC, TDS, major ions (Ca^{2+} , Mg^{2+} , Na^+ , K^+ , NH_4^+ , NO_2^- , Cl^- , NO_3^-). The obtained results were compared with the Water Framework Directive (DKU-WFD, 2000/60) and fulfil the criteria imposed from this directive. Inductively coupled plasma optical emission spectroscopy (ICP-AES) has been used for the analysis of heavy metals. In the water samplingsites, the concentration of Fe as the highest presented element is; 0.897 to 0.485 mg/L, Zn varies from 0.513 to 0.392 mg/L, Ni from 0.174 to the highest of 0.235 mg/L, Mn 0.141-0.194 mg/L, Pb 0.142-0.254 mg/L, whereas As, Cd, Co, Al and Co, were under limit detection in all of the water samples. Also, in the sludge ones the highest concentration element is Fe, followed by Zn, Mn, Ni and Pb. The highest concentration of Fe is in sample M3. The concentration varies from 0.985 mg/kg to the lowest of 0.698 mg/kg, Zn from 0.913 to 0.565 mg/kg, Mn from the highest of 0.413 to the lowest of 0.186 mg/kg, Ni 0.212 to 0.185 mg/kg, Pb 0.187 mg/kg to 0.143 mg/kg, followed by Cu, Co and Al. Even in the soil samples, iron varies from; 0.652 mg/kg to the highest of 0.989 mg/kg, Zn starts from 0.589 to 0.798 mg/kg, Mn from 0.119 to 0.189 mg/kg, Ni 0.139 to 0.178 mg/kg and Pb 0.163 to 0.189. The concentration of Co was observed in thre soil samples from 0.033 to 0.064 mg/kg, whereas, Al is presented from 0.045 to 0.054 mg/kg followed by Cu from 0.049 to 0.098 mg/kg. The study shows that we are dealing with moderate pollution with these elements in the river, but to have a firm conclusion, it is advisable to examine more the zone of study.

Key words: The Lumbardhi River, soil, sludge, water, pollution, ICP-AES technique.

INTRUDUCTION

For some time now, surface water in Kosovo has been polluted, and Kosovo cities still do not have a program for the treatment of urban water and wastewater. Kosovo has problems with water in many respects; first, Kosovo has a problem with water as a natural resource, as Kosovo waters in general, going on out its territory, [MUCHUWETI et al. 2006]. We live on a planet where the aquatic environment predominates, so water is a chemical compound, with extraordinary properties and fundamental importance to the environment [MUCHUWETI et al. 2006, JUSUFI et al. 2017]. Rapid industrialization and urbanization have caused contamination

of the environment by these substances, and studies have shown that it is very serious concern for humans and environment in general, [JUSUFI et al. 2017, BAJRAKTARI et al. 2019].

The presence of clean water is essential for life on Earth, because the specific properties of liquid water, vapor water and solid water, determine the environmental conditions that make life possible on this continent, [FERATI et al. 2015, MARKOVIĆ et al. 2020]. Also, the extraordinary properties of water as a solvent, condition the chemical erosion of rock formations, which is a natural phenomenon, which leads to the formation of the Earth's surface layer, the transfer of nutrients from the Earth to plants, and then to living- organic species, [GASHI et al. 2017]. This paper is a brief summary of physical and chemical parameters and heavy metals in the water of the Lumbardhi in municipality of Prizren. It is also mentioned on different researches previously that the presence of these elements is quite high in different areas of the country [MARKOVIĆ et al. 2020, GASHI et al. 2017] and that heavy metals can cause various diseases and different anomalies [THOMSEN et al. 2019, HAZRAT et al. 2019], so this kind of study and constant repetition of these researches are inalienable.

Nowadays, qualitative and quantitative determination of total metals and distribution of all their physical and chemical species in trace amounts (speciation) in natural water resources is to be considered as the main challenge for most scientists [MALIQI et al. 2020]. Based on the results of such studies it will be possible in the future to propose protection and detoxification measures of affected river waters and general protection and remediation of ecosystems. Therefore the watershed of Lumbardhi River in Prizren, which belongs to the basin of Drini Bardhë, the richest basin with an annual flow of 2.200.00 million m³ and with the longest surface of 4.622 km² in the territory of the republic of Kosovo [MEMIM 2016].

The Lumbardhi River flows in the Sharr Mountains and overflows into the White Drin [MEMIM 2016]. It runs through the middle of the city of Prizren. There are discharges of rural and urban waters onto it, without any prior treatment. They are today the largest pollutant of water resources. Urban discharge waters originate from the production process and include: water from processes, sanitation waters and water from the purification of special equipment for each industry [MEMIM 2016]. Unlike municipal wastewater, whose composition is well known, the discharge waters from various industries and laundries, it is difficult to distinguish the great diversity of pollutants and their specific ingredients. Based on the laboratory analysis, the state of the Lumbardhi River ecosystem was assessed by polluters for the period September of 2018.

MATERIALS AND METHODS

Lumbardhi of Prizren, is a river in Kosovo, where it flows through the villages of Srečka and Prizren, while it flows into Drini Bardhë river. Lumbardhi of Prizren is 18 km long, and has a basin area, of: 158 km² [MEMIM 2016]. In order to have accurate data during water monitoring and analysis, we should also know the temperature and climate, since it plays crucial role in water composition. According to climate in Republic of Kosovo, the weather in Kosovo is considered continental with warm summers and cold snowy winters, with temperature from -10°C to -26°C in the winter and from 20°C to 37°C in the summer [MEMIM 2016].

The dry season begins in March and lasts until September and the prolonged wet season between October to February [MALIQI et al. 2020]. For this study, the samples were collected in September of 2018 in dry season. Water samples were composite, by mixing water from different depth from locations: Streams of the 40th Wells M1; Andrra M2 and City Park M3. The number of sampling spots was 3 and at every sampling spot samples were taken in order to determine the

chemical parameters and heavy metals. The sampling spots of water in the river of Lumbardhi Prizren, were marked by codes M1, M2 and M3. Also, sludge and soil samples were taken at the same sampling site.

DETERMINATION OF PHYSICO-CHEMICAL PARAMETERS

The Sampling tools were washed with water and dried before the next sample was collected. The collected samples were stored in polythene plastic containers. Sample preparation was done according to standard methods for surface water analysis [APHA. AWWA. WEF. 1998]. The study area with the sampling locations is shown in Figure 1 and the details about all sampling sites are presented in Table 1. Geographical positions were determined by GPS, using model “geko 201, 12 channel”.



Fig. 1. Sampling sites in the study area.

The determination of physico-chemical parameters for determination of the quality parameters of the water, we have used standard methods for water analysis including classical and modern methods [WHO 2011]. Temperature of water was measured immediately after sampling, using a digital thermometer, model “Quick 63142”. Measurements of pH were performed immediately after sampling using a pH/ion-meter, model “Hanna Instruments, pH & EC” [WHO 2011, WHO 1993]. Electric conductivity was measured by a “HANNA Instrument HI 8424” conductivity meter. Total hardness of water was determined by EDTA titration using Mercurochrome black T indicator and chemicals of p.a. purity. Chlorides were determined using argentometric methods.

Some physico-chemical parameters (NH_4^+ , NO_3^- , PO_4^{3-}) were determined by UV-VIS spectrometry. “WTW S12 photometer”, “SECOMAM Prim Light spectrophotometer” and

“SECOMAM Pastel UV RS232 spectrophotometer” were used with a monochromatic irradiation in the spectral range of 190-1100 nm [WHO 1993, EPA 2007]. The measurement region, in a cuvette of 10 mm, was 340-800 nm, for the analysis of drinking waters, discharged and sea water [ZHUSHI et al. 2020].

SAMPLE TREATMENT

Water sampling was done by inserting the glass bottle in the vertical direction of water flow, carefully removing the impurities that float on the surface of water on the both sides of the river bed. Samples were taken in 2 L glass bottles. Also, an additional bottle was filled and treated with 2 ml of HNO₃ for the determination of heavy metals, by the ICP-AES methode. The same procedure was applied at all three points, where samples were taken. The water samples were treated according to EPA 6010C standard [U.S. EPA 2007].

Soil samples were taken in the vicinity of the river. Each sample was taken in plastic bag around 1-2 kg. Initially they were left to dry in room temperature for few days, continuing grinding and treatment according to the EPA 3051A standard [U.S. EPA 2007].

Sludge samples were taken aproximately around 250 mg and sent to laboratory for further treatment and testing according to EPA 3051A standard [U.S. EPA 2007].

All analyzed elements (As, Cd, Co, Al, Cu, Fe, Mn, Ni, Pb and Zn) were determined by atomic emission spectrometry with inductively coupled plasma, ICP-AES technique methode. Calculation and presentation of statistical charts was done using the Minitab 19 software program.

RESULTS AND DISCUSSION

The primary goal of this study is to look into the influence of industrial and antopogjenic impact on water, soil and sludge pollution in the study area. Therefore, the results of the physico-chemical analysis are presented in Table 1. The obtained results were compared with the Water Framework Directive [DKU-WFD 2000/60, DKU-WFD 2000], and fulfil the criteria imposed from this directive.

Table 1. Physico-chemical properties of water samples in Lumbardh River, Kosovo

Parameter s	M1	M2	M3	Parameter s	M1	M2	M3
Temp	13.4 °C	11.7 °C	12.3 °C	PO ₄ ³⁻	0.035	0.055	0.069
DO mg/l	8.6	8.4	6.8	P _{tot}	0.101	0.103	0.113
O ₂ %	115	86.5	86	SO ₄ ²⁻	8.6	7.62	7.99
EC (19°C)	389 µScm ⁻¹	387µScm ⁻¹	425 µScm ⁻¹	Cl ⁻	3.19	1.4	2.1
pH	6.44	6.81	6.87	F ⁻	0.3	0.2	0.1
TDS	159	169	178	FT d ⁰ H	11.63	11.09	11.3
TMS	21	19.9	55.3	F _{Ca} d ⁰ H	13.6	12.8	12.2
COD	28.4	35.8	59	F _{Mg} d ⁰ H	17.4	13.6	15.9
BOD	16.2	20.9	42.1	Ca	98.6	99.8	101
TOC	9.3	11.8	19.89	Mg	19.84	16.8	16.9
NO ₃ ⁻	0.5	0.5	0.5	M _A	14.11	10.25	10.35
SUR	<0.2	<0.2	<0.2	HCO ₃ ⁻	426.35	584.6	548.63
NH ₄ ⁺	0.08	0.06	0.28	TUR	3.8	3.4	3.6
NO ₂ ⁻	0.01	0.01	0.01	KMnO ₄	5.69	12.352	10.43
N _{in}	0.152	0.236	0.223	N _{tot}	0.221	0.231	0.259

While physico-chemical qualities provide some insight into water quality, they do not provide a complete picture of water pollution. The water classification of this basin (river) was determined by comparing many water quality indicators at several sampling locations to the UNECE-recommended parameters in Table 2.

Table 2. Classification of river quality by UNECE (content, mg/L)

Category	P. Total	NO ₃ ⁻	OT	BOD ₅	COD	NH ₄ ⁺
I	<10	<5	>7	<3	<3	<0.1
II	10–25	5–25	7–6	3–5	3–10	0.1–0.5
III	25–50	25–50	6–4	5–9	10–20	0.5–2
IV	50–125	50–80	4–3	9–15	20–30	2–8
V	>125	>80	<3	>15	>30	>8

The present study was carried out for three sampling points of water, sludge and three soil samples in the vicinity of the river. The following table (Tab.1), presents the water sampling points, physical and chemical properties of the water samples.

Also, (Tab.1) shows several physico-chemical parameters measured in the water of Lumbardhi river, Prizren: air temperature, water temperature, pH, electrical conductivity (EC), dissolved oxygen, BOD₅, total hardness, content of sulfates, nitrites, ammonium and phosphates. Temperature is a biologically significant factor which plays an important role in the metabolic activities of organisms [ZHUSHI et al. 2020]. It is also an important parameter in determining water quality, as it influences pH, alkalinity, acidity and dissolved oxygen (DO), [EU's DRINKING WATER STANDARDS 1998].

The temperature values recorded in the water samples from the study area range between 11.7°C (M2) and 13.4 °C (M1), as summarized in Table 1 with a mean temperature of 12.46 °C. The recorded temperature values were within the WHO standard for drinking water [EU's DRINKING WATER STANDARDS 1998]. The pH is a measure of the acidity or alkalinity and measures the concentration of hydrogen ions in water. Basically, pH is determined by the amount of dissolved carbon dioxide (CO₂) which forms carbonic acid in the water. The pH values of the surface water sampled in the area varied from 6.44 to 6.81 with a mean value of 6.70 (the WHO standard range is 6.50-8.50), [WHO 2011].

From these data we can see that the water of the river Lumbardhi Prizren is neutral from pH. The minimum TDS value of 159 mg dm⁻³ was recorded at M1 while the maximum value of 178 mg dm⁻³ was recorded at M3. No limit has been set by WHO for drinking water and water for domestic uses but water with values similar to these has previously been described as good [WHO 2011]. Electrical conductivity (EC) is a measure of water capacity to convey electric current. It is a determination of levels of inorganic constituents in water [EU's DRINKING WATER STANDARDS 1998, WHO 2004]. EC values obtained for the samples were in the range of 378-425 µScm⁻¹, which is below the WHO recommended value of 400 µScm⁻¹ indicating a low amount of dissolved inorganic substances in ionized form.

Dissolved oxygen (DO) is an important parameter in water quality assessment and reflects the physical and biological processes prevailing in the water. The DO values indicate the degree of pollution in water bodies. DO values, as shown in Table 1, varied from 6.8 to 8.6 mg dm⁻³.

The values for biochemical demand shown in Table 1 range from 16.2 (M1) to 42.1 mg dm⁻³ (M3) with a mean of 26.4 mg dm⁻³. The values are quite higher than the standard of 10 mg dm⁻³ recommended by WHO.

The total hardness was 11.3 (sampling spots M3), 11.9 (sampling spot M2), 11.63 (sampling spots M3). Sulfate content higher than 100 mg dm⁻³ tends to give water a bitter taste and has a laxative effect on people not adapted to the water [WHO 2011, WHO 1993]. Also ailments like catarrh, dehydration and gastrointestinal irritation have been linked with high sulfate concentration.

The results revealed that all analyzed water samples have a low sulfate content ranging from 7.62 to 8.6 mg dm⁻³ (Table 1). So, the concentration of sulfates is below the maximum value allowed by the WHO and the EU [EU's DRINKING WATER STANDARDS 1998, WHO 2004].

Nitrate content in the analyzed water samples in the three samplesite, it is 0.5 (M1, M2 and M3). These fall within the allowable value when compared to the WHO recommended guidelines. Nitrate fouls the water system and epidemiological studies have shown that exposure to nitrate causes methemoglobinemia disease [EU's DRINKING WATER STANDARDS 1998, WHO 2004]. The amounts of Cl⁻, range from 1.4 to 3.19 mg dm⁻³, PO₄³⁻ ions range from 0.035 to 0.069 and NH₄⁺ ions range from 0.06 to 0.28 mg dm⁻³. Whereas, all other parameters are within the allowed limits, according to WHO and EU standards [EU's DRINKING WATER STANDARDS 1998, WHO 2004].

The following table (Table 3), summarizes the results of water, sludge and sediment samples. Water results are expressed in mg/L, while those of soil and sludge in mg/kg.

Table 3. The measured results of water (mg/L), sludge and sediment samples (mg/kg).

Elements	M1. Water	M2. Water	M3. Water	M1. Sludge	M2. Sludge	M3. Sludge	M1. Soil	M2. Soil	M3. Soil
As	nd	nd	nd	nd	nd	nd	nd	nd	nd
Cd	nd	nd	nd	nd	nd	nd	nd	nd	nd
Co	0.018	0.019	0.014	0.072	0.068	0.085	0.033	0.064	0.041
Al	0.029	0.038	0.086	0.064	0.089	0.095	0.045	0.054	0.049
Cu	0.038	0.028	0.069	0.095	0.098	0.111	0.049	0.089	0.098
Fe	0.485	0.661	0.897	0.698	0.858	0.985	0.895	0.989	0.652
Mn	0.141	0.168	0.194	0.186	0.198	0.413	0.168	0.189	0.119
Ni	0.174	0.189	0.235	0.185	0.193	0.212	0.156	0.178	0.139
Pb	0.142	0.159	0.254	0.158	0.187	0.143	0.163	0.018	0.165
Zn	0.392	0.428	0.513	0.565	0.802	0.913	0.589	0.798	0.758

E*-Elements (Variables), W*-Water samples, nd-under limit detection

The following table (Tab. 4), is a summary of all results in the form of statistical analyzes of measurements made on water, soil and sludge samples in three sampling points (M1-M3). The results are presented as mean, standard deviation, variance, minimum, maximum, Q1, Q3, median and range for Co, Al, Cu, Fe, Mn, Ni, Pb and Zn, the following (Tab. 4).

Table 4. Descriptive statistics of heavy metals presented in water, sludge and soil samples.

Variable	Mean	StDev	Variance	Min	Q1	Median	Q3	Max	Range
Co	0.02735	0.02269	0.00048	0.011	0.014	0.022	0.0338	0.084	0.072
Al	0.0489	0.0182	0.0002	0.029	0.030	0.045	0.066	0.067	0.034
Cu	0.0343	0.0272	0.0006	0.01	0.0179	0.024	0.045	0.085	0.073
Fe	0.7897	0.1784	0.0318	0.449	0.650	0.871	0.931	0.979	0.528
Mn	0.1436	0.1469	0.0211	0.020	0.049	0.081	0.229	0.481	0.458
Zn	0.51	0.1968	0.0379	0.298	0.3689	0.541	0.6988	0.890	0.589

The elements measured (Tab. 3), showed that the concentrations of As, Cd, Co, Al and Cu was below the limit of detection. Similar case was observed in the case of Ni in the samples, where it was present only in sampling point (M2) while in the sampling points M1 and M3 were under limit of detection. According to World Health Organization [WHO 1993], other elements, such as: Fe, Mn, Ni, Pb and Zn, are higher values, if compared to international standards, for surface water (river water).

The concentration of copper in water in different places has shows different results. For example, the presence of this element in USA from different studies varied from 0.0005 to 1 mg/L [ATSDR 2005], in United Kingdom (0.003 to 0.019 mg/L) and in India with lower concentrations, strating from 0.0008 to 0.01 mg/L [ATSDR 2005]. WHO cited that concentration of copper in drinking-water may vary of a water characteristics, such as pH, hardness and copper availability in the distribution system [EU's DRINKING WATER STANDARDS 1998, ATSDR 2005]. Similar to our study, this element had low concentration, varied from 0.028 mg/L in water samples to 0.111 mg/L in sludge samples.

Zinc is an element that is found naturally in environment, but also anthropogenic activities can raise its concentration. Zinc is an element with relatively low toxicity, restricted to taking

high doses. The amount of this element in USA in the samples of air is lower than $1 \mu\text{g}/\text{m}^3$, but this amount can vary near cities, closer to urban ones it varies from 0.1 to $1.7 \mu\text{g}/\text{m}^3$ [IARC 1978]. Environmental Protection Agency (EPA) has stated that drinking water should not contain more than 5 mg of zinc per liter of water (5 mg/L or 5 ppm) because of taste, [U.S. EPA 2007].

In our measured samples, zinc had relatively low concentrations for all of the cases. In water samples, its concentration was below EPA recommendations (less than 5 ppm) in all of the measured cases.

The last elements that were present in our study were iron and manganese. Both of these elements are counted as essential substances that must be present in body to function properly. These elements can often be found as such due to similar valence in physiological conditions, ionic radius, etc [CHANDRA et al. 2020]. According to the division of toxicants by US EPA, it is suggested that both of these elements (Fe and Mn) are non-carcinogens. World Health Organization (WHO) has established water guideline for iron as 0.3 mg/L, and manganese as 0.4 mg/L [KORÇA et al. 2020].

The concentration of iron in our samples is slightly higher than World Health Organization [EU's DRINKING WATER STANDARDS 1998, WHO 2004], recommended, respectively it ranges from 0.485- 0.897 mg/L in water samples, almost double concentration that the recommended one. As for manganese, we have lower concentrations within recommended norms ranging from 0.174 mg/L to 0.235 mg/L, [KORÇA et al. 2020].

Figures above (Fig. 2- Fig. 4) are built based on the findings of these elements in water, sludge and soil samples. The diagrams are divided for each case where the highest concentration of each element in the measured samples is shown. The following figures show the concentration of heavy metals which have been observed in water samples (Fig. 2), sludge samples (Fig. 3) and soil samples (Fig. 4).

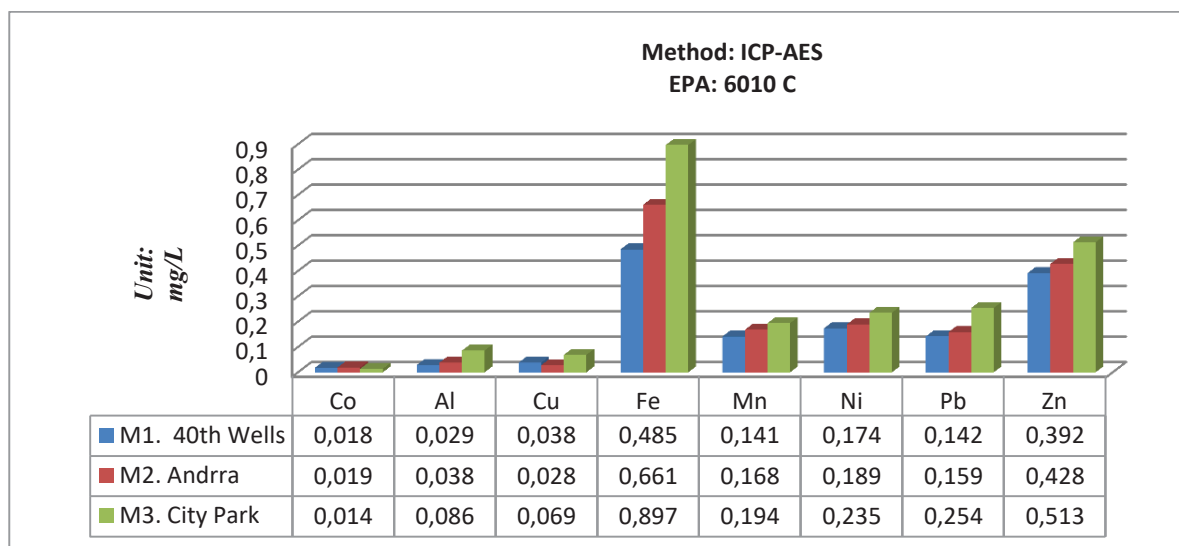


Fig. 2. The presence of heavy metals in water samples (mg/L).

If we compare the highest concentrations of elements in water, we observe that concentration of Fe is maximum in the measured samples, followed by Zn, Ni, Mn and Pb, continuing with a very small difference to the other elements.

The concentration of Fe as the highest presented element is 0.897 to 0.485 mg/L, Zn varies

from 0.513 to 0.392 mg/L, Ni from 0.174 to the highest of 0.235 mg/L, Mn 0.141-0.194 mg/L, Pb 0.142-0.254 mg/L. Whereas, arsenic, cadmium, cobalt, aluminum and copper, were under limit detection in all of the water samples.

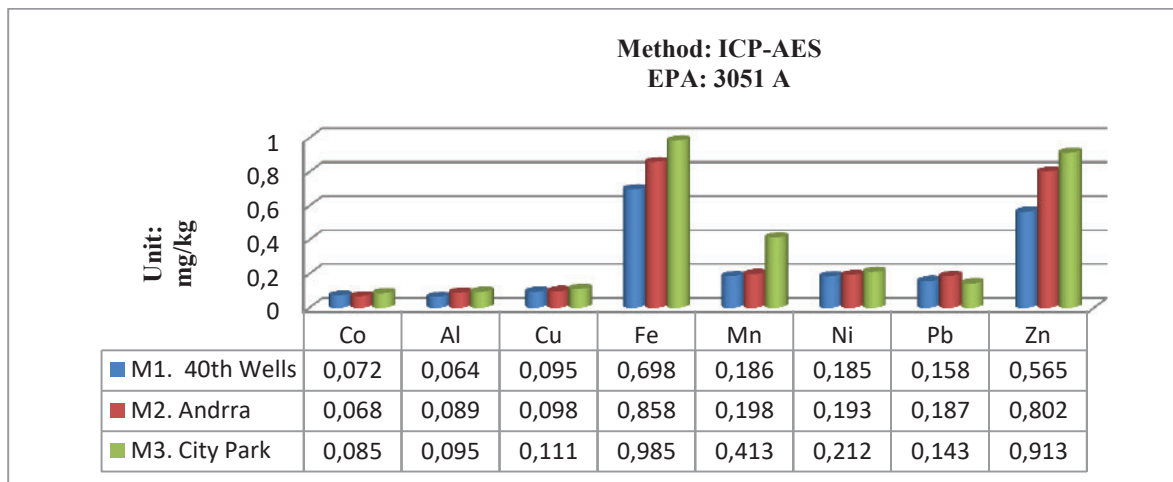


Fig. 3. The presence of heavy metals in sludge samples (mg/kg).

Similar to water samples, also in the sludge ones the highest concentration element is Fe, followed by Zn, Mn, Ni and Pb. The highest concentration of Fe is in sample M3. The concentration varies from 0.985 mg/kg to the lowest of 0.698 mg/kg, Zn from 0.913 to 0.565 mg/kg, Mn from the highest of 0.413 to the lowest of 0.186 mg/kg, Ni 0.212 to 0.185 mg/kg, Pb 0.187 mg/kg to 0.143 mg/kg, followed by Cu, Co and Al. Similarly, arsenic and cadmium were under limit detection in all of the sludge samples.

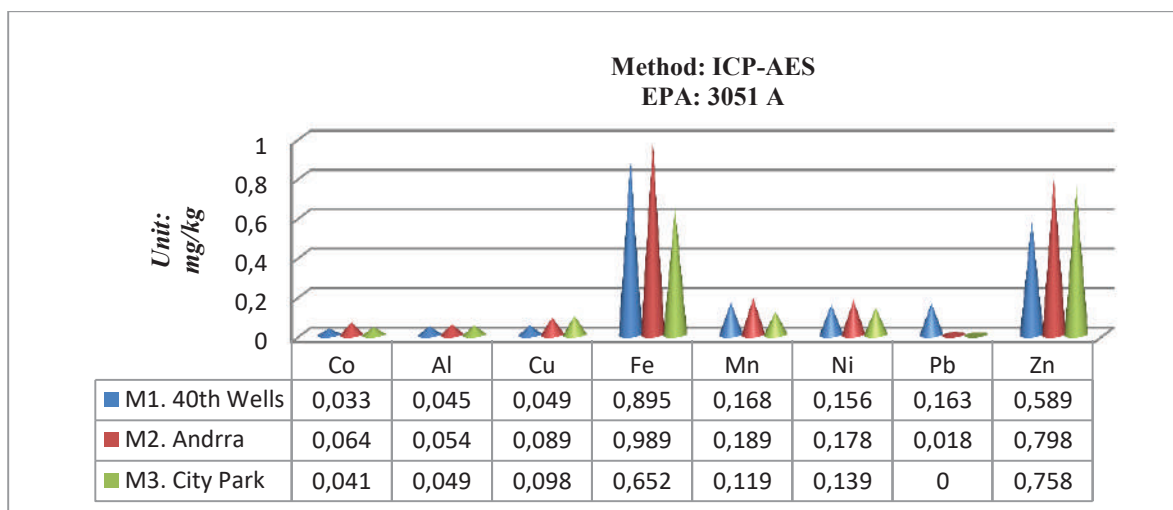


Fig. 4. The presence of heavy metals in soil samples (mg/kg).

In the figure above (Fig. 4), there are presented the elements observed in soil samples in the vicinity of Lumbardhi River. Even in the case of soil samples, the highest concentration of elements is arranged according to the decrease of their concentration: Fe > Zn > Mn > Ni > Pb. Even in this case presented, the concentrations of As and Cd, is below the detection limit, while, Co, Al and Cu, are presented as low values, to comment.

Iron varies in soil samples from 0.652 mg/kg to the highest of 0.989 mg/kg, Zn starts from

0.589 to 0.798 mg/kg, Mn from 0.119 to 0.189 mg/kg, Ni 0.139 to 0.178 mg/kg and Pb 0.163 to 0.189. The concentration of Co was observed in three soil samples from 0.033 to 0.064 mg/kg, whereas, Al is presented from 0.045 to 0.054 mg/kg followed by Cu from 0.049 to 0.098 mg/kg.

Table 5. Classification of heavy metals in sludge and in soils according to Dutch Intervention values.

Elements in sludge	Non polluted (ppm)	Moderate polluted (ppm)	Heavily polluted (ppm)	Elements in soil	Target value (mg/kg)	Intervention value (mg/kg)
Cu	>25	25-50	>50	Cu	36	190
Zn	>90	90-200	>200	Zn	140	720
Ni	>20	20-50	>50	Ni	35	210
Cd	-	-	-	Cd	0.8	12
Pb	-	-	-	Pb	85	530

If we compare our results that we obtained (Tab. 3) with the recommendations of maximum amount allowed of these elements in sludge and soils that are presented in Table 5 [KORÇA et al. 2020], we see that our samples are below the maximum amount allowed concentrations. Our results compared with table 5, show that we are dealing with much lower concentrations than the maximum amount allowed target for each element, and much lower than the case on an intervention, (ATSDR 2004). Similar, we have the same in the case of the sludge samples, where their concentration is much lower than what is classified in the table as polluted and highly polluted [KORÇA et al. 2020, ATSDR 2004]. In all of our cases, our measured sludge results falls into the non-polluted category compared with table 5 as recommended.

CONCLUSIONS

The present investigation demonstrates the presence of physico-chemical parameters in the water, and heavy metals (Co, Al, Cu, Fe, Mn, Ni, Pb and Zn) in water, soil and sludge samples, measured with ICP-AES technique.

If we give a conclusion with the results presented, we are optimistic that the presence of contamination is not enormous comparing the physico-chemical parameters, properties of water, and heavy metal presence in water, sludge and soil.

Our analyses of the water of the river Lumbardhi of Prizren relate the water quality as good, except for some spots where anthropogenic pollutants probably appear. The physico-chemical parameters, are in accordance with the Water Framework Directive (DKU-WFD) 2000/60 and classification of river quality by UNECE (content, mg/L).

The results of heavy metals show that their concentrations are approximately within international standards, except for some spots where higher concentrations of some heavy metals are observed.

Based on WHO and EU standards for drinking water the Lumbardhi water was classified in the second class according to the concentration of iron, zinc, nickel, lead and manganese, whereas the presence of these elements in sludge and soil, is within any standard international.

Also, it is advisable that concentrations of pesticide should be measured too, since farmers in our country use these substances without any recommended quality and quantity, but it is very necessary that bacteriological parameters should be measured constantly in water samples.

Although Kosovo has no legislative prohibition for exceeded concentrations of toxic metals in the natural water resources until now, the results from this study represent a small contribution to gain a clear overview of the state in this field of environmental quality assurance. We have thus concluded that water resources of Kosovo's are put at risk by anthropogenic pollution. It is advisable to keep the continuous monitoring and analysis of the study area.

REFERENCES

- MUCHUWETI M., BIRKETT J.W., CHINYANGA R., M.D ZVAUYA., SCRIMSHAW LESTER J.N. 2006. Heavy metal content of vegetables irrigated with mixtures of wastewater and sewage sludge in Zimbabwe, Implications for human health. *Agriculture, Ecosystems & Environment*, Volume 112, Issue 1, pp. 41- 48.
- JUSUFI K., STAFILOV T., VASJARI M., KORCA B., HALILI J and BERISHA A. 2017. Measuring the presence of heavy metals and their bioavailability in potato crops around Kosovo's power plants, *Fresenius Environmental Bulletin* 26(2a/2017a), pp. 1682-1686.
- BAJRAKTARI N., MORINA I., DEMAKU S. 2019. Assessing the Presence of Heavy Metals in the Area of Gllloogoc (Kosovo) by Using Mosses as a Bioindicator for Heavy Metals, *Journal of Ecological Engineering*, Volume 20, Issue 6, pp. 135-140.
- FERATI F & KEROLLI-MUSTAFA M & KRAJA-YLLI A. 2015. Assessment of heavy metal contamination in water and sediments of Trepça and Sitnica rivers, Kosovo, using pollution indicators and multivariate cluster analysis, *Environ Monit Assess*, 187:338 <https://doi.org/10.1007/s10661-015-4524-4>.
- MARKOVIĆ S., VUČKOVIĆ B., NIKOLIĆ-BUJANOVIĆ L. 2020. Heavy metals and radon content in spring water of Kosovo, *Sci Rep* 10, 10359. <https://doi.org/10.1038/s41598-020-67371-1>.
- GASHI F., FRANČIŠKOVIĆ-BILINSKI S., BILINSKI H., SHALA A and GASHI A. 2017. Impact of Kishnica and Badovci Flotation Tailing Dams on Levels of Heavy Metals in Water of Graçanica River (Kosovo), *Journal of Chemistry*, Volume-Article: ID 5172647, 10 pages <https://doi.org/10.1155/2017/517264>.
- THOMSEN S. T., HERRERA J A.R., JAKOBSEN L., FAGT S., PIRES S.M. 2019. Burden of disease of heavy metals in population clusters: towards targeted public health strategies, *European Journal of Public Health*, Volume 29, Issue 4.
- HAZRAT A., EZZAT K and IKRAM I. 2019 Environmental Chemistry and Ecotoxicology of Hazardous Heavy Metals, Environmental Persistence, Toxicity and Bioaccumulation, *Journal of Chemistry*, Volume, 14 pages, <https://doi.org/10.1155/2019/6730305>.
- MALIQI E., JUSUFI K & KUMAR SINGH S. 2020. Assessment and Spatial Mapping of Groundwater Quality Parameters Using Metal Pollution Indices, Graphical Methods and Geoinformatics", *Analytical Chemistry Letters*, 10 (2), pp. 152-180.
- KESTNER R. 1975. Chemical speciation in sea water, in: E. D. Goldberg (Ur.), *The nature of sea water*, Dahlem Konferenzen, Berlin, p.172.
- MEMIM. 2016. Encyclopedia. Retrieved 29 April "Bistrica (Kosovo)".
- APHA., AWWA., WEF. 1998. Standard methods for the examination of water and wastewater (20th ed.) Washington DC, 1998.
- ZHUSHI E.F., ÇARDAKU H., BYTYÇI A., KUÇI T., DESKU A., YMERI P., BYTYÇI P. 2020. Correlation between physical and chemical parameters of water and biotic indices: The case

- study the White Drin River basin, Kosovo. *Journal of Water and Land Development*. No. 46 (VII–IX) p. 229–241. DOI 10.24425/jwld.2020.134585.
- WHO. 2011. Guidelines for drinking-water quality. 4th edition. WHO, Geneva, Switzerland.
- WHO. 1993. World Health Organization. Guidelines for Drinking Water Quality. World Health Organization, Geneva, Switzerland.
- EPA. 2007. "Method 6010C (SW-846): Inductively Coupled Plasma-Atomic Emission Spectrometry," Revision 3.
- U.S. EPA. 2007. "Method 3051A (SW-846): Microwave Assisted Acid Digestion of Sediments, Sludges, and Oils," Revision 1. Washington, DC.
- DKU-WFD. 2000. Water Framework Directive (DKU-WFD, 2000/60).
- WHO. 2011. Guidelines for drinking-water quality. 4th edition. WHO, Geneva, Switzerland.
- EU's drinking water standards. 1998. Council Directive 98/83/EC on the quality of water intended for human consumption.
- WHO. 2004. World Health Organization. Copper in drinking water.
- ATSDR. 2005-Public Health Statment, Zinc CAS#: 7440-66-6.
- IARC. 1978. Working Group on the Evaluation of Carcinogenic Risks to Humans, & World Health Organization. Overall evaluations of carcinogenicity: an updating of IARC monographs volumes 1 to 42 (Vol. 7). World Health Organization.
- CHANDRA GHOSH G., JAHED HASSAN KHAN MD., KUMAR CHAKRABORTY T., ZAMAN S., ENAMUL KABIR A.H.M & TANAKA HUMAN H. 2020. Health risk assessment of elevated and variable iron and manganese intake with arsenic safe groundwater in Jashore, Bangladesh, *Scientific Reports Nature*, 10:5206.
- KORÇA B., DEMAKU S. 2020. Evaluating the Presence of Heavy Metals in the Vicinity of an Industrial Complex, *Pol. J. Environ. Stud.* Vol. 29, No. 5 pp. 3643-3649.
- ATSDR. 2004. Public Health Statment, Cobalt CAS#: 7440-48-4.

EFFECT OF THE MAGNETIC FIELD ON MIXED CONVECTION IN A CAVITY HEATED FROM THE TOP FILLED WITH A NANOFLUID

EL HATTAB Mohamed

Mechanics, Process of Energy and Environment Laboratory, Ibn Zohr University, ENSA, Agadir,
Morocco

Research Team, Energy and Sustainable Development, ESTG, Ibn Zohr University, Morocco

LAFDAILI Zakaria

Mechanics, Process of Energy and Environment Laboratory, Ibn Zohr University, ENSA, Agadir,
Morocco

ABSTRACT

In this paper, we present a numerical study of mixed convection in a square lid-driven cavity heated from top and filled with water-Cu nanofluid and subjected to a magnetic field oriented at an angle α with respect to the x axis. The transport equations are solved with finite volume method using the SIMPLE algorithm. Comparisons with previously published works are performed and found to be in good agreement. The influence of Grashof and Hartmann numbers as well as the volume fraction of nanoparticles on the hydrodynamic and thermal characteristics of the nanofluid is illustrated and discussed in terms of streamlines, isotherms and mean Nusselt number. Two orientations of the magnetic field ($\alpha = 0^\circ$ and 90°) were considered to control the flow.

Keywords: Mixed convection, Heat transfer, Magnetic field, Water-Cu nanofluid

PRODUCTION OF INDUSTRIAL BIOMOLECULES BY ACTINOMYCETES ISOLATED FROM SOIL IN SAUDI ARABIA

Maha Fahad Algouraibi

Department of Biology, College of Science and Arts at Khulis, University of Jeddah,
Jeddah, Saudi Arabia.

Nashwa Ibrahim Hagagy

Department of Biology, College of Science and Arts at Khulis, University of Jeddah,
Jeddah, Saudi Arabia.

Lobna Abdelkefi-Mesrati

Department of Biology, College of Science and Arts at Khulis, University of Jeddah,
Jeddah, Saudi Arabia.

In Saudi Arabia industry, many enzymes with higher efficiency and low cost were needed. For that different screening programs were done to search the most suitable microorganisms producing the high quality enzymes. Moreover, many medical problems appeared such as the resistance of different bacteria to antibiotics which encourage us the search of new active biomolecules. In the present study, we decided to investigate unexplored areas of Saudi Arabia to isolate actinomycetes with probably promising features.

After isolation of 59 actinomycetes from different soil cities in Saudi Arabia, we investigated their morphological properties and their ability to produce extracellular enzymes on solid culture media containing specific substrates as a sole source of utilization. Different types of enzymes were detected in the new bacterial collection. In fact, out of fifty nine actinomycetes, 44 isolates (74%) showed amylase activity, 45 isolates (76%) produced cellulase enzymes, 44 isolates (74%) were classified as positive to catalase, 29 isolates (49%) were found positive for lipase activity and 40 isolates (67%) were able to produce protease enzymes.

After comparison between promising stains showing diverse characters including color of aerial mycelium, reverse side color, and ability to produce diffusible pigments, we conducted an identification study. The sequencing and alignment of rDNA of the chosen isolates permitted the identification of the genus *Streptomyces*.

Some strains exhibited a significant antimicrobial activity against two Gram-negative bacteria (*Escherichia coli* and *Klebsiella pneumonia*), two Gram-positive bacteria (*Staphylococcus aureus* and *Bacillus subtilis*) and one yeast (*Candida albicans*). The results indicated that *Streptomyces* sp. strain JS1 and strain JS2 showed high inhibitory activity (5.5, 7.5 mm) against *B. subtilis* and *C. albicans*, respectively. Moreover, MIC of their extracts revealed that they have good inhibitory activity against Gram-positive, Gram-negative and fungal pathogens with MIC values ranged between 30 and 45 µg/ml.

Keywords: Actinomycetes, biomolecule, enzyme, antimicrobial activity.

REMOVAL OF SULFATE FROM LEATHER INDUSTRY WASTEWATER WITH DIFFERENT ACTIVATED CARBON ADSORPTIONS

Assoc. Prof. Ali Rıza DİNÇER

Department of Environmental Engineering, Çorlu Faculty of Engineering, Tekirdağ Namık Kemal University, Tekirdağ, Turkey ORCID:0000-0002-9294-0643

MSc. Elçin GENÇ

Çevre Gıda ve Endüstriyel Analiz Laboratuvarı, Merkez Mah. Tatlıpınar Sok. Mert Plaza, No:13, k:1-2, 34406, Kağıthane-İstanbul

Assist Prof. Dr. İbrahim Feda ARAL

Department of Civil Engineering, Çorlu Faculty of Engineering, Tekirdağ Namık Kemal University, Tekirdağ, Turkey ORCID:0000-0002-9294-0643

Abstract

The characterization of wastewater originating from the leather industry has a complex structure and contains high amounts of organic and inorganic substances. Many treatment methods have been tried in the literature for the treatment of leather wastewater. In this study, sulphate removal was investigated by adsorption method. Solutions were prepared by adding 0.5 g, 1 g and 2 g granular activated carbon to the waste water. Adsorption was carried out on an orbital shaker for 30 min, 45 min, 60 min, 90 min and 120 min. At the end of the adsorption process, sulfate determination was carried out in the samples. The removal efficiencies of these activated carbons were compared by using two different types of activated carbon as adsorbent. Adsorbents were added to wastewater in different doses, at different times and at different pH, and their effect on the adsorption was investigated in these variables. As a result of the study, it was determined that the removal efficiency obtained as a result of the adsorption with granular activated carbon as the adsorbent was higher than the coconut activated carbon at pH=4, where removal was high in both adsorbents. Maximum sulphate removal coefficient (Q_0) in granular activated carbon and coconut activated carbon was found as 2.44978 ($R^2=2.44978$) and 2.747253 mg/g ($R^2=2.747253$), respectively.

Key words: Adsorption, Leather, Sulfate, Wastewater

1. Introduction

With the increasing industrialization, the removal of pollutants in wastewater is one of the subjects that have been studied. Industrial facilities have to treat their wastewater in a way that will not harm the environment and be below the determined discharge limits.

A series of processes are carried out for the final product obtained in the leather industry. Sulphate, which is among the polluting parameters in the wastewater formed as a result of the processes, causes negative effects. Sulphate is reduced to hydrogen sulfide by the effect of bacteria in concrete channels where industrial wastewater is conveyed under anaerobic conditions, and the resulting H_2S oxidizes to form H_2SO_4 with moisture. Thus, it causes

corrosion of concrete pipes. It is also known to cause odor at low pH due to the presence of H_2S (Duranoğlu, 2011).

Various studies have been carried out in our country on physical, chemical, biological, advanced treatment and combinations of these treatment methods for the removal of SO_4^{2-} in leather industry wastewater. In this study, the removal of SO_4^{2-} by adsorption method was investigated. During the processing of raw hide, leather; pre-processes such as wetting, calcining, hair removal. At this stage, the skin is freed from the pieces of meat on it, making it easier for chemicals used in advanced processes to penetrate the skin (Küçükpelvan et al., 2017).

After the pre-treatments are applied, the leather is made ready for the tanning process. The tanning process is carried out with the help of tanning agents to give the leather a stable form and to provide high heat resistance. The substances used in tanning can be listed as mineral, vegetable and synthetic organic substances. Chromium is the most widely used mineral tanning agent with its unique properties to leather (Özgünay et al., 2007).

Wet finishing processes consist of neutralization, bleaching, retanning, dyeing and lubrication steps, and these processes are usually carried out in a single process (Karabay, 2008).

Crust undergoing retanning, dyeing and drying processes is subjected to a few more processes. The purpose of these processes is to make the leather softer and to close minor faults. By processing the leather with organic solvent or water-based paint and varnish, the resistance of the leather is increased, its appearance is improved and the surface becomes homogeneous. After this process, the leather is given its final shape and the process is completed with the garment stage (Küçükpelvan et al., 2017).

Wastes from the leather industry are among the most important industrial wastewaters. The polluting parameters are Cr^{+6} , SO_4^{2-} , total chromium, COD, BOD, AKM, sulfur, oil and grease (Pehlivanoğlu et al., 1998). When these polluting parameters are carried to surface waters by wastewater, they precipitate over time and form sludge at the bottom, which causes many problems such as filling lakes and dams, deterioration of oxygen balance and turbidity. In addition, chromium has toxic and carcinogenic effects, as well as a tendency to accumulate in living organisms (Tunay et al., 1991).

In the leather industry, mostly chromium salts are used to make animal skins non-perishable and usable, that is, tanning. Although various alternative materials have been developed for tanning in recent years, the reasons such as the fact that chromium salts are more economical and that no substance alone can replace the properties that chromium salts give to leather make chromium salts indispensable in the tanning process (Çetinkaya et al., 2010). SO_4^{2-} passes into wastewater due to the intensive use of sulfuric acid (Küçükpelvan et al., 2017). Pollutant parameters in wastewater originating from leather industry; COD, BOD, Total Suspended Solids, pH, Oil and Grease, Ammonia, TKN, Sulfur, Total Dissolved Solids, SO_4^{2-} , Cr^{+6} , Surfactant etc. can be counted as In order to make the treatment system simpler and more effective, wastewater containing chromium and sulfur is collected separately and pre-treated during the processing of the leather and then combined with other wastewaters (Küçükpelvan et al., 2017).

Sulfurous wastewater; It is formed as a result of washing water during the hair removal process, and sulfur oxidation, neutralization and carbonization processes are generally applied after balancing in the treatment of these wastewaters (Kabdaşlı et al., 1992).

By pre-treatment of chrome-containing wastewater, chromium is recovered and hazardous waste generation is reduced. While the simple precipitation process is sufficient in case of separation, chemical precipitation is applied for chrome removal if it is not done (Kabdaşlı et al., 1992).

It is preferred that leather production is carried out in Organized Industrial Zones so that leather wastewater can be treated in common treatment facilities. It is preferred to construct a central treatment plant for industrial wastewater, as each industrial establishment requires a separate treatment plant and requires huge investments. The initial investment and operating cost in Organized Industrial Zones, and the selection of the appropriate treatment plant are important for calculating the participation shares of the industries in the region (Küçükpelvan, 2019).

2. Material and Methods

Analysis of the adsorption data was performed according to the Langmuir isotherm.

The Langmuir isotherm explains better than other isotherms whether the retention that occurs in active adsorption areas on solid surfaces is physical or chemical adsorption. In the Langmuir isotherm; adsorption increases linearly with the initial adsorbent concentration. At the maximum saturation point, the surface is covered with a single layer and the amount of adsorbent adsorbed on the surface remains constant. In the Langmuir isotherm, the adsorption energy is uniform. The adsorption rate is directly proportional to the adsorbent concentration and the empty adsorption areas on the surface (Beyhan, 2003).

The Langmuir isotherm model assumes that adsorption takes place on a homogeneous surface and in a monolayer. At the same time, Langmuir acknowledges that all active sites have the same energy and equal affinity for the molecules to be adsorbed (Langmuir, 1918).

$$C_e \text{ (mg l}^{-1}\text{)} / q_e \text{ (mg g}^{-1}\text{)} = 1/(Q_0 \cdot K_L) + (1/Q_0 \text{ (g)}) \cdot C_e \text{ (mg l}^{-1}\text{)} \quad (1)$$

In these equations, C_e (mg l⁻¹) value is the concentration of SO₄⁻² and Cr⁺⁶ in the equilibrium solution, q_e (mg g⁻¹) value is the amount of adsorbed SO₄⁻² and Cr⁺⁶, K_L value is Langmuir constant, Q_0 (g) is adsorbed. It gives the maximum amount of SO₄⁻² and Cr⁺⁶ that can be produced. Since the equation specifies a line between C_e/q_e and C_e values, the slope of the line gives the value of $1/Q_0$, and the point where the line intersects on the y-axis gives the value of $1/Q_0 \cdot K_L$ (Namasivayam et al., 2001).

2.1. Preparation of Samples

Activated carbon weighings used in the study were made on analytical balance. The balance is a device that has an accuracy of 0.0001 grams and can automatically calibrate itself.

0.5 g, 1 g and 2 g activated carbon were added to 100 ml wastewater samples used in the study, and adsorption was carried out in an orbital shaker for 30 minutes, 60 minutes, 45 minutes, 90 minutes and 120 minutes.

The adsorption of the samples prepared in an orbital shaker, whose shaking speed can be adjusted optically-electronically, was carried out by circular mixing method at a rotational speed of 150 rpm.



Figure 1. Mixing process of samples in orbital shaker

Sulphate analyzes in the study were performed with a 2100N model Hach-Lange turbidimeter. The turbidimeter has a measuring range of 0 - 4000 NBB.

2.3. Determination of Sulphate

SO_4^{-2} is widely distributed in nature and can be found in natural waters in concentrations ranging from a few mg/l to g/l (Stieg et al., 1997).

The SO_4^{-2} determination in the wastewater sample used in this study was analyzed by the SM 4500- SO_4^{-2} :E method.

In the analysis principle, SO_4^{-2} ions precipitate with BaCl_2 forming BaSO_4 crystals of uniform size. The light absorbance of the BaSO_4 suspension is measured with a photometer and the SO_4^{-2} concentration is determined by comparison with the generated standard curve (Stieg et al., 1997).

The wastewater sample used in this study was stored at 4 °C since bacteria can reduce SO_4^{-2} to S^{-2} if organic substances are present in the sample during the study.

The pH value of the sample used in the study was measured as 7.74. The adsorption process was carried out at two different pH values: mixing with the addition of activated carbon on the sample without changing the pH value of 7.74, and adding activated carbon after the pH value was adjusted to 4 with HCl.

A buffer solution was prepared by dissolving 30 g of $\text{MgCl}_2 \cdot 6\text{H}_2\text{O}$, 5 g of $\text{CH}_3\text{COONa} \cdot 3\text{H}_2\text{O}$, 1 g of KNO_3 , 20 ml of CH_3COOH in 500 ml of water and completing it with distilled water to 1000 ml.

The wastewater sample used in this study was diluted 10 times during the analysis and the calculations were made by considering the dilution rate.

5 ml of sample on 45 ml of water was filtered with a 0.45 μm filter with the help of an injector. A 50 ml sample was taken into a 100 ml beaker and 10 ml of Buffer-A solution was added to it. The turbidity of the sample was recorded as the first reading value by placing it in the turbidimeter cuvette. A spatula full of BaCl_2 was added to the sample taken out of the cuvette and then mixed for 1 minute on a magnetic stirrer. The mixed sample was put back into the turbidimeter cuvette and the value in the turbidimeter was recorded at the end of 5 minutes.

Subsequently, a calibration curve was created by plotting SO_4^{-2} concentrations.

3.Results and Discussion

Solutions were prepared by adding 0.5 g, 1 g and 2 g granular activated carbon to the waste water. Adsorption was carried out on an orbital shaker for 30 min, 45 min, 60 min, 90 min and 120 min. At the end of the adsorption process, sulfate determination was carried out in the samples. The results are shown in the Figures below. The highest SO_4^{-2} removal was achieved in 60 minutes in the adsorption experiment performed with 0.5 g granular activated carbon for variable times. 318.7 mg/l, 298.5 mg/l, 267.1 mg/l, 300.1 mg/l at pH=7.74 adsorption time of 30 min, 45 min, 60 min, 90 min and 120 min, respectively and sulfate values of 325.1 mg/l were obtained.

During the 90 and 120 min adsorption period, the sulfate concentration increased above 300 mg/l. In this case, it was determined that the activated carbon gave back the sulphate that it had held during the long mixing process. The same study was repeated as 30 min, 45 min, 60 min, 90 min and 120 min adsorption trial with 1 g granular activated carbon. At pH=7.74, the effluent sulfate concentrations were 272.3 mg/l, 266.4 mg/l, 254.3 mg/l, 268.2, respectively, at 30 min, 45 min, 60 min, 90 min and 120 min adsorption times. Compared to 0.5 g activated carbon adsorption values, higher efficiency was obtained in 1 g activated carbon adsorption. The effluent sulfate concentrations increased at 90 and 120 min adsorption times. When examined, the highest SO_4^{-2} removal was achieved in 60 minutes in the adsorption experiment performed with 1 g granular activated carbon for variable times. The same study was repeated with 2 g granular activated carbon for 30 min, 45 min, 60 min, 90 min and 120 min adsorption trial. The results are given in Figure 2. In the adsorption experiment performed with 2 g granular activated carbon with variable durations, the highest SO_4^{-2} removal was achieved in 60 minutes. At the same pH value, at the adsorption times of 30 min, 45 min, 60 min, 90 min and 120 min, the effluent sulphate concentration decreased in the first 60 min time period, and the effluent sulphate concentrations increased again at the end of 90 and 120 min.

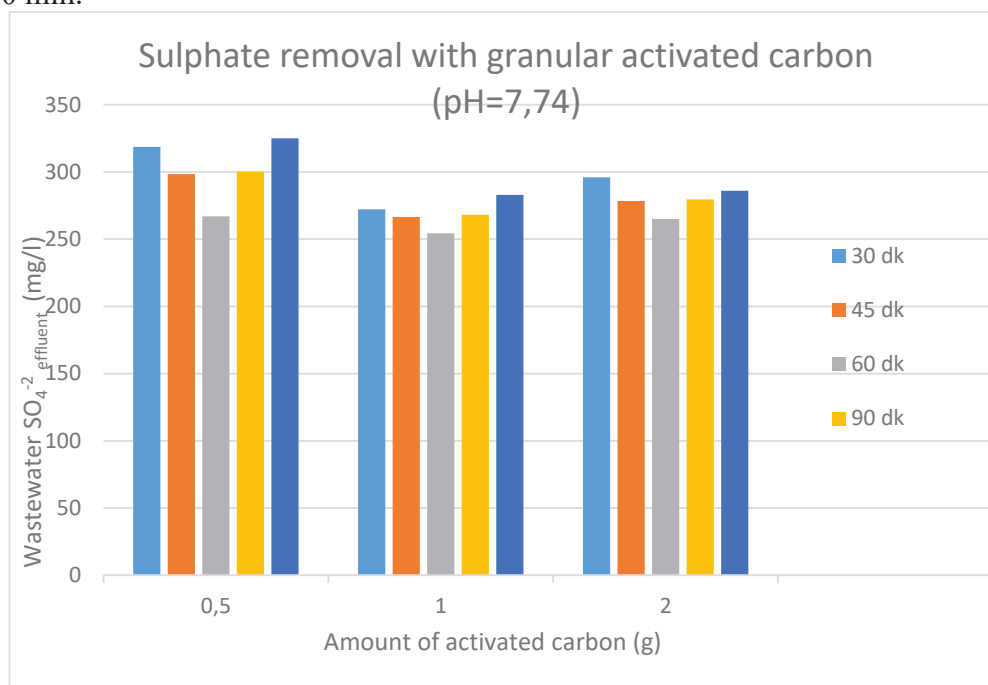


Figure 2. SO_4^{-2} removal with granular activated carbon (pH=7.74)

When the Figure 3 is examined, the highest SO_4^{-2} removal was achieved in 60 minutes in the adsorption experiment performed with 0.5 g granular activated carbon for variable times. At pH=4, 277.2 mg/l, 251.4 mg/l, 220.8 mg/l, 230.4 mg/l and 225 adsorption times, respectively,

at 30 min, 45 min, 60 min, 90 min and 120 min adsorption time. As a result of adsorption, the highest adsorption occurred in the first 60 min time period. The sulfate concentration increased during the 90 and 120 min adsorption process. In this case, it was determined that the activated carbon gave back the sulphate that it had held during the long mixing process. The same study was repeated as 30 min, 45 min, 60 min, 90 min and 120 min adsorption trial with 1 g granular activated carbon. At pH=4, the effluent sulfate concentrations were 252.1 mg/l, 231.8 mg/l, 206.2 mg/l, 218.0 mg, respectively, at adsorption times of 30 min, 45 min, 60 min, 90 min and 120 min. /l and 224.0 mg/l were found. Compared to 0.5 g activated carbon adsorption values, higher efficiency was obtained in 1 g activated carbon adsorption. The yield reached the highest value at 60 min adsorption time. The effluent sulfate concentrations increased at 90 and 120 min adsorption times. When examined, the highest SO_4^{-2} removal was achieved in 60 minutes in the adsorption experiment performed with 1 g granular activated carbon for variable times. The same study was repeated with 2 g granular activated carbon in the form of 30 min, 45 min, 60 min, 90 min and 120 min adsorption trial at pH=4. In the adsorption experiment performed with 2 g granular activated carbon with variable durations, the highest SO_4^{-2} removal was achieved in 60 minutes. At the same pH value, at the adsorption times of 30 min, 45 min, 60 min, 90 min and 120 min, the effluent sulphate concentration decreased in the first 60 min time period, and the effluent sulphate concentrations increased again at the end of 90 and 120 min.

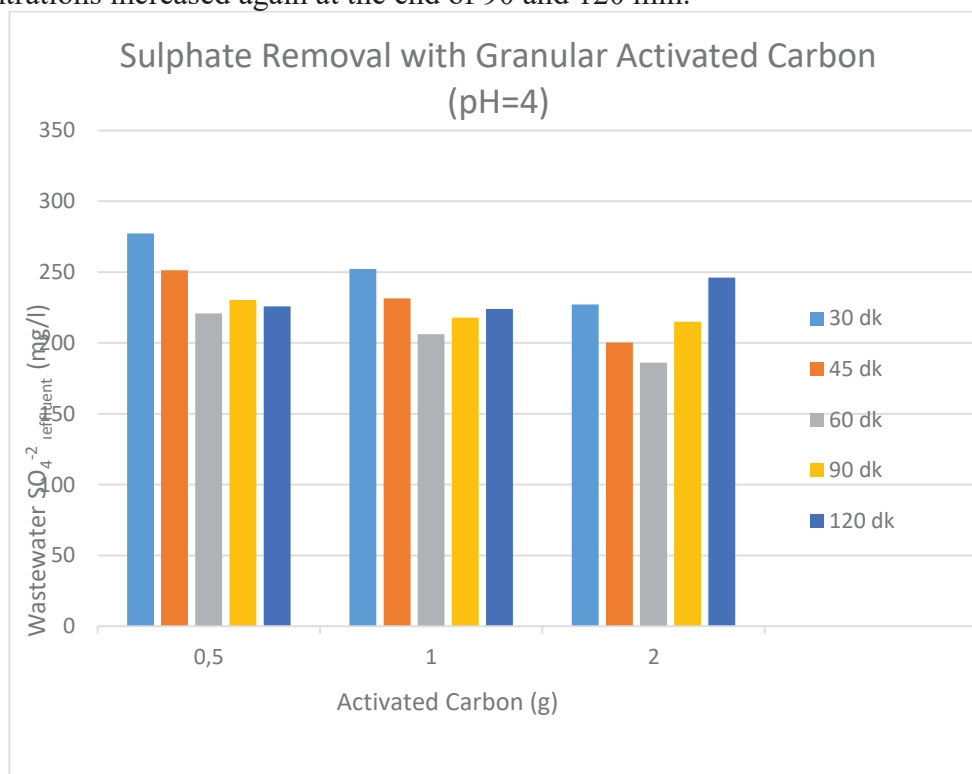


Figure 3. SO_4^{-2} removal with granular activated carbon (pH=4)

3.1. Sulphate Removal with Coconut Activated Carbon

Solutions were prepared by adding 0.5 g, 1 g and 2 g of coconut activated carbon to the waste water. Adsorption was carried out on an orbital shaker for 30 min, 45 min, 60 min, 90 min and 120 min. At the end of the adsorption process, sulfate determination was carried out in the samples. When Figure 4 is examined, the highest SO_4^{-2} removal was achieved in 60 minutes in the adsorption experiment performed with 0.5 g coconut activated carbon for variable

times. 274.0 mg/l, 263.7 mg/l, 256.9 mg/l, 269.2 mg/l at pH=7.74 adsorption time of 30 min, 45 min, 60 min, 90 min and 120 min, respectively and 282.5 mg/l sulfate values were obtained. As a result of adsorption, the highest adsorption occurred in the first 60 min time period.

The sulfate concentration increased during the 90 and 120 min adsorption process. In this case, it was determined that the activated carbon gave back the sulphate that it had held during the long mixing process. The same study was repeated as 30 min, 45 min, 60 min, 90 min and 120 min adsorption trial with 1 g coconut activated carbon. The results are shown in figure 4. At pH=7.74, the effluent sulfate concentrations were 263.7 mg/l, 260.4 mg/l, 258.5 mg/l, 261, respectively, at the adsorption times of 30 min, 45 min, 60 min, 90 min and 120 min. 2 mg/l and 269.4 mg/l were found. The yield reached the highest value at 60 min adsorption time. The effluent sulfate concentrations increased at 90 and 120 min adsorption times. When Figure 4 is examined, the highest SO_4^{2-} removal was achieved in 60 minutes in the adsorption experiment performed with 1 g coconut activated carbon for variable times. The same study was repeated with 2 g granular activated carbon for 30 min, 45 min, 60 min, 90 min and 120 min adsorption trial. In the adsorption experiment performed with 2 g coconut activated carbon for variable times, the highest SO_4^{2-} removal was achieved in 60 minutes. At the same pH value, at the adsorption times of 30 min, 45 min, 60 min, 90 min and 120 min, the effluent sulphate concentration decreased in the first 60 min time period, and the effluent sulphate concentrations increased again at the end of 90 and 120 min.

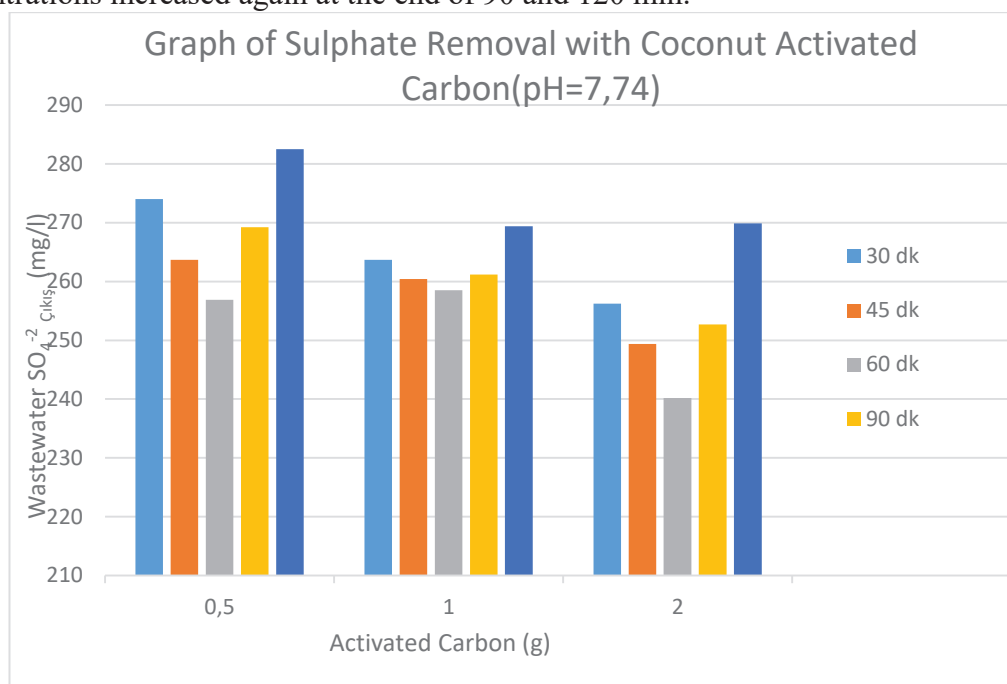


Figure 4. SO_4^{2-} removal with Coconut activated carbon (pH=7.74)

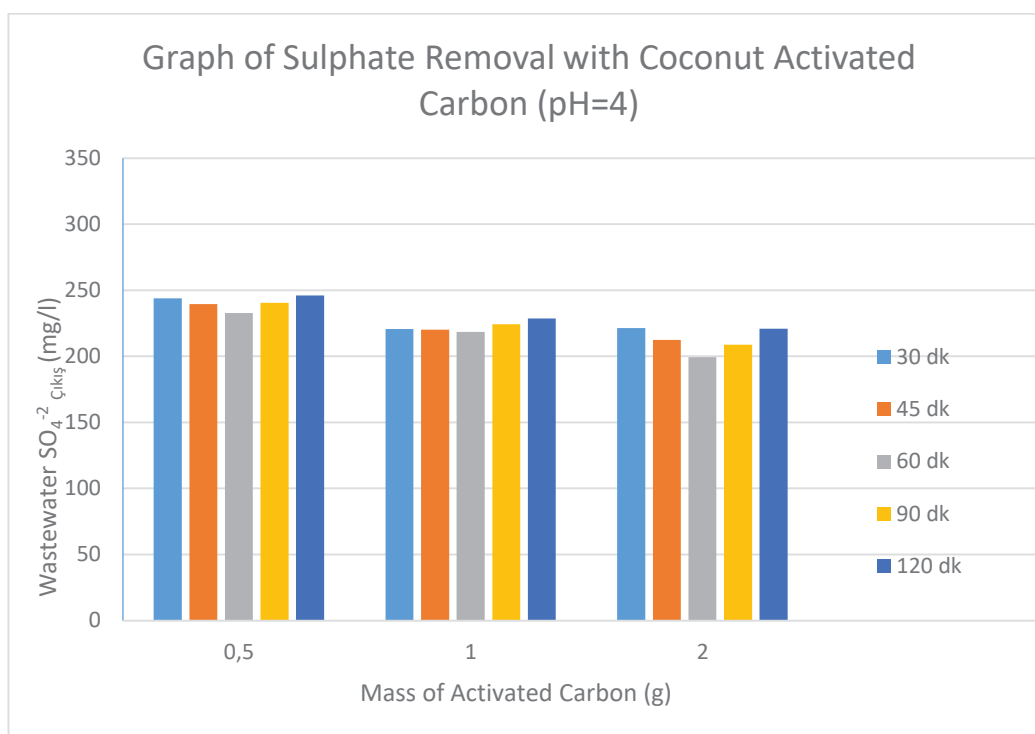


Figure 5. Effluent sulphate concentrations are shown at pH=4 at 0.5 g, 1 g and 2 g activated carbon concentrations at 30 min, 45 min, 60 min, 90 min and 120 min adsorption times.

The highest adsorption efficiencies were achieved with the use of 1 g and 2 g activated carbon. The optimum dose for sulfate adsorption was determined as 2 g at pH=4. At low adsorbent ratio, effluent sulfate concentrations increase. It was found that the sulfate retained in the activated carbon was desorbed again during the long mixing time. It was determined that the maximum removal was at acidic pH.

As a result of the SO_4^{2-} removal study with coconut activated carbon, the highest SO_4^{2-} removal efficiency was obtained when adsorption was performed with 2 g of activated carbon at pH=4 for 60 minutes. The results with the highest removal efficiency are given in Figure 5. Increasing the amount of activated carbon from 0.5 g to 1 g in adsorption with coconut activated carbon at pH = 4 for 60 minutes allowed 3% in SO_4^{2-} removal, while increasing it from 1 g to 2 g yielded 6%.

Due to the low SO_4^{2-} removal efficiency, 1.0353 g of Na_2SO_4 chemical was added to the distilled water in order to be able to evaluate, and a sample with a SO_4^{2-} result of 346.7 mg/l was obtained. As a result of the study, since the efficiency of SO_4^{2-} removal with granular activated carbon is higher than that of coconut activated carbon, the evaluation study was carried out with granular activated carbon at pH=4 and pH=7. As in the study on the wastewater sample, in the trial study with pure water, the highest SO_4^{2-} removal efficiency was achieved in 60 minutes of adsorption using 2 g of activated carbon at pH=4.

Langmuir adsorption model was used in the mathematical description of SO_4^{2-} removal obtained as a result of adsorption with 2 g of activated carbon at pH=4 where the removal is high in both adsorbents. Graphics of isotherms are given in Figure 6.

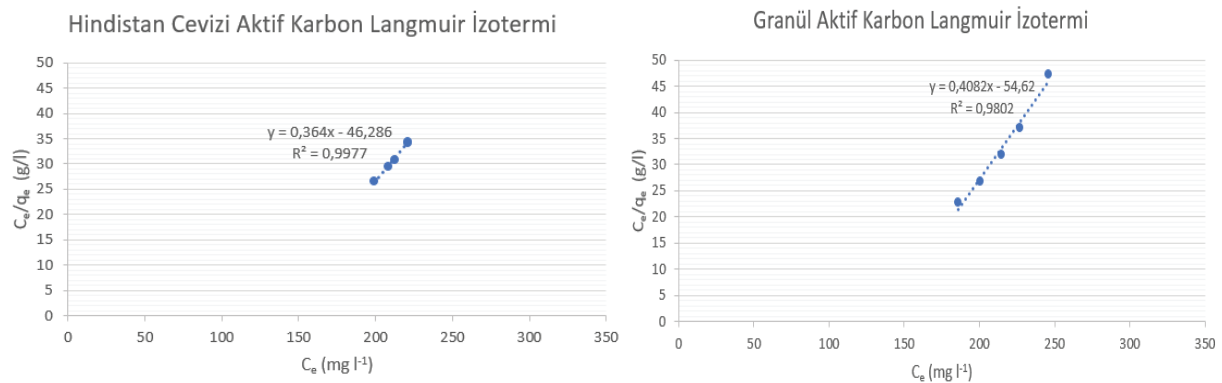


Figure 6. Langmuir isotherm plot for SO_4^{2-} removal

Langmuir adsorption isotherm constants were calculated and the results were given in Table 1. Langmuir adsorption model was used in the mathematical description of SO_4^{2-} removal obtained as a result of adsorption with 2 g of activated carbon at pH=4 where the removal is high in both adsorbents. Graphics of isotherms are given in Figure 6.

Namasivayam et al. (2007), in their studies on anion removal, determined that the amount of SO_4^{2-} in water can be reduced by means of activated carbon obtained by using coconut shell fibers.

As reported by Bingöl (2013), when the effect of the initial pH on the equilibrium adsorption capacity was investigated, it was observed that the highest adsorption capacity was reached at pH = 4.5. The reason is related to the positive loading of the chitosan particle adsorbent surface. Adsorption of SO_4^{2-} ions from water increases with decreasing pH value. The effect of adsorbent concentration on SO_4^{2-} adsorption with chitosan particles was investigated at different adsorbent amounts, and it was observed that the amount of SO_4^{2-} removed from the environment increased with the increase in adsorbent concentration.

As reported by Arslan (2009), one of the most important factors affecting the adsorption process is the contact time between the adsorbent and the solution. The adsorbent rapidly adsorbs the material in the liquid film layer surrounding it, and the adsorption rate is high at the first contact. As the contact time increases, the adsorption rate decreases. Because at the end of a certain time, an equilibrium is established between the adsorbed substance and the substance in the

Table 1. Langmuir coefficients and adsorption distribution constants of SO_4^{2-} adsorption

adsorbent	Langmuir Isotherm		
	Q_0 (mg g ⁻¹)	K_L (l mg ⁻¹)	R^2
Granular Activated Carbon	2,44978	0,007473	0,9802
Coconut Activated Carbon	2,747253	0,007864	0,9977

In SO_4^{2-} adsorption, Langmuir adsorption equation is obeyed for both adsorbents ($R^2 > 0.98$).

4. References

- Arslan S. (2009). Bitkisel Kaynaklı Aktif Karbon ile Pestisit Giderimi, (Yüksek Lisans Tezi), Y.T.Ü. Fen Bilimleri Enstitüsü, İstanbul.
- Beyhan M. (2003). Atık çamurlar ve doğal malzemeler ile sulardan florür iyonu gideriminin araştırılması (Doktora Tezi), Yıldız Teknik Üniversitesi, İstanbul.
- Bingöl İS. (2013). Kitosan partikül ile atık sulardan SO₄-2 giderilmesi (Yüksek Lisans Tezi), Hacettepe Üniversitesi Kimya Mühendisliği Ana Bilim Dalı, Ankara.
- Çetinkaya F., Çetinkaya Y. (2010). Derinin Tabaklanması İşleminde Maskeleye Maddeleri Kullanımının Krom Alımı Üzerine Etkisinin Araştırılması. Hayvansal Üretim, 51(1), 40-47.
- Duranoğlu D. (2012). Sulfate removal from wastewater by chemical precipitation method. Journal of Engineering and Natural Sciences Mühendislik ve Fen Bilimleri Dergisi, 30, 39-55.
- Kabdaşlı I., Tünay, O. (1992). Deri Endüstrisinde Arıtma Uygulamaları, İTÜ 3. Endüstriyel Kirlenme Sempozyumu.
- Karabay S. (2008). Waste Management İn Leather Industry, M.Sc.Thesis, Dokuz Eylül Üniversitesi.
- Küçükpelvan H., Yarıntepe C.C., Öz N.A. (2017). Deri atıksunun arıtım metotları. Çanakkale Onsekiz Mart Üniversitesi Fen Bilimleri Enstitüsü Dergisi, 3, 1, 59-96
- Langmuir I. (1918). The adsorption of gases on plane surfaces of glass, mica and platinum, Journal of the American Chemical Society, 40, 1361–1403.
- Namasivayam C., Sangeetha D. (2007). Application of coconut coir pith for the removal of sulfate and other anions from water. WOS.
- Namasivayam C., Radhika R., Suba S. (2001). Uptake of dyes by a promising locally available agricultural solid waste: coir pith. Waste Manage. 21, 381–387.
- Özgünay H., Çolak S., Mutlu M. M., Akyüz F. (2007). Characterization Of Leather Industry Wastes, Polish J. Of Environ. Stud. 16, 6, 867-873.
- Pehlivanoglu E., Ertas T. T., Tanik A., Kutahya A. (1998). Chemical Treatability Of Dyeing Bath Wastewaters in Textile Industry, First International Workshop on Enviromental Quality and Enviromental Engineering in The Middle East Region, 671-677.
- Stieg S., Fisher B.R., Mathre O. B., Wright T.M. (1997). 4500-SO₄²⁻ Sulfate. Approved by Standard Methods Committee, Editorial revisions, 2011.
- Tunay O., Ovez S., Alp K., Sakar S., Sunter İ. (1991). Endüstriyel Atıksuların Ön Arıtılması, Teknoloji İletimi Semineri No: 1, İSO-SKATMK.

A CASE OF PERICARDITIS FIBRINOSA CAUSED BY HISTOPHILUS SOMNI IN A TWO-MONTH-OLD SIMMENTAL BREED CALF

Mehmet TUZCU

Selcuk University Faculty of Veterinary Medicine Department of Pathology Selcuklu/KONYA
ORCID: 0000-0003-3118-1054

Nevin TUZCU

Selcuk University Faculty of Pharmacy Department of Pharmaceutical Microbiology
Selcuklu/KONYA ORCID: 0000-0002-1017-718X

Zeynep CELIK

Selcuk University Faculty of Veterinary Medicine Department of Pathology Selcuklu/KONYA
ORCID: 0000-0002-9667-5728

Gokhan AKCAKAVAK

Yozgat Bozok University Faculty of Veterinary Medicine Department of Pathology
Sorgun/YOZGAT ORCID: 0000-0001-5949-4752

Abstract

In this presentation, a case of pericarditis fibrinosa associated with *Histophilus somni* in a 2-month-old female Simmental calf brought to our pathology laboratory with a request for necropsy was evaluated pathologically and microbiologically. Macroscopically, severe fibrinous inflammation was found in the pleura and pericardial sac. It was observed that the liver was quite swollen and in a crunchy consistency, and the gall bladder was quite full. While multifocal collapsed areas were determined in the cortex region of the kidneys, severe hyperemia and focal bleeding areas were found in the abomasum. Severe thickening of the microscopic pericardium and inflamed cells, mostly neutrophils, were observed. Masson trichrome stainings showed that this thickening consisted of dense connective tissue components and fibrin. Severe hyperemia, alveolar emphysema, alveolar macrophages in the interalveolar septum of the lung, as well as inflammatory infiltration areas containing dense connective tissue and neutrophils in some areas of the pleura were determined. It was noted that the remark cords in the liver were dissociated, hepatocytes were different from each other in appearance, and large vacuoles in their cytoplasm. In the kidneys, necrosis, degeneration and desquamation of the tubular epithelium, hemorrhages and mononuclear cell infiltrations in the intertubular areas were observed, while a pink homogeneous material was found in the Bowman capsule. According to the findings obtained in pathological and microbiological examinations, the case was diagnosed as pericarditis fibrinosa due to *Histophilus somni*. This result reveals that *Hemophilus somni* should also be considered in determining the etiology of fibrinous pericarditis in calves.

Keywords: Fibrinous pericarditis, *Histophilus somni*, Fibrinous pleuritis.

1. INTRODUCTION

Pericarditis is inflammation of the visceral and parietal leaves of the pericardial sac. Pericardial inflammations rarely occur locally, commonly during the course of systemic diseases. Fibrinous pericarditis usually occurs by the hematogenous route, but sometimes in inflammatory events in the surrounding tissues, they can come to the pericardium with the lymphatic system and cause inflammation. In fibrinous pericarditis, the pericardial tissue is rough, granular, and there are fibrin deposition and adhesions on the epicardial surface [1,20].

Histophilus group microorganisms are found in all animal species. As they form part of the normal bacterial flora, they cause specific infections in various animals and are also secondary to some other infections. The most important infections caused by Histophilus group microorganisms are equine contagious metritis, chicken infectious coryza, sheep bronchopneumonia and swine influenza [2,18,16].

Histophilus somni (Histophilus ovis, Haemophilus agni, Haemophilus somnus) is an opportunistic pathogenic bacterium in the form of gram-negative coccobacillus that causes systemic infections [17]. The agent was first described in 1960 as a Haemophilus-like organism that causes meningoencephalitis in beef cattle in California [10,8]. Infection is common in cattle in North America, Western Europe and Scandinavia, causing serious economic problems [6]. Histophilus somni causes meningoencephalitis, arthritis, pleuritis, bronchopneumonia, otitis, mastitis and myocarditis in cattle [16,14,7].

Histophilosis is a sporadic disease of cattle worldwide. Predisposing factors for the disease are stress, weather, diet-related factors and mixing of cattle with different herds [15]. The agent causes thrombotic meningoencephalitis especially in young beef cattle. Although there is insufficient information about the invasion of the vessels in the pathogenesis of the disease, the main site of invasion of the vessels is considered to be the respiratory system. After the invasion of the agent into the vessels, it causes septicemia and creates vasculitis in many organs. The disease mostly occurs shortly after winter feeding and return from pasture. The disease progresses in subacute, chronic and lethal or non-lethal forms [20,4]. The disease cannot be fully diagnosed clinically. Vaccination is known to be the most effective and appropriate method to prevent disease [11].

Hemophilus show a different growth requirement from other microorganisms. They do not grow on routine artificial media in the laboratory. They need growth factors for their reproduction. Microorganisms adapted to the medium after initial isolation can grow without growth factor [19,16].

Coagulative necrosis, neutrophilic inflammation, bleeding and fibrous exudates in the heart are frequently reported pathologically in myocarditis cases of calves with Histophilus somni in the etiology. Bacterial colonies consisting of coccobacilli were also reported in Gram staining performed on these sections. Areas of necrosis have been reported to be surrounded by an infiltrate of inflammatory cells predominantly composed of neutrophils, lymphocytes, plasma cells, and macrophages. Thrombosis and vasculitis have been identified in medium and small diameter arteries and veins. Fibrinous pericarditis has also been reported in some cases with areas of acute infarction in the heart. Bronchopneumonia with multifocal necrosis with moderate, diffuse congestion in the lungs and alveolar exudation of fibrin and neutrophils has been reported. Fibrin effusion with entangled neutrophils and macrophages in the pleura has been reported [3,9,13].

In this presentation, a case of pericarditis fibrinosa associated with Histophilus somni in a 2-month-old female Simmental calf brought to our pathology laboratory with a request for necropsy was evaluated pathologically and microbiologically.

2. MATERIAL AND METHOD

2.1 Case Report

The material of this case report consists of tissues of a 2-month-old dead calf belonging to a breeder who applied to our department with the complaint of blood in the stool, respiratory distress and death. Tissue samples taken after autopsy of the calf were processed with known laboratory methods and stained with Hematoxylin Eosin and special staining methods. The culture of tissue samples were performed 10% blood agar and chocolate agar, and incubated for 72 hours at 37 °C in an aerobic and microaerophilic environment, Microscopic photographs (Olympus, DP12) were taken from the necessary preparations as a result of microscopic examinations.

3. RESULTS AND DISCUSSION

In the necropsy performed on the calf brought to our department with the complaints of hemorrhagic enteritis and respiratory distress, a severe fibrinous inflammation was found in the pleura and pericardial sac macroscopically (Figure 1.A). This fibrinous inflammation was also observed in the parenchyma tissue of the lung. In addition, hard hepatizing pneumonia foci were seen in the lung (Figure 1.C). It was observed that the liver was quite swollen and in a crunchy consistency, and the gallbladder was quite full (Figure 1.A). While multifocal collapsed areas were detected in the cortex region of the kidneys (Figure 1.C), severe hyperemia and focal bleeding areas were observed in the abomasum (Figure 1.F).

Microscopic examinations revealed hyperemia in the myocardium, as well as degeneration and necrosis in myocytes. In addition, severe thickening of the pericardium and inflamed cells mostly composed of neutrophil granulocytes were observed (Figure 2.A). In the Masson trichrome stainings, it was observed that this thickening consisted of dense connective tissue components and fibrin (Figure 2.F). In addition to severe hyperemia, alveolar emphysema, alveolar macrophages in the interalveolar septum of the lung, inflammatory infiltration areas containing dense connective tissue and neutrophils were detected in some areas of the pleura (Figure 2.B-C). It was noted that the remark cords in the liver were dissociated, hepatocytes were different from each other in appearance, and large vacuoles in their cytoplasm (Figure 2.D). In addition, areas of focal necrosis were also found in some areas. In the kidneys, necrosis, degeneration and desquamation of the tubular epithelium, hemorrhages and mononuclear cell infiltrations in the intertubular areas were observed, while a pink homogeneous material was found in the Bowmann's capsule (Figure 2.E).

In microbiological examinations, immobile, Gram (-), catalase (-), oxidase (+), indole (-), H₂S (-), urea (-), ONPG (+), with yellow pigmented, round shaped flat colony growing in microaerophilic environment, VP (-), coccobacillus bacteria with citrate reaction (-) were identified as *Histophilus somni*.

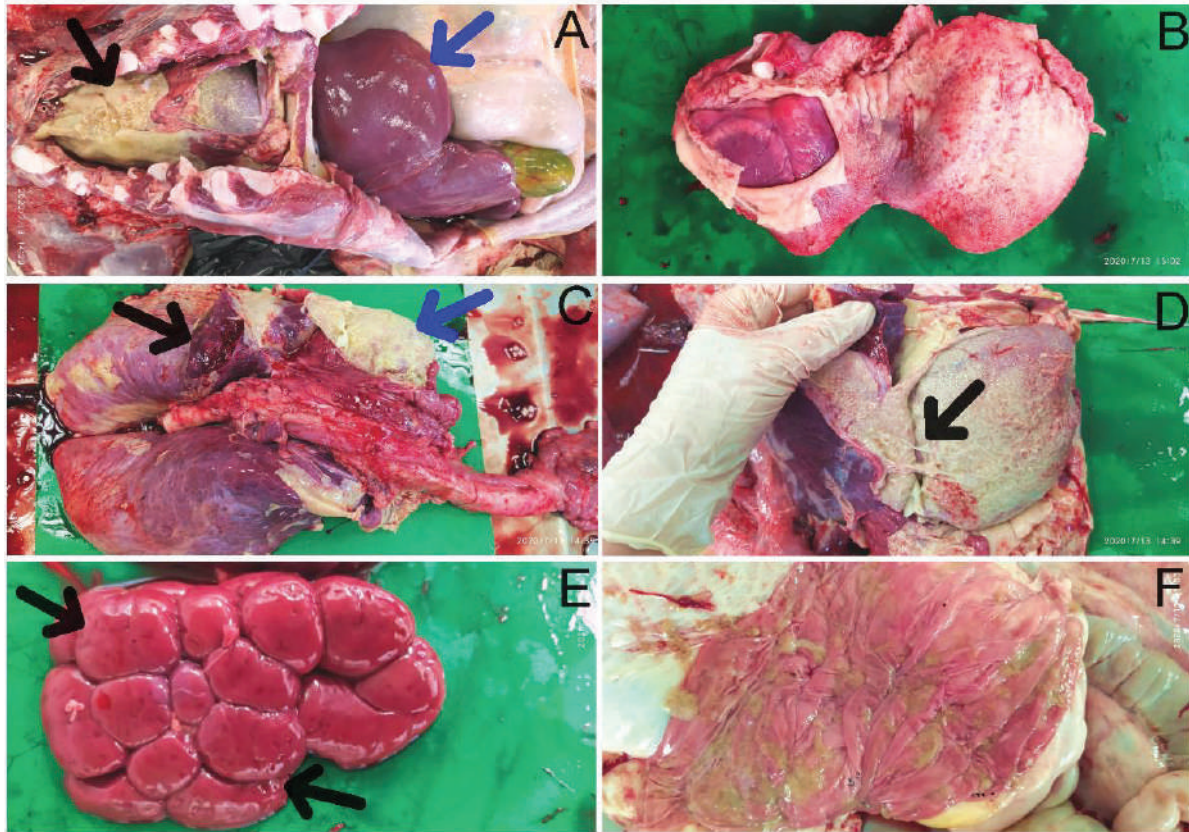


Figure 1. A. Dense fibrin mass in thoracic cavity organs (black arrow) and liver very swollen and friable (blue arrow), B. Dense fibrin mass in pericardium, C. Fibrin masses in cranial lobes of lung (blue arrow) and pneumonia area (black arrow), D. Dense fibrin masses in the pericardium and epicardium (arrow), E. Multifocal sunken areas (arrows) in the renal cortex region, F. Hyperemia and focal bleeding areas in the abomasum mucosa.

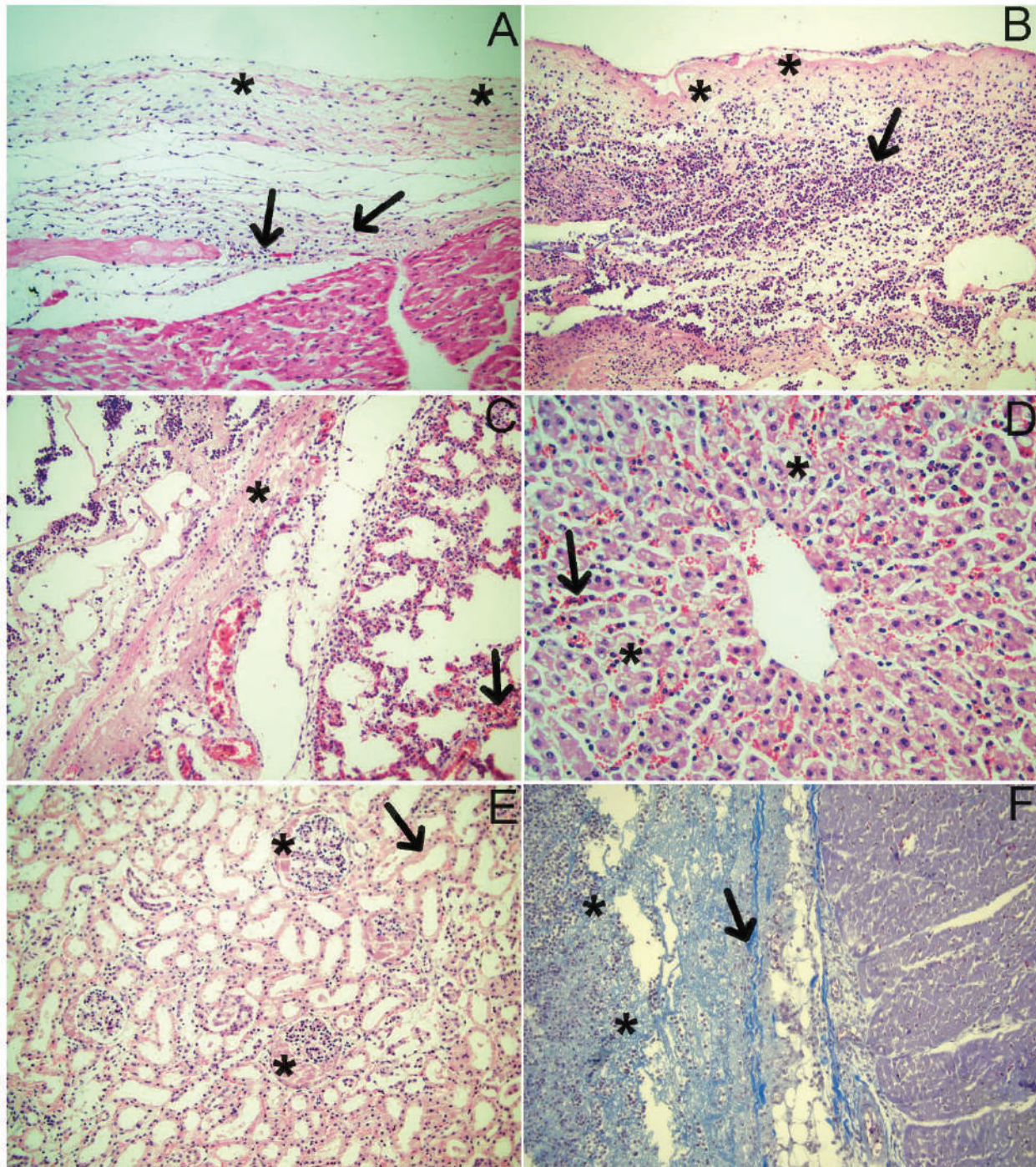


Figure 2. **A.** Inflammatory cell infiltrates (arrows) and fibrin structures (stars) in the pericardium of the heart, H.E, x200. **B.** Inflammatory cell infiltrates (arrow) and fibrin structures (asterisks) in pleura in the lung, H.E, x400. **C.** Hyperemia (arrow) in the interalveolar septum in the lung and fibrin structures (star) in the pleura, x200. **D.** Dissociation of remark cords in liver, large vacuoles (stars) in hepatocyte cytoplasm and hyperemia (arrow) in sinusoids, H.E, x400. **E.** Degenerative and necrotic changes (arrow) in tubular epithelium in kidney with pink homogeneous material (stars) in Bowmann's capsule, H.E, x200. **F.** Fibrin structures (stars) and connective tissue (arrows) in the pericardium of the heart, Massom trichrome, x200.

This case was diagnosed with cardiac histophilosis based on pathological and microbiological findings. *Trueperella pyogenes*, *Listeria monocytogenes*, *Escherichia coli*, *Pseudomonas* spp. or *Streptococcus* spp. Embolic pyogenic or opportunistic bacterial pathogens such as embolic

pyogenic or opportunistic bacterial pathogens can also cause myocarditis in cattle, but such lesions tend to be randomly distributed and outbreaks are rare [12].

In our country, there is very little published information about cardiac histophylosis in the remote areas. Most reports of cardiac histophilosis originate in Canada and, to a lesser extent, the United States and the United Kingdom [5,12]. The calf that constitutes our case belongs to a farm in Eskil district of Aksaray province. There are no previous reports of cardiac histophylosis in our region. In a study conducted in Canada, it was reported that *H. somni* was responsible for 76% of myocardial diseases detected in beef cattle in Canada [5].

4. CONCLUSION

According to the findings obtained in pathological and microbiological examinations, the case was diagnosed as pericarditis fibrinosa due to *Histophilus somni*. This result reveals that *Histophilus somni* should be considered in determining the etiology of fibrinous pericarditis in calves.

REFERENCES

- [1]. H. Athar, J. Parrah, B. Moulvi, M. Singh, F. Dedmari. "Pericarditis in bovines-a review." International Journal of Advanced Veterinary Science and Technology, 1, 1, 19-27.
- [2]. E. Biberstein. "Haemophilus and Taylorella. In: Diagnostic Procedure in Veterinary Bacteriology and Mycology." Eds: Elsevier, p. 151-64. 2012. 1990.
- [3]. SF. Elswaifi. "The molecular characterization of phosphorylcholine (ChoP) on *Histophilus somni* lipooligosaccharide: contribution of ChoP to bacterial virulence and pathogenesis." Virginia Tech. 2006.
- [4]. H. Erer, MK. Çiftçi, M. Ortatatlı, F. Hatipoğlu, Ö. Özdemir. "Veteriner Sistemik Patoloji" II.Cilt. 4. 2020.
- [5]. DM. Haines, KM. Moline, RA. Sargent, JR. Campbell, DJ. Myers, PA. Doig. "Immunohistochemical study of *Hemophilus somnus*, *Mycoplasma bovis*, *Mannheimia hemolytica*, and bovine viral diarrhoea virus in death losses due to myocarditis in feedlot cattle." The Canadian Veterinary Journal, 45, 3, 231. 2004.
- [6]. FW. Harris, ED. Janzen. "The *Haemophilus somnus* disease complex (hemophilosis): a review." The Canadian Veterinary Journal, 30, 10, 816. 1989.
- [7]. SA. Headley, AH. Pereira, LC. Balbo, GWD. Santia, AP. Bracarense, LF. Cunha, J. Schade, W. Okano, PF. Pereira, F. Morotti. "Histophilus somni-associated syndromes in sheep from Southern Brazil." Brazilian Journal of Microbiology, 49, 591-600. 2018.
- [8]. PC. Kennedy, EL. Biberstein, J. Howarth, LM. Frazier, D. Dungworth. "Infectious meningo-encephalitis in cattle, caused by a haemophilus-like organism." American journal of veterinary research, 21, 403-9. 1960.

- [9]. A. Kessell, J. Finnie, P. Windsor. "Neurological diseases of ruminant livestock in Australia. III: bacterial and protozoal infections." *Australian veterinary journal*, 89, 8, 289-96. 2011.
- [10]. G. LA. "Infectious embolic meningo-encephalitis in cattle." *Journal of the American Veterinary Medical Association*, 129, 9, 417-21. 1956.
- [11]. RL. Larson, D. Step. "Evidence-based effectiveness of vaccination against *Mannheimia haemolytica*, *Pasteurella multocida*, and *Histophilus somni* in feedlot cattle for mitigating the incidence and effect of bovine respiratory disease complex." *Veterinary Clinics: Food Animal Practice*, 28, 1, 97-106. e7. 2012.
- [12]. CA. Margineda, D. O'Toole, M. Prieto, FA. Uzal, GC. Zielinski. "Histophilus somni myocarditis and leptomeningitis in feedlot cattle: case report and occurrence in South America." *Journal of Veterinary Diagnostic Investigation*, 31, 6, 893-8. 2019.
- [13]. D. O'Toole, K. Sondgeroth. "Histophilosis as a natural disease." *Histophilus somni*, 15-48. 2015.
- [14]. Y. Pan. "An Investigation of *Histophilus somni* Virulence Factors in Pathogenesis and Diagnosis." *Virginia Polytechnic Institute and State University*. 2014.
- [15]. Y. Pan, B. Subhadra, I. Sandal, A. Dickerman, TJ. Inzana. "The role of *uspE* in virulence and biofilm formation by *Histophilus somni*." *Veterinary Microbiology*, 109267. 2021.
- [16]. PJ. Quinn, BK. Markey, FC. Leonard, P. Hartigan, S. Fanning, E. Fitzpatrick. "Veterinary microbiology and microbial disease." *John Wiley & Sons*. 2011.
- [17]. I. Sandal, TJ. Inzana. "A genomic window into the virulence of *Histophilus somni*." *Trends in microbiology*, 18, 2, 90-9. 2010.
- [18]. JG. Songer, KW. Post. "Veterinary microbiology-E-book: bacterial and fungal agents of animal disease." *Elsevier Health Sciences*. 2004.
- [19]. L. Stephens, J. Humphrey, P. Little, D. Barnum. "Morphological, biochemical, antigenic, and cytochemical relationships among *Haemophilus somnus*, *Haemophilus agni*, *Haemophilus haemoglobinophilus*, *Histophilus ovis*, and *Actinobacillus seminis*." *Journal of Clinical Microbiology*, 17, 5, 728-37. 1983.
- [20]. JF. Zachary, MD. McGavin. "Pathologic Basis of Veterinary Disease." *Elsevier Health Sciences*. 2012.

SUBCUTANEOUS MULTIPLE MASTOCYTOMA IN AN 8-YEAR-OLD MALE ENGLISH SETTER

Ozgur OZDEMIR

Selcuk University, Faculty of Veterinary Medicine, Department of Pathology, Konya, Turkey.
ORCID: 0000-0002-1595-0557

Mehmet Burak ATES

Selcuk University, Faculty of Veterinary Medicine, Department of Pathology, Konya, Turkey,
ORCID: 0000-0003-1297-426X

Mehmet TUZCU

Selcuk University, Faculty of Veterinary Medicine, Department of Pathology, Konya, Turkey,
ORCID: 0000-0003-3118-1054

Abstract

In this presentation, mast cell tumors were described in 2 subcutaneous masses located in the femoral region of the hind leg in a male English Setter dog. In 8-year-old male dogs brought to the veterinary clinic with the complaint of lameness, 2 masses of 2x1.5x1.5 and 1.5x1.5x1 cm were detected in the distal right femoral region, subcutaneous tissue and feeling embedded in the muscle tissue. It was observed that the totally extirpated masses were brownish-black in appearance and had a hard structure. The cross-sectional faces of the masses were grayish-white and cloudy in appearance. Sections prepared after routine tissue fixation and follow-up procedures were stained with Hematoxylated-Eosin (HE), Methyl Green Pyronin (MGG), Dominici and Congo Red (CR). The preparations were examined under a light microscope. In microscopic examination; Tumoral masses with unclear borders and progressing from the dermis into the muscle tissue were observed. In these areas, there were similar cells with oval or round shape, prominent nuclei, abundant and prominent cytoplasm with bluish colored granules, arranged in cords. It was determined that cytoplasmic granules showed methochromasia in staining with Dominici Dye. In addition, cytoplasmic granules in pink color were determined in staining with MGG. A large number of eosinophil granulocytes were found among the tumoral cells. In addition, amyloid deposits with a pink homogeneous appearance and positive staining with Congo Red were found among the tumor cells. As a result, the case was defined as subcutaneous multiple mastocytoma. Since multiple tumors are not common in dogs, it was deemed appropriate to present them.

Keywords: Subcutaneous mastocytoma, English Setter, pathology, amyloidosis

1.

2. INTRODUCTION

Mast cell tumors can be found ubiquitously in pet species. Tumors may be nodular or multicentric, mostly in the skin. In addition to the skin, it can also be seen in internal organs such as the liver, spleen, and intestines. Although the location and biological behavior differ by species, the similarities are greater. Mast cell tumors (MCTs) are quite common in dogs. It is less common in cats, but rare in other species. Mast cell tumors constitute 21% of skin neoplasms in dogs and are

the most frequently diagnosed malignant skin tumor in dogs. Although there is no gender or age preference, its incidence increases with age. The mean age of MCT is reported as 9 [1- 3].

The breeds in which mastocytomas are most common in dogs are boxers, shar-peis, bulldogs, labrador and golden retrievers, pit bull terriers, Boston terriers, , fox terriers, weimaraners, cocker spaniels, Rhodesian ridgebacks, dachshunds, Australian cattle dogs, pug dogs, beagles, schnauzers. Boxers and pug dogs tend to develop MCTs that are less biologically aggressive, while shar-peis tend to develop MCTs that often behave more aggressively at a younger age. The majority of MCTs in animals occur as single nodules in the skin. Subcutaneous MCTs should be distinguished from cutaneous MCTs in dogs as they have opposing biological behaviors. Mastocytomas can develop anywhere on the body. However, it commonly occurs in the skin and subcutaneous tissue. It has been reported to be more common in the hind legs in Boxers and Terriers. It has been reported frequently on the tail in Rhodesian ridgebacks, and on the head and hind legs in English setters [1- 2].

Subcutaneous mastocytomas can be located in the subcutis anywhere in the body. However, in most of the cases (60%), it is located on the back, chest and legs. 95% of tumors are in the form of a single mass. While swelling is seen on the skin, ulceration rarely occurs. It is usually seen as a lipoma-like, fleshy soft masses with undefined borders [2].

Microscopically, tumoral cells are oval or spherical in shape, with a prominent round nucleus, and pale pink cytoplasm with bluish granules on staining with hematoxylin-eosin. Among these cells, abundant eosinophil granulocytes are found. In addition, findings such as collagenolysis, sclerosis, edema, necrosis, and secondary inflammation are quite common in mast cell tumors, and in cases where these findings are very intense, neoplastic cells may be masked by them. Diagnosis is easy because cytoplasmic granules are prominent in most of the cases. These granules are stained pink with giemsa and purple with Dominici [3-5].

2. MATERIALS AND METHODS

2.1. CASE HISTORY

In 8-year-old male dogs brought to the veterinary clinic with the complaint of lameness, 2 masses of 2x1.5x1.5 and 1.5x1.5x1 cm diameter were detected in the distal right femoral region, subcutaneous tissue and feeling embedded in the muscle tissue (Fig. 1). It was observed that the totally extirpated masses had a hard structure with a brownish-black appearance. The cross-sectional faces of the masses were grayish-white and cloudy in appearance.

2.2. METHODS

The extirpated masses were fixed in 10% formaldehyde solution for 24 hours. Slides prepared after routine tissue follow-up were stained with Hematoxylated-Eosin (HE), Methyl Green Pyronin (MGG), Dominici and Congo Red (CR) dyes ([6]). Preparations were examined under a light microscope (Olympus BX51, Tokyo, Japan).

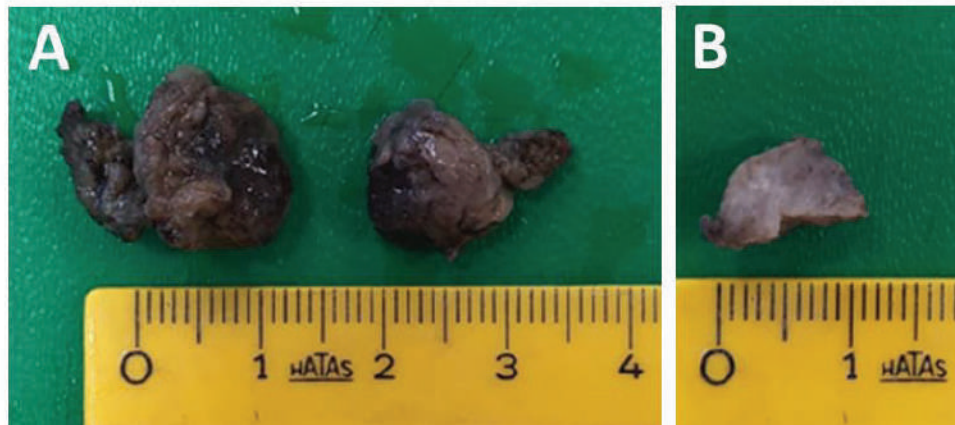


Figure 1. Masses extirpated from the hind leg (A) and cross-sectional face (B).

3. RESULTS AND DISCUSSION

In microscopic examination; Tumoral masses with unclear borders, advancing from the dermis into the muscle tissue were observed. In these areas, there were similar cells with broad and well-defined cytoplasm, which were arranged in cords, oval or round in shape, with a prominent nucleus, with bluish colored granules inside. It was determined that cytoplasmic granules showed methochromasia in staining with Dominici stain (Fig 3A-B). In addition, pink colored cytoplasmic granules were detected in staining with MGP (Fig 3C-D). Abundant eosinophil granulocytes were found among the tumoral cells. In addition, amyloid deposits with a pink homogeneous appearance and positive staining with Congo Red were found among the tumor cells.

Mast cell tumors are one of the most common skin tumors in dogs, and they are frequently seen between 8 and 10 years of age. They can develop anywhere on the body, but the hind legs, abdomen, and chest are the most common sites. It is more common in the hind legs in Boxers and Terriers, and in the head and hind legs in English setters [2]. In this study, tumors were found in the hind leg of the English setter dog, as reported in the literature. Although it is generally reported as single masses [2], 2 masses were extirpated in this case. In this case, the tumor was defined as a rare multiple form.

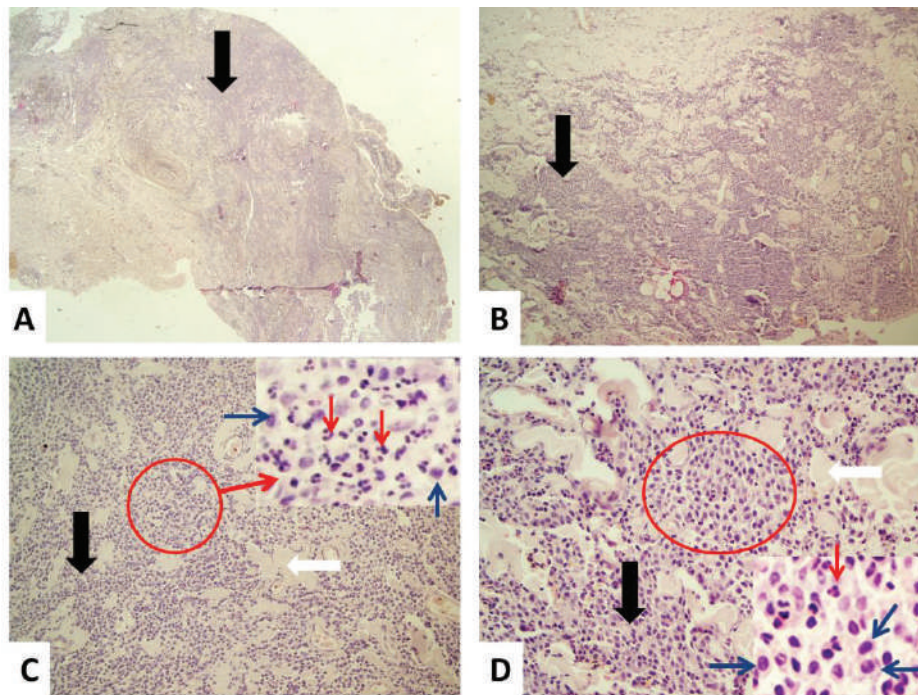


Figure 2. A-B. Tumoral infiltration (black arrow) extending from dermis into muscle tissue, H&E. C-D. Mast cells lined up in cords (black arrow) and hyalinized collagen (white arrow), Small Pictures: Mast cells with basophilic granules (blue arrow), Eosinophil granulocyte (red arrow) H&E.

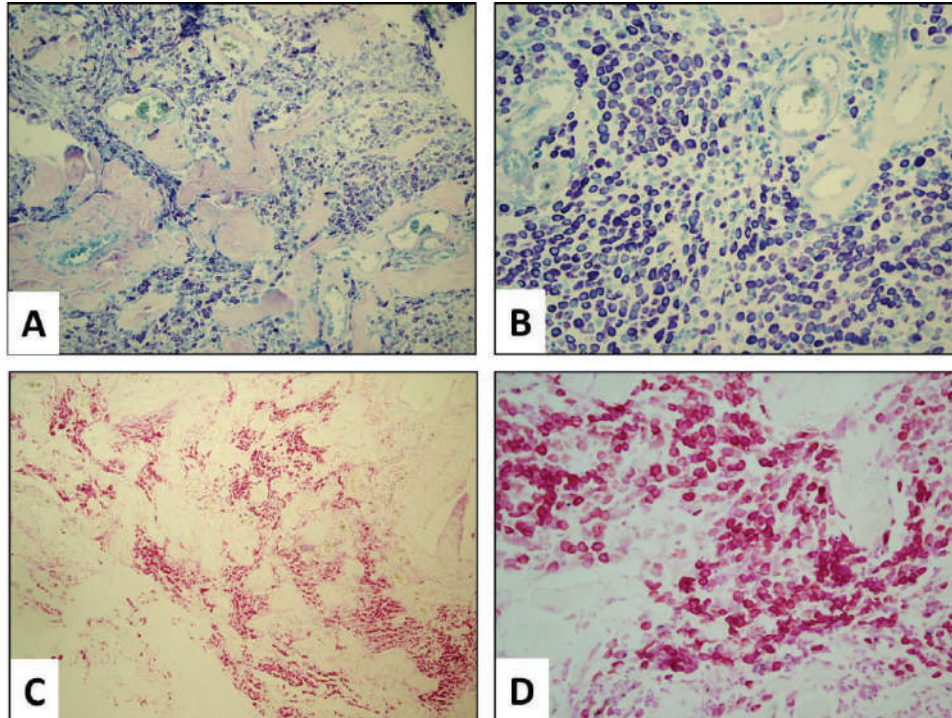


Figure 3. A-B. Mast cells with purple granules in their cytoplasm, Dominici Stain. CD. Mast cells with purple granules in their cytoplasm, MGP Stain.

In microscopic examination, the arrangement of the tumor in cords separated by thin bands, cell shape and cytoplasmic bluish granules in hematoxylin-eosin staining were consistent with the literature [5]. In the histochemical stainings performed to confirm the case, the granules were seen in purple color in Domici's Mast cell staining, and pink in color with Giemsa stain. With these data, it was defined as mastocytoma. In dogs, mastocytomas are usually in the epidermis and are called cutaneous mastocytomas. When tumor cells extend into the dermis and into the subcutaneous insertions, it is called a subcutaneous mastocytoma. In previous studies, it has been reported that subcutaneous mastocytomas were named as grade 2 cutaneous mastocytomas and were incorrectly evaluated [2]. In this case, because the tumor cells invaded from the dermis to the muscle tissue, it was evaluated as subcutaneous mastocytoma. Since subcutaneous mastocytomas do not have exact borders and invade into the tissues, the tumoral mass is not completely removed, and it is reported that it frequently recurs and metastasizes [7]. In this case, it was evaluated that due to the spread of tumor cells into the muscle tissue, there was no complete extirpation and possibly recurrence.

Abundant eosinophil granulocytes are common in tumoral areas ([3]). In addition, it has been reported that findings such as collagenolysis, sclerosis, edema, necrosis, and secondary inflammation may be encountered [2-5]. In this report, as well as hyalinized collagen deposits with abundant eosinophil granulocytes among tumor cells, amyloid deposits stained positively with Congo red were seen. It was evaluated that this may be the result of the slow and long-lasting development of tumoral masses.

4. CONCLUSION

As a result, the case was defined as subcutaneous multiple mastocytoma. Since multiple tumors are not common in dogs, it was deemed appropriate to present them.

REFERENCES

- [1]. A. Aydoğan, and N. Metin, (2013) Köpek yumuşak doku tümörlerinde patolojik tanı: derleme. MAKÜ Sag Bil Enst Derg, vol. 1 (2), pp. 86-105, 2013.
- [2]. M. Kiupel M, Mast cell tumor In: Tumors in domestic animals. 5th ed., Donald J. Meuten Ed., Ames, Iowa : John Wiley & Sons Inc, 2017.
- [3]. H. Erer and M. Kiran, Veteriner Onkoloji, 6th ed, Güler Ofset, Konya, 2019.
- [4]. S. Atalay Vural and Y. Aydın, Köpeklerin Mast Hücre Tümörleri: 19 Olguya Ait Patolojik Survey. Turk J Vet Anim Sci, vol. 25, pp. 887-893, 2001.
- [5]. F. Hatipoglu, M.B. Ates, M.K. Ciftci, O. Ozdemir, E. Oruc, F. Terzi , G. Akcakavak and M. Ortatatli, Multicentric Cutaneous Mast Cell Tumor in a Male Pitbull Dog. EurasianBioChem 2018, 26 - 27 April 2018, Ankara / TURKEY, pp.125, 2018.
- [6]. L.G. Luna, Manual of histologic staining methods of the Armed Forces Institute of Pathology. 3rd Edition, McGraw-Hill, New York. 1968
- [7]. A.E. Villalobos. (2021) Tumors of the Skin in Dogs in: MSD Manual (Veterinary Manual). [Online]. Available: <https://www.msdsmanual.com/dog-owners/skin-disorders-of-dogs/tumors-of-the-skin-in-dogs#v3207530>.

HEMANGIOPERICYTOMA IN A 17-YEAR-OLD FEMALE GOLDEN RETRIEVER DOG**Ertan Oruc**

Selcuk University, Faculty of Veterinary Medicine, Department of Pathology, Konya, Turkey.

ORCID: 0000-0003-4234-8219

Ozgur Ozdemir

Selcuk University, Faculty of Veterinary Medicine, Department of Pathology, Konya, Turkey.

ORCID: 0000-0002-1595-0557

Mehmet Burak Ates

Selcuk University, Faculty of Veterinary Medicine, Department of Pathology, Konya, Turkey.

ORCID: 0000-0003-1297-426X

Abstract

Hemangiopericytoma is one of the most common subcutaneous soft tissue tumors of dogs. The neoplasm is histopathologically characterized by spindle-shaped cells arranged in whorls around the blood vessels and characterized by the appearance of neoplastic cells as a "fingerprint" pattern. In this report, we described a case of hemangiopericytoma in a Golden Retriever dog. In the anamnesis of female dog, it was 17 years old and firstly noted by the owner about 3 years ago that the swelling noticed in the subcutaneous region of the distal humerus was about 0,5 cm in size. Due to the swelling getting bigger in the course of time (about three years), the mass was resected and submitted to Pathology Laboratory of the Faculty of Veterinary Medicine, Selcuk University. Biopsy materials in 2 pieces were measured as 6.5X4.5X5 and 2.5X2X2 cm in diameter. Grossly, the cross-sectional face of the large piece, cream-colored and viscous, had a layered appearance. The smaller one had a hard consistency and the cross-sectional face had a red and white mottled appearance. After the routine histopathology process, Tissue sections were stained with hematoxylin and eosine (HE) and Masson's Trichrome (MT) stains and examined under the light microscope. Microscopically, the neoplasm was multilobular and composed of pleomorphic spindle-shaped cells. The neoplastic cells had vesicular nuclei and contained round nucleoli. The neoplastic tissue cells were arranged in multiple helices which is separated by stromal collagen. There was mild hemorrhages and some necrotic area. Mitotic figures were seen in these sections. Considering that it develops slowly and remains localized for a long time, it was found appropriate to present it as a case report.

Keywords: Hemangiopericytoma, Golden Retriever Dog, Histopathology

1. INTRODUCTION

Hemangiopericytoma, first described by Stout and Murray in 1942 is one of the most common subcutaneous soft tissue tumors of dogs. It is rare and aggressive mesenchymal tumors which arises from Zimmermann pericytes surrounding the endothelial lining of capillaries and venules [1,2]. There is no significant difference between Breeds or in the sex distribution of affected dogs in terms of tumor preference. It is reported 74% of the tumors developed on the extremities and recurrence rates were 60% with surgical excision combined with radiotherapy and 31% with only surgical excision [3].

Hemangiopericytoma is characterized by spindle-shaped cells with cytoplasmic process arranged in whorls around blood vessels in microscopy. The structure formed by neoplastic cells gives the tumor a "fingerprint" pattern [4]. The neoplasm is generally local infiltrative and metastasizes are seldom [5]. In a study conducted in dogs treated with postoperative radiation; The survival time was determined as 2.5-55 months. It has been reported that 40.9% of the dogs did not re-grow for 24 months. It was determined that 40% of the dogs died from tumor recurrence or tumor-related causes [6]. In this presentation, a case of slowly developing hemangiopericytoma in a 17-year-old female dog is discussed.

2. MATERIAL AND METHOD

In the anamnesis of female dog, it was 17 years old and firstly noted by the owner about 3 years ago that the swelling noticed in the subcutaneous region of the distal humerus was about 0,5 cm in size. Due to the swelling getting bigger in the course of time (about three years), the mass was resected and submitted to Pathology Laboratory of the Faculty of Veterinary Medicine, Selcuk University. After the routine histopathology process, Tissue sections were stained with hematoxylin and eosine (HE) and Masson's Trichrome (MT) stains [7] and examined under the light microscope.

3. RESULTS AND DISCUSSION

Biopsy materials in 2 pieces were measured as 6.5X4.5X5 and 2.5X2X2 cm in diameter. Grossly, the cross-sectional face of the large piece, cream-colored and viscous, had a layered appearance. the smaller one had a hard consistency and the cross-sectional face had a red and white mottled appearance (Figure 1). Microscopically, the neoplasm was multilobular and composed of pleomorphic spindle-shaped cells (Figure 2-3). The neoplastic cells had vesicular nuclei and contained round nucleoli. The neoplastic tissue cells were arranged in multiple helices which is separated by stromal collagen. There were mild hemorrhages and some necrotic area. Mitotic figures were seen in these sections (Figure 4).

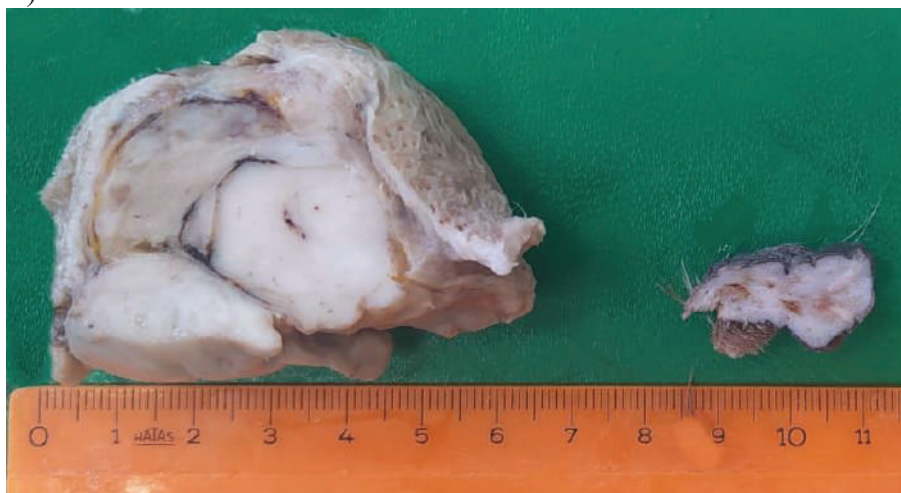


Figure 1. Cross-sectional face of the large piece, cream-colored and viscous, had a layered appearance. the smaller one had a hard consistency and the cross-sectional face had a red and white mottled appearance

In histopathological examination, the neoplasm was multilobular and composed of pleomorphic spindle-shaped cells. Tumor cells had vesicular nuclei and contained round nucleoli. The neoplastic tissue cells were arranged in multiple helices which is separated by stromal collagen. There were mild hemorrhages and some necrotic area. Mitotic figures were seen in these sections.

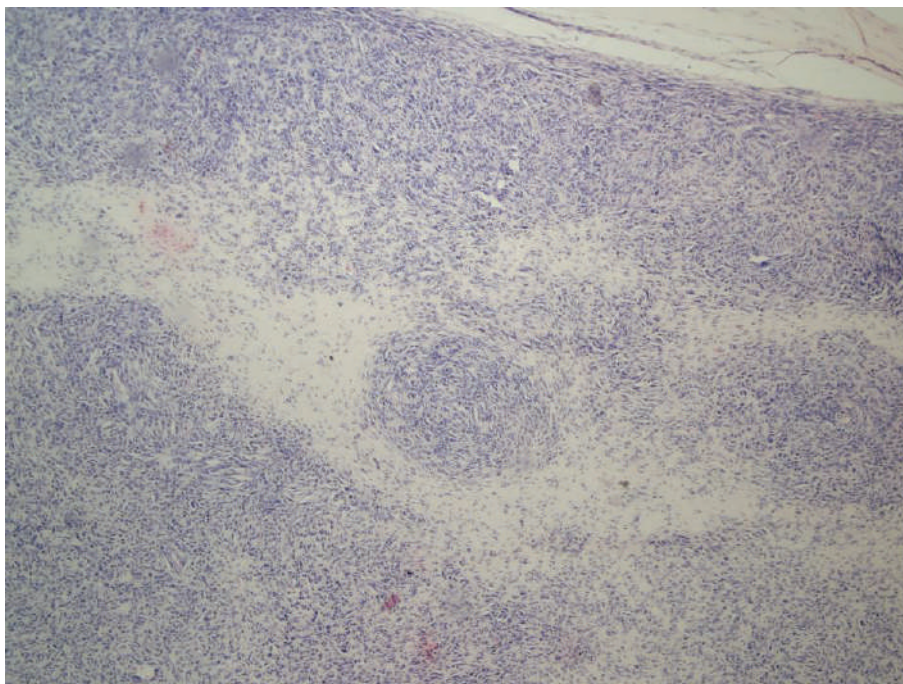


Figure 2. Multilobular arranged tumor section and multiple helices view. HE

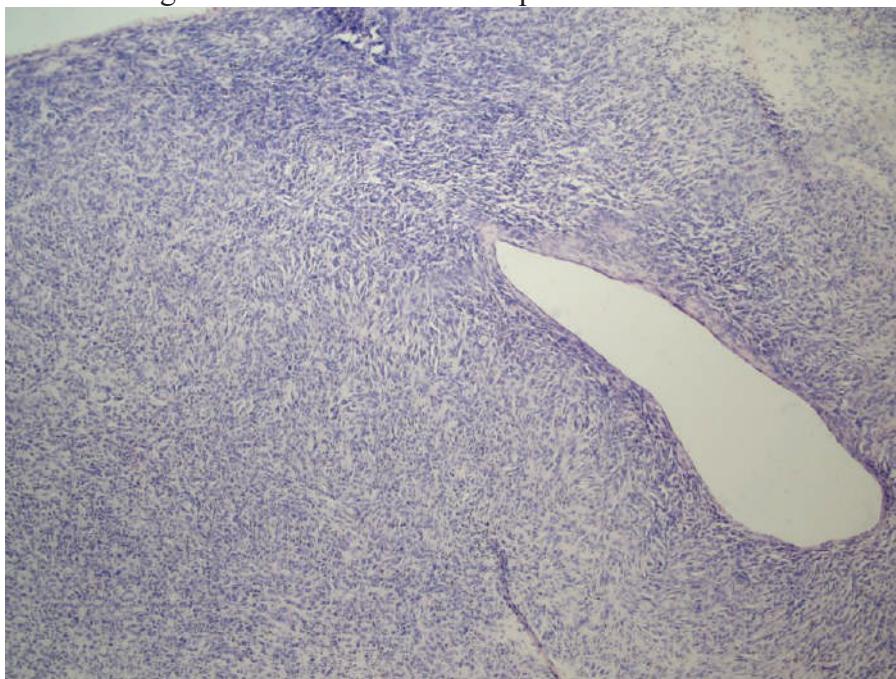


Figure 3. Another view of multiple helices structures. HE

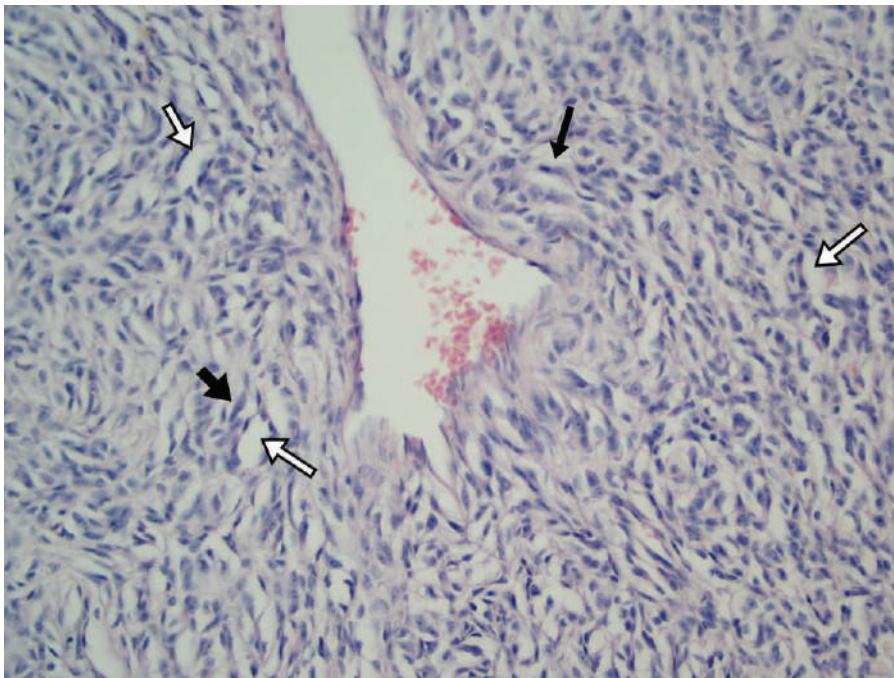


Figure 4. Pleomorphic spindle-shaped tumor cells (thick black arrow). They have vesicular nuclei. The neoplastic tissue cells were arranged in multiple helices which is separated by stromal collagen and many capillaries (white arrows) and mitosis (thin black arrow). HE

Average age of hemangiopericytomas is 7 to 10 years (middle-aged or older dogs) [8]. In previous reports of our department, 2 more cases of hemangiopericytoma were reported. One of them was observed on the posterior left extremity plantar face of a 9-year-old German Shepherd dog [9] and the other was observed on the left anterior extremity of a 4-year-old cross-breed dog [10]. In the present case, the dog was 17 years old Golden Retriever and this lesion was first noticed on distal humerus for 3 years ago. Hemangiopericytomas are generally found in subcutaneous layer of integument of the extremities [11]. Similarly, location of the tumor was subcutaneous region of the distal humerus. According to the morphology, Three subtypes of hemangiopericytoma were described as epithelioid, storiform and perivascular [12]. Tumor cells arranged concentrically around the central lumen in this case and named as perivascular form.

4. CONCLUSION

In conclusion, considering that it develops slowly and remains localized for a long time, it was found appropriate to present it as a case report.

REFERENCES

- [1]. AP Stout, & MR Murray, "Hemangiopericytoma: a vascular tumor featuring Zimmermann's pericytes". *Annals of surgery*, 116(1), 26, 1942.
- [2]. A Ghose, G Guha, R Kundu, J Tew, & R Chaudhary, "CNS hemangiopericytoma. *American journal of clinical oncology*, 40(3), 223-227, 2017.
- [3]. GM Graves, DE Bjorling, E Mahaffey, "Canine hemangiopericytoma: 23 cases (1967-1984)" *Journal of the American Veterinary Medical Association*, 192(1):99-102, 1988.
- [4]. LT Pulley, AA Stannard, *Tumors of the skin and soft tissues*. In: *Tumors in domestic animals*, 3rd ed., pp. 48–51. University of California Press, Berkeley, CA. 1990.
- [5]. E Handharyani, K Ochiai, T Kadosawa, T Kimura, & T Umemura "Canine hemangiopericytoma: an evaluation of metastatic potential" . *Journal of Veterinary Diagnostic Investigation*, 11(5), 474-478, 1999.
- [6]. SM Evans, *Canine hemangiopericytoma: a retrospective analysis of response to surgery and orthovoltage radiation*. *Veterinary Radiology*, 28(1), 13-16, 1987.
- [7]. Luna
- [8]. DJ Meuten, *Tumors in domestic animals*. John Wiley & Sons, 2020
- [9]. MK Çiftçi, F. Hatipoğlu, S Avki, "Bir Alman kurt köpeğinde hemangiopericytoma olgusu", *Vet. Bil. Derg.* 12,2: 153-157, 1996.
- [10]. MB Ates, MK Ciftci M Ortatatli, F Hatipoglu, A case of hemangiopericytoma in a crossbred dog 6 th International Conference on Sustainable Agriculture and Environment October 3-5, 2019, Konya, Turkey, 2019.
- [11]. F Namazi, MA Hasiri, A Oryan, A Moshiri, "Hemangiopericytoma in a young dog: Evaluation of histopathological and immunohistochemical features". In *Veterinary research forum: an international quarterly journal* (Vol. 5, No. 2, p. 157). Faculty of Veterinary Medicine, Urmia University, Urmia, Iran.
- [12]. MH Goldschmidt., MJ Hendrick, *Tumors of the Skin and Soft Tissue*. DJ Meuten, Eds. *Tumors of Domestic Animals*. 4.ed. Iowa: Iowa State Press, 45-117, 2002

INFILTRATIVE RENAL LYMPHOMA IN A 1-YEAR-OLD MALE STRAY CAT**Mustafa ORTATATLI**Selcuk University, Faculty of Veterinary Medicine, Department of Pathology, Konya, Turkey,
ORCID: 0000-0002-3713-813X**Ertan ORUC**Selcuk University, Faculty of Veterinary Medicine, Department of Pathology, Konya, Turkey.
ORCID: 0000-0003-4234-8219**Ozgur OZDEMIR**Selcuk University, Faculty of Veterinary Medicine, Department of Pathology, Konya, Turkey.
ORCID: 0000-0002-1595-0557

Abstract

A 1-year-old male stray cat adopted by animal lovers was previously taken to a private Veterinary Clinic in Istanbul with complaints of severe kidney failure, loss of appetite and weight loss. After the clinical examinations, it was informed that the animal was decided to be euthanized and necropsy was performed there. In the necropsy, it was reported that the kidneys were quite enlarged and pale in color, and 5 tissue pieces taken from the kidneys were sent to our Pathology Department within formaldehyde solution. In macroscopic examination, it was noted that the outer surface of the organ included dark brown areas in places, but was generally light and pale gray-white in color. It was observed, on the cut surfaces, that the capsule was quite thickened and contained bleeding areas, and there were pale, whitish areas extending from the cortex to the medulla, but the cortico-medullary border was not clear.

In the histopathological examination, it was noticed that the capsule, cortex and medulla were covered with diffuse, infiltratively extending, mostly dark-hyperchromatic, round-nucleated and small cytoplasm, generally round uniform-looking lymphoid type tumor cells. It was noted that the tumor cells were of blastic type and there were many mitotic figures. The glomeruli and tubules were detached and degenerative due to tumor tissue that spread infiltratively in the renal interstitium and did not have a separate stroma. Thanks to the typical lymphoblastic structure of the tumor cells, the case was diagnosed as lymphoma, which can be widely seen in the kidneys of cats.

Despite the knowledge that renal lymphomas are usually metastatic and may not only be limited to the kidneys but also spread to lymph nodes and other lymphoid organs, we could not obtain information about the prevalence/distribution in this animal since the necropsy was not performed by us. It was thought that it would be appropriate to present the case in order to draw attention to the need for a more careful and systematic necropsy examination and to take tissue samples from all suspicious organs for histopathological examination.

Key Words: renal lymphoma, cat, pathology, oncology

1. INTRODUCTION

Tumors originating from lymphoid cells are defined as lymphoma, lymphosarcoma, or malignant lymphoma. It is one of the most common tumors in cats. One-third of all feline tumors have been reported as lymphoma. It is 2 times more common in male cats than females. It has been reported to be seen even in younger cats than 6 months of age because it mostly has a viral etiology (Feline Leukemie Virus). Alimentar, mediastinal,

multicentric, leukemic and solitary (renal) types of lymphoma are common in cats, with the most alimentary type being seen [3,6].

Renal Lymphoma, as in all species, is one of the most common tumors in the kidneys of cats. When it is found solitary in the kidneys, if investigated, it has been reported not only in the kidney, but also in the related and other lymph nodes. The tumor causes renal dysfunction by suppressing the kidney parenchyma [4,5,7]. Feline Leukemie Virus was found positive in 50% of renal lymphomas [1]. Clinically, symptoms such as loss of appetite, excessive water consumption, weight loss and vomiting are seen [2].

Macroscopically, the kidneys are usually enlarged, multiple masses of different sizes and whitish colors are seen in the appearance of protruding from the surface. Histologically, lymphoblastic type cells with prominent round nuclei and little cytoplasm are seen in the renal interstitium and are referred to as "typical" lymphoma cells [3,5,7].

2. CASE HISTORY and MACROSCOPIC EXAMINATION

In this presentation, infiltrative type lymphosarcoma was described in the kidney of a young cat. A 1-year-old male stray cat adopted by animal lovers was previously taken to a private Veterinary Clinic in Istanbul with complaints of severe kidney failure, loss of appetite and weight loss. After the clinical examinations, it was reported that the animal was decided to be euthanized and necropsy was performed. Because it was noticed that the kidneys were quite enlarged and pale in color in the necropsy examination, 5 tissue pieces taken from the kidneys with the suspicion of a tumor were sent to the Selcuk University, Veterinary Faculty, Pathology Department Laboratory for pathological examination.

In the macroscopic examination of the kidney pieces, the largest of which is 5x3x2 cm and the smallest 2,5x2x1.5 cm, delivered to our department within formaldehyde solution, it was noted that the outer surface of the organ included dark brown areas in places, but was generally light and pale gray-white in color (Figure 1A). On the section surface, the capsule and the bleeding areas underneath were dark brown in places due to the effect of formaldehyde, the capsule was quite thickened, and there were pale, whitish areas extending from the cortex to the medulla. The cortico-medullary border was not clear (Figure 1B).

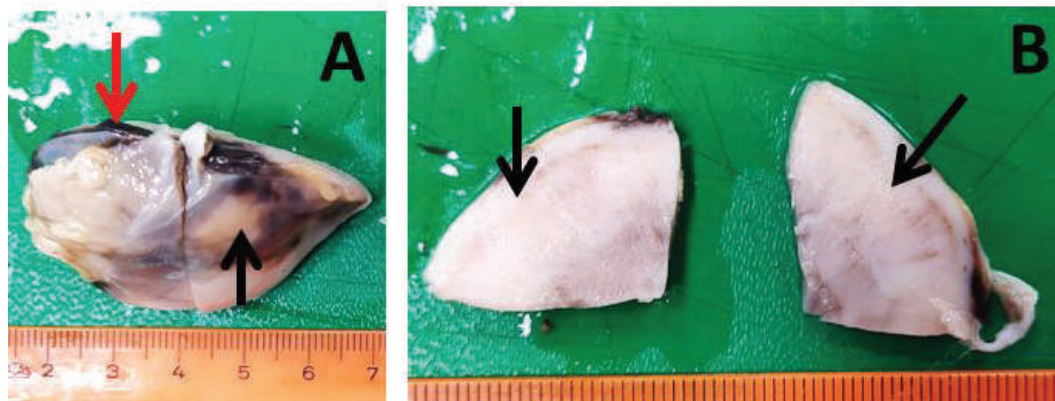


Figure 1. A. Bleeding areas under the capsule (red arrow), whitish tumoral areas with protruding surface appearance (black arrow). B. Corticomedullary borders are lost due to diffuse tumoral infiltration (black arrows) on cut surfaces.

3. METHODS

Tissue pieces were thinned to a thickness of 4-5 mm and then fixed in 10% formaldehyde solution for 24 hours again. After routine tissue processing procedures, the preparations were stained with Hematoxylin-Eosin (HE) (Luna 1968). The slides were examined under a light microscope (Olympus BX51, Tokyo, Japan).

4. MICROSCOPIC FINDINGS AND DISCUSSION

On the histopathological examination of the sections, it was noticed that the capsule, cortex, and medulla were covered with diffuse and infiltratively extending tumor cells, which are mostly dark-hyperchromatic, round-nucleated and prominent but small cytoplasm, generally round-oval shaped uniform-looking lymphoid type cells (Figure 2.A-F). It was noted that the tumor cells were of blastic type and there were many mitotic figures (Figure 2F). It was observed that the glomerulus and tubules were separated and degenerative due to tumor cells that did not have a distinct stroma and were noticed to have spread infiltratively in the renal interstitium. Bowmann's cavities and tubules contained a protein-rich fluid (Figure 2.D-E). In addition, diffuse bleeding was observed under the capsule. Owing to the typical lymphoblastic structure of the tumor cells, the case was diagnosed as lymphoma, which can be widely seen in the kidneys of cats.

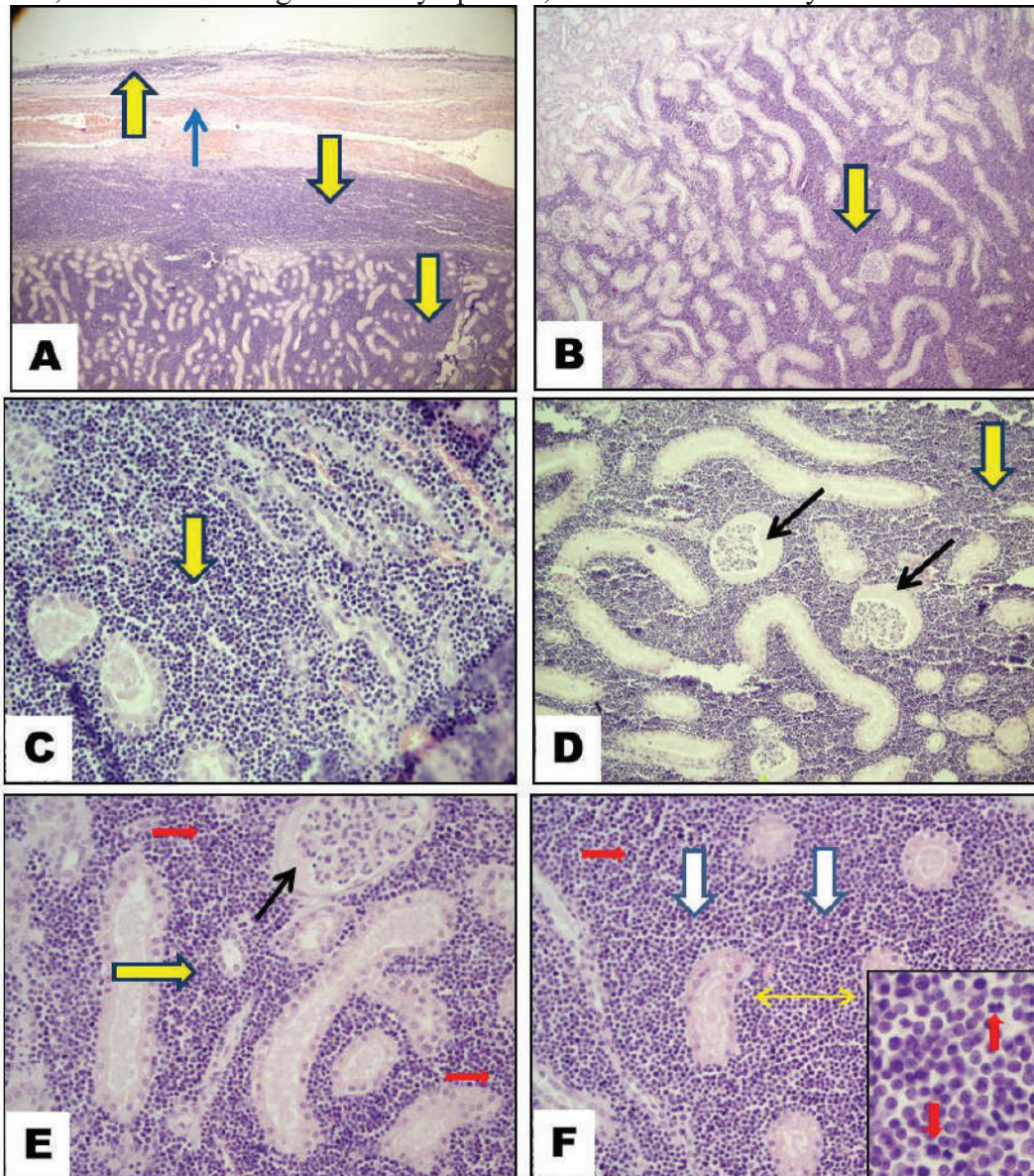


Figure 2. A. Aggregation of tumoral cells in subcapsular and cortical areas of kidney (yellow arrows) and subcapsular hemorrhage (blue thin arrow), HxE, x4, B. Infiltrating tumoral cells into kidney interstitium (yellow arrow). HxE, x10, C. Dark-hyperchromatic and round-nucleated tumoral lymphoid cells in the interstitium (yellow arrow). HxE, x20, D. glomerulus and tubules were separated and degenerative due to tumor cells (yellow arrow) and proteinous fluid in Bowmann's space (black thin arrows). HxE, x20, E. tumor cells in tubules (yellow arrow) and hemorrhage (red arrows). HxE, x20, F. tumor cells (yellow arrow) and mitotic figures (red arrows). HxE, x20, inset shows a high magnification of mitotic figures (red arrows).

E.Uniform-looking tumoral lymphoid cells in the interstitium (yellow arrow) and proteinous fluid in Bowmann's space (black thin arrow). HxE, x40, F. Tumor tissue has not a distinct stroma (white arrows) and separates tubules (yellow thin arrow) HxE, x40, mitotic figures (red arrows) are seen in inset. HxE.

It is reported that renal lymphoma is the most common tumor among kidney tumors and causes renal dysfunction due to tumoral infiltrations [3,4,5]. In this case, it was interpreted that tumoral infiltrates enlarged in the interstitium by putting pressure on the glomerular and tubular areas, thus causing renal dysfunction. Macroscopically, the appearance of whitish multiple masses protruding from the surface [3,4,6] was also seen in this case, and it was also noted that the corticomedullary border disappeared due to tumoral infiltration. As stated in the literature [1,6,7], in microscopic examinations, the presence of lymphoblastic type cells with dark hyperchromatic nuclei and low cytoplasm led to the diagnosis of lymphoma. In addition, the presence of many mitotic figures in the tumoral area was associated with the aggressiveness of the tumor.

The clinical findings reported in the anamnesis were found to be compatible with the literature data [2]. In cases where renal lymphomas are found, if other tissues are investigated, it has been reported that tumors are also found in the lymph nodes, which are not alone, and half of the renal tumors are associated with Feline Leukemie virus [1,5,7]. In this case, since only the kidney tissue was sent to our laboratory, no comment could be made regarding the presence of tumors in other tissues. In addition, no research on viral etiology could be conducted.

5. CONCLUSION

Despite the knowledge that renal lymphomas are usually metastatic and may have spread not only to the kidneys but also to the lymph nodes and other lymphoid organs, we could not obtain information about the prevalence and organ involvement in this animal since necropsy was not performed by us. It was thought that it would be appropriate to present the case in order to draw attention to the need for a more careful and systematic necropsy examination and to take tissue samples from all suspicious organs for histopathological examination, especially in lymphoma cases, which has an important place among kidney tumors in cats.

REFERENCES

- [1]. Barnette (2021) Lymphoma in Cats. [Online]. Available: <https://vcahospitals.com/know-your-pet/lymphoma-in-cats>
- [2]. Brooks W (2021) Lymphoma in Cats. [Online]. Available: <https://veterinarypartner.vin.com/default.aspx?pid=19239&id=4951906>.
- [3]. Erer H, Kiran M (2019) Veteriner Onkoloji. 6. Baskı, Güler Ofset, Konya.
- [4]. Finotello, R, Vasconi, ME, Sabattini, S. (2018) Feline large granular lymphocyte lymphoma: an Italian Society of Veterinary Oncology (SIONCOV) retrospective study. *Vet Comp Oncol* 2018; 16: 159–166
- [5]. Meuten DJ and Meuten TLK M (2017) Tumors of the Urinary System In: Tumors in domestic animals. Edited by Donald J. Meuten, Fifth edition. Ames, Iowa : John Wiley & Sons Inc.
- [6]. Moulton JE, Harvey JW (1990) Tumors of the lymphoid and hemato-poietic tissues. In: Moulton JE, ed. *Tumors in Domestic animals*, 3rd edition. Berkeley, CA: University of California.
- [7]. Vail DV, Moore AS, Ogilvie GK, Volk LM (1998) Feline Lymphoma (145 Cases): Proliferation Indices, Cluster of Differentiation 3 Immunoreactivity, and Their Association with Prognosis in 90 Cats *J Vet Intern Med* 1998;12:349-354

EXTRAMEDULLARY PLASMACYTOMA IN SPLEEN OF 12-YEAR-OLD FEMALE GOLDEN RETRIEVER DOG

Mustafa ORTATATLI

Selcuk University, Faculty of Veterinary Medicine, Department of Pathology, Konya, Turkey.
ORCID: 0000-0002-3713-813X

Ertan ORUC

Selcuk University, Faculty of Veterinary Medicine, Department of Pathology, Konya, Turkey.
ORCID: 0000-0003-4234-8219

Zeynep CELIK

Selcuk University, Faculty of Veterinary Medicine, Department of Pathology, Konya, Turkey.
ORCID: 0000-0002-9667-5728

Fatih HATİPOĞLU

Selcuk University, Faculty of Veterinary Medicine, Department of Pathology, Konya, Turkey.
ORCID: 0000-0002-0103-5868

Kyrgyz-Turkish Manas University, Faculty of Veterinary Medicine, Department of Pathology, Bishkek, Kyrgyzstan, ORCID: 0000-0002-0103-5868

Abstract

Extramedullary plasmacytomas (EMP) are rare and solitary plasmacytic tumors of soft tissues in dogs and cats. It is characterized by a localized proliferation of neoplastic monoclonal plasma cells. In this report, extramedullary plasmacytoma in spleen tissue was grossly and histopathologically described in a 12-year-old female Golden Retriever dog. After the surgical total extirpation of spleen because of splenomegaly, whole organ submitted to our laboratory. In the macroscopic examination, the organ was measured as 35x21x10 cm. Numerous irregular gray-white foci were observed on the surface of the spleen, which were prominent under the capsule and occasionally protruding from the capsule. In addition to the gray-white foci on the cut surface, bloody leakage was noted. For histopathology, tissue sections were taken from the spleen and routinely processed. Paraffin sections were stained with Hematoxylin and Eosine (HE), Dominici Stain (DS), Methylene Green Pyronin (MGP) and Congo Red Stain (CRS) and examined under the light microscopy. Histopathologically, it is noncapsulated and tumor cells were especially seen in sinusoids. The tumour cells were round to oval shaped and there were limited anisocytosis and anisokaryosis. The nuclei were eccentrically located, clumped chromatin resembling mature plasma cells in many areas. Mitotic figures were observed in some microscopic area. DC stain was negative for mast cell tumor. In MGP stain, cytoplasm of tumor cells were pale pink and amyloid-like material was observed in sinusoidal spaces in CR stain. According to histopathology results tumor was described as extramedullary plasmacytoma and it was found appropriate to present it as a case report, since it is rarely an extramedullary plasmacytoma located in the spleen.

Keywords: extramedullary plasmacytoma, spleen, Golden retriever dog, histopathology

1. INTRODUCTION

Extramedullary plasmacytoma (EMP) refers to tumors occurring outside of the bone marrow, in soft tissues or organs that may be focal, spread to regional lymph nodes, or metastasize to distant areas [1]. In a large veterinary case study (751 cases); the most common EMP location in the dog was cutaneous sites (86%), followed by mucous membranes (9%), and the rectum and colon (4%). Other sites, including the stomach, spleen, genitalia, eyes, uterus, and liver made up the remaining 1% of cases [6]. Unlike cutaneous and oral EMP, the EMP seen in the organs can metastasize to regional lymph nodes [8].

Extramedullary plasmacytomas (EMPs) comprise about 2.5% of all neoplasms in dogs and occur most commonly in middle-aged to older dogs (mean 8 to 10 years) [4]. Overrepresented breeds include cocker spaniels, certain terrier breeds (West Highland white, Yorkshire, and Airedale terriers), boxers, and golden retrievers [4].

2. CASE HISTORY

12-year-old Golden Retriever dog was diagnosed with splenomegaly in Selcuk University Veterinary Faculty Animal Hospital Surgery Department, and the spleen was removed by total extirpation and sent to the Pathology Department of the same faculty.

3. MATERIAL AND METHOD

Samples taken from different parts of the spleen were fixed in 10% formaldehyde solution for 48 hours. After routine laboratory procedures, 5 μ thick sections were taken from the paraffin blocks prepared with a microtome (Leica RM 2125RT). Stained with Hematoxylin-Eosin, Methyl Green Pyronin (MGP), Dominici and Congo Red (CR). The slides were examined under a light microscope (Olympus BX51, Tokyo, Japan) and photographed (Olympus EP50).

4. RESULT AND DISCUSSION

4.1. Macroscopic findings

In the macroscopic examination, it was determined that the spleen was 35x21x10 in size, swollen, friable, and some parts were hemorrhagic (Figure 1A, B). Numerous irregular gray-white foci were seen on the external surface (Figure 1A,B) and cut surface of the spleen. In addition, it was noted that there was a large amount of blood leakage on the cut surface of the spleen.

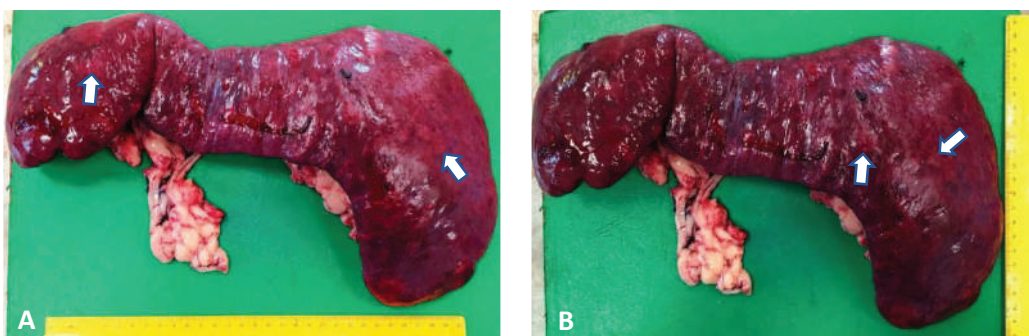


Figure 1. A. B. Macroscopic appearance of the spleen. Swollen and some parts were hemorrhagic. Irregular gray-white foci (arrows) on the external surface.

4.2. Microscopic findings

In the histopathological examination, it was determined that there was no capsule around the tumoral mass, and it was observed that the tumor cells were especially collected in the sinusoids (Figure 2). It was noted that these cells were round-oval shaped and nuclei were located eccentrically in the cytoplasm of these cells. In addition, free globules with hyaline appearance were observed in the sinusoidal spaces in some areas (Figure 3). Anisocytosis, anisokaryosis and mitotic figures (Figure 4) were determined in these tumor cells, albeit in small amounts. Plasma cells cytoplasm were seen in pink color in Methyl Green Pyronin stain for plasma cells. Dominici stain was negative for mast cell tumor. In the Congo Red staining performed to determine the amyloid deposits, it was observed that there were amyloid-like deposits that were stained brick red, especially in the sinusoidal spaces (Figure 5). After the Congo red staining showed amyloid-like deposits staining brick red in the sinusoidal spaces, logol and 1% sulfuric acid were poured onto the cut surface of the spleen tissue pieces fixed in formol. After this procedure, dark brown-black foci, which are signs of amyloid deposition, were noted especially in the subcapsular region of the spleen (Figure 6).

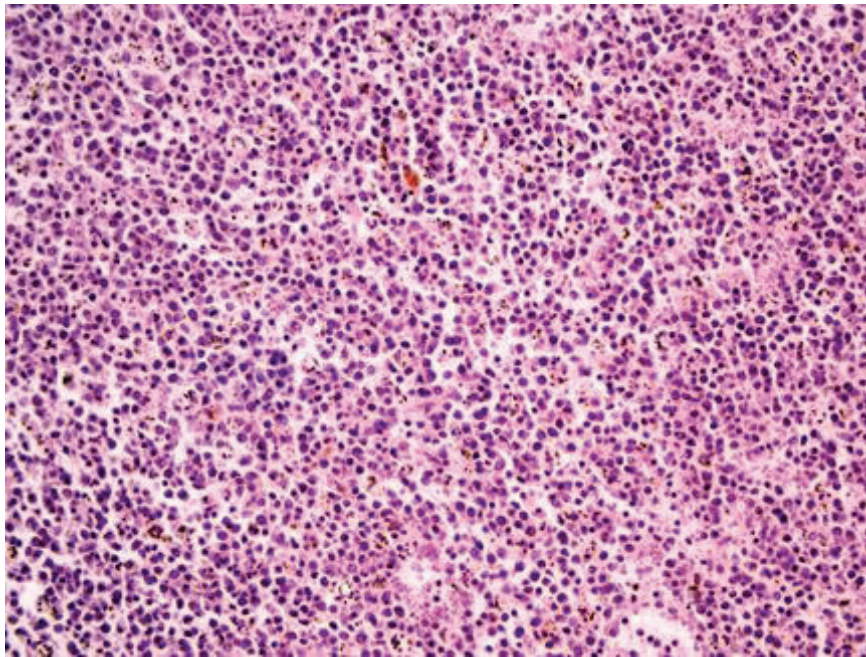


Figure 2. General appearance of tumor cells. No capsule around the tumoral mass and Tumor cells in the sinusoids, 40X, H&E,

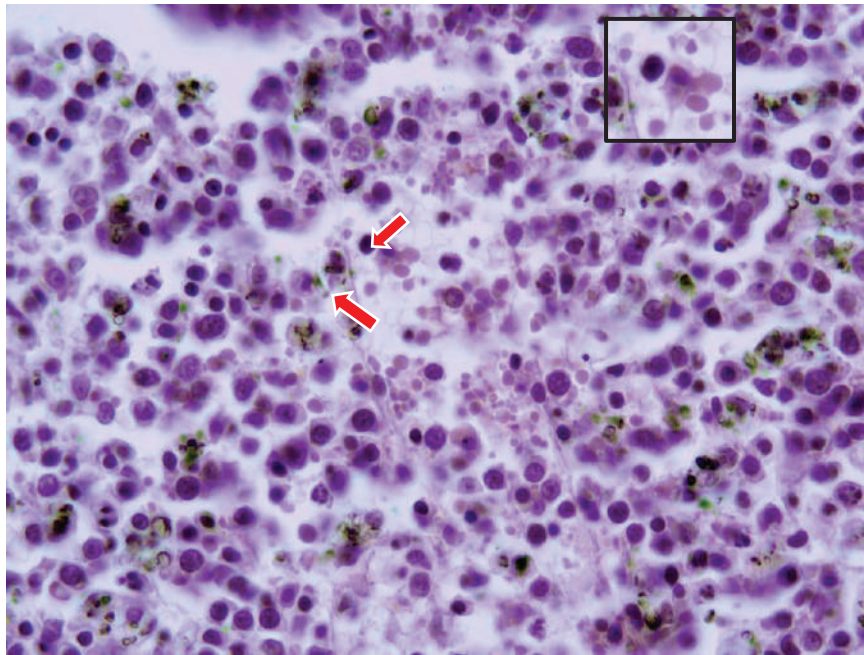


Figure 3 . Round-oval shaped tumor cells and nuclei eccentrically in the cytoplasm. Free globules (arrows and insert) with hyaline appearance in the sinusoidal spaces, 100X, H&E.

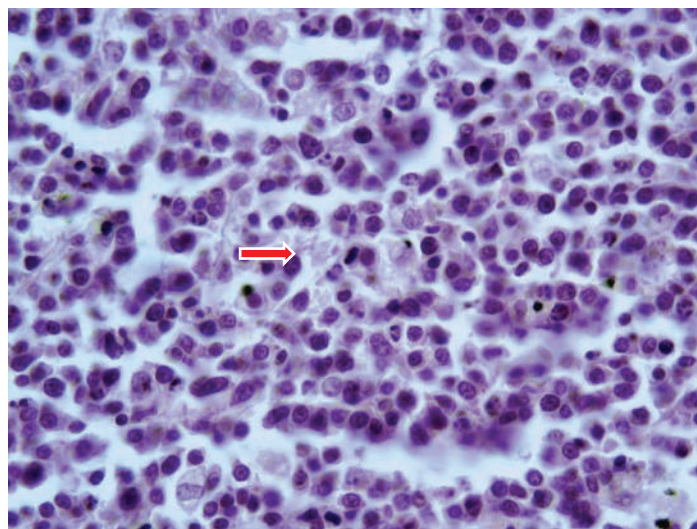


Figure 4. Tumor cells and mitotic figure (arrow), HE, X100

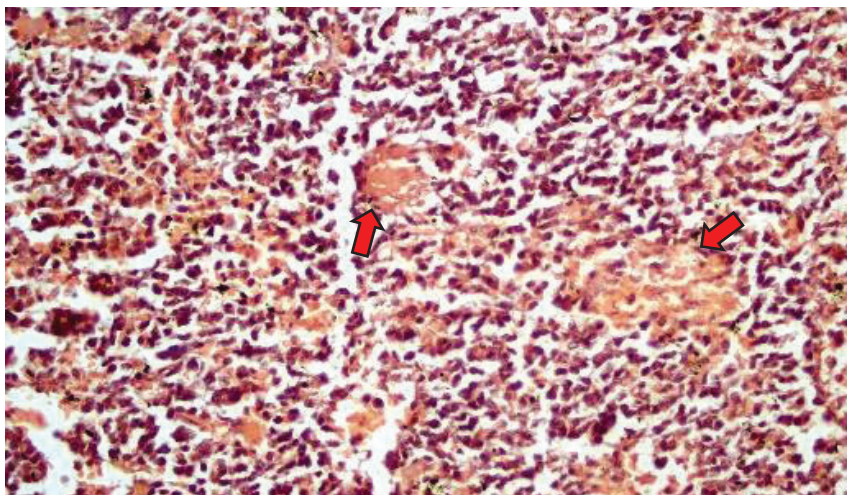


Figure 5. Brick red colored amyloid-like deposits (arrows) in the sinusoidal spaces, 40X Congo Red.

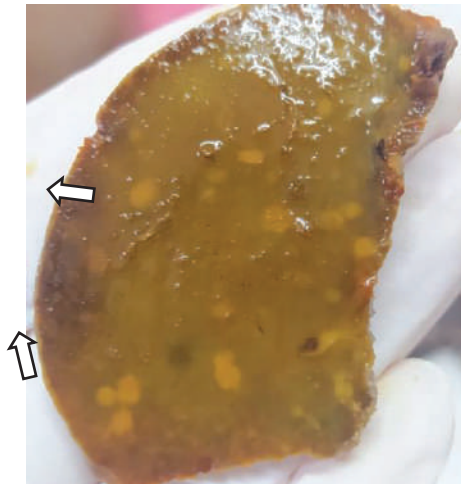


Figure 6. Dark brown-black foci (arrows) on cut surface of subcapsular region in the spleen (Logol and 1% sulfuric acid proceses after formol fixation)

EMPs occur most commonly in middle-aged to older dogs (mean 8 to 10 years). Overrepresented breeds include cocker spaniels, certain terrier breeds (West Highland white, Yorkshire, and Airedale terriers), boxers, and golden retrievers [4]. In our case, the dog was 12-year-old and Golden Retriever. The most common EMP location in the dog was cutaneous sites (86%), followed by mucous membranes (9%), and the rectum and colon (4%). Other sites, including the stomach, spleen, genitalia, eyes, uterus, and liver made up the remaining 1% of cases [6]. Although it has been reported that the most common EMP site is cutaneous sites, no tumor-related findings were observed in the skin and other parts and organs of the body in the presented case. Only the spleen was affected.

It has been reported that basosquamous carcinoma is also seen in cutaneous plasmacytoma cases [2] and in another case [3], focal amyloid deposition was also observed together with cutaneous plasmacytoma. In the presented case, focal amyloid deposits were also observed in the spleen together with EMP.

Amyloid of immunoglobulin lambda light chain origin, demonstrated by either thioflavine T or Congo red staining, has been described in association with extramedullary plasmacytomas in dogs, cats, and horses. Amyloid detection has some diagnostic usefulness: 60 percent of canine extramedullary plasmacytomas had thioflavine T staining, while other round cell tumors did not stain [9]. In the presented case, the presence of amyloid deposits together with the EMP detected in the spleen supports the statements in sources.

The incidence of EMP in cats is low, and few case reports exist. Affected cats are usually older, with a mean age of 8.5 years. Skin is the most common site affected, but other reported sites include the oral cavity, gastrointestinal tract, retroperitoneum, brain, and orbit [5,10,7].

In general, EMPs often have a benign clinical course in dogs and cats and may be cured with complete surgical excision. Noncutaneous, non-oral EMP may have a more aggressive behavior; however, dogs treated with surgery alone or a combination of surgery and adjuvant systemic chemotherapy can have extended survival times [11].

In general, EMPs often have a benign clinical course in dogs and cats and may be cured with complete surgical excision. Noncutaneous, non-oral EMP may have a more aggressive behavior;

however, dogs treated with surgery alone or a combination of surgery and adjuvant systemic chemotherapy can have extended survival times [11].

5. CONCLUSION

As a result of the examinations, the case was diagnosed as extramedullary plasmacytoma. Although EMP can occur in many organs and tissues, this case is worth presenting because its incidence in the spleen is very low. As in this case, it was aimed to draw the attention of clinicians to the subject, since tumors in the spleen also cause splenomegaly.

REFERENCES

- [1]. L. Adelman, V. Larson, T. Sissener, T. Spotswood. "Extramedullary plasmacytoma in the lung of a Doberman pinscher dog." *The Canadian veterinary journal*, 55(1), 1237-40. 2014.
- [2]. MB. Ates, M. Ortatatli, F. Hatipoglu, O. Ozdemir, "Concomitant Two Tumours In A German Shepherd Dog: Cutaneous Plasmacytoma And Basosquamous Carcinoma." 2nd Erasmus International Academic Research Symposium, October 11-13, 2019, p.79-85, Paris, France. 2019.
- [3]. MB. Ates, M. Ortatatli, E. Oruc, F. Hatipoglu. "A Case of Cutaneous Plasmacytoma With Focal Amyloid Deposition in A Maltese Poodle BreedDog." IV. International Scientific and Vocational Studies Congress – Science and Health (BILMES SH 2019- ANKARA), 7-10 November 2019, p.222-226, Ankara, Turkey. 2019.
- [4]. GN. Clark, H. Berg, SJ. Engler, et al. "Extramedullary plasmacytomas in dogs: results of surgical excision in 131 cases." *J Am Anim Hosp Assoc*. 28:105-111. 1992.
- [5]. F. Hatipoglu, MK. Çiftçi, F. Terzi, MB. Ateş, Ö. Özdemir, M. Ortatatlı. "Extramedullary Plasmacytoma of Oral Cavity a 7-Year-Old Male Tekir Cat." 3rd International Conference On Science, Ecology And Technology (ICONSETE), 14-16 August 2017, Rome, Italy, Pp:43. 2017.
- [6]. PA. Kupanoff, CA. Popovitch, MH. Goldschmidt. "Colorectal Plasmacytomas: A Retrospective Study of Nine Dogs." *Journal of the American Animal Hospital Association*, 42(1), 37-43. doi:10.5326/0420037 2006.
- [7]. M. Majzoub, W. Breuer, SJ. Platz, et al. "Histopathologic and immunophenotypic characterization of extramedullary plasmacytomas in nine cats." *Vet Pathol*, 40(3):249-253. 2003.
- [8]. JM. Meis, JJ. Butler, BM. Osborne, NG. Ordóñez. "Solitary plasmacytomas of bone and extramedullary plasmacytomas. A clinicopathologic and immunohistochemical study." *Cancer*, 59(8), 1475-85.
- [9]. DJ. Meuten. "Tumors in Domestic Animals." 5 th Ed., John Wiley & Sons, 2017.
- [10]. PJ. Mellor, S. Haugland, S. Murphy, et al. "Myeloma-related disorders in cats commonly present as extramedullary neoplasms in contrast to myeloma in human patients: 24 cases with clinical follow-up." *J Vet Intern Med.*, 20(6):1376-1383. 2006
- [11]. R. Sternberg, J. Wypig, AM. Barger. "Extramedullary and solitary osseous plasmacytomas in dogs and cats." 2009. (<https://www.dvm360.com/view/extramedullary-and-solitary-osseous-plasmacytomas-dogs-and-cats>)

HISTOPATHOLOGICAL CHARACTERIZATION OF HEPATOCELLULAR CARCINOMA IN A DOG

Mehmet Burak ATES

Selcuk University, Faculty of Veterinary Medicine, Department of Pathology, Konya, Turkey,
ORCID: 0000-0003-1297-426X,

Mehmet TUZCU

Selcuk University, Faculty of Veterinary Medicine, Department of Pathology, Konya, Turkey,
ORCID: 0000-0003-3118-1054,

Mustafa ORTATATLI

Selcuk University, Faculty of Veterinary Medicine, Department of Pathology, Konya, Turkey,
ORCID: 0000-0002-3713-813X

Abstract

A 10-year-old castrated male German Shepherd Dog with complaints of loss of appetite, vomiting, and exhaustion was referred to a private veterinary clinic. After the clinical examination, an increase in the levels of liver serum enzymes (AST: 62 U/L, ALT: 201 U/L, ALP: 441 U/L, and GGT: 219 U/L) was detected. Ultrasonographic imaging revealed a mass of approximately 9 cm in diameter in the right posterior lobe of the liver. This tumor in the liver was removed in two sections through laparotomy. These masses were taken into 10% formol solution and directed to the Selcuk University, Faculty of Veterinary Medicine, Department of Pathology. Macroscopically, it was observed that the first mass was 4x3x1 cm and the second mass was 5x4x1.5 cm, dark red/brown in color, fragile consistency, and grey-white irregular areas on it. Routine tissue processing processes were applied to the samples taken from these masses. Then, sections with a thickness of 5 microns were taken with a microtome and stained with hematoxylin-eosin, Periodic Acid-Schiff, and Congo Red. In the microscopic examination, numerous tumor islets were observed, surrounded by a thin stroma that spread over large areas. It was determined that the cells resembling the hepatocytes in these tumor islets exhibited atypical cell features, especially anisonucleosis and anisocytosis. The nuclei of most tumor cells were found to be condensed with chromatin, and some of them were binucleated. The mitotic index of tumor cells was also found to be high. It was noted that atypical hepatocytes sometimes came together and developed acinar structure/arrangement. Enlargement and proteinaceous deposits were observed in the sinusoids. Some tumor cells were found to be in a solid location without a sinusoidal structure. Turbidity and vacuole formations were observed in the cytoplasm of some hepatocytes. It was revealed that some vessels were invaded by tumor cells. Also, large areas of hemorrhage in the liver and focal necrotic foci within these areas were determined. In conclusion, in the light of its histopathological character; it was diagnosed that three different forms of hepatocellular carcinoma (trabecular, pseudoglandular, solid) were present simultaneously in the case.

Keywords: Liver tumors, Hepatocellular carcinoma, Dog, Oncology

1. INTRODUCTION

Hepatocellular carcinoma is a rare tumor, although it has been reported in many animal species (dogs, cats, horses, cattle, sheep and pigs)[1]. Although the incidence of hepatocellular carcinoma (HCC) has been reported to be higher in dogs compared to other species, this rate is less than 0.5% of all necropsies and less than 1% of all neoplasms [1-3]. HCC is the most frequent primary liver tumor seen in dogs, out of all the malignant tumors seen in the liver and gallbladder, including bile duct carcinoma, carcinoids, and sarcomas [1]. However, due to a paucity of current studies describing the prevalence of HCC, new investigations utilizing modern diagnostic criteria are required to assess the incidence of HCC in dogs and other species.

HCC is more common in dogs at the age of 10 years or later [1]. However, reporting HCC in a 25-month-old dog can be considered as an indication that it can be observed at an earlier age [4]. There is no breed predisposition [1, 2]. Although there is information that it is observed more frequently in male, this has not been proven yet [5].

Clinical manifestations of HCC in dogs are mostly nonspecific. The most common findings: anorexia, vomiting, lethargy, weight loss, while less frequently abdominal tension, diarrhea, icterus, polyuria, polydipsia, and melena can be observed. Sometimes hepatomegaly can be felt by palpation. In some cases, no clinical findings may be observed [1, 6]. Increases in serum activities of AST, ALT, ALP and GGT are observed in dogs with hepatocellular neoplasia. However, this condition is not specific to HCC. In some cases, decreases in blood albumin and glucose levels, and increases in globulin and bile acids can be observed [1, 4, 6, 7]. In a study investigating HCC in dogs, nonspecific haematological abnormalities such as leukocytosis (21 of 32) and anemia (14 of 26) were reported [8].

Radiographic imaging findings of HCC are nonspecific. However, ultrasound examination allows it to easily detect masses in the liver. The limitation of this technique is that it cannot distinguish hyperplastic lesions from neoplastic lesions. Therefore, this technique should be combined with fine-needle aspiration, biopsy, or laparotomy [1, 9, 10].

HCC is observed macroscopically in solid, nodular, or diffuse forms. The solid form is most common in dogs. Numerous small nodules may be present within the solid mass covering single or adjacent liver lobes [2, 5]. Although the color of HCC masses is mostly variable, they may be close to normal liver color and the consistency may be soft, hard, or fragile. Sometimes, necrotic or bleeding areas may also be observed, related to its histological pattern [1].

The histological appearance of hepatocellular carcinomas is classified as trabecular, pseudoglandular, solid, and scirrhous, depending on the degree of differentiation of hepatocytes and the histological arrangement of the cells [1, 2].

The number of recent studies on hepatocellular carcinoma, which is rarely observed in dogs but is the most observed among liver neoplasms, is very few. In this respect, there is a need for studies that are combined with new imaging techniques in such cases in dogs. In this study, which was planned for this purpose, the histopathological characterization of the mass determined by ultrasonography was made and it was thought that it would contribute to the field of veterinary oncology.

2. CASE HISTORY

In this study, a case of hepatocellular carcinoma in a 10-year-old male German Shepherd Dog was described histopathologically. This dog, known to have been castrated in his past, was brought to a private veterinary clinic with non-specific signs of loss of appetite, vomiting, lethargy.

There was no negative finding in the preliminary clinical examination performed in the veterinary clinic. Blood samples were taken for the evaluation of biochemical parameters. Upon the results, ultrasound examination was deemed appropriate because liver disease was suspected. As a result of this examination, a mass was observed in the liver. Later, the mass, which was removed in two parts

by laparotomy, was referred to Selcuk University, Veterinary Faculty, Pathology Department for histopathological examination.

3. MATERIAL AND METHODS

After the surgical operation, the mass extirpated from the liver was fixed in 10% formol solution for 48 hours. After trimming the mass, it was taken into tissue cassettes and subjected to routine tissue processing. Then, after cooling the paraffin-embedded samples, sections were taken with a thickness of 5 micrometers by means of a microtome. The obtained materials were stained according to the methods mentioned below. It was then examined under a light microscope and photographs were taken if deemed necessary.

3.1. Hematoxylin-Eosin Stain

Samples deparaffinized with xylol and then graded alcohols are stained with hematoxylin for 5 minutes, then dipped in acid alcohol. Tissues passed through ammoniacal water were washed in running water. Then, the tissues were stained with eosin for 2 minutes, washed in running water, passed through series of alcohol and xylol and covered with Entellan (Merck Millipore, Germany) [11].

3.2. Periodic acid-Schiff Stain (PAS)

Following deparaffinization, the sections were immersed in a 0.5 percent periodic acid solution for 5 minutes. After washing in distilled water, the sections were submerged in Schiff reagent for 15 minutes. These were rinsed for 5 minutes with tap water, then counterstained with Mayer's haematoxylin, dehydrated, and sealed with Entellan (Merck Millipore, Germany) [11].

3.3. Congo Red Stain

Tissues were stained with congo red to be examined for amyloid deposition. 8–10-micron thick sections were deparaffinized and stained in Congo Red working solution for 15 minutes. After immersion in distilled water, the sections were passed through alkaline alcohol. Then, counterstaining was performed with hematoxylin for one minute. After passing through ammonia water, it was dehydrated with alcohol series. Covered with mounting medium [11].

4. RESULTS AND DISCUSSION

In this study, it was seen that clinical findings such as anorexia, vomiting and lethargy, which were observed intensely in dogs with hepatocellular carcinoma, were not sufficient for diagnosis [1, 4, 6]. There is no information about the patient's age and race as well as being prone to HCC. Serum biochemical parameters are presented in Table 1. When these data were examined, an increase in the amounts of AST (62 U/L), ALT (201 U/L), ALP (441 U/L), and GGT (219 U/L) was noted. It has been suggested that the increase in liver enzyme levels in HCC cases may aggravate the biological behavior of the tumor [12]. Similarly, these increases have been associated with poor prognosis [12]. The increase in the amount of GGT and total bilirubin in this case was thought to be associated with cholestasis shaped by the pressure of the tumor mass on the bile ducts. It has been reported that the amount of glucose close to the lower limit, and the amount of albumin and protein decreased, can be observed in some HCC cases [1, 4, 6, 7]. When serum biochemical parameters were evaluated together, it was determined that liver dysfunction could be suspected but not specific for HCC.

In the abdominal ultrasonographic imaging performed on the patient, a mass of approximately 9 cm in diameter was detected in the right posterior lobe of the liver (Figure 1). In a study with 41 dogs, the left liver lobe was affected in 28 (68.3%) dogs, the central liver lobe was affected in 8 (19.5%) dogs,

and the right liver lobe was affected in 5 (12.2%) [12]. The probable reason for the higher intraoperative mortality rate of neoplasms in the right lobe of the liver was associated with its connection to the caudal vena cava. For this reason, more detailed imaging of tumors localized on the right side of the liver is required [12].

Table 1. Serum Biochemical Parameters

Parameter		Reference ranges
AST	62 U/L ↑	14 - 44
ALT	201 U/L ↑	10 – 100
ALP	441 U/L ↑	6 – 102
Amylase	925 U/L	100 – 1000
Glucose	69 mg/dL	64 – 170
Magnesium	2.1 mg/dL	1.5 – 2.5
Total bilirubin	0.6 mg/dL ↑	0.1 – 0.4
Direct bilirubin	0.3 mg/dL	0 – 0.4
Phosphorus	5.1 mg/dL	2.4 – 8.2
Cholesterol	215 mg/dL	75 – 220
Albumin	1.3 g/dL ↓	2.5 – 3.9
Calcium	9.1 mg/dL	8.2 – 10.8
Triglycerides	155 mg/dL	25 – 160
GGT	219 U/L ↑	1 – 10
Protein	3.4 g/dL ↓	5.2 – 8.8
BUN	11.4 mg/dL	14 – 36
Creatinine	1.5 mg/dL	0.6 – 2.4

The liver mass detected by ultrasound was extirpated in two sections by laparotomy. In the macroscopic examination, the first mass was 4x3x1 cm, the second mass was 5x4x1.5 cm, dark red/brown colored, fragile consistency, and gray-white irregular areas on it (Figure 2). It has been reported that the color close to the normal liver color and fragile consistency in this type of tumors is important in distinguishing it from cholangiosarcomas, which are generally hard and gray-white, yellow-brown [1].

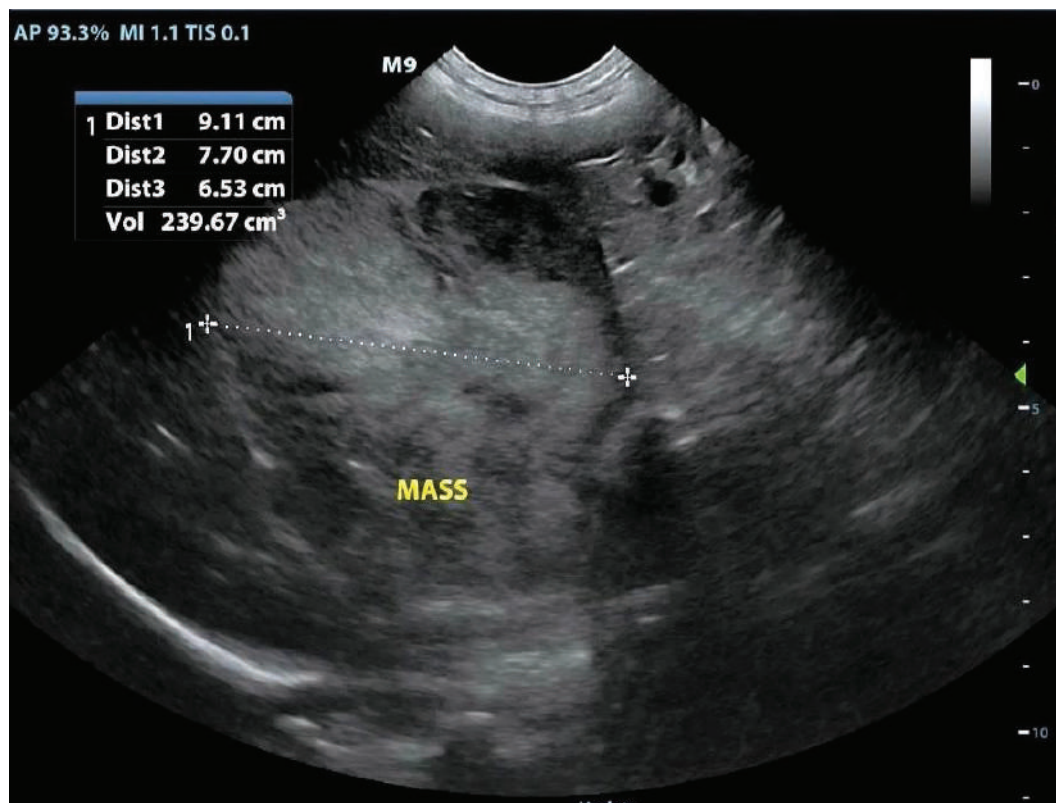


Figure 1. Image of the mass with ultrasound.

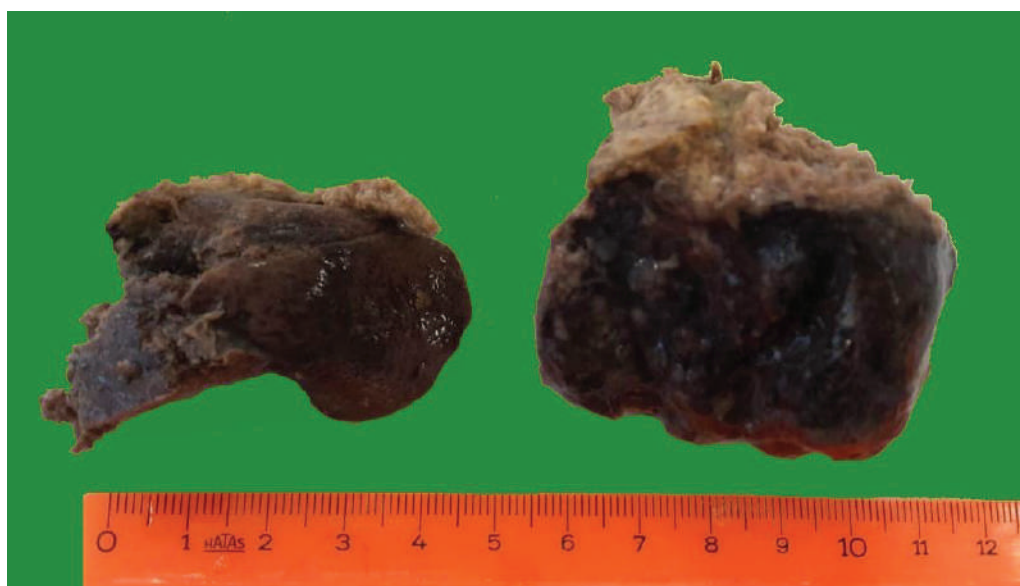


Figure 2. Macroscopic images of the masses

The histological appearance of hepatocellular carcinomas is classified as trabecular, pseudoglandular, solid, and scirrhous form. In the microscopic examination of this study material, numerous tumor islets were observed, surrounded by a thin stroma that spread over large areas. It was determined that the cells resembling the hepatocytes in these tumor islets exhibited atypical cell features, especially anisonucleosis and anisocytosis. The nuclei of most tumor cells were found to be condensed with chromatin, and some of them were binucleated. The mitotic index of tumor cells was also found to be

high. It was noted that atypical hepatocytes sometimes came together and developed acinar structure/arrangement. Enlargement and proteinaceous deposits were observed in the sinusoids and disse space. The deposits were evaluated as amyloid units in Congo-red staining. Some tumor cells were found to be in a solid location without a sinusoidal structure. Turbidity and vacuole formations were observed in the cytoplasm of some hepatocytes (Clear cell pattern). It was revealed that some vessels were invaded by tumor cells. Also, large areas of hemorrhage in the liver and focal necrotic foci within these areas were determined (Figure 3). In the light of its histopathological character, it was diagnosed that three different forms of hepatocellular carcinoma (trabecular, pseudoglandular, solid) were present simultaneously in the case. Trabeculae form is the most common type in dogs [1, 13]. But in this case, it is interesting that several forms were observed together. It is important to differentiate HCC cases from hepatic adenomas. In this case, this distinction was made by the presence of severe atypical character of the tumor cells or multinucleation, severe mitotic activity and vascular invasion. In addition, the absence of PAS-positive mucin helped to differentiate from cholangiocarcinoma [1].

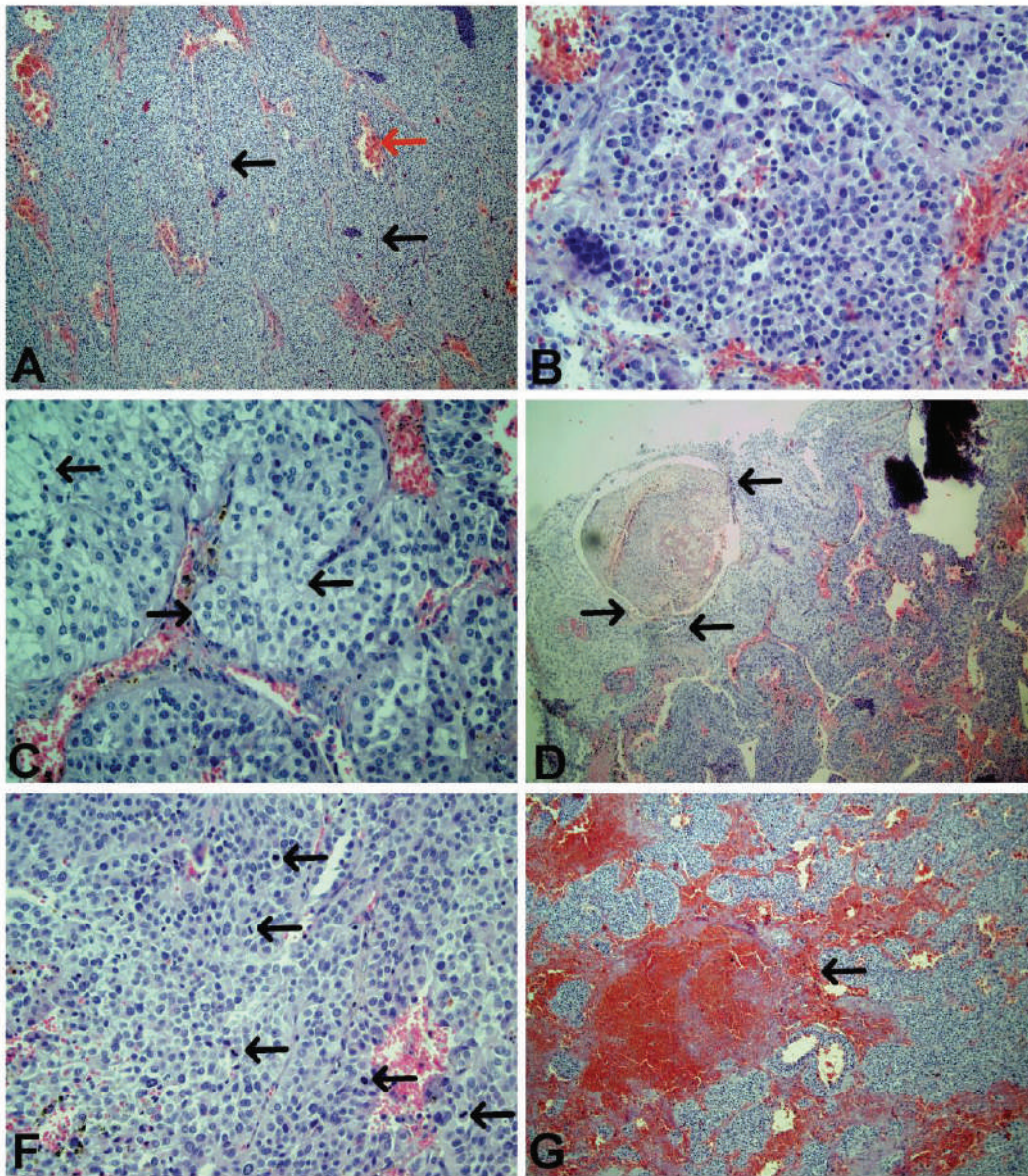


Figure 3. A: Numerous tumor islets surrounded by a thin stroma (black arrows) and hemorrhage between islets (red arrow), 4X, HE; B: Atypical tumor cells

within the islets, 40X, HE; **C:** Turbidity and vacuole formations in the cytoplasm of some hepatocytes, Clear cell pattern (arrows), 40X, HE; **D:** Vascular invasion of tumor cells (arrows) and thrombosis, 20X, HE; **F:** Atypical tumor cells and mitosis (arrows), 20X, HE; **G:** Foci of necrosis with large areas of hemorrhage (arrow), 10X, HE.

5. CONCLUSION

Hepatocellular carcinoma cases, especially localized in the right lobe, are very rare in dogs. In this case, it was emphasized that clinical findings, physical examination, and serum biochemical parameters were non-specific. It was defended that ultrasound imaging technique provides very useful data in detecting the presence of such masses, but it must be combined with histopathology for a definitive diagnosis. In addition, it was concluded that histopathological classification cannot always be uniform, sometimes several forms can coexist in a single mass, and therefore, the classification can be made according to the form that dominates the mass.

ACKNOWLEDGMENT

We would like to thank Veterinarian Okan Kahraman who followed the patient and provided the necessary information for the preparation of this case report.

REFERENCES

- [1]. Cullen, J.M., Tumors of the liver and gallbladder, in Tumors in domestic animals, D.J. Meuten, Editor. 2016, John Wiley & Sons, Inc. p. 602-631.
- [2]. Trigo, F.J., et al., The pathology of liver tumours in the dog. *J Comp Pathol*, 1982. **92**(1): p. 21-39.
- [3]. Bastianello, S.S., A survey on neoplasia in domestic species over a 40-year period from 1935 to 1974 in the Republic of South Africa. VI. Tumours occurring in dogs. *Onderstepoort J Vet Res*, 1983. **50**(3): p. 199-220.
- [4]. Teshima, T., et al., Hepatocellular carcinoma in a young dog. *The Canadian veterinary journal = La revue veterinaire canadienne*, 2013. **54**(9): p. 845-848.
- [5]. Patnaik, A.K., A.I. Hurvitz, and P.H. Lieberman, Canine hepatic neoplasms: a clinicopathologic study. *Vet Pathol*, 1980. **17**(5): p. 553-64.
- [6]. Balkman, C., Hepatobiliary Neoplasia in Dogs and Cats. *Veterinary Clinics of North America: Small Animal Practice*, 2009. **39**(3): p. 617-625.

- [7]. Center, S.A., et al., Diagnostic efficacy of serum alkaline phosphatase and gamma-glutamyltransferase in dogs with histologically confirmed hepatobiliary disease: 270 cases (1980-1990). J Am Vet Med Assoc, 1992. **201**(8): p. 1258-64.
- [8]. Patnaik, A.K., et al., Canine Hepatocellular Carcinoma. Veterinary Pathology, 1981. **18**(4): p. 427-438.
- [9]. Braun, U., et al., Clinical and ultrasonographic findings in four cows with liver tumours. Vet Rec, 2005. **157**(16): p. 482-4.
- [10]. Warren-Smith, C.M., et al., Lack of associations between ultrasonographic appearance of parenchymal lesions of the canine liver and histological diagnosis. J Small Anim Pract, 2012. **53**(3): p. 168-73.
- [11]. Luna, L.G., Routine Staining Procedures, in Manual of histologic staining methods of the Armed Forces Institute of Pathology. 1968, McGraw-Hill Book Company: United States of America. p. 32-44.
- [12]. Liptak, J.M., et al., Massive hepatocellular carcinoma in dogs: 48 cases (1992-2002). J Am Vet Med Assoc, 2004. **225**(8): p. 1225-30.
- [13]. Moyer, J., et al., Factors associated with survival in dogs with a histopathological diagnosis of hepatocellular carcinoma: 94 cases (2007-2018). Open Vet J, 2021. **11**(1): p. 144-153.

THE CASE OF EPIDERMAL INCLUSION CYST IN A 2-YEARS-OLD HOUND DOG

Zeynep CELIK

Selcuk University, Faculty of Veterinary Medicine, Department of Pathology, Konya, Turkey.
ORCID: 0000-0002-9667-5728

Osman DAGAR

Selcuk University, Faculty of Veterinary Medicine, Department of Pathology, Konya, Turkey,
ORCID: 0000-0003-2209-7512

Aysegul BULUT

Selcuk University, Faculty of Veterinary Medicine, Department of Pathology, Konya, Turkey,
ORCID: 0000-0002-0085-3586

Rabia SALIK

Selcuk University, Faculty of Veterinary Medicine, Department of Pathology, Konya, Turkey,
ORCID: 0000-0002-0364-697X

Gokhan AKCAKAVAK

Bozok University, Faculty of Veterinary Medicine, Department of Pathology, Yozgat, Turkey,
ORCID: 0000-0001-5949-4752

Aysenur TURAL

Selcuk University, Faculty of Veterinary Medicine, Department of Pathology, Konya, Turkey,
ORCID: 0000-0003-1585-3359

Beatriz PADRON PEREZ

Selcuk University, Faculty of Veterinary Medicine, Department of Microbiology, Konya, Turkey,
ORCID: 0000-0003-1020-9636

Fatih HATIPOGLU

Selcuk University, Faculty of Veterinary Medicine, Department of Pathology, Konya, Turkey.
ORCID: 0000-0002-0103-5868

Kyrgyz-Turkish Manas University, Faculty of Veterinary Medicine, Department of Pathology,
Bishkek, Kyrgyzstan. ORCID: 0000-0002-0103-5868

Abstract

In this case, an epidermal inclusion cyst was described in a 2-year-old female hound dog. In the anamnesis, the dog was brought to the Department of Surgery, Faculty of Veterinary, Selcuk University, by its owner, with masses ranging from 0,5 cm to 2 cm in diameter, appearing in increasing numbers in many parts of the body in a period of a year. After the examinations, the mass in the neck region, of approximately 2x1x1 cm in size, was surgically extirpated and sent to the Department of Pathology, Faculty of Veterinary Medicine, Selcuk University. It was determined that the mass, whose macroscopic examinations and measurements were made in our department, was white in colour and had a hard consistency. On the cross-sectional surface of the mass, it was observed that there was a structure with a diameter of about 1 cm, clearly circumscribed around it, and a mottled white colour with a granular surface. Histopathological examinations revealed a solitary cystic structure surrounded by stratified squamous cells in the middle of the dermis layer. It was determined that these squamous cells showed a granular structure from the outside to the inside

of the cyst, and the contents of the cyst consisted of loose and lamellated keratin. While no lesion was found in the epidermis layer, it was determined that some hair follicles were filled with a foreign substance considered to belong to *Demodex* parasite mite sections. No findings were found in the preliminary microbiological examination. Apart from the fact that epidermal inclusion cysts are common in all species, considering that the diagnosis is very important in terms of being different from dermoid cysts as they are not congenital and they can transform into squamous cell cancer, although it is rare, this case is deemed worthy of presentation.

Keywords: Epidermal inclusion cyst, hound dog, pathology

1. INTRODUCTION

Epidermal inclusion cysts also called epidermoid, epidermal, and infundibular cysts, are common skin lesions in many species [5,6]. Although the highest incidence in dogs is reported to be between the ages of 4 and 8 years, no gender predisposition has been reported [5,6]. It has been suggested that epidermal cysts, previously thought to be congenital, occur secondary to the traumatic displacement of epithelial tissue [3,4]. Although there are reports about the transformation of inclusion cysts into squamous cell cancer in humans, no such data have been found in animals yet [1,2]. Macroscopically, even if the lesion is in the dermis, it can sometimes be connected to the surface of the epidermis. They are usually found as solitary lesions of 0.3-2.0 cm in diameter, soft consistency and well-circumscribed [3]. Microscopically, a lesion surrounded by hyperplastic epithelium is seen in the dermis. The epithelial layer on the cyst wall is mostly granular. The inside of the cyst is seen as covered with loose keratin layers. In long-term cases, the layers of keratin can be seen in a higher number and more compactly. Sometimes, hair loss in the epidermis layer above these lesions may also occur [3,5].

2. CASE HISTORY

A 2-year-old, non-infertile sloughi female dog was brought to Selcuk University, Veterinary Faculty, Animal Hospital Surgery Clinic by the owner after 0.5-2.0 cm diameter, hard-consistent masses (Figure 1.A,B) were observed in many parts of the body (approximately 8-10). In the clinical examination, no findings such as pain or itching related to the masses were reported. After the largest of the masses was surgically removed, it was sent to Selcuk University, Faculty of Veterinary Medicine, Department of Pathology. In the anamnesis taken from the owner, it was reported that the dog was adopted from the street when it was about 1 year old and that these masses were present, despite in reduced numbers, when it was first adopted. The owner of the patient also stated that the number of masses increased after moving to another house, that all the lesions were seen in areas covered with white hairs and that the lesions decreased in winter months.



Figure 1. A.B. The appearance of the mass on the skin.

3. MATERIAL AND METHOD

3.1. Histopathologic examination

The obtained biopsy sample was fixed in a 10% formaldehyde solution for 24 hours. After the fixation process was completed, it was followed on an automatic tissue processor device (Leica TP 1020) and embedded in paraffin. Then, sections of 5 μ thickness were obtained from these paraffin blocks with a microtome (Leica RM 2125RT) and stained with Hematoxylin-Eosin (H&E) stain. The obtained preparations were examined under a light microscope (Olympus BX51, Tokyo, Japan) and photographed (Olympus EP50).

3.2. Microbiologic examination

A skin scraping was obtained from the area over the lesion and examined in terms of mycotic and bacterial agents. After the direct microscopic examination, it was cultured on Sabouraud dextrose agar (SDA) and incubated at room temperature for 15 days. In addition, blood agar containing 5% sheep blood was inoculated and incubated for 48 hours at 37°C both aerobically and microaerobically.

3.3. Parasitologic examination

A scraping was recovered from the location of the mass and placed on a slide. After adding 1-2 drops of 10% potassium hydroxide, it was kept for 45 minutes and examined under a light microscope (40X objective).

4. RESULT AND DISCUSSION

4.1. Macroscopic result

In the macroscopic examination, it was determined that the mass was approximately 2x1x1 cm in size, white in colour and with a hard consistency (Figure 2A). On the cross-sectional surface of the mass, a clearly circumscribed structure with a diameter of approximately 1 cm, a mottled surface and a granular appearance was noticed (Figure 2B).



Figure 2. The external surface of the mass (A) and the mottled and granular structure on the cut-sectional surface (B).

4.2. Microscopic result

The histopathological examination revealed a solitary cystic structure surrounded by stratified squamous cells in the middle of the dermis layer (Figure 3). It was noted that these stratified squamous cells showed a granular structure from the outside of the cyst to the inside, while the contents of the cyst consisted of loose and lamellated keratin (Figure 4). No lesions were found in the epidermis layer, but it was determined that some hair follicles were filled with a foreign substance, which was considered to belong to Demodex parasite mite sections but no results were obtained in the parasitological or microbiological examination.

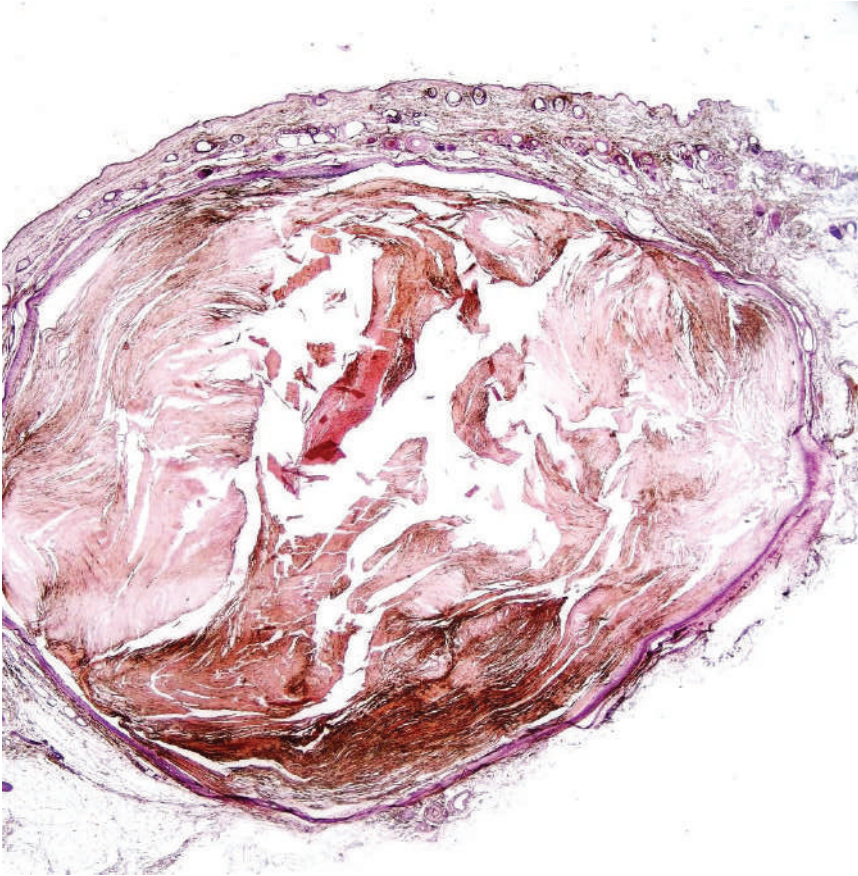


Figure 3. General view of the cyst in the dermis layer, 4X, H&E.

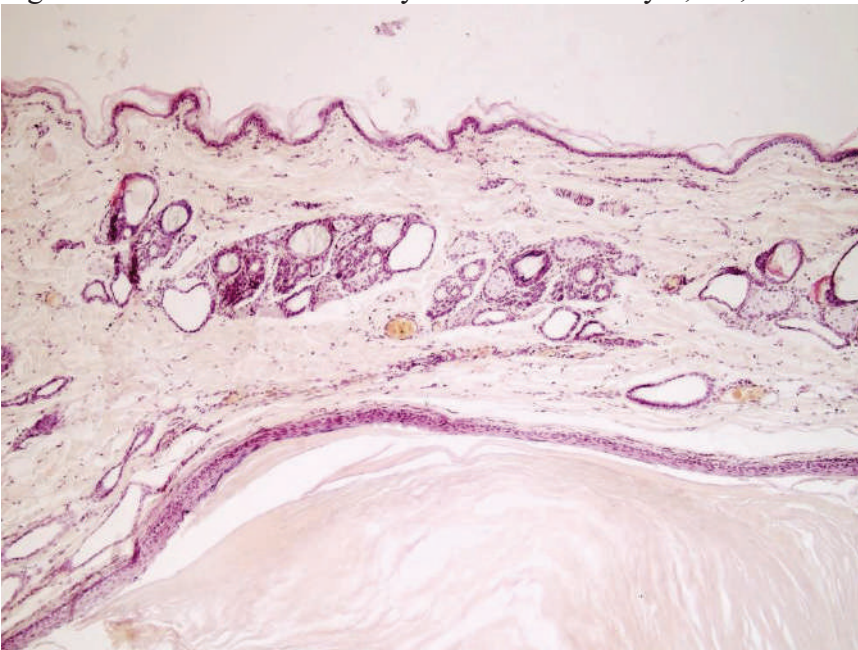


Figure 4. The epidermis with a normal appearance and the part of the cyst close to the epidermis, 10X, H&E.

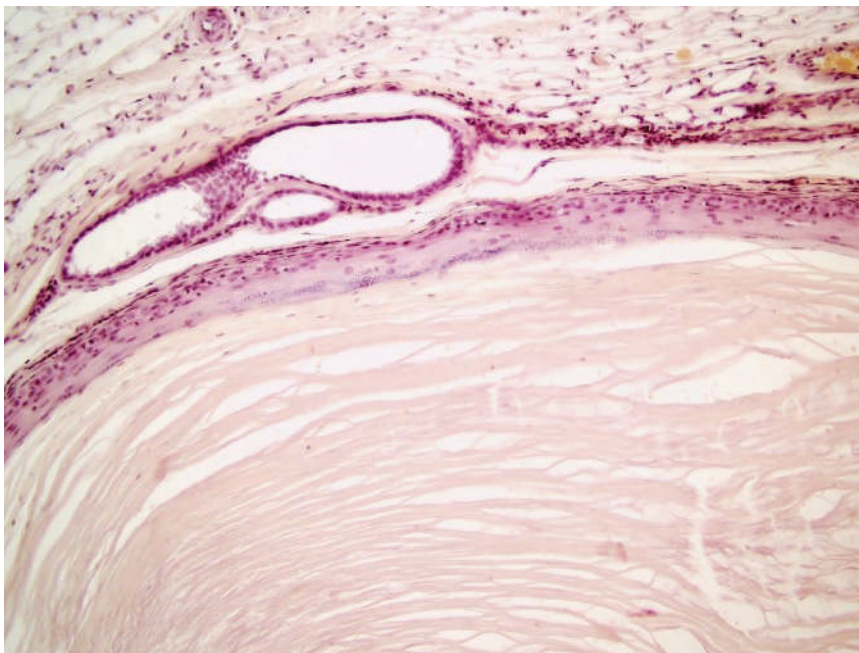


Figure 5. The cyst wall, consisting of stratified squamous cells, and loose and lamellar structures within the cyst, 20X, H&E.

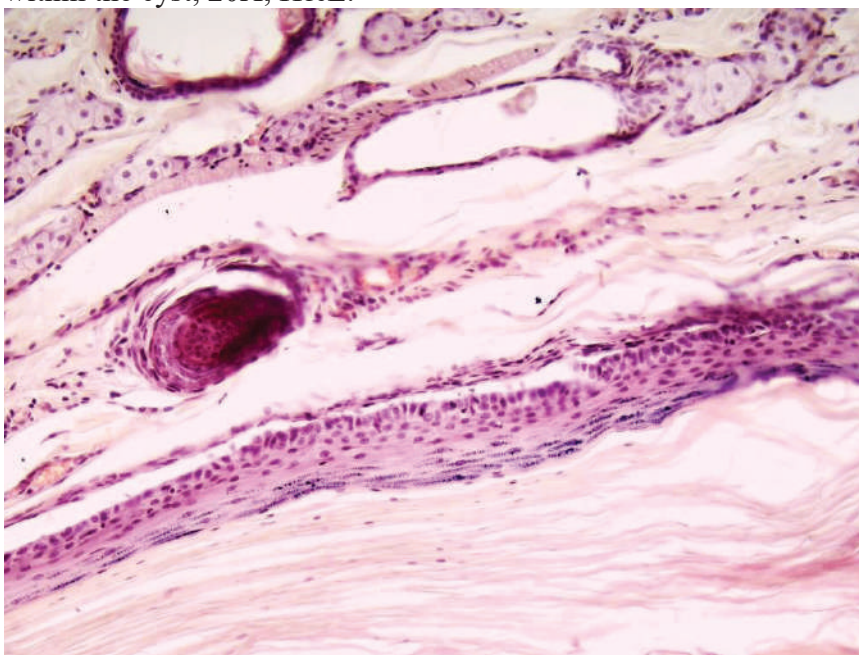


Figure 6. The stratified squamous epithelial layer and granular structures in the cyst wall and pink lamellar structures in the lumen, 40X, H&E.

4.3. Microbiologic result

No growth was detected as a result of the microbiological examination.

4.4. Parasitologic result

No parasitic agents were found as a result of the parasitological examination.

It has been reported that epidermal inclusion cysts occur as a result of the displacement of epithelial tissue due to trauma, and because of this displacement, cysts consisting of keratin surrounded by an epithelial layer and showing lamellarity develop [3,5,6]. The findings obtained as a result of the histopathological examinations were similar to the data found in the literature. According to the information received from the owner, it was found that during the winter months, the dog was walked with clothes and that it especially liked walking on fields. An answer to the question of why these

masses increase in summer may be that in this season, the dog goes outdoors without clothes, that, because of its breed, its skin is thin and its hair very short, and that traumatic factors (such as dry grass) are present in the areas where it walks. The fact that no results were obtained in the microbiological and parasitological examinations also strengthened the thought that, in this case, the lesions developed due to traumatic reasons. In addition, the question of whether the sun has an effect on the aetiology of the inclusion cyst or not has arisen as the lesions are only found in areas covered with white hairs, and the number decreases in winter.

5. CONCLUSION

As a result of the macroscopic and histopathological examinations, the mass was diagnosed as an epidermal inclusion cyst. It was considered worthy of being presented in order to contribute to the diagnosis and treatment and to help general practitioners since it can be confused with neoplastic formations of cutaneous and subcutaneous tissues in terms of appearance.

REFERENCES

- [1]. I. Antón-Badiola, P. San Miguel-Fraile, A. Peteiro-Cancelo, JA. Ortiz-Rey. "Squamous Cell Carcinoma Arising on an Epidermal Inclusion Cyst: A Case Presentation and Review of the Literature." *Actas Dermo-Sifiliográficas* (English Edition), 101(4), 349-53. doi:[https://doi.org/10.1016/S1578-2190\(10\)70646-6](https://doi.org/10.1016/S1578-2190(10)70646-6) 2010.
- [2]. E. Frank, D. Macias, B. Hondorp, J. Kerstetter, JC. Inman. "Incidental squamous cell carcinoma in an epidermal inclusion cyst: a case report and review of the literature." *Case reports in dermatology*, 10(1), 61-68. 2018.
- [3]. MH. Goldschmidt, FS. Shofer. "Skin tumors of the dog and cat." Pergamon Press Ltd. 1992
- [4]. LL. Hillyer, AP Jackson, GC. Quinn, MJ. Day. "Epidermal (infundibular) and dermoid cysts in the dorsal midline of a three-year-old thoroughbred-cross gelding." *Veterinary Dermatology*, 14(4), 205-09. doi:<https://doi.org/10.1046/j.1365-3164.2003.00345.x> 2003.
- [5]. DJ Meuten. *Tumors in domestic animals*: John Wiley & Sons. 2020
- [6]. WM. Parker. "Multiple (more than two thousand) epidermal inclusion cysts in a dog." *The Canadian veterinary journal = La revue veterinaire canadienne*, 36(6), 386-87. 1995

“A SURVEY STUDY OF INSECT PEST ORDERS AND THEIR MANAGEMENT STRATEGIES IN DIFFERENT AREAS OF VIDARBHA REGION”.

Badiye V.H.

PG Department of Zoology SMM College of Science, Nagpur (Maharashtra, India)

Gajbe P.U

PG Department of Zoology SMM College of Science, Nagpur (Maharashtra, India)

Saha R.S.

PG Department of Zoology SMM College of Science, Nagpur (Maharashtra, India)

Insects are the most dominant species on the earth and a very important and integral part of the ecosystem belongs to the phylum Arthropoda. They are beneficial for human society but some of them are very harmful to growing crops, stored products. They attack crops either by directly eating them or infecting them by the transmission of bacteria or viruses. During the present survey study, many hemipteran and lepidopteran species were observed in the various crop field. Implementation of Integrated pest management strategies mainly depends upon various factors such as education, economic status, Govt. policies, availability of working tools, etc. There is a major issue for the scientists to make cost-effective pest management strategies and awareness programs for the farmers to avoid crop damage and financial loss. The insect pest's management strategies include several methods such as traditional methods, mechanical methods, chemical methods, and the use of biological agents as parasitoids or the predators for management of pests. However, most of the farmers from various study fields were found to be practicing traditional methods and hazardous chemical (Insecticides, pesticide) methods as compared to the other methods and the practices of pest control. Financial crunch, non-availability of resources, lack of scientific knowledge and methodology might be the reason for depending upon the insecticides and pesticides rather than using the other methods.

Keywords: Insect pests, Lepidoptera, Hemiptera, IPM Strategies.

EDIBLE ORNAMENTAL FLOWERS SEED COLLECTION – PRESENT STATUS AND FUTURE PERSPECTIVES AT CENTER FOR BIODIVERSITY AND CONSERVATION, UASVM CLUJ-NAPOCA, ROMANIA

Corina CĂTANĂ

University of Agricultural Sciences and Veterinary Medicine, Center for Biodiversity and Conservation, Department of Horticulture and Landscaping, Cluj-Napoca, Romania.
ORCID ID: <https://orcid.org/0000-0002-6041-215X>

Alina MITROI

University of Agricultural Sciences and Veterinary Medicine, Center for Biodiversity and Conservation, Department of Horticulture and Landscaping, Cluj-Napoca, Romania.

Paula BOBOC (OROS)

University of Agricultural Sciences and Veterinary Medicine, Center for Biodiversity and Conservation, Department of Horticulture and Landscaping, Cluj-Napoca, Romania.
ORCID ID: <https://orcid.org/0000-0003-3760-5460>

ABSTRACT

In the international context of developing services that include providing edible flowers to consumers, whether it is gastronomy, floral arrangements or organizing events on this topic, this paper aims to establish the first documented collection in Romania of ornamental plants with edible flowers. The Center for Biodiversity and Conservation (CBC) is included in the research and didactic activity of the research institute “Institute of Advanced Horticultural Research of Transylvania (ICHAT). The CBC has as a priority area of definition and activity: biodiversity and bioconservation of plant species of horticultural interest (horticulture, forestry), the priority objective being the collection, conservation and study of the germplasm fund for horticultural and forestry species. The collection of edible ornamental flower seeds is an innovative one. The collection is 80% completed and covers morphological analysis, indexing (preparation of passport forms according to national and international standards) and the storage. Some species and genera are characterized by a high degree of edibility, for human consumption using other plant organs besides flowers. Whether they are crystallized violets and used as a decoration under the name of Toulouse violets, or they are used as a raw material for obtaining violet syrup (*Viola wittrochiana*), the reputation of these delicacies is constantly increasing, while the plates decorated with rose flowers (*Rosa* sp.) and aromatic water with peony petals (*Paeonia* sp.) are on an upward trend in the preferences of haute cuisine consumers. In order to obtain flowers smaller than those characteristic of the species, in order to be used also as decorations in the culinary arts, the planting distances practiced in the experiment were generally smaller than those used in classical cultures. A notable result in this regard is the miniature form of *Celosia argentea* var. *plumosa* L., in which the flowers have a size of about 2 cm.

Keywords: germplasm collection, edible ornamentals, seeds, bulbs

THE GENOMIC AND TRANSCRIPTOMIC APPROACHES IN OPIUM POPPY

Tuğba Gürkök Tan

Çankırı Karatekin University, Eldivan Vocational School of Health Services,
Department of Medical Laboratory Techniques, Çankırı, Turkey.
ORCID ID: <https://orcid.org/0000-0003-0599-5628>

Gülşen Güçlü

Sivas Cumhuriyet University, Vocational School of Health Services,
Department of Health Care Services, Sivas, Turkey.
ORCID ID: <https://orcid.org/0000-0002-3599-213X>

Abstract

Papaver somniferum L. (opium poppy), which is traditionally cultivated in our country, has been grown in Central Anatolia since the Hittites period. The poppy plant has economic, commercial and medicinal value in terms of both seeds and capsules. It is known that the poppy capsule, which has been used as a medicinal plant since ancient times, produces about 30 different alkaloids, as well as benzyloquinoline alkaloids (BIA) with pharmaceutical properties such as narcotic analgesic morphine, anti-cancer noscapine, cough suppressant codeine, antimicrobial sanguarine, blood vessel dilator papaverine. The biosynthesis pathway of these secondary metabolites is quite complex and has long been searched by genomic, transcriptomic and metabolomic approaches. Although studies on genes associated with BIA biosynthesis and their functioning have been going on for many years, genomic and transcriptomic studies have accelerated with the recent releasing of the genome sequence of the poppy plant. In this study, both the BIA biosynthesis pathways in poppy will be explained and the genomic and transcriptomic approaches for the determination of the genes in this pathway and the functions of these genes will be presented. The resulting total data are expected to guide the production of transgenic plants with increased secondary metabolites through gene silencing and over-expression in the future of poppy plant.

Keywords: *Papaver somniferum* L., Opium poppy, Benzyloquinoline alkaloids, Genomic, Transcriptomic

INTRODUCTION

Papaver somniferum L., which is traditionally cultivated in Turkey, is in the *Papaver* genus of the *Papaveraceae* family of the *Papaverales* order. Turkey is considered very rich in terms of *Papaver* species. Species in the genus *Papaver* are systematically grouped into 9 sections. Of these 9 sections, 3 are perennial, 4 are annual, and there are species belonging to a total of 7 sections in our country (Boissier, 1867).

In the world, poppy cultivation is done legally in Turkey, India, Australia, France, Spain, Hungary as the main producer under the supervision of the United Nations (UN) Organization. Turkey and India are recognized as traditional poppy producer countries by the UN. Poppy has been grown in Central Anatolia since the Hittite period (Ertem, 1974).

In addition to being used as food for its seeds and oil, poppy is also considered as an ornamental plant due to its flowers and dry capsules. It is a versatile plant that is also used for medicinal purposes due to its Benzyloquinoline alkaloids (BIA) it produces. Poppy, which has been used as a medicinal plant since the Hittites, produces BIAs with pharmaceutical properties such as narcotic analgesic morphine, anti-cancer agent noscapine, antitussive codeine, antimicrobial sanguarine, vasodilating papaverine (Desgagné-Penix et al., 2010).

Besides, thebaine is used both to produce codeine and morphine, which are natural poppy products, and to produce semi-synthetic alkaloids naltrexone and hydrocodone (Pei et al., 2021). BIAs are not suitable for commercial production by synthetic or recombinant biotechnological approaches, thus poppy is the only source of BIAs (Nakagawa et al., 2016). The BIA has approximately 2,500 known members and has potential pharmacological properties. Like other secondary or specialized metabolites, they are produced not for normal growth and development in the plant, but for defense against other herbivores and pathogens. While these alkaloids are mostly found in Papaveraceae, Ranunculaceae, Berberidaceae, Menispermaceae families; the most studied species are *Papaver somniferum*, *Eschscholzia californica*, *Thalictrum flavum*, *Coptis japonica* (Ziegler and Facchini, 2008).

BIA Biosynthesis in Opium Poppy

Common pathway for BIA:

BIA biosynthesis basically starts with the decarboxylation, ortho-hydroxylation and deamination of tyrosine to both dopamine and 4-hydroxyphenylacetaldehyde molecule by the enzyme tyrosinecarboxylase (TYDC) (Figure 1). TYDC has a large gene family; about 15 members are also in poppy (Facchini and De Luca, 1994; Facchini et al., 2007). The first committed step of the BIA synthesis pathway is catalyzed by norcoclaurine synthase (NCS) (Samanani and Facchini, 2001). NCS combines dopamine and 4-hydroxyphenylacetaldehyde to form (S)-norcoclaurine with the formation of the C-C bridge. (S)-norcoclaurine is the central precursor molecule for all BIA synthetic plants (Stadler et al., 1989). NCS also thought to regulate BIA biosynthesis due to substrate concentration sensitivity (Lichman et al., 2015). BIA biosynthesis consists of several methylation and hydroxylation steps. The first methylation step is the conversion of (S)-norcoclaurine to (S)-coclaurine by norcoclaurine-6-O-methyltransferase (6OMT) (Ounaroon et al., 2003). Following steps are catalyzed by Cochlaurine N-methyltransferase (CNMT) (Choi et al., 2002), (S)-N-methylcoclaurine 3'-hydroxylase (NMCH) (Park et al., 2018) and 3'-hydroxy-N-methylcoclaurine 4'-O-methyltransferase (4'OMT) which converts (S)-3'-hydroxy-N-methylcoclaurine to (S)-reticuline (Morishige et al., 2000). (S)-reticuline is the central intermediate in most BIA synthesis pathways. Not only are they produced by dimeric bisbenzylisoquinoline alkaloids (S)-reticuline. Another branch in BIA biosynthesis in which (S)-reticuline does not act as an intermediate is papaverine biosynthesis (Ziegler and Facchini, 2008).

After (S)-reticuline biosynthesis, the pathway divides into different branches to synthesize several BIAs such as morphine, sanguinarine, papaverine and noscapine.

a. *Papaverine route:*

The papaverine biosynthesis pathway in opium poppy is still unclear, but several hypotheses exist. Two different pathways have been suggested for the synthesis of papaverine. The first begins with the conversion of (S)-norcoclaurine to (S)-coclaurine by the 6'OMT enzyme. It is the O-methylation of (S)-norreticuline to (S)-norlaudanine by the N7OMT enzyme and after a few steps, papaverine is formed. Pienkny et al. (2009) found a new O-methyltransferase enzyme, which they named norreticuline-7-O-methyltransferase (N7OMT). This enzyme belongs to the class II O-methyltransferase protein family. They stated that the synthesis of papaverine with this enzyme can occur in two different ways (Pienkny et al., 2009). The second pathway is the formation of papaverine by the conversion of (S)-N-Methylcoclaurine (with O-methylations) from (S)-coclaurine to laudanone via the CNMT enzyme. However, Virus Induced Gene Silencing (VIGS) studies on this pathway support the first pathway (Desgagné-Penix and Facchini, 2012).

In contrast, Pathak et al. (2013), in their transcriptome study with natural papaverine mutants, determined that 6'OMT, 4'OMT, and N7OMT were overexpressed, but 7'OMT was decreased. Based on this, they obtained results showing that the biosynthesis of papaverine continues via (S)-coclaurine, that is, the intermediate product in this pathway is (S)-coclaurine (Pathak et al., 2013).

b. Sanguinarine route:

This pathway continues with the formation of two methylenedioxy bridges that result in (S)-chelantipholine and (S)-stylopin. Both reactions are catalyzed by P450-linked monooxygenases. Two cDNAs encoding the stylopin synthase enzyme were cloned from the *E. californica* plant and classified as Cyp719A2 and Cyp719A3 (Ikezawa et al., 2007). Cyp719A2 converts (S)-keliantifolin to (S)-stylopin. (S)-stylopin is then N-methylated by the TNMT enzyme (Liscombe and Facchini, 2007). Cytochrome p450-dependent monooxygenase (S)-cis-N-methylstylopin 14-hydroxylase (MSH) enzyme synthesizes protopine by hydroxylation, and then protopine is hydroxylated with cytochrome p450-linked monooxygenase 6-hydroxylase (P6H) to form dihydroxysanguinarine spontaneously by intramolecular rearrangement (Facchini et al., 2007). The last step in this route is the conversion of Dihydrosanguinarin to sanguinarine by Dihydrobenzophenanthridine oxidase (DBOX) enzyme.

c. Noscapine route:

The noscapine pathway is partially similar to the formation of the berberine intermediate. Eleven enzymatic steps are required to convert (S)-reticuline to noscapine (Park et al., 2018). The noscapine pathway begins with conversion of (S) reticuline to (S)-scoulerine by Berberine bridge enzyme (BBE). Although the pathway is common to the (S)-cannadine molecule, the enzyme tetrahydroprotoberberine cis-N-methyltransferase (TNMT), which is also involved in the sanguinarine pathway, methylates the (S)-cannadine to (S)-N-methylcannadine (Dang and Facchini, 2012). 10 out of the 12 biosynthetic genes existed in the noscapine pathway as a cluster. The last step is catalyzed by Noscapine synthase (NOS) to yield noscopine (Winzer et al., 2012).

d. Morphine route:

Although most biochemical reactions in BIA pathway continues with (S)-reticuline molecule, for morphinan alkaloid biosynthesis the formation of the (R)-reticuline is the first stable step (Facchini et al., 2007). Reticuline epimerase (REPI) enzyme is responsible for the epimerization of the reticuline molecules (Farrow et al., 2015). (R)-reticuline is converted into salutaridine by salutaridine synthase (SalSyn) (Gesell et al., 2009), which is then reduced by salutaridine reductase to yield salutaridinol (Grothe et al., 2001). The subsequent step is the conversion of salutaridinol to thebaine by salutaridinol 7-O-acetyltransferase (SalAT) (Ziegler et al., 2006). Besides, a novel enzyme called thebaine synthase (THS) which produce thebaine was isolated from the latex of opium poppy (Chen et al., 2018). In the last step of morphine biosynthesis, there are two different routes from thebaine to morphine. In one of the route oripavine, morphinone and morphine synthesized from thebaine, respectively with the enzymes codeine O-demethylase (CODM), thebaine 6-O-demethylase (T6ODM) and codeinone reductase (COR). The other route goes on thebaine, codeinone, codeine and morphine. The enzymes taking part in this route are T6ODM, COR and CODM, respectively (Unterlinner et al., 1999).

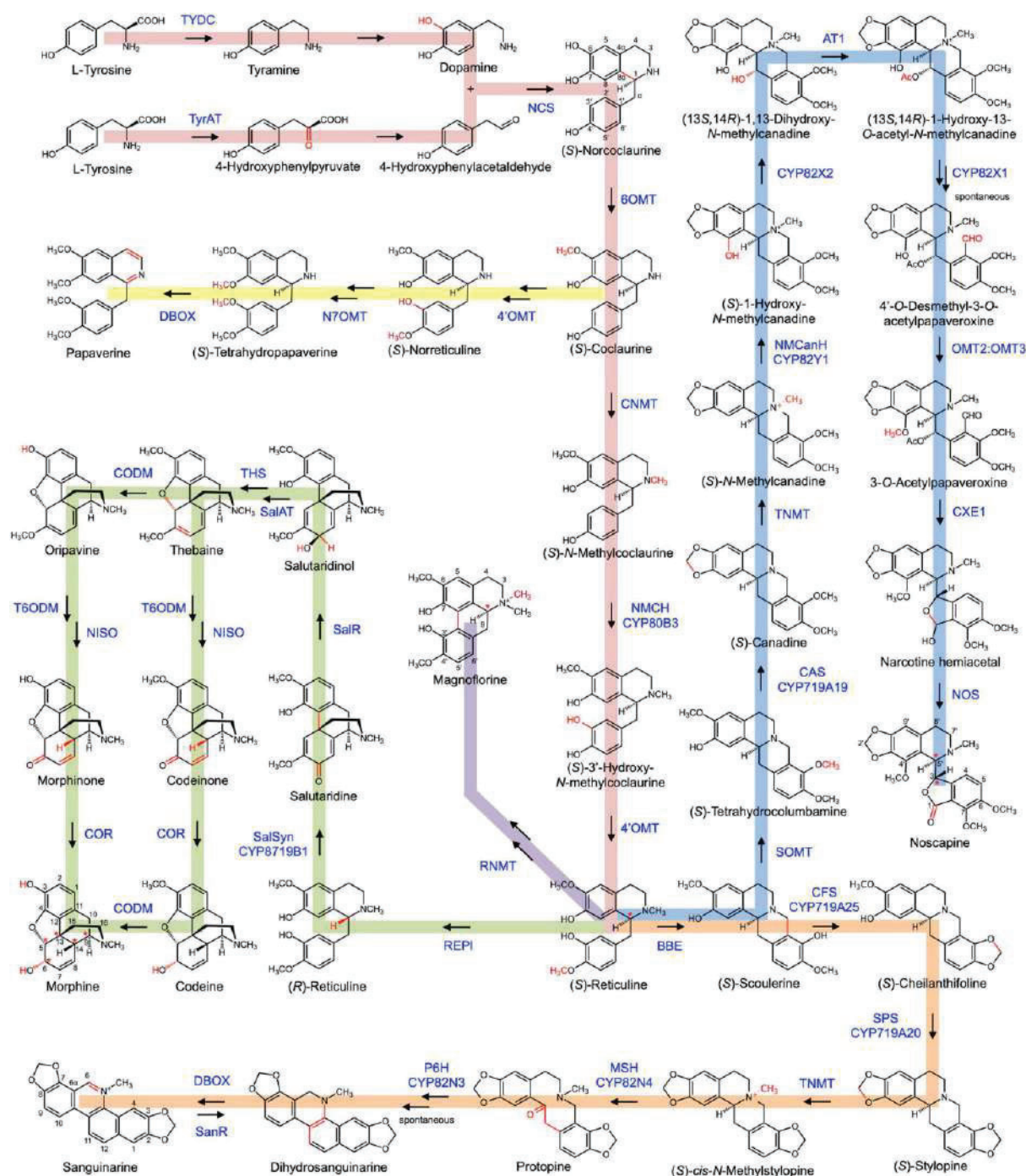


Figure 1. Major BIA biosynthetic pathways in opium poppy (Singh et al., 2019).

Genomic approaches:

Whole genome sequencing:

Whole genome sequencing of opium poppy is important because of BIAs. We know that *P. somniferum* is the only source of medically and economically important morphine. The exploration of the genome sequence led us to brighten genetic and physiologic basis of this miraculous plant. In addition, the genome sequences of poppy facilitate to understand the evolution of BIA synthesis genes.

To date two variety of opium poppy whole genome sequencing was performed. The high noscapine variety of *P. somniferum* (HN1) and 'Chinese Herbal Medicine' (CHM) (Guo et al., 2018)

Among Papaveraceae family *P. somniferum* genome size is found to be the largest. In HN1 genome size detected as 2,72 Gb while in CHM it was found as 2,62 Gb. The reason why poppy has the largest genome is explained by the burst of repetitive elements. In CHM 65.79% of the genome is composed of transposable elements and the majority of the transposable elements are the members of long terminal repeats (LTR). Among LTRs Ty3/*Gypsy* elements are predominant. Both whole genome sequencing analysis revealed that about 80,000 genes predicted as protein coding. In CHM, 5226 transfer RNA genes, 1404 miRNA genes, 2076 small nuclear RNA genes, and 1129 ribosomal RNA genes were detected (Pei et al., 2021).

Functional Genomics:

It is aimed to increase morphinan alkaloids by over-expression of COR enzyme by using RNAi in *P. somniferum* plant. A significant increase was observed in the amount of alkaloids in the capsules of transgenic lines grown both in the greenhouse and in the field after 4 years. The increase in the total amount of alkaloids can be attributed to the increase in the amount of morphine, codeine and thebaine. With the increase in the amount of COR enzyme, an increase in morphine and codeine can be expected, but the increase in thebaine is unpredictable. It has been stated that the reason for the increase in the amount of thebaine may be the feedback inhibition of the demethylation steps as a result of the increase in the amount of morphine and codeine, or the prevention of the transition of thebaine to the vesicles that accumulate morphine and codeine (Larkin et al., 2007).

Regulation of *SalAT* gene expression also caused changes in the alkaloid content of poppy. Over-expression of the *SalAT* transgene increased the overall alkaloid content by approximately 40%. On the other hand, silencing of *SalAT* transcripts with RNAi to approximately one-tenth of the normal level resulted in unexpected accumulation of the salutaridine molecule. They stated that this event can be explained as the conversion of salutaridinol, the substrate of *SalAT*, to salutaridine by the reversible *SalIR* enzyme (Allen et al., 2008). VIGS-mediated suppression of transcript levels of the *DBOX* enzyme in poppy, reducing the amount of sanguinarine, dihydroxysanguinarine and papaverine in roots supports the function of this enzyme in different pathways (Hagel and Facchini, 2013).

Hagel and Facchini (2010) isolated thebaine T6OMD and COMD enzymes using functional genomics. In the study, the stem transcriptomes of *Top1* (thebaine oripavine poppy 1) mutants containing high thebaine and oripavine but not morphine and codeine were compared with 3 different cultivars that accumulate morphine. Metabolic functions of T6OMD and COMD enzymes were determined by VIGS (Hagel and Facchini, 2010).

In opium poppy when *REPI* gene transcripts were silenced via VIGS it was found that (R)-reticuline and morphinan alkaloids decreased on the other hand (S)-reticuline abundance was increased. This study supports that *REPI* plays a key role in morphine biosynthesis (Farrow et al., 2015).

4OMT2 has a critical role in BIA biosynthesis hence VIGS-mediated gene silencing of this gene. When 4'*OMT* gene was suppressed via VIGS in a morphine rich variety, the total alkaloid content reduced in stem tissues, but significantly increased total alkaloid content in the capsule. Silencing of reticuline 7-O-methyltransferase (7OMT) that converts (S)-reticuline to (S)-laudanine, also reduced not only total alkaloid content in stem, but also reduced the several selected BIA biosynthesis genes in different tissues. Over-expression of 4'*OMT* increased expression of *CNMT*, *SalAT* and 7OMT and decreased *COR* gene expression in the stem. 7OMT gene over-expression increased *COR*, *SAT*, 6OMT and 4'*OMT* transcript level in the stem but decreased *CNMT*, 6OMT and *COR* transcript levels in the capsule of opium poppy (Gurkok et al., 2016).

The new gene editing technology has recently been applied to opium poppy. When *CRISPR/Cas9* gene editing technology used to mutate *4'OMT2* gene it reduces morphine biosynthesis (Alagoz et al., 2016).

Transcriptomic approaches

All of the RNAs created against external stimuli in a tissue or living thing at a certain time are called transcriptome (Kogenaru et al., 2012). Although the genomes of cells in an organism are the same, their transcriptome profiles can vary (Tang et al., 2011).

Transcriptome studies are established as a first step to identify gene expression patterns in organisms. Gene expression patterns and alkaloid profiles can give important clues about BIA biosynthesis pathway.

Pathak et al. (2013) carried out a transcriptome profiling study to shed light the papaverine pathway. Their results suggest that papaverine biosynthesis may proceed differently from the previously identified pathway. As well as they also revealed that a set of methyl transferase and dehydrogenase enzymes play role in this route (Pathak et al., 2013).

Using microarray gene expression analyzes, in different time points, were conducted in methyl jasmonate treated opium poppy capsules. In this study also the alkaloid accumulation was detected. According to the results of microarray analysis, the number of transcripts whose expression changed compared to the control at the 12th hour, found the most. Besides, morphine and noscapine amounts were determined to be higher than other alkaloids in all time periods (Gurkok et al., 2015).

CONCLUSION

As a result, with this study, the pathways described so far on the poppy plant and the genomic and transcriptomic studies determined in this pathway are presented in a wide scope. In light of these pathways, genomic and transcriptomic research is expected to gain momentum. With future comprehensive studies, the possibility of developing transgenic plants of *P. somniferum*, which has economic, medical and agricultural importance, will increase.

REFERENCES

- Alagoz, Y., Gurkok, T., Zhang, B., & Unver, T. (2016). Manipulating the biosynthesis of bioactive compound alkaloids for next-generation metabolic engineering in opium poppy using CRISPR-Cas 9 genome editing technology. *Scientific reports*, 6(1), 1-9.
- Allen, R. S., Miller, J. A., Chitty, J. A., Fist, A. J., Gerlach, W. L., & Larkin, P. J. (2008). Metabolic engineering of morphinan alkaloids by over-expression and RNAi suppression of salutaridinol 7-O-acetyltransferase in opium poppy. *Plant biotechnology journal*, 6(1), 22-30.
- Boissier, E. (1867). *Flora Orientalis: Thalamiflorae* (Vol. 1). apud H. Georg.
- Chen, X., Hagel, J. M., Chang, L., Tucker, J. E., Shiigi, S. A., Yelapaala, Y., ... & Facchini, P. J. (2018). A pathogenesis-related 10 protein catalyzes the final step in thebaine biosynthesis. *Nature chemical biology*, 14(7), 738-743.
- Choi, K. B., Morishige, T., Shitan, N., Yazaki, K., & Sato, F. (2002). Molecular cloning and characterization of coclaurinen-methyltransferase from cultured cells of *Coptis japonica*. *Journal of Biological Chemistry*, 277(1), 830-835.
- Dang, T. T. T., & Facchini, P. J. (2012). Characterization of three O-methyltransferases involved in noscapine biosynthesis in opium poppy. *Plant physiology*, 159(2), 618-631.
- Desgagné-Penix, I., Khan, M. F., Schriemer, D. C., Cram, D., Nowak, J., & Facchini, P. J. (2010). Integration of deep transcriptome and proteome analyses reveals the components of alkaloid metabolism in opium poppy cell cultures. *BMC plant biology*, 10(1), 1-17.
- Desgagné-Penix, I., & Facchini, P. J. (2012). Systematic silencing of benzylisoquinoline alkaloid biosynthetic genes reveals the major route to papaverine in opium poppy. *The Plant Journal*, 72(2), 331-344.

- Ertem, H. (1974). Boğazköy metinlerine göre Hititler devri Anadolu'sunun florası. *Türk Tarih Kurumu yayınlarından*/7.
- Facchini, P. J., & De Luca, V. (1994). Differential and tissue-specific expression of a gene family for tyrosine/dopa decarboxylase in opium poppy. *Journal of Biological Chemistry*, 269(43), 26684-26690.
- Facchini, P. J., Hagel, J. M., Liscombe, D. K., Loukanina, N., MacLeod, B. P., Samanani, N., & Zulak, K. G. (2007). Opium poppy: blueprint for an alkaloid factory. *Phytochemistry Reviews*, 6(1), 97-124.
- Farrow, S. C., Hagel, J. M., Beaudoin, G. A., Burns, D. C., & Facchini, P. J. (2015). Stereochemical inversion of (S)-reticuline by a cytochrome P450 fusion in opium poppy. *Nature Chemical Biology*, 11(9), 728-732.
- Gesell, A., Rolf, M., Ziegler, J., Chávez, M. L. D., Huang, F. C., & Kutchan, T. M. (2009). CYP719B1 is salutaridine synthase, the CC phenol-coupling enzyme of morphine biosynthesis in opium poppy. *Journal of Biological Chemistry*, 284(36), 24432-24442.
- Grothe, T., Lenz, R., & Kutchan, T. M. (2001). Molecular characterization of the salutaridinol 7-O-acetyltransferase involved in morphine biosynthesis in opium poppy *Papaver somniferum*. *Journal of Biological Chemistry*, 276(33), 30717-30723.
- Gurkok, T., Turktas, M., Parmaksiz, I., & Unver, T. (2015). Transcriptome profiling of alkaloid biosynthesis in elicitor induced opium poppy. *Plant Molecular Biology Reporter*, 33(3), 673-688.
- Gurkok, T., Ozhuner, E., Parmaksiz, I., Özcan, S., Turktas, M., Ipek, A., ... & Unver, T. (2016). Functional characterization of 4' OMT and 7OMT genes in BIA biosynthesis. *Frontiers in plant science*, 7, 98.
- Hagel, J. M., & Facchini, P. J. (2010). Dioxygenases catalyze the O-demethylation steps of morphine biosynthesis in opium poppy. *Nature chemical biology*, 6(4), 273-275.
- Hagel, J. M., & Facchini, P. J. (2013). Benzylisoquinoline alkaloid metabolism: a century of discovery and a brave new world. *Plant and Cell Physiology*, 54(5), 647-672.
- Ikezawa, N., Iwasa, K., & Sato, F. (2007). Molecular cloning and characterization of methylenedioxy bridge-forming enzymes involved in stylophine biosynthesis in *Eschscholzia californica*. *The FEBS journal*, 274(4), 1019-1035.
- Kogenaru, S., Yan, Q., Guo, Y., & Wang, N. (2012). RNA-seq and microarray complement each other in transcriptome profiling. *BMC genomics*, 13(1), 1-16.
- Larkin, P. J., Miller, J. A., Allen, R. S., Chitty, J. A., Gerlach, W. L., Frick, S., ... & Fist, A. J. (2007). Increasing morphinan alkaloid production by over-expressing codeinone reductase in transgenic *Papaver somniferum*. *Plant biotechnology journal*, 5(1), 26-37.
- Lichman, B. R., Gershtater, M. C., Lamming, E. D., Pesnot, T., Sula, A., Keep, N. H., ... & Ward, J. M. (2015). 'Dopamine-first' mechanism enables the rational engineering of the norcoclaurine synthase aldehyde activity profile. *The FEBS journal*, 282(6), 1137-1151.
- Liscombe, D. K., & Facchini, P. J. (2007). Molecular cloning and characterization of tetrahydropprotoberberine cis-N-methyltransferase, an enzyme involved in alkaloid biosynthesis in opium poppy. *Journal of Biological Chemistry*, 282(20), 14741-14751.
- Morishige, T., Tsujita, T., Yamada, Y., & Sato, F. (2000). Molecular characterization of the S-adenosyl-L-methionine: 3'-hydroxy-N-methylcoclaurine 4'-O-methyltransferase involved in isoquinoline alkaloid biosynthesis in *Coptis japonica*. *Journal of Biological Chemistry*, 275(30), 23398-23405.
- Nakagawa, A., Matsumura, E., Koyanagi, T., Katayama, T., Kawano, N., Yoshimatsu, K., ... & Minami, H. (2016). Total biosynthesis of opiates by stepwise fermentation using engineered *Escherichia coli*. *Nature communications*, 7(1), 1-8.
- Ounaroon, A., Decker, G., Schmidt, J., Lottspeich, F., & Kutchan, T. M. (2003). (R, S)-Reticuline 7-O-methyltransferase and (R, S)-norcoclaurine 6-O-methyltransferase of *Papaver*

- somniferum–cDNA cloning and characterization of methyl transfer enzymes of alkaloid biosynthesis in opium poppy. *The plant journal*, 36(6), 808-819.
- Park, M. R., Chen, X., Lang, D. E., Ng, K. K., & Facchini, P. J. (2018). Heterodimeric O-methyltransferases involved in the biosynthesis of noscapine in opium poppy. *The Plant Journal*, 95(2), 252-267.
- Pathak, S., Lakhwani, D., Gupta, P., Mishra, B. K., Shukla, S., Asif, M. H., & Trivedi, P. K. (2013). Comparative transcriptome analysis using high papaverine mutant of *Papaver somniferum* reveals pathway and uncharacterized steps of papaverine biosynthesis. *PloS one*, 8(5), e65622.
- Pei, L., Wang, B., Ye, J., Hu, X., Fu, L., Li, K., ... & Cong, B. (2021). Genome and transcriptome of *Papaver somniferum* Chinese landrace CHM indicates that massive genome expansion contributes to high benzyloquinoline alkaloid biosynthesis. *Horticulture Research*, 8(1), 1-13.
- Pienkny, S., Brandt, W., Schmidt, J., Kramell, R., & Ziegler, J. (2009). Functional characterization of a novel benzyloquinoline O-methyltransferase suggests its involvement in papaverine biosynthesis in opium poppy (*Papaver somniferum* L). *The Plant Journal*, 60(1), 56-67.
- Samanani, N., & Facchini, P. J. (2001). Isolation and partial characterization of norcoclaurine synthase, the first committed step in benzyloquinoline alkaloid biosynthesis, from opium poppy. *Planta*, 213(6), 898-906.
- Singh, A., Menéndez-Perdomo, I. M., & Facchini, P. J. (2019). Benzyloquinoline alkaloid biosynthesis in opium poppy: An update. *Phytochemistry Reviews*, 18(6), 1457-1482.
- Stadler, R., Kutchan, T. M., & Zenk, M. H. (1989). (S)-Norcoclaurine is the central intermediate in benzyloquinoline alkaloid biosynthesis. *Phytochemistry*, 28(4), 1083-1086.
- Tang, F., Lao, K., & Surani, M. A. (2011). Development and applications of single-cell transcriptome analysis. *Nature methods*, 8(4), S6-S11.
- Unterlinner, B., Lenz, R., & Kutchan, T. M. (1999). Molecular cloning and functional expression of codeinone reductase: the penultimate enzyme in morphine biosynthesis in the opium poppy *Papaver somniferum*. *The Plant Journal*, 18(5), 465-475.
- Winzer, T., Gazda, V., He, Z., Kaminski, F., Kern, M., Larson, T. R., ... & Graham, I. A. (2012). A *Papaver somniferum* 10-gene cluster for synthesis of the anticancer alkaloid noscapine. *Science*, 336(6089), 1704-1708.
- Ziegler, J., Voigtländer, S., Schmidt, J., Kramell, R., Miersch, O., Ammer, C., ... & Kutchan, T. M. (2006). Comparative transcript and alkaloid profiling in *Papaver* species identifies a short chain dehydrogenase/reductase involved in morphine biosynthesis. *The Plant Journal*, 48(2), 177-192.
- Ziegler, J., & Facchini, P. J. (2008). Alkaloid biosynthesis: metabolism and trafficking. *Annu. Rev. Plant Biol.*, 59, 735-769.

DERIVATIONS PERIOD 2 OF PRIME RINGS

Mehsin Jabel Atteya

Department of Mathematics, College of Education, Al-Mustansiriyah University,
Baghdad, Iraq

ORCID NO: 0000-0001-7380-6951

ABSTRACT

The main purpose of this paper is to introduce and study the definition of derivations period 2 via associative ring R and U be a nonzero ideal of R . Accurately, we prove the derivation is commuting of U of a ring R that satisfied certain conditions.

KEY WORDS: Derivations, map period 2, generalized derivation, prime ring, 2-torsion free.
(2010) Mathematics Subject Classification: 16W25, 16W10, 16U80.

1 INTRODUCTION

The modern definition of abstract ring appeared in 1914 in Fraenkel's paper which under title "On zero divisors and the decomposition of ring". One of the natural questions of Ring Theory is to determine conditions implying commutativity of the ring. A systematic study of non-commutative rings started in the 20th century while commutative rings have appeared though in a covered way much before, and as many other theories, go back to Fermat's Last Theorem. In 1847, a French mathematician Lamé stated a solution of this problem. Unlike commutative rings, which grew from number theory, non-commutative rings originated from an idea of Hamilton, who endeavoured to generalize the complex numbers as a two-dimensional algebra over the reals to a four-dimensional algebra of quaternions. Other natural noncommutative objects are matrices. In 1850, they were introduced by Cayley, together with their laws of addition and multiplication and, in 1870, Pierce noted that the modern ring axioms held for square matrices. During the last two decades, the commutativity of associative rings with derivations have become one of the focus points of several authors and a significant work has been done in this direction. Basically, the study of derivation was initiated during the 1950s and 1960s. Derivations of rings got a tremendous development in 1957, when Posner [13] established two very striking results in the case of prime rings. A considerable amount of work has been done on derivations and related maps during the last decades (see, e.g., [1,3,4, 14-17] and references therein). In 1957 Herstein proved that if $\text{char } R \neq 2$, then any Jordan derivation of R is a derivation (see [23, Theorem 3.1]). We refer the reader to [22] and [21] for the 2-torsion free semiprime case. For the case $\text{char } R = 2$, Herstein proved that if R is not a commutative integral domain, then a Jordan derivation δ of R satisfying $\delta(xy) = \delta(x)y + x\delta(y)$ for all $x, y \in R$.

Indeed, in [12] M.N. Daif, proved that, let R be a semiprime ring and d a derivation of R with $d^3 \neq 0$. If $[d(x), d(y)] = 0$ for all $x, y \in R$, then R contains a non-zero central ideal. M.N. Daif and H.E. Bell [20] proved that, let R be a semiprime ring admitting a derivation d for which either $xy + d(xy) = yx + d(yx)$ for all $x, y \in R$ or $xy - d(xy) = yx - d(yx)$ for all $x, y \in R$, then R is

commutative. On the other hand, DeFilippis [11] proved that, when R be a prime ring let d a non-zero derivation of R , $U \neq (0)$ a two-sided ideal of R , such that $d([x,y])=[x,y]$ for all $x,y \in U$, then R is commutative. Abdelkarim Boua in [8] studied the commutativity of 3-prime near-rings admitting homoderivations which satisfy certain differential identities on near-rings. Homoderivation has diversity notions in agreement with reference [10] where Eszter Gselmann and Gergely Kiss investigated the (different) notions of homoderivations. The effect of a homoderivation on ideals studied by E. F. Alhare and N. M. Muthana [9]. They proved that U is a non-zero left ideal in a prime ring R that admits a homoderivation h which is zero power valued on U satisfying $xy + h(xy) = yx + h(yx)$ for all $x, y \in U$. Then R is commutative. Also, Ahmad Al-Kenani, Asmaa Melaibari and Najat Muthana [5] showed that R is a prime ring and U is a non-zero ideal of R . If $x \in R$ and x centralizes U , then $x \in Z(R)$. Asmaa Melaibari, Najat Muthana and Ahmad Al-Kenani [7] pointed out that R is any ring with no non-zero central ideals. If $H: R \rightarrow R$ is a zero-power valued CE-homoderivation (i.e., centrally extended homoderivation), then H is additive.

The main purpose of this paper is to introduce and study the definition of derivations period 2 via associative ring R and U be a nonzero ideal of R .

2 PRELIMINARIES

Let R be an associative ring with center $Z(R)$. Let $x, y, z \in R$. We write the notation $[y, x]$ for the commutator $yx - xy$ and $x \circ y$ for anticommutator $xy + yx$ also make use of the identities $[xy, z] = [x, z]y + x[y, z]$ and $[x, yz] = [x, y]z + y[x, z]$. Recall that R is semiprime if $aRa = 0$ implies $a = 0$ and R is prime if $aRb = 0$ implies $a = 0$ or $b = 0$. Every prime ring is semiprime ring, but the converse is not true always. R is said to be commutative if $xy = yx$ for all $x, y \in R$. An analogous notion is that of anticommutativity of rings. A ring R is said to be n -torsion free if for $x \in R$, $nx = 0$ implies $x = 0$. A map $d: R \rightarrow R$ is said to be n -commuting on R if $[d(x), x^n] = 0$ holds for all $x \in R$. It is said that a map $d: R \rightarrow R$ is n -centralizing on R if $[d(x), x^n] \in Z(R)$ is fulfilled for all $x \in R$. An additive map $d: R \rightarrow R$ is called a derivation if the Leibniz's rule $d(xy) = d(x)y + xd(y)$ holds for all $x, y \in R$.

Also, an additive mapping $D: R \rightarrow R$ is called a generalized derivation if there exists an additive mapping d on R such that $D(xy) = D(x)y + xd(y)$ for all $x, y \in R$. Let S be a nonempty subset of R . A map $f: R \rightarrow R$ is said to be of period 2 on S if $f^2(x) = x$ for all $x \in S$.

We first fix the following fact which shall be used frequently throughout the text.

Lemma 1 [18, Lemma 2.1] Let R be a semiprime ring, U a nonzero two-sided ideal of R and $a \in R$ such that $axa = 0$ for all $x \in U$, then $a = 0$.

3. THE MAIN RESULTS

Theorem 3.1. Let R be a prime ring and U be a nonzero ideal of R . If D is a generalized derivation with associated d derivation period 2 of R such that

- (i) $d(x) \circ D(y) = 0$ for all $x, y \in U$,
- (ii) $d(x) \circ D(y) \mp x \circ y = 0$ for all $x, y \in U$, then d is commuting of U .

Proof: (i) From our hypothesis, we have $d(x) \circ D(y) = 0$ for all $x, y \in U$. (3.1)

Replacing y by yz in (3.1), we have

$$d(x) \circ yd(z) + D(y)[z, d(x)] = 0 \text{ for all } x, y, z \in U. \quad (3.2)$$

Substitute $zd(x)$ for z in (3.2), we find that

$$d(x) \circ yzd^2(x) = 0 \text{ for all } x, y, z \in U. \quad (3.3)$$

Moreover,

$$d(x)yzd^2(x) = -yzd^2(x)d(x) \text{ for all } x, y, z \in U. \quad (3.4)$$

Replacing y by ry in (3.4) and use (3.4), we obtain

$$[d(x), r]yzd^2(x) = 0 \text{ for all } x, y, z \in U, r \in R. \quad (3.5)$$

This implies that $[d(x), r]Ryzd^2(x) = (0)$ for all $x, y, z \in U$ and $r \in R$.

Furthermore,

$$[d(x), y]d^2(x)R[d(x), y]d^2(x)R[d(x), y]d^2(x) = (0) \text{ for all } x, y \in U.$$

Due to R is semiprime, we obtain $[d(x), y]d^2(x) = 0$ for all $x, y \in U$.

Linearization this relation gives us

$$[d(x), y]d^2(z) + [d(z), y]d^2(x) = 0 \text{ for all } x, y, z \in U. \quad (3.6)$$

Substitute yu for y in relation (3.6), we obtain

$$[d(x), y]ud^2(z) + [d(z), y]ud^2(x) = 0 \text{ for all } x, y, z, u \in U. \quad (3.7)$$

Replace u by $ud^2(x)w[d(z), y]u$ in (3.7), we show

$$[d(x), y]udz(x)w[d(z), y]ud^2(x) + [d(z), y]udz(x)w[d(z), y]ud^2(x) = 0$$

for all $x, y, z, w, u \in U$. (3.8)

This relation yields

$$[d(z), y]ud^2(x)w[d(z), y]ud^2(x) = 0 \text{ for all } x, y, z, w, u \in U. \quad (3.11)$$

Substitute wr for w in (3.11) and using semiprimeness of R , we deduce

$[d(z), y]ud^2(x)w = 0$ for all $y, z, u, w \in U$. Replacing w by $r[d(z), y]u$ with using the fact that of R is semiprime ring, we conclude that

$$[d(z), y]ud^2(x) = 0 \text{ for all } x, y, z, u \in U. \quad (3.12)$$

Due to d is period 2, we conclude that

$$[d(z), y]ux = 0 \text{ for all } x, y, z, u \in U. \text{ Replacing } x \text{ by } d(z)y, \text{ we obtain}$$

$$[d(z), y]ud(z)y = 0 \text{ for all } x, y, z, u \in U. \quad (3.13)$$

Again, putting $u = yd(z)$ in relation (3.13) and subtracting this result from relation (3, 13), we arrive at

$$[d(z), y]u[d(z), y] = 0 \text{ for all } x, y, z, u \in U.$$

Employing Lemma 1, we conclude that d is commuting of U .

The proof of the branch (ii) is similar as the branch (i).

Theorem 3.2: Let R be a prime ring and U be a nonzero ideal of R . If D is a generalized derivation with associated d derivation period 2 of R such that

- (i) $d(x) \circ D(y) - xy = 0$ for all $x, y \in U$,
- (ii) $d(x) \circ D(y) - [x, y] = 0$ for all $x, y \in U$, then d is commuting of U .

Proof: (i) From our hypothesis $d(x) \circ D(y) - xy = 0$ for all $x, y \in U$.

Replacing y by yz , we find that

$$(d(x) \circ D(y))z + d(x) \circ yd(z) + D(y)[z, d(x)] - xyz = 0 \text{ for all } x, y, z \in U. \quad (3.14)$$

This relation leads to

$$d(x) \circ yd(z) + D(y)[z, d(x)] = 0 \text{ for all } x, y, z \in U. \quad (3.15)$$

Putting $zd(x)$ for z in (3.15) to get $d(x) \circ yzd^2(x) = 0$ for all $x, y, z \in U$. i.e.,

$$d(x)yzd^2(x) + yzd^2(x)d(x) = 0 \text{ for all } x, y, z \in U. \quad (3.16)$$

Replacing y by ry in (3.16) with use (3.16), we get $[d(x), r]yzd^2(x) = 0$ for all $x, y, z \in U$ and $r \in R$. This implies that $[d(x), r]Ryzd^2(x) = (0)$ for all $x, y, z \in U$ and $r \in R$. Using similar manner as in the proof of Theorem 3. 1, we get the required result.

The proof of the branch (ii) is similar as the branch (i).

Theorem 3.3: Let R be a prime ring and U be a nonzero ideal of R . If D is a generalized derivation with associated d derivation period 2 of R such that $[d(x), D(y)] = 0$ for all $x, y \in U$ then d is commuting of U .

Proof. By hypothesis, we have the relation $[d(x), D(y)] = 0$ for all $x, y \in U$.

Replacing y by yz , we find that

$$[d(x), D(y)][z + D(y)[d(x), z] + [d(x), y]d(z) + y[d(x), d(z)] = 0 \text{ for all } x, y, z \in U. \quad (3.17)$$

This yields the relation

$$D(y)[d(x), z] + [d(x), y]d(z) + y[d(x), d(z)] = 0 \text{ for all } x, y, z \in U. \quad (3.18)$$

Again, replacing z by $zd(x)$ in (3.18), we show

$$D(y)[d(x), zd(x)] + [d(x), y]d(zd(x)) + y[d(x), d(zd(x))] = 0 \text{ for all } x, y, z \in U. \quad (3.19)$$

Employing (3.18) on relation (3.19), we arrive to

$$[d(x), y]zd^2(x) + yz[d(x), d^2(x)] + y[d(x), z]d^2(x) = 0 \text{ for all } x, y, z \in U. \quad (3.20)$$

Substitute ry for y in (3.20) to get $[d(x), r]yzd^2(x) = 0$ for all $x, y, z \in U$ and $r \in R$.

Applying the same arguments as we have done in the proof of Theorem 3.1, we get the required result.

ACKNOWLEDGEMENTS

The author is grateful to Al-Mustansiriya University, the Republic of Iraq and beholden to the reviewer(s) for his/ their accuracy with professionally reading the article.

REFERENCES

- [1] H. E Bell and W. S Matindale III, Centralizing mappings of semiprime rings, *Canad. Math. Bull.*, 30(1), (1987), 42-60.
- [2] Xiaowei Xu, Yang Liu, and Wei Zhang, Skew n -Derivations on semiprime rings, *Bull. Korean Math. Soc.* 5 (2013), No. 6, pp. 1863-1871, <http://dx.doi.org/10.4134/BKMS.2013.50.6.1863>.
- [3] I. N. Herstein, *Rings with Involution*. The University of Chicago Press, 1976.
- [4] Mehsin Jabel Atteya, Commutativity with Derivations of Semiprime Rings, *Discussiones Mathematicae General Algebra and Applications* 40(2020)165–175doi:10.7151/dmgaa.1333
- [5] Ahmad Al-Kenani, Asmaa Melaibari and Najat Muthana, Homoderivations and commutativity of prime rings, *East-West J. of Mathematics*, Vol. 17, No. 2 (2015), pp. 117-126.
- [6] E. F. Alhare and N. M. Muthana, On homoderivations and commutativity of rings, *Bulletin of the International Mathematical Virtual Institute*, 9(2), (2019), 301 { 304.
- [7] Asmaa Melaibari, Najat Muthana and Ahmad Al-Kenani, Centrally extended homoderivations on rings, *Gulf Journal of Mathematics*, Vol.4, Issue 2, (2016), pp.62-70.
- [8] Abdelkarim Boua, Homoderivations and Jordan right ideals in 3-prime near-rings AIP Conference Proceedings 2074, 020010 (2019); <https://doi.org/10.1063/1.5090627>.
- [9] E. F. Alhare and N. M. Muthana, The commutativity of prime rings with homoderivations, *International Journal of Advanced and Applied Sciences*, 5 (5) 2018, Pages: 79-81.
- [10] Eszter Gselmann and Gergely Kiss, Remarks on the notion of homo-derivations February 6, 2020, arXiv:2001.03439v3 [math.RA].
- [11] V. De Filippis, Automorphisms and derivations in prime rings, *Rendiconti di Matematica, Serie VII*, Vol.19, Roma(1999), 393 -404.
- [12] M.N. Daif Commutativity results for semiprime rings with derivations, *Internat. J. Math. and Math. Sci.* Vol.21(3) (1998), 471- 474.
- [13] E. C. Posner, Derivations in prime rings, *Proc. Amer. Math. Soc.* 8 (1957), 1093- 1100.
- [14] Asma Ali, Mehsin Jabel Atteya, Phool Miyan and Farhat Ali, Semigroup ideals and permuting 3-generalized derivations in prime near rings, *Italian Journal of Pure and Applied Mathematics*, n.35(2015), 207-226.

- [15] Ajda Fošner and Mehsein Jabel Atteya, Semigeneralized semiderivations of semiprime rings, AIP Conference Proceedings 2037, 020010 (2018), <https://doi.org/10.1063/1.5078465>. Published Online: 14 November (2018).
- [16] Ajda Fošner and Mehsein Jabel Atteya, Study of (σ, τ) -generalized derivations with their composition of semiprime rings, Kragujevac Journal of Mathematics, Vol. 43(4) (2019), Pages 535-558.
- [17] Mehsein Jabel Atteya, New types of permuting n -derivations with their applications to associative rings, Symmetry, 12, (2020) 46; doi:10.3390/sym12010046, www.mdpi.com/journal/symmetry.
- [18] M.S. Samman and A.B. Thaheem, Derivations of semiprime rings, International Journal of Pure and Applied Mathematics, Volume 5 No. 4 (2003), 465-472.
- [19] P.M. Cohn, Further algebra and applications, Springer-Verlag London Berlin Heidelberg, 1st edition, SBN 978-1-4471-1120-7, (2003).
- [20] M.N. Daif and H.E. Bell, Remarks on derivations on semiprime rings Internat. J. Math. and Math. Sci. 15, 205- 206(1992).
- [21] M. Brešar, Jordan derivations on semiprime rings, Proc. Amer. Math. Soc. 104(4) (1988) 1003–1006.
- [22] J. M. Cusack, Jordan derivations on rings, Proc. Amer. Math. Soc. 53(2) (1975) 321–324.
- [23] I. N. Herstein, Jordan derivations of prime rings, Proc. Amer. Math. Soc. 8 (1957) 1104–1110.

THE EFFECT OF HEAT TREATMENT STRATEGIES ON THERMAL STABILIZATION OF POLYACRYLONITRILE FIBERS IN CARBON FIBER PRODUCTION

Kemal Şahin TUNÇEL

Department of Traditional Crafts, Siirt University, Siirt, Turkey

ORCID ID: 0000-0001-5095-6543

Md. Mahbubor RAHMAN

Bangladesh University of Textiles, Tejgaon, Dhaka, Bangladesh

ORCID ID: 0000-0001-7104-9459

Tuba DEMİREL

Department of Mechanical Engineering, Erciyes University, Kayseri, Turkey

ORCID ID: 0000-0002-5760-3705

Ismail KARACAN

Department of Textile Engineering, Erciyes University, Kayseri, Turkey

ORCID ID: 0000-0002-9047-1011

ABSTRACT

The thermal stabilization stage is the most important stage of carbon fiber production in terms of the ability of Polyacrylonitrile (PAN) fibers to resist high temperatures throughout the carbonization stage. The degree of stabilization of the PAN fibers determines the final carbon fiber strength. Here, insufficient stabilization and excessive stabilization adversely affect the mechanical properties. For optimum thermal stabilization, it is necessary to effectively use the basic process parameters such as temperature, time, and heating rate. In this study, PAN fibers were passed through a 15% guanidine carbonate aqueous solution to accelerate the process before thermal stabilization. Then, thermal stabilization was carried out using two different heat treatment procedures, single-step (SS) and multi-step (MS). While SS heat treatment was carried out isothermally at 250 °C, MS heat treatment was carried out at temperatures between 200 and 250 °C. Both heat treatment procedures include three different stabilization times of 15, 45, and 75 minutes. The changes in linear density, fiber thickness, density, and mechanical properties of PAN fibers after thermal stabilization are given comparatively for two different heat treatment procedures. Differential scanning calorimetry (DSC) technique was used to examine the change in the thermal properties of the samples after heat treatment. While the DSC conversion index value increased up to 60% as a result of SS heat treatment, it increased up to 94% as a result of MS heat treatment. Similarly, the mechanical properties obtained as a result of MS heat treatment were found to be higher than the mechanical properties obtained as a result of SS heat treatment.

Keywords: Polyacrylonitrile, Guanidine Carbonate, Thermal Stabilization, Carbon Fiber.

1. INTRODUCTION

The thermal stabilization stage is seen as the most important stage in carbon fiber production. At this stage, the precursor fiber turns into a structure resistant to high temperatures during carbonization [1-5]. Thermal processes during thermal stabilization cause some chemical changes in the PAN polymer chains. This provides the formation of a condensed cyclic structure with a carbon-nitrogen double bond ($C=N$) [6,7]. This structure makes the polymer much more thermally stable compared to the old nitrile bond ($C\equiv N$) [8]. In addition to all the transformations, the thermal stabilization stage is shown as the one that consumes the most energy and takes a lot of time [9-12]. For this reason, PAN fibers were passed through guanidine carbonate aqueous solution before the thermal stabilization process to both reduce the time required for thermal stabilization of PAN fibers and accelerate the process [13], accordingly.

Optimum stabilization can only be achieved by choosing the best parameters during thermal stabilization. It is important that parameters such as residence time of the fibers in the oven, stabilization temperature, and heating rate are used in a balanced pattern [14-17]. During stabilization in an air atmosphere, oxygen generally diffuses from the outer surface of the fibers to the inner parts. In some cases, due to the inhomogeneity of the oxygen distribution in the fiber, the skin-core effect occurs [18], resulting in fibers with low mechanical properties. Therefore, a gradual increase in temperature will be more effective than single-step heat treatment, especially during the use of thicker fibers.

This research includes a series of preliminary studies in which both single-step and multi-step heat treatments were applied to examine the effect of the heat treatment procedure on the thermal stabilization of the fibers obtained after guanidine carbonate impregnation. The data obtained from both heat treatment results were evaluated by comparing them with each other.

2. MATERIAL AND METHOD

Before chemical treatment, PAN fibers were kept in 5% aqueous ethanol solution to remove the spin-finish oils they were exposed to during their production, and then washed and dried. Some properties of untreated PAN fibers are listed in Table 1. Heat treatment procedures applied to PAN fibers are given in Fig. 1 and Fig. 2.

Table 1 Some properties of untreated PAN fibers

Precursor	Linear density (Tex)	Density (g/cm^3)	Fiber thickness (μm)	Tensile strength (MPa)	Tensile modulus (GPa)	Elongation at break (%)
PAN	59.7	1.18	22	262.2	13.9	11.6



Figure 1 Single-step heat treatment procedure

In both heat treatment procedures, the rate at all steps of thermal stabilization (i.e, heating and cooling) was determined as 2°C/min.

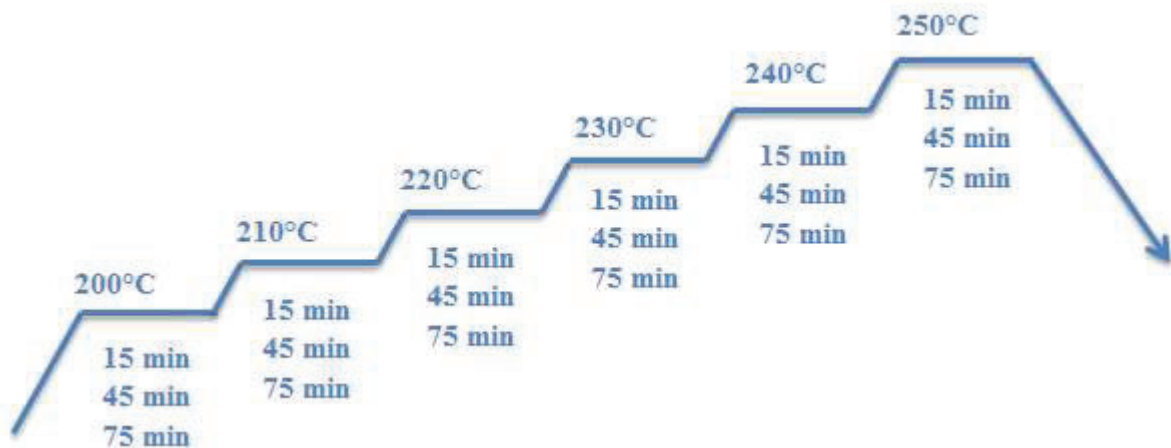


Figure 2 Multi-step heat treatment procedure

2.1. Linear Density Measurements

The linear density of all samples was calculated as Tex. It refers to the weight in grams of 1000 meters of yarn.

2.2. Fiber Thickness Measurements

Fiber thickness measurements of all samples were carried out using an Olympus brand CX31 model optical microscope. To calculate the fiber thickness, the measurements were made at 20 different points along the fiber axis of five randomly selected filaments and the result was expressed as the mean value.

2.3. Density Measurements

For density measurements, solutions with known densities were prepared by using isopropyl alcohol (0.786 g/cm³) and perchloroethylene (1.62 g/cm³) liquids. The prepared samples were left in these density solutions and waited for a certain period of time to reach the equilibrium position. All density values were obtained using these density solutions.

2.4. Measurements of Mechanical Properties

The mechanical properties of all samples were measured using a Prowhite brand tensile strength tester at a tensile speed of 5 mm/min and a gauge distance of 20 mm. Results were given by averaging 20 measurements.

2.5. DSC Measurements

A Perkin Elmer Diamond DSC system was used to examine the thermal properties of PAN samples after heat treatments. The test was carried out using a temperature between 50 and 400°C and a heating rate of 10°C/min. The nitrogen flow rate was determined as 50 ml/min. The weight of the samples used for the test is about 5 mg. For the thermally stabilized samples, the DSC conversion index was calculated using Eq. (1),

$$\text{DSC – Conversion index (\%)} = \frac{\Delta H_0 - \Delta H}{\Delta H_0} \times 100\% \quad (1)$$

ΔH_0 is the exothermic heat for raw PAN and ΔH is the exothermic heat for PAN that is thermally stabilized after heat treatments.

3. RESULTS AND DISCUSSION

3.1. Evaluation of Linear Density Measurements

The linear density gives an idea about the mass change in the polymer structure in general. In Figure 3, the change in linear density as a result of both SS and MS heat treatment is shown.

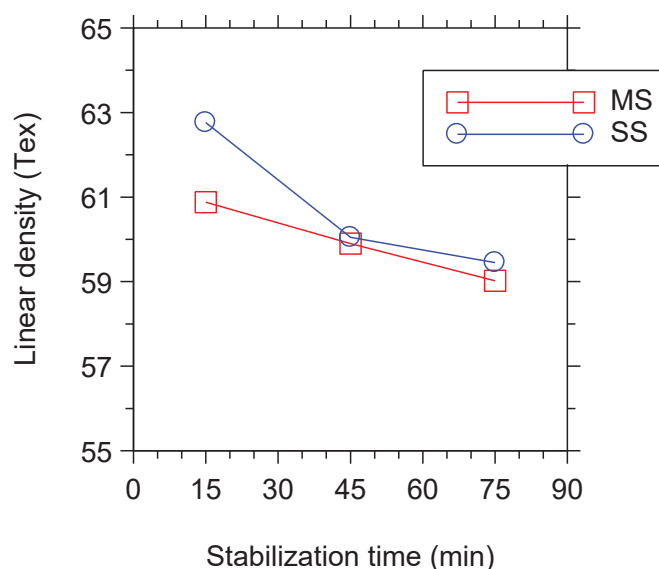


Figure 3 Change in linear density after heat treatments

The linear density of the PAN samples impregnated with 15% guanidine carbonate aqueous solution increased by approximately 14% and was calculated as 68.1 tex. Then, as a result of both heat treatments, a decrease in linear density was observed depending on the mass loss with the effect of temperature and time. However, in MS heat treatment, more mass loss was observed as the waiting time of the samples in the furnace was longer.

3.2. Evaluation of Fiber Thickness Measurements

Fiber thickness is an important parameter to ensure homogeneity during thermal stabilization. Figure 4 shows the change in fiber thickness as a result of both SS and MS heat treatment. The fiber thickness tended to decrease due to the mass losses in the fiber after thermal treatments. The fiber thickness of the raw sample was 22 μm and increased slightly after guanidine carbonate impregnation. However, it decreased due to the increase in stabilization time and stabilization temperature during heat treatments. This situation supports the change in linear density. It was observed that the results obtained from both heat treatment procedures were close to each other. After 75 minutes of stabilization, the average fiber thickness values were 17.9 μm with SS heat treatment and 17.5 μm with MS heat treatment. Thus, as a result of MS heat treatment, the fiber thickness value decreased by 20.5% compared to the untreated sample.

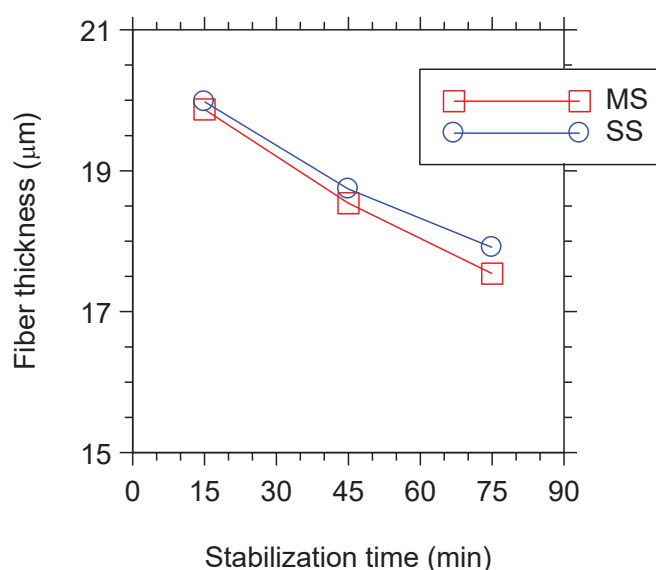


Figure 4 Change in fiber thickness after heat treatments

3.3. Evaluation of Density Measurements

To obtain carbon fiber with good mechanical properties from PAN-based fibers, the thermal stabilization stage must be fulfilled at an optimum level. Therefore, it is important to know the fiber densities of the samples obtained after heat treatments. Looking at the literature, it has been stated that the fiber density of the samples should be between 1.34 – 1.40 g/cm^3 for optimum thermal stabilization of PAN-based fibers [19].

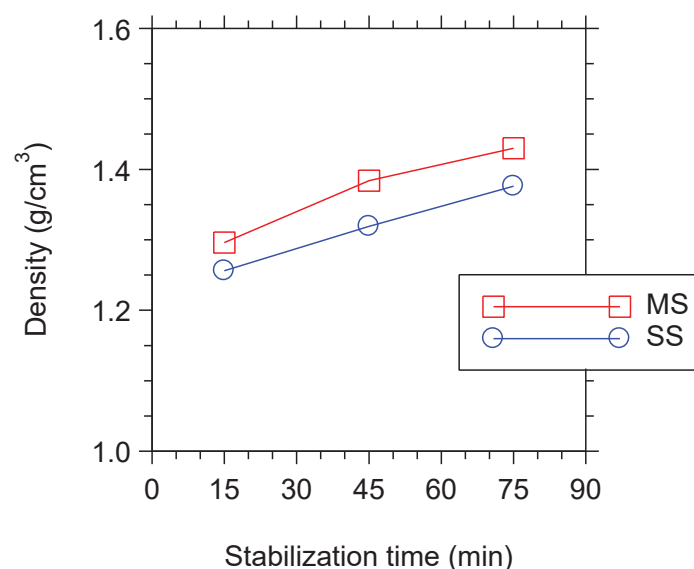


Figure 5 Change in fiber density after heat treatments

Figure 5 shows the change in fiber density as a result of both SS and MS heat treatment. With the increase of the stabilization time, the density values increased in all heat treatments. The increase in the density values after thermal stabilization is interpreted as the closer packing of the macromolecule chains to each other due to the cyclization of the nitrile groups in the PAN polymer structure [20]. After 75 minutes of stabilization, the density value increased up to 1.37 g/cm³ with SS heat treatment, while it increased up to 1.43 g/cm³ with MS heat treatment.

3.4. Evaluation of Mechanical Properties

Figures 6-8 show the change in mechanical properties as a result of both SS and MS heat treatment during the thermal stabilization of PAN fibers.

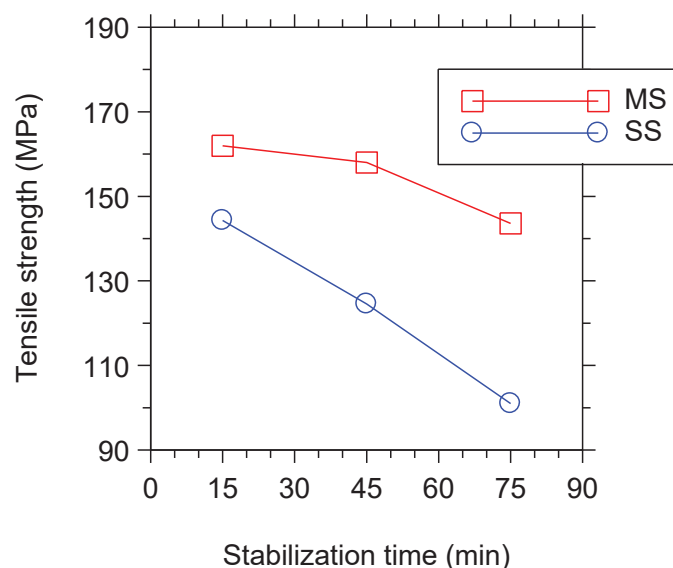


Figure 6 Change in tensile strength after heat treatments

To produce a carbon fiber with the desired level of mechanical properties, PAN-based fibers must be fully stabilized before the carbonization stage. While excessive stabilization may

adversely affect the mechanical properties, insufficient stabilization also negatively affects the mechanical properties. Especially when compared to the initial tensile strength values, a decrease in tensile strength is likely due to thermal degradation. However, higher tensile strength values were obtained with MS heat treatment. The important thing is to keep the reduction in tensile strength at an optimum level.

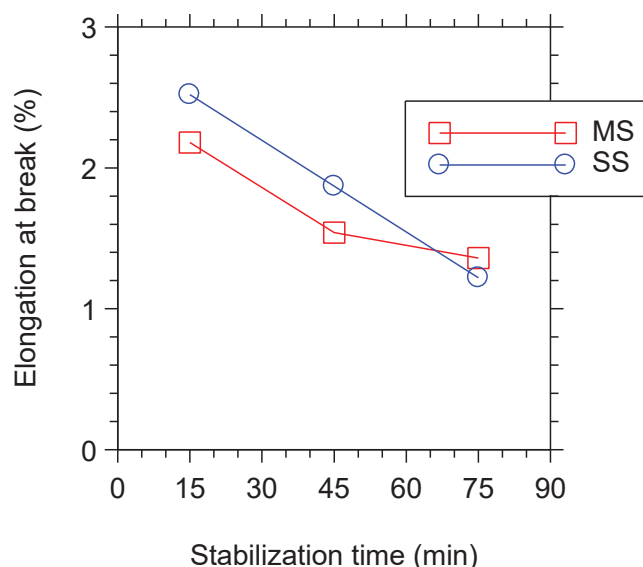


Figure 7 Change in elongation at break after heat treatments

The tensile strength values vary between 144 and 101 MPa as a result of SS heat treatment, while it varies between 162 and 143 MPa as a result of MS heat treatment. Similarly, higher modulus values were obtained as a result of MS heat treatment. On the other hand, we can say that guanidine carbonate makes the structure more brittle and thus the elongation at break decreases more.

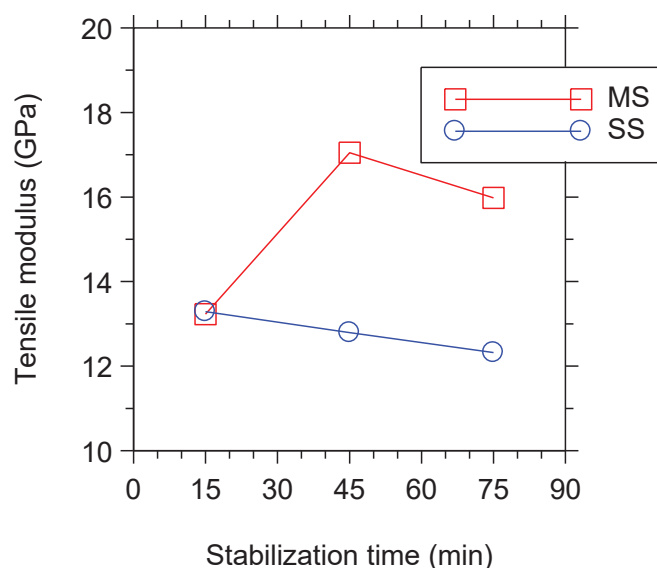


Figure 8 Change in tensile modulus after heat treatments

3.5. Evaluation of DSC Measurements

DSC thermograms contain important information about the change in thermal properties of PAN fibers throughout the process. The thermograms obtained from DSC in Figure 9 show comparatively the change in thermal properties of PAN fibers as a result of both SS and MS heat treatment. As a result of both heat treatments, the exothermic peak area and height gradually and continuously decrease with the increase of the heat treatment time, but it is seen that the peak width increase.

In Figure 9, when the DSC thermograms obtained after 45 minutes of stabilization are examined, the difference between the two different heat treatments is seen most clearly and it is understood that the MS heat treatment is more effective in a short time. The reduction of the area of peak supports the cyclization of nitrile ($C\equiv N$) groups present in the untreated PAN fiber.

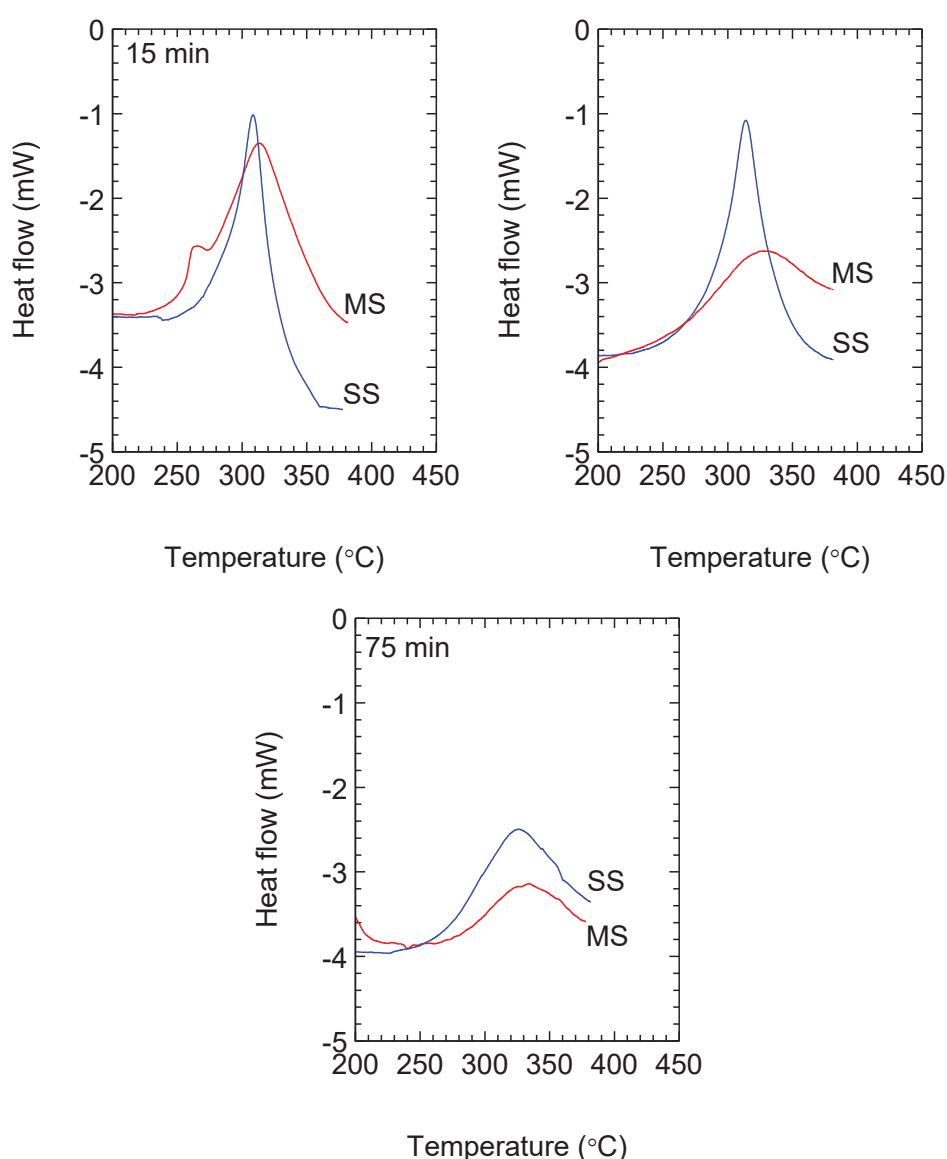


Figure 9 Change in thermograms obtained from DSC

Peak height value for 75 min stabilization as a result of MS heat treatment decreased by 97.5% compared to the untreated sample (see Figure 10).

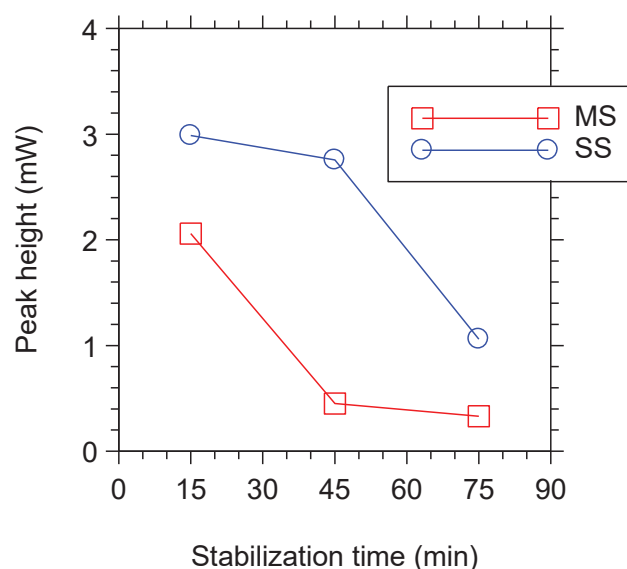


Figure 10 Change in peak heights obtained from DSC thermograms

DSC conversion index [21] values obtained using Eq. 1 are given in Figure 11. It was observed that the DSC conversion index increased continuously throughout stabilization. At the end of thermal stabilization, DSC conversion index values of the samples stabilized by SS and MS heat treatment increased up to 60% and 94%, respectively. This shows that MS heat treatment is more effective in terms of the thermal stability of PAN fiber.

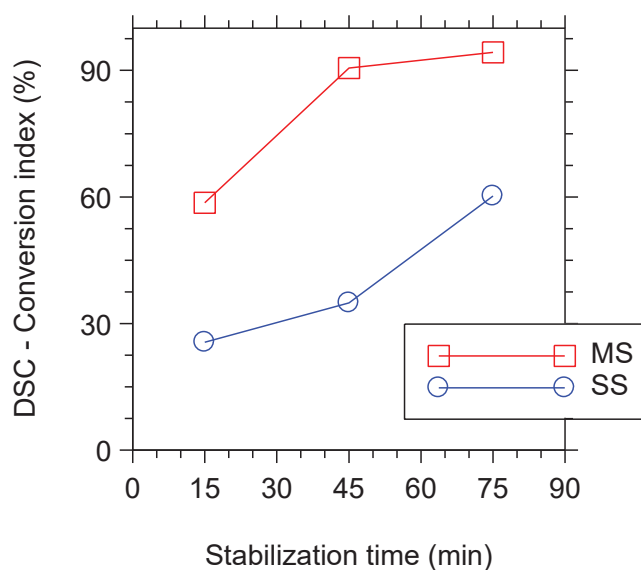


Figure 11 DSC conversion index values

4. CONCLUSIONS

To reduce the time required for the thermal stability of the PAN fibers, the samples passed through the guanidine carbonate aqueous solution were then thermally stabilized by both SS and MS heat treatments. To examine the differences between the heat treatments, the samples were subjected to a series of tests as a result of the process. Although the linear density and fiber thickness values tend to decrease due to mass losses due to temperature and time, the

density values tend to increase. Density values vary between 1.26 and 1.37 g/cm³ in the samples obtained as a result of SS heat treatment, while it changes between 1.30 and 1.43 g/cm³ with MS heat treatment. On the other hand, the mechanical properties obtained as a result of MS heat treatment were found to be higher than the mechanical properties obtained as a result of SS heat treatment. Similarly, the information obtained from DSC supports that MS heat treatment is more effective than SS heat treatment. It has been observed that MS heat treatment has a more positive effect on the thermal stabilization of PAN-based fibers compared to SS heat treatment. It is foreseen that it will be a heat treatment procedure that is much more suitable especially for the thermal stabilization of thick fibers.

REFERENCES

1. Clarke, A.J., Bailey, J.E., (1973). Oxidation of Acrylic Fibres for Carbon Fibre Formation, *Nature*, 243: 146–150. <https://doi.org/10.1038/243146a0>
2. Jain, M.K., Balasubramanian, M., Desai, P., Abhiraman, A.S., (1987). Conversion of Acrylonitrile-based Precursors to Carbon Fibres, *J. Mater. Sci.*, 22: 301–312. <https://doi.org/10.1007/BF01160585>
3. Ogawa, H., Saito, K., (1995). Oxidation Behavior of Polyacrylonitrile Fibers Evaluated by New Stabilization Index, *Carbon N.Y.*, 33: 783–788. [https://doi.org/10.1016/0008-6223\(95\)00007-Z](https://doi.org/10.1016/0008-6223(95)00007-Z)
4. Liu, J., Xiao, S., Shen, Z., Xu, L., Zhang, L., Peng, J., (2018). Study on the Oxidative Stabilization of Polyacrylonitrile Fibers by Microwave Heating, *Polymer Degradation and Stability*, 150, 86–91. <https://doi.org/10.1016/j.polymdegradstab.2018.02.017>
5. Tajaddod, N., Li, H., Minus, M.L., (2018). Low-temperature Graphitic Formation Promoted by Confined Interphase Structures in Polyacrylonitrile/Carbon Nanotube Materials, *Polymer*, 137, 346–357. <https://doi.org/10.1016/j.polymer.2018.01.007>
6. Farsani, R.E., Shokuhfar, A., Sedghi, A., (2007). Conversion of Modified Commercial Polyacrylonitrile Fibers to Carbon Fibers, *Journal of Optoelectronics and Advanced Materials*. <https://doi.org/10.5281/zenodo.1058913>
7. Rahaman, M.S.A., Ismail, A.F., Mustafa, A., (2007). A Review of Heat Treatment on Polyacrylonitrile Fiber, *Polymer Degradation and Stability*, 92(8), 1421–1432. <https://doi.org/10.1016/j.polymdegradstab.2007.03.023>
8. Damodaran, S., Desai, P., Abhiraman, A.S., (1990). Chemical and Physical Aspects of the Formation of Carbon Fibres from PAN-based Precursors, *The Journal of The Textile Institute*, 81(4): 384–420. <https://doi.org/10.1080/00405009008658719>

9. Badii, K., Naebe, M., Golkarnarenji, G., et al (2014). Energy Saving in Electric Heater of Carbon Fiber Stabilization Oven, In: 2014 4th International Conference on Artificial Intelligence with Applications in Engineering and Technology, IEEE, 109–114. <https://doi.org/10.1109/ICAJET.2014.27>
10. Khayyam, H., Naebe, M., Zabihi, O., Zamani, R., Atkiss, S., Fox, B., (2015). Dynamic Prediction Models and Optimization of Polyacrylonitrile (PAN) Stabilization Processes for Production of Carbon Fiber, IEEE Transactions on Industrial Informatics, 11(4), 887–896. <https://doi.org/10.1109/TII.2015.2434329>
11. Golkarnarenji, G., Naebe, M., Badii, K., et al (2018). Production of Low Cost Carbon-Fiber through Energy Optimization of Stabilization Process, Materials, 11: 385. <https://doi.org/10.3390/ma11030385>
12. Golkarnarenji, G., Naebe, M., Badii, K., et al, (2018). Support Vector Regression Modelling and Optimization of Energy Consumption in Carbon Fiber Production Line, Comput. Chem. Eng., 109:276–288. <https://doi.org/10.1016/j.compchemeng.2017.11.020>
13. Karacan, İ., Erdoğan, G., (2011). An Investigation on Structure Characterization of Thermally Stabilized Polyacrylonitrile Precursor Fibers Pretreated with Guanidine Carbonate prior to Carbonization, Polymer Engineering & Science, 52(5), 937–952. <https://doi.org/10.1002/pen.22160>
14. Fitzer, E., Frohs, W., Heine, M., (1986). Optimization of Stabilization and Carbonization Treatment of PAN Fibres and Structural Characterization of the Resulting Carbon Fibres, Carbon N.Y., 24: 387–395. [https://doi.org/10.1016/0008-6223\(86\)90257-5](https://doi.org/10.1016/0008-6223(86)90257-5)
15. Jing, M., Wang, C., Bai, Y., et al (2007). Effect of Temperatures in the Rearmost Stabilization Zone on Structure and Properties of PAN-based Oxidized Fibers, Polym. Bull., 58: 541–551. <https://doi.org/10.1007/s00289-006-0692-2>
16. Duan, Q., Wang, B., Wang, H., (2012). Effects of Stabilization Temperature on Structures and Properties of Polyacrylonitrile (PAN)-based Stabilized Electrospun Nanofiber Mats, J. Macromol. Sci., Part B, 51: 2428–2437. <https://doi.org/10.1080/00222348.2012.676415>
17. Rahman M. M., Demirel T., Tunçel K. Ş., Karacan I., (2021). The effect of the ammonium persulfate and a multi-step annealing approach during thermal stabilization of polyacrylonitrile multifilament prior to carbonization. J. Mater. Sci. 56:14844-14865. <https://doi.org/10.1007/s10853-021-06209-1>
18. Nunna, S., Naebe, M., Hameed, N., Fox, B.L., Creighton, C., (2017). Evolution of Radial Heterogeneity in Polyacrylonitrile Fibres during Thermal Stabilization: An Overview,

Polymer Degradation and Stability, 136, 20-30.
<https://doi.org/10.1016/j.polymdegradstab.2016.12.007>

19. Soulis, S., Konstantopoulos, G., Koumoulos, E., Charitidis, C., (2020), Impact of Alternative Stabilization Strategies for the Production of PAN-based Carbon Fibers with High Performance, *Fibers*, 8(6): 33. <https://doi.org/10.3390/fib8060033>
20. Bajaj, P., Roopanwal, A.K., (1997). Thermal Stabilization of Acrylic Precursors for the Production of Carbon Fibers: An Overview, *Journal of Macromolecular Science, Part C: Polymer Reviews*, 37(1), 97–147. <https://doi.org/10.1080/15321799708014734>
21. Tsai, J-S., Hsu, H-N., (1992). Determination of the Aromatization Index for Oxidized Polyacrylonitrile Fibre by the Differential Scanning Calorimetry Method, *Journal of Materials Science Letters*, 11: 1403–1405. <https://doi.org/10.1007/BF00729641>

EVALUATION OF THEORETICAL AND EXPERIMENTAL PROPERTIES OF 3-METHYL-4-(3-ACETOXY-4-METHOXY-BENZYLIDENAMINO)-4,5-DIHYDRO-1H-1,2,4-TRIAZOL-5-ONE

Instructor Önder Albayrak^{1,*}, Assoc.Prof. Dr. Murat Beytur², Prof. Dr. Haydar Yüksek²

¹ Kafkas University, Atatürk Vocational School of Health Services, 36100, Kars, Turkey

² Kafkas University, Faculty of Science and Letters, Department of Chemistry, 36100, Kars, Turkey

ABSTRACT

3-methyl-4-(3-acetoxy-4-methoxy-benzylidenamino)-4,5-dihydro-1H-1,2,4-triazol-5-one was obtained in excellent yields through 3-methyl-4-amino-4,5-dihydro-1H-1,2,4-triazol-5-one with 3-acetoxy-4-methoxy-benzaldehyde. The 3-methyl-4-(3-acetoxy-4-methoxy-benzylidenamino)-4,5-dihydro-1H-1,2,4-triazol-5-one has been optimized using B3LYP/6-311G(d) basis set. ¹H-NMR and ¹³C-NMR isotropic shift values were calculated by the method of GIAO using the program package Gaussian G09. Experimental and theoretical values were inserted into the graphic according to equation of $\delta_{\text{exp}} = a + b \cdot \delta_{\text{calc}}$. The standard error values were found via SigmaPlot program with regression coefficient of a and b constants. Theoretically calculated IR data are multiplied with appropriate adjustment factors and the data obtained according to DFT method are formed using theoretical infrared spectrum. IR absorption frequencies of this compound were calculated by same method. The veda4f program was used in defining IR data which were calculated theoretically. The thermodynamic parameters, electronic properties (total energy, dipole moment), HOMO and LUMO energies, Mulliken atomic charges of titled compound has been investigated by using Gaussian 09W program. The spectroscopic and structural data of this compound has been calculated by using 6-311G(d) basis set with density functional method (DFT/B3LYP) and compared with experimental values.

Keywords: Schiff base, B3LYP, spectroscopic, electronic, thermodynamic.

1. Introduction

Heterocyclic bases are defined as cyclic compounds consisting of carbon and heteroatom(s) within a ring [1]. They exhibit a variety of chemical [2-4] and biological applications as a result of their structural diversity [2, 5-7]. In the present study, 3-methyl-4-(3-acetoxy-4-methoxy-benzylidenamino)-4,5-dihydro-1H-1,2,4-triazol-5-one was optimized by using 6-311G(d) basis set of the B3LYP method [8, 9]. ¹H-NMR and ¹³C-NMR isotropic shift values were calculated by the method of GIAO. Experimental and theoretical values were inserted into the graphic according to equation of $\delta_{\text{exp}} = a + b \cdot \delta_{\text{calc}}$. The standard error values were found via SigmaPlot program with regression coefficient of a and b constants. The vibrational frequencies, atomic charges and frontier molecule orbitals (HOMO and LUMO) of the titled compound have been calculated by using B3LYP method with 6-311G(d) basis set. All quantum chemical calculations were carried out by using Gaussian09W program package and the GaussView molecular visualization program [8,9]. The vibrational calculations of the molecule was computed by using B3LYP [10] density functional method with 6-311G(d) basis set in ground state. IR absorption frequencies of the titled compound were calculated by the same basis set. Then, they were compared with experimental data [11] which are shown to be accurate. Infrared spectrum was composed by using the data obtained from the method. The assignments of fundamental vibrational modes of the titled compound were performed on the basis of total energy distribution (TED) analysis by using veda4f program [12]. Also, the molecular structure, the highest occupied molecular orbital-lowest unoccupied molecular orbital (HOMO-LUMO), ionization potential, electron affinity, energy gap, electronegativity,

molecular hardness, molecular softness, chemical potential, electrophilic index and nucleophilic index and Mulliken atomic charges of the titled compound have been investigated by the same basis set. Thermodynamic properties of analyzed molecule were calculated by the same basis set.

2. Materials and Methods

Gaussian09W program package was used for the DFT calculations [8]. The visualization for the verification of the optimized molecular structure was performed using the Gaussview program [9]. The geometry optimization of the titled compound was performed by using B3LYP method with 6-311G(d) basis set. The GIAO (Gauge-Including Atomic Orbital) ^1H and ^{13}C NMR chemical shift values in DMSO were calculated by the same basis set. The standard error rate was calculated according to $\delta_{\text{calc}} = a \delta_{\text{exp}} + b$ formula. The spectral data of the titled compound were carried out with the same basis set. The veda4f program was used for identification of calculated IR data [12]. Then, theoretically, the electronic property (ionization potential, electron affinity, energy gap, electronegativity, molecular hardness, molecular softness, chemical potential, electrophilic index and nucleophilic index), Mulliken atomic charges, the atomic charges, dipole moments, energy and thermodynamical parameters were calculated.

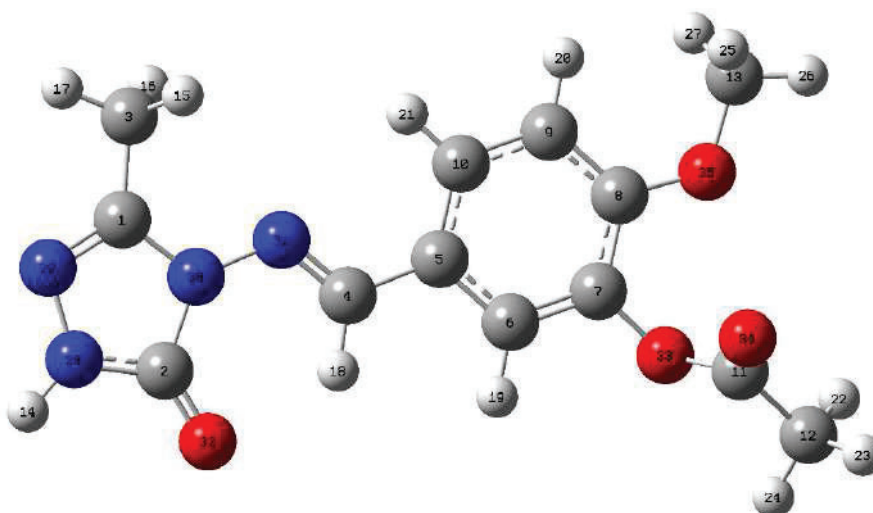


Figure 1. Optimized molecular structure of titled compound with B3LYP/ 6-311G(d) level.

3. Results and Discussion

3.1. NMR spectral analysis

In nuclear magnetic resonance (NMR) spectroscopy, the isotropic chemical shift analysis allows us to identify relative ionic species and to calculate reliable magnetic properties which provide the accurate predictions of molecular geometries [13-15]. In this framework, the optimized molecular geometry of the titled compound was obtained by using B3LYP method with 6-311G(d) basis level in DMSO solvent. By considering the optimized molecular geometry of the titled compound the ^1H and ^{13}C NMR chemical shift values were calculated at the same level by using Gauge-Independent Atomic Orbital (GIAO) method. Theoretically and experimentally values [11] were plotted according to $\delta_{\text{exp}} = a \delta_{\text{calc}} + b$, Eq. a and b constants regression coefficients with a standard error values were found using the SigmaPlot program.

Table 1. The calculated and experimental ^{13}C and ^1H NMR isotropic chemical shifts of the titled compound

No	Experim.	DFT/6311(d) DMSO	Diff./DMSO
1C	144.70	150.01	-5.31
2C	153.44	153.63	-0.19
3C	11.57	12.36	-0.79
4C	151.73	151.83	-0.10
5C	128.60	130.72	-2.12
6C	126.75	129.82	-3.07
7C	140.18	145.66	-5.48
8C	154.82	159.91	-5.09
9C	113.35	113.69	-0.34
10C	121.21	126.25	-5.04
11C	168.95	173.95	-5.00
12C	20.83	20.30	0.53
13C	56.57	54.30	2.27
14H	11.57	6.67	4.90
15H	2.26	2.05	0.21
16H	2.26	2.06	0.20
17H	2.26	1.70	0.56
18H	9.60	9.43	0.17
19H	7.61	6.75	0.86
20H	7.24	6.63	0.61
21H	7.67	7.82	-0.15
22H	2.28	2.10	0.18
23H	2.28	1.36	0.92
24H	2.28	2.01	0.27
25H	3.85	3.32	0.53
26H	3.85	3.76	0.09
27H	3.85	3.47	0.38

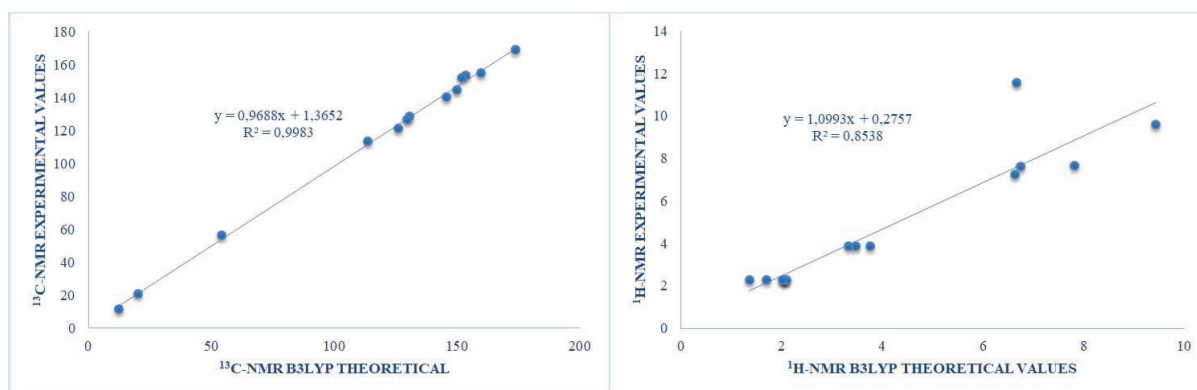


Figure 2. The correlation graphics for ^{13}C -NMR (DMSO), ^1H -NMR (DMSO), chemical shifts of the titled compound.

3.2. Vibrational frequencies

The titled compound has 35 atoms and the number of the normal vibrations are 99. The observed and calculated vibrational frequencies, the calculated IR intensities and assignments of vibrational frequencies for titled compound are summarized in Table 2.

Table 2. The calculated and experimental frequency values of the titled compound

Vibrational Frequencies	Experimental	B3LYP
ν CC (17), ν OC (51)	1273	1271
ν NC (57), ν CC (17)	1608	1591
ν NC (54), ν CC (22)	1608	1608
ν OC (77), ν NC (11)	1710	1736
ν OC (92)	1757	1778
ν NH (100)	3179	3520

ν , stretching; δ , bending; γ , out-of-plane bending; τ , torsion

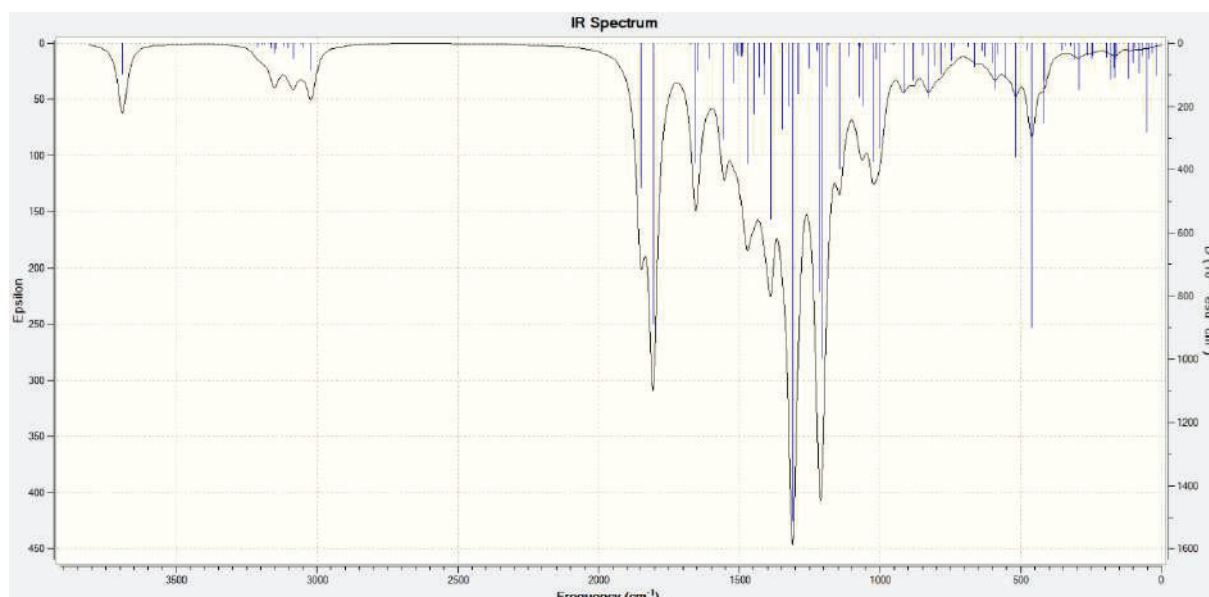


Figure 3. The IR spectrum of the titled compound

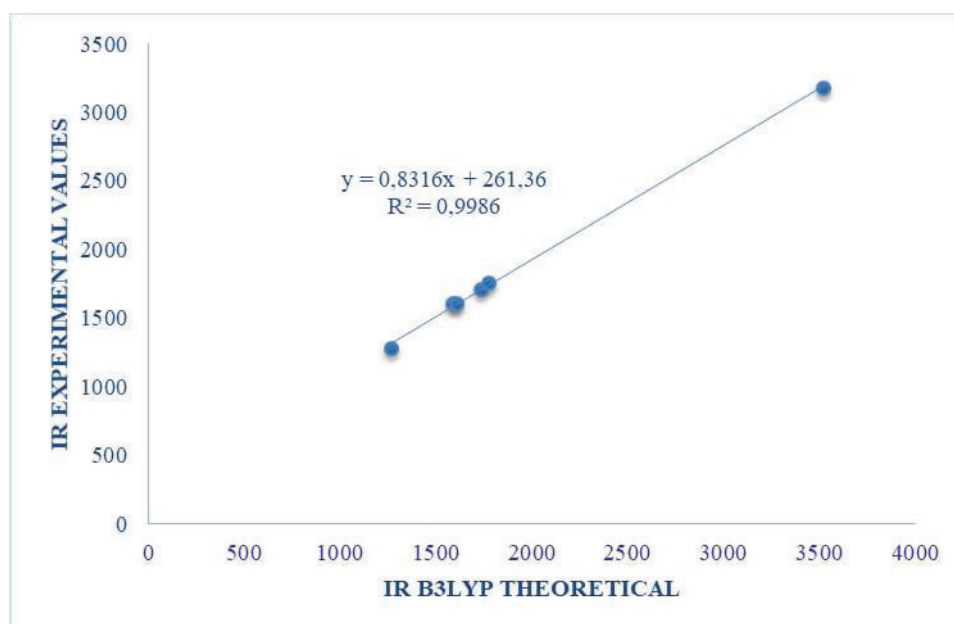
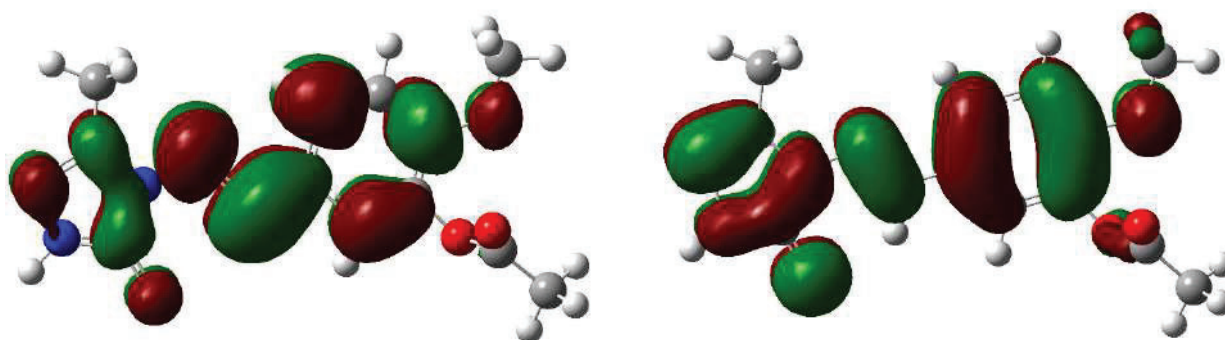


Figure 4. The correlation graphic for vibrational frequencies of the titled compound.

3.3. Electronic and Thermodynamic Properties

Theoretical, the molecular structure, the highest occupied molecular orbital-lowest unoccupied molecular orbital (HOMO-LUMO) (Figure 5), ionization potential, electron affinity, energy gap, electronegativity, molecular hardness, molecular softness, chemical potential, electrophilic index and nucleophilic index (Table 3), Mulliken atomic charges (Table 4) and thermodynamical parameters (Table 5) of the titled compound has been investigated Tables 3-5.



E_{LUMO} (B3LYP): -1.628 eV

E_{LUMO} (HF) : -5.943 eV

Figure 4. The calculated HOMO-LUMO energies of the titled compound according to DFT/B3LYP/6-311G(d) level

Table 7. The electronic properties of the titled compound

Electronic Properties	B3LYP (eV)
E _{LUMO}	-1.628
E _{HOMO}	-5.943
I; Ionization Potential	5.943
A; Electron Affinity	1.628

ΔE ; Energy Gap	4.315
χ ; Electronegativity	3.786
η ; Molecular Hardness	4.315
S ; Molecular Softness	2.158
μ ; Chemical Potential	-3.786
ω ; Electrophilic Index	0.0418
ε ; Nucleophilic Index	-0.600
μ_x (Debye)	1.9736
μ_y (Debye)	2.8921
μ_z (Debye)	-1.1064
μ_{Toplam} (Debye)	3.6720

Table 4. Mulliken atomic charges of the titled compound

Atoms	B3LYP	Atoms	B3LYP		B3LYP
1C	0.4045	13C	-0.4625	25H	0.2213
2C	0.5819	14H	0.3703	26H	0.2337
3C	-0.6698	15H	0.2352	27H	0.2126
4C	-0.6048	16H	0.2345	28N	-0.4962
5C	-0.0142	17H	0.2379	29N	-0.1996
6C	-0.2261	18H	0.2583	30N	-0.3621
7C	0.2080	19H	0.2099	31N	-0.2124
8C	0.2731	20H	0.2184	32O	-0.3939
9C	-0.2705	21H	0.2092	33O	-0.3551
10C	-0.1567	22H	0.2409	34O	-0.3158
11C	0.3913	23H	0.2387	35O	-0.3335
12C	-0.6885	24H	0.2376		

Table 6. The thermodynamic properties of the titled compound

Rotational temperatures (Kelvin)	B3LYP
A	0.0336
B	0.0059
C	0.0051
Rotational constants (GHZ)	
A	0.7003
B	0.1225
C	0.1070
Zero-point vibrational energy (Kcal/Mol)	168.2196
Thermal correction to Energy	0.2883
Thermal correction to Enthalpy	0.2892
Thermal correction to Gibbs Free Energy	0.2170
Sum of electronic and zero-point Energies	-1023.6634
Sum of electronic and thermal Energies	-1023.6432
Sum of electronic and thermal Enthalpies	-1023.6423
Sum of electronic and thermal Free Energies	-1023.7146
Thermal Energies E(Kcal/mol)	
Translational	0.889
Rotational	0.889
Vibrational	179.123
Total	180.900
Thermal Capacity CV(Cal/Mol-Kelvin)	
Translational	2.981

Rotational	2.981
Vibrational	67.641
Total	73.603
Entropy S (Cal/Mol-Kelvin)	
Translational	42.893
Rotational	34.814
Vibrational	74.408
Total	152.114

4. Conclusions

In the present study, the structure of the 3-methyl-4-(3-acetoxy-4-methoxy-benzylidenamino)-4,5-dihydro-1H-1,2,4-triazol-5-one is characterized by using ^1H , ^{13}C NMR and FT-IR, spectroscopic methods. The ^1H , ^{13}C NMR chemicals shifts, vibrational frequencies, HOMO and LUMO analyses and atomic charges of titled molecule synthesized have been calculated by using DFT/B3LYP method. By considering the results of experimental works it can be easily stated that the ^1H and ^{13}C NMR chemical shifts, vibrational frequencies spectroscopic parameters obtained theoretically are in a very good agreement with the experimental data. Also, the electronic structure of titled compound are determined electronic structure identifiers such as the Energy of the Highest Occupied Molecular Orbital, Energy of the Lowest Unoccupied Molecular Orbital, ionization potential, electron affinity, energy gap, electronegativity, molecular hardness, molecular softness, chemical potential, electrophilic index and nucleophilic index and dipole moment. Finally, thermodynamical parameters were calculated.

5. References

- [1] M. Beytur, Z. T. Irak, S. Manap, H. Yüksek, 'Synthesis, characterization and theoretical determination of corrosion inhibitor activities of some new 4, 5-dihydro-1H-1, 2, 4-Triazol-5-one derivatives', Heliyon 2019, 5, e01809.
- [2] M. Beytur, I. Avinca, 'Molecular, Electronic, Nonlinear Optical and Spectroscopic Analysis of Heterocyclic 3-Substituted-4-(3-methyl-2-thienylmethylenamino)-4, 5-dihydro-1H-1, 2, 4-triazol-5-ones: Experiment and DFT Calculations', Heterocycl Comm 2021, 27, 1-16.
- [3] M. Erdoğan, P. Taslimi, B. Tuzun, 'Synthesis and docking calculations of tetrafluoronaphthalene derivatives and their inhibition profiles against some metabolic enzymes', Arch Pharm 2021, 354, 2000409.
- [4] M. Beytur, 'Fabrication Of Platinum Nanoparticle/Boron Nitride Quantum Dots/6-Methyl-2-(3-Hydroxy-4-Methoxybenzylidenamino)-Benzothiazole (Ils) Nanocomposite For Electrocatalytic Oxidation Of Methanol', J. Chil. Chem. Soc. 2020, 65, 4929-4933.
- [5] Ş. Bahçeci, N. Yıldırım, Ö. Gürsoy-Kol, S. Manap, M. Beytur, H. Yüksek, 'Synthesis, characterization and antioxidant properties of new 3-alkyl (aryl)-4-(3-hydroxy-4-methoxybenzylidenamino)-4, 5-dihydro-1H-1, 2, 4-triazol-5-ones', Rasayan J Chem 2016, 9, 494-501.
- [6] Ö. Aktaş-Yokuş, H. Yüksek, S. Manap, F. Aytemiz, M. Alkan, M. Beytur, Ö. Gürsoy-Kol, 'In-vitro biological activity of some new 1, 2, 4-triazole derivatives with their potentiometric titrations', Bulg Chem Commun 2017, 49, 98-106.
- [7] K. Evren, H. Yüksek, M. Beytur, O. Akyildirim, M. Akçay, C. Beytur, 'Heterosiklik 4, 5-dihidro-1H-1, 2, 4-triazol-5-on Türevinin Antioksidan Özelliğinin Erkek Ratlarda (Wistar albino) İn vivo Olarak Belirlenmesi', Bitlis Eren Üniversitesi Fen Bilimleri Dergisi, 9, 542-548.
- [8] Frisch, M.J., Trucks, G.W., Schlegel, H.B., Scuseria, G.E., Robb, M.A., Cheeseman, J.R., Scalmani, G., Barone, V., Mennucci, B., Petersson, G.A., Nakatsuji, H., Caricato, M.; Li, X., Hratchian, H.P., Izmaylov, A.F., Bloino, J., Zheng, G., Sonnenberg, J.L., Hada, M., Ehara, M., Toyota, K., Fukuda, R., Hasegawa, J., Ishida, M., Nakajima, T., Honda, Y., Kitao, O., Nakai, H., Vreven, T.,

- Montgomery, J.A., Jr.Vreven, T., Peralta, J.E., Ogliaro, F., Bearpark, M., Heyd, J.J., Brothers, E., Kudin, N., Staroverov, V.N., Kobayashi, R., Normand, J., Raghavachari, K., Rendell, A., Burant, J.C., Iyengar, S.S., Tomasi J., Cossi, M., Rega, N., Millam, J.M., Klene, M., Knox, J.E., Cross J.B., Bakken, V., Adamo, C., Jaramillo, J., Gomperts, R., Stratmann, R.E., Yazyev, O., Austin, A.J., Cammi, R., Pomelli, C., Ochterski, J.W., Martin; L.R., Morokuma, K., Zakrzewski, V.G., Voth, G.A., Salvador, P., Dannenberg, J.J., Dapprich, S.; Daniels A.D., Farkas, O.; Foresman, J.B., Ortiz, J.V., Cioslowski, J., and Fox, D.J. (2009). Gaussian Inc., Wallingford, CT.
- [9] Frisch, A., Nielson, A.B., & Holder, A.J. (2003).Gaussview User Manual, Gaussian, Inc., Wallingford, CT, [3] Wolinski, K., Hilton, J.F., Pulay, P. (1990). *J. Am. Chem. Soc.*, 112, 512.
- [10] Becke A.D. (1993). Density functional thermochemistry. III. The role of exact exchange. *The Journal of Chemical Physics*. 98, 5648.
- [11] Ş. Bahçeci, N. Yıldırım, M. Alkan, H. Ö. Gürsoy-Kol, Manap, M. Beytur, Yüksek, S. Investigation of Antioxidant, Biological and Acidic Properties of New 3-Alkyl(Aryl)-4-(3-acetoxy-4-methoxybenzylidenamino)-4,5-dihydro-1H-1,2,4-triazol-5-ones, *The Pharmaceutical and Chemical Journal*. 2017, 4 (4), 91-101.
- [12] Jamróz, M.H. (2004). Vibrational Energy Distribution Analysis: VEDA 4 program, Warsaw.
- [13] Rani, A.U.; Sundaraganesan, N.; Kurt, M.; Çınar, M.; Karabacak, M., (2010), *Spectrochim. Acta Part A*, 75, 1523–1529.
- [14] Subramanian, N.; Sundaraganesan, N.; Jayabharathi, (2010), *J., Spectrochim Acta Part A*, 76, 259–269.
- [15] Wade, Jr. L.G. (2006).Organic Chemistry, 6nd ed.; Pearson Prentice Hall: New Jersey.

PARTICLE-LADEN FLOW in a POROUS CHANNEL: ENTRY and BOUNDARY CONDITIONS

M.H. Hamdan

Professor, Department of Mathematics and Statistics
University of New Brunswick
100 Tucker Park Road, Saint John, New Brunswick, E2L 4L5
Canada

ABSTRACT

In this work we provide analysis and sub-classification of a particle-laden fluid flow model through isotropic porous media. Boundary conditions associated with particle-laden flow models are analyzed when the medium porosity is constant, and compatible inlet conditions to a two-dimensional channel are derived.

Keywords: Porous media, dusty gases, channel boundary and inlet conditions

1. INTRODUCTION

Interest in the study of particle-laden flow through porous media stems from a number of practical applications that include the design of deep bed filtration systems, [1], [2], and liquid-dust separators, [3]; sub-surface transport of contaminants into repositories; movement of nutrients into plant roots; and the transport of slurries through porous structures (*cf.* Awartani and Hamdan [4] and the references therein).

A further important application is found in oil reservoir analysis wherein a porous layer is impaired by the settling of particles on the solid porous matrix constituents, thus constricting the pores and resulting in permeability reduction, with adverse effects on reservoir yield (*cf.* Wong and Mettananda [5], Civan and Rasmussen [6], and the references therein). Furthermore, in recent years there has been interest in dusty gas flow with pressure-dependent viscosity due to the importance of this type of flow in enhance oil recovery and carbon sequestration, [7].

The above applications have been dealt with extensively with emphasis on modeling (theoretically and experimentally) the flow phenomena and analyzing initial and boundary value problems associated with the flow, in addition to estimating the permeability reduction due to the clogging of the pore (*cf.* Sharma and Yortsos [2] and the references therein).

Of particular interest to the current work are mathematical models that describe the flow of a dusty gas through porous media, and based on the continuum approach and the averaging of Saffman's dusty gas flow equations, Saffman [8], over a representative elementary porous

volume. In free space, Saffman's model assumes the presence of a small concentration, by volume, of dust particles in the mixture, and the forces exerted by the phases on each other are proportional to their relative velocities. When a particle-laden flow is considered through a porous structure, a further interaction exists between the phases involved and the porous matrix, Siyyam and Hamdan [9]. The effects of the porous matrix on the flowing phases depend on the porous matrix microstructure, which can be modeled through idealized geometric descriptions, (such as the descriptions of isotropic granular and consolidated media that have been based on the concept of a representative unit cell, developed by Du Plessis and Masliyah [10].

A number of models have been reported in the work of Hamdan and co-workers (cf. [11-14] and the references therein). These models describe various flows in porous media. Governing equations are the continuity and momentum equations for each phase. These models may be of interest in the transport of particulates or dilute slurries in porous sediments or pipes. At the outset, in analyzing dusty gas flows in natural and industrial settings, proper boundary conditions need to be imposed. Three types of conditions are imperative in bounded domains:

- i) boundary conditions imposed on a macroscopic boundary;
- ii) entry or inlet conditions to a porous layer or channel; and
- iii) interface conditions in cases of fluid flow over a porous layer.

In case of single phase flow through porous structures, these conditions have been sufficiently analyzed and the concept of a macroscopic boundary has been properly defined (cf. Alazmi and Vafai [15], and Prat [16]. Conditions associated with the dusty gas flow through a porous structure, governed by the model equations (1)-(4), above, need some attention to facilitate a better understanding of the flow model and the behavior of the phases involved, and to shed light on validity and limitation of model parameters. The case of interfacial conditions between a dusty gas and a porous layer has been discussed by Roach et.al. [17].

In this work, therefore, we will consider a model of dusty gas flow in porous media and provide its classifications in a number of porous settings, then derive appropriate entry conditions to a porous channel in two space dimensions. Entry conditions to a channel must be compatible with the model itself. In addition, modified forms of Darcy's and Brinkman's equations are deduced from the model equations to account for the significant particle-phase inertial effects. As is well-known, Darcy's and Brinkman's equations ignore inertial effects in the case of a single fluid in the flow field. The modified forms of these equations, as developed in the current work, are expected to be valid when a particle phase is introduced in the flow field and the particle-phase inertial terms are significant.

2. MODEL EQUATIONS

Particle-laden flow through an isotropic porous structure of variable porosity is governed by the following coupled set of equations, written here for each phase in their steady-state forms, [11, 12]

Fluid-phase:

$$\nabla \cdot \phi \vec{u} = 0 \quad (1)$$

$$\rho \nabla \cdot \phi \vec{u} \vec{u} = -\phi \nabla P + \mu \nabla^2 \phi \vec{u} + K \phi N [\vec{v} - \vec{u}] - f \mu \vec{u} \quad (2)$$

Particle-phase:

$$\nabla \cdot \phi N \vec{v} = -\varepsilon S \quad (3)$$

$$\nabla \cdot \phi N \vec{v} \vec{v} = \frac{K}{m} \phi N [\vec{u} - \vec{v}] + \frac{K}{m} \phi \vec{\delta} [N - N_d] \quad (4)$$

wherein \vec{u} is the fluid-phase velocity field, \vec{v} is the particle-phase velocity field, P is the pressure, ρ is the density, μ is the viscosity, N is the particle number density (number of particles per unit volume), m is the mass of a dust particle, K is the Stokes' coefficient of resistance, ϕ is the medium porosity, ε is the particle settling rate (mass transfer coefficient), S is the surface area of the solid matrix in contact with the fluid in a control volume, N_d is a reference particle distribution, $\vec{\delta}$ is a diffusion coefficient vector, and f is a friction factor that depends on the porous microstructure. Different forms of f will be discussed in Section 4 of this work.

Model equations (1)-(4) may be of interest in the transport of particulates or dilute slurries in porous sediments or pipes. They represent a determinate system of eight scalar equations in the eight unknown functions of position, \vec{u} , \vec{v} , P and N . All other functions and constants in the above system are assumed to be known.

In what follows, we provide classification of the above model and obtain governing equations for different regiments.

2.1. Flow through a Porous Medium with Constant Porosity

If porosity, ϕ , is constant, equations (1)-(4) take the following forms, respectively, where $\mu^* = \mu/\phi$ is the effective viscosity (or viscosity of the fluid in the porous medium):

Fluid-phase:

$$\nabla \cdot \vec{u} = 0 \quad (5)$$

$$\rho \nabla \cdot \vec{u} \vec{u} = -\nabla P + \mu^* \nabla^2 \vec{u} + K N [\vec{v} - \vec{u}] - \frac{f}{\phi} \mu \vec{u} \quad (6)$$

Particle-phase:

$$\nabla \cdot N \vec{v} = -\varepsilon S \quad (7)$$

$$\nabla \cdot N \vec{v} \vec{v} = \frac{K}{m} N [\vec{u} - \vec{v}] + \frac{K}{m} \vec{\delta} [N - N_d] \quad (8)$$

Equations (5)-(8) are valid when ε is constant and when the porous matrix is rigid (does not sediment) and dust-particle settling does not alter contribute to changes in porosity.

2.2. Flow in the Absence of Particle Diffusion

If settling is insignificant then $\varepsilon = 0$ in (7). In addition, if particle diffusion is ignored, then $\vec{\delta} = \vec{0}$ in (8). Under these restrictions, equations (7) and (8) are replaced, respectively, by

$$\nabla \cdot N \vec{v} = 0 \quad (9)$$

$$\nabla \cdot N \vec{v} \vec{v} = \frac{K}{m} N [\vec{u} - \vec{v}] \quad (10)$$

If the particle number density, N , is constant or the particle distribution is uniform, equations (9) and (10) take the following forms, respectively

$$\nabla \cdot \vec{v} = 0 \quad (11)$$

$$\nabla \cdot \vec{v} \vec{v} = \frac{K}{m} [\vec{u} - \vec{v}] \quad (12)$$

The governing equations will then be (5), (6), (11) and (12). These represent an over-determined system of eight equations in the seven unknowns, \vec{u} , \vec{v} , and P .

In order to render the system of equations determinate, we introduce a dust-phase partial pressure, P_d , interpreted as the pressure necessary to maintain a uniform distribution of dust particles. We write (12) as:

$$\nabla \cdot \vec{v} \vec{v} = -\nabla P_d + \frac{K}{m} [\vec{u} - \vec{v}] \quad (13)$$

2.3. Single-phase Flow

In the absence of a particle phase, the dust-phase continuity and momentum equations vanish, and equations (5) and (6) reduce to the following equations, respectively, where we have taken $N = 0$:

$$\nabla \cdot \vec{u} = 0 \quad (14)$$

$$\rho \nabla \cdot \vec{u} \vec{u} = -\nabla P + \mu^* \nabla^2 \vec{u} - \frac{f}{\phi} \mu \vec{u} \quad (15)$$

Equation (15) governs the flow of a single-phase fluid through a constant porosity, isotropic porous medium. If f is identified with the ratio of porosity to permeability, η , equation (15) reduces to the well-known Darcy-Lapwood-Brinkman equation, [11], namely

$$\rho \nabla \cdot \vec{u} \vec{u} = -\nabla P + \mu^* \nabla^2 \vec{u} - \frac{\mu}{\eta} \vec{u} \quad (16)$$

The Left-Hand-Side of (16) represents the macroscopic convective acceleration of the fluid. When the flow is fully-developed, with no macroscopic stream-wise fluid velocity gradients, inertial effects may be ignored and equation (16) reduces to Brinkman's equation, namely

$$\mu^* \nabla^2 \vec{u} - \frac{\mu}{\eta} \vec{u} = \nabla P \quad (17)$$

Equations (16) and (17) are valid when macroscopic boundary effects are important and porosity is high; that is, when macroscopic cross-stream velocity gradients are present, and a no-slip condition is imposed on macroscopic, solid boundary.

In the absence of macroscopic cross-stream velocity gradients, and the presence of stream-wise velocity gradients, equation (16) reduces to the following equation, known as the Darcy-Lapwood equation:

$$\rho \nabla \cdot \vec{u} \vec{u} = -\nabla P - \frac{\mu}{\eta} \vec{u} \quad (18)$$

In the absence of stream-wise velocity gradients, the Left-Hand-Side of (18) vanishes, and the following Darcy's equation results:

$$\frac{\mu}{\eta} \vec{u} = -\nabla P \quad (19)$$

Equation (19) is not compatible with the presence of a macroscopic solid boundary where viscous shear effects are significant, and on which the no-slip velocity condition is imposed. Typically, this equation is valid in cases where the flow is over a quiescent layer of fluid and a slip velocity is encountered.

3. PARALLEL FLUID AND PARTICLE VELOCITIES

When a dusty fluid flows through a porous matrix, the fluid-phase enjoys a no-slip condition on fluid-phase velocity on macroscopic, solid walls. For the dust-phase, the macroscopic cross-

stream velocity gradients are absent (due to the absence of dust viscosity and hence the absence of dust viscous shear effects) while the stream-wise velocity gradients are always present. This is attributed to the fact that in the presence of an impermeable boundary, dust particles settle on the macroscopic boundary, set into motion particles already settled, or reflect back into the flow field and assume a stream-wise velocity gradient, [11]. In other words, the presence of a macroscopic boundary gives rise to an impenetrability condition on the dust particles whose macroscopic inertia is permanently present and hence the dust-phase convective term always survives.

In order to simplify analysis of boundary conditions, some authors assume that the dust-phase velocity is everywhere parallel to the fluid-phase velocity field, [14]. This assumption works well when dealing with inlet conditions to a channel. Allan and Hamdan [14] provided the following model for the case of parallel velocity fields,

Letting β be a function of position, and assuming that

$$\vec{v} = \beta \vec{u} \quad (20)$$

Then the flow is governed by

$$\nabla \cdot \beta \vec{u} = 0 \quad (21)$$

$$\rho(\vec{u} \cdot \nabla) \vec{u} + mN(\vec{u} \cdot \nabla) \beta^2 \vec{u} = -\nabla P + \mu^* \nabla^2 \vec{u} - \mu f \vec{u} \quad (22)$$

The Left-Hand-Sides of (22) involve the fluid-phase macroscopic convective inertial term in addition to a macroscopic inertial term that arises due to the presence of dust particles. They are valid when both macroscopic cross-stream and stream-wise fluid-phase velocity gradients are present. They emphasize the permanent presence of particle-phase stream-wise velocity gradients and the absence of particle-phase viscous shear.

Equation (22) gives rise to the following forms of Darcy's and Brinkman's equations in describing fluid motion in the presence of a dust phase. When the flow is fully-developed with no macroscopic stream-wise fluid velocity gradients, fluid inertial effects are insignificant while particle stream-wise velocity gradients are present, hence the dust-phase macroscopic convective term is present, and equation (22) reduces to

$$mN(\vec{u} \cdot \nabla) \beta^2 \vec{u} = -\nabla P + \mu^* \nabla^2 \vec{u} - \mu f \vec{u} \quad (23)$$

Equation (23) represents the Brinkman equation-equivalent for dusty gas flow through porous media, valid when macroscopic cross-stream fluid-phase velocity gradients are present, and a no-slip fluid velocity condition is imposed on the macroscopic boundary.

If the particle-phase is absent, $N = 0$, equation (23) reduces to Brinkman's equation (17) that governs single-phase flow through porous media.

When macroscopic boundary effects are not important, that is when the macroscopic cross-stream fluid-phase velocity gradients are absent, Equation (22) reduces to

$$\rho(\vec{u} \cdot \nabla)\vec{u} + mN(\vec{u} \cdot \nabla)\beta^2\vec{u} = -\nabla P - \mu f\vec{u} \quad (24)$$

Equation (24) is the Darcy-Lapwood equation-equivalent for dusty gas flow through a sparse distribution of particles fixed in space.

In the absence of both macroscopic cross-stream and stream-wise fluid-phase velocity gradients, equation (22) takes the following form

$$mN(\vec{u} \cdot \nabla)\beta^2\vec{u} = -\nabla P - \mu f\vec{u} \quad (25)$$

Equation (25) is the Darcy equation-equivalents for dusty gas flow through porous media. In the absence of a particle-phase, the Left-Hand-Side of (25) is identically zero, and Darcy's equation is recovered. It is evident from the above analysis that the model developed in Allan and Hamdan, [14], provides a partial answer to the question of how the fluid-phase velocity field is modified in the presence of a particle-phase, and explains the effect of the particle-phase on the fluid-phase through the introduction of a macroscopic inertial term that is expressed in terms of the fluid-phase velocity.

4. INLET CONDITIONS TO TWO-DIMENSIONAL CHANNELS

In the study of two-dimensional flow through a porous channel bounded by macroscopic, solid boundary on which a no-slip condition is imposed, entry velocity profile to the channel must be compatible with the equations governing the flow. This can be accomplished by considering a Poiseuille flow in the configuration shown in Fig. 1, where the fully-developed flow of a dusty gas is through a straight channel of depth D filled with porous material and bounded from above and below by solid, macroscopic walls.

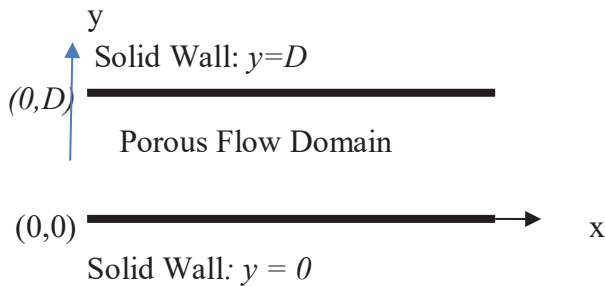


Fig. 1: Representative Sketch

Assuming that the porous matrix is of constant porosity, and the flow is driven by a constant pressure gradient, the flow is governed by equations (14) and (22). For flow in two dimensions, equation (14) takes the following components' form:

$$u_x + v_y = 0 \quad (26)$$

where u and v are the fluid-phase tangential and normal velocity components, respectively, and subscript notation denotes partial differentiation. Momentum equation (24) takes the following components' form:

$$\rho[uu_x + vv_y] + mN[u(\beta^2 u)_x + v(\beta^2 u)_y] = -P_x + \mu^*[u_{xx} + u_{yy}] - \mu f u \quad (27)$$

$$\rho[uv_x + vv_y] + mN[u(\beta^2 v)_x + v(\beta^2 v)_y] = -P_y + \mu^*[v_{xx} + v_{yy}] - \mu f v \quad (28)$$

Assuming parallel flow at entrance to the channel, then $v = v_x = v_y = u_x = 0$. Hence, $u = u(y)$. Equation (28) is automatically satisfied and (27) reduces to:

$$mN[u(\beta^2 u)_x] = -P_x + \mu^* u_{yy} - \mu f u \quad (29)$$

Now, since the dust-phase velocity is proportional to the fluid-phase velocity, equation (20) can be written in the following components' form

$$(u_d, v_d) = (\beta u, \beta v) \quad (30)$$

where u_d and v_d are the dust-phase tangential and normal velocity components, respectively.

At channel entrance, $v = 0$ and $u = u(y)$. Equation (30) thus yields $v_d = 0$ and

$$u_d = \beta u(y) \quad (31)$$

Differentiating (31) with respect to x , and using the fact that $u = u(y)$, we obtain

$$(u_d)_x = u\beta_x \quad (32)$$

Using (11), (20) and (26), we obtain

$$u\beta_x + v\beta_y = 0 \quad (33)$$

Equation (33) implies that β is constant on the fluid-phase streamlines.

Since $v = 0$ at channel entrance, equation (33) yields

$$u\beta_x = 0 \quad (34)$$

Since $u = u(y)$ is not identically zero, it follows from (34) that $\beta_x = 0$, or $\beta = \beta(y)$. Equation (31) then yields

$$u_d = u_d(y) = \beta(y)u(y) \quad (35)$$

With $\beta = \beta(y)$ and $u = u(y)$, equation (29) takes the form

$$u_{yy} - \frac{\mu}{\mu^*} f u = \frac{P_x}{\mu^*} \quad (36)$$

Assuming a constant pressure gradient and constant viscosity coefficients, we solve equation (36) satisfying

$u(0) = u(D) = 0$ admits the following solution:

$$u(y) = c_1 \text{Exp}(-Ay) + c_2 \text{Exp}(Ay) - \frac{P_x}{\mu f} \quad (37)$$

where

$$A = \sqrt{\mu f / \mu^*} \quad (38)$$

$$c_1 = \left\{ 1 - \frac{\text{Exp}(DA) - 1}{\text{Exp}(2DA) - 1} \right\} \frac{P_x}{\mu f} \quad (39)$$

$$c_2 = \left\{ \frac{\text{Exp}(DA) - 1}{\text{Exp}(2DA) - 1} \right\} \frac{P_x}{\mu f} \quad (40)$$

Equation (37) represents the fluid-phase inlet velocity profile to the channel. This profile is compatible with the flow governing equations and can be used as a condition in boundary value problems involving flow through two-dimensional porous channels.

Once the fluid-phase inlet velocity is determined, the dust-phase inlet velocity can be determined from (35). The choice of $\beta(y)$ that renders (11) satisfied influences the form of particle inlet velocity condition. However, regardless of the choice of $\beta(y)$, the dust-phase inlet velocity, u_d will be zero at the solid boundary points at channel entrance (points $(x, y) = (0, 0)$ and $(x, y) = (0, D)$ in Fig. 1) in light of condition (35) for the model at hand, and the no-slip assumption on the fluid-phase velocity.

Friction factor, f , appearing in (36) is microstructure and material-dependent. For different materials, f depends on porosity and tortuosity of the medium, and on the microscopic characteristics length (such as the average pore diameter or the average diameter of a particle). **Table 1**, below, shows the expressions of f for granular and consolidated matter. It also shows expressions of permeability, $\eta = \varphi / f$ for the two types of materials listed. With the knowledge of porosity, tortuosity and microscopic length, d , values of f can be calculated and used in the solution, above.

5. CONCLUSION

In this work we have provided analysis of a dusty gas model of flow through isotropic porous media. We relied on the model with a uniform distribution of dust in the flow field, with the dust-phase and fluid-phase velocity fields being everywhere parallel, to provide classification of porous media models.

A sub-classification of the model has been provided for both variable porosity and constant porosity media. For

Granular Media	Consolidated Media (Sponges and Metallic Foams)
$f = \frac{36(1 - \varphi)^{\frac{2}{3}}}{d^2[1 - (1 - \varphi)^{\frac{1}{3}}][1 - (1 - \varphi)^{\frac{2}{3}}]}$	$f = \frac{36\tau(\tau - 1)}{d^2\varphi}$ $\tau \approx \frac{1 + 2\varphi}{3}$
	$\eta = \frac{\varphi}{f} = \frac{d^2\varphi^2}{36\tau(\tau - 1)}$

$\eta = \frac{\varphi}{f}$ $= \frac{d^2 \varphi [1 - (1 - \varphi)^{\frac{1}{3}}] [1 - (1 - \varphi)^{\frac{2}{3}}]}{36(1 - \varphi)^{\frac{2}{3}}}$	
--	--

Table 1. Friction Factor for Granular and Consolidated Media

constant porosity media, we used the model to deduce modified forms of Darcy's law, Brinkman's equation, the Darcy-Lapwood equation, and the Darcy-Lapwood-Brinkman model, which govern the flow of a single phase fluid flow. The modified forms take into account particle inertia that is always significant, and may be of utility when analyzing the flow of a dusty fluid with constant number density and parallel fluid and particle velocity fields, through similar configurations where the above single phase flow equations are valid. In addition, we have also derived an inlet condition to a two-dimensional channel that is compatible with the governing equations. This inlet condition can be used in realistic computations involving the models at hand.

ACKNOWLEDGMENT

The author wishes to express sincere gratitude to Prof. Dr. M.T. Kamel (retired) for his assistance in this work.

REFERENCES

- [1]. C. Choo and C. Tien, "Analysis of transient behavior of deep-bed filtration," *J. Colloid Interface Science*, vol. 169, pp. 13–33, 1995.
- [2]. M.M. Sharma and Y.C. Yortsos, "A network model for deep bed filtration processes," *AIChE J.*, vol. 33(10), pp. 1644–1652, 1987.
- [3]. D.C. Mays and J.R. Hunt, "Hydrodynamic aspects of particle clogging in porous media," *J. Environmental Science and Technology*, vol. 39, pp. 577–584, 2005.
- [4]. M.M. Awartani and M.H. Hamdan, "Some admissible geometries in the study of steady plane flow of a dusty fluid through porous media," *J. Applied Mathematics and Computation*, vol. 100(1), pp. 85–92, 1999.
- [5]. R.C. K. Wong and D.C.A. Mettananda, "Permeability reduction in Qishn sandstone specimens due to particle suspension injection," *J. Transport in Porous Media*, vol. 81, pp. 105–122, 2010.
- [6]. F. Civan and M.L. Rasmussen, "Analytical models for porous media impairment by particles in rectilinear and radial flows," In *Handbook of Porous Media, second edition*, K. Vafai Ed., Taylor and Francis, New York, pp. 485–542, 2005.
- [7]. M.S. Abu Zaytoon and M.H. Hamdan, "Effects of the porous microstructure on drag coefficient in flow of a fluid with pressure-dependent viscosity," *International Journal of Mechanics*, vol 15, pp. 136–144, 2021.

- [8]. P.G. Saffman, "On the stability of laminar flow of a dusty gas," *J. Fluid Mechanics*, vol. 13(1), pp. 120-129, 1962.
- [9]. H.I. Siyyam and M.H. Hamdan, "Analysis of particulate behaviour in porous media," *J. Applied Mathematics and Mechanics*, vol. 29(4), pp. 511-516, 2008.
- [10]. J.P. Du Plessis and J.H. Masliyah, "Flow through isotropic granular porous media," *J. Transport in Porous Media*, vol. 6, pp. 207-221, 1991.
- [11]. M.H. Hamdan and R.M. Barron, "On the Darcy-Lapwood-Brinkman-Saffman dusty fluid flow models in porous media. Part I: models development," *Applied Mathematics and Computation*, vol. 54(1), pp. 65-79, 1993.
- [12]. S.M. Alzahrani and M.H. Hamdan, "Mathematical modelling of dusty gas flow through isotropic porous media with Forchheimer effects," *Int. J. of Enhanced Research in Science, Technology & Engineering*, vol. 5(5), pp. 116-124, 2016.
- [13]. D.C. Roach, M.S. Abu Zaytoon and M.H. Hamdan, "On the flow of dusty gases with pressure -dependent viscosities through porous structures," *Int. J. Enhanced Research in Science, Technology & Engineering*, vol. 5(9), pp. 46-54, 2016.
- [14]. F.M. Allan and M.H. Hamdan, "Fluid-particle model of flow through porous media: The case of uniform particle distribution and parallel velocity fields", *J. Applied Mathematics and Computation*, 183(2), pp. 1208-1213, 2006.
- [15]. B. Alazmi and K. Vafai, "Analysis of fluid flow and heat transfer interfacial conditions between a porous medium and a fluid layer", *Int. J. Heat and Mass Transfer*, 44, pp. 1735-1749, 2001.
- [16]. M. Prat, "On the boundary conditions at the macroscopic level", *J. Transport in Porous Media*, 54, pp. 259-280, 1989.
- [17]. M.H. Hamdan, D.C. Roach, Roberto Silva-Zea, Romel Erazo-Bone, Fidel Chuchuca-Aguilar, and Kenny Escobar-Segovia, "On the flow of a dusty gas through a channel over a porous layer saturated with a dusty gas", *IOSR Journal of Engineering*, Vol. 10(9), pp. 35-44, 2020.

THE HONEY OF RHODENDRON**ORMAN GÜLÜ BALI**

Dr. Öğretim Üyesi Münire TURHAN

Orcid: 0000-0003-3373-1400

Bingöl Üniversitesi Gıda Tarım ve Hayvancılık Meslek Yüksek Okulu Bitkisel ve Hayvansal Üretim Bölümü Arıcılık Programı

ÖZET

Bal, yüzyıllar boyu, insanoğlu için en önemli besin kaynaklarından biri olmuştur. Türkiye, uygun ekolojik yapısı, zengin bitki florası, arı materyalindeki genetik varyasyonu ile arıcılıkta günümüzde söz sahibi olması muhtemel bir ülke konumundadır Arıların farklı kaynaklardan ürettikleri bal, insanoğlunun en eski ve ortak besin maddesinden biridir. Tamamen doğada üretildiği gibi kullanılabilen balın oluşumu ve bileşimi bölgelere göre önemli farklılıklar göstermektedir. Oldukça farklı ekolojik yapısı nedeniyle ülkemizde çok çeşitli ballar üretilmektedir. Balın kalitesini ve biyokimyasal özelliklerini nektar kaynağı başta olmak üzere, olgunlaşması, üretim şekli, iklim koşulları, işleme ve depolama şartları belirler. Türkiye’de ballar kaynağına, üretim ve pazarlama şekline, rengine ve nem içeriğine göre değerlendirilmektedir. Tamamen doğaya bağımlı halde elde edilen balın kimyasal bileşimi yörelere ve balın çeşidine göre incelendiğinde farklılıklar göstermektedirler. Genel olarak bal yaklaşık %80 oranında farklı şekerler, %17 oranında sudan oluşmaktadır. Geriye kalan %3'lük kısım enzimler başta olmak üzere değerli bileşenlerden oluşmaktadır Orijinine göre; arıların bitki çiçeklerindeki nektarlardan ürettikleri bal çiçek balı (ıhlamur balı, yonca balı, turuncgil balı, pamuk balı, üçgül balı, kekik balı, püren balı, akasya balı, funda balı gibi); bitkilerin canlı kısımlarından veya bitki üzerinde yaşayan canlıların salgılarından ürettikleri bal ise salgı balı (çam balı, meşe balı, köknar balı, yaprak balı gibi) olarak adlandırılır.

Fundagiller ailesi (Ericaceae) kuzey ve güney yarımkürenin ılıman bölgelerinde yayılmış yaklaşık 128

cins ile temsil edilir. Çalı veya ağaç şeklinde, nadir olarak otsu bitkilerden oluşur. Ormangülleri Çin,Tibet, Burma, Nepal, Yeni Gine, Tropik Asya, Avrupa ve Kuzey Amerika’da yayılış gösteren 700 türesahiptir. Yaşam alanları deniz seviyesinden başlayarak 4000 m yüksekliğe kadar çıkmaktadır. Türleri20 cm ile 30 metre arasında değişen çalı ve ağaç formlardan oluşmaktadır. Ormangülleri nem oranı yüksek, organik madde bakımından zengin, derin ve iyi drenaja sahip asidik topraklarda iyi gelişim göstermektedir.

Ülkemizde ise deniz seviyesinde 3200 m yüksekliğe kadar yayılış gösteren *R. ponticum*, *R. luteum*, *R.*

ungernii, *R. smirnovii* ve *R. caucasicum* olmak üzere 5 türü ve bunlara bağlı 12 taksonu bulunmaktadır.

Halk arasında Ağu yada komar olarak da adlandırılan orman gülleri Batı Karadeniz’den Doğu Karadeniz’e kadar sahil ormanları veya orman arasındaki açıklıklarda geniş bir yayılışa sahiptir.Deli bal, yüksek oranda grayanotoksin içeren Sapindaceae familyası ve Ericaceae familyasının *Rhododendron ponticum* ve *Rhododendron luteum* türlerinin nektarının bal arıları tarafından toplanması,

dehidre edilip, olgunlaşması sonucu oluşturulan doğal bir üründür.

Anahtar kelimeler: *Bal, Deli Bal, Fundagiller*

ABSTRACT

For centuries, honey has been one of the most important food sources for human beings. Turkey is a country that is likely to have a say in beekeeping with its suitable ecological structure, rich plant flora, genetic variation in bee material. The formation and composition of honey, which can be used as it is produced in nature, shows significant differences according to the regions. Due to its quite different ecological structure, a wide variety of honey is produced in our country. The quality and biochemical properties of honey, especially the nectar source, its maturation, production method, climatic conditions, processing and storage conditions determine. In Turkey, honey is evaluated according to its source, production and marketing method, color and moisture content. In Turkey, honey is evaluated according to its source, production and marketing method, color and moisture content. When the chemical composition of honey, which is obtained completely dependent on nature, is examined according to the regions and the type of honey, they show differences. In general, honey consists of about 80% different sugars and 17% water. The remaining 3% consists of valuable components, especially enzymes.

According to its origin; honey produced by bees from nectar in plant flowers, flower honey (such as linden honey, clover honey, citrus honey, cotton honey, clover honey, thyme honey, puree honey, acacia honey, heather honey); The honey produced from the living parts of plants or from the secretions of the living things living on the plant is called secretory honey (such as pine honey, oak honey, fir honey, leaf honey).

The heathaceae family (Ericaceae) is distributed in temperate regions of the northern and southern hemispheres. represented by gender. It consists of shrubs or trees, rarely herbaceous plants. Rhododendrons have 700 species distributed in China, Tibet, Burma, Nepal, New Guinea, Tropical Asia, Europe and North America. Their habitats start from sea level and go up to 4000 m altitude. The species consists of shrub and tree forms ranging from 20 cm to 30 meters. Rhododendrons grow well in acidic soils with high moisture content, rich in organic matter, deep and well drained shows.

In our country, *R. ponticum*, *R. luteum*, *R. unguernii*, *R. smirnovii* and *R. caucasicum*, and 12 taxa related to them.

Rhododendrons, also called agu or komar among the people, have a wide distribution in the clearings between the coastal forests or forests from the Western Black Sea to the Eastern Black Sea. Crazy honey is the honey of the nectar of the Sapindaceae family and Ericaceae family *Rhododendron ponticum* and *Rhododendron luteum* species that contain high levels of grayanotoxin. collected by bees, It is a natural product created as a result of dehydrated and ripening.

Keywords: *Honey, Mad Honey, Rhododendrons*

GİRİŞ

Arı ürünlerinin tedavi amaçlı kullanılmasıyla ilgili ilk kalıntılar antik Mısır dönemine 6000 yıl öncesine dayanmaktadır. Ayrıca, Romalılar ve Yunanlılarda arı ürünlerini tıbbi amaçlar için kullanmışlardır (Molan, 2006). Geleneksel bir tedavi yöntemi olarak kullanılan arı ürünleri başta yara ve yanıklar olmak üzere çeşitli enfeksiyon hastalıkları, soğuk algınlıkları, kalp ve damar rahatsızlıkları gibi birçok hastalığın tedavisinde kullanılmaktadır. Ayrıca, son yıllarda yapılan araştırmalarda bazı kanser hastalıklarında da arı ürünlerinin etkili sonuç verdiği belirtilmiştir (Dustmann 1993; FAO 1996; Mundo ve ark., 2004). Apiterapi, bu arı ürünlerinin bilinçsiz bir şekilde kullanılmasından ziyade hem sağlığın korunması hem de tedavi amaçlı olarak bilinçli ve sistemli bir şekilde uygulanan alternatif tıp tekniği olarak uygulanması esasına dayanır. Arı ürünlerinin bir besin kaynağı olarak kullanılmasının yanında biyoaktif özelliğe de sahiptirler. Bu biyoaktif karakterleri yapılarında yer alan fenolik bileşenlerden ileri gelmektedir. Bu bileşenler bitkiler tarafından üretilen birer sekonder metabolit olup, miktarları ve türleri toplandıkları bitki florasına, coğrafi özelliklere, arı ürünlerinin üretim şekline ve hasat zamanına bağlı farklılıklar göstermektedir (Tezcan ve ark., 2011).

Bal protein kaynağı bir besin maddesi olarak tanımlanmasa da baldaki aminoasitler balın orijini açısından önemlidir. Balda miktarı en fazla olan aminoasit prolin aminoasitidir. Prolin, bitkilerde çeşitli miktarlarda (Akasyada 222 mg/kg, kekikte 956 mg/kg) bulunan bir aminoasit olmasından dolayı prolin miktarı, şeker grubu ile beslenen arılardan elde edilen bal ile nektardan elde edilen balın ayrılmasında bir kriter olarak kullanılmaktadır (Bogdanov ve ark., 2000; Güler ve ark., 2007).

Bileşikler birçok gıdanın antioksidan, antiinflamatuvar ve antibakteriyel özellikleri gibi çeşitli özellikleriyle ilişkilidir. Bu gıdalara örnek olarak bal, polen, propolis ve arı sütünü verebiliriz. Çünkü bu arı ürünleri, arıların çiçeklerden topladıkları nektarlarda bulunan fenolik ve flavonoid bileşikler içerirler (Marcucci ve ark.; Fiorani ve ark., 2006). Hastalıkların bazıları hücrelerde oksidatif hasar sonucu oluştuğundan arı ürünlerinin iyileştirici özelliğinin içerdiği antioksidan kapasitesinden geldiği belirtilmektedir (Buratti ve ark., 2007). Apiterapi özellikler, Çin, Kore, Rusya, Doğu Avrupa ve Güney Amerika'da hala yaygın olarak uygulanmaktadır (Christopher ve Kim, 1997).

Bal, flavonoidler (luteolin, kuersetin, apigenin, galangin vd.), fenolik asitler (kafeik asit, ferulik asit vd.) ve bu maddelerin türevlerini içermekte olup antioksidan aktiviteye sahiptir. Yapısında bulunan bu tür polifenoller balın görünüşü ve fonksiyonel özellikleri üzerine de etkili olmaktadır. Balın fenolik bileşen miktarı nektar kaynağına coğrafi ve ekolojik şartlara göre değişiklik göstermekle birlikte koyu renkli balların açık renkli ballara göre daha fazla fenolik içeriğe ve antioksidan aktiviteye sahip olduğu belirtilmektedir (Karadal ve Yıldırım, 2012; Escuredo ve ark., 2012). Balın antioksidan aktivitesi ve toplam fenolik içeriği arasında pozitif bir ilişki bulunmakta ve antioksidan aktivite esas olarak fenolik bileşiklerden kaynaklanmaktadır. Koyu renkli ballarda bol miktarda bulunan fenolik bileşiklerin, askorbik asit ve E vitamini göre daha güçlü antioksidan aktivite gösterdiği bilinmektedir (Sarıkaya, 2009). Balların sınıflandırılması, üretim ve pazarlama şekline göre, rengine göre yapılabildiği gibi elde edilen kaynağına göre de yapılmaktadır. Balın rengine göre sınıflandırılmasında 6 standart bulunmakta olup ballar açık su beyazından siyah ambere kadar sınıflandırma yapılmaktadır. Yararlanılan kaynağına göre ballar, çiçek ve salgı balları olarak sınıflandırılır.

Çiçek ballarına örnek arıların yararlandıkları çiçek kaynağına göre ıhlamur, yonca, pamuk balı vs. şeklinde isimlendirilir. Salgı balları ise arıların bitkilerin salgılarından veya bazı

böceklerin salgılarından elde ettikleri ballar olup, alındıkları kaynağa göre çam balı veya yaprak balı olarak isimlendirilir (Doğaroğlu, 2004).

Balın antioksidan özelliği nektarların toplandığı bitkisel kaynağa, mevsimsel ve çevresel faktörlere bağlıdır (Bertocelj ve ark., 2007). Bala antioksidan özelliğini veren maddeler: flavanoidler, fenolik asitler, tiamin, riboflavin, α -tokoferol, askorbik asit gibi vitaminler, glukoz oksidaz, katalaz, peroksidaz gibi enzimler olduğu belirtilmektedir (Aljadi ve ark., 2004; Alvarez-Suarez ve ark., 2010; Bertocelj ve ark., 2007). Yapay balın antioksidan aktivitesi doğal ballara göre daha düşüktür (Alvarez-Suarez ve ark., 2010).

Balın vitamin ve enzim içeriğine bağlı antioksidan aktivitesi taze ballarda daha yüksek olacağı belirtilmektedir. Bu maddeler ısıtma işlemi, ışık ve uygunsuz saklama koşullarına göre oldukça duyarlı olmaktadır (Alvarez-Suarez ve ark., 2010; Nagai ve ark., 2001). Koyu renkli balların mineral madde içeriği açık renkli ballara göre daha fazladır (Nombre ve ark., 2010). Buna ilave olarak, Antioksidan ve antibakteriyel özellikleri de daha fazladır (Alvarez-Suarez ve ark., 2010; Bertocelj ve ark., 2007; Brundzynski ve ark., 2011). Ancak bu ballarda HMF miktarı da doğal olarak yüksek olması beklenmektedir. HMF miktarı belirlenen limitlerin üzerinde olabilir (Fallico ve ark., 2004; Turhan ve ark., 2008).

Silici ve ark., (2010), Karadeniz bölgesinde farklı illerden toplanan 50 adet orman gülü balının antioksidan özelliklerini farklı metotlar uygulayarak analiz etmişler ve orman gülü balının geniş çaplı bir araştırmasını yaparak antioksidan ve antimikrobiyal özelliklerini açıklamaya çalışmışlardır. Polat (2007), farklı orijinlere sahip 26 adet bal örneklerinin fizikokimyasal ve mineral madde içeriklerini incelemiş ve bal örneklerinde serbest asitlik, pH, HMF, iletkenlik ve mineral madde içeriklerini tespit ederek birbirleriyle karşılaştırmıştır.

1. Balın İnsan Sağlığı Üzerine Etkileri

1.1. Antimikrobiyal Etki

Bal yapısında bulunan hidrojen peroksit, flavonoid ve fenolik asit bileşiklerinin varlığıyla antibakteriyel etkiye sahiptir. Bu özelliğinden dolayı bal, insanlarda hastalık oluşumuna neden olan patojen bakterilerin gelişmesine ve çoğalmasına engelleyici bir ortam oluşturmaktadır. Yapılan son araştırmalarda balın sadece bakteriler üzerine değil aynı zamanda virüsler, mantarlar ve parazitlere karşı da inhibe edici özelliklerinin olduğu belirtilmiştir. Bu amaçla yapılan bir araştırmada hidatik kiste (ekinokokkoz) sebep olan *Echinococcus granulosus* paraziti üzerine uygulanan %10'luk bal konsantrasyonunun üçüncü dakikadan itibaren parazitler üzerine inhibe edici etki gösterdiği tespit edilmiştir (Karadal ve ark., 2012). Bir başka çalışmada ise Bingöl yöresinden toplanan bal örneklerinin *Candida albicans* ve *Rhodotorula rubra* gibi mantar türlerinin gelişmesini durdurduğu belirtilmiştir (Aksoy ve ark., 2006).

1.2. Antioksidan Etki

Bal, doğal bir antioksidan etkiye sahip besin maddesidir. Balın antioksidan madde içeriği; nektarın bitkisel kaynağına, mevsimsel ve çevresel faktörlere bağlı olarak değişiklikler göstermektedir (Spilioti ve ark., 2014). Balın antioksidan karakteri yapısında bulunan glukoz oksidaz, katalaz, peroksidaz gibi enzimlerin yanında flavonoidler, fenolik asitler (benzoik asit, ferulik asit, kumarik asit ve kafeik asit) gibi bileşenlerden kaynaklandığı belirtilmiştir (İsidorov ve ark., 2015). Başka bir çalışmada ise balın antioksidan özellik göstermesinde

karotenoidler, tokoferoller ve tiamin, riboflavin ve askorbik asit gibi vitaminlerinde etkili olduğu belirtilmiştir (Khalil ve ark., 2012). Balın antioksidan özelliği ile toplam fenolik madde içeriğinin birbiriyle ilişkili olduğu ve toplam fenolik madde artışının balın antioksidan özelliğini de artırdığı belirtilmiştir (Alzahrani ve ark., 2012). Başka bir araştırmada ise koyu renkli balların toplam fenolik madde içeriklerinin açık renkli ballara göre daha fazla olduğu, buna bağlı olarak da daha yüksek antioksidan aktivite gösterdikleri belirtilmiştir (Ajibola ve ark., 2012). Bunların ilave olarak, bal serbest radikal oluşumunu hızlandıran metal iyonlarını da tutma özelliğine sahiptir (Manyi-Loh ve ark., 2011).

1.3. Sindirim Sistemine Etki

Balın sindirim sistemi üzerine etkisi çeşitli araştırmalarda açıklanmaya çalışılmıştır. Balın, mide ülserine sebep olan *Helicobacter pylori* bakterisi üzerine etkili olduğu ve bu bakterinin gelişmesini inhibe ettiği belirtilmiştir (Ajibola ve ark., 2012).

1.4. Kansere Hücreleri Üzerine Etki

Balın içerisinde bulunan fenolik asit ve flavonoid gibi biyoaktif bileşenler, kansere neden olan serbest radikal oluşumunu ve oksidatif stresi engelleyerek kanser hücrelerini inhibe edici özellikleri olduğu belirtilmiştir (Othman, 2012). Balın bu özelliklerine bağlı olarak yapılan birçok çalışmada da mide, kolon, karaciğer kanserlerinin tedavisinde de etkili olduğu tüketiminin faydalı olduğu belirtilmiştir (Abdel-Latif, 2015).

2.ORMAN GÜLÜ BALI (RHODODENDRON)

2.1 Fitokimyasal özellikleri

Quiang vd. (2011) Rhododendron türlerinde çoğunluğu flavonoid ve diterpenlerden oluşan 208 bileşik tanımlamıştır. Cinsin değişik türlerinde kaempferol, quercitrin, hyperoside, farrerol ve polystachoside gibi 65 ten fazla flavonoid tanımlanmıştır. Çiçeklerin cyanidin, peonidin, azaleatin gibi ntocyanidinleri ve fenollerini içerdiği belirlenmiştir. Bu cinsten bulunan ikinci önemli kimyasal sınıfı diterpenoidlerdir ve 30 dan fazla diterpenoid tespit edilmiştir. Bunların çoğunluğu grayane-type diterpenoidler olup bitkinin toksitesinden sorumludurlar. Bu bitkilerin yaprak, çiçek ve meyvesinden elde edilen esansiyel yağlar alfa-pinene, beta-pinene, limonene, borneol, myrcene ve p-cymene'dir. Bu cinsten izole edilen diğer bileşikler phenol türevleri, bir alkaloid ve lignin, hirsutine, pinoselin, 4-O-beta-glucopyranoside ve bir beta carotene'dir. Çiçek ve yapraklarda çeşitli karbonhidratlarda tespit edilmiştir. Tasdemir vd. (2003), toksik olan iki rhododendron türünün 11 farklı organında HS-SPME bağlı GC-MS kullanarak uçucu bileşikler tespit etmiştir (Tasdemir ve ark., 2005). *R. Ponticum* yapraklarının n-hexane ekstraktı 14 uçucu bileşik içermiştir; bu bileşikler içinde temel bileşimler, tricyclic diterpene 5,15-rosadiene (% 42.8), 2-ethyl hexanol (% 13.3) ve styrene (% 10.0) dir. Yaprakların CH₂Cl₂ ekstraktından ise 8 bileşik izole edilmiştir ve bu bileşikler arasında majör bileşik 1-butanol dır. İlginç bir şekilde, mor pembe renkli çekici çiçekleri de hoş olmayan bir kokuya sahip olan 1-methyl-2-pyrrolidone en fazla bulunan uçucu iken (% 79.7), bu bileşik yapraklarda tespit edilmemiştir. *R. Luteum* türünün n hexane ekstraktının uçucu profili *R. ponticum* 'a benzer bulunmuştur. Ethyl acetate (% 13.3), 6-methyl-5-hepten-2-one (% 11.1), 2-ethyl hexanol ve alpha terpineol major bileşikler olarak tespit edilmiştir. Bitkinin CH₂Cl₂ekstratının analiziyle belirlenen 1-butanol, benzyl alcohol ve phenylethyl alcohol bitkide bulunan toplam uçucuların %82.5'ni oluşturan bileşiklerdir. Çiçeklerde benzyl alcohol,limonene ve p-cymene tespit edilen major bileşiklerdir. Bu araştırmada

hidrokarbonlar, alkoller, ester ve ketonlar da belirlenmiştir, ancak grayanotoksin belirlenmemiştir. Çünkü bu diterpenler ısıtma konusunda stabil değildir, düşük basınç uygulaması isterler ve GC analizinden önce türevlendirmeye ihtiyaç duyulur (Teraï et al.1993).

2.2. Farmakolojik Aktiviteleri

Rhododendron cinsi çoğunluğu flavonoid ve diterpenlerden oluşan 200 den fazla bileşik içermektedir. Özellikle flavonoidler; antiinflamatuvar, analjezik, antibakteriyel, antioksidan ve antidiyabetik aktivitesinden, triterpenler; immunomodülatör, antidiyabetik ve sitostatik özelliklerinden diterpenler; toksik, insektisidal ve sitotoksik aktivitelerinden, kumarinler; antibakteriyel, tirozinaz inhibitör ve sitotoksik aktivitesinden fenolik bileşikler ise; antiviral ve immunomodülatör aktivitesinden sorumlu olarak gösterilmişlerdir (Harborne et al. 1971). Rhododendron cinsi çok sayıda flavonoid içermektedir. Flavonoidlerin biyolojikaktiviteleri iyi bilindiğinden daha çok araştırmalar bu yöne kaymıştır. Spesifik bileşikler göz önünde tutulduğunda ise; flavonoid grubundan hyperoside anti-inflammatuar etki ve analjezik aktiviteden, quercitrin, rutin ve isoquercitrin anti-inflammatuar ve analjezik aktiviteden sorumlu olduğu rapor edilmiştir. Esansiyel yağ komponentleri ile daphnetin ve rhodonetin in vitro antimikrobiyel aktivite gösterirken, daurichromenic acid, rhododaurichromenic acid A güçlü antiviral aktiviteye sahip olduğu belirlenmiştir. Bu cinsin türlerinde tespit edilen ursolic acid, corosolic acid, 23-hydroxyursolic acid ve rhododendric acid in vitro antidiyabetik aktivite gösterirken arjulinik asidin tirozinaz aktivite inhibitörü olduğu tespit edilmiştir. Bununla birlikte grayanotoxin, secorhodomolloide B ve ferruginene C 'nin hepatom ve lösemi gibi kanser hücrelerinde selektivite, ve/yada in vitro sitotoksikite gösterdiği belirlenmiştir. Rhodojaponin III, rhodomolin A ve rhodomollein I ise insektisidal aktivite gösteren bileşiklerdir (Popescu et al. 2013).

2.2.1. Anti İnflamatuvar Aktivite

Rhododendron türlerinin yarından fazlası geleneksel tıpta artirit, romatoidal hastalıklar ve bronşit ile ilgili inflamasyonlara karşı kullanılmaktadır. Bu konuda yapılan araştırmaların önemli bir kısmı deli bal üretimine bitkisel kaynak oluşturan *R. ponticum* ve *R. luteum* ile ilgilidir. Bir araştırmada, *R. ponticum* yapraklarının etanolik ekstraktı farelerde karagenan indüklü pençe ödemi modeli üzerinde çalışılmıştır (Erdemoğlu ve ark., 2003). Bu araştırmada Indometacin (10 mg/kg) referans olarak kullanılmış, bitki ekstraktı ise 500 mg/kg dozda verilmiştir. Önerilen ekstrak bu dozda herhangi bir gastroülserojenik etki göstermemiş, güçlü antiinflamatuvar etki göstermiştir. Daha sonra araştırmacılar *R. Ponticum* yapraklarının etil asetat ekstraktlarından anti inflammatuar etkiden sorumlu olduğunu düşündükleri hyperoside, quercitrin, isoquercitrin gibi bileşikler izole etmişlerdir. Bu bileşikler daha önceki araştırmalardakullanılann test modelinde % 26.8-30.7 oranında inhibisyon gösterirken,TPA indüklü kulak ödemi modelinde % 32.8-44.7 oranında inhibisyon göstermiştir. Bu bileşiklerden en güçlü olanın flavonolün glikozitler olduğu rapor edilmiştir (Rylski et al. 1979)

2.2.2. Anti-Nosiseptif Aktivite

R. ponticum'un (500 mg/kg) etanol ekstraktının farelerde benzoquinone indüklü abdominal konstriksiyon modelinde anti-nosiseptif etki gösterdiği bildirilmiştir (Zhang, et al.2010). Araştırmacılar bitkinin etil asetat ekstraktından izole ettikleri hyperoside 4, quercitrin ve isoquercitrin'in güçlü analjezik bileşikler olduğunu tespit etmişlerdir. Bu bileşiklerden

hyperoside ve isoquercitrin 97.31 mg/kg dozda % 25.8 inhibitör etkiye sahipken, quercitrinin 65.24 mg/kg dozda % 29.9 inhibisyon gösterdiği tespit edilmiştir. Nitekim *R. ponticum*'dan hyperoside bileşiğinin izole edildiği, antinflamatuar ve analjezik etki gösterdiği daha önceki araştırmalarda da gösterilmiştir (Rylski et al, 1979). Bu bileşiğin aynı zamanda nöron kültürlerinde nöroprotektif ve antiaapoptotik etki gösterdiği de rapor edilmiştir (Zhang, et al.2010, Hu et al. 2009)

2.2.3. Anti-Mikrobiyel Aktivite

R. luteum çiçeklerinden elde edilen esansiyel yağın *Serratia marcescens*, *Enterococcus faecalis* ve *Staphylococcus aureus* bakterileri üzerine moderate etki gösterdiği belirlenmiştir (Usta ve ark. 2012).

2.2.4. Antiprotozoal ve Anti-Viral Aktivite

Rhododendron türlerinin *Leishmania donovani* ve *Plasmodium falciparum*'a karşı antiprotozoal etki gösterdiği tespit edilmiştir (Tasdemir, ve ark. 2004). Miltefosine (IC₅₀:0.103 ug/mL)'nin standart olarak kullanıldığı bir araştırmada, *R. luteum* ile endemik bir tür olan *Rhododendron x sochadzea* Charadze & Davlianidze yapraklarının kloroform ekstraktı IC₅₀ değeri 2.3 ve 4.5 ug/mL konsantrasyonda Alamar Blue testinde leişmenisidal etki göstermiştir. Artemisin(IC₅₀:0.0027 ug/mL) standart olarak kullanıldığı başka bir araştırmada, *R. luteum*, *R. ponticum*, *R. smirnowii* Trautv., *Rhododendron x sochadzeae* Charadze & Davlianidze, *R. ungerii* Trautv. ekstraktlarının antiplasmodiyal aktivite gösterdiği tespit edilmiştir (Tasdemir, ve ark. 2004)

2.2.5. Asetilkolinesteraz İnhibitör Aktivite

Alzheimer hastalığının patogenezi, beyindeki nörotransmitter acethylcoline seviyesindeki yoksunluk olarak bilinmektedir. Asetilkolin eseraz inhibitörleri asetilkolin yıkımını önlemekte bu nedenle Alzheimer tedavisinde kullanılmaktadır. 1 mg/mL *R. ponticum* ve *R. luteum* ekstraktı AChE aktivitesini % 93 ve 76 oranında inhibe etmiştir (Orhan ve ark. 2004)

2.3. Rhododendron Türlerinin Geleneksel Tıpta Kullanımı

Etnomedikal Rhododendron türlerinin çoğu geleneksel Çin tıbbında artirit, akut ve kronik bronşit ve astım tedavisinde kullanılmıştır (Zhao et al. 2012). *R. dauricum* ve *R. molle* Çin farmakopesinde soğuk algınlığı, migren, düşme kaynaklı yaralanmalarda gelişen ağrı ve şişlik ile "inatçı stubborn tinea"da kullanılmak üzere yerini almıştır (Pharmacopoeia of the Peoples Republic of China (PPRC). 2010). Hindistan'da *R. arboretum*, *R. anthopogon*, *R. campanulatum* ve *R. lepidotum* ayurvedik tedavide kullanılan Rhododendron türleridir (Bhattacharyya, 2011). Bu bölgede özellikle *R. arboretum* çiçekleri dizanteri, dyspepsia, diyare, burun kanaması için tavsiye edilmektedir (Uniyal, et al. 2006). Japonya'nın kuzeyinde Rhododendron cinsine ait türler dismenorea ve kolit tedavisinde kullanılırken, Sibiry'a da eksternal olarak diş tedavisinde, eklem ağrısında kullanılırken böcek kovucu olarak kullanımı da vardır (Popescu et al. 2013). Kore'de *R. brachycarpium* en çok araştırılan Rhododendron türü olup, diyabet, artirit, baş ağrısı ve hipotansiyon tedavisinde kullanılmıştır (Choi et al. 2002). *R. Aureum* bitkisinin yaprakları Kore ve Uzak Doğu ile Rusya'da erupsiyon, romatoid artirit, kusma, diyare tadavisi ile diüretik olarak kullanılmıştır (Kim et al.2008). Tibet'te geleneksel phyoterapide *R. anthopogon* ve *R. anthopogonoides*'in yaprak ve çiçekleri

inflamasyon, akciğer ve cilt hastalıklarında kullanılmaktadır (Guleria et al. 2011). *R. caucasicum* yaprakları Kafkaslarda narkotik ve diaforetik olarak kullanılmaktadır (Sreevidya et al 2003). Kuzey Amerika’da bu cinsin türleri yaygın olarak tedavi amaçlı kullanılmaktadır. *R. calendulaceum* romatik ve kadın hastalıkları tedavisinde, *R. maximum* analjezik ve antiromatik olarak, *R. Albiforum* soğuk algınlığı, gastrointestinal hastalıklar, cilt problemleri boğaz ağrısı için *R. viscosum* narkotik olarak ve *R. tomentosum* dan elde edilen çay tonik olarak kullanılmakta, Kanada’da ise *R. groenlandicum* antidiyabetik ajan olarak kullanılmaktadır (Jhonson et al 1999, Tam, et al. 2009). Avrupa’da ise özellikle Almanya’da *R. Ferrugineum* yaprakları romatizma, hipertansiyon, kas ağrısı ve metabolik hastalıkların tedavisinde kullanılmaktadır (Louis et al. 2010). Bu bitkinin yaprak, çiçek ve galleri, diüretik, üriner antiseptik, antidiyaretik, yara iyileştirici ve ekspektoran olarak önerilmektedir (Sreevidya et al 2003). Romanya’da *R. Kotschy* romatik ve akciğer hastalıkları, öksürük için kullanılırken, Türkiye’de *R. luteum* ve *R. ponticum* yaprakları fitoterapide kullanılmaktadır. Özellikle *R. luteum* Sweet yaprakları diüretik, analjezik, romatizmal ağrılar, fungal ayak enfeksiyonları için *R. ponticum* L. yaprakları ise ödem, soğuk algınlığı, diş ağrısı, romatizmal ağrılar, diüretik, fungal ayak enfeksiyonları ve narkotik amaçlı kullanılmaktadır (Louis et al. 2010).

Avusturya halk tıbbında da Rhododendron türlerinin kullanımı oldukça yaygındır. Bitkiden solunum sistemi, kardiyovasküler, gastrointestinal ve üriner sistem rahatsızlıklarında faydalanılmakta, *R. Ferrugineum* yaprakları mesane rahatsızlıkları, gut ve romatizmaya karşı çay olarak önerilmektedir (Erdemoğlu ve ark. 2008).

2.4. Orman Güülü (Rhododendron Balı, Deli Bal, Kumar Balı, Acı Bal, Tutan Bal) Balı

Kaynaklara bilinen ilk biyolojik savaş olarak geçmiştir; tarihi kaynaklarda belirtildiğine göre; Romalı askerlerin perslerden kaçarken (M.Ö. 434-354) Doğu Karadeniz bölgesinde yedikleri bal anlatıcının ifadesiyle şu şekildedir: “ az yiyenler sarhoş gibiydiler, mideleri bulandı ve sersemleştiler, çok yiyenler ise bir çılgın gibiydiler. Bir güne kalmadan askerlerin bir kısmı uyanamadı bir kısmı ise hiçbir iz bırakmaksızın ayağa kalktılar. Yine de bu bizim bozguna uğramış görüntümüzü değiştirmedir” şeklinde Xenophon tarafından hikaye edilmektedir (Lampe,1988). Deli bal ile ilgili araştırmaların bir kısmı balın kimyasal yapısı, GTX içeriği ve medikal faydalı özellikleri üzerine yoğunlaşırken bir kısmı da zehirlenme üzerine vaka bildirimleri ile ilgilidir.

3.Deli bal zehirlenmesi ile ilgili vaka bildirimleri

Silici ve Atayoğlu’nun 2015 yılında Food and Chemical Toxicology dergisinde yayımlanan araştırmalarında 1989 yılından 2015 yılına kadar yapılan deli bal zehirlenmesi ile ilgili vaka bildirimleri derlenmiş 1003 vaka bulgusu değerlendirilmiştir (Silici ve Atayoğlu 2015). Yaklaşık 26 yıllık vaka bildirimleri değerlendirildiğinde, zehirlenmenin daha çok erkeklerde (%73.98) ve 15-64 yaşlarda olduğu, en çok zehirlenme vakalarının 1989-2014 tarihleri arasında rapor edildiğibelirlenmiştir. Bildirimi yapılan 1009 vakanın 746 ‘sı erkek (% 74.13) ve 261’i kadındır (25.87). Yaş aralıkları ise % 0.78’i 0-14 yaş grubunda, % 96.70’i 14-65 yaş grubunda ve % 2.52’ si ise 65 yaş üzerinde olduğu bildirilmiştir. Hastaların hikâyesi sorgulandığında, tüketilen bal miktarı değişkendir, bir çay kaşığından 10 yemek kaşığına kadar değişebilmektedir. Bu değer en az 5 g en çok 300 g şeklinde rapor edilmiştir.

Bal zehirlenmesi ile oluşan yaygın şikâyetlerin baş dönmesi (% 21.39), bulantı (% 17.47), kusma (% 12.95), halsizlik (% 10.04), bulanık görme (% 8.03), sinkop (%5.32) olduğu, EKG sonuçlarının SB: 155 (% 67.10), CAVB:16 (% 6.93), NR: 14 (% 6.06), AVB: 15 (% 6.49) şeklinde olduğu tespit edilmiştir. 1003 vakanın değerlendirilmesi sonucu zehirlenme sonucu

ölüm vakası görülmediği ve hastaların yaygın olarak 0.5 (% 24.49) ve 1 mg (% 25.51) atropine ile salin (iv fluid) 29 (% 29.59) ile tedavi edildiği ve genelde 24 saatte iyileşmenin görülerek taburcu edildiği belirlenmiştir. Bal zehirlenmesinin teşhis ve tedavisinin iyi anlaşılması hem etkin ve erken tedavi için hem de gereksiz tedavi masraflarının yapılmaması için önem kazanmaktadır.

KAYNAKLAR

Akgün N. 2017. Ordu İlinde Üretilen Kestane Balı, Akasya Balı, Orman Gülü Ve Yayla Ballarının Fiziksel Ve Kimyasal Aktiviteleri İle Antioksidan Aktivitelerinin İncelenmesi. Ordu Üniversitesi Fen Bilimleri Enstitüsü.

Aljadi, A.M., Kamaruddin, M.Y. 2004. Evaluation of the phenolic contents and antioxidant capacities of two Malaysian floral honeys. Food Chemistry, 85: 513-518.

Alvarez-Suarez J.M., Tulipani S., Diaz D., Estevez Y., Romandini S., Giampieri F, Damiani E., Astolfi P., Bompadre S., Battino M. 2010. Antioxidant and antimicrobial capacity of several monofloral Cuban honeys and their correlation with color, polyphenol content and other chemical compounds. Food Chem. Toxicol. 48: 2490-2499.

Bhattacharyya, D. 2011. *Rhododendron* Species and Their Uses with Special Reference to Himalayas – a Review. Assam University Journal of Science & Technology, 7(1), 161-167.

Bertocelj, J., Dobersek, U., Jamnik, M. 2007 Golob T. Evaluation of the phenolic content, antioxidant activity and colour of Slovenian honey. Food Chemistry, 105:822–828.

Bogdanov, S., Lullmann, C., Martin, P., Russmann, H., Vorwohl, G. 2000. Honey quality, methods of analysis and international regulatory standards: Review of the work of the international honey commission, Swiss Bee Research Centre, FAM, Liebefeld, Switzerland. www.agroscope.admin.ch; Erişim Tarihi: (8 Haziran 2016).

Buratti, S., Benedetti, S., Cosia, M.S. 2007. Evaluation of the antioxidant power of honey, propolis and royal jelly by amperometric flow injection analysis, Talanta, 71, 1387-1392.

Choi, Y.S., Jang, I.S., Kim, B.H., Kwon, N.Y., Kim, J.D., Lee, M.Y., et al. 2002. A case of severe bradyarrhythmia after ingestion of *Rhododendron brachycarpum*. Korean Circulation Journal, 32: 268–270.

Christopher, M.H., Kim, M.D. 1997. Potentiating health and crisis of the immune system. Plenum pres. New York, chapter. 24, 243-270.

De Loose, R. Nieuwe cultivar op kompost van Azalea indica L.: een bonte sport van cv. De waele's favorite bekommen door bestraling. Verbondsnieuws Belg. Sierteelt, 18 (4): 125-129.

Doğaroğlu, M. 2004. Modern arıcılık teknikleri 2.baskı. Doğa Arıcılık Tic. Ltd. Şti. Tekirdağ.

Dustman, J.H. 1993. Honey quality and its control. American Bee Journal. 133(9):648-651.

- Erdemoğlu, N., Akkol, E.A., Yeşilada, E., Çalış, I. 2008. Bioassay-guided evaluation of anti inflammatory and antinociceptive activities of *Rhododendron ponticum* L. leaves. *Journal of Ethnopharmacology*, 119: 172–178.
- Erdemoğlu, N., Küplei, E., Yeşilada, E. 2003. Anti-inflammatory and antinociceptive activity assessment of plants used as remedy in Turkish folk medicine. *Journal of Ethnopharmacology*, 89(1):123-129.
- Escuredo, O., Dobre, I., Fernández-González, M., Seijo, M.C. 2014. Contribution of botanical origin and sugar composition of honeys on the crystallization phenomenon. *Food Chemistry*, 149: 84-90.
- Fallico, B., Zappala, M., Arena, E., Verzera, A. 2004. Effects of conditioning on HMF content in unifloral honeys. *Food Chemistry*, 85: 305-313.
- Fiorani, M., Accorsi, A., Blasa, M., Diamantini, G., Piatti, E. 2006. Flavonoids from Italian multifloral honeys reduce the extracellular ferricyanide in human red blood cells, *J. Agric. Food Chemistry*, 54, 8328-34.
- Guleria, S., Tikku, A.K., Singh, G., Vyas, D., Bhardwaj, A. 2011. Antioxidant activity and protective effect against plasmid DNA strand scission of leaf, bark, and heartwood extracts from *Acacia catechu*. *Journal of Food Science*, 76: C959–C964.
- Guler, A., Bakan, A., Nisbet, C., Yavuz, O. 2007. Determination of important biochemical properties of honey to discriminate pure and adulterated honey with sucrose (*Saccharum officinarum* L.) syrup. *Food Chemistry*, 105: 1119-1125.
- Harborne, J.B., Williams, C.A. 1971. Leaf survey of flavonoids and simple phenols in the genus *Rhododendron* *Phytochemistry*, 10(11): 2727-2744.
- Hu, J., Wang, Z., Guo, Y. Y., Zhang, X. N., Xu, Z.H., Liu, S. B., Zhao, M. G. 2009. A role of periaqueductal grey NR2B-containing NMDA receptor in mediating persistent inflammatory pain. *Molecular pain*, 5(1), 71.22.
- Jhonson, B.J., Miller, G.H., Fogel, M.L., Magee, J.W., Gagan, M.K., Chivas, A.R. 1999. 65,000 Years of Vegetation Change in Central Australia and the Australian Summer Monsoon. *Science*, 284, 1150-1152.
- Karadal, F., Yıldırım, Y. 2012. Balın kalite nitelikleri, beslenme ve sağlık açısından önemi. *Erciyes Üniversitesi Veterinerlik Fakültesi Dergisi*, 9(3): 197-209.
- Kim, C., Kim, D.S., Lee, H.W., Ahn, Y.M., Uhm, J.H. 2008. A case of grayanotoxin intoxication presenting with mental changes and vomiting. *Korean Journal of Pediatric Gastroenterology and Nutrition*, 11: 223–225.
- Lampe, K.F. 1988. *Rhododendrons, Mountain laurel, and mad honey*. *JAMA*, 259(13): 2009.
- Louis, A., Petereit, F., Lechtenberg, M., Deters A., Hensel, A. 2010. Phytochemical characterization of *Rhododendron ferrugineum* and in vitro assessment of an aqueous extract on cell toxicity. *Planta Medica*, 76 (14); 1550.

- Louis, A., Petereit, F., Canigoeral, S., Hensel, A. 2009. Phytochemical characterisation of the leaves of *Rhododendron ferrugineum*. *Planta Medica*, 75 (09): 1550-1557.
- Molan, P.C. 2006. The evidence supporting the use honey as a wound dressing, *Int. J. Low Extrem Wounds*, 5, 40-54.
- Nagai, T., Sakai, M., Inoue, R., Inoue, H., Suzuki, N. 2001. Antioxidative activities of some commercially honeys, royal jelly, and propolis. *Food Chemistry*, 75:237–240.
- Nombre, I., Schweitzer, P., Boussim, J.I, Rasolodimby, J.M. 2010. Impacts of storage conditions on physicochemical characteristics of honey samples from Burkina Faso. *Afr. J. Food Sci.* 4(7): 458 –463.
- Orhan, I., Şener, B., Choudhary, M.I., Khalid, A. 2004. Acetylcholinesterase and butyrylcholinesterase inhibitory activity of some Turkish medicinal plants” *J. Ethnopharm.* 91: 57-60.
- Pharmacopoeia of the Peoples Republic of China (PPRC). 2010. 3 volumes China.
- Polat, G. 2007. Farklı lokasyon ve orijinlere sahip balların reolojik, fizikokimyasal karakteristikleri ve mineral içeriklerinin belirlenmesi. Yüksek Lisans Tezi, Selçuk Üniversitesi, Fen Bilimleri Enstitüsü, Gıda Mühendisliği Anabilim Dalı, Konya.
- Popescu, R., Kopp, B. 2013. The genus *Rhododendron*: an ethnopharmacologic
- Rylski, M., Duriasz-Rowinska, H., Rewerski, W. 1979. The analgesic action of some flavonoids in the hot plate test. *Acta Physiol Pol*, 30: 385–388.
- Silici, S. 2019. Orman Gülü Balı (Deli Bal) Toksikasyonu, *Türk Bilimsel Derlemeler Dergisi* E-ISSN: 2146-0132, 12 (2): 35-44, 2019
- Silici, S., Atayoğlu, A.T. 2015. Mad honey intoxication: A systematic review on the 1199 cases. *Food Chem Toxicol*, 86: 282-90.
- Silici, S., Sagdic, O., Ekici, L. 2010. Total phenolic content, antiradical, antioxidant and antimicrobial activities of *Rhododendron* honeys. *Food Chemistry*, 121, 238-243
- Sreevidya, N., Mehrotra, S. 2003. Spectrophotometric method for estimation of alkaloids precipitable with Dragendorff's reagent in plant materials. *J AOAC*, 86(6):1124-27.
- Tam, T.W., Liu, R., Arnason, J.T., Krantis, A., Staines, W.A., Haddad, P.S., Foster, B.C. 2009. Actions of ethnobotanically selected Cree anti-diabetic plants on human cytochrome P450 isoforms and flavin-containing monooxygenase 3. *J Ethnopharmacol*, 29;126(1): 119-26.
- Tasdemir, D., Brun, R., Perozoo, R., Dönmez, A.A. 2005. Evaluation of antiprotozoal and plasmodial enoyl-ACP reductase inhibition potential of Turkish medicinal plants, 19(2): 162-166.

Tasdemir, D., Dönmez, A.A., Çalı, I., Rüedi, P. 2004. Evaluation of biological activity of Turkish plants. Rapid screening for the antimicrobial, antioxidant, and acetylcholinesterase inhibitory potential by TLC bioautographic methods” J.Pharm Biol, 42 (4-5), 374-383.

Terai, T., Tanaka, S. 1993. Gas chromatographic determination on grayatoxins. Chem Express, 8: 381-384.

Tezcan , F., Kolaylı , S., Şahin, H., Ulusoy, E. 2011. Evaluation of organic acid, saccharide composition and antioxidant properties of some authentic Turkish honey, J. Food Nutr. Res. 50, 33-40.

Turhan, I., Tetik, N., Karhan, M., Gurel, F., Tavukcuoglu, H.R. 2008. Quality of honeys influenced by thermal treatment. Lebensm Wiss Technol. 41:1396– 1399.

Uniyal, S.K., Singh, K.N., Jamwal, P., Lal, B. 2006. Traditional use of medicinal plants among the tribal communities of Chhota Bhangal, Western Himalaya. Journal of Ethnobiology and Ethnomedicine, 2: 14.

Usta, A., Yaylı, B., Kahrınman, N., Karaoğlu, S.A., Yaylı, N. 2012. Composition and Antimicrobial Activity of Essential Oil from the Flower of *Rhododendron luteum* Sweet. Asian Journal of Chemistry, Vol. 24, No. 5.

Zhao, B., Yin, Z.F., Xu, M., Wang, Q.C. 2012. AFLP analysis of genetic variation in wild populations of five *Rhododendron* species in Qinling Mountain in China. Biochem. Syst. Ecol, 45: 198-20.

Zhang, S., Chen, F., Peng, S., Ma, W., Korpelainen, H., Li, C. 2010. Comparative physiological, ultrastructural and proteomic analyses reveal sexual differences in the responses of *Populus cathayana* under drought stress. Proteomics, 10, 2661–2677.

INVESTIGATION OF THE USAGE OF CORAL WASTE FISH SCALS AS A CATALYST IN PRODUCTION OF BIODIESEL

Gediz UĞUZ

0000-0002-6796-6067

Ondokuz Mayıs University, Engineering Faculty, Chemical Engineering, Samsun, Turkey.

Abstract

In recent years, clean and alternative energy sources such as wind, solar, biomass and biodiesel have become an important research area due to the energy resources consumed with the increasing energy need and the energy crises that have arisen accordingly. In this study, a catalyst was synthesized from coral (*pagrus pagrus*) fish flakes to be used in the production of biodiesel from waste fish flakes and used as a catalyst in the transesterification reaction in biodiesel production. For this purpose, calcined catalysts were synthesized from coral (*pagrus pagrus*) fish scales to be used in biodiesel production in order to increase the reaction rate and to evaluate fish wastes. For this purpose, fish scales were washed and dried to remove residues and other substances. The dried flakes were first ground into fine powder and then calcined at different temperatures (900 and 1000 °C). The synthesized catalyst was characterized by the Thermogravimetric analysis method (TGA). When the catalysts calcined at different temperatures were characterized, it was determined that the best transformation was observed using the X-ray diffraction method (XRD). The morphological properties of the best catalyst were determined by Scanning Electron Microscopy and Energy Dispersion Spectrometer (SEM-EDS) technique. Conventional biodiesel was produced using the best catalyst. Biodiesel yield was calculated and the results were evaluated.

Keywords: Biodiesel, Catalyst, Coral fish, SEM-EDS, TGA, XRD.

Introduction

To deal with rising energy demand, depletion of fossil fuel supplies and environmental issues caused by fossil fuel consumption, governments seeking to reduce their reliance on petroleum-exporting countries are exploring alternative energy sources such as biofuels. Mr. Rudolph Diesel pioneered the use of vegetable oils in compression ignition engines in the early 19th century (Orchard, Jon and John, 2007). Vegetable oils are easy to produce as they are obtained by simple pressing of oil-bearing biomass prior to decanting and filtration. However, using vegetable oils in diesel engines designed to run on diesel fuel raises certain problems. Indeed, due to their high viscosity and low cetane number in comparison to diesel fuel, vegetable oils are more difficult to pump, inject, and ignite in diesel engines. Furthermore, owing to the presence of phospholipids in the fuel, the use of vegetable oils may cause the buildup of gums in the inner sections of the diesel engine, depending on the pressing temperature and the nature of the biomass utilized upstream. Some modifications, therefore, have to be made to the engine. The goal of the adjustments is to keep the vegetable oil at a high temperature in order to reduce viscosity and increase ignition, ensuring long-term engine running. The use of vegetable oils as fuel is especially well suited to static engines. Once started, the sort of engine is designed to run continuously at a high regime, and hence at high temperatures. Vegetable oil, on the other hand, is difficult to utilize in car engines, which experience significant swings in load, resulting in huge temperature differences inside the combustion chamber.

To improve the market value of biodiesel, it is required to make its manufacturing feasible. Biodiesel costs can be reduced by using less valued raw materials such as oils, fats, and leftover frying oils. However, due to the high FFA concentration of these feedstocks, the transesterification process cannot be applied directly to them. Because of the high saturation level, the cold-flow characteristics of biodiesel derived from such sources, particularly lipids, are very poor. As a result, research should

concentrate on enhancing the cold flow properties of biodiesel generated from low-cost raw sources. By using blends of oils and animal fats such as beef tallow and chicken fat is an opportunity to produce biodiesel.

To avoid modifying car engines, one option is to create biodiesel by chemically modifying vegetable oils through transesterification. This biofuel has fuel properties similar to diesel fuel. It may thus be used as a pure fuel or combined with diesel fuel in diesel engines without requiring extensive engine changes. Because biodiesel is a great rubber solvent, just a few seals or hose modifications may be required. As a result, biodiesel is a very appealing alternative to diesel fuel. It contributes toward sustainable development as i) it makes it possible to use locally available, renewable resources and ii) it reduces greenhouse gas emissions when compared to diesel fuel, without sacrificing engine performance.

Biodiesel is made up of mono-alkyl esters derived from many sources such as vegetable oils, animal fats, greases, oil and fat wastes, or a combination of multiple feedstocks (Ma and Hanna, 1999). It is most often utilized as a fuel in engines and heating systems. Biodiesel is a non-toxic, biodegradable biofuel that is also lucrative for the environment. That is one of the reasons why biodiesel has gained popularity; also, petroleum supplies are decreasing, necessitating the search for alternate energy sources (Fukuda, Kondo and Noda, 2001).

Biodiesel is created by transesterifying oils, fats, or mixes of these with alcohol utilizing appropriate catalysis. Despite the comparatively low cost of the biodiesel production method, the high cost of its raw materials is a key barrier to its widespread commercialization; biodiesel derived from biomass is typically 10 to 50 percent more expensive than diesel derived from petroleum (Leung and Guo, 2006). Fortunately, waste frying oils (WFOs) have remained low-cost feedstocks, making biodiesel manufacturing more viable in comparison to fossil-fuel-based diesel production (Gonzalez Gomez, Howard-Hildige, Leahy and Rice, 2002).

In the transesterification procedure, triacylglycerides (also known as triglycerides) in vegetable oils are transformed into fatty acid alkyl esters known as "biodiesel" in the presence of short-chain alcohol and a catalyst, with glycerol as a byproduct (**Figure 1**). In general, a catalyst is used to speed up the transesterification reaction. Catalysts used for the transesterification of triacylglycerides are often classed as homogeneous, heterogeneous, or enzymatic, depending on the mechanism.

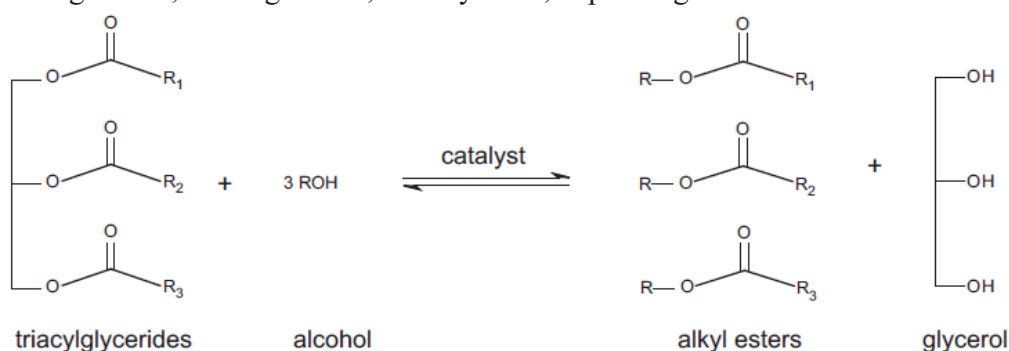


Figure 1. The reaction equation of biodiesel production

In this study, a catalyst was synthesized from coral (*pagrus pagrus*) fish flakes to be used in the production of biodiesel from waste fish flakes and used as a catalyst in the transesterification reaction in biodiesel production. For this purpose, calcined catalysts were synthesized from coral (*pagrus pagrus*) fish scales to be used in biodiesel production in order to increase the reaction rate and to evaluate fish wastes. For this purpose, fish scales were washed and dried to remove residues and other substances. The dried flakes were first ground into fine powder and then calcined at different temperatures (900 and 1000 °C). The synthesized catalyst was characterized by the Thermogravimetric analysis method

(TGA). When the catalysts calcined at different temperatures were characterized, it was determined that the best transformation was observed using the X-ray diffraction method (XRD). The morphological properties of the best catalyst were determined by Scanning Electron Microscopy and Energy Dispersion Spectrometer (SEM-EDS) technique. Conventional biodiesel was produced using the best catalyst. Biodiesel yield was calculated and the results were evaluated.

Materials and Methods

Materials

Safflower oil (*Carthamus Tinctorius*) was supported from Kayseri, in Turkey for biodiesel production. The fatty acid contents of safflower oil were determined by using GC and was shown in Table 3. Coral fish (*pagrus pagrus*) scales were taken from fish market in Black Sea, Turkey. Methanol (>99% purity) was purchased from Sigma Aldrich for biodiesel production.

Synthesis of the heterogeneous catalyst

In this study, natural heterogeneous catalyst synthesized from coral waste fish scales by using calcination technique. Firstly, waste fish scales were cleaned several times with distilled water to remove various contaminants and other substances. The waste scales were dried in an oven for approximately 6 hours at 100 °C. The dried scales were ground to a fine powder and calcined in a muffle furnace at different temperatures (900 and 1000 °C) for 2 hours. The thermal properties of waste fish scales were determined by Thermogravimetric Analysis (TGA). The novel waste coral fish scale catalyst was named as CFWS. The best calcination temperature was determined by using XRD technique. The morphology of the novel catalyst was defined by SEM. The thermal properties of waste fish scales were determined by Thermogravimetric Analysis (TGA). Finally, the novel synthesized catalysts (CFWS) were used for biodiesel production from safflower oil.

Characterization Methods

The produced novel CFWS properties were evaluated by using some characterization techniques. XRD patterns were obtained (Rigaku Smart Lab Co., Japan) using Cu K β source equipped with an SC-70 Page 7/16 detector. The analysis was performed at 2 θ ranging from 2° to 80° at a scanning speed of 1° min⁻¹. The surface morphology of the synthesized catalyst by using JEOL-SEM JSM 7001F model device has been used at 15 kV. Thermogravimetric analysis of the coral fish (*pagrus pagrus*) scales (TGA) is conducted with the TA Instrument SDTQ600 analyzer. 10 mg of sample was loaded into pans. The temperature ranges from 20 to 800 °C with a heating rate of 15 °C/min under nitrogen (N₂) atmosphere of 150 mL /min to determine the thermal properties of seabass fish scales.

Biodiesel Production

In the present study, safflower oil was reacted with 25% (v/v oil) methanol (6:1 molar ratio) and 1% (m/m oil) CFWS. Safflower oil was heated to remove water and humidity. The reaction was carried out nearly at 60 °C for 1 hour and 400 rpm stirring speed. The methyl ester was washed introduced into a rotary evaporator to remove the excess water and methanol. Finally, the product was filtered by using filter paper and bottled in darkness ambient.

Results & Discussions

Coral fish scales are combined of various matters such as water, organics, inorganics, minerals. The TGA was carried out for quantitative estimation of contents of waste fish scales. The effects of calcination conditions on weight change on fish scales were determined by the TGA method. The weight changes of fish scales were revealed in **Figure 2**. over the temperature range from 20 to 800 °C. The interpretation of TGA curve was explained in **Table 1**.

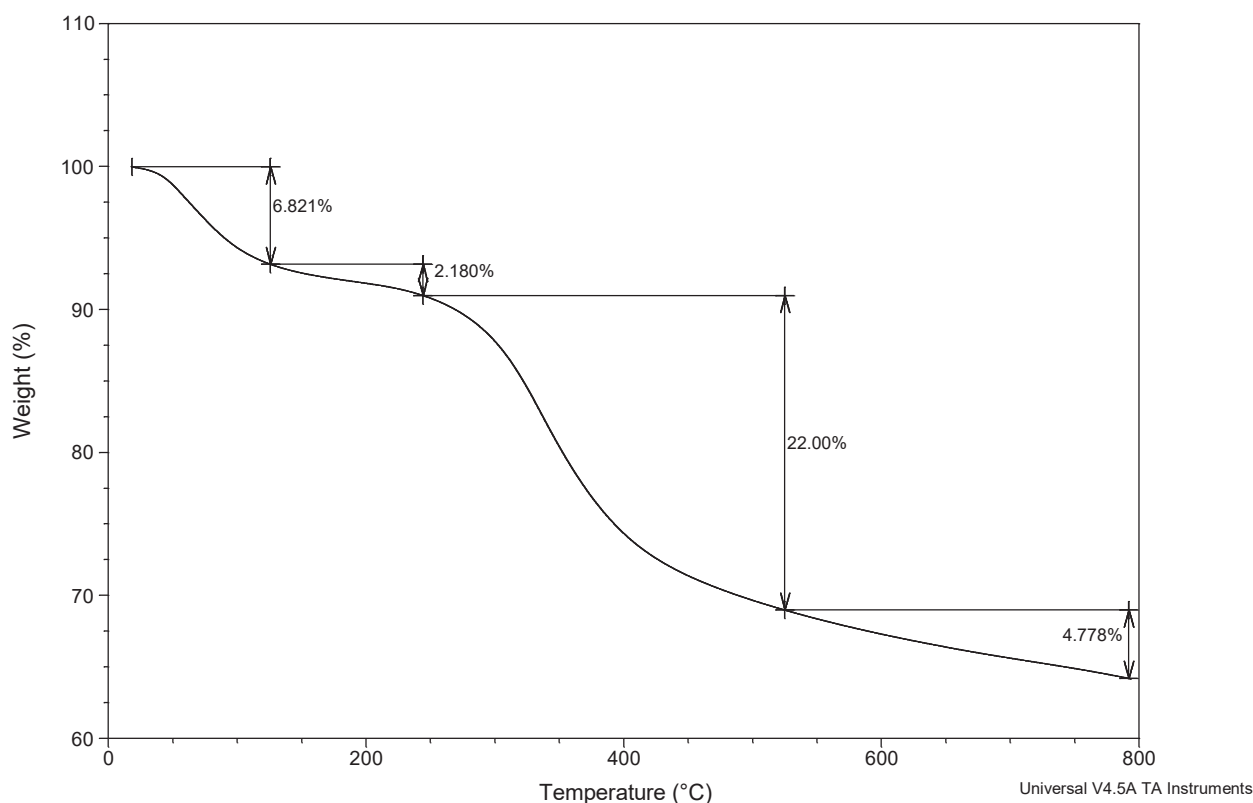


Figure 2. TGA curve of waste fish scale (Coral) between 20 – 800 °C

Table 1. The weight change of fish scale (Coral)

Stage	Temperature Range (°C)	Weight Loss (%)	Causes
1	20 - 125	6.82	Evaporation of adsorbed water
2	125 - 245	2.18	Loss of the lattice water
3	250 - 525	22.00	Macromolecules fragmentation
4	525 - 800	4.77	Formation of gaseous

In **Figure 2.**, the initial 6.82% weight loss corresponding to the temperature range of 20 - 125 °C indicating the evaporation of adsorbed water occurred between 125 and 245 °C because of the loss of the lattice water. The weight loss of 22.00% resulted in the temperature range of 245 - 525 °C, which can be attributed to fragmentation of macromolecules and loss of guanine and the other organic matters. In additionally, 4.77% steady weight loss up to 800 °C due to formation of gaseous elements. The total weight loss was determined as nearly 36 % for calcined waste fish scale.

The XRD patterns for the CFWS samples were obtained over a calcination temperature 900 and 1000 °C as shown in Figure below.

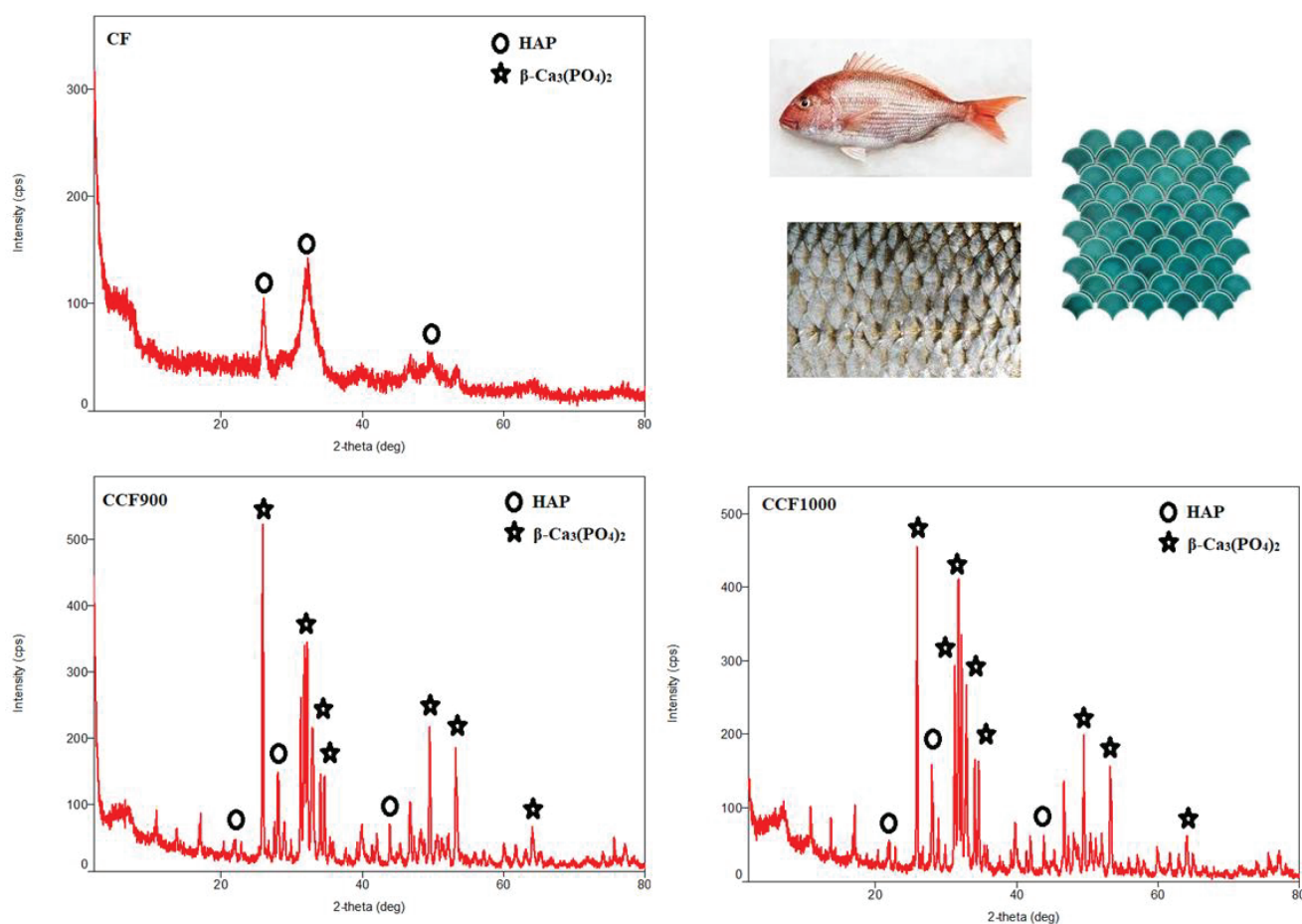


Figure 3. XRD patterns of waste Coral (*pagrus pagrus*) fish scales derived catalysts by calcination at different temperatures (900, and 1000 °C).

Figure 3. shows the XRD patterns for the waste coral fish scales samples obtained over a calcination temperatures 900 and 1000 °C. In Figure 3, small peaks of hydroxyapatite (HAP) at 25 °C. Prominent peaks of HAP can be seen after 900 °C and the formation of β - $\text{Ca}_3(\text{PO}_4)_2$ conforming to transformation of HAP can be seen at 900 and 1000 °C. The catalyst that produced at 1000 °C act as a base catalyst. Narrow and highly intense peaks of the calcined waste fish scales referred the crystalline structure of the novel catalyst. SEM micrograph of catalyst samples exhibited the existence of circular holes distributed over the catalyst surface at a calcination temperature of 1000 °C as shown in **Figure 4.** below.

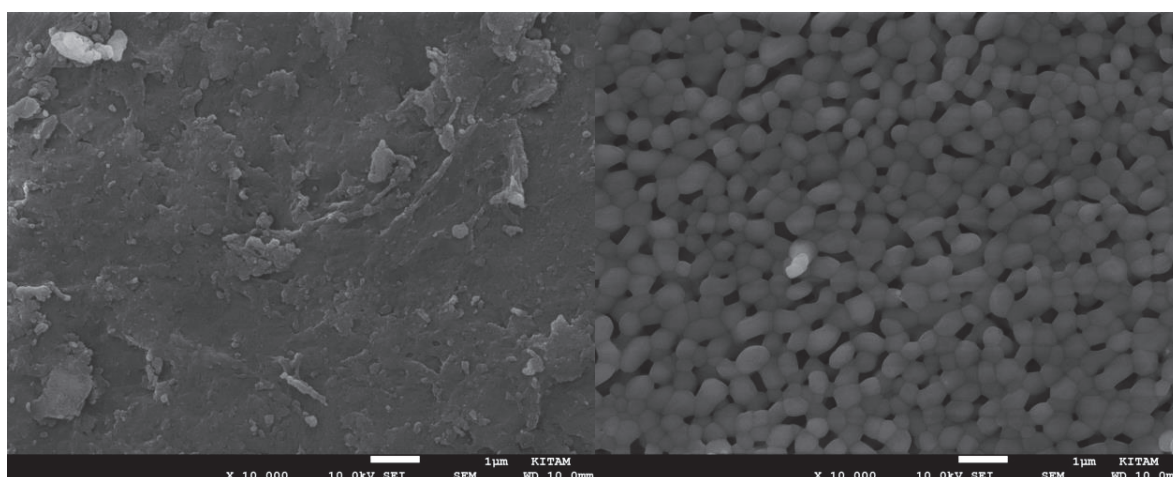


Figure 4. SEM images of the waste fish scale before and after calcination process a) 25 °C, b) 1000 °C

SEM micrograph (**Figure 4**) of catalyst samples exhibited the existence of circular holes distributed over the catalyst surface at calcination temperature of 1000 °C. As depicted in **Figure 4b**, the internal layer of the WFSC (**Figure 4b**) exhibited regular oval-shaped particles having tapered ends. After the preparation catalyst, it was used for biodiesel production. Biodiesel yield was calculated as 70 %. It was concluded that the novel catalyst could be improve after some restorations.

Conclusions

In the present study, it was depicted the prosperous application of calcined was fish scale (coral) as an efficient heterogeneous catalyst for biodiesel production in transesterification of safflower oil. $\beta\text{Ca}_3(\text{PO}_4)_2$ was generated from the HAP in coral fish scale with high temperatures with calcination process. The novel product could effectively catalyze the methanolysis of refined safflower oil to yield FAME (biodiesel). The best novel catalyst was prepared in 1000 °C. The yield of methyl ester conversion in the study which catalysed by the CFWS was reported to be 70 % from safflower oil.

Acknowledgements

The authors would like to thank to Dr. Nalan TÜRKÖZ KARAKULLUKÇU, Aysun KARACA AYLÇIN and Yunis GEDİK in KİTAM, Ondokuz Mayıs University, Samsun, Turkey, for the TGA, XRD and SEM analysis.

References

- Karmakar A, Karmakar S, Mukherjee S. Properties of various plants and animals feedstocks for biodiesel production. *Bioresource Technology* 2010;101:7201e10.
- Knothe G. Biodiesel and renewable diesel: a comparison. *Progress in Energy and Combustion Science* 2010;36:364e73.
- Sidibé SS, Blin J, Vaitilingom G, Azoumah Y. Use of crude filtered vegetable oil as a fuel in diesel engines state of the art: literature review. *Renewable and Sustainable Energy Reviews* 2010;14:2748e59.
- Atadashi IM, Aroua MK, Aziz AA. High quality biodiesel and its diesel engine application: a review. *Renewable and Sustainable Energy Reviews* 2010;14:1999e2008.
- Demirbas A. Biodiesel production from vegetable oils via catalytic and noncatalytic supercritical methanol transesterification methods. *Progress in Energy and Combustion Science* 2005;31:466e87.
- Nigam PS, Singh A. Production of liquid biofuels from renewable resources. *Progress in Energy and Combustion Science* 2011;37:52e68.

- Qi DH, Geng LM, Chen H, Bian YZ, Liu J, Ren XC. Combustion and performance evaluation of a diesel engine fueled with biodiesel produced from soybean crude oil. *Renewable Energy* 2009;34:2706e13.
- Agarwal AK. Biofuels (alcohols and biodiesel) applications as fuels for internal combustion engines. *Progress in Energy and Combustion Science* 2007;33:233e71.
- Lam MK, Lee KT, Mohamed AR. Homogeneous, heterogeneous and enzymatic catalysis for transesterification of high free fatty acid oil (waste cooking oil) to biodiesel: a review. *Biotechnology Advances* 2010;28:500e18.
- Vyas AP, Verma JL, Subrahmanyam N. A review on FAME production processes. *Fuel* 2010;89:1e9.
- Ma, F. and Hanna, M.A., 1999. Biodiesel production: a review, *Bioresource Technology*, 70, 1-15.
- Leung, D.Y.C. and Guo, Y., 2006. Transesterification of neat and used frying oil: optimization for biodiesel production. *Fuel Process Technol*, 87, 883–90.
- Gonzalez Gomez, M.E., Howard-Hildige, R., Leahy, J.J., and Rice, B., 2002. Winterization of waste cooking oil methyl ester to improve cold temperature fuel properties. *Fuel*, 81, 33–39.
- Fukuda, H., Kondo, A. and Noda, H., 2001. Biodiesel fuel production by transesterification of oils, *Journal of Bioscience and Bioengineering*, 92, 405–416.